UNIVERSITAT DE BARCELONA

Yacimientos de ámbar del Cretácico de la Cuenca del Maestrazgo: tafonomía, bioinclusiones y paleoecología

Sergio Álvarez Parra

Yacimientos de ámbar del Cretácico de la Cuenca del Maestrazgo: tafonomía, bioinclusiones y paleoecología

Sergio Álvarez Parra

Directores: Xavier Delclòs Martínez y Enrique Peñalver Mollá

Universitat de Barcelona
Facultat de Ciències de la Terra
Departament de Dinàmica de la Terra i de l'Oceà

Programa de Doctorat en Ciències de la Terra, 2023

TESIS DOCTORAL

Yacimientos de ámbar del Cretácico de la Cuenca del Maestrazgo: tafonomía, bioinclusiones y paleoecología

Sergio Álvarez Parra

Directores:

Xavier Delclòs Martínez

Enrique Peñalver Mollá

Programa de Doctorat en Ciències de la Terra

Departament de Dinàmica de la Terra i l'Oceà

Facultat de Ciències de la Terra

Universitat de Barcelona

2023

Portada: El autor de la Tesis Doctoral con una pieza de ámbar del yacimiento de San Just, julio de 2021. Foto: Fundación Conjunto Paleontológico de Teruel-Dinópolis. Autora: Silvia Sánchez.

Contraportada: Ejemplar excepcionalmente conservado de avispa de la familia Scelionidae (Hymenoptera) en ámbar del yacimiento de Ariño (Albiense inferior).
Ejemplar con sigla AR-1-A-2019.95.3.

UNIVERSITAT DE BARCELONA

Yacimientos de ámbar del Cretácico de la Cuenca del Maestrazgo: tafonomía, bioinclusiones y paleoecología

Memoria de Tesis Doctoral presentada por Sergio Álvarez Parra, dirigida por Xavier Delclòs (Universitat de Barcelona) y Enrique Peñalver (Instituto Geológico y Minero de España-CSIC), para optar al título de doctor por la Universitat de Barcelona. Esta memoria se ha realizado dentro del Programa de Doctorat en Ciències de la Terra HDK09 de la Universitat de Barcelona y se enmarca en el proyecto *Cretaceous Resin Event: global bioevent of massive resin production at the initial diversification of modern forest ecosystems* CGL2017-84419 (IPs: Xavier Delclòs y Eduardo Barrón) del Ministerio de Ciencia e Innovación del Gobierno de España. El periodo de realización de la Tesis Doctoral ha sido financiado durante tres años y cinco meses por el programa de *Ajuts per a la contractació de personal investigador en formació-FI* de la Secretaria d'Universitats i Recerca de la Generalitat de Catalunya y el Fondo Social Europeo (2019FI_B 00330, 2020FI_B1 00002, 2021FI_B2 00003). El candidato forma parte del Institut de Recerca de la Biodiversitat (IRBio) y del grupo y proyecto de investigación *Geologia Sedimentària* 2017SGR-824 (IPs: Anna Travé y Telm Bover) de la Agència de Gestió d'Ajuts Universitaris i de Recerca de la Generalitat de Catalunya. Se ha recibido financiación para estancias y actividades de investigación y formación por parte de las *Ajuts de recerca de la Facultat de Ciències de la Terra* (Universitat de Barcelona), *Ajuts per a la realització d'activitats formatives en relació als Ajuts per a la contractació de personal investigador en formació-FI* (Agència de Gestió d'Ajuts Universitaris i de Recerca, Generalitat de Catalunya), *Ajuts per a la realització d'estades formatives a Espanya i l'estranger dirigida a doctorands de la Universitat de Barcelona* (Fundació Montcelimar, Universitat de Barcelona) y la empresa pública EL SOPLAO S.L. (acuerdo de investigación #20963 con la Universitat de Barcelona, VAPC 20225428 con IGME-CSIC, Consejería de Industria, Turismo, Innovación, Transporte y Comercio del Gobierno de Cantabria).

Sergio Álvarez Parra

Barcelona, noviembre de 2022

Instituto Geológico y Minero de España

IRBio Institut de Recerca de la Biodiversitat UNIVERSITAT DE BARCELONA

GRUP DE GEOLOGIA SEDIMENTÀRIA

Generalitat de Catalunya Departament d'Empresa i Coneixement Secretaria d'Universitats i Recerca

Unió Europea Fons social europeu L'FSE inverteix en el teu futur

Amberia

Not all those who wander are lost.

"No todos los que vagan están perdidos".

The Riddle of Strider, La Comunidad del Anillo
J.R.R. Tolkien, 1954

"Nada tiene sentido en Biología
si no es a la luz de la evolución".

Theodosius Dobzhansky, 1973

Algunas veces olvidada, muchas veces obviada.
La tafonomía es la disciplina, dentro de la Paleontología,
que se encarga del estudio de los procesos de fosilización
y la formación de yacimientos. Es esta disciplina la que
da respuesta a una pregunta tan básica y fundamental
como por qué tenemos este fósil delante de nosotros.
Por ello, me tomo la libertad de versionar
la famosa frase del Prof. Dobzhansky.

"Nada tiene sentido en Paleontología
si no es a la luz de la tafonomía".

Agradecimientos

El tiempo, ese gran misterio. El pasado no existe, el futuro no existe, el presente es inalcanzable. Desde siempre he sentido fascinación por el tiempo, por el tiempo futuro, pero más aún por el tiempo pasado. Muchas preguntas. ¿Qué ocurrió? ¿Cómo era? ¿Por qué? Hasta ahora. Ya ha llegado el momento. Ya estoy escribiendo estas líneas que simbolizan el final de una etapa, y el comienzo de otra. Todo esto viene de largo, desde aquel niño de cinco años que se divertía imitando sonidos de dinosaurios, que después creció, y finalmente ha podido trabajar en lo que le apasiona. Y hasta aquí no habría llegado si no es por la ayuda y el apoyo de muchas personas que me han acompañado en un momento u otro, de una forma u otra.

Comenzaré con las personas que se ocuparon de mi educación y formación. Muchos profesores me impulsaron a seguir con lo que me gustaba, en particular José Luis Díaz León, que me llevó a conocer el increíble mundo de la Biología.

Durante los años de la carrera de Biología en la Universidad Autónoma de Madrid pude acércame por primera vez a la Paleontología. Agradezco muchísimo a los profesores José Luis Sanz, Ángela Delgado, Jesús Marugán y Fran Poyato que me transmitieran su fascinación por esta disciplina.

Cursar el paleomáster de la Universitat de València y la Universitat d'Alacant fue una de las mejores experiencias de mi vida. Me adentré aún más en la Paleontología y pude conocer a personas estupendas. Muchas gracias a todos, profesores y compañeros. En especial a Héctor Botella y Carlos Martínez, por vuestro apoyo y confianza.

Algo que nunca puede faltar en el camino son los amigos. Durante estos últimos tres años he sentido que me he despegado de muchos de ellos, ligado tanto a la distancia como a cierta situación sanitaria global. Pero, deciros que me he acordado mucho de vosotros y me alegra que podamos seguir viéndonos aunque sea cada varios meses. Los amigos de siempre, Andrés, Javi, Luis y Rubén, que sepáis que recordar los buenos momentos con vosotros me ha ayudado a iluminarme en las épocas más oscuras. Los amigos biólogos, muchos buenos momentos tanto en las clases de la universidad como de viaje en el extranjero. Y no podía olvidarme, por supuesto, del Paleoteam: Andreu, Esther, Mavi y Óscar (me olvido de una persona, pero seguro que aparece más adelante). Me encantó el grupo y la amistad que formamos, ojalá más reencuentros.

Agradezco a los compañeros de la Fundación Conjunto Paleontológico de Teruel-Dinópolis que nos hayan brindado la posibilidad de trabajar en el yacimiento de Ariño. En particular, quiero agradecer a Luis Alcalá (ahora en el Parque de las Ciencias de Andalucía-Granada), Eduardo Espílez y Luis Mampel su colaboración y continuo apoyo.

El trabajo de campo en los yacimientos de ámbar de Teruel se ha realizado gracias a los permisos de la Dirección General de Patrimonio Cultural del Gobierno de Aragón.

Particularmente, agradezco la gestión y el trato cercano de Juan Carlos García Pimienta. También, considero que la difusión social es una parte esencial del trabajo científico, por lo que he de agradecer el interés de Javier Millán, de Diario de Teruel, por nuestro trabajo a lo largo del periodo de mi Tesis Doctoral.

I would like to thank the nice experience during my stay at the Muséum national d'Histoire naturelle in Paris. I could work in an amazing place with good people. Merci beaucoup André, Patricia, Romain, Corentin, Elvis et Nyniane. I am eager to come back! Especially, I am indebted to André, thanks a lot for helping me so much.

The city of dreaming spires, Oxford. Really, it has been a dream to enjoy the opportunity of living in this city for almost three months (in two stages). I cannot express how big my gratitude is to Erin. Thank you so much for your welcome and for everything that I have learnt. An unforgettable experience. I also want to thank Leonidas, an amazing guy and friend. And, of course, I cannot forget the person who was my housemate during more than two months. Thank you so much for your good company and interesting conversations, Sotiria. Many scares at the haunted Museum Lodge.

Muchas gracias, Mónica, por brindarme la posibilidad de hacer una estancia en el Museo Senckenberg de Frankfurt, y de volver en el futuro cercano, además de por tu apoyo a lo largo de estos años. Muchas gracias también a Mélanie, merci!

Durante los más de tres años que he estado en el despacho 327 de la Facultat de Ciències de la Terra he podido conocer a muchas personas que me han acompañado en el día a día, haciéndolo todo mucho más agradable. Muchas gracias a Aixa, Camille, Constanza, Elvan, Lucia, Maria y Maxime, espero que la amistad continúe por muchos años. En especial, quiero agradecer a Jordi el apoyo mutuo en los malos y buenos momentos. También, quiero recordar a los compañeros paleontólogos con los que me cruzado por el pasillo tantas veces durante este tiempo: Alejandro Gallardo, Carles Ferrández, Carles Martín, Josep Sanjuan, Raquel Villalonga y Zain Belaústegui, además del resto de miembros del Departament de Dinàmica de la Terra i l'Oceá.

Al comenzar el Doctorado tuve la gran oportunidad de unirme al grupo AMBERIA, de lo que estoy muy orgulloso y agradecido. Tengo el placer de decir que todos vosotros sois unas grandes personas y desde el principio me he sentido integrado y muy a gusto. Es curioso, a muchos de vosotros os conozco desde hace poco más de tres años, pero tengo la sensación de que nos conocemos desde hace mucho. Es un placer trabajar con vosotros y os agradezco mucho que me hayáis hecho partícipe. Mención especial a Rafael López del Valle, el preparador de ámbar por antonomasia; sin tu trabajo mi Tesis Doctoral no habría salido adelante. También, quiero destacar la ayuda y el inestimable apoyo de Eduardo Barrón, David Peris, Alba Sánchez, Toni Monleón y Telm Bover a lo largo de estos últimos años.

Si mis directores se podrían considerar como mis “padres científicos”, a ti tendría que considerar como mi “hermano mayor científico”. Muchas gracias, Ricardo. En estas líneas no hay espacio suficiente para mostrarte toda mi gratitud. No solo recuerdo todo lo que he aprendido de ti desde el punto de vista científico, sino también los buenos momentos. Porque comer en una calle de Oxford una comida exótica cuyo nombre soy incapaz de pronunciar o un turno de noche en el sincrotrón amenizado por joyas musicales, son experiencias vitales difíciles de olvidar.

Y ahora es el turno de las dos personas que me han guiado durante todo este periodo. Xavier, muchas gracias por darme la oportunidad de trabajar a tu lado, de enseñarme tanto y de transmitirme tu pasión por el estudio del ámbar. Recuerdo todas las charlas distendidas que hemos compartido y que tanto me han ayudado. Quique, aún me acuerdo de la primera vez que nos vimos allá por principios de 2016 cuando conversamos en la biblioteca del IGME. Para mí eres una fuente de sabiduría, y no solo eso, sino que me contagias la pasión por el saber. De ti he aprendido cómo poder ver y entender todo desde otro punto vista. Gracias a los dos, tanto por ser mis directores, como por ser mis amigos.

Agradecimiento infinito a aquellas personas que han estado conmigo toda mi vida, a mi familia. No os puedo nombrar aquí a todos, tías, tíos, primas y primos, pero sabed que vuestro apoyo constante, a pesar de la distancia, me ha ayudado mucho más de lo que imagináis.

Muchas gracias a mi abuela Isabel. La persona que ha estado conmigo prácticamente cada día de mi vida y con la que he crecido. Cada visita, cada llamada, me aporta una felicidad indescriptible. Muchas gracias por todo, y es decir poco. Abuelo Aquilino, abuela Vicenta y abuelo Antonio, aunque ya no estéis, seguís acompañándome y os recuerdo mucho.

La persona que está conmigo y que me apoya día tras día, la que aguanta mis rayaditas, la que soporta mis charlas no solicitadas de taxonomía de psocópteros y con la que disfruto cada segundo que comparto con ella. Pocas cosas me hacen más feliz que ir a un restaurante, a una cafetería, de viaje o simplemente ver una película contigo. Mireia, muchísimas gracias.

Y por último, las dos personas responsables de que tengáis delante de vosotros un tocho sobre bichos muertos hace millones de años. Mamá, papá, os lo debo todo. Muchísimas gracias por llevarme a ver cualquier yacimiento arqueológico con el que nos topábamos, por llevarme a cada museo en el que hubiera dinosaurios, por animarme a seguir con lo que me apasiona, por aguantar todos mis “¿por qué?”, por lo que me habéis dado y enseñado. En realidad, os tengo que dar las gracias por todo.

I’m simply saying that life… finds a way.

Índice

Resumen

El objetivo de esta Tesis Doctoral es el estudio de los yacimientos de ámbar de la Cuenca del Maestrazgo con foco en la tafonomía, el paleoambiente, el contenido paleobiológico y la paleoecología. En esta cuenca se ha hallado ámbar con contenido paleobiológico, es decir bioinclusiones, en cuatro yacimientos: Ariño (Albiense inferior), San Just (Albiense superior), Arroyo de la Pascueta (Albiense superior) y La Hoya (Cenomaniense inferior). Las diferencias de edades entre ellos ofrecen una oportunidad excepcional para conocer los cambios de las características de los bosques resiníferos y su biota asociada a lo largo de un intervalo temporal de unos 10 millones de años.

Una de las principales líneas de investigación ha sido el estudio tafonómico del ámbar del nivel AR-1 de Ariño. Este nivel se localiza en la Mina Santa María (Ariño, Teruel), se ha asignado a la Formación Escucha, se ha interpretado como una llanura pantanosa bajo un clima tropical o subtropical y ha proporcionado un rico y diverso registro fósil, que incluye dos especies de dinosaurios. Además, en este nivel se han diferenciado una capa inferior con piezas de ámbar de raíz interpretadas como *in situ* en relación con el lugar de producción de la resina, y una capa superior rica en ámbar aéreo con contenido paleobiológico. El registro de bioinclusiones del ámbar de Ariño incluye insectos de 11 órdenes diferentes, un fragmento de pluma de dinosaurio y el pelo de mamífero más antiguo conocido en ámbar, entre otros restos. Las características tafonómicas del registro fósil del yacimiento de Ariño, correspondiente al nivel AR-1, han permitido tipificarlo como autóctono-parautóctono. Las peculiaridades geoquímicas y de conservación del ámbar de Ariño podrían apuntar hacia un paleoambiente en el que los árboles resiníferos vivieron bajo un fuerte estrés ambiental, quizás relacionado con encharcamientos o inundaciones seguidos de desecaciones de forma periódica. El estudio pluridisciplinar del registro fósil del yacimiento de Ariño ha proporcionado información clave sobre sus características paleoecológicas.

Los yacimientos de ámbar de San Just (Utrillas, Teruel), Arroyo de la Pascueta (Rubielos de Mora, Teruel) y La Hoya (Cortes de Arenoso, Castellón) se han asignado al "Grupo Utrillas" y comparten características tafonómicas y paleoambientales. Los tres yacimientos se han interpretado como parautóctonos y sus paleoambientes se han relacionado con lagunas costeras bajo un clima árido. El ámbar de San Just es el más rico en bioinclusiones de la Cuenca del Maestrazgo, e incluye insectos de 12 órdenes diferentes y fragmentos de plumas de dinosaurio, entre otros restos. Además, el yacimiento de San Just es la localidad tipo de 26 especies de artrópodos. Los ámbares de Arroyo de la Pascueta y La Hoya son pobres en bioinclusiones.

Se han observado diferencias entre los registros de bioinclusiones de los ámbares de Ariño y San Just, probablemente debido a las diferencias en sus edades y paleoambientes. Se

han identificado coocurrencias taxonómicas a nivel de especie, por una parte, entre los registros de los ámbares de El Soplao y Ariño y, por otra parte, entre los de los ámbares de El Soplao, Peñacerrada I, San Just y Arroyo de la Pascueta, lo que puede indicar una posible conexión entre los bosques resiníferos de estas áreas. Curiosamente, como se ha indicado en investigaciones anteriores, los registros de bioinclusiones de los ámbares de la península ibérica en general, y de la Cuenca del Maestrazgo en particular, muestran coocurrencias de géneros de insectos con los ámbares del Barremiense del Líbano y del Cenomaniense de Myanmar.

A partir de los análisis espectroscópicos y geoquímicos de los ámbares de la Cuenca del Maestrazgo se ha inferido que los árboles productores de resina en esta región durante la mitad del Cretácico pertenecieron a la familia de coníferas Araucariaceae.

Se ha evidenciado que el Cretácico fue un periodo en el que se dieron las condiciones ambientales adecuadas para la producción en masa de resina, además del depósito de las piezas de resina resultantes, al menos en algunas regiones, como en la Cuenca del Maestrazgo durante la mitad del Cretácico. Los factores abióticos y bióticos implicados probablemente estuvieron interrelacionados. La aplicación de técnicas bioinformáticas, como el modelado de nicho ecológico, en el estudio de la distribución de bosques resiníferos, tanto en la actualidad como en el pasado, podría proporcionar nueva información sobre los factores clave involucrados en la producción en masa de resina.

Abstract

The objective of this PhD Thesis is the study of the amber-bearing outcrops from the Maestrazgo Basin with a focus on the taphonomy, palaeoenvironment, palaeobiological content and palaeoecology. In this basin, amber with palaeobiological content, *i.e.,* bioinclusions, has been found in four localities: Ariño (lower Albian), San Just (upper Albian), Arroyo de la Pascueta (upper Albian) and La Hoya (lower Cenomanian). The difference of ages between them offers an exceptional opportunity to understand the changes in the characteristics of resiniferous forests and their associated biota over a time interval of about 10 million years.

One of the main research lines has been the taphonomic study of the amber from the level AR-1 of Ariño. This level is located in the Santa María Mine (Ariño, Teruel), it has been assigned to the Escucha Formation, it has been interpreted as a swamp plain under a tropical or subtropical climate, and it has provided a rich and diverse fossil record, including two dinosaur species. In addition, a lower layer with root amber pieces, interpreted as *in situ* in relation to the place of resin production, and an upper layer rich in aerial amber with palaeobiological content, have been differentiated in this level. The Ariño amber bioinclusion

record includes insects of 11 orders, a fragment of a dinosaur feather, and the oldest known mammalian hair in amber, among other remains. The taphonomic characteristics of the fossil record from the Ariño site, corresponding to the level AR-1, have allowed it to be classified as autochthonous-parautochthonous. The geochemical and taphonomic peculiarities of the Ariño amber could point at a palaeoenvironment in which resiniferous trees lived under high environmental stress, perhaps related to ponding or flooding followed by periodic drying. The multidisciplinary study of the fossil record from the Ariño site has provided key information on its palaeoecological characteristics.

The amber outcrops of San Just (Utrillas, Teruel), Arroyo de la Pascueta (Rubielos de Mora, Teruel) and La Hoya (Cortes de Arenoso, Castellón) have been assigned to the "Utrillas Group" and share the same taphonomic and palaeoenvironmental characteristics. These three outcrops have been interpreted as parautochthonous, and their palaeoenvironments have been related to coastal lagoons under an arid climate. The San Just amber is the richest in bioinclusions from the Maestrazgo Basin, including insects from 12 orders and fragments of dinosaur feathers, among other remains. In addition, San Just is the type locality of 26 arthropod species. The ambers from Arroyo de la Pascueta and La Hoya are poor in bioinclusions.

The bioinclusion records of the Ariño and San Just ambers show differences, probably due to their different ages and palaeoenvironments. Taxonomic co-occurrences have been identified at the species level, on the one hand, between the records of the ambers from El Soplao and Ariño and, on the other hand, between those of the ambers from El Soplao, Peñacerrada I, San Just and Arroyo de la Pascueta, which may indicate a possible connection between the resiniferous forests of these areas. Interestingly, as previous works pointed out, the bioinclusion records of the ambers from the Iberian Peninsula in general, and from the Maestrazgo Basin in particular, show co-occurrences of insect genera with the ambers from the Barremian of Lebanon and the Cenomanian of Myanmar.

The spectroscopic and geochemical analyses of the ambers from the Maestrazgo Basin have allowed to infer that the resin-producing trees in this region during the 'mid-Cretaceous' belonged to the Araucariaceae coniferous family.

The evidence shows that the Cretaceous was a period in which suitable environmental conditions for the resin mass production occurred, in addition to the preservation of the resulting resin pieces, at least in some regions, such as in the Maestrazgo Basin during the 'mid-Cretaceous'. The abiotic and biotic factors involved in it were probably interrelated. The application of bioinformatics techniques (such as Ecological Niche Modelling) on the study of the resiniferous forest distribution, both today and in the Past, may provide new information on the key factors involved in the resin mass production.

1. Introducción

1.1. El ámbar: definición y origen

El ámbar es resina fósil. En ocasiones, la resina fosilizada recibe el nombre de resinita, generalmente cuando se presenta en tamaño micrométrico en depósitos de carbón (Stach, 1982). Históricamente, en la península ibérica se utilizaba el nombre *succino* para denominar a la resina fósil (Cavanilles, 1797). En griego antiguo se llamaba *ἤλεκτρον* (*élektron*), relacionado con el significado "sol radiante" (Lambert y Poinar, 2002). El ámbar ha tenido una destacada relación con las culturas humanas de todo el mundo desde el Paleolítico, dado que se ha usado como joya y elemento de prestigio social, como sustancia curativa e incluso a modo de incienso para la producción aromas y fragancias (Lambert y Poinar, 2002; Peñalver, 2012; Murillo-Barroso *et al.*, 2018).

Las resinas son sustancias producidas por células especializadas de las plantas cuya composición es una mezcla compleja de terpenoides, tanto volátiles como no volátiles, fenoles y otros compuestos (Fig. 1) (Langenheim, 1969, 2003; Labandeira, 2014). La resina se secreta por medio de canales, huecos, cavidades, tricomas o el tejido epidérmico (Langenheim, 2003). Las plantas producen otras sustancias que se pueden confundir con la resina, como gomas, mucílagos, ceras, grasas y látex (Langenheim, 2003), algunas de ellas también presentes en el registro fósil (Roberts *et al.*, 2020). En ocasiones, se confunde la savia, fluido cuya función principal es el transporte interno de nutrientes (Jensen *et al.*, 2016), con la resina. Las plantas productoras de resina forman parte de las coníferas (gimnospermas) y las angiospermas (Langenheim, 1969). Se conocen al menos 66 géneros actuales de coníferas, incluidos en siete familias diferentes, con especies productoras de resina, mientras que entre las angiospermas se conocen al menos 153 géneros actuales, de 29 familias diferentes, que incluyen especies resinosas (Langenheim, 2003). A pesar de ello, solo las especies de unos pocos géneros producen resina en cantidad copiosa, entre los que cabe destacar el género de coníferas *Agathis*, de la familia Araucariaceae, y el género de angiospermas *Hymenaea*, de la familia Fabaceae (Langenheim, 1995).

Tradicionalmente, se ha considerado que la resina es una sustancia defensiva y protectora que es secretada por ciertas plantas como resultado de un daño físico, el ataque por animales o infestación por microorganismos, es decir, situaciones de estrés ambiental (Langenheim, 1969, 2003; Martínez-Delclòs *et al.*, 2004; Labandeira, 2014; Seyfullah *et al.*, 2018a). Sin embargo, su fisiología ha sido poco explorada y las causas de su producción en masa se desconocen en gran medida y muy posiblemente se puedan relacionar con factores abióticos o bióticos, o una combinación de ambos (Hoffmann *et al.*, 1984; Langenheim, 2003; Martínez-Delclòs *et al.*, 2004; Labandeira, 2014; McCoy *et al.*, 2017; Seyfullah *et al.*, 2018a; Delclòs *et al.*, en preparación). Algunos de los factores abióticos, muchos de ellos interrelacionados, que pueden condicionar, limitar o estimular la producción en masa de

resina son la temperatura, la precipitación, la composición de gases atmosféricos, la radiación solar, la actividad volcánica global, la fluctuación del nivel del mar, las corrientes marinas (y los fenómenos climáticos extremos asociados, como tormentas y monzones) y los incendios forestales (Langenheim, 2003; Martínez-Delclòs *et al.*, 2004; Labandeira, 2014; Seyfullah *et al.*, 2018; Delclòs *et al.*, en preparación). Mientras que entre los factores bióticos se consideran las enfermedades de los árboles causadas por virus o microorganismos y los ataques o daños causados por insectos (Langenheim, 2003; Martínez-Delclòs *et al.*, 2004; Labandeira, 2014; Seyfullah *et al.*, 2018a; Peris *et al.*, 2021; Delclòs *et al.*, en preparación).

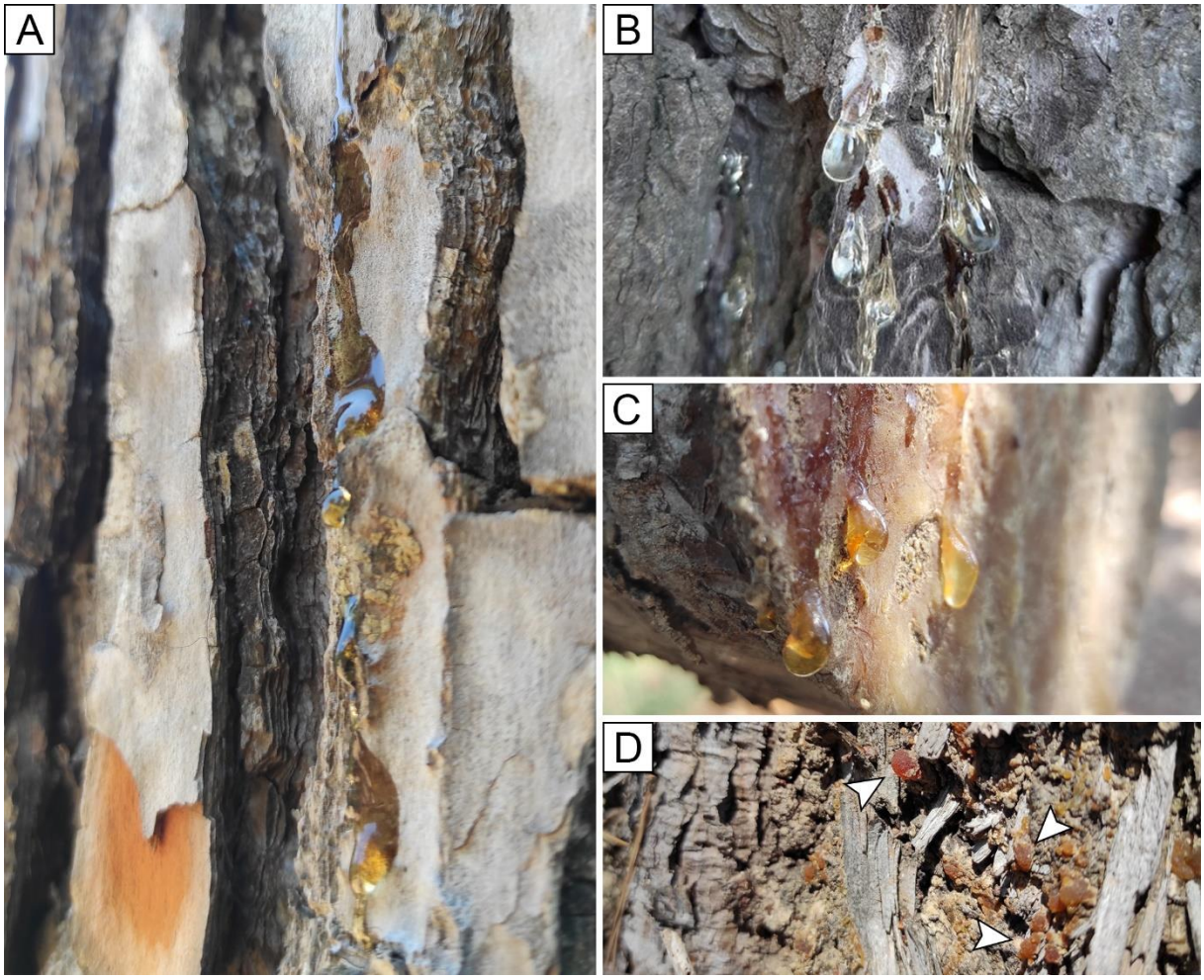

Figura 1. Resina producida en troncos de *Pinus halepensis* Miller, 1768 (Pinaceae). A) Colada de resina de coloración amarillenta, Lloret de Mar (Catalunya), junio de 2021; B) Gotas de resina de coloración blanquecina, Mallorca (Illes Balears), agosto de 2020; C) Gotas de resina de coloración amarillenta en un tronco cortado, Xàbia (Comunitat Valenciana), agosto de 2022; D) Gotas de resina endurecida (flechas), Lloret de Mar, junio de 2021.

Una de las características más llamativas del ámbar es la capacidad de conservación excepcional y en tres dimensiones de organismos fósiles en su interior, generalmente pequeños artrópodos (Labandeira, 2014; Grimaldi, 2019). Estos organismos conservados en su interior

se denominan bioinclusiones. En el caso de que se encuentren dos o más bioinclusiones en la misma pieza de ámbar, se denominan sininclusiones. En sentido estricto, el ámbar es un fósil indirecto (resto fósil de la actividad de los árboles resiníferos) que a su vez contiene fósiles directos. El ámbar no es el único de este tipo, ya que se ha confirmado la conservación de insectos en otros fósiles indirectos, como los coprolitos (*e.g.*, Qvarnström *et al.*, 2021). Las resinas difieren mucho en la probabilidad de capturar organismos, ya que esta capacidad depende tanto de las características de la propia resina como de los organismos. Principalmente, las dos propiedades que posibilitan o no la captura es el tiempo de endurecimiento y la viscosidad de la resina (Martínez-Delclòs *et al.*, 2004; Labandeira, 2014). Una resina que tarde en endurecerse varios días tiene más posibilidades de capturar organismos que otra resina que se endurezca más rápidamente. De igual modo, una resina fluida es más fácil que capture organismos que otra más viscosa. Ambas propiedades tienen relación tanto con la afinidad taxonómica del árbol productor como con las condiciones ambientales (Langenheim, 2003).

La resina con una mayor probabilidad de capturar organismos es aquella secretada en las partes aéreas del árbol, es decir, ramas y tronco (Martínez-Delclòs *et al.*, 2004), pues está en contacto directo con la biota que habita en o alrededor del árbol. Además, en ocasiones esta resina es secretada por medio de diferentes flujos de coladas, y cada uno de ellos cubre las superficies de desecación de las coladas previas, lo que causa la inclusión rápida de organismos que se habían quedado pegados en la superficie anterior pegajosa (Martínez-Delclòs *et al.*, 2004). La resina producida en las raíces de los árboles raramente captura organismos, debido a la formación de una corteza externa, a causa de la desecación, su crecimiento desde dentro hacia fuera y que en el subsuelo habitan menos organismos que en la superficie (Langenheim, 2003; Martínez-Delclòs *et al.*, 2004). La captura en resina depende del tamaño del organismo, dado que es más fácil que un organismo de pequeño tamaño (unos pocos milímetros) quede incluido en resina antes que otro de mayor tamaño (Henwood, 1993; Martínez-Delclòs *et al.*, 2004). La captura en resina podría estar sesgada hacia organismos que se sientan atraídos por el aroma de la resina, frente a otros que les repela (Labandeira, 2014; Solórzano Kraemer *et al.*, 2018). También, la posibilidad de que un organismo acabe incluido en resina depende de su modo de vida y su hábitat dentro de los bosques. Se ha demostrado con experimentos actualísticos que el registro de bioinclusiones en resina representa principalmente la artropodofauna que habita en el árbol resinífero o cerca de él, en lugar de representar la del bosque en general (Solórzano Kraemer *et al.*, 2018). Así, los insectos que viven en la corteza de los árboles, como los psocópteros, se encuentran sobrerrepresentados como bioinclusiones en resina, mientras que los artrópodos que habitan en el suelo del bosque se encuentran infrarrepresentados (Solórzano Kraemer *et al.*, 2018). A pesar de ello, los organismos del suelo también pueden ser capturados en resina de hojarasca, es decir, producida en la parte baja del

tronco de los árboles (Perrichot, 2004; Sánchez García, 2017). Aunque habitualmente se considera que las bioinclusiones en ámbar muestran una conservación excepcional, no es siempre así. En el momento de la captura en resina, el organismo lucha por escapar y en este proceso es posible que se desprendan partes corporales (Martínez-Delclòs *et al.*, 2004). Además, la resina puede capturar fragmentos orgánicos e inorgánicos que dificulten la posterior observación de la bioinclusión en cuestión y, en función de las características del árbol resinífero o las condiciones ambientales, es posible que la resina sea muy turbia, incluso opaca, lo que impida la visualización de bioinclusiones (Martínez-Delclòs *et al.*, 2004).

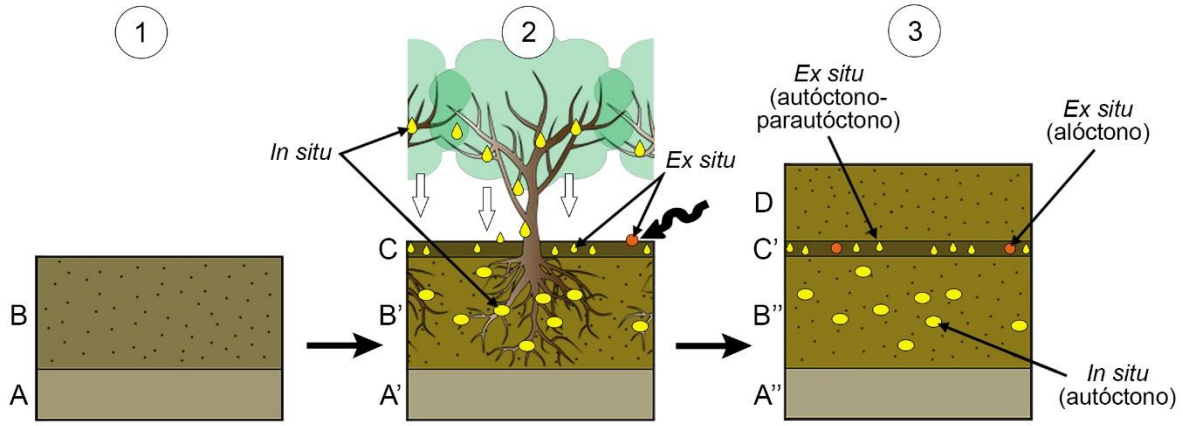

Figura 2. Diagrama de las fases de formación de un yacimiento de ámbar autóctono-parautóctono. 1) Ambiente deposicional original; 2) Establecimiento del bosque resinífero y pedogénesis, presencia de resina *in situ* tanto en las ramas como en las raíces; 3) Fosildiagénesis de las piezas de resina, lo que resulta en una capa inferior con piezas de ámbar de raíz *in situ* en relación con el lugar de producción de la resina y una capa superior con una combinación de piezas de ámbar *ex situ* principalmente autóctonas-parautóctonas, aunque no se puede descartar la presencia de piezas alóctonas. Las letras A-D indican las diferentes capas del suelo. Imagen modificada de Álvarez-Parra *et al.* (2021b).

El proceso de fosilización de la resina se denomina ambarización (Labandeira, 2014). Este proceso comienza con la polimerización de los compuestos que forman la resina, lo que a su vez causa su endurecimiento (Langenheim, 2003; Labandeira, 2014). La polimerización es fotoiniciada y empieza a suceder tan pronto como la resina es secretada (Langenheim, 2003). La resina producida en las partes aéreas de los árboles cae por gravedad al suelo del bosque, y puede ser enterrada superficialmente (Martínez-Delclòs *et al.*, 2004). Normalmente, la resina, tanto de las partes aéreas del árbol como de las raíces, es transportada por medio de la escorrentía a medios transicionales, como deltas o pantanos costeros, donde tiene lugar su enterramiento y comienza la fosildiagénesis (Martínez-Delclòs *et al.*, 2004). La mayor parte de los yacimientos de ámbar se consideran parautóctonos o alóctonos, dado que la resina sufrió transporte bioestratinómico, ya sea en el mismo medio donde se produjo (parautoctonía) o en

medios alejados de aquellos donde tuvo lugar la producción (aloctonía) (Martínez-Delclòs *et al.*, 2004; Seyfullah *et al.*, 2018a). Se han identificado algunos yacimientos de ámbar autóctonos-parautóctonos (Fig. 2), es decir, la mayor parte de la resina se enterró en el medio donde se produjo sin sufrir transporte bioestratinómico (excluyendo la caída gravitatoria desde las partes aéreas de los árboles), aunque una parte de la resina pudo sufrir transporte dentro del mismo medio (Seyfullah *et al.*, 2018b; Álvarez-Parra *et al.*, 2021b). El ámbar también puede conservarse *in situ* en relación con la planta productora, si se encuentra en contacto con el resto fósil de la planta (Labandeira, 2014), e *in situ* en relación con el lugar de producción de la resina (Álvarez-Parra *et al.*, 2021b). El primer caso es compatible con autoctonía, parautoctonía y aloctonía, mientras que el segundo solo es compatible con autoctonía. Tras el enterramiento definitivo de la resina, tienen lugar los procesos fosildiagenéticos afectando tanto a la resina, como a sus bioinclusiones, aunque éstas últimas pueden empezar a sufrir la diagénesis, como deshidratación, carbonización y emisión de fluidos y gases internos, desde su inclusión en la resina (Martínez-Delclòs *et al.*, 2004). Las piezas de resina pueden experimentar deformación o fracturación debido a procesos tectónicos y las bioinclusiones habitualmente se conservan huecas, con escaso rastro de caracteres anatómicos internos, debido a la actividad de enzimas y microorganismos, además de perder la coloración externa original (Henwood *et al.*, 1993; Martínez-Delclòs *et al.*, 2004; Labandeira, 2014; Jiang *et al.*, 2022), aunque se conocen excepciones de conservación de color (Cai *et al.*, 2020). En ocasiones puede producirse reelaboración de las piezas de ámbar, lo que se corresponde con un desenterramiento y un posterior enterramiento secundario en depósitos más modernos (Martínez-Delclòs *et al.*, 2004). Las piezas de ámbar resultantes se clasifican como ámbar arriñonado o de raíz, relacionado con la resina producida en las raíces de los árboles, y como ámbar aéreo, relacionado con la resina producida en las partes aéreas de los árboles (Álvarez-Parra *et al.*, 2021b). Las piezas de ámbar aéreo se presentan con diferentes morfologías, como gotas, estalactitas y coladas (Fig. 3) (Martínez-Delclòs *et al.*, 2004). Además, el ámbar aéreo de hojarasca se relaciona con resina de hojarasca producida en la parte baja de los árboles (Perrichot, 2004; Sánchez García, 2017).

Tradicionalmente, se ha diferenciado entre resina, copal y ámbar, en función de su estado de maduración o fosilización. A pesar de ello, los límites entre los tres conceptos son problemáticos, dado que diferentes autores han establecido diferentes definiciones relativamente arbitrarias (Langenheim, 2003; Martínez-Delclòs *et al.*, 2004; Labandeira, 2014). Generalmente, se considera que el copal es resina subfósil que inició recientemente el proceso de ambarización, mientras el ámbar es resina en un estado de ambarización avanzado (Vávra, 2009). Se ha establecido una nueva clasificación cronológica de muestras de resinas y resinas fósiles en colecciones museísticas que pueden datarse mediante análisis de radiocarbono (Solórzano-Kraemer *et al.*, 2020). De este modo, se considera resina de

Defaunación a aquella resina producida después del año 1760 AD, copal a la resina producida durante el Pleistoceno y el Holoceno hasta el año 1760 AD y ámbar a la resina producida antes del Pleistoceno (Solórzano-Kraemer *et al.*, 2020). Sin embargo, esta clasificación no tiene en cuenta el estado de ambarización de la resina, por lo que resulta complejo extrapolarla al pasado y clasificar las resinas fósiles desde un punto de vista tafonómico.

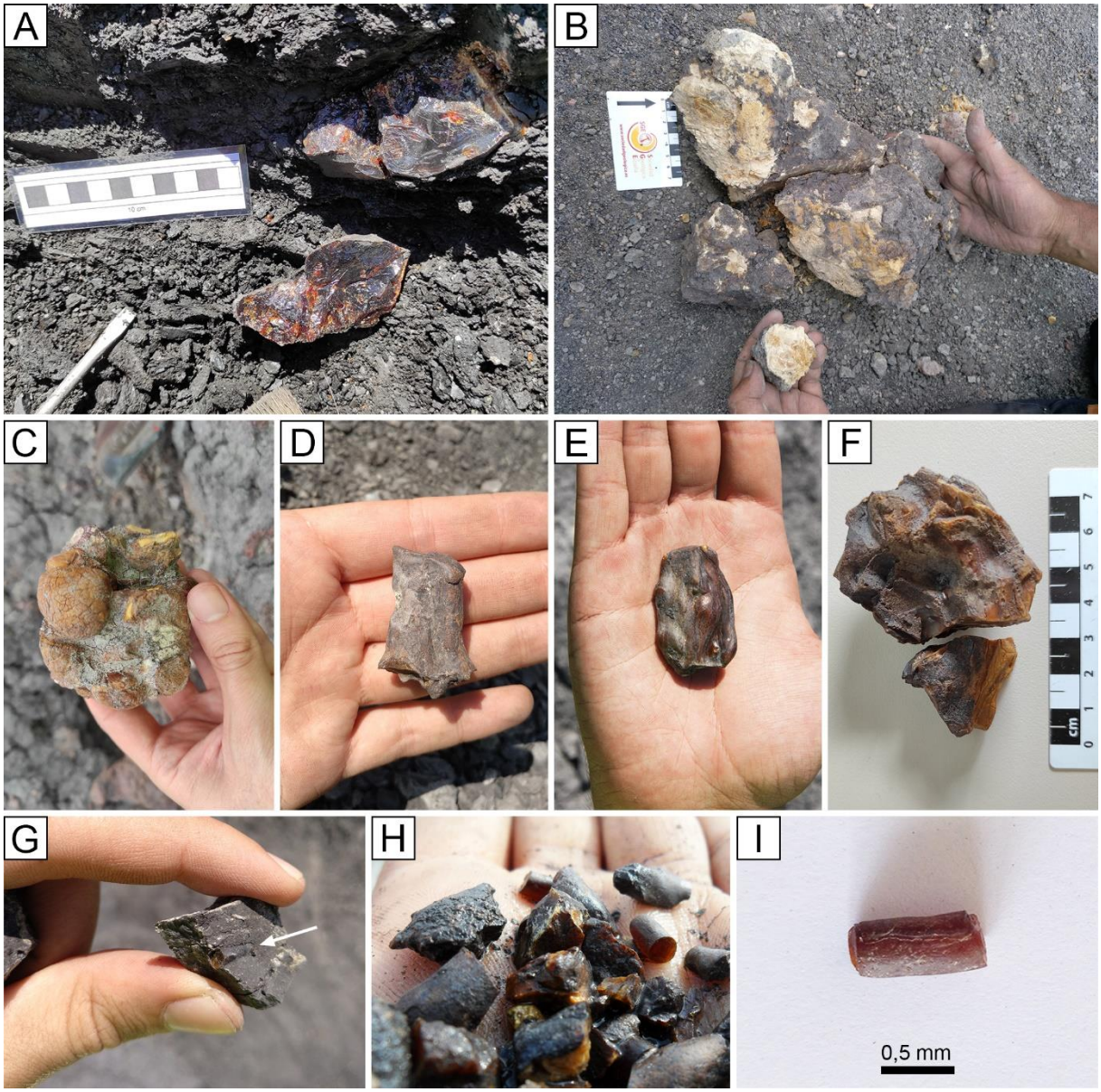

Figura 3. Ámbar con diferentes morfologías. A) Pieza de ámbar de raíz de gran tamaño en el yacimiento de San Just, año 2021; B) Pieza de ámbar de raíz de gran tamaño en el yacimiento de Ariño, año 2019; C) Pieza de ámbar de raíz de pequeño tamaño y con protuberancias del yacimiento de Ariño, año 2021; D, E) Piezas de ámbar aéreo en forma de colada del yacimiento de Ariño, E fotografía de Enrique Peñalver, año 2019; F) Pieza de ámbar aéreo de gran tamaño en forma de colada del yacimiento de San Just, año 2021; G-I) Piezas de ámbar aéreo en forma de estalactita y gota del yacimiento de Ariño, H fotografía de Ricardo Pérez de la Fuente, año 2019.

Los registros de ámbar más antiguos datan del Carbonífero (Bray y Anderson, 2009). Se ha hallado ámbar del Triásico en diferentes lugares del mundo como Estados Unidos, España, Italia, Lesoto y Australia, aunque es de pequeño tamaño y en poca cantidad (*e.g.*, Litwin y Ash, 1991). En ámbar triásico de Dolomitas (Italia) se han descrito las bioinclusiones en ámbar más antiguas conocidas (Schmidt *et al.*, 2012). El registro de ámbar del Jurásico es muy escaso a nivel mundial (Neri *et al.*, 2016), aunque se han documentado depósitos de carbón ricos en resinita (*e.g.*, Bojesen-Koefoed *et al.*, 1996). Los yacimientos de ámbar más antiguos en los que las piezas de ámbar son abundantes y el ámbar aéreo es rico en bioinclusiones son los del Barremiense del Líbano (Maksoud y Azar, 2020). Los yacimientos de ámbar más estudiados del Cenozoico datan del Eoceno, como los ámbares de Oise en Francia (Nel y Brasero, 2010), del Báltico (Weitschat y Wichard, 2002), de Cambay en India (Rust *et al.*, 2010) y de Fushun en China (Wang *et al.*, 2014), y del Mioceno, como los ámbares de México (Solórzano Kraemer, 2010), República Dominicana (Penney, 2010) y Zhangpu en China (Wang *et al.*, 2021). Los árboles productores de resina en masa durante el Cretácico se han asociado principalmente a las familias de coníferas Araucariaceae, †Cheirolepidiaceae, Cupressaceae, Pinaceae y Podocarpaceae (Pereira *et al.*, 2009; Menor-Salván *et al.*, 2016; McCoy *et al.*, 2021), aunque también se han sugerido otros grupos como †Erdtmanithecales (Seyfullah *et al.*, 2020). Los ámbares del Cenozoico se han relacionado tanto con árboles resiníferos pertenecientes a grupos de angiospermas (*e.g.*, Nohra *et al.*, 2015; Wang *et al.*, 2021), como con coníferas (*e.g.*, Wolfe *et al.*, 2009; Wang *et al.*, 2014).

1.2. El ámbar cretácico en el mundo

Los yacimientos de ámbar cretácicos son muy numerosos y se encuentran ampliamente distribuidos (Fig. 4). Los yacimientos de ámbar prebarremienses son escasos y no muy bien conocidos. El ámbar hallado en la Formación Maracangalha de Brasil podría tener una edad desde Berriasiense hasta Barremiense (Pereira *et al.*, 2009). En el sur de Inglaterra se han documentado dos yacimientos de ámbar, uno cercano a Hastings datado como Berriasiense superior-Valanginiense inferior y otro cercano a Bexhill datado como Valanginiense medio o superior (Brasier *et al.*, 2009). En el ámbar de Hastings se describieron posibles telarañas y microbioinclusiones (Brasier *et al.*, 2009). En la Formación Kirkwood de Sudáfrica, datada como Valanginiense, se ha encontrado ámbar en un nivel con restos de plantas en forma de cutículas que se corresponde con una acumulación alóctona (Gomez *et al.*, 2002b). Varios yacimientos de ámbar de Israel han sido datados como Valanginiense-Hauteriviense (Nissembaum y Horowitz, 1992). El ámbar cretácico más antiguo en el que se ha hallado un insecto como bioinclusión es el ámbar del Hauteriviense de Golling en Austria (Borkent, 1997).

El registro de ámbar del Barremiense está representado principalmente por los más de 450 yacimientos de ámbar localizados en el Líbano, entre los que se incluyen al menos 29 en los que se han identificado bioinclusiones (Maksoud y Azar, 2020). Los ámbares del Líbano han proporcionado insectos de 21 órdenes diferentes (Maksoud *et al.*, 2022). Como se ha comentado anteriormente, los ámbares del Libano son los más antiguos conocidos en los que las bioinclusiones son abundantes y diversas taxonómicamente, principalmente de artrópodos y plantas, aunque también restos de vertebrados (Maksoud y Azar, 2020). Se han documentado otros ámbares de edad barremiense en Siria (Choufani *et al.*, 2015) y la Isla de Wight en Inglaterra (Jarzembowski *et al.*, 2008), ambos con bioinclusiones. Los yacimientos de ámbar del Aptiense son escasos, aunque distribuidos mundialmente, ya que se han encontrado en Brasil, Congo, Portugal, Francia, Rusia, China y Japón, aunque entre ellos solo los ámbares de los yacimientos de Doumanga en Congo y Choshi en Japón han proporcionado bioinclusiones (Bouju y Perrichot, 2020; Perkovsky *et al.*, 2020). Los yacimientos de ámbar del Albiense son numerosos en la península ibérica, varios de ellos con bioinclusiones, como se comentará más adelante. Otros ámbares albienses se han hallado en el sur de Francia (Saint Martin *et al.*, 2021), norte de Italia (Trevisani y Ragazzi, 2013), Taimyr en Rusia (Rasnitsyn *et al.*, 2016) y Hkamti en Myanmar (Xing y Qiu, 2020), este último rico en bioinclusiones.

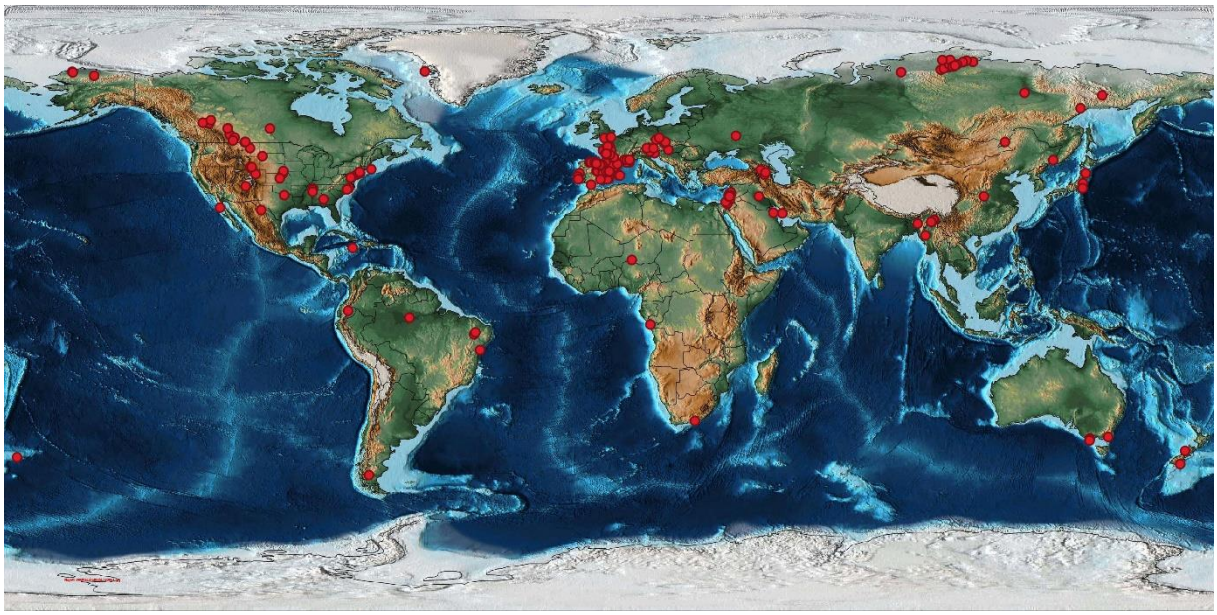

Figura 4. Mapa del mundo en la actualidad con la localización georreferenciada de 299 yacimientos de ámbar del Cretácico (círculos rojos). Mapa obtenido de Scotese (2001).

Numerosos yacimientos de ámbar del Cenomaniense se han hallado en la costa oeste y el área noroccidental de Francia, varios de ellos con bioinclusiones (Perrichot *et al.*, 2007; Girard *et al.*, 2013b). Uno de los yacimientos de ámbar cretácico de Francia con mayor relevancia es Archingeay-Les Nouillers, datado como Albiense superior-Cenomaniense

inferior (Néraudeau *et al.*, 2002), que ha proporcionado bioinclusiones de crustáceos, miriápodos, arácnidos, insectos de 13 órdenes diferentes y otros hexápodos, plumas de dinosaurio, registro de piel de reptil y pelos de mamífero (Perrichot *et al.*, 2007; Vullo *et al.*, 2010). También en Europa, se ha documentado ámbar cenomaniense sin bioinclusiones en Alemania y Chequia (Schmidt *et al.*, 2001; Havelcová *et al.*, 2016). Entre los yacimientos de Taimyr en Rusia, el ámbar de Nizhnyaya Agapa es rico en bioinclusiones y se ha datado como Cenomaniense superior (Rasnitsyn *et al.*, 2016). El ámbar del yacimiento cenomaniense de Agdzhakend en Azerbaiyán también es rico en bioinclusiones (Rasnitsyn *et al.*, 2016). El ámbar más conocido del Cretácico es el extraído de las minas del valle de Hukawng, en la región de Kachin al norte de Myanmar, cuyos niveles con ámbar se han datado como Cenomaniense inferior (Shi *et al.*, 2012). Su registro en bioinclusiones es muy rico y diverso, generalmente con una conservación excepcional (Grimaldi *et al.*, 2002). A partir de bioinclusiones en este ámbar se han descrito especies de plantas, moluscos, crustáceos, arácnidos, hexápodos (entre los que se incluyen 28 órdenes de insectos) y vertebrados (Ross, 2022). Algunos de los hallazgos más llamativos son una concha de amonites (Yu *et al.*, 2019), cuyo registro en ámbar es altamente improbable dado su hábitat marino, y restos esqueléticos de dinosaurio (Xing *et al.*, 2016). Yacimientos de ámbar cenomaniense sin bioinclusiones se han documentado a lo largo de América, como en el oeste de Canadá, Texas en Estados Unidos y Argentina (*e.g.*, Friedman *et al.*, 2018), y en las islas Chatham en Nueva Zelanda (Stilwell *et al.*, 2020).

Los yacimientos de ámbar del Turoniense más estudiados se encuentran en la costa este de Estados Unidos, principalmente en Nueva Jersey, como el yacimiento de Sayreville (Grimaldi *et al.*, 1989). El yacimiento de La Garnache en Francia, probablemente del Turoniense, ha proporcionado bioinclusiones (Néraudeau *et al.*, 2017). Otros yacimientos de ámbar turonienses se localizan en el sur de Australia (Quinney *et al.*, 2015; Stilwell *et al.*, 2020). Solo se conocen dos yacimientos de ámbar del Coniaciense, uno en Azerbaiyán (Zherikhin y Eskov, 1999) y otro, denominado Shavarshavan, en Armenia; este último ha proporcionado bioinclusiones (Rasnitsyn *et al.*, 2016). Los yacimientos de ámbar del Santoniense más estudiados, algunos con bioinclusiones, se encuentran en el sur de Francia (Saint Martin *et al.*, 2021), en Taimyr en Rusia (Rasnitsyn *et al.*, 2016), entre los que destaca el yacimiento de Yantardakh, y en Japón (Lambert *et al.*, 2016). La mayoría de los yacimientos de ámbar del Campaniense se localizan en América del Norte, como los del oeste de Canadá, incluyendo los destacados yacimientos de Grassy Lake y Cedar Lake (McKellar *et al.*, 2008), y en la costa este de Estados Unidos (Szadziewski *et al.*, 2018). El yacimiento de Tilin, en el oeste de Myanmar, ha proporcionado una amplia y diversa colección de bioinclusiones (Zheng *et al.*, 2018). Se conocen varios yacimientos de ámbar del Maastrichtiense, sin embargo han sido poco estudiados. Algunos de estos yacimientos se encuentran en Wyoming en Estados Unidos (Grimaldi *et al.*, 2000), el oeste de Canadá (McKellar *et al.*, 2008) e India (Dutta *et al.*, 2011).

El yacimiento maastrichtiense de Bonne Butte, en Dakota del Norte en Estados Unidos, es el único de esta edad que ha proporcionado ámbar con bioinclusiones (Nel *et al.*, 2010a).

1.3. El ámbar en la península ibérica y su protección patrimonial

Los yacimientos de ámbar son numerosos en la península ibérica (Fig. 5) (Peñalver y Delclòs, 2010). La presencia de ámbar se ha documentado desde hace más de dos siglos *(e.g.*, Casal, 1762; Cavanilles, 1797). También, se ha hallado en yacimientos arqueológicos, lo que evidencia la relación de los antiguos pobladores de la península ibérica con el ámbar y sus posibles usos por las culturas antiguas (Álvarez-Fernández *et al.*, 2005; Murillo-Barroso *et al.*, 2018). El investigador Enrique Peñalver (Instituto Geológico y Minero de España-CSIC) ha recopilado menciones de más de 150 posibles yacimientos de ámbar en la península ibérica, aunque en muchos de ellos no se ha confirmado la presencia de ámbar, y en algunas ocasiones ni la existencia del yacimiento por tratarse de explotaciones de carbón abandonadas y desaparecidas. Por el momento, se ha hallado ámbar en al menos 67 yacimientos de España y nueve yacimientos de Portugal (Fig. 5) (Delclòs *et al.*, 2007; Peñalver y Delclòs, 2010; Peñalver *et al.*, 2018a; Silvéiro y Madeira, 2018). El ámbar más antiguo de la península ibérica se ha encontrado en un yacimiento dentro del término municipal de Xixona en Alicante, situado en facies Keuper de edad Ladiniense-Rhaetiense (Triásico), aunque por el momento no se ha estudiado (Peñalver y Delclòs, 2010). La mayoría de los ámbares de la península ibérica se encuentran en estratos del Cretácico Inferior y, en menor medida, del Cretácico Superior (Peñalver y Delclòs, 2010). Entre los del Cretácico Superior, cabe destacar el yacimiento de ámbar de Soto del Real (Comunidad de Madrid), datado como Turoniense, y varios yacimientos de ámbar maastrichtiense del prepirineo catalán (Peñalver y Delclòs, 2010). Curiosamente, también se han documentado piezas de ámbar de muy pequeño tamaño en los yacimientos de compresión del Barremiense de La Hoyas (Cuenca) y del Mioceno de Rubielos de Mora (Teruel) y La Rinconada en Ribesalbes (Castellón).

Los yacimientos de ámbar del Cretácico de la península ibérica se corresponden de forma general con las zonas costeras del oeste, norte y este de la paleoisla de Iberia (Peñalver y Delclòs, 2010; Peñalver *et al.*, 2018a). Estos yacimientos se han interpretado como registros de medios transicionales como deltas o pantanos costeros, donde las piezas de resina se acumulaban tras un breve transporte bioestratinómico, lo que relaciona a los yacimientos con acumulaciones parautóctonas (Delclòs *et al.*, 2007; Peñalver y Delclòs, 2010). Durante la mitad del Cretácico, la paleoisla de Iberia se situaba a latitudes bajas de 25-30ºN bajo un clima subtropical-tropical junto el desarrollo de ambientes áridos a nivel local (Heimhofer *et al.*, 2012; Csiki-Sava *et al.*, 2015). Por el momento se han hallado bioinclusiones únicamente en el ámbar de 12 yacimientos de la península ibérica (Fig. 6): Cascais-Estoril (Lisboa, Portugal), La

Rodada, El Caleyu, Pola de Siero (los tres en Asturias), El Soplao (Cantabria), Peñacerrada I (Burgos), Peñacerrada II, Salinillas de Buradón (los dos en Álava), Ariño, San Just, Arroyo de la Pascueta (los tres en Teruel) y La Hoya (Castellón). Todos ellos se han datado como Albiense, excepto La Hoya como Cenomaniense inferior (Peñalver y Delclòs, 2010; Peñalver *et al.*, 2018b; Álvarez-Parra *et al.*, 2021b; Barrón *et al.*, enviado).

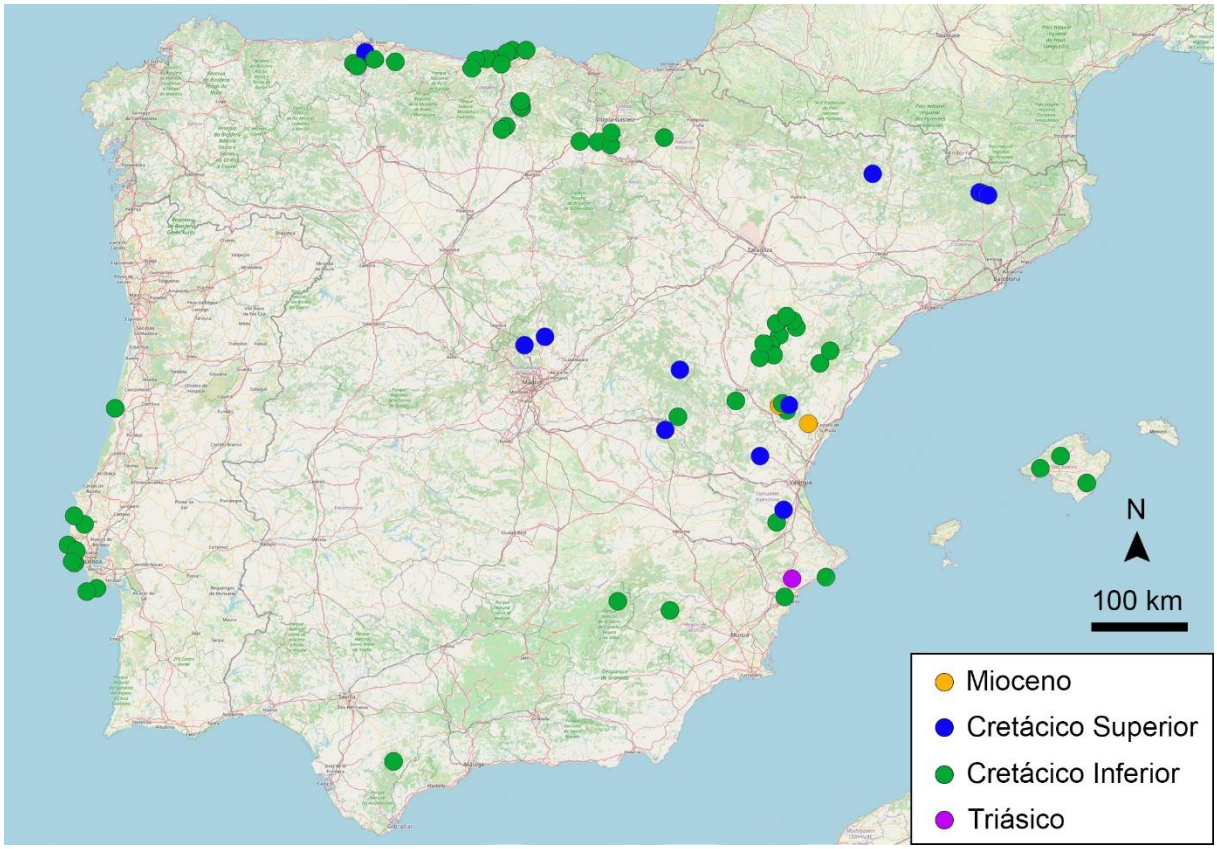

Figura 5. Mapa de la península ibérica con las localizaciones georreferenciadas de yacimientos de ámbar del Triásico (uno), Cretácico Inferior (60), Cretácico Superior (13) y Mioceno (dos). Mapa modificado del complemento QuickMapServices de QGIS (mapa OSM Standard).

El ámbar de Cascais-Estoril, geológicamente procedente de la Cuenca Lusitánica, es el único ámbar portugués con contenido paleobiológico. La única bioinclusión conocida de este ámbar se trata de un díptero nematócero que se encuentra en una colección privada (Peñalver *et al.*, 2018a). Los tres yacimientos asturianos indicados anteriormente se localizan en la Depresión Central Asturiana y han proporcionado pocas bioinclusiones (Peñalver y Delclòs, 2010; Arillo *et al.*, 2020). El Caleyu y Pola de Siero se han asignado a la Formación Ullaga del Albiense superior (Peñalver y Delclòs, 2010), mientras que La Rodada se ha incluido en la Formación El Caleyu del Albiense superior-Cenomaniense inferior (Arillo *et al.*, 2020). Los yacimientos de El Soplao, Peñacerrada I, Peñacerrada II y Salinillas de Buradón se localizan en la Cuenca Vasco-Cantábrica. El yacimiento de ámbar de El Soplao, ha proporcionado una

diversa colección de artrópodos como bioinclusiones en el ámbar, además de otros restos fósiles (Najarro *et al.*, 2009, 2010; Pérez de la Fuente, 2012). Se ha incluido en la Formación Las Peñosas, de edad Albiense inferior-medio (García-Mondéjar, 1982), y los resultados preliminares del contenido palinológico del nivel con ámbar indican una edad Albiense medio. El medio sedimentario se ha relacionado con un delta-estuario de influencia marina (Najarro *et al.*, 2009). Los yacimientos de ámbar de Peñacerrada I, Peñacerrada II, llamados en conjunto ámbar de Álava, y Salinillas de Buradón, se han asignado al "Grupo Utrillas" y su datación es Albiense superior (Barrón *et al.*, 2015). El ámbar de Peñacerrada I es el más rico y diverso en bioinclusiones de la península ibérica (Alonso *et al.*, 2000; Peñalver y Delclòs, 2010). Mientras que los ámbares de Peñacerrada II y Salinillas de Buradón son más pobres en bioinclusiones (Arillo *et al.*, 2008b; Martínez-Torres *et al.*, 2011). El medio sedimentario se ha relacionado con ambientes fluvio-lacustres en deltas con influencia marina (Alonso *et al.*, 2000; Barrón *et al.*, 2015). En la Cuenca del Maestrazgo, también denominada Cuenca del Maestrat, se han documentado más de 30 yacimientos de ámbar, sin embargo no se ha podido confirmar la presencia de ámbar en todos ellos, y solo se han hallado bioinclusiones en el ámbar de cuatro, como se comentará en extenso más adelante: Ariño, San Just, Arroyo de la Pascueta y La Hoya (Peñalver y Delclòs, 2010; Álvarez-Parra *et al.*, 2021b). La mención más antigua a posibles bioinclusiones en ámbar de la península ibérica se refiere al ámbar hallado cerca de Linares de Mora en Teruel (Boscá, 1910), aunque no se ha podido confirmar.

Los ámbares cretácicos de la península ibérica se han asociado a resinas producidas por árboles de las familias Araucariaceae y †Cheirolepidiaceae (Peñalver y Delclòs, 2010; Menor-Salván *et al.*, 2010, 2016; Dal Corso *et al.*, 2013; Kvaček *et al.*, 2018; Álvarez-Parra *et al.*, 2021b; McCoy *et al.*, 2021). Estos resultados se sustentan en hallazgos de restos fósiles de estos grupos en los niveles con ámbar y en la geoquímica de los ámbares (Menor-Salván *et al.*, 2016; McCoy *et al.*, 2021). Son abundantes los restos fósiles del género *Agathoxylon* de la familia Araucariaceae y los del género *Frenelopsis* de la familia †Cheirolepidiaceae en los niveles con ámbar, sin embargo solo las araucariáceas están representadas como bioinclusiones (Kvaček *et al.*, 2018). Los análisis geoquímicos de cromatografía de gases/espectrometría de masas (GC-MS) indican que los árboles productores de resina que dieron lugar a la resina relacionada con los ámbares de Peñacerrada I, Ariño, San Just y La Hoya pertenecían a la familia Araucariaceae (Chaler y Grimalt, 2005; Menor-Salván *et al.*, 2016; Álvarez-Parra *et al.*, 2021b), mientras que los de los ámbares de El Soplao y El Caleyu se correspondían con la familia †Cheirolepidiaceae (Menor-Salván *et al.*, 2016). El caso del ámbar de El Soplao es peculiar, ya que la geoquímica lo relaciona con †Cheirolepidiaceae o quizás con árboles relacionados con Cupressaceae (Menor-Salván et al., 2010, 2016), mientras que los hallazgos paleobotánicos apuntan a Araucariaceae (Kvaček *et al.*, 2018). El ámbar turoniense de Soto del Real se ha relacionado con árboles de la familia Pinaceae (Menor-Salván *et al.*, 2016).

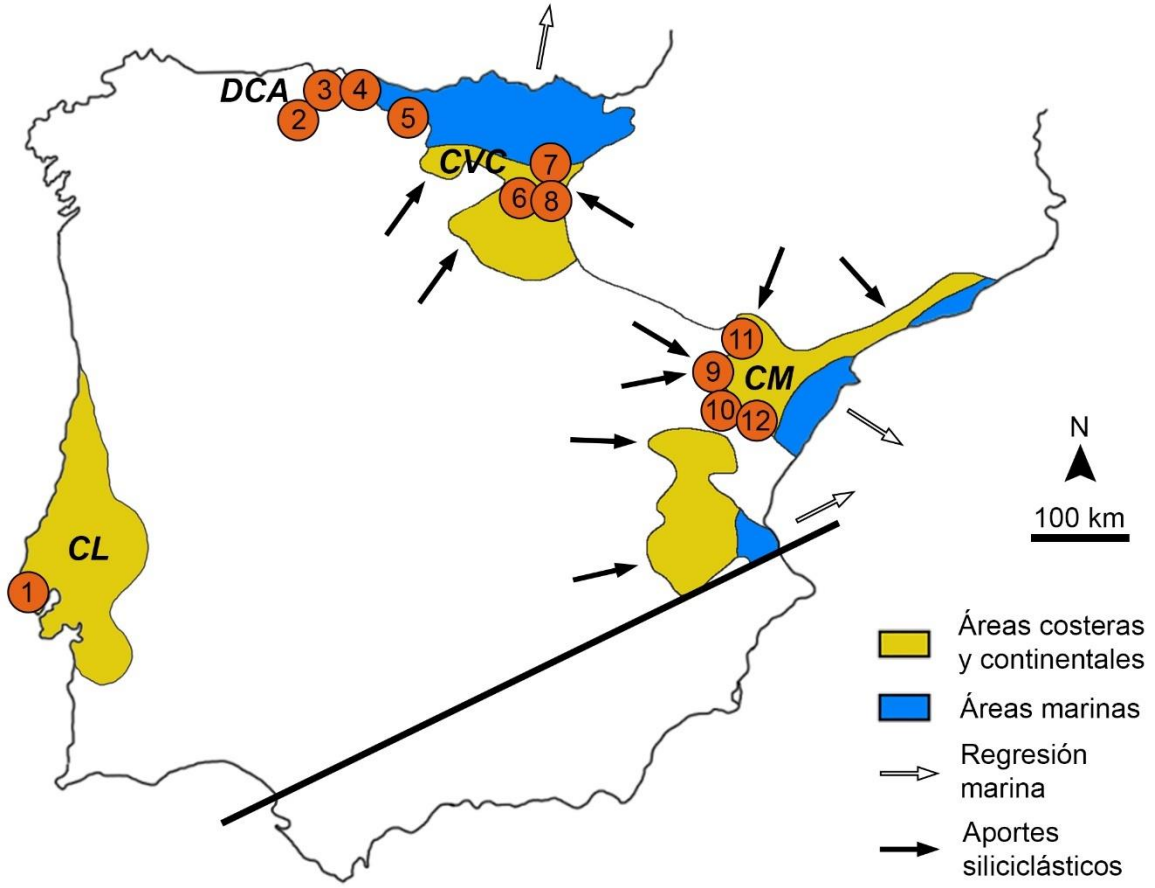

Figura 6. Mapa de la península ibérica que muestra las cuencas sedimentarias durante el Albiense inferior-medio con indicación de los 12 yacimientos de ámbar con bioinclusiones de España y Portugal. Cuenca Lusitana (*CL*), Depresión Central Asturiana (*DCA*), Cuenca Vasco-Cántabra (*CVC*) y Cuenca del Maestrazgo (*CM*). Estoril-Cascais (1), El Caleyu (2), La Rodada (3), Pola de Siero (4), El Soplao (5), Salinillas de Buradón (6), Peñacerrada I (7), Peñacerrada II (8), San Just (9), Arroyo de la Pascueta (10), Ariño (11), La Hoya (12). Mapa modificado de Mas *et al.* (2004).

El patrimonio paleontológico de España aparece mencionado en la Ley 16/1985 de Patrimonio Histórico Español y la Ley 42/2007 de Patrimonio Natural y de la Biodiversidad, además de la Ley 33/2015, modificación de la última (Vegas *et al.*, 2018). Sin embargo, la gestión y protección del patrimonio paleontológico depende de las leyes propias de Patrimonio Cultural de cada comunidad autónoma (Vegas *et al.*, 2018). Por ello, el estatus legal de los yacimientos de ámbar de España depende de la comunidad autónoma en la que se encuentran, lo que conlleva unas medidas y acciones de protección diferentes en cada caso (Rodrigo *et al.*, 2018). Por el momento, el único yacimiento de ámbar de España bajo una figura protección es Peñacerrada II, designado tanto Bien de Interés Cultural (BIC) como Bien Cultural Calificado (Rodrigo *et al.*, 2018). Se ha planteado la designación como BIC de los yacimientos de ámbar de El Soplao y San Just, aunque el proceso burocrático se encuentra detenido (Rodrigo *et al.*, 2018). Además, varios yacimientos de ámbar se han considerado bajo la figura de Lugar de

Interés Geológico (LIG), o se localizan geográficamente dentro de uno de ellos, y están incluidos en el Inventario Español de Lugares de Interés Geológico desarrollado por el Instituto Geológico y Minero de España. Esta consideración no proporciona protección a los yacimientos, sino que destaca su relevancia dentro del patrimonio geológico español, además de valorar su vulnerabilidad (García-Cortés y Cabrera Ferrero, 2021). Los yacimientos de ámbar considerados como LIGs son: El Caleyu (CA010, Yacimiento de ámbar cretácico de El Caleyu), El Soplao (incluido en CV004, Yacimientos de Zn-Pb de La Florida y Cueva de El Soplao), Peñacerrada I (CV010, Ámbar de Peñacerrada I. Moraza), Peñacerrada II (PV129, Yacimientos de ámbar de Peñacerrada), San Just (IB204, Localidades tipo de las Fms Escucha y Utrillas y ámbar de San Just), Arroyo de la Pascueta [incluido en IB214, Yacimiento paleobotánico del Cretácico del Arroyo de la Pascueta (Rubielos de Mora)] y La Hoya (IB076, Yacimiento de ámbar La Hoya del Cretácico en Cortes de Arenoso). Entre los yacimientos de ámbar españoles con bioinclusiones, algunos se encuentran protegidos por un vallado, como El Soplao y Peñacerrada II, o por vigilancia activa de la Guardia Civil y el SEPRONA, como San Just, mientras que otros se encuentran cubiertos de forma premeditada tras su excavación, como Peñacerrada I, o su acceso es complejo debido a su localización aislada, como Arroyo de la Pascueta y La Hoya (Rodrigo *et al.*, 2018). El yacimiento de Ariño es un caso especial, ya que se encuentra en una mina de propiedad privada, por lo que su acceso depende de las propias actividades y trabajos en la mina (Alcalá *et al.*, 2012). Los yacimientos de ámbar de Portugal, por el momento, no se encuentran bajo protección de ninguna designación patrimonial (Rodrigo *et al.*, 2018).

1.4. Objetivos e hipótesis de trabajo

El objetivo principal de la Tesis Doctoral es establecer la relevancia de los ámbares cretácicos de la Cuenca del Maestrazgo y, particularmente, estudiar por primera vez y de forma pluridisciplinar el ámbar procedente del yacimiento de Ariño. Para desarrollarlo se ha requerido investigar la tafonomía y las características paleoambientales de los diferentes yacimientos, además de estudiar el contenido paleobiológico del ámbar, lo que, en conjunto, ha ofrecido una visión general de la paleoecología del ecosistema. A continuación, se listan las hipótesis de trabajo del proyecto de Tesis Doctoral, junto con los objetivos asociados:

Hipótesis 1: El estudio tafonómico del ámbar de los yacimientos de la Cuenca del Maestrazgo permite diferenciar si su origen es principalmente autóctono, parautóctono o alóctono y proporciona información sobre las características paleoambientales de los bosques resiníferos.

Objetivo: Inferir los medios sedimentarios de los yacimientos de ámbar a partir de la información estratigráfica y sedimentológica y las características de los ámbares.

Hipótesis 2: El registro paleobotánico del yacimiento de Ariño y las características espectroscópicas y geoquímicas del ámbar apuntan a que los árboles de la familia Araucariaceae fueron los productores de la resina, al igual que se ha inferido para otros ámbares cretácicos de Iberia.

Objetivo: Estudiar los restos fusinizados de plantas del yacimiento de Ariño y realizar análisis espectroscópicos y geoquímicos para obtener información sobre la afinidad taxonómica de los árboles productores de resina.

Hipótesis 3: El ámbar de Ariño es rico en bioinclusiones de artrópodos, las cuales muestran diferencias taxonómicas con las de San Just, Arroyo de la Pascueta y La Hoya debido a las diferentes edades y características paleoambientales de estos yacimientos.

Objetivo: Iniciar el estudio taxonómico del registro de artrópodos en los ámbares de Ariño y La Hoya, continuar el del registro de los ámbares de San Just y Arroyo de la Pascueta y realizar una comparación taxonómica.

Hipótesis 4: El registro de bioinclusiones de artrópodos en los ámbares de la Cuenca del Maestrazgo muestra diferencias taxonómicas con el de los ámbares de la Cuenca Vasco-Cantábrica debido a las diferentes características paleoambientales en cada área.

Objetivo: Evaluar las diferencias y similitudes del registro de artrópodos en los ámbares de los yacimientos de la Cuenca del Maestrazgo con respecto a los de la Cuenca Vasco-Cantábrica.

Hipótesis 5: El registro de bioinclusiones de artrópodos en los ámbares de la Cuenca del Maestrazgo muestra más similitudes taxonómicas con el de los ámbares del Albiense-Cenomaniense de Francia que con el de los ámbares cretácicos de otras regiones debido a su cercanía paleográfica.

Objetivo: Comparar las coocurrencias a nivel de género de artrópodos de los ámbares de la Cuenca del Maestrazgo con ámbares cretácicos de otras regiones.

Hipótesis 6: El diverso registro fósil del yacimiento de Ariño permite considerar el yacimiento como un *Konservat-Lagerstätte* de importancia mundial dadas sus características únicas, lo que permite una detallada reconstrucción del paleoecosistema boscoso durante el Albiense.

Objetivo: Integrar la nueva información obtenida a partir del estudio tafonómico del ámbar y de las bioinclusiones con la información bibliográfica previa del yacimiento de Ariño y realizar una reconstrucción paleoambiental y paleoecológica del ecosistema.

Hipótesis 7: Durante el Cretácico se dio una combinación de factores abióticos y bióticos que propiciaron la producción en masa de resina en determinadas regiones del mundo, como en la Cuenca del Maestrazgo desde el Albiense inferior al Cenomaniense inferior.

Objetivo: Evaluar las posibles causas de producción en masa de resina durante el Cretácico y aplicar la metodología del modelado de nicho ecológico sobre la distribución de bosques resiníferos en este periodo.

1.5. Justificación de la Tesis Doctoral

La línea de investigación en la que se centra la presente Tesis Doctoral es el estudio de los ámbares cretácicos de la Cuenca del Maestrazgo. El estudio de los ámbares de la península ibérica se lleva desarrollando desde hace más de dos décadas; sin embargo, el foco principal de las investigaciones ha sido los ámbares de la Cuenca Vasco-Cantábrica y la Depresión Central Asturiana. En cuanto al estudio científico de los ámbares de la Cuenca del Maestrazgo, éste se ha centrado principalmente en el registro de bioinclusiones del ámbar del yacimiento de San Just. El hallazgo de ámbar en el yacimiento de Ariño por parte del equipo de la Fundación Conjunto Paleontológico de Teruel-Dinópolis y el elevado potencial del mismo de contener bioinclusiones, junto con sus peculiares características tafonómicas, circunstancias ya reconocidas tras una primera prospección por mis directores, fueron la motivación principal para enfocar la presente Tesis Doctoral hacia el estudio de los ámbares de la Cuenca del Maestrazgo.

La relevancia del proyecto de Tesis Doctoral radica en que se inicia el estudio del ámbar del yacimiento de Ariño y, además, se proporciona información sobre los yacimientos de ámbar de Arroyo de la Pascueta y La Hoya. Se conocía desde hace tiempo la presencia de bioinclusiones en los ámbares de estos dos yacimientos, sin embargo han permanecido a la espera de un estudio detallado. El ámbar de San Just es uno de los más importantes del Cretácico Inferior dada su riqueza en bioinclusiones, algunas de ellas poco comunes. Por ello, el desarrollo de la presente Tesis Doctoral centrada en parte en este ámbar está justificada y ayuda a incrementar aún más su relevancia.

Durante el proyecto de Tesis Doctoral se ha abordado el estudio de la tafonomía y el contenido paleobiológico de los ámbares y la inferencia del paleoambiente y la paleoecología de los correspondientes ecosistemas. Además, se ha realizado una aproximación a los factores que pudieron estar implicados en la producción en masa de resina durante el Cretácico

mediante la aplicación del modelado de nicho ecológico. La presente Tesis Doctoral se compone de ocho artículos publicados en revistas indexadas en el *Journal Citation Reports*, tres enviados y tres en preparación, todos ellos indicados en el Anexo 8.1. Estos trabajos tratan las siguientes temáticas para conseguir testar las hipótesis presentadas inicialmente:

- Tafonomía del ámbar: anexos 8.1.3 y 8.1.10.
- Tafonomía de las bioinclusiones: anexos 8.1.2, 8.1.5 y 8.1.13.
- Taxonomía de las bioinclusiones: anexos 8.1.1, 8.1.3, 8.1.4, 8.1.5, 8.1.6, 8.1.7, 8.1.8, 8.1.10, 8.1.11, 8.1.12 y 8.1.13.
- Paleoambiente y paleoecología: anexos 8.1.3 y 8.1.9.
- Paleoautoecología de las bioinclusiones: anexos 8.1.1, 8.1.2, 8.1.3, 8.1.4, 8.1.5, 8.1.6, 8.1.7, 8.1.8, 8.1.10, 8.1.11, 8.1.12 y 8.1.13.
- Producción en masa de resina: anexo 8.1.14.

El trabajo del Anexo 8.1.3 se considera central en la Tesis Doctoral por su enfoque pluridisciplinar, ya que aborda tanto la tafonomía y el contenido paleobiológico del ámbar de Ariño, como la inferencia del paleoambiente y la paleoecología del ecosistema. El estudio de las bioinclusiones se ha centrado en los órdenes de insectos Psocodea e Hymenoptera, aunque también se han realizado contribuciones sobre los ácaros Oribatida y el orden de insectos Diptera, además de restos de vertebrados, como plumas de dinosaurio y pelos de mamífero. Los listados de bioinclusiones en los ámbares de la Cuenca del Maestrazgo se encuentran en el Anexo 8.2. La limitación de tiempo hace inviable un estudio taxonómico más amplio dentro del marco de una Tesis Doctoral. Los estudios previos sobre Psocodea se habían centrado en unos pocos ejemplares en el ámbar de Peñacerrada I, por lo que es relevante extender su conocimiento a otros ámbares de la península ibérica. La abundancia y diversidad de los ejemplares de Hymenoptera en los ámbares de la Cuenca del Maestrazgo, junto con la escasa información previa que se tenía, justifica su estudio taxonómico. Cabe destacar que durante la Tesis Doctoral se ha trabajado con bioinclusiones en ámbares del Cretácico y el Eoceno de otras regiones del mundo, como ha sido el caso de los anexos 8.1.1 y 8.1.8. Este tipo de trabajos son esenciales, ya que ayudan a responder cuestiones paleoecológicas y evolutivas, además de servir como marco comparativo. Por ejemplo, el trabajo del Anexo 8.1.1 ha proporcionado información clave sobre la estasis evolutiva en el orden Psocodea, mientras que el trabajo del Anexo 8.1.8 ha ayudado a explicar cuestiones paleobiogeográficas del mismo grupo taxonómico.

Durante la Tesis Doctoral se ha prestado especial atención a la divulgación y la difusión social tanto de las campañas de excavación como de los resultados de las investigaciones. Un resumen de estas actividades se recoge en el Anexo 8.3.

2. Material y metodología

2.1. Material de estudio y colecciones museísticas

Durante el proyecto de Tesis Doctoral se han examinado piezas de ámbar, copal y resina de Defaunación (*sensu* Solórzano-Kraemer *et al.*, 2020) procedentes de diferentes lugares que están depositadas en ocho instituciones científicas públicas. La mayor parte de las piezas de ámbar estudiadas procede de yacimientos de España, aunque también se han estudiado ejemplares en ámbares de otros lugares del mundo con propósitos comparativos. La correspondencia de las siglas de los ámbares de la Cuenca del Maestrazgo se puede comprobar en el Anexo 8.2. También, se han revisado ejemplares actuales de psocópteros, el grupo de insectos más intensamente estudiado en la Tesis Doctoral, de diversas regiones del mundo de la Colección de Entomología Hope del Oxford University Museum of Natural History (Oxford, Reino Unido).

Las instituciones donde se encuentra depositado el material estudiado son:

- Museo Aragonés de Paleontología (Fundación Conjunto Paleontológico de Teruel-Dinópolis) en Teruel, Aragón (España): ámbar de Ariño, San Just y Arroyo de la Pascueta.
- Museu de la Universitat de València d'Història Natural en Burjassot, Comunitat Valenciana (España): ámbar de La Hoya.
- Museo de Ciencias Naturales de Álava en Vitoria-Gasteiz, País Vasco (España): ámbar de Peñacerrada I y Peñacerrada II.
- Colección Institucional del Laboratorio de la Cueva El Soplao en Celis, Cantabria (España): ámbar de El Soplao.
- Museu de Ciències Naturals de Barcelona en Barcelona, Cataluña (España): ámbar de Kachin (Myanmar).
- Departamento de Geociencias y Museo de la Université de Rennes 1 en Rennes, Bretaña (Francia): ámbar de Archingeay-Les Nouillers (Francia) y ámbar de Doumanga (Congo).
- Muséum national d'Histoire naturelle en París, Isla de Francia (Francia): ámbar de Oise (Francia) y ámbar de Totolapa (México).
- Senckenberg Forschungsinstitut und Naturmuseum de Frankfurt (Alemania): ámbar del Báltico y copal y resina de Defaunación de Tanzania.

2.2. Trabajo de campo: obtención de permisos y extracción de ámbar

La prospección y excavación de yacimientos es esencial en Paleontología, ya que proporcionan el material de estudio. La búsqueda de potenciales yacimientos de ámbar comienza con la revisión bibliográfica de mapas geológicos de la zona elegida. El ámbar suele

ser abundante en niveles de lutitas, limolitas y margas con elevado contenido en materia orgánica, la cual le da al nivel estratigráfico un color grisáceo o negruzco. En ocasiones, también se puede encontrar ámbar en niveles de carbón de minas a cielo abierto. Estos niveles estratigráficos se relacionan con un medio sedimentario transicional, adecuado para la acumulación y fosilización de la resina y la conservación del ámbar (Martínez-Delclòs *et al.*, 2004). En concreto, en la Cuenca del Maestrazgo se hallan niveles de carbón en la Formación Escucha y algunos niveles de menor potencia en el "Grupo Utrillas" (*sensu* Rodríguez-López *et al.*, 2009), que han sido tradicionalmente explotados para combustible. Los cuatro yacimientos de ámbar con bioinclusiones de la cuenca se encuentran en estos estratos.

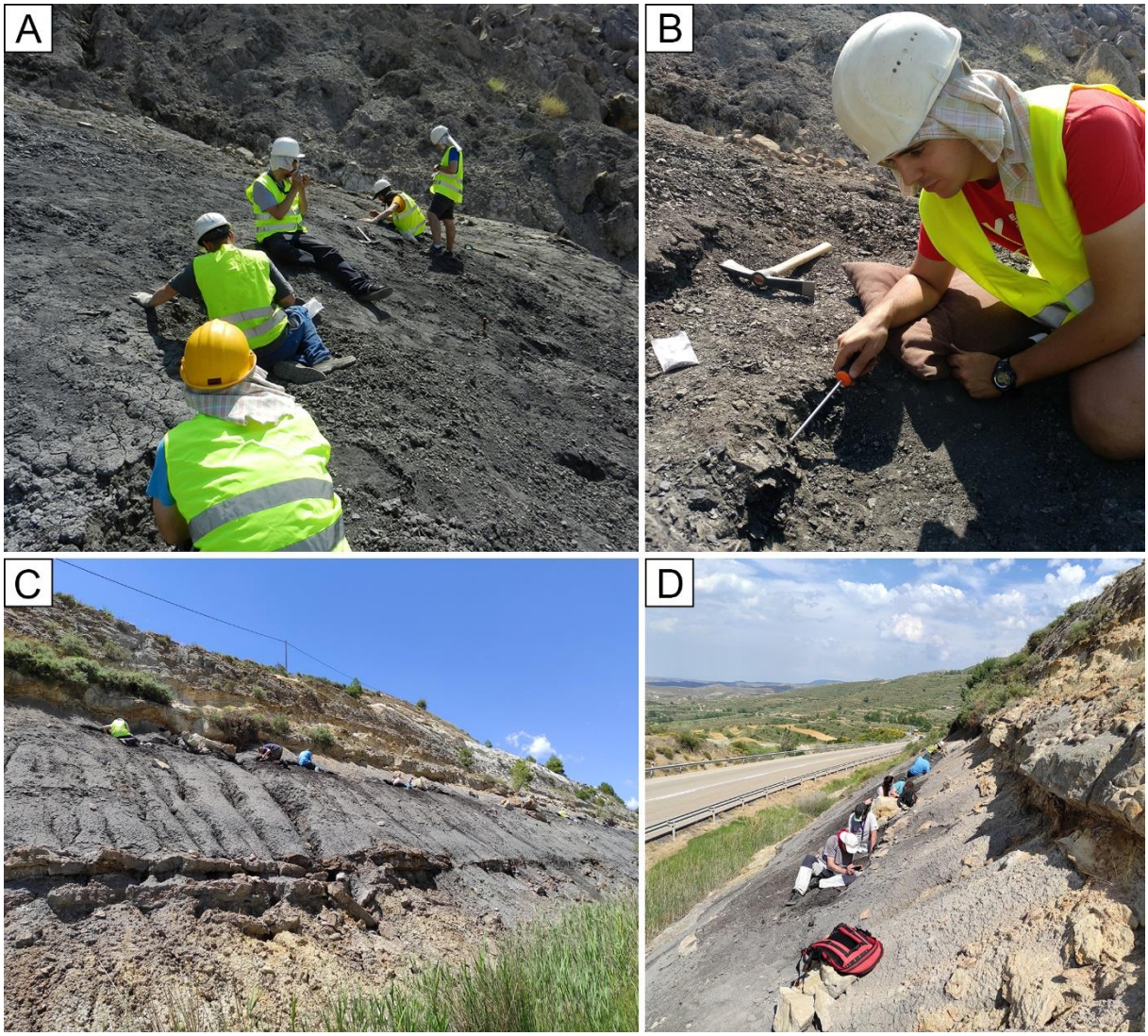

Figura 7. Trabajo de campo en los yacimientos de ámbar de Ariño en 2019 (A, B) y San Just en 2021 (C, D). A) Excavación y observación de muestras, fotografía de Xavier Delclòs; B) Metodología de excavación en la matriz rocosa con un destornillador de punta plana; C, D) Excavación a lo largo del nivel rico en ámbar.

Durante el desarrollo de la Tesis Doctoral, se han realizado dos prospecciones y una excavación en el yacimiento de Ariño (Teruel), una prospección en el yacimiento de la Mina La Dehesa (Teruel), una excavación en San Just (Teruel) y visitas a La Hoya (Castellón), Arroyo de la Pascueta y Son del Puerto (ambos en Teruel). Las prospecciones (2019 y 2021) y la excavación (2019) en Ariño se han realizado con permisos de la Dirección General de Patrimonio Cultural del Gobierno de Aragón (DGPC) obtenidos por el equipo de la Fundación Conjunto Paleontológico de Teruel-Dinópolis. La prospección en la Mina La Dehesa (2021) se realizó con permiso de la DGPC y en colaboración con la empresa Paleoymás. La excavación en San Just (2021) fue codirigida por Sergio Álvarez Parra, Xavier Delclòs y Luis Alcalá, con el permiso 500/20-2021 emitido por la DGPC. Las visitas a La Hoya (2021), Arroyo de la Pascueta (2022) y Son del Puerto (2022) únicamente consistieron en observaciones geológicas y estratigráficas junto con toma de fotografías. El material obtenido en cada una de estas actuaciones ha sido depositado en la institución indicada por la autoridad autonómica correspondiente.

El trabajo de extracción en el yacimiento comienza con la búsqueda del nivel rico en ámbar (Fig. 7). El ámbar se puede encontrar, o bien en una matriz arcillosa blanda que se puede retirar con destornillador de punta plana y cepillo, o bien en una matriz arcillosa dura, para la que se requiere el uso de una piqueta. En días soleados, el ámbar destaca por su brillo intenso y usualmente es hallado en superficie tras el lavado del nivel por el agua de lluvia. Las piezas de ámbar extraídas se han de guardar en bolsitas correctamente etiquetadas con indicación del nombre del yacimiento, nivel y fecha. En el caso de que haya piezas que se fragmenten durante la extracción, se han de guardar todos los fragmentos juntos, y separados de las otras piezas, por si aparecieran en ellos bioinclusiones. En ocasiones se pueden encontrar grandes masas de ámbar de raíz o piezas aéreas de colada de cierta longitud; en estos casos, es recomendable cubrir la pieza con papel para evitar fragmentación y daños. En yacimientos de ámbar en los que sea complicada la extracción o la abundancia de piezas sea baja, se puede usar la técnica de extracción por flotación (Corral *et al.*, 1999). Esta técnica consiste en la introducción de la roca arcillosa blanda que contiene el ámbar en una hormigonera. La roca se disgrega en el agua, ya que se disuelven las arcillas, por lo que el ámbar flota y se facilita su separación. En el caso de las excavaciones efectuadas, no fue necesario el uso de esta técnica ya que el ámbar se encontraba y extraía fácilmente durante el trabajo directo en el nivel (Fig. 7).

2.3. Preparación en el laboratorio de ámbar con bioinclusiones

Una vez se han recogido las piezas de ámbar del yacimiento, comienza la laboriosa fase de búsqueda de bioinclusiones y preparación de las piezas. El geólogo y gemólogo Rafael López del Valle, especializado en preparación de ámbar, es el encargado de realizar esta tarea tras los

muestreos o excavaciones en yacimientos españoles organizadas por nuestro equipo de investigación AMBERIA (acrónimo de Ámbar de Iberia). La metodología está especificada en Corral *et al.* (1999), aunque trabajos posteriores incluyen algunas modificaciones de la técnica (Nascimbene y Silverstein, 2000; Sadowski *et al.*, 2021).

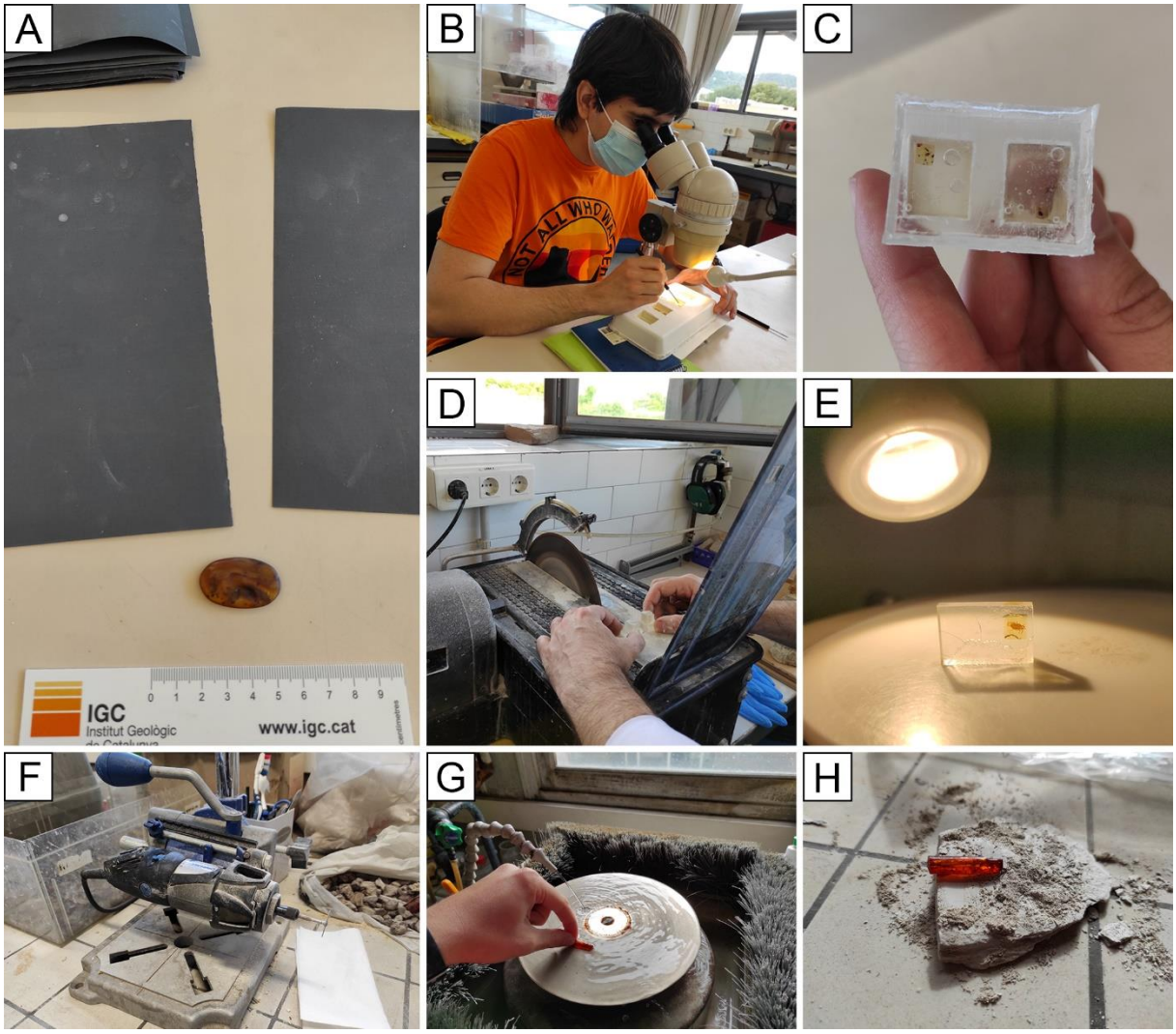

Figura 8. Procedimiento de preparación de piezas de ámbar con bioinclusiones. A) Lijas y pieza de ámbar a preparar; B) Colocación de la pieza de ámbar, tras su cortado y lijado, en resina epoxi; C) Prisma de resina epoxi endurecida con la pieza de ámbar; D) Cortado del prisma de resina epoxi con una sierra eléctrica; E) Pieza de ámbar con un ácaro como bioinclusión preparada en resina epoxi; F) Sierra eléctrica utilizada para cortar ámbar; G) Lijado de una pieza de ámbar con una lija mecánica con agua; H) Pulido de la superficie de una pieza de ámbar con una roca diatomita de grano muy fino. Las fotografías A-E se han tomado en el Laboratori de Paleontologia del Departament de Dinàmica de la Terra i de l'Oceà de la Facultat de Ciències de la Terra de la Universitat de Barcelona; las fotografías F-H se han tomado en el Muséum national d'Histoire naturelle de París.

El proceso realizado por nuestro equipo sigue siempre el mismo protocolo. Se requiere el lavado de las piezas de ámbar para separarlas de la matriz de roca. Posteriormente, se separan las piezas de ámbar de raíz de las de ámbar aéreo. Son estas últimas las que tienen un alto potencial de contener bioinclusiones. Cada pieza de ámbar aéreo se observa bajo una lupa binocular en busca de posibles bioinclusiones, principalmente pequeños artrópodos. Algunos artrópodos pueden medir incluso menos de 1 mm, por lo que las piezas de ámbar más pequeñas también pueden contener bioinclusiones. Es posible que algunas piezas de ámbar requieran ser cortadas y/o pulidas en caso de que la parte más externa sea opaca.

Tras localizar las piezas con bioinclusiones, es necesaria su preparación. La preparación de piezas de ámbar no solo facilita el estudio científico de las bioinclusiones, sino que las protege y permite su preservación en colecciones museísticas. Durante el desarrollo de la Tesis Doctoral se han preparado piezas de ámbar junto con Alejandro Gallardo (Universitat de Barcelona) en el Laboratori de Paleontologia del Departament de Dinàmica de la Terra i de l'Oceà de la Facultat de Ciències de la Terra de la Universitat de Barcelona (Fig. 8A-E), siguiendo la metodología indicada a continuación y basada en Corral *et al.* (1999): 1) selección de los planos adecuados para el estudio anatómico y taxonómico de la bioinclusión, se suele obtener una pieza con forma de prisma; 2) desgaste de la pieza de ámbar con papel de lija mojado con agua —se recomienda cambiar periódicamente la dirección de lijado para evitar la aparición de rayas y surcos en la superficie—; 3) pulido de la superficie del ámbar con gel limpiador de vitrocerámica sobre un trapo de algodón —este gel contiene partículas muy finas que facilitan el pulido—; 4) inserción de la pieza de ámbar en un molde de silicona con resina epoxi (EPO-TEK 301) —previamente se requiere la preparación de la resina epoxi por medio de un catalizador—; 5) colocación del molde de silicona con resina epoxi y la pieza de ámbar en una cámara de vacío, la cual evita que se formen burbujas, durante unas 24 horas hasta su endurecimiento; 6) extracción del prisma de resina epoxi con la pieza de ámbar del molde de silicona; y 7) desgaste mecánico y manual del prisma y posterior pulido con gel limpiador de vitrocerámica.

Durante una estancia en el Muséum national d'Histoire naturelle (MNHN) de París, relacionada con la Tesis Doctoral, se realizó la preparación de piezas de ámbar del Eoceno de Oise (Fig. 8F-H). La metodología difiere ligeramente con la explicada anteriormente. En un primer lugar, se corta la pieza de ámbar seleccionada con una sierra eléctrica de pequeño tamaño, posteriormente se desgasta mecánicamente con una lija circular teniendo en cuenta los planos apropiados para el estudio de la bioinclusión y, por último, se pule la superficie con una roca diatomita de grano muy fino, lo que permite la correcta visualización de la bioinclusión. Algunos grupos de investigación prefieren preservar la pieza de ámbar en aceites minerales o en bálsamo de Canadá, en vez de en resina epoxi.

2.4. Espectroscopía de infrarrojos para la caracterización de muestras de ámbar

La espectroscopía infrarroja transformada de Fourier (IRTF) es una técnica que permite la caracterización de muestras orgánicas a partir de su grado de absorción de luz infrarroja en función de su composición química, su organización espacial y la naturaleza de sus enlaces (Beck *et al.*, 1964; Edwards y Farwell, 1996). El espectro de transmitancias obtenido a partir del análisis del ámbar de un yacimiento permite la comparación con otros ámbares coetáneos de otras regiones del mundo o de edades diferentes, ya que varía en función del árbol resinífero y el grado de maduración (Langenheim y Beck, 1965; Grimalt *et al.*, 1988; McKellar *et al.*, 2008). Además, esta técnica también se ha usado en ocasiones para diferenciar ámbar de otros restos geológicos similares y de imitaciones (Kosmowska-Ceranowicz, 2015). En este proyecto, se han realizado análisis IRTF del ámbar aéreo de Ariño, San Just, Arroyo de la Pascueta y La Hoya con el objetivo de compararlos entre ellos y con los ámbares de la Cuenca Vasco-Cantábrica en busca de diferencias en los espectros que pudieran indicar diferencias en su origen.

Los análisis IRTF se han realizado en la Unidad de Espectroscopía Molecular de los Centros Científicos y Tecnológicos de la Universitat de Barcelona (CCiTUB) (Fig. 9). Se han llevado a cabo con un espectrómetro IR Perkin Elmer Frontier que utiliza un sistema ATR de diamante con un detector DTGS de temperatura estabilizada y un divisor de haz CsI. En primer lugar, se requiere seleccionar las piezas de ámbar que se quieren analizar. Es importante tener en cuenta que la metodología es parcialmente destructiva, por lo que las piezas seleccionadas no deberían contener bioinclusiones. Alternativamente, en el caso de que la pieza de ámbar tenga dos superficies planas paralelas, se puede analizar sin necesidad de destruirla parcialmente. Con ayuda de un escalpelo se corta la pieza para obtener uno o varios fragmentos pequeños, que posteriormente se trituran en un mortero de ágata hasta obtener un polvo fino. Un fragmento de 1 cm^3 es suficiente para realizar el análisis. Finalmente, el polvo obtenido se usa para cubrir completamente la lente del detector del espectrómetro, se aplasta con un instrumento metálico y se realiza el análisis. Es muy importante limpiar con etanol los instrumentos utilizados tras cada análisis para evitar contaminaciones y obtener resultados erróneos. El espectrómetro puede realizar los análisis en transmitancia o en absorbancia; en el caso del ámbar se suelen realizar los análisis en transmitancia por consenso para así facilitar las comparaciones.

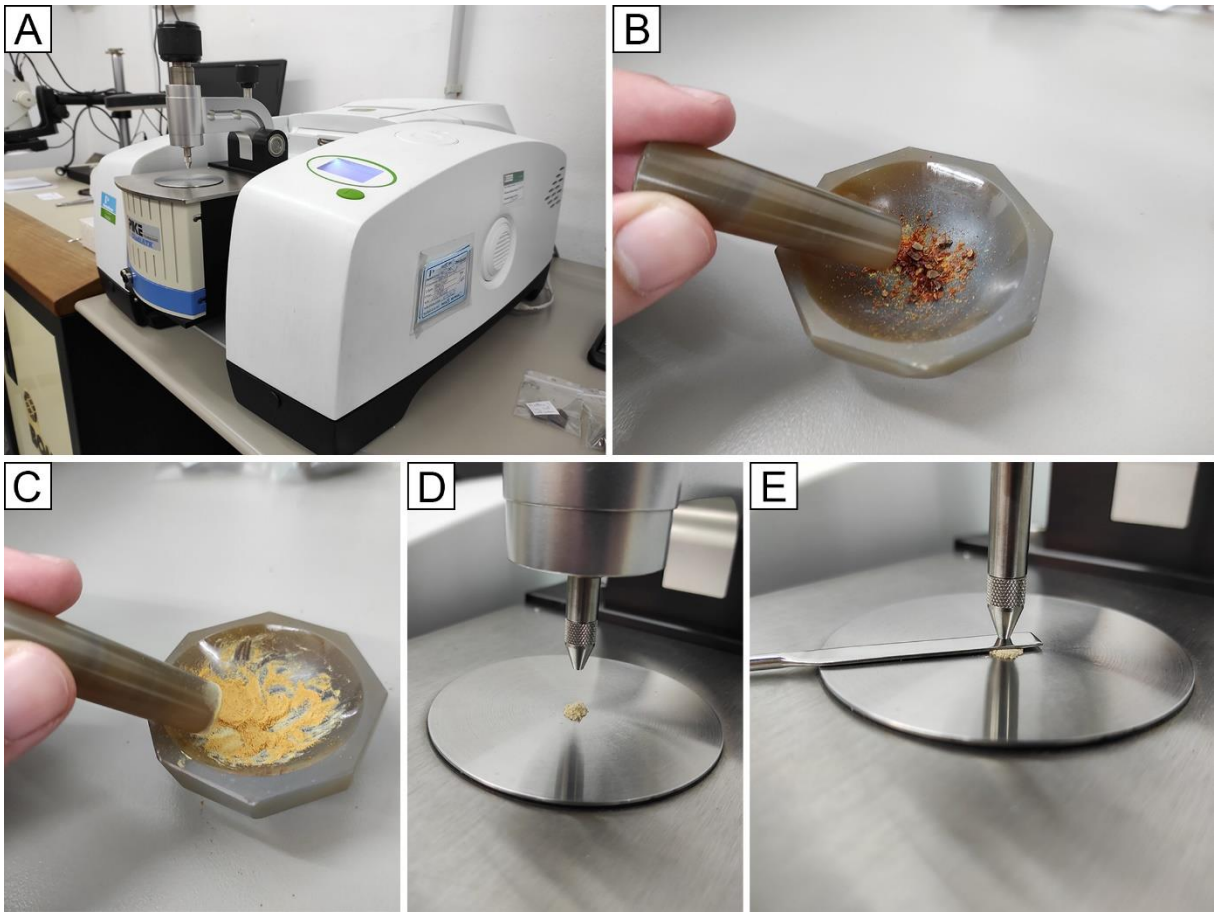

Figura 9. Procedimiento para realizar análisis IRTF de piezas de ámbar en la Unidad de Espectroscopía Molecular de los Centros Científicos y Tecnológicos de la Universitat de Barcelona. A) Espectrómetro IR Perkin Elmer Frontier; B) Fragmentos de ámbar cortados con escalpelo; C) Polvo fino de ámbar obtenido al triturarlo con un mortero de ágata; D) Lente del detector del espectrómetro cubierto con polvo fino de ámbar; E) Espectrómetro listo para iniciar el análisis IRTF de la muestra de ámbar.

2.5. Microscopio electrónico de barrido: aplicación en estudios tafonómicos

La Microscopía Electrónica de Barrido (MEB) es una técnica que permite la obtención de imágenes en alta resolución de la superficie de una muestra mediante la emisión de un haz de electrones (Zhou *et al.*, 2007). Esta técnica no destructiva es ampliamente usada para el examen en detalle y el fotografiado de microfósiles (Sandberg y Hay, 1967) o de partes de fósiles mayores. Además, la MEB se puede aplicar a estudios tafonómicos mediante la observación de trazas, de origen orgánico u inorgánico, en restos fósiles (Shipman, 1981). En el presente proyecto de Tesis Doctoral se ha utilizado la MEB con el objetivo de visualizar y fotografiar la superficie de piezas de ámbar de raíz del yacimiento de Ariño y así obtener información tafonómica que indique si las piezas de resina sufrieron transporte durante la etapa bioestratinómica (Álvarez-Parra *et al.*, 2021b). También, se han fotografiado

bioinclusiones que han quedado expuestas en la superficie de piezas de ámbar aéreo tras su preparación (Fig. 10). Previamente ya se había aplicado la MEB a estudios sobre ámbar y bioinclusiones superficiales (Ascaso *et al.*, 2003; Speranza *et al.*, 2015), pero no con el objetivo de interpretar las piezas desde el punto de vista tafonómico relativo a transporte bioestratinómico.

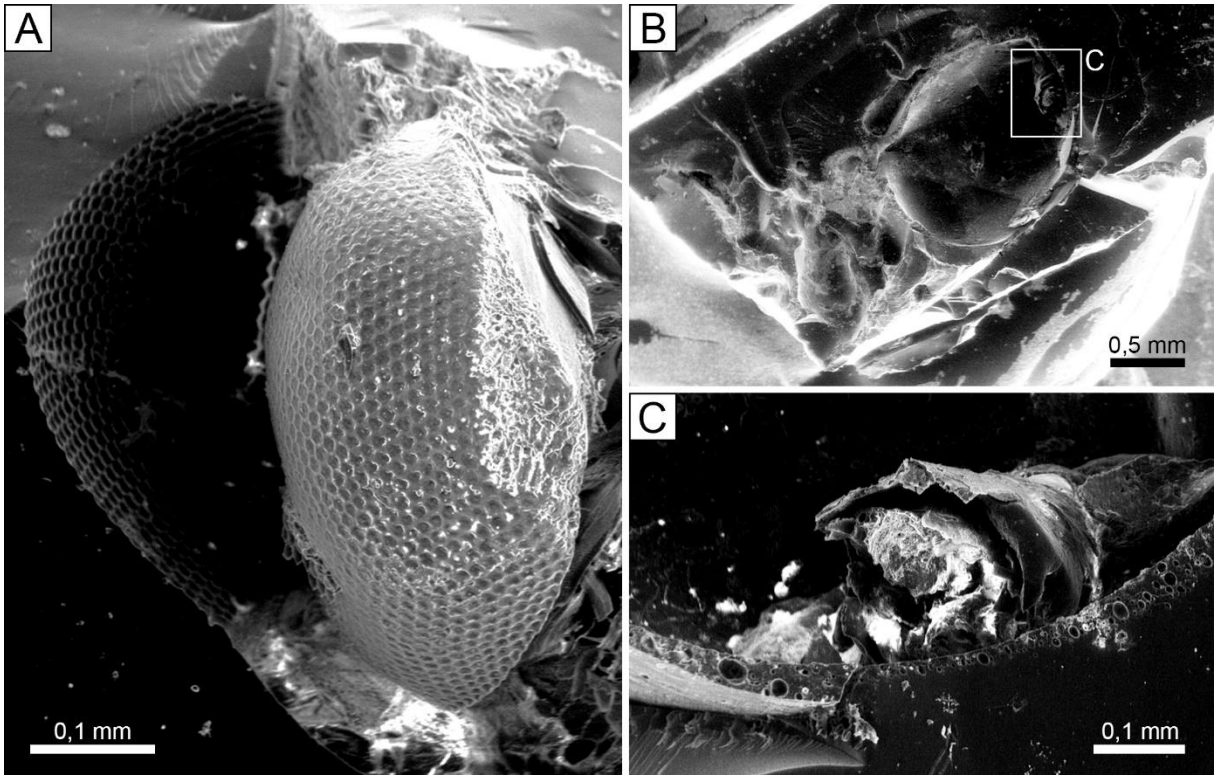

Figura 10. Imágenes obtenidas mediante MEB en la Unidad de Microscopía Electrónica de los Centros Científicos y Tecnológicos de la Universitat de Barcelona de bioinclusiones en ámbar de Ariño expuestas en superficie. A) Ojo de díptero (AR-1-A-2018.2.1) en el que se observan los omatidios; B) Araña (AR-1-A-2019.76) en la que se diferencia el prosoma, junto con porciones de patas, y el opistosoma, se indica la localización de la subfigura C con un recuadro; C) Estructuras que podrían estar relacionadas con las hileras en la parte distal del opistosoma.

La MEB se ha realizado en la Unidad de Microscopía Electrónica de los CCiTUB mediante un microscopio electrónico de barrido Quanta 200. El fragmento de ámbar de raíz objeto del estudio tafonómico se sumergió durante un día en agua destilada y se sometió, incluido en una bolsita de plástico con agua destilada para evitar daños, a cuatro ciclos de baño ultrasónico. Todas las muestras examinadas se adhirieron a una base con pegamento para evitar su movimiento al introducirlas en el microscopio. La visualización de las muestras requiere que estén secas y, además, en ocasiones se recubren con metales para mejorar su conductividad (Zhou *et al.*, 2007). En este caso, las piezas se recubrieron con grafito en una cámara de vacío.

Adicionalmente, una pieza de ámbar del yacimiento de Ariño con tres pelos de mamífero como bioinclusiones se visualizó y fotografió mediante un microscopio electrónico de barrido Hitachi S4800 del Servicio Central de Apoyo a la Investigación Experimental de la Universitat de València (Álvarez-Parra *et al*., 2020a).

2.6. Visualización, fotografiado y dibujo de bioinclusiones

Las bioinclusiones en el ámbar suelen ser de pequeño tamaño, menos de 1 cm de longitud. Algunos ejemplares de avispas parasitoides halladas en ámbar pueden medir incluso alrededor de 0,5 mm de longitud. Por ello, es esencial el uso de lupa binocular y microscopio óptico de campo claro para el examen y estudio de las bioinclusiones (Fig. 11). La correcta visualización requiere del uso de luz reflejada y/o transmitida. En el caso del ámbar, debido a su transparencia, la segunda opción es la más útil, aunque usualmente se trabaja combinando ambas. El uso de microscopio óptico permite utilizar elevados aumentos (4×, 10×, 20× y 50×) para facilitar la observación de caracteres anatómicos de reducido tamaño.

Además de la propia visualización de la bioinclusión, se requiere la toma de fotografías para ilustrar las observaciones. Esto se realiza mediante una cámara digital incorporada a la lupa binocular o microscopio óptico. Cada cámara digital lleva asociado un *software* especializado para la toma de fotografías. Una característica del ámbar es la conservación tridimensional de las bioinclusiones, por ello es necesaria la toma de varias fotografías en diferentes planos focales y su posterior combinación. La combinación fotográfica se ha realizado mediante el *software* Photoshop CS6 (https://www.adobe.com), y Helicon Focus 7.6.1 (https://www.heliconsoft.com/) en el caso del trabajo realizado en el MNHN de París.

El estudio de bioinclusiones en ámbar generalmente viene acompañado de la realización de un dibujo, esquemático o detallado, de la morfología del ejemplar. Esto se realiza mediante la técnica clásica de dibujo a cámara clara. Una lupa binocular o microscopio óptico equipado con tubo de cámara clara permite superponer la imagen del ejemplar a estudiar con la de un folio, por lo que es posible dibujar el ejemplar a la manera de un calco. Esta técnica ayuda a representar los caracteres anatómicos mediante el cambio de plano focal. A diferencia de las fotografías, los dibujos a cámara clara son interpretativos y se complementan con aquellas.

La mayor parte del trabajo realizado durante el proyecto de Tesis Doctoral se ha acometido con una lupa binocular Leica Wild M3Z y con un microscopio óptico Olympus CX41, ambos equipados con cámara clara y cámara digital sCMEX-20, en el Departament de Dinàmica de la Terra i de l'Oceà de la Facultat de Ciències de la Terra de la Universitat de Barcelona. Durante la estancia en el MNHN de París se utilizó una lupa Nikon SMZ25 equipada con cámara digital Nikon D800 y una lupa binocular Leica M205 equipada con cámara clara. El trabajo en el Oxford University Museum of Natural History se realizó con una lupa binocular

ZEISS SteREO Discovery.V12 equipada con cámara clara. Finalmente, se ha realizado el procesamiento digital de las fotografías y los dibujos mediante Photoshop CS6 para la preparación de figuras que permitan una buena visualización e interpretación de los ejemplares estudiados para su publicación en artículos científicos.

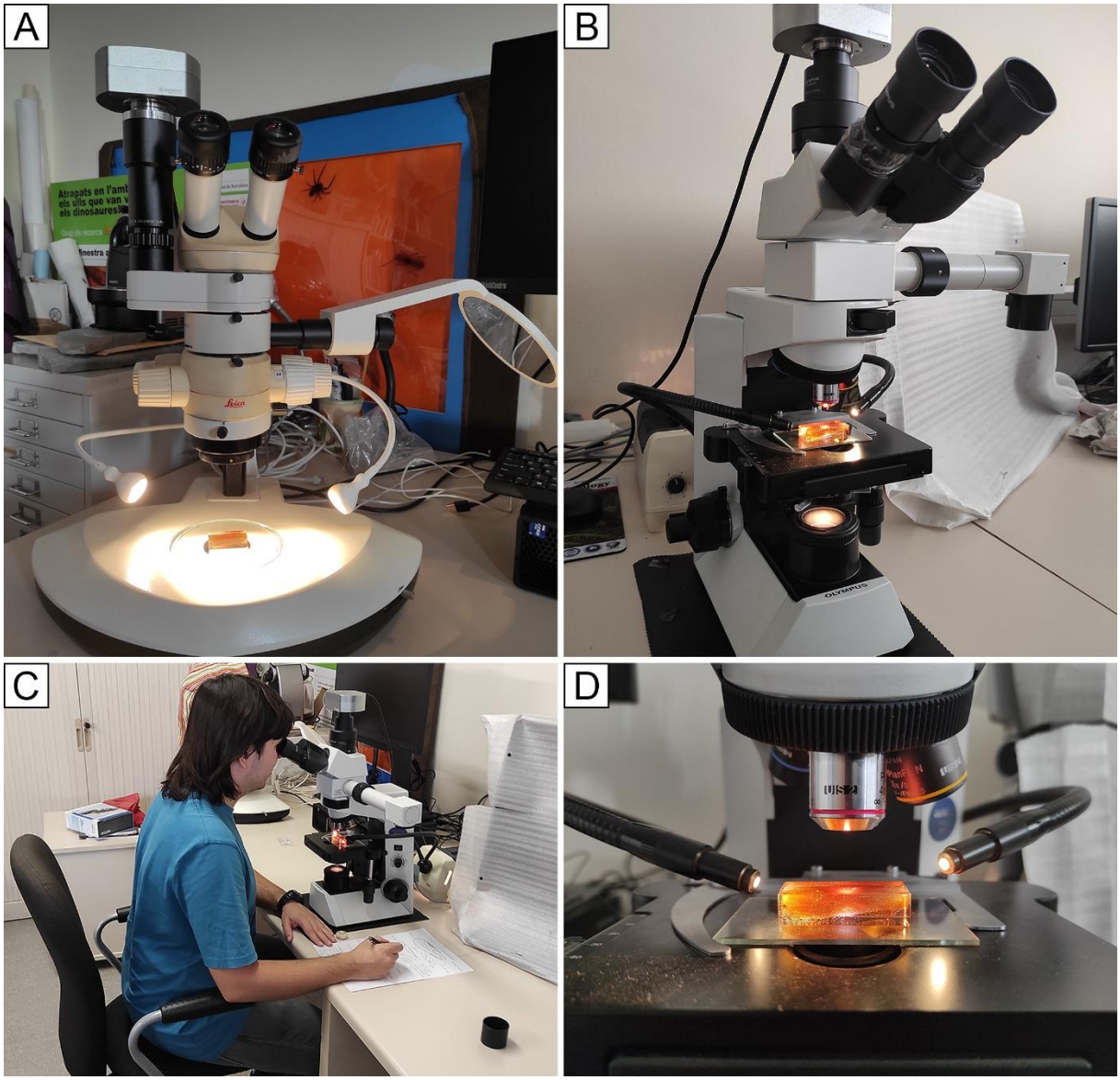

Figura 11. Procedimiento de visualización, fotografiado y dibujo de bioinclusiones en ámbar. A) Lupa binocular Leica Wild M3Z, con iluminación reflejada y transmitida, con una muestra de ámbar en epoxi; B) Microscopio óptico Olympus CX41, con iluminación reflejada y transmitida, con una muestra de ámbar en epoxi; C) Proceso de dibujo a cámara clara de una bioinclusión en ámbar, en ocasiones se requiere iluminación del folio en donde se dibuja el ejemplar; D) Muestra de ámbar en epoxi colocada en la base de un microscopio óptico Olympus CX41 con iluminación reflejada y transmitida. Fotografías tomadas en el Departament de Dinàmica de la Terra i de l'Oceà de la Facultat de Ciències de la Terra de la Universitat de Barcelona.

2.7. Microtomografía computarizada y por contraste de fase con luz sincrotrón de bioinclusiones en ámbar

La tomografía computarizada (CT) es una técnica no destructiva de escaneado y reconstrucción tridimensional que consiste en un haz de rayos-X que atraviesa una muestra en diferentes ángulos y proporciona una imagen en función de la absorción de los rayos por cada material del que se compone la muestra (Ritman, 2011). Esta técnica se usa habitualmente con propósitos médicos y para la observación de estructuras internas que no son visibles desde el exterior de forma convencional. En el caso de muestras de pequeño tamaño se usa un escáner micro-CT, el cual se caracteriza por una alta resolución y un funcionamiento por el cual la muestra gira y la fuente y detector de rayos están fijos (Dierick *et al.*, 2007; Ritman, 2011). La técnica de micro-CT se ha usado para la obtención de imágenes que permiten la reconstrucción tridimensional de bioinclusiones en ámbar, principalmente aquellas en las que la observación mediante microscopio óptico es difícil (Dierick *et al.*, 2007; Kypke y Solodovnikov, 2020; Peris *et al.*, 2022). A pesar de ello, en muchas ocasiones el contraste entre la bioinclusión y el ámbar no es muy alto y no se pueden obtener imágenes que permitan diferenciar la bioinclusión del ámbar que lo rodea, posiblemente debido a causas tafonómicas o a características del ámbar como matriz. Durante la Tesis Doctoral se ha usado un escáner micro-CT Bruker Skyscan 1272 con generador de 10 W y 20-100 kV, detector de 11 Mpx y resolución máxima de 0,45 μm del Centro de Investigación en Ciencia e Ingeniería Multiescala de la Universitat Politècnica de Catalunya en Barcelona (Fig. 12A-D). Se han escaneado piezas de ámbar de diferentes regiones y edades con una resolución de 4 μm, a pesar de ello los resultados no fueron los esperados y no se pudieron obtener imágenes de suficiente contraste que permitieran crear modelos tridimensionales. Se creó el modelo tridimensional preliminar de un fragmento de pluma del ámbar de San Just (SJ-10-13) escaneado con micro-CT previamente a la Tesis Doctoral mediante el *software* VGStudioMax 2.1 (https://www.volumegraphics.com).

Se ha participado en un proyecto de investigación para el escaneado de bioinclusiones en ámbar y copal mediante contraste de fase con luz sincrotrón en el Deutsches Elecktronen-Synchrotron (DESY) de Hamburgo (Alemania) en octubre de 2022 (Fig. 12E, F). Los análisis se han llevado a cabo en el *Beamline*-IBL P05 en PETRA III del DESY, usando los parámetros: 3.601 proyecciones, 18 keV de energía, 50 mm de distancia de la muestra al detector y un tamaño efectivo de píxel de 0.64 μm. Esta técnica ya se ha aplicado previamente a estudios sobre bioinclusiones en ámbar y proporciona una mayor resolución que los escaneados mediante micro-CT (Soriano *et al.*, 2010). Los resultados preliminares obtenidos son más prometedores que los conseguidos mediante escáner micro-CT.

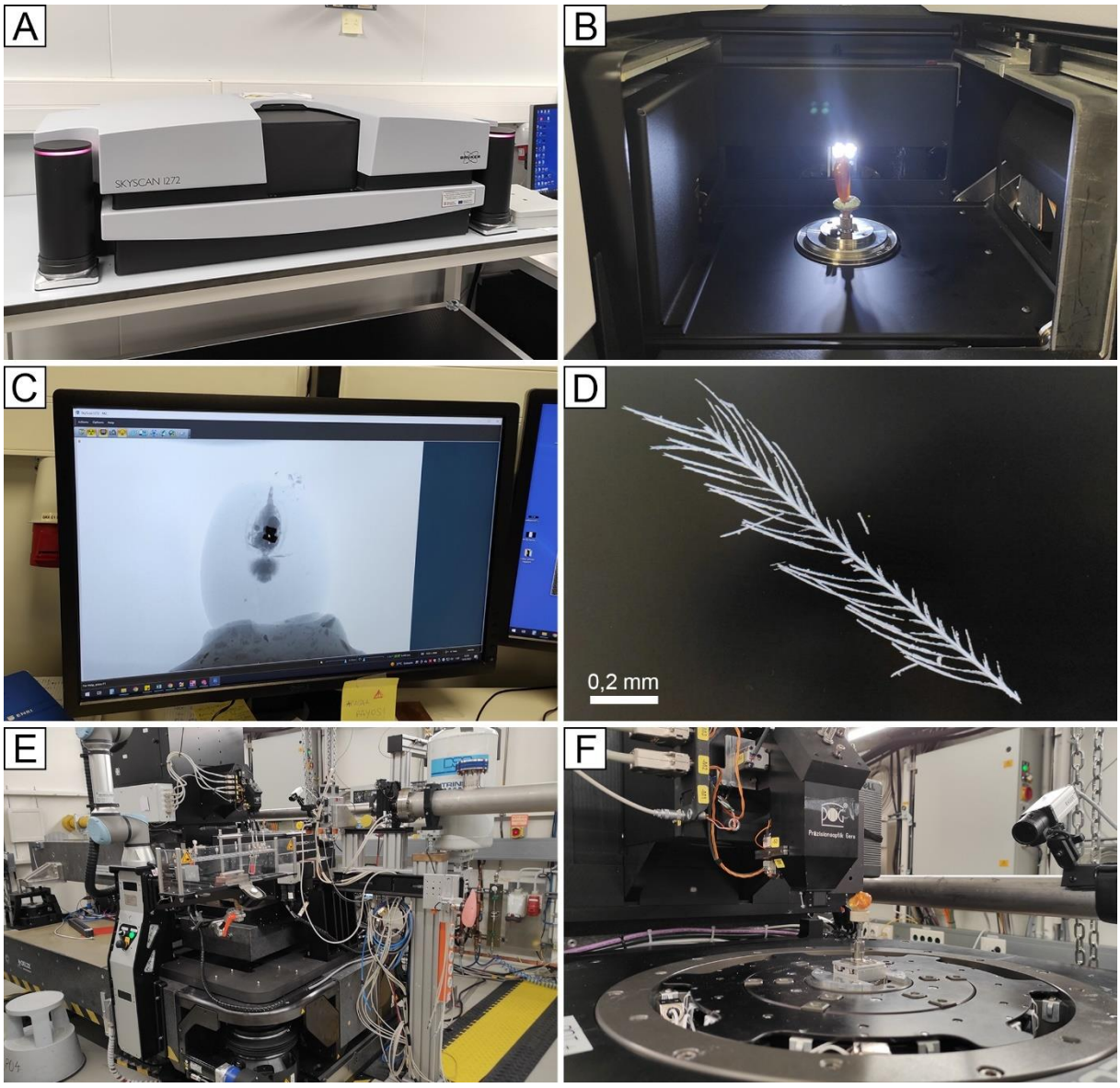

Figura 12. Escaneado de bioinclusiones en ámbar mediante micro-CT en el Centro de Investigación en Ciencia e Ingeniería Multiescala de la Universitat Politècnica de Catalunya y contraste de fase con luz sincrotrón en el Deutsches Elecktronen-Synchrotron (DESY) de Hamburgo (Alemania). A) Escáner micro-CT Bruker Skyscan; B) Pieza de ámbar colocada en la base del escáner lista para ser escaneada; C) Imagen obtenida mediante escáner micro-CT; D) Modelo tridimensional de un fragmento de pluma en ámbar de San Just (SJ-10-13); E) *Beamline*-IBL P05 en PETRA III del DESY; F) Pieza de copal colocada en la base del *beamline* lista para iniciar el escaneado.

2.8. Modelado de nicho ecológico

El modelado de nicho ecológico (*Ecological Niche Modelling*, ENM) es una técnica que permite estimar la distribución geográfica de los taxones en el espacio y en el tiempo mediante la correlación de los datos de presencia y los parámetros ambientales asociados (Franklin, 2010; Townsend Peterson *et al.*, 2011; Guisan *et al.*, 2017). Es decir, permite generar un

modelo ecológico de un taxón a partir de la información conocida sobre su distribución y estimar la probabilidad de que ese taxón se encuentre en otros lugares en función de las condiciones ambientales que necesita para vivir. Esta técnica ha empezado a aplicarse recientemente a la fauna y flora actual, principalmente con el objetivo de conocer la distribución de una especie en el futuro, teniendo en cuenta los pronósticos del Cambio Climático Global (Saupe *et al.*, 2011; Sillero y Carbonero, 2013). Así, se puede estimar la probabilidad de que una especie se extinga en un corto plazo de tiempo si la temperatura global aumenta. Otra función del ENM es conocer el nicho potencial de una especie actual a partir de la distribución conocida y de las variables ambientales que la condicionan (Chefaoui *et al.*, 2016). Curiosamente, el objeto de estudio del ENM no tienen por qué ser especies o grupos de más alto rango taxonómico, también se pueden modelar distribuciones de, por ejemplo, enfermedades (Wint *et al.*, 2002), atropellos de fauna (Ramp *et al.*, 2005), murciélagos estrellados contra molinos de viento (Santos *et al.*, 2013) o mordeduras de serpiente (Yañez-Arenas *et al.*, 2014). Una aproximación todavía poco explorada del ENM es su aplicación a especies fósiles o PaleoENM (Myers *et al.*, 2015). La principal diferencia metodológica entre el ENM y el PaleoENM es la obtención de información ambiental. Para trabajar sobre especies actuales es fácil obtener datos ambientales de lugares donde está presente una especie, pero el PaleoENM requiere obtener estos datos a partir de aproximaciones sedimentológicas y geoquímicas. Sin embargo, ya existen modelos climáticos y ambientales del pasado creados a partir de estos datos por paleoclimatólogos y es posible trabajar de forma precisa con esta información. La técnica del PaleoENM ya se ha aplicado eficientemente para modelar la distribución potencial en el pasado de diferentes grupos taxonómicos, como corales (Pohl *et al.*, 2019), équidos (Maguire y Stigall, 2009) y dinosaurios (Chiarenza *et al.*, 2022).

La aplicación del PaleoENM a estudios sobre ámbar permitiría explicar las características ambientales que condicionaron la presencia de bosques resiníferos. Dentro del presente proyecto de Tesis Doctoral se ha abordado la modelización de la distribución potencial de bosques resiníferos (o puntos de producción en masa de resina) durante el Cretácico, junto con la investigadora Erin E. Saupe (University of Oxford), con el objetivo de averiguar las causas de la existencia de numerosos yacimientos de ámbar de esa edad en la península ibérica, en general, y la Cuenca del Maestrazgo en particular. Se ha recopilado una extensa lista de coordenadas de 299 yacimientos cretácicos de ámbar a nivel mundial a partir de búsqueda bibliográfica. También se dispone de seis capas de variables ambientales a nivel global para cada piso del Cretácico obtenidas gracias a la colaboración con el grupo de investigación BRIDGE de la University of Bristol (https://www.paleo.bristol.ac.uk/resources/simulations/): temperatura media anual, temperatura media en el mes más cálido, temperatura media en el mes más frío, precipitación media anual, precipitación medial en el mes más húmedo y precipitación media en el mes más

seco. La metodología comienza con la rotación de las coordenadas actuales de cada yacimiento de ámbar a las paleocoordenadas correspondientes mediante los *softwares* R 4.0.4 (https://www.r-project.org/) y GPlates 2.2.0 (https://www.gplates.org/). Posteriormente, se requiere la preparación de los datos (puntos con paleocoordenadas); para ello, se selecciona un solo punto de paleocoordenadas por celda de las capas de variables ambientales (*unique occurrences*). Se requiere la separación en datos de prueba y datos de entrenamiento, normalmente un 25% de los datos son de prueba y el restante 75%, de entrenamiento. También se requiere la obtención de regiones de calibración de las variables ambientales. El procesamiento del PaleoENM se ha realizado usando el *software* R, con el *software* MaxEnt (Philips *et al.*, 2006) integrado, por medio del paquete kuenm (Cobos *et al.*, 2019). La visualización de mapas se ha realizado mediante el *software* QGIS 3.22.3 (https://www.qgis.org/en/site/). El procesamiento del paquete kuenm permite obtener un modelo de distribución potencial para una edad, teniendo en cuenta los datos (yacimientos de ámbar) y las capas de variables ambientales de esa edad correspondiente, y proyectar el modelo sobre otras edades. El evaluador del modelo empleado es el valor AUC [el área bajo la curva ROC (*Receiver Operating Characteristic*)]. Si el modelo es adecuado (valor AUC > 0,8), el modelo debería predecir la presencia de bosques resiníferos (equivalentes a yacimientos de ámbar) para otras edades.

3. Contexto geológico

3.1. La Cuenca del Maestrazgo

La Cuenca del Maestrazgo se corresponde con la parte suroriental de la rama aragonesa de la cordillera ibérica. Tuvo su origen en procesos *rifting* que se desarrollaron desde el Jurásico Superior hasta el Cretácico Inferior (Salas y Guimerà, 1996; Salas *et al.*, 2001, 2019). Durante este periodo, la Cuenca del Maestrazgo correspondía a un golfo en la parte oriental de la paleoisla de Iberia, en el archipiélago europeo, abierto al Tetis (Salas y Guimerà, 1996; Salas *et al.*, 2001). Esta cuenca, considerada como la zona de enlace entre la cordillera ibérica y la cordillera costero-catalana, probablemente estuvo conectada a la Cuenca de Garraf hasta la apertura del Mediterráneo occidental a partir del Oligoceno superior (Salas *et al.*, 2019). La formación de la Cuenca del Maestrazgo se debe al desarrollo de fallas lístricas en relación con la apertura del margen occidental del Tetis, la bahía de Vizcaya y el Atlántico norte (Antolín-Tomás *et al.*, 2007; Tugend *et al.*, 2015; Salas *et al.*, 2019). El final de la fase de *rifting* durante el Albiense fue simultáneo al desarrollo de depocentros en las zonas marginales de la cuenca, que conllevó un incremento en la tasa de sedimentación relacionada con aportes fluviales y depósitos deltaicos ricos en materia orgánica, lo que dio lugar al desarrollo de la Formación Escucha (Salas *et al.*, 2019). La potencia sedimentaria del Jurásico Superior-Cretácico Inferior llega a superar los 2,5 km en algunas zonas de la cuenca (Fig. 13) (Salas y Guimerà, 1996; Bover-Arnal *et al.*, 2016). Durante el Paleógeno, la orogenia alpina, debida a la colisión entre las placas ibérica y europea, causó la inversión de la Cuenca del Maestrazgo (Salas *et al.*, 2001). Nueve subcuencas mesozoicas son reconocidas dentro de la Cuenca del Maestrazgo (Salas *et al.*, 2019): Oliete, Las Parras, Galve, Cedramán, Penyagolosa, Orpesa, Salzedella, Morella y El Perelló.

Los niveles ricos en ámbar de la Cuenca del Maestrazgo se corresponden estratigráficamente con la Formación Escucha y el "Grupo Utrillas" (*sensu* Rodríguez-López *et al.*, 2009). La Formación Escucha, también conocida como Formación Lignitos de Escucha (Pardo, 1974), consiste en una alternancia de lutitas, areniscas y carbón, estos últimos explotables económicamente, sobre calizas y margas de la Plataforma Urgoniana del Aptiense (Cervera *et al.*, 1976; Pardo y Villena, 1979; Querol, 1990; Querol *et al.*, 1992). Esta formación se ha relacionado con un ambiente costero de sistema delta-estuario con registros sedimentarios de pantanos de agua dulce y presencia periódica de agua salobre e influencia mareal bajo un clima subtropical (Querol, 1990; Querol *et al.*, 1992; Peyrot *et al.*, 2007). Los niveles de la Formación Escucha se dataron como Aptiense superior-Albiense inferior a partir del contenido palinológico (Peyrot *et al.*, 2007), pero más tarde la datación de su base se precisó como Albiense inferior mediante bioestratigrafía de amonites e isotopía de estroncio (Bover-Arnal *et al.*, 2016).

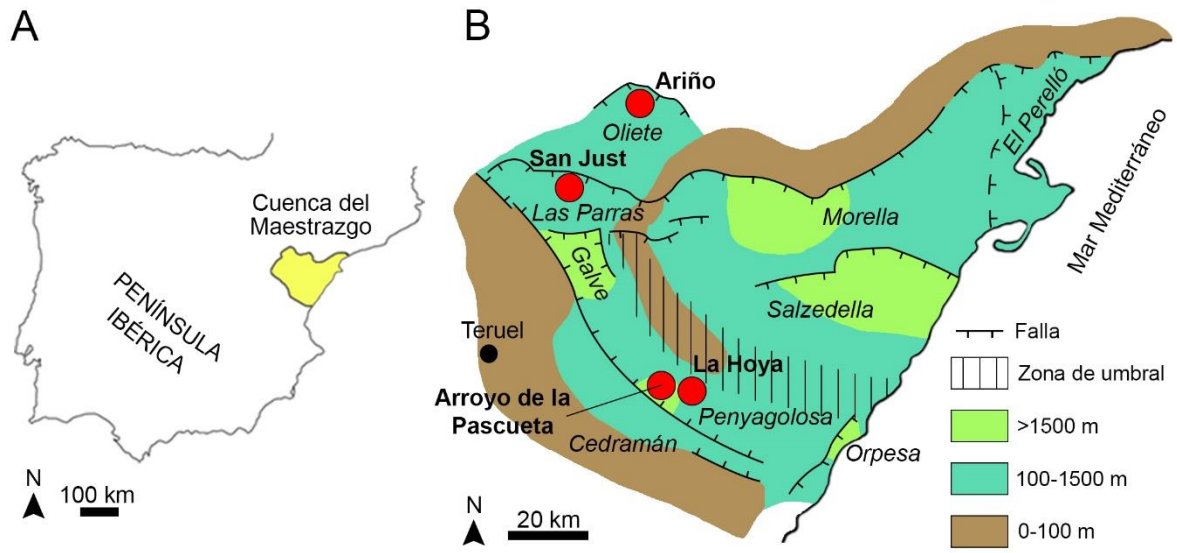

Figura 13. Localización de los yacimientos de ámbar de Ariño, San Just, Arroyo de la Pascueta y La Hoya. A) Localización de la Cuenca del Maestrazgo en la península ibérica; B) Mapa simplificado de la Cuenca del Maestrazgo con los espesores sedimentarios junto con la localización de las nueve subcuencas (en cursiva) y los cuatro yacimientos de ámbar (en negrita). Mapa modificado de Salas *et al.* (2019).

El "Grupo Utrillas", por ahora no formalmente definido, está formado por estratos de areniscas, limolitas y lutitas, y localizado estratigráficamente por encima del miembro medio de la Formación Escucha y por debajo de las unidades carbonáticas del Cretácico Superior (Pardo y Villena, 1979; Salas *et al.*, 2019; Bueno-Cebollada *et al.*, 2022). El "Grupo Utrillas" incluye el miembro superior de la Formación Escucha y la previamente descrita Formación Utrillas (Rodríguez-López *et al.*, 2009; Bueno-Cebollada *et al.*, 2022), también conocida como Formación Arenas de Utrillas (Pardo, 1974). La Formación Utrillas fue interpretada inicialmente como el registro sedimentario de un ambiente fluvial y aluvial (Pardo, 1979; Pardo *et al.*, 1991). Sin embargo, estudios recientes relacionan el "Grupo Utrillas" con un sistema de erg, correspondiente a un desierto de dunas eólicas que se extendió al menos 16.000 km^2, que incluye alternancias de ambientes aluviales *back*-erg y *fore*-erg de interacción marina (Rodríguez-López *et al.*, 2008, 2009, 2010, 2012; Bueno-Cebollada *et al.*, 2022). Para estos autores, los niveles lutíticos ricos en materia orgánica y ámbar corresponderían a registros de bosques resiníferos en lagunas costeras bajo un clima árido (Rodríguez-López *et al.*, 2020, 2021; Barrón *et al.*, enviado). El contenido palinológico ha permitido datar el "Grupo Utrillas" como Albiense medio-Cenomaniense inferior (Bueno-Cebollada *et al.*, 2021).

3.2. Estratigrafía y registro paleontológico de los yacimientos de ámbar estudiados

3.2.1. Yacimiento de Ariño (Albiense inferior)

El yacimiento de Ariño se sitúa en una mina a cielo abierto, la Mina Santa María de Ariño del Grupo SAMCA, que explotaba los depósitos de carbón de la Formación Escucha (Fig. 14A). La Mina Santa María se encuentra al este del municipio de Ariño, en la provincia de Teruel (Aragón). Desde el punto de vista geológico, se sitúa en la Subcuenca de Oliete, en el extremo noroeste de la Cuenca del Maestrazgo y muy cercano a la falla de Oliete (Alcalá *et al.*, 2012; Álvarez-Parra *et al.*, 2021b). La sedimentación en la Subcuenca de Oliete comenzó durante el Barremiense y en ella se registró una alternancia de depósitos continentales, transicionales y marinos hasta el Albiense medio correspondientes a las formaciones Blesa, Alacón, Forcall, Oliete, Escucha y el "Grupo Utrillas" (Meléndez *et al.*, 2000; Aurell *et al.*, 2018; García-Penas *et al.*, 2022). El yacimiento se corresponde con el nivel más rico en fósiles de la mina, que se denomina AR-1 (Fig. 14C), con una superficie reconocida de 600.000 m^2 y ha asignado a la Formación Escucha, y que está compuesto por margas grises y oscuras con alto contenido en materia orgánica que en algunas áreas se encuentra en forma de carbón (Alcalá *et al.*, 2012; Tibert *et al.*, 2013; Villanueva-Amadoz *et al.*, 2015; Vajda *et al.*, 2016; Álvarez-Parra *et al.*, 2021b). El nivel AR-1 se sitúa estratigráficamente por debajo el primer nivel de carbón explotado comercialmente (Fig. 15A) (Alcalá *et al.*, 2012). En el nivel AR-1 se han diferenciado una capa inferior de color grisáceo rica en ámbar de raíz y otra superior de color negro rica en ámbar aéreo; solo la superior contiene también fusinita asignada a la araucariácea *Agathoxylon* sp. (Fig. 15A) (Álvarez-Parra *et al.*, 2021b). La fusinita es un tipo de inertinita que se corresponde con restos carbonizados de plantas en relación con paleoincendios (Scott, 2000). El nivel AR-1 se superpone a un nivel de carbonatos de origen lacustre oligotrófico que muestra el desarrollo de paleosuelos en su parte superior, incluyendo bioturbación por raíces (Álvarez-Parra *et al.*, 2021b). El registro fósil del nivel AR-1 es prolífico e incluye microfósiles y más de 10.000 macrofósiles: carofitas, restos de helechos y coníferas, polen de gimnospermas y angiospermas, invertebrados como bivalvos, gasterópodos y ostrácodos, restos de peces condrictios y osteíctios, acumulaciones de esqueletos articulados o semiarticulados de tortugas, cocodrilos y dinosaurios (ornitópodos y anquilosaurios) y dientes aislados de dinosaurios carnívoros alosauroideos (Alcalá *et al.*, 2012, 2018; McDonald *et al.*, 2012; Buscalioni *et al.*, 2013; Kirkland *et al.*, 2013; Pérez-García *et al.*, 2015, 2020; Villanueva-Amadoz *et al.*, 2015; Álvarez-Parra *et al.*, 2021b), además de icnofósiles como coprolitos (Vajda *et al.*, 2016). Además, el ámbar del yacimiento ha proporcionado numerosas bioinclusiones, principalmente de artrópodos, junto con pelos de mamífero y un fragmento de

pluma de dinosaurio (Álvarez-Parra *et al.*, 2021b). El nivel AR-1 está datado como Albiense inferior a partir del estudio de carofitas, polen y ostrácodos (Tibert *et al.* 2013; Villanueva-Amadoz *et al.*, 2015; Vajda *et al.*, 2016; Álvarez-Parra *et al.*, 2021b).

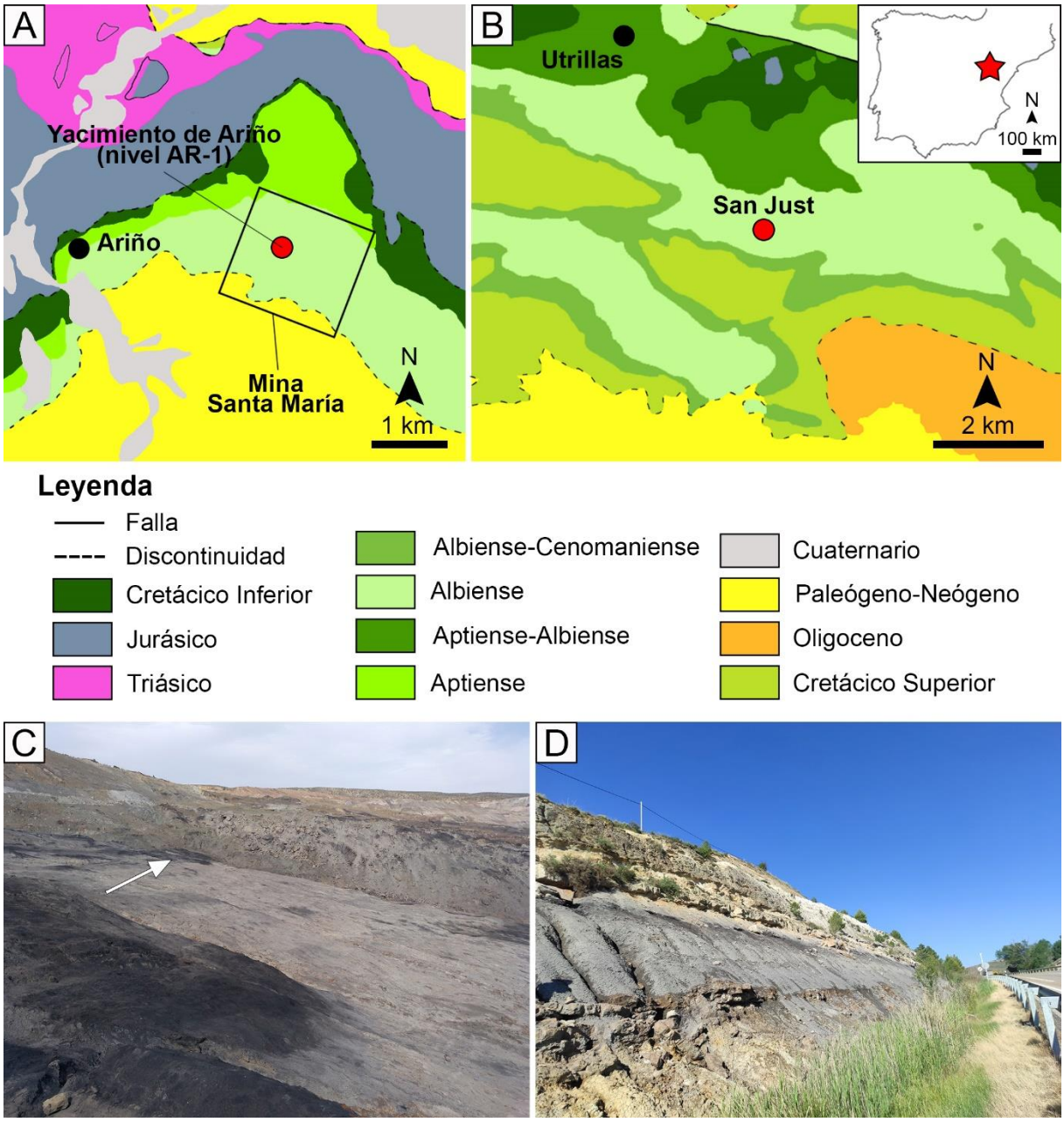

Figura 14. Los yacimientos de ámbar de Ariño y San Just. A) Mapa geológico simplificado con la localización del yacimiento de Ariño, modificado de Alcalá *et al.* (2012) y Álvarez-Parra *et al.* (2021b); B) Mapa geológico simplificado con la localización del yacimiento de ámbar de San Just, modificado de Santer *et al.* (2022); C) Fotografía del nivel AR-1 en la Mina Santa María de Ariño, la flecha indica uno de los lugares donde el ámbar aéreo es abundante; D) Fotografía de la sección de San Just. La estrella roja en la silueta de la península ibérica indica la localización de ambos yacimientos.

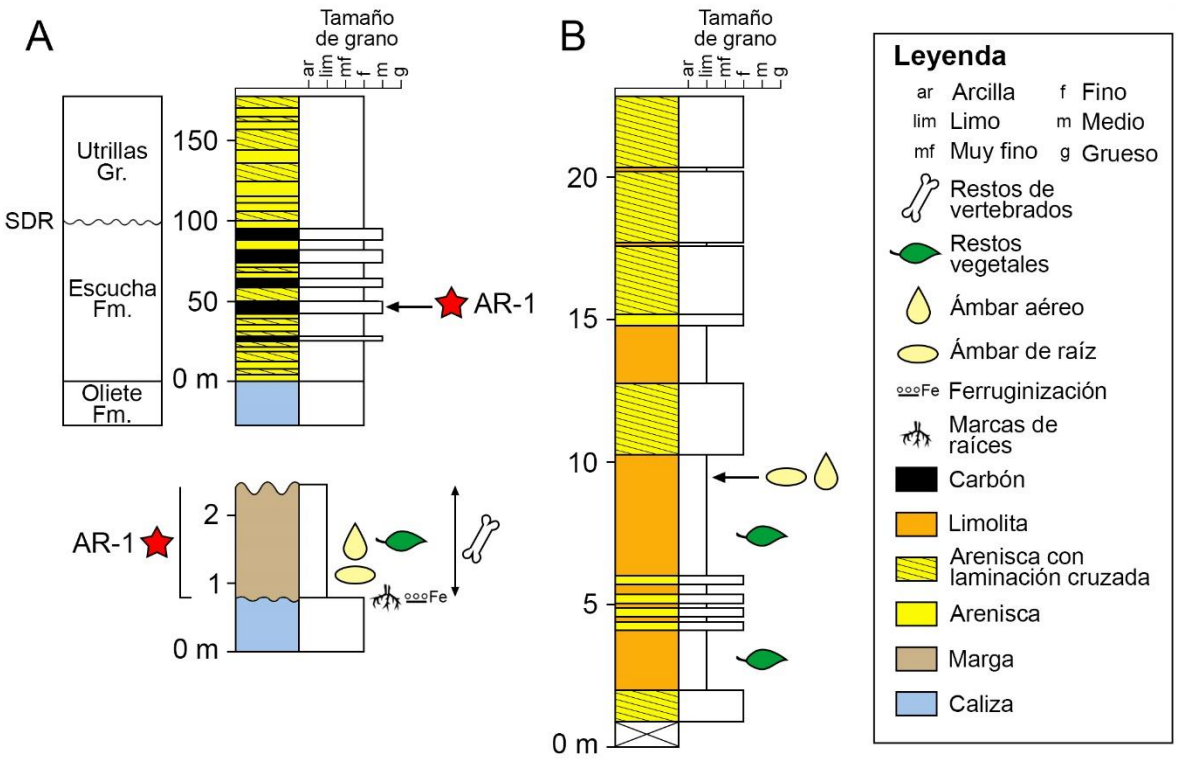

Figura 15. Estratigrafía de los yacimientos de ámbar de Ariño y San Just. A) Columna estratigráfica de la Subcuenca de Oliete (arriba) y columna estratigráfica en detalle del nivel AR-1 (abajo), SDR = Superficie de Discontinuidad Regional, modificado de Kirkland *et al.* (2013) y Álvarez-Parra *et al.* (2021b); B) Columna estratigráfica de la sección donde se encuentra el yacimiento de ámbar de San Just, modificado de Barrón *et al.* (enviado).

3.2.2. Yacimiento de San Just (Albiense superior)

El yacimiento de ámbar de San Just se localiza en la Subcuenca de Aliaga según Salas y Guimerà (1996), considerada como Subcuenca de Las Parras según Salas *et al.* (2019). Se encuadra dentro del término municipal de Utrillas, en la provincia de Teruel, en la ladera norte de la sierra de San Just, de la que el yacimiento toma el nombre (Fig. 14B) (Peñalver *et al.*, 2007). La sección de San Just se asignó previamente al miembro medio de la Formación Escucha (Peñalver *et al.*, 2007; Villanueva-Amadoz *et al.*, 2010), y el estudio del contenido palinológico de angiospermas indicó una edad Albiense medio-superior inferior (Villanueva-Amadoz *et al.*, 2010). El estudio palinológico completo de la sección ha permitido su datación como Albiense superior y el estudio estratigráfico indica que se corresponde con el "Grupo Utrillas" (Barrón *et al.*, enviado). La sección muestra una alternancia de niveles de areniscas de grano fino con laminación cruzada y niveles de limolitas oscuras con alto contenido en materia orgánica originadas por sedimentos depositados en un medio de baja energía (Figs. 14D, 15B) (Barrón *et al.*, enviado). Estructuras relacionadas con deformación por agua, como s*lumps*, se observan en los niveles de areniscas de la parte inferior de la sección del yacimiento

(Barrón *et al.*, enviado). A mitad de sección, en la parte superior de un estrato de limolitas negras, se encuentra un nivel más oscuro y muy rico en ámbar de unos 40 centímetros de potencia, con piezas aéreas y también de raíz. En este estrato también se encuentra fusinita y otros restos de plantas; por ejemplo, la especie de conífera *Frenelopsis justae* Barral, Gomez, Daviero-Gomez, Lécuyer, Mendes & Ewin, 2019 fue descrita a partir de muestras de San Just (Barral *et al.*, 2019). Las piezas de ámbar aéreo suelen ser muy transparentes. Las piezas de ámbar de raíz presentan una corteza originada por el desarrollo de hongos resinícolas durante el Cretácico (Speranza *et al.*, 2015). Se han documentado las icnoespecies *Teredolites clavatus* Leymerie, 1842 y *Apectoichnus longissimus* (Kelly & Bromley, 1984), correspondientes a perforaciones de bivalvos de la familia Pholadidae, en varias piezas de ámbar (Mayoral *et al.*, 2020). El registro de bioinclusiones del ámbar de San Just es muy amplio y contiene hongos, plantas, coprolitos de artrópodos, telarañas, arácnidos, 12 órdenes de insectos y plumas de dinosaurio (Peñalver *et al.*, 2007; Peñalver y Delclòs, 2010).

3.2.3. Yacimiento de Arroyo de la Pascueta (Albiense superior)

El yacimiento de ámbar de Arroyo de la Pascueta se encuentra en la Subcuenca de Penyagolosa, en el área conocida como Mas del Paso dentro del término municipal de Rubielos de Mora, en la provincia de Teruel (Fig. 16A) (Peñalver y Martínez-Delclòs, 2002). Inicialmente, desde un punto de vista estratigráfico, el yacimiento se incluyó en la Formación Escucha y se dató como Albiense inferior-medio a partir de la presencia del foraminífero *Mesorbitolina* gr. *subconcava* Leymerie, 1878 (Gomez *et al.*, 2000). Sin embargo, un nuevo estudio estratigráfico y palinológico ha permitido asignar esta sección al "Grupo Utrillas" y precisar su datación como Albiense superior (Barrón *et al.*, enviado). La sección Arroyo de la Pascueta consiste en una alternancia de areniscas de grano fino, que muestran laminación cruzada, de 10 metros de espesor y niveles oscuros de limolitas y lutitas, además de niveles heterolíticos de arcillitas y areniscas de grano fino (Fig. 17A) (Barrón *et al.*, enviado). El ámbar es abundante en un nivel lutítico oscuro con un alto contenido en materia orgánica, en la parte superior de la sección Arroyo de la Pascueta (Fig. 16B) (Barrón *et al.*, enviado). El registro paleobotánico de la sección se estudió extensamente (Gomez *et al.*, 1999, 2000, 2002a; Daviero *et al.*, 2001; Gomez, 2002), e incluye fusinita, restos fósiles de coníferas de los géneros *Agathoxylon* (Araucariaceae), *Brachyphyllum* (Araucariaceae), *Pagiophyllum* (Araucariaceae), *Frenelopsis* (†Cheirolepidiaceae), *Classostrobus* (†Cheirolepidiaceae) y *Mirovia* (†Miroviaceae), del orden †Bennettitales como *Pseudocycas* y del orden Ginkgoales como *Nehvizdya*. Además, a partir del registro de la sección se describieron las especies *Nehvizdya* (=*Erethmophyllum*) *penalveri* Gomez, 2000, *Frenelopsis turolensis* Gomez, 2002, *Classostrobus turolensis* Gomez, 2002 y *Mirovia gothanii* Gomez, 2002. El ámbar encontrado

en Arroyo de la Pascueta incluye piezas de raíz y piezas aéreas, ambos tipos en el mismo nivel estratigráfico. El ámbar aéreo es de color amarillento y suele ser bastante transparente. El registro de bioinclusiones se corresponde con dos psocópteros, un hemíptero, un blátido, una larva de rafidióptero, cuatro dípteros y cinco himenópteros.

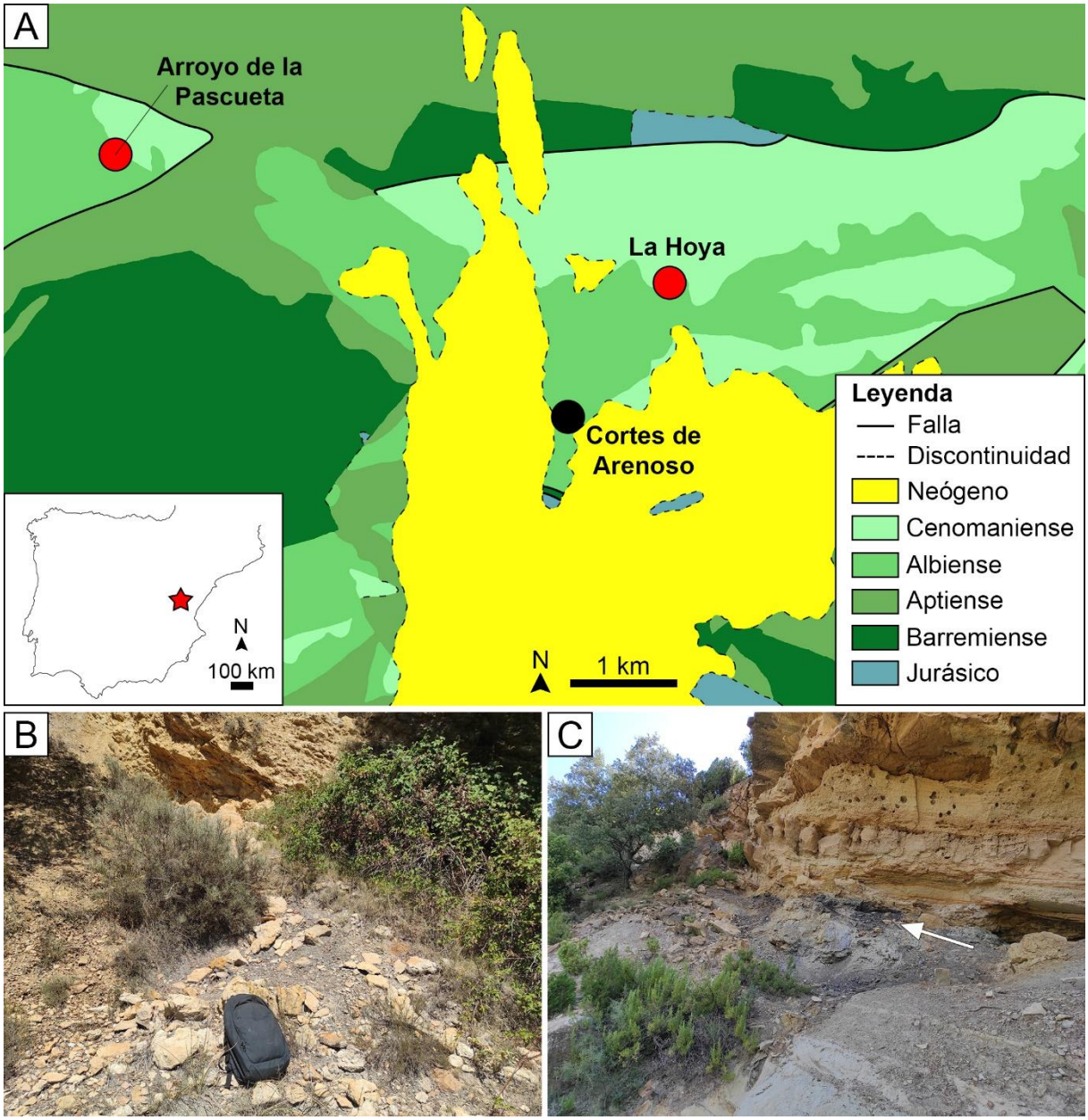

Figura 16. Los yacimientos de ámbar de Arroyo de la Pascueta y La Hoya. A) Mapa geológico simplificado con la localización de los yacimientos de ámbar de Arroyo de la Pascueta y La Hoya, modificado de Solórzano-Kraemer *et al.* (enviado); B) Fotografía del yacimiento de ámbar de Arroyo de la Pascueta, en la actualidad parcialmente cubierto y de difícil acceso; C) Fotografía del yacimiento de ámbar de La Hoya, la flecha indica el nivel rico en ámbar, modificado de Solórzano-Kraemer *et al.* (enviado).

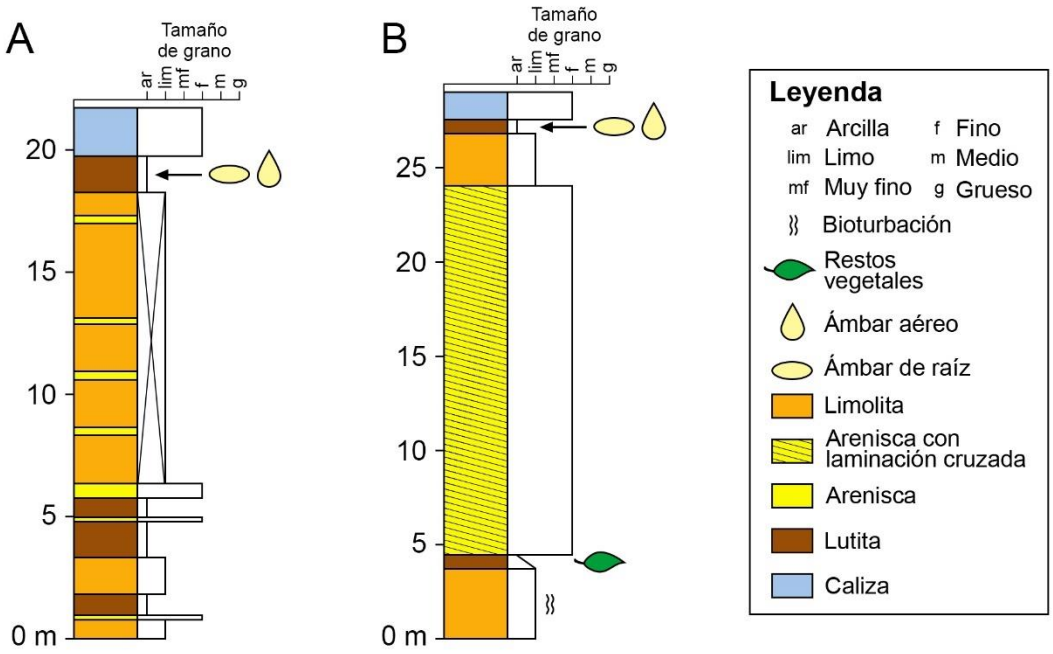

Figura 17. Estratigrafía de los yacimientos de ámbar de Arroyo de la Pascueta y La Hoya. A) Columna estratigráfica de la parte superior de la sección de Arroyo de la Pascueta, donde se encuentra el yacimiento de ámbar, modificado de Barrón *et al.* (enviado); B) Columna estratigráfica de la parte superior de la sección de Cortes de Arenoso, donde se encuentra el yacimiento de ámbar de La Hoya, modificado de Barrón *et al.* (enviado). Para ver las secciones completas, consultar el trabajo de Barrón *et al.* (enviado).

3.2.4. Yacimiento de La Hoya (Cenomaniense inferior)

El yacimiento de ámbar de La Hoya se localiza también en la Subcuenca de Penyagolosa, muy cerca del municipio de Cortes de Arenoso, en la provincia de Castellón (Comunitat Valenciana). El yacimiento de Arroyo de la Pascueta se encuentra a unos pocos kilómetros de distancia del yacimiento de La Hoya (Fig. 16A) (Solórzano-Kraemer *et al.*, enviado). Toma su nombre del barranco de Font de l'Hoya. Estratigráficamente se sitúa en la sección Cortes de Arenoso, incluida en el "Grupo Utrillas" y datada como Albiense superior-Cenomaniense inferior a partir del contenido palinológico (Barrón *et al.*, enviado), aunque inicialmente el yacimiento se asignó a la Formación Escucha y se dató preliminarmente como Albiense inferior-medio (Peñalver y Delclòs, 2010). Esta sección consiste en una alternancia de estratos de areniscas de grano fino, que muestran laminación cruzada, y estratos de lutitas y limolitas de color oscuro (Barrón *et al.*, enviado). El ámbar de La Hoya, tanto de raíz como aéreo, es rico en un nivel de lutitas grises-negras rico en materia orgánica de unos 50 cm de potencia que incluye fusinita, por encima de un nivel de limolitas grises de unos 3 m de potencia (Fig. 16C, Fig. 17B) (Solórzano-Kraemer *et al.*, enviado). Estas lutitas se localizan en la parte más superior de la sección y su contenido palinológico indica una edad Cenomaniense inferior,

debido a la presencia de los palinomorfos *Echinipollis cenomanensis* Pacltová, 1969, *Polypodiisporonites cenomanianus* (Singh, 1983) y *Senectotetradites grossus* Singh, 1983 (Barrón *et al.*, enviado). Por debajo del nivel de limolitas se encuentra un nivel de areniscas con laminación cruzada, mientras que por encima del nivel de lutitas se encuentran calizas. Otros niveles de la sección también son fosilíferos y han proporcionado restos de plantas y algunos huesos de dinosaurio. El ámbar es de color rojizo-amarillento y se fragmenta fácilmente, además, la matriz rocosa es dura, por lo que la extracción de ámbar es complicada. Se corresponde con el único ámbar con bioinclusiones de la Comunitat Valenciana. Sus bioinclusiones son escasas y no muy bien conservadas, y su registro incluye dos blátidos, un himenóptero, tres dípteros y unos pocos restos de insectos indeterminados (Solórzano-Kraemer *et al.*, enviado).

4. Resultados

4.1. Aspectos tafonómicos y bosques resiníferos durante el Cretácico

4.1.1. Tafonomía de los yacimientos de ámbar de la Cuenca del Maestrazgo

4.1.1.1. Características espectroscópicas y geoquímicas de los ámbares

Los análisis de espectroscopía IRTF realizados de los ámbares de Ariño, San Just, Arroyo de la Pascueta y La Hoya muestran prácticamente los mismos espectros, con solo diferencias menores (Fig. 18) (Peñalver *et al.*, 2007; Dal Corso *et al.*, 2013; Álvarez-Parra *et al.*, 2021b; Solórzano-Kraemer *et al.*, enviado). En todos ellos se aprecian bandas a alrededor de 2.950 cm^{-1}, 1.700 cm^{-1} y 1.450 cm^{-1}, características del ámbar (Grimalt *et al.*, 1988).

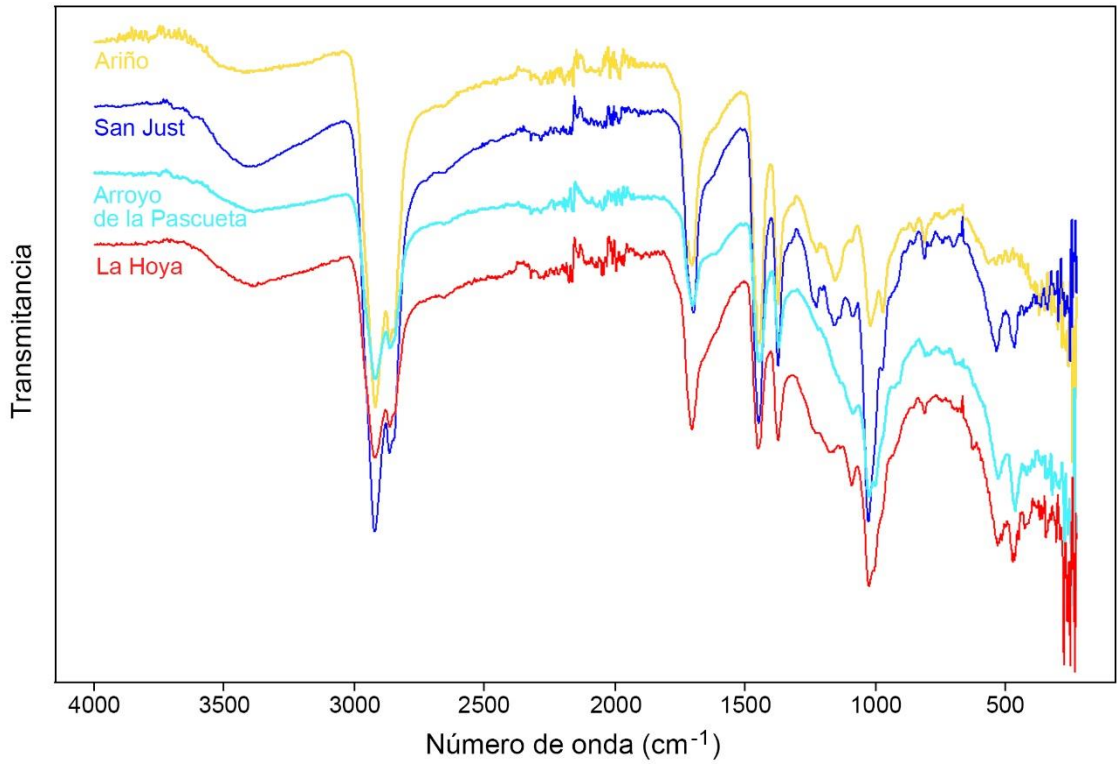

Figura 18. Espectros de infrarrojos (IRTF) de los ámbares de Ariño, San Just, Arroyo de la Pascueta y La Hoya. Resolución = 4 cm^{-1}.

Los análisis geoquímicos GC-MS de los ámbares de la Cuenca del Maestrazgo, realizados por el geoquímico César Menor Salván (Universidad de Alcalá), muestran similitudes importantes y apuntan a que el árbol productor en masa de la resina en la región durante el Albiense y Cenomaniense perteneció a la familia Araucariaceae (Menor-Salván *et al.*, 2016; Álvarez-Parra *et al.*, 2021b). En relación con la clasificación quimiosistemática del ámbar, los ámbares de Ariño y San Just se han asignado al Tipo 1, mientras que el ámbar de La Hoya, al

Tipo 3, siendo ambos tipos de ámbares caracterizados por una elevada concentración de ambareno (Menor-Salván *et al*., 2016; Álvarez-Parra *et al*., 2021b). Hasta el momento no se ha un realizado análisis geoquímico GC-MS del ámbar de Arroyo de la Pascueta. La composición geoquímica del ámbar de Ariño está en estudio por César Menor Salván y, por el momento, cabe destacar la posible presencia de kujigamberol, un compuesto hasta ahora únicamente hallado en el ámbar santoniense de Kuji en Japón (Kimura *et al*., 2012), posiblemente relacionado con el estado de maduración del ámbar y procesos diagenéticos.

4.1.1.2. Captura en resina y conservación de las bioinclusiones

El registro en resina de la entomofauna de los bosques se encuentra sesgado por varios factores, tanto en relación con la propia resina, como su fluidez o viscosidad y tiempo de endurecimiento, como en relación con los organismos, por ejemplo el lugar donde habitan respecto a los árboles resiníferos y su atracción o repulsión a los componentes químicos de la resina (Rasnitsyn y Quicke, 2002; Martínez-Delclòs *et al*., 2004; Solórzano Kraemer *et al*., 2018). Por ello, no todas las resinas atrapan organismos como bioinclusiones y no todos los ámbares fosilíferos son igual de ricos en bioinclusiones. El ámbar de Ariño destaca a nivel mundial por su elevada proporción de bioinclusiones, con unas 145 bioinclusiones por kg de ámbar aéreo. En comparación, el ampliamente conocido ámbar cenomaniense de Myanmar contiene unas 46 bioinclusiones por kg de ámbar (Grimaldi *et al*., 2002). En cuanto a los yacimientos de ámbar de Francia, el ámbar de Archingeay-Les Nouillers proporciona unos 80 artrópodos por kg de ámbar (Néraudeau *et al*., 2002), mientras que el ámbar de Fourtou, unos 17,5 artrópodos por kg de ámbar (Girard *et al*., 2013a). El ámbar con mayor proporción de bioinclusiones es el del yacimiento cenomaniense de Agdzhakend en Azerbaiyán, con alrededor de 560 insectos por kg de ámbar (Rasnitsyn y Quicke, 2002). El ámbar extraído tras la excavación de San Just de 2021 contiene una proporción de 42 bioinclusiones por kg de ámbar aéreo. Una nueva revisión del ámbar sin preparar de Arroyo de la Pascueta ha mostrado una proporción de siete bioinclusiones por kg de ámbar aéreo, mientras que la de ámbar sin preparar de La Hoya no ha proporcionado ninguna bioinclusión en 0,7 kg de ámbar aéreo.

El establecimiento de un criterio común en relación con el conteo de bioinclusiones es esencial para implementar un marco de comparación de riqueza de bioinclusiones entre diferentes ámbares. En primer lugar, se debería evitar el conteo en los casos de identificación compleja como telarañas, coprolitos, tricomas, fibras indeterminadas, restos fúngicos, fragmentos muy parciales de artrópodos y microbioinclusiones. En segundo lugar, es muy importante la separación del ámbar de raíz, sin bioinclusiones, durante el pesado del ámbar aéreo, potencialmente con bioinclusiones. El estudio del potencial de atrapamiento de resinas del pasado, en consideración de la riqueza y proporción de bioinclusiones en relación con la

geoquímica del ámbar, es una línea de investigación prometedora, pero poco desarrollada. El establecimiento de un criterio común de conteo de bioinclusiones es un primer paso, dado que en cada investigación se utiliza un criterio distinto (no separación del ámbar de raíz antes del pesado o conteo únicamente de insectos o artrópodos), y está el hecho de que en muchos estudios sobre yacimientos de ámbar se obvia esta información.

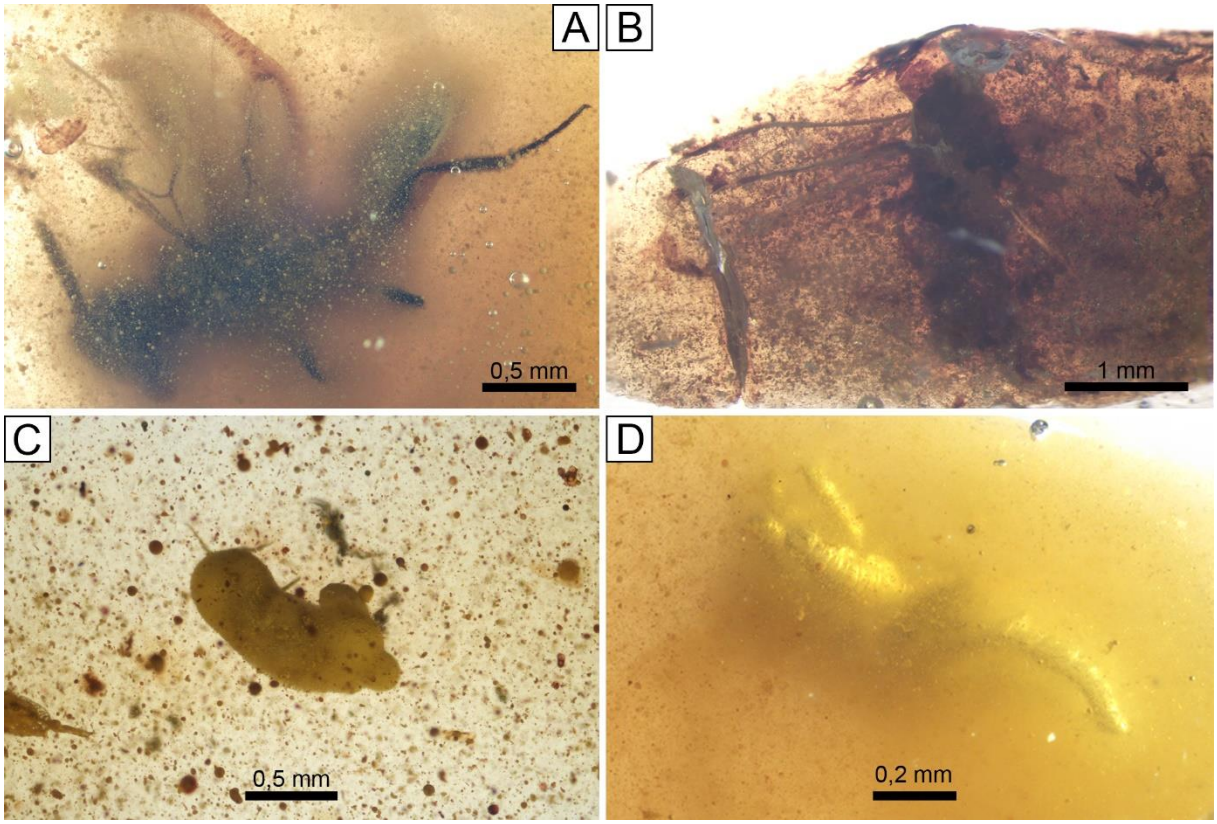

Figura 19. Bioinclusiones en ámbar con características de conservación que dificultan su visualización y estudio. A) Pieza de ámbar turbio del yacimiento de Ariño con una avispa de la familia †Serphitidae (Hymenoptera), AR-1-A-2019.94.5; B) Pieza de ámbar turbio, con muchos fragmentos orgánicos e inorgánicos, del yacimiento de Ariño con una avispa indeterminada, AR-1-A-2019.98.1; C) Un tisanóptero (Thysanoptera) recubierto por diminutas burbujas blanquecinas en ámbar de Ariño, AR-1-A-2019.114.1, imagen tomada de Álvarez-Parra *et al.* (2021b); D) Avispa *Diameneura marveni* Santer & Álvarez-Parra, 2022 de la familia †Spathiopterygidae (Hymenoptera) en ámbar de San Just con las patas recubiertas por burbujas, imagen tomada de Santer *et al.* (2022).

La conservación de bioinclusiones es muy diferente incluso en piezas de ámbar del mismo yacimiento. De forma general, las bioinclusiones en el ámbar de San Just muestran una conservación excepcional en piezas bastante transparentes. Sin embargo, las bioinclusiones del ámbar de Ariño generalmente se encuentran deficientemente conservadas en piezas turbias y con muchos fragmentos orgánicos e inorgánicos que dificultan su visualización (Fig. 19A, B). Además, en el ámbar de Ariño se han hallado algunos casos de insectos cubiertos por diminutas

burbujas blanquecinas (Fig. 19C), de forma similar a muchas bioinclusiones en ámbar Báltico; estas cubiertas han sido interpretadas como la reacción de fluidos emitidos durante el proceso de descomposición de los organismos atrapados con la resina todavía sin polimerizar (Martínez-Delclòs *et al.*, 2004). Curiosamente, un ejemplar de avispa del ámbar de San Just, conservada en una pieza de ámbar turbio, muestra las patas cubiertas por burbujas que se han relacionado con gases emitidos durante la descomposición del insecto (Fig. 19D) (Santer *et al.*, 2022). La turbidez del ámbar, probablemente debida a la presencia de numerosas gotas diminutas de savia elaborada, podría estar asociada a producción de resina bajo condiciones de estrés (McKellar *et al.*, 2011b; Lozano *et al.*, 2020). Las bioinclusiones del ámbar de Arroyo de la Pascueta muestran una conservación similar a las del ámbar de San Just, en cambio, las del ámbar de La Hoya generalmente muestran una deficiente conservación y difícil visualización. Sin embargo, el pequeño número de bioinclusiones de ambos ámbares impide una comparación adecuada. Recientemente, se ha evidenciado la mineralización por calcita, calcedonia y cuarzo de tejidos de insectos en ámbar cenomaniense de Myanmar, debido a la entrada de fluidos tras el enterramiento de la resina (Jiang *et al.*, 2022). Por ahora no se ha realizado una investigación similar sobre las bioinclusiones del ámbar de España, pero es una interesante línea de investigación, ya que es posible que estos procesos fosildiagenéticos se den también en otros ámbares.

4.1.1.3. Bioestratinomía y fosildiagénesis del ámbar

El yacimiento de Ariño es peculiar desde el punto de vista tafonómico, ya que se encuentran restos esqueléticos de dinosaurios en el mismo nivel que el ámbar, cuyas piezas aéreas contienen bioinclusiones (Álvarez-Parra *et al.*, 2021b). Esta coocurrencia es poco común (Cockx *et al.*, 2020). Como se ha comentado anteriormente, en este nivel se observa una capa inferior con piezas de ámbar de raíz y una capa superior con fusinita y piezas de ámbar aéreo con bioinclusiones. Las piezas de ámbar de raíz se encuentran distribuidas por toda la capa y muestran morfologías irregulares (Fig. 20A). Estas piezas generalmente están siempre completas cuando se excavan. Al examinarse mediante MEB, las piezas de ámbar de raíz muestran pequeños salientes y protuberancias en la microestructura de la costra externa y no se encuentra evidencia de surcos lineales (Álvarez-Parra *et al.*, 2021b). Además, estas piezas no muestran la corteza constituida por hongos resinícolas observada en otros ámbares (Speranza *et al.*, 2015). El investigador Rafael P. Lozano (Instituto Geológico y Minero de España-CSIC) ha hallado inclusiones en forma de burbujas monofásicas (sólido), bifásicas (sólido y líquido) y trifásicas (sólido, líquido y gas) (Fig. 21A), junto con cristalizaciones minerales en el interior de piezas de ámbar de raíz. Uno de estos minerales fue identificado preliminarmente como szomolnokita (Fig. 21B) (Álvarez-Parra *et al.*, 2021b). También se han

observado cuboctaedros de pirita (Fig. 21C, D) (Álvarez-Parra *et al.*, 2021b). Se ha confirmado la presencia de otros minerales poco comunes, algunos no descritos todavía como especies minerales, que se podrían relacionar con las características del ambiente en el que se encontraba la resina original, o con la entrada de fluidos externos y/o procesos diagenéticos (Jiang *et al.*, 2022). Estas peculiaridades del ámbar de Ariño están en proceso de estudio dentro de una investigación dirigida por Rafael P. Lozano. El ámbar aéreo presente en la capa superior se encuentra con morfologías de gota, estalactita o colada, usualmente con superficies internas y/o externas de desecación (Álvarez-Parra *et al.*, 2021b). El yacimiento de Ariño se ha interpretado como autóctono-parautóctono, y las piezas de ámbar de raíz se han tipificado como *in situ*, es decir, se encuentran en el lugar donde se produjo la resina original en el suelo del bosque resinífero, caso único en el registro fósil. Una pieza hallada en la capa superior del nivel AR-1 es de color negro y muestra surcos lineales milimétricos y oquedades (AR-1-A-2019.79), por lo que no se puede descartar la presencia de unas pocas muestras alóctonas. La tafonomía del yacimiento de Ariño se presentó en detalle en el trabajo de Álvarez-Parra *et al.* (2021b).

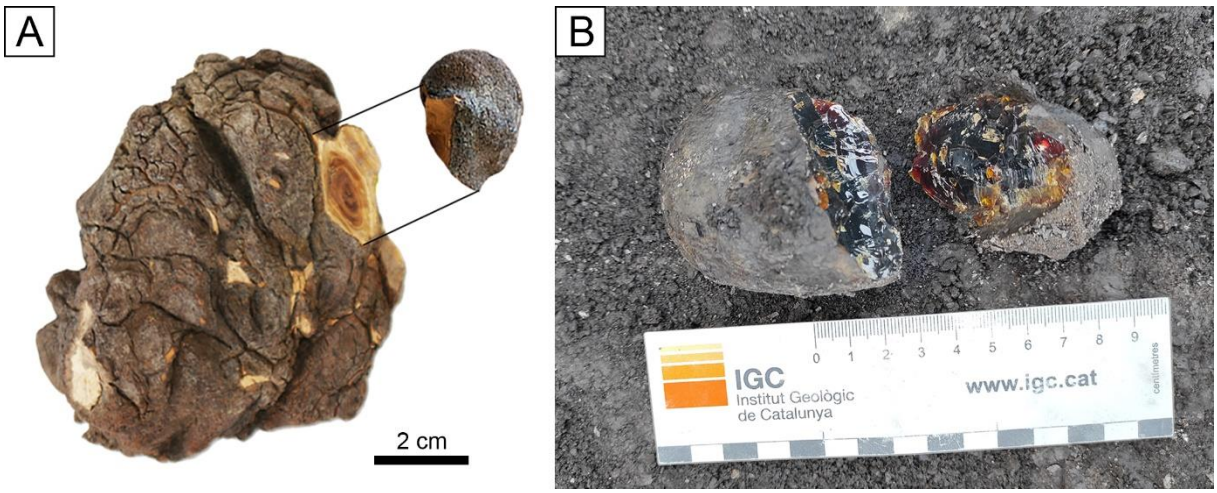

Figura 20. Ejemplos de piezas de ámbar de raíz. A) Pieza hallada en la capa inferior del nivel AR-1 del yacimiento de Ariño con morfología irregular y protuberancias; B) Pieza hallada en el yacimiento de San Just con morfología regular y sin protuberancias.

A diferencia del yacimiento de Ariño, los ámbares de los yacimientos de San Just, Arroyo de la Pascueta y La Hoya se encuentran en capas en las que se hallan en conjunto piezas de raíz, generalmente de morfología regular (Fig. 20B), y piezas aéreas. Por ello, estos yacimientos de ámbar se han interpretado como parautóctonos, con algunos posibles elementos alóctonos, al igual que la mayoría de los yacimientos de ámbar conocidos (Martínez-Delclòs *et al.*, 2004).

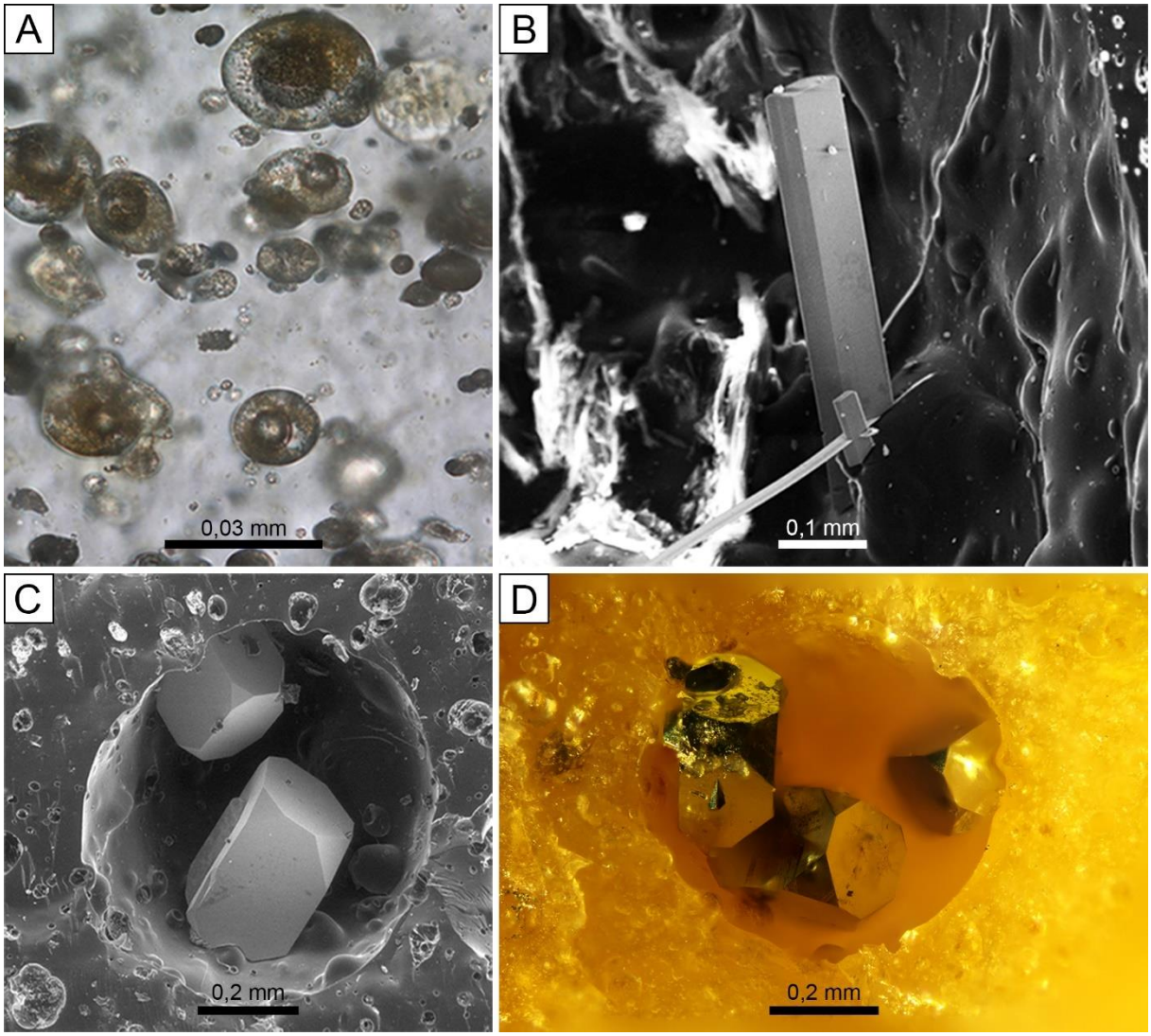

Figura 21. Estructuras halladas en el interior del ámbar de Ariño. A) Inclusiones en forma de burbujas trifásicas en la pieza AR-1-A-2019.130, probablemente relacionadas con secreciones del árbol productor de resina; B) Imagen de microscopio electrónico de barrido de cristales de un sulfato de hierro en la pieza AR-1-A-2019.129, probablemente szomolnokita, creciendo hacia el interior de un espacio hueco del ámbar; C, D) Cuboctaedros de pirita en el interior de un espacio hueco del ámbar (AR-1-A-2019.86), C se corresponde con la imagen del microscopio electrónico de barrido, D se corresponde con una fotografía realizada con un microscopio óptico antes de la preparación de la pieza para el microscopio electrónico de barrido. Imágenes A-C tomadas de Álvarez-Parra *et al*. (2021b).

4.1.2. Nuevos yacimientos de ámbar

Durante el presente proyecto de Tesis Doctoral se han estudiado dos nuevos yacimientos de ámbar de la Cuenca del Maestrazgo: Mina La Dehesa de Estercuel y Son del Puerto, ambos en la provincia de Teruel. El ámbar de estos yacimientos fue hallado por investigadores que lo

notificaron a la DGPC. El objetivo respecto a estos yacimientos es realizar una primera aproximación paleontológica de ambos y valorar su potencial en bioinclusiones.

4.1.2.1. Mina La Dehesa de Estercuel

La Mina La Dehesa es una mina de arcillitas a cielo abierto del Grupo SAMCA localizada al este del municipio de Estercuel (Teruel). Los estudios paleontológicos previos de la Mina La Dehesa han proporcionado un amplio y diverso registro paleobotánico, datado como Albiense superior, de la Unidad "Margas de Transición" entre la Formación Utrillas y la Formación Mosqueruela (Villanueva-Amadoz *et al.*, 2011, 2014; Sender *et al.*, 2012, 2019; Estévez-Gallardo *et al.*, 2019), pero hasta el momento no se había documentado la presencia de ámbar. El hallazgo de ámbar en octubre de 2019 fue notificado por el paleontólogo Cristóbal Rubio (Paleoymás) a la DGPC, y se puso en contacto con Sergio Álvarez Parra en enero de 2020. Como se ha comentado anteriormente, se visitó la Mina La Dehesa en julio de 2021, momento en el que se localizó el nivel con ámbar, se recogieron muestras y se realizó la interpretación estratigráfica preliminar (Fig. 22A-C). El ámbar es relativamente abundante en un nivel de limolitas negras y grisáceas parcialmente cementado, a diferencia de otros yacimientos de la Cuenca del Maestrazgo, como Ariño o San Just, donde la roca matriz que contiene el ámbar está suelta. En este nivel, se encuentran numerosas piezas de ámbar de raíz de morfologías aplanada y redondeada, además de escasas piezas de ámbar de posible origen aéreo con morfología de gota. La matriz rocosa cementada es similar a la del yacimiento de La Hoya, pero en este último el ámbar se fragmenta fácilmente, a diferencia del de la Mina La Dehesa.

En el nivel con ámbar también se han hallado restos carbonizados de plantas en forma de cutículas que corresponden a *Frenelopsis* y *Brachyphyllum*, y se ha observado que carece de fusinita. También se han hallado ostreidos, otros bivalvos y gasterópodos, algunos de ellos a pocos centímetros de piezas de ámbar. Tras el examen del contenido micropaleontológico de la roca del nivel con ámbar se han hallado moluscos de tamaño milimétrico, espículas de erizo y restos de plantas en forma de cutículas. Por ello, es posible que el medio donde se depositó la resina correspondiera a un área transicional con influencia marina, o a una zona marina poco profunda; es decir, se trataría de una acumulación parautóctona o alóctona. Hasta el momento, no se han encontrado bioinclusiones en las escasas piezas de ámbar de posible origen aéreo. Por debajo del nivel con ámbar se encuentran unas calizas rojizas por oxidación con algunas piezas a techo de ámbar de raíz, y bajo estas calizas existe otro nivel de limolitas grisáceas, en cuya base se localiza un nivel de arenisca limosa rojiza con trazas de paleoraíces (rizocreciones). A techo del nivel con ámbar se encuentra un delgado nivel de limolitas blanquecinas, sobre los que se sitúan otros niveles de limolitas grisáceas. Y a techo de todo ello se hallan calizas ocres posiblemente cenomanienses.

Estas observaciones son preliminares y se requiere una nueva visita a la Mina La Dehesa para revisar la interpretación estratigráfica y sedimentológica, recoger más muestras de ámbar y realizar posteriormente un examen en detalle del contenido micropaleontológico del nivel con ámbar.

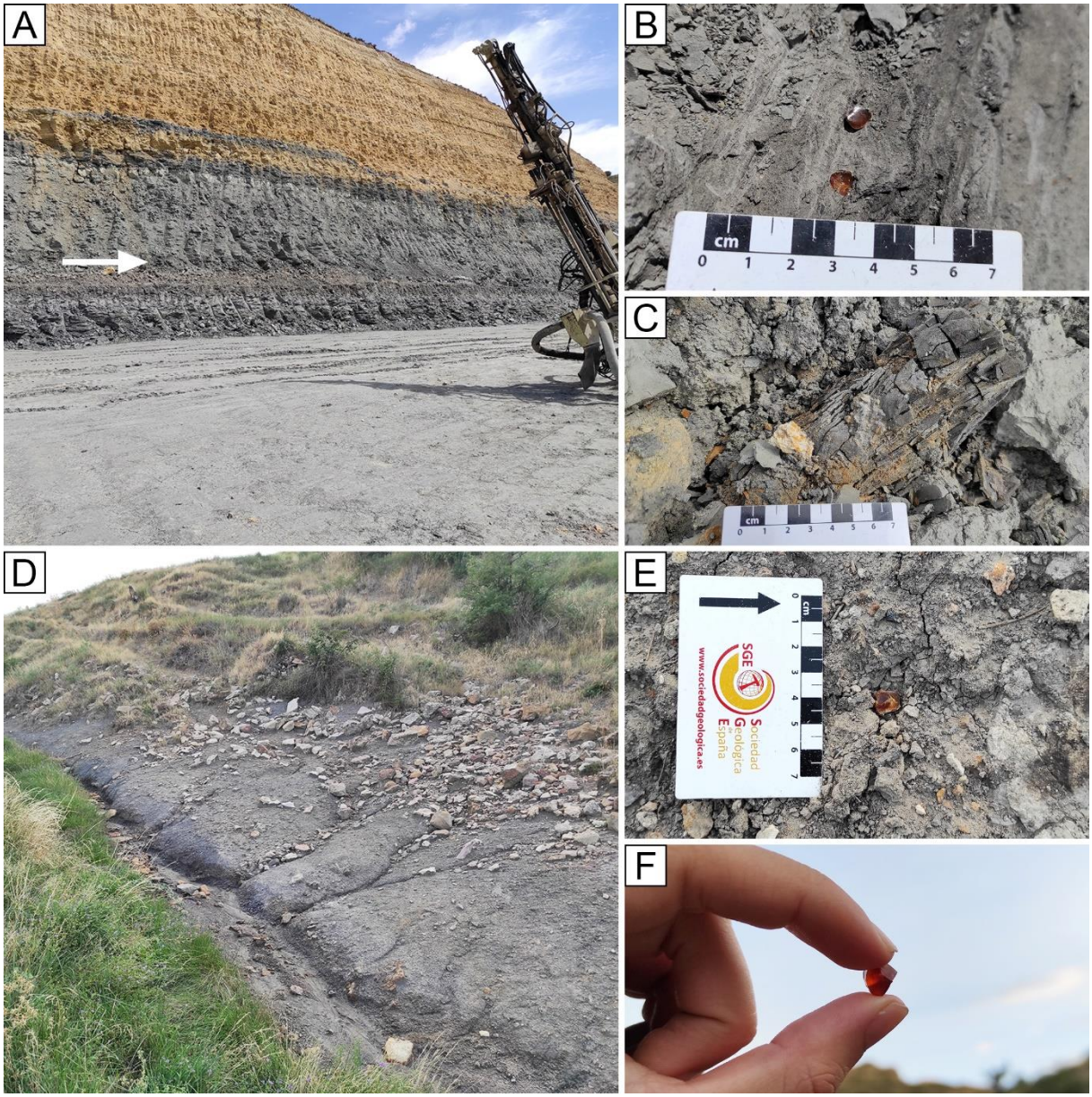

Figura 22. Yacimientos de ámbar de Mina La Dehesa de Estercuel en el año 2021 (A-C) y Son del Puerto en el año 2022 (D-F). A) Sección de la Mina La Dehesa donde se encuentra el nivel con ámbar, indicado con una flecha blanca; B) Pieza de ámbar, posiblemente aéreo, en la matriz rocosa; C) Resto carbonizado de planta; D) Nivel de limolitas negras y grisáceas que se corresponde con el yacimiento de Son del Puerto; E) Pieza de ámbar en la matriz rocosa; F) Pieza de ámbar translúcido sin bioinclusiones.

4.1.2.2. Son del Puerto

El yacimiento de Son del Puerto se encuentra muy cerca de la pedanía del mismo nombre, perteneciente al municipio de Rillo (Teruel). El hallazgo de ámbar fue notificado a la DGPC por el paleontólogo Diego Castanera (Fundación Conjunto Paleontológico de Teruel-Dinópolis) en relación con la instalación de infraestructuras eólicas. La DGPC se puso en contacto con Sergio Álvarez Parra, con relación al yacimiento, en marzo de 2022. Al lado izquierdo de la carretera de salida de Son del Puerto hacia Valdeconejos se localiza un nivel de limolitas negras y grisáceas donde se encuentra ámbar (Fig. 22D-F). Este nivel es de difícil interpretación estratigráfica ya que el afloramiento es muy pequeño y, en algunas zonas, se encuentra cubierto por suelo actual y vegetación y, en otras, por rocas calizas y areniscas, además de fragmentos de cerámica, procedentes de muros situados por encima. Al otro lado de la carretera, el nivel está cubierto por cultivos y es inaccesible. Aparentemente, muestra una potencia de alrededor de un metro y se sitúa a base de rocas del "Grupo Utrillas", por lo que es posible que el nivel con ámbar sea del Albiense superior, similar al cercano yacimiento de San Just. En este nivel la roca no está cementada y, en algunas zonas, parece finamente laminada con color blanquecino. Se observan numerosos cristales y maclas de yeso y restos fósiles carbonizados de plantas, además de algunos moldes internos de bivalvos. Se han encontrado fragmentos de ámbar de raíz, además de algunas piezas posiblemente de ámbar aéreo. Las piezas de ámbar se encuentran parcialmente enterradas, pero al excavar ligeramente no se encontraron más piezas. Este nuevo yacimiento de ámbar es de interés y se requiere un estudio estratigráfico detallado. El fácil acceso al yacimiento implica un peligro desde el punto de vista patrimonial dado el riesgo de expolio.

4.1.3. Distribución de los bosques resiníferos durante el Cretácico

Como se ha comentado anteriormente, durante la Tesis Doctoral se ha llevado a cabo una recopilación bibliográfica de 299 yacimientos de ámbar cretácicos a nivel mundial, con indicación de las coordenadas geográficas y su datación. Recopilaciones similares se han realizado previamente (*e.g.*, Martínez-Delclòs *et al.*, 2004; Seyfullah *et al.*, 2018a), aunque hasta ahora no se había incluido un número tan elevado de yacimientos. Estos datos proporcionan información sobre la distribución de los bosques resiníferos en el pasado. Se ha evidenciado un sesgo de muestreo de yacimientos de ámbar en el Hemisferio Sur, ya que son desproporcionadamente más numerosos en el Hemisferio Norte. Del mismo modo, se conocen muchos yacimientos en las regiones donde existen grupos de investigación especializados en el ámbar, como en el oeste de Canadá, España, Francia o Líbano. Durante el proceso de recopilación de datos, en ocasiones, ha resultado complejo obtener una información concreta

sobre la edad de los yacimientos, ya que pocos se han estudiado desde el punto de vista bioestratigráfico y a menudo únicamente se indica la presencia de ámbar sin profundizar en ello. Además, desafortunadamente, no es habitual indicar las coordenadas o incluir mapas detallados de dónde se encuentran los yacimientos.

Tras la rotación a paleocoordenadas y la visualización en paleomapas, se observa que algunos puntos caen en zonas marinas, normalmente cerca de la costa (Fig. 23). Esto se puede explicar en relación con el medio de depósito de la resina, que suele corresponder con medios transicionales como pantanos costeros o deltas (Martínez-Delclòs *et al.*, 2004), en conjunto con falta de precisión en algunas regiones de los paleomapas. Una vez calculadas las paleocoordenadas, el objeto de estudio y los datos no se corresponden con "yacimientos de ámbar", sino con "bosques resiníferos", o más bien, "áreas de producción en masa de resina". Al tener en cuenta esta información, se puede apreciar que los bosques resiníferos durante el Cretácico se encontraban en zonas costeras, principalmente del Hemisferio Norte, aunque esto podría estar relacionado con los sesgos comentados anteriormente. Los bosques resiníferos son relativamente escasos antes del Albiense, a excepción del área norte de Gondwana durante el Barremiense que hoy se corresponde con el Líbano. Durante el Albiense, Cenomaniense y Turoniense, estos bosques se podían encontrar en latitudes altas, sin embargo, la mayor parte de ellos ocupaba zonas entre las latitudes 20º y 40º (Fig. 23). Curiosamente, el registro de bosques resiníferos del Coniaciense está únicamente representado en la actualidad por dos yacimientos de ámbar, lo que resalta con las cifras del resto de edades del Cretácico Superior y podría evidenciar un hueco en el registro, quizás relacionado con cambios ambientales. Durante el Santoniense, Campaniense y Maastrichtiense, los bosques resiníferos estaban presentes principalmente entre las latitudes 40º a 60º (Fig. 23).

La aplicación del ENM se ha empleado para modelar la distribución de bosques resiníferos o áreas de producción en masa de resina durante las edades del Cretácico y es la primera vez que se usa esta metodología en investigación sobre el ámbar. Se han obtenido los primeros resultados; sin embargo, no son los esperados, ya que la distribución potencial mostrada no se corresponde con todos o la mayoría de los puntos de presencia de bosques resiníferos (Fig. 24). Es decir, existen puntos de presencia en zonas donde el modelo indica que la probabilidad de que haya bosques resiníferos es muy baja, y por lo tanto el modelo no es capaz de predecir la presencia de bosques resiníferos. Sucede de igual modo al proyectar un modelo obtenido para una edad sobre un paleomapa de otra edad. Cabe destacar que estos resultados se han obtenido de modelos con un valor AUC > 0,8, y por ello deberían de ser precisos.

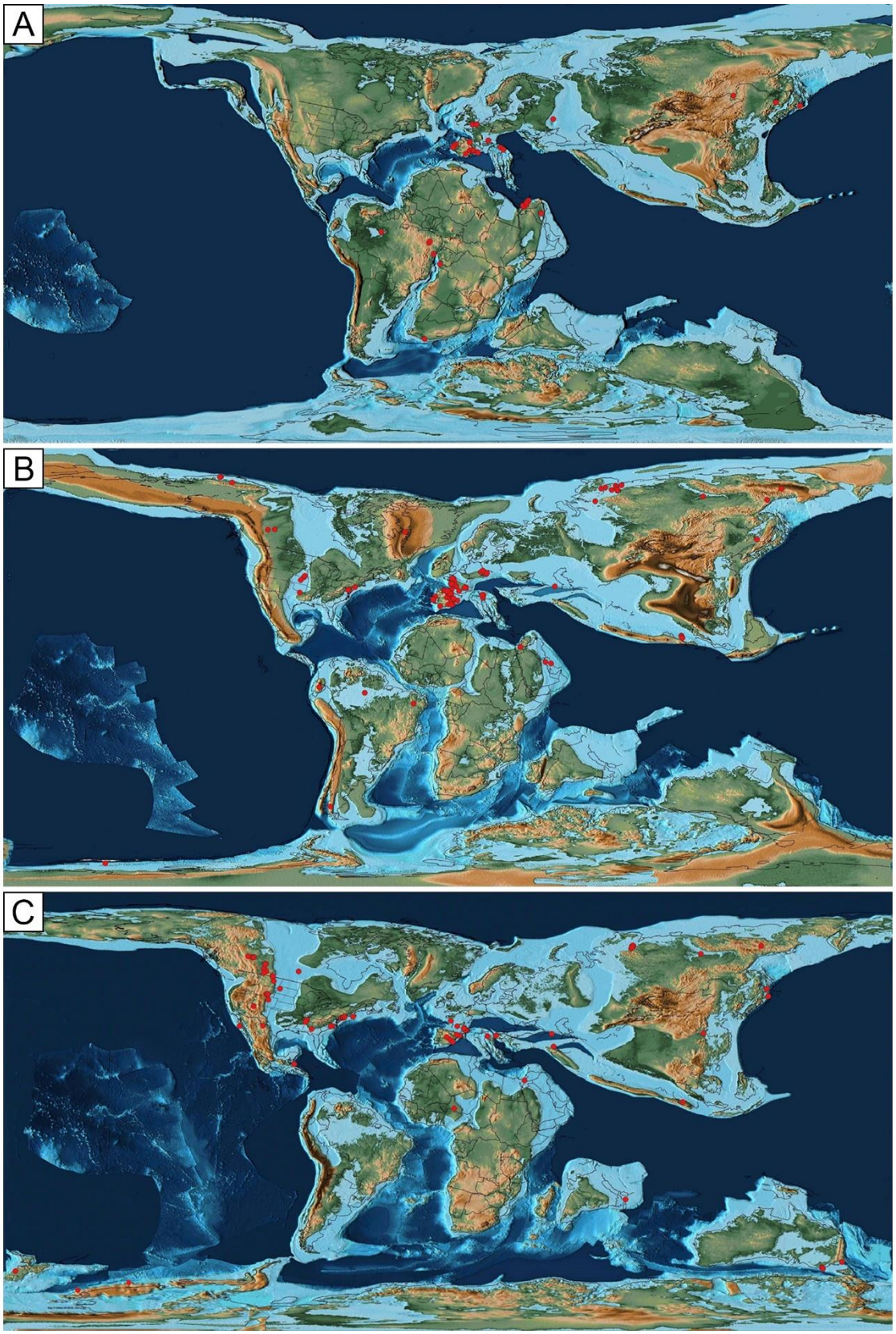

Figura 23. Paleomapas del Cretácico con la distribución de bosques resiníferos (círculos rojos) en cada intervalo temporal. A) Cretácico Inferior, Berriasiense-Aptiense; B) Mitad del Cretácico, Albiense-Cenomaniense; C) Cretácico Superior, Turoniense-Maastrichtiense. Paleomapas obtenidos de Scotese (2001).

Una de las causas potenciales que podría explicar estos resultados poco prometedores es el sesgo de muestreo e investigación de yacimientos de ámbar comentado anteriormente. Además, es importante tener en cuenta la tafonomía del ámbar, ya que la mayoría de los yacimientos son parautóctonos o alóctonos, dado que la resina se suele depositar finalmente en un medio de transición (Martínez-Delclòs *et al.*, 2004). Por este motivo es posible que las paleocoordenadas obtenidas no se correspondan con precisión al lugar donde se encontraba el bosque resinífero. En este proceso se ha considerado la presencia de yacimientos de ámbar sin tener en cuenta la planta productora, y es probable que cada grupo taxonómico de árboles resiníferos produjera resina en masa bajo diferentes condiciones ambientales en el caso de que varios grupos estuvieran implicados. Desafortunadamente, no se han realizado estudios tafonómicos de muchos yacimientos de ámbar, al igual que tampoco se conoce la planta productora de resina de muchos ámbares. A pesar de que se han recopilado 299 yacimientos de ámbar, el número de yacimientos para cada edad no es muy elevado. Las edades del Cretácico con mayor número de yacimientos de ámbar son Barremiense, Albiense y Cenomaniense. Con relación a ello, los modelos de distribución obtenidos a partir de los datos de ambas edades son los que tienen un valor AUC más alto. Aun así, el número de datos en estas edades no es suficiente para generar un modelo adecuado y así predecir la distribución de los bosques resiníferos.

La recopilación bibliográfica fue exhaustiva y se indicaron todas las posibles presencias de ámbar a lo largo del Cretácico. Por ello, el problema con relación al bajo número de datos por edad no se puede solucionar por ahora. Sin embargo, a pesar de que los primeros resultados no sean prometedores, el proyecto puede continuar. El siguiente paso de este estudio es repetir el proceso modificando los parámetros seleccionados inicialmente, por ejemplo usar 10% de datos de prueba y 90% de entrenamiento (en vez de 25% y 75%, respectivamente). También es posible cambiar el enfoque del proyecto y realizar un análisis estadístico multivariante de coocurrencia a partir del número de yacimientos de ámbar para cada edad y los valores cuantitativos correspondientes, como son el intervalo temporal, concentración de CO_2 y O_2 atmosférico, luminosidad solar, temperatura global media y precipitación global media. Mediante este enfoque, se podría obtener un algoritmo que explique el número de yacimientos de ámbar para cada edad. Hasta el momento, no se había realizado una investigación sobre la distribución de bosques resiníferos del pasado en función de las variables ambientales mediante técnicas informáticas o estadísticas como las aquí descritas. Por ello, esta es una aproximación que podría proporcionar información clave para conocer los condicionantes de producción en masa de resina en el pasado.

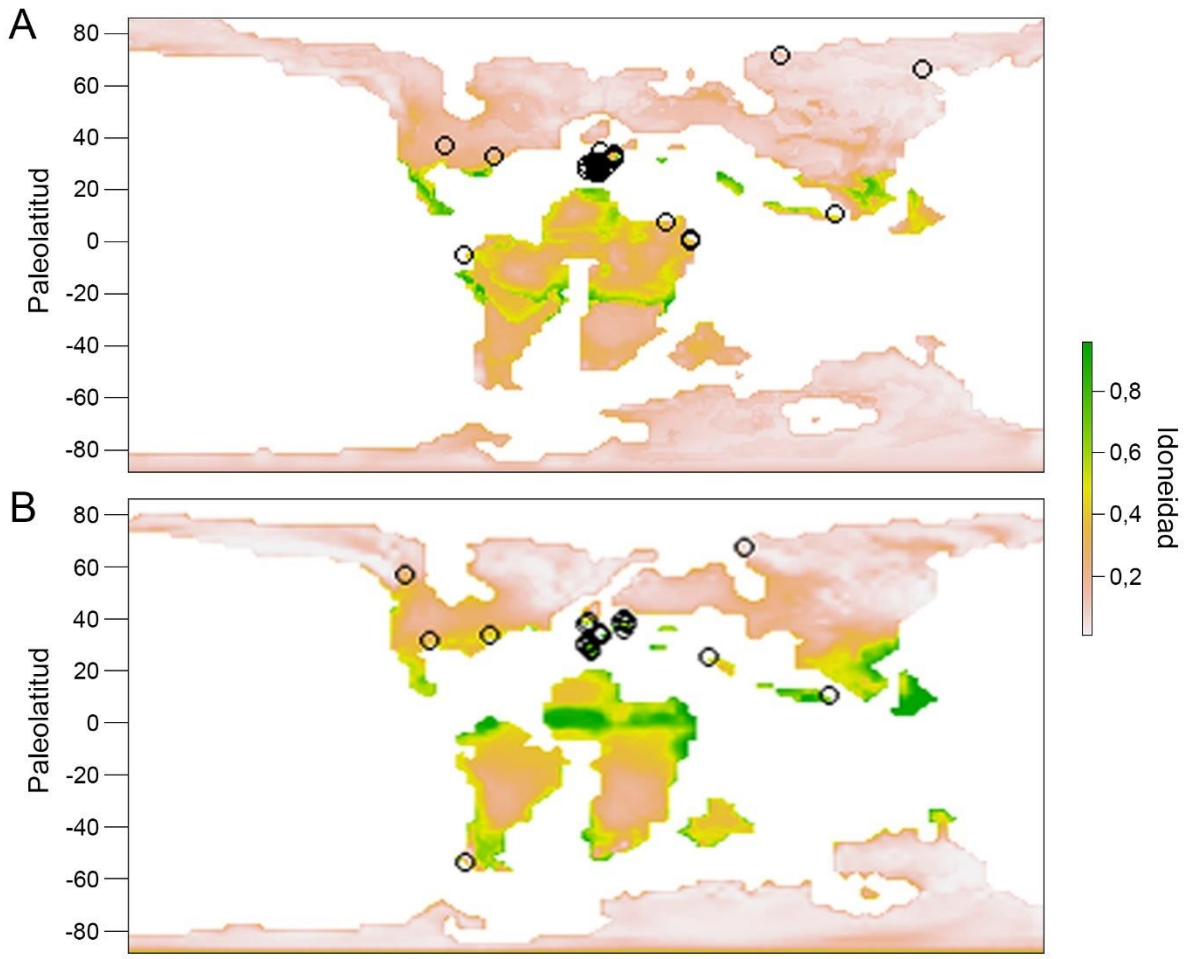

Figura 24. Resultados preliminares de la aplicación del modelado de nicho ecológico (ENM) sobre la distribución potencial de bosques resiníferos durante el Cretácico. A) Modelo obtenido a partir de los puntos de presencia y variables ambientales del Albiense y proyectado en un paleomapa de esa misma edad, valor AUC = 0,873, desviación estándar = 0,030; B) Modelo obtenido a partir de los puntos de presencia y variables ambientales del Cenomaniense y proyectado en un paleomapa de esa misma edad, valor AUC = 0,861, desviación estándar = 0,040. Los círculos se corresponden con los puntos de presencia de bosques resiníferos del Albiense y el Cenomaniense inferidos a partir de la localización de los yacimientos de ámbar. Nótese que, a pesar del elevado valor AUC en ambos modelos, se pueden observar puntos de presencia de bosques resiníferos donde los modelos indican que el ambiente es poco idóneo.

4.2. Bioinclusiones de los ámbares de la Cuenca del Maestrazgo: taxonomía y sistemática

4.2.1. Criterios y problemáticas

El estudio taxonómico y sistemático de las bioinclusiones halladas en ámbar es clave para conocer la diversidad y las relaciones ecológicas en los bosques resiníferos del pasado. Los yacimientos de ámbar de Ariño, San Just, Arroyo de la Pascueta y La Hoya proporcionan un registro a lo largo de un rango temporal desde el Albiense inferior hasta el Cenomaniense inferior en la Cuenca del Maestrazgo, por lo que el estudio comparativo de sus bioinclusiones ayuda a conocer la evolución de la paleodiversidad en esta región. Los yacimientos de ámbar con bioinclusiones del Cretácico Inferior no son numerosos, y Ariño y San Just se encuentran entre los más importantes de esta época a nivel mundial dada su riqueza y diversidad.

Los taxones y las relaciones filogenéticas que se establecen para los artrópodos son relativamente inestables, tanto a nivel orden y familia como a nivel de género y especie, lo que conlleva algunas problemáticas. Los estudios filogenéticos continuamente proporcionan nueva información sobre las relaciones filogenéticas a nivel de orden y por ello muchos taxones cambian de rango o resultan ser parafiléticos o polifiléticos, y por lo tanto inválidos en sistemática cladista (Giribet y Edgecombe, 2012; Misof *et al.*, 2014; Tihelka *et al.*, 2021). En ocasiones, los análisis filogenéticos morfológicos y moleculares dan lugar a resultados contradictorios (Johnson *et al.*, 2018). Por ejemplo, tradicionalmente se consideraban los órdenes de insectos 'Psocoptera' y 'Blattaria', sin embargo, ambos han resultado ser parafiléticos (Misof *et al.*, 2014). 'Psocoptera' se ha fusionado con Phthiraptera para formar el orden Psocodea (de Moya *et al.*, 2021), mientras que 'Blattaria' se ha unido con Isoptera para dar lugar al orden Blattodea (Inward *et al.*, 2007). En cambio, aunque de forma similar, Mecoptera *sensu stricto* se ha considerado parafilético y se ha propuesto fusionarlo con Siphonaptera, pero manteniendo el nombre Mecoptera para el clado que los agrupa (Tihelka *et al.*, 2020). Existe controversia en cuanto al rango taxonómico adecuado para algunos grupos, como los arácnidos Acariformes y los hexápodos Collembola y †Lophioneurida. En algunos órdenes de insectos, como Hymenoptera, la sistemática interna es reorganizada con frecuencia y, por ejemplo, algunos géneros se transfieren a otras familias o se sinonimizan taxones (*e.g.*, Rasnitsyn y Öhm-Kühnle, 2020).

En este apartado se muestra un resumen taxonómico y sistemático de las bioinclusiones halladas en los ámbares de la Cuenca del Maestrazgo. Se ha seguido la disposición de Grimaldi y Engel (2005) para exponer los órdenes de insectos y se han tenido en cuenta las relaciones filogenéticas mostradas en el trabajo de Tihelka *et al.* (2021). Las arañas (Araneae), pseudoescorpiones (Pseudoscorpiones) y ácaros (Acari) son arácnidos, que se incluyen en

Chelicerata. Los Hexapoda históricamente se han dividido en 'Entognatha' (Collembola, Protura y Diplura) e Insecta, en función de la presencia de piezas bucales entognatas o ectognatas, respectivamente. Los órdenes de insectos Archaeognatha y Thysanura se consideran en el grupo 'Apterygota', debido a la ausencia primitiva de alas, y el resto de los insectos forman el clado Pterygota, que poseen alas o las han perdido de forma secundaria. Los representantes de los órdenes Ephemeroptera y Odonata se han agrupado tradicionalmente en Palaeoptera, junto con otros grupos de insectos paleozoicos, dado que carecen de la habilidad para plegar las alas sobre el abdomen, aunque podría ser una agrupación parafilética. El resto de los insectos alados, Neoptera, se dividen en Polyneoptera, Acercaria y Holometabola. Desde el punto de vista del modo de desarrollo y crecimiento de los hexápodos (Grimaldi y Engel, 2005), se considera que Entognatha, Archaeognatha y Thysanura son ametábolos, ya que no sufren metamorfosis, es decir, los ejemplares inmaduros crecen en tamaño gradualmente hasta la forma adulta sin un notable cambio morfológico. Los insectos Polyneoptera y Acercaria son hemimetábolos, dado que experimentan una metamorfosis incompleta caracterizada por la fase de ninfa con morfología general similar al adulto, en la que el ejemplar no posee alas ni órganos sexuales funcionales y sufre varias mudas hasta la fase de imago (adulto). Finalmente, los Holometabola desarrollan una metamorfosis completa en la que la larva muestra una morfología diferente a la del adulto y existe una fase de pupa entre la larva y el imago.

A la hora de organizar este apartado, se ha optado por indicar los órdenes de insectos presentes en los ámbares de la Cuenca del Maestrazgo, además de otros grupos de artrópodos, plantas, hongos, icnofósiles y vertebrados. En taxonomía ocasionalmente se prefiere usar nomenclatura abierta (Bengtson, 1988), y así se ha empleado aquí con la especie *Jantardachus* cf. *reductus* Vishniakova, 1981 (†Lophioneurida). En cada sección de este apartado se han comentado las bioinclusiones por yacimiento siguiendo el orden de mayor a menor número de bioinclusiones totales (San Just, Ariño, Arroyo de la Pascueta y La Hoya). También, se incluye una introducción biológica y sistemática de cada grupo taxonómico, además de una comparación con el registro de otros yacimientos de ámbar de España. En caso de que el registro en otros ámbares de España sea escaso, se ha indicado la presencia del grupo taxonómico en yacimientos de compresión. La identificación y determinación de las bioinclusiones se ha realizado en colaboración con mis directores y otros especialistas del grupo AMBERIA.

		Ariño		San Just		Arroyo de la Pascueta		La Hoya	
Arachnida	Araneae	1	1,03%	17	4,71%	-	-	-	-
	Pseudoscorpiones	-	-	1	0,28%	-	-	-	-
	Acari	5	5,15%	19	5,26%	-	-	-	-
Insecta	Archaeognatha	1	1,03%	1	0,28%	-	-	-	-
	Orthoptera	2	2,06%	1	0,28%	-	-	-	-
	Blattodea	1	1,03%	21	5,82%	1	7,14%	2	33,33%
	†Umenocoleidae	1	1,03%	-	-	-	-	-	-
	Mantodea	-	-	1	0,28%	-	-	-	-
	Psocodea	7	7,22%	9	2,49%	2	14,29%	-	-
	†Lophioneurida	-	-	1	0,28%	-	-	-	-
	Thysanoptera	11	11,35%	13	3,60%	-	-	-	-
	Hemiptera	6	6,19%	30	8,31%	1	7,14%	-	-
	Raphidioptera	-	-	-	-	1	7,14%	-	-
	Neuroptera	3	3,09%	8	2,21%	-	-	-	-
	Coleoptera	5	5,15%	23	6,37%	-	-	-	-
	Hymenoptera	34	35,05%	111	30,75%	5	35,71%	1	16,67%
	Diptera	19	19,59%	105	29,08%	4	28,58%	3	50%
	Lepidoptera	1	1,03%	-	-	-	-	-	-
	Total	**96**	100%	**361**	100%	**14**	100%	**6**	100%

Tabla 1. Artrópodos en los ámbares de la Cuenca del Maestrazgo. En la columna de la izquierda de cada ámbar se indica el número de ejemplares por taxón, mientras que en la columna de la derecha se indica la abundancia relativa. En los conteos no se han considerado los ejemplares con una identificación dudosa, por lo que los valores indicados en "Total" no se corresponden con el total de bioinclusiones en cada ámbar. Las representaciones gráficas de las abundancias relativas se encuentran en la Fig. 25. Para comprobar el registro completo de bioinclusiones, ver el Anexo 8.2.

Durante la Tesis Doctoral se han estudiado diferentes grupos taxonómicos, aunque se ha profundizado en mayor medida en los órdenes Psocodea e Hymenoptera, entre estos últimos principalmente los miembros de 'Parasitica' y algunos ejemplares de familias parasitoides de Aculeata. El estudio de estos dos órdenes de insectos en el ámbar de España se inició hace años, aunque centrado sobre todo en el registro del ámbar de Peñacerrada I. Por ello, se ha decidido continuar su estudio, pero enfocado en el registro de los ámbares de la Cuenca del Maestrazgo. En el caso de Psocodea, también se han estudiado ejemplares en ámbares eocenos con interés comparativo. Aparte de estos dos órdenes, también cabe destacar la investigación, en menor medida, sobre otros grupos de artrópodos en los ámbares de la Cuenca del Maestrazgo, como Acari y Diptera.

4.2.2. Paleobiodiversidad

El ámbar con mayor número de bioinclusiones de la Cuenca del Maestrazgo es el del yacimiento San Just, seguido por los de los yacimientos de Ariño, Arroyo de la Pascueta y La Hoya. Por el momento, se han descrito dos especies de artrópodos a partir de bioinclusiones

del ámbar de Ariño (Anexo 8.2). El yacimiento de ámbar de San Just es la localidad tipo de 26 especies de artrópodos, mientras que el yacimiento de ámbar de Arroyo de la Pascueta es la localidad tipo de una especie de avispas (Anexo 8.2). Los órdenes de artrópodos con un mayor número de ejemplares en los ámbares de Ariño, San Just y Arroyo de la Pascueta son Hymenoptera y Diptera (Tabla 1; Fig. 25). Las abundancias relativas de artrópodos en los ámbares de San Just y Ariño muestran valores similares, aunque cabe destacar la abundancia relativa de ácaros, blattodeos, hemípteros y coleópteros en el ámbar de San Just, y de tisanópteros en el ámbar de Ariño (Tabla 1; Fig. 25). El pequeño número de bioinclusiones de los ámbares de Arroyo de la Pascueta y La Hoya dificulta la comparación taxonómica con otros ámbares.

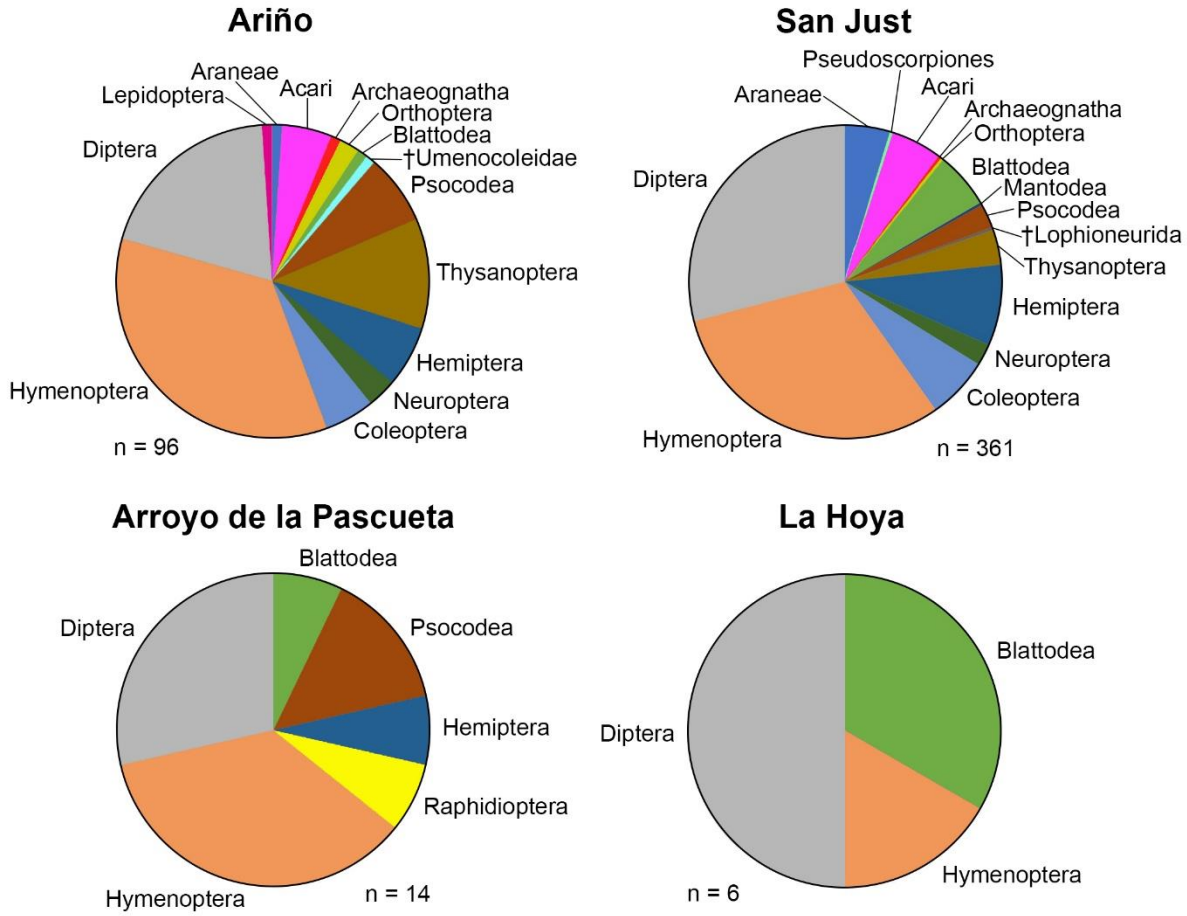

Figura 25. Artrópodos en los ámbares de la Cuenca del Maestrazgo. Abundancia relativa por taxón en cada uno de los ámbares. Los datos numéricos se encuentran en la Tabla 1.

4.2.3. Restos de plantas y hongos

La presencia de restos de plantas como bioinclusiones en ámbar es habitual (*e.g.*, Sadowski *et al.*, 2014; Li *et al.*, 2022a). En relación con el ámbar de España, se han hallado restos de plantas en Peñacerrada I y El Soplao (Delclòs *et al.*, 2007; Kvaček *et al.*, 2018), en este último cabe destacar dos restos foliares (Pérez de la Fuente, 2012). Al menos 10 restos indeterminados se han identificado en el ámbar de San Just. Un peculiar resto de planta fue hallado en el ámbar de Ariño (Fig. 26A) (Álvarez-Parra *et al.*, 2021b). En el yacimiento de Ariño se hallaron restos de tejidos de plantas rellenos de ámbar que podrían corresponder con súber (Álvarez-Parra *et al.*, 2021b). En la mayoría de los ámbares de España se observan bioinclusiones de tricomas y fibras, y también están presentes en San Just y Ariño. Los tricomas de San Just tienen entre dos y seis expansiones, mientras que los de Ariño presentan tres o cuatro (Fig. 26B). Estos tricomas son de difícil adscripción taxonómica y podrían proceder de helechos o coníferas (Peñalver *et al.*, 2007). Entre las bioinclusiones de plantas también se incluyen fibras indeterminadas y granos de polen (Peñalver *et al.*, 2007).

Restos filamentosos en ámbar podrían corresponder a hifas fúngicas, como se han documentado en diferentes ámbares del mundo y de España (Delclòs *et al.*, 2007; Peñalver *et al.*, 2007; Halbwachs, 2019). Se han identificado estructuras fúngicas como bioinclusiones en los ámbares de San Just, Arroyo de la Pascueta y La Hoya (Speranza *et al.*, 2010; Delclòs *et al.*, 2010). Además, se ha documentado que las piezas de ámbar de raíz de San Just, Arroyo de la Pascueta y La Hoya, a diferencia de las de Ariño, poseen una corteza debida al desarrollo de hongos resinícolas originada cuando la resina aún no se había endurecido completamente (Peñalver *et al.*, 2007; Speranza *et al.*, 2015).

4.2.4. Icnofósiles

El ámbar, en ocasiones, también puede conservar restos de actividad de los organismos del pasado, es decir, icnofósiles. En el ámbar de la Cuenca del Maestrazgo se han hallado icnofósiles representados por coprolitos y telarañas. Los coprolitos son una fuente clave de información paleoecológica, ya que su estudio permite inferir redes tróficas del pasado (Richter y Baszio, 2001). Sin embargo, se ha profundizado poco en la investigación sobre coprolitos, y su composición, en ámbar. Se han documentado coprolitos de artrópodos en ámbar cuya morfología y composición han permitido inferir fungivoría (Schmidt *et al.*, 2010), alimentación basada en líquenes (Schmidt *et al.*, 2022) y polinivoría (Hinkelman y Vršanská, 2020). También se han encontrado coprolitos de termitas en niveles estratigráficos con ámbar (Colin *et al.*, 2011). En el ámbar de San Just se han hallado siete piezas con uno o más coprolitos, además de coprolitos de termita, caracterizados por su sección hexagonal, en la

matriz rocosa del nivel. En el ámbar de Ariño se ha hallado un coprolito aislado (Fig. 26C) de morfología cilíndrica irregular de algo más de 0,5 mm de longitud que podría mostrar hifas fúngicas en superficie y una pieza con un conjunto de al menos 20 coprolitos (Fig. 26D) relativamente esféricos e irregulares de menos de 0,5 mm de diámetro. La identificación de los artrópodos productores de estos coprolitos es compleja dado que no se encuentran sininclusiones en las piezas y se requeriría de un estudio comparativo con coprolitos de otros ámbares y con muestras fecales de artrópodos actuales.

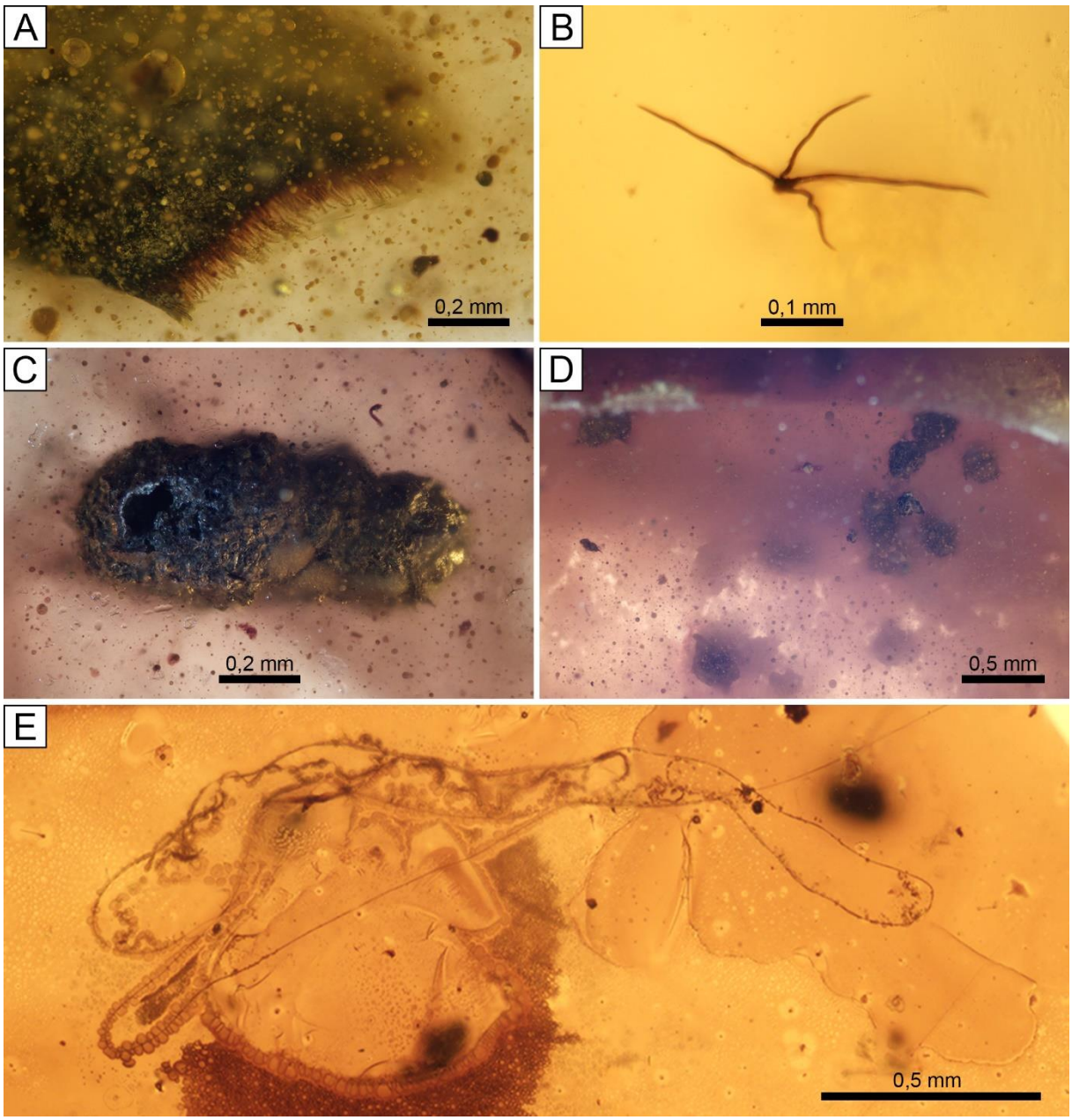

Figura 26. Restos de plantas, icnofósiles y telarañas en el ámbar de Ariño. A) Resto de planta indeterminado, AR-1-A-114.3, imagen tomada de Álvarez-Parra *et al.* (2021b); B) Tricoma, AR-1-A-2019.95.8; C) Coprolito aislado, AR-1-A-2019.73; D) Conjunto de coprolitos, AR-1-A-2019.77; E) Porción de telaraña, AR-1-A-2019.95.5, imagen tomada de Álvarez-Parra *et al.* (2021b).

Las arañas son arácnidos caracterizados por tener la capacidad de secretar seda a partir de unas estructuras especializadas denominadas hileras, la cual puede tener diferentes funciones (Foelix, 2011; Ludwig *et al.*, 2018). Algunas arañas son capaces de construir estructuras llamadas telarañas, en ocasiones de gran tamaño, usualmente con la función de capturar presas (Foelix, 2011; Ludwig *et al.*, 2018). Se han documentado hebras aisladas de telaraña y porciones de telarañas, en ocasiones con organismos atrapados, en ámbares cretácicos (Dunlop *et al.*, 2018). La supuesta telaraña más antigua conocida se ha descrito de ámbar del Berriasiense superior-Valanginiense inferior de Hastings (Brasier *et al.*, 2009). Uno de los hallazgos más relevantes del ámbar de España es una telaraña con presas en una pieza de ámbar de San Just (Peñalver *et al.*, 2006). En total, se han identificado nueve piezas de ámbar de San Just, tres de Ariño (Fig. 26E) (Álvarez-Parra *et al.*, 2021b) y una de Arroyo de la Pascueta con telarañas, porciones de telaraña o hebras aisladas. Se ha iniciado el estudio de las telarañas en ámbar de España junto con la determinación de los criterios para identificar telarañas en ámbar, ya que es común su confusión con otros restos orgánicos, como hifas fúngicas o fracturas del propio ámbar (Peñalver *et al.*, 2021a).

Filo Arthropoda

Subfilo Chelicerata: Clase Arachnida

4.2.5. Orden Araneae

Las arañas son un grupo diverso de arácnidos con más de 50.000 especies actuales (Dunlop *et al.*, 2022). Son casi en su totalidad depredadoras y se distribuyen ampliamente por una gran variedad de hábitats en el mundo (Foelix, 2011). Algunas especies de arañas tienen la capacidad de producir telarañas y veneno para la captura de presas (Foelix, 2011). El registro fósil más antiguo de arañas es del Carbonífero (Selden, 2021). Se encuentran como bioinclusiones en diversos ámbares cretácicos (Guo *et al.*, 2022). Se han identificado numerosos ejemplares de arañas en los ámbares de España (Delclòs *et al.*, 2007), sin embargo solo unos pocos de ellos se han estudiado taxonómicamente debido a la dificultad de su estudio anatómico. Se han identificado las familias Oonopidae y †Lagonomegopidae en los ámbares de El Soplao, Peñacerrada I y San Just (Saupe *et al.*, 2012; Pérez-de la Fuente *et al.*, 2013). La familia Oonopidae está representada por el género de araña saltadora *Orchestina* en los tres yacimientos (Saupe *et al.*, 2012). En el ámbar de Peñacerrada II se han descrito una especie de la familia Araneidae y otra de †Lagonomegopidae (Penney, 2006; Penney y Ortuño, 2006). El registro del ámbar de San Just está constituido por 17 ejemplares (Fig. 27A, B), aunque solo dos de ellos han sido estudiados taxonómicamente y corresponden a *Orchestina* especie

informal 2 (Oonopidae) y *Spinomegops aragonesis* Pérez-de la Fuente, Saupe & Selden, 2013 (†Lagonomegopidae) (Saupe *et al.*, 2012; Pérez-de la Fuente *et al.*, 2013). En el ámbar de Ariño se han hallado dos ejemplares parciales cuya identificación como arañas es dudosa. Solo un ejemplar puede ser identificado con certidumbre como una araña (AR-1-A-2019.76), en el que se observan unas estructuras que podrían estar relacionadas con las hileras (apéndices encargados de la secreción de seda) en el interior del opistosoma (Fig. 10B, C) (Álvarez-Parra *et al.*, 2021b).

4.2.6. Orden Pseudoscorpiones

Los pseudoescorpiones son un grupo de pequeños arácnidos con una morfología que recuerda a la de los escorpiones, ya que poseen pedipalpos terminados en forma de quela o pinza, pero carecen del metasoma y aguijón característicos de los escorpiones (Weygoldt, 1969). Todos los pseudoescorpiones son depredadores, principalmente de otros artrópodos, y suelen formar parte de la edafofauna de los bosques, aunque algunos de ellos actualmente habitan zonas intermareales o cuevas (Weygoldt, 1969). En ocasiones, algunas especies de pseudoescorpiones desarrollan interacciones biológicas de comensalismo por medio de foresis en insectos (Poinar *et al.*, 1998). Se conocen fósiles desde el Devónico y posiblemente fuera uno de los primeros grupos de artrópodos en colonizar zonas continentales (Harms y Dunlop, 2017). Su registro fósil está representado principalmente por inclusiones en ámbar a partir del Cretácico, y cabe destacar los numerosos registros en ámbar cretácico de Myanmar y eoceno del Báltico (Harms y Dunlop, 2017). El único ejemplar de pseudoescorpión conocido del ámbar de la Cuenca del Maestrazgo es SJNB2012-44 (Fig. 27C), procedente del yacimiento de San Just, que se corresponde con un pedipalpo posiblemente perteneciente a la familia Pseudogarypidae y actualmente está en estudio por miembros del grupo AMBERIA. Además, se han documentado otros dos ejemplares de pseudoescorpiones en el ámbar de Peñacerrada I (Delclòs *et al.*, 2007; Rodrigo *et al.*, 2018).

4.2.7. Subclase Acari

Los ácaros (Acari) son arácnidos de pequeño tamaño que habitan en una enorme variedad de hábitats en todos los continentes con diversos modos de vida, ya que se han documentado ácaros detritívoros, depredadores y parásitos (Krantz y Walter, 2009). Actualmente se conocen alrededor de 55.000 especies, aunque se estima la existencia de muchas más (Arribas *et al.*, 2020). Es posible que sean el grupo hermano de los solífugos (Pepato y Klimov, 2015) o de los pseudoescorpiones (Sharma *et al.*, 2014).

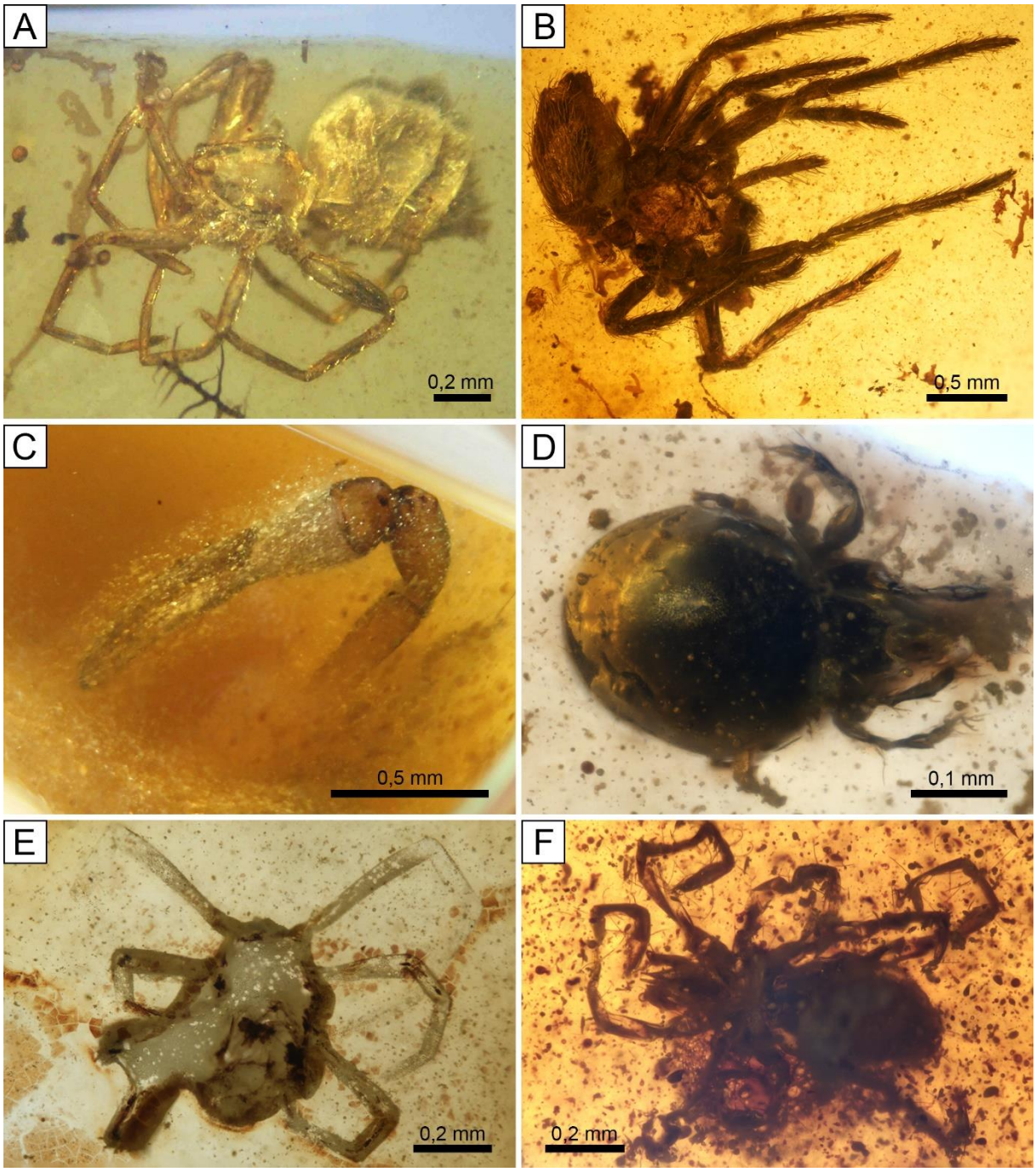

Figura 27. Arácnidos en los ámbares de la Cuenca del Maestrazgo. A) Araña *Orchestina* sp. (Oonopidae) en ámbar de San Just, CPT-4100, imagen de Xavier Delclòs; B) Araña de la familia †Lagonomegopidae en ámbar de San Just, SJNB2012-12-07, imagen tomada de Barrón *et al.* (enviado); C) Pedipalpo de pseudoescorpión en ámbar de San Just, SJNB2012-44, imagen de Enrique Peñalver; D) Holotipo del ácaro *Liacarus* (*Procorynetes*) *shtanchaevae* (Oribatida: Liacaridae) en ámbar de Ariño, AR-1-A-2019.45, imagen tomada de Arillo *et al.* (2022); E) Larva de ácaro en ámbar de Ariño, AR-1-A-2019.62; F) Ácaro de la familia Rhagidiidae en ámbar de Ariño, AR-1-A-2019.71, imagen tomada de Álvarez-Parra *et al.* (2021b).

La sistemática de los ácaros es muy debatida a nivel de alto rango taxonómico y es posible que no formen un grupo monofilético (Arribas *et al.*, 2020), a pesar de ello tradicionalmente se han dividido en Acariformes y Parasitiformes, ambos tratados como superórdenes u órdenes por diferentes investigadores (Mironov y Bochkov, 2009; Arribas *et al.*, 2020). Dentro de Acariformes se consideran los clados Trombidiformes y Sarcoptiformes, en este último se incluyen los oribátidos (Oribatida) (Arribas *et al.*, 2020). El registro fósil más antiguo de ácaros es del Devónico Inferior (Dunlop y Garwood, 2018). Los oribátidos más antiguos datan del Devónico (Subías y Arillo, 2002). Los oribátidos son miembros habituales de la edafofauna y su alimentación es principalmente detritívora, pero se conocen algunas especies depredadoras (Schatz y Behan-Pelletier, 2008).

Los ácaros cretácicos, a pesar de ser relativamente abundantes en ámbar, han sido poco estudiados y el registro mejor conocido es el del ámbar de España, estudiado por los investigadores Antonio Arillo y Luis S. Subías (ambos de la Universidad Complutense de Madrid). El único ácaro parásito (garrapata) conocido del ámbar de España se ha encontrado en el ámbar de El Soplao y se corresponde con una nueva especie del género *Deinocroton* dentro de la familia †Deinocrotonidae (Peñalver *et al.*, 2022a). En relación con los acariformes, se ha documentado un ácaro *Leptus* sp. (Trombidiformes) parasitando a un díptero de la familia †Archizelmiridae en el ámbar de San Just (Arillo *et al.*, 2018). En este ámbar se han identificado otros tres ejemplares que podrían asignarse también al género *Leptus*, asimismo presente en los ámbares de El Soplao y Peñacerrada I (Pérez de la Fuente, 2012), además de un ejemplar que podría corresponder a la familia Bdellidae (Trombidiformes). En cuanto a los oribátidos, cabe destacar que de las 17 especies conocidas de este grupo en ámbar cretácico, 13 de ellas lo son a partir de ejemplares del ámbar de España (Arillo *et al.*, 2020, 2022): La Rodada, 1; El Soplao, 3; Peñacerrada I, 2; Salinillas de Buradón, 1; San Just, 5; y Ariño, 1. Las cinco especies de oribátidos descritas del ámbar de San Just son *Trhypochthonius lopezvallei* Arillo, Subías & Shtanchaeva, 2012 (Trhypochthoniidae), *Cretaceobodes martinezae* Arillo, Subías & Shtanchaeva, 2010 (Otocepheidae), *Ametroproctus valeriae* Arillo, Subías & Shtanchaeva, 2009 (Ametroproctidae), *Tenuelamellarea estefaniae* Arillo & Subías, 2016 (Lamellareidae) e *Hypovertex hispanicus* Arillo & Subías, 2016 (Scutoverticidae) (Arillo *et al.*, 2009b, 2010, 2012, 2016). Aparte de los cinco trombidiformes y cinco oribátidos identificados en el ámbar de San Just hay que tener en cuenta el hallazgo de otros nueve ácaros no determinados. La primera especie descrita del ámbar de Ariño fue el oribátido *Liacarus* (*Procorynetes*) *shtanchaevae* Arillo & Subías, 2022 de la familia Liacaridae (Fig. 27D) (Arillo *et al.*, 2022). Esta especie pertenece a un subgénero viviente, único caso en el registro cretácico del grupo, además, 13 de las 17 especies de oribátidos conocidas de ámbares cretácicos han sido asignadas a géneros vivientes (Arillo *et al.*, 2022). Por lo tanto, se constata una elevada estasis morfológica en oribátidos, algo usual entre grupos de artrópodos habitantes del suelo

de los bosques (Arillo *et al.*, 2022). En el ámbar de Ariño también se han documentado una larva de ácaro (AR-1-A-2019.62), caracterizada por tener seis patas (Fig. 27E), y un ejemplar (AR-1-A-2019.71) de la familia Rhagidiidae (Trombidiformes) (Fig. 27F) (Álvarez-Parra *et al.*, 2021b). Como se ha comentado anteriormente, se han encontrado restos mal conservados que podrían ser de ácaros o arañas. Además, al registro de ácaros se podrían añadir un resto parcial indeterminado y un ejemplar completo diminuto (AR-1-A-2019.95.4) que podría asignarse a la familia Pyemotidae (Trombidiformes) o ser un insecto indeterminado, ya que no se puede discernir el número exacto de patas.

Subfilo Hexapoda

4.2.8. Clase Collembola

Los colémbolos son hexápodos no insectos caracterizados por, al igual que Protura y Diplura, presentar piezas bucales entognatas (Rusek, 1998). Este grupo cuenta con más de 8.000 especies actuales; tienen tamaño muy pequeño y habitan en todos los continentes (Hopkin, 1997). Existen especies detritívoras, herbívoras y depredadoras, y suelen formar parte de la edafofauna, aunque también pueden vivir en otros hábitats (Rusek, 1998). Se considera que los colémbolos son el grupo de hexápodos más numeroso del planeta (Hopkin, 1997). La posición filogenética del grupo es controvertida, ya que unos análisis filogenéticos lo agrupan junto con Protura, aunque otros incluso lo excluyen de Hexapoda (Luan *et al.*, 2005). Su registro fósil más antiguo data del Devónico Inferior (Grimaldi y Engel, 2005). Se conocen colémbolos en varios ámbares cretácicos, como los de Canadá y Myanmar (Sánchez-García y Engel, 2016). Se han descrito ocho especies de colémbolos del ámbar de Peñacerrada I y se han identificado tres ejemplares del ámbar de El Soplao (Pérez de la Fuente, 2012; Sánchez-García y Engel, 2016, 2017). Además, se ha inferido comportamiento de cortejo y gregarismo a partir de algunos ejemplares de Peñacerrada I (Sánchez-García *et al.*, 2018). Los colémbolos del ámbar de España, al igual que otros taxones de la edafofauna, fueron estudiados por la paleontóloga Alba Sánchez García (Universitat de València) durante su Tesis Doctoral (Sánchez García, 2017). En el ámbar de San Just se han hallado cuatro ejemplares de colémbolos de identificación dudosa (CPT-4064, CPT-4115, MAP-7754 y SJE-2012-46-01).

4.2.9. Orden Diplura

Los dipluros, con algo más de 1.000 especies conocidas, son hexápodos ciegos con piezas bucales entognatas y podrían ser el grupo hermano de los insectos (Dallai *et al.*, 2011). Forman parte de la edafofauna, aunque algunas especies habitan en cuevas, y muestran diferentes

preferencias de alimentación, ya que se encuentran especies detritívoras y otras depredadoras (Sendra *et al.*, 2021). Su registro fósil es muy escaso, conocido únicamente por unos pocos ejemplares, y su representante más antiguo data del Carbonífero (Kukalová-Peck, 1987). En el ámbar de San Just se ha encontrado un resto parcial (SJ-10-44) que podría corresponder a este orden.

Clase Insecta

4.2.10. Orden Archaeognatha

Los arqueognatos son insectos ametábolos que retienen varios caracteres plesiomórficos, como, por ejemplo, la ausencia de alas (Sturm y Machida, 2001). Forman parte de la edafofauna, dado que viven en la hojarasca, en materia orgánica en descomposición y bajo rocas, y su alimentación consta de algas, líquenes y materia orgánica en descomposición (Sturm y Machida, 2001). Su registro fósil no es muy numeroso y los más antiguos representantes datan del Carbonífero (Rasnitsyn *et al.*, 2004). Se conocen ejemplares de los ámbares cretácicos de Myanmar y Líbano (Sánchez-García *et al.*, 2019), y también están presentes en el ámbar de España. Se han hallado 10 ejemplares en el ámbar de Peñacerrada I y, además, otro ejemplar en el ámbar de San Just (SJE-2012-45-09) y un resto parcial en el ámbar de Ariño (AR-1-A-2019.46) (Fig. 28A).

4.2.11. Orden Orthoptera

Los ortópteros son insectos hemimetábolos pertenecientes al clado Polyneoptera junto con Blattodea, Mantodea y otros órdenes (Grimaldi y Engel, 2005). Es un grupo muy diverso entre los polineópteros, con más de 20.000 especies actuales descritas (Gutjahr y de Souza Braga, 2018). Se caracterizan por sus patas posteriores alargadas y adaptadas para el salto, además, muchas especies poseen la capacidad de estridular, es decir, producir sonidos como llamada de apareamiento (Gutjahr y de Souza Braga, 2018). La mayoría de las especies de ortópteros son herbívoras y en ocasiones forman grandes enjambres que pueden dar lugar a plagas (Gutjahr y de Souza Braga, 2018). El registro fósil conocido de los ortópteros es muy amplio y sus representantes más antiguos datan del Carbonífero (Grimaldi y Engel, 2005). Se han descrito tres especies en el ámbar de Peñacerrada I pertenecientes a la familia †Elcanidae (Peñalver y Grimaldi, 2010). Esta familia se caracteriza por la presencia de espolones móviles en la superficie dorsal de la tibia de las patas posteriores y usualmente se ha agrupado junto con †Permelcanidae en la superfamilia †Elcanoidea, aunque es posible que el primero sea un taxón parafilético (Peñalver y Grimaldi, 2010). La posición filogenética de †Elcanoidea es muy

controvertida y podrían ser el grupo hermano del resto de ortópteros (Peñalver y Grimaldi, 2010). Los ortópteros solo están representados por un resto parcial en el ámbar de San Just (CPT-4083) y dos ejemplares en el ámbar de Ariño (AR-1-A-2019.36 y AR-1-A-2019.108) que podrían corresponder a la familia †Elcanidae (Fig. 28B, C).

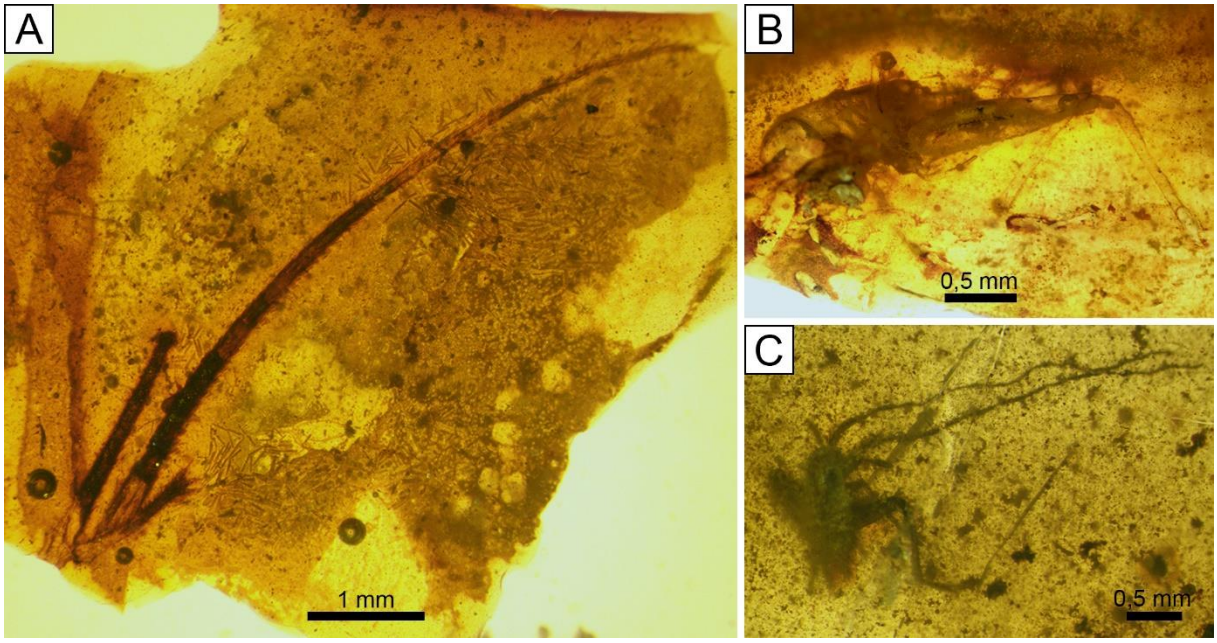

Figura 28. Restos y ejemplares de Archaeognatha y Orthoptera en el ámbar de Ariño. A) Cercos y filamento terminal de Archaeognatha, AR-1-A-2019.46; B) Ejemplar preliminarmente asignado a la familia †Elcanidae (Orthoptera), AR-1-A-2019.36; C) Ejemplar posiblemente inmaduro que podría pertenecer a la familia †Elcanidae (Orthoptera), AR-1-A-2019.108.

4.2.12. Orden Blattodea

El orden Blattodea es un grupo de insectos hemimetábolos que incluye a las cucarachas y a las termitas, anteriormente reconocidos como órdenes propios, 'Blattaria' e Isoptera respectivamente (Grimaldi y Engel, 2005). Los análisis filogenéticos indican que en realidad las termitas son cucarachas eusociales (Inward *et al.*, 2007; Wang *et al.*, 2017). En la actualidad se conocen más de 4.000 especies de cucarachas que habitan en diversos hábitats por todo el mundo, muchas de ellas forman parte de la edafofauna de los bosques y en ocasiones algunas especies pueden llegar a considerarse plaga, principalmente en áreas urbanas (Bell *et al.*, 2007). Se conocen especies herbívoras, depredadores y omnívoras, además, tienen un papel importante en los ecosistemas como recicladores de materia orgánica (Bell *et al.*, 2007). El registro fósil más antiguo de cucarachas es del Carbonífero Superior (Zhang *et al.*, 2013). Se han hallado cucarachas en los ámbares de El Soplao, Peñacerrada I, Ariño, San Just, Arroyo de la Pascueta y La Hoya, y su estudio taxonómico preliminar lo ha iniciado la paleontóloga Lucia Šmídová (Univerzita Karlova, Praga, Chequia). En la colección

de El Soplao se incluyen siete ejemplares y en la de Peñacerrada I se han identificado 65 ejemplares, aunque es posible que algunos de ellos correspondan a otros grupos de Polyneoptera como Grylloblattodea, †Umenocoleidae o †Alienopteridae. Se han identificado 15 ejemplares en San Just, entre ellos miembros de las familias †Blattulidae, †Mesoblattinidae y Corydiidae, junto con ejemplares que podrían adscribirse a las familias †Skokidae y †Liberiblattinidae, además de algunos ejemplares indeterminados. En el ámbar de Ariño se ha hallado un único ejemplar asignado a la familia †Blattulidae (AR-1-A-2019.38.1) (Fig. 29A). La única cucaracha de Arroyo de la Pascueta se ha identificado como perteneciente a Corydiidae (Fig. 29B). Por último, de los dos ejemplares de La Hoya, uno podría pertenecer a †Mesoblattinidae (Fig. 29C) y el otro es un inmaduro indeterminado. Se han hallado morfotipos en los ámbares de El Soplao y Peñacerrada I, similares a los de San Just.

En cuanto a las termitas, se conocen alrededor de 3.000 especies actuales. Habitan en poblaciones sociales y poseen un sistema de castas con diferentes morfotipos, además, muchas especies se alimentan de la celulosa de la madera, por lo que también participan en el reciclaje de materia orgánica en los ecosistemas (Engel *et al.*, 2009; Krishna *et al.*, 2013). El registro fósil más antiguo de termitas y su diferenciación en castas data del Barremiense (Martínez-Delclòs y Martinell, 1995), aunque es posible que derivasen de las cucarachas durante el Jurásico Superior (Engel *et al.*, 2009; Krishna *et al.*, 2013). Las termitas se consideran el grupo de insectos eusociales más antiguo (Bignell *et al.*, 2010). Se han hallado termitas en diversos ámbares cretácicos del mundo, como Líbano (Barremiense), Francia (Albiense-Cenomaniense), Myanmar (Cenomaniense) y Canadá (Campaniense), además se han descrito cuatro géneros monoespecíficos en el ámbar de España, tres de Peñacerrada I y uno de San Just (Engel y Delclòs, 2010, Sánchez-García *et al.*, 2020). En el ámbar de El Soplao se han hallado dos ejemplares fragmentarios (Sánchez-García *et al.*, 2020). La especie descrita del ámbar de San Just es *Aragonitermes teruelensis* Engel & Delclòs, 2010 (Fig. 29D), clasificada como *incertae sedis* al igual que las especies de Peñacerrada I, ya que muestran características primitivas de difícil adscripción a nivel de familia (Engel y Delclòs, 2010; Sánchez-García *et al.*, 2020). Además, hay otros cinco restos parciales de San Just asignados a termitas (Fig. 29E).

4.2.13. Orden *incertae sedis*: Familia †Umenocoleidae

Los umenocoleidos son un grupo de insectos hemimetábolos extintos cuya posición filogenética, junto con la de los alienoptéridos, ha generado mucho debate en los últimos años. Los análisis filogenéticos indican que †Umenocoleidae y †Alienopteridae son grupos hermanos y forman parte del superorden Dictyoptera (Luo *et al.*, 2022b). Los alienoptéridos fueron inicialmente descritos como un nuevo orden (Bai *et al.*, 2016), a pesar de ello, actualmente se ha reducido su categoría taxonómica (Luo *et al.*, 2022a). Por otro lado, los umenocoleidos, en

un principio, se consideraron miembros de Coleoptera, aunque las investigaciones recientes apuntan a que deben agruparse en Dictyoptera y su aspecto similar a los escarabajos se debe a evolución convergente (Luo *et al.*, 2022b). Existe controversia en cuanto al nombre usado para el clado que agrupa a las familias †Umenocoleidae y †Alienopteridae, dado que algunos autores proponen †Umenocoleoidea (Vršanský *et al.*, 2021), mientras que otros proponen †Alienoptera (Luo *et al.*, 2022a). De cualquier modo, los análisis filogenéticos indican que este clado es el grupo hermano del orden Mantodea (Luo *et al.*, 2022a, b).

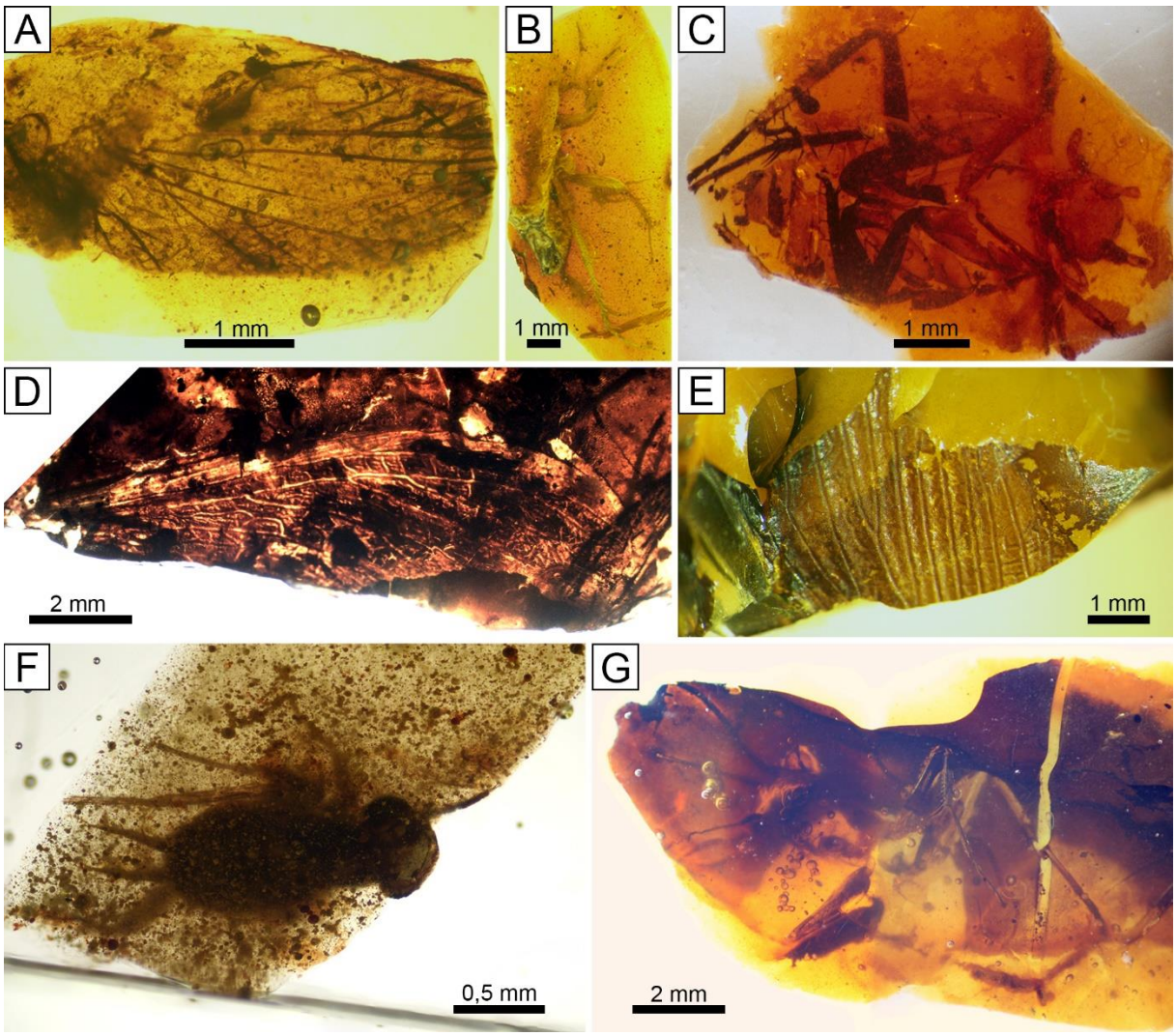

Figura 29. Dictiópteros en los ámbares de la Cuenca del Maestrazgo. A) Restos alares asignados a la familia †Blattulidae (Blattodea) en el ámbar de Ariño, AR-1-A-2019.38.1; B) Ejemplar perteneciente a la familia Corydiidae (Blattodea) en el ámbar de Arroyo de la Pascueta, AP-11.3; C) Ejemplar de la familia †Mesoblattinidae (Blattodea) en el ámbar de La Hoya, LH-1; D) Holotipo de *Aragonitermes teruelensis* (Blattodea: Isoptera) en el ámbar de San Just, CPT-4065, imagen de Xavier Delclòs; E) Resto alar parcial de termita (Blattodea: Isoptera) en el ámbar de San Just, SJNB2021-50; F) Ejemplar de la familia †Umenocoleidae en el ámbar de Ariño, AR-1-A-2019.128.3; G) Holotipo de *Aragonimantis aenigma* (Mantodea) en el ámbar de San Just, SJ-10-17, imagen de Enrique Peñalver.

El registro fósil de †Umenocoleidae se restringe al Cretácico e incluye tanto ejemplares en ámbar como en compresión en yacimientos desde el Berriasiense hasta el Cenomaniense, y su diversidad no es elevada, ya que incluye únicamente 17 especies en 10 géneros (Luo *et al.*, 2022a). Los umenocoleidos durante el Cretácico Inferior mostraron una amplia distribución geográfica (Luo *et al.*, 2022a), y junto con los alienoptéridos, es posible que ocupasen un nuevo nicho ecológico peculiar entre los dictiópteros, pero se ha sugerido que desaparecieron debido a la competencia con otros grupos de insectos tras la radiación de las angiospermas (Luo *et al.*, 2022b). Se ha encontrado un ejemplar de umenocoleido en el ámbar de Ariño (AR-1-A-2019.128.3) (Fig. 29F), durante un estudio en colaboración con Lucia Šmídová. Se trata de una ninfa con morfología similar a la del género *Jantaropterix*, principalmente por la forma de la cabeza y los cercos, perteneciente a †Umenocoleidae (Vršanský, 2003; Mlynský *et al.*, 2019; Vršanský *et al.*, 2021). Sin embargo, Luo *et al.* (2022a, b) excluyen este género de †Umenocoleidae.

4.2.14. Orden Mantodea

Los miembros del orden Mantodea, comúnmente conocidos como mantis, son insectos hemimetábolos depredadores caracterizados por sus patas anteriores raptoras y con una amplia distribución ocupando diversos hábitats (Prete *et al.*, 1999). En la actualidad se conocen unas 2.400 especies (Zhang, 2011). El registro fósil de mantis no es abundante y no está muy estudiado debido a que usualmente los adultos miden varios centímetros de longitud y, por lo tanto, su registro en ámbar es fragmentario. Mientras que el de compresión no suele conservar detalles anatómicos que ayuden a su clasificación, dado que principalmente son restos alares (Martínez-Delclòs *et al.*, 2004; Schubnel y Nel, 2019). Los representantes más antiguos del grupo son del Cretácico Inferior (Delclòs *et al.*, 2016), aunque posiblemente surgieran en el Jurásico o incluso antes (Béthoux y Wieland, 2009). Este grupo solo está representado en el registro fósil de la península ibérica por la especie *Aragonimantis aenigma* Delclòs, Peñalver, Arillo, Engel, Nel, Azar & Ross, 2016 (familia *incertae sedis*) (Fig. 29G), del yacimiento de San Just (Delclòs *et al.*, 2016). Además, Vršanský (2002) indica la presencia de dos ejemplares, depositados en una colección privada, asignados al género *Cretophotina* (familia *incertae sedis*) del yacimiento de compresión del Cretácico Inferior del Montsec (Lleida, España).

4.2.15. Orden Psocodea

Los psocópteros son insectos hemimetábolos de pequeño tamaño (Fig. 30A), conocidos comúnmente como piojos de las cortezas, que se caracterizan por sus piezas bucales masticadoras (Mockford, 1993). Se conocen al menos 5.720 especies actuales de psocópteros que habitan en diferentes hábitats, principalmente como miembros de la edafofauna, también en cortezas de los árboles, rocas, cuevas, nidos de aves y mamíferos e, incluso, en zonas domésticas (Smithers, 1972; New, 1987; Zhang, 2011). Son herbívoros o detritívoros y se alimentan principalmente de restos orgánicos en descomposición o microorganismos como algas, líquenes y hongos (New, 1987). Cumplen un papel fundamental en los ecosistemas como recicladores de la materia orgánica (New, 1987). Tradicionalmente, se consideraban como un orden propio, 'Psocoptera', muy relacionado con los piojos parásitos que forman el clado Phthiraptera (Smithers, 1972). Los estudios filogenéticos apuntan a que los piojos parásitos son el grupo hermano de los psocópteros de la familia Liposcelididae, conocidos como piojos de los libros (Johnson *et al.*, 2018; de Moya *et al.*, 2021). Por ello, los psocópteros se corresponden con el grupo parafilético 'Psocoptera' que, junto con los piojos parásitos, considerados como infraorden Phthiraptera, forman el orden Psocodea (Johnson *et al.*, 2018; de Moya *et al.*, 2021). El orden Psocodea se incluye en el grupo Acercaria, anteriormente llamado Paraneoptera, junto con los órdenes †Permopsocida, †Miomoptera, †Hypoperlida, †Lophioneurida, Thysanoptera y Hemiptera (Prokop *et al.*, 2017). Curiosamente, recientes estudios filogenéticos moleculares sitúan a Psocodea como grupo hermano de los insectos holometábolos (Holometabola), por ello Acercaria pasaría a ser una agrupación parafilética (Misof *et al.*, 2014; Johnson *et al.*, 2018). Sin embargo, los mapeos de caracteres morfológicos no han permitido reconocer ninguna apomorfía que soporte el hipotético clado [Psocodea+Holometabola], y en cambio sí se han hallado 14 potenciales caracteres apomórficos que sustentan la monofilia de Acercaria (Johnson *et al.*, 2018).

En el orden Psocodea se reconocen los subórdenes Trogiomorpha, Troctomorpha (incluido Phthiraptera) y Psocomorpha (de Moya *et al.*, 2021). En la actualidad, el suborden Psocomorpha es el más diverso con alrededor de 3.600 especies descritas (Yoshizawa y Johnson, 2014). En el suborden Trogiomorpha se incluyen las familias †Cormopsocidae (no se considera dentro de ningún infraorden), Prionoglarididae (infraorden Prionoglaridetae), Psyllipsocidae (infraorden Psyllipsocetae), †Empheriidae, Lepidopsocidae, Psoquilidae y Trogiidae (las cinco en el infraorden Atropetae) (Yoshizawa *et al.*, 2006; Yoshizawa y Lienhard, 2020). El suborden Troctomorpha engloba a las familias Amphientomidae, Compsocidae, †Electrentomidae, Manicapsocidae, Musapsocidae, Troctopsocidae y Protroctopsocidae (las siete en el infraorden Amphientometae), Sphaeropsocidae (infraorden Sphaeropsocetae), Pachytroctidae (infraorden Pachytroctetae) y Liposcelididae (infraorden Liposcelidetae),

además del infraorden Phthiraptera (de Moya *et al.*, 2021). Por último, en el suborden Psocomorpha se consideran los infraórdenes Archipsocetae (una familia), Caeciliusetae (seis familias), Homilopsocidae (cinco familias), Philotarsetae (tres familias), Epipsocetae (cuatro familias) y Psocetae (cuatro familias) (Yoshizawa y Johnson, 2014).

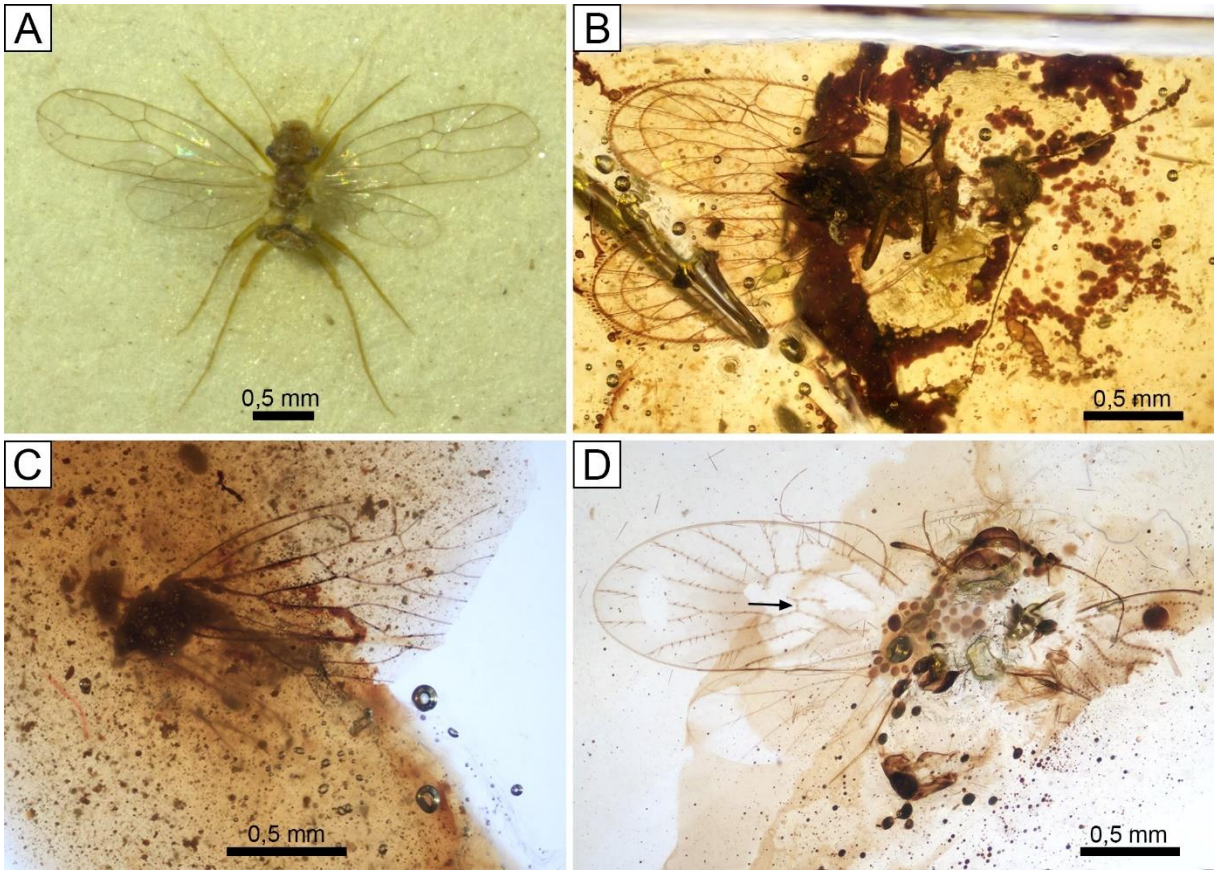

Figura 30. Ejemplares del suborden Trogiomorpha (Psocodea). A) Ejemplar actual de *Psyllipsocus ramburii* Selys-Longchamps, 1872 (Psyllipsocidae) de la Colección de Entomología Hope del Oxford University Museum of Natural History (ejemplar en cajón nº 26234); B) Ejemplar de *Archaeatropos alavensis* (†Empheriidae) en el ámbar de San Just, MAP-7812, imagen tomada de Álvarez-Parra *et al.* (2022b); C) Holotipo de *Libanoglaris hespericus* (†Empheriidae) en el ámbar de Ariño, AR-1-A-2019.35, imagen tomada de Álvarez-Parra *et al.* (2022b); D) Ejemplar de la familia †Empheriidae en el ámbar de Arroyo de la Pascueta, AP-10, la vena transversal rs-m está indicada con una flecha.

El registro fósil más antiguo de Psocodea data del Carbonífero Superior (Nel *et al.*, 2013), aunque es en el Cretácico cuando los psocópteros experimentan una destacada diversificación (Mockford *et al.*, 2013; Álvarez-Parra *et al.*, 2020b). Los Phthiraptera están representados en el registro fósil por una sola especie (Dalgleish *et al.*, 2006). Trogiomorpha es el suborden con un mayor número de especies cretácicas, lo que contrasta con la diversidad actual, dado que es el suborden menos diverso (Álvarez-Parra *et al.*, 2022b). Es posible que los Trogiomorpha pasaran a ocupar hábitats marginales, donde se suelen encontrar en la actualidad, debido a

competencia de nicho tras la diversificación de los Psocomorpha (Álvarez-Parra *et al.*, 2022b). Esta competencia con los Psocomorpha pudo llevar a la extinción de las familias †Cormopsocidae y †Empheriidae (Álvarez-Parra *et al.*, 2022b). Algunos miembros de Trogiomorpha muestran una elevada estasis morfológica, incluso desde el Cretácico, típica de grupos de hábitats marginales (Álvarez-Parra *et al.*, 2020b). Se han descrito especies de psocópteros en ámbares cretácicos de Canadá, Nueva Jersey en Estados Unidos, España, Francia, Líbano, Taimyr en Rusia y Myanmar (Álvarez-Parra *et al.*, 2020b, 2022b). Se ha profundizado poco en el conocimiento de la paleobiología de los psocópteros cretácicos, aunque se supone que pudo ser similar a la biología de los representantes actuales del grupo. Curiosamente, los psocópteros son más abundantes en yacimientos de ámbar como bioinclusiones que en yacimientos de compresión, hecho relacionado con cuestiones tafonómicas o paleoecológicas (Álvarez-Parra *et al.*, 2022b).

Taxón	El Soplao	Peñacerrada I	Peñacerrada II	San Just	Ariño	Arroyo de la Pascueta
Trogiomorpha						
†Empheriidae						
Archaeatropos alavensis	X	X		X		X
Empheropsocus margineglabrus		X				
Empheropsocus arilloi		X				
Preempheria antiqua		X		X		
Preempheria sp. nov.?		X				
Libanoglaris hespericus	X				X	
Gen. et sp. nov.	X		X			X
Trogiidae						
Gen. et sp. nov.?		X?				
Troctomorpha						
Incertae sedis						
Gen. et sp. nov.	X	X	X	X		
Compsocidae						
Burmacompsocus sp. nov.	X					
Manicapsocidae						
Azarpsocus sp. nov.	X				X	
Manicapsocidus enigmaticus		X				
Psocomorpha						
Incertae sedis						
Gen. et sp. nov.					X?	

Tabla 2. Coocurrencia de los taxones del orden Psocodea hallados en los ámbares de España. Los tres ámbares de la Cuenca Vasco-Cantábrica se encuentran a la izquierda, y los tres ámbares de la Cuenca del Maestrazgo a la derecha. Los subórdenes están indicados en azul y las familias en verde.

Los psocópteros del ámbar de España se encuentran en los ámbares de El Soplao (17 ejemplares), Peñacerrada I (84 ejemplares), Peñacerrada II (24 ejemplares), San Just (9 ejemplares), Ariño (7 ejemplares) y Arroyo de la Pascueta (2 ejemplares). Todos estos

ejemplares se han revisado en relación con la Tesis Doctoral. Muchos de ellos tienen una deficiente conservación, pero otros ejemplares se han podido determinar a nivel de especie (Tabla 2). Dos ejemplares hallados en piezas de ámbar de San Just tras la excavación de 2021 permanecen pendientes de revisión detallada. El suborden Trogiomorpha está representado en el ámbar de Peñacerrada I por las especies *Archaeatropos alavensis* Baz & Ortuño, 2000, *Empheropsocus margineglabrus* Baz & Ortuño, 2001, *Empheropsocus arilloi* Baz & Ortuño, 2001, *Preempheria antiqua* Baz & Ortuño, 2001 (las cuatro pertenecientes a †Empheriidae) (Baz y Ortuño, 2000, 2001b). Tras una revisión preliminar, se comprobó que la especie *A. alavensis* es la más numerosa entre los psocópteros del ámbar de Peñacerrada I. Además, se ha confirmado su presencia en los ámbares de El Soplao, San Just (Fig. 30B) y Arroyo de la Pascueta, lo que evidencia su amplia distribución espacial y temporal (Álvarez-Parra *et al.*, 2022b). Esta especie fue inicialmente incluida en la familia '†Archaeatropidae', pero recientemente un estudio filogenético ha indicado que dicha familia es polifilética y ha sido sinonimizada bajo †Empheriidae (Li *et al.*, 2022b). La especie *P. antiqua* también se ha identificado en el ámbar de San Just (Álvarez-Parra *et al.*, 2022b). En el ámbar de Ariño se ha descrito la especie *Libanoglaris hespericus* Álvarez-Parra, Peñalver, Nel & Delclòs, 2022 (†Empheriidae) (Fig. 30C), también presente en el ámbar de El Soplao (Álvarez-Parra *et al.*, 2022b). Una ninfa de psocóptero con conservación excepcional del ámbar de San Just se ha relacionado con la familia †Empheriidae, lo que proporciona nuevos datos anatómicos de la ontogenia de esta familia extinta (Álvarez-Parra *et al.*, 2022b). Otras ninfas de psocóptero se han identificado preliminarmente en el ámbar de Peñacerrada I, pero ni estas ni la de San Just muestran transporte de detritus, como se ha observado en ninfas de otros ámbares cretácicos (Álvarez-Parra *et al.*, 2022b; Kiesmüller *et al.*, 2022).

Además de estos ejemplares descritos de Trogiomorpha, se ha iniciado el estudio de otros representantes del suborden. Dos ejemplares del ámbar de Peñacerrada I podrían describirse como una nueva especie del género *Preempheria*. Se han hallado cuatro ejemplares en el ámbar de El Soplao, uno en el de Peñacerrada II y otro en el de Arroyo de la Pascueta con una venación alar bastante peculiar (Fig. 30D), ya que las venas Rs y M de las alas anteriores no se encuentran fusionadas, sino unidas por una vena transversal rs-m. Preliminarmente, estos seis ejemplares se incluirán en un nuevo género dentro de la familia †Empheriidae. Tres ejemplares del ámbar de Peñacerrada I podrían pertenecer a la familia Trogiidae.

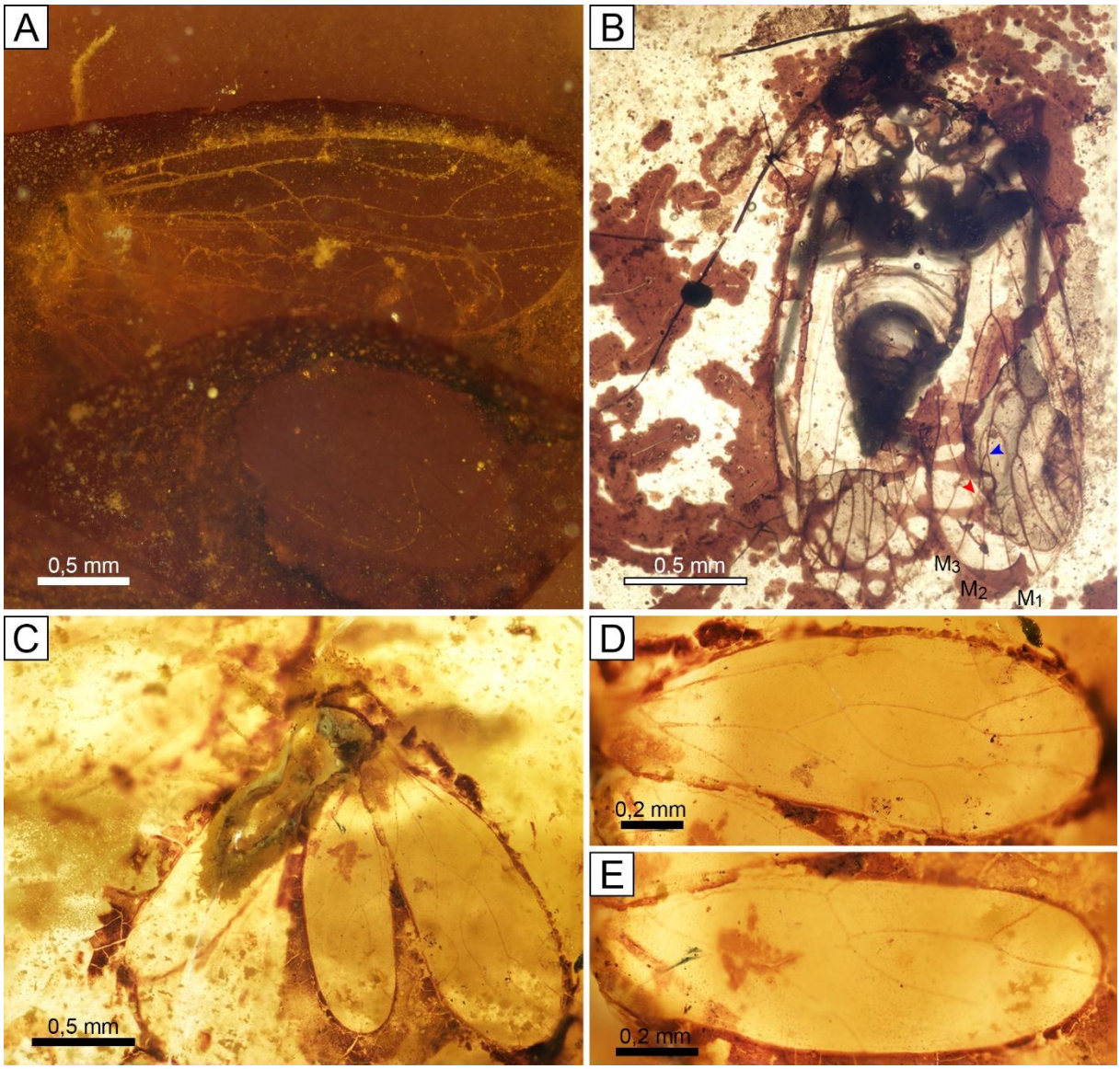

Figura 31. Ejemplares de los subórdenes Troctomorpha y Psocomorpha (Psocodea) en los ámbares de la Cuenca del Maestrazgo. A) Ejemplar identificado como una nueva especie del género *Azarpsocus* (Troctomorpha: Manicapsocidae) en el ámbar de Ariño, AR-1-A-2019.60.1; B) Ejemplar que podría asignarse a las familias Manicapsocidae o Compsocidae (Troctomorpha) en el ámbar de San Just, SJNB2012-12-03, la flecha azul indica la separación de M_1 y M_2+M_3, la flecha roja indica la separación de M_2 y M_3, ambas del ala anterior; C) Ejemplar del ámbar de Ariño que podría incluirse en el suborden Psocomorpha, AR-1-A-2019.50.3; D, E) Ala anterior y posterior, respectivamente, del ejemplar en C. Imágenes A, C-E tomadas de Álvarez-Parra *et al.* (en preparación 1).

Los psocópteros del suborden Troctomorpha se han identificado en los ámbares de El Soplao, Peñacerrada I, Peñacerrada II, San Just y Ariño. La primera especie de este suborden del ámbar de España se describió en Peñacerrada I, *Manicapsocidus enigmaticus* Baz & Ortuño, 2001, incluida en la familia Manicapsocidae (Baz y Ortuño, 2001a). Una nueva especie del género *Azarpsocus*, también perteneciente a Manicapsocidae, se podría describir a partir de un ejemplar del ámbar de El Soplao y dos del ámbar de Ariño (Fig. 31A) (Álvarez-Parra *et*

al., en preparación 1). El único representante de la familia Compsocidae del ámbar de España se corresponde con un ejemplar que se ha asignado al género *Burmacompsocus* (Álvarez-Parra *et al.*, en preparación 1). Cinco ejemplares, un ejemplar en cada uno de los ámbares de El Soplao, Peñacerrada I, Peñacerrada II, San Just y ámbar cenomaniense de Archingeay-Les Nouillers, todos con una venación alar similar, se encuentran actualmente en estudio (Fig. 31B). Comúnmente, la vena M del ala anterior de los psocópteros se separa proximalmente en M_3 y M_1+M_2, en cambio, en estos cuatro ejemplares, la vena M se separa proximalmente en M_1 y M_2+M_3. Este hecho ya se ha descrito en especies cretácicas de las familias Manicapsocidae y Compsocidae (Azar *et al.*, 2016; Hakim *et al.*, 2020), por lo que es probable que los ejemplares en estudio pertenezcan a una de estas dos familias, aunque por el momento se consideran *incertae sedis* en Troctormorpha. También, es posible que todas las especies con este característico patrón de venación se agrupen en un clado, aunque se requeriría un análisis filogenético que confirme esta hipótesis.

Los psocópteros del suborden Psocomorpha son raros en ámbar cretácico. Se ha descrito una especie en ámbar del Cenomaniense-Santoniense de Francia, dos especies en ámbar santoniense de Taimyr en Rusia y una especie en ámbar cenomaniense de Myanmar (Azar *et al.*, 2015; Yoshizawa y Yamamoto, 2021). Un ejemplar del ámbar de Ariño podría describirse como un nuevo género y una nueva especie de Psocomorpha (Fig. 31C-E) (Álvarez-Parra *et al.*, en preparación 1). Este ejemplar sería el psocomorfo más antiguo conocido y, curiosamente, muestra similitudes con el género *Scottiella* (Pseudocaeciliidae), actualmente viviente en las islas Seychelles (Álvarez-Parra *et al.*, en preparación 1). A pesar de ello, sus peculiaridades anatómicas y la ausencia de caracteres clave impedirían su adscripción a una familia concreta (Álvarez-Parra *et al.*, en preparación 1).

Taxón	Líbano	España	Francia	Myanmar	EEUU	Rusia	Canadá
Trogiomorpha	X	X	X	X	X	X	X
†Empheriidae	X	X	X	X	X	X	
Archaeatropos	X	X					
Libanoglaris	X	X					
Trogiidae		X?				X	X
Troctomorpha	X	X	X	X		X	X
Compsocidae		X		X			
Burmacompsocus		X		X			
Manicapsocidae		X		X			
Azarpsocus		X		X			
Psocomorpha		X?	X	X		X	

Tabla 3. Coocurrencia de los taxones del orden Psocodea hallados en los ámbares de España y otros ámbares cretácicos. Los ámbares están ordenados de más antiguo a la izquierda, a más moderno a la derecha. Los subórdenes están indicados en azul, las familias en verde, y los géneros en amarillo.

El estudio de los psocópteros en el ámbar de España ha abierto una nueva oportunidad de comparación paleofaunística con el registro de otros ámbares cretácicos. Al igual que se ha indicado previamente sobre coleópteros, himenópteros y dípteros (Peris *et al.*, 2016), se ha evidenciado la coocurrencia de los mismos géneros en ámbar de España en comparación con los del Líbano y Myanmar (Tabla 3) (Álvarez-Parra *et al.*, en preparación 1). Y en cambio, se han hallado pocas similitudes con el registro de bioinclusiones del ámbar del Albiense-Cenomaniense de Francia. Este hecho es sorprendente dada la cercanía geográfica y temporal del ámbar de España con el ámbar de Francia.

Durante el proyecto de Tesis Doctoral se han revisado las colecciones de psocópteros en ámbar de Oise (Eoceno inferior) y del Báltico (Eoceno superior). Estas revisiones han permitido una comparación taxonómica que ha proporcionado información sobre la diversidad relativa de cada suborden de psocópteros entre ámbares cretácicos y eocenos. Además, se ha podido profundizar en taxonomía y en los posibles factores que caracterizan la distribución de psocópteros, tanto en el presente como en el pasado (Álvarez-Parra y Nel, 2022). En el ámbar de Oise los psocópteros del suborden Psocomorpha son los más numerosos en cuanto a número de ejemplares, aunque solo hay dos especies determinadas de este suborden y la mayoría de los ejemplares se pueden asignar a la especie *Eolachesilla eocenica* Nel, Prokop, De Ploëg & Millet, 2005 (familia Lachesillidae) (Nel *et al.*, 2005). En contraste, en el ámbar Báltico los psocópteros del suborden Psocomorpha son los más diversos (20 de 31 especies descritas) y abundantes. La continuación de este enfoque de estudio en ámbares más recientes (Mioceno), e incluso en copal y resina de Defaunación, podría dar las claves para inferir las causas de estas diferencias y proporcionar información sobre la evolución de los psocópteros en un amplio rango temporal.

4.2.16. Orden †Lophioneurida

Los lofionéuridos son un raro grupo de insectos fósiles con representantes desde el Carbonífero Superior al Cretácico Superior y que forman parte del superorden Thripida junto con el orden Thysanoptera (Nel *et al.*, 2014). Tradicionalmente se han considerado como grupo cercano filogenéticamente a los tisanópteros, aunque su posición y composición son muy debatidas. Nel *et al.* (2012, 2014) consideran que †Lophioneurida incluye a las familias †Lophioneuridae (12 géneros y 27 especies) y †Moundthripidae (un género y una especie).

Los lofionéuridos poseían un cono bucal corto con estiletes maxilares y mandibulares relativamente simétricos (Vishniakova, 1981; Wang *et al.*, 2009), aunque en algunos ejemplares fueron aparentemente asimétricos (Grimaldi y Engel, 2005) o carecían de la mandíbula derecha (Nel *et al.*, 2007, 2012). Seguramente fueron omnívoros con un hábito de alimentación de perforador-succionador en los tejidos de las plantas, y quizás facultativamente

polinívoros, aunque se descarta su papel en la polinización debido a la ausencia de estructuras corporales relacionadas con el transporte de polen (Zherikhin, 2002). Los lofionéuridos se han sugerido como los posibles causantes de perforaciones en esporas del Pérmico asociadas a plantas vasculares del orden †Noeggerathiales (Wang *et al.*, 2009).

Aunque los lofionéuridos son relativamente diversos en yacimientos de compresión, los únicos conocidos en ámbar cretácico son una especie en el ámbar barremiense del Líbano, una especie en ámbar cenomaniense de Myanmar y dos especies en ámbar santoniense de Taimyr (Rasnitsyn y Quicke, 2002). Durante el proyecto de Tesis Doctoral tuvo lugar el descubrimiento del primer lofionéurido en el ámbar de la península ibérica, en concreto en ámbar albiense de San Just (Álvarez-Parra *et al.*, 2021a). Inicialmente, el ejemplar MAP-7751 estaba etiquetado como 'Psocoptera', aunque una revisión en detalle pudo proporcionar las claves para su correcta identificación en el enigmático orden †Lophioneurida. El ejemplar no está bien conservado y el ámbar es muy oscuro, incluso opaco en algunas áreas (Fig. 32A). Curiosamente, las alas se pueden observar correctamente y el ámbar en el área que ocupan las alas es claro (Fig. 32B). Esto se debe posiblemente al modo en que el ejemplar quedó incluido en la resina, ya que las alas debieron cubrir parte de la superficie externa de la resina fluida, lo que evitó su desecación superficial y diferencial respecto al resto de la superficie de la resina. En este ejemplar se pueden observar la cabeza, las alas y las patas. La venación alar es prácticamente idéntica a la de la especie *Jantardachus reductus* del ámbar santoniense de Yantardakh en Taimyr (Vishniakova, 1981), unos 20 millones de años más reciente que el ámbar de San Just. El ejemplar aún requiere un estudio taxonómico detallado y comparativo, aunque de forma preliminar se ha determinado como *Jantardachus* cf. *reductus*, debido a la ausencia de caracteres que se pudieran asociar a variabilidad interespecífica. Esta determinación implicaría un elevado grado de estasis morfológica y, aunque sería novedoso en este grupo, no sería raro al tener en cuenta que se ha observado un elevado grado de estasis morfológica en otros grupos de insectos de Acercaria, como los psocópteros (Álvarez-Parra *et al.*, 2020b), los tisanópteros (Nel *et al.*, 2021) y los hemípteros (Andersen *et al.*, 1993).

4.2.17. Orden Thysanoptera

Los tisanópteros son insectos hemimetábolos de pequeño tamaño que cuentan con más de 6.000 especies actuales con distribución mundial (Mound y Hastenpflug-Vesmanis, 2021). Se consideran el grupo hermano de los hemípteros (Johnson *et al.*, 2018). Su principal característica anatómica es poseer piezas bucales asimétricas de tipo perforador (Mound, 2005). La mayor parte de las especies se alimentan de plantas u hongos, aunque también se conocen especies depredadoras (Mound, 2005). Estos insectos tienen una gran importancia en los ecosistemas ya que algunas especies participan en la polinización de gimnospermas y

angiospermas, y también algunas especies pueden producir plagas, entre ellas unas pocas pueden actuar como vectores de virus que afectan a las plantas (Mound, 2005). El registro fósil más antiguo de tisanópteros es del Triásico Superior, pero es en el Cretácico cuando su diversidad comienza a incrementarse (Grimaldi *et al*., 2004). Los tisanópteros están representados en el ámbar de España por *Tethysthrips hispanicus* Nel, Peñalver, Azar, Hodebert & Nel, 2010 (Thripidae) de El Soplao (Nel *et al*., 2010b), *Gymnopollisthrips minor* Peñalver, Nel & Nel, 2012 y *Gymnopollisthrips maior* Peñalver, Nel & Nel, 2012 (Melanthripidae) de Peñacerrada I (Peñalver *et al*., 2012), *Alavathrips moralesi* Peñalver, Nel & Nel, 2022 (Phlaeothripidae) de Peñacerrada II (Peñalver *et al*., 2022c) e *Hispanothrips utrillensis* Peñalver & Nel, 2010 (Stenurothripidae) de San Just (Peñalver y Nel, 2010). Se han encontrado granos de polen de la gimnosperma *Cycadopites*, cuyo árbol productor pudo pertenecer a las Ginkgoales o Cycadales, en contacto con los ejemplares del género *Gymnopollisthrips*, lo que demuestra la polinización de gimnospermas por tisanópteros ya durante el Cretácico Inferior (Peñalver *et al*., 2012). En el ámbar de San Just se han identificado 13 tisanópteros, tres de ellos asignados a la especie *H. utrillensis*, y en el ámbar de Ariño, 11 ejemplares, uno de ellos un inmaduro con buena conservación (Fig. 32C, D) (Álvarez-Parra *et al*., 2021b). Desde el punto de tafonómico, cabe destacar un tisanóptero del ámbar de Ariño recubierto con pequeñas burbujas blanquecinas similares a las que se encuentran en ámbar eoceno del Báltico (Fig. 19C) (Álvarez-Parra *et al*., 2021b).

4.2.18. Orden Hemiptera

Los hemípteros son insectos hemimetábolos caracterizados por su aparato bucal perforador-succionador que facilita su alimentación por medio de la absorción de fluidos de plantas o animales (Schwertner *et al*., 2021). La mayoría de las especies de hemípteros son fitófagas, aunque se han documentado especies depredadoras y hematófagas (Schwertner *et al*., 2021). Se conocen más de 100.000 especies actuales, por lo que son el grupo de insectos hemimetábolos más diverso (Zhang, 2011). Entre los hemípteros, los pertenecientes al suborden Heteroptera se caracterizan por sus alas anteriores, llamadas hemiélitros, divididas en una sección proximal muy quitinizada y una sección distal membranosa, mientras que el resto de los hemípteros (anteriormente agrupados en el taxón, ahora considerado parafilético, Homoptera) poseen alas anteriores y posteriores completamente membranosas (Schwertner *et al*., 2021). Actualmente, se aceptan los subórdenes Sternorrhyncha, Coleorrhyncha, Auchenorryncha y Heteroptera (Johnson *et al*., 2018). Cabe destacar que se ha documentado comunicación vibracional acústica y no acústica en algunos grupos de hemípteros (Davranoglou *et al*., 2019, 2020). El registro fósil más antiguo conocido de hemípteros data del Carbonífero Superior (Nel *et al*., 2013).

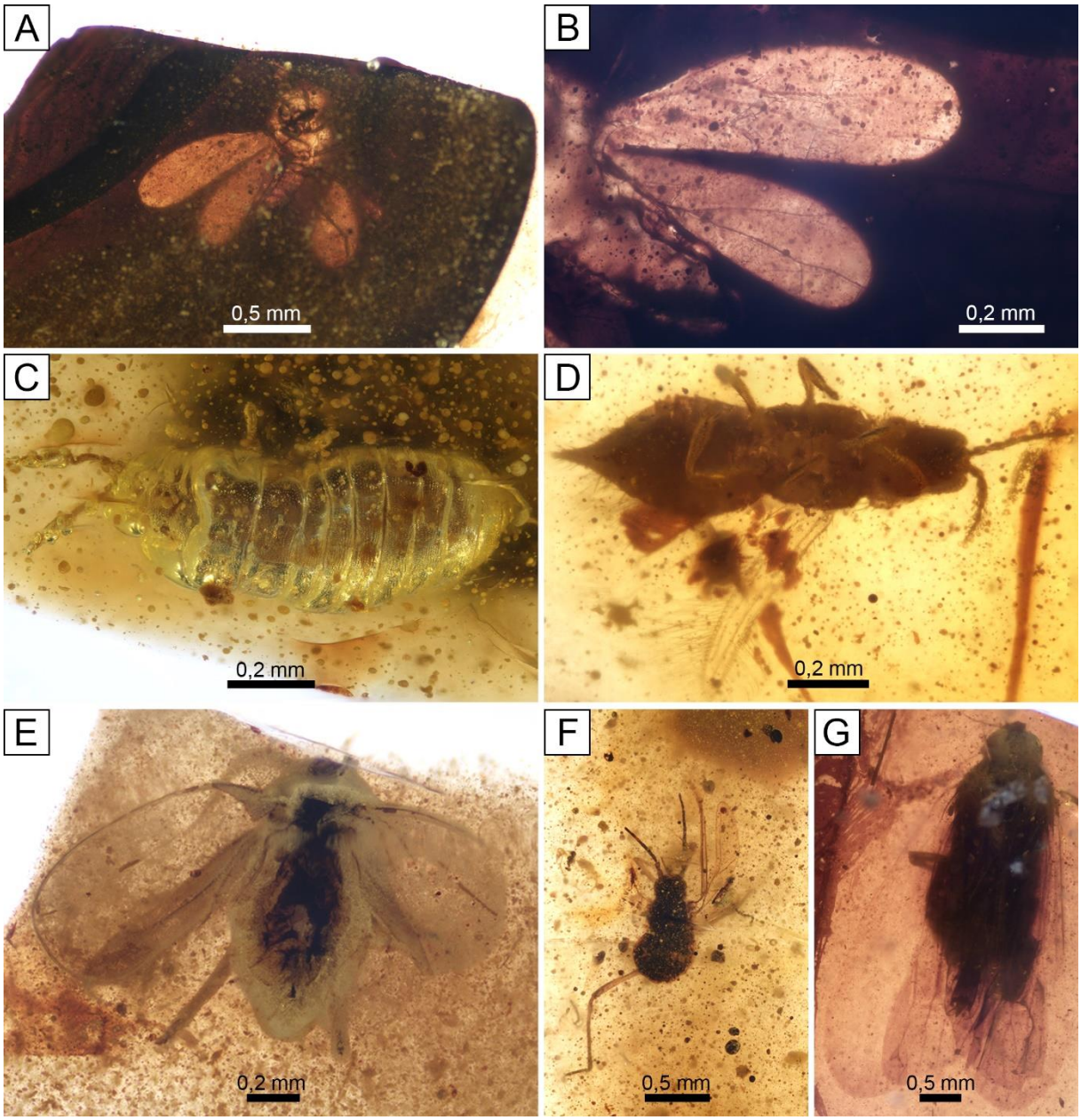

Figura 32. Ejemplares de †Lophioneurida, Thysanoptera y Hemiptera en los ámbares de la Cuenca del Maestrazgo. A) Ejemplar determinado como *Jantardachus* cf. *reductus* (†Lophioneurida: †Lophioneuridae) en el ámbar de San Just, MAP-7751; B) Alas de *Jantardachus* cf. *reductus* con la venación visible; C) Inmaduro de tisanóptero (Thysanoptera) en el ámbar de Ariño, AR-1-A-2019.114.2, imagen tomada de Álvarez-Parra *et al.* (2021b); D) Ejemplar de tisanóptero en el ámbar de Ariño, AR-1-A-2019.40, imagen tomada de Álvarez-Parra *et al.* (2021b); E) Ejemplar asignado a la subfamilia Aleurodicinae (Hemiptera: Aleirodidae) en el ámbar de Ariño, AR-1-A-2019.100.1, imagen tomada de Álvarez-Parra *et al.* (2021b); F) Ejemplar de Aphidoidea (Hemiptera) en el ámbar de Ariño, AR-1-A-2019.103, imagen tomada de Álvarez-Parra *et al.* (2021b); G) Ejemplar preliminarmente incluido en la familia Cixiidae (Hemiptera) en el ámbar de Arroyo de la Pascueta, CPT-3334.

En el ámbar de España se han hallado varios hemípteros, aunque muchos de ellos están pendientes de estudio. Se han descrito cinco especies en el ámbar de Peñacerrada I, una de ellas también presente en Peñacerrada II, pertenecientes a los subórdenes Sternorrhyncha (familia †Burmitaphididae) y Heteroptera (familias †Hispanocaderidae, Hydrometridae y Mesoveliidae) (Peñalver y Wegierek, 2008; Golub *et al*., 2012; Sánchez-García *et al*., 2016, 2017). En el ámbar de El Soplao se han identificado 16 ejemplares de los subórdenes Sternorrhyncha, Auchenorrhyncha y Heteroptera (Pérez de la Fuente, 2012). *Iberofoveopsis miguelesi* Peñalver & Szwedo, 2010 es la única especie de hemíptero descrita del ámbar de San Just (Peñalver y Szwedo, 2010). Se incluyó en la familia †Perforissidae (Auchenorrhyncha) y se observó la presencia de posibles órganos sensitivos en la cabeza y el tórax cuya función pudo ser la detección de humedad ambiental (Peñalver y Szwedo, 2010). Además, se han identificado otros 29 ejemplares de hemípteros en el ámbar de San Just, aunque se requiere su estudio para una precisa asignación taxonómica. Los hemípteros son escasos en el ámbar de Ariño y solo se han identificado cuatro ejemplares pertenecientes a Sternorrhyncha y otros dos indeterminados (Álvarez-Parra *et al*., 2021b). Tres de los esternorinchos se encuentran como sininclusiones en la misma pieza (AR-1-A-2019.100) y pertenecen a la subfamilia Aleurodicinae (Aleyrodidae) (Fig. 32E), mientras que el último es asignado a Aphidoidea (Fig. 32F) (Álvarez-Parra *et al*., 2021b). Además, un único hemíptero, que podría corresponder a la familia Cixiidae (Auchenorrhyncha), fue hallado en el ámbar de Arroyo de la Pascueta (CPT-3334) (Fig. 32G). Este ejemplar de Arroyo de la Pascueta, junto con otros Auchenorrhyncha del resto de ámbares de España están actualmente en estudio (Peñalver *et al*., 2021b).

4.2.19. Orden Raphidioptera

Los rafidiópteros son insectos holometábolos que se caracterizan por su protórax alargado, lo que explica su nombre común de moscas serpiente; además, las hembras tienen un ovopositor alargado (Aspöck, 2002). Curiosamente, el estadio pupal es móvil y depredador, al igual que la forma adulta (Aspöck, 2002). El registro fósil más antiguo de rafidióptero data del Jurásico y cabe destacar que la diversidad y disparidad de este grupo durante el Cretácico era mucho mayor que en la actualidad, que cuenta con solo unas 250 especies (Grimaldi y Engel, 2005). Su distribución actual se encuentra relegada a zonas templadas y frías del Hemisferio Norte, mientras que en el pasado los rafidiópteros tuvieron una distribución mucho mayor habitando zonas tropicales y el Hemisferio Sur (Grimaldi y Engel, 2005). Se han hallado representantes de este grupo en varios ámbares cretácicos y son relativamente abundantes en el ámbar de El Soplao. Hasta el momento, se han descrito una especie de la familia †Baissopteridae y dos especies y dos morfotipos indeterminados de la familia †Mesoraphidiidae de Peñacerrada I y tres especies y un morfotipo indeterminado de la familia

†Mesoraphidiidae de El Soplao (Pérez-de la Fuente *et al.*, 2010, 2012b). A pesar de la diversidad y abundancia de rafidiópteros en los ámbares de la Cuenca Vasco-Cantábrica, no se ha encontrado ningún ejemplar en el extenso registro de San Just. El único ejemplar de rafidióptero fósil en la Cuenca del Maestrazgo se trata de una larva (AP-11.2) en una pieza de ámbar de Arroyo de la Pascueta (Fig. 33A), y se corresponde con el único rafidióptero del ámbar de España que no es adulto, en estudio en colaboración con el paleoentomólogo Ricardo Pérez de la Fuente (Oxford University Museum of Natural History). El ejemplar se caracteriza por: antenas de tres segmentos con dos setas apicales, palpos cortos, ojos con cinco omatidios, sutura ecdisial claramente visible en la parte dorsal de la cápsula cefálica, protórax inclinado pero más corto que la cabeza (cabeza 1,5× más larga que el protórax), nueve segmentos abdominales, segmento abdominal 8 más largo y estrecho que los anteriores y segmentos abdominales cubiertos por setas. Las mandíbulas se pueden ver por transparencia del resto de piezas bucales. Es posible que corresponda a la familia †Mesoraphidiidae, al igual que otros ejemplares cretácicos, aunque se requiere de un estudio anatómico más detallado. Se han encontrado larvas de rafidióptero en ámbares del Líbano, Francia, Myanmar y Nueva Jersey en Estados Unidos (Engel, 2002; Perrichot y Engel, 2007; Grimaldi y Nascimbene, 2010; Haug *et al.*, 2020; Lu y Liu, 2021).

4.2.20. Orden Neuroptera

Los neurópteros son insectos holometábolos que en la actualidad poseen piezas bucales masticadoras y cuatro alas de similar longitud con venación compleja de estructura reticular compuesta por numerosas venas longitudinales y transversales (Aspöck *et al.*, 2012). Se conocen más de 5.800 especies actuales, la mayoría de ellas depredadoras, aunque se han documentado especies polinívoras (Zhang, 2011; Aspöck *et al.*, 2012). Sus larvas son depredadoras, caracterizadas por sus piezas bucales prominentes (Beutel *et al.*, 2010). Se agrupan en el superorden Neuropterida junto con Megaloptera y Raphidioptera (Engel *et al.*, 2018). Los ejemplares de neurópteros más antiguos conocidos datan del Pérmico (Ponomarenko y Shcherbakov, 2004). Los neurópteros son abundantes en el registro fósil del Cretácico, tanto en yacimientos de compresión como en ámbar (Makarkin *et al.*, 2012; Lu y Liu, 2021). En el ámbar de El Soplao se han descrito dos especies de las familias Berothidae y Coniopterygidae a partir de ejemplares adultos (Pérez-de la Fuente *et al.*, 2019, 2021), y una especie de la superfamilia Chrysopoidea a partir de un ejemplar inmaduro, este último mostrando evidencias de interacción planta-insecto y estrategia de camuflaje (Pérez-de la Fuente *et al.*, 2012a). Se han identificado una larva y cuatro adultos de la familia Berothidae en el ámbar de Peñacerrada I (Pérez-de la Fuente *et al.*, 2020, 2021).

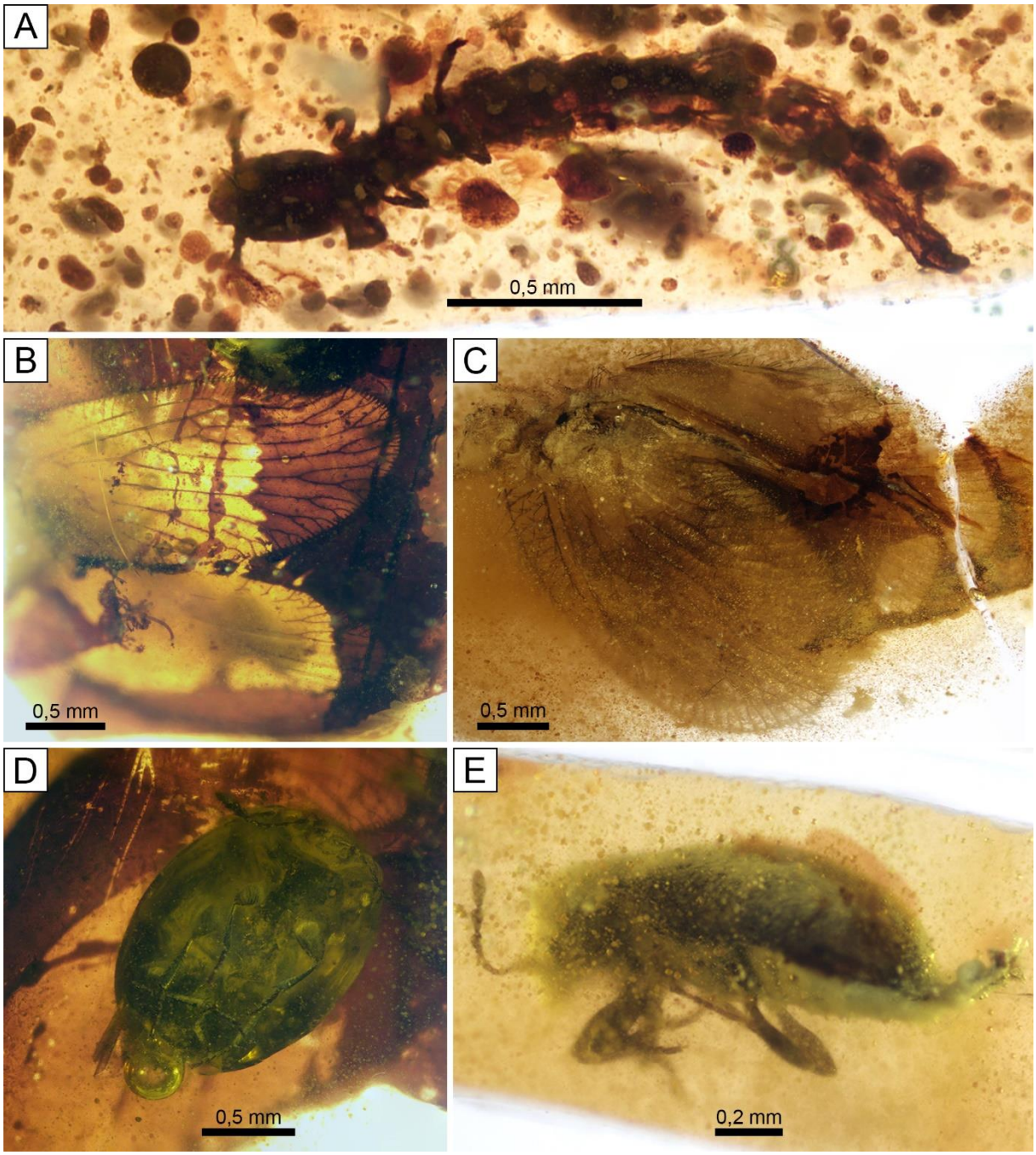

Figura 33. Ejemplares de Raphidioptera, Neuroptera y Coleoptera en los ámbares de la Cuenca del Maestrazgo. A) Larva de Raphidioptera en el ámbar de Arroyo de la Pascueta, AP-11.2; B) Restos alares preliminarmente identificados como pertenecientes a la subfamilia †Paradoxosisyrinae (Neuroptera: Sisyridae) en el ámbar de San Just, SJNB2021-32.1; C) Ejemplar asignado a la subfamilia †Paradoxosisyrinae en el ámbar de Ariño, AR-1-A-2019.128.1; D) Ejemplar de Coleoptera en el ámbar de San Just, SJNB2021-32.2; E) Ejemplar preliminarmente asignado a la familia Ptinidae (Coleoptera) en el ámbar de Ariño, AR-1-A-2019.44. Imágenes C y E tomadas de Álvarez-Parra *et al.* (2021b).

Se han hallado ocho ejemplares de neurópteros en el ámbar de San Just, entre ellos una larva que podría asignarse a la familia Berothidae, otra larva con afinidades a las superfamilias

Mantispoidea y Dilaroidea (Pérez-de la Fuente *et al.*, 2020), unos restos alares que podrían estar relacionados con la subfamilia †Paradoxosisyrinae dentro de la familia Sisyridae (Fig. 33B) y un adulto de la familia Mantispidae descrito como *Aragomantispa lacerata* Pérez-de la Fuente & Peñalver, 2019, el cual ha proporcionado información clave sobre la evolución de las patas anteriores raptoras características de los mantíspidos (Pérez-de la Fuente y Peñalver, 2019). Los neurópteros del ámbar de Ariño están representados por dos impresiones alares en la superficie del ámbar que podrían corresponder a miembros de la familia Berothidae y un adulto completo (AR-1-A-2019.128.1) perteneciente a la subfamilia †Paradoxosisyrinae (Fig. 33C) (Álvarez-Parra *et al.*, 2021b). Este último ejemplar está actualmente en estudio, junto con otros ejemplares de la misma subfamilia de otros ámbares de España, en colaboración con Ricardo Pérez de la Fuente.

4.2.21. Orden Coleoptera

Los coleópteros, conocidos comúnmente con el nombre de escarabajos, son insectos holometábolos que habitan en una amplia diversidad de ecosistemas por todo el mundo y muestran una enorme disparidad morfológica (Crowson, 1981). Se trata del grupo de insectos más diverso, con más de 380.000 especies conocidas, aunque se estima que aún quedan muchas por descubrir (Ślipiński *et al.*, 2011). La mayoría de las especies son herbívoras y algunas de ellas pueden llegar a considerarse plagas (Crowson, 1981), además hay especies que actúan como polinizadores tanto de gimnospermas como de angiospermas. Son considerados como uno de los primeros grupos de polinizadores (Peris *et al.*, 2017, 2020). Su estructura anatómica más característica es la presencia de alas anteriores endurecidas, llamadas élitros (Crowson, 1981). El registro fósil más antiguo de coleópteros procede del Pérmico Inferior, aunque los estudios filogenéticos estiman su origen en el Carbonífero (McKenna *et al.*, 2019). Se conocen muchas especies de coleópteros fósiles de diferentes ámbares cretácicos del mundo (Peris, 2020; Peris y Rust, 2020). En los ámbares de la península ibérica se han identificado ejemplares que han sido estudiados, o están en estudio, por el paleontólogo David Peris (Universitat de Barcelona) que realizó su Tesis Doctoral sobre este grupo de insectos (Peris, 2015). Se han hallado 23 ejemplares de coleópteros en el ámbar de San Just (Fig. 33D), entre ellos las especies *Arra legalovi* Peris, Davis & Delclòs, 2014 de la familia Nemonychidae (también presente en el ámbar de El Soplao) y *Actenobius magneoculus* Peris, Philips & Delclòs, 2015 de la familia Ptinidae (Peris *et al.*, 2014, 2015). La especie *A. legalovi* pudo haberse alimentado de polen o fluidos de gimnospermas Araucariaceae (Peris *et al.*, 2014). Además, en el ámbar de San Just se han identificado las familias Cryptophagidae, Dermestidae, Eucinetidae, Silvanidae y Staphylinidae (Peris *et al.*, 2016). Cabe destacar el hallazgo en los ámbares de El Soplao, Peñacerrada I y San Just de larvas de coleóptero

identificadas como posibles miembros de Dermestidae en asociación con plumas de dinosaurio que han llevado a inferir una interacción simbiótica entre estas larvas y los dinosaurios (Peñalver *et al*., enviado). En el ámbar de Ariño se han encontrado cinco ejemplares de coleópteros con deficiente conservación (Álvarez-Parra *et al*., 2021b), aunque dos de ellos se podrían identificar como Ptinidae (AR-1-A-2019.44) (Fig. 33E) y Cantharidae (AR-1-A-2019.118.1).

4.2.22. Orden Hymenoptera

Los himenópteros son insectos holometábolos entre los que se incluyen las avispas, las abejas, los abejorros y las hormigas. Este grupo se corresponde con el cuarto orden de insectos más diverso, con más de 150.000 especies actuales descritas (Aguiar *et al*., 2013). La mayoría de los himenópteros poseen piezas bucales masticadoras, aunque algunas especies tienen una probóscide que les permite alimentarse de néctar (Goulet y Huber, 1993; Grimaldi y Engel, 2005). Una de las características anatómicas de los himenópteros es la presencia de hamuli, diminutos ganchos situados en las alas posteriores que permiten su acoplamiento con las alas anteriores (Grimaldi y Engel, 2005). Al final del abdomen de las hembras se encuentra el ovopositor, que en algunos grupos ha evolucionado en un aguijón venenoso (Goulet y Huber, 1993; Grimaldi y Engel, 2005). Muestran una amplia distribución y cumplen importantes roles en los ecosistemas, además se conocen especies herbívoras, depredadoras, parasitoides y polinizadoras (Peters *et al*., 2017). Los estudios filogenéticos sitúan a Hymenoptera como grupo hermano del resto de insectos holometábolos (Misof *et al*., 2014). Históricamente, se han considerado los grupos 'Symphyta' y Apocrita, los segundos caracterizados por un estrechamiento llamado peciolo entre el primer segmento del abdomen (fusionado al tórax) y el segundo segmento del abdomen (Sharkey *et al*., 2012). Dentro de los Apocrita, se han diferenciado los 'Parasitica' y los Aculeata, los últimos caracterizados por la presencia de un aguijón en las hembras (Sharkey *et al*., 2012). Sin embargo, tanto 'Symphyta' como 'Parasitica' han resultado ser agrupaciones parafiléticas (Sharkey *et al*., 2012). Los 'Parasitica' fueron agrupados debido a su biología parasitoide, aunque algunos grupos de Aculeata también muestran este modo de vida (Peters *et al*., 2017).

El parasitoidismo es un tipo de parasitismo, es decir, una interacción biológica en la que un organismo se beneficia mientras que el otro quedo perjudicado, por el cual una fase adulta tiene vida libre dispersiva, pero su fase larvaria es parasita y se alimenta de su huésped (u hospedador) tras la ovoposición, hasta llevarlo o no a su muerte, para finalmente emerger en fase adulta (Labandeira y Li, 2021). En el caso de que la larva del parasitoide se desarrolle fuera del huésped se denomina ectoparasitoidismo, mientras que si la larva se desarrolla en el interior del huésped se trata de endoparasitoidismo (Labandeira y Li, 2021). Si el huésped

permanece vivo y puede alimentarse y continuar su desarrollo tras la ovoposición del parasitoide se denomina parasitoidismo koinobionte y usualmente es la salida del adulto la que produce la muerte del huésped (Labandeira y Li, 2021). En cambio, si el huésped muere o es paralizado, sin poder continuar su desarrollo, tras la ovoposición del parasitoide, se corresponde con parasitoidismo idiobionte (Labandeira y Li, 2021). Cabe destacar que se pueden dar varios niveles de parasitoidismo (hiperparasitoidismo), es decir, las larvas de un parasitoide se desarrollan en larvas de otro parasitoide (Poelman *et al.*, 2022). Se conocen especies parasitoides que pueden llevar a cabo la ovoposición en un huésped durante la fase de huevo, larva, pupa o adulto (Labandeira y Li, 2021). Hasta 10 órdenes de insectos contienen miembros parasitoides, pero el 75% de las especies de insectos parasitoides forman parte de Hymenoptera, comúnmente llamadas avispas parásitas o parasitoides (Quicke, 1997; Labandeira y Li, 2021). Se ha debatido ampliamente sobre el origen evolutivo del parasitoidismo en Hymenoptera y se considera que surgió una sola vez, por lo que todas las avispas parasitoides serían descendientes de un linaje que apareció en el Pérmico (Peters *et al.*, 2017). Otros modos de vida presentes en representantes de Apocrita surgieron secundariamente (Quicke, 1997; Peters et al., 2017). Es posible que un representante de 'Symphyta', los cuales usualmente ponen sus huevos en madera, cambiase hacia una ovoposición en o sobre larvas de escarabajos que habitasen en la madera (Quicke, 1997). Un análisis filogenético indica que los grupos más diversos de avispas parasitoides forman el clado Parasitoida (Peters *et al.*, 2017). El parasitoidismo ha podido llevar a la reducción extrema de tamaño en algunos himenópteros, como el que se da en los grupos de Chalcidoidea, en el que se incluye el insecto adulto más pequeño conocido con 0,139-0,240 mm de longitud (machos de *Dicopomorpha echmepterygis* Mockford, 1997, Mymaridae), parasitoide de huevos de psocópteros (Mockford, 1997).

Hymenoptera es uno de los grupos de insectos con mayor número de especies fósiles conocidas (Aguiar *et al.*, 2013). Su registro fósil más antiguo data del Triásico (Grimaldi y Engel, 2005). Los himenópteros son uno de los grupos de insectos más abundantes y diversos en ámbar cretácico (Zhang *et al.*, 2018; Rasnitsyn y Öhm-Kühnle, 2021). Los himenópteros también son numerosos en los ámbares de España y se ha comprobado su gran diversidad, a pesar de ello, muchos ejemplares aún no se han estudiado taxonómicamente. La familia Scelionidae (Platygastroidea) se ha documentado en los ámbares de El Caleyu y La Rodada (Arbizu *et al.*, 1999; Peñalver *et al.*, 2018b). Algunos autores consideran esta familia como una subfamilia dentro de Platygastridae, dado que podría ser polifilética (Sharkey, 2007; Murphy *et al.*, 2007). Sin embargo, aquí se prefiere considerar Scelionidae como familia, tras seguir el criterio en artículos más recientes (Zhang *et al.*, 2018; Talamas *et al.*, 2019; Rasnitsyn y Öhm-Kühnle, 2021).

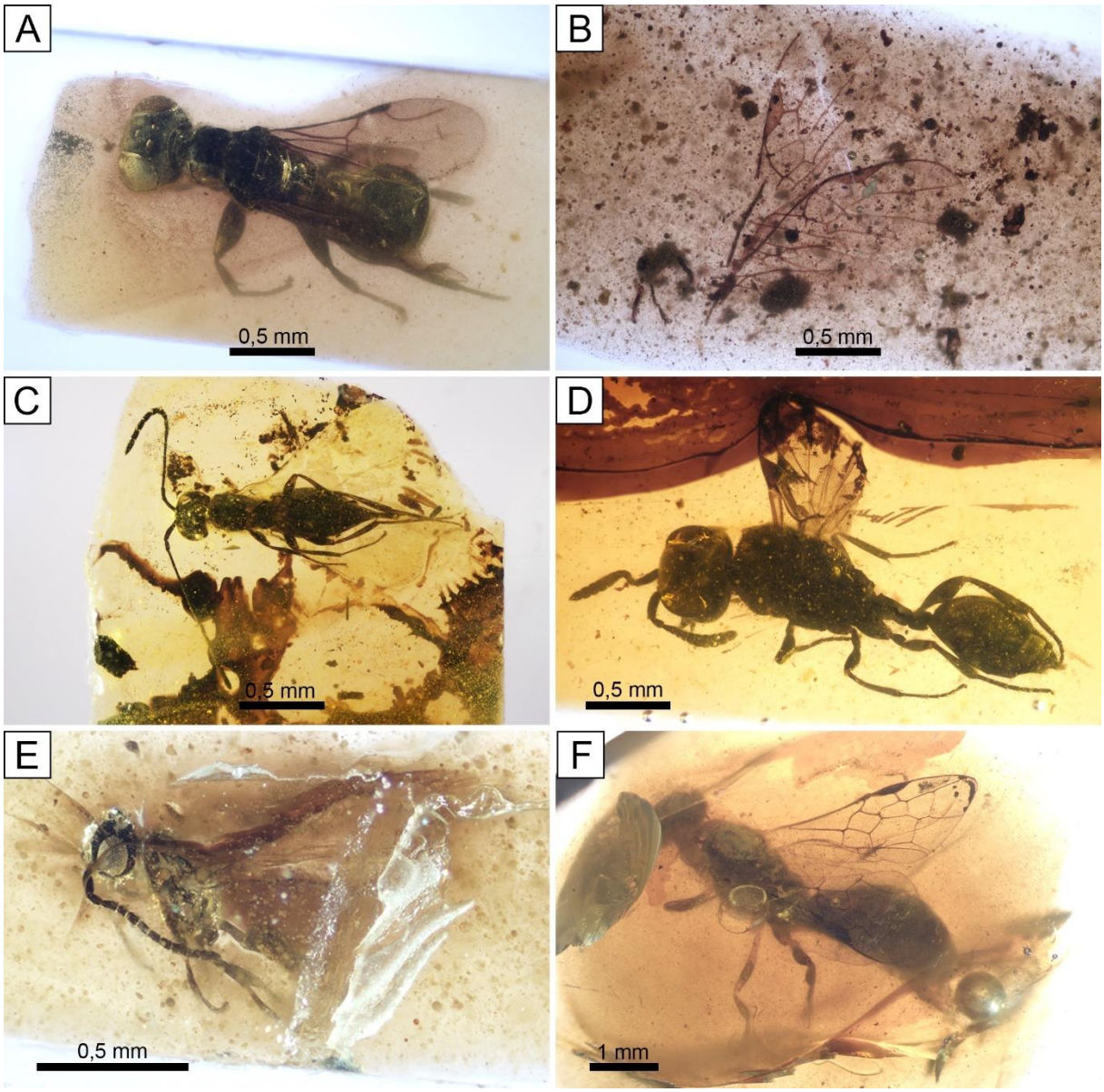

Figura 34. Himenópteros (Hymenoptera) en el ámbar de San Just. A) Ejemplar de la familia †Stigmaphronidae, CPT-4157; B) Holotipo de *Utrillabracon electropteron* (Braconidae), MAP-7819; C) Ejemplar asignado a la especie *Mymaropsis turolensis* (†Spathiopterygidae), CPT-4097, imagen tomada de Santer *et al.* (2022); D) Ejemplar perteneciente al género *Serphites* (†Serphitidae), SJNB2021-17, imagen tomada de Álvarez-Parra *et al.* (en preparación 2); E) Ejemplar que podría ser incluido en †Serphitoidea o Mymarommatoidea, CPT-4179; F) Ejemplar preliminarmente considerado como perteneciente a la familia Sapygidae, SJ-10-09.

En el ámbar de El Soplao, en relación con el grupo 'Parasitica', se han identificado cuatro especies, una en cada una de las familias Evaniidae (Evanioidea), Megalyridae (Megalyroidea), Mymarommatidae (Mymarommatoidea) y †Serphitidae (†Serphitoidea) (Ortega-Blanco *et al.*, 2011d, e; Pérez-de la Fuente *et al.*, 2012c, d), y también se ha indicado la presencia de las familias Braconidae (Ichneumonoidea), †Maimetshidae (Trigonalyoidea), Scelionidae, †Stigmaphronidae (superfamilia *incertae sedis*), y quizás Mymaridae (Chalcidoidea) (Pérez de

la Fuente, 2012). Además, durante la Tesis Doctoral se ha identificado un ejemplar que muy posiblemente pertenezca a la familia Rotoitidae (Chalcidoidea), conocida en la actualidad solo por dos especies presentes en Chile y Nueva Zelanda, aunque con una mayor diversidad durante el Cretácico (Gumovsky *et al.*, 2018). Las únicas tres familias de Aculeata reconocidas en el ámbar de El Soplao son Bethylidae, Chrysididae (ambas en Chrysidoidea) y Tiphiidae (Tiphioidea) (Pérez de la Fuente, 2012). El ámbar de Peñacerrada I es el que contiene el mayor número de familias y especies de Hymenoptera entre los ámbares de España, con un total de 18 familias y 39 especies identificadas, dado que fue la línea de investigación del investigador Jaume Ortega Blanco (Ortega Blanco, 2010). Entre ellas se incluye la única especie de 'Symphyta' del ámbar de España, perteneciente a la familia Anaxyelidae (Anaxyeloidea) (Ortega-Blanco *et al.*, 2008), cuyos representantes actuales tienen la particularidad de que las hembras ponen los huevos en madera recién quemada. En relación con 'Parasitica', se han reconocido una especie de †Alavarommatidae (Mymarommatoidea), dos especies de Braconidae, una especie de Diapriidae (Diaprioidea), dos especies de Evaniidae, una especie de †Gallorommatidae (Mymarommatoidea), dos especies de †Maimetshidae, dos especies de Megalyridae, una especie de †Proteropsceliopsidae (Platygastroidea), una especie de Mymarommatidae, una especie de †Radiophronidae (superfamilia *incertae sedis*), ocho especies de Scelionidae, dos especies de †Serphitidae (†Serphitoidea), una especie de †Spathiopterygidae (Diaprioidea) y siete especies de †Stigmaphronidae (Ortega-Blanco *et al.*, 2009, 2010, 2011a, b, d, e, 2014; Perrichot, 2009; Peñalver *et al.*, 2010; Perrichot *et al.*, 2011; Engel *et al.*, 2013b). En cuanto a Aculeata, se han identificado tres especies de Bethylidae, una especie de Embolemidae y una especie de Scolebythidae, las tres pertenecientes a Chrysidoidea (Ortega-Blanco *et al.*, 2011c; Engel *et al.*, 2013a; Ortega-Blanco y Engel, 2013).

Los himenópteros están presentes en los cuatro yacimientos de ámbar con bioinclusiones de la Cuenca del Maestrazgo. El registro de este grupo en el ámbar de San Just es muy numeroso, ya que incluye 111 ejemplares, y solo se ha estudiado taxonómicamente una pequeña parte. En este ámbar se han descrito siete especies de cinco familias (Braconidae, Evaniidae, †Gallorommatidae, †Serphitidae y †Spathiopterygidae), además de la presencia de dos especies de otras familias (†Alavarommatidae y †Stigmaphronidae). Los miembros de la familia Evaniidae, dentro del grupo 'Parasitica', son parasitoides de cucarachas, se caracterizan por un tener un estrecho peciolo en la región posterodorsal del mesosoma y se encuentran representados en el ámbar de San Just por las especies *Cretevania alcalai* Peñalver, Ortega-Blanco, Nel & Delclòs, 2010 y *Cretevania montoyai* Peñalver, Ortega-Blanco, Nel & Delclòs, 2010 (Peñalver *et al.*, 2010). La familia †Stigmaphronidae se conoce únicamente por ejemplares cretácicos y su biología es desconocida, aunque se sugiere que fueron parasitoides (Ortega-Blanco *et al.*, 2011b). En el ámbar de San Just se ha identificado la especie *Burmaphron jentilak* Ortega-Blanco, Delclòs & Engel, 2011 (Ortega-Blanco *et al.*, 2011), y es

posible que otros cuatro ejemplares también se correspondan con esta familia (Fig. 34A). A pesar de que tanto †Stigmaphronidae como †Radiophronidae se consideraron miembros de la superfamilia Ceraphronoidea, un estudio comparativo ha demostrado que ambas familias no muestran los caracteres diagnósticos de Ceraphronoidea y es posible que sean miembros de Aculeata, e incluso es probable que †Stigmaphronidae sea una agrupación polifilética (Mikó *et al.*, 2018). Las familias de las otras seis especies descritas se incluyen en el clado Parasitoida (Peters *et al.*, 2017). La familia Braconidae es la segunda entre los himenópteros con un mayor número de especies actuales descritas, solo por detrás de Ichneumonidae, ambas incluidas en Ichneumonoidea (Chen y van Achterberg, 2019). Los bracónidos son parasitoides de larvas de Coleoptera, Diptera, Lepidoptera y, más raramente, otros insectos, e incluso de algunos adultos (Chen y van Achterberg, 2019). En San Just están representados por la especie *Utrillabracon electropteron* Álvarez-Parra & Engel, 2022 (Fig. 34B), asignada a la subfamilia †Protorhyssalinae (Álvarez-Parra *et al.*, 2022a). Es probable que esta subfamilia sea un grupo parafilético o polifilético, pero se requiere un análisis filogenético que lo confirme (Álvarez-Parra *et al.*, 2022a). La familia †Spathiopterygidae solo incluye especies conocidas en ámbares cretácicos y podría estar relacionada con la familia Diapriidae dentro la superfamilia Diaprioidea, aunque muestra caracteres anatómicos peculiares y su biología se desconoce (Engel *et al.*, 2013a; Santer *et al.*, 2022). En el ámbar de San Just se han descrito las especies *Mymaropsis turolensis* Engel & Ortega-Blanco, 2013, conocida por un posible macho y una hembra (Fig. 34C), y *Diameneura marveni* Santer & Álvarez-Parra, 2022 (Santer *et al.*, 2022). En esta familia las alas posteriores se encuentran muy reducidas o incluso ausentes en algunas especies, algo poco común en Hymenoptera (Santer *et al.*, 2022). Las familias †Alavarommatidae, †Dipterommatidae, †Galloromatidae, Mymarommatidae (las cuatro en Mymarommatoidea), †Archaeoserphitidae y †Serphitidae (estas dos últimas en †Serphitoidea), forman el clado Bipetiolarida, cuya característica principal es la presencia de un peciolo dividido en dos segmentos (Engel, 2015). En el ámbar de San Just se describieron las especies *Cretaceomma turolensis* (Ortega-Blanco, Peñalver, Delclòs & Engel, 2011) (†Gallorommatidae) (Ortega-Blanco *et al.*, 2011e), originalmente en el género *Galloromma* (Ortega-Blanco *et al.*, 2011e; Rasnitsyn *et al.*, 2022), y *Serphites silban* Ortega-Blanco, Delclòs, Peñalver & Engel, 2011 (†Serphitidae) (Ortega-Blanco *et al.* 2011d), además de la presencia de la especie *Alavaromma orchamum* Ortega-Blanco, Peñalver, Delclòs & Engel, 2011 (†Alavarommatidae), descrita a partir de un ejemplar del ámbar de Peñacerrada I (Ortega-Blanco *et al.*, 2011e). La biología de estas familias, solo presentes en ámbares cretácicos, es desconocida (Engel, 2015). La única familia viviente de Bipetiolarida, Mymarommatidae, incluye al menos una especie parasitoide de huevos de psocópteros (Honsberger *et al.*, 2022).

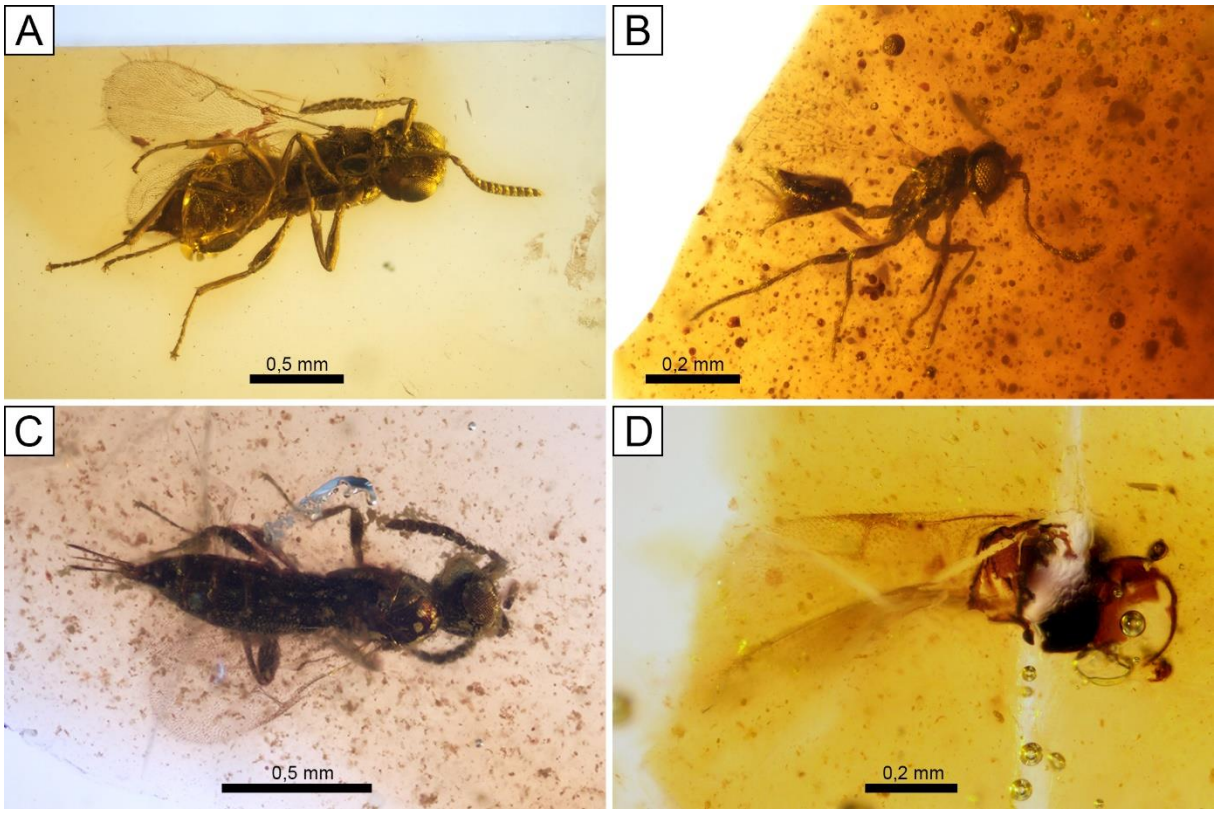

Figura 35. Himenópteros (Hymenoptera) en los ámbares de la Cuenca del Maestrazgo. A) Ejemplar de la familia Scelionidae en el ámbar de Ariño, AR-1-A-2019.95.3, imagen tomada de Álvarez-Parra *et al.* (2021b); B) Ejemplar preliminarmente determinado como *Cretaceomma turolensis* (†Gallorommatidae) en el ámbar de Ariño, AR-1-A-2019.61, imagen tomada de Álvarez-Parra *et al.* (2021b); C) Ejemplar asignado a la familia Scelionidae en el ámbar de Arroyo de la Pascueta, CPT-3338; D) Ejemplar asignado a la familia Scelionidae en el ámbar de La Hoya, LH-2.

Se ha iniciado el estudio de tres ejemplares del ámbar de San Just asignados a †Serphitidae (Álvarez-Parra *et al.*, 2021c, en preparación 2), los cuales se han determinado preliminarmente como *Serphites* sp. (SJ-10-03), una nueva especie de *Serphites* (SJNB2012-17) (Fig. 34D) y un nuevo género y especie (SJ-10-12). Un ejemplar (CPT-4179) se encontraba originalmente etiquetado como Scelionidae, sin embargo, tras un examen detallado se ha identificado como un miembro de Bipetiolarida, ya que se pueden observar los dos segmentos del peciolo (Fig. 34E). Este ejemplar posee varias características peculiares, ya que parecen "intermedias" entre Mymarommatoidea y †Serphitoidea. Su tamaño se encuentra entre los de los ejemplares de †Alavarommatidae y †Archaeoserphitidae, las dos familias consideradas más "primitivas" en sus correspondientes superfamilias. Su habitus recuerda al de las especies de Mymarommatoidea, a pesar de ello, posee algunas venas y pterostigma en las alas anteriores (ausentes en Mymarommatoidea) y alas posteriores desarrolladas (muy reducidas en Mymarommatoidea). El número de segmentos antenales no se corresponde con el de †Archaeoserphitidae. En conclusión, es posible que o bien este ejemplar se asigne a la familia

†Archaeoserphitidae, o que pertenezca a una nueva familia de Mymarommatoidea. Se han identificado preliminarmente 65 ejemplares como miembros de Scelionidae, aunque se requiere un estudio taxonómico comparativo. Esta familia es numerosa en ámbares cretácicos (Zhang *et al.*, 2018) y sus representantes actuales son parasitoides idiobiontes de huevos de arañas y diferentes órdenes de insectos (Goulet y Huber, 1993). Entre los Aculeata se ha hallado un ejemplar asignado a la familia Sierolomorphidae (Tiphioidea), dos a la familia Bethylidae y tres que podrían pertenecer a Sapygidae (Pompiloidea) o a otras familias filogenéticamente cercanas (Fig. 34F). La biología de Sierolomorphidae es poco conocida, aunque se considera que podrían ser ectoparasitoides de insectos (Goulet y Huber, 1993). La familia Bethylidae es muy numerosa en la actualidad, son parasitoides principalmente de larvas de Coleoptera y Lepidoptera, y se conocen formas adultas depredadoras (Goulet y Huber, 1993). Se conocen pocos ejemplares fósiles de Sapygidae y los representantes actuales de la familia son cleptoparasitoides de abejas de las subfamilias Megachilinae (Megachilidae) y Apinae (Apidae), es decir, depositan sus huevos en nidos de estas abejas y la larva se alimenta tanto de la larva huésped como del alimento proporcionado por la abeja adulta (Bennet y Engel, 2005).

En el ámbar de Ariño se han identificado 34 himenópteros, la mayoría de ellos mal conservados o incompletos (Álvarez-Parra *et al.*, 2021b). Entre ellos, 14 ejemplares se han asignado preliminarmente a Scelionidae (Fig. 35A), tres a †Stigmaphronidae, tres a †Serphitidae, uno a †Gallorommatidae y uno a Mymarommatoidea. Los tres †Serphitidae, actualmente en estudio junto con los del ámbar de San Just, posiblemente se describan como una nueva especie del género *Serphites* (Álvarez-Parra *et al.*, 2021c, en preparación 2). El representante de Gallorommatidae muestra un morfotipo similar al de la especie del ámbar de San Just *Cretaceomma turolensis* (Álvarez-Parra *et al.*, 2021b), por lo que es posible que se trate de la misma especie o una nueva especie del mismo género (Fig. 35B). Arroyo de la Pascueta es localidad tipo de la especie *Cretevania rubusensis* Peñalver, Ortega-Blanco, Nel & Delclòs, 2010, de la familia Evaniidae (Peñalver *et al.*, 2010). Además, se han identificado cuatro representantes de Scelionidae (Fig. 35C). Por último, en el ámbar de La Hoya también se ha hallado un ejemplar de la familia Scelionidae (Fig. 35D).

4.2.23. Orden Diptera

Los dípteros son insectos holometábolos caracterizados por la presencia de únicamente las alas anteriores, ya que las anteriores se encuentran transformadas en halterios, estructuras relacionadas con el movimiento durante el vuelo (McAlpine, 1981; Yeates y Wiegmann, 2005). Son uno de los grupos de insectos más conocidos y estudiados, ya que se consideran el segundo orden de insectos más diverso con alrededor de 160.000 especies descritas con modos de vida

muy diversos y distribuidas ampliamente por hábitats terrestres y acuáticos, e incluso marinos (Yeates y Wiegmann, 2005; Zhang, 2011; Pak *et al.*, 2021). Se conocen especies detritívoras, herbívoras, carroñeras y depredadoras, además algunas han desarrollado polinivoría y hematofagia (Yeates y Wiegmann, 2005). Los dípteros se consideran muy importantes por su implicación en plagas, polinización y transmisión de enfermedades (Ssymank *et al.*, 2008; Badii *et al.*, 2015; Arellano *et al.*, 2022). Tradicionalmente, los dípteros se han dividido en el taxón parafilético 'Nematocera' y el clado Brachycera (Yeates *et al.*, 2007). La sistemática a nivel suprafamiliar de los dípteros es inestable y está en continua reorganización (Yeates *et al.*, 2007; Zhang *et al.*, 2022).

Los dípteros más antiguos conocidos datan del Triásico Medio (Peñalver *et al.*, en prensa). Al igual que en otros ámbares cretácicos, este grupo es abundante y diverso en el ámbar de España, y se han hallado representantes en ámbares de nueve yacimientos de la península ibérica. Un díptero nematócero indeterminado es la única bioinclusión conocida en ámbar de Portugal (Peñalver *et al.*, 2018a). Una especie de la familia Atelestidae fue descrita en el ámbar de El Caleyu (Peñalver y Arillo, 2007). En el ámbar de El Soplao se han registrado ejemplares de 12 familias (Atelestidae, Cecidomyiidae, Ceratopogonidae, †Chimeromyiidae, Chironomidae, Dolichopodidae, Hybotidae, Phoridae, Psychodidae, Ptychopteridae, Rhagionidae y †Zhangsolvidae) e identificado ocho especies (Pérez-de la Fuente *et al.*, 2011; Pérez de la Fuente, 2012; Arillo *et al.*, 2015; Lukashevich y Arillo, 2016; Peñalver *et al.*, 2022b). El ámbar de Peñacerrada I ha proporcionado registro de 19 familias (Atelestidae, Cecidomyiidae, Ceratopogonidae, †Chimeromyiidae, Chironomidae, Dolichopodidae, Ironomyiidae, Keroplatidae, Limoniidae, Lonchopteridae, Mycetophilidae, Phoridae, Psychodidae. Rhagionidae, Stratiomyidae, Tanyderidae, †Tethepomyiidae, Xylomyidae y Xylophagidae) y se han identificado 21 especies (Szadziewski y Arillo, 1998, 2003; Arillo y Mostovski, 1999; Waters y Arillo, 1999; Arillo y Nel, 2000; Blagoderov y Arillo, 2002; Grimaldi y Arillo, 2008; Grimaldi *et al.*, 2009, 2011; Skibińska *et al.*, 2017; Kania-Kłosok *et al.*, 2021a, b), mientras que en Peñacerrada II solo se ha descrito una especie de la familia Limoniidae (Krzemiński y Arillo, 2007). Este orden también se ha identificado en los ámbares de San Just (11 familias), Ariño (siete familias), Arroyo de la Pascueta (dos familias) y La Hoya (una familia).

El yacimiento de San Just es la localidad tipo de seis especies de dípteros. Además, se ha confirmado la presencia de otras dos especies. El registro total de dípteros del ámbar de San Just es de 105 ejemplares. Entre los nematóceros se encuentran representadas las familias Ceratopogonidae, Chironomidae (ambas en el infraorden Culicomorpha), Anisopodidae, †Archizelmiridae, Keroplatidae, Mycetophilidae (las cuatro en el infraorden Bibionomorpha), Scatopsidae (infraorden Psychodomorpha) y Limoniidae (infraorden Tipulomorpha). Los ceratopogónidos son habitantes comunes de hábitats con elevada humedad, además, las

hembras de algunas especies se caracterizan por la hematofagia como modo de alimentación (Pérez-de la Fuente *et al*., 2011). En el ámbar de San Just se han identificado 26 ceratopogónidos y se han identificado las especies *Leptoconops zherikhini* Szadziewski & Arillo, 2003, *Archiculicoides skalskii* (Szadziewski & Arillo, 1998) [especie incluida en el género *Gerontodacus* según Borkent (2019)], *Protoculicoides hispanicus* Szadziewski & Arillo, 2016 y *Protoculicodes sanjusti* Szadziewski & Arillo, 2016 [ambas especies incluidas en el género *Atriculicoides* según Borkent (2019)] (Arillo *et al*., 2008a; Szadziewski *et al*., 2016). La especie *A. skalskii* está presente también tanto en el ámbar de El Soplao como en el de Peñacerrada I (Szadziewski y Arillo, 1998; Pérez-de la fuente *et al*., 2011), y *L. zherikhini* se describió inicialmente en el ámbar de Peñacerrada I (Szadziewski y Arillo, 2003). Se han hallado 13 quironómidos, aunque por el momento no se han estudiado taxonómicamente. El ámbar de San Just ha proporcionado dos ejemplares de la familia †Archizelmiridae, grupo hallado raramente en ámbar. Estos ejemplares se describieron como *Burmazelmira grimaldii* Arillo, Blagoderov & Peñalver, 2018 y, curiosamente, uno de ellos mostraba un ácaro *Leptus* sp. adherido a una de sus patas, lo que evidencia una relación de parasitismo (Arillo *et al*., 2018). Esta familia ha sido incluida en la superfamilia Sciaroidea, aunque las relaciones filogenéticas con otras familias son poco claras y su biología es desconocida (Grimaldi *et al*., 2003). Las familias Anisopodidae (un ejemplar), Keroplatidae (cuatro ejemplares), Mycetophilidae (un ejemplar) y Scatopsidae (un ejemplar), aunque han sido identificadas, aun no se ha iniciado el estudio taxonómico. La familia Limoniidae se encuentra representada por la especie *Helius turolensis* Kania-Kłosok, Krzemiński & Arillo, 2021, cuyo género contiene especies vivientes de áreas bajo clima cálido, y pudo alimentarse de néctar o polen (Kania-Kłosok *et al*., 2021a). En relación con los braquíceros, se han identificado las familias Rhagionidae (en el infraorden Tabanomorpha), Dolichopodidae, †Chimeromyiidae, Lonchopteridae y Phoridae (las cuatro en el clado Eremoneura). La familia Rhagionidae está representada por cinco ejemplares y dos de ellos se han identificado como *Litoleptis fossilis* Arillo, Peñalver & García-Gimeno, 2009 (originalmente adscrito a la familia Spaniidae), que pudo ser hematófaga (Arillo *et al*., 2009a). Nueve ejemplares han sido identificados como pertenecientes a la familia Dolichopodidae, todos ellos asignados al género *Microphorites*, aunque solo uno de ellos se ha descrito como *Microphorites utrillensis* Peñalver, 2008 (Arillo *et al*., 2008a). Este género extinto se ha asociado a un ambiente de playa arenosa en la costa bajo clima cálido (Nel *et al*., 2004; Arillo *et al*., 2008a). Se han hallado dos ejemplares de la familia †Chimeromyiidae, conocida únicamente por ejemplares cretácicos. La posición filogenética de esta familia entre los eremoneuros es imprecisa y su paleobiología es desconocida. Un ejemplar recientemente descubierto (SJNB2021-37) muestra una conservación excepcional y de forma preliminar se ha determinado como *Chimeromyia alava* Grimaldi & Arillo, 2009 (Fig. 36A), especie presente en el ámbar de Peñacerrada I (Grimaldi

et al., 2009), a partir de las similitudes en la genitalia masculina y la venación alar; a pesar de ello, se está estudiando en detalle en colaboración con Antonio Arillo y Mónica Solórzano-Kraemer (Senckenberg Forschungsinstitut und Naturmuseum) y es posible que se describa como una nueva especie. Por último, las familias Lonchopteridae y Phoridae, pertenecientes al clado Cyclorrhapha dentro de Eremoneura, se han identificado preliminarmente a partir de uno y tres ejemplares respectivamente, los cuales aún no han sido estudiados.

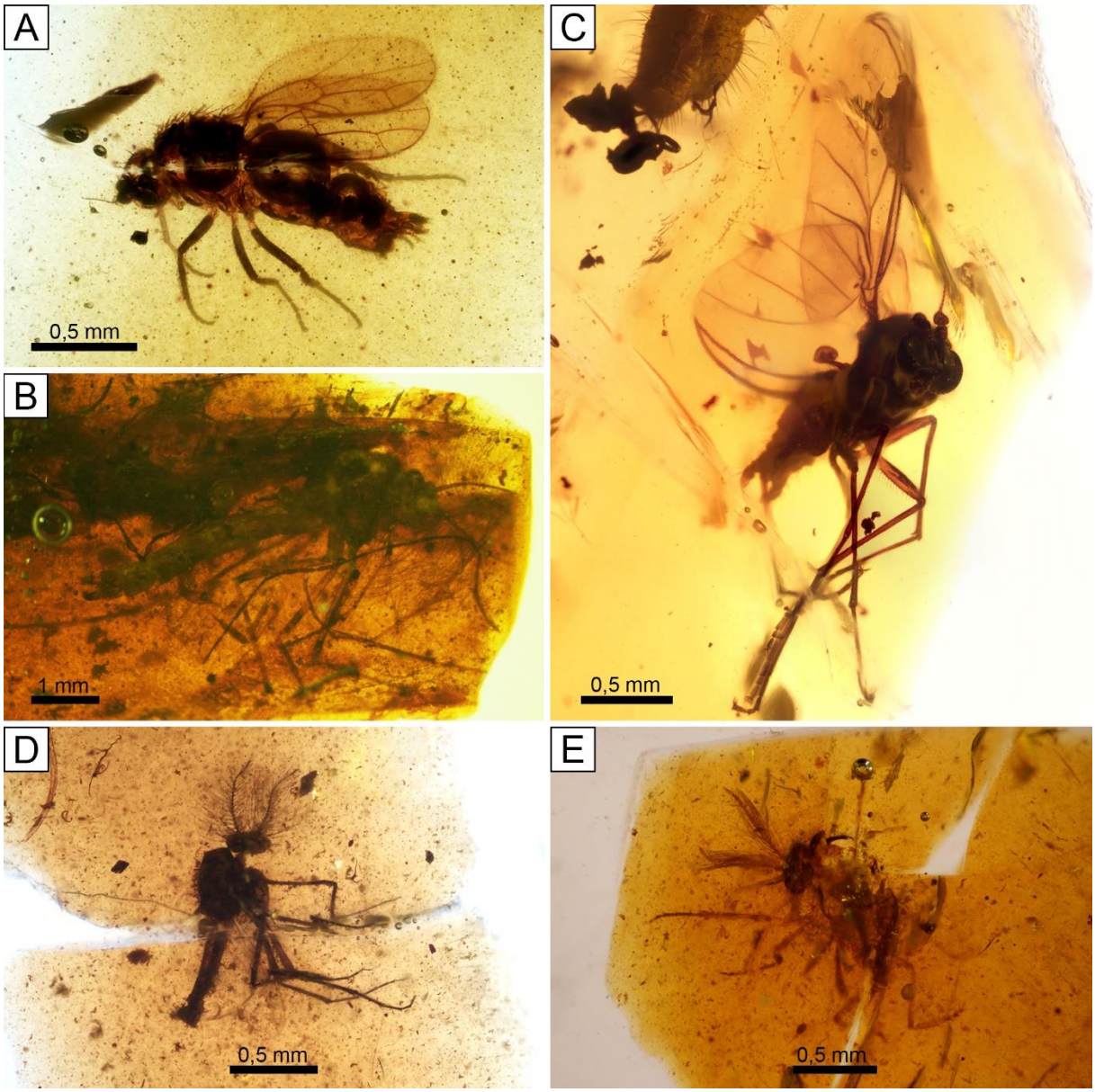

Figura 36. Dípteros (Diptera) en los ámbares de la Cuenca del Maestrazgo. A) Ejemplar preliminarmente determinado como *Chimeromyia alava* (†Chimeromyiidae) en el ámbar de San Just, SJNB2021-37; B) Ejemplar de la familia Chironomidae en el ámbar de Ariño, AR-1-A-2019.47.1; C) Ejemplar de *Burmazelmira* sp. (†Archizelmiridae) en el ámbar de Ariño, AR-1-A-2019.95.2, imagen tomada de Álvarez-Parra *et al.* (2021b); D) Ejemplar de la familia Chironomidae en el ámbar de Arroyo de la Pascueta, AP-9; E) Ejemplar de la familia Chironomidae en el ámbar de La Hoya, LH-3.

El registro de dípteros del ámbar de Ariño está representado por 19 ejemplares, la mayoría con deficiente conservación (Fig. 36B). Sin embargo, se han identificado las familias de nematóceros †Archizelmiridae, Cecidomyiidae, Ceratopogonidae, Chironomidae, Mycetophilidae, Rhagionidae, Scatopsidae y, con dudas, Psychodidae. Cada una de estas familias representadas únicamente por un ejemplar, aunque se han identificado con dudas un ejemplar adicional de Cecidomyiidae y otro de Ceratopogonidae, y dos de Rhagionidae. De entre estos ejemplares, el ejemplar macho asignado a la familia †Archizelmiridae (AR-1-A-2019.95.2) muestra una conservación excepcional, actualmente está en estudio en colaboración con Antonio Arillo y Enrique Peñalver, y se ha determinado preliminarmente como *Burmazelmira* sp. (Fig. 36C). Muy posiblemente se describa como una nueva especie, dadas sus diferencias anatómicas con las otras especies del género, principalmente en las antenas y la venación alar (Grimaldi *et al.*, 2003; Arillo *et al.*, 2018). En el ámbar de Arroyo de la Pascueta se han identificado cuatro dípteros, uno de ellos se trata de un miembro de la familia Chironomidae en una pieza de ámbar junto con una telaraña (Fig. 36D). Además, otro ejemplar podría pertenecer a la familia Ceratopogonidae. En el ámbar de La Hoya también se han identificado tres dípteros, uno de la familia Chironomidae (Fig. 36E) y dos de la familia Hybotidae (Brachycera: Eremoneura). Los dos hibótidos, una hembra y otro de sexo no conocido, se encuentran como sininclusiones en la misma pieza de ámbar y se han determinado como especie 2 de un nuevo género (Solórzano-Kraemer *et al.*, enviado). Este nuevo género también se ha encontrado en el ámbar de El Soplao, donde se ha descrito una nueva especie a partir de tres machos y otra especie no nombrada a partir de una hembra. Al no encontrase ejemplares machos con morfotipo similar a la nueva especie en el ámbar de La Hoya, se ha preferido no describir una nueva especie (Solórzano-Kraemer *et al.*, enviado). El nuevo género muestra similitudes anatómicas con *Trichinites*, del ámbar barremiense del Líbano, y *Eccomocydromia*, del ámbar Cenomaniense de Francia. Estos tres taxones no se han asignado a ninguna subfamilia de hibótidos y podrían agruparse en un clado propio, a pesar de ello, se requiere un análisis filogenético de las especies de la familia, que considere tanto fósiles como actuales, para poder resolver las relaciones entre las subfamilias (Solórzano-Kraemer *et al.*, enviado).

4.2.24. Orden Lepidoptera

Los lepidópteros son insectos holometábolos que incluyen a las mariposas y a las polillas (Goldstein, 2017). Se trata del tercer orden de insectos más diverso, con al menos 157.000 especies descritas, aunque se estima que aún quedan muchas especies pendientes de describir (Whalberg *et al.*, 2013). La mayoría de las especies de lepidópteros son herbívoras y cumplen un papel fundamental en la polinización de angiospermas, aunque algunas son depredadoras

(Pierce, 1995; Goldstein, 2017). Su registro fósil atribuido al grupo más antiguo data del Triásico Superior (van Eldijk *et al.*, 2018). Se conocen varias especies de lepidópteros en ámbares cretácicos (Zhang *et al.*, 2020). Hasta el momento, la única especie descrita de lepidóptero del registro fósil de la península ibérica es *Zygaena*? *turolensis* Fernández-Rubio, Peñalver & Martínez-Delclòs, 1991 (Zygaenidae) del yacimiento mioceno de compresión de Rubielos de Mora (Fernández-Rubio *et al.*, 1991). Además, se han identificado 25 ejemplares de lepidópteros en el ámbar de Peñacerrada I (Delclòs *et al.*, 2007) y cinco en el ámbar de El Soplao (Pérez de la Fuente, 2012). Estos ejemplares están en estudio por el entomólogo Víctor Sarto i Monteys (Institut de Ciència i Tecnologia Ambientals, Universitat Autònoma de Barcelona) y casi todos, si no todos, pertenecen a la familia Micropterigidae. El único lepidóptero conocido del ámbar de la Cuenca del Maestrazgo se corresponde con una oruga (larva) completa y relativamente bien conservada hallada en el ámbar de Ariño (AR-1-A-2019.95.1) (Fig. 37). Este ejemplar se identificó de forma preliminar como perteneciente al clado Ditrysia (Álvarez-Parra *et al.*, 2021b) y está en estudio en colaboración con Ricardo Pérez de la Fuente y Víctor Sarto i Monteys. Se observan claramente los diferentes segmentos corporales y las propatas, además, posiblemente se consigan observar los ganchos en algunas de ellas, característicos de Lepidoptera (Stehr, 1987). Su tamaño de alrededor de 5 mm de longitud excluye su asignación a la familia Micropterigidae (Stehr, 1987), lo que es interesante, ya que la mayor parte del registro fósil mundial de lepidópteros cretácicos se corresponde con esta familia. Solo se han hallado 13 orugas de lepidóptero en ámbares cretácicos y se ha propuesto que estos insectos inmaduros pudieron servir de alimento a aves cretácicas (Gauweiler *et al.*, 2022).

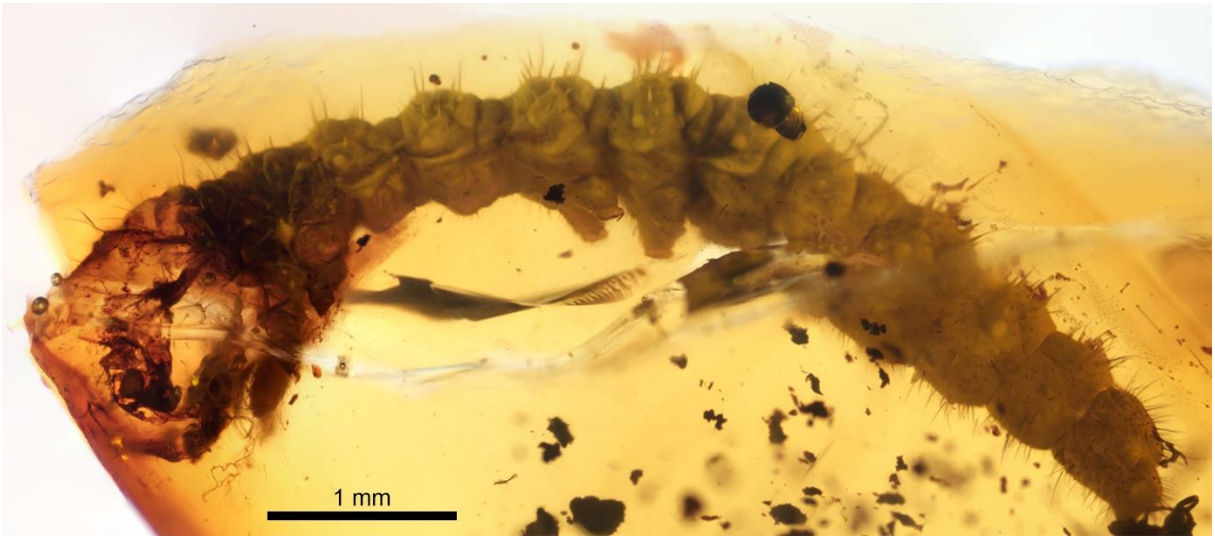

Figura 37. Oruga de Lepidoptera, preliminarmente asignada al clado Ditrysia, en el ámbar de Ariño, AR-1-A-2019.95.1. Imagen tomada de Álvarez-Parra *et al.* (2021b).

Filo Chordata: Subfilo Vertebrata: Clado Amniota

4.2.25. Clado Dinosauria

El registro de dinosaurios en ámbar cretácico es relativamente abundante, representado principalmente por plumas (Xing *et al.*, 2020), aunque de forma excepcional también se han encontrado restos esqueléticos (Xing *et al.*, 2016). Incluso, se han descrito artrópodos parásitos asociados a plumas de dinosaurio en ámbar cretácico (Peñalver *et al.*, 2017; Chitimia-Dobler *et al.*, 2022). Se han hallado plumas en ámbares cretácicos de todo el mundo (Perrichot *et al.*, 2008; McKellar *et al.*, 2011a; Xing *et al.*, 2020), y también están presentes en el ámbar de la península ibérica, aunque hasta el momento no se han estudiado desde los puntos de vista morfológico y taxonómico.

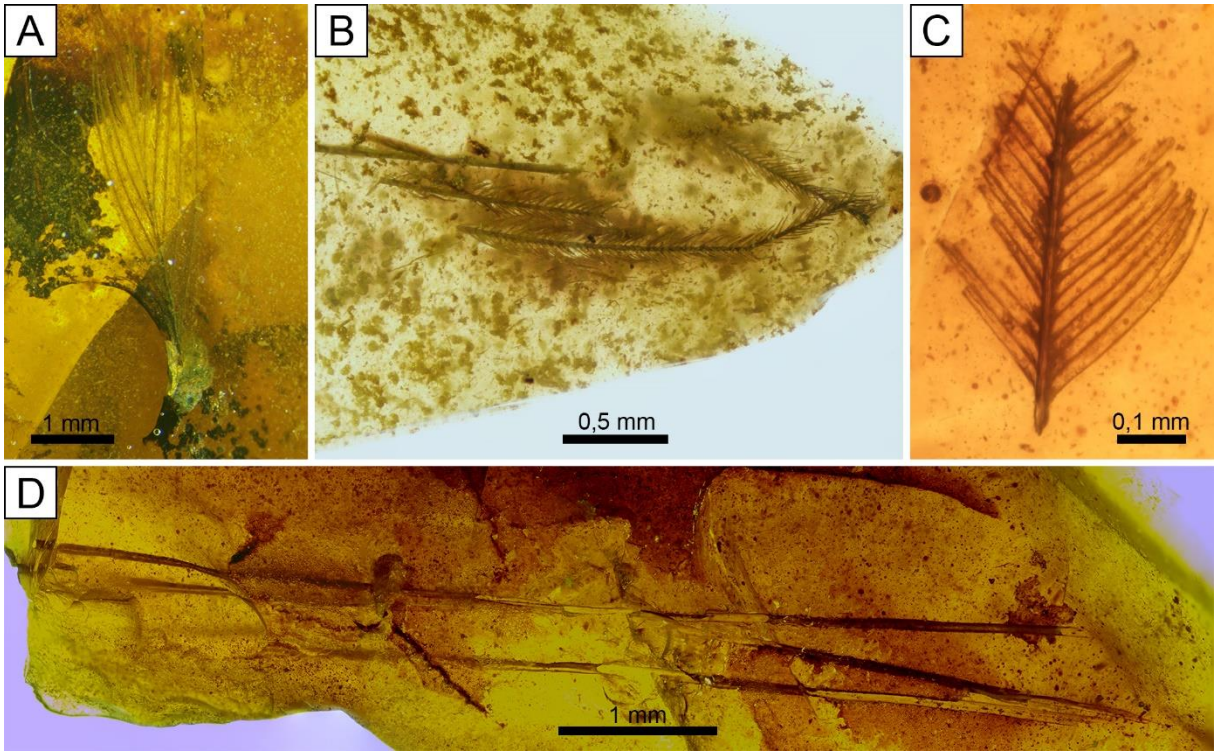

Figura 38. Restos tegumentarios de vertebrados en los ámbares de la Cuenca del Maestrazgo. A) Fragmento de pluma en el ámbar de San Just, SJNB2021-21.1; B) Conjunto de barbas de plumas en el ámbar de San Just, SJNB2021-3; C) Fragmento de pluma en el ámbar de Ariño; AR-1-A-2019.53, imagen tomada de Álvarez-Parra *et al.* (2021b); D) Mechón de tres pelos en el ámbar de Ariño, AR-1-A-2019.88.1, imagen tomada de Álvarez-Parra *et al.* (2020a).

Varias plumas se han hallado en el ámbar de Peñacerrada I (Delclòs *et al.*, 2007), mientras que se han identificado solo dos en el ámbar de El Soplao (Pérez de la Fuente, 2012). En San Just se han encontrado ocho piezas de ámbar con registro de plumas (Fig. 38A, B),

algunos de ellos son fragmentos aislados, mientras que otros son asociaciones de varios fragmentos (Álvarez-Parra *et al.*, 2020a). Un solo fragmento de pluma se ha identificado en el ámbar de Ariño (Fig. 38C) (Álvarez-Parra *et al.*, 2021b). Las plumas del ámbar de la Cuenca del Maestrazgo, al ser solo fragmentos, son de difícil asignación taxonómica, aunque podrían pertenecer a aves †Enantiornithes, dada su abundancia en otros ámbares cretácicos (Álvarez-Parra *et al.*, 2020a; Xing *et al.*, 2020). La interpretación tafonómica de la asociación de plumas de la pieza de ámbar de San Just CPT-4200, junto con una pieza con un mechón de pelo de mamífero del ámbar de Ariño, permitió describir el proceso de arrancamiento de vestidura (*pull off vestiture*), relacionado con la captura y conservación en resina de pelos o plumas arrancadas cuando el animal estaba vivo (Álvarez-Parra *et al.*, 2020a). Como se han comentado anteriormente, el estudio detallado de la pieza SJNB2012-31-01, con fragmentos de plumas de dinosaurio, ha permitido inferir una asociación simbiótica entre estos vertebrados y larvas de coleópteros (Peñalver *et al.*, enviado).

4.2.26. Clase Mammalia

El registro fósil de mamíferos en ámbar es muy raro. Únicamente se han hallado algunos pelos aislados en ámbares cretácicos, aunque el registro en ámbares cenozoicos es algo más abundante (Weitschat y Wichard, 2002; Peñalver y Grimaldi, 2005; Sidorchuk *et al.*, 2019). Se han descrito restos óseos de un mamífero solenodóntido en ámbar mioceno de República Dominicana (MacPhee y Grimaldi, 1996). El registro de pelos en ámbar cretácico es muy escaso, ya que solo se han descrito dos pelos aislados en una misma pieza de ámbar de Archingeay-Les Nouillers en Francia (Vullo *et al.*, 2010), aunque también hay menciones de pelos aislados en otros ámbares (*e.g.*, Zherikhin y Sukatsheva, 1973). Un descubrimiento excepcional fue el hallazgo de tres pelos de mamífero formando un pequeño mechón (AR-1-A-2019.88.1) en ámbar de Ariño (Fig. 38D) (Álvarez-Parra *et al.*, 2020a). Se corresponden con el registro de mamífero en ámbar más antiguo del mundo. El patrón superficial de escamas de queratina de los pelos del ámbar de Ariño es similar al que presentan los pelos de algunos mamíferos actuales, como los mustélidos (Álvarez-Parra *et al.*, 2020a). Como se ha comentado anteriormente, la interpretación tafonómica de este mechón de pelo, junto con una pieza con plumas de dinosaurio del ámbar de San Just, permitió describir el proceso tafonómico de arrancamiento de vestidura (*pull off vestiture*).

5. Discusión

5.1. Características paleoambientales de los yacimientos de ámbar de la Cuenca del Maestrazgo

El estudio del contenido paleobiológico de los ámbares de la Cuenca del Maestrazgo complementa los resultados obtenidos a partir de los estudios tafonómicos y estratigráficos, lo que ayuda a inferir el paleoambiente en el que se desarrollaron los bosques resiníferos. Los yacimientos de ámbar de esta cuenca abarcan un amplio rango temporal, desde el Albiense inferior (Ariño) hasta el Cenomaniense inferior (La Hoya).

Profundizar en la tafonomía de los yacimientos de ámbar es clave para poder comprender e interpretar los datos que se obtienen a partir del ámbar y sus bioinclusiones, y para conocer el grado de transporte bioestratinómico del conjunto paleobiológico. Como se ha comentado anteriormente, la captura de organismos en resina está sesgada por varios factores, por lo que no todos los organismos que habitan en un bosque resinífero tienen la misma probabilidad de acabar atrapados en resina, ni en la misma proporción que en el ecosistema (Solórzano Kraemer *et al.*, 2018). Además, tras su formación, las piezas de resina pueden sufrir transporte antes de su enterramiento final (Martínez-Delclòs *et al.*, 2004). Por ello, averiguar si el ámbar de un yacimiento es autóctono o es el resultado de una acumulación parautóctona o alóctona, o una combinación de materiales parautóctonos y alóctonos, es esencial antes de abordar la reconstrucción paleoecológica a partir de las bioinclusiones.

El yacimiento de Ariño, considerado un *Konservat-Lagerstätte*, es único a nivel mundial, dado que el nivel AR-1 ha proporcionado un registro fósil muy diverso, que incluye restos esqueléticos de dinosaurios y ámbar aéreo rico en bioinclusiones, lo que ha permitido conocer su paleoecología de un modo sin precedentes (Fig. 39) (Álvarez-Parra *et al.*, 2021b). El estudio tafonómico del ámbar y el resto de los fósiles del nivel AR-1 indica que es un registro principalmente autóctono con algunos materiales parautóctonos y unos pocos alóctonos (Alcalá *et al.*, 2012; Tibert *et al.*, 2013; Villanueva-Amadoz *et al.*, 2015; Vajda *et al.*, 2016; Álvarez-Parra *et al.*, 2021b). Solo se ha hallado una pieza de ámbar para la que se ha inferido un origen alóctono (AR-1-A-2019.79) (Álvarez-Parra *et al.*, 2021b), al igual que se ha inferido para restos de madera carbonizada del mismo nivel (Villanueva-Amadoz *et al.*, 2015). El hallazgo de piezas de ámbar de raíz *in situ* en relación con el lugar en el que se produjo la resina permite inferir que el nivel AR-1 se corresponde con el paleosuelo de una llanura pantanosa costera donde se desarrolló un bosque resinífero de araucariáceas (Álvarez-Parra *et al.*, 2021b). En esta zona pantanosa se desarrollaban lagos someros alcalinos que experimentaban variaciones en los niveles de salinidad debido a aportes marinos esporádicos bajo un clima tropical o subtropical (Tibert *et al.*, 2013; Villanueva-Amadoz *et al.*, 2015; Vajda *et al.*, 2016; Álvarez-Parra *et al.*, 2021b). Gracias a la naturaleza principalmente autóctona del ámbar, e incluso *in situ* en relación con el lugar de producción de resina, Ariño es un yacimiento ideal

para estudiar el proceso de producción de resina durante el Cretácico y los cambios químicos debidos a procesos diagenéticos tempranos.

La producción en masa de resina está relacionada con árboles sometidos a situaciones de estrés ambiental (Langenheim, 2003). El suelo del bosque resinífero de Ariño pudo estar encharcado o inundado, al menos ocasionalmente, lo que causaría la producción de resina en masa por parte de las araucariáceas. A su vez, este hecho explicaría la conservación diferencial entre el ámbar *in situ* y las raíces, dado que éstas pudieron pudrirse muy fácilmente en el suelo encharcado (Álvarez-Parra *et al.*, 2021b). Sin embargo, es posible que la producción en masa de resina en Ariño se debiera a múltiples factores. Muchas piezas de ámbar aéreo de este yacimiento son turbias, con muchos fragmentos orgánicos e inorgánicos, e incluso, algunas de ellas opacas, lo que dificulta o impide la visualización de bioinclusiones. Además, el hallazgo de burbujas monofásicas, bifásicas y trifásicas en el ámbar de raíz implicaría la producción de otras secreciones junto con la resina, quizás ligadas a un estrés ambiental extremo. La presencia de compuestos poco comunes, como kujigamberol, y mineralizaciones en forma de pequeños cristales, como la probable szomolnokita (Fig. 21B), en el ámbar de Ariño puede deberse a procesos diagenéticos ocurridos durante el Cretácico, poco después de la producción de la resina. Una hipótesis que podría explicar las peculiares características del ámbar de Ariño es que las piezas de resina se sometieron a muy altas temperaturas de forma relativamente contemporánea a su producción, como indica la investigación en proceso dirigida por Rafael P. Lozano. La presencia de fusinita se ha relacionado con el desarrollo de paleoincendios (Scott, 2000), los cuales fueron muy comunes y estuvieron ampliamente distribuidos a nivel global durante el Aptiense y el Albiense en relación con la elevada concentración de O_2 en la atmósfera (Wang *et al.*, 2019). La capa superior del nivel AR-1 de Ariño contiene abundante fusinita (Álvarez-Parra *et al.*, 2021b), al igual que los niveles con ámbar de otros yacimientos de la península ibérica (Peñalver y Delclòs, 2010). Por ello, es probable que el bosque de Ariño sufriera incendios ocasionales, lo que también se ha relacionado con la producción en masa de resina (Martínez-Delclòs *et al.*, 2004; Seyfullah *et al.*, 2018a). En caso de que fuera así, las piezas de ámbar aéreo de Ariño, principalmente autóctonas, se encontrarían con la superficie quemada y la visualización de bioinclusiones sería muy compleja. Sin embargo, el aspecto del ámbar aéreo de Ariño no se corresponde con ello, sino que su turbidez y opacidad estaría más relacionada con otras secreciones de los árboles resiníferos junto con la resina (McKellar *et al.*, 2011b; Lozano *et al.*, 2020). Por ello, a pesar de que la presencia de fusinita evidencie el desarrollo de paleoincendios en superficie, es posible que no fueran recurrentes en el bosque resinífero, o sucedieran en áreas algo más alejadas.

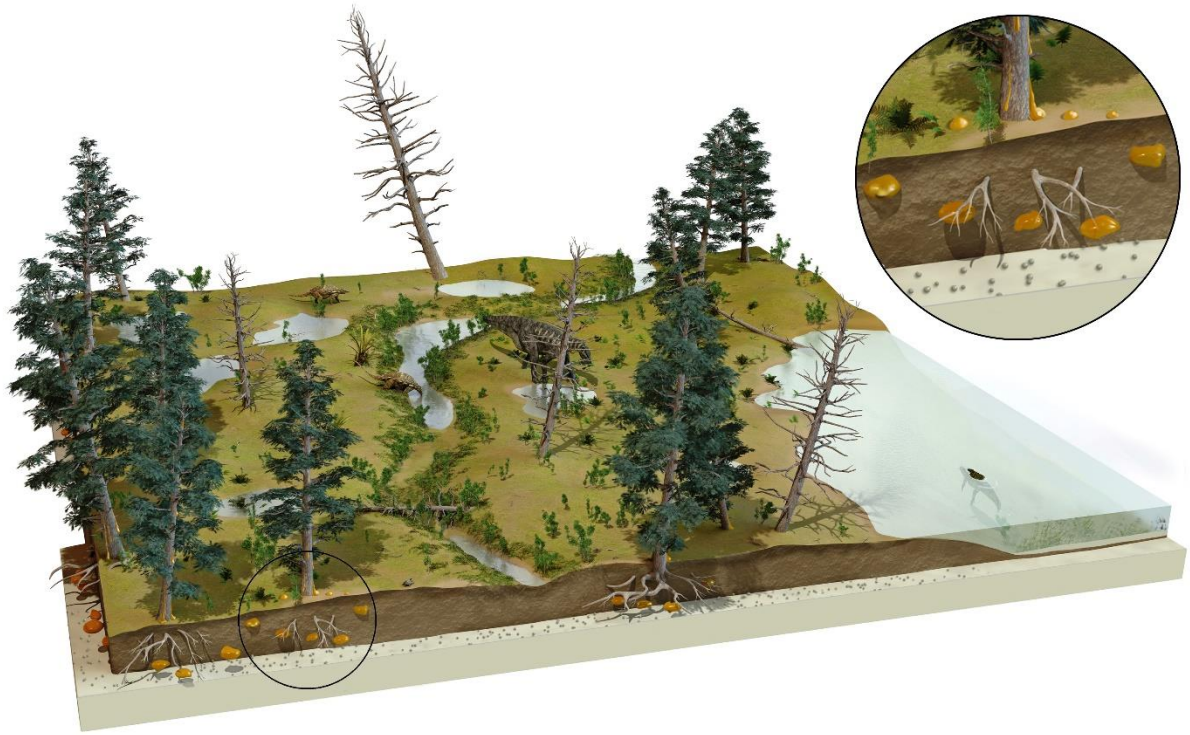

Figura 39. Reconstrucción artística del paleoambiente pantanoso de Ariño (Albiense inferior) con representación de los organismos inferidos a partir del registro fósil. Arriba a la derecha se puede observar la parte inferior de una araucariácea (Araucariaceae) con producción de resina aérea y de raíz. Autor: José Antonio Peñas. Imagen tomada de Álvarez-Parra *et al.* (2021b).

Una explicación alternativa para las altas temperaturas a las que estuvieron sometidas las piezas de resina y que explicaría las características peculiares del ámbar podría ser el desarrollo de combustiones espontáneas subterráneas debido a desecaciones, de forma similar a como ocurre actualmente en Las Tablas de Daimiel en Ciudad Real (Moreno *et al.*, 2011). En este contexto, es posible que el paleoambiente de Ariño sufriera encharcamientos o inundaciones de forma periódica u ocasional, lo que causaría la producción en masa de resina debido al estrés ambiental de los árboles resiníferos, seguido por periodos de desecación, cuando se producirían combustiones subterráneas que afectarían a las piezas de resina de raíz. La ausencia de corteza constituida de hongos resinícolas en las piezas de ámbar de raíz podría estar relacionada con las combustiones subterráneas, que impedirían el desarrollo de estos hongos. A su vez, las altas temperaturas del subsuelo pudieron influir en la aparición de compuestos poco comunes y mineralizaciones en el ámbar. La turbidez de muchas de las piezas de ámbar aéreo y la presencia de burbujas monofásicas, bifásicas y trifásicas del ámbar de raíz podría estar ligado al estrés ambiental extremo al que estuvieron sometidos los árboles resiníferos debido a los periodos de encharcamiento o inundación de la zona pantanosa, lo cual provocaría la producción de otras secreciones junto con la resina (Lozano *et al.*, 2020).

La interpretación paleoambiental del ecosistema de Ariño, y su relación con la producción de resina y las características del ámbar, es una línea de investigación en proceso que aún requiere de más observaciones, experimentación y resultados. Las explicaciones aquí expuestas son preliminares, dado que el estudio de las mineralizaciones y la geoquímica del ámbar de Ariño se está iniciando. No se puede descartar la posibilidad de que las piezas de ámbar hayan estado sometidas a altas temperaturas en periodos recientes o incluso actuales debido a combustiones espontáneas de los depósitos de carbón, como se ha documentado en la Mina Santa María de Ariño (Laita *et al.*, 2019). En cualquier caso, el ámbar de Ariño muestra rasgos peculiares, diferentes a los de los otros ámbares de la península ibérica, probablemente en relación con su edad ligeramente más antigua, el paleoambiente donde se produjo la resina y las características tafonómicas.

Los yacimientos de ámbar de San Just, Arroyo de la Pascueta y La Hoya comparten características tafonómicas y paleoambientales. Como se ha comentado anteriormente, el ámbar de los tres yacimientos se considera parautóctono junto con posible material de origen alóctono; es decir, tras la producción de resina, las piezas sufrieron transporte, principalmente en el mismo medio donde se produjo, antes de depositarse y enterrarse, dado que se encuentran piezas de ámbar de raíz y aéreo mezcladas en el mismo nivel. El paleoambiente de los tres yacimientos se ha interpretado como una laguna costera con árboles de la familia Araucariaceae correspondientes a los productores de resina (Menor-Salván *et al.*, 2016; Barrón *et al.*, enviado). Los paleoambientes inferidos a partir del estudio estratigráfico y paleobotánico muestran diferentes ecosistemas con amplia diversidad de plantas en un contexto árido (Barrón *et al.*, enviado). Por ello, los ambientes donde se desarrollaron los bosques resiníferos de araucariáceas en el este de Iberia fueron bastante diferentes desde el Albiense inferior, representado por la zona pantanosa bajo un clima tropical o subtropical de Ariño, hasta el Albiense superior y Cenomaniense inferior, representados por lagunas costeras bajo un clima árido de San Just, Arroyo de la Pascueta y La Hoya, lo que explicaría las diferentes características observadas en el ámbar de Ariño en relación con los otros ámbares de la cuenca. Sin embargo, cabe destacar la similitud en el espectro de infrarrojos entre los cuatro ámbares (Fig. 18), probablemente en relación con un origen común por árboles de la familia Araucariaceae.

La búsqueda y el estudio de otros yacimientos de ámbar en la Cuenca del Maestrazgo ayudaría a comprender mejor los cambios ambientales de los ecosistemas en los que se desarrollaron los bosques resiníferos. El hallazgo de ámbar, con o sin bioinclusiones, de edad Albiense inferior y asociado a la Formación Escucha, en otros yacimientos permitía averiguar si las características del ámbar de Ariño son únicas en la cuenca o se deben a factores más ampliamente distribuidos.

5.2. Contenido paleobiológico de los ámbares de la Cuenca del Maestrazgo: comparación taxonómica y paleobiogeografía

A pesar de los más de 30 yacimientos de ámbar documentados en la Cuenca del Maestrazgo, solo se han hallado bioinclusiones en el ámbar de cuatro de ellos. Este hecho no implica que la presencia de bioinclusiones en los ámbares del Maestrazgo sea limitada, sino que se han encontrado bioinclusiones únicamente en el ámbar de aquellos yacimientos que se han excavado de forma más intensa y se han estudiado en detalle. Por ello, es muy probable que a corto o medio plazo se encuentren otros ámbares con contenido paleobiológico en la cuenca, lo que incrementa la importancia del estudio de yacimientos de ámbar recién descubiertos como la Mina La Dehesa de Estercuel y Son del Puerto.

Los ámbares de Ariño y San Just son los más ricos en bioinclusiones de la Cuenca del Maestrazgo, mientras que los ámbares de Arroyo de la Pascueta y La Hoya han proporcionado pocas bioinclusiones, de forma similar a los ámbares de la Depresión Central Asturiana (Peñalver y Delclòs, 2010; Arillo *et al.*, 2020). Las bioinclusiones del ámbar de San Just, de forma general, muestran una mejor conservación que las de los otros ámbares de la cuenca, además de que este ámbar es generalmente transparente, lo que facilita la visualización de las bioinclusiones. El contenido paleobiológico de los ámbares de Arroyo de la Pascueta y La Hoya, al ser tan pobre, hace que la comparación taxonómica sea compleja y no tenga una validez estadística. Sin embargo, en estos dos ámbares se han encontrado representantes de Hymenoptera y Diptera, en concordancia con lo esperado, dado que son los órdenes de insectos más numerosos y comúnmente hallados en ámbar del Cretácico (*e.g.*, Perrichot *et al.*, 2007). También, tanto el ámbar de Arroyo de la Pascueta como de La Hoya incluyen registro de cucarachas (Blattodea) que podrían ser habitantes del suelo del bosque, lo que implicaría que, a pesar del escaso registro de ámbar con bioinclusiones, en ambos yacimientos se encuentran piezas de ámbar de hojarasca (Perrichot, 2004; Sánchez García, 2017).

Los valores de abundancia relativa de cada grupo de artrópodos en el ámbar de Ariño se encuentran sesgados debido a la conservación de sus bioinclusiones, ya que varias de ellas son fragmentos o su visualización es compleja, por lo que no se han podido asignar con certeza a un grupo taxonómico. Sin embargo, de forma general, la abundancia relativa de cada grupo de artrópodos en el ámbar de Ariño es similar a la del ámbar de San Just (Tabla 1; Fig. 25). Algunas diferencias quedan reflejadas en grupos como Araneae, Blattodea y Diptera, más abundantes en proporción en el ámbar de San Just, y Psocodea y Thysanoptera, más abundantes en proporción en el ámbar de Ariño. Estas diferencias podrían relacionarse con los diferentes paleoambientes de cada yacimiento, aunque también podrían deberse a un sesgo de muestreo, por lo que se requeriría identificar un mayor número de bioinclusiones en el ámbar de Ariño para obtener resultados concluyentes.

Los valores de abundancia relativa de cada grupo de artrópodos en los ámbares de El Soplao y Peñacerrada I, ambos en la Cuenca Vasco-Cantábrica, fueron presentados por Pérez de la Fuente (2012), lo que permite llevar a cabo la comparación taxonómica, puesto que no se han realizado excavaciones posteriores en estos yacimientos. Los representantes de Araneae, Blattodea y Hemiptera muestran abundancias relativas más elevadas en el ámbar de San Just que en los ámbares de El Soplao y Peñacerrada I, mientras que en el ámbar de Ariño se encuentran sobrerrepresentados los miembros de Psocodea y Thysanoptera, al igual que se ha comentado anteriormente en comparación con el ámbar de San Just. Los himenópteros son bastante más numerosos que los dípteros en el ámbar de El Soplao, al igual que en el ámbar de Ariño. En cambio, en el ámbar de Peñacerrada I los dípteros son bastante más abundantes que los himenópteros. Curiosamente, los himenópteros y los dípteros muestran abundancias relativas similares en el ámbar de San Just. Cabe destacar el hallazgo de una oruga de Lepidoptera en el ámbar de Ariño (Fig. 37) y una larva de Raphidioptera en el ámbar de Arroyo de la Pascueta (Fig. 33A), únicos inmaduros de ambos grupos identificados en el ámbar de la península ibérica y no muy comunes en otros ámbares cretácicos (Perrichot y Engel, 2007; Gauweiler *et al.*, 2022). Además, la presencia de un representante de †Lophioneurida en el ámbar de San Just (Fig. 32A, B) es destacable, dada su rareza en ámbar cretácico (Rasnitsyn y Quicke, 2002).

De forma preliminar, se aprecian diferencias a nivel de géneros y especies entre el ámbar de Ariño y de San Just, aunque se requiere un estudio taxonómico detallado de los ejemplares. En relación con los psocópteros, grupo ampliamente estudiado en la Tesis Doctoral, cabe destacar que ninguno de los morfotipos presentes en el ámbar de San Just se ha encontrado en el ámbar de Ariño (Álvarez-Parra *et al.*, 2022b). Sin embargo, sí se han hallado similitudes, incluso a nivel de especie, entre los ámbares de Ariño y El Soplao, como *Libanoglaris hespericus* (Psocodea: †Empheriidae) y una nueva especie del género *Azarpsocus* (Psocodea: Manicapsocidae) (Álvarez-Parra *et al.*, 2022b, en preparación 1). Similitudes entre los ámbares de Ariño y de San Just son el género *Burmazelmira* (Diptera: †Archizelmiridae) (Arillo *et al.*, 2018; Álvarez-Parra *et al.*, 2021b), aunque posiblemente el ejemplar del ámbar de Ariño corresponda a una nueva especie (Fig. 36C), el género *Serphites* (Hymenoptera: †Serphitidae) (Fig. 34D), aunque corresponden a especies diferentes en cada yacimiento (Álvarez-Parra *et al.*, 2021c, en preparación 2), y la especie *Cretaceomma turolensis* (Hymenoptera: †Gallorommatidae), dado que preliminarmente no se han encontrado diferencias anatómicas que justifiquen su adscripción a otra especie (Fig. 35B) (Ortega-Blanco *et al.*, 2011e; Álvarez-Parra *et al.*, 2021b). Hasta siete especies presentes en el ámbar de San Just están también presentes en otros ámbares de la península ibérica: *Alavaromma orchamum* (Hymenoptera; presente en el ámbar de Peñacerrada I), *Archaeatropos alavensis* (Psocodea; presente en los ámbares de El Soplao, Peñacerrada I y Arroyo de la Pascueta),

Archiculicoides skalskii (Diptera; presente en los ámbares de El Soplao y Peñacerrada I), *Arra legalovi* (Coleoptera; presente en el ámbar de El Soplao), *Burmaphron jentilak* (Hymenoptera; presente en el ámbar de Peñacerrada I), *Leptoconops zherikini* (Diptera; presente en el ámbar de El Soplao) y *Preempheria antiqua* (Psocodea; presente en el ámbar de Peñacerrada I).

Curiosamente, el ámbar de San Just comparte especies con los ámbares de El Soplao, Peñacerrada I y Arroyo de la Pascueta, mientras que el ámbar de Ariño con el de El Soplao. Este hecho podría tener relación con las dataciones de cada uno de los ámbares, dado que el ámbar de Ariño es Albiense inferior (Álvarez-Parra *et al.*, 2021b), mientras que los de Peñacerrada I, San Just y Arroyo de la Pascueta son Albiense superior (Barrón *et al.*, 2015, enviado). La datación de Albiense medio del ámbar de El Soplao explicaría la presencia de especies del resto de ámbares, dado que se sitúa "intermedio" en edad. La coocurrencia de especies entre los ámbares de la Cuenca del Maestrazgo y la Cuenca Vasco-Cantábrica implicaría una posible conexión de los bosques a lo largo de la costa norte y este de Iberia durante la mitad del Cretácico que facilitara una distribución amplia de los géneros y especies.

En cuanto a la comparación taxonómica con otros ámbares cretácicos, los ámbares de la Cuenca del Maestrazgo tienen en común con ellos la elevada abundancia de ejemplares de la familia Scelionidae entre los himenópteros (*e.g.*, Ortega-Blanco *et al.*, 2014; Zhang *et al.*, 2018). Se han encontrado similitudes a nivel de familia con otros ámbares cretácicos, aunque cabe destacar la coocurrencia de géneros en ámbares alejados espacial y temporalmente. Por ejemplo, los géneros *Orchestina* (Oonopidae), *Leptoconops* (Diptera), *Microphorites* (Diptera), *Protoculicoides* (Diptera) *Cretevania* (Hymenoptera) y *Serphites* (Hymenoptera) se encuentran ampliamente distribuidos durante el Cretácico (Arillo *et al.*, 2008a; Peñalver *et al.*, 2010; Ortega-Blanco *et al.*, 2011d; Saupe *et al.*, 2012; Szadziewski *et al.*, 2016). Sin embargo, un dato peculiar es la coocurrencia de géneros entre los ámbares de la Cuenca del Maestrazgo y los ámbares barremiense del Líbano y cenomaniense de Myanmar. Ejemplos de ello son los géneros *Archaeatropos* (Psocodea; presente en el ámbar del Líbano), *Burmaphron* (Hymenoptera; presente en el ámbar de Myanmar), *Burmazelmira* (Diptera; presente en el ámbar de Myanmar), *Cretaceomma* (Hymenoptera; presente en el ámbar del Líbano), *Helius* (Diptera; presente en los ámbares del Líbano y Myanmar), *Libanoglaris* (Psocodea; presente en el ámbar del Líbano) y *Mymaropsis* (Hymenoptera; presente en el ámbar del Líbano). Además, también se han identificado los géneros *Azarpsocus* (Psocodea), en los ámbares de El Soplao y Ariño, y *Burmacompsocus* (Psocodea), en el ámbar de El Soplao, los cuales se describieron a partir de ejemplares en ámbar cenomaniense de Myanmar (Nel y Waller, 2007; Maheu y Nel, 2020; Álvarez-Parra *et al.*, en preparación 1). En general, se aprecia una similitud con estos dos ámbares bastante distanciados geográfica y temporalmente, al contrario que con el cercano ámbar Albiense-Cenomaniense de Francia. Esta peculiaridad ya se había indicado

anteriormente (Peris, 2015; Peris *et al.*, 2016), y podría tener relación con las características paleoambientales y paleoclimáticas en cada región (Peris *et al.*, 2016), factores paleogeográficos debido al aislamiento de Iberia con Laurasia (Peris *et al.*, 2016) y la existencia de paleocorrientes oceánicas entre el Tetis y el Atlántico norte que dificultasen el intercambio de artropodofauna entre Iberia y Laurasia (Álvarez-Parra *et al.*, en preparación 1), de forma similar a como ocurre en el Canal de Mozambique entre África continental y Madagascar (Samonds *et al.*, 2012).

5.3. Producción en masa de resina durante el Cretácico

La formación de yacimientos de ámbar está condicionada principalmente por dos factores (Delclòs *et al.*, en preparación): 1) desarrollo de un bosque compuesto por árboles con la capacidad de producir resina en masa en respuesta a diversos factores, y 2) existencia de un medio sedimentario adecuado para la conservación de resinas a lo largo del tiempo. En la actualidad se conocen especies de árboles productores de resina distribuidas prácticamente a nivel global, a excepción de la Antártida (Langenheim, 2003). Sin embargo, la mayoría de estas especies no tiene la capacidad de producir resina en cantidades copiosas. Algunas de las regiones donde se conocen bosques compuestos por árboles que producen resina en masa son la costa este de África y Madagascar, donde están presentes bosques de árboles del género de angiospermas *Hymenaea* (familia Fabaceae) (Delclòs *et al.*, 2020), y el archipiélago de Nueva Caledonia y la Isla Norte de Nueva Zelanda, donde se localizan bosques de árboles del género de gimnospermas *Agathis* (familia Araucariaceae) (Seyfullah *et al.*, 2018a). En algunas regiones se ha documentado un elevado número de yacimientos de ámbar del Cretácico (Fig. 23), como por ejemplo en el Líbano del Barremiense, en el norte y este de Iberia del Albiense, en la costa este de Estados Unidos del Turoniense o en el oeste de Canadá del Campaniense. Aunque también se conocen yacimientos de ámbar en otras regiones de cada una de estas edades. Por ello, se podría suponer que las condiciones ambientales que propiciaron la producción en masa de resina durante el Cretácico, y su depósito en medios sedimentarios, se encontraban principalmente limitadas a algunas regiones, al igual que ocurre en la actualidad.

La Cuenca del Maestrazgo, en el margen oriental de Iberia, se corresponde con una de las regiones donde se dieron los factores requeridos para la formación de numerosos yacimientos de ámbar, a partir del depósito de resina en un intervalo de tiempo desde el Albiense inferior al Cenomaniense inferior (aproximadamente 10 millones de años). Es decir, había árboles con capacidad de producir resina en masa, en este caso de la familia Araucariaceae como indican los análisis geoquímicos, y existían los medios sedimentarios adecuados para su depósito y registro, como la zona pantanosa correspondiente al nivel AR-1 de Ariño y las lagunas costeras correspondientes a los niveles con ámbar de San Just, Arroyo

de la Pascueta y La Hoya. Hay varios factores que pueden condicionar la producción en masa de resina, tanto abióticos como bióticos (Langenheim, 2003; Martínez-Delclòs *et al.*, 2004; Seyfullah *et al.*, 2018a). Como se expone en el trabajo de Delclòs *et al.* (en preparación), entre los abióticos, algunos de los factores son a nivel global, como la composición de gases atmosféricos, la radiación solar y la fluctuación del nivel del mar, y otros a nivel regional, como la actividad volcánica y las condiciones climáticas, estas últimas relacionadas a su vez con la circulación oceánica. Los factores bióticos tendrían influencia principalmente a nivel regional, como las enfermedades causadas por virus y microorganismos o el ataque por insectos (Langenheim, 2003; Peris *et al.*, 2021).

Se conoce registro de ámbar desde el Carbonífero, sin embargo los depósitos precretácicos no son ricos en ámbar, las piezas son de muy pequeño tamaño y raramente contienen bioinclusiones. Cabe destacar el ámbar del Triásico de Dolomitas en Italia dado que, aunque su contenido paleobiológico es escaso, contiene las bioinclusiones más antiguas conocidas (Schmidt *et al.*, 2012). Curiosamente, el ámbar de Dolomitas y otros ámbares del Triásico coinciden con el intervalo temporal del Episodio Pluvial del Carniense (*Carnian Pluvial Episode*) (Seyfullah *et al.*, 2018b; Roghi *et al.*, 2022). Se conocen muchos yacimientos de ámbar del Cenozoico, aunque la mayor parte de ellos se han datado como Eoceno y Mioceno (Solórzano-Kraemer *et al.*, 2020). Es por ello por lo que se pueden diferenciar intervalos temporales en los que la producción en masa de resina y su tasa de depósito se incrementan a nivel global: Carniense (Triásico), Cretácico, Eoceno y Mioceno. El Cretácico es un periodo clave para comprender la producción de resina en el pasado, dado que es a partir del Barremiense cuando se comienzan a formar depósitos ricos en piezas de resina, en muchas ocasiones con bioinclusiones. Además, durante el Cretácico y el Paleógeno tiene lugar el evento Revolución Terrestre de las Angiospermas (*Angiosperm Terrestrial Revolution*) (Benton *et al.*, 2022), que incluye el evento Revolución Terrestre del Cretácico (*Cretaceous Terrestrial Revolution*) (Lloyd *et al.*, 2008). La Revolución Terrestre de las Angiospermas se corresponde con el efecto macroecológico sobre la biota terrestre global causado por el origen y diversificación de las angiospermas y que condujo al desarrollo de la biodiversidad moderna (Benton *et al.*, 2022). Teniendo esto en cuenta, cabe la posibilidad de que la diversificación de las angiospermas, ya desde el Cretácico Inferior, pudiera haber tenido influencia en la producción en masa de resina por parte de las gimnospermas.

La distribución espacial de las especies depende de diversos factores, entre ellos su nicho ecológico y la competencia con otras especies (Hutchinson, 1957). El nicho fundamental de una especie es el conjunto de condiciones ambientales en las que esa especie puede vivir potencialmente, mientras que el nicho realizado es el conjunto de condiciones ambientales en las que esa especie vive efectivamente debido a la competencia con otras especies (Hutchinson, 1957). Generalmente, el nicho realizado se encuentra incluido en el nicho fundamental,

aunque puede haber casos en los que el nicho realizado se encuentre fuera de los límites del nicho fundamental, es decir, la especie vive bajo condiciones ambientales teóricamente no adecuadas (Pulliam, 2000). Otros casos, más habituales, son aquellos en los que una especie habita bajo unas condiciones ambientales adecuadas, pero no óptimas; es decir, su nicho realizado se encuentra limitado a las condiciones ambientales extremas dentro del rango de condiciones ambientales adecuadas (Pulliam, 2000). La hipótesis sobre la relación entre la diversificación de las angiospermas y la producción en masa de resina por gimnospermas durante el Cretácico Inferior implicaría que las angiospermas habrían desplazado a algunos grupos de coníferas hacia hábitats no óptimos, cuya consecuencia habría sido la producción en masa de resina debido al estrés ambiental. Se ha evidenciado que en diferentes momentos del Cretácico Inferior se dieron condiciones áridas en el interior de los continentes (Föllmi, 2012), lo que también se ha interpretado en la Cuenca del Maestrazgo (Barrón *et al.*, enviado). Por ello, también es posible que el desplazamiento de las especies de coníferas con la capacidad de producir resina en masa hacia hábitats no óptimos pudiera haberse debido a la expansión del clima árido. En cualquier caso, la producción en masa de resina implica que el árbol productor sufre estrés ambiental (Langenheim, 2003). Los factores abióticos y bióticos que lo estimularon durante el Cretácico probablemente estaban interrelacionados y se requiere un mayor estudio, principalmente tafonómico y geoquímico, de los ámbares para poder obtener resultados concluyentes. Además, se requieren estudios actuotafonómicos sobre la producción en masa de resina en los bosques de araucariáceas de Nueva Caledonia y Nueva Zelanda que puedan desvelar los factores clave.

6. Conclusiones

Conclusiones

Los yacimientos de ámbar del Cretácico con origen en coníferas son numerosos en la Cuenca del Maestrazgo. A pesar de ello, solo en el ámbar de cuatro de ellos se han hallado bioinclusiones. Estos cuatro yacimientos se incluyen en un intervalo temporal que va desde el Albiense inferior hasta el Cenomaniense inferior. Por ello se interpreta que, al menos durante este intervalo, se dieron las circunstancias adecuadas, a su vez relacionadas con factores abióticos y bióticos, para la producción en masa de resina. Los paleoambientes de los yacimientos que han proporcionado ámbar con bioinclusiones difieren de un medio pantanoso bajo un clima tropical o subtropical (Ariño; Formación Escucha) a medios de lagunas costeras bajo un clima árido (San Just, Arroyo de la Pascueta y La Hoya; "Grupo Utrillas"). La Cuenca del Maestrazgo es un área relevante para conocer los cambios de las características de los bosques resiníferos y su biota asociada a lo largo de varios millones de años en el este de Iberia.

El estudio tafonómico del ámbar del yacimiento de Ariño, y las investigaciones tafonómicas previas de otros restos fósiles, han permitido interpretar este yacimiento como autóctono-parautóctono, con un escaso porcentaje de elementos alóctonos, y con piezas de ámbar de raíz *in situ* en relación con el lugar de producción de la resina. En cambio, los yacimientos de ámbar de San Just, Arroyo de la Pascueta y La Hoya se han interpretado como parautóctonos, con algunas piezas de posible origen alóctono. Estos estudios facilitan las claves para poder diferenciar yacimientos de diferente naturaleza tafonómica y aportan nueva información para dilucidar cómo se forman tanto los yacimientos de ámbar autóctonos-parautóctonos como los parautóctonos y alóctonos, y las características de los correspondientes paleoambientes.

Los análisis espectroscópicos y geoquímicos de los ámbares, además del estudio paleobotánico de los niveles con ámbar, han permitido evidenciar que los ámbares de la Cuenca del Maestrazgo se asocian a resina producida por coníferas de la familia Araucariaceae. Otros ámbares de la península ibérica también se han asociado a árboles de esta familia como productores de resina. Así se puede concluir que se dieron las condiciones adecuadas para que estos árboles produjeran resina en masa, al menos desde el Albiense inferior hasta el Cenomaniense inferior, en varias áreas a lo largo de la costa norte y este de Iberia.

El desarrollo de la Tesis Doctoral ha permitido iniciar el estudio taxonómico de las bioinclusiones de los ámbares de Ariño y La Hoya, además de proseguir el de las bioinclusiones de los ámbares de San Just y Arroyo de la Pascueta. La fauna de artrópodos registrada como bioinclusiones en los ámbares de la Cuenca del Maestrazgo es diversa, e incluye arácnidos de tres grupos diferentes (Araneae, Pseudoscorpiones y Acari), posibles hexápodos no insectos (Collembola y Diplura) e insectos de 14 órdenes diferentes (Archaeognatha, Orthoptera, Blattodea, Mantodea, Psocodea, †Lophioneurida, Thysanoptera, Hemiptera, Raphidioptera,

Neuroptera, Coleoptera, Hymenoptera, Diptera y Lepidoptera). Cabe destacar el hallazgo de insectos poco comunes en ámbares cretácicos, como un representante del orden †Lophioneurida en el ámbar de San Just, una larva de Raphidioptera en el ámbar de Arroyo de la Pascueta y una oruga de Lepidoptera en el ámbar de Ariño. Además, el ámbar de Ariño ha proporcionado los pelos de mamífero más antiguos como bioinclusiones en ámbar, y tanto el ámbar de Ariño como el de San Just contienen fragmentos de plumas de dinosaurio. La poca cantidad de bioinclusiones en los ámbares de Arroyo de la Pascueta y La Hoya dificulta su comparación taxonómica con otros ámbares. Los contenidos paleobiológicos de los ámbares de Ariño y San Just muestran diferencias taxonómicas entre sí, probablemente debido a la diferencia en las edades y en los paleoambientes. A pesar de las diferencias en las características paleoambientales de estos yacimientos, se han identificado coocurrencias de especies, por una parte, entre los ámbares de Ariño y El Soplao y, por otra parte, entre los ámbares de El Soplao, Peñacerrada I, San Just y Arroyo de la Pascueta. Ello puede indicar una posible conexión entre los bosques resiníferos de estas áreas durante la mitad del Cretácico que facilitara la distribución de la entomofauna. Curiosamente, a pesar de la separación espacial y temporal, se han observado más similitudes taxonómicas a nivel de género entre la entomofauna de los ámbares de la Cuenca del Maestrazgo y la de los ámbares del Barremiense del Líbano y del Cenomaniense de Myanmar, que con la entomofauna de los geográficamente cercanos ámbares del Albiense-Cenomaniense de Francia. Esto podría deberse a factores paleoambientales, paleoclimáticos y paleogeográficos o a corrientes oceánicas que favoreciesen o dificultasen el intercambio de entomofauna entre Laurasia y la paleoisla de Iberia.

El yacimiento de Ariño es único a nivel mundial debido a que se encuentran restos de vertebrados, entre ellos dinosaurios, en el mismo nivel que contiene ámbar aéreo rico en bioinclusiones, lo que proporciona información paleobiológica y paleoecológica a partir de dos tipos complementarios de conservación. Este hecho, unido a su tipificación como yacimiento autóctono-parautóctono, permite su consideración como *Konservat-Lagerstätte* y hace que tenga una relevancia mundial entre los yacimientos paleontológicos del Cretácico Inferior. El estudio pluridisciplinar de su registro fósil ha proporcionado información sin precedentes sobre la paleoecología de su ecosistema. La integración de los resultados permite inferir una red paleoecológica con varios niveles que muestra inferencias de interacción de los organismos entre ellos y con su medio.

Durante el Cretácico se dieron las condiciones ambientales adecuadas para la producción en masa de resina y el depósito de las piezas resultantes, al menos en algunas regiones, como fue el caso de la Cuenca del Maestrazgo. Los factores, tanto abióticos como bióticos, que causaron la producción en masa de resina durante este periodo probablemente estuvieron interrelacionados. Un posible factor pudo ser la diversificación de las angiospermas durante el

Cretácico Inferior, la cual pudo haber influido en el desplazamiento de algunos grupos de coníferas a ambientes no óptimos, lo que causaría la producción en masa de resina debido al estrés ambiental. Se requieren investigaciones sobre los factores que condicionan la producción en masa de resina en la actualidad. La aplicación de estudios de ENM y el análisis multivariante de coocurrencias podrían proporcionar información sobre los factores clave en la producción en masa de resina en el presente y el pasado.

Conclusions

Cretaceous amber deposits, with origin on conifers, are numerous in the Maestrazgo Basin. Nonetheless, bioinclusions have only been found in the amber from four of them. These four outcrops are included in a time interval from the lower Albian to the lower Cenomanian. Therefore, at least during this interval, the suitable conditions for the resin mass production occurred, in relation to abiotic and biotic factors. The palaeoenvironments of the outcrops providing amber with bioinclusions were a swamp plain under a tropical or subtropical climate (Ariño; Escucha Formation) and coastal lagoons under an arid climate (San Just, Arroyo de la Pascueta and La Hoya; “Utrillas Group"). The Maestrazgo Basin is a relevant area to know the changes in the characteristics of resiniferous forests and their associated biota over several million years in eastern Iberia.

The taphonomic study of the amber from the Ariño site, together with previous taphonomic investigations on other fossil remains, have allowed to interpret it as autochthonous-parautochthonous, with a few allochthonous elements, and with root amber pieces *in situ* in relation to the place of resin production. The amber-bearing outcrops of San Just, Arroyo de la Pascueta, and La Hoya have been interpreted as parautochthonous, with some pieces of possible allochthonous origin. These studies are key to differentiate outcrops of different taphonomic characteristics and provide new information to elucidate how the autochthonous-parautochthonous and the parautochthonous and allochthonous amber-bearing outcrops are formed, besides the characteristics of the corresponding palaeoenvironments.

The spectroscopic and geochemical analyses of the ambers, in addition to the palaeobotanical study of the levels with amber, have allowed to infer that the ambers from the Maestrazgo Basin are related to resin-producing conifers belonging to the family Araucariaceae. Other ambers from the Iberian Peninsula have also been related to trees of this family as resin producers. Thus, it is evidenced that the suitable conditions for resin mass production of araucariacean trees were present, at least from the lower Albian to the lower Cenomanian, in several areas along the northern and eastern coast of Iberia.

The research work of the PhD Thesis has allowed to start the taxonomic study of the bioinclusions in the Ariño and La Hoya ambers, in addition to carry on that of the bioinclusions in the San Just and Arroyo de la Pascueta ambers. The arthropod fauna recorded as bioinclusions in the ambers from the Maestrazgo Basin is diverse, and includes arachnids of three groups (Araneae, Pseudoscorpiones, and Acari), possible non-insect hexapods (Collembola and Diplura) and insects of 14 orders (Archaeognatha, Orthoptera, Blattodea, Mantodea, Psocodea, †Lophioneurida, Thysanoptera, Hemiptera, Raphidioptera, Neuroptera, Coleoptera, Hymenoptera, Diptera, and Lepidoptera). It is significant to note the finding of unusual insects in Cretaceous ambers, such as a representative of the order †Lophioneurida in San Just amber, a Raphidioptera larva in Arroyo de la Pascueta amber, and a Lepidoptera caterpillar in Ariño amber. Futhermore, Ariño amber has provided the oldest mammalian hairs as bioinclusions in amber, and both Ariño and San Just ambers contain fragments of dinosaur feathers. The low quantity of bioinclusions in the ambers from Arroyo de la Pascueta and La Hoya hinders their taxonomic comparisons with other ambers. The palaeobiological contents of the Ariño and San Just ambers show taxonomic differences between them, probably due to the difference in ages and paleoenvironments. Despite the differences in the palaeoenvironmental characteristics of these outcrops, species co-occurrences have been identified, on the one hand, between the Ariño and El Soplao ambers and, on the other hand, between the El Soplao, Peñacerrada I, San Just and Arroyo de la Pascueta ambers. This fact may indicate a possible connection between the resiniferous forests of these areas during the 'mid-Cretaceous', affecting to the distribution of the entomofauna. Interestingly, despite the spatial and temporal separations, more taxonomic similarities at the genus level have been observed between the entomofauna of the Maestrazgo Basin ambers and that of the Barremian ambers of Lebanon and the Cenomanian amber of Myanmar, than with the entomofauna from the geographically close Albian–Cenomanian ambers of France. This might be explained based on palaeoenvironmental, palaeoclimatic, and palaeogeographic factors or ocean currents that favoured or hindered the exchange of entomofauna between Laurasia and the palaeoisland of Iberia.

The Ariño site is unique worldwide because of the presence of vertebrate remains, including dinosaurs, aerial amber rich in bioinclusions found in the same level, providing palaeobiological and palaeoecological information from two complementary types of conservation. This fact, together with its identification as autochthonous-paraautochthonous, allows to consider it as a *Konservat-Lagerstätte* with relevance among the palaeontological sites of the Lower Cretaceous. The multidisciplinary study of its fossil record has provided unprecedented information on the palaeoecology of its ecosystem. The integration of the results allows to infer a palaeoecological web with several levels showing inference of interactions between the organisms and with their environment.

During the Cretaceous, the suitable environmental conditions for the resin mass production and the deposit of the resulting pieces occurred, at least in some regions, such as the Maestrazgo Basin. The factors, both abiotic and biotic, involved in the resin mass production during this period were probably interrelated. A possible factor could be the diversification of angiosperms during the Lower Cretaceous, which could have influenced the displacement of some conifer groups conifer to non-optimal environments, causing the resin mass production due to environmental stress. Additional studies are required to know the factors involved in the resin mass production today. The application of ENM studies and multivariate co-occurrence analyses may provide insights into the key factors involved in resin mass production at Recent and Past.

7. Bibliografía

Aguiar, A.P., Deans, A.R., Engel, M.S., Forshage, M., Huber, J.T., Jennings, J.T., Johnson, N.F., Lelej, A.S., Longino, J.T., Lohrmann, V., Mikó, I., Ohl, M., Rasmussen, C., Taeger, A., Yu, D.S.K. 2013. Order Hymenoptera. En: Zhang, Z.-Q. (Ed.), *Animal biodiversity: an outline of higher-level classification and survey of taxonomic richness (Addenda 2013)*. *Zootaxa*, **3703**(1), 51-62.

Alcalá, L., Espílez, E., Mampel, L., Kirkland, J.I., Ortiga, M., Rubio, D., González, A., Ayala, D., Cobos, A., Royo-Torres, R., Gascó, F., Pesquero, M.D. 2012. A new Lower Cretaceous vertebrate bonebed near Ariño (Teruel, Aragón, Spain); found and managed in a joint collaboration between a mining company and a palaeontological park. *Geoheritage*, **4**, 275-286.

Alcalá, L., Espílez, E., Mampel, L. 2018. Ariño: la mina de los dinosaurios. En: Zamora, S. (Ed), *Fósiles: nuevos hallazgos paleontológicos en Aragón*. Institución «Fernando el Católico», pp. 111-141.

Alonso, J., Arillo, A., Barrón, E., Corral, J.C., Grimalt, J., López, J.F., López, R., Martínez-Delclòs, X., Ortuño, V., Peñalver, E., Trincão, P.R. 2000. A new fossil resin with biological inclusions in Lower Cretaceous deposits from Álava (Northern Spain, Basque-Cantabrian Basin). *Journal of Paleontology*, **74**(1), 158-178.

Álvarez Fernández, E., Peñalver Mollá, E., Delclòs, X. 2005. La presencia de ámbar en los yacimientos prehistóricos (del Paleolítico Superior a la Edad del Bronce) de la Cornisa Cantábrica y sus fuentes de aprovisionamiento. *Zephyrus*, **58**, 159-182.

Álvarez-Parra, S., Nel, A. 2022. A new genus of setose-winged barklice (Psocodea: Trogiomorpha: Lepidopsocidae) from the Eocene amber of Oise with notes on the biogeography of Thylacellinae. *Historical Biology*, 1-10.

Álvarez-Parra, S., Delclòs, X., Solórzano-Kraemer, M.M., Alcalá, L., Peñalver, E. 2020a. Cretaceous amniote integuments recorded through a taphonomic process unique to resins. *Scientific Reports*, **10**, 19840.

Álvarez-Parra, S., Peñalver, E., Nel, A., Delclòs, X. 2020b. The oldest representative of the extant barklice genus *Psyllipsocus* (Psocodea: Trogiomorpha: Psyllipsocidae) from the Cenomanian amber of Myanmar. *Cretaceous Research*, **113**, 104480.

Álvarez-Parra, S., Peñalver E., Nel, P., Nel, A., Delclòs, X. 2021a. A representative of the controversial order †Lophioneurida (Insecta: Thripida) in Albian Spanish amber. En: Vlachos, E., Cruzado-Caballero, P., Crespo, V.D., Ríos Ibañez, M., Arnal, F.A.M., Herraiz, J.L., Gascó-Lluna, F., Guerrero-Arenas, R., Ferrón, H.G. (Eds.), *3rd Palaeontological Virtual Congress Book of Abstracts: palaeontology in the virtual era*, p. 187.

Álvarez-Parra, S., Pérez-de la Fuente, R., Peñalver, E., Barrón, E., Alcalá, L., Pérez-Cano, J., Martín-Closas, C., Trabelsi, K., Meléndez, N., López Del Valle, R., Lozano, R.P., Peris, D., Rodrigo, A., Sarto i Monteys, V., Bueno-Cebollada, C.A., Menor-Salván, C., Philippe, M., Sánchez-García, A., Peña-Kairath, C., Arillo, A., Espílez, E., Mampel, L., Delclòs, X. 2021b. Dinosaur bonebed amber from an original swamp forest soil. *eLife*, **10**, e72477.

Álvarez-Parra, S., Santer, M., Peñalver, E., Engel, M.S., Delclòs, X. 2021c. The wasp family †Serphitidae (Hymenoptera) from Lower Cretaceous Spanish ambers. En: Vlachos, E., Cruzado-Caballero, P., Crespo, V.D., Ríos Ibañez, M., Arnal, F.A.M., Herraiz, J.L., Gascó-Lluna, F., Guerrero-Arenas, R., Ferrón, H.G. (Eds.), *3rd Palaeontological Virtual Congress Book of Abstracts: palaeontology in the virtual era*, p. 188.

Álvarez-Parra, S., Peñalver, E., Delclòs, X., Engel, M.S. 2022a. A braconid wasp (Hymenoptera, Braconidae) from the Lower Cretaceous amber of San Just, eastern Iberian Peninsula. *ZooKeys*, **1103**, 65-78.

Álvarez-Parra, S., Peñalver, E., Nel, A., Delclòs, X. 2022b. New barklice (Psocodea, Trogiomorpha) from Lower Cretaceous Spanish amber. *Papers in Palaeontology*, **8**(3), e1436.

Álvarez-Parra, S., Peñalver, E., Nel, A., Delclòs, X. en preparación 1. Barklice (Insecta: Psocodea) from Early Cretaceous resiniferous forests of Iberia (Spanish amber): new Troctomorpha and the oldest Psocomorpha.

Álvarez-Parra, S., Santer, M., *et al*. en preparación 2. Serphitid wasps (Hymenoptera: Serphitidae) from Early Cretaceous amber of eastern Spain with comments on the evolution and palaeobiology of Serphitoidea.

Andersen, N.M., Spence, J.R., Wilson, M.V.H. 1993. 50 million years of structural stasis in water striders (Hemiptera: Gerridae). *American Entomologist*, **39**(3), 174-176.

Antolín-Tomás, B., Liesa, C.L., Casas, A., Gil-Peña, I. 2007. Geometry of fracturing linked to extension and basin formation in the Maestrazgo Basin (Eastern Iberian Chain, Spain). *Revista de la Sociedad Geológica de España*, **20**(3-4), 351-365.

Arbizu, M., Bernárdez, E., Peñalver, E., Prieto, M.A. 1999. El ámbar de Asturias (España). *Estudios del Museo de Ciencias Naturales de Álava*, **14**(Núm. Espec. 2), 245-254.

Arellano, A.A., Sommer, A.J., Coon, K.L. 2022. Beyond canonical models: why a broader understanding of Diptera-microbiota interactions is essential for vector-borne disease control. *Evolutionary Ecology*.

Arillo, A., Mostovski, M.B. 1999. A new genus of Prioriphorinae (Diptera, Phoridae) from the Lower Cretaceous amber of Alava (Spain). *Studia Dipterologica*, **6**(2), 251-255.

Arillo, A., Nel, A. 2000. Two new fossil cecidomyiids flies from the Lower Cretaceous amber of Alava (Spain) (Diptera, Cecidomyiidae). *Bulletin de la Societé Entomologique de France*, **105**(3), 285-288.

Arillo, A., Peñalver, E., Delclòs, X. 2008a. *Microphorites* (Diptera: Dolichopodidae) from the Lower Cretaceous amber of San Just (Spain), and the co-occurrence of two ceratopogonid species in Spanish amber deposits. *Zootaxa*, **1920**(1), 29-40.

Arillo, A., Subías, L.S., Shtanchaeva, U. 2008b. A new fossil oribatid mite, *Ommatocepheus nortoni* sp. nov. (Acariformes, Oribatida, Cepheidae), from a new outcrop of Lower Cretaceous Álava amber (northern Spain). *Systematic and Applied Acarology*, **13**(3), 252-255.

Arillo, A., Peñalver, E., García-Gimeno, V. 2009a. First fossil *Litoleptis* (Diptera: Spaniidae) from the Lower Cretaceous amber of San Just (Teruel Province, Spain). *Zootaxa*, **2026**(1), 33-39.

Arillo, A., Subías, L.S., Shtanchaeva, U. 2009b. A new fossil species of oribatid mite, *Ametroproctus valeriae* sp. nov. (Acariformes, Oribatida, Ametroproctidae), from the Lower Cretaceous amber of San Just, Teruel Province, Spain. *Cretaceous Research*, **30**(2), 322-324.

Arillo, A., Subías, L.S., Shtanchaeva, U. 2010. A new genus and species of oribatid mite, *Cretaceobodes martinezae* gen. et sp. nov., from the Lower Cretaceous amber of San Just (Teruel Province, Spain) (Acariformes, Oribatida, Otocepheidae). *Paleontological Journal*, **44**(3), 287-290.

Arillo, A., Subías, L.S., Shtanchaeva, U. 2012. A new species of fossil oribatid mite (Acariformes, Oribatida, Trhypochthoniidae) from the Lower Cretaceous amber of San Just (Teruel Province, Spain). *Systematic and Applied Acarology*, **17**(1), 106-112.

Arillo, A., Peñalver, E., Pérez-de la Fuente, R., Delclòs, X., Criscione, J., Barden, P.M., Riccio, P.M., Grimaldi, D.A. 2015. Long-proboscid brachyceran flies in Cretaceous amber (Diptera: Stratiomyomorpha: Zhangsolvidae). *Systematic Entomology*, **40**, 242-267.

Arillo, A., Subías, L.S., Sánchez-García, A. 2016. New species of fossil oribatid mites (Acariformes, Oribatida), from the Lower Cretaceous amber of Spain. *Cretaceous Research*, **63**, 68-76.

Arillo, A., Blagoderov, V., Peñalver, E. 2018. Early Cretaceous parasitism in amber: a new species of *Burmazelmira* fly (Diptera: Archizelmiridae) parasitized by a *Leptus* sp. mite (Acari, Erythraeidae). *Cretaceous Research*, **86**, 24-32.

Arillo, A., Subías, L.S., Peñalver, E. 2020. A new species of fossil Oribatid mite (Acariformes, Oribatida: Caleremaeidae) from a new Cretaceous amber outcrop in Asturias, Spain. *Cretaceous Research*, **109**, 104382.

Arillo, A., Subías, L.S., Álvarez-Parra, S. 2022. First fossil record of the oribatid family Liacaridae (Acariformes: Gustavioidea) from the lower Albian amber-bearing site of Ariño (eastern Spain). *Cretaceous Research*, **131**, 105087.

Arribas, P., Andújar, C., Moraza, M.L., Linard, B., Emerson, B.C., Vogler, A.P. 2020. Mitochondrial metagenomics reveals the ancient origin and phylodiversity of soil mites and provides a phylogeny of the Acari. *Molecular Biology and Evolution*, **37**(3), 683-694.

Ascaso, C., Wierzchos, J., Corral, J.C., López, R., Alonso, J. 2003. New applications of light and electron microscopic techniques for the study of microbiological inclusions in amber. *Journal of Paleontology*, **77**(6), 1182-1192.

Aspöck, H. 2002. The biology of Raphidioptera: a review of present knowledge. *Acta Zoologica Academiae Scientiarum Hungaricae*, **48**(Suppl. 2), 35-50.

Aspöck, U., Haring, E., Aspöck, H. 2012. The phylogeny of the Neuropterida: long lasting and current controversies and challenges (Insecta: Endopterygota). *Arthropod Systematics & Phylogeny*, **70**(2), 119-129.

Aurell, M., Soria, A.R., Bádenas, B., Liesa, C.L., Canudo, J.I., Gasca, J.M., Moreno-Azanza, M., Medrano-Aguado, E., Meléndez, A. 2018. Barremian synrift sedimentation in the Oliete sub-basin (Iberian Basin, Spain): palaeogeographical evolution and distribution of vertebrate remains. *Journal of Iberian Geology*, **44**(2), 285-308.

Azar, D., Nel, A., Perrichot, V. 2015. Diverse barklice (Psocodea) from Late Cretaceous Vendean amber. *Paleontological Contributions*, **2014**(10C), 9-15.

Azar, D., Hakim, M., Huang, D. 2016. A new compsocid booklouse from the Cretaceous amber of Myanmar (Psocodea: Troctomorpha: Amphientometae: Compsocidae). *Cretaceous Research*, **68**, 28-33.

Badii, K.B., Billah, M.K., Afreh-Nuamah, K., Obeng-Ofori, D., Nyarko, G. 2015. Review of the pest status, economic impact and management of fruit-infesting flies (Diptera: Tephritidae) in Africa. *African Journal of Agricultural Research*, **10**(12), 1488-1498.

Bai, M., Beutel, R.G., Klass, K.D., Zhang, W., Yang, X., Wipfler, B. 2016. †Alienoptera — a new insect order in the roach–mantodean twilight zone. *Gondwana Research*, **39**, 317-326.

Barral, A., Gomez, B., Daviero-Gomez, V., Lécuyer, C., Mendes, M.M., Ewin, T.A. 2019. New insights into the morphology and taxonomy of the Cretaceous conifer *Frenelopsis* based on a new species from the Albian of San Just, Teruel, Spain. *Cretaceous Research*, **95**, 21-36.

Barrón, E., Peyrot, D., Rodríguez-López, J.P., Meléndez, N., López del Valle, R., Najarro, M., Rosales, I., Comas-Rengifo, M.J. 2015. Palynology of Aptian and upper Albian (Lower Cretaceous) amber-bearing outcrops of the southern margin of the Basque-Cantabrian basin (northern Spain). *Cretaceous Research*, **52**, 292-312.

Barrón, E., Peyrot, D., Bueno-Cebollada, C.A., Kvaček, J., Álvarez-Parra, S., Altolaguirre, Y., Meléndez, N. enviado. Biodiversity of ecosystems in an arid setting: the late Albian plant communities and associated biota from eastern Iberia. *PLOS One*.

Baz, A., Ortuño, V.M. 2000. Archaeatropidae, a new family of Psocoptera from the Cretaceous amber of Alava, Northern Spain. *Annals of the Entomological Society of America*, **93**(3), 367-373.

Baz, A., Ortuño, V.M. 2001a. A new electrentomoid psocid (Psocoptera) from the Cretaceous amber of Alava (Northern Spain). *Deutsche Entomologische Zeitschrift*, **48**(1), 27-32.

Baz, A., Ortuño, V.M. 2001b. New genera and species of empheriids (Psocoptera: Empheriidae) from the Cretaceous amber of Alava, northern Spain. *Cretaceous Research*, **22**(5), 575-584.

Beck, C.W., Wilbur, E., Meret, S. 1964. Infra-red spectra and the origin of amber. *Nature*, **201**(4916), 256-257.

Bell, W.J., Roth, L.M., Nalepa, C.A. 2007. *Cockroaches: ecology, behavior, and natural history*. The Johns Hopkins University Press, 248 pp.

Bengtson, P. 1988. Open nomenclature. *Palaeontology*, **31**(1), 223-227.

Bennett, D.J., Engel, M.S. 2005. A primitive sapygid wasp in Burmese amber (Hymenoptera: Sapygidae). *Acta Zoologica Cracoviensia*, **48**(3-4), 1-9.

Benton, M.J., Wilf, P., Sauquet, H. 2022. The Angiosperm Terrestrial Revolution and the origins of modern biodiversity. *New Phytologist*, **233**(5), 2017-2035.

Béthoux, O., Wieland, F. 2009. Evidence for Carboniferous origin of the order Mantodea (Insecta: Dictyoptera) gained from forewing morphology. *Zoological Journal of the Linnean Society*, **156**(1), 79-113.

Beutel, R.G., Friedrich, F., Aspöck, U. 2010. The larval head of Nevrorthidae and the phylogeny of Neuroptera (Insecta). *Zoological Journal of the Linnean Society*, **158**(3), 533-562.

Bignell D.E., Roisin, Y. Lo, N. 2010. *Biology of termites: a modern synthesis*. Springer, 576 pp.

Blagoderov, V.A., Arillo, A. 2002. New Sciaroidea (Insecta: Diptera) in Lower Cretaceous amber from Spain. *Studia Dipterologica*, **9**(1), 31-40.

Bojesen-Koefoed, J.A., Christiansen, F.G., Petersen, H.I., Piasecki, S., Stemmerik, L., Nytoft, H.P. 1996. Resinite-rich coals of northeast Greenland-a hitherto unrecognized, highly oil-prone Jurassic source rock. *Bulletin of Canadian Petroleum Geology*, **44**(3), 458-473.

Borkent, A. 1997. Upper and Lower Cretaceous biting midges (Ceratopogonidae: Diptera) from Hungarian and Austrian amber and the Koonwarra fossil bed of Australia. *Stuttgarter Beiträge zur Naturkunde Serie B (Geologie un Paläontologie)*, **249**, 1-10.

Borkent, A. 2019. The phylogenetic relationships of Cretaceous biting midges, with a key to all known genera (Diptera: Ceratopogonidae). *American Museum Novitates*, **3921**, 1-48.

Boscá, A. 1910. Cuenca calaminífera de Linares de Aragón. *Asociación Española para el Progreso de las Ciencias*, **4**, 171-181.

Bouju, V., Perrichot, V. 2020. A review of amber and copal occurrences in Africa and their paleontological significance. *Bulletin de la Société Géologique de France*, **191**, 17.

Bover-Arnal, T., Moreno-Bedmar, J.A., Frijia, G., Pascual-Cebrian, E., Salas, R. 2016. Chronostratigraphy of the Barremian-Early Albian of the Maestrat Basin (E Iberian Peninsula): integrating strontium-isotope stratigraphy and ammonoid biostratigraphy. *Newsletters on Stratigraphy*, **49**, 41-68.

Brasier, M., Cotton, L., Yenney, I. 2009. First report of amber with spider webs and microbial inclusions from the earliest Cretaceous (c. 140 Ma) of Hastings, Sussex. *Journal of the Geological Society*, **166**(6), 989-997.

Bray, P.S., Anderson, K.B. 2009. Identification of Carboniferous (320 million years old) class Ic amber. *Science*, **326**(5949), 132-134.

Bueno-Cebollada, C.A., Barrón, E., Peyrot, D., Meléndez, N. 2021. Palynostratigraphy and palaeoenvironmental evolution of the Aptian to lower Cenomanian succession in the Serranía de Cuenca (Eastern Spain). *Cretaceous Research*, **128**, 104956.

Bueno-Cebollada, C.A., Fregenal-Martínez, M., Meléndez, N. 2022. Along-strike sedimentological variability and architectural patterns of the transgression of a "mid"-Cretaceous braidplain system (Iberian Basin, eastern Spain): a tool for depicting eustatic and tectonic signatures within the framework of a global transgression. *Sedimentary Geology*, **429**, 106082.

Buscalioni, Á.D., Alcalá, L., Espílez, E., Mampel, L. 2013. European Goniopholididae from the Early Albian Escucha Formation in Ariño (Teruel, Aragón, Spain). *Spanish Journal of Palaeontology*, **28**(1), 103-122.

Cai, C., Tihelka, E., Pan, Y., Yin, Z., Jiang, R., Xia, F., Huang, D. 2020. Structural colours in diverse Mesozoic insects. *Proceedings of the Royal Society B*, **287**(1930), 20200301.

Casal, G. 1762. *Succini Asturici, à Doctore Gafpar Cafal, Almae Eclefiae Cathedralis Ovetenfis Medico, reperti, folertique ejufdem cura probati, & examinati, Hiftoria*. Servicio de Publicaciones, Historia Natural y Médica del Principado de Asturias, Ed. Facsímil 1998, 480 pp.

Cavanilles, A.J. 1797. *Observaciones sobre la historia natural, geografía, agricultura, población y frutos del Reyno de Valencia*. Imprenta Real de Madrid, Tomo II, 339 pp.

Cervera, A., Pardo, G., Villena, J. 1976. Algunas precisiones litoestratigráficas sobre la formación 'Lignitos de Escucha'. *Tecniterrae*, **14**, 25-33.

Chaler, R., Grimalt, J.O. 2005. Fingerprinting of Cretaceous higher plant resins by infrared spectroscopy and gas chromatography coupled to mass spectrometry. *Phytochemical Analysis*, **16**(6), 446-450.

Chefaoui, R.M., Assis, J., Duarte, C.M., Serrão, E.A. 2016. Large-scale prediction of seagrass distribution integrating landscape metrics and environmental factors: the case of *Cymodocea nodosa* (Mediterranean–Atlantic). *Estuaries and Coasts*, **39**(1), 123-137.

Chen, X.X., van Achterberg, C. 2019. Systematics, phylogeny, and evolution of braconid wasps: 30 years of progress. *Annual Review of Entomology*, **64**(1), 335-358.

Chiarenza, A.A., Mannion, P.D., Farnsworth, A., Carrano, M.T., Varela, S. 2022. Climatic constraints on the biogeographic history of Mesozoic dinosaurs. *Current Biology*, **32**(3), 570-585.

Chitimia-Dobler, L., Mans, B.J., Handschuh, S., Dunlop, J.A. 2022. A remarkable assemblage of ticks from mid-Cretaceous Burmese amber. *Parasitology*, **149**(6), 820-830.

Choufani, J., El-Halabi, W., Azar, D., Nel, A. 2015. First fossil insect from Lower Cretaceous Lebanese amber in Syria (Diptera: Ceratopogonidae). *Cretaceous Research*, **54**, 106-116.

Cobos, M.E., Townsend Peterson, A., Barve, N., Osorio-Olvera, L. 2019. kuenm: an R package for detailed development of ecological niche models using Maxent. *PeerJ*, **7**, e6281.

Cockx, P., McKellar, R., Tappert, R., Vavrek, M., Muehlenbachs, K. 2020. Bonebed amber as a new source of paleontological data: the case of the Pipestone Creek deposit (Upper Cretaceous), Alberta, Canada. *Gondwana Research*, **81**, 378-389.

Colin, J.P., Néraudeau, D., Nel, A., Perrichot, V. 2011. Termite coprolites (Insecta: Isoptera) from the Cretaceous of western France: a palaeoecological insight. *Revue de Micropaléontologie*, **54**(3), 129-139.

Corral, J.C., López Del Valle, R., Alonso, J. 1999. El ámbar cretácico de Álava (Cuenca Vasco-Cantábrica, norte de España). Su colecta y preparación. *Estudios del Museo de Ciencias Naturales de Álava*, **14**, 7-21.

Crowson, R.A. 1981. *The biology of the Coleoptera*. Academic Press, 802 pp.

Csiki-Sava, Z., Buffetaut, E., Ősi, A., Pereda-Suberbiola, X., Brusatte, S.L. 2015. Island life in the Cretaceous-faunal composition, biogeography, evolution, and extinction of land-living vertebrates on the Late Cretaceous European archipelago. *ZooKeys*, **469**, 1-161.

Dal Corso, J., Roghi, G., Ragazzi, E., Angelini, I., Giaretta, A., Soriano, Delclòs, X., Jenkyns, H.C. 2013. Physico-chemical analysis of Albian (Lower Cretaceous) amber from San Just (Spain): implications for palaeoenvironmental and palaeoecological studies. *Geologica Acta*, **11**(3), 359-370.

Dalgleish, R.C., Palma, R.L., Price, R.D., Smith, V.S. 2006. Fossil lice (Insecta: Phthiraptera) reconsidered. *Systematic Entomology*, **31**(4), 648-651.

Dallai, R., Mercati, D., Carapelli, A., Nardi, F., Machida, R., Sekiya, K., Frati, F. 2011. Sperm accessory microtubules suggest the placement of Diplura as the sister-group of Insecta ss. *Arthropod Structure & Development*, **40**(1), 77-92.

Daviero, V., Gomez, B., Philippe, M. 2001. Uncommon branching pattern within conifers: *Frenelopsis turolensis*, a Spanish Early Cretaceous Cheirolepidiaceae. *Canadian Journal of Botany*, **79**(12), 1400-1408.

Davranoglou, L.-R., Cicirello, A., Taylor, G.K., Mortimer, B. 2019. Planthopper bugs use a fast, cyclic elastic recoil mechanism for effective vibrational communication at small body size. *PLOS Biology*, **17**(3), e3000155.

Davranoglou, L.-R., Mortimer, B., Taylor, G.K., Malenovský, I. 2020. On the morphology and evolution of cicadomorphan tymbal organs. *Arthropod Structure & Development*, **55**, 100918.

de Moya, R.S., Yoshizawa, K., Walden, K.K., Sweet, A.D., Dietrich, C.H., Kevin P.J. 2021. Phylogenomics of parasitic and nonparasitic lice (Insecta: Psocodea): combining sequence data and exploring compositional bias solutions in next generation data sets. *Systematic Biology*, **70**(4), 719-738.

Delclòs, X., Arillo, A., Peñalver, E., Barrón, E., Soriano, C., López Del Valle, R., Bernárdez, E., Corral, C., Ortuño, V.M. 2007. Fossiliferous amber deposits from the Cretaceous (Albian) of Spain. *Comptes Rendus Palevol*, **6**(1-2), 135-149.

Delclòs, X., Peñalver, E., Arillo, A., Engel, M.S., Nel, A., Azar, D., Ross, A. 2016. New mantises (Insecta: Mantodea) in cretaceous ambers from Lebanon, Spain, and Myanmar. *Cretaceous Research*, **60**, 91-108.

Delclòs, X., Peñalver, E., Ranaivosoa, V., Solórzano-Kraemer, M.M. 2020. Unravelling the mystery of "Madagascar copal": age, origin and preservation of a Recent resin. *PLOS One*, **15**(5), e0232623.

Delclòs, X., Peñalver, E., Barrón, E., Pérez-de la Fuente, R., Grimaldi, D.A., Holz, M., Labandeira, C., Scotese, C.R., Solórzano-Kraemer, M.M., Álvarez-Parra, S., *et al*., Peris, D. en preparación. Amber and the Cretaceous Resinous Interval: hypotheses on causes.

Dierick, M., Cnudde, V., Masschaele, B., Vlassenbroeck, J., Van Hoorebeke, L., Jacobs, P. 2007. Micro-CT of fossils preserved in amber. *Nuclear Instruments and Methods in Physics Research Section A: Accelerators, Spectrometers, Detectors and Associated Equipment*, **580**(1), 641-643.

Dunlop, J.A., Selden, P.A., Pfeffer, T., Chitimia-Dobler, L. 2018. A Burmese amber tick wrapped in spider silk. *Cretaceous Research*, **90**, 136-141.

Dunlop, J.A., Garwood, R.J. 2018. Terrestrial invertebrates in the Rhynie chert ecosystem. *Philosophical Transactions of the Royal Society B: Biological Sciences*, **373**(1739), 20160493.

Dunlop, J.A., Penney, D., Jekel, D. 2022. A summary list of fossil spiders and their relatives. En: *World spider catalog, v.23.5*. Natural History Museum Bern. Disponible *online* en http://wsc.nmbe.ch (consultado el 30/08/2022).

Dutta, S., Mallick, M., Kumar, K., Mann, U., Greenwood, P.F. 2011. Terpenoid composition and botanical affinity of Cretaceous resins from India and Myanmar. *International Journal of Coal Geology*, **85**(1), 49-55.

Edwards, H.G., Farwell, D.W. 1996. Fourier transform-Raman spectroscopy of amber. *Spectrochimica Acta Part A: Molecular and Biomolecular Spectroscopy*, **52**(9), 1119-1125.

Engel, M.S. 2002. The smallest snakefly (Raphidioptera: Mesoraphidiidae): a new species in Cretaceous amber from Myanmar, with a catalog of fossil snakeflies. *American Museum Novitates*, **3363**, 1-22.

Engel, M.S. 2015. A new family of primitive serphitoid wasps in Lebanese amber (Hymenoptera: Serphitoidea). *Novitates Paleoentomologicae*, **13**, 1-22.

Engel, M.S., Delclòs, X. 2010. Primitive termites in Cretaceous amber from Spain and Canada (Isoptera). *Journal of the Kansas Entomological Society*, **83**(2), 111-128.

Engel, M.S., Grimaldi, D.A., Krishna, K. 2009. Termites (Isoptera): their phylogeny, classification, and rise to ecological dominance. *American Museum Novitates*, **3650**, 1-27.

Engel, M.S., Ortega-Blanco, J., McKellar, R.C. 2013a. New scolebythid wasps in Cretaceous amber from Spain and Canada, with implications for the phylogeny of the family (Hymenoptera: Scolebythidae). *Cretaceous Research*, **46**, 31-42.

Engel, M.S., Ortega-Blanco, J., Soriano, C., Grimaldi, D.A., Delclòs, X. 2013b. A new lineage of enigmatic diaprioid wasps in Cretaceous amber (Hymenoptera: Diaprioidea). *American Museum Novitates*, **3771**, 1-23.

Engel, M.S., Winterton, S.L., Breitkreuz, L.C. 2018. Phylogeny and evolution of Neuropterida: where have wings of lace taken us? *Annual Review of Entomology*, **63**, 531-551.

Estévez-Gallardo, P., Sender, L.M., Mayoral, E., Diez, J.B. 2017. First evidence of insect herbivory on Albian aquatic angiosperms of the NE Iberian Peninsula. *Earth and Environmental Science Transactions of the Royal Society of Edinburgh*, **108**(4), 429-435.

Fernández-Rubio, F., Peñalver, E., Martínez-Delclòs, X. 1991. *Zygaena*? *turolensis*, una nueva especie de lepidóptera zygaenidae del mioceno de Rubielos de Mora (Teruel): descripción y filogenia. *Estudios del Museo de Ciencias Naturales de Álava*, **6**, 77-93.

Franklin, J. 2010. *Mapping species distributions: spatial inference and prediction*. Cambridge University Press, 320 pp.

Friedman, V., Lambert, J.B., Contreras, T.A., Stout, E., Kaur, S., Mitamura, H. 2018. Late Cretaceous amber in Texas: chemical characterization and paleoenvironment. *Life: The Excitement of Biology*, **5**(3), 132-154.

Foelix, R.F. 2011. *Biology of spiders*. Oxford University Press, Third Edition, 432 pp.

Föllmi, K.B. 2012. Early Cretaceous life, climate and anoxia. *Cretaceous Research*, **35**, 230-257.

García-Cortés, A., Cabrera Ferrero, A. 2021. El Inventario Español de Lugares de Interés Geológico (IELIG): metodología y reflexiones para su futura actualización. *Revista de la Sociedad Española para la Defensa del Patrimonio Geológico y Minero*, **36**, 53-68.

García-Penas, A., Aurell, M., Zamora, S. 2022. Progressive opening of a shallow-marine bay (Oliete Subbasin, Spain) and the record of possible eustatic fall events near the Barremian-Aptian boundary. *Palaeogeography, Palaeoclimatology, Palaeoecology*, **594**, 110938.

Gauweiler, J., Haug, C., Müller, P., Haug, J.T. 2022. Lepidopteran caterpillars in the Cretaceous: were they a good food source for early birds? *Palaeodiversity*, **15**(1), 45-59.

Girard, V., Breton, G., Perrichot, V., Bilotte, M., Le Loeuff, J., Nel, A., Philippe, M., Thevenard, F. 2013a. The Cenomanian amber of Fourtou (Aude, Southern France): taphonomy and palaeoecological implications. *Annales de Paléontologie*, **99**(4), 301-315.

Girard, V., Néraudeau, D., Breton, G., Morel, N. 2013b. Palaeoecology of the Cenomanian amber forest of Sarthe (western France). *Geologica Acta*, **11**(3), 321-330.

Giribet, G., Edgecombe, G.D. 2012. Reevaluating the arthropod tree of life. *Annual Review of Entomology*, **57**, 167-186.

Goldstein, P.Z. 2017. Diversity and significance of Lepidoptera: a phylogenetic perspective. En: Foottit, R.G., Adler, P.H. (Eds.), *Insect biodiversity: science and society*. John Wiley & Sons, pp. 463-495.

Golub, V.B., Popov, Y., Arillo, A. 2012. Hispanocaderidae n. fam. (Hemiptera: Heteroptera: Tingoidea), one of the oldest lace bugs from the Lower Cretaceous Álava amber (Spain). *Zootaxa*, **3270**(1), 41-50.

Gomez, B. 2002. A new species of *Mirovia* (Coniferales, Miroviaceae) from the Lower Cretaceous of the Iberian Ranges (Spain). *Cretaceous Research*, **23**(6), 761-773.

Gomez, B., Barale, G., Martín-Closas, C., Thévenard, F., Philippe, M. 1999. Découverte d'une flore à Ginkgoales, Bennettitales et Coniférales dans le Crétacé inférieur de la Formation Escucha (Chaîne Ibérique Orientale, Teruel, Espagne). *Neues Jahrbuch für Geologie und Paläontologie, Monatshefte*, **11**, 661-675.

Gomez, B., Martín-Closas, C., Barale, G., Thévenard, F. 2000. A new species of *Nehvizdya* (Ginkgoales) from the Lower Cretaceous of the Iberian Ranges (Spain). *Review of Palaeobotany and Palynology*, **111**(1-2), 49-70.

Gomez, B., Martín-Closas, C., Barale, G., Solé de porta, N., Thévenard, F., Guignard, G. 2002a. *Frenelopsis* (Coniferales: Cheirolepidiaceae) and related male organ genera from the Lower Cretaceous of Spain. *Palaeontology*, **45**(5), 997-1036.

Gomez, B., Martínez-Delclòs, X., Bamford, M., Philippe, M. 2002b. Taphonomy and palaeoecology of plant remains from the oldest African Early Cretaceous amber locality. *Lethaia*, **35**(4), 300-308.

Goulet, H., Huber, J.T. 1993. *Hymenoptera of the world: an identification guide to families*. Research Branch Agriculture Canada, 668 pp.

Grimaldi, D.A. 2019. Amber. *Current Biology*, **29**(18), R861-R862.

Grimaldi, D.A., Arillo, A. 2008. The Tethepomyiidae, a new family of enigmatic Cretaceous Diptera. *Alavesia*, **2**, 259-265.

Grimaldi D.A., Engel M.S. 2005. *Evolution of the insects*. Cambridge University Press, 755 pp.

Grimaldi, D.A., Nascimbene, P.C. 2010. Raritan (New Jersey) Amber. En: Penney, D. (Ed.), *Biodiversity of fossils in amber from the major world deposits*. Siri Scientific Press, pp. 167-191.

Grimaldi, D.A., Beck, C.W., Boon, J.J. 1989. Occurrence, chemical characteristics, and paleontology of the fossil resins from New Jersey. *American Museum Novitates*, **2948**, 1-28.

Grimaldi, D.A., Lillegraven, J.A., Wampler, T.W., Bookwalter, D., Shedrinsky, A. 2000. Amber from Upper Cretaceous through Paleocene strata of the Hanna Basin, Wyoming, with evidence for source and taphonomy of fossil resins. *Rocky Mountain Geology*, **35**(2), 163-204.

Grimaldi, D.A., Engel, M.S., Nascimbene, P.C. 2002. Fossiliferous Cretaceous amber from Myanmar (Burma): its rediscovery, biotic diversity, and paleontological significance. *American Museum Novitates*, **3361**, 1-71.

Grimaldi, D.A., Amorim, D.D.S., Blagoderov, V. 2003. The Mesozoic family Archizelmiridae (Diptera: Insecta). *Journal of Paleontology*, **77**(2), 368-381.

Grimaldi, D.A., Shmakov, A., Fraser, N. 2004. Mesozoic thrips and early evolution of the order Thysanoptera (Insecta). *Journal of Paleontology*, **78**(5), 941-952.

Grimaldi, D.A., Cumming, J.M., Arillo, A. 2009. Chimeromyiidae, a new family of Eremoneuran Diptera from the Cretaceous. *Zootaxa*, **2078**(1), 34-54.

Grimaldi, D.A., Arillo, A., Cumming, J.M., Hauser, M. 2011. Brachyceran Diptera (Insecta) in Cretaceous ambers, part IV, significant new orthorrhaphous taxa. *ZooKeys*, **148**, 293-332.

Grimalt, J.O., Simoneit, B.R.T., Hatcher, P.G., Nissenbaum, A. 1988. The molecular composition of ambers. *Organic Geochemistry*, **13**(4-6), 677-690.

Guisan, A., Thuiller, W., Zimmermann, N.E. 2017. *Habitat suitability and distribution models: with applications in R*. Cambridge University Press, 300 pp.

Gumovsky, A., Perkovsky, E., Rasnitsyn, A. 2018. Laurasian ancestors and “Gondwanan” descendants of Rotoitidae (Hymenoptera: Chalcidoidea): what a review of Late Cretaceous *Baeomorpha* revealed. *Cretaceous Research*, **84**, 286-322.

Guo, X., Selden, P.A., Ren, D. 2022. New specimens from mid-Cretaceous Myanmar amber illuminate the phylogenetic placement of Lagonomegopidae (Arachnida: Araneae). *Zoological Journal of the Linnean Society*, **195**(2), 399-416.

Gutjahr, A.L.N., de Souza Braga, C.E. 2018. Order Orthoptera. En: Hamada, N., Thorp, J.H., Rogers, D.C. (Eds.), *Thorp and covich's freshwater invertebrates*. Academic Press, Volumen 3, pp. 143-168.

Hakim, M., Azar, D., Huang, D. 2020. A unique manicapsocid (Psocodea: Amphientometae) from the mid-Cretaceous Burmese amber. *Cretaceous Research*, **107**, 104278.

Halbwachs, H. 2019. Fungi trapped in amber—a fossil legacy frozen in time. *Mycological Progress*, **18**(7), 879-893.

Harms, D., Dunlop, J.A. 2017. The fossil history of pseudoscorpions (Arachnida: Pseudoscorpiones). *Fossil Record*, **20**(2), 215-238.

Haug, J.T., Müller, P., Haug, C. 2020. A 100 million-year-old snake-fly larva with an unusually large antenna. *Bulletin of Geosciences*, **95**(2), 167-177.

Havelcová, M., Machovič, V., Linhartová, M., Lapčák, L., Přichystal, A., Dvořák, Z. 2016. Vibrational spectroscopy with chromatographic methods in molecular analyses of Moravian amber samples (Czech Republic). *Microchemical Journal*, **128**, 153-160.

Heimhofer, U., Hochuli, P.A., Burla, S., Oberli, F., Adatte, T., Dinis, J.L., Weissert, H. 2012. Climate and vegetation history of western Portugal inferred from Albian near-shore deposits (Galé Formation, Lusitanian Basin). *Geological Magazine*, **149**(6), 1046-1064.

Henwood, A. 1993. Recent plant resins and the taphonomy of organisms in amber: a review. *Modern Geology*, **19**(1), 35-59.

Hinkelman, J., Vršanská, L. 2020. A Myanmar amber cockroach with protruding feces contains pollen and a rich microcenosis. *The Science of Nature*, **107**, 13.

Hoffmann, J.J., Kingsolver, B.E., McLaughlin, S.P., Timmermann, B.N. 1984. Production of resins by arid-adapted Astereae. En: Timmermann, B.M., Steelink, C., Loewus, F.A. (Eds.), *Phytochemical adaptations to stress*. Springer, pp. 251-271.

Honsberger, D.N., Huber, J.T., Wright, M.G. 2022. A new *Mymaromma* sp. (Mymarommatoidea, Mymarommatidae) in Hawai'i and first host record for the superfamily. *Journal of Hymenoptera Research*, **89**, 73-87.

Hopkin, S.P. 1997. *Biology of the springtails (Insecta: Collembola)*. Oxford University Press, 340 pp.

Hutchinson, G.E. 1957. Concluding Remarks. *Cold Spring Harbor Symposia on Quantitative Biology*, **22**(0), 415-427.

Inward, D., Beccaloni, G., Eggleton, P. 2007. Death of an order: a comprehensive molecular phylogenetic study confirms that termites are eusocial cockroaches. *Biology Letters*, **3**(3), 331-335.

Jarzembowski, E., Azar, D., Nel, A. 2008. A new chironomid (Insecta: Diptera) from Wealden amber (Lower Cretaceous) of the Isle of Wight (UK). *Geologica Acta*, **6**(3), 285-291.

Jensen, K.H., Berg-Sørensen, K., Bruus, H., Holbrook, N.M., Liesche, J., Schulz, A., Zwieniecki, M.A., Bohr, T. 2016. Sap flow and sugar transport in plants. *Reviews of Modern Physics*, **88**(3), 035007.

Jiang, H., Tomaschek, F., Drew Muscente, A., Niu, C., Nyunt, T.T., Fang, Y., Schmidt, U., Chen, J., Lönartz, M., Mähler, B., Wappler, T., Jarzembowski, E.A., Szwedo, J., Zhang, H., Rust, J., Wang, B.

2022. Widespread mineralization of soft-bodied insects in Cretaceous amber. *Geobiology*, **20**(3), 363-376.

Johnson, K.P., Dietrich, C.H., Friedrich, F., Beutel, R.G., Wipfler, B., Peters, R.S., Allen, J.M., Petersen, M., Donath, A., Walden, K.K.O., Kozlov, A.M., Podsiadlowski, L., Mayer, C., Meusemann, K., Vasilikopoulos, A., Waterhouse, R.M., Cameron, S.L., Weirauch, C., Swanson, D.R., Percy, D.M., Hardy, N.B., Terry, I., Liu, S., Zhou, X., Misof, B., Robertson, H.M., Yoshizawa, K. 2018. Phylogenomics and the evolution of hemipteroid insects. *Proceedings of the National Academy of Sciences*, **115**(50), 12775-12780.

Kania-Kłosok, I., Krzemiński, W., Arillo, A. 2021a. Two new long-rostrum cranefly species from the Cretaceous Iberian amber (Diptera, Limoniidae, *Helius*). *Scientific Reports*, **11**, 12851.

Kania-Kłosok, I., Krzemiński, W., Kopeć, K., Arillo, A. 2021b. The oldest evolutionary lineage of *Trichoneura* Loew, 1850 (Diptera, Limoniidae) and the first evidence of this genus in Cretaceous Spanish amber. *Insects*, **12**(5), 411.

Kiesmüller, C., Haug, J.T., Müller, P., Hörnig, M.K. 2022. Debris-carrying behaviour of bark lice immatures preserved in 100 million years old amber. *PalZ*, **96**(2), 231-258.

Kimura, K.I., Minamikawa, Y., Ogasawara, Y., Yoshida, J., Saitoh, K.I., Shinden, H., Ye, Y.Q., Takahashi, S., Miyakawa, T., Koshino, H. 2012. Kujigamberol, a new dinorlabdane diterpenoid isolated from 85 million years old Kuji amber using a biotechnological assay. *Fitoterapia*, **83**(5), 907-912.

Kirkland, J.I., Alcalá, L., Loewen, M.A., Espílez, E., Mampel, L., Wiersma, J.P. 2013. The basal nodosaurid ankylosaur *Europelta carbonensis* n. gen., n. sp. from the Lower Cretaceous (lower Albian) Escucha Formation of northeastern Spain. *PLOS One*, **8**(12), e80405.

Kosmowska-Ceranowicz, B. 2015. Infrared spectra atlas of fossil resins, subfossil resins and selected imitations of amber. En: Kosmowska-Ceranowicz, B., Vávra, N. (Eds.), *Infrared spectra of the world's resin–holotype characteristics*. PAS Museum of Earth, pp. 7-214.

Krantz, G.W., Walter, D.E. 2009. *A manual of acarology*. Texas Tech University Press, 816 pp.

Krishna, K., Grimaldi, D.A., Krishna, V., Engel, M.S. 2013. Treatise on the Isoptera of the world. *Bulletin of the American Museum of Natural History*, **377**, 1-2704.

Krzemiński, W., Arillo, A. 2007. *Alavia neli* n. gen. and n. sp. —the first Limoniidae (Diptera) from the Lower Cretaceous amber of Alava (Spain). *Alavesia*, **1**, 11-13.

Kukalová-Peck, J. 1987. New Carboniferous Diplura, Monura, and Thysanura, the hexapod ground plan, and the role of thoracic side lobes in the origin of wings (Insecta). *Canadian Journal of Zoology*, **65**(10), 2327-2345.

Kvaček, J., Barrón, E., Heřmanová, Z., Mendes, M.M., Karch, J., Žemlička, J., Dudak, J. 2018. Araucarian conifer from late Albian amber of northern Spain. *Papers in Palaeontology*, **4**(4), 643-656.

Kypke, J.L., Solodovnikov, A. 2020. Every cloud has a silver lining: X-ray micro-CT reveals *Orsunius* rove beetle in Rovno amber from a specimen inaccessible to light microscopy. *Historical Biology*, **32**(7), 940-950.

Labandeira, C.C. 2014. Amber. En: Laflamme, M., Schiffbauer, J.D., Darroch, S.A.F. (Eds.), *Reading and writing of the fossil record: preservational pathways to exceptional fossilization*. The Paleontological Society Papers, 20, pp. 163-217.

Labandeira, C.C., Li, L. 2021. The history of insect parasitism and the Mid-Mesozoic Parasitoid Revolution. En: De Baeths, K., Huntley, J.W. (Eds.), *The evolution and fossil record of parasitism: identification and macroevolution of parasites*. Springer, Topics in Geobiology, 49(11), pp. 377-533.

Laita, E., Bauluz, B., Yuste, A. 2019. High-temperature mineral phases generated in natural clinkers by spontaneous combustion of coal. *Minerals*, **9**(4), 213.

Lambert, J.B., Poinar, G.O., Jr. 2002. Amber: the organic gemstone. *Accounts of Chemical Research*, **35**(8), 628-636.

Lambert, J.B., Levy, A.J., Rueb, N.R., Nguyen, T.V., Wu, Y., Santiago-Blay, J.A. 2016. Amber from Japan: a nuclear magnetic resonance study. *Life: The Excitement of Biology*, **3**(4), 231-253.

Langenheim, J.H. 1969. Amber: a botanical inquiry. *Science*, **163**(3872), 1157-1169.

Langenheim, J.H. 1995. Biology of amber-producing trees: focus on case studies of *Hymenaea* and *Agathis*. En: Anderson, K.B., Crelling, J.C. (Eds.), *American Chemical Society symposium series*. American Chemical Society, 617, pp. 1-31.

Langenheim, J.H. 2003. *Plant resins: chemistry, evolution, ecology, and ethnobotany*. Timber Press, 586 pp.

Langenheim, J.H., Beck, C.W. 1965. Infrared spectra as a means of determining botanical sources of amber. *Science*, **149**(3679), 52-55.

Li, Y., Li, Y. D., Wang, Y.D., Schneider, H., Shi, G.L. 2022a. Re-appraisal of lacewing mimicry of liverworts from the mid-Cretaceous Kachin amber, Myanmar with a description of *Selaginella cretacea* sp. nov. (Selaginellales, Selaginellaceae). *Cretaceous Research*, **133**, 105143.

Li, S., Yoshizawa, K., Wang, Q., Ren, D., Bai, M., Yao, Y. 2022b. New genus and species of †Empheriidae (Insecta: Psocodea: Trogiomorpha) and their implication for the phylogeny of infraorder Atropetae. *Frontiers in Ecology and Evolution*, **10**, 907903.

Litwin, R.J., Ash, S.R. 1991. First early Mesozoic amber in the western hemisphere. *Geology*, **19**(3), 273-276.

Lloyd, G.T., Davis, K.E., Pisani, D., Tarver, J.E., Ruta, M., Sakamoto, M., Hone, D.W.E., Jennings, R., Benton, M.J. 2008. Dinosaurs and the Cretaceous terrestrial revolution. *Proceedings of the Royal Society B: Biological Sciences*, **275**(1650), 2483-2490.

Lozano, R.P., Pérez-de la Fuente, R., Barrón, E., Rodrigo, A., Viejo, J.L., Peñalver, E. 2020. Phloem sap in Cretaceous ambers as abundant double emulsions preserving organic and inorganic residues. *Scientific Reports*, **10**, 9751.

Lu, X., Liu, X. 2021. The Neuropterida from the mid-Cretaceous of Myanmar: a spectacular palaeodiversity bridging the Mesozoic and present faunas. *Cretaceous Research*, **121**, 104727.

Luan, Y.X., Mallatt, J.M., Xie, R.D., Yang, Y.M., Yin, W.Y. 2005. The phylogenetic positions of three basal-hexapod groups (Protura, Diplura, and Collembola) based on ribosomal RNA gene sequences. *Molecular Biology and Evolution*, **22**(7), 1579-1592.

Ludwig, L., Barbour, M.A., Guevara, J., Avilés, L., González, A.L. 2018. Caught in the web: spider web architecture affects prey specialization and spider–prey stoichiometric relationships. *Ecology and Evolution*, **8**(13), 6449-6462.

Lukashevich, E.D., Arillo, A. 2016. New *Eoptychoptera* (Insecta: Diptera, Ptychopteridae) from the Lower Cretaceous of Spain. *Cretaceous Research*, **58**, 254-264.

Luo, C., Beutel, R.G., Engel, M.S., Liang, K., Li, L., Li, J., Xu, C., Vršanský, P., Jarzembowski, E.A., Wang, B. 2022a. Life history and evolution of the enigmatic Cretaceous–Eocene Alienopteridae: a critical review. *Earth-Science Reviews*, **225**, 103914.

Luo, C.-H., Beutel, R.G., Thomson, U.R., Zheng, D.R., Li, J.-H., Zhao, X.-Y., Zhang, H.-C., Wang, B. 2022b. Beetle or roach: systematic position of the enigmatic Umenocoleidae based on new material from Zhonggou Formation in Jiuquan, Northwest China, and a morphocladistic analysis. *Palaeoworld*, **31**(1), 121-130.

MacPhee, R.D.E., Grimaldi, D.A. 1996. Mammal bones in Dominican amber. *Nature*, **380**, 489-490.

Maguire, K.C., Stigall, A.L. 2009. Using ecological niche modeling for quantitative biogeographic analysis: a case study of Miocene and Pliocene Equinae in the Great Plains. *Paleobiology*, **35**(4), 587-611.

Maheu, A., Nel, A. 2020. A new fossil booklouse (Psocodea: Troctomorpha: Amphientometae: Manicapsocidae) from the mid-Cretaceous amber of northern Myanmar. *Cretaceous Research*, **106**, 104222.

Makarkin, V.N., Yang, Q., Peng, Y., Ren, D. 2012. A comparative overview of the neuropteran assemblage of the Lower Cretaceous Yixian Formation (China), with description of a new genus of Psychopsidae (Insecta: Neuroptera). *Cretaceous Research*, **35**, 57-68.

Maksoud, S., Azar, D. 2020. Lebanese amber: latest updates. *Palaeoentomology*, **3**(2), 125-155.

Maksoud, S., Granier, B.R., Azar, D. 2022. Palaeoentomological (fossil insects) outcrops in Lebanon. *Carnets de Géologie*, **22**(16), 699-743.

Martínez-Delclòs, X., Martinell, J. 1995. The oldest known record of social insects. *Journal of Paleontology*, **69**(3), 594-599.

Martínez-Delclòs, X., Briggs, D.E., Peñalver, E., 2004. Taphonomy of insects in carbonates and amber. *Palaeogeography, Palaeoclimatology, Palaeoecology*, **203**(1-2), 19-64.

Martínez-Torres, L.M., Alonso, J., Valle, J.M. 2011. The upper Aptian–lower Albian amber deposit of the Peñacerrada II geosite (Basque-Cantabrian Basin, Northern Spain): geological context and protection. *Geoheritage*, **3**(1), 55-61.

Mas, R., García, A., Salas, R., Meléndez, A., Alonso, A., Aurell, M., Bádenas, B., Benito, M.I., Carenas, B., García-Hidalgo, J.F., Gil, J., Segura, M. 2004. Segunda fase de rifting: Jurásico Superior-Cretácico Inferior. En: Vera, J.A. (Ed.), *Geología de España*. Sociedad Geológica de España e Instituto Geológico y Minero de España, pp. 503-551.

Mayoral, E., Santos, A., Vintaned, J.G., Wisshak, M., Neumann, C., Uchman, A., Nel, A. 2020. Bivalve bioerosion in Cretaceous-Neogene amber around the globe, with implications for the ichnogenera *Teredolites* and *Apectoichnus*. *Palaeogeography, Palaeoclimatology, Palaeoecology*, **538**, 109410.

McAlpine, J.F. 1981. Morphology and terminology – adults. En: McAlpine, J.F., Peterson, B.V., Shewell, G.E., Teskey, H.J., Vockeroth, J.R., Wood, D.M. (Eds.), *Manual of Nearctic Diptera Volume 1*. Research Branch Agriculture Canada, Monograph No. 27, pp. 9-63.

McCoy, V.E., Boom, A., Solórzano Kraemer, M.M., Gabbott, S.E. 2017. The chemistry of American and African amber, copal, and resin from the genus *Hymenaea*. *Organic Geochemistry*, **113**, 43-54.

McCoy, V.E., Barthel, H.J., Boom, A., Peñalver, E., Delclòs, X., Solórzano-Kraemer, M.M. 2021. Volatile and semi-volatile composition of Cretaceous amber. *Cretaceous Research*, **127**, 104958.

McDonald, A.T., Espílez, E., Mampel, L., Kirkland, J.I., Alcalá, L. 2012. An unusual new basal iguanodont (Dinosauria: Ornithopoda) from the Lower Cretaceous of Teruel, Spain. *Zootaxa*, **3595**, 61-76.

McKellar, R.C., Wolfe, A.P., Tappert, R., Muehlenbachs, K. 2008. Correlation of Grassy Lake and Cedar Lake ambers using infrared spectroscopy, stable isotopes, and palaeoentomology. *Canadian Journal of Earth Sciences*, **45**(9), 1061-1082.

McKellar, R.C., Chatterton, B.D., Wolfe, A.P., Currie, P.J. 2011a. A diverse assemblage of Late Cretaceous dinosaur and bird feathers from Canadian amber. *Science*, **333**(6049), 1619-1622.

McKellar, R.C., Wolfe, A.P., Muehlenbachs, K., Tappert, R., Engel, M.S., Cheng, T., Sánchez-Azofeifa, G.A. 2011b. Insect outbreaks produce distinctive carbon isotope signatures in defensive resins and fossiliferous ambers. *Proceedings of the Royal Society B: Biological Sciences*, **278**(1722), 3219-3224.

McKenna, D.D., Shin, S., Ahrens, D., Balke, M., Beza-Beza, C., Clarke, D.J., Donath, A., Escalona, H.E., Friedrich, F., Letsch, H., Liu, S., Maddison, D., Mayer, C., Misof, B., Murin, P.J., Niehuis, O., Peters, R.S., Podsiadlowski, L., Pohl, H., Scully, E.D., Yan, E.V., Zhou, X., Ślipiński, S.A., Beutel, R.G. 2019. The evolution and genomic basis of beetle diversity. *Proceedings of the National Academy of Sciences*, **116**(49), 24729-24737.

Meléndez, A., Soria, A.R., Meléndez, N. 2000. A coastal lacustrine system in the Lower Barremian from the Oliete Sub-basin, central Iberian Range, northeastern Spain. En: Gierlowski-Kordesch, E.H., Kelts, K.R. (Eds.), *Lake basins through space and time*. The American Association of Petroleum Geologists, Studies in Geology 46, pp. 279-284.

Menor-Salván, C., Najarro, M., Velasco, F., Rosales, I., Tornos, F., Simoneit, B.R.T. 2010. Terpenoids in extracts of lower cretaceous ambers from the Basque-Cantabrian Basin (El Soplao, Cantabria, Spain): paleochemotaxonomic aspects. *Organic Geochemistry*, **41**(10), 1089-1103.

Menor-Salván, C., Simoneit, B.R.T., Ruiz-Bermejo, M., Alonso, J. 2016. The molecular composition of Cretaceous ambers: identification and chemosystematic relevance of 1,6-dimethyl-5-alkyltetralins and related bisnorlabdane biomarkers. *Organic Geochemistry*, **93**, 7-21.

Mikó, I., van de Kamp, T., Trietsch, C., Ulmer, J.M., Zuber, M., Baumbach, T., Deans, A.R. 2018. A new megaspilid wasp from Eocene Baltic amber (Hymenoptera: Ceraphronoidea), with notes on two non-ceraphronoid families: Radiophronidae and Stigmaphronidae. *PeerJ*, **6**, e5174.

Mironov, S.V., Bochkov, A.V. 2009. Modern conceptions concerning the macrophylogeny of acariform mites (Chelicerata, Acariformes). *Entomological Review*, **89**(8), 975-992.

Misof, B., Liu, S., Meusemann, K., Peters, R.S., Donath, A., *et al.* 2014. Phylogenomics resolves the timing and pattern of insect evolution. *Science*, **346**(6210), 763-767.

Mlynský, T., Wu, H., Koubova, I. 2019. Dominant Burmite cockroach *Jantaropterix ellenbergeri* sp. n. might laid isolated eggs together. *Paleontographica Abteilung A*, 314, 69-79.

Mockford, E.L. 1993. *North American Psocoptera (Insecta)*. Sandhill Crane Press, 455 pp.

Mockford, E.L. 1997. A new species of *Dicopomorpha* (Hymenoptera: Mymaridae) with diminutive, apterous males. *Annals of the Entomological Society of America*, **90**(2), 115-120.

Mockford, E.L., Lienhard, C., Yoshizawa, K. 2013. Revised classification of' 'Psocoptera' from Cretaceous amber, a reassessment of published information. *Insecta Matsumurana*, **69**, 1-26.

Moreno, L., Jiménez, M.E., Aguilera, H., Jiménez, P., de la Losa, A. 2011. The 2009 smouldering peat fire in Las Tablas de Daimiel National Park (Spain). *Fire Technology*, **47**(2), 519-538.

Mound, L.A. 2005. Thysanoptera: diversity and interactions. *Annual Review of Entomology*, **50**, 247-269.

Mound, L.A., Hastenpflug-Vesmanis, A. 2021. All genera of the world: order Thysanoptera (Animalia: Arthropoda: Insecta). *Megataxa*, **6**(1), 2-69.

Murillo-Barroso, M., Peñalver, E., Bueno, P., Barroso, R., de Balbín, R., Martinon-Torres, M. 2018. Amber in prehistoric Iberia: new data and a review. *PLOS One*, **13**(8), e0202235.

Murphy, N.P., Carey, D., Castro, L.R., Dowton, M., Austin, A.D. 2007. Phylogeny of the platygastroid wasps (Hymenoptera) based on sequences from the 18S rRNA, 28S rRNA and cytochrome oxidase I genes: implications for the evolution of the ovipositor system and host relationships. *Biological Journal of the Linnean Society*, **91**(4), 653-669.

Myers, C.E., Stigall, A.L., Lieberman, B.S. 2015. PaleoENM: applying ecological niche modeling to the fossil record. *Paleobiology*, *41*(2), 226-244.

Najarro, M., Peñalver, E., Rosales, I., Pérez-de la Fuente, R., Daviero-Gomez, V., Gómez, B., Delclòs, X. 2009. Unusual concentration of Early Albian arthropod-bearing amber in the Basque-Cantabrian Basin (El Soplao, Cantabria, Northern Spain): palaeoenvironmental and palaeobiological implications. *Geologica Acta*, **7**(3), 363-387.

Najarro, M., Peñalver, E., Pérez-de la Fuente, R., Ortega-Blanco, J., Menor-Salván, C., Barrón, E., Soriano, C., Rosales, I., López del Valle, R., Velasco, F., Tornos, F., Daviero-Gomez, B., Delclòs, X. 2010. Review of the El Soplao amber outcrop, early Cretaceous of Cantabria, Spain. *Acta Geologica Sinica (English Edition)*, **84**(4), 959-976.

Nascimbene, P., Silverstein, H. 2000. The preparation of fragile Cretaceous ambers for conservation and study of organismal inclusions. En: Grimaldi, D. (Ed.), *Studies on fossils in amber, with particular reference to the Cretaceous of New Jersey*. Backhuys Publishers, pp. 93-102.

Nel, A., Brasero, N 2010. Oise amber. En: Penney, D. (Ed.), *Biodiversity of fossils in amber from the major world deposits*. Siri Scientific Press, pp. 137-148.

Nel, A., Waller, A. 2007. The first fossil Compsocidae from Cretaceous Burmese amber (Insecta, Psocoptera, Troctomorpha). *Cretaceous Research*, **28**(6), 1039-1041.

Nel, A., Perrichot, V., Daugeron, C., Néraudeau, D. 2004. A new *Microphorites* in the Lower Cretaceous amber of the southwest of France (Diptera: Dolichopodidae, "Microphorinae"). *Annales de la Société Entomologique de France*, **40**(1), 23-29.

Nel, A., Prokop, J., De Ploëg, G., Millet, J. 2005. New Psocoptera (Insecta) from the lowermost Eocene amber of Oise, France. *Journal of Systematic Palaeontology*, **3**(4), 371-391.

Nel, P., Azar, D., Nel, A. 2007. A new 'primitive' family of thrips from Early Cretaceous Lebanese amber (Insecta, Thysanoptera). *Cretaceous Research*, **28**(6), 1033-1038.

Nel, A., DePalma, R.A., Engel, M.S. 2010a. A possible hemiphlebiid damselfly in Late Cretaceous amber from South Dakota (Odonata: Zygoptera). *Transactions of the Kansas Academy of Science*, **113**(3/4), 231-234.

Nel, P., Peñalver, E., Azar, D., Hodebert, G., Nel, A. 2010b. Modern thrips families Thripidae and Phlaeothripidae in early Cretaceous amber (Insecta: Thysanoptera). *Annales de la Société Entomologique de France*, **46**(1-2), 154-163.

Nel, P., Azar, D., Prokop, J., Roques, P., Hodebert, G., Nel, A. 2012. From Carboniferous to Recent: wing venation enlightens evolution of thysanopteran lineage. *Journal of Systematic Palaeontology*, **10**(2), 385-399.

Nel, A., Roques, P., Nel, P., Prokin, A.A., Bourgoin, T., Prokop, J., Szwedo, J., Azar, D., Desutter-Grandcolas, L., Wappler, T., Garrouste, R., Coty, D., Huang, D., Engel, M.S., Kirejtshuk, A.G. 2013. The earliest known holometabolous insects. *Nature*, **503**, 257-261.

Nel, P., Retana-Salazar, A.P., Azar, D., Nel, A., Huang, D.-Y. 2014. Redefining the Thripida (Insecta: Paraneoptera). *Journal of Systematic Palaeontology*, **12**(7), 865-878.

Nel, P., Schubnel, T., Perrichot, V., Nel, A. 2021. *Ankothrips*, the most ancient extant thrips genus (Thysanoptera, Melanthripidae). *Papers in Palaeontology*, **7**(2), 825-837.

Néraudeau, D., Perrichot, V., Dejax, J., Masure, E., Nel, A., Philippe, M., Moreau, P., Guillocheau, F., Guyot, T. 2002. A new fossil locality with insects in amber and plants (likely uppermost Albian): Archingeay (Charente-Maritime, France). *Geobios*, **35**(2), 233-240.

Néraudeau, D., Perrichot, V., Batten, D.J., Boura, A., Girard, V., Jeanneau, L., Nohra, Y.A., Polette, F., Saint Martin, S., Saint Martin, J.-P, Thomas, R. 2017. Upper Cretaceous amber from Vendée, north-western France: age dating and geological, chemical, and palaeontological characteristics. *Cretaceous Research*, **70**, 77-95.

Neri, M., Roghi, G., Ragazzi, E., Papazzonia, C.A. 2016. First record of Pliensbachian (Lower Jurassic) amber and associated palynoflora from the Monti Lessini (northern Italy). *Geobios*, **50**, 49-63.

New, T.R. 1987. Biology of the Psocoptera. *Oriental Insects*, **21**(1), 1-109.

Nissenbaum, A., Horowitz, A. 1992. The Levantine amber belt. *Journal of African Earth Sciences (and the Middle East)*, **14**(2), 295-300.

Nohra, Y.A., Perrichot, V., Jeanneau, L., Le Pollès, L., Azar, D. 2015. Chemical characterization and botanical origin of French ambers. *Journal of Natural Products*, **78**(6), 1284-1293.

Ortega Blanco, J, 2010. *Diversidad de himenópteros del ámbar Cretácico Inferior de España*. Tesis Doctoral, Universidad de Barcelona.

Ortega-Blanco, J., Engel, M.S. 2013. Bethylidae from Early Cretaceous Spanish amber (Hymenoptera: Chrysidoidea). *Journal of the Kansas Entomological Society*, **86**(3), 264-276.

Ortega-Blanco, J., Rasnitsyn, A.P., Delclòs, X. 2008. First record of anaxyelid woodwasps (Hymenoptera: Anaxyelidae) in Lower Cretaceous Spanish amber. *Zootaxa*, **1937**(1), 39-50.

Ortega-Blanco, J., Bennett, D.J., Delclòs, X., Engel, M.S. 2009. A primitive aphidiine wasp in Albian amber from Spain and a Northern Hemisphere origin for the subfamily (Hymenoptera: Braconidae: Aphidiinae). *Journal of the Kansas Entomological Society*, **82**(4), 273-282.

Ortega-Blanco, J., Rasnitsyn, A.P., Delclòs, X. 2010. A new family of ceraphronoid wasps from Early Cretaceous Álava amber, Spain. *Acta Palaeontologica Polonica*, **55**(2), 265-276.

Ortega-Blanco, J., Delclòs, X., Engel, M.S. 2011a. A protorhyssaline wasp in Early Cretaceous amber from Spain (Hymenoptera: Braconidae). *Journal of the Kansas Entomological Society*, **84**(1), 51-57.

Ortega-Blanco, J., Delclòs, X., Engel, M.S. 2011b. Diverse stigmaphronid wasps in Early Cretaceous amber from Spain (Hymenoptera: Ceraphronoidea: Stigmaphronidae). *Cretaceous Research*, **32**(6), 762-773.

Ortega-Blanco, J., Delclòs, X., Engel, M.S. 2011c. The wasp family Embolemidae in Early Cretaceous amber from Spain (Hymenoptera: Chrysidoidea). *Journal of the Kansas Entomological Society*, **84**(1), 36-42.

Ortega-Blanco, J., Delclòs, X., Peñalver, E., Engel, M.S. 2011d. Serphitid wasps in early Cretaceous amber from Spain (Hymenoptera: Serphitidae). *Cretaceous Research*, **32**(2), 143-154.

Ortega-Blanco, J., Peñalver, E., Delclòs, X., Engel, M.S. 2011e. False fairy wasps in early Cretaceous amber from Spain (Hymenoptera: Mymarommatoidea). *Palaeontology*, **54**(3), 511-523.

Ortega-Blanco, J., McKellar, R.C., Engel, M.S. 2014. Diverse scelionid wasps from Early Cretaceous Álava amber, Spain (Hymenoptera: Platygastroidea). *Bulletin of Geosciences*, **89**(3), 553-571.

Pak, N., Wu, S., Gibson, J.F. 2021. The evolution of marine dwelling in Diptera. *Ecology and Evolution*, **11**(16), 11440-11448.

Pardo, G. 1974. Nota previa sobre las características litoestratigráficas de las formaciones «Arenas de Utrillas» y «Lignitos de Escucha». *Acta Geológica Hispánica*, **IX**(2), 62-66.

Pardo, G., Villena, J. 1979. Características sedimentológicas y paleogeográficas de la Formación Escucha. *Cuadernos de Geología Ibérica*, **5**, 407-418.

Penney, D. 2006. The oldest lagonomegopid spider, a new species in Lower Cretaceous amber from Álava, Spain. *Geologica Acta*, **4**(3), 377-382.

Penney, D. 2010. Dominican amber. En: Penney, D. (Ed), *Biodiversity of fossils in amber from the major world deposits*. Siri Scientific Press, pp. 22-41.

Penney, D., Ortuño, V.M. 2006. Oldest true orb-weaving spider (Araneae: Araneidae). *Biology Letters*, **2**(3), 447-450.

Peñalver, E. 2012. *Ámbar: la historia de un material que ha fascinado a la humanidad*. Los Libros de la Catarata, 134 pp.

Peñalver, E., Arillo, A. 2007. A new species of the family Hybotidae in the Lower Cretaceous amber of El Caleyu (Asturias, Spain); *Alavesia prietoi* n. sp. *Alavesia*, **1**, 63-68.

Peñalver, E., Delclòs, X. 2010. Spanish amber. En: Penney, D. (Ed), *Biodiversity of fossils in amber from the major world deposits*. Siri Scientific Press, pp. 236-270.

Peñalver, E., Grimaldi, D. 2005. Assemblages of mammalian hair and blood-feeding midges (Insecta: Diptera: Psychodidae: Phlebotominae) in Miocene amber. *Earth and Environmental Science Transactions of The Royal Society of Edinburgh*, **96**(2), 177-195.

Peñalver, E., Grimaldi, D.A. 2010. Latest occurrences of the Mesozoic family Elcanidae (Insecta: Orthoptera), in Cretaceous amber from Myanmar and Spain. *Annales de la Société Entomologique de France*, **46**(1-2), 88-99.

Peñalver, E., Martínez-Delclòs, X. 2002. Importancia patrimonial de Arroyo de la Pascueta, un yacimiento de ámbar cretácico con insectos fósiles en Rubielos de Mora. En: Meléndez Hevia, G., Peñalver Mollá, E. (Eds.), *El patrimonio paleontológico de Teruel: I Jornadas sobre el patrimonio de la provincia de Teruel. Paleontología*. Instituto de Estudios Turolenses, pp. 201-208.

Peñalver, E., Nel, P. 2010. *Hispanothrips* from Early Cretaceous Spanish amber, a new genus of the resurrected family Stenurothripidae (Insecta: Thysanoptera). *Annales de la Société Entomologique de France*, **46**(1-2), 138-147.

Peñalver, E., Szwedo, J. 2010. Perforissidae (Hemiptera: Fulgoroidea) from the Lower Cretaceous San Just amber (Eastern Spain). *Alavesia*, **3**, 97-103.

Peñalver, E., Wegierek, P. 2008. A new genus and species of the family Tajmyraphididae (Hemiptera: Sternorrhyncha) in Early Cretaceous amber from Peñacerrada I (Spain). *Alavesia*, **2**, 187-192.

Peñalver, E., Grimaldi, D.A., Delclòs, X. 2006. Early Cretaceous spider web with its prey. *Science*, **312**(5781), 1761-1761.

Peñalver, E., Delclòs, X., Soriano, C. 2007. A new rich amber outcrop with palaeobiological inclusions in the Lower Cretaceous of Spain. *Cretaceous Research*, **28**(5), 791-802.

Peñalver, E., Ortega-Blanco, J., Nel, A., Delclòs, X. 2010. Mesozoic Evaniidae (Insecta: Hymenoptera) in Spanish amber: reanalysis of the phylogeny of the Evanioidea. *Acta Geologica Sinica-English Edition*, **84**(4), 809-827.

Peñalver, E., Labandeira, C.C., Barrón, E., Delclòs, X., Nel, P., Nel, A., Tafforeau, P., Soriano, C. 2012. Thrips pollination of Mesozoic gymnosperms. *Proceedings of the National Academy of Sciences*, **109**(22), 8623-8628.

Peñalver, E., Arillo, A., Delclòs, X., Peris, D., Grimaldi, D.A., Anderson, S.R., Nascimbene, C., Pérez-de la Fuente, R. 2017. Ticks parasitised feathered dinosaurs as revealed by Cretaceous amber assemblages. *Nature Communications*, **8**, 1924.

Peñalver, E., Barrón, E., Delclòs, X., Álvarez-Fernández, E., Arillo, A., López Del Valle, R., Lozano, R.P., Murillo-Barroso, M., Pérez-de la Fuente, R., Peris, D., Rodrigo, A., Sánchez-García, A., Sarto i Monteys, V., Viejo, J.L., Vilaça, R. 2018a. Amber in Portugal: state of the art. En: Vaz, N., Sá, A.A. (Eds.), *Yacimientos paleontológicos excepcionales en la Península Ibérica*. Cuadernos del Museo Geominero, 27, pp. 279-287.

Peñalver, E., Gónzalez-Fernández, R., López Del Valle, R., Barrón, E., Lozano, R.P., Rodrigo, A., Pérez-de la Fuente, R., Menéndez-Casares, E., Sarto i Monteys, V. 2018b. Un nuevo yacimiento de ámbar cretácico en Asturias (norte de España): resultados preliminares de la excavación paleontológica de 2017 en La Rodada (La Manjoya). En: Vaz, N., Sá, A.A. (Eds.), *Yacimientos paleontológicos excepcionales en la Península Ibérica*. Cuadernos del Museo Geominero, 27, 289-299.

Peñalver, E., Álvarez-Parra, S., Pérez-de la Fuente, R., López del Valle, R., Delclòs, X. 2021a. Spider web remains in Cretaceous amber. En: Vlachos, E., Cruzado-Caballero, P., Crespo, V.D., Ríos Ibañez, M., Arnal, F.A.M., Herraiz, J.L., Gascó-Lluna, F., Guerrero-Arenas, R., Ferrón, H.G. (Eds.), *3rd Palaeontological Virtual Congress Book of Abstracts: palaeontology in the virtual era*, p. 218.

Peñalver, E., Viejo J.L, Álvarez-Parra, S. 2021b. Una visión preliminar sobre los insectos fulgoroideos (Hemiptera) en el ámbar cretácico de España. En: García-Forner, A., Conejero-Ortega, N., Díaz Acha, Y. (Eds.), *Libro de resúmenes XXIV Bienal de la Real Sociedad Española de Historia Natural: la huella humana en la naturaleza*, pp. 228-229.

Peñalver, E., Álvarez-Parra, S., Arillo, A., Delclòs, X., Estrada-Peña, A., Pérez-de la Fuente, R. 2022a. Anatomía y paleobiología de la garrapata más antigua conocida, hallada en el ámbar cretácico de Rábago-El Soplao (Cantabria). En: Blanco, F., Blanco-Moreno, C., Buscalioni, A.D., de la Cita, L.,

Llandres, M., Martín-Abad, H., Marugán-Lobón, J., Monleón, M.A., Navalón, G., Nebreda, S.M., Prieto, I., San Román, C. (Eds.), *Libro de resúmenes de las XXXVII Jornadas SEP y V Congreso Ibérico de Paleontología*. Sociedad Española de Paleontología, Palaeontological Publications Nº2, p. 139.

Peñalver, E., Arillo, A., Nel, A. 2022b. A review of the Cretaceous genus *Eltxo* (Diptera: Cecidomyiidae) with description of the new species *Eltxo grimaldii* from El Soplao amber. *Palaeoentomology*, **5**(5), 461-467.

Peñalver, E., Nel, A., Nel, P. 2022c. An apterous Tubulifera (Insecta, Thysanoptera, Phlaeothripidae) preserved in Spanish Cretaceous amber. *Historical Biology*, **34**(8), 1381-1387.

Peñalver, E., Matamales-Andreu, R., Nel, A., Pérez-de la Fuente R. en prensa. Early adaptations of true flies (Diptera) to moist and aquatic continental environments. *Papers in Palaeontology*.

Peñalver, E., Peris, D., Álvarez-Parra, S., Grimaldi, D.A., Arillo, A., Chiappe, L., Delclòs, X., Alcalá, L., Sanz, J.L., Solórzano-Kraemer, M.M., Pérez-de la Fuente, R. enviado. Symbiosis between Cretaceous dinosaurs and feather-feeding beetles. *Proceedings of the National Academy of Sciences*.

Pepato, A.R., Klimov, P.B. 2015. Origin and higher-level diversification of acariform mites–evidence from nuclear ribosomal genes, extensive taxon sampling, and secondary structure alignment. *BMC Evolutionary Biology*, **15**, 178.

Pereira, R., de Souza Carvalho, I., Simoneit, B.R., de Almeida Azevedo, D. 2009. Molecular composition and chemosystematic aspects of Cretaceous amber from the Amazonas, Araripe and Recôncavo basins, Brazil. *Organic Geochemistry*, **40**(8), 863-875.

Pérez de la Fuente, R. 2012. *Paleobiología de los artrópodos del ámbar cretácico de El Soplao (Cantabria, España)*. Tesis Doctoral, Universitat de Barcelona.

Pérez-de la Fuente, R., Peñalver, E. 2019. A mantidfly in Cretaceous Spanish amber provides insights into the evolution of integumentary specialisations on the raptorial foreleg. *Scientific Reports*, **9**, 13248.

Pérez-de la Fuente, R., Nel, A., Peñalver, E., Delclòs, X. 2010. A new Early Cretaceous snakefly (Raphidioptera: Mesoraphidiidae) from El Soplao amber (Spain). *Annales de la Société Entomologique de France*, **46**(1-2), 108-115.

Pérez-de la Fuente, R., Delclòs, X., Peñalver, E., Arillo, A. 2011. Biting midges (Diptera: Ceratopogonidae) from the Early Cretaceous El Soplao amber (N Spain). *Cretaceous Research*, **32**(6), 750-761.

Pérez-de la Fuente, R., Delclòs, X., Peñalver, E., Speranza, M., Wierzchos, J., Ascaso, C., Engel, M.S. 2012a. Early evolution and ecology of camouflage in insects. *Proceedings of the National Academy of Sciences*, **109**(52), 21414-21419.

Pérez-de la Fuente, R., Peñalver, E., Delclòs, X., Engel, M.S. 2012b. Snakefly diversity in Early Cretaceous amber from Spain (Neuropterida, Raphidioptera). *ZooKeys*, **204**, 1-40.

Pérez-de fa Fuente, R., Peñalver, E., Ortega-Blanco, J. 2012c. A new species of the diverse Cretaceous genus *Cretevania* Rasnitsyn, 1975 (Hymenoptera: Evaniidae) from Spanish amber. *Zootaxa*, **3514**(1), 70-78.

Pérez-de la Fuente, R., Perrichot, V., Ortega-Blanco, J., Delclòs, X., Engel, M.S. 2012c. Description of the male of *Megalava truncata* Perrichot (Hymenoptera: Megalyridae) in Early Cretaceous amber from El Soplao (Spain). *Zootaxa*, **3274**(1), 29-35.

Pérez-de la Fuente, R., Saupe, E.E., Selden, P.A. 2013. New lagonomegopid spiders (Araneae: †Lagonomegopidae) from Early Cretaceous Spanish amber. *Journal of Systematic Palaeontology*, **11**(5), 531-553.

Pérez-de la Fuente, R., Delclòs, X., Engel, M.S., Peñalver, E. 2019. A new dustywing (Neuroptera: Coniopterygidae) from the Early Cretaceous amber of Spain. *Palaeoentomology*, **2**(3), 279-288.

Pérez-de la Fuente, R., Engel, M.S., Delclòs, X., Peñalver, E. 2020. Straight-jawed lacewing larvae (Neuroptera) from Lower Cretaceous Spanish amber, with an account on the known amber diversity of neuropterid immatures. *Cretaceous Research*, **106**, 104200.

Pérez-de la Fuente, R., Peñalver, E., Engel, M.S. 2021. Beaded lacewings (Neuroptera: Berothidae) in amber from the Lower Cretaceous of Spain. *Cretaceous Research*, **119**, 104705.

Pérez-García, A., Espílez, E., Mampel, L., Alcalá, L. 2015. A new European Albian turtle that extends the known stratigraphic range of the Pleurosternidae (Paracryptodira). *Cretaceous Research*, **55**, 74-83.

Pérez-García, A., Espílez, E., Mampel, L., Alcalá, L. 2020. A new basal turtle represented by the two most complete skeletons of Helochelydridae in Europe. *Cretaceous Research*, **107**, 104291.

Peris, D. 2015. *Paleobiología de los escarabajos (Insecta: Coleoptera) de los ámbares cretácicos del oeste europeo*. Tesis Doctoral, Universitat de Barcelona.

Peris, D. 2020. Coleoptera in amber from Cretaceous resiniferous forests. *Cretaceous Research*, **113**, 104484.

Peris, D., Rust, J. 2020. Cretaceous beetles (Insecta: Coleoptera) in amber: the palaeoecology of this most diverse group of insects. *Zoological Journal of the Linnean Society*, **189**(4), 1085-1104.

Peris, D., Davis, S.R., Engel, M.S., Delclòs, X. 2014. An evolutionary history embedded in amber: reflection of the Mesozoic shift in weevil-dominated (Coleoptera: Curculionoidea) faunas. *Zoological Journal of the Linnean Society*, **171**(3), 534-553.

Peris, D., Philips, T.K., Delclòs, X. 2015. Ptinid beetles from the Cretaceous gymnosperm-dominated forests. *Cretaceous Research*, **52**, 440-452.

Peris, D., Ruzzier, E., Perrichot, V., Delclòs, X. 2016. Evolutionary and paleobiological implications of Coleoptera (Insecta) from Tethyan-influenced Cretaceous ambers. *Geoscience Frontiers*, **7**(4), 695-706.

Peris, D., Pérez-de la Fuente, R., Peñalver, E., Delclòs, X., Barrón, E., Labandeira, C.C. 2017. False blister beetles and the expansion of gymnosperm-insect pollination modes before angiosperm dominance. *Current Biology*, **27**(6), 897-904.

Peris, D., Labandeira, C.C., Barrón, E., Delclòs, X., Rust, J., Wang, B. 2020. Generalist pollen-feeding beetles during the mid-Cretaceous. *iScience*, **23**, 100913.

Peris, D., Delclòs, X., Jordal, B. 2021. Origin and evolution of fungus farming in wood-boring Coleoptera–a palaeontological perspective. *Biological Reviews*, **96**(6), 2476-2488.

Peris, D., Mähler, B., Kolibáč, J. 2022. Review of the family Thanerocleridae (Coleoptera: Cleroidea) and the description of *Thanerosus* gen. nov. from Cretaceous amber using micro-CT scanning. *Insects*, **13**(5), 438.

Perkovsky, E.E., Martynova, K.V., Mita, T., Olmi, M., Zheng, Y., Müller, P., Zhang, Q., Gantier, F., Perrichot, V. 2020. A golden age for ectoparasitoids of Embiodea: Cretaceous Sclerogibbidae (Hymenoptera, Chrysidoidea) from Kachin (Myanmar), Charentes (France) and Choshi (Japan) ambers. *Gondwana Research*, **87**, 1-22.

Perrichot, V. 2004. Early Cretaceous amber from south-western France: insight into the Mesozoic litter fauna. *Geologica Acta*, **2**(1), 9-22.

Perrichot, V. 2009. Long-tailed wasps (Hymenoptera: Megalyridae) from Cretaceous and Paleogene European amber. *Paleontological Contributions*, **2009**(1), 1-19.

Perrichot, V., Engel, M.S. 2007. Early Cretaceous snakefly larvae in amber from Lebanon, Myanmar, and France (Raphidioptera). *American Museum Novitates*, **3598**, 1-11.

Perrichot, V., Neraudeau, D., Nel, A., De Ploëg, G. 2007. A reassessment of the Cretaceous amber deposits from France and their palaeontological significance. *African Invertebrates*, **48**(1), 213-227.

Perrichot, V., Marion, L., Néraudeau, D., Vullo, R., Tafforeau, P. 2008. The early evolution of feathers: fossil evidence from Cretaceous amber of France. *Proceedings of the Royal Society B: Biological Sciences*, **275**(1639), 1197-1202.

Perrichot, V., Ortega-Blanco, J., McKellar, R.C., Delclòs, X., Azar, D., Nel, A., Tafforeau, P., Engel, M.S. 2011. New and revised maimetshid wasps from Cretaceous ambers (Hymenoptera, Maimetshidae). *ZooKeys*, **130**, 421-453.

Peters, R.S., Krogmann, L., Mayer, C., Donath, A., Gunkel, S., Meusemann, K., Kozlov, A., Podsiadlowski, L., Petersen, M., Lanfear, R., Diez, P.A., Heraty, J., Kjer, K.M., Klopfstein, S., Meier, R., Polidori, C., Schmitt, T., Liu, S., Zhou, X., Wappler, T., Rust, J., Misof, B., Niehuis, O. 2017. Evolutionary history of the Hymenoptera. *Current Biology*, **27**, 1013-1018.

Peyrot, D., Rodríguez-López, J.P., Lassaletta, L., Meléndez, N., Barrón, E. 2007. Contributions to the palaeoenvironmental knowledge of the Escucha Formation in the Lower Cretaceous Oliete Sub-basin, Teruel, Spain. *Comptes Rendus Palevol*, **6**(6-7), 469-481.

Phillips, S.J., Anderson, R.P., Schapire, R.E. 2006. Maximum entropy modeling of species geographic distributions. *Ecological Modelling*, **190**(3-4), 231-259.

Pierce, N.E. 1995. Predatory and parasitic Lepidoptera: carnivores living on plants. *Journal of the Lepidopterists' Society*, **49**(4), 412-453.

Poelman, E.H., Cusumano, A., De Boer, J.G. 2022. The ecology of hyperparasitoids. *Annual Review of Entomology*, **67**, 143-161.

Pohl, A., Laugié, M., Borgomano, J., Michel, J., Lanteaume, C., Scotese, C.R., Frau, C., Poli, E., Donnadieu, Y. 2019. Quantifying the paleogeographic driver of Cretaceous carbonate platform development using paleoecological niche modeling. *Palaeogeography, Palaeoclimatology, Palaeoecology*, **514**, 222-232.

Poinar, G.O., Jr., Curcic, B.P., Cokendolpher, J.C. 1998. Arthropod phoresy involving pseudoscorpions in the past and present. *Acta Arachnologica*, **47**(2), 79-96.

Ponomarenko, A.G., Shcherbakov, D.E. 2004. New lacewings (Neuroptera) from the terminal Permian and basal Triassic of Siberia. *Paleontological Journal*, **38**(Suppl. 2), S197-S203.

Prete, F.R., Wells, H., Hurd, L.E., Wells, P.H. 1999. *The praying mantids*. The John Hopkins University Press, 400 pp.

Prokop, J., Pecharová, M., Garrouste, R., Beattie, R., Chintauan-Marquier, I.C., Nel, A. 2017. Redefining the extinct orders Miomoptera and Hypoperlida as stem acercarian insects. *BMC Evolutionary Biology*, **17**(1), 205.

Pulliam, H.R. 2000. On the relationship between niche and distribution. *Ecology Letters*, **3**(4), 349--361.

Querol, X. 1990. *Distribución de la materia mineral y azufre en los carbones de la Fm. Escucha. Relación con los factores geológicos, sedimentológicos y diagenéticos*. Tesis Doctoral, Universitat de Barcelona.

Querol, X., Salas, R., Pardo, G., Ardevol, L. 1992. Albian coal-bearing deposits of the Iberian Range in northeastern Spain. En: McCabe, P.J., Parrish, J.T. (Eds.), *Controls on the distribution and quality of Cretaceous coals*. The Geological Society of America, Special paper 267, pp. 193-208.

Quicke, D.L.J. 1997. *Parasitic wasps*. Champman & Hall, 470 pp.

Quinney, A., Mays, C., Stilwell, J.D., Zelenitsky, D.K., Therrien, F. 2015. The range of bioinclusions and pseudoinclusions preserved in a new Turonian (~90 Ma) amber occurrence from Southern Australia. *PLOS One*, **10**(5), e0121307.

Qvarnström, M., Fikáček, M., Wernström, J.V., Huld, S., Beutel, R.G., Arriaga-Varela, E., Niedźwiedzki, G. (2021). Exceptionally preserved beetles in a Triassic coprolite of putative dinosauriform origin. Current Biology, 31(15), 3374-3381.

Ramp, D., Caldwell, J., Edwards, K.A., Warton, D., Croft, D.B. 2005. Modelling of wildlife fatality hotspots along the snowy mountain highway in New South Wales, Australia. *Biological Conservation*, **126**(4), 474-490.

Rasnitsyn, A.P., Öhm-Kühnle, C. 2020. Taxonomic revision of the infraorder Proctotrupomorpha (Hymenoptera). *Palaeoentomology*, **3**(3), 223-234.

Rasnitsyn, A.P., Öhm-Kühnle, C. 2021. Non-aculeate hymenoptera in the Cretaceous ambers of the world. *Cretaceous Research*, **124**, 104805.

Rasnitsyn, A.P., Quicke, D.L.J. 2002. *History of insects*. Kluwer Academic Publishers, 517 pp.

Rasnitsyn, A.P., Aristov, D.S., Gorochov, A.V., Rowland, J.M., Sinitshenkova, N.D. 2004. Important new insect fossils from Carrizo Arroyo and the Permo-Carboniferous faunal boundary. *New Mexico Museum of Natural History and Science Bulletin*, **25**, 215-246.

Rasnitsyn, A.P., Bashkuev, A.S., Kopylov, D.S., Lukashevich, E.D., Ponomarenko, A.G., Popov, Y.A., Rasnitsyn, D.A., Rhyzkova, O.V., Sidorchk, E.A., Sukatsheva, I.D., Vorontsov, D.D. 2016. Sequence and scale of changes in the terrestrial biota during the Cretaceous (based on materials from fossil resins). *Cretaceous Research*, **61**, 234-255.

Rasnitsyn, A.P., Maalouf, M., Maalouf, R., Azar, D. 2022. New Serphitidae and Gallorommatidae (Insecta: Hymenoptera: Microprocta) in the Early Cretaceous Lebanese amber. *Palaeoentomology*, **5**(2), 120-136.

Richter, G., Baszio, S. 2001. Traces of a limnic food web in the Eocene Lake Messel — a preliminary report based on fish coprolite analyses. *Palaeogeography, Palaeoclimatology, Palaeoecology*, **166**(3-4), 345-368.

Ritman, E.L. 2011. Current status of developments and applications of micro-CT. *Annual Review of Biomedical Engineering*, **13**, 531-552.

Roberts, E.A., Seyfullah, L.J., Loveridge, R.F., Garside, P., Martill, D.M. 2020. Cretaceous gnetalean yields first preserved plant gum. *Scientific Reports*, **10**, 3401.

Rodrigo, A., Peñalver, E., Lopez del Valle, R., Barrón, E., Delclòs, X. 2018. The heritage interest of the Cretaceous amber outcrops in the Iberian Peninsula, and their management and protection. *Geoheritage*, **10**(3), 511-523.

Rodríguez-López, J.P. 2008. *Sedimentología y evolución del sistema desértico arenoso (erg) desarrollado en el margen occidental del Tethys durante el Cretácico Medio, Cordillera Ibérica. Provincias de Teruel y Zaragoza*. Tesis Doctoral, Universidad Complutense de Madrid.

Rodríguez-López, J.P., Meléndez, N., De Boer, P.L., Soria, A.R. 2008. Aeolian sand sea development along the Mid-Cretaceous Western Tethyan Margin (Spain): erg sedimentology and palaeoclimate implications. *Sedimentology*, **55**, 1253-1292.

Rodríguez-López, J.P., Meléndez, N., Soria, A.R., De Boer, P. 2009. Reinterpretación estratigráfica y sedimentológica de las formaciones Escucha y Utrillas de la Cordillera Ibérica. *Revista de la Sociedad Geológica de España*, **22**, 163-219.

Rodríguez-López, J.P., Meléndez, N., de Boer, P.L., Soria, A.R. 2010. The action of wind and water in a back erg margin system close to the Variscan Iberian Massif. *Sedimentology*, **57**, 1315-1356.

Rodríguez-López, J.P., Melendez, N., De Boer, P.L., Soria, A.R. 2012. Controls on marine–erg margin cycle variability: aeolian-marine interaction in the mid-Cretaceous Iberian Desert System, Spain. *Sedimentology*, **59**(2), 466-501.

Rodríguez-López, J.P., Peyrot, D., Barrón, E. 2020. Complex sedimentology and palaeohabitats of Holocene coastal deserts, their topographic controls, and analogues for the mid-Cretaceous of northern Iberia. *Earth-Science Reviews*, **201**, 103075.

Rodríguez-López, J.P., Barrón, E., Peyrot, D., Hughes, G.B. 2021. Deadly oasis: recurrent annihilation of Cretaceous desert bryophyte colonies; the role of solar, climate and lithospheric forcing. *Geoscience Frontiers*, **12**(1), 1-12.

Roghi, G., Gianolla, P., Kustatscher, E., Schmidt, A.R., Seyfullah, L.J. 2022. An exceptionally preserved terrestrial record of LIP effects on plants in the Carnian (Upper Triassic) amber-bearing section of the Dolomites, Italy. *Frontiers in Earth Science*, **10**, 900586.

Ross, A.J. 2022. Supplement to the Burmese (Myanmar) amber checklist and bibliography, 2021. *Palaeoentomology*, **5**(1), 27-45.

Rusek, J. 1998. Biodiversity of Collembola and their functional role in the ecosystem. *Biodiversity & Conservation*, **7**(9), 1207-1219.

Rust, J., Singh, H., Rana, R.S., McCann, T., Singh, L., Anderson, K., Sarkar, N., Nascimbene, P.C., Stebner, F., Thomas, J.C., Solórzano Kraemer, M., Williams, C.J., Engel, M.S., Shani, A., Grimaldi, D. 2010. Biogeographic and evolutionary implications of a diverse paleobiota in amber from the early Eocene of India. *Proceedings of the National Academy of Sciences*, **107**(43), 18360-18365.

Sadowski, E.M., Seyfullah, L.J., Sadowski, F., Fleischmann, A., Behling, H., Schmidt, A.R. 2014. Carnivorous leaves from Baltic amber. *Proceedings of the National Academy of Sciences*, **112**(1), 190-195.

Sadowski, E.M., Schmidt, A.R., Seyfullah, L.J., Solórzano-Kraemer, M.M., Neumann, C., Perrichot, V., Hamann, C., Milke, R., Nascimbene, P.C. 2021. Conservation, preparation and imaging of diverse ambers and their inclusions. *Earth-Science Reviews*, **220**, 103653.

Saint Martin, J.-P., Dutour, Y., Ebbo, L., Frau, C., Mazière, B., Néraudeau, D., Saint Martin, S., Tortosa, T., Turini, E., Valentin, X. 2021. Reassessment of amber-bearing deposits of Provence, southeastern France. *Bulletin de la Société Géologique de France*, **192**, 5.

Salas, R., Guimerà, J. 1996. Rasgos estructurales principales de la cuenca cretácica inferior del Maestrazgo (Cordillera Ibérica oriental). *Geogaceta*, **20**(7), 1704-1706.

Salas, R., Guimerà, J., Mas, R., Martín-Closas, C., Meléndez, A., Alonso, A. 2001. Evolution of the Mesozoic Central Iberian Rift System and its Cainozoic inversion (Iberian chain). *Mémoires du Muséum National d'Histoire Naturelle*, **186**, 145-185.

Salas, R., Guimerà, J., Bover-Arnal, T., Nebot, M. 2019. The Iberian-Catalan linkage: the Maestrat and Garraf basins. En: Quesada, C., Oliveira, J.T. (Eds.), *The geology of Iberia: a geodynamic approach*. Springer, Volume 3: The Alpine Cycle, pp. 228-230.

Samonds, K.E., Godfrey, L.R., Ali, J.R., Goodman, S.M., Vences, M., Sutherland, M.R., Irwin, M.T., Krause, D.W. 2012. Spatial and temporal arrival patterns of Madagascar's vertebrate fauna explained by distance, ocean currents, and ancestor type. *Proceedings of the National Academy of Sciences*, **109**(14), 5352-5357.

Sánchez García, A. 2017. *Paleobiología de los artrópodos edáficos y acuáticos del ámbar del Cretácico Inferior de España*. Tesis Doctoral, Universitat de Barcelona.

Sánchez-García, A., Engel, M.S. 2016. Springtails from the Early Cretaceous amber of Spain (Collembola: Entomobryomorpha), with an annotated checklist of fossil Collembola. *American Museum Novitates*, **3862**, 1-47.

Sánchez-García, A., Engel, M.S. 2017. Long-term stasis in a diverse fauna of Early Cretaceous springtails (Collembola: Symphypleona). *Journal of Systematic Palaeontology*, **15**(7), 513-537.

Sánchez-García, A., Arillo, A., Nel, A. 2016. The first water measurers from the Lower Cretaceous amber of Spain (Heteroptera, Hydrometridae, Heterocleptinae). *Cretaceous Research*, **57**, 111-121.

Sánchez-García, A., Nel, A., Arillo, A., Solórzano Kraemer, M.M. 2017. The semi-aquatic pondweed bugs of a Cretaceous swamp. *PeerJ*, **5**, e3760.

Sánchez-García, A., Peñalver, E., Delclòs, X., Engel, M.S. 2018. Mating and aggregative behaviors among basal hexapods in the Early Cretaceous. *PLOS One*, **13**(2), e0191669.

Sánchez-García, A., Peñalver, E., Delclòs, X., Engel, M.S. 2019. Jumping bristletails (Insecta, Archaeognatha) from the Lower Cretaceous amber of Lebanon. *Papers in Palaeontology*, **5**(4), 679-697.

Sánchez-García, A., Peñalver, E., Delclòs, X., Engel, M.S. 2020. Early Cretaceous termites in amber from northern Spain (Isoptera). *Cretaceous Research*, **110**, 104385.

Sandberg, P.A., Hay, W.W. 1967. Study of microfossils by means of the scanning electron microscope. *Journal of Paleontology*, **41**(4), 999-1001.

Santer, M., Álvarez-Parra, S., Nel, A., Peñalver, E., Delclòs, X. 2022. New insights into the enigmatic Cretaceous family Spathiopterygidae (Hymenoptera: Diaprioidea). *Cretaceous Research*, **133**, 105128.

Santos, H., Rodrigues, L., Jones, G., Rebelo, H. 2013. Using species distribution modelling to predict bat fatality risk at wind farms. *Biological Conservation*, **157**, 178-186.

Saupe, E.E., Papes, M., Selden, P.A., Vetter, R.S. 2011. Tracking a medically important spider: climate change, ecological niche modeling, and the brown recluse (*Loxosceles reclusa*). *PLOS One*, **6**(3), e17731.

Saupe, E.E., Pérez-de la Fuente, R., Selden, P.A., Delclòs, X., Tafforeau, P., Soriano, C. 2012. New *Orchestina* Simon, 1882 (Araneae: Oonopidae) from Cretaceous ambers of Spain and France: first spiders described using phase-contrast X-ray synchrotron microtomography. *Palaeontology*, **55**(1), 127-143.

Schatz, H., Behan-Pelletier, V. 2008. Global diversity of oribatids (Oribatida: Acari: Arachnida). *Hydrobiologia*, **595**, 323-328.

Schmidt, A.R., von Eynatten, H., Wagreich, M. 2001. The Mesozoic amber of Schliersee (southern Germany) is Cretaceous in age. *Cretaceous Research*, **22**(4), 423-428.

Schmidt, A.R., Dörfelt, H., Struwe, S., Perrichot, V. 2010. Evidence for fungivory in Cretaceous amber forests from Gondwana and Laurasia. *Palaeontographica Abteilung B: Palaeobotany - Palaeophytology*, **283**(4-6), 157-173.

Schmidt, A.R., Jancke, S., Lindquist, E.E., Ragazzi, E., Roghi, G., Nascimbene, P.C., Schmidt, K., Wappler, T., Grimaldi, D.A. 2012. Arthropods in amber from the Triassic Period. *Proceedings of the National Academy of Sciences*, **109**(37), 14796-14801.

Schmidt, A.R., Steuernagel, L., Behling, H., Seyfullah, L.J., Beimforde, C., Sadowski, E.M., Rikkinen, J., Kaasalainen, U. 2022. Fossil evidence of lichen grazing from Palaeogene amber. *Review of Palaeobotany and Palynology*, **302**, 104664.

Schubnel, T., Nel, A. 2019. New Paleogene mantises from the Oise amber and their evolutionary importance. *Acta Palaeontologica Polonica*, **64**(4), 779-786.

Schwertner, C.F., Carrenho, R., Moreira, F.F., Cassis, G. 2021. Hemiptera sampling methods. En: Santos, J.C., Fernandes, G.W. (Eds.), *Measuring arthropod biodiversity*. Springer, pp. 289-313.

Scotese, C.R. 2001. *Atlas of Earth History, Volume 1, Paleogeography*. PALEOMAP Project, 52 pp.

Scott, A.C. 2000. The Pre-Quaternary history of fire. *Palaeogeography, Palaeoclimatology, Palaeoecology*, **164**(1-4), 281-329.

Selden, P.A. 2021. New spiders (Araneae: Mesothelae), from the Carboniferous of New Mexico and England, and a review of Paleozoic Araneae. En: Lucas, S.G., DiMichele, W.A., Allen, B.D. (Eds.), *Kinney Brick Quarry Lagerstätte*. New Mexico Museum of Natural History and Science Bulletin 84, pp. 317-358.

Sender, L.M., Villanueva-Amadoz, U., Diez, J.B., Sanchez-Pellicer, R., Bercovici, A., Pons, D., Ferrer, J. 2012. A new uppermost Albian flora from Teruel province, northeastern Spain. *Geodiversitas*, **34**(2), 373-397.

Sender, L.M., Doyle, J.A., Upchurch Jr, G.R., Villanueva-Amadoz, U., Diez, J.B. 2019. Leaf and inflorescence evidence for near-basal Araceae and an unexpected diversity of other monocots from the late Early Cretaceous of Spain. *Journal of Systematic Palaeontology*, **17**(15), 1313-1346.

Sendra, A., Jiménez-Valverde, A., Selfa, J., Reboleira, A.S.P.S. 2021. Diversity, ecology, distribution and biogeography of Diplura. *Insect Conservation and Diversity*, **14**(4), 415-425.

Seyfullah, L.J., Beimforde, C., Dal Corso, J., Perrichot, V., Rikkinen, J., Schmidt, A.R. 2018a. Production and preservation of resins – past and present. *Biological Reviews*, **93**(3), 1684-1714.

Seyfullah, L.J., Roghi, G., Dal Corso, J., Schmidt, A.R. 2018b. The Carnian Pluvial Episode and the first global appearance of amber. *Journal of the Geological Society*, **175**(6), 1012-1018.

Seyfullah, L.J., Roberts, E.A., Schmidt, A.R., Ragazzi, E., Anderson, K.B., Rodrigues do Nascimento, Jr., D., Ferreira da Silva Filho, W., Kunzmann, L. 2020. Revealing the diversity of amber source plants from the Early Cretaceous Crato Formation, Brazil. *BMC Evolutionary Biology*, **20**(1), 107

Sharkey, M.J. 2007. Phylogeny and classification of Hymenoptera. *Zootaxa*, **1668**(1), 521-548.

Sharkey, M.J., Carpenter, J.M., Vilhelmsen, L., Heraty, J., Liljeblad, J., Dowling, A.P.G., Schulmeister, S., Murray, D., Deans, A.R., Ronquist, F., Krogmann, L., Wheeler, W.C. 2012. Phylogenetic relationships among superfamilies of Hymenoptera. *Cladistics*, **28**(1), 80-112.

Sharma, P.P., Kaluziak, S.T., Pérez-Porro, A.R., González, V.L., Hormiga, G., Wheeler, W.C., Giribet, G. 2014. Phylogenomic interrogation of Arachnida reveals systemic conflicts in phylogenetic signal. *Molecular Biology and Evolution*, **31**(11), 2963-2984.

Shi, G., Grimaldi, D.A., Harlow, G.E., Wang, Ji., Wang, Ju., Yang, M., Yang, M., Lei, W., Li, Q., Li, X. 2012. Age constraint on Burmese amber based on U–Pb dating of zircons. *Cretaceous Research*, **37**, 155-163.

Shipman, P. 1981. Applications of scanning electron microscopy to taphonomic problems. *Annals of the New York Academy of Sciences*, **376**(1), 357-385.

Sidorchuk, E.A., Bochkov, A.V., Weiterschan, T., Chernova, O.F. 2019. A case of mite-on-mammal ectoparasitism from Eocene Baltic amber (Acari: Prostigmata: Myobiidae and Mammalia: Erinaceomorpha). *Journal of Systematic Palaeontology*, **17**(4), 331-347.

Sillero, N., Carretero, M.A. 2013. Modelling the past and future distribution of contracting species. The Iberian lizard *Podarcis carbonelli* (Squamata: Lacertidae) as a case study. *Zoologischer Anzeiger-A Journal of Comparative Zoology*, **252**(3), 289-298.

Silvéiro, G., Madeira, J. 2018. Âmbar português: o caso de estudo do Apciano da Praia da Bafureira (Cascais, Portugal). *Geonovas*, **31**, 67-72.

Skibińska, K., Krzemiński, W., Arillo, A. 2017. The first Tanyderidae (Diptera) from Lower Cretaceous Álava amber (Spain). *Historical Biology*, **31**(7), 872-878.

Ślipiński, S.A., Leschen, R.A.B., Lawrence, J.F. 2011. Order Coleoptera Linnaeus, 1758. En: Zhang, Z.-Q. (Ed.), *Animal biodiversity: an outline of higher-level classification and survey of taxonomic richness*. *Zootaxa*, **3148**, 203-208.

Smithers, C.N. 1972. The classification and phylogeny of the Psocoptera. *Australian Museum Memoir*, **14**, 1-349.

Solórzano Kraemer, M.M. 2010. Mexican amber. En: Penney, D. (Ed), *Biodiversity of fossils in amber from the major world deposits*. Siri Scientific Press, pp. 42-56.

Solórzano Kraemer, M.M., Delclòs, X., Clapham, M.E., Arillo, A., Peris, D., Jäger, P., Stebner, F., Peñalver, E. 2018. Arthropods in modern resins reveal if amber accurately recorded forest arthropod communities. *Proceedings of the National Academy of Sciences*, **115**(26), 6739-6744.

Solórzano-Kraemer, M.M., Delclòs, X., Engel, M.S., Peñalver, E. 2020. A revised definition for copal and its significance for palaeontological and Anthropocene biodiversity-loss studies. *Scientific Reports*, **10**, 19904.

Solórzano-Kraemer, M.M., Sinclair, B.J., Arillo, A., Álvarez-Parra, S. enviado. A new genus of dance flies (Diptera: Empidoidea: Hybotidae) from Cretaceous Spanish ambers and introduction to the fossiliferous amber outcrop of La Hoya (Castellón Province, Spain). *PeerJ*.

Soriano, C., Archer, M., Azar, D., Creaser, P., Delclòs, X., Godthelp, H., Hand, S., Jones, A., Nel, A., Néraudeau, D., Ortega-Blanco, J., Pérez-de la Fuente, R., Perrichot, V., Saupe, E., Solórzano-Kraemer, M., Tafforeau, P. 2010. Synchrotron X-ray imaging of inclusions in amber. *Comptes Rendus Palevol*, **9**(6-7), 361-368.

Speranza, M., Wierzchos, J., Alonso, J., Bettucci, L., Martín-González, A., Ascaso, C. 2010. Traditional and new microscopy techniques applied to the study of microscopic fungi included in amber. *Microscopy: Science, Technology, Application and Education*, **2**, 1135-1145.

Speranza, M., Ascaso, C., Delclòs, X., Peñalver, E. 2015. Cretaceous mycelia preserving fungal polysaccharides: taphonomic and paleoecological potential of microorganisms preserved in fossil resins. *Geologica Acta*, **13**(4), 363-385.

Ssymank, A., Kearns, C.A., Pape, T., Thompson, F.C. 2008. Pollinating flies (Diptera): a major contribution to plant diversity and agricultural production. *Biodiversity*, **9**(1-2), 86-89.

Stach, E. 1982. The macerals of coal. En: Stach, E., Mackowsky, M., Teichmüller, M., Taylor, G.H., Chandra, D., Teichmüller, R. (Eds.), *Stach's textbook of coal petrology*. Gebrüder Borntraeger, pp. 87-140.

Stehr, F.W. 1987. Order Lepidoptera. En: Stehr, F.W. (Ed.), *Immature insects*. Kendall/Hunt Publishing Company, pp. 288-596.

Stilwell, J.D., Langendam, A., Mays, C., Sutherland, L.J., Arillo, A., Bickel, D.J., De Silva, W.T., Pentland, A.H., Roghi, G., Price, G.D., Cantrill, D.J., Quinney, A., Peñalver, E. 2020. Amber from the Triassic to Paleogene of Australia and New Zealand as exceptional preservation of poorly known terrestrial ecosystems. *Scientific Reports*, **10**, 5703.

Sturm, H., Machida, R. 2001. Archaeognatha. En: Kristensen, N.P., Beutel, R.G. (Eds.), *Handbuch der Zoologie, Band IV, Arthropoda: Insecta, Teilband 37*. Walter de Gruyter, pp. 1-213.

Subías, L.S., Arillo, A. 2002. Oribatid fossil mites from the Upper Devonian of South Mountain, New York and the Lower Carboniferous of County Antrim, North Ireland (Acariformes, Oribatida). *Estudios del Museo de Ciencias Naturales de Álava*, **17**, 93-106.

Szadziewski, R., Arillo, A. 1998. Biting midges (Diptera: Ceratopogonidae) from the lower Cretaceous amber from Alava, Spain. *Polskie Pismo Entomologiczne*, **67**(4), 291-298.

Szadziewski, R., Arillo, A. 2003. The oldest fossil record of the extant subgenus *Leptoconops* (*Leptoconops*) (Diptera: Ceratopogonidae). *Acta Zoologica Cracoviensia*, **46**(suppl.–Fossil Insects), 271-275.

Szadziewski, R., Arillo, A., Urbanek, A., Sontag, E. 2016. Biting midges of the extinct genus *Protoculicoides* Boesel from Lower Cretaceous amber of San Just, Spain and new synonymy in recently described fossil genera (Diptera: Ceratopogonidae). *Cretaceous Research*, **58**, 1-9.

Szadziewski, R., Krynicki, V.E., Krzemiński, W. 2018. The latest record of the extinct subfamily Eoptychopterinae (Diptera: Ptychopteridae) from Upper Cretaceous amber of North Carolina. *Cretaceous Research*, **82**, 147-151.

Talamas, E.J., Johnson, N.F., Shih, C., Ren, D. 2019. Proterosceliopsidae: a new family of Platygastroidea from Cretaceous amber. *Journal of Hymenoptera Research*, **73**, 3-38.

Tibert, N.E., Colin, J.P., Kirkland, J.I., Alcalá, L., Martín-Closas, C. 2013. Lower Cretaceous nonmarine ostracodes from an Escucha Formation dinosaur bonebed in eastern Spain. *Micropaleontology*, **59**(1), 83-91.

Tihelka, E., Giacomelli, M., Huang, D.-Y., Pisani, D., Donoghue, P.C.J., Cai, C.-Y. 2020. Fleas are parasitic scorpionflies. *Palaeoentomology*, **3**(6), 641-653.

Tihelka, E., Cai, C., Giacomelli, M., Lozano-Fernandez, J., Rota-Stabelli, O., Huang, D., Engel, M.S., Donoghue, P.C.J., Pisani, D. 2021. The evolution of insect biodiversity. *Current Biology*, **31**(19), R1299-R1311.

Townsend Peterson, A., Soberón, J., Pearson, R.G., Anderson, R.P., Martínez-Meyer, E., Nakamura, M., Araújo, M.B. 2011. *Ecological niches and geographic distributions*. Princeton University Press, 314 pp.

Trevisani, E., Ragazzi, E. 2013. L'ambra nelle Alpi Meridionali: stato delle conoscenze. *Quaderni del Museo di Storia Naturale di Ferrara*, **1**, 25-32.

Tugend, J., Manatschal, G., Kusznir, N.J. 2015. Spatial and temporal evolution of hyperextended rift systems: implication for the nature, kinematics, and timing of the Iberian-European plate boundary. *Geology*, **43**(1), 15-18.

Vajda, V., Pesquero Fernández, M.D., Villanueva-Amadoz, U., Lehsten, V., Alcalá, L. 2016. Dietary and environmental implications of Early Cretaceous predatory dinosaur coprolites from Teruel, Spain. *Palaeogeography, Palaeoclimatology, Palaeoecology*, **464**, 134-142.

van Eldijk, T.J., Wappler, T., Strother, P.K., van der Weijst, C.M., Rajaei, H., Visscher, H., van de Schootbrugge, B. 2018. A Triassic-Jurassic window into the evolution of Lepidoptera. *Science Advances*, **4**(1), e1701568.

Vávra, N. 2009. Amber, fossil resins, and copal — contributions to the terminology of fossil plant resins. *Denisia*, **26**, 213-222.

Vegas, J., Delvene, G., Menéndez, S., Rábano, I, García-Cortés, Á., Díaz-Martínez, E., Jiménez, R. 2018. El patrimonio paleontológico en España: una necesidad de consenso sobre su gestión y marco legal. *Revista PH: Boletín del Instituto Andaluz del Patrimonio Histórico*, **94**, 326-329.

Villanueva-Amadoz, U., Pons, D., Diez, J.B., Ferrer, J., Sender, L.M. 2010. Angiosperm pollen grains of San Just site (Escucha Formation) from the Albian of the Iberian Range (north-eastern Spain). *Review of Palaeobotany and Palynology*, **162**(3), 362-381.

Villanueva-Amadoz, U., Sender, L.M., Diez, J.B., Ferrer, J., Pons, D. 2011. Palynological studies of the boundary marls unit (Albian-Cenomanian) from northeastern Spain. Paleophytogeographical implications. *Geodiversitas*, **33**(1), 137-176.

Villanueva-Amadoz, U., Sender, L.M., Diez, J.B., Ferrer, J.J., Pons, D. 2014. A new isoetalean microsporophyll from the latest Albian of northeastern Spain: diversity in the development and dispersal strategies of microspores. *Acta Palaeontologica Polonica*, **59**(2), 479-490.

Villanueva-Amadoz, U., Sender, L.M., Alcalá, L., Pons, D., Royo-Torres, R., Diez, J.B. 2015. Paleoenvironmental reconstruction of an Albian plant community from the Ariño bonebed layer (Iberian Chain, NE Spain). *Historical Biology*, **27**(3-4), 430-441.

Vishniakova, V.N. 1981. New Palaeozoic and Mesozoic Lophioneuridae (Thripida). En: Vishniakova, V.N., Dlussky, G.M., Pritykina, L.N. (Eds.), *New fossil insects from the territory of the USSR*. Trudy Paleontologicheskogo Instituta Academii Nauk SSSR, pp. 43-63 [en ruso].

Vršanský, P. 2002. Origin and the early evolution of mantises. *AMBA Projekty*, **6**(1), 1-16.

Vršanský, P. 2003. Umenocoleoidea—an amazing lineage of aberrant insects (Insecta, Blattaria). *Amba Projekty*, **7**(1), 1-32.

Vršanský, P., Sendi, H., Hinkelman, J., Hain, M. 2021. *Alienopterix* Mlynský *et al*., 2018 complex in North Myanmar amber supports Umenocoleoidea/ae status. *Biologia*, **76**(8), 2207-2224.

Vullo, R., Girard, V., Azar, D., Néraudeau, D. 2010. Mammalian hairs in Early Cretaceous amber. *Naturwissenschaften*, **97**(7), 683-687.

Wahlberg, N., Wheat, C.W., Peña, C. 2013. Timing and patterns in the taxonomic diversification of Lepidoptera (butterflies and moths). *PLOS One*, **8**(11), e80875.

Wang, J., Labandeira, C.C., Zhang, G., Bek, J., Pfefferkorn, H.W. 2009. Permian *Circulipuncturites discinisporis* Labandeira, Wang, Zhang, Bek et Pfefferkorn gen. et spec. nov. (formerly *Discinispora*) from China, an ichnotaxon of a punch-and-sucking insect on Noeggerathialean spores. *Review of Palaeobotany and Palynology*, **156**(3-4), 277-282.

Wang, B., Rust, J., Engel, M.S., Szwedo, J., Dutta, S., Nel, A., Fang, Yo., Meng, F., Shi, G., Jarzembowsky, E.A., Wappler, T., Stebner, F., Fang, Ya., Mao, L., Zheng, D., Zhang, H. 2014. A diverse paleobiota in Early Eocene Fushun amber from China. *Current Biology*, **24**(14), 1606-1610.

Wang, Z., Shi, Y., Qiu, Z., Che, Y., Lo, N. 2017. Reconstructing the phylogeny of Blattodea: robust support for interfamilial relationships and major clades. *Scientific Reports*, **7**, 3907.

Wang, S., Shao, L.Y., Yan, Z.M., Shi, M.J., Zhang, Y.H. 2019. Characteristics of Early Cretaceous wildfires in peat-forming environment, NE China. *Journal of Palaeogeography*, **8**(1), 1-13.

Wang, B., Shi, G., Xu, C., Spicer, R.A., Perrichot, V., Schmidt, A.R., Feldberg, K., Heinrichs, J., Chény, C., Pang, H., Liu, X., Gao, T., Wang, Z., Ślipiński, A., Solórzano-Kraemer, M.M., Heads, S.W., Thomas, M.J., Sadowski, E.-M., Szweso, J., Azar, D., Nel, A., Chen, J., Zhang, Qi, Zhang, Qin., Luo, C., Yu, T., Zheng, D., Zhang, H., Engel, M.S. 2021. The mid-Miocene Zhangpu biota reveals an outstandingly rich rainforest biome in East Asia. *Science Advances*, **7**(18), eabg0625.

Waters, S.B., Arillo, A. 1999. A new genus of Hybotidae (Díptera, Empidoidea) from Lower Cretaceous amber of Alava (Spain). *Studia Dipterologica*, **6**(1), 59-66.

Weitschat, W., Wichard, W. 2002. *Atlas of plants and animals in Baltic amber*. Verlag Dr. Friedrich Pfeil, 256 pp.

Weygoldt, P. 1696. *The biology of pseudoscorpions*. Harvard University Press, 145 pp.

Wint, G.W., Robinson, T.P., Bourn, D.M., Durr, P.A., Hay, S.I., Randolph, S.E., Rogers, D.J. 2002. Mapping bovine tuberculosis in Great Britain using environmental data. *Trends in Microbiology*, **10**(10), 441-444.

Wolfe, A.P., Tappert, R., Muehlenbachs, K., Boudreau, M., McKellar, R.C., Basinger, J.F., Garrett, A. 2009. A new proposal concerning the botanical origin of Baltic amber. *Proceedings of the Royal Society B: Biological Sciences*, **276**(1672), 3403-3412.

Xing, L., Qiu, L. 2020. Zircon UPb age constraints on the mid-Cretaceous Hkamti amber biota in northern Myanmar. *Palaeogeography, Palaeoclimatology, Palaeoecology*, **558**, 109960.

Xing, L., McKellar, R.C., Xu, X., Li, G., Bai, M., Scott Persons IV, W., Miyashita, T., Benton, M.J., Zhang, J., Wolfe, A.P., Yi, Q., Tseng, K., Ran, H, Currie, P.J. 2016. A feathered dinosaur tail with primitive plumage trapped in mid-Cretaceous amber. *Current Biology*, **26**(24), 3352-3360.

Xing, L., Cockx, P., McKellar, R.C. 2020. Disassociated feathers in Burmese amber shed new light on mid-Cretaceous dinosaurs and avifauna. *Gondwana Research*, **82**, 241-253.

Yañez-Arenas, C., Townsend Peterson, A., Mokondoko, P., Rojas-Soto, O., Martínez-Meyer, E. 2014. The use of ecological niche modeling to infer potential risk areas of snakebite in the Mexican state of Veracruz. *PLOS One*, **9**(6), e100957.

Yeates, D.K., Wiegmann, B.M. 2005. *The evolutionary biology of flies*. Columbia University Press, 430 pp.

Yeates, D.K., Wiegmann, B.M., Courtney, G.W., Meier, R., Lambkin, C., Pape, T. 2007. Phylogeny and systematics of Diptera: two decades of progress and prospects. *Zootaxa*, **1668**(1), 565-590.

Yoshizawa, K., Johnson, K.P. 2014. Phylogeny of the suborder Psocomorpha: congruence and incongruence between morphology and molecular data (Insecta: Psocodea: 'Psocoptera'). *Zoological Journal of the Linnean Society*, **171**(4), 716-731.

Yoshizawa, K., Lienhard, C. 2020. †Cormopsocidae: a new family of the suborder Trogiomorpha (Insecta: Psocodea) from Burmese amber. *Entomological Science*, **23**(2), 208-215.

Yoshizawa, K., Yamamoto, S. 2021. The earliest fossil record of the suborder Psocomorpha (Insecta: Psocodea) from mid-Cretaceous Burmese amber, with description of a new genus and species. *Insecta Matsumurana*, **77**, 1-15.

Yoshizawa, K., Lienhard, C., Johnson, K.P. 2006. Molecular systematics of the suborder Trogiomorpha (Insecta: Psocodea: 'Psocoptera'). *Zoological Journal of the Linnean Society*, **146**(2), 287-299.

Yu, T., Thomson, U., Mu, L., Ross, A., Kennedy, J., Broly, P., Xia, F., Zhang, H., Wang, B., Dilcher, D. 2019. An ammonite trapped in Burmese amber. *Proceedings of the National Academy of Sciences*, **116**(23), 11345-11350.

Zhang, Z.-Q. 2011. Phylum Arthropoda von Siebold, 1848. En: Zhang, Z.-Q. (Ed.), *Animal biodiversity: an outline of higher-level classification and survey of taxonomic richness*. *Zootaxa*, **3148**, 99-103.

Zhang, Z., Schneider, J.W., Hong, Y. 2013. The most ancient roach (Blattodea): a new genus and species from the earliest Late Carboniferous (Namurian) of China, with a discussion of the phylomorphogeny of early blattids. *Journal of Systematic Palaeontology*, **11**(1), 27-40.

Zhang, Q., Rasnitsyn, A.P., Wang, B., Zhang, H. 2018. Hymenoptera (wasps, bees and ants) in mid-Cretaceous Burmese amber: a review of the fauna. *Proceedings of the Geologists' Association*, **129**(6), 736-747.

Zhang, W., Deng, P., Wang, J., Zhang, P., Guo, Z., Ren, D. 2020. A new jaw-moth (Lepidoptera: Micropterigidae) from mid-Cretaceous Burmese amber. *Cretaceous Research*, **116**, 104609.

Zhang, X., Yang, D., Kang, Z. 2022. New data on the mitochondrial genome of Nematocera (lower Diptera): features, structures and phylogenetic implications. *Zoological Journal of the Linnean Society*.

Zheng, D., Chang, S.C., Perrichot, V., Dutta, S., Rudra, A., Mu, L., Kelly, R.S., Li, S., Zhang, Qi, Zhang, Qin., Wong, J., Wang, J., Wang, H, Fang, Y., Zhang, H., Wang, B. 2018. A Late Cretaceous amber biota from central Myanmar. *Nature Communications*, **9**, 3170.

Zherikhin, V.V. 2002. Order Thripida. En: Rasnitsyn, A.P., Quicke, D.L.J. (Eds.), *History of insects*. Kluwer Academic Publishers, pp. 133-143.

Zherikhin, V.V., Eskov, K.Y. 1999. Mesozoic and lower Tertiary resins in former USSR. *Estudios del Museo de Ciencias Naturales de Álava*, **14**, 119-131.

Zherikhin, V.V., Sukatsheva, I.D. 1973. On the Cretaceous insectiferous “ambers” (retinits) in the North Siberia. En: Narchuk, E.P. (Ed.), *Problems of the insect palaeontology. Lectures on the 24th Annual Readings in Memory of NA Kholodkovsky*. Nauka, pp. 3-48 [en ruso].

Zhou, W., Apkarian, R., Wang, Z.L., Joy, D. 2007. Fundamentals of Scanning Electron Microscopy (SEM). En: Zhou, W., Wang, Z.L. (Eds.), *Scanning microscopy for nanotechnology*. Springer, pp 1-40.

8. Anexos

8.1. Publicaciones y trabajos que constituyen el presente proyecto de Tesis Doctoral

El asterisco * indica el autor de correspondencia.

8.1.1. **Álvarez-Parra, S.***, Peñalver, E., Nel, A., Delclòs, X. 2020. The oldest representative of the extant barklice genus *Psyllipsocus* (Psocodea: Trogiomorpha: Psyllipsocidae) from the Cenomanian amber of Myanmar. *Cretaceous Research*, **113**, 104480.

8.1.2. **Álvarez-Parra, S.***, Delclòs, X., Solórzano-Kraemer, M.M., Alcalá, L., Peñalver, E. 2020. Cretaceous amniote integuments recorded through a taphonomic process unique to resins. *Scientific Reports*, **10**, 19840.

8.1.3. **Álvarez-Parra, S.***, Pérez-de la Fuente, R., Peñalver, E., Barrón, E., Alcalá, L., Pérez-Cano, J., Martín-Closas, C., Trabelsi, K., Meléndez, N., López Del Valle, R., Lozano, R.P., Peris, D., Rodrigo, A., Sarto i Monteys, V., Bueno-Cebollada, C.A., Menor-Salván, C., Philippe, M., Sánchez-García, A., Peña-Kairath, C., Arillo, A., Espílez, E., Mampel, L., Delclòs, X. 2021. Dinosaur bonebed amber from an original swamp forest soil. *eLife*, **10**, e72477.

8.1.4. Arillo, A., Subías, L.S., **Álvarez-Parra, S.*** 2022. First fossil record of the oribatid family Liacaridae (Acariformes: Gustavioidea) from the lower Albian amber-bearing site of Ariño (eastern Spain). *Cretaceous Research*, 131, 105087.

8.1.5. Santer, M., **Álvarez-Parra, S.***, Nel, A., Peñalver, E., Delclòs, X. 2022. New insights into the enigmatic Cretaceous family Spathiopterygidae (Hymenoptera: Diaprioidea). *Cretaceous Research*, **133**, 105128.

8.1.6. **Álvarez-Parra, S.***, Peñalver, E., Nel, A., Delclòs, X. 2022. New barklice (Psocodea, Trogiomorpha) from Lower Cretaceous Spanish amber. *Papers in Palaeontology*, **8**(3), e1436.

8.1.7. **Álvarez-Parra, S.***, Peñalver, E., Delclòs, X., Engel, M.S. 2022. A braconid wasp (Hymenoptera: Ichneumonoidea: Braconidae) from the Lower Cretaceous amber of San Just (E Iberian Peninsula). *ZooKeys*, **1103**, 65-78.

8.1.8. **Álvarez-Parra, S.***, Nel, A. 2022. A new genus of setose-winged barklice (Psocodea: Trogiomorpha: Lepidopsocidae) from the Eocene amber of Oise with notes on the biogeography of Thylacellinae. *Historical Biology*, 1-10.

8.1.9. Barrón, E.*, Peyrot, D., Bueno-Cebollada, C.A., Kvaček, J., **Álvarez-Parra, S.**, Altolaguirre, Y., Meléndez, N. enviado tras revisión. Biodiversity of ecosystems

in an arid setting: the late Albian plant communities and associated biota from eastern Iberia. *PLOS One*.

8.1.10. Solórzano-Kraemer, M.M.*, Sinclair, B.J., Arillo, A., **Álvarez-Parra, S.** enviado tras revisión. A new genus of dance flies (Diptera: Empidoidea: Hybotidae) from Cretaceous Spanish ambers and introduction to the fossiliferous amber outcrop of La Hoya (Castellón Province, Spain). *PeerJ*.

8.1.11. Peñalver, E.*, Peris, D., **Álvarez-Parra, S.**, Grimaldi, D.A., Arillo, A., Chiappe, L., Delclòs, X., Alcalá, L., Sanz, J.L., Solórzano-Kraemer, M.M., Pérez-de la Fuente, R.* en revisión. Symbiosis between Cretaceous dinosaurs and feather-feeding beetles. *Proceedings of the National Academy of Sciences*.

8.1.12. **Álvarez-Parra, S.***, Peñalver, E., Nel, A., Delclòs, X. en preparación. Barklice (Insecta: Psocodea) from Early Cretaceous resiniferous forests of Iberia (Spanish amber): new Troctomorpha and the oldest Psocomorpha.

8.1.13. **Álvarez-Parra, S.***, Santer, M., *et al*. en preparación. Serphitid wasps (Hymenoptera: Serphitidae) from Early Cretaceous amber of eastern Spain with comments on the evolution and palaeobiology of Serphitoidea.

8.1.14. Delclòs, X.*, Peñalver, E., Barrón, E., Pérez-de la Fuente, R., Grimaldi, D.A., Holz, M., Labandeira, C., Scotese, C.R., Solórzano-Kraemer, M.M., **Álvarez-Parra, S.**, *et al.*, Peris, D. en preparación. Amber and the Cretaceous Resinous Interval: hypotheses on causes.

Anexo 8.1.1

The oldest representative of the extant barklice genus *Psyllipsocus* (Psocodea: Trogiomorpha: Psyllipsocidae) from the Cenomanian amber of Myanmar

Álvarez-Parra, S., Peñalver, E., Nel, A., Delclòs, X. 2020. The oldest representative of the extant barklice genus *Psyllipsocus* (Psocodea: Trogiomorpha: Psyllipsocidae) from the Cenomanian amber of Myanmar. *Cretaceous Research*, **113**, 104480.

DOI: https://doi.org/10.1016/j.cretres.2020.104480

Revista científica: *Cretaceous Research*
Factor de impacto: 2,176 (2020)
Categoría: *Paleontology*, Q1 (2020)

Cretaceous Research 113 (2020) 104480

Contents lists available at ScienceDirect

Cretaceous Research

journal homepage: www.elsevier.com/locate/CretRes

Short communication

The oldest representative of the extant barklice genus *Psyllipsocus* (Psocodea: Trogiomorpha: Psyllipsocidae) from the Cenomanian amber of Myanmar

Sergio Álvarez-Parra [a, *], Enrique Peñalver [b], André Nel [c], Xavier Delclòs [a]

[a] Departament de Dinàmica de la Terra i de l'Oceà and Institut de Recerca de la Biodiversitat (IRBio), Facultat de Ciències de la Terra, Universitat de Barcelona, c/ Martí i Franquès s/n, 08028, Barcelona, Spain
[b] Instituto Geológico y Minero de España (Museo Geominero), c/ Cirilo Amorós 42, 46004, Valencia, Spain
[c] Institut de Systématique, Évolution, Biodiversité, ISYEB - UMR 7205 – CNRS, MNHN, UPMC, EPHE, Muséum national d'Histoire naturelle, Sorbonne Universités, 57 rue Cuvier, CP 50, Entomologie, F-75005, Paris, France

ARTICLE INFO

Article history:
Received 9 October 2019
Received in revised form
15 February 2020
Accepted in revised form 4 April 2020
Available online 20 April 2020

Keywords:
Psocodea
Psyllipsocidae
Psyllipsocus
New species
Burmese amber

ABSTRACT

We describe *Psyllipsocus yoshizawai* sp. nov., the oldest and first Cretaceous species of the extant genus *Psyllipsocus* (Psocodea: Trogiomorpha: Psyllipsocidae). This is the fifth genus and sixth species to be identified within the family Psyllipsocidae from the Cretaceous and the third genus and fourth species of psyllipsocids from the Cenomanian amber of Myanmar (Burmese amber, in Tanai). Its taxonomic affinities with the other fossil and living psyllipsocid genera are discussed. The attribution to the extant genus *Psyllipsocus* is based on the absence of any significant differences with this genus that could not correspond to a specific level. This situation is rare but not exceptional, as some other extant insect genera have already been recorded from the Burmese amber. It suggests a high morphological stability of the genus over time. A checklist of the known Cretaceous psocodean species from amber is given.

1. Introduction

Psocodea is an insect order that includes the Phthiraptera (parasitic lice) and the 'Psocoptera' (booklice and barklice), the latter being considered a paraphyletic group (Johnson et al., 2018). To date, around 10,800 living species have been described in this order (Zhang, 2011). The oldest stem representative of Psocodea is *Westphalopsocus pumilio* Azar et al., in Nel et al., 2013 from the Upper Carboniferous (Pennsylvanian) (Nel et al., 2013), but diversification of the crown group seems to have occurred during the Cretaceous (Mockford et al., 2013). To date, 53 species of the three psocid suborders have been described from amber of this period (Table 1).

The family Psyllipsocidae (Trogiomorpha) comprises six fossil species in five extinct genera, although *Parapsyllipsocus vergereaui* Perrichot et al., 2003 (early Cenomanian, Charentese amber, France) might also be a psyllipsocid (sensu Perrichot et al., 2003), and 71 extant species in five living genera (Hakim et al., 2018), one of which (*Psyllipsocus* Selys-Longchamps, 1872) includes two fossil representatives as commented below. *Libanopsyllipsocus alexanderasnitsyni* Azar and Nel, 2011 (early Barremian, Hammana-Mdeyrij amber, Lebanon) was transferred to the family Pachytroctidae by Mockford et al. (2013) but reasserted as a psyllipsocid by Hakim et al. (2018). The three earliest Cenomanian taxa *Annulipsyllipsocus andreneli* Hakim et al., 2018, *Annulipsyllipsocus inexspectatus* Hakim et al., 2018, and *Concavapsocus parallelus* Wang et al., 2019, are described from the Tanai (= Danai) amber in Myanmar. Lastly, the Santonian *Khatangia inclusa* Vishniakova, 1975 was described from the Taimyr amber in the Russian Federation (Yantardakh locality). Wang et al. (2019) proposed that *Globopsocus aquilonius* Azar and Engel, 2008 from the latest Cenomanian of the Taimyr Peninsula (Agapa locality) could be a psyllipsocid closely related to *C. parallelus*; this taxon was first identified as a Sphaeropsocidae (Troctomorpha) (Azar and Engel, 2008) but later reasserted as incertae sedis within Electrentomoidea (Troctomorpha) by Mockford et al. (2013), and therefore a revision of the holotype specimen is required. *Psyllipsocus eocenicus* Nel et al., 2005 (Oise amber, France) and *Sinopsyllipsocus fushunensis* Zhang et al., 2016

* Corresponding author.
E-mail address: sergio.alvarez-parra@ub.edu (S. Álvarez-Parra).

https://doi.org/10.1016/j.cretres.2020.104480
0195-6671/

Table 1
Checklist of the known species of Psocodea from Cretaceous amber and their provenance. The specimen described in this paper is shown in bold. The presence of an asterisk in the reference indicates that the taxonomic determination was modified by Mockford et al. (2013).

Suborder	Infraorder	Superfamily	Family	Genus and species	Provenance	Reference
Trogiomorpha				*Empheriopsis vulnerata*	Yantardakh, Taimyr Peninsula (Russian Federation)	Vishniakova (1975) *
				Parapsyllipsocus vergereaui	Archingeay-Les Nouillers, Charente-Maritime (France)	Perrichot et al. (2003)
	Atropetae		Archaeatropidae	*Archaeatropos alavensis*	Peñacerrada I, Burgos (Spain)	Baz and Ortuño (2000)
				Archaeatropos perantiqua	Tanai, Kachin (Myanmar)	Cockerell (1919) *
				Archaeatropos randatae	Jezzine, Caza Jezzine (Lebanon)	Azar and Nel (2004) *
				Bcharreglaris amunobi	Bcharreh, Caza Bcharreh (Lebanon)	Azar and Nel (2004) *
				Libanoglaris chehabi	Hammana-Mdeyrij, Caza Baabda (Lebanon)	Azar and Nel (2004) *
				Libanoglaris mouawadi	Hammana-Mdeyrij, Caza Baabda (Lebanon)	Perrichot et al. (2003) *
				Proprionoglaris axioperierga	La Garnache, Vendée (France)	Azar et al. (2015b)
				Proprionoglaris guyoti	Archingeay-Les Nouillers, Charente-Maritime (France)	Perrichot et al. (2003) *
				Prospeleketor albianensis	Archingeay-Les Nouillers, Charente-Maritime (France)	Perrichot et al. (2003) *
				Setoglaris reemae	Hammana-Mdeyrij, Caza Baabda (Lebanon)	Azar and Nel (2004) *
			Empheriidae	*Empheropsocus arilloi*	Peñacerrada I, Burgos (Spain)	Baz and Ortuño, 2001a
				Empheropsocus margineglabrus	Peñacerrada I, Burgos (Spain)	Baz and Ortuño, 2001a
				Jerseyempheria grimaldii	Sayreville, New Jersey (USA)	Azar et al. (2010b)
				Preempheria antiqua	Peñacerrada I, Burgos (Spain)	Baz and Ortuño, 2001a
			Trogiidae	*Cretolepinotus tankei*	Pipestone Creek, Alberta (Canada)	Cockx et al. (2020)
				Eolepinotus pilosus	Yantardakh, Taimyr Peninsula (Russian Federation)	Vishniakova (1975)
	Prionoglaridetae		Prionoglarididae	*Palaeosiamoglaris burmica*	Tanai, Kachin (Myanmar)	Azar et al. (2017b)
				Palaeosiamoglaris inexpectata	Tanai, Kachin (Myanmar)	Azar et al. (2017b)
				Palaeosiamoglaris lienhardi	Tanai, Kachin (Myanmar)	Azar et al. (2017b)
	Psyllipsocetae		Psyllipsocidae	*Annulipsyllipsocus andreneli*	Tanai, Kachin (Myanmar)	Hakim et al. (2018)
				Annulipsyllipsocus inexspectatus	Tanai, Kachin (Myanmar)	Hakim et al. (2018)
				Concavapsocus parallelus	Tanai, Kachin (Myanmar)	Wang et al. (2019)
				Khatangia inclusa	Yantardakh, Taimyr Peninsula (Russian Federation)	Vishniakova (1975)
				Libanopsyllipsocus alexanderasnitsyni	Hammana-Mdeyrij, Caza Baabda (Lebanon)	Azar and Nel (2011)
				***Psyllipsocus yoshizawai* sp. nov.**	Tanai, Kachin (Myanmar)	Álvarez-Parra et al. herein
Troctomorpha	Amphientometae			*Scocompus atelisus*	La Garnache, Vendée (France)	Azar et al. (2015b)
			Manicapsocidae	*Azarpsocus perreaui*	Tanai, Kachin (Myanmar)	Maheu and Nel (2020)
				Palaeomanicapsocus fouadi	Tanai, Kachin (Myanmar)	Azar et al. (2017a)
				Palaeomanicapsocus margoae	Tanai, Kachin (Myanmar)	Azar et al. (2017a)
				Paramanicapsocus longiantennatus	Tanai, Kachin (Myanmar)	Hakim et al. (2020)
		Electrentomoidea		*Globopsocus aquilonius*	Agapa, Taimyr Peninsula (Russian Federation)	Azar and Engel (2008) *
				Libanomphientomum nudus	Hammana-Mdeyrij, Caza Baabda (Lebanon)	Choufani et al. (2011) *
			Electrentomidae	*Manicapsocidus enigmaticus*	Peñacerrada I, Burgos (Spain)	Baz and Ortuño (2001b) *
				Paramesopsocus lu	Hammana-Mdeyrij, Caza Baabda (Lebanon)	Azar et al. (2008) *
			Compsocidae	*Burmacompsocus banksi*	Tanai, Kachin (Myanmar)	Cockerell (1916) *
				Burmacompsocus coniugans	Tanai, Kachin (Myanmar)	Sroka and Nel (2017)
				Burmacompsocus perreaui	Tanai, Kachin (Myanmar)	Nel and Waller (2007)
				Burmacompsocus pouilloni	Tanai, Kachin (Myanmar)	Ngô-Muller et al. (2020)
				Paraelectrentomopsis chenyangcaii	Tanai, Kachin (Myanmar)	Azar et al. (2016)
		Amphientomoidea	Amphientomidae	*Arcantipsocus courvillei*	Archingeay-Les Nouillers, Charente-Maritime (France)	Azar et al. (2009) *
				Proamphientomum cretaceum	Yantardakh, Taimyr Peninsula (Russian Federation)	Vishniakova (1975)
	Nanopsocetae		Liposcelididae	*Cretoscelis burmitica*	Tanai, Kachin (Myanmar)	Grimaldi and Engel (2006a)
			Pachytroctidae	*Atapinella garroustei*	Tanai, Kachin (Myanmar)	Azar et al. (2015a)
				Burmipachytrocta singularis	Tanai, Kachin (Myanmar)	Azar et al. (2015a)
				Libaneuphoris jantopi	Falougha, Caza Baabda (Lebanon)	Azar et al. (2015a)
			Sphaeropsocidae	*Asphaeropsocites neli*	Hammana-Mdeyrij, Caza Baabda (Lebanon)	Azar et al. (2010a)
				Sphaeropsocites lebanensis	Jezzine, Caza Jezzine (Lebanon)	Grimaldi and Engel (2006b)

Table 1 (*continued*)

Suborder	Infraorder	Superfamily	Family	Genus and species	Provenance	Reference
				Sphaeropsocoides canadensis	Cedar Lake, Manitoba (Canada)	Grimaldi and Engel (2006b)
Psocomorpha				*Cretapsocus capillatus*	Yantardakh, Taimyr Peninsula (Russian Federation)	Vishniakova (1975) *
	Homilopsocidea		Lachesillidae	*Archaelachesis granulosa*	Yantardakh, Taimyr Peninsula (Russian Federation)	Vishniakova (1975)
			Mesopsocidae	*Mesopsocoides dupei*	La Garnache, Vendée (France)	Azar et al. (2015b)

(Fushun amber, China) were discovered in early Eocene deposits. A nymph of *Psyllipsocus* sp. was described from Mexican amber (Simojovel de Allende) which is early-middle Miocene in age (Mockford, 1969). The five living genera of Psyllipsocidae are *Dorypteryx* Aaron, 1883, *Pseudopsyllipsocus* Li, 2002, *Pseudorypteryx* García Aldrete, 1984, *Psocathropos* Ribaga, 1899 and *Psyllipsocus* (for species, see Hakim et al., 2018), although *Pseudopsyllipsocus* might be a lepidopsocid, as indicated by Mockford (2011).

Here, we describe a new species of *Psyllipsocus* from the Tanai amber (northern Myanmar) that is Cenomanian in age. It is the fifth genus and sixth species within the Psyllipsocidae to be identified in Cretaceous amber and the third genus and fourth species from the Tanai amber.

2. Material and methods

The studied material is included in an amber piece that came from mines in the Hukawng Valley (Kachin State, northern Myanmar), near Tanai Village (see Grimaldi et al., 2002: fig. 1), and is early Cenomanian in age, 98.79 ± 0.62 Ma (Shi et al., 2012) based on volcanic zircons. Although recent works debate about an older age for the Burmese amber based on palaeontological dating (see Mao et al., 2018; Smith and Ross, 2018). The amber piece containing the specimen was cut and polished and the specimen was examined with a Motic BA310 compound microscope using reflected and transmitted light. The photographs were taken with a Moticam 2500 attached to the compound microscope and processed using Motic Images Plus 2.0 ML software. A compound microscope Olympus CX41 equipped with a camera lucida tube was used to make the drawings. Adobe Photoshop CS6 software was used to obtain the measurements and prepare the figures. The specimen is housed at the *Museu de Ciències Naturals de Barcelona* (MCNB) with the accession number MGB 89665.

The remarkable preservation of the studied specimen has enabled an accurate anatomical description and comparison. The works of Lienhard (1998) and Mockford (1993) are followed for wing venation nomenclature and body terminology. The works of Mockford (1993) and Smithers (1972, 1990) are followed for the systematics of the psocids.

This manuscript has been registered in ZooBank under the number urn:lsid:zoobank.org:pub:0A9DC056-F388-4157-AA1F-D9D1B9CFAA99.

3. Systematic palaeontology

Suborder Trogiomorpha Roesler, 1944
Infraorder Psyllipsocetae Smithers, 1972
Family Psyllipsocidae Kolbe, 1884
Genus *Psyllipsocus* Selys-Longchamps, 1872

Psyllipsocus yoshizawai sp. nov.
Figs. 1–3

This new species has been registered in ZooBank under the number urn:lsid:zoobank.org:act:E26812C1-3242-46A9-8BB7-59DC679C4506.

Holotype. Probably a female, MGB 89665, housed at the *Museu de Ciències Naturals de Barcelona* (MCNB).
Locality and horizon. Hukawng Valley, near Tanai (=Danai) Village, northern Myanmar, lowermost Cenomanian.
Etymology. In honour of Dr. Kazunori Yoshizawa from the Hokkaido University for his outstanding contributions to the study of the taxonomy, morphology and phylogeny of Psocodea.
Diagnosis. Macropterous, probably a female. Antennomeres not secondarily annulated; prominent, gibbous postclypeus; maxillary palps four-segmented without visible sensillum on any palpomere, second and fourth palpomeres of similar lengths, fourth palpomere distally broadened and with rounded apex; transparent and well-developed wings with complete venation; forewings with straight costal margin; margin glabrous except for the proximal part of costal margin; rows of setae above veins; Sc ending free; elongated pterostigma; six-angled radial cell as long as wide; Rs two-branched; M three-branched; elongated areola postica bounded by Cu_{1a} much longer than Cu_{1b}; nodulus present; only one anal vein; hindwings glabrous; R_1 showing sigmoidal path; Rs and M two-branched; four-angled, elongated basi-radial cell; Cu_1 simple and with a pronounced curve at the point of separation with M; A bifurcating into 1A and 2A near wing base; two distal spurs on tibiae; tarsi three-segmented with two pretarsal claws, without pulvillus or preapical teeth.
Description. Complete specimen (Fig. 1A, B), macropterous with complete venation (Fig. 2A, B), probably a female. Brown body 1.11 mm long. Elongated head, 0.29 mm wide, with epicranial suture between two prominent compound eyes globular in shape, diameter 0.11 mm; antennae poorly preserved with around 16 antennomeres, not secondarily annulated, covered by fine hairs (Fig. 3A); scape and pedicel not well visible. Lengths of preserved antennomeres of right antenna: I 0.03 mm, II 0.15 mm, III 0.08 mm, IV 0.07 mm, V 0.06 mm, VI incomplete; ocelli not visible; front with prominent, gibbous postclypeus; left lacinia and galea poorly visible, lacinia apparently displaying two small apical teeth (Fig. 3B); labial palps not visible; maxillary palps four-segmented, 0.33 mm long, covered with fine hairs; lengths of palpomeres of left maxillary palpus: I 0.04 mm, II 0.11 mm, III 0.06 mm, IV 0.11 mm, fourth palpomere distally widened and with round apex, no sensillum in second palpomere (Fig. 3C). Thorax well preserved with a conspicuous pronotum; mesonotum raised above level of head and pronotum; metanotum much lower. Both right wings twisted and deformed; measurements and description of venation taken from left wings. Peculiarly, several veins appear duplicated due to a reflection. Forewing 1.12 mm long and 0.51 mm wide, with complete venation (Fig. 2A), transparent with glabrous margin, except for presence of several hairs on anteriormost part of costal margin, and rows of setae along veins, straight costal margin, round apex, without flattened scales; Sc long, ending free in wing membrane without reaching costal margin or R; Sc' without several very

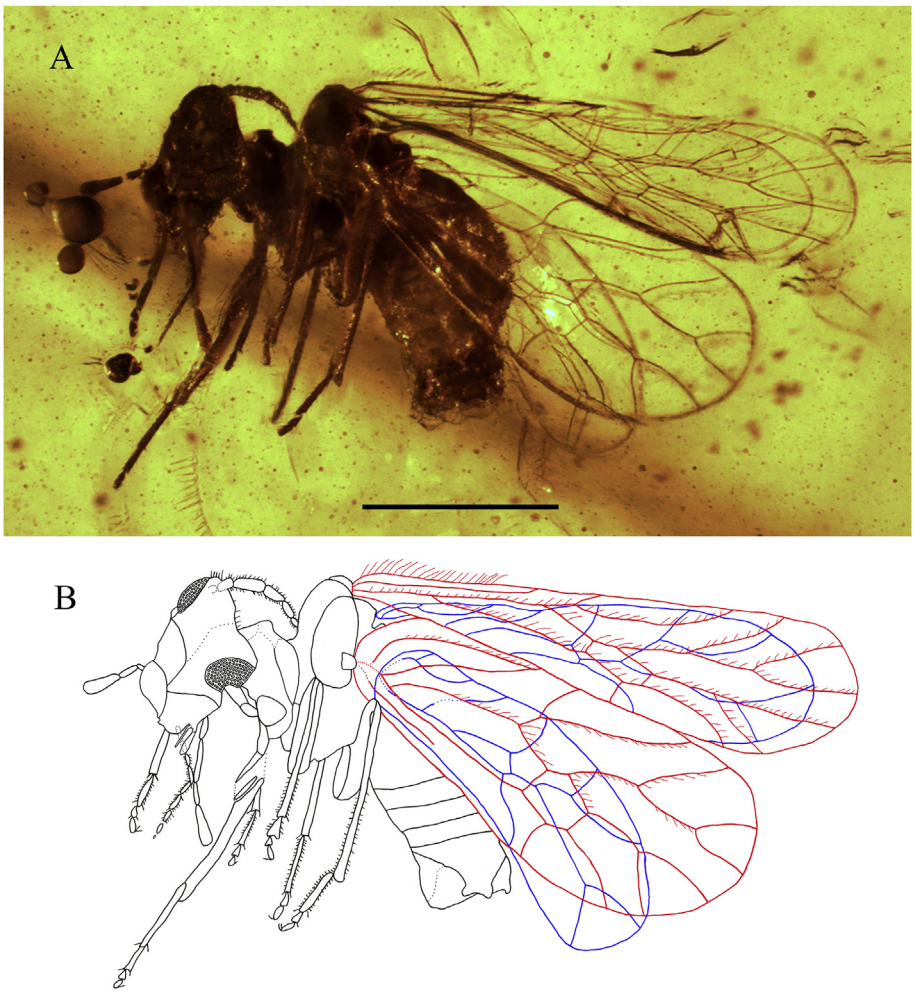

Fig. 1. Habitus of *Psyllipsocus yoshizawai* sp. nov. (Psocodea: Trogiomorpha: Psyllipsocidae), holotype, MGB 89665, probably a female: A) photograph; B) drawing (forewings in red and hindwings in blue). Both at the same scale. Scale bar = 0.5 mm. (For interpretation of the references to colour in this figure legend, the reader is referred to the Web version of this article.)

small spines; elongated pterostigma 0.25 mm in breadth, of same colour as rest of wing, bounded by Sc' and R_1; bifurcation of R and M + Cu_1 close to wing base at 0.19 mm; bifurcation of R_1 and Rs at 0.69 mm from wing base; Rs fused with M for a short distance of 0.05 mm; Rs divided into R_{2+3} and R_{4+5} at 0.85 mm from wing base, reaching wing margin at 0.95 mm and 1.06 mm respectively, R_{4+5} slightly curved; radial cell between R_1 and Rs closed and six-angled, as long as wide and with vein edges of similar lengths; M + Cu_1 splits into M and Cu_1 at 0.44 mm from wing base; M_3 emerging from M at 0.79 mm from wing base and reaching wing margin at 0.96 mm following a slightly sigmoidal path; furthermore, M displays another bifurcation at 0.97 mm from wing base, M_1 and M_2 reaching wing margin at 1.11 mm and 1.09 mm from wing base, respectively; Cu_1 splits into Cu_{1a} and Cu_{1b} at 0.48 mm from wing base, Cu_{1a} much longer than Cu_{1b}, straight and with a slight curve before reaching wing margin at 0.85 mm from wing base, Cu_{1b} with an accentuated curve just before reaching wing margin at 0.57 mm from wing base, areola postica long, 0.28 mm wide; a straight Cu_2 distally fused with a curved A near posterior wing margin, a nodulus at 0.41 mm from wing base (Fig. 3D). Hindwing slightly deformed in costal region (Fig. 2B), transparent and with complete venation, 0.92 mm long and 0.32 mm wide, glabrous margin, round apex, without flattened scales or setae; sigmoidal R_1 reaching wing margin at 0.57 mm from wing base; elongated, four-angled, narrow basi-radial cell broadened distally, triangular in shape; Rs and M fused for 0.07 mm then bifurcating again at 0.48 mm from wing base; Rs extending straight and divided into R_{2+3} and R_{4+5} at 0.75 mm from wing base, reaching wing margin at 0.84 mm and 0.91 mm from wing base, respectively; M slightly curving and splitting into M_1 and M_2 at 0.59 mm from wing base, M_1 curved, ending at 0.78 mm, M_2 straight and joining wing margin at 0.61 mm; M + Cu_1 emerging straight but strongly curved at point of separation between M and Cu_1, Cu_1 continuing this curve and ending at 0.44 mm from wing base; Cu_2 poorly preserved but may have shown a sigmoidal path, reaching wing margin at 0.33 mm; A bifurcating into 1A and 2A near wing base. All legs completely preserved, covered by sparse fine hairs, with coxae and trochanters obscure (only visible in left foreleg), femora thick and long, tibiae thin and long, three-segmented tarsi; combined length of tibia and tarsus 0.69 mm; all tibiae with two lateral distal spurs (Fig. 3E); tarsus 0.16 mm long overall, lengths of tarsomeres 0.09 mm, 0.03 mm and 0.04 mm from proximal to distal ones; distal tarsomere with two pretarsal claws without preapical tooth, pulvillus absent (Fig. 3F). Abdomen 0.63 mm long with several visible segments ventrally. Probably female genitalia poorly preserved with tongue-shaped subgenital plate 0.08 mm wide (Fig. 3G).

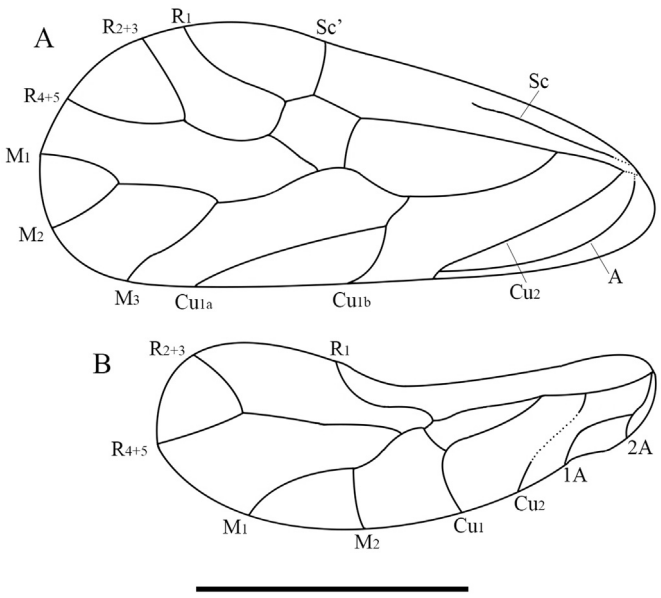

Fig. 2. Drawings of left wings of *Psyllipsocus yoshizawai* sp. nov. (Psocodea: Trogiomorpha: Psyllipsocidae), holotype, MGB 89665, probably a female: A) forewing; B) hindwing. Scale bar = 0.5 mm.

4. Discussion

Psyllipsocus yoshizawai sp. nov. can be included in the Psyllipsocidae on the basis of the following characters according to the key to families provided by Smithers (1990): 1) body and wings without flattened scales, 2) lacinia normal, present, 3) maxillary palps without sensillum on second segment, 4) macropterous, 5) forewing membranous, 6) forewing venation more complex than two parallel, partially evanescent, longitudinal veins, 7) pterostigmal area not more opaque than rest of wing membrane, 8) forewing with Cu_2 and A joined with a nodulus, 9) forewing with one anal vein and 10) tarsi three-segmented. The same conclusion is reached according to the key to psocid families provided by Lienhard (1998), on the basis of: 1) body and wings without scales, 2) elongated head, 3) gibbous postclypeus and lacinia well-developed, 4) no conical sensillum on second segment of maxillary palps, 5) presence of nodulus and 6) tibia and tarsus longer than abdomen. Furthermore, *P. yoshizawai* corresponds to Psyllipsocidae based on Smithers (1972) because of: 1) elongated head and long antennae without secondary annulations, 2) narrow lacinia with few apical teeth, 3) maxillary palps without sensillum on second segment, 4) forewing pterostigma not thickened, 5) a cross-vein r_1-rs, 6) long areola postica bounded by Cu_{1b} shorter than Cu_{1a}, 7) presence of nodulus joining Cu_2 and A, 8) hindwing with M two-branched, 9) tarsi three-segmented and 10) pretarsal claws without preapical teeth. Smithers (1972) also referred to features such as ocelli, labial palps and genitalia, but these structures are poorly preserved or not visible in the studied specimen. Finally, the preserved and visible features of *P. yoshizawai* fit the diagnosis of Psyllipsocidae provided by Mockford (1993): 1) body and wings without scales but often with setae, 2) second segment of maxillary palps without sensory spur, 3) forewing with bifurcation of R and M + Cu_{1a} close to wing base, 4) M + Cu_{1a} divided about one-third distance from wing base to wing up in forewing and 5) no pulvillus in pretarsal claws. Nonetheless, this diagnosis also refers to the labrum and genitalia, not well visible in the studied specimen; moreover, the presence in this diagnosis of a preapical tooth on the pretarsal claw diverges from the list of characters for the family provided by Smithers (1972), which includes claws without a preapical tooth. The absence of a preapical tooth on the pretarsal claw in *P. yoshizawai* may indicate that this is an unreliable diagnostic character for the family as suggested by Wang et al. (2019). As such, *P. yoshizawai* is included in the Psyllipsocidae (Trogiomorpha: Psyllipsocetae), although the impossibility of determining the total number of antennomeres, the complete mouthpart anatomy or the genitalia structures hinders a definitive identification.

Psyllipsocus yoshizawai sp. nov. differs from *Libanopsyllipsocus alexanderasnitsyni*, which possesses forewing with M two-branched, areola postica more elongated, no pterostigma, hindwing with R_1 absent, M simple and presence of preapical tooth on pretarsal claws (Azar and Nel, 2011). The probable psyllipsocid *Parapsyllipsocus vergereaui* displays a very different wing venation to *P. yoshizawai*, for example forewing with Sc reaching anterior wing margin, Sc' long and distally directed, radial cell distally opened and hindwing with Rs simple and basi-radial cell three-angled (Perrichot et al., 2003). The diagnosis of the genus *Annulipsyllipsocus* includes antennomeres with secondary annulations, wings with colour pattern, forewing with bulged costal margin and triangular pterostigma (Hakim et al., 2018); *P. yoshizawai* does not share these features. *Concavapsocus parallelus* possesses different characters to *P. yoshizawai*, such as narrow vertex, forewing with inwardly concave apex, setae in posterior wing margin, M and Cu_1 not branched, hindwing triangular, posterior margin with dense setae, R and M not branched and Cu_1 bifurcating into Cu_{1a} and Cu_{1b} near middle hindwing (Wang et al., 2019). Likewise, *P. yoshizawai* differs from *Khatangia inclusa*, because the latter possesses antennomeres with secondary annulations, forewing with triangular pterostigma, absence of nodulus and presence of pretarsal claws with preapical teeth (Vishniakova, 1975). The Eocene psyllipsocid *Sinopsyllipsocus fushunensis* displays secondary annulations on antennae, long sensillum on the second segment of the maxillary palps, forewing with triangular pterostigma, proximal part of Sc not reaching radius and a single, small preapical tooth on pretarsal claws (Zhang et al., 2016).

Considering the extant genera of Psyllipsocidae, *Psyllipsocus yoshizawai* sp. nov. fits within the genus *Psyllipsocus* on the basis of the characters of the psyllipsocid genera keyed by Smithers (1990): 1) macropterous with evident veins on forewings and 2) forewing with margin glabrous and few setae above the veins disposed in a row; moreover, the characters of the forewing, such as Rs branched and Cu_{1a} several times longer than Cu_{1b}, are indicated as typical of *Psyllipsocus*. The key to the genera of Psyllipsocidae by Mockford (1993) indicates the following characters for *Psyllipsocus*: 1) forewing wide with Rs and M branched distally, 2) forewing broader, at most length/greatest width of 2.76 (in the studied specimen this ratio corresponds to 2.20) and 3) vertex (distance between eyes/greatest width of postclypeus) broad and mesonotum and metanotum scarcely, if at all, raised above the level of the head; all of the above fit with *P. yoshizawai*. Furthermore, *P. yoshizawai* presents a very similar morphology to that of *Psyllipsocus eocenicus* (Oise amber, the only fossil adult *Psyllipsocus* described to date). They share similar wing venation, despite differences such as a more triangular-shaped pterostigma, slightly elongated radial cell on the forewing and straight R_1 and three-angled basi-radial cell on the hindwing of *P. eocenicus* (see Nel et al., 2005). The most important difference is the presence of a single preapical tooth on the pretarsal claws of *P. eocenicus*. The diagnosis for *Psyllipsocus* by Mockford (1993) and the emended diagnosis by Mockford (2011) include a broad vertex, the mesonotum of winged forms raised above the level of the head, the metanotum much lower and a forewing and hindwing venation similar to *P. yoshizawai*, but Mockford (1993, 2011) also mentioned characters that cannot be observed in *P. yoshizawai*, such as the antennal pedicel usually with

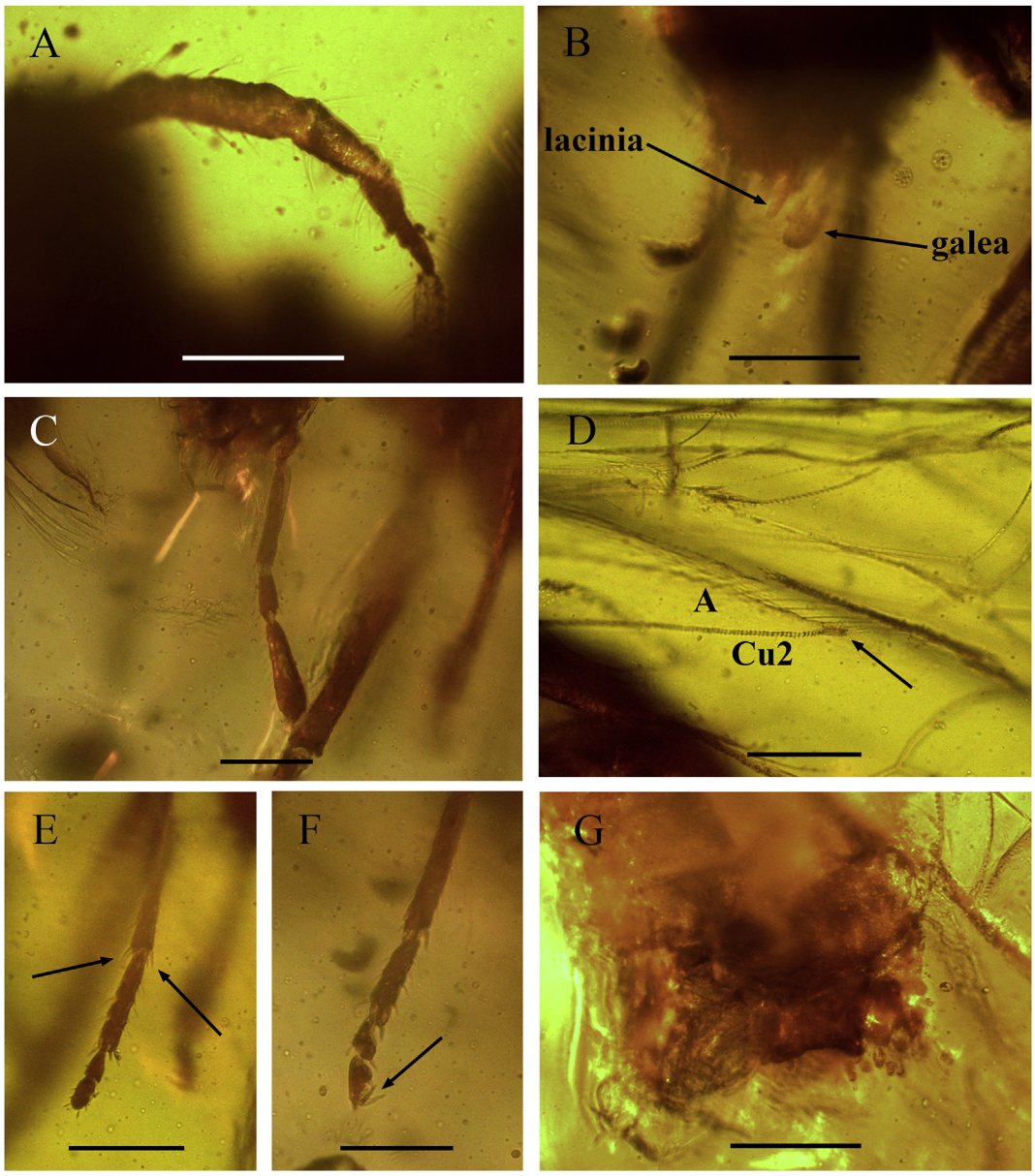

Fig. 3. *Psyllipsocus yoshizawai* sp. nov. (Psocodea: Trogiomorpha: Psyllipsocidae), holotype, MGB 89665, probably a female: A) right antenna, lacking secondary annulations; B) lacinia and galea, indicated with arrows; C) left maxillary palpus; D) nodulus, indicated with an arrow, joining Cu2 and A in left forewing; E) right mid-tibia, showing two distal spurs, indicated with arrows; F) distal foreleg, showing three-segmented tarsus and pretarsal claws, the latter indicated with an arrow; G) genitalia in ventral view, most probably of a female. Scale bars = 0.1 mm.

a minute distal sense peg, the coxal rasp present and characters of the genitalia. The genus *Dorypteryx* can be excluded based on the reduced forewings with R and M veins unbranched; *Pseudorypteryx* has a large sensillum on the fourth segment of the maxillary palps and usually displays forewings reduced to slender traps; *Psocathropos* displays a narrow vertex, the mesonotum and metanotum considerably raised above the level of the head and hindwings with M simple (Mockford, 1993; Smithers, 1972, 1990).

Notwithstanding the great antiquity of *Psyllipsocus yoshizawai* sp. nov., we propose including it in this extant genus because of the lack of any significant differences that could justify a new genus. *Psyllipsocus eocenicus* is almost 'midway' (earliest Eocene, temporary distance ca. 53 Ma, Nel et al., 1999) between the extant *Psyllipsocus* species and *P. yoshizawai* sp. nov. (early Cenomanian, ca. 98 Ma old, Shi et al., 2012). Both fossils show a high morphological stability of the genus over time. Furthermore, it is the first extant genus of Psocodea with representatives dating back to the Cretaceous to date.

The extant 'Psocoptera' feed on microorganisms such as algae, lichens and fungi and are considered cosmopolitan, but require a constantly warm and humid habitat. They show a high diversity and great abundance in intertropical areas (New, 1987). The representatives of Psyllipsocidae, called cave barklice, are found in caves, rock outcrops, leaf litter and rodent nests (New, 1987; Mockford, 2011). The Cretaceous psyllipsocids have been found in amber sites from Lebanon (Barremian), Myanmar (Cenomanian) and the Russian Federation (Taimyr Peninsula; Santonian); all of them lived in warm and humid forest environments (Azar, 2007; Cruickshank and Ko, 2003; Golovneva, 2012), which also applies to the French site of Archingeay-Les Nouillers (Charentese amber), where the probable psyllipsocid *Parapsyllipsocus vergereaui* was found (Néraudeau et al., 2002) (Fig. 4). The presence of these

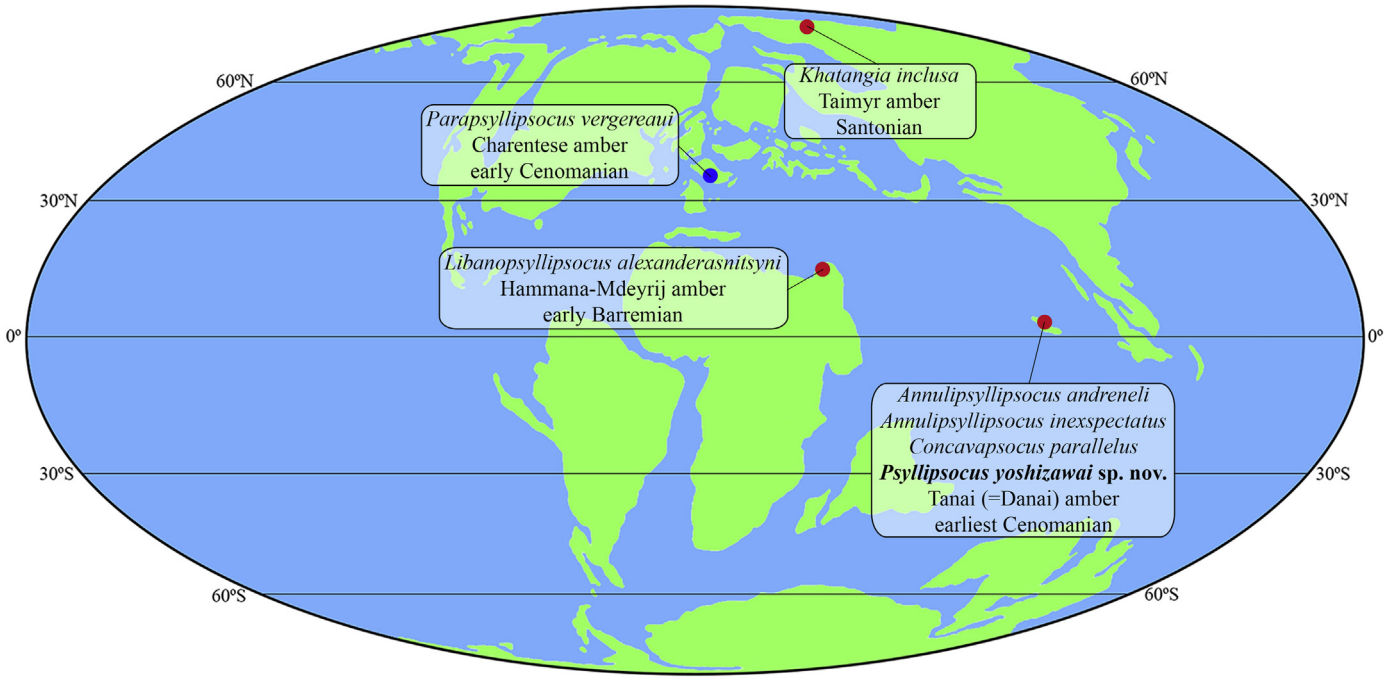

Fig. 4. Global palaeogeographic reconstruction during the Late Cretaceous (100 Ma) showing the provenance of the known Cretaceous psyllipsocids (Psocodea: Trogiomorpha: Psyllipsocidae) in red circles, and the probable psyllipsocid *Parapsyllipsocus vergereaui* in a blue circle. Modified from Blakey (2011). (For interpretation of the references to colour in this figure legend, the reader is referred to the Web version of this article.)

psyllipsocid fossil species in these palaeoenvironments and the vast geographical and temporal distances that separate them suggest that the autoecology of the Cretaceous psyllipsocids may have been similar to that of the living representatives and that they were already widely distributed during this period.

Polymorphism affects several families of psocids, viz., the size of the compound eyes or the development of the wings in one or both sexes; this phenomenon is observed in the extant psyllipsocid genera *Dorypteryx*, *Pseudorypteryx*, *Psocathropos* and *Psyllipsocus* (see Kučerová, 1997, 1998). Furthermore, Badonnel (1959) observed an environmental influence on wing development in extant *Psyllipsocus ramburii* Selys-Longchamps, 1872, whereby nymphs become brachypterous adults when reared in isolation or in small groups at a temperature above 25 °C, but become macropterous adults when reared in small groups at below 25 °C (New, 1987); similar observations were noted by Kučerová (1997) for *Dorypteryx domestica* Smithers, 1958. Polymorphism has recently been indicated for the fossil species *Annulipsyllipsocus andreneli* from the Cenomanian Tanai amber (Myanmar), suggesting that polymorphism may have been present in the Psyllipsocidae very early on in the family's history (Hakim et al., 2018). Besides wing polymorphism, asymmetrical wing venation has been reported in this family, as in a specimen of *Concavapsocus parallelus*; therefore, the identification of species based solely on wing venation may be unreliable (Wang et al., 2019).

5. Conclusions

Psyllipsocus yoshizawai sp. nov. increases our knowledge about the palaeodiversity of the family Psyllipsocidae in the Cretaceous. To date, five genera and six species of psyllipsocids are known from this period. The newly studied specimen corresponds to the third genus and fourth species identified within the Psyllipsocidae from Tanai amber (Myanmar), which has provided most of the known Cretaceous palaeodiversity of this family.

Psyllipsocus yoshizawai sp. nov. is attributed to the extant genus *Psyllipsocus*, indicating a high morphological stability over time in this genus. This is rare but not unique among the Upper Cretaceous insects from Burmese amber, viz. there are 22 records of extant genera for more than 700 genera currently described (ca. 3% of the genera), according to the catalogue by Ross (2019). Future findings of new fossil psyllipsocid specimens could shed further light on the obscure palaeobiology and palaeoautoecology of the family.

Acknowledgements

We thank Eduardo Koutsoukos and two anonymous reviewers for their useful and helpful comments that have improved the manuscript. The first author has a grant funded by the Secretary of Universities and Research of the Government of Catalonia (Spain) and the European Social Fund (2019FI_B00330). This study is a contribution to the Spanish Ministry of Science, Innovation and Universities Project CRE CGL2017-84419 (Spain, AEI/FEDER, UE).

References

Aaron, S.F., 1883. Description of new Psocidae in the collection of the American Entomological Society. Transactions of the American Entomological Society and Proceedings of the Entomological Section of the Academy of Natural Sciences 11 (1), 37–40.

Azar, D., 2007. Preservation and accumulation of biological inclusions in Lebanese amber and their significance. Comptes Rendus Palevol 6 (1–2), 151–156. https://doi.org/10.1016/j.crpv.2006.10.004.

Azar, D., Engel, M.S., 2008. A sphaeropsocid bark louse in Late Cretaceous amber from Siberia (Psocoptera: Sphaeropsocidae). Transactions of the Kansas Academy of Science 111 (1), 141–147. https://doi.org/10.1660/0022-8443(2008)111[141:ASBLIL]2.0.CO;2.

Azar, D., Nel, A., 2004. Four new Psocoptera from Lebanese amber (Insecta: Psocomorpha: Trogiomorpha). Annales de la Société Entomologique de France 40 (2), 185–192. https://doi.org/10.1080/00379271.2004.10697415.

Azar, D., Nel, A., 2011. The oldest psyllipsocid booklice, in Lower Cretaceous amber from Lebanon (Psocodea, Trogiomorpha, Psocathropetae, Psyllipsocidae). ZooKeys 130, 153–165. https://doi.org/10.3897/zookeys.130.1430.

Azar, D., Hajar, L., Indary, C., Nel, A., 2008. Paramesopsocidae, a new Mesozoic psocid family (Insecta: Psocodea "Psocoptera": Psocomorpha). Annales de la

Société Entomologique de France 44 (4), 459–470. https://doi.org/10.1080/00379271.2008.10697581.
Azar, D., Nel, A., Néraudeau, D., 2009. A new Cretaceous psocodean family from the Charente-Maritime amber (France) (Insecta, Psocodea, Psocomorpha). Geodiversitas 31 (1), 117–128. https://doi.org/10.5252/g2009n1a10.
Azar, D., Engel, M.S., Grimaldi, D.A., 2010a. A new genus of sphaeropsocid bark lice from the Early Cretaceous amber of Lebanon (Psocodea: Sphaeropsocidae). Annales de la Société Entomologique de France 46 (1–2), 103–107. https://doi.org/10.1080/00379271.2010.10697643.
Azar, D., Nel, A., Petrulevičius, J.F., 2010b. First Psocodean (Psocodea, Empheriidae) from the Cretaceous Amber of New Jersey. Acta Geologica Sinica-English Edition 84 (4), 762–767. https://doi.org/10.1111/j.1755-6724.2010.00255.x.
Azar, D., Huang, D., Cai, C., Nel, A., 2015a. The earliest records of pachytroctid booklice from Lebanese and Burmese Cretaceous ambers (Psocodea, Troctomorpha, Nanopsocetae, Pachytroctidae). Cretaceous Research 52, 336–347. https://doi.org/10.1016/j.cretres.2014.04.005.
Azar, D., Nel, A., Perrichot, V., 2015b. Diverse barklice (Psocodea) from Late Cretaceous Vendean amber. Paleontological Contributions 2014 (10C), 9–16. https://doi.org/10.17161/PC.1808.15983.
Azar, D., Hakim, M., Huang, D., 2016. A new compsocid booklouse from the Cretaceous amber of Myanmar (Psocodea: Troctomorpha: Amphientometae: Compsocidae). Cretaceous Research 68, 28–33. https://doi.org/10.1016/j.cretres.2016.08.003.
Azar, D., Hakim, M., Huang, D., Cai, C., Nel, A., 2017a. New fossil booklice from the Cretaceous amber of Myanmar (Psocodea: Troctomorpha: Amphientometae: Manicapsocidae). Cretaceous Research 70, 8–14. https://doi.org/10.1016/j.cretres.2016.09.013.
Azar, D., Huang, D., El-Hajj, L., Cai, C., Nel, A., Maksoud, S., 2017b. New Prionoglaridae from Burmese amber (Psocodea: Trogiomorpha: Prionoglaridetae). Cretaceous Research 75, 146–156. https://doi.org/10.1016/j.cretres.2017.03.028.
Badonnel, A., 1959. Développement des ailes de *Psyllipsocus ramburi* Sel. Long.: Essai d'interprétation. Bulletin de la Societe Zoologique de France 84, 91–98.
Baz, A., Ortuño, V.M., 2000. Archaeatropidae, a new family of Psocoptera from the Cretaceous amber of Alava, Northern Spain. Annals of the Entomological Society of America 93 (3), 367–373. https://doi.org/10.1603/0013-8746(2000)093[0367:AANFOP]2.0.CO;2.
Baz, A., Ortuño, V.M., 2001a. New genera and species of empheriids (Psocoptera: Empheriidae) from the Cretaceous amber of Alava, northern Spain. Cretaceous Research 22 (5), 575–584. https://doi.org/10.1006/cres.2001.0275.
Baz, A., Ortuño, V.M., 2001b. A new electrentomoid psocid (Psocoptera) from the Cretaceous amber of Alava (Northern Spain). Deutsche Entomologische Zeitschrift 48 (1), 27–32. https://doi.org/10.1002/dez.200100004.
Blakey, R.C., 2011. Global paleogeographic views of earth history: Late Precambrian to Recent accessed 29 06 2019. http://cpgeosystems.com/paleomaps.html.
Choufani, J., Azar, D., Nel, A., 2011. The oldest amphientomete booklouce from Lower Cretaceous amber of Lebanon (Psocodea: Troctomorpha). Insect Systematics and Evolution 42 (2), 149–159. https://doi.org/10.1163/187631211X579405.
Cockerell, T.D.A., 1916. Insects in Burmese Amber. American Journal of Science 42, 135–138.
Cockerell, T.D.A., 1919. Insects in Burmese Amber. Entomologist 52, 241–243.
Cockx, P., McKellar, R., Tappert, R., Vavrek, M., Muehlenbachs, K., 2020. Bonebed amber as a new source of paleontological data: The case of the Pipestone Creek deposit (Upper Cretaceous), Alberta, Canada. Gondwana Research 81, 378–389. https://doi.org/10.1016/j.gr.2019.12.005.
Cruickshank, R.D., Ko, K., 2003. Geology of an amber locality in the Hukawng Valley, northern Myanmar. Journal of Asian Earth Sciences 21 (5), 441–455. https://doi.org/10.1016/S1367-9120(02)00044-5.
García Aldrete, A.N., 1984. Trogiomorpha (Psocoptera) of Chamela, Jalisco, Mexico. Folia Entomologica Mexicana 59, 25–69.
Golovneva, L.B., 2012. The Late Cretaceous flora of the Khatanga depression (northern Siberia). Paleobotanika 3, 32–61.
Grimaldi, D., Engel, M.S., 2006a. Fossil Liposcelididae and the lice ages (Insecta: Psocodea). Proceedings of the Royal Society B: Biological Sciences 273 (1586), 625–633. https://doi.org/10.1098/rspb.2005.3337.
Grimaldi, D., Engel, M.S., 2006b. Extralimital fossils of the "Gondwanan" family Sphaeropsocidae (Insecta: Psocodea). American Museum Novitates 2006 (3523), 1–18. https://doi.org/10.1206/0003-0082(2006)3523[1:EFOTGF]2.0.CO;2.
Grimaldi, D.A., Engel, M.S., Nascimbene, P.C., 2002. Fossiliferous Cretaceous amber from Myanmar (Burma): its rediscovery, biotic diversity, and paleontological significance. American Museum Novitates 3361, 1–72. https://doi.org/10.1206/0003-0082(2002)361<0001:FCAFMB>2.0.CO;2.
Hakim, M., Azar, S., Maksoud, S., Huang, D., Azar, D., 2018. New polymorphic psyllipsocids from Burmese amber (Psocodea: Psyllipsocidae). Cretaceous Research 84, 389–400. https://doi.org/10.1016/j.cretres.2017.11.027.
Hakim, M., Azar, D., Huang, D., 2020. A unique manicapsocid (Psocodea: Amphientometae) from the mid-Cretaceous Burmese amber. Cretaceous Research 107, 104278. https://doi.org/10.1016/j.cretres.2019.104278.
Johnson, K.P., Dietrich, C.H., Friedrich, F., Beutel, R.G., Wipfler, B., Peters, R.S., Allen, J.M., Petersen, M., Donath, A., Walden, K.K.O., Kozlov, A.M., Podsiadlowski, L., Mayer, C., Meusemann, K., Vasilikopoulos, A., Waterhouse, R.M., Cameron, S.L., Weirauch, C., Swanson, D.R., Percy, D.M., Hardy, N.B., Terry, I., Liu, S., Zhou, X., Misof, B., Robertson, H.M., Yoshizawa, K., 2018. Phylogenomics and the evolution of hemipteroid insects. Proceedings of the National Academy of Sciences 115 (50), 12775–12780. https://doi.org/10.1073/pnas.1815820115.
Kolbe, H.J., 1884. Der Entwickelungsgang der Psociden im Individuum und in der Zeit. Berliner Entomologische Zeitschrift 28, 35–38.
Kučerová, Z., 1997. Macropterous form of *Dorypteryx domestica* (Psocoptera: Psyllipsocidae). European Journal of Entomology 94 (4), 567–573.
Kučerová, Z., 1998. Wing polymorphism in *Dorypteryx domestica* (Smithers) (Psocoptera: Psyllipsocidae). Insect Systematics and Evolution 29 (4), 451–457.
Li, F.S., 2002. Psocoptera of China. National Natural Science Foundation of China, Science Press, Beijing xlvi + 1976 pp. (2 volumes).
Lienhard, C., 1998. Psocoptères Euro-Méditerranéens, vol. 83. Fédération Française des Sociétés de Sciences Naturelles, Faune de France, p. 533.
Maheu, A., Nel, A., 2020. A new fossil booklouse (psocodea: Troctomorpha: Amphientometae: Manicapsocidae) from the mid-Cretaceous amber of northern Myanmar. Cretaceous Research 106, 104222. https://doi.org/10.1016/j.cretres.2019.104222.
Mao, Y.Y., Liang, K., Su, Y.T., Li, J.G., Rao, X., Zhang, H., Xia, F.Y., Fu, Y.Z., Cai, C.Y., Huang, D.Y., 2018. Various amberground marine animals on Burmese amber with discussions on its age. Palaeoentomology 1 (1), 91–93. https://doi.org/10.11646/palaeoentomology.1.1.11.
Mockford, E.L., 1969. Fossil insects of the order Psocoptera from Tertiary amber of Chiapas, Mexico. Journal of Paleontology 43 (5), 1267–1273.
Mockford, E.L., 1993. North American Psocoptera (Insecta), vol. 10. Sandhill Crane Press, p. 455. Flora & Fauna Handbook.
Mockford, E.L., 2011. New species of *Psyllipsocus* (Psocoptera: Psyllipsocidae) from North and Middle America with a key to the species of the region. Transactions of the American Entomological Society 137 (1–2), 15–48. https://doi.org/10.3157/061.137.0115.
Mockford, E.L., Lienhard, C., Yoshizawa, K., 2013. Revised classification of 'Psocoptera' from Cretaceous amber, a reassessment of published information. Insecta Matsumurana New series 69, 1–26.
Nel, A., Waller, A., 2007. The first fossil Compsocidae from Cretaceous Burmese amber (Insecta, Psocoptera, Troctomorpha). Cretaceous Research 28 (6), 1039–1041. https://doi.org/10.1016/j.cretres.2007.02.002.
Nel, A., de Plöeg, G., Dejax, J., Dutheil, D., de Franceschi, D., Gheerbrant, E., Godinot, M., Hervet, S., Menier, J.J., Augé, M., Bignot, G., Cavagnetto, C., Duffaud, S., Gaudant, J., Hua, S., Jossang, A., de Lapparent de Broin, F., Pozzi, J.P., Paicheler, J.C., Beuchet, F., Rage, J.C., 1999. Un gisement sparnacien exceptionnel à plantes, arthropodes et vertébrés (Éocène basal, MP7): Le Quesnoy (Oise, France). Comptes Rendus de l'Academie des Sciences - Series IIA: Earth and Planetary Science 329 (1), 65–72. https://doi.org/10.1016/S1251-8050(99)80229-8.
Nel, A., Prokop, J., De Ploëg, G., Millet, J., 2005. New Psocoptera (Insecta) from the lowermost Eocene amber of Oise, France. Journal of Systematic Palaeontology 3 (4), 371–391. https://doi.org/10.1017/S1477201905001598.
Nel, A., Roques, P., Nel, P., Prokin, A.A., Bourgoin, T., Prokop, J., Szwedo, J., Azar, D., Desutter-Grandcolas, L., Wappler, T., Garrouste, R., Coty, D., Huang, D., Engel, M.S., Kirejtshuk, A.G., 2013. The earliest known holometabolous insects. Nature 503 (7475), 257–261. https://doi.org/10.1038/nature12629.
Néraudeau, D., Perrichot, V., Dejax, J., Masure, E., Nel, A., Philippe, M., Moreau, P., Guillocheau, F., Guyot, T., 2002. Un nouveau gisement à ambre insectifère et à végétaux (Albien terminal probable): Archingeay (Charente-Maritime, France). Geobios 35 (2), 233–240. https://doi.org/10.1016/S0016-6995(02)00024-4.
New, T.R., 1987. Biology of the Psocoptera. Oriental Insects 21 (1), 1–109.
Ngô-Muller, V., Garrouste, R., Nel, A., 2020. Small but important: a piece of mid-Cretaceous Burmese amber with a new genus and two new insect species (Odonata: Burmaphlebiidae & 'Psocoptera': Compsocidae). Cretaceous Research 110, 104405. https://doi.org/10.1016/j.cretres.2020.104405.
Perrichot, V., Azar, D., Néraudeau, D., Nel, A., 2003. New Psocoptera in the Lower Cretaceous ambers of southwestern France and Lebanon (Insecta: Psocoptera: Trogiomorpha). Geological Magazine 140 (6), 669–683. https://doi.org/10.1017/S0016756803008355.
Ribaga, C., 1899. Descrizione di un nuovo genere e di una nuova specie di Psocidi trovato in Italia. Rivista di Patologia Vegetale 8, 156–159.
Roesler, R., 1944. Die Gatungen der Copeognatha. Stettiner Entomologisches Zeitung 105, 117–166.
Ross, A.J., 2019. Burmese (Myanmar) amber checklist and bibliography 2018. Palaeoentomology 2, 22–84. https://doi.org/10.11646/palaeoentomology.2.1.5.
Selys-Longchamps, E.D., 1872. Notes on two new genera of Psocidae. Entomologist Monthly Magazine 9, 145–146.
Shi, G., Grimaldi, D.A., Harlow, G.E., Wang, Ji, Wang, Ju, Yang, M., Lei, W., Li, Q., Li, X., 2012. Age constraint on Burmese amber based on U–Pb dating of zircons. Cretaceous Research 37, 155–163. https://doi.org/10.1016/j.cretres.2012.03.014.
Smith, R.D., Ross, A.J., 2018. Amberground pholadid bivalve borings and inclusions in Burmese amber: implications for proximity of resin-producing forests to brackish waters, and the age of the amber. Earth and Environmental Science Transactions of the Royal Society of Edinburgh 107 (2–3), 239–247. https://doi.org/10.1017/S1755691017000287.
Smithers, C.N., 1958. A new genus and species of domestic psocid (Psocoptera) from Southern Rhodesia. Journal of the Entomological Society of Southern Africa 21 (1), 113–116.
Smithers, C.N., 1972. The classification and phylogeny of the Psocoptera, vol. 14. Australian Museum Memoir, p. 349.
Smithers, C.N., 1990. Keys to the family and genera of Psocoptera (Arthropoda: Insecta). Technical Reports of the Australian Museum 2, 1–82.
Sroka, P., Nel, A., 2017. New species of Compsocidae (Insecta, Psocodea) from Cretaceous Burmese amber. Zootaxa 4320 (3), 597–600. https://doi.org/10.11646/zootaxa.4320.3.1.

Vishniakova, V.N., 1975. Psocoptera in Late-Cretaceous insect-bearing resins from the Taimyr. Entomological Review 54, 63–75.
Wang, R., Li, S., Ren, D., Yao, Y., 2019. New genus and species of the Psyllipsocidae (Psocodea: Trogiomorpha) from mid-Cretaceous Burmese amber. Cretaceous Research 104, 104178. https://doi.org/10.1016/j.cretres.2019.07.008.
Zhang, Z.Q., 2011. Animal biodiversity: An outline of higher-level classification and survey of taxonomic richness. Zootaxa 3148, 1–237.
Zhang, Q., Nel, A., Azar, D., Wang, B., 2016. New Chinese psocids from Eocene Fushun amber (Insecta: Psocodea). Alcheringa: An Australasian Journal of Palaeontology 40 (3), 366–372. https://doi.org/10.1080/03115518.2016.1144952.

Anexo 8.1.2

Cretaceous amniote integuments recorded through a taphonomic process unique to resins

Álvarez-Parra, S., Delclòs, X., Solórzano-Kraemer, M.M., Alcalá, L., Peñalver, E. 2020. Cretaceous amniote integuments recorded through a taphonomic process unique to resins. *Scientific Reports*, **10**, 19840.

DOI: https://doi.org/10.1038/s41598-020-76830-8

Revista científica: *Scientific Reports*
Factor de impacto: 4,380 (2020)
Categoría: *Multidisciplinary Sciences*, Q1 (2020)

scientific reports

Check for updates

OPEN

Cretaceous amniote integuments recorded through a taphonomic process unique to resins

Sergio Álvarez-Parra[1]✉, Xavier Delclòs[1], Mónica M. Solórzano-Kraemer[2], Luis Alcalá[3] & Enrique Peñalver[4]

Fossil records of vertebrate integuments are relatively common in both rocks, as compressions, and amber, as inclusions. The integument remains, mainly the Mesozoic ones, are of great interest due to the panoply of palaeobiological information they can provide. We describe two Spanish Cretaceous amber pieces that are of taphonomic importance, one bearing avian dinosaur feather remains and the other, mammalian hair. The preserved feather remains originated from an avian dinosaur resting in contact with a stalactite-shaped resin emission for the time it took for the fresh resin to harden. The second piece shows three hair strands recorded on a surface of desiccation, with the characteristic scale pattern exceptionally well preserved and the strands aligned together, which can be considered the record of a tuft. These assemblages were recorded through a rare biostratinomic process we call "pull off vestiture" that is different from the typical resin entrapment and embedding of organisms and biological remains, and unique to resins. The peculiarity of this process is supported by actualistic observations using sticky traps in Madagascar. Lastly, we reinterpret some exceptional records from the literature in the light of that process, thus bringing new insight to the taphonomic and palaeoecological understanding of the circumstances of their origins.

Amber is fossilised resin originating in ancient forests, with a high capacity for exceptional and three-dimensional preservation of biological remains, providing an outstanding source of information from past ecosystems[1]. Arthropods are the most common bioinclusions in amber[2,3], although vertebrate remains are also often found, including those from Amphibia (e.g.,[4]) and crown group Reptilia (e.g.,[5]), such as body fossils and dinosaur feathers (e.g.,[6,7]). Dinosaur feathers and mammalian hair are keratin integumentary structures which constitute the different forms of vertebrate vestiture[8]. The term vestiture is used in this paper for the plumage and pelage of amniotes, thus excluding other dermal structures as scales or glands. Cretaceous amber is an important source of knowledge about feathers, in which they are particularly abundant, providing a panoply of palaeobiological evidence (e.g.,[6,7,9,10]). Recently, a new study has shown feather-like structures in pterosaurs, so these structures could appear in an archosaur ancestor of dinosaurs and pterosaurs or independently in these two groups[11]. Feathers are β-keratin integumentary structures[12] which are present in avian and some non-avian dinosaurs and whose origin has been widely studied[13]. The feather structure is composed by medulla, cortex and cuticle (inner to outer)[14]. Feathers show high morphological variability, even in the same specimen, so their determination is challenging[14].

Mammalian remains are rare in amber, and even more so in amber from the Cretaceous[15,16]. A partial mammalian skeleton which could correspond to a solenodontid was reported from the Miocene amber of the Dominican Republic[17], but this is a unique finding since mammals are usually represented in amber by hairs, as in, for example, two records of abundant solenodontid-like hair also found in Dominican amber[18]. Hair is an α-keratin integumentary structure occurring since before the emergence of crown mammals[19,20]. Like feathers, the hair structure is composed of three layers; medulla, cortex and cuticle, going from innermost to outermost[21–23]. The hair cuticle consists of approximately rectangular, flattened, keratin scales composed of an exocuticle rich in sulphur and an endocuticle with low sulphur content[21,23]. The overlapping of the keratin scales provides the characteristic surface scale pattern (cuticular pattern) of mammalian hair[22,23]. The diverse hair surface scale

[1]Departament de Dinàmica de la Terra i de l'Oceà and Institut de Recerca de la Biodiversitat (IRBio), Facultat de Ciències de la Terra, Universitat de Barcelona, c/ Martí i Franquès S/N, 08028 Barcelona, Spain. [2]Paläontologie und Historische Geologie, Senckenberg Forschungsinstitut und Naturmuseum, Senckenberganlage 25, 60325 Frankfurt am Main, Germany. [3]Fundación Conjunto Paleontológico de Teruel-Dinópolis/Museo Aragonés de Paleontología, Av. Sagunto s/n, 44002 Teruel, Spain. [4]Instituto Geológico y Minero de España (Museo Geominero), c/ Cirilo Amorós 42, 46004 Valencia, Spain. ✉email: sergio.alvarez-parra@ub.edu

patterns can provide information for the determination of mammalian taxa[18,22,23]. The scale pattern can differ between mammalian species, between individual strands of the same specimen, between stages of ontogenesis and along the length of a single strand depending on relative proximity to the basal region or the tip[21,24]. Furthermore, it is also possible for different species to show similar patterns[21,24]. The cuticular scale pattern is genetically controlled[23,25]. Its morphology and arrangement depend on biomechanical forces, which act on the cells during their hardening through the keratinisation process, and on growing speed[26]. Until now, the oldest described mammalian hair in amber corresponds to two strands from the late Albian French amber of Archingeay-Les Nouillers[16]. Mammalian hair is also reported from the early Cenomanian Burmese amber (northern Myanmar), even retaining the scale pattern[27]. One specimen of filamentous structure from the Santonian amber of Yantardakh (Taimyr, Russia) could also be a mammalian hair strand[15]. The youngest Cretaceous mammalian hair comes from the late Campanian amber of Grassy Lake in Canada[6], but it is still undescribed. The record of mammalian hair in Cenozoic amber is comparatively richer (e.g., [18,28,29]).

Based on its molecular composition, the preservation potential of feathers and hair is high[30], although the keratin protein has a low fossilisation potential[10,31]. Dinosaur feathers from compression sites are well-known[30], although the three-dimensional preservation in amber allows an exceptional visualisation of their anatomic structure[7]. Mammalian hair in Mesozoic mammaliaforms found in compression sites has been preserved as a halo of carbonised fur or tufts (e.g.,[19,32]), but usually the scale pattern is obscure or poorly preserved (e.g.,[33]). Furthermore, the taphonomic conditions that facilitated the preservation of vestitures in amber are little-known, and they have been usually related to resin flows produced near the forest floor (or 'litter amber' sensu[34]), requiring at least a contact of the individual before escaping[7]. In contrast, the taphonomic processes of insect preservation in amber have been widely studied[35,36]. Actualistic methods as sticky traps have been previously used to evaluate the accuracy of the record of forest arthropods in resin and amber[3,37], but this kind of traps also records vertebrate vestitures and can provide an example of how resin traps these remains.

Here, we report on two Cretaceous amber pieces from Spain, containing a grouping of avian dinosaur feather remains and three strands of mammalian hair, respectively, resulting from the recording of vertebrate vestiture through a distinct biostratinomic process that we describe for the first time and that is unique to resins.

Results

Avian dinosaur feather remains. A small flake (4.1 mm long and 2.8 mm at its greatest width) of an aerial, stalactite-shaped amber piece (CPT-4200, from San Just outcrop, Teruel, Spain) contains abundant feather remains (the barbs are easily recognised) of an avian dinosaur (Fig. 1). The flake piece is curved in cross section, with the convex (external) surface being dark and the concave one being of the same colour and transparency as the rest of the piece (Fig. 1a). These features indicate that it is a fragment of one of the concentric layers, originating from a resin flow; both the internal core of the piece and a potential later layer (or layers) were lost. The external surface is darker due to original desiccation under aerial conditions. This surface is completely covered by feather barbs dispersed at random without preferential orientation. The barbs (at least a few millimetres long and ca. 0.29 mm wide, with barbules ca. 0.26 mm long; Fig. 1a–d) are not impressions in the surface, but conserved original organic matter, although some small patches are missing (Fig. 1c). Barbs and barbules are well preserved, including the nodes and internodes of the pennula (Fig. 1e,f). The sticky external resin layer must have already been somewhat hardened when the feathers came into contact with it because it does not show deformation from contact and the barbules did not penetrate the resin but are present over the whole original convex surface, as preserved.

Mammalian hair strands. Three mostly parallel-aligned strands of mammalian hair are present in the fragment AR-1-A-2019.88.1 (from Ariño outcrop, Teruel, Spain) (Figs. 2a, S1) (see the description of the whole amber piece AR-1-A-2019.88 in the Supplementary information). They are named X, Y and Z and are exceptionally well preserved, even showing the surface scale pattern (Fig. 2b–d). The scale pattern is easily observed due to the piece having been broken during its extraction, which has facilitated its drawing and SEM imaging (Fig. 3), in contrast to the two hair strands in the French amber, which are poorly preserved[16], and the hair records found in compression sites (e.g.,[19,33]). The three hair strands are brown and straight, and apparently they were rigid. Strand Y is broken, and it is possible that the two fragments are actually from two different strands. There is a discontinuous gap between them where the amber piece seems to be broken, but as they are in the same plane below strand X, we treat them as two fragments of the same strand. The strands are incomplete, and the tips and hair follicles are not preserved, so the orientation of the scale arrangement is not possible to determine. The scale pattern can be partly seen in the external brown surface, but the transparency of the amber fragment facilitates visualisation of the scale pattern mainly as impressions (or cast prints) in the amber, as shown on the internal surfaces of the broken sections. Strand X is 6.72 mm long and around 0.07 mm in diameter; broken strand Y is composed of two strand fragments which are 3.26 mm and 3.20 mm long, respectively, with a diameter of around 0.07 mm, and strand Z is 6.19 mm long and around 0.07 mm in diameter. The cross section of the hair strands cannot be visualised, so medulla and cortex cannot be seen, and are possibly not preserved along the strands, although they could be in those parts where the brown surface of the cuticle is present. An accurate description of the scale pattern was achieved based on the clearly marked scale margins appearing as impressions in the amber.

The scale pattern and proportions of the three hair strands are similar. Scales are wider than they are long and are in a transverse position in relation to the hair longitudinal axis (Figs. 2b–d, 3). Scale length varies between 5–7 µm. The surface scale pattern is wavy in all three strands, mostly regular in strand Y and slightly irregular in strands X and Z. Scale margins are smooth and close together. Following the terminology of Chernova[23], the

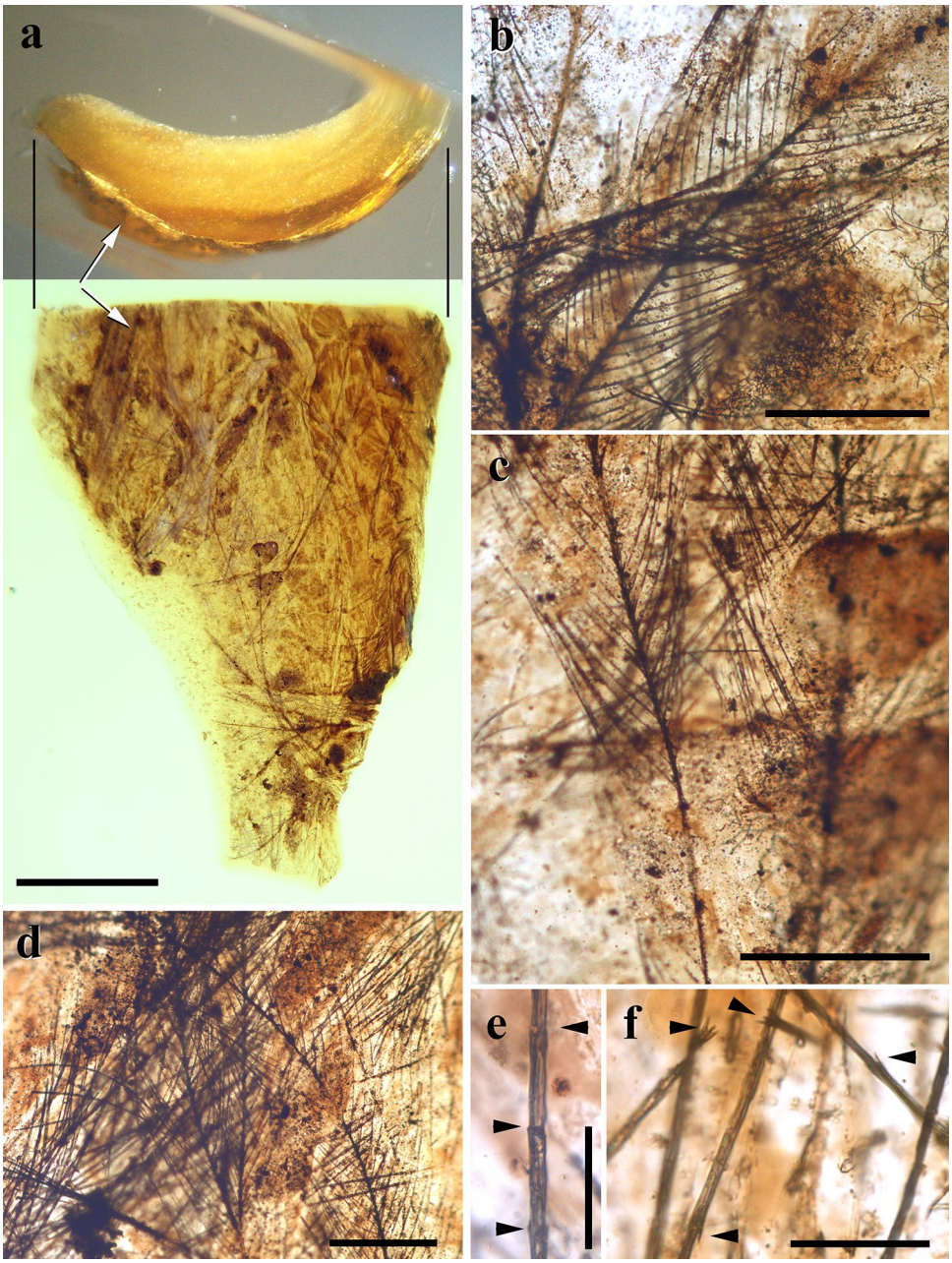

Figure 1. Avian dinosaur feather remains densely covering the convex surface of a flake fragment detached from a stalactite-shaped aerial amber piece (CPT-4200) found in the middle–earliest late Albian San Just outcrop (Utrillas, Teruel, Spain). (**a**) Two views of the stalactite-shaped aerial amber piece at the same scale showing the convex, external surface covered with feather remains (arrows: note that the surface is darkened, corresponding to a surface of desiccation). (**b–d**) Details of the dense, chaotic assemblage of feather remains (barbs) in the convex surface (note the left barb in (**c**) differentially preserved along its axis). (**e**, **f**) Details of some barbules showing the nodes of the pennulum (arrowheads in **e**), and spines in the internodes (arrowheads in **f**). Scale bars 1 mm (**a**), 0.2 mm (**b–d**), 0.05 mm (**e**, **f**). (**a–d**, **f**) are image compositions (Photoshop CS2, version 9.0; www.adobe.com).

cuticular pattern corresponds to a non-annular morphotype, adhering and tegular, with more than one scale embracing the shaft, to which they are strongly attached, and clearly imbricate.

Actualistic data. Mammalian hair was recorded in sticky traps located at different heights in the trunk of the angiosperms *Hymenaea verrucosa* Gaertner, 1791 and *Canarium madagascariense* Engler, 1883 in Madagascar (Figs. 4, 5). Isolated strands are found in several sticky traps, although even tufts are present in others. Mammalian hair corresponds to the 0.11% and 0.01% of the total remains adhered to sticky traps in *H. verrucosa* and

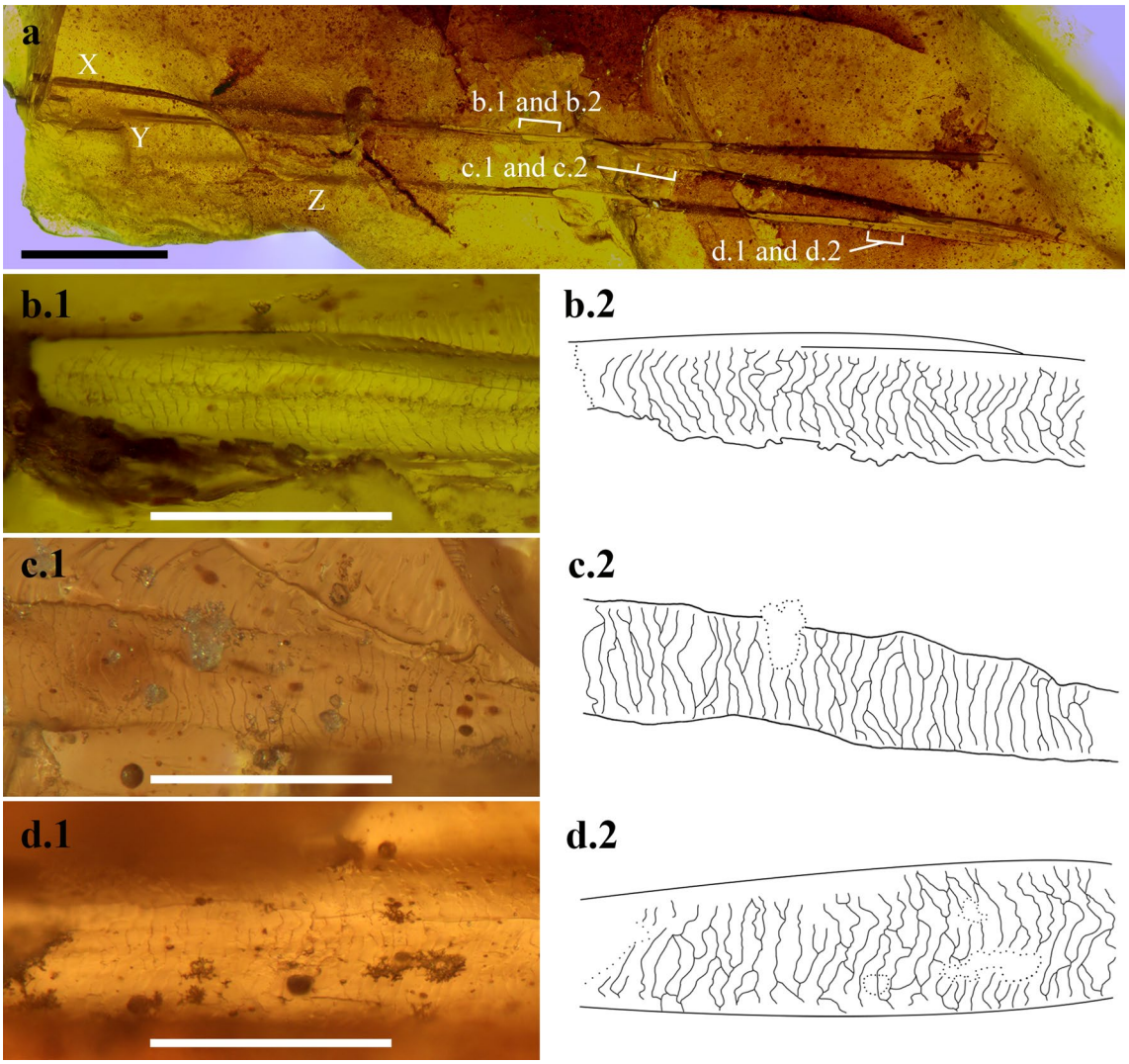

Figure 2. Hair strands aligned in the amber fragment AR-1-A-2019.88.1. (Ariño, Teruel, Spain), dated as early Albian. (**a**) Image composition of the general view of the three strands named X, Y and Z, indicating the locations of the following images and drawings. (**b–d**) Superficial scale patterns as cast prints in the amber, illustrated as micrographs and camera lucida drawings from X, Y and Z strands, respectively, all at the same scale. Scale bars 1 mm (**a**), 0.1 mm (**b–d**). Image composition and drawings prepared with Photoshop CS6, version 13.0 (www.adobe.com).

C. madagascariense, respectively. The strands were pulled off retaining the proximal and distal portions. Sticky traps located at 0 m high in the trees recorded hair strands and tufts of rodents that are most likely non-arboreal (Fig. 5e); several of these sticky traps were even gnawed (Fig. 5c,d). Hair, most likely from lemurs, is found in sticky traps at 2 m high in *C. madagascariense* (Figs. 4h, 5g). In contrast, feathers are not found adhered to the traps.

Discussion

Most isolated feathers found in Burmese amber have been determined as belonging to Enantiornithes based on the presence of skeletal remains with associated feathers of this group (e.g., 38), although this hypothesis is controversial due to the many feather morphotypes that are not associated with skeletal remains[7]. The San Just feather remains could be consistent with this taxonomic affinity, but the absence of enantiornithine skeletal records in Spanish amber precludes even a tentative determination. Filamentous elongated remains are often found in amber and they can be confused with hair strands. Fungal mycelia have been reported in ambers from different deposits, showing hyphae of 2–8 µm diameter (e.g.,[39,40]), as opposed to the Ariño strands which are around 70 µm in diameter. Undetermined plant fibres also appear in amber, but they are usually distinct from hair-like structures, as they can be very irregular in shape. The key characteristic of hair strands is their scale pattern[22,23], although Chernova[14] noticed a similarity between the microstructures of determined hairs and feathers as a result of morphological convergence. The Ariño strands clearly correspond to mammalian hair as their scale pattern is very similar to others from fossil (Mesozoic and Cenozoic) and extant hair specimens (Figs. 5e–g, 6).

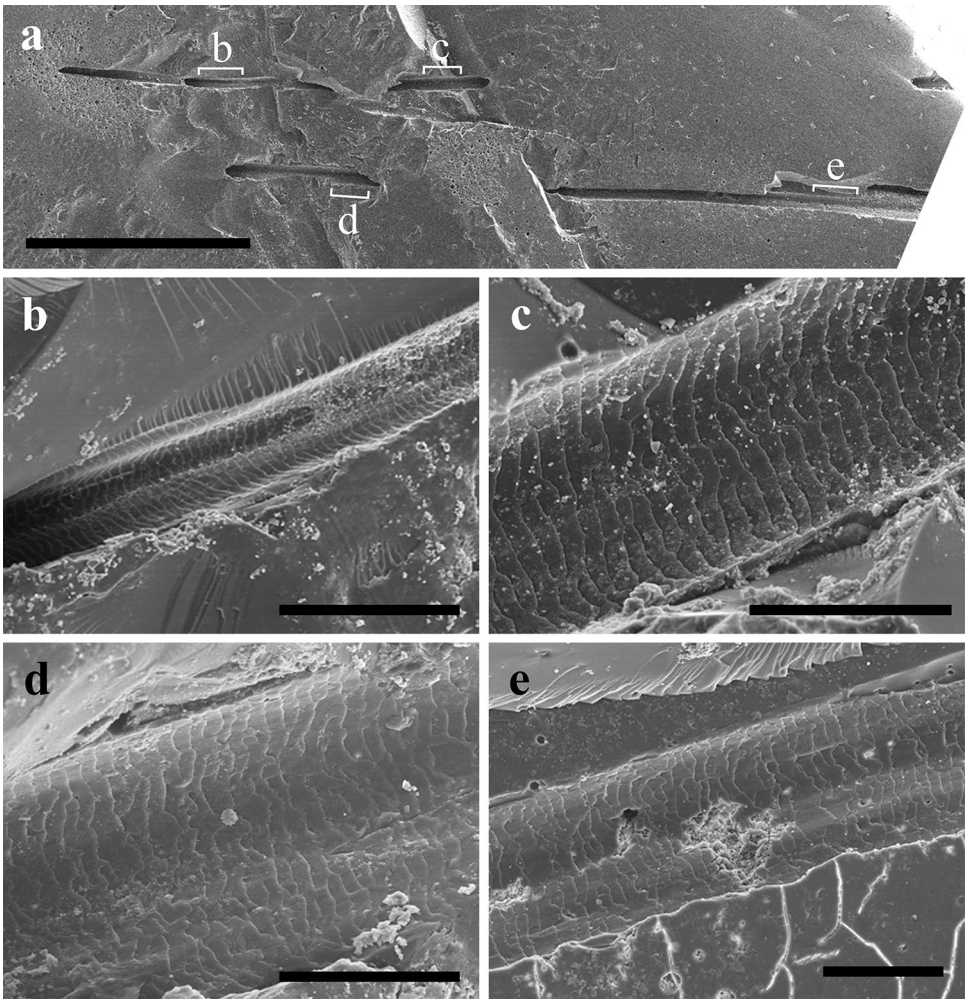

Figure 3. SEM images of the scale pattern of hair strands as cast prints in the amber fragment AR-1-A-2019.88.1 (Ariño, Teruel, Spain), dated as early Albian (see Fig. 2). (**a**) General view of the amber surface and the hair strands, indicating the locations of the following images. (**b**, **c**) Scale patterns of the hair strand X. (**d**, **e**) Scale patterns of the hair strand Z. Scale bars 1 mm (**a**), 0.1 mm (**b**), 0.05 mm (**c**–**e**).

Accurate determination of isolated hair in deep time is especially difficult, if not impossible. In the Early Cretaceous Spanish localities of the Galve area, near Ariño, mammalian remains belonging to Dryolestida, Multituberculata (Eobaataridae, Paulchoffatiidae, Pinheirodontidae, Plagiaulacidae/Eobaataridae), Symmetrodonta (Spalacotheriidae) and the Peramuridae family have been identified[41]; these taxa are extinct and information about their hair scale pattern is obscure. An exceptionally well-preserved specimen from the late Barremian Las Hoyas locality (Cuenca, Spain), identified as *Spinolestes xenarthrosus* Martin et al. 2015 (Eutriconodonta: Gobiconodontidae) has provided important information about the eutriconodont fauna, including integumentary structures, as this specimen has preserved the hair scale pattern[33]. Hair strands of *S. xenarthrosus* include two morphotypes of scale patterns, as the primary hairs show imbricate, ovate scales forming an irregular mosaic and the secondary hairs possess annular scales embracing the shaft with simple or serrated free margins (extended data Fig. 5 in[33]). The scale pattern of the Ariño hair strands does not correspond to the morphotypes of the Las Hoyas specimen, as more than one scale embraces the shaft and the pattern is wavy with smooth margins. Considering extant taxa, the scale pattern of mustelids (Carnivora: Mustelidae) is very similar to that of the Ariño hair strands, for example, *Martes martes* Linnaeus, 1758 (plate 72–80 in[22]) and the wavy pattern at the pars basalis of *Lutra lutra* Linnaeus, 1958 (Fig. 7 in[42]). Despite all the above knowledge, accurate determination of the hair strands from Ariño is not also possible, due to the poorly preserved scale pattern of fossil hair in Cretaceous mammalian specimens. The Ariño hair strands from the early Albian are the oldest mammalian record in amber and increase the previous known Cretaceous record of mammalian hair confined to late Albian–early Cenomanian ambers[16,27]. New descriptions of scale patterns of hair in Cretaceous amber, whose preservation capacity is exceptionally high, as seen in the Ariño hair strands, could shed further light on the evolution of this mammalian character through time.

Based on the matching scale pattern and proportions of the three hair strands, their proximity and alignment in the amber piece, we assume that they were a tuft. Although they are only three strands, their disposition and the lateral similarity in diameter and scale pattern support our inference that they are not randomly detached

Figure 4. Examples of non-natural "pull off vestiture" process in actuotaphonomic research in Madagascar using yellow sticky traps on trunks of the resiniferous tree species *Hymenaea verrucosa* (Fabaceae) and *Canarium madagascariense* (Burseraceae). (**a**) Three sticky trap lines at 0, 1 and 2 m height, respectively, in *H. verrucosa*, in Sacaramy area (Antsiranana), tree 2H2 (2R2), campaign 2015. (**b–d**) Sticky traps with abundant trapped hair, in *H. verrucosa* tree 2, at 1 m, 2 m and 0 m heights, respectively, in Ambahy community (Nosy Varika, Mananjary region), campaign 2013 (see arrowheads in **c** indicating tufts and inset in **d** showing the tuft enlarged). (**e**) Detail of tuft and small portion of lizard skin in sticky trap of *H. verrucosa* tree 1 at 1 m height, Ambahy community, campaign 2013. (**f**) *H. verrucosa* tree 2H1 (2R1) at 2 m height, Sacaramy area, campaign 2015. (**g**) *H. verrucosa* tree 3R5 (3H4) at 1 m height, Analamandrofo forest in Andranotsara, at 40 km south of Sambava city, campaign 2017. (**h**) Hair (arrowheads), most likely of the abundant lemurs in the canopy of the research area, sticky trap in *C. madagascariense* tree 3 at 2 m height, Ranomafana National Park, campaign 2013. (**i**) Sticky trap with abundant lizard skin (geckos) from *H. verrucosa* tree 2 at 0 m height, Ambahy community, campaign 2013. Sticky traps measure ca. 20×7.5 cm. Scale bars 1 cm (**e–h**).

strands. This is a unique record in the Cretaceous, as other hair strands in amber (France and Myanmar) appear as isolated specimens[16,27]. The two hair strands in French amber are in the same piece, separated by only 1 mm, but they cannot be confirmed as a tuft because of their poor preservation[16]. Therefore, the Ariño hair strands show more similarities with the record of tufts in the Eocene Baltic amber (e.g.,[28,29]) (Fig. 6).

Both amber pieces presented in this study correspond to resin flows exposed to aerial conditions for a time, based on their morphology and the presence of surfaces of desiccation. Despite the small size of the amber piece CPT-4200 (showing feather remains), the manner in which the barbs cover the whole surface of desiccation, as preserved, indicates that this record was not the consequence of contact between a detached feather, or feathers, and the sticky resin emission. This record can best be explained thus: an avian dinosaur made contact with the

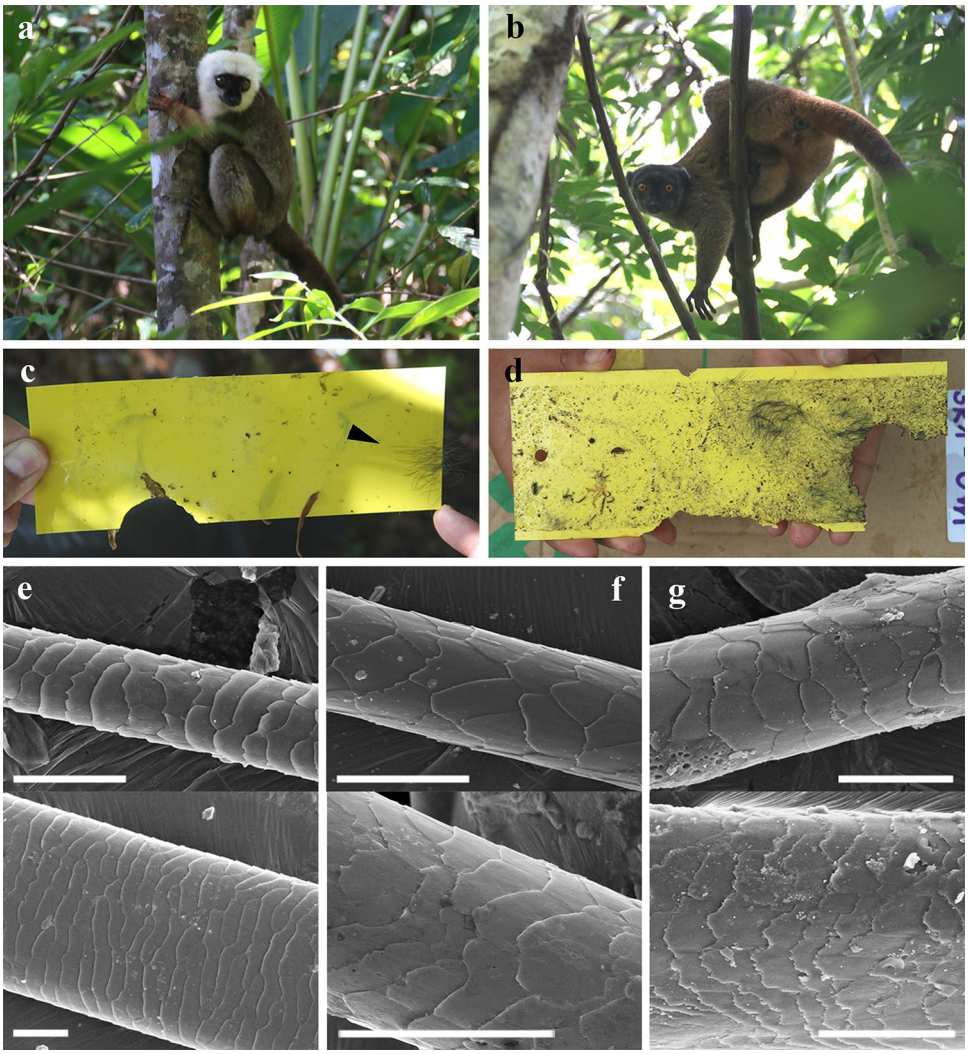

Figure 5. Images from actualistic data obtained in Malagasy forests. (**a**, **b**) Two lemur species in the tree canopy in the Ranomafana National Park. (**c**, **d**) Sticky traps with adhered hair tufts (indicated with an arrowhead in **c**) and gnaw marks, from *Hymenaea verrucosa* tree 1 at 2 m height, in Ambahy community (Nosy Varika, Mananjary region), campaign 2013, and *H. verrucosa* tree 3R1 at 0 m height, in Analamandrofo forest in Andranotsara, at 40 km south of Sambava city, campaign 2017, respectively. (**e**–**g**) SEM images of hair strands from *H. verrucosa* tree 2 at 0 m height, most likely of a rodent, in Ambahy community, campaign 2013 (sticky trap from Fig. 4d), *H. verrucosa* tree 1 at 1 m height, Ambahy community, campaign 2013 (sticky trap from Fig. 4e), and *Canarium madagascariense* tree 3 at 2 m height, most likely of a lemur, Ranomafana National Park, campaign 2013 (sticky trap from Fig. 4h), respectively. Sticky traps measure ca. 20 × 7.5 cm. Scale bars 0.02 mm (**e**), 0.04 mm (**f**), 0.03 mm (**g**).

resin emission, resting there for the necessary amount of time, for example during sleep, for the more external barbs of its vestiture to become firmly fixed in the hardened resin. Later, with the movement of the animal, the fixed barbs detached. However, it can be observed that some portions of the barbs were apparently better fixed than others as there is differential preservation along the barbs (Fig. 1c). Regarding the amber fragment AR-1-A-2019.88.1 (showing the hair tuft), the hair strands could have become embedded slowly while the mammal in question was resting or sleeping near the resin source, in similar fashion to the feathers in piece CPT-4200.

The two amber records described herein are very peculiar and their origins are far from the common process for generation of bioinclusions in resins that are preserved as amber or copal. Typically, a bioinclusion originates when an animal or a detached organismal remnant makes contact with fresh, sticky resin and is thus trapped and then embedded. Here, we present the "pull off vestiture" biostratinomic process unique to resins, which we define as follows: "the entrapment of external portions of vertebrate vestiture, more specifically small portions of plumage and pelage, of living individuals that had rested for a time in contact with a fresh, sticky resin emission that hardened and retained those vestiture portions". Note that this process does not imply the death of the animal. The process requires a type of resin that can harden very quickly after being exuded. Such a feature has been observed in extant resins from *Agathis australis* (D. Don) Loudon, 1829 (gymnosperm) in New Zealand

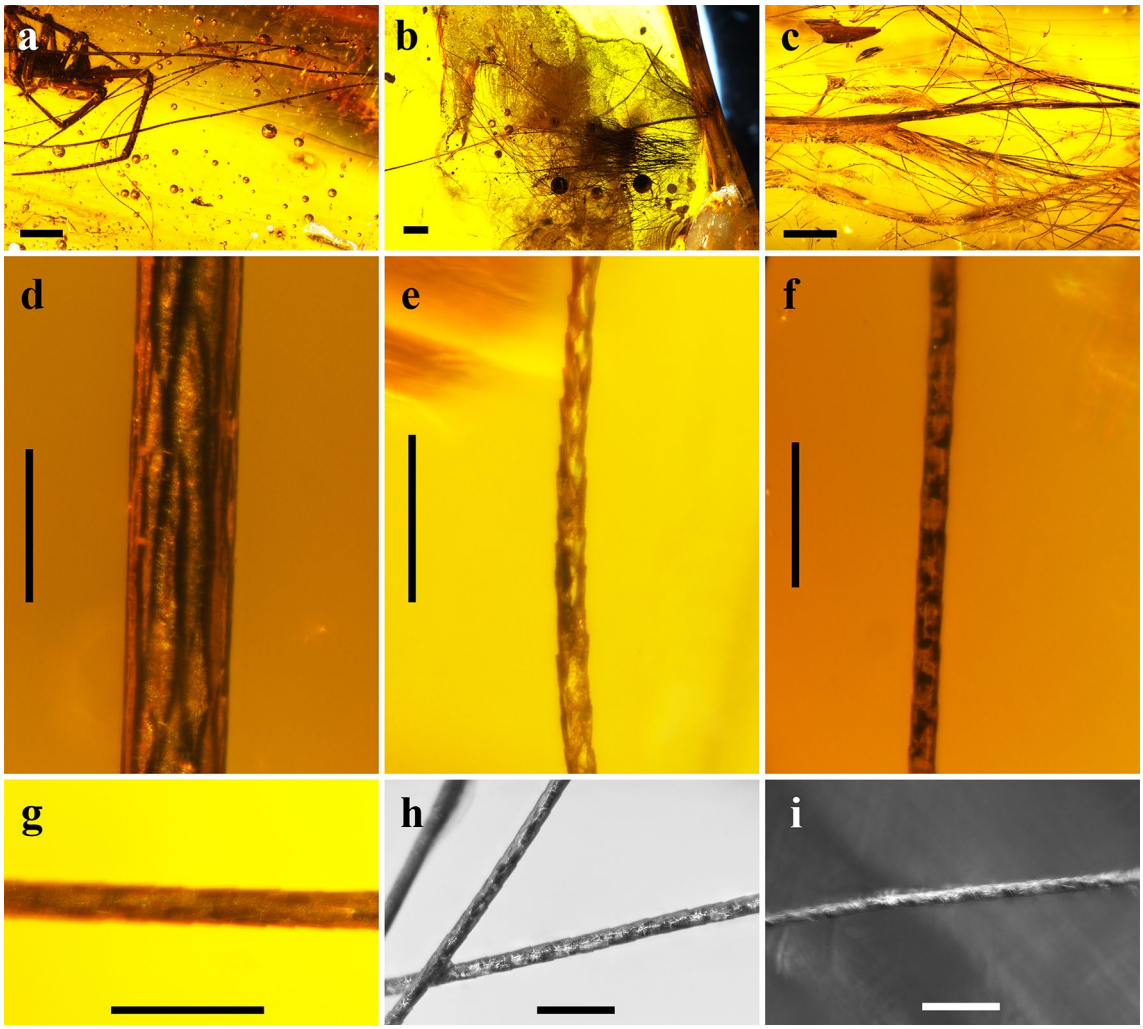

Figure 6. Mammalian hair in Eocene Baltic amber. (**a–c**) Tufts in pieces SMF-Be-5160 (showing a spider as syninclusion), SMF-Be-8362 and SMF-Be-365, respectively. (**d–i**) Details of hair strands in pieces SMF-Be-5160, SMF-Be-365, SMF-Be-8362, SMF-Be-5160, SMF-Be-365 and SMF-Be-5161, respectively. Scale bars 1 mm (**a–c**), 0.1 mm (**d–i**).

and *Hymenaea verrucosa* in Madagascar, but not under all conditions (own observations). Furthermore, actualistic observations using sticky traps in *H. verrucosa* and *Canarium madagascariense* in Madagascar support this hypothesis (Figs. 4, 5). These records are similar to those of the natural "pull off vestiture" process of resins, although the trapping capacity of the sticky traps is much higher. Hair would be trapped immediately in the sticky traps with minimal contact, whereas the "pull off vestiture" process involving resin requires contact to be sustained for the time it takes for the resin to harden. Squamate reptile scaly skin was also recorded on the sticky traps (Fig. 4i), as has been found in Cretaceous amber from France, Lebanon and Myanmar[43–46], but these kinds of record would be recorded differently as they could be explained by detached portions of lizard moults which do not require high stickiness.

The "pull off vestiture" biostratinomic process described herein is unique to resins and clarifies some intriguing findings in Cretaceous and Cenozoic ambers. Other semi-fluid preservative materials, like asphalt (highly viscous liquid or a semi-solid form of petroleum) or tar seeps, do not pull off vertebrate vestiture while allowing the survival of the individual[47]. Paired ornamental feathers of enantiornithine tails in the manner of their distal parts in relative live position (each pair) from the Burmese amber record have been reported[48,49]. Xing et al.[48] commented that the paired feathers, which they found abundantly, could easily be removed, maybe as a sacrificial gesture in defensive behaviour. The record of these abundant findings could be related to the "pull off vestiture" process, as are other enantiornithine feather records in amber (e.g.,[7]). The tail feathers could become stuck in the resin while the individual was resting or sleeping close to the resin source in the tree, and after a time, when the resin was hardened and the individual left, the feathers were removed, similar to the biostratinomic process of the San Just and Ariño records in this work (Fig. 7). The tufts found in Eocene Baltic amber only preserve the distal parts of the strands[29] and are coincident with the "pull off vestiture" process (Fig. 7). The basal parts of the hairs (including the follicles) are not preserved in the amber pieces because typically only the distal parts contacted and became embedded in the resin emissions to undergo the "pull off vestiture" process. Records of mammalian hair strands in Miocene Dominican amber correspond to isolated strands with different orientations,

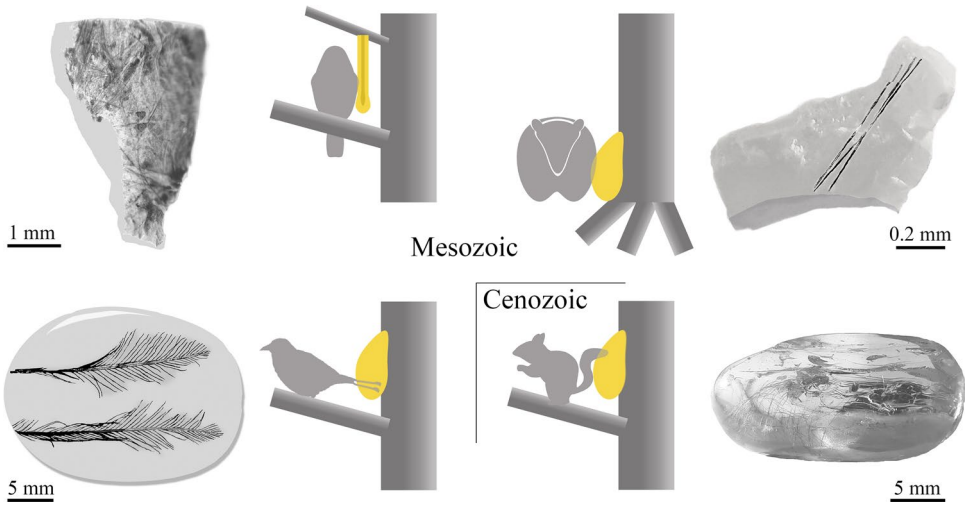

Figure 7. Schema of the two examples studied and another two from the literature of the "pull off vestiture" process as interpreted. From upper left to lower right: Spanish pieces CPT-4200, containing feather remains and AR-1-A-2019.88.1 containing hair tuft of an indeterminate mammal, Burmese piece DIP-V-17194 (modified from[48]) containing a pair of feathers from tail plumage, most likely with ornamental function, and Baltic piece SMF-Be-2009 containing mammalian hair. Illustration created using Adobe Photoshop CS2, version 9.0 (www.adobe.com).

not forming tufts, and even retaining basal parts (e.g.,[18,50]), so they could have been blown by the wind or shed randomly by the mammalian individual and do not correspond to a "pull off vestiture" process. The rich record of mammalian tufts in Baltic amber could be related to the presence of arboreal mammals such as sciuromorph rodents[51], although Sidorchuk et al.[29] proposed the floor-dwellers, erinaceomorph amphilemurids. The extreme scarcity of hair in Cretaceous amber suggests that the arboreal mammals did not inhabit the resiniferous forests during this period, although an arboreal lifestyle has been suggested for gliding Mesozoic mammals from compression sites (e.g.,[32,52]). The new biostratinomic approach described herein can explain records of vertebrates in amber and provide new inferences of palaeoecological information about the ancient resiniferous forests.

Material and methods

The San Just outcrop is located near Utrillas (Teruel, Spain) and corresponds geologically to the Middle or Upper Member of the Escucha Formation[53,54]. It has been dated as middle–earliest late Albian based on palynological data, and related to a swamp plain environment[55]. It is the type-locality of 23 species and its diverse record of bioinclusions contains coprolites, fungi, plants, arachnids, 12 insect orders and dinosaur feathers[53,54]. More data about the amber piece CPT-4200 are available in the Supplementary information.

The Ariño amber outcrop is in the Santa María opencast mine near Ariño (Teruel, Spain), which has provided a diverse fossil record from the bonebed layer AR-1, including coprolites, algae, plants, molluscs, ostracods, fish, turtles, crocodiles and dinosaurs[56], and is the type-locality of nine new taxa to date. This layer, belonging to the Middle Member of the Escucha Formation, has been dated as early Albian based on the charophyte assemblage[57] and related to a freshwater swamp plain in a deltaic-estuarine system with salinity variations due to marine inputs under subtropical-tropical climate conditions[58]. The amber piece AR-1-A-2019.88 with the mammalian hair studied herein was found in AR-1, composed of marls within an alternation of marl and limestone levels with alkaline oligotrophic origin, pond or shallow lake, and was unearthed from the layer in separate fragments; a description of the piece is available in the Supplementary information (Fig. S1).

The San Just piece CPT-4200 was photographed with a digital camera Olympus Camedia MODEL N.C5050 ZOOM attached to an Olympus SZX9 stereomicroscope, and the detailed micrographs of the barbules, using a ColorView IIIu Soft Imaging System attached to an Olympus BX51 compound microscope; the frontal view of the feather remains (Fig. 1a) was taken using a digital camera Canon EOS 650D and z-stacked automatically by the software Macrofotografía version 1.1.0.5 (www.macrorail.com). A compound microscope Olympus CX41 equipped with an attached camera lucida tube and a digital camera sCMEX-20 was used to make the drawings and the micrographs of the mammalian hair strands and other syninclusions in piece AR-1-A-2019.88; these micrographs were processed with ImageFocusAlpha version 1.3.7.12967.20180920 (www.euromex.com). SEM images of the fossil and extant hair strands with gold sputtering were obtained with a Hitachi S4800 Electronic Microscope at the Microscopy Services (SCSIE) of the University of Valencia (Spain). Figures were prepared with Photoshop CS2 version 9.0 (www.adobe.com) and Photoshop CS6 version 13.0 (www.adobe.com). The description of the scale pattern of the hair strands follows the nomenclature of Teerink[22] and Chernova[23].

Regarding the Baltic amber pieces (Fig. 6), they are housed at the Senckenberg Research Institute and Natural History Museum (SMF) in Frankfurt (Germany). The colour photographs and Z-stacks images were performed under a Nikon SMZ25 microscope, using Nikon SHR Plan Apo 0.5x and SHR Plan Apo 2x objectives with a microscope camera Nikon DS-Ri2 and the NIS-Element software version 4.51.00 (www.microscope.healthcare

.nikon.com). Infrared reflected photomicrographs (black and white) were taken with a Nikon Eclipse ME600D. All these methods were undertaken at the SMF.

The actualistic data were obtained in Madagascar with sticky traps following the methodology of Solórzano Kraemer et al.[3]. The sticky traps were located around 12 trees of the species *Hymenaea verrucosa* (Fabaceae) and four trees of the species *Canarium madagascariense* (Burseraceae) at 0, 1 and 2 m high during eight days in Sacaramy area (Antsiranana), Ambahy community (Nosy Varika, Mananjary region), Analamandrofo forest, in Andranotsara at 40 km south of Sambava city and Ranomafana National Park, during the 2013, 2015 and 2017 campaigns[59] and were photographed with a Canon EOS 40D digital camera. *Hymenaea* is a genus of resiniferous tree that originated amber deposits in several places such as Mexico and Dominican Republic. Nowadays, representatives of this genus are found in Madagascar, where an actuotaphonomic work was addressed to study how the resin traps biological remains using sticky traps. The resiniferous genus *Canarium* occurs in Malagasy forests with dissimilar environmental conditions, thus allowing the comparison of resin trapping in different ecosystems.

Data availability

All data that support this study are available in the main text or in the Supplementary information. Institutions that host the Spanish amber pieces are indicated in the Supplementary information. Actualistic data from sticky traps are available at the SMF in Frankfurt (Germany).

Received: 28 July 2020; Accepted: 3 November 2020
Published online: 16 November 2020

References

1. Labandeira, C. C. Amber. In *Reading and Writing of the Fossil Record: Preservational Pathways to Exceptional Fossilization* (eds. Laflamme, M., Schiffbauer, J. D. & Darroch, S. A. F.) 163–217 (The Paleontological Society Papers, Boulder, 20, 2014).
2. Martínez-Delclòs, X., Briggs, D. E. G. & Peñalver, E. Taphonomy of insects in carbonates and amber. *Palaeogeogr. Palaeoclimatol. Palaeoecol.* **203,** 19–64 (2004).
3. Solórzano Kraemer, M. M. *et al*. Arthropods in modern resins reveal if amber accurately recorded forest arthropod communities. *Proc. Natl. Acad. Sci. USA* **115,** 6739–6744 (2018).
4. Xing, L., Stanley, E. L., Bai, M. & Blackburn, D. C. The earliest direct evidence of frogs in wet tropical forests from Cretaceous Burmese amber. *Sci. Rep.* **8**, 8770 (2018).
5. Daza, J. D., Stanley, E. L., Wagner, P., Bauer, A. M. & Grimaldi, D. A. Mid-Cretaceous amber fossils illuminate the past diversity of tropical lizards. *Sci. Adv.* **2**, e1501080 (2016).
6. McKellar, R. C., Chatterton, B. D. E., Wolfe, A. P. & Currie, P. J. A diverse assemblage of Late Cretaceous dinosaur and bird feathers from Canadian amber. *Science* **333**, 1619–1622 (2011).
7. Xing, L., Cockx, P. & McKellar, R. C. Disassociated feathers in Burmese amber shed new light on mid-Cretaceous dinosaurs and avifauna. *Gondwana Res.* **82**, 241–253 (2020).
8. Chuong, C. -M. & Homberger, D. G. Development and evolution of the amniote integument: current landscape and future horizon. *J. Exp. Zool. (Mol. Dev. Evol.)* **298B,** 1–11 (2003).
9. Perrichot, V., Marion, L., Néraudeau, D., Vullo, R. & Tafforeau, P. The early evolution of feathers: fossil evidence from Cretaceous amber of France. *Proc. R. Soc. B Biol. Sci.* **275**, 1197–1202 (2008).
10. McCoy, V. E. *et al.* Ancient amino acids from fossil feathers in amber. *Sci. Rep.* **9**, 6420 (2019).
11. Yang, Z. *et al.* Pterosaur integumentary structures with complex feather-like branching. *Nat. Ecol. Evol.* **3**, 24–30 (2019).
12. Sawyer, R. H. & Knapp, L. W. Avian skin development and the evolutionary origin of feathers. *J. Exp. Zool. (Mol. Dev. Evol.)* **298B,** 57–72 (2003).
13. Benton, M. J., Dhouailly, D., Jiang, B. & McNamara, M. The early origin of feathers. *Trends Ecol. Evol.* **34**, 856–869 (2019).
14. Chernova, O. F. One more example of morphological convergence: Similarity between the architectonics of feather and hair. *Dokl. Biol. Sci.* **405**, 446–450 (2005).
15. Zherikhin, V. V. & Sukatsheva, I. D. On the Cretaceous insectiferous "ambers" (retinits) in the North Siberia. In *Problems of the Insect Palaeontology. Lectures on the 24th Annual Readings in Memory of NA Kholodkovsky* (ed. Narchuk, E. P.) 3–48 (Nauka, Leningrad, 1973) (in Russian).
16. Vullo, R., Girard, V., Azar, D. & Néraudeau, D. Mammalian hairs in Early Cretaceous amber. *Naturwissenschaften* **97**, 683–687 (2010).
17. MacPhee, R. D. E. & Grimaldi, D. A. Mammal bones in Dominican amber. *Nature* **380**, 489–490 (1996).
18. Peñalver, E. & Grimaldi, D. Assemblages of mammalian hair and blood-feeding midges (Insecta: Diptera: Psychodidae: Phlebotominae) in Miocene amber. *Trans. R. Soc. Edinb. Earth Sci.* **96**, 177–195 (2006).
19. Ji, Q., Luo, Z.-X., Yuan, C.-X. & Tabrum, A. R. A swimming mammaliaform from the Middle Jurassic and ecomorphological diversification of early mammals. *Science* **311**, 1123–1127 (2006).
20. Eliason, C. M., Hudson, L., Watts, T., Garza, H. & Clarke, J. A. Exceptional preservation and the fossil record of tetrapod integument. *Proc. R. Soc. B Biol. Sci.* **284**, 20170556 (2017).
21. Chapman, R. E. Hair, wool, quill, nail, claw, hoof, and horn. In *Biology of the Integument Vertebrates*, Vol. 2 (eds. Bereiter-Hahn J., Gedeon Matoltsy, A. & Sylvia Richards, K.) 293–317 (Springer, Berlin, 1986).
22. Teerink, B. J. (ed.) *Hair of West-European Mammals: Atlas and Identification Key* (Cambridge University Press, Over Wallop, 1991).
23. Chernova, O. F. Architectonic and diagnostic significance of hair cuticle. *Biol. Bull.* **29**, 238–247 (2002).
24. Noback, C. R. Morphology and phylogeny of hair. *Ann. N. Y. Acad. Sci.* **53**, 476–492 (1951).
25. Rogers, G. E. *et al.* (eds) *The Biology of Wool and Hair* (Chapman and Hall Ltd., London, 1989).
26. Kassenbeck, P. Morphology and fine structure of hair. In *Hair Research* (eds. Orfanos, C. E., Montagna, W. & Stüttgen, G.) 52–64 (Springer, Berlin, 1981).
27. Poinar, G. & Poinar, R. (eds) *What Bugged the Dinosaurs? Insects, Disease, and Death in the Cretaceous* (Princeton University Press, Princeton and Oxford, 2008).
28. Weitschat, W. & Wichard, W. (eds) *Atlas of Plants and Animals in Baltic Amber* (Verlag Dr. Friedrich Pfeil, Munich, 2002).
29. Sidorchuk, E. A., Bochkov, A. V., Weiterschan, T. & Chernova, O. F. A case of mite-on-mammal ectoparasitism from Eocene Baltic amber (Acari: Prostigmata: Myobiidae and Mammalia: Erinaceomorpha). *J. Syst. Palaeontol.* **17**, 331–347 (2019).
30. Schweitzer, M. H. Soft tissue preservation in terrestrial Mesozoic vertebrates. *Annu. Rev. Earth Pl. Sc.* **39**, 187–216 (2011).
31. Saitta, E. T. *et al.* Low fossilization potential of keratin protein revealed by experimental taphonomy. *Palaeontology* **60**, 547–556 (2017).
32. Meng, Q.-J. *et al.* New gliding mammaliaforms from the Jurassic. *Nature* **548**, 291–296 (2017).

33. Martin, T. *et al.* A Cretaceous eutriconodont and integument evolution in early mammals. *Nature* **526**, 380–384 (2015).
34. Perrichot, V. Early Cretaceous amber from south-western France: insight into the Mesozoic litter fauna. *Geol. Acta* **2**, 9–22 (2004).
35. McCoy, V. E., Soriano, C. & Gabbott, S. E. A review of preservational variation of fossil inclusions in amber of different chemical groups. *Earth Environ. Sci. Trans. R. Soc. Edinb.* **107,** 203–211 (2018).
36. McCoy, V. E. *et al.* Unlocking preservation bias in the amber insect fossil record through experimental decay. *PLoS ONE* **13**, e0195482. https://doi.org/10.1371/journal.pone.0195482 (2018).
37. Solórzano Kraemer, M. M., Kraemer, A. S., Stebner, F., Bickel, D. J. & Rust, J. Entrapment bias of arthropods in Miocene amber revealed by trapping experiments in a tropical forest in Chiapas Mexico. *PLoS ONE* **10**, e0118820. https://doi.org/10.1371/journal.pone.0118820 (2015).
38. Xing, L. *et al.* A fully feathered enantiornithine foot and wing fragment preserved in mid-Cretaceous Burmese amber. *Sci. Rep.* **9**, 927 (2019).
39. Rikkinen, J. & Poinar, G. O. Jr. Fossilised fungal mycelium from Tertiary Dominican amber. *Mycol. Res.* **105**, 890–896 (2001).
40. Speranza, M., Ascaso, C., Delclòs, X. & Peñalver, E. Cretaceous mycelia preserving fungal polysaccharides: taphonomic and paleoecological potential of microorganisms preserved in fossil resins. *Geol. Acta* **13**, 363–385 (2015).
41. Badiola, A., Canudo, J. I. & Cuenca-Bescós, G. A systematic reassessment of Early Cretaceous multituberculates from Galve (Teruel, Spain). *Cretaceous Res.* **32**, 45–57 (2011).
42. Kuhn, R. A. & Meyer, W. Comparative hair structure in the Lutrinae (Carnivora: Mustelidae). *Mammalia* **74**, 291–303 (2010).
43. Grimaldi, D. A., Engel, M. S. & Nascimbene, P. C. Fossiliferous Cretaceous amber from Myanmar (Burma): its rediscovery, biotic diversity, and paleontological significance. *Am. Mus. Novit.* **3361**, 1–71 (2002).
44. Arnold, E. N., Azar, D., Ineich, I. & Nel, A. The oldest reptile in amber: a 120 million year old lizard from Lebanon. *J. Zool.* **258**, 7–10 (2002).
45. Perrichot, V. & Néraudeau, D. Reptile skin remains in the Cretaceous amber of France. *C. R. Palevol* **4**, 47–51 (2005).
46. Azar, D. Preservation and accumulation of biological inclusions in Lebanese amber and their significance. *C. R. Palevol* **6**, 151–156 (2007).
47. Spencer, L. M., Van Valkenburgh, B. & Harris, J. M. Taphonomic analysis of large mammals recovered from the Pleistocene Rancho La Brea tar seeps. *Paleobiology* **29**, 561–575 (2003).
48. Xing, L., Cockx, P., McKellar, R. C. & O´Connor, J. Ornamental feathers in Cretaceous Burmese amber: resolving the enigma of rachis-dominated feather structure. *J. Palaeogeog.* **7,** 13 (2018).
49. Carroll, N. R., Chiappe, L. M. & Bottjer, D. J. Mid-Cretaceous amber inclusions reveal morphogenesis of extinct rachis-dominated feathers. *Sci. Rep.* **9**, 18108 (2019).
50. Lewis, R. E. & Grimaldi, D. A pulicid flea in Miocene amber from the Dominican Republic (Insecta, Siphonaptera, Pulicidae). *Am. Mus. Novit.* **3205**, 1–9 (1997).
51. Voigt, E. Ein Haareinschluss mit Phthirapteren-Eiern im Bernstein. *Mitt. Geol. Staatsinst. Hamburg* **21**, 59–74 (1952).
52. Han, G., Mao, F., Bi, S., Wang, Y. & Meng, J. A Jurassic gliding euharamiyidan mammal with an ear of five auditory bones. *Nature* **551**, 451–456 (2017).
53. Peñalver, E., Delclòs, X. & Soriano, C. A new rich amber outcrop with palaeobiological inclusions in the Lower Cretaceous of Spain. *Cretaceous Res.* **28**, 791–802 (2007).
54. Peñalver, E. & Delclòs, X. Spanish amber. In *Biodiversity of Fossils in Amber from the Major World Deposits* (ed. Penney, D.) 236–270 (Siri Scientific Press, Manchester, 2010).
55. Villanueva-Amadoz, U., Pons, D., Diez, J. B., Ferrer, J. & Sender, L. M. Angiosperm pollen grains of San Just site (Escucha Formation) from the Albian of the Iberian Range (north-eastern Spain). *Rev. Palaeobot. Palyno.* **162**, 362–381 (2010).
56. Alcalá, L. *et al.* A new Lower Cretaceous vertebrate bonebed near Ariño (Teruel, Aragón, Spain); found and managed in a joint collaboration between a mining company and a palaeontological park. *Geoheritage* **4**, 275–286 (2012).
57. Tibert, N. E., Colin, J.-P., Kirkland, J. I., Alcalá, L. & Martín-Closas, C. Lower Cretaceous nonmarine ostracodes from an Escucha Formation dinosaur bonebed in eastern Spain. *Micropaleontology* **59**, 83–91 (2013).
58. Villanueva-Amadoz, U. *et al.* Paleoenvironmental reconstruction of an Albian plant community from the Ariño bonebed layer (Iberian Chain, NE Spain). *Hist. Biol.* **27**, 430–441 (2015).
59. Delclòs, X., Peñalver, E., Ranaivosoa, V. & Solórzano-Kraemer, M. M. Unravelling the mystery of "Madagascar copal': age, origin and preservation of a recent resin. *PLoS ONE* **15**, e0232623. https://doi.org/10.1371/journal.pone.0232623 (2020).
60. Nascimbene, P. & Silverstein, H. The preparation of fragile Cretaceous ambers for conservation and study of organismal inclusions. In *Studies on Fossils in Amber, with Particular Reference to the Cretaceous of New Jersey* (ed. Grimaldi, D.) 93–102 (Backhuys Publishers, Leiden, 2000).
61. Lozano, R. P. *et al.* Phloem sap in Cretaceous ambers as abundant double emulsions preserving organic and inorganic residues. *Sci. Rep.* **10**, 9751 (2020).
62. Bell, W. J. *et al.* (eds) *Cockroaches: Ecology, Behavior, and Natural History* (The Johns Hopkins University Press, Baltimore, 2007).

Acknowledgements

We thank the SAMCA Group, which has been extracting coal in Ariño since 1919, for allowing us to enter into the opencast mine and to obtain the amber. We also thank the General Directorate of Cultural Heritage of the Government of Aragon (Spain) for the permission to excavate in the San Just (code of permission 171/2007 of the Government of Aragon) and Ariño (code of permission 201/10-2019 of the Government of Aragon) localities. The Ministry of Environment, Ecology and Forests (Madagascar) gave us the permissions to work in the Malagasy protected areas (192/13/MEF/SG/DGF/DCB.SAP/SCB, 060/15/MEEF/SG/DGF/DCB.SAP/SCB and 192/17/MEEF/SG/DGF/DSAP/SCB.Re). The authors wish to acknowledge the team of the Malagasy Institute for the Conservation of Tropical Environments (ICTE/MICET) for their assistance with aspects of the administrative development of our work in Madagascar. We thank the Malagasy Centre ValBio in Ranomafana National Park and Ambahy Community for their support. We are grateful to Eduardo Espílez and Luis Mampel for field logistics in Ariño and to Rafael López del Valle for the preparation of the Spanish amber pieces. We are indebted to Enrique Navarro Raga and Plini Montoya for their support with the SEM imaging at the Microscopy Services (SCSIE) of the University of Valencia (Spain) and to Robin Kunz (SMF, Frankfurt, Germany) for support with some of the amber pictures. We thank the editors, Michael J. Benton and other anonymous reviewer for their helpful comments that have improved the original manuscript. For their financial support, we thank the Department of Education, Culture and Sport of the Government of Aragon, Research Group E04_20R FOCONTUR (financed by the Department of Science, University and Society of Knowledge of the Government of Aragon and FEDER funds ´Construyendo Europa desde Aragón´), Instituto Aragonés de Fomento (Spain) and Dinópolis (Spain). We thank the Spanish Ministry of Economy, Industry and Competitiveness (Project CGL2014-52163), the Spanish Government (Project AEI/FEDER, UE CGL2017-84419), the National Geographic Global Exploration Fund

Northern Europe (Project GEFNE 127-14) and the German Volkswagen Foundation (Project N. 90946) for financial support in Madagascar. This study is a contribution to the Spanish Ministry of Science, Innovation and Universities (Spain, AEI/FEDER, UE) Project CRE CGL2017-84419 and Project PGC2018-094034-B-C22. This study forms part of the first author's (S.Á.-P.) doctoral thesis, supported by a grant from the Secretary of Universities and Research of the Government of Catalonia (Spain) and the European Social Fund (2019FI_B00330).

Author contributions

S.Á.-P., X.D. and E.P. designed the project. All authors conducted the field work. S.Á.-P., X.D., M.M.S.-K. and E.P. studied the amber assemblages. S.Á.-P., X.D., M.M.S.-K. and E.P. did the imaging. S.Á.-P. and E.P. did the illustrations. All the authors analysed the data and contributed to the discussion. S.Á.-P. and E.P. wrote the manuscript with input from the rest of the authors.

Competing interests

The authors declare no competing interests.

Additional information

Supplementary information is available for this paper at https://doi.org/10.1038/s41598-020-76830-8.

Correspondence and requests for materials should be addressed to S.Á.-P.

Reprints and permissions information is available at www.nature.com/reprints.

Publisher's note Springer Nature remains neutral with regard to jurisdictional claims in published maps and institutional affiliations.

Supplementary information

Cretaceous amniote integuments recorded through a taphonomic process unique to resins

Sergio Álvarez-Parra*, Xavier Delclòs, Mónica M. Solórzano-Kraemer, Luis Alcalá & Enrique Peñalver

*sergio.alvarez-parra@ub.edu

Supplementary material and methods

Amber piece CPT-4200

The small amber flake is embedded in a prism of epoxy resin important for the preservation of amber pieces with bioinclusions (*60*). It was found during an excavation in the San Just amber-bearing outcrop near Utrillas (Teruel, Spain) in 2007. It is housed at the Museo Aragonés de Paleontología (Fundación Conjunto Paleontológico de Teruel-Dinópolis, Teruel) with the accession number CPT-4200. Its primary field number was SJ-07-147.

Amber piece AR-1-A-2019.88

The piece was found during an excavation in the Santa María opencast mine near Ariño (Teruel) in 2019 and is housed at the Museo Aragonés de Paleontología (Fundación Conjunto Paleontológico de Teruel-Dinópolis, Teruel). It is made up of seven fragments (AR-1-A-2019.88.1 to 88.7). Three strands of mammalian hair are in one of these fragments (AR-1-A-2019.88.1) and the other two bioinclusions (syninclusions) are in two different fragments, one being a partial undetermined insect antenna (AR-1-A-2019.88.2) and the other an undetermined arthropod (AR-1-A-2019.88.3) (Fig. S1a). Four of these fragments are less than 1 mm long and do not include visible fossil remains. The fossiliferous fragments AR-1-A-2019.88.1 and AR-1-A-2019.88.2 are around 1 mm long, and AR-1-A-2019.88.3 is 1.45 mm long. None are embedded in epoxy resin. The amber is brownish-yellow with abundant dark microscopic inclusions corresponding to double emulsions of phloem sap typically present in Cretaceous ambers (*61*), so these characteristics give a slightly opaque aspect to the fragments, mostly in the case of AR-1-A-2019.88.3.

Fragment AR-1-A-2019.88.2 includes a partial insect antenna (Fig. S1b). It corresponds to a filiform morphotype, with four setose and long antennomeres, maybe of the apical section. Each antennomere is 0.30 mm long (although one of them seems to be incomplete and is 0.26 mm long) and 0.06 mm wide. This type of antenna could correspond to Blattodea (*62*), but an accurate determination is not possible because of the poor and partial preservation. This fragment shows a surface of desiccation (Fig. S1c), indicating that the resin was under aerial conditions for a time in the resiniferous tree, but there is no evidence from which to infer an approximate height. It was possibly close to the litter.

Fragment AR-1-A-2019.88.3 is very opaque with abundant double emulsions of sap. An undetermined fossil remnant shows in an edge of the fragment (Fig. S1d). It could be a partial body remain of an arthropod, but its poor preservation prevents identification. An emerging long structure could correspond to an antenna.

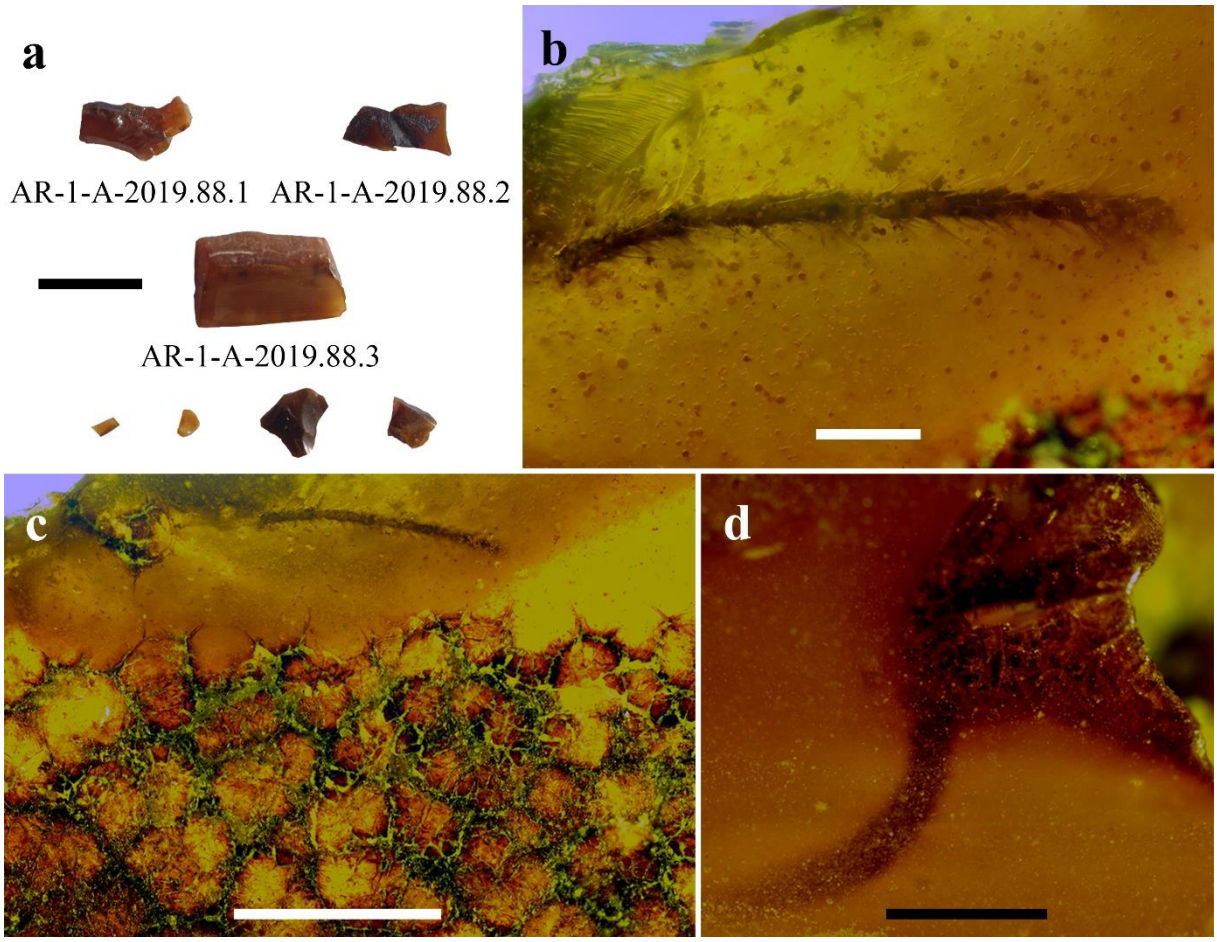

Supplementary Figure S1. Fragmented amber piece AR-1-A-2019.88 from Ariño outcrop (Teruel, Spain), dated as early Albian. (**a**) All the fragments at the same scale. (**b**) Insect antenna in AR-1-A-2019.88.2. (**c**) Surface of desiccation in AR-1-A-2019.88.2. (**d**) Image composition of an arthropod in AR-1-A-2019.88.3. Scale bars 1 mm (a, c, d), 0.2 mm (b).

References (Supplementary information)

60. Nascimbene, P. & Silverstein, H. The preparation of fragile Cretaceous ambers for conservation and study of organismal inclusions. In *Studies on Fossils in Amber, with Particular Reference to the Cretaceous of New Jersey* (ed. Grimaldi, D.) 93–102 (Backhuys Publishers, Leiden, 2000).

61. Lozano, R. P. *et al*. Phloem sap in Cretaceous ambers as abundant double emulsions preserving organic and inorganic residues. *Sci. Rep.* **10,** 9751 (2020).

62. Bell, W. J., Roth, L. M. & Nalepa, C. A. Eds, *Cockroaches: ecology, behavior, and natural history*. (The Johns Hopkins University Press, Baltimore, 2007).

Anexo 8.1.3

Dinosaur bonebed amber from an original swamp forest soil

Álvarez-Parra, S., Pérez-de la Fuente, R., Peñalver, E., Barrón, E., Alcalá, L., Pérez-Cano, J., Martín-Closas, C., Trabelsi, K., Meléndez, N., López Del Valle, R., Lozano, R.P., Peris, D., Rodrigo, A., Sarto i Monteys, V., Bueno-Cebollada, C.A., Menor-Salván, C., Philippe, M., Sánchez-García, A., Peña-Kairath, C., Arillo, A., Espílez, E., Mampel, L., Delclòs, X. 2021. Dinosaur bonebed amber from an original swamp forest soil. *eLife*, **10**, e72477.

DOI: https://doi.org/10.7554/eLife.72477

Revista científica: *eLife*
Factor de impacto: 8,713 (2021)
Categoría: *Biology*, Q1 (2021)

RESEARCH ARTICLE

Dinosaur bonebed amber from an original swamp forest soil

Sergio Álvarez-Parra[1]*, Ricardo Pérez-de la Fuente[2], Enrique Peñalver[3], Eduardo Barrón[3], Luis Alcalá[4], Jordi Pérez-Cano[1], Carles Martín-Closas[1], Khaled Trabelsi[5,6,7], Nieves Meléndez[8], Rafael López Del Valle[9], Rafael P Lozano[3], David Peris[1], Ana Rodrigo[3], Víctor Sarto i Monteys[10], Carlos A Bueno-Cebollada[3], César Menor-Salván[11,12], Marc Philippe[13], Alba Sánchez-García[14,15], Constanza Peña-Kairath[1], Antonio Arillo[16], Eduardo Espílez[4], Luis Mampel[4], Xavier Delclòs[1]

[1]Departament de Dinàmica de la Terra i de l'Oceà and Institut de Recerca de la Biodiversitat (IRBio), Facultat de Ciències de la Terra, Universitat de Barcelona, c/ Martí i Franquès s/n, 08028, Barcelona, Spain; [2]Oxford University Museum of Natural History, Oxford, United Kingdom; [3]Museo Geominero (IGME, CSIC), c/ Ríos Rosas 23, Madrid, Spain; [4]Fundación Conjunto Paleontológico de Teruel-Dinópolis/Museo Aragonés de Paleontología, Av. Sagunto s/n, Teruel, Spain; [5]Université de Sfax, Faculté des Sciences de Sfax, Sfax, Tunisia; [6]Université de Tunis El Manar II, Faculté des Sciences de Tunis, LR18 ES07, Tunis, Tunisia; [7]Department of Geology, University of Vienna, UZA 2, Vienna, Austria; [8]Departamento de Geodinámica, Estratigrafía y Paleontología, Facultad de Ciencias Geológicas, Universidad Complutense de Madrid, Ciudad Universitaria, Madrid, Spain; [9]Museo de Ciencias Naturales de Álava, c/ Siervas de Jesús 24, 01001, Vitoria-Gasteiz, Spain; [10]Institut de Ciència i Tecnologia Ambientals (ICTA), Edifici Z – ICTA-ICP, Universitat Autònoma de Barcelona, Barcelona, Spain; [11]School of Chemistry and Biochemistry, Georgia Institute of Technology, Atlanta, United States; [12]Departamento de Biología de Sistemas/ Instituto de Investigación Química "Andrés del Río" (IQAR), Universidad de Alcalá, 28805, Alcalá de Henares, Madrid, Spain; [13]Univ. Lyon, Université Claude Bernard Lyon 1, CNRS, ENTPE, UMR 5023 LEHNA, Villeurbanne, France; [14]Departament de Botànica i Geologia, Facultat de Ciències Biològiques, Universitat de València, c/ Dr. Moliner 50, Burjassot, Spain; [15]Division of Invertebrate Zoology, American Museum of Natural History, New York, United States; [16]Departamento de Biodiversidad, Ecología y Evolución, Facultad de Biología, Universidad Complutense de Madrid, c/ José Antonio Novais 12, Madrid, Spain

***For correspondence:** sergio.alvarez-parra@ub.edu

Competing interest: The authors declare that no competing interests exist.

Funding: See page 20

Received: 25 July 2021
Preprinted: 16 September 2021
Accepted: 08 November 2021
Published: 30 November 2021

Reviewing Editor: Min Zhu, Chinese Academy of Sciences, China

Abstract Dinosaur bonebeds with amber content, yet scarce, offer a superior wealth and quality of data on ancient terrestrial ecosystems. However, the preserved palaeodiversity and/or taphonomic characteristics of these exceptional localities had hitherto limited their palaeobiological potential. Here, we describe the amber from the Lower Cretaceous dinosaur bonebed of Ariño (Teruel, Spain) using a multidisciplinary approach. Amber is found in both a root layer with amber strictly in situ and a litter layer mainly composed of aerial pieces unusually rich in bioinclusions, encompassing 11 insect orders, arachnids, and a few plant and vertebrate remains, including a feather. Additional palaeontological data—charophytes, palynomorphs, ostracods— are provided. Ariño arguably represents the most prolific and palaeobiologically diverse locality in which fossiliferous amber and a dinosaur bonebed have been found in association, and the only one known

where the vast majority of the palaeontological assemblage suffered no or low-grade pre-burial transport. This has unlocked unprecedentedly complete and reliable palaeoecological data out of two complementary windows of preservation—the bonebed and the amber—from the same site.

Editor's evaluation

In an integrative way, the authors introduced an exceptional Konservat-Lagerstätte jointly preserving dinosaur remains and fossiliferous amber. Impressively, this is the first time that strictly in situ amber is reported, and the key claims of the manuscript are well supported by the paleontological and geochemical data. This manuscript will be of broad interest to scientists, including paleontologists, geobiologists, ecologists and geologists, as well as the public.

Introduction

Localities preserving either vertebrate bonebeds or fossilised plant resin (amber) are among the most valuable sources of information on past terrestrial ecosystems (***Rogers et al., 2007***; ***Seyfullah et al., 2018***). Yet, when a bonebed and fossilised resin are found jointly in the same site, and there is certainty that they originally belonged to the same biocoenosis, the potential for extracting and integrating palaeobiological data is barely unmatched in palaeontology. Although amber from the Cretaceous is often found together with other fossils such as plant and, more infrequently, vertebrate remains, fossiliferous amber associated with bonebeds including dinosaurs has been previously reported in only three occasions. Firstly, the lower Cenomanian (ca. 96–100.5 Ma) locality of Fouras/Bois Vert (Charente-Maritime, France) yielded diverse vertebrate remains, including about 50 dinosaur bone fragments, alongside plant macroremains, molluscs, and amber lumps, a few of which were fossiliferous (***Néraudeau et al., 2003***). From the latter, ~110 bioinclusions belonging to arachnids, springtails and, at least four insect orders have been reported, including several species described (***Perrichot et al., 2007***; ***Tihelka et al., 2021***). Secondly, amber is known from the upper Campanian (~73 Ma) Pipestone Creek bonebed (Alberta, Canada) (***Tanke, 2004***; ***Currie et al., 2008***). Although >99% of the 3000 individual fossils recovered from this site belong to *Pachyrhinosaurus*, other dinosaurs, fish, turtles, lizards, and crocodilians were also found (***Currie et al., 2008***; ***Bell and Currie, 2016***; ***Cockx et al., 2020***). Six bioinclusions recovered from ca. 50 cm^3 of typically <1 cm amber pieces were described (***Cockx et al., 2020***). Lastly, fossiliferous amber was found in Stratum 11 from the uppermost Maastrichtian (ca. 67–66 Ma) Bone Butte bonebed site (South Dakota, USA) (***DePalma, 2010***). This site, belonging to the intensively studied Hell Creek Formation, provided ~3000 mostly disarticulated fossils representing >50 species of dinosaurs and other vertebrates; the non-vertebrate material included molluscs, ichnofossils, and plant macroremains, and was mostly found together with the fossiliferous amber (***DePalma, 2010***; ***DePalma et al., 2015***). The palaeodiversity recovered from the latter, in contrast, was rather scarce, with 22 bioinclusions found in 400 g of collected amber (***DePalma, 2010***; ***DePalma et al., 2010***; ***Nel et al., 2010***). Other Bone Butte strata yielded non-fossiliferous amber (***DePalma, 2010***). In addition, a hadrosaur jaw with an amber piece originally attached to it and containing an inclusion was reported from the uppermost Campanian Dinosaur Park Formation in Alberta (***McKellar et al., 2019***). Further Upper Cretaceous bonebed localities from western Canada yielded amber but lacking bioinclusions (***Cockx et al., 2021***).

The Ariño deposit represents one of the most important Lower Cretaceous dinosaur sites from Europe (***Alcalá et al., 2012***). This outcrop, located within the Santa María open-pit coal mine (Ariño municipality, Teruel Province, Spain), takes part in the Oliete Sub-basin of the Maestrazgo Basin (eastern Iberian Peninsula) (***Salas and Guimerà, 1996***). This extensional sub-basin was infilled with sediments deposited in palaeoenvironments ranging from marine to continental during the early Barremian to middle Albian (***Meléndez et al., 2000***). In this sub-basin, the siliciclastic Escucha Formation, early Albian in age (***Peyrot et al., 2007***; ***Bover-Arnal et al., 2016***), was deposited overlying Aptian marine carbonates (***Cervera et al., 1976***). This formation represents coastal environments that included barrier-island systems with back-barrier marshes and flood-tidal deltas (***Rodríguez-López et al., 2009***). The AR-1 level of the Ariño locality, with ca. 600,000 m^2 of surveyed surface, consists of marls with a high concentration of organic matter occasionally forming coal, which underlie the lowest level of coal exploited in the Santa María mine (***Figure 1***, ***Video 1***; ***Alcalá et al., 2012***). The

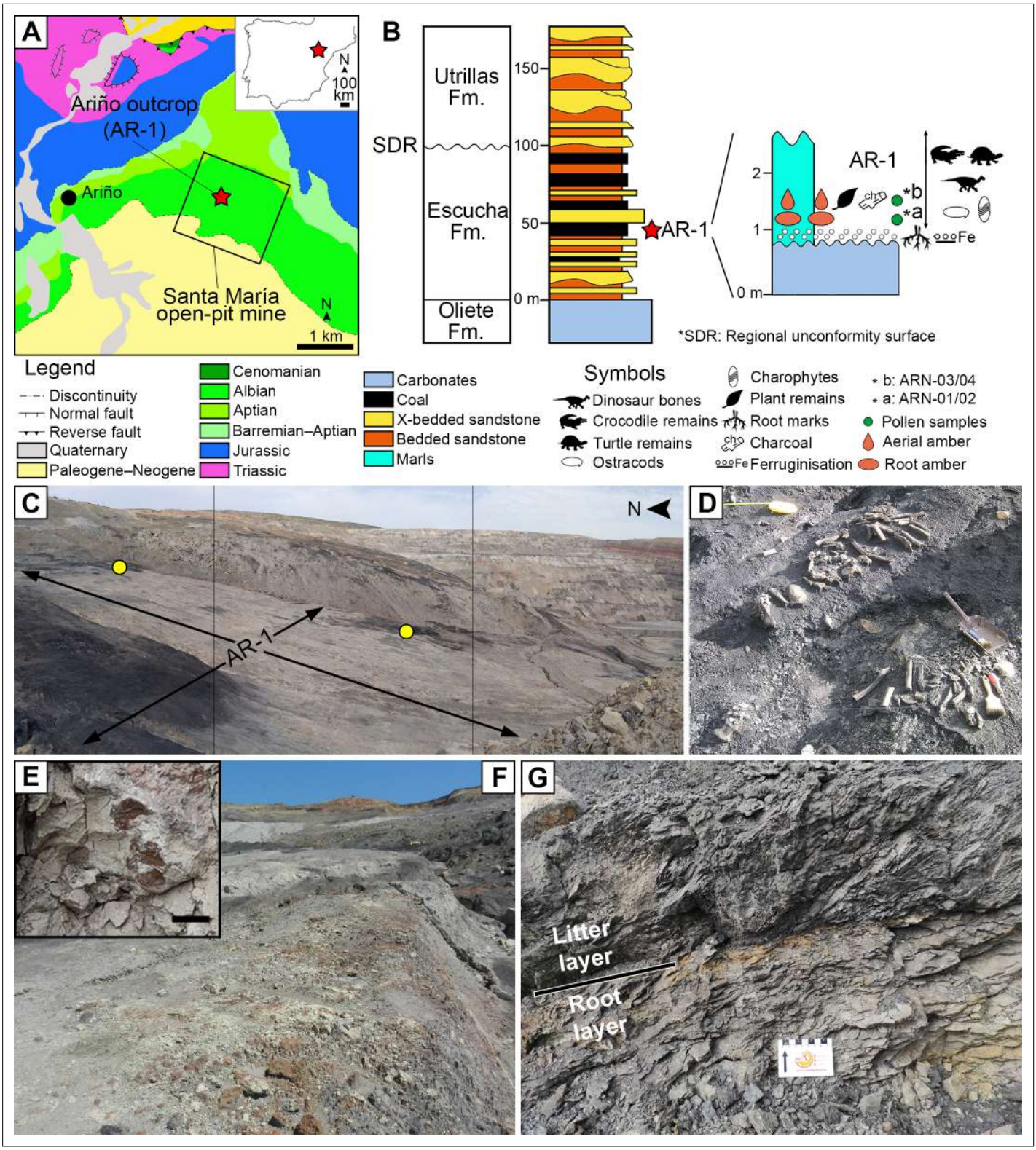

Figure 1. The Lower Cretaceous vertebrate bonebed and amber site of Ariño. (**A**) Geographical and geological location; modified from ***Alcalá et al., 2012*** (**B**) Stratigraphic location of the level AR-1; general stratigraphic log from the Oliete Sub-basin, modified from ***Kirkland et al., 2013***, is shown at the left, together with the location of the level AR-1 (red star); a section of the latter, including the stratigraphic location of the amber deposit studied herein, is shown at the right. (**C**) Santa María open-pit coal mine with indication of the level AR-1 and the two excavated areas rich in aerial amber (yellow dots); the bottom of the open-pit coal is at the right. (**D**) One of the 160+ bone concentrations found in Ariño, AR-1/10, during vertebrate fieldwork in

Figure 1 continued on next page

Figure 1 continued

2010, showing the holotype of the nodosaurid *Europelta carbonensis*; metal dustpan ~30 cm long. (**E**) Root marks at the top of the carbonates below the level AR-1; scale bar, 1 cm. (**F**) Carbonates right below the level AR-1, displaying edaphic features at the top. (**G**) Detail photograph of the level AR-1 showing the lower root layer (with amber from resin exuded by roots) and the upper litter layer (with amber from resin exuded by trunk and branches); centimetric scale. See also ***Video 1***.

AR-1 level has yielded a rich and diverse vertebrate fossil record representing more than 10,000 fossils namely found in more than 160 mono- or bitaxic concentrations of usually well-preserved, articulated or semi-articulated partial skeletons (***Alcalá et al., 2012***; ***Alcalá et al., 2018***; ***Buscalioni et al., 2013***; ***Villanueva-Amadoz et al., 2015***). From these, new species of freshwater and terrestrial turtles, crocodilians, and ornithischian dinosaurs–that is, the ornithopod *Proa valdearinnoensis* and the nodosaurid *Europelta carbonensis*– have been described (***McDonald et al., 2012***; ***Buscalioni et al., 2013***; ***Kirkland et al., 2013***; ***Pérez-García et al., 2015***; ***Pérez-García et al., 2020***). Predatory dinosaurs were also present in the Ariño ecosystem, as evidenced by coprolites, ichnites, and isolated allosauroidean teeth (***Alcalá et al., 2012***; ***Alcalá et al., 2018***; ***Vajda et al., 2016***). Chondrichthyan and osteichthyan fish remains have also been occasionally found (***Alcalá et al., 2012***). Regarding the invertebrate record, three ostracod species (***Tibert et al., 2013***), as well as freshwater bivalves and gastropods, were reported (***Alcalá et al., 2012***; ***Kirkland et al., 2013***). From the palaeobotanical standpoint, two charophyte species, fern remains, conifer twigs, taxonomically unassigned charcoalified wood remains, undetermined cuticles, and palynomorphs found in both the marls and coprolites (spores, gymnosperm, and angiosperm pollen grains) were previously known (***Tibert et al., 2013***; ***Villanueva-Amadoz et al., 2015***; ***Vajda et al., 2016***). Based on the former geological and palaeontological data, the Ariño palaeoenvironment was inferred as a freshwater swamp plain with perennial alkaline shallow lakes subjected to salinity fluctuations due to marine influence under a tropical–subtropical climate (***Alcalá et al., 2012***; ***Tibert et al., 2013***; ***Villanueva-Amadoz et al., 2015***). The level AR-1 was dated as early Albian (ca. 110 Ma) based on charophyte, palynological, and ostracod assemblages (***Tibert et al., 2013***; ***Villanueva-Amadoz et al., 2015***; ***Vajda et al., 2016***).

The presence of indeterminate amounts of amber in the AR-1 level from Ariño was first noted by ***Alcalá et al., 2012***, with later works only adding that amber pieces were abundant and sometimes large (***Alcalá et al., 2018***). The only previously described bioinclusion from Ariño amber was a tuft of three remarkably well-preserved mammalian hair strands corresponding to the oldest hair reported in amber (***Álvarez-Parra et al., 2020a***).

In the Iberian Peninsula, amber is found in Triassic (Ladinian–Rhaetian) and Cretaceous (Albian–Maastrichtian) deposits; those having yielded abundant amber with bioinclusions are mostly late Albian in age, namely from the Basque-Cantabrian (e.g. Peñacerrada I and El Soplao) and Maestrazgo basins (e.g. San Just) (***Alonso et al., 2000***; ***Delclòs et al., 2007***; ***Peñalver et al., 2007***; ***Najarro et al., 2009***; ***Peñalver and Delclòs, 2010***).

Here, we characterise the amber deposit associated with the dinosaur bonebed AR-1 of Ariño from a multidisciplinary standpoint, describing its morphological, geochemical, palaeofaunistic, and taphonomic features, all of which allow us to recognise the palaeontological singularity of this site. Together with complementary palaeontological data (charophytes, palynomorphs, ostracods), our integrative results enable a complete reconstruction of the Ariño biota.

Video 1. Amber excavation in the lower Albian bonebed level AR-1 of Ariño during May 2019 and extraction of two strictly in situ (autochthonous) kidney-shaped amber pieces from the root layer. See also Figures 1 and 2.
https://elifesciences.org/articles/72477/figures#video1

Results

Amber characteristics

Two distinct amber-bearing layers, a lower one and an upper one, are present in the Ariño AR-1 level (***Figures 1 and 2***, ***Figure 2—figure supplements 1 and 2***). The lower layer overlies a level of carbonates of oligotrophic lacustrine origin showing the development of palaeosols at its

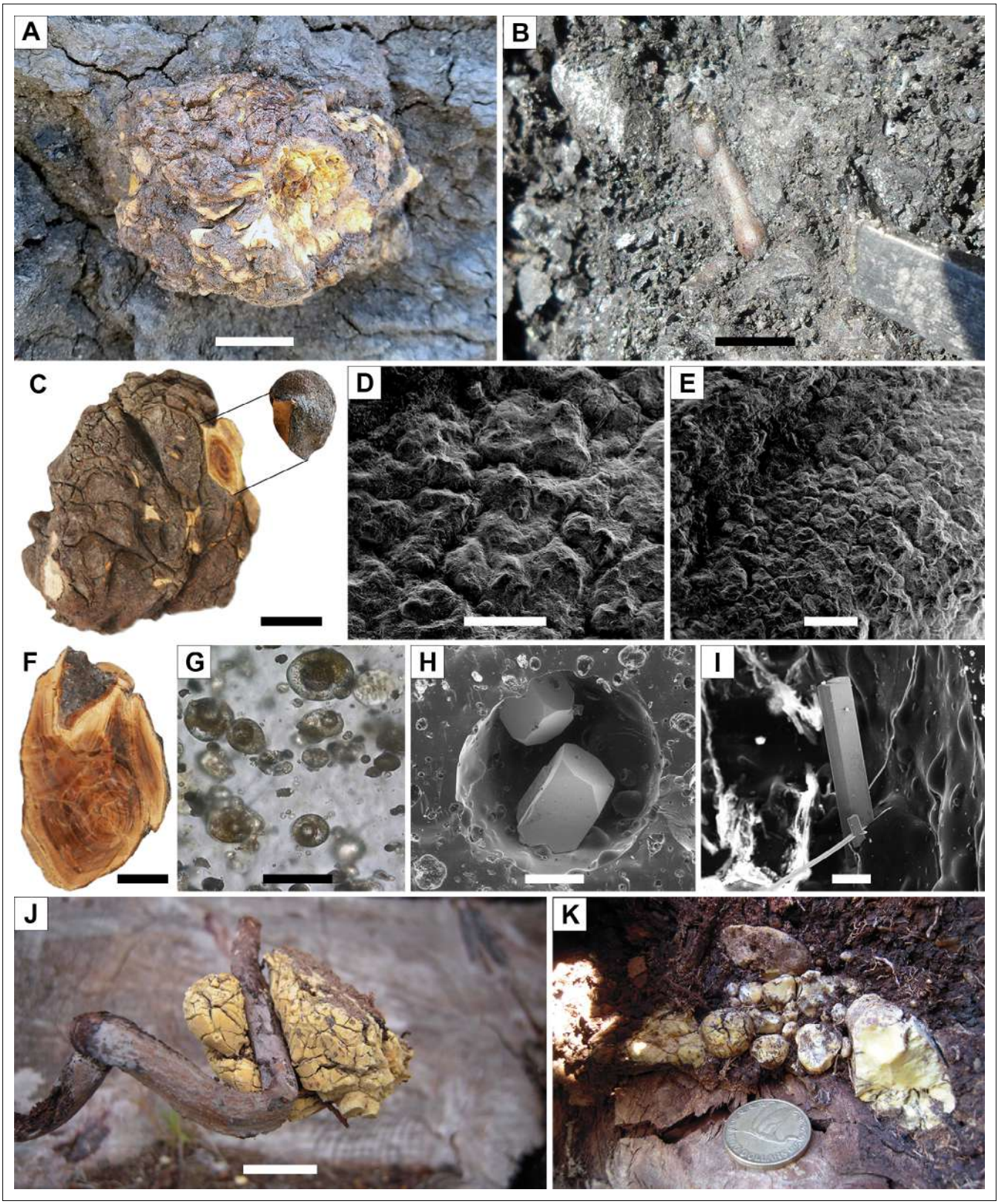

Figure 2. Diversity of amber pieces from the AR-1 level and Pleistocene copal pieces for comparison. (**A**) Kidney-shaped amber piece (root layer). (**B**) Aerial amber piece (litter layer), corresponding to a resin flow, after partially removing surrounding rock during fieldwork. (**C**) Kidney-shaped amber piece (AR-1-A-2019.93) from the root layer. (**D, E**) Two different areas of the external surface from a fragment detached from the piece in (**C**), showing the preserved delicate surface microprotrusions and no evidence of linear grooves. (**F**) Kidney-shaped amber piece (root layer) showing the internal banding

Figure 2 continued on next page

Figure 2 continued

pattern (AR-1-A-2019.132). (**G**) Triphasic (solid+ liquid + gas) bubble-like inclusions in a kidney-shaped amber piece (AR-1-A-2019.130). (**H**) Two pyrite cuboctahedrons in an alleged empty space left by a fluid inclusion (amber piece AR-1-A-2019.86). (**I**) Needle-shaped crystals from an iron sulphate (likely szomolnokite) growing inward from the walls in an alleged empty space left by a fluid inclusion (amber piece AR-1-A-2019.129). (**J**) Kidney-shaped piece of Pleistocene copal associated to an *Agathis australis* root from an overturned stump in Waipapakauri (North Island, New Zealand). (**K**) Pleistocene copal pieces associated to the root system of the same *A. australis* stump; coin 2.65 cm in diameter. Scale bars, 2 cm (**A–C**, **F, J**), 0.5 mm (**D**), 1 mm (**E**), 0.03 mm (**G**), 0.2 mm (**H**), and 0.1 mm (**I**). See also ***Video 1***.

The online version of this article includes the following figure supplement(s) for figure 2:

Figure supplement 1. Strictly in situ (autochthonous) kidney-shaped amber pieces from the root layer of the lower Albian bonebed level AR-1 of Ariño.

Figure supplement 2. Litter layer of the lower Albian bonebed level AR-1 of Ariño.

Figure supplement 3. Amber pieces with taphonomic interest from the level AR-1 of Ariño.

top, including root marks (***Figure 1E and F***). This layer is characterised by abundant, irregular amber lumps (i.e., kidney-shaped) 10–40 cm in length with protrusions, an opaque crust, an inner banding pattern, and lacking bioinclusions (***Figure 2A, C and F***, ***Figure 2—figure supplement 1***). Aerial amber and charcoalified plant remains are absent in this layer. The kidney-shaped amber pieces are distributed along the exposed area of the AR-1 level and, if not partially exposed due to weathering, are complete. The opaque crust from the amber pieces has an irregular morphology and its ultrastructure shows delicate microprotrusions and no evidence of linear grooves (***Figure 2C–E***). The banding patterns are formed by variable densities of abundant bubble-like inclusions of different sizes, which are monophasic (solid), biphasic (solid+ liquid), or triphasic (solid+ liquid + gas) (***Figure 2G***). Mineral crystals have been detected growing inwards within allegedly empty spaces left by larger bubble-like inclusions—these include pyrite cuboctahedrons and needle-shaped crystals from an iron sulphate mineral according to EDS analysis (likely szomolnokite, $Fe^{2+}SO_4 \cdot H_2O$) (***Figure 2H,I***, ***Figure 2—figure supplement 3A***).

The upper layer from the Ariño AR-1 level is rich in amber pieces of flow-, droplet-, and stalactite-shaped morphologies, which often show external and/or internal desiccation surfaces (***Figure 2B***, ***Figure 2—figure supplement 2***). Small, almost spherical amber pieces about 1–5 cm in diameter, with an opaque crust similar to the kidney-shaped amber pieces, are also present in this layer, yet rare; their surface is polished and more regular in patterning (***Figure 2—figure supplement 3B-D***). Amber pieces range from translucent to opaque, and from light yellow to dark reddish in colour. One peculiar piece showed subtle, multidirectional surface microscopic scratches and borings, the latter filled with an undetermined material, neither calcium carbonate nor gypsum (***Figure 2—figure supplement 3E***).

The FTIR spectra of two stalactite-shaped amber pieces from Ariño are dominated by a small C-H stretching band at 2925 cm^{-1}, an intense C-H band at 1457 cm^{-1}, and an intense carbonyl band at 1707 cm^{-1} (***Figure 3A***, ***Figure 3—source data 1***, ***Figure 3—source data 2***, ***Figure 3—source data 3***), all characteristic of amber (***Grimalt et al., 1988***). Hydroxyl bands near 3500 cm^{-1} are present. The Ariño amber spectra are very similar to those from San Just amber, their main difference being the presence of a small band near 1200 cm^{-1} in the latter. On the other hand, the composition of the organic solvent-extractable materials obtained by GC-MS, comprising the 32.5 % of the Ariño amber, is dominated by labdane resin acids and its diagenetic derivatives, with amberene (**I**; 1,6-dimethyl-5-isopentyltetralin) being the major component in the bulk extract (***Figure 3B***, ***Figure 3—figure supplement 1***, ***Figure 3—source data 4***). The labdan-18-oic acids are dominant in the polar fraction of the organic extract from the amber. The identification of the clerodane-family diterpene **VI** is noteworthy. The analyses show no evidence of significant terpenes of the pimarane/abietane family and discount the presence of ferruginol. The Ariño amber does not show a significant content of either 15-homoamberene (**III**) or 1-methylamberene (**X**) (***Figure 3B***, ***Figure 3—figure supplement 1***; ***Kawamura et al., 2018***). This could point to a lack of the corresponding labdanoid alcohols or non-oxidised C18/C19 labdanoids in the precursor resin, as the diagenesis of these molecules could lead to 1-methylamberene. The decarboxylation of the labdan-18-oic acids prevailing in the Ariño amber polar fraction could be the first step in the diagenesis to amberene and its related compounds, especially isomers of the labdanoid **VI**, found as a rich distribution of peaks with M^+=246.

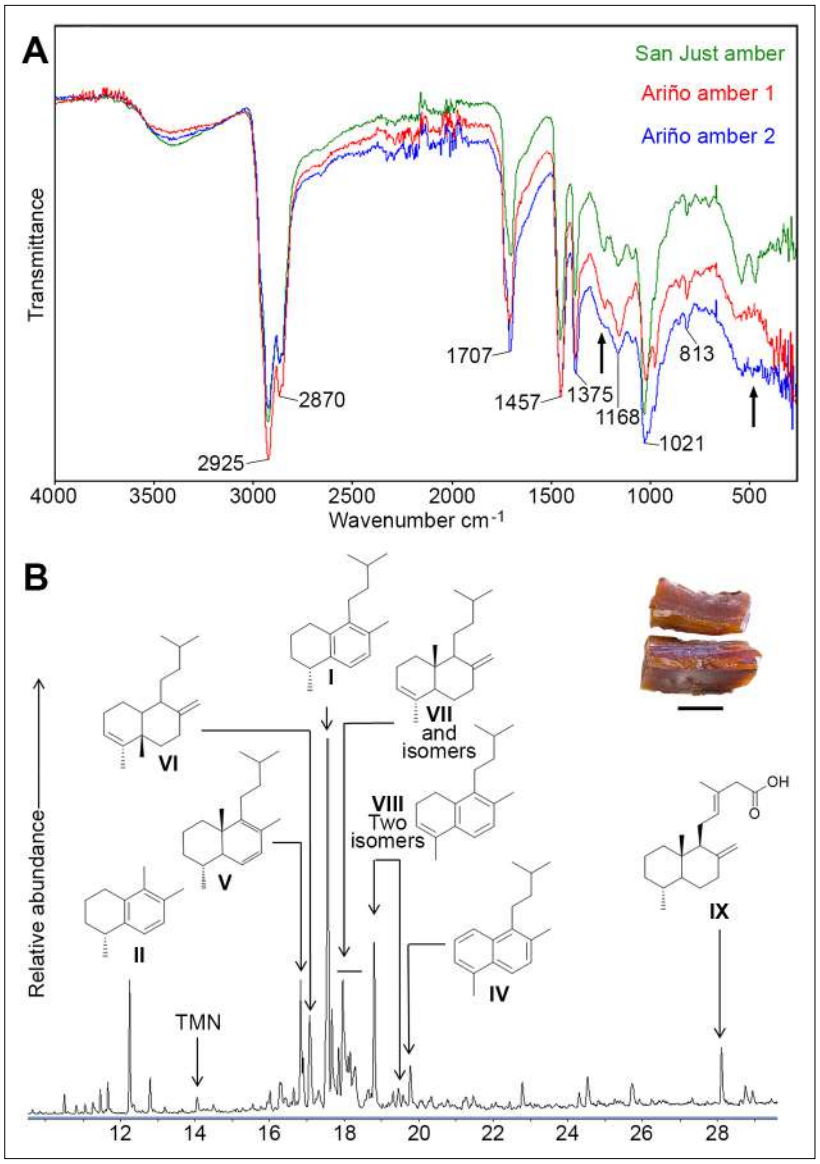

Figure 3. Physicochemical characterisation of the Lower Cretaceous amber from Ariño. (**A**) Infrared (FTIR) spectra obtained from two aerial amber pieces (litter layer); a spectrum from San Just amber (upper Albian) is provided for comparison; arrows indicate the main differences between Ariño and San Just ambers, at around 1200 and 500 cm^{-1}; resolution = 4 cm^{-1}. (**B**) Gas chromatography-mass spectrometry (GC-MS) trace for the underivatised total solvent extract of aerial amber, showing the structures of the main identified terpenoids, referred herein using Roman numerals (full formulation provided in ***Figure 3—figure supplement 1B***); TMN = trimethylnaphthalenes; the analysed aerial amber is shown at the top right (scale bar 0.5 mm).

The online version of this article includes the following figure supplement(s) for figure 3:

Source data 1. FTIR data of the Ariño amber 1.

Source data 2. FTIR data of the Ariño amber 2.

Source data 3. FTIR data of the San Just amber.

Source data 4. GC-MS data of the Ariño amber.

Figure supplement 1. Physicochemical characterisation of the Lower Cretaceous amber from Ariño.

Bioinclusions

A total of 166 bioinclusions were obtained out of 918 g of aerial amber (***Figure 4***, ***Figure 4—figure supplement 1***, ***Figure 4—figure supplement 2***); about one third of them are well to exceptionally well preserved. Plant inclusions are present, such as numerous fern or conifer trichomes (not considered in the inclusion count) and other undetermined remains (***Figure 4—figure supplement 1A-E***). The diverse assemblage is chiefly composed of arthropods or remains of their activity, such as spiderweb threads (***Figure 4—figure supplement 1F,G***) and coprolites, but also a few vertebrate integumentary remains. Arthropods are represented by arachnids and 11 insect orders. Arachnid inclusions belong to mites (Acari) and spiders (Araneae). Mites include a rare trombidiform of the family Rhagidiidae, an oribatid, and an undetermined six-legged larva (***Figure 4A***). One spider offers taphonomic insights (***Figure 4—figure supplement 1H***). Five amber pieces with arthropods as syninclusions have spiderwebs preserved; although all are isolated strands, one tangled sample might correspond to a partial web (***Figure 4—figure supplement 1F***). In the latter, glue droplets on several strands suggest it belonged to an orb web (***Figure 4—figure supplement 1G***). The insect orders found in the Ariño amber are jumping bristletails (Archaeognatha), crickets (Orthoptera), cockroaches (Blattodea), barklice (Psocodea), thrips (Thysanoptera), whiteflies and aphids (Hemiptera), lacewings (Neuroptera), beetles (Coleoptera), moths (Lepidoptera), gnats, midges, and other flies (Diptera), and wasps (Hymenoptera). Archaeognaths are represented by the inclusion of a cercus and a medial caudal filament. Two orthopterans are poorly preserved, but one could belong to †Elcanidae. A blattodean nymph and an adult have been found, as well as several remains such as probably blattodean isolated antennae. Among the seven psocodeans discovered, new taxa probably within the †Archaeatropidae and Manicapsocidae have been recognised. Thysanopterans are the third most abundant insect order in the Ariño amber, with 11 specimens (***Figure 4B and C***); three amber pieces contain more than one thrips as syninclusions. One isolated thrips shows a thin milky coating (***Figure 4—figure supplement 1I***), also found in other inclusions, and an infrequent nymph is unusually well preserved (***Figure 4B***). Hemipterans comprise four representatives of Sternorrhyncha and two incomplete undetermined specimens. Three of the former have been identified as Aleyrodidae, probably belonging to the Aleurodicinae (***Figure 4D***), and are preserved in the same amber piece as syninclusions. In addition, an Aphidoidea specimen (***Figure 4—figure supplement 2A***) has been found in an amber piece with spiderweb strands. The neuropteran record consists of two wing impressions on amber surfaces probably belonging to Berothidae (***Figure 4—figure supplement 2B***) and a complete specimen, which could correspond to a †Paradoxosisyrinae (Sisyridae) (***Figure 4—figure supplement 2C***). Five coleopteran specimens have been discovered, two tentatively identified as belonging to Ptinidae (***Figure 4—figure supplement 2D***) and Cantharidae (***Figure 4—figure supplement 2E***). A ditrysian lepidopteran larva, yet incomplete anteriorly, is remarkably well preserved (***Figure 4E***). Dipterans (***Figure 4F***) are represented by 19 specimens of the families †Archizelmiridae, Cecidomyiidae, Ceratopogonidae (including at least one female), Chironomidae, Mycetophilidae, Rhagionidae, Scatopsidae, and probably Psychodidae. The first group is represented by a well-preserved male within the genus *Burmazelmira* (***Figure 4F***). Lastly, hymenopterans are the most abundant insects in Ariño amber, accounting for 34 specimens belonging to the Platygastroidea, Mymarommatoidea, †Serphitidae, and †Stigmaphronidae (***Figure 4G–I***). Furthermore, a new vertebrate inclusion is represented by a basal feather barb portion with a pennaceous structure (***Figure 4J***).

Palaeobotanical and ostracod assemblages

Charophytes sampled from the level AR-1 comprise four species belonging to the families †Clavatoraceae and Characeae. The assemblage is dominated by †Clavatoraceae, particularly by well-preserved fructifications of *Atopochara trivolvis* var. *trivolvis* (***Figure 5A-D***, ***Figure 5—figure supplement 1A,B***) and *Clavator harrisii* var. *harrisii* (***Figure 5E-J***, ***Figure 5—figure supplement 1C-E***) (n > 100 for each species). The former is represented by large utricles showing a characteristic triradiate symmetry and displaying flame-shaped cells at positions a1, a3, b1, and c1 (***Grambast, 1968***); such a configuration is variable in other populations of the same species. Five morphotypes of *C. harrisii* var. *harrisii* have been distinguished based on the cell disposition at the abaxial side of the utricle, showing the phylloid imprint flanked at the base by two small cells and bearing above a complex of 5–11 cells (***Figure 5—figure supplement 1F-J***); although this variety had been previously identified in Ariño, none of the morphotypes described herein for the first time in the variety were evident (***Tibert et al., 2013***).

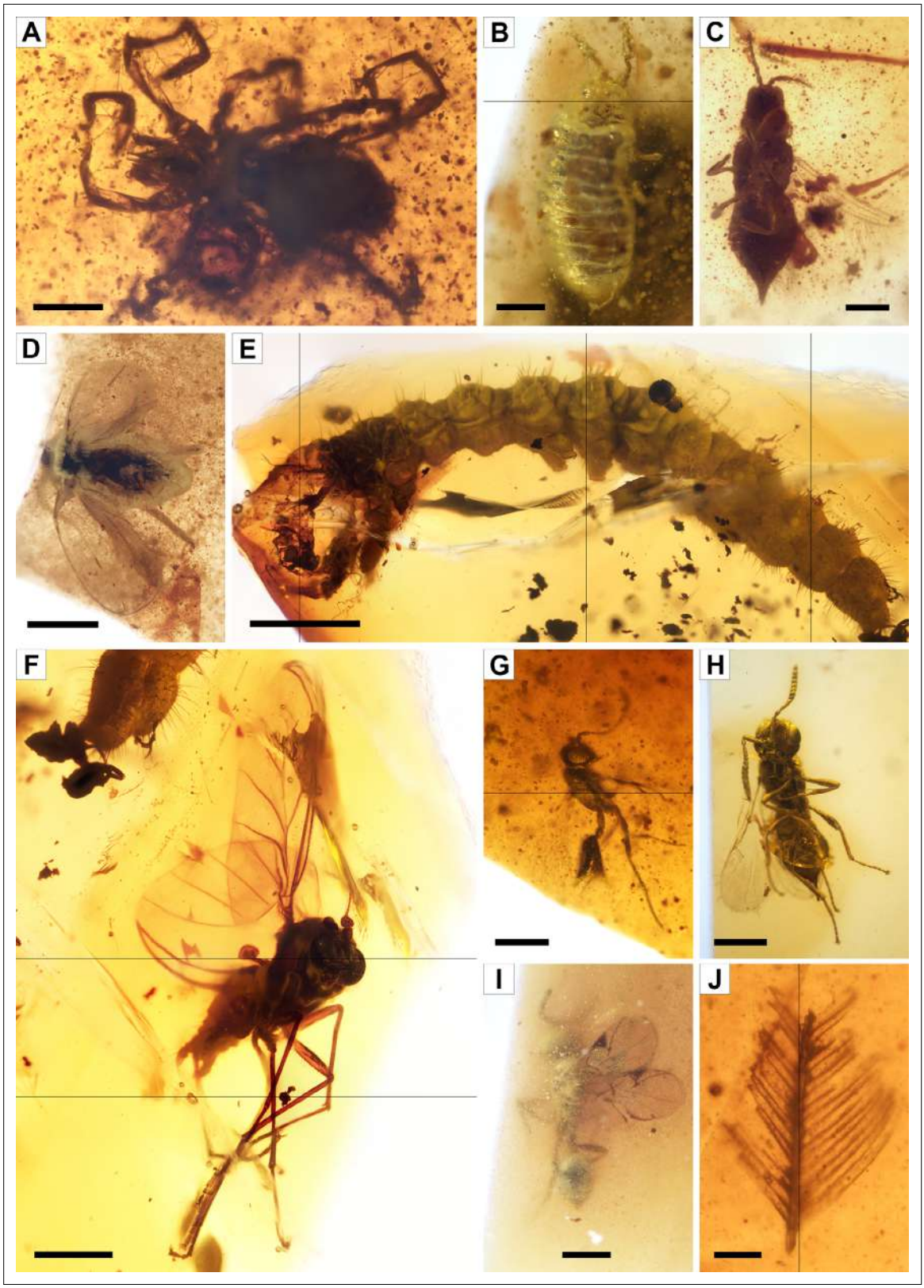

Figure 4. Faunal bioinclusions from the Lower Cretaceous bonebed amber of Ariño. (**A**) A rhagidiid mite, the oldest known (Acari: Rhagidiidae; AR-1-A-2019.71). (**B**) An immature thrips (Thysanoptera; AR-1-A-2019.114.2). (**C**) An adult thrips (Thysanoptera; AR-1-A-2019.40). (**D**) A whitefly (Hemiptera: Aleyrodidae; AR-1-A-2019.100.1). (**E**) A ditrysian lepidopteran larva (AR-1-A-2019.95.1). (**F**) A *Burmazelmira* sp. fly (Diptera: †Archizelmiridae: AR-1-A-2019.95.2). (**G**) A false fairy wasp, the oldest known (Hymenoptera: Mymarommatoidea; AR-1-A-2019.61). (**H**) A superbly preserved platygastroid wasp

Figure 4 continued on next page

Figure 4 continued

(Hymenoptera: Platygastroidea; AR-1-A-2019.95.3). (**I**) A serphitid wasp, the oldest known (Hymenoptera: †Serphitidae; AR-1-A-2019.94.8). (**J**) A feather barb fragment with pennaceous structure (Theropoda; AR-1-A-2019.53). Scale bars, 0.2 mm (**A–C**, **G**), 0.5 mm (**D, F, H, I**), 1 mm (**E**), and 0.1 mm (**J**).

The online version of this article includes the following figure supplement(s) for figure 4:

Figure supplement 1. Diverse bioinclusions in amber from the level AR-1 of Ariño.

Figure supplement 2. Insect bioinclusions in amber from the level AR-1 of Ariño.

Moreover, several (n = 10) portions of clavatoracean thalli belonging to *Clavatoraxis* sp. have been recovered (***Figure 5K***). Lastly, rare occurrences (n = 3) of small characean gyrogonites with affinities to *Mesochara harrisii* are also present (***Figure 5L***); their determination remains somewhat uncertain due to the lack of a basal plate (***Martín-Closas et al., 2018***).

Charcoalified plant remains (fusinite/inertinite) are abundant in the upper amber layer (***Figure 2—figure supplement 2A***). These correspond to secondary xylem with strongly araucariacean (1) 2 (3) seriate intertracheary radial pitting and araucarioid cross-fields. Although they are similar to the araucariacean *Agathoxylon gardoniense*, we prefer to identify these samples as *Agathoxylon* sp. due to preservation. Other charcoalified wood remains likely belonging to other taxonomic groups have also been found. Furthermore, a rare sample of amber-filled plant tissue shows cells elliptic to rounded in cross-section and elongate in longitudinal section, blunt tips, 20–50 µm in diameter, and with thin walls (somewhat collenchymatous). Cells are arranged radially, but without evidence of growth rings. These characteristics suggest that this fossilised tissue might represent suber (cork) (***Figure 4—figure supplement 1B-E***).

The four studied palynological samples (ARN-01–ARN-04) have provided highly diverse, well-preserved assemblages that include a total of 72 different palynomorph taxa, that is, two from freshwater algae, 38 from spores of ferns and allied groups, 21 from gymnosperm pollen grains, and 11 from angiosperm pollen grains (***Figure 5M-T***, ***Figure 5—figure supplement 1K-P***, ***Supplementary file 1***). Aquatic palynomorphs, consisting of zygnematacean freshwater algae, are a small proportion of the samples except for ARN-04, characterised by the abundance of *Chomotriletes minor* (3.87 % of the total palynomorph sum) (***Figure 5M***). Spores numerically dominate the assemblages except for ARN-01. Overall, fern spores such as *Appendicisporites* spp. (***Figure 5N***), *Cicatricosisporites* spp., *Cyathidites australis*, *Cyathidites minor* (***Figure 5O***), and *Gleicheniidites senonicus*, predominate (13.48–38.42%) over those of bryophytes and lycophytes (1.44–2.38%). Gymnosperms are namely represented by *Inaperturopollenites dubius* (12.79–20.36%) (***Figure 5P***), related to taxodioid conifers (***Stuchlik et al., 2002***), and the genus *Classopollis* (9.39–15.95%) (***Figure 5Q***), produced by †Cheirolepidiaceae conifers (***Taylor and Alvin, 1984***). Araucariacean and bisaccate pollen show low amounts except for the araucariacean *Araucariacites* spp. (***Figure 5R***), which is particularly abundant in ARN-01 (12.79%). The abundance of *Eucommiidites* spp., assigned to †Erdtmanithecaceae gymnosperms, is also relevant (2.90%–8.00%) (***Figure 5S***). '*Liliacidites*' *minutus* (***Figure 5T***) was the most abundant angiosperm pollen in the assemblages (up to 12 % in ARN-01).

The ostracod fauna recovered from the level AR-1 is comprised of four species belonging to the families Limnocytheridae, †Cyprideidae, and Cyprididae (***Figure 5U–EE***, ***Figure 5—figure supplement 1Q–Y***). Specimens show mostly closed carapaces and are generally well preserved. The Limnocytheridae are represented by *Theriosynoecum* cf. *fittoni* (***Figure 5U and V***) (n = 20) and *Rosacythere denticulata* (n > 70) (***Figure 5W–BB***). Although the latter species was previously identified in Ariño (***Tibert et al., 2013***), three variants have now been detected: one with a faint pitting and extremely small rosette ornamentation (***Figure 5W***), one with a well-developed rosette (***Figure 5X, Y and AA***, ***Figure 5—figure supplement 1Q–U***), and one with strongly developed rosette and spine-like nodes locally generated at the postero-dorsal and postero-ventral parts of the carapace (***Figure 5Z and BB***, ***Figure 5—figure supplement 1V–Y***). †Cyprideidae and Cyprididae are found for the first time in Ariño, represented by the species *Cypridea* cf. *clavata* (n = 35) (***Figure 5CC and DD***) and *Mantelliana* sp. (n = 12) (***Figure 5EE***), respectively.

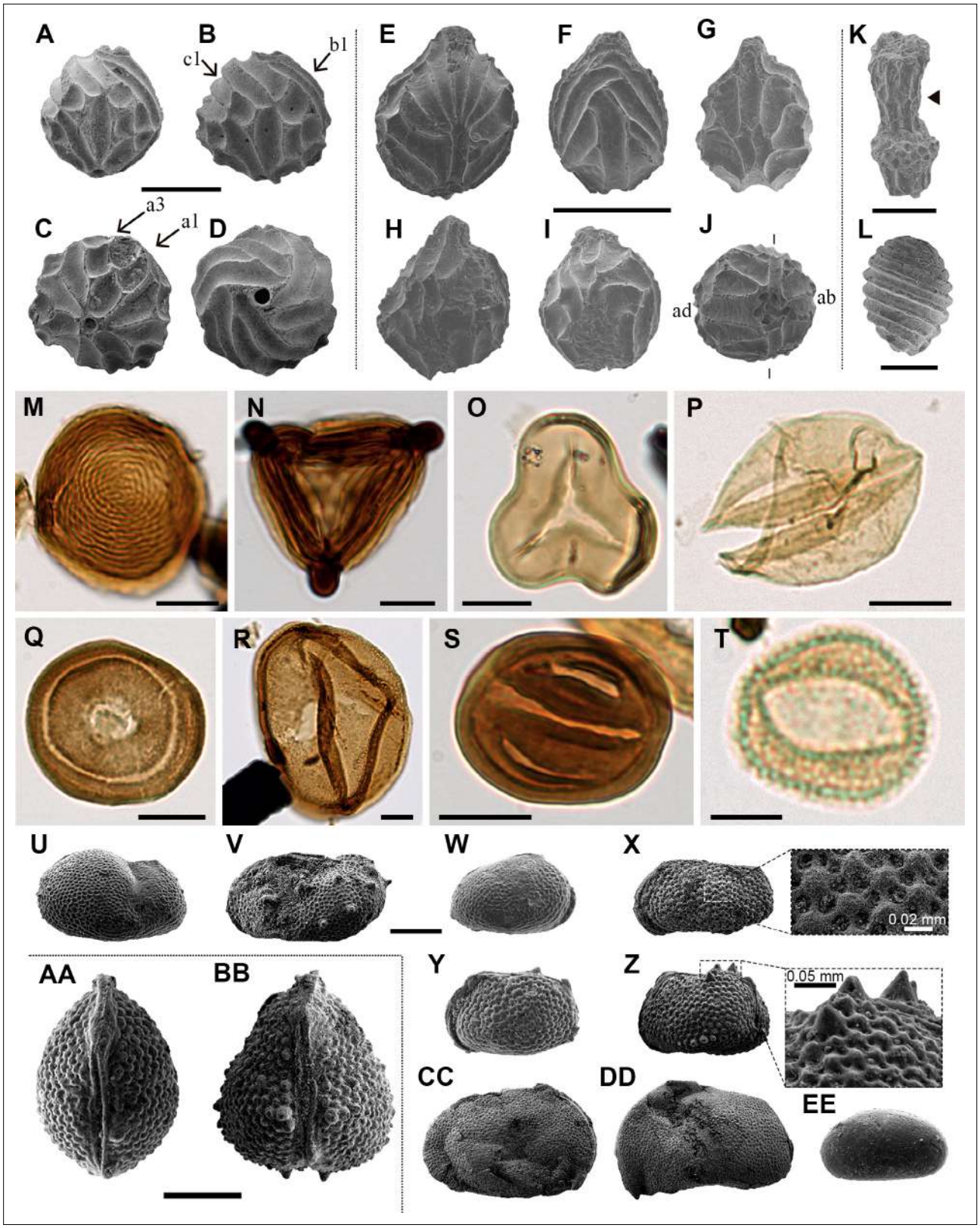

Figure 5. Charophyte (A–L), palynomorph (M–T), and ostracod (U–EE) records sampled from level AR-1 of Ariño. (**A–D**) *Atopochara trivolvis* var. *trivolvis* (†Clavatoraceae): (**A, B**) Lateral views (AR-1-CH-004 and AR-1-CH-005, respectively); (**C**) Basal view (AR-1-CH-007); (**D**) Apical view (AR-1-CH-008); cell lettering after ***Grambast, 1968***. (**E–J**) *Clavator harrisii* var. *harrisii* (†Clavatoraceae): (**E**) Lateral view (AR-1-CH-009); (**F**) Adaxial view (AR-1-CH-011); (**G**) Abaxial view morphotype II (AR-1-CH-013); (**H**) Abaxial view morphotype III (AR-1-CH-014); (**I**) Abaxial view morphotype IV (AR-1-CH-015); (**J**) Basal

Figure 5 continued on next page

Figure 5 continued

view (AR-1-CH-017) with indication of adaxial (ad) and abaxial (ab) sides. (**K**) *Clavatoraxis* sp. (†Clavatoraceae) (AR-1-CH-019); the arrowhead indicates the zig-zag line at the central part of the internode. (**L**) aff. *Mesochara harrisii* (Characeae) in lateral view (AR-1-CH-001). (**M**) *Chomotriletes minor* (ARN-03). (**N**) *Appendicisporites tricornitatus* (ARN-01). (**O**) *Cyathidites minor* (ARN-02). (**P**) *Inaperturopollenites dubius* (ARN-04). (**Q**) *Classopollis* sp. (ARN-02). (**R**) *Araucariacites hungaricus* (ARN-01). (**S**) *Eucommiidites minor* (ARN-01). (**T**) "*Liliacidites*" *minutus* (ARN-01). (**U, V**) *Theriosynoecum* cf. *fittoni* (Limnocytheridae): (**U**) Right lateral view, female carapace (AR-1-OS-001); (**V**) Left lateral view, male carapace (AR-1-OS-002). (**W–BB**) *Rosacythere denticulata* (Limnocytheridae): (**W**) Female? carapace, right lateral view, variant with extremely small rosette ornamentation (simply reticulated form) (AR-1-OS-006); (**X**) Male carapace of the variant with well-developed rosette ornamentation, left lateral view (AR-1-OS-011), and detail of the ornamentation; (**Y**) Female carapace of the variant with well-developed rosette ornamentation, left lateral view (AR-1-OS-007); (**Z**) Female carapace of the variant with strongly developed rosette ornamentation and spine-like nodes, left lateral view (AR-1-OS-015), and detail of the spine-like node ornamentation; (**AA**) Female carapace of the variant with well-developed rosette ornamentation, dorsal view (AR-1-OS-012); (**BB**) Female carapace of the variant with strongly developed rosette ornamentation and spine-like nodes, dorsal view (AR-1-OS-018), showing intraspecific variability. (**CC**), (**DD**) *Cypridea* cf. *clavata* (†Cyprideidae): (**CC**) Specimen in right lateral view (AR-1-OS-004); (**DD**) Specimen in left lateral view (AR-1-OS-005). (**EE**) *Mantelliana* sp. (Cyprididae) (AR-1-OS-003), right lateral view. Scale bars, 0.5 mm (**A–J**), 0.25 mm (**K**), 0.2 mm (**L, U–EE**), 0.01 mm (**M–S**), and 0.005 mm (**T**). See also ***Supplementary file 1***.

The online version of this article includes the following figure supplement(s) for figure 5:

Figure supplement 1. Additional charophyte (A–J), palynomorph (K–P), and ostracod (Q–Y) records sampled from level AR-1 of Ariño.

Discussion

Taphonomy

The kidney-shaped, bioinclusion-lacking amber pieces from AR-1's lower amber-bearing layer were produced by roots. Subterranean accumulations from both Recent/subfossil resin in modern forests and amber in geological deposits have been partly attributed to roots (***Langenheim, 1967***; ***Langenheim, 2003***; ***Henwood, 1993***; ***Martínez-Delclòs et al., 2004***; ***Seyfullah et al., 2018***). Although the resiniferous capacity of roots is well known (***Langenheim, 2003***), observations of resin attached and/or associated with roots from both angiosperms and gymnosperms have been occasional (***Langenheim, 1967***; ***Seyfullah et al., 2018***). Our field observations of late Pleistocene copal pieces produced and still attached to roots, covered by original soil, in an *Agathis australis* overturned stump, which was formerly referred to but not figured (***Najarro et al., 2009***; ***Speranza et al., 2015***), show similar morphologies to the Ariño kidney-shaped amber pieces (***Figure 2J and K***). The Ariño's lower amber layer is interpreted as a root layer where the abundant and complete amber pieces are strictly in situ, that is, they are located exactly where the roots of the resiniferous trees exuded this resin in the subsoil (***Figure 6A***). This level immediately overlies carbonates that display edaphic features at the top (***Figure 1E and F***). It has high lateral continuity and lacks aerial amber or charcoalified plant remains (***Figures 1 and 2***, ***Figure 2—figure supplement 1***). Also, the fragile surface protrusions and microprotrusions of the kidney-shaped amber pieces from this layer would not have preserved even if minimal biostratinomic transport or other processes entailing abrasion had occurred (***Figure 2C–E***). This is the first time strictly in situ amber is reported; the scarcely fossiliferous, autochthonous-parautochthonous Triassic amber droplets from the Dolomites are preserved in a palaeosol (***Schmidt et al., 2012***; ***Seyfullah et al., 2018***), but they are strictly ex situ, as the resin at least fell by gravity from their aboveground exudation location to the forest floor (***Figure 6A***). Although other amber-bearing outcrops from the Iberian Peninsula have commonly yielded kidney-shaped amber pieces (***Alonso et al., 2000***; ***Peñalver et al., 2007***; ***Najarro et al., 2009***), these appear fragmented and in pockets together with aerial amber and generally have smoother surfaces and more regular morphologies than those from Ariño. The kidney-shaped amber pieces have further noteworthy characteristics. Firstly, the amber pieces show marked internal bands composed of variable densities of mono-, bi-, or triphasic bubble-like inclusions (***Figure 2F and G***). Although these microscopic inclusions likely correspond to fossilised sap-resin emulsions (***Lozano et al., 2020***), at least partially, they show more complex and previously undocumented morphologies and arrangements. These microinclusions have the potential to provide key data on taphonomy and the conditions under which resin production occurred. Moreover, pyrite cuboctahedrons (***Figure 2H***) are usually found as mineralisations in the alleged empty spaces left by fluid bubble-like inclusions within amber (***Alonso et al., 2000***); they have been related to early diagenesis in reducing environments produced by anaerobic bacteria (***Allison, 1990***). In contrast, the iron sulphate minerals growing in these spaces (***Figure 2I***, ***Figure 2—figure supplement 3A***) have not been previously reported; they could have formed during late diagenesis under oxidising

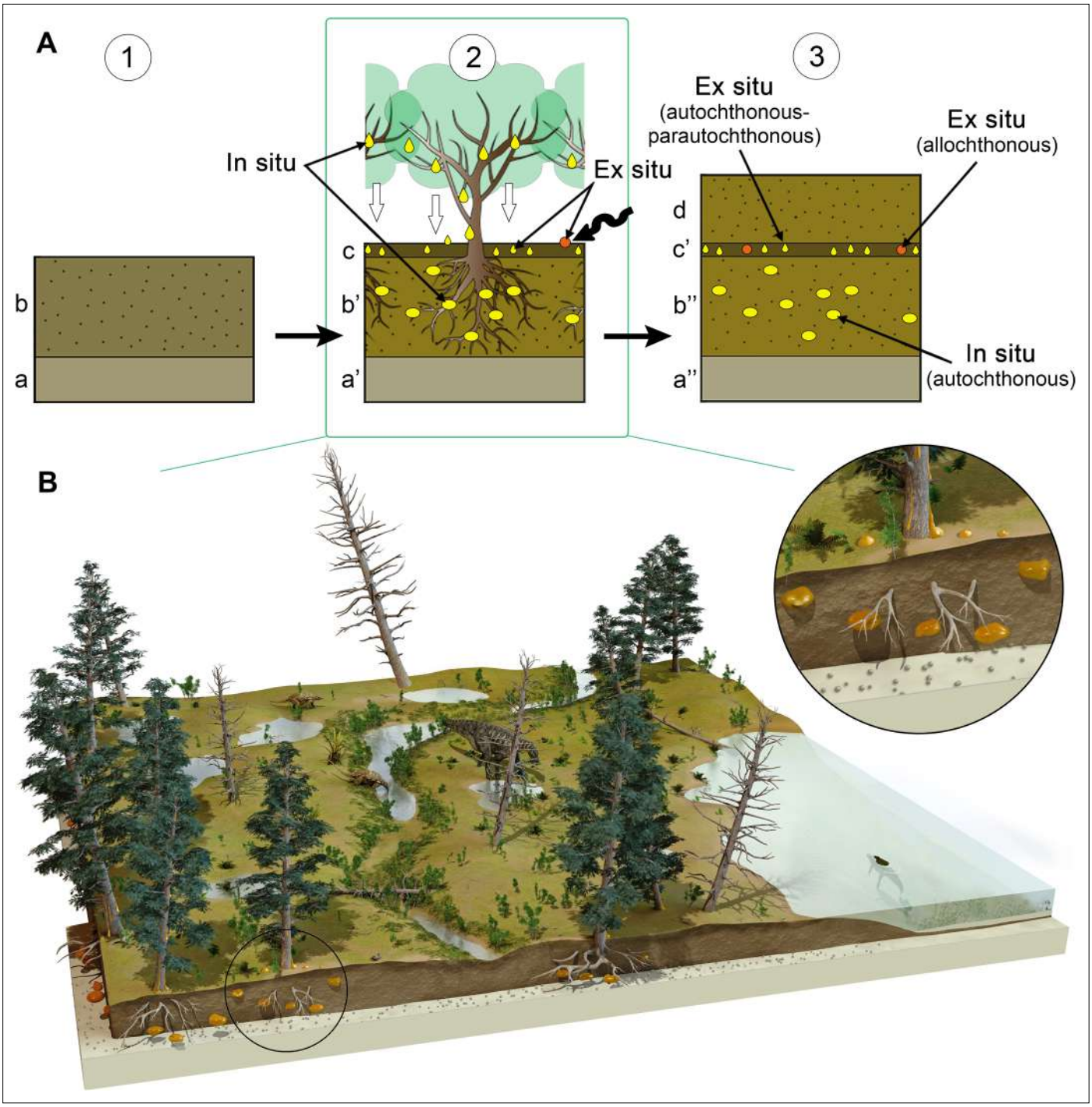

Figure 6. Formation of the amber deposit of Ariño. (**A**) Idealised diagrams depicting (1) the original depositional environment (a, carbonates; b, soil prior to tree installation); (2) resiniferous forest installation and pedogenesis; concentration of in situ kidney-shaped resin pieces produced by the roots in a root horizon (b'); accumulation of aerial resin pieces fallen from the branches and trunk and a few resin pieces dragged after transport (wavy arrow) in a litter horizon (c); and (3) fossil diagenesis of the resin pieces, resulting in a layer containing strictly in situ autochthonous kidney-shaped amber pieces produced by roots (b''), and a layer mostly composed of strictly ex situ autochthonous-parautochthonous aerial amber pieces and a few potentially allochthonous amber pieces (c'); level AR-1 corresponds to a single cycle of forest floor installation-destruction. (**B**) Artistic reconstruction of the coastal freshwater swamp ecosystem of Ariño, with emphasis on the depositional environment of the resin. The resiniferous trees are araucariaceans (extant model used: *Agathis australis*), tentatively identified as the resin source of Ariño; other depicted terrestrial plants are undetermined vegetation included for artistic purpose. Charophytes and a crocodile (*Hulkepholis plotos*) inhabit the shallow water body on the right; two nodosaurids (*Europelta carbonensis*), an iguanodontian (*Proa valdearinnoensis*), and a turtle (*Aragochersis lignitesta*) are shown on land; these vertebrate species were erected based on the Ariño bonebed material. Artist of the illustration in (**B**): José Antonio Peñas.

conditions after the input of oxygenated water into the amber (**Allison, 1990**). Secondly, the kidney-shaped amber pieces from Ariño lack the coating of resinicolous fungal mycelia otherwise common in Cretaceous ambers (**Speranza et al., 2015**). Both the mono- to multiphasic inclusions and the lack of fungal coating might be related to the likely partial flooding of the Ariño forest soil, typical of swampy environments. Although resin can solidify on or within the forest soil in tropical or subtropical climate environments (**Henwood, 1993**), plant macrofossils are usually highly altered and poorly preserved in soils and coal deposits (**Delclòs et al., 2020**). The absence of roots associated with the kidney-shaped amber pieces in the root layer could be explained by their differential fossilisation in the partly flooded soil. The inside-out growth pattern of the resin produced by roots, based on our field observations, is incompatible with the inclusion of surrounding soil particles in the outer surface of the resin, as the opaque crust readily hardens and pushes back the sediment around it.

The upper amber-bearing layer from Ariño's AR-1 level is rich in aerial amber pieces (**Figure 2B**, **Figure 2—figure supplement 2**). This amber type results from fluid resin falling on the ground from the trunk or branches (**Martínez-Delclòs et al., 2004**). The aerial amber pieces commonly have delicate morphologies and preserve external desiccation surfaces, both elements indicating very limited transport. Overall, the upper layer is interpreted as a litter layer namely resulting from the autochthonous-parautochthonous accumulation of strictly ex situ aerial amber pieces, but also occasionally containing amber pieces showing surface polishing or scratching and thus likely being more allochthonous in nature, that is, transported and deposited far away from their production environment (**Figure 6A**). Moreover, the absence of strictly in situ kidney-shaped amber pieces in the litter layer suggests that AR-1 corresponds to a single cycle of forest floor installation-destruction. Charcoalified wood remains are abundant in this layer; these were previously found in Ariño and were related to wildfires (**Villanueva-Amadoz et al., 2015**; **Vajda et al., 2016**), which have been deemed as promoters of resin production and accumulation (**Najarro et al., 2010**; **Seyfullah et al., 2018**). On the other hand, the aerial amber is highly fossiliferous, with 145 bioinclusions/kg (excluding coprolites, spiderwebs, and undetermined bioinclusions). Although determining amber bioinclusion richness is prone to multiple biases (e.g., bioinclusion occurrence data should be ideally limited to aerial amber, as kidney-shaped amber fragments were almost certainly devoid of bioinclusions), this value is among the highest reported worldwide. Richness data from other Cretaceous Albian to Cenomanian amber localities range from about 10–80 inclusions/kg (**Grimaldi et al., 2002**; **Néraudeau et al., 2002**; **Girard et al., 2013**; **Peñalver et al., 2018**; **Zheng et al., 2018**), although values surpassing the 500 insects/kg have been exceptionally reported (**Rasnitsyn and Quicke, 2002**). A few bioinclusions are covered by a white foam consisting of microscopic bubbles produced by decomposition fluids during early diagenesis (**Figure 4—figure supplement 1I**), similar to that commonly observed in the Eocene Baltic amber (**Martínez-Delclòs et al., 2004**), but otherwise rare among Cretaceous ambers.

The charophyte, palynological, and ostracod data provided herein are also indicative of a very limited transport of these remains prior to burial. The utricles of the two clavatoracean charophytes found are well preserved and abundant, suggesting that these remains are autochthonous or parautochthonous. The occurrence of clavatoracean portions of thalli associated with the fructifications supports this inference. The studied palynological samples show conspicuous abundances of pollen related to araucariacean trees and angiosperms in ARN-01 (root layer), which could indicate parautochthony based on their limited pollen production and dispersal potential (**Taylor and Hu, 2010**). Samples ARN-03 and ARN-04 (litter layer) contain low araucariacean and angiosperm pollen and high amounts of allochthonous wind-transported miospores such as *Cyathidites* spp., *Inaperturopollenites dubius*, and *Classopollis* spp., which suggest chiefly allochthonous assemblages. In contrast, ARN-02 (at the top of the root layer) shows a parautochthonous-allochthonous transitional assemblage based on an increase of fern spores and erdtmanithecalean pollen, as well as lower values of araucariacean pollen than ARN-03 and ARN-04. The previous palaeobotanical accounts from Ariño concluded parautochthony based on the good palynomorph preservation, with some samples even showing their original tetrad configuration, although they recognised that some charcoalified wood remains could be allochthonous (**Villanueva-Amadoz et al., 2015**; **Vajda et al., 2016**). Lastly, the studied ostracods constitute a relatively rich assemblage characterised by abundant specimens with closed carapaces (**Figure 5AA and BB**), which together with the low percentage of broken individuals points towards autochthonous remains (**Trabelsi et al., 2021**).

The previous taphonomic accounts on the Ariño vertebrates indicated the absence or lowest grade of biostratinomic transport. The abundant vertebrate fossils are namely found in monotaxic (occasionally bitaxic) concentrations of well-preserved, articulated, or semi-articulated remains (**Alcalá et al., 2012**; **Alcalá et al., 2018**; **Buscalioni et al., 2013**; **Villanueva-Amadoz et al., 2015**). Coprolites, likely dinosaurian, show a palynomorph composition similar to that of the rock (**Vajda et al., 2016**). By integrating all the taphonomic data from the diverse palaeobiological elements from Ariño, we can conclude that the great majority of the assemblage, except for some pollen and charcoalified plant material, as well as a small percentage of the amber, had an autochthonous or parautochthonous origin, and therefore roughly inhabited or was produced in the same area where it fossilised. This circumstance, although critical for inferring reliable data on the palaeoecosystem (**Martínez-Delclòs et al., 2004**), remains infrequent among palaeontological deposits, particularly those jointly preserving dinosaur remains and fossiliferous amber. Indeed, the three previously reported localities where fossiliferous amber was found associated with dinosaur bonebeds, all from the Late Cretaceous, show clear signs of being either allochthonous or clearly mixed assemblages in which at least a substantial part of the vertebrate remains suffered significant transport prior to burial (**Néraudeau et al., 2003**; **Currie et al., 2008**; **DePalma, 2010**): (1) Fouras/Bois Vert (="Plage de la Vierge") was interpreted as resulting from a catastrophic event such as a storm in a coastal estuarine environment, with the fragmentary bones showing evidence of considerable pre-burial transport; however, amber was assumed to be not heavily transported due to the lack of rounding (**Néraudeau et al., 2003**); (2) the Pipestone Creek monodominant vertebrate assemblage corresponds to disarticulated bones formed by a fluvial allochthonous accumulation in a vegetated floodplain, and interpreted as a mass mortality event; no taphonomic assessment for the amber was provided (**Tanke, 2004**; **Currie et al., 2008**; **Cockx et al., 2020**); and (3) Bone Butte's Stratum 11 was reconstructed as a mixed (~70/30) autochthonous/allochthonous vertebrate assemblage deposited in a river oxbow lake; amber showed no signs of significant transport (**DePalma, 2010**). From the diagenetic standpoint, a high maturity of the Ariño amber samples is inferred based on the absence of exocyclic methylenic bands at 880 cm^{-1}, 1640 cm^{-1}, and 3070 cm^{-1} in the FTIR spectra, in accordance with their Cretaceous age (**Grimalt et al., 1988**). Furthermore, there is no significant difference in the distribution of trimethylnaphthalene isomers between the Ariño amber and the other ambarene-rich Cretaceous Iberian ambers in the GC-MS analyses (**Menor-Salván et al., 2016**), suggesting a similar thermal and diagenetic history (**Strachan et al., 1988**).

Age of the level AR-1

Our charophyte, palynological, and ostracod data support the dating of the level AR-1 as early Albian in age (around 110 Ma), as previously proposed for Ariño and, more generally, the whole Escucha Formation (**Alcalá et al., 2012**; **Tibert et al., 2013**; **Villanueva-Amadoz et al., 2015**; **Bover-Arnal et al., 2016**; **Vajda et al., 2016**). The whole timespan of the co-occurrence of the charophytes *Atopochara trivolvis* var. *trivolvis* and *Clavator harrisii* var. *harrisii* is late Barremian–early Albian. However, in the late Barremian–early Aptian timespan, these species are associated to *A. trivolvis* var. *triquetra* (**Pérez-Cano et al., 2020**). Based on the occurrence of homogeneous populations of *A. trivolvis* var. *trivolvis*, the studied assemblage is assigned to the upper Aptian–lower Albian European Clavator grovesii var. corrugatus (= Clavator grovesii var. lusitanicus) biozone of **Riveline et al., 1996**. This view is complementary to that based on the previously found co-occurrence in Ariño of *Clavator harrisii* var. *harrisii* and *Clavator harrisii* var. *zavialensis* indicating an early Albian age (**Tibert et al., 2013**). The oldest occurrence of *A. trivolvis* var. *trivolvis* has recently been reported from the upper Barremian (**Pérez-Cano et al., 2020**), but this variety is more characteristic of upper Aptian–Albian deposits (**Martín-Closas, 2000**). Regarding the palynomorphs, and in accordance with the age inferred by **Peyrot et al., 2007**, the occurrence of *Retimonocolpites dividuus* (**Figure 5—figure supplement 1N**) in ARN-03 indicates an age not older than late Aptian (**Burden and Hills, 1989**), and the low occurrence of *Tricolpites* sp. (**Figure 5—figure supplement 1P**) indicates a lower Albian age for the studied level (**Tanrikulu et al., 2018**).

Resin-producing tree

Identifying which plant sources created the resin accumulations that led to the present amber deposits is still contentious, and different conifer groups have been proposed for the Cretaceous:

†Cheirolepidiaceae, Araucariaceae, and Cupressaceae in Laurasia and other groups such as †Erdtmanithecales in Gondwana (**Menor-Salván et al., 2016**; **Seyfullah et al., 2020**). The GC-MS results (**Figure 3B**, **Figure 3—figure supplement 1**) classify the Ariño amber among the amberene-rich group of Cretaceous Iberian ambers. In that regard, Ariño shows the same distribution as other Iberian ambers such as those from Peñacerrada I and San Just in terpenes **I**, **II**, **V**, **VI**, and the alkylnaphthalene **IV**, resulting from the labdane aromatisation, as well as in the overall diterpene composition (**Menor-Salván et al., 2016**). This amberene-rich group is distinguished from the abietane-rich group of Cretaceous Iberian ambers (e.g. El Soplao amber) in the lack of significant terpenes from the pimarane/abietane family as well as ferruginol, a common biomarker of extant Cupressaceae (**Menor-Salván et al., 2016**). Instead, the clerodane-family diterpene **VI** found in Ariño amber, a biomarker of the family Araucariaceae (**Cox et al., 2007**), could indicate that the botanical source of the amber is related to *Araucaria*/*Agathis*. In fact, the resin of *Araucaria bidwillii* is rich in kolavenic acid (**Cox et al., 2007**), which might be a biological precursor of **VI**. The Ariño amber differs from extant Araucariaceae in the lack of pimarane/abietane-class terpenoids. It is possible that early Araucariaceae lacked the biochemical routes of tricyclic diterpenoids that extant representatives possess (**Menor-Salván et al., 2016**). In any case, the most plausible stance for now is to regard the Ariño amber as resulting from araucariacean resin. The finding of charcoalified *Agathoxylon* sp. supports this interpretation, although other types of charcoalified wood likely belonging to other taxonomic groups have been found in Ariño. The presence of araucariacean remains as bioinclusions in Albian amber from the Peñacerrada I locality was proposed as evidence for an araucariacean resin-producing tree (**Kvaček et al., 2018**). Araucariaceans have also been proposed as the source of other Lower Cretaceous ambers such as those from Lebanon, Myanmar, or France (**Poinar et al., 2007**; **Perrichot et al., 2010**; **Seyfullah et al., 2018**).

Palaeoecology

The palaeoecological reconstruction of the coastal swamp forest of Ariño that the data herein presented has allowed is remarkably complete. Floristically, the ecosystem was composed of mixed communities of gymnosperms (namely taxodioids and cheirolepids, but also araucariaceans), ferns, and angiosperms as indicated by the palynological assemblages previously obtained (**Villanueva-Amadoz et al., 2015**; **Vajda et al., 2016**) and the more diverse account presented herein, which is based on larger (or complementary in some aspects) data sampling. Based on coprolite contents, such plants were consumed by the ornithopod and nodosaurid dinosaurs described from the site (**Alcalá et al., 2012**; **Vajda et al., 2016**). As extant taxodioids are chiefly comprised of species with a high water requirement, these trees possibly were subjected to periodic flooding similarly to the bald cypress in modern swamps (**Farjon, 2005**). The extinct cheirolepids ranged from succulent, shrubby xerophytes to tall forest trees adapted to a wide range of habitats, from coasts to uplands slopes, particularly in hot and/or dry climates from lower latitudes (**Anderson et al., 2007**). Moreover, the Ariño swamp local flora was also likely encompassed by anemiacean, dicksoniacean, and/or cyatheacean ferns growing as riparian or in the understorey (**Van Konijnenburg-Van Cittert, 2002**). †Erdtmanithecales, and angiosperms, particularly those of lauralean and chloranthacean affinity, inhabited disturbed and riparian areas (**Doyle et al., 2008**). The diversity of the charophyte and ostracod fauna studied herein is higher than the previously described by **Tibert et al., 2013**, which so far can be explained based on palaeoecological constraints, notably the water salinity parameter, or sampling differences. Both charophytes and ostracods lived in shallow permanent water bodies from the freshwater swamp and were well adapted to fluctuating salinities resulting from marine inputs. The presence of the *Theriosynoecum-Cypridea-Mantelliana* ostracod association strongly evidences freshwater to slightly saline permanent water bodies (**Horne, 2009**). The intraspecific variability observed on the carapace ornamentation within the *Rosacythere denticulata* specimens is regarded as ecophenotypic (**Sames, 2011**), and could indicate an episodic increase in salinity and/or a variation of salinity, evolving towards brackish conditions.

The terrestrial arthropod community of the Ariño swamp forest was very diverse. Spiders, free-roaming or sit-and-wait lurking predators on the forest canopy or floor (**Foelix, 2011**), inhabited the palaeoecosystem, some likely using orbicular webs to hunt the abundant flying insects. The soil-dwelling arthropod fauna consisted of at least mites, jumping bristletails, cockroaches, and psocids, all of which were important for nutrient recycling (**Levings and Windsor, 1985**). The finding of a

rhagidiid mite (**Figure 4A**) is extraordinary, as the fossil record of this predatory group was limited to a few specimens in Eocene amber (**Judson and Wunderlich, 2003**). The Ariño psocid fauna differs from those previously described from other Iberian ambers, and some specimens will be described as new taxa. Extant psocids feed on algae, lichens, and fungi from diverse warm and humid habitats; such autoecology was likely already present in the group during the Cretaceous, rendering them common inhabitants of the resiniferous forests (**Álvarez-Parra et al., 2020b**). The Ariño amber insect groups with phytophagous feeding habits include thrips, hemipterans, and orthopterans. The presence of several thrips as syninclusions could suggest aggregative behaviour. The three aleyrodid hemipterans found are also preserved as syninclusions (**Figure 4I**); the extant relatives of these small sap-sucking insects mostly inhabit angiosperms (**Martin et al., 2000**), contrary to the gymnosperm affinity of the Cretaceous resiniferous trees. Fossil immature thysanopterans are rare, and the Ariño immature specimen could represent an early-stage nymph based on habitus, size, and antennal annulations and microtrichia (**Figure 4B**; **Vance, 1974**).

Holometabolous insects, overwhelmingly diverse and ecologically paramount in modern ecosystems, are well represented in Ariño amber. The exceptional discovery of a lepidopteran caterpillar, rarely encountered in Cretaceous ambers (**Haug and Haug, 2021**) and unprecedented in Iberian amber, implies herbivory not only by adults but also by immature insects in the palaeoecosystem (**Figure 4E**). The two beetle groups tentatively identified, ptinids and cantharids, have been previously found in Iberian amber (**Peris, 2020**). These, according to the habits of extant relatives, are good candidates for having engaged in trophic or even reproductive interactions with plants, as Cretaceous beetles —including some from Iberian amber— are known to have fed on pollen from both gymnosperm and angiosperms, acting as pollinators (**Peris et al., 2020**). The identified dipteran groups presently show various feeding habits, including phytophagy, mycophagy, predation, and ectoparasitism (**McAlpine et al., 1981**). Regarding the latter, female ceratopogonids likely fed on vertebrate blood, probably that from Ariño's dinosaurs according to data from other Iberian ambers (**Pérez-de la Fuente et al., 2011**). As the larval stages and adults of most of the identified dipteran groups chiefly inhabit warm and moist, often aquatic, environments such as diverse wetlands (**McAlpine et al., 1981**), these insects likely thrived in the tropical-subtropical swamp of Ariño. The genus *Burmazelmira* is currently composed of two species from younger ambers; although the discovered *Burmazelmira* sp. male (**Figure 4F**) is similar to *B. grimaldii* from San Just amber (**Arillo et al., 2018**), it shows morphological differences that could warrant describing a new taxon. Lastly, the hymenopteran groups found in Ariño amber are comprised of small to minute forms generally assumed to be idiobiont parasitoids of insect eggs. Platygastroids are the most abundant hymenopterans in Ariño amber, several of them superbly preserved (**Figure 4H**); their predominance is consistent with that observed in other Cretaceous ambers (**Ortega-Blanco et al., 2014**). One mymarommatoid specimen (**Figure 4G**) is similar to *Galloromma turolensis* (†Gallorommatidae) from San Just amber (**Ortega-Blanco et al., 2011**). The Ariño serphitids and mymarommatoids represent the oldest records worldwide for these groups. The Ariño amber has also yielded vertebrate remains, such as the oldest known mammalian hair preserved in amber (**Álvarez-Parra et al., 2020a**) and the pennaceous feather fragment reported herein (**Figure 4J**). These instances showcase the potential of this amber to provide integumentary remains of the vertebrates otherwise preserved as skeleton material in the site's rocks.

Conclusions

Considering the extraordinary abundance and diversity of fossils that both the rocks and the amber have yielded, Ariño can be regarded as the most significant locality to date in which fossiliferous amber has been found associated with a dinosaur bonebed (**Figure 6B**). Although the amber palaeodiversity from Fouras/Bois Vert (France) could potentially match that of Ariño (**Perrichot et al., 2007**; **Tihelka et al., 2021**), the known vertebrate record from Ariño is two orders of magnitude richer, and more complete (**Néraudeau et al., 2003**). The opposite occurs in both the Pipestone Creek (Canada) and the Bone Butte (USA) localities —whereas their vertebrate/dinosaur records are at least comparable (clearly superior for Bone Butte) to those from Ariño, the palaeodiversity described as inclusions from the Ariño amber is one order of magnitude higher, with the fossiliferous potential of the amber probably being significantly greater as well (**Tanke, 2004**; **Currie et al., 2008**; **Nel et al., 2010**; **DePalma, 2010**; **Cockx et al., 2020**). Indeed, the aerial amber from Ariño stands out for being unusually highly fossiliferous, and it has already revealed a remarkable diversity in spite of the early

stages of its study, including morphotypes that will be described as new taxa. Furthermore, Ariño is the first known locality yielding fossiliferous amber and dinosaur remains in which both elements and the remaining palaeontological assemblage assessed —except some pollen and plant macroremains— generally suffered no or low-grade transport prior to burial (autochthony/parautochthony), and from which amber strictly in situ has been reported for the first time. This has enabled a reliable palaeoecological reconstruction and, more importantly, will keep allowing the extraction of sound palaeoecological inferences from upcoming material. Last but not least, Ariño is the oldest known locality preserving fossiliferous amber in a dinosaur bonebed —the only one hitherto described from the Early Cretaceous—, and it also provides the oldest fossiliferous amber from the Iberian Peninsula. All these characteristics render Ariño one of a kind, offering one of the most complete and integrated pictures from an ancient coastal ecosystem through two diverse and complementary taphonomic windows. This unique 'dual' site will remain of interest across many palaeobiological disciplines, and will be of particular significance at promoting studies in emerging fields such as deep-time arthropod-vertebrate interactions.

Materials and methods

Key resources table

Reagent type (species) or resource	Designation	Source or reference	Identifiers	Additional information
Chemical compound, drug	BSTFA + TMCS, 99:1	Merck/Supelco		
Chemical compound, drug	Dichloromethane Optima for HPLC and GC	Fisher Scientific		
Chemical compound, drug	Methanol Optimafor HPLC and GC	Fisher Scientific		
Software, algorithm	ImageFocusAlpha v. 1.3.7.12967.20180920	Euromex		
Software, algorithm	Adobe Photoshop CS6	Adobe Systems	RRID:SCR_014199	
Software, algorithm	Agilent MassHunter Quantitative Analysis B.06.00	Agilent	RRID:SCR_015040	
Software, algorithm	Microsoft Excel v. 16.0.14131.20278	Microsoft Corporation	RRID:SCR_016137	

Fieldwork and material

Amber samples were collected from the level AR-1 of the Ariño outcrop in the Santa María open-pit coal mine, near Ariño village (Teruel Province, Aragón, Spain). The amber excavation was carried out in July 2019, after two previous palaeontological amber surveys in July 2018 and May 2019 (permissions 201/10–2018 and 201/10–2019 of the Aragon Government, Spain). Excavation of aerial amber pieces was carried out at two locations from the AR-1 level (***Figure 1C***), near the AR-1/154, AR-1/156, AR-1/157, and AR-1/158 vertebrate concentrations. The acronyms of the amber pieces and bioinclusions are AR-1-A-(number). Field observations on copal associated with *Agathis australis*, herein used for comparison, were conducted at a private property in Waipapakauri, close to State Highway 1, North Island of New Zealand, by EP and XD, during a campaign in 2011 and with the permission of the landowner. Macrophotographs of the Ariño site and material were made using a Canon EOS70D.

Amber preparation and imaging

Most of the amber pieces with bioinclusions were embedded in epoxy resin (Epo-tek 301) following ***Corral et al., 1999*** to facilitate their preservation and observation. Several amber pieces were cut to observe the fluid inclusions and mineralisations. The amber piece AR-1-A-2019.129 was imaged and analysed with a SEM JEOL 6010 PLUS/LA 20 kV with RX (EDS) detector at the Instituto Geológico y Minero de España laboratories (Tres Cantos, Spain). The sample AR-1-A-2018.1 of amber-infilled plant tissue was cleaved in several fragments and thin sections were made to obtain both longitudinal and transversal views of the cellular structure; other non-prepared samples were examined with a Leica Wild M3Z stereozoom microscope, equipped with a x2 frontal lens and a 0.5–40 zoom, under tangential light. Microphotographs of the amber inclusions and thin sections of amber-filled plant tissue were made with a sCMEX20 digital camera attached to an Olympus CX41 compound microscope taken through ImageFocusAlpha version 1.3.7.12967.20180920; images were processed using Photoshop CS6; fine black lines in figures indicate composition of photographs; ***Figure 4C, E and F***,

Figure 4—figure supplement 1A,G,H, and *Figure 4—figure supplement 2C* are formed by stacking. SEM images of amber-infilled plant tissue preserving the cellular structure and charcoalified wood were obtained with a Quanta 200 electronic microscope at the Museo Nacional de Ciencias Naturales (Madrid, Spain). SEM imaging of the amber pieces with taphonomic importance was carried out with a Quanta 200 electronic microscope at the Scanning Electron Microscopy Unit of the CCiTUB (Universitat de Barcelona); all pieces, except AR-1-A-2019.79, were sputtered with graphite. The amber piece AR-1-A-2019.79 was first submerged in a 50 % solution of 37 % HCl for 2 min and then in distilled water for 1 day to remove calcium carbonate and gypsum, respectively, from the surface of the piece. The amber piece AR-1-A-2019.93 was carefully unearthed in the field, although a small protruding fragment around 3 cm long was detached. The amber piece and the small fragment were protected to avoid friction on their surface during extraction, transport, and handling. Both were submerged in distilled water for 1 day. The small fragment was treated with four ultrasonic cleaning cycles of 30 s each; it was placed in a plastic pocket bag with distilled water to avoid friction on its surface. This methodology allows an accurate visualisation of its unaltered surface at the SEM to check if it suffered abrasion.

Amber characterisation

The FTIR (Fourier Transform Infrared Spectroscopy) analyses of the Ariño and San Just ambers were conducted using an IR PerkinElmer Frontier spectrometer that utilises a diamond ATR system with a temperature stabilised DTGS detector and a CsI beam splitter at the Molecular Spectrometry Unit of the CCiTUB. The study of molecular composition and chemotaxonomy was performed after extraction with CH_2Cl_2:CH_3OH (DCM:MeOH 2:1) in a Soxhlet extractor using 2.3858 g of crushed stalactite-type aerial amber pieces, selected for showing the highest transparency and the least possible weathering and inclusion content. After extraction, 1.6126 g of polymeric, organic-insoluble material remained. The crude extract was directly analysed by gas chromatography-mass spectrometry (GC-MS), concentrated to 5 ml at a rotovap, and fractionated using silica gel column chromatography. Successive elution was performed using n-hexane, n-hexane:DCM 3:1 (fraction 1), DCM (fraction 2), and methanol (fraction 3). Fraction one contained the aliphatic and tetralin-rich fraction, and fraction two contained the aromatic fraction, both were analysed by GC-MS after concentration to 1 ml by evaporation in a nitrogen stream. Fraction three was dried, forming a creamy white pulverulent residue containing polar terpenoids and resin acids, analysed after conversion to trimethylsilyl derivatives by reaction with N,O-bis-(trimethylsilyl)trifluoroacetamide containing 1 % trimethylchlorosilane at 65 °C for 3 hr. GC-MS analyses were performed with an Agilent 6,850 GC coupled to an Agilent 5975 C quadrupole mass spectrometer. Separation was performed on a HP-5MS column coated with (5%-phenyl)-methylpolysiloxane (30 m long, 0.25 mm inner diameter, 0.25 μm film thickness). The operating conditions were as follows: 8 psi He carrier gas pressure, initial temperature hold at 40 °C for 1.5 min, increased from 40°C to 150°C at a rate of 15 °C/min, hold for 2 min, increased from 150°C to 255°C at a rate of 5 °C/min, held isothermal for 20 min, and finally increased to 300 °C at a rate of 5 °C/min. The sample was injected in the split mode at 50:1 with the injector temperature at 290 °C. The mass spectrometer was operated in the electron impact mode at an ionisation energy of 70 eV and scanned from 40 to 700 Da. The temperature of the ion source was 230 °C and the quadrupole temperature was 150 °C. Data were acquired and processed using the Agilent MassHunter software, and percentages were calculated by normalising the peak areas of the corresponding compounds in the total extracts. Identification of compounds was based on authentic standards and comparison of mass spectra with standard libraries and literature.

Charophytes and ostracods

Specimens were obtained from the level AR-1 after picking the rock associated with the amber. The acronyms of the charophytes and ostracods are AR-1-CH-(number) and AR-1-OS-(number), respectively. The microfossil preparation followed standard methods in micropalaeontology as applied to charophytes (***Pérez-Cano et al., 2020***). Scanning Electron Microscope (SEM) images of selected charophyte and ostracod specimens were obtained using the Quanta 200 scanning electron microscope at the Scanning Electron Microscopy Unit of the CCiTUB. Additional SEM images of ostracods were obtained using a JEOL 6400 device at the Faculty of Earth Sciences, Geography and Astronomy, University of Vienna (Austria). Clavatoracean utricular nomenclature follows that of ***Grambast, 1968***.

Palynology

Four consecutive samples from the level AR-1 (ARN-01–ARN-04) were prepared for palynological studies by the Geologischer Dienst NRW (Germany) (https://www.gd.nrw.de). ARN-01 and ARN-02 were obtained from the lower (root) layer rich in kidney-shaped amber pieces (ARN-02 closer to the upper layer), and ARN-03 and ARN-04 were gathered from the upper (litter) layer rich in aerial amber pieces (***Figure 1B***). The rock samples were treated following standard palynological preparation techniques (***Traverse, 2007***) consisting of acid attack with HCl, HF, and diluted HNO_3 and sieving with different grid sizes (500, 250, 75, 50, and 12 µm). Samples were studied with an Olympus BX51 bright-field light microscope attached to a ColorView IIIu camera. The percentage ranges provided in the results show the lowest and the highest abundance of the corresponding taxon in the four samples.

Material availability

All the material obtained prior and during the amber excavation in Ariño is housed at the Museo Aragonés de Paleontología (Fundación Conjunto Paleontológico de Teruel-Dinópolis, Teruel Province, Spain).

The copal pieces for comparison are housed at the Museo Geominero of the Instituto Geológico y Minero de España (IGME) and Universitat de Barcelona (UB).

Acknowledgements

We are grateful to the SAMCA Group for its collaboration and to the Dirección General de Patrimonio Cultural del Gobierno de Aragón (Spain) for permissions to excavate. We thank Alejandro Gallardo (Laboratory of Palaeontology-UB), Telm Bover-Arnal (UB), Guillermo Rey, José Antonio Peñas, and the technicians of the CCiTUB. Thanks are also due to the editor and the reviewers Min Zhu and Andrew Ross, as well as an anonymous referee, for their constructive comments. Equipment has been partly funded by FEDER (IGME13-4E-1518). We are grateful to the Departamento de Ciencia, Innovación y Sociedad del Conocimiento, Gobierno de Aragón (Grupo de Investigación de Referencia E04_20 R) y Ministerio de Ciencia e Innovación, Gobierno de España (Unidad de Paleontología de Dinosaurios de Teruel and AMBERIA Team). This study is a contribution to the projects CRE CGL2017-84419, PGC2018-094034-B-C22 (both from the Ministerio de Ciencia, Innovación y Universidades, Spain, AEI/FEDER, UE), BIOGEOEVENTS CGL2015-69805-P (Ministerio de Economía y Competitividad, Spain, and the European Regional Development Fund), 2017SGR-824 (AGAUR, Generalitat de Catalunya, Spain), UNESCO IGCP Project 661 of the Austrian Academy of Sciences, and LR18 ES07 (Faculty of Sciences, Université de Tunis El Manar). JP-C acknowledges the support from the Ministerio de Ciencia e Innovación (BES-2016–076469). AS-G is funded by an APOSTD2019 Research Fellowship (Generalitat Valenciana, Spain) and the European Social Fund. RP-dlF is funded by a Museum Research Fellowship (Oxford University Museum of Natural History, UK). This study forms part of the first author's (SÁ-P) doctoral thesis, supported by a grant from the Secretaria d'Universitats i Recerca de la Generalitat de Catalunya and the European Social Fund (2020FI_B1 00002).

Additional information

Funding

Funder	Grant reference number	Author
Ministerio de Ciencia, Innovación y Universidades	CGL2017-84419	Eduardo Barrón Xavier Delclòs
Ministerio de Ciencia, Innovación y Universidades	PGC2018-094034-B-C22	Luis Alcalá
Ministerio de Economía y Competitividad	CGL2015-69805-P	Carles Martín-Closas
Generalitat de Catalunya	2017SGR-824	Carles Martín-Closas Xavier Delclòs

Funder	Grant reference number	Author
Generalitat de Catalunya	2020FI_B1 00002	Sergio Álvarez-Parra
Oxford University	Museum Research Fellowship	Ricardo Pérez-de la Fuente
Ministerio de Ciencia, Innovación y Universidades	BES-2016-076469	Jordi Pérez-Cano
Austrian Academy of Sciences	Project 661	Khaled Trabelsi
Université de Tunis	LR18 ES07	Khaled Trabelsi
Generalitat Valenciana	APOSTD2019	Alba Sánchez-García
European Regional Development Fund	IGME13-4E-1518	Rafael P Lozano

The funders had no role in study design, data collection and interpretation, or the decision to submit the work for publication.

Author contributions

Sergio Álvarez-Parra, Conceptualization, Fieldwork, Investigation, Methodology, Supervision, Writing - original draft, Writing - review and editing; Ricardo Pérez-de la Fuente, Conceptualization, Fieldwork, Investigation, Writing - original draft, Writing - review and editing; Enrique Peñalver, Conceptualization, Fieldwork, Investigation, Supervision, Writing - review and editing; Eduardo Barrón, Fieldwork, Investigation, Methodology, Project administration; Luis Alcalá, Fieldwork, Investigation, Project administration; Jordi Pérez-Cano, Carles Martín-Closas, Khaled Trabelsi, César Menor-Salván, Marc Philippe, Investigation, Methodology; Nieves Meléndez, Rafael P Lozano, Fieldwork, Investigation, Methodology; Rafael López Del Valle, Fieldwork, Methodology; David Peris, Eduardo Espílez, Fieldwork, Investigation; Ana Rodrigo, Víctor Sarto i Monteys, Constanza Peña-Kairath, Fieldwork; Carlos A Bueno-Cebollada, Alba Sánchez-García, Antonio Arillo, Investigation; Luis Mampel, Investigation, Fieldwork; Xavier Delclòs, Conceptualization, Fieldwork, Investigation, Project administration, Supervision, Writing - review and editing

Author ORCIDs

Sergio Álvarez-Parra http://orcid.org/0000-0002-0232-1647
Ricardo Pérez-de la Fuente http://orcid.org/0000-0002-2830-2639
Enrique Peñalver http://orcid.org/0000-0001-8312-6087
Eduardo Barrón http://orcid.org/0000-0003-4979-1117
Luis Alcalá http://orcid.org/0000-0002-6369-6186
Jordi Pérez-Cano http://orcid.org/0000-0002-1782-5346
Carles Martín-Closas http://orcid.org/0000-0003-4349-738X
Khaled Trabelsi http://orcid.org/0000-0003-0207-9819
Rafael López Del Valle http://orcid.org/0000-0002-7164-9558
David Peris http://orcid.org/0000-0003-4074-7400
Ana Rodrigo http://orcid.org/0000-0001-7201-9286
Víctor Sarto i Monteys http://orcid.org/0000-0003-2701-6558
Carlos A Bueno-Cebollada http://orcid.org/0000-0003-0367-4177
Marc Philippe http://orcid.org/0000-0002-4658-617X
Alba Sánchez-García http://orcid.org/0000-0003-0911-2001
Constanza Peña-Kairath http://orcid.org/0000-0002-4877-7754
Xavier Delclòs http://orcid.org/0000-0002-2233-5480

Decision letter and Author response

Decision letter https://doi.org/10.7554/eLife.72477.sa1
Author response https://doi.org/10.7554/eLife.72477.sa2

Additional files

Supplementary files

- Supplementary file 1. List of palynomorphs recorded from the lower Albian bonebed level AR-1 of Ariño and their relative abundances. ARN-01 and ARN-02 were obtained from the lower root layer with kidney-shaped amber pieces, and ARN-03 and ARN-04 from the upper litter layer rich in aerial amber pieces, all of them within the level AR-1. See also ***Figure 5*** and ***Figure 5—figure supplement 1***.
- Transparent reporting form

Data availability

All data generated or analysed during this study are included in the manuscript and supporting files. Palynomorphs taxa and their abundances are available in Supplementary File 1. Source data of FTIR analyses are available in Figure 3-source data 1-3. Source data of GC-MS are available in Figure 3-source data 4.

References

Alcalá L, Espílez E, Mampel L, Kirkland JI, Ortiga M, Rubio D, González A, Ayala D, Cobos A, Royo-Torres R, Gascó F, Pesquero MD. 2012. A New Lower Cretaceous Vertebrate Bonebed Near Ariño (Teruel, Aragón, Spain); Found and Managed in a Joint Collaboration Between a Mining Company and a Palaeontological Park. *Geoheritage* **4**: 275–286. DOI: https://doi.org/10.1007/s12371-012-0068-y

Alcalá L, Espílez E, Mampel L. 2018. Ariño: La mina de los dinosaurios. Zamora S (Ed). *Fósiles: Nuevos Hallazgos Paleontológicos En Aragón*. Zaragoza, Spain: Institución «Fernando el Católico». p. 111–141.

Allison PA. 1990. Diagenesis. Pyrite. Briggs DEG, Crowther PR (Eds). *Palaeobiology: A Synthesis*. Hoboken, USA: Blackwell Science. p. 253–255.

Alonso J, Arillo A, Barrón E, Corral JC, Grimalt J, López JF, López R, Martínez-delclòs X, Ortuño V, Peñalver E, Trincão PR. 2000. A new fossil resin with biological inclusions in lower cretaceous deposits from álava (northern spain, basque-cantabrian basin). *Journal of Paleontology* **74**: 158–178. DOI: https://doi.org/10.1666/0022-3360(2000)074<0158:ANFRWB>2.0.CO;2

Álvarez-Parra S, Delclòs X, Solórzano-Kraemer MM, Alcalá L, Peñalver E. 2020a. Cretaceous amniote integuments recorded through a taphonomic process unique to resins. *Scientific Reports* **10**: 19840. DOI: https://doi.org/10.1038/s41598-020-76830-8, PMID: 33199731

Álvarez-Parra S, Peñalver E, Nel A, Delclòs X. 2020b. The oldest representative of the extant barklice genus Psyllipsocus (Psocodea: Trogiomorpha: Psyllipsocidae) from the Cenomanian amber of Myanmar. *Cretaceous Research* **113**: 104480. DOI: https://doi.org/10.1016/j.cretres.2020.104480

Anderson JA, Anderson HM, Cleal CJ. 2007. Brief History of the Gymnosperms: Classification, Biodiversity, Phytogeography and Ecology. Pretoria, South Africa: South African National Biodiversity Institute.

Arillo A, Blagoderov V, Peñalver E. 2018. Early Cretaceous parasitism in amber: A new species of Burmazelmira fly (Diptera: Archizelmiridae) parasitized by a Leptus sp. mite (Acari, Erythraeidae). *Cretaceous Research* **86**: 24–32. DOI: https://doi.org/10.1016/j.cretres.2018.02.006

Bell PR, Currie PJ. 2016. A high-latitude dromaeosaurid, Boreonykus certekorum, gen. et sp. nov. (Theropoda), from the upper Campanian Wapiti Formation, west-central Alberta. *Journal of Vertebrate Paleontology* **36**: e1034359. DOI: https://doi.org/10.1080/02724634.2015.1034359

Bover-Arnal T, Moreno-Bedmar JA, Frijia G, Pascual-Cebrian E, Salas R. 2016. Chronostratigraphy of the Barremian – Early Albian of the Maestrat Basin (E Iberian Peninsula): integrating strontium-isotope stratigraphy and ammonoid biostratigraphy. *Newsletters on Stratigraphy* **49**: 41–68. DOI: https://doi.org/10.1127/nos/2016/0072

Burden ET, Hills LV. 1989. Illustrated key to genera of Lower Cretaceous terrestrial palynomorphs (excluding megaspores) of Western Canada. *American Association of Stratigraphic Palynologists Foundation, Contribution Series* **21**: 1–147.

Buscalioni ÁD, Alcalá L, Espílez E, Mampel L. 2013. European Goniopholididae from the Early Albian Escucha Formation in Ariño (Teruel, Aragón, Spain). *Spanish Journal of Palaeontology* **28**: 103. DOI: https://doi.org/10.7203/sjp.28.1.17835

Cervera A, Pardo G, Villena J. 1976. Algunas precisiones litoestratigráficas sobre la formación 'Lignitos de Escucha. *Tecniterrae* **14**: 25–33.

Cockx P, McKellar R, Tappert R, Vavrek M, Muehlenbachs K. 2020. Bonebed amber as a new source of paleontological data: The case of the Pipestone Creek deposit (Upper Cretaceous), Alberta, Canada. *Gondwana Research* **81**: 378–389. DOI: https://doi.org/10.1016/j.gr.2019.12.005

Cockx P, Tappert R, Muehlenbachs K, Somers C, McKellar RC. 2021. Amber from a Tyrannosaurus rex bonebed (Saskatchewan, Canada) with implications for paleoenvironment and paleoecology. *Cretaceous Research* **125**: 104865. DOI: https://doi.org/10.1016/j.cretres.2021.104865

Corral JC, López Del Valle R, Alonso J. 1999. El ámbar cretácico de Álava (Cuenca Vasco-Cantábrica, norte de España). Su colecta y preparación. *Estudios Del Museo de Ciencias Naturales de Álava* **14**:7–21.

Cox RE, Yamamoto S, Otto A, Simoneit BRT. 2007. Oxygenated di- and tricyclic diterpenoids of southern hemisphere conifers. *Biochemical Systematics and Ecology* **35**: 342–362. DOI: https://doi.org/10.1016/j.bse.2006.09.013
Currie PJ, Langston W, Tanke DH. 2008. A New Horned Dinosaur from an Upper Cretaceous Bone Bed in Alberta. NRC Research Press. DOI: https://doi.org/10.1139/9780660198194
Delclòs X, Arillo A, Peñalver E, Barrón E, Soriano C, Valle RLD, Bernárdez E, Corral C, Ortuño VM. 2007. Fossiliferous amber deposits from the Cretaceous (Albian) of Spain. *Comptes Rendus Palevol* **6**: 135–149. DOI: https://doi.org/10.1016/j.crpv.2006.09.003
Delclòs X, Peñalver E, Ranaivosoa V, Solórzano-Kraemer MM. 2020. Unravelling the mystery of "Madagascar copal": Age, origin and preservation of a Recent resin. *PLOS ONE* **15**: e0232623. DOI: https://doi.org/10.1371/journal.pone.0232623, PMID: 32421746
DePalma RA. 2010. Geology, Taphonomy, and Paleoecology of a Unique Upper Cretaceous Bonebed near the Cretaceous-Tertiary Boundary in South Dakota. University of Kansas.
DePalma R, Cichocki F, Dierick M, Feeney R. 2010. Preliminary notes on the first recorded amber insects from the Hell Creek Formation. *The Journal of Paleontological Sciences* **10**: C0001.
DePalma RA, Burnham DA, Martin LD, Larson PL, Bakker RT. 2015. The first giant raptor (Theropoda: Dromaeosauridae) from the Hell Creek Formation. *Paleontological Contributions* **14**: 1–16. DOI: https://doi.org/10.17161/paleo.1808.18764
Doyle JA, Endress PK, Upchurch GR. 2008. Early Cretaceous monocots: a phylogenetic evaluation. *Acta Musei Nationalis Pragae Series B - Historia Naturalis* **64**: 59–87. DOI: https://doi.org/10.5167/uzh-11654
Farjon A. 2005. A Monograph of Cupressaceae and Sciadopitys. London, UK: Royal Botanic Gardens.
Foelix RF. 2011. Biology of Spiders. Oxford, UK: Oxford University Press.
Girard V, Breton G, Perrichot V, Bilotte M, Le Loeuff J, Nel A, Philippe M, Thevenard F. 2013. The Cenomanian amber of Fourtou (Aude, Southern France): Taphonomy and palaeoecological implications. *Annales de Paléontologie* **99**: 301–315. DOI: https://doi.org/10.1016/j.annpal.2013.06.002
Grambast L. 1968. Evolution of the utricle in the Charophyte genera Perimneste Harris and Atopochara Peck. *Journal of the Linnean Society of London, Botany* **61**: 5–11. DOI: https://doi.org/10.1111/j.1095-8339.1968.tb00099.x
Grimaldi DA, Engel MS, Nascimbene PC. 2002. Fossiliferous Cretaceous amber from Myanmar (Burma): its rediscovery, biotic diversity, and paleontological significance. *American Museum Novitates* **3361**: 1–71. DOI: https://doi.org/10.1206/0003-0082(2002)3612.0.CO;2
Grimalt JO, Simoneit BRT, Hatcher PG, Nissenbaum A. 1988. The molecular composition of ambers. *Organic Geochemistry* **13**: 677–690. DOI: https://doi.org/10.1016/0146-6380(88)90089-7
Haug JT, Haug C. 2021. A 100 million-year-old armoured caterpillar supports the early diversification of moths and butterflies. *Gondwana Research* **93**: 101–105. DOI: https://doi.org/10.1016/j.gr.2021.01.009
Henwood A. 1993. Recent plant resins and the taphonomy of organisms in amber: a review. *Modern Geology* **19**: 35.
Horne DJ. 2009. Purbeck–Wealden. Whittaker JE, Hart MB (Eds). *Ostracods in British Stratigraphy*. London, UK: The Geological Society of London. p. 289–308.
Judson M, Wunderlich J. 2003. Rhagidiidae (Acari, Eupodoidea) from Baltic amber. *Acta Zoologica Cracoviensia* **46**:147–152.
Kawamura T, Koshino H, Nakamura T, Nagasawa Y, Nanao H, Shirai M, Uesugi S, Ohno M, Kimura K. 2018. Amberene and 1-methylamberene, isolated and identified from Kuji amber (Japan). *Organic Geochemistry* **120**: 12–18. DOI: https://doi.org/10.1016/j.orggeochem.2018.02.014
Kirkland JI, Alcalá L, Loewen MA, Espílez E, Mampel L, Wiersma JP. 2013. The basal nodosaurid ankylosaur Europelta carbonensis n. gen., n. sp. from the Lower Cretaceous (lower Albian) Escucha Formation of northeastern Spain. *PLOS ONE* **8**: e80405. DOI: https://doi.org/10.1371/journal.pone.0080405, PMID: 24312471
Kvaček J, Barrón E, Heřmanová Z, Mendes MM, Karch J, Žemlička J, Dudák J. 2018. Araucarian conifer from late Albian amber of northern Spain. *Papers in Palaeontology* **4**: 643–656. DOI: https://doi.org/10.1002/spp2.1223
Langenheim JH. 1967. Preliminary investigations of Hymenaea courbaril as a resin producer. *Journal of the Arnold Arboretum* **48**: 203–230. DOI: https://doi.org/10.5962/p.185723
Langenheim JH. 2003. Plant Resins: Chemistry, Evolution, Ecology, and Ethnobotany. Portland, USA: Timber Press.
Levings SC, Windsor DM. 1985. Litter arthropod populations in a tropical deciduous forest: relationships between years and arthropod groups. *The Journal of Animal Ecology* **54**: 61–69. DOI: https://doi.org/10.2307/4620
Lozano RP, Pérez-de la Fuente R, Barrón E, Rodrigo A, Viejo JL, Peñalver E. 2020. Phloem sap in Cretaceous ambers as abundant double emulsions preserving organic and inorganic residues. *Scientific Reports* **10**: 9751. DOI: https://doi.org/10.1038/s41598-020-66631-4, PMID: 32546844
Martin JH, Mifsud D, Rapisarda C. 2000. The whiteflies (Hemiptera: Aleyrodidae) of Europe and the Mediterranean Basin. *Bulletin of Entomological Research* **90**: 407–448. DOI: https://doi.org/10.1017/s0007485300000547, PMID: 11082558
Martín-Closas C. 2000. Els Caròfits Del Juràssic Superior i Cretaci Inferior de La Península Ibèrica. Barcelona, Spain: Institut d'Estudis Catalans, Arxius de les Seccions de Ciències, vol. 125.

Martín-Closas C, Vicente A, Pérez-Cano J, Sanjuan J, Bover-Arnal T. 2018. On the earliest occurrence of Tolypella section Tolypella in the fossil record and the age of major clades in extant Characeae. *Botany Letters* **165**: 23–33. DOI: https://doi.org/10.1080/23818107.2017.1387078

Martínez-Delclòs X, Briggs DE, Peñalver E. 2004. Taphonomy of insects in carbonates and amber. *Palaeogeography, Palaeoclimatology, Palaeoecology* **203**: 19–64. DOI: https://doi.org/10.1016/S0031-0182(03)00643-6

McAlpine JF, Peterson BV, Shewell GE, Teskey HJ, Vockeroth JR, Wood DM. 1981. Manual of Nearctic Diptera. Ottawa, Canada: Research Branch Agriculture Canada.

McDonald AT, Espílez E, Mampel L, Kirkland JI, Alcalá L. 2012. An unusual new basal iguanodont (Dinosauria: Ornithopoda) from the Lower Cretaceous of Teruel, Spain. *Zootaxa* **3595**: 61–76. DOI: https://doi.org/10.11646/zootaxa.3595.1.3

McKellar RC, Jones E, Engel MS, Tappert R, Wolfe AP, Muehlenbachs K, Cockx P, Koppelhus EB, Currie PJ. 2019. A direct association between amber and dinosaur remains provides paleoecological insights. *Scientific Reports* **9**: 17916. DOI: https://doi.org/10.1038/s41598-019-54400-x, PMID: 31784622

Meléndez A, Soria AR, Meléndez N. 2000. A coastal lacustrine system in the Lower Barremian from the Oliete Sub-basin, central Iberian Range, northeastern Spain. In: Gierlowski-Kordesch EH, Kelts KR (Eds), Lake Basins Through Space and Time. Tulsa, USA: The American Association of Petroleum Geologists. *Studies in Geology* **46**:279–284.

Menor-Salván C, Simoneit BRT, Ruiz-Bermejo M, Alonso J. 2016. The molecular composition of Cretaceous ambers: identification and chemosystematic relevance of 1,6-dimethyl-5-alkyltetralins and related bisnorlabdane biomarkers. *Organic Geochemistry* **93**: 7–21. DOI: https://doi.org/10.1016/j.orggeochem.2015.12.010

Najarro M, Peñalver E, Rosales I, Pérez-de la Fuente R, Daviero-Gomez V, Gomez B, Delclòs X. 2009. Unusual concentration of Early Albian arthropod-bearing amber in the Basque-Cantabrian Basin (El Soplao, Cantabria, Northern Spain): palaeoenvironmental and palaeobiological implications. *Geologica Acta* **7**: 363–387. DOI: https://doi.org/10.1344/105.000001443

Najarro M, Peñalver E, Pérez-de la Fuente R, Ortega-Blanco J, Menor-Salván C, Barrón E, Soriano C, Rosales I, López Del Valle R, Velasco F, Tornos F, Daviero-Gomez V, Gomez B, Delclòs X. 2010. Review of the El Soplao amber outcrop, Early Cretaceous of Cantabria, Spain. *Acta Geologica Sinica* **84**: 959–976. DOI: https://doi.org/10.1111/j.1755-6724.2010.00258.x

Nel A, DePalma RA, Engel MS. 2010. A Possible Hemiphlebiid Damselfly in Late Cretaceous Amber from South Dakota (Odonata: Zygoptera). *Transactions of the Kansas Academy of Science* **113**: 231. DOI: https://doi.org/10.1660/062.113.0312

Néraudeau D, Perrichot V, Dejax J, Masure E, Nel A, Phillipe M, Moreau P, Guillocheau F, Guyot T. 2002. A new fossil locality with insects in amber and plants (likely Uppermost Albian): Archingeay (Charente-Maritime, France. *Geobios* **35**: 233–240. DOI: https://doi.org/10.1016/S0016-6995(02)00024-4

Néraudeau D, Allain R, Perrichot V, Videt B, de Lapparent de Broin F, Guillocheau F, Philippe M, Rage JC, Vullo R. 2003. Découverte d'un dépôt paralique à bois fossiles, ambre insectifère et restes d'Iguanodontidae (Dinosauria, Ornithopoda) dans le Cénomanien inférieur de Fouras (Charente-Maritime, Sud-Ouest de la France). *Comptes Rendus Palevol* **2**: 221–230. DOI: https://doi.org/10.1016/S1631-0683(03)00032-0

Ortega-Blanco J, Peñalver E, Delclòs X, Engel MS. 2011. False fairy wasps in early Cretaceous amber from Spain (Hymenoptera: Mymarommatoidea. *Palaeontology* **54**: 511–523. DOI: https://doi.org/10.1111/j.1475-4983.2011.01049.x

Ortega-Blanco J, McKellar RC, Engel MS. 2014. Diverse scelionid wasps from Early Cretaceous Álava amber, Spain (Hymenoptera: Platygastroidea. *Bulletin of Geosciences* **89**: 553–571. DOI: https://doi.org/10.3140/bull.geosci.1463

Peñalver E, Delclòs X, Soriano C. 2007. A new rich amber outcrop with palaeobiological inclusions in the Lower Cretaceous of Spain. *Cretaceous Research* **28**: 791–802. DOI: https://doi.org/10.1016/j.cretres.2006.12.004

Peñalver E, Delclòs X. 2010. Spanish amber. Penney D (Ed). *Biodiversity of Fossils in Amber from the Major World Deposits*. Rochdale, UK: Siri Scientific Press. p. 236–270.

Peñalver E, González-Fernández B, López Del Valle R, Barrón E, Lozano RP, Rodrigo A, Pérez-de la Fuente R, Menéndez-Casares E. 2018. Un nuevo yacimiento de ámbar cretácico en Asturias (norte de España): Resultados preliminares de la excavación paleontológica de 2017 en La Rodada (La Manjoya. Vaz N, Sá AA (Eds). *Yacimientos Paleontológicos Excepcionales En La Península Ibérica*. Madrid, Spain: Instituto Geológico y Minero de España, Cuadernos del Museo Geominero. p. 289–299.

Pérez-Cano J, Bover-Arnal T, Martín-Closas C. 2020. Barremian charophytes from the Maestrat Basin. *Cretaceous Research* **115**: 104544. DOI: https://doi.org/10.1016/j.cretres.2020.104544

Pérez-de la Fuente R, Delclòs X, Peñalver E, Arillo A. 2011. Biting midges (Diptera: Ceratopogonidae) from the Early Cretaceous El Soplao amber (N Spain). *Cretaceous Research* **32**: 750–761. DOI: https://doi.org/10.1016/j.cretres.2011.05.003

Pérez-García A, Espílez E, Mampel L, Alcalá L. 2015. A new European Albian turtle that extends the known stratigraphic range of the Pleurosternidae (Paracryptodira. *Cretaceous Research* **55**: 74–83. DOI: https://doi.org/10.1016/j.cretres.2015.02.007

Pérez-García A, Espílez E, Mampel L, Alcalá L. 2020. A new basal turtle represented by the two most complete skeletons of Helochelydridae in Europe. *Cretaceous Research* **107**: 104291. DOI: https://doi.org/10.1016/j.cretres.2019.104291

Peris D. 2020. Coleoptera in amber from Cretaceous resiniferous forests. *Cretaceous Reseach* **113**: 104484. DOI: https://doi.org/10.1016/j.cretres.2020.104484
Peris D, Labandeira CC, Barrón E, Delclòs X, Rust J, Wang B. 2020. Generalist Pollen-Feeding Beetles during the Mid-Cretaceous. *IScience* **23**: 100913. DOI: https://doi.org/10.1016/j.isci.2020.100913, PMID: 32191877
Perrichot V, Néraudeau D, Nel A, De Ploeg G. 2007. A reassessment of the Cretaceous amber deposits from France and their palaeontological significance. *African Invertebrates* **48**: 213–227.
Perrichot V, Néraudeau D, Tafforeau P. 2010. Charentese amber. Penney D (Ed). *Biodiversity of Fossils in Amber from the Major World Deposits*. Rochdale, UK: Siri Scientific Press. p. 193–208.
Peyrot D, Rodríguez-López JP, Barrón E, Meléndez N. 2007. Palynology and biostratigraphy of the Escucha Formation in the Early Cretaceous Oliete Sub-basin, Teruel, Spain. *Revista Española de Micropaleontología* **39**:135–154.
Poinar G, Lambert JB, Wu Y. 2007. Araucarian source of fossiliferous Burmese amber: spectroscopic and anatomical evidence. *Journal of the Botanical Research Institute of Texas* **1**:449–455.
Rasnitsyn AP, Quicke DLJ. 2002. History of Insects. Kluwer Academic Publishers. DOI: https://doi.org/10.1007/0-306-47577-4
Riveline J, Berger JP, Feist M, Martín-Closas C, Schudack M, Soulié-Märsche I. 1996. European Mesozoic-Cenozoic charophyte biozonation. *Bulletin de La Société Géologique de France* **167**: 453–468.
Rodríguez-López JP, Meléndez N, Soria AR, De Boer PL. 2009. Reinterpretación estratigráfica y sedimentológica de las formaciones Escucha y Utrillas de la Cordillera Ibérica. *Revista de La Sociedad Geológica de España* **22**:163–219.
Rogers RR, Eberth DA, Fiorillo AR. 2007. Bonebeds. Genesis, Analysis and Paleobiological Significance. The University of Chicago Press. DOI: https://doi.org/10.7208/chicago/9780226723730.001.0001
Salas R, Guimerà J. 1996. Rasgos estructurales principales de la cuenca cretácica inferior del Maestrazgo (Cordillera Ibérica oriental. *Geogaceta* **20**: 1704–1706.
Sames B. 2011. Early Cretaceous Theriosynoecum Branson 1936 in North America and Europe. *Micropaleontology* **57**:291–344.
Schmidt AR, Jancke S, Lindquist EE, Ragazzi E, Roghi G, Nascimbene PC, Schmidt K, Wappler T, Grimaldi DA. 2012. Arthropods in amber from the Triassic Period. *PNAS* **109**: 14796–14801. DOI: https://doi.org/10.1073/pnas.1208464109, PMID: 22927387
Seyfullah L.J, Beimforde C, Dal Corso J, Perrichot V, Rikkinen J, Schmidt AR. 2018. Production and preservation of resins - past and present. *Biological Reviews of the Cambridge Philosophical Society* **93**: 1684–1714. DOI: https://doi.org/10.1111/brv.12414, PMID: 29726609
Seyfullah LJ, Roberts EA, Schmidt AR, Ragazzi E, Anderson KB, Rodrigues do Nascimento D Jr, Ferreira da Silva Filho W, Kunzmann L. 2020. Revealing the diversity of amber source plants from the Early Cretaceous Crato Formation, Brazil. *BMC Evolutionary Biology* **20**: 107. DOI: https://doi.org/10.1186/s12862-020-01651-2, PMID: 32819273
Speranza M, Ascaso C, Delclòs X, Peñalver E. 2015. Cretaceous mycelia preserving fungal polysaccharides: taphonomic and paleoecological potential of microorganisms preserved in fossil resins. *Geologica Acta* **13**: 363–385. DOI: https://doi.org/10.1344/GeologicaActa2015.13.4.8
Strachan MG, Alexander R, Kagi RI. 1988. Trimethylnaphthalenes in crude oils and sediments: effects of source and maturity. *Geochimica et Cosmochimica Acta* **52**: 1255–1264. DOI: https://doi.org/10.1016/0016-7037(88)90279-7
Stuchlik L, Ziembińska-Tworzydło M, Kohlman-Adamska A, Grabowska I, Ważyńska H, Sadowska A. 2002. Atlas of Pollen and Spores of the Polish Neogene Vol. 2, Gymnosperms. Warsaw, Poland: Polish Academy of Sciences.
Tanke DH. 2004. Mosquitoes and mud: the 2003 Royal Tyrrell Museum of Palaeontology expedition to the Grande Praire region (Northwestern Alberta, Canada). *Alberta Paleontological Society Bulletin* **19**:3–31.
Tanrikulu S, Doyle JA, Delusina I. 2018. Early Cretaceous (Albian) spores and pollen from the Glen Rose Formation of Texas and their significance for correlation of the Potomac Group. *Palynology* **42**: 438–456. DOI: https://doi.org/10.1080/01916122.2017.1374309
Taylor TN, Alvin KL. 1984. Ultrastructure and development of mesozoic pollen: classopollis. *American Journal of Botany* **71**: 575–587. DOI: https://doi.org/10.1002/j.1537-2197.1984.tb12543.x
Taylor DW, Hu S. 2010. Coevolution of early angiosperms and their pollinators: Evidence for pollen. *Palaeontographica Abteilung B* **283**: 103–135. DOI: https://doi.org/10.1127/palb/283/2010/103
Tibert NE, Colin JP, Kirkland JI, Alcalá L, Martín-Closas C. 2013. Lower Cretaceous nonmarine ostracodes from an Escucha Formation dinosaur bonebed in eastern Spain. *Micropaleontology* **59**:83–91.
Tihelka E, Huang D, Perrichot V, Cai C. 2021. A previously missing link in the evolution of dasytine soft-winged flower beetles from Cretaceous Charentese amber (Coleoptera, Melyridae). *Papers in Palaeontology* **12**: 1360. DOI: https://doi.org/10.1002/spp2.1360
Trabelsi K, Sames B, Nasri A, Piovesan EK, Elferhi F, Skanji A, Houla Y, Soussi M, Wagreich M. 2021. Ostracods as proxies for marginal marine to non-marine intervals in the mid-Cretaceous carbonate platform of the Central Tunisian Atlas (North Africa): response to major short-term sea-level falls. *Cretaceous Research* **117**: 104581. DOI: https://doi.org/10.1016/j.cretres.2020.104581
Traverse A. 2007. Paleopalynology. Springer. DOI: https://doi.org/10.1007/978-1-4020-5610-9
Vajda V, Pesquero Fernández MD, Villanueva-Amadoz U, Lehsten V, Alcalá L. 2016. Dietary and environmental implications of Early Cretaceous predatory dinosaur coprolites from Teruel, Spain. *Palaeogeography, Palaeoclimatology, Palaeoecology* **464**: 134–142. DOI: https://doi.org/10.1016/j.palaeo.2016.02.036

Van Konijnenburg-Van Cittert JHA. 2002. Ecology of some Late Triassic to Early Cretaceous ferns in Eurasia. *Review of Palaeobotany and Palynology* **119**: 113–124. DOI: https://doi.org/10.1016/S0034-6667(01)00132-4

Vance TC. 1974. Larvae of the Sericothripini (Thysanoptera: Thripidae), with reference to other larvae of the Terebrantia, of Illinois. *Illinois Natural History Survey Bulletin* **31**: 144–208. DOI: https://doi.org/10.21900/j.inhs.v31.149

Villanueva-Amadoz U, Sender LM, Alcalá L, Pons D, Royo-Torres R, Diez JB. 2015. Paleoenvironmental reconstruction of an Albian plant community from the Ariño bonebed layer (Iberian Chain, NE Spain). *Historical Biology* **27**: 430–441. DOI: https://doi.org/10.1080/08912963.2014.895826

Zheng D, Chang S-C, Perrichot V, Dutta S, Rudra A, Mu L, Kelly RS, Li S, Zhang Q, Zhang Q, Wong J, Wang J, Wang H, Fang Y, Zhang H, Wang B. 2018. A Late Cretaceous amber biota from central Myanmar. *Nature Communications* **9**: 3170. DOI: https://doi.org/10.1038/s41467-018-05650-2, PMID: 30093646

RESEARCH ARTICLE

Figures and figure supplements

Dinosaur bonebed amber from an original swamp forest soil

Sergio Álvarez-Parra *et al*

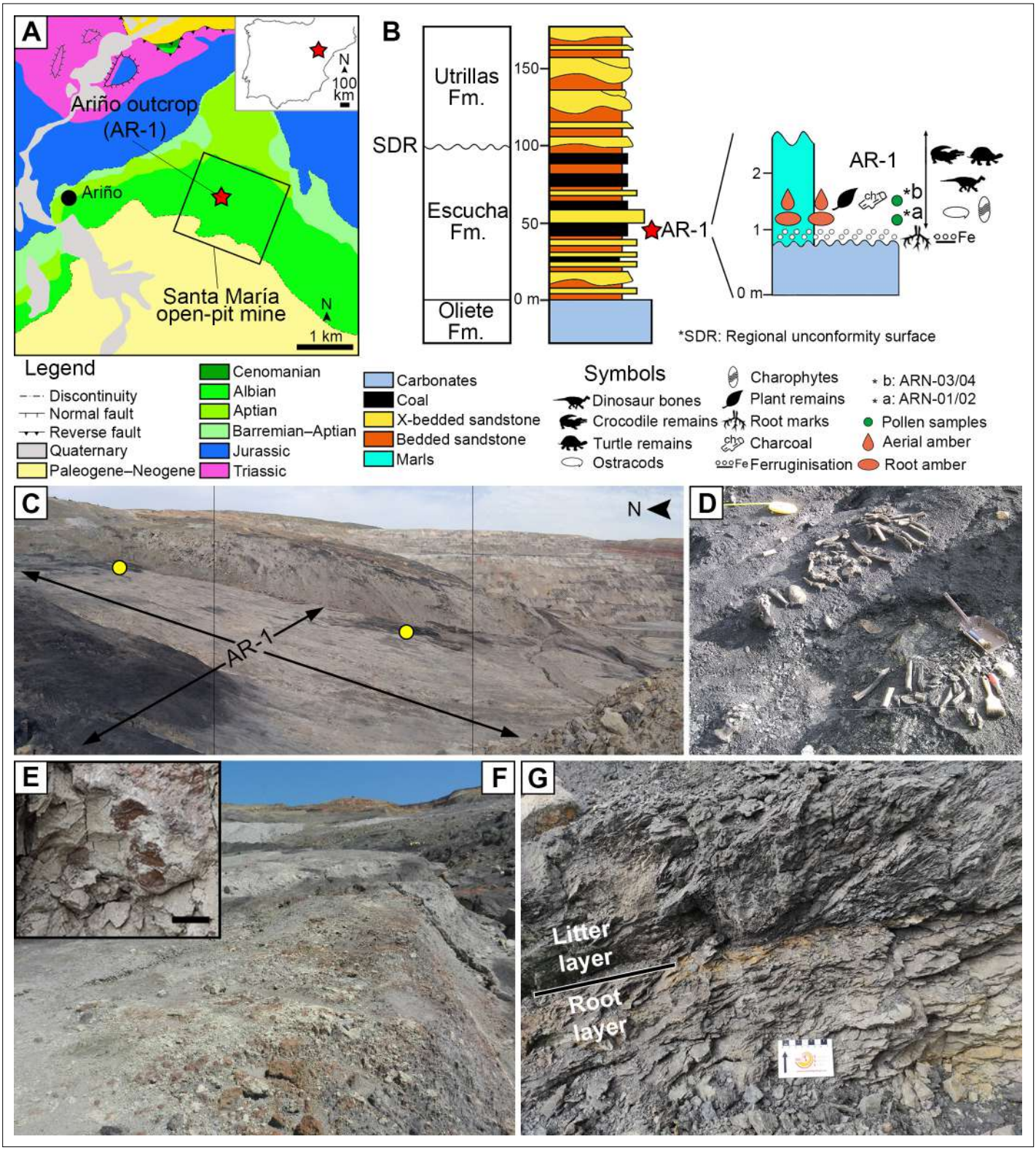

Figure 1. The Lower Cretaceous vertebrate bonebed and amber site of Ariño. (**A**) Geographical and geological location; modified from ***Alcalá et al., 2012*** (**B**) Stratigraphic location of the level AR-1; general stratigraphic log from the Oliete Sub-basin, modified from ***Kirkland et al., 2013***, is shown at the left, together with the location of the level AR-1 (red star); a section of the latter, including the stratigraphic location of the amber deposit studied herein, is shown at the right. (**C**) Santa María open-pit coal mine with indication of the level AR-1 and the two excavated areas rich in aerial amber (yellow dots); the bottom of the open-pit coal is at the right. (**D**) One of the 160+ bone concentrations found in Ariño, AR-1/10, during vertebrate fieldwork in

Figure 1 continued on next page

Figure 1 continued

2010, showing the holotype of the nodosaurid *Europelta carbonensis*; metal dustpan ~30 cm long. (**E**) Root marks at the top of the carbonates below the level AR-1; scale bar, 1 cm. (**F**) Carbonates right below the level AR-1, displaying edaphic features at the top. (**G**) Detail photograph of the level AR-1 showing the lower root layer (with amber from resin exuded by roots) and the upper litter layer (with amber from resin exuded by trunk and branches); centimetric scale. See also ***Video 1***.

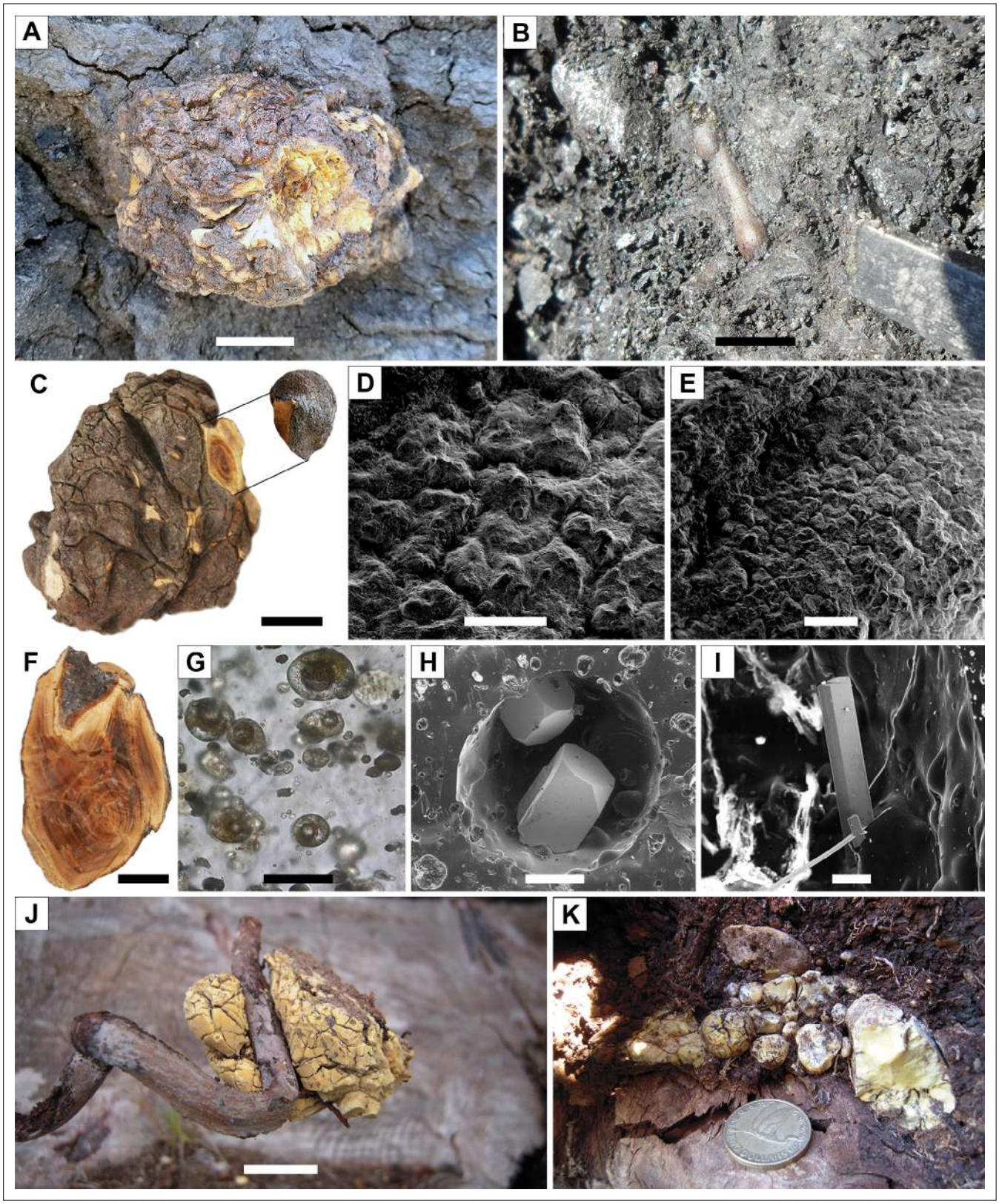

Figure 2. Diversity of amber pieces from the AR-1 level and Pleistocene copal pieces for comparison. (**A**) Kidney-shaped amber piece (root layer). (**B**) Aerial amber piece (litter layer), corresponding to a resin flow, after partially removing surrounding rock during fieldwork. (**C**) Kidney-shaped amber piece (AR-1-A-2019.93) from the root layer. (**D, E**) Two different areas of the external surface from a fragment detached from the piece in (**C**), showing the preserved delicate surface microprotrusions and no evidence of linear grooves. (**F**) Kidney-shaped amber piece (root layer) showing the internal banding

Figure 2 continued on next page

Figure 2 continued

pattern (AR-1-A-2019.132). (**G**) Triphasic (solid+ liquid + gas) bubble-like inclusions in a kidney-shaped amber piece (AR-1-A-2019.130). (**H**) Two pyrite cuboctahedrons in an alleged empty space left by a fluid inclusion (amber piece AR-1-A-2019.86). (**I**) Needle-shaped crystals from an iron sulphate (likely szomolnokite) growing inward from the walls in an alleged empty space left by a fluid inclusion (amber piece AR-1-A-2019.129). (**J**) Kidney-shaped piece of Pleistocene copal associated to an *Agathis australis* root from an overturned stump in Waipapakauri (North Island, New Zealand). (**K**) Pleistocene copal pieces associated to the root system of the same *A. australis* stump; coin 2.65 cm in diameter. Scale bars, 2 cm (**A–C**, **F, J**), 0.5 mm (**D**), 1 mm (**E**), 0.03 mm (**G**), 0.2 mm (**H**), and 0.1 mm (**I**). See also ***Video 1***.

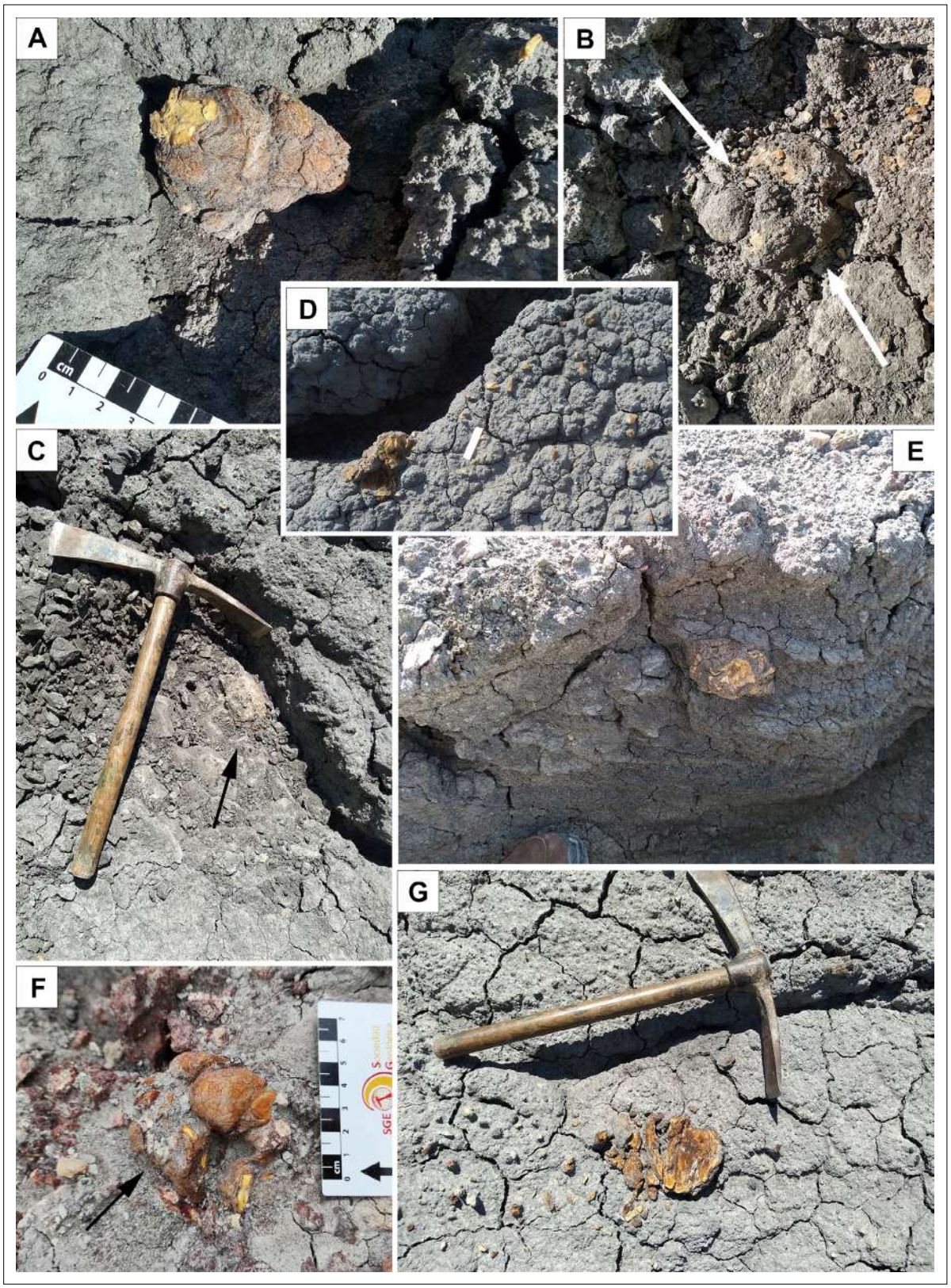

Figure 2—figure supplement 1. Strictly in situ (autochthonous) kidney-shaped amber pieces from the root layer of the lower Albian bonebed level AR-1 of Ariño. (**A**) Slightly elongate piece exposed by the weathering, but not moved, lacking a detached small surface fragment (left). (**B, C**) Two rounded and slightly elongate pieces (white arrows in (**B**) and black arrow in (**C**)) partially exposed during excavation (piece diameter in (**B**) = 9 cm; pickaxe length in (**C**) = 35 cm). (**D**) Strictly in situ piece fragmented by the weathering, and fragments of another piece on the right (paper strip = 4 cm). (**E**)

Figure 2—figure supplement 1 continued on next page

Figure 2—figure supplement 1 continued

Piece partially exposed in the sidewall of a small gully excavated by rain (piece diameter = ca. 7.5 cm). (**F**) Irregular in situ piece indicated with an arrow; centimetric scale. (**G**) Crumbled amber piece (pickaxe length = 35 cm). (**D, E**) excavated during July 2018 and the rest during May 2019.

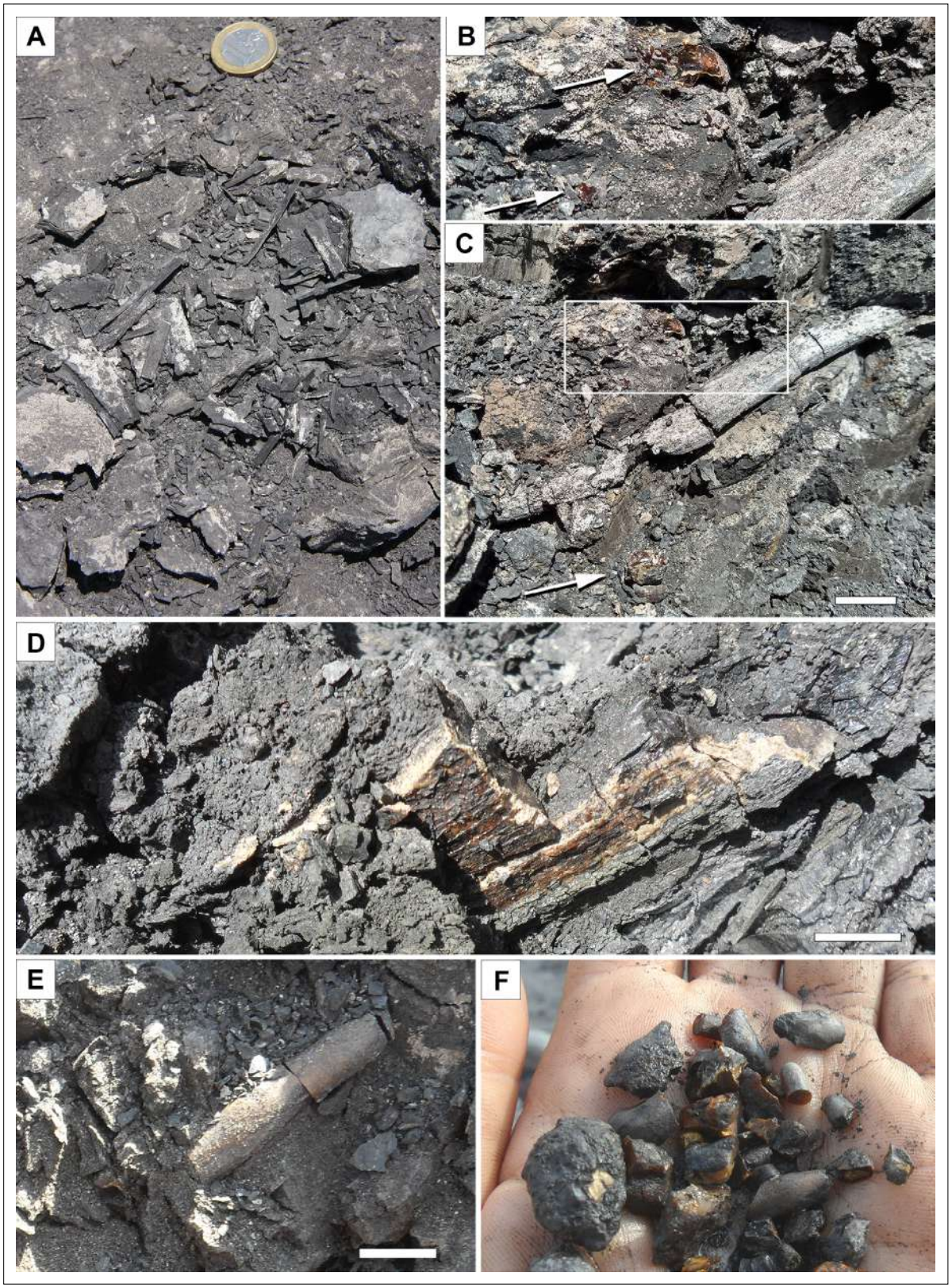

Figure 2—figure supplement 2. Litter layer of the lower Albian bonebed level AR-1 of Ariño. (**A**) Plant remains, most likely elongate charcoalified wood pieces (coin diameter = 2.3 cm). (**B, C**) Strictly ex situ (autochthonous) aerial amber pieces (arrows) and elongate woody remains ((**B**) is the enlarged inset in (**C**)). (**D**) Strictly ex situ flattened amber piece most likely originated from resin coating the trunk or infilling a broken trunk. (**E**) Strictly ex situ stalactite-shaped aerial amber piece. (**F**) Assortment of aerial amber piece fragments. (A, D–F) excavated during July 2019 and the rest during May 2019. Scale bars, 2 cm (**C**), and 1 cm (**D, E**).

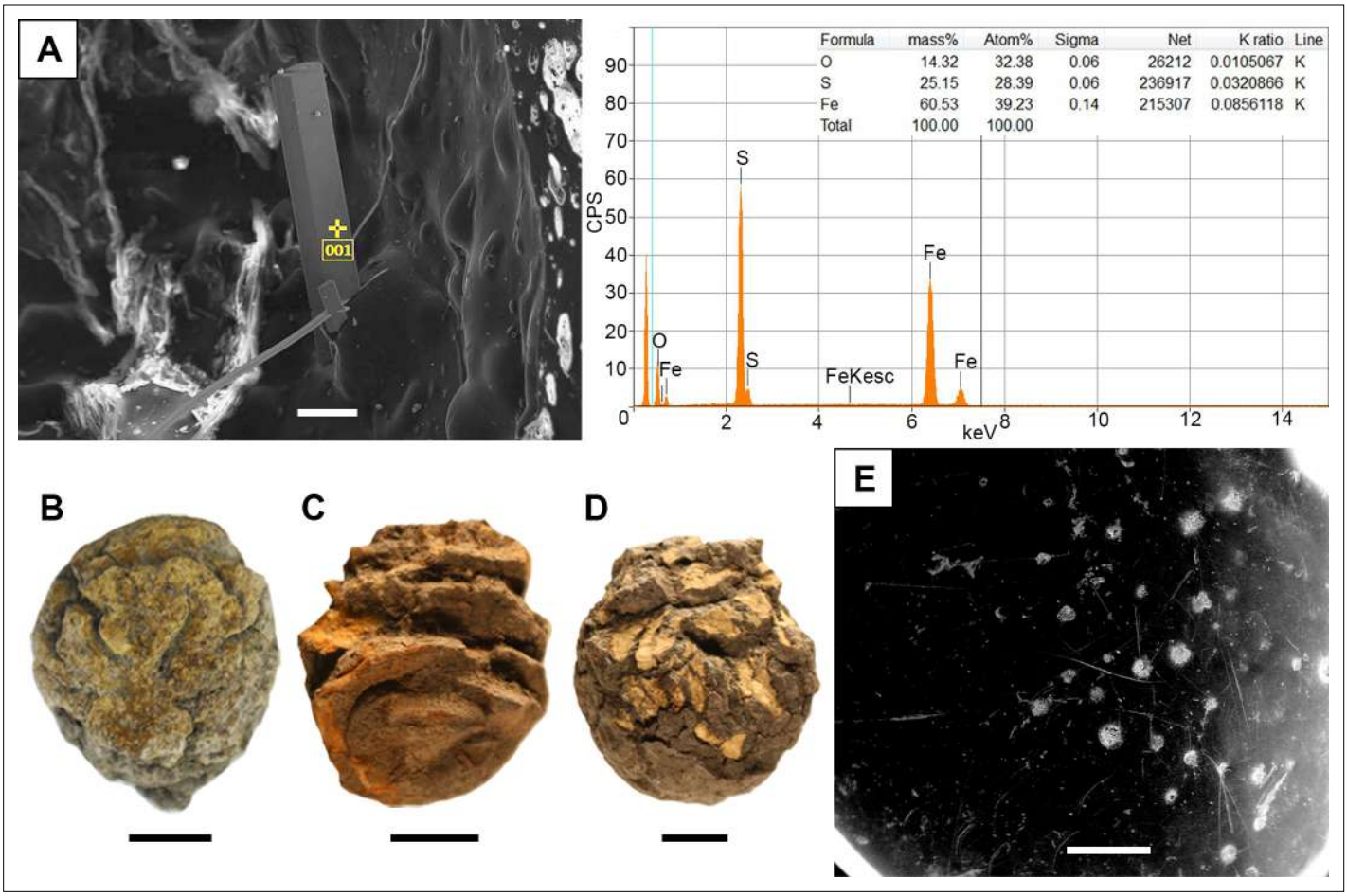

Figure 2—figure supplement 3. Amber pieces with taphonomic interest from the level AR-1 of Ariño. (**A**) EDS analysis of the needle-shaped crystals from an iron sulphate (likely szomolnokite) growing inward from the walls in the alleged empty space left by a fluid bubble-like inclusion of an amber piece (AR-1-A-2019.129). (**B–D**) Small, almost spherical amber masses from the litter layer (AR-1-A-2019.131, AR-1-A-2019.134 and AR-1-A-2019.133, respectively). (**E**) Surface of a peculiar amber piece found in the litter layer, showing surface borings and linear grooves (AR-1-A-2019.79). Scale bars, 0.1 mm (**A**), 5 mm (**B**), 1 cm (**C, D**), and 1 mm (**E**).

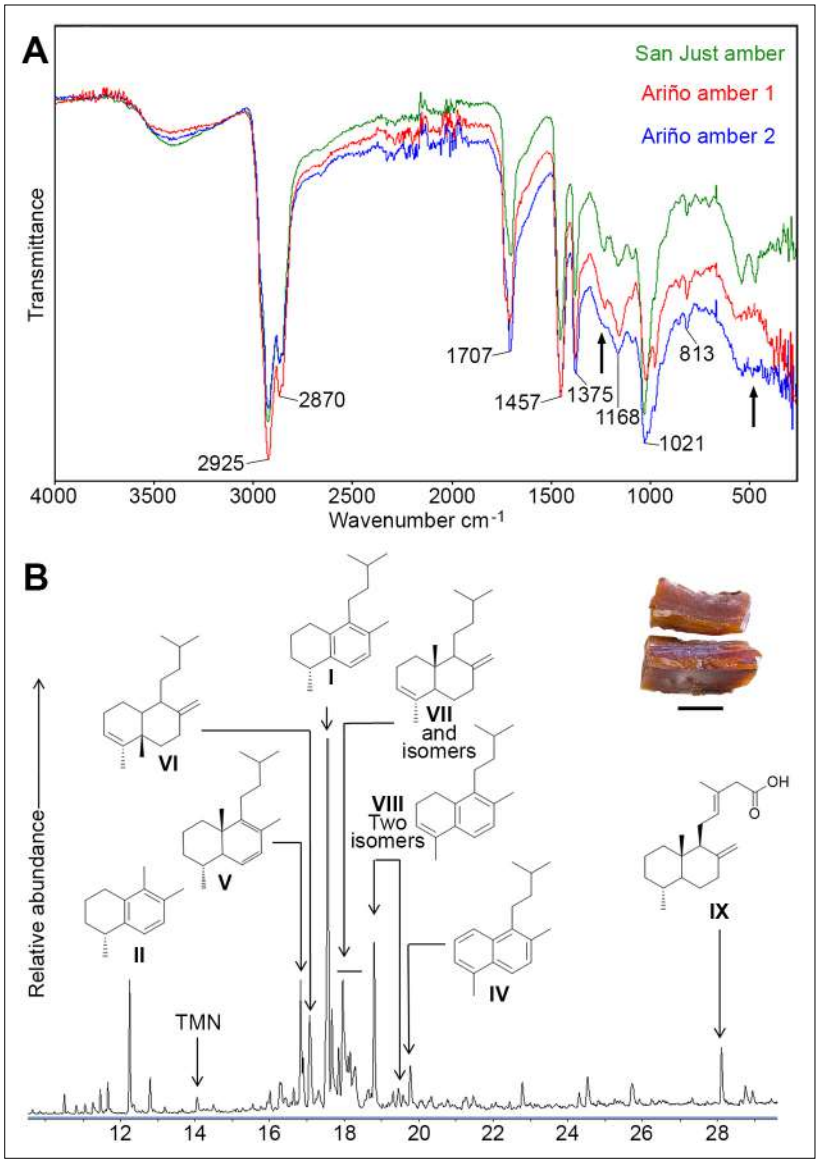

Figure 3. Physicochemical characterisation of the Lower Cretaceous amber from Ariño. (**A**) Infrared (FTIR) spectra obtained from two aerial amber pieces (litter layer); a spectrum from San Just amber (upper Albian) is provided for comparison; arrows indicate the main differences between Ariño and San Just ambers, at around 1200 and 500 cm^{-1}; resolution = 4 cm^{-1}. (**B**) Gas chromatography-mass spectrometry (GC-MS) trace for the underivatised total solvent extract of aerial amber, showing the structures of the main identified terpenoids, referred herein using Roman numerals (full formulation provided in ***Figure 3—figure supplement 1B***); TMN = trimethylnaphthalenes; the analysed aerial amber is shown at the top right (scale bar 0.5 mm).

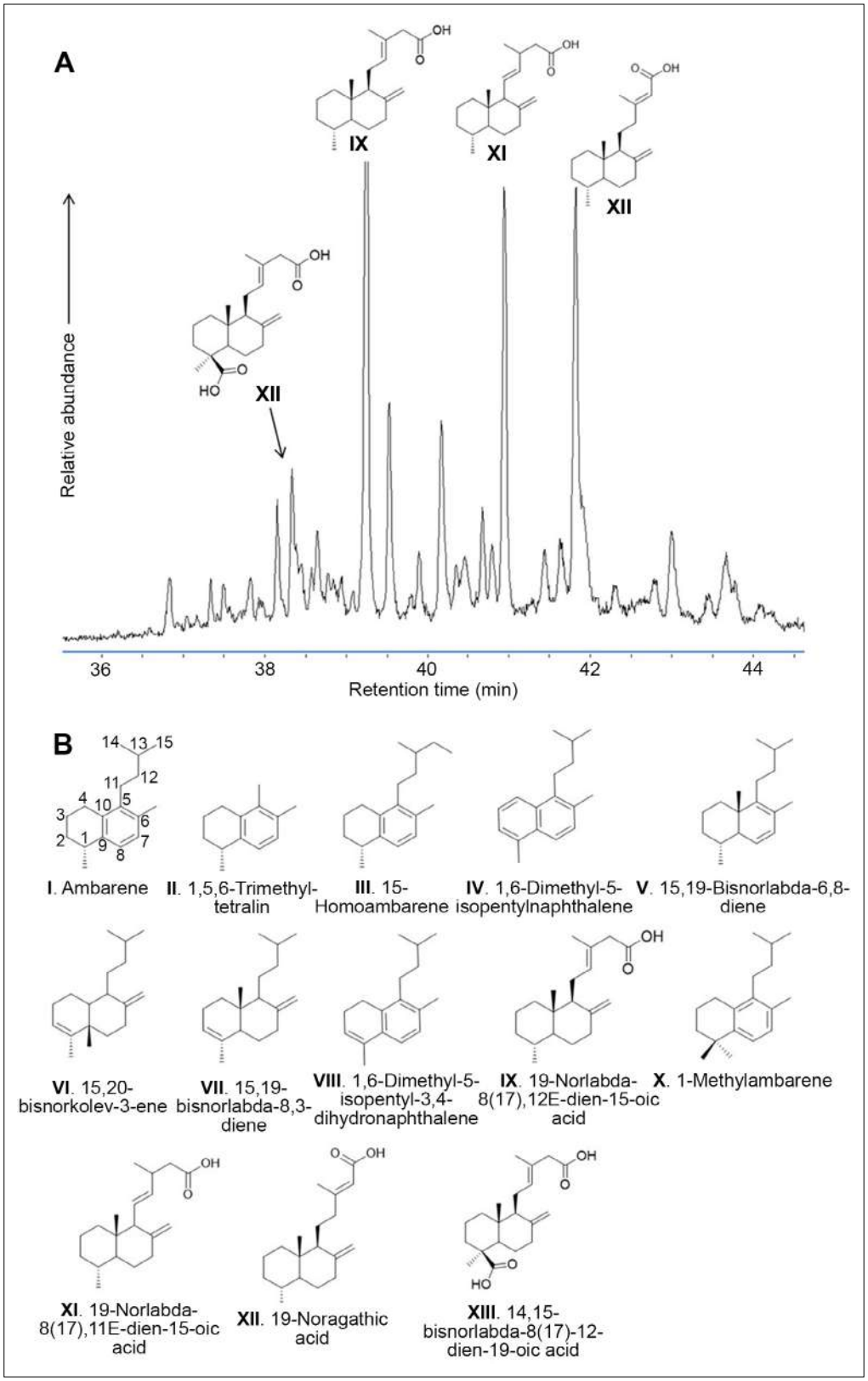

Figure 3—figure supplement 1. Physicochemical characterisation of the Lower Cretaceous amber from Ariño. (**A**) Gas chromatography-mass spectrometry (GC-MS) chromatogram corresponding to the polar fraction of the organic extract of the Ariño amber, showing labdanoic acids as main components; decarboxylation and disproportionation of labdanoic acids lead to the main hydrocarbons found, diterpenes of the labdane family. (**B**) Chemical structures cited in the work.

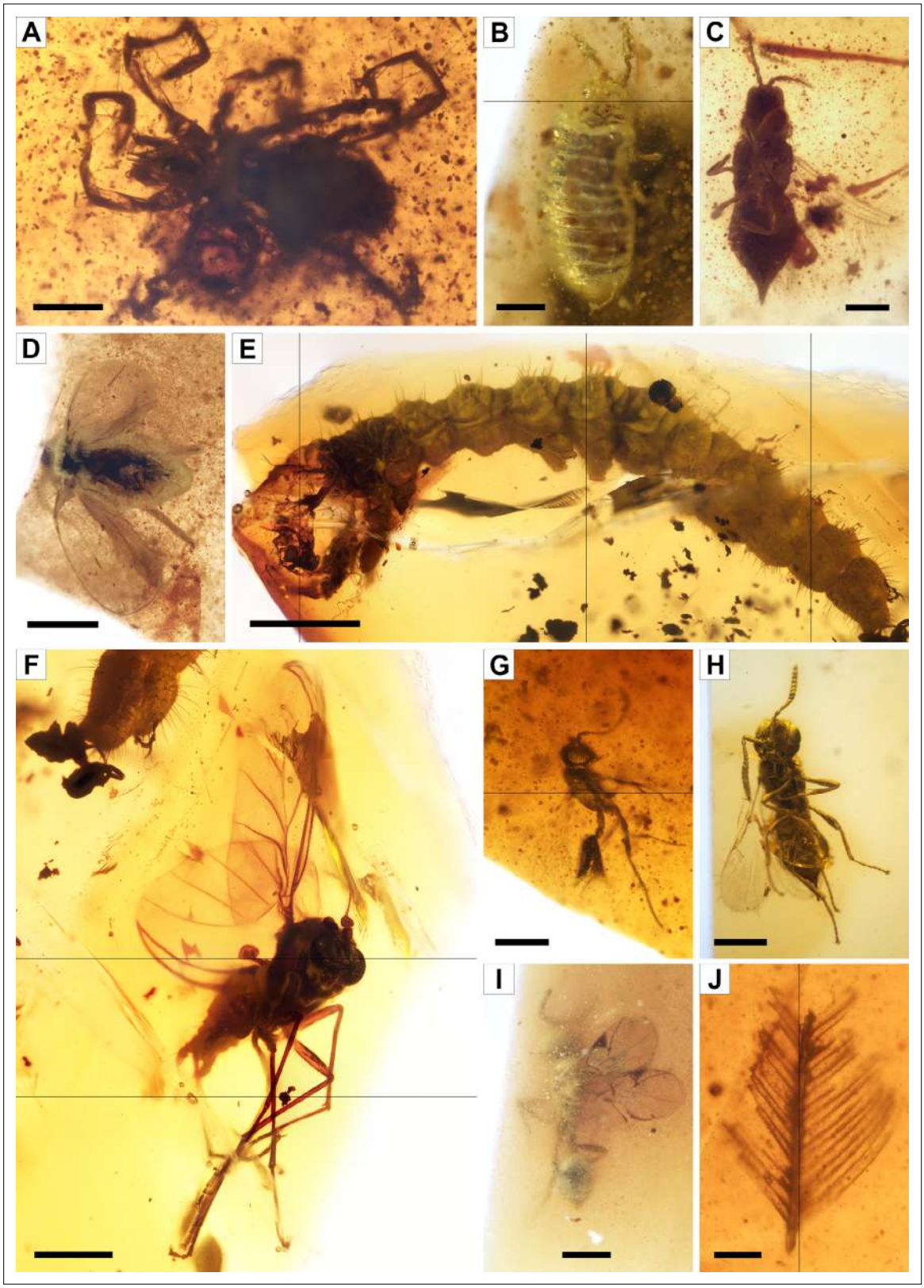

Figure 4. Faunal bioinclusions from the Lower Cretaceous bonebed amber of Ariño. (**A**) A rhagidiid mite, the oldest known (Acari: Rhagidiidae; AR-1-A-2019.71). (**B**) An immature thrips (Thysanoptera; AR-1-A-2019.114.2). (**C**) An adult thrips (Thysanoptera; AR-1-A-2019.40). (**D**) A whitefly (Hemiptera: Aleyrodidae; AR-1-A-2019.100.1). (**E**) A ditrysian lepidopteran larva (AR-1-A-2019.95.1). (**F**) A *Burmazelmira* sp. fly (Diptera: †Archizelmiridae: AR-1-A-2019.95.2). (**G**) A false fairy wasp, the oldest known (Hymenoptera: Mymarommatoidea; AR-1-A-2019.61). (**H**) A superbly preserved platygastroid wasp

Figure 4 continued on next page

Figure 4 continued

(Hymenoptera: Platygastroidea; AR-1-A-2019.95.3). (**I**) A serphitid wasp, the oldest known (Hymenoptera: †Serphitidae; AR-1-A-2019.94.8). (**J**) A feather barb fragment with pennaceous structure (Theropoda; AR-1-A-2019.53). Scale bars, 0.2 mm (**A–C**, **G**), 0.5 mm (**D, F, H, I**), 1 mm (**E**), and 0.1 mm (**J**).

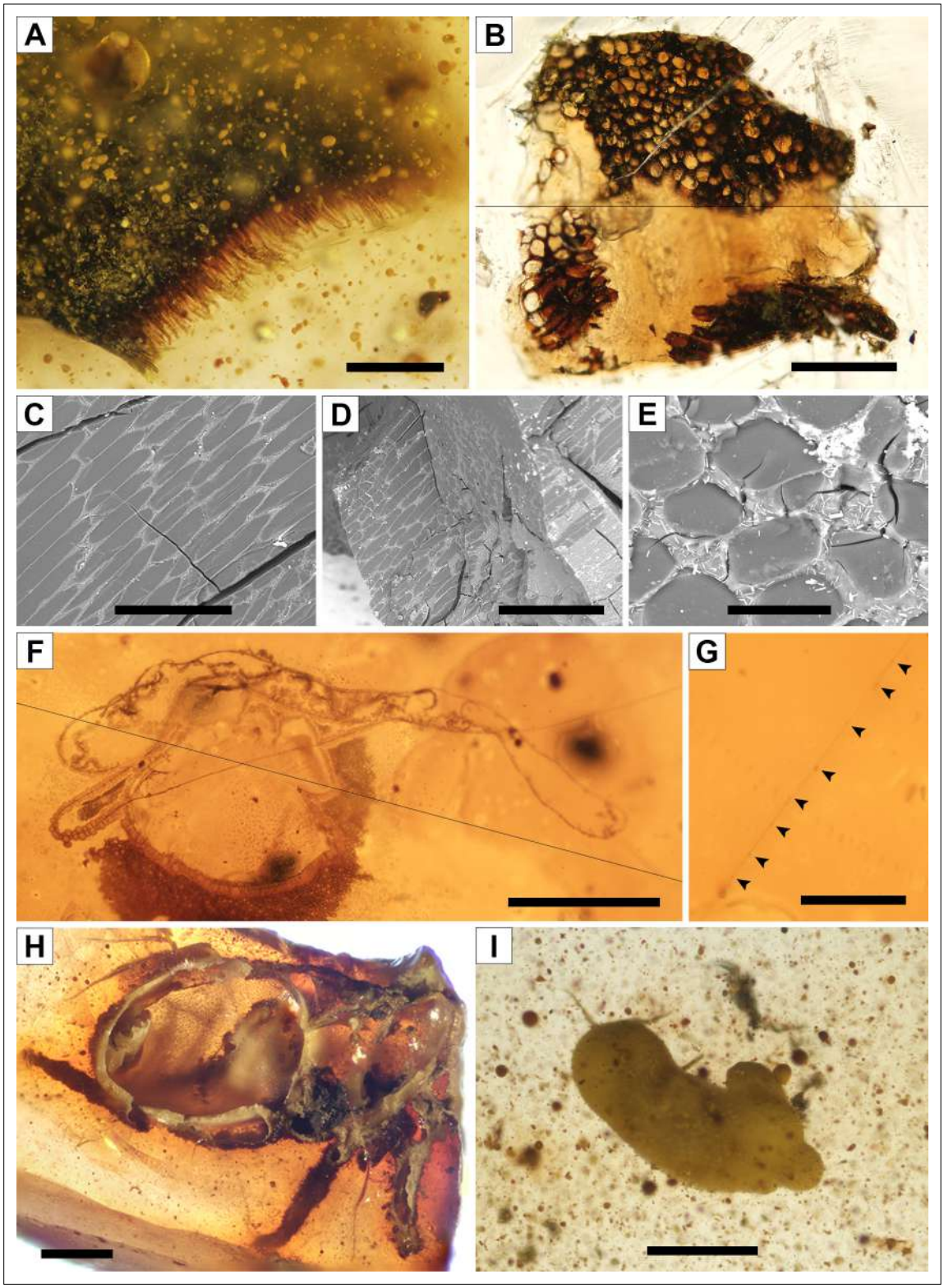

Figure 4—figure supplement 1. Diverse bioinclusions in amber from the level AR-1 of Ariño. (**A**) Plant remain (AR-1-A-2019.114.3). (**B–E**) Amber-infilled plant tissue preserving the cellular structure that could correspond to suber (cork) (AR-1-A-2018.1): (**B**) Preparation (transversal view); (**C–E**) SEM images: (**C**) in longitudinal and oblique view, (**D**) in transversal and oblique view, and (**E**) in transversal view. (**F**) A tangled spiderweb portion (AR-1-A-2019.95.5). (**G**) Detail photograph of a spiderweb strand found in the former, with glue droplets marked with arrowheads. (**H**) Spider showing the inner body structure in the surface of a broken amber piece (AR-1-A-2019.76). (**I**) Thrips showing a thin milky coat (AR-1-A-2019.114.1). Scale bars, 0.2 mm (**A, C**), 0.5 mm (**B, F, H, I**), 0.3 mm (**D**), 0.02 mm (**E**), and 0.05 mm (**G**).

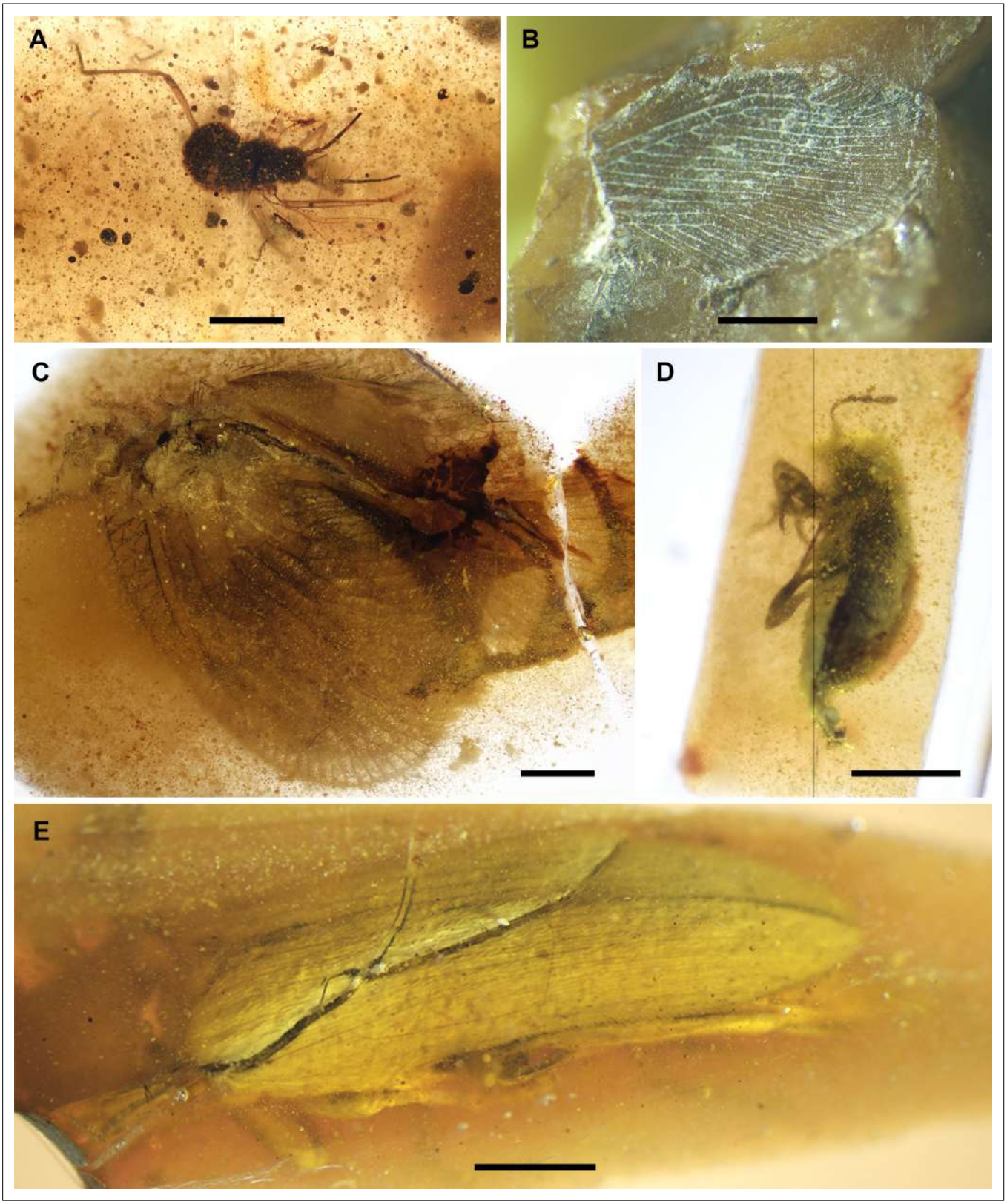

Figure 4—figure supplement 2. Insect bioinclusions in amber from the level AR-1 of Ariño. (**A**) An aphidoid (Hemiptera; AR-1-A-2019.103). (**B**) Wing impression on amber surface probabñy belonging to Berothidae (Neuroptera; AR-1-A-2019.83). (**C**) A tentative †Paradoxosisyrinae specimen (Neuroptera: Sisyridae; AR-1-A-2019.128.1). (**D**) A probable Ptinidae specimen (Coleoptera; AR-1-A-2019.44). (**E**) A probable Cantharidae specimen (Coleoptera; AR-1-A-2019.118.1). Scale bars, 0.5 mm (**A, C, D**), and 1 mm (**B, E**).

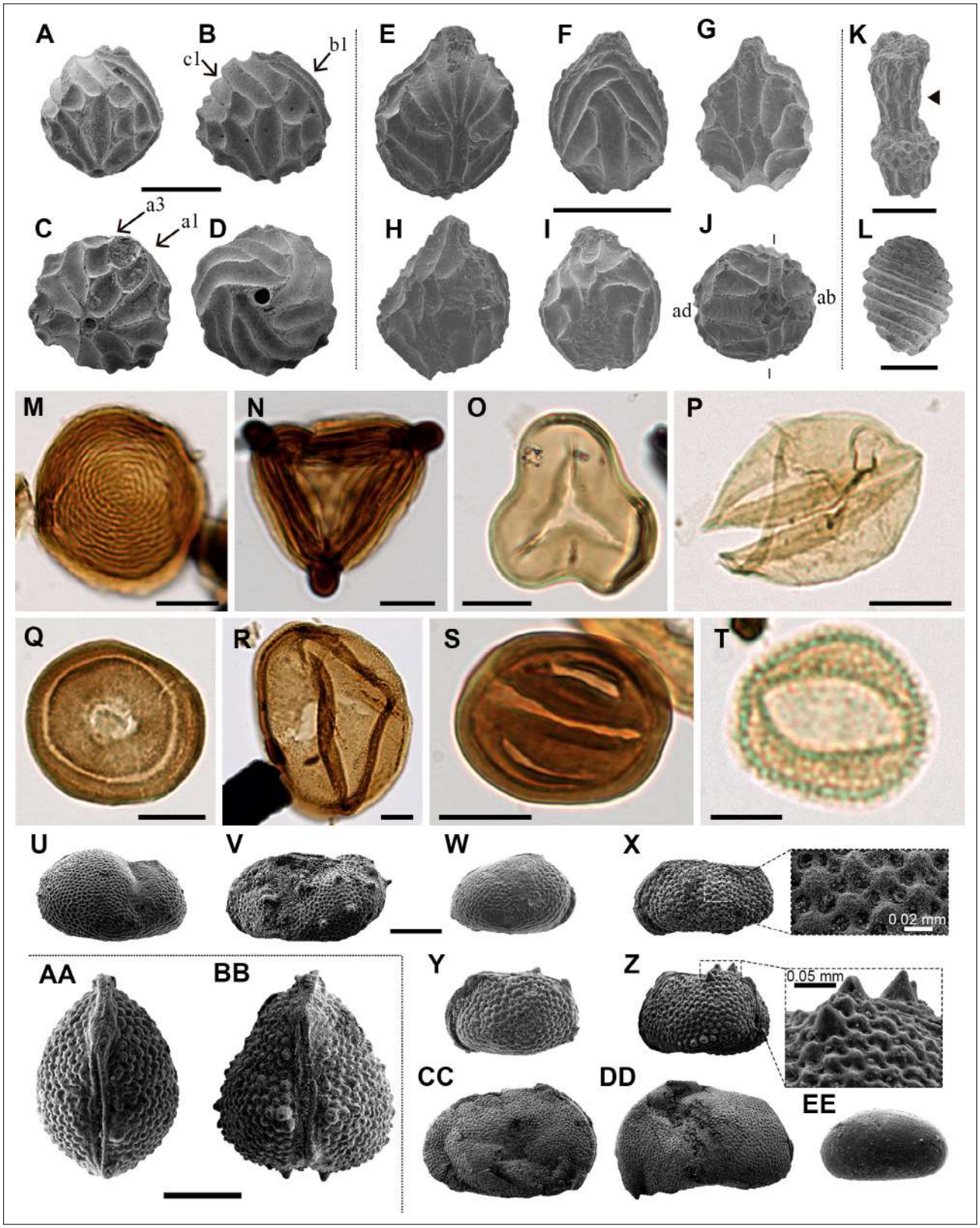

Figure 5. Charophyte (A–L), palynomorph (M–T), and ostracod (U–EE) records sampled from level AR-1 of Ariño. (**A–D**) *Atopochara trivolvis* var. *trivolvis* (†Clavatoraceae): (**A, B**) Lateral views (AR-1-CH-004 and AR-1-CH-005, respectively); (**C**) Basal view (AR-1-CH-007); (**D**) Apical view (AR-1-CH-008); cell lettering after ***Grambast, 1968***. (**E–J**) *Clavator harrisii* var. *harrisii* (†Clavatoraceae): (**E**) Lateral view (AR-1-CH-009); (**F**) Adaxial view (AR-1-CH-011); (**G**) Abaxial view morphotype II (AR-1-CH-013); (**H**) Abaxial view morphotype III (AR-1-CH-014); (**I**) Abaxial view morphotype IV (AR-1-CH-015); (**J**) Basal

Figure 5 continued on next page

Figure 5 continued

view (AR-1-CH-017) with indication of adaxial (ad) and abaxial (ab) sides. (**K**) *Clavatoraxis* sp. (†Clavatoraceae) (AR-1-CH-019); the arrowhead indicates the zig-zag line at the central part of the internode. (**L**) aff. *Mesochara harrisii* (Characeae) in lateral view (AR-1-CH-001). (**M**) *Chomotriletes minor* (ARN-03). (**N**) *Appendicisporites tricornitatus* (ARN-01). (**O**) *Cyathidites minor* (ARN-02). (**P**) *Inaperturopollenites dubius* (ARN-04). (**Q**) *Classopollis* sp. (ARN-02). (**R**) *Araucariacites hungaricus* (ARN-01). (**S**) *Eucommiidites minor* (ARN-01). (**T**) "*Liliacidites*" *minutus* (ARN-01). (**U, V**) *Theriosynoecum* cf. *fittoni* (Limnocytheridae): (**U**) Right lateral view, female carapace (AR-1-OS-001); (**V**) Left lateral view, male carapace (AR-1-OS-002). (**W–BB**) *Rosacythere denticulata* (Limnocytheridae): (**W**) Female? carapace, right lateral view, variant with extremely small rosette ornamentation (simply reticulated form) (AR-1-OS-006); (**X**) Male carapace of the variant with well-developed rosette ornamentation, left lateral view (AR-1-OS-011), and detail of the ornamentation; (**Y**) Female carapace of the variant with well-developed rosette ornamentation, left lateral view (AR-1-OS-007); (**Z**) Female carapace of the variant with strongly developed rosette ornamentation and spine-like nodes, left lateral view (AR-1-OS-015), and detail of the spine-like node ornamentation; (**AA**) Female carapace of the variant with well-developed rosette ornamentation, dorsal view (AR-1-OS-012); (**BB**) Female carapace of the variant with strongly developed rosette ornamentation and spine-like nodes, dorsal view (AR-1-OS-018), showing intraspecific variability. (**CC**), (**DD**) *Cypridea* cf. *clavata* (†Cyprideidae): (**CC**) Specimen in right lateral view (AR-1-OS-004); (**DD**) Specimen in left lateral view (AR-1-OS-005). (**EE**) *Mantelliana* sp. (Cyprididae) (AR-1-OS-003), right lateral view. Scale bars, 0.5 mm (**A–J**), 0.25 mm (**K**), 0.2 mm (**L, U–EE**), 0.01 mm (**M–S**), and 0.005 mm (**T**). See also ***Supplementary file 1***.

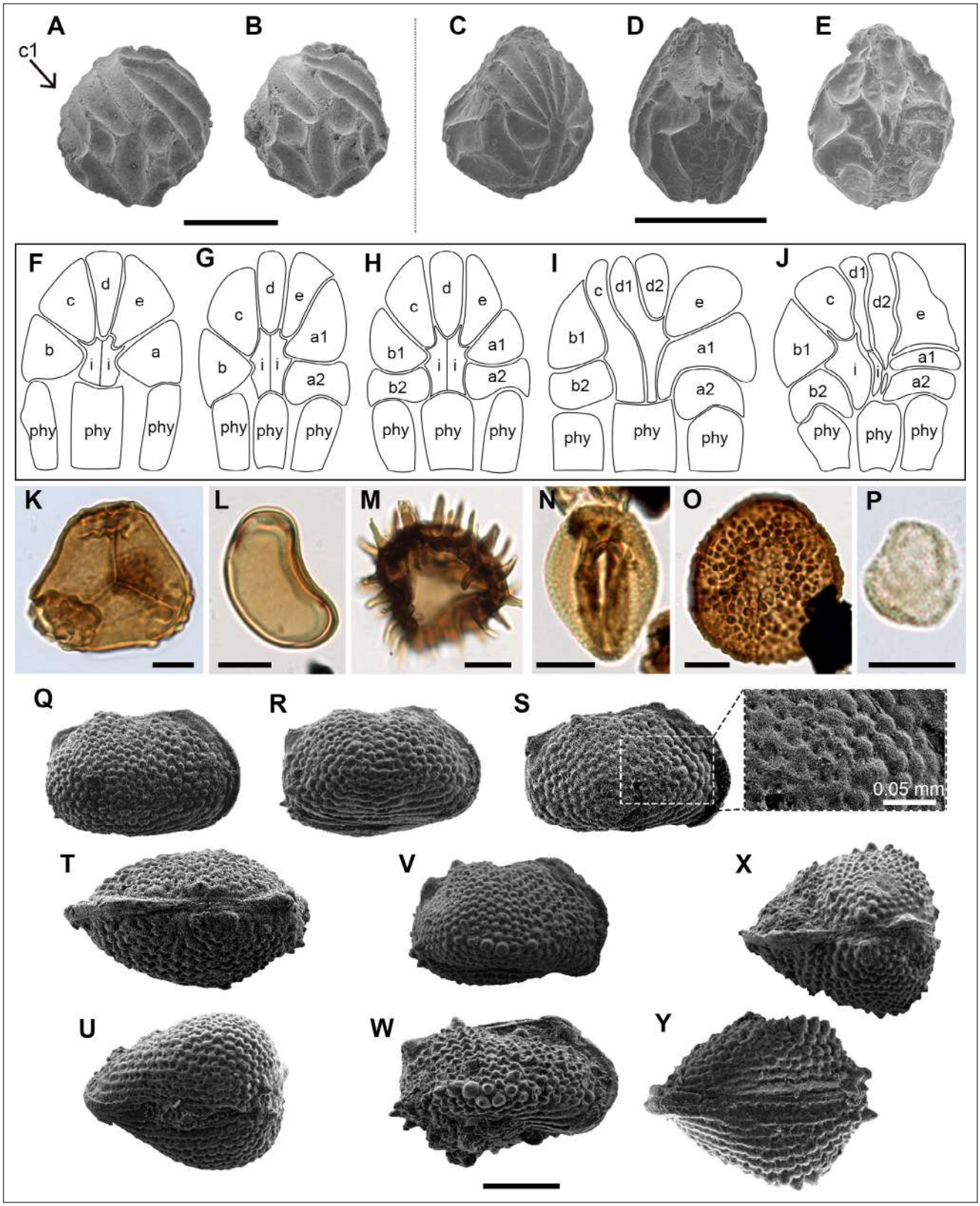

Figure 5—figure supplement 1. Additional charophyte (A–J), palynomorph (K–P), and ostracod (Q–Y) records sampled from level AR-1 of Ariño. (**A, B**) *Atopochara trivolvis* var. *trivolvis* (†Clavatoraceae) lateral views (AR-1-CH-003 and AR-1-CH-006, respectively); cell lettering after ***Grambast, 1968***. (**C–E**) *Clavator harrisii* var. *harrisii* (†Clavatoraceae): (**C**) Lateral view (AR-1-CH-010); (**D**) Abaxial view morphotype I (AR-1-CH-012); (**E**) Abaxial view morphotype V (AR-1-CH-016). (**F–J**) Morphotypes of the abaxial part of the utricle of *Clavator harrisii* var. *harrisii*: (**F**) Morphotype I showing the impression of

Figure 5—figure supplement 1 continued on next page

Figure 5—figure supplement 1 continued

the phylloid cortical cells (phy), two intermediate cells (i) and an adaxial fan with five cells, two lateral cells (a and b) and three apical cells (c, d, e); (**G**) Morphotype II showing the adaxial fan with six cells by subdivision of the a cell; (**H**) Morphotype III showing the adaxial fan with seven cells by subdivision of a and b cells; (**I**) Morphotype IV showing an adaxial fan with eight cells by subdivision of d cell in addition to the other subdivisions already found in morphotype II, fusion of fan cells and intermediate cells is also observed; (**J**) Morphotype V with the same number of fan cells as in morphotype IV but showing different cell shapes and no fusion between intermediate and fan cells. (**K**) *Trilobosporites purverulentus* (ARN-02). (**L**) *Laevigatosporites haardti* (ARN-01). (**M**) *Ceratosporites* sp. (ARN-02). (**N**) *Retimonocolpites dividuus* (ARN-03). (**O**) *Foraminisporis* cf. *undulatus* (ARN-01). (**P**) *Tricolpites* sp. (ARN-04). (**Q–Y**) *Rosacythere denticulata* (Limnocytheridae): (**Q–U**) Variant with well-developed rosette ornamentation: (**Q–S**) Female carapaces, right lateral views and detail of the ornamentation (AR-1-OS-008, AR-1-OS-009 and AR-1-OS-010, respectively); (**T**) Male carapace, dorsal view (AR-1-OS-013); (**U**) Female carapace, ventral view (AR-1-OS-014); (**V–Y**) Variant with well-developed rosette ornamentation and spine-like node: (**V, W**) Female and male carapace respectively, right lateral views (AR-1-OS-016 and AR-1-OS-017, respectively); (**X**) Female carapace, dorsal view (AR-1-OS-019); (**Y**) Female carapace, ventral view (AR-1-OS-20). Scale bars, 0.05 mm (**A–E**), 0.01 mm (**K–P**), and 0.2 mm (**Q–Y**).

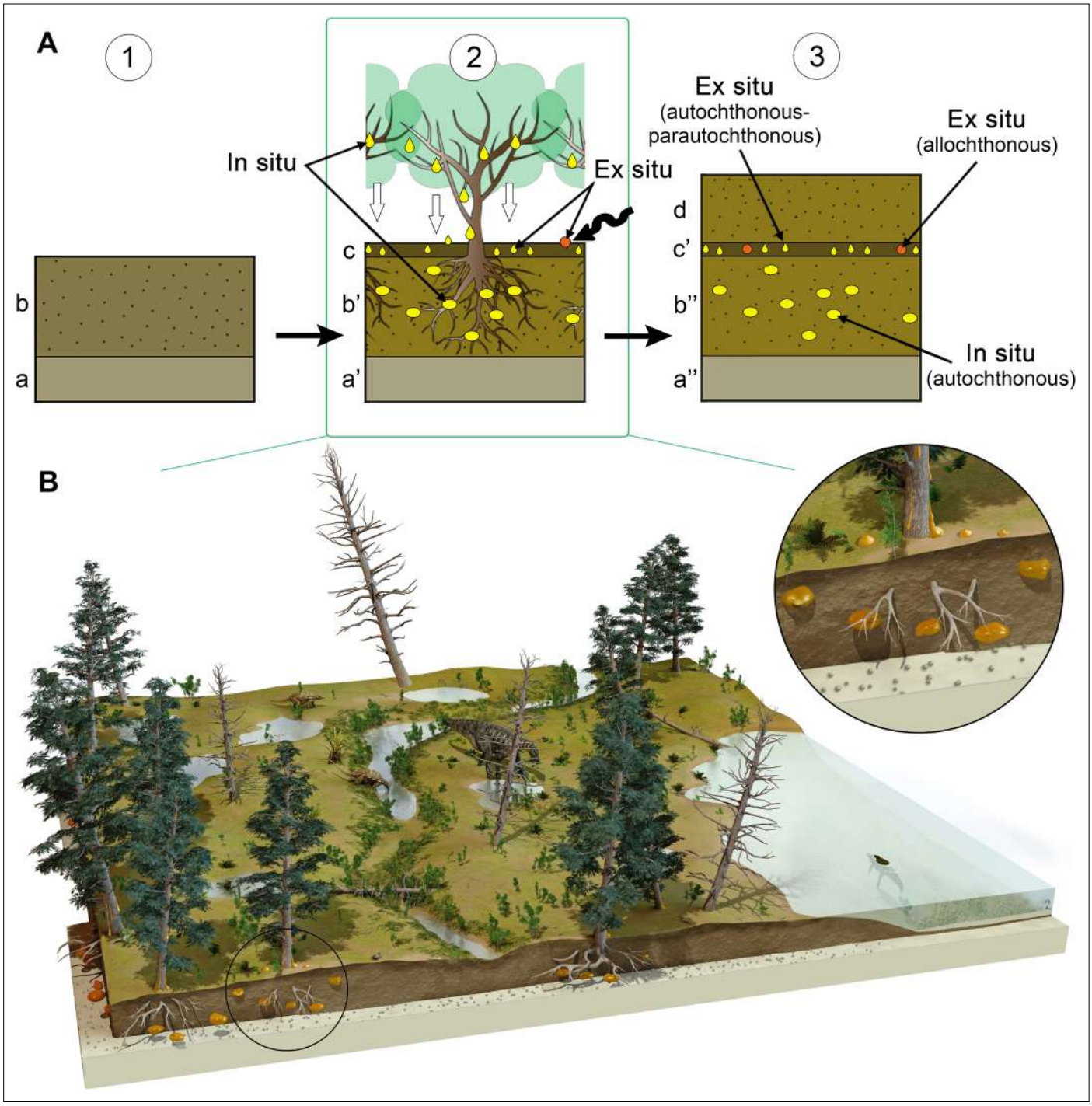

Figure 6. Formation of the amber deposit of Ariño. (**A**) Idealised diagrams depicting (1) the original depositional environment (a, carbonates; b, soil prior to tree installation); (2) resiniferous forest installation and pedogenesis; concentration of in situ kidney-shaped resin pieces produced by the roots in a root horizon (b'); accumulation of aerial resin pieces fallen from the branches and trunk and a few resin pieces dragged after transport (wavy arrow) in a litter horizon (c); and (3) fossil diagenesis of the resin pieces, resulting in a layer containing strictly in situ autochthonous kidney-shaped amber pieces produced by roots (b''), and a layer mostly composed of strictly ex situ autochthonous-parautochthonous aerial amber pieces and a few potentially allochthonous amber pieces (c'); level AR-1 corresponds to a single cycle of forest floor installation-destruction. (**B**) Artistic reconstruction of the coastal freshwater swamp ecosystem of Ariño, with emphasis on the depositional environment of the resin. The resiniferous trees are araucariaceans (extant model used: *Agathis australis*), tentatively identified as the resin source of Ariño; other depicted terrestrial plants are undetermined vegetation included for artistic purpose. Charophytes and a crocodile (*Hulkepholis plotos*) inhabit the shallow water body on the right; two nodosaurids (*Europelta carbonensis*), an iguanodontian (*Proa valdearinnoensis*), and a turtle (*Aragochersis lignitesta*) are shown on land; these vertebrate species were erected based on the Ariño bonebed material. Artist of the illustration in (**B**): José Antonio Peñas.

Anexo 8.1.4

First fossil record of the oribatid family Liacaridae (Acariformes: Gustavioidea) from the lower Albian amber-bearing site of Ariño (eastern Spain)

Arillo, A., Subías, L.S., **Álvarez-Parra, S.** 2022. First fossil record of the oribatid family Liacaridae (Acariformes: Gustavioidea) from the lower Albian amber-bearing site of Ariño (eastern Spain). *Cretaceous Research*, **131**, 105087.

DOI: https://doi.org/10.1016/j.cretres.2021.105087

Revista científica: *Cretaceous Research*
Factor de impacto: 2,432 (2021)
Categoría: *Paleontology*, Q1 (2021)

Cretaceous Research 131 (2022) 105087

Contents lists available at ScienceDirect

Cretaceous Research

journal homepage: www.elsevier.com/locate/CretRes

Short communication

First fossil record of the oribatid family Liacaridae (Acariformes: Gustavioidea) from the lower Albian amber-bearing site of Ariño (eastern Spain)

Antonio Arillo [a], Luis S. Subías [a], Sergio Álvarez-Parra [b, *]

[a] Departamento de Biodiversidad, Ecología y Evolución, Facultad de Biología, Universidad Complutense, c/ José Antonio Novais, 12, 28040 Madrid, Spain
[b] Departament de Dinàmica de la Terra i de l'Oceà and Institut de Recerca de la Biodiversitat (IRBio), Facultat de Ciències de la Terra, Universitat de Barcelona, c/ Martí i Franquès s/n, 08028 Barcelona, Spain

ARTICLE INFO

Article history:
Received 5 August 2021
Received in revised form
3 November 2021
Accepted in revised form 3 November 2021
Available online 11 November 2021

Keywords:
Cretaceous
Spanish amber
Mite
Oribatida
Liacarus (*Procorynetes*) *shtanchaevae* sp. nov.
Bradytely

ABSTRACT

We describe the first beetle mite (Oribatida) found in the lower Albian (Lower Cretaceous) amber-bearing site of Ariño, located in the Teruel Province (eastern Iberian Peninsula). It represents the first fossil record of the family Liacaridae (Acariformes: Oribatida: Gustavioidea). A new species, *Liacarus* (*Procorynetes*) *shtanchaevae* Arillo and Subías sp. nov., is described and compared with the living species of the subgenus *Liacarus* (*Procorynetes*). Notes on its biogeography and palaeobiology are provided. It corresponds to the first Cretaceous record of an extant oribatid subgenus and bears witness to the wide range of distribution that the ancient representatives of the subgenus may have had. Most of the oribatid species from Cretaceous ambers belong to living genera, which reflects the high degree of morphological stasis, or bradytely, over the evolutionary history of oribatid mites since the Early Cretaceous.

1. Introduction

Beetle mites (Oribatida) are common in almost all terrestrial ecosystems, and comprise more than 10,000 described species (Subías, 2004, updated online version 2019). Some estimations have placed the number of oribatid species in the world fauna as high as 50,000–100,000 (Schatz and Behan-Pelletier, 2008). However, because of their minute size, they are rarely found in the fossil record, especially in pre-Cenozoic strata, and are mostly associated with amber deposits from the Cretaceous onwards. The oldest oribatid mites date from the Middle Devonian (Norton et al., 1988; Subías and Arillo, 2002). Only 16 oribatid species have been described in Cretaceous ambers from Lebanon, Spain, Taimyr, and Canada (Arillo et al., 2016, 2019, 2020); the species from Lebanon (Barremian) corresponds to the oldest oribatid in amber (Arillo et al., 2019). Regarding the oribatid fossil record, an outstanding upper Albian amber outcrop is San Just (Maestrazgo Basin, Teruel Province, Spain), which contains five species (Arillo et al., 2009, 2010, 2012, 2016): *Trhypochthonius lopezvallei* Arillo, Subías and Shtanchaeva, 2012, *Cretaceobodes martinezae* Arillo, Subías and Shtanchaeva, 2010, *Ametroproctus valeriae* Arillo, Subías and Shtanchaeva, 2009, *Tenuelamellarea estefaniae* Arillo and Subías, 2016 (in Arillo et al., 2016), and *Hypovertex hispanicus* Arillo and Subías, 2016 (in Arillo et al., 2016).

Nowadays, oribatids inhabit a wide range of habitats, such as plant litter, soil, mosses, lichens, rock surfaces, bark, and leaves (Schatz and Behan-Pelletier, 2008).

Liacaridae is a forest soil dwelling family of oribatids with an almost cosmopolitan distribution, being present in all continents, except for Antarctica and Australia. It is included in the superfamily Gustavioidea. Four fossil species and one subspecies belonging to the Gustavioidea are known: three species of the family Astegistidae (*Cultroribula jurassica* Krivolutsky, 1977 (in Krivolutsky and Krasilov, 1977) from the Tithonian, in the Burea River Basin, in Far East Russia, and *Cultroribula lauta* Sellnick, 1931 and *Cultroribula superba* Sellnick, 1931, both from Eocene Baltic amber), one species of the family Xenillidae, *Xenillus tegeocraniformis* (Sellnick, 1919) from Baltic amber, and one subspecies of the family Ceratoppiidae, *Ceratoppia bipilis fossilis* Sellnick, 1919 from Baltic amber. To date,

* Corresponding author.
E-mail addresses: arillo@educa.madrid.org (A. Arillo), subias@bio.ucm.es (L.S. Subías), sergio.alvarez-parra@ub.edu (S. Álvarez-Parra).

https://doi.org/10.1016/j.cretres.2021.105087

the families Metrioppiidae, Tenuialidae, Gustaviidae and Multoribulidae lack any fossil record. Some living species of oribatids are found as subfossils, as it is the case of the liacarid species *Adoristes* (*Adoristes*) *ovatus* (Koch, 1839) and *Liacarus* (*Liacarus*) *coracinus* (Koch, 1841) from Quaternary deposits of northern Europe (Dunlop et al., 2012).

Here, we describe a new oribatid species from the lower Albian (Lower Cretaceous) amber-bearing site of Ariño, which belongs to a living genus and subgenus of the family Liacaridae and represents the first fossil record of the family worldwide.

2. Systematics of Liacaridae

The systematics of the family Liacaridae is controversial. Woolley (1972) proposed to group it under the superfamily Liacaroidea with Astegistidae, Metrioppiidae, Xenillidae, and Tenuialidae, but Subías (2004, updated online version 2019) grouped these five families alongside Gustaviidae, Ceratoppiidae and Multoribulidae inside the superfamily Gustavioidea. Xenillidae was erected as a family that shares anatomical features with Liacaridae (Woolley and Higgins, 1966), although some authors consider it as a synonym of the latter (e.g., Weigmann, 2006; Norton and Behan-Pelletier, 2009; Dunlop et al., 2012). Nonetheless, we prefer to follow the systematics established by Subías (2004, updated online version 2019), and consider Liacaridae and Xenillidae as different families based on the body sculpture, the morphology of the histerosomal setae and the depth of the rostral grooves (Ryabinin and Zaitsev, 2019).

Analysis of the 18S rRNA gene (Schaefer and Caruso, 2019) does not shed light on the phylogeny of Gustavioidea; *Xenillus* seems to be linked to *Euzetes* Berlese, 1908 (Ceratozetoidea: Ceratozetidae) and *Ceratoppia* (Gustavioidea: Ceratoppiidae) seems to be outside the clade of the superfamily, closer to *Banksinoma* Oudemans, 1930 (Oppioidea: Thyrisomidae).

The inner systematics of the family has also changed over time. Woolley (1972) included six genera (*Liacarus* Michael, 1898, *Adoristes* Hull, 1916, *Opsioristes* Woolley, 1967, *Rhaphidosus* Woolley, 1969, *Dorycranosus* Woolley, 1969, and *Procorynetes* Woolley, 1969). Later, Subías (2004, updated online version 2019) considered *Rhaphidosus*, *Dorycranosus* and *Procorynetes* as subgenera of *Liacarus*, thus recognising six genera: *Liacarus* (with four subgenera, *Liacarus*, *Rhaphidosus*, *Dorycranosus*, and *Procorynetes*), *Adoristes* (with two subgenera, *Adoristes* and *Gordeeviella* Shtanchaeva, Subías and Arillo, 2010), *Birsteinius* Krivolutsky, 1965, *Opsioristes*, *Planoristes* Iturrondobeitia and Subías, 1978, and *Scarabacarus* Shtanchaeva and Subías, 2010.

Currently, the subgenus *Liacarus* (*Procorynetes*) is considered to include eight species (Subías, 2004, updated online version 2019). These are *Liacarus* (*Procorynetes*) *altaicus* (Krivolutsky, 1974), *Liacarus* (*Procorynetes*) *andinus* (P. Balogh, 1984), *Liacarus* (*Procorynetes*) *breviclavatus* Aoki, 1970, *Liacarus* (*Procorynetes*) *clavatus* Fujikawa and Aoki, 1970, *Liacarus* (*Procorynetes*) *espeletiae* (P. Balogh, 1984), *Liacarus* (*Procorynetes*) *globifer* (Kramer, 1897), *Liacarus* (*Procorynetes*) *huvsgulensis* Bayartogtokh, 2010, and *Liacarus* (*Procorynetes*) *nigerrimus* Berlese, 1916. The subgenus *Liacarus* (*Liacarus*) is the most diverse of the genus, comprising 61 species and three

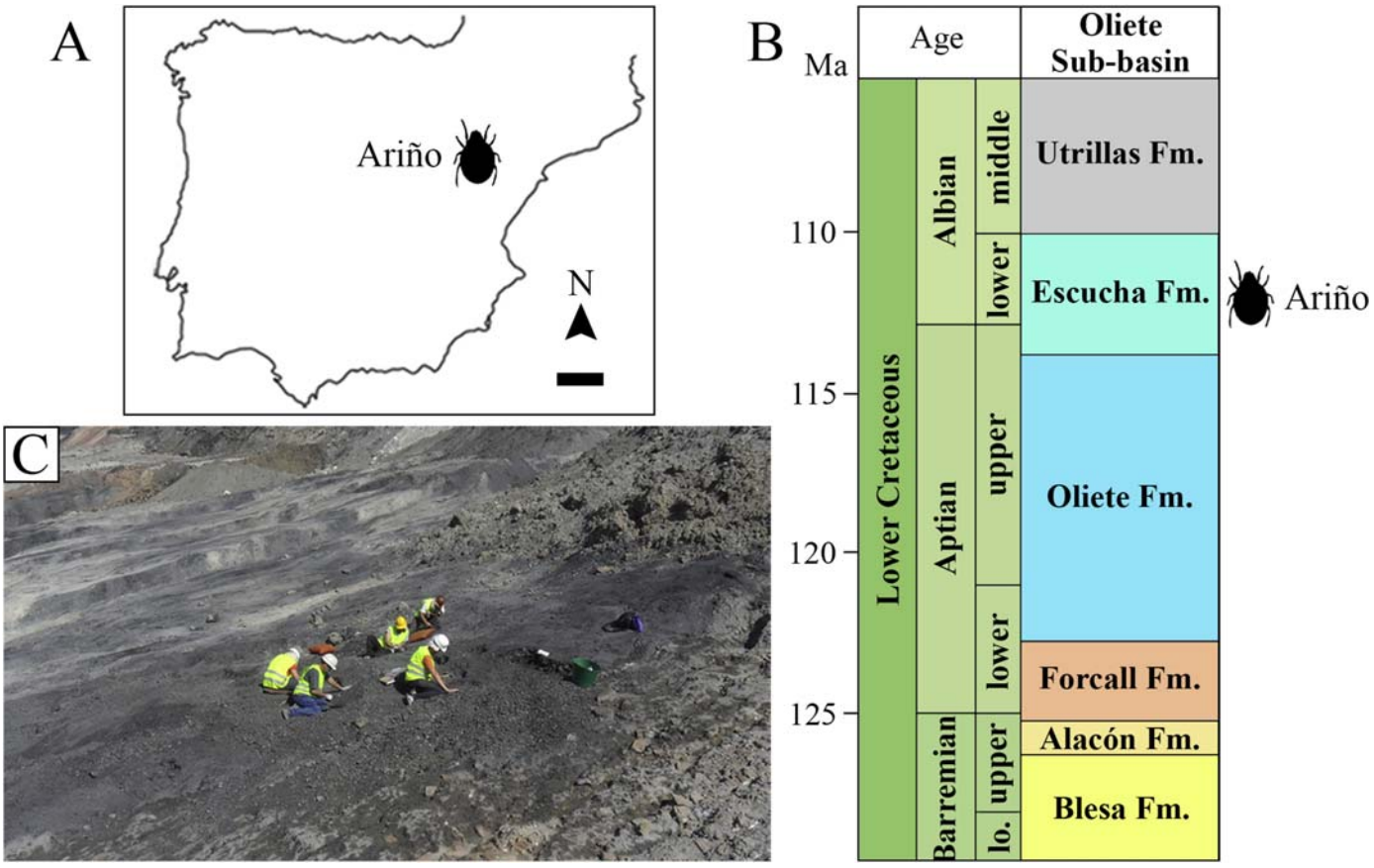

Fig. 1. Geographical and stratigraphic location of the lower Albian amber-bearing site of Ariño (Teruel Province, Spain); type locality of the oribatid species described: A) map of the Iberian Peninsula showing the location of Ariño (41° 1′ N, 0° 33′ W); B) approximate location of the Ariño site in the Lower Cretaceous stratigraphy of the Oliete Sub-basin, based on Aurell et al. (2018); C) amber excavation in the bonebed level AR-1 of Ariño, July 2019. Scale bar = 100 km (A).

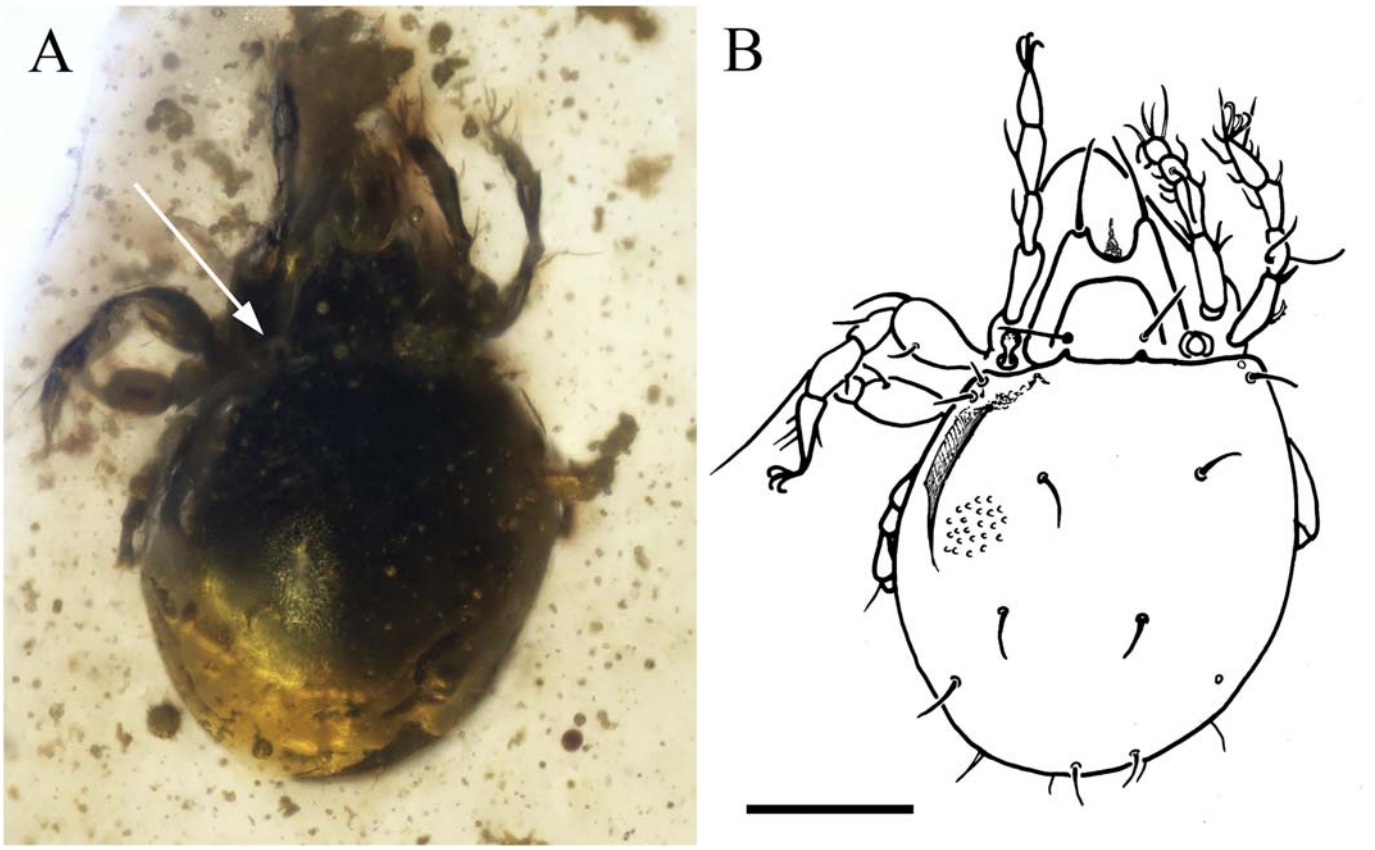

Fig. 2. *Liacarus* (*Procorynetes*) *shtanchaevae* sp. nov. (Oribatida: Liacaridae), from the lower Albian amber-bearing site of Ariño (Teruel Province, Spain), holotype AR-1-A-2019.45: A, B) photograph and drawing from dorsal view, both at the same scale, arrow in A indicates the sensilla. Scale bar = 100 μm.

subspecies, while the subgenera *Liacarus* (*Dorycranosus*) and *Liacarus* (*Rhaphidosus*) include 36 (and one subspecies) and seven species respectively (Subías, 2004, updated online version 2019).

3. Material and methods

Fossiliferous Cretaceous amber from the Maestrazgo Basin (eastern Spain) has been known since Boscá (1910) mentioned the first apparent bioinclusions from calamine mines in the locality of Linares de Mora. To date, 31 amber-bearing outcrops have been reported in the basin, but only four of them show bioinclusions (Delclòs et al., 2007; Peñalver and Delclòs, 2010; Álvarez-Parra et al., 2021): Arroyo de la Pascueta, La Hoya, San Just and Ariño. The latter was excavated in 2019 and turned out to be a deposit that was very rich in bioinclusions, yielding the specimen studied here (Fig. 1).

The Ariño site is located in the Santa María open-pit mine (Ariño, Teruel, Spain). Geologically, it is in the Oliete Sub-basin of the Maestrazgo Basin, belonging to the Aragonese Branch of the Iberian Chain (Salas and Guimerà, 1996). The amber was found in the bonebed level AR-1 (Fig. 1), belonging to the middle member of the Escucha Formation and dated as lower Albian based on the charophyte, ostracod, and palynological assemblages (Tibert et al., 2013; Villanueva-Amadoz et al., 2015; Álvarez-Parra et al., 2021). This fossil site is highly significant as it has provided a diverse fossil record of plants, molluscs, ostracods, fish, turtles, crocodilians, and dinosaurs (Alcalá et al., 2012). It is the type locality of six vertebrate species, including two ornithischian dinosaurs, three ostracod species, and the mite species described here. The level AR-1 is mainly constituted of marls rich in organic matter (Álvarez-Parra et al., 2021). The Ariño palaeoenvironment is inferred as a freshwater swamp plain with permanent alkaline shallow lakes, with salinity fluctuations due to marine influence, under a tropical or subtropical climate (Tibert et al., 2013; Villanueva-Amadoz et al., 2015). The presence of amber rich in arthropod inclusions in the bonebed level is interesting, as it increases the palaeoecological information about the habitat of the dinosaurs and other vertebrates (Álvarez-Parra et al., 2020a, 2021). The taphonomic conditions of this Konservat-Lagerstätte are under study and emphasize the significance of the fossil record found in this site (Álvarez-Parra et al., 2021).

The amber piece containing the fossil mite was cut and embedded in an epoxy resin prism measuring 20 × 13 mm following the methodology of Corral et al. (1999). This technique provides stabilisation and protection to the piece. The photograph of the specimen was taken using an Olympus CX41 compound microscope with an attached digital camera sCMEX-20, through the software ImageFocusAlpha version 1.3.7.12967.20180920. Drawings were made with the aid of an Olympus U-DA drawing tube attached to an Olympus BX50 compound microscope. The figures were prepared using Photoshop CS6 and GIMP 2.10. The specimen is housed at the Museo Aragonés de Paleontología (Fundación Conjunto Paleontológico de Teruel-Dinópolis, Teruel, Spain) with the fieldwork number AR-1-A-2019.45.

This manuscript has been registered in ZooBank under the number urn:lsid:zoobank.org:pub:FCEC0E9A-5AF3-49F5-87D0-420408C4F9E9.

4. Systematic palaeontology

Order Acariformes Zakhvatkin, 1952
Suborder Oribatida Dugès, 1834

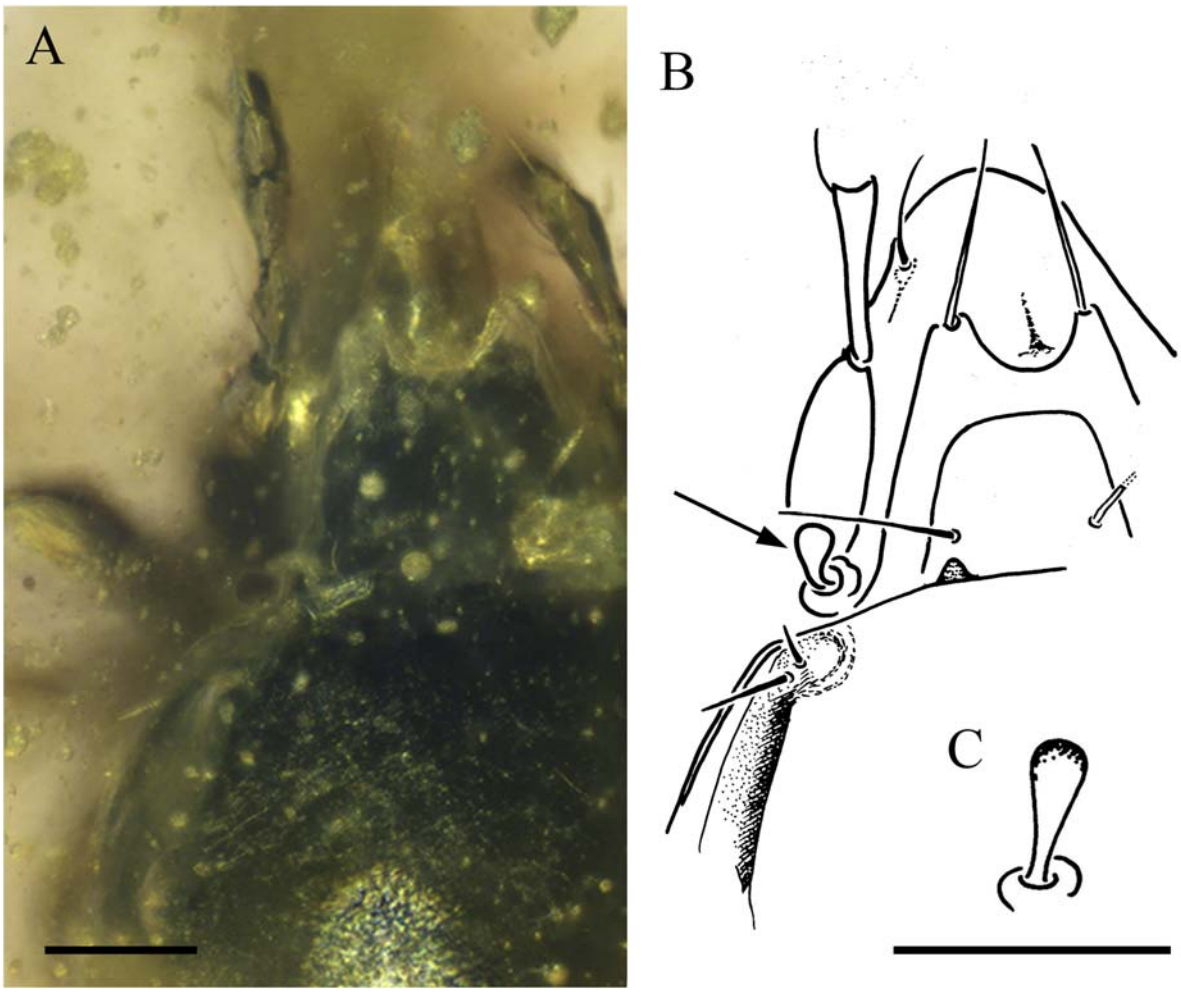

Fig. 3. *Liacarus* (*Procorynetes*) *shtanchaevae* sp. nov. (Oribatida: Liacaridae), from the lower Albian amber-bearing site of Ariño (Teruel Province, Spain), holotype AR-1-A-2019.45: A, B) photograph and drawing of the prodorsum region and anterior part of the notogaster, both at the same scale, arrow in B indicates the sensilla; C) drawing of the short and clubbed sensilla. Scale bars = 50 μm.

Infraorder Brachypilina Hull, 1918
Superfamily Gustavioidea Oudemans, 1900
Family Liacaridae Sellnick, 1928

Genus *Liacarus* Michael, 1898
(=*Leiosoma* Nicolet, 1855 *nom. praeoc.*)
(=*Leuroxenillus* Woolley and Higgins, 1966)
(=*Stenoxenillus* Woolley and Higgins, 1966)
Subgenus *Liacarus* (*Procorynetes*) Woolley, 1969
Type species: *Liacarus* (*Procorynetes*) *nigerrimus* Berlese, 1916

Liacarus* (*Procorynetes*) *shtanchaevae Arillo and Subías sp. nov. (Figs. 2 and 3)
This new species has been registered in ZooBank under the number urn:lsid:zoobank.org:act:B70B5EB4-193B-4135-9E41-CF16BBB14088.

Holotype. Specimen number AR-1-A-2019.45, housed at the Museo Aragonés de Paleontología (Fundación Conjunto Paleontológico de Teruel-Dinópolis, Teruel, Spain).
Locality and horizon. Bonebed level AR-1 of the Ariño site, in the Santa María open-pit mine, Teruel, Spain. Maestrazgo Basin, middle interval of the lower sedimentary succession of the Escucha Formation, lower Albian (Alcalá et al., 2012; Álvarez-Parra et al., 2021).

Etymology. The specific epithet is named after our oribatologist colleague Umukusum Ya. Shtanchaeva.
Diagnosis. *Liacarus* (*Procorynetes*) species with short lamellae and well-developed translamella. Short and clubbed sensilla.
Description. *Measurements:* Body length 397 μm, body width 244 μm (Figs. 2A and B).
Prodorsum: Anterior edge rounded. Short lamellae ending far from the anterior edge without cuspis at the base of the lamellar setae. Well-developed translamella with arched anterior margin, without central tooth (Fig. 3A and B). Rostral, lamellar and interlamellar setae smooth and well developed. Exobothridial setae no visible. Short tailed sensilla with clubbed head slightly truncated (Fig. 3C). Tutorium absent.
Notogaster: Rounded and slightly punctuated. Seven pairs of smooth setae are visible (including two humeral pairs). Humeral region rounded, without pteromorphs. Porose area absent.
Ventral side: Poorly preserved and obscured. Distant anal and genital plates. Three pairs of adanal setae preserved, pair ad_1 being in post-anal position. Anal plates seem to bear two pairs of anal setae. Genital setae not visible. Epimeral region not visible.
Legs and chaetotaxy: Legs tridactylous. Legs I, II and III with slightly swollen femora. Chaetotaxy of legs partially preserved. Setae in femorae I slightly barbulated. Solenidia on Tibiae I and II visible.

5. Discussion

5.1. Taxonomy

The systematics of the genus *Liacarus* is mainly based on the shape of the sensillae. The new species clearly belongs to the subgenus *Liacarus* (*Procorynetes*), in view of the short tail and the clubbed head, slightly truncated, on its apex. Species within this subgenus present different types of lamellar shape. In some species, such as *L.* (*P.*) *huvsgulensis*, *L.* (*P.*) *clavatus*, *L.* (*P.*) *altaicus*, *L.* (*P.*) *andinus*, and *L.* (*P.*) *espeletiae*, the lamellae are very close to each other, without any translamellar development. Other species develop a short translamella with a medial tooth on its anterior margin, such as *L.* (*P.*) *breviclavatus* and *L.* (*P.*) *nigerrimus*. While *L.* (*P.*) *globifer* has a short translamella without medial tooth. Dubinina et al. (1966) noted that the shape of lamellae and lamellar cuspis and the presence or absence of translamellar tooth have strong intraspecific variability (even in the same population) in the genus *Liacarus*.

Liacarus (*Procorynetes*) *shtanchaevae* sp. nov. is close to *L.* (*P*). *globifer* but easily distinguished from that species by its developed translamella, shorter lamellae and shorter lamellar and interlamellar setae. Furthermore, the size of the new species is around 400 μm, while *L.* (*P*). *globifer* is about 900 μm.

5.2. *Distribution of the* Liacarus (Procorynetes) *spp.*

Living *Liacarus* (*Procorynetes*) spp. seem to show a cold climate distribution (Fig. 4). Palaearctic species are found in boreal areas or at high elevations. *Liacarus* (*Procorynetes*) *altaicus* was described from elfin woodlands of *Pinus sibirica* and tundra in Altai Republic (Krivolutsky, 1974) and later, Behan-Pelletier (1978) found this species in different arctic and subarctic localities in Canada. Furthermore, *L.* (*P.*) *huvsgulensis* was discovered in the banks of the river Borsog in the east side of Lake Khuvsgul (Khövsgöl) at a height of 1645 m in samples of mosses and litter from forests of *Larix sibirica* (Bayartogtokh, 2010).

Concerning the Japanese species, *L.* (*P.*) *breviclavatus* was discovered in *Abies veitchii* var. *sikokana* smoking trees with insecticides on Mount Ishizuchi (1890 m) in the island of Shikoku (Aoki, 1970), and *L.* (*P.*) *clavatus* was described in a Glehn's spruce (*Picea glehnii*) forest near Obihiro in the island of Hokkaido (Fujikawa and Aoki, 1970).

The fifth Palaearctic species, *L.* (*P.*) *globifer*, was described from Greenland and later recorded in shrub samples from Kandalaksha on the shores of the White Sea (Dzhaparidze, 1987).

The two Neotropical species, *L.* (*P.*) *andinus* and *L.* (*P.*) *espeletiae*, were sampled in *Espeletia hartwegiana* dead leaves in Huila, Colombia, at a height of 3700 m (Balogh, 1984).

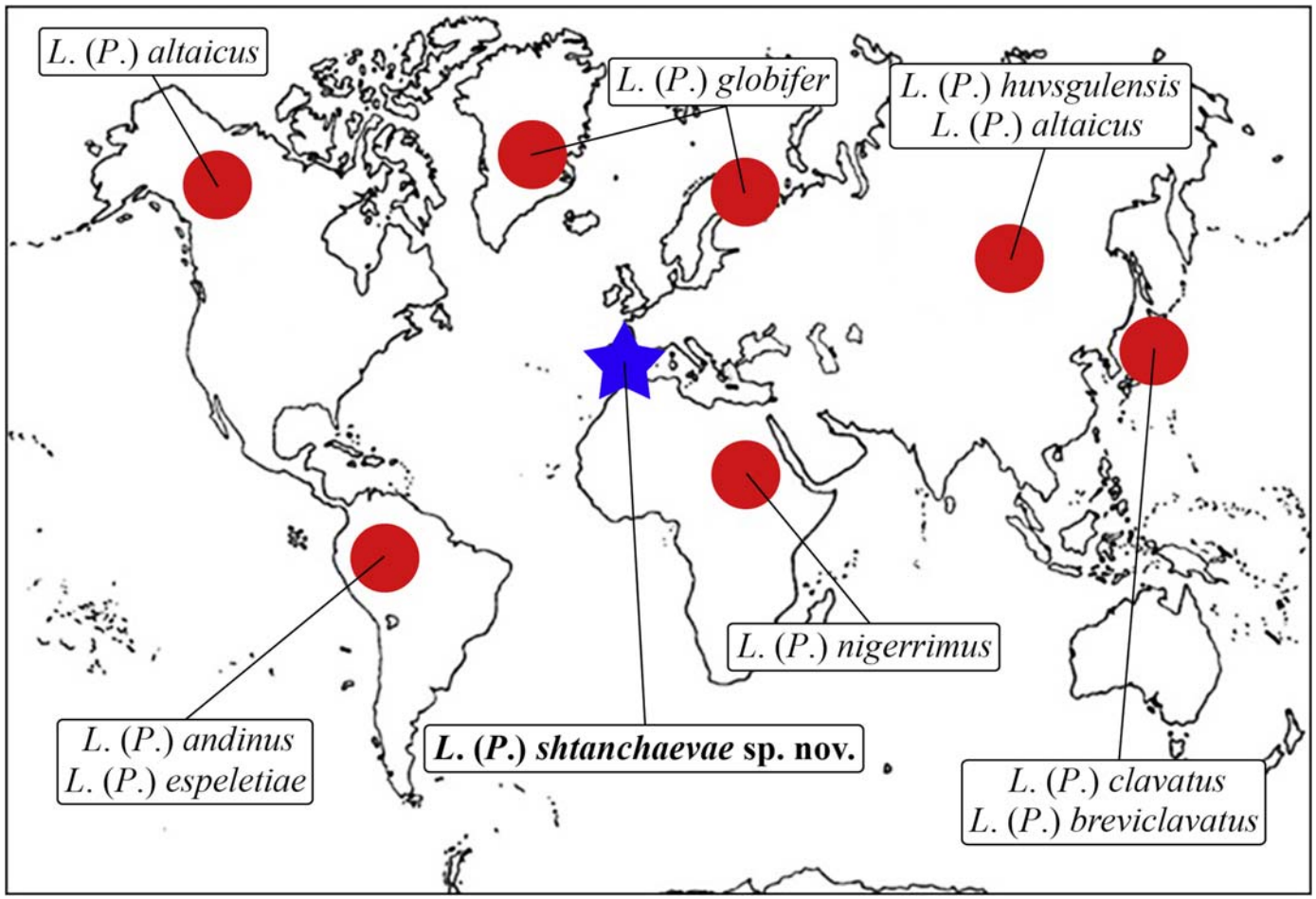

Fig. 4. Distribution of the *Liacarus* (*Procorynetes*) spp. (Oribatida: Liacaridae). Red dots correspond to the living species, and the blue star represents the type locality of the new fossil species from the lower Albian (Lower Cretaceous) amber-bearing site of Ariño. (For interpretation of the references to color in this figure legend, the reader is referred to the Web version of this article.)

Finally, the only African species, *L.* (*P.*) *nigerrimus*, was described from "East Africa", the label of the holotype reading "Africa Orientale, Alluaud et Jeannel" (Castagnoli and Pegazzano, 1985). We know that Charles A. Alluaud and René Jeannel made an expedition to East Africa in 1911–1912 to study equatorial alpine fauna and they collected samples in both Mount Kenya and Mount Kilimanjaro. Therefore, the holotype must come from one of these mountains.

The presence of *L.* (*P.*) *shtanchaevae* sp. nov. during the early Albian of the Iberian Peninsula is interesting, as it corresponds to the only species of the subgenus living under a warm climate and at low altitude where the resiniferous forest thrived. Therefore, the *Liacarus* (*Procorynetes*) spp. seems to follow a common pattern of a relict distribution which was wider in the past, and today is restricted to cold areas or high elevations in the Holarctic and high mountains in the Afrotropical and Neotropical ecozones (Fig. 4).

5.3. Morphological stasis in oribatid mites

The new species described here belongs not just to a living genus, but to a living subgenus. This is the only case so far of a specimen of a living oribatid subgenus in the Cretaceous. However, its finding is not surprising, as oribatid mites are an important example of bradytely within arthropods: that is, long-term morphological stasis over the geological time (Simpson, 1944). Most of them have preserved a highly similar habitus and morphology since the Cretaceous that makes them almost indistinguishable from the living representatives. To date, 17 oribatid species have been described from Cretaceous ambers, 15 of them listed by Arillo et al. (2020), with the additions of the species from Lebanese amber (Arillo et al., 2019) and the species described here. Interestingly, 13 of these species belong to living genera – that is, 76% of the oribatid species from Cretaceous ambers – suggesting bradytely for these genera in particular and oribatids in general. The only four extinct oribatid genera recorded in Cretaceous ambers are: *Eocamisia* Bulanova-Zachvatkina, 1974 (Santonian, Russia), *Rasnitsynella* Krivolutsky, 1976 (in Krivolutsky and Ryabinin, 1976) (Santonian, Russia), *Strieremaeus* Sellnick, 1919 (Albian, Spain, also recorded in Eocene Baltic and Rovno ambers), and *Cretaceobodes* Arillo, Subías and Shtanchaeva, 2010 (Albian, Spain). Bradytely has usually been related to groups inhabiting mesic microhabitats, such as the leaf litter on forest soil (Yamamoto et al., 2017). Besides the oribatids, some beetles, psocids, and springtails are leaf litter habitants with Cretaceous species belonging to living genera (Sánchez-García and Engel, 2016; Yamamoto et al., 2017; Álvarez-Parra et al., 2020b). The body plan and general habitus of the oribatids have remained stable and almost unchanged at least since the Early Cretaceous, occupying a similar litter habitat to their living representatives. However, the evolutionary patterns over the history of the oribatids are not well known, and the description of new fossil species may draw attention to the outstanding morphological stability of this group.

6. Concluding remarks

Liacarus (*Procorynetes*) *shtanchaevae* sp. nov., from the lower Albian amber-bearing site of Ariño, represents the first fossil record of the Liacaridae, and the first Cretaceous species belonging to a living oribatid subgenus. It is the seventeenth oribatid species from Cretaceous amber described to date, and thus increases the known palaeodiversity of the group. Considering the biology of the extant representatives of the family, it may be a leaf litter dweller of the resiniferous forest community. However, the environmental conditions of its ecosystem, close to the sea and under a tropical or subtropical climate, differ from those of the living species of the subgenus, which inhabit cold environments at high latitudes or high mountains at middle latitudes. Therefore, the new species shows that the living species of the subgenus may be relict, since the ancient representatives occupied a wider range of habitats and distribution.

Acknowledgements

We thank our colleagues who participated in the palaeontological excavation in Ariño, and the SAMCA Group and Fundación Conjunto Paleontológico de Teruel-Dinópolis for their collaboration. We also thank the Dirección General de Patrimonio Cultural of the Aragón Government (Spain) for permission to excavate in Ariño (permit 201/10-2019 of the Aragón Government). We are grateful to Mr. Rafael López del Valle for the preparation of the amber piece. We thank the editor Dr Eduardo Koutsoukos and two anonymous reviewers for their helpful comments and suggestions that have improved the manuscript. This study is a contribution to the project CRE CGL2017-84419 funded by the Spanish AEI/FEDER, UE. The co-author S.Á.-P. thanks his Ph.D. Thesis advisers, Dr Xavier Delclòs (Universitat de Barcelona) and Dr Enrique Peñalver (Instituto Geológico y Minero de España-CSIC), and acknowledges the support of the Secretary of Universities and Research of the Government of Catalonia (Spain) and the European Social Fund (2020FI_B1 00002).

References

Alcalá, L., Espílez, E., Mampel, L., Kirkland, J.I., Ortiga, M., Rubio, D., González, A., Ayala, D., Cobos, A., Royo-Torres, R., Gascó, F., Pesquero, M.D., 2012. A new Lower Cretaceous vertebrate bonebed near Ariño (Teruel, Aragón, Spain); found and managed in a joint collaboration between a mining company and a palaeontological park. Geoheritage 4 (4), 275–286. https://doi.org/10.1007/s12371-012-0068-y.

Álvarez-Parra, S., Delclòs, X., Solórzano-Kraemer, M.M., Alcalá, L., Peñalver, E., 2020a. Cretaceous amniote integuments recorded through a taphonomic process unique to resins. Scientific Reports 10, 19840. https://doi.org/10.1038/s41598-020-76830-8.

Álvarez-Parra, S., Peñalver, E., Nel, A., Delclòs, X., 2020b. The oldest representative of the extant barklice genus *Psyllipsocus* (Psocodea: Trogiomorpha: Psyllipsocidae) from the Cenomanian amber of Myanmar. Cretaceous Research 113, 104480. https://doi.org/10.1016/j.cretres.2020.104480.

Álvarez-Parra, S., Pérez-de la Fuente, R., Peñalver, E., Barrón, E., Alcalá, L., Pérez-Cano, J., Martín-Closas, C., Trabelsi, K., Meléndez, N., López Del Valle, R., Lozano, R.P., Peris, D., Rodrigo, A., Sarto i Monteys, V., Bueno-Cebollada, C.A., Menor-Salván, C., Philippe, M., Sánchez-García, A., Peña-Kairath, C., Arillo, A., Espílez, E., Mampel, L., Delclòs, X., 2021. Dinosaur bonebed amber from an original swamp forest soil. eLife 10, e72477. https://doi.org/10.7554/eLife.72477.

Aoki, J., 1970. Descriptions of oribatid mites collected by smoking of trees with insecticides. I. Mt. Ishizuchi and Mt. Odaigahara. Bulletin of the National Science Museum, Tokyo 13, 585–602.

Arillo, A., Subías, L.S., Shtanchaeva, U., 2009. A new fossil species of oribatid mite, *Ametroproctus valeriae* sp. nov. (Acariformes, Oribatida, Ametroproctidae), from the Lower Cretaceous amber of San Just, Teruel Province, Spain. Cretaceous Research 30 (2), 322–324. https://doi.org/10.1016/j.cretres.2008.07.013.

Arillo, A., Subías, L.S., Shtanchaeva, U., 2010. A new genus and species of oribatid mite, *Cretaceobodes martinezae* gen. et sp. nov. from the Lower Cretaceous amber of San Just (Teruel Province, Spain) (Acariformes, Oribatida, Otocepheidae). Paleontological Journal 44, 287–290. https://doi.org/10.1134/S003103011003007X.

Arillo, A., Subías, L.S., Shtanchaeva, U., 2012. A new species of fossil oribatid mite (Acariformes, Oribatida, Trhypochthoniidae) from the Lower Cretaceous amber of San Just (Teruel Province, Spain). Systematic & Applied Acarology 17 (1), 106–112. https://doi.org/10.11158/saa.17.1.16.

Arillo, A., Subías, L.S., Sánchez-García, A., 2016. New species of fossil oribatid mites (Acariformes, Oribatida), from the Lower Cretaceous amber of Spain. Cretaceous Research 63, 68–76. https://doi.org/10.1016/j.cretres.2016.02.009.

Arillo, A., Subías, L.S., Chaves da Rocha, G., Azar, D., 2019. First fossil oribatid mite from Lebanese amber (Acariformes, Oribatida, Neoliodidae). Palaeoentomology 2 (6), 611–617. https://doi.org/10.11646/palaeoentomology.2.6.12.

Arillo, A., Subías, L.S., Peñalver, E., 2020. A new species of fossil Oribatid mite (Acariformes, Oribatida: Caleremaeidae) from a new Cretaceous amber outcrop in Asturias, Spain. Cretaceous Research 109, 104382. https://doi.org/10.1016/j.cretres.2020.104382.

Aurell, M., Soria, A.R., Bádenas, B., Liesa, C.L., Canudo, J.I., Gasca, J.M., Moreno-Azanza, M., Medrano-Aguado, E., Meléndez, A., 2018. Barremian synrift

sedimentation in the Oliete sub-basin (Iberian Basin, Spain): palaeogeographical evolution and distribution of vertebrate remains. Journal of Iberian Geology 44 (2), 285–308. https://doi.org/10.1007/s41513-018-0057-3.
Balogh, P., 1984. Oribatid mites from Colombia II (Acari). Acta Zoologica Academiae Scientiarum Hungaricae 30 (3–4), 315–326.
Bayartogtokh, B., 2010. Oribatid mites of Mongolia (Acari: Oribatida). KMK Scientific Press, Russian Academy of Sciences, Moscow, p. 371 [in Russian].
Behan-Pelletier, V.M., 1978. Diversity, distribution and feeding habits of North American arctic soil Acari. Unpublished Ph.D. thesis. McGill University, Montreal, p. 428.
Berlese, A., 1908. Elenco di generi e specie nuove di Acari. Redia 5, 1–15.
Berlese, A., 1916. Centuria terza di Acari nuovi. Redia 12, 289–338.
Boscá, A., 1910. Cuenca calaminífera de Linares de Aragón. Asociación Española para el Progreso de la Ciencia 4 (1), 171–181.
Bulanova-Zachvatkina, Y.M., 1974. A new genus of mite (Acariformes, Oribatei) from the Upper Cretaceous of Taymyr. Paleontological Journal 8, 247–250.
Castagnoli, M., Pegazzano, F., 1985. Catalogue of the Berlese acaroteca. Istituto Sperimentale per la Zoologia Agraria, Firenze, p. 490.
Corral, J.C., López Del Valle, R., Alonso, J., 1999. El ámbar cretácico de Álava (Cuenca Vasco-Cantábrica, norte de España). Su colecta y preparación. Estudios del Museo de Ciencias Naturales de Alava 14 (2), 7–21.
Delclòs, X., Arillo, A., Peñalver, E., Barrón, E., Soriano, C., López del Valle, R., Bernárdez, E., Corral, C., Ortuño, V.M., 2007. Fossiliferous amber deposits from the Cretaceous (Albian) of Spain. Comptes Rendus Palevol 6 (1–2), 135–149. https://doi.org/10.1016/j.crpv.2006.09.003.
Dugès, A.L., 1834. Recherches sur l'ordre des Acariens I–III. Annales des Sciences Naturelles Zoologie 2 (2), 18–63.
Dubinina, E.V., Sosnina, E.F., Vysotskaya, S.O., Markov, G.N., Atanasov, L.K., 1966. Oribatid mites (Oribatea) from rodent nests of Mt Vitosha. Izvestiya na Zoologicheskiya Institut s Muzei (Sofia) 22, 81–139.
Dunlop, J.A., Penney, D., Jekel, D., 2012. A summary list of fossil spiders and their relatives. World Spider Catalog. Natural History Museum Bern, version 20.5. https://wsc.nmbe.ch/resources/fossils/Fossils20.5.pdf. (Accessed 16 December 2020).
Dzhaparidze, N.I., 1987. Oribatid mites of the genera *Raphidosus* and *Procorynetes* found in the Soviet Union fauna. Bulletin of the Academy of Sciences of the Georgian SSR 125 (1), 141–143 [in Russian].
Fujikawa, T., Aoki, J., 1970. Five species of the genus *Liacarus* Michael (Acari: Liacaridae). Taxonomic notes on oribatid mites of Hokkaido. III. Annotationes Zoologicae Japonenses 43, 158–165.
Hull, J.E., 1916. Terrestrial Acari of the Tyne province, I: Oribatidae. Transactions of the Natural History Society of Northumberland, Durham and Newcastle (New Series) 4, 381–410.
Hull, J.E., 1918. Terrestrial Acari of the Tyne province. Transactions of the Natural History Society of Northumberland, Durham and Newcastle (New Series) 5, 13–88.
Iturrondobeitia, J.C., Subías, L.S., 1978. Contribución al conocimiento de los oribátidos (Acarida, Oribatida) del PaísVasco, II. Boletín de la Asociación Española de Entomología 2, 87–90.
Koch, C.L., 1839. Deutschlands Crustaceen, Myriapoden und Arachniden. Friedrich Pustet, Regensburg, pp. 28–30.
Koch, C.L., 1841. Deutschlands Crustaceen, Myriapoden und Arachniden. Friedrich Pustet, Regensburg, pp. 31–32.
Kramer, P., 1897. Grönlandische Milben. Bibliotheca Zoologica 20 (3), 77–83.
Krivolutsky, D.A., 1965. Some notes on the system of the family Liacaridae Sell., 1928 (Oribatei, Acariformes). Otcyel Biologicseszkij 70 (2), 118–120.
Krivolutsky, D.A., 1974. New oribatid mites of the URSS. Zoologicheskii Zhurnal 53 (12), 1880–1884 [in Russian].
Krivolutsky, D.A., Ryabinin, N.A., 1976. Oribatid mites in Siberian and Far East amber. Reports of the Academy of Science of the USSR 230, 945–948 [in Russian].
Krivolutsky, D.A., Krasilov, B.A., 1977. Oribatid mites from Upper Jura deposits of USSR. In: Skarlato, O.A., Balashov, Y.S. (Eds.), Morphology and Diagnostics of Mites. Zoological Institute, Leningrad, pp. 16–24 [in Russian].
Michael, A.D., 1898. Oribatidae. In: Schulze, F.E. (Ed.), Das Tierreich, Lief. 3 (Acarina), vol. 8. Friedländer und Sohn, Berlin, pp. 1–93.
Nicolet, H., 1855. Histoire naturelle des acariens qui se troven aux environs de Paris. Archives du Muséum National d'Histoire Naturelle Paris 7, 381–482.
Norton, R.A., Bonamo, P.M., Grierson, J.D., Shear, W.A., 1988. Oribatid mite fossils from a terrestrial Devonian deposit near Gilboa, New York. Journal of Paleontology 62, 259–269.
Norton, R.A., Behan-Pelletier, V.M., 2009. Suborder Oribatida. In: Krantz, G.W., Walter, D.E. (Eds.), A Manual of Acarology, vol. 15. Texas Tech University Press, Lubbock, pp. 430–564.
Oudemans, A.C., 1900. Remarks on the denomination of the genera and higher groups in "Das Tierreich, Oribatidae". Tijdschrift voor Entomologie 43 (1–2), 140–149.
Oudemans, A.C., 1930. Acarologische Aanteekeningen CIII. Entomologische Berichten 8, 97–101.
Peñalver, E., Delclòs, X., 2010. Spanish amber. In: Penney, D. (Ed.), Biodiversity of fossils in amber from the major world deposits, vol. 13. Siri Scientific Press, Manchester, pp. 236–270.
Ryabinin, N.A., Zaitsev, A.S., 2019. New species of oribatid mites (Acari, Oribatida) from Sakhalin Island. Entomological Review 99 (4), 560–564. https://doi.org/10.1134/S0013873819040183.
Salas, R., Guimerà, J., 1996. Rasgos estructurales principales de la cuenca cretácica inferior del Maestrazgo (Cordillera Ibérica oriental). Geogaceta 20 (7), 1704–1706.
Sánchez-García, A., Engel, M.S., 2016. Springtails from the Early Cretaceous amber of Spain (Collembola: Entomobryomorpha), with an annotated checklist of fossil Collembola. American Museum Novitates 3862, 1–47. https://doi.org/10.1206/3862.1.
Schaefer, I., Caruso, T., 2019. Oribatid mites show that soil food web complexity and close aboveground-belowground linkages emerged in the early Paleozoic. Communications Biology 2, 387. https://doi.org/10.1038/s42003-019-0628-7.
Schatz, H., Behan-Pelletier, V., 2008. Global diversity of oribatids (Oribatida: Acari: Arachnida). Hydrobiologia 595, 323–328. https://doi.org/10.1007/s10750-007-9027-z.
Sellnick, M., 1919. Die Oribatiden der Bernsteinsammlung der Universität Königsberg i. Pr. Schriften der Physikalisch-Ökonomischen Gesellschaft zu Königsberg 59, 21–42.
Sellnick, M., 1928. Formenkreis: Hornmilben, Oribatei. In: Brohmer, P., Ehrmann, P., Ulmer, G. (Eds.), Die Tierwelt Mitteleuropas, vol. 3. Quelle und Meyer, Leipzig, pp. 1–42 (4), IX.
Sellnick, M., 1931. Milben im Berstein. Bernsteinforschung 2, 148–180.
Shtanchaeva, U.Y., Subías, L.S., 2010. A new genus and species of oribatid mites *Scarabacarus longisensillus* gen. et sp. n. (Acariformes, Liacaridae) from the Caucasus. Entomological Review 90 (8), 1111–1114. https://doi.org/10.1134/S0013873810080166.
Shtanchaeva, U.Y., Subías, L.S., Arillo, A., 2010. New taxa of oribatid mites of the family Liacaridae (Acariformes: Oribatida) from the Caucasus. Entomologica Fennica 20 (4), 245–248. https://doi.org/10.33338/ef.84485.
Simpson, G., 1944. Tempo and Mode in Evolution. Columbia University Press, New York, p. 237.
Subías, L.S., 2004. Listado sistemático, sinonímico y biogeográfico de los ácaros oribátidos (Acariformes, Oribatida) del mundo (1758–2002). Graellsia 60, 3–305. https://doi.org/10.3989/graellsia.2004.v60.iExtra.218 (14th update 2019).
Subías, L.S., Arillo, A., 2002. Oribatid fossil mites from the Upper Devonian of South Mountain, New York and the Lower Carboniferous of County Antrim, North Ireland (Acariformes, Oribatida). Estudios del Museo de Ciencias Naturales de Alava 17, 93–106.
Tibert, N.E., Colin, J.P., Kirkland, J.I., Alcalá, L., Martín-Closas, C., 2013. Lower Cretaceous nonmarine ostracodes from an Escucha Formation dinosaur bonebed in eastern Spain. Micropaleontology 59 (1), 83–91.
Villanueva-Amadoz, U., Sender, L.M., Alcalá, L., Pons, D., Royo-Torres, R., Diez, J.B., 2015. Paleoenvironmental reconstruction of an Albian plant community from the Ariño bonebed layer (Iberian Chain, NE Spain). Historical Biology 27 (3–4), 430–441. https://doi.org/10.1080/08912963.2014.895826.
Weigmann, G., 2006. Hornmilben (Oribatida). In: Die Tierwelt Deutschlands, vol. 76. Verlag Goecke & Evers, Keltern, p. 520.
Woolley, T.A., 1967. North American Liacaridae, I: *Adoristes* and a related new genus (Acari: Cryptostigmata). Journal of the Kansas Entomological Society 40 (3), 270–276.
Woolley, T.A., 1969. North American Liacaridae, III: new genera and species (Acari: Cryptostigmata). Journal of the Kansas Entomological Society 42 (2), 183–194.
Woolley, T.A., 1972. The systematics of the Liacaroidea (Acari: Cryptostigmata). Acarologia 14 (2), 250–257.
Woolley, T.A., Higgins, H.G., 1966. Xenillidae, a new family of oribatid mites (Acari: Cryptostigmata). Journal of the New York Entomological Society 74 (4), 201–221.
Yamamoto, S., Takahashi, Y., Parker, J., 2017. Evolutionary stasis in enigmatic jacobsoniid beetles. Gondwana Research 45, 275–281. https://doi.org/10.1016/j.gr.2016.12.008.
Zakhvatkin, A.A., 1952. Subdivision of the mites (Acarina) into orders and the position of these in the system of Chelicerata. Parazitologicheskii Sbornik Zoologicheskii Institut Akademii Nauk SSSR 12, 5–46.

Anexo 8.1.5

New insights into the enigmatic Cretaceous family Spathiopterygidae (Hymenoptera: Diaprioidea)

Santer, M., **Álvarez-Parra, S.**, Nel, A., Peñalver, E., Delclòs, X. 2022. New insights into the enigmatic Cretaceous family Spathiopterygidae (Hymenoptera: Diaprioidea). *Cretaceous Research*, **133**, 105128.

DOI: https://doi.org/10.1016/j.cretres.2021.105128

Revista científica: *Cretaceous Research*
Factor de impacto: 2,432 (2021)
Categoría: *Paleontology*, Q1 (2021)

Cretaceous Research 133 (2022) 105128

Contents lists available at ScienceDirect

Cretaceous Research

journal homepage: www.elsevier.com/locate/CretRes

New insights into the enigmatic Cretaceous family Spathiopterygidae (Hymenoptera: Diaprioidea)

Maxime Santer [a], Sergio Álvarez-Parra [b, *], André Nel [c], Enrique Peñalver [d], Xavier Delclòs [b]

[a] Univ. Rennes, CNRS, Géosciences Rennes, UMR 6118, Rennes, F-35000, France
[b] Departament de Dinàmica de la Terra i de l'Oceà and Institut de Recerca de la Biodiversitat (IRBio), Facultat de Ciències de la Terra, Universitat de Barcelona, c/Martí i Franquès s/n, Barcelona, 08028, Spain
[c] Institut de Systématique, Évolution, Biodiversité (ISYEB) Muséum national d'Histoire naturelle, CNRS, Sorbonne Université, EPHE, Université des Antilles, CP50, 57 rue Cuvier Paris, 75005 France
[d] Museo Geominero (IGME, CSIC), c/Cirilo Amorós 42, Valencia, 46004, Spain

ARTICLE INFO

Article history:
Received 8 September 2021
Received in revised form
21 December 2021
Accepted in revised form 21 December 2021
Available online 28 December 2021

Keywords:
Albian
Amber
Palaeobiology
Parasitoidism
Wasps

ABSTRACT

The Cretaceous family Spathiopterygidae (Hymenoptera: Diaprioidea), containing five species in four genera, showed a wide distribution from the upper Barremian to the Turonian. We describe two new representatives of the family from the upper Albian San Just outcrop in the eastern Iberian Peninsula that correspond to *Diameneura marveni* gen. et sp. nov. Santer and Álvarez-Parra and to a female member of *Mymaropsis turolensis* Engel and Ortega-Blanco, 2013. The forewing venation of *Diameneura marveni* gen. et sp. nov. is interpreted, allowing an appropriate comparison for future descriptions. Furthermore, we provide a diagnosis for *Mymaropsis baabdaensis* since no diagnosis was proposed in the initial paper. We indicate the taphonomic characteristics of the newly described specimens, discuss the interrelationships of the family, and provide new insights about the sexual dimorphism and palaeobiology of spathiopterygids.

1. Introduction

Hymenoptera is a diverse insect order containing more than 153,000 living species that play a panoply of ecological roles in the environment, such as herbivory, pollination, predation, and parasitoidism (Peters et al., 2017). It has shown outstanding diversity since the Triassic, with more than 3607 extinct species described to date (Fossilworks, available at http://fossilworks.org, accessed 13 December 2021). Moreover, its members are common bioinclusions in amber deposits worldwide (e.g., Zhang et al., 2018). The Cretaceous shows an impressive diversity of these insects thank to the specimens found in Burmese amber. Among this diversity, several extinct hymenopteran families are restricted to the Cretaceous, such as Serphitidae, Aptenoperissidae, and Ohlhoffiidae (Ortega-Blanco et al., 2011a; Rasnitsyn et al., 2017; Jouault et al., 2021c). Their studies are crucial to understand the diversification and palaeobiology of hymenopterans during the early evolution of the Recent ecosystems.

Spathiopterygidae is a poorly known Cretaceous family of tiny wasps. It currently includes four genera and five species identified from deposits of Lebanon, Spain, Myanmar, and the USA, spanning from the upper Barremian to the Turonian (Engel et al., 2013, 2015; Krogmann et al., 2016). *Cretapria tsukadai* Fujiyama, 1994, from the Aptian Choshi amber, could also belong to this family (Rasnitsyn and Öhm-Kühnle, 2020). Interestingly, these wasps appear to be rare, mostly being only represented by the holotype specimens. Therefore, their intraspecific variability and sexual dimorphism are unclear. Until now, only one female specimen has been described (Krogmann et al., 2016). The study of these wasps is important to gain further knowledge on their hypothesised parasitoid lifestyle (Engel et al., 2015). It is expected that this known palaeodiversity will be increased through the description of new specimens, as some from the Cenomanian Burmese amber are currently pending investigation (Zhang et al., 2018). It is likely that additional specimens are also present in more Cretaceous amber deposits, such as in French and Burmese ambers (Corentin Jouault pers. comm.).

* Corresponding author.
E-mail address: sergio.alvarez-parra@ub.edu (S. Álvarez-Parra).

https://doi.org/10.1016/j.cretres.2021.105128

Spathiopterygidae is currently included in the superfamily Diaprioidea (Engel et al., 2013) and in the infraorder Proctotrupomorpha alongside several other groups of parasitoid wasps (Sharkey, 2007; Sharkey et al., 2012; Peters et al., 2017). The superfamily Diaprioidea was originally proposed to include the extant families Diapriidae, Monomachidae, and Maamingidae (Dowton and Austin, 2001: fig. 2; Sharkey, 2007). Later, the family Ismaridae was added after it was raised from the rank of diapriid subfamily to that of family (Sharkey et al., 2012). The reduced wing venation of Diapriidae, Maamingidae, and Spathiopterygidae suggests a grouping of these families, when considering the relative complete venation of Monomachidae as a plesiomorphic state character (Engel et al., 2013). The sister group of Spathiopterygidae could be Maamingidae (Engel et al., 2013), a monogeneric family that includes only two species from New Zealand (Early et al., 2001a), but no cladistic analyses prove that. Recently, in the revision of Proctotrupomorpha by Rasnitsyn and Öhm-Kühnle (2020), a new clade called Microprocta was proposed to comprise the groups Chalcidoidea, Diaprioidea, Platygastroidea, and Bipetiolarida (embracing Serphitoidea and Mymarommatoidea). Furthermore, the families Monomachidae and Maamingidae were excluded from Diaprioidea, Diapriidae being the putative sister group of Spathiopterygidae (Rasnitsyn and Öhm-Kühnle, 2020).

Here, we describe a new genus and species belonging to Spathiopterygidae and the first known female of *Mymaropsis turolensis*. Both specimens were identified in amber pieces from the upper Albian San Just amber-bearing outcrop (eastern Iberian Peninsula). The new genus and species correspond to the fifth genus and sixth species known for this enigmatic Cretaceous family of tiny wasps. We discuss its phylogenetic position within the family and provide new comments about the presumable palaeobiology of the spathiopterygids. Furthermore, we provide the first diagnosis for *Mymaropsis baabdaensis* originally described from the Barremian Lebanese amber.

2. Geological setting

The San Just amber-bearing outcrop (Fig. 1) is located near Utrillas (Teruel Province, Spain) in the Aliaga Sub-basin within the Maestrazgo Basin in the Aragonese Branch of the Iberian Chain (Salas and Guimerà, 1996). There are more than 30 amber-bearing outcrops in the Maestrazgo Basin, although only four of them have yielded bioinclusions to date (Álvarez-Parra et al., 2021): Ariño, San Just, Arroyo de la Pascueta, and La Hoya. The stratigraphic section of San Just belongs to the middle member (Regachuelo Member) of the Escucha Formation (Peñalver et al., 2007). The age of onset of the Escucha Formation was first established as late Aptian–early Albian based on palynological data (Peyrot et al., 2007), although a chronostratigraphic study supported by ammonoid biostratigraphy and strontium isotope stratigraphy suggested early Albian as the oldest age (Bover-Arnal et al., 2016). The San Just amber is found in a layer of grey-black marls containing high amounts of organic matter, charcoal, and fusinite (Peñalver et al., 2007). The San Just locality has been dated middle–earliest late Albian based on the palynological assemblage (Villanueva-Amadoz et al., 2010), although a new, extensive palynological study has constrained the dating to the late Albian based on unpublished data. The amber could be parautochthonous in a depositional environment that has been proposed to have been a freshwater swamp plain (Peñalver et al., 2007; Villanueva-Amadoz et al., 2010).

San Just is the amber-bearing outcrop with the highest number of bioinclusions in the Maestrazgo Basin, including coprolites, Araneae orbwebs, fungi, plants, arachnids, 12 insect orders, and dinosaur feathers (Peñalver et al., 2006, 2007; Peñalver and Delclòs, 2010). It is the type locality of 25 arthropod species (including the new species described herein). Hymenopterans are one of the most abundant insect orders in San Just amber, but only eight species have been identified so far belonging to the families Alavarommatidae, Evaniidae, Gallorommatidae, Serphitidae, Spathiopterygidae, and Stigmaphronidae.

3. Material and methods

The studied material corresponds to the bioinclusions of two amber pieces from the San Just amber-bearing outcrop (Teruel, Aragon, Spain) obtained during fieldwork in 2007. The pieces were

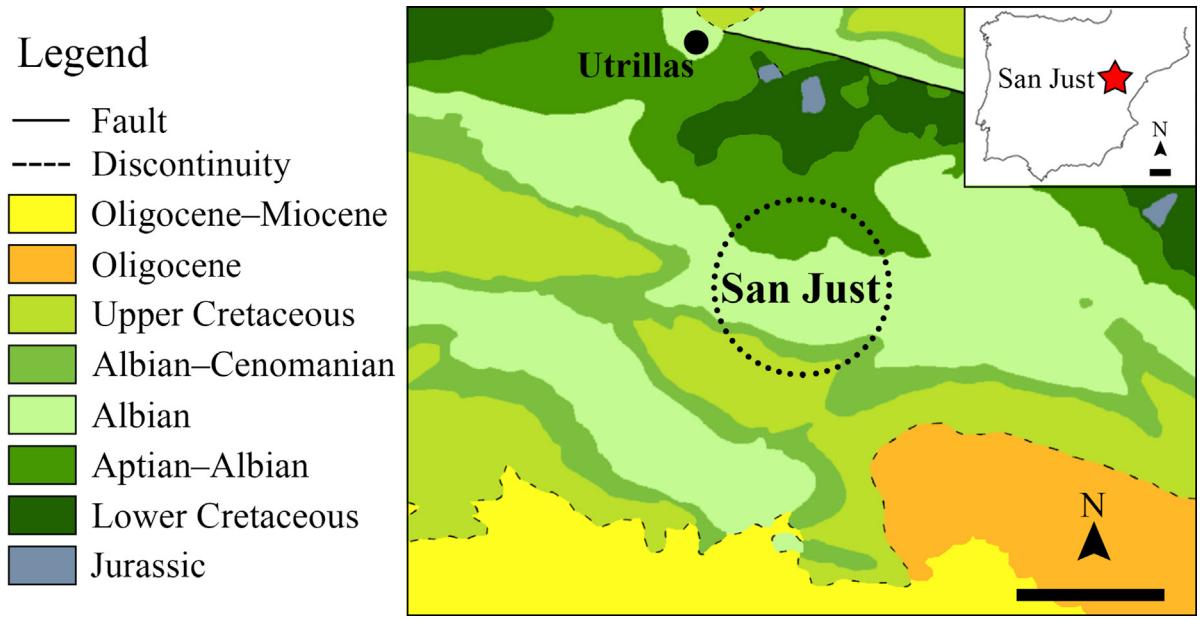

Fig. 1. Geographical and geological location of the upper Albian San Just amber-bearing outcrop (Teruel Province, Spain); modified from Canerot et al. (1977) and Martín Fernández and Canerot (1977). Scale bars = 100 km (Iberian Peninsula), 2 km (geological map).

cut, polished, and embedded in epoxy resin following the methodology of Corral et al. (1999). This is important for the stabilisation and protection of the amber pieces. An Olympus CX41 compound microscope with an attached camera lucida and the digital camera sCMEX-20 was used to make the drawings and take the photographs of the specimens. Photographs were taken with ImageFocusAlpha version 1.3.7.12967.20180920. The figures were prepared using Photoshop CS6. The 3D reconstruction and animation were performed with Blender 2.91.2. The anatomical nomenclature follows the work of Engel et al. (2013). The diagnosis for *Mymaropsis baabdaensis* has been made following the description provided in work of Krogmann et al. (2016). The forewing venation nomenclature corresponds to: Sc+R = subcostal and radial; B = basal; R = radial; Rs = radial sector; M = medial; Rs+M = radial sector and medial; M+Cu = medial and cubital; Cu = cubital.

The specimens are housed at the Museo Aragonés de Paleontología (Fundación Conjunto Paleontológico de Teruel-Dinópolis) in Teruel, Spain. Regarding the fossil notation, CPT is the official number at the museum and SJ-07 is the field notation for the excavation in 2007 (administrative permission code: 171/2007).

This manuscript has been registered in ZooBank under the number urn:lsid:zoobank.org:pub:6B175995-DBB6-4AE8-B2E4-839ADC05168C.

4. Results

4.1. Systematic palaeontology

Order Hymenoptera Linnaeus, 1758
Superfamily Diaprioidea Haliday, 1833
Family Spathiopterygidae Engel and Ortega-Blanco, 2013 (in Engel et al., 2013)

Type genus: *Spathiopteryx* Engel and Ortega-Blanco, 2013 (in Engel et al., 2013)
Other genera: *Mymaropsis* Engel and Ortega-Blanco, 2013 (in Engel et al., 2013), *Spathopria* Engel, Ortega-Blanco and Grimaldi, 2013 (in Engel et al., 2013), *Diaspathion* Engel and Huang, 2015 (in Engel et al., 2015), and *Diameneura* gen. nov. More information provided in Table 1.

Genus ***Diameneura*** gen. nov. Santer and Álvarez-Parra
This new genus has been registered in ZooBank under the number urn:lsid:zoobank.org:act:F092F27C-BF78-41D3-91ED-8FC7B7E6E20A.
Type species: *Diameneura marveni* sp. nov., by present designation and monotypy.

Etymology. The new generic name is composed of the Greek terms '*diamesos*' (meaning 'median') and '*neura*' (meaning 'venations'), referring to the fact that the forewing has longitudinal veins as well as a sclerotised part of the margin. Gender feminine.
Diagnosis. Compound eyes not bulging, with number of ommatidia over 120 each; polygonal rugulose microsculpture present on back of head and mesoscutum; forewing membrane wrinkled; margin densely covered with stiff setae; visible venation, but mainly nebulous; setae disposition on membrane not homogeneous, with positive gradient from base to apex; highly sclerotised mid-basal section of costal margin (thick parastigma); sclerotised M+Cu covered with rough, stiff setae; Rs+M not contacting M+Cu; Rs not contacting Rs+M; Rs well defined and well distant from R.

Diameneura marveni sp. nov. Santer and Álvarez-Parra
Figs. 2, 3, Fig. S1

This new species has been registered in ZooBank under the number urn:lsid:zoobank.org:act:6ADB8802-C684-467A-9596-C71E926F59E7.

Material. Holotype only, CPT-4095 (SJ-07-41), sex unknown, from San Just amber. Housed at Museo Aragonés de Paleontología (Fundación Conjunto Paleontológico de Teruel-Dinópolis) in Teruel, Spain. Specimen preserved in a milky amber piece prepared in an epoxy prism of 23 × 15 mm.
Locality and horizon. San Just amber-bearing outcrop, Teruel, Spain; Escucha Formation, upper Albian (Peñalver et al., 2007).
Etymology. The specific epithet *marveni* is a patronym honouring Nigel Marven, a British wildlife TV presenter known for his appearances in several palaeontology documentaries; and is to be treated as a noun in a genitive case.
Diagnosis. Same as that for the genus (see above).
Description. Integument black to dark brown, sex unknown (Fig. 2A–D). Head globular-ovoid, 0.19 mm long and 0.30 mm wide; three ocelli visible; compound eyes not bulging and occupying large portion of head lateral surface, with number of dorsally visible ommatidia over 120 each and distance between eyes 0.13 mm wide; antennae 0.96 mm long, densely covered by small bubbles; scape about twice as long as pedicel and slightly curved; elongate pedicel not globular, 1.5 × longer than wide, with a rimmed distal margin; flagellomeres covered with curved setae, distal flagellomere tapering toward apex; antennomeres lengths: scape 0.11 mm and pedicel 0.06 mm, with only two distal flagellomeres completely visible (0.08 mm and 0.11 mm long, respectively). Mesosoma with bulging mesoscutum 0.21 mm long and 0.24 mm wide. Polygonal rugulose microsculpture present on back of head and mesoscutum (Fig. 2E); notauli if present not visible or only

Table 1
Checklist of the known genera and species of Spathiopterygidae, with the known sex, age, and provenance indicated. In bold: new genus and species described herein. The information about the resin-producing tree and Burmese amber is from McCoy et al. (2021) and Ross et al. (2010), respectively.

Genus and species	Known sex	Age	Provenance	Resin-producing tree	Reference
Spathopria sayrevillensis Engel, Ortega-Blanco and Grimaldi, 2013	♂	Turonian	Sayreville, USA	Cupressaceae	Engel et al. (2013)
Diaspathion ortegai Engel and Huang, 2015	♂	early Cenomanian	Hukawng Valley, Myanmar	Araucariaceae or Dipterocarpaceae	Engel et al. (2015)
Spathiopteryx alavarommopsis Engel and Ortega-Blanco, 2013	♂	late Albian	Peñacerrada I, Spain	Araucariaceae	Engel et al. (2013)
Diameneura marveni gen. et sp. nov. Santer and Álvarez-Parra	Unknown	late Albian	San Just, Spain	Cheirolepidiaceae	This paper
Mymaropsis turolensis Engel and Ortega-Blanco, 2013	♂?, ♀	late Albian	San Just, Spain	Cheirolepidiaceae	Engel et al. (2013); this paper
Mymaropsis baabdaensis Krogmann, Azar, Rajaei and Nel, 2016	♀	late Barremian	Hammana-Mdeyrij, Lebanon	Conifers (Araucariaceae, Cheirolepidiaceae or Podocarpaceae)	Krogmann et al. (2016); this paper

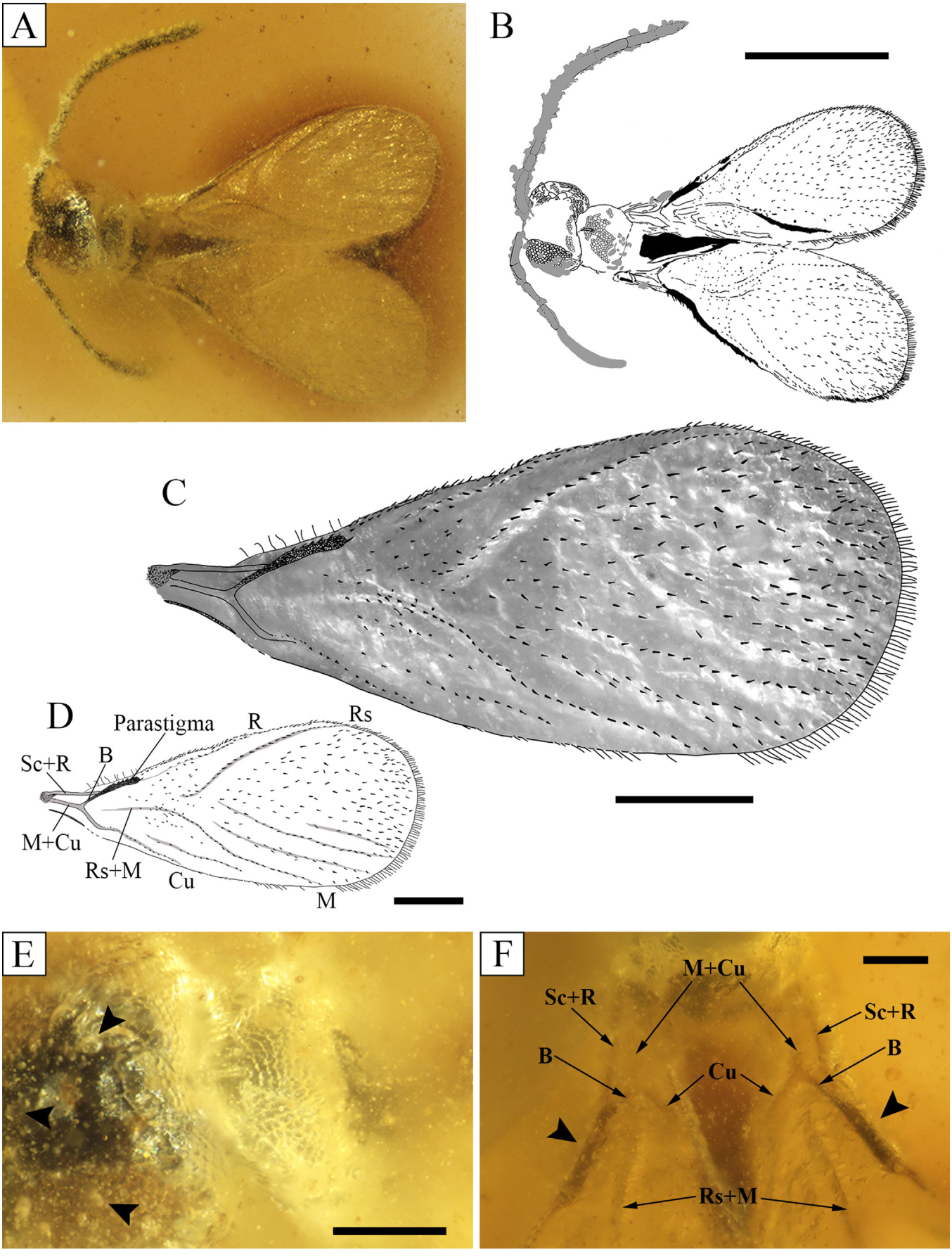
A
B
C
D
Parastigma
R
Rs
Sc+R
B
M+Cu
Rs+M
Cu
M
E
F
M+Cu
Sc+R
Sc+R
B
B
Cu
Rs+M

Fig. 3. Artistic 3D reconstruction of *Diameneura marveni* gen. et sp. nov. (Hymenoptera: Spathiopterygidae). Unknown parts of the body taken from other species in the family; presence of hind wings speculative. Forewing 1.05 mm long. Author: Maxime Santer. Animation of the supposed living behaviour in Video 1.

anteriorly. Forewings surpassing metasoma (Fig. 2C, D), whitish, 1.05 mm long and 0.43 mm wide; membrane wrinkled, and moderately covered with setae, with a positive gradient from base to apex of wing; margin densely covered with stiff fringe setae; highly sclerotised mid-basal section of costal margin (thick parastigma) (Fig. 2F); Sc+R present in anterior part near wing base; sclerotised M+Cu at base of wings, covered with rough, stiff setae; diverging into B and Cu at 0.11 mm from wing base; R reaching margin at 0.62 mm from wing base; Rs+M horizontal not contacting with M+Cu; Rs not contacting Rs+M; Rs well defined and well distant from R; Rs reaching wing margin at 0.88 mm from wing base; M reaching wing margin at 0.84 mm from wing base; Cu present, parallel to M, reaching wing margin at 0.44 mm from wing base; anal vein difficult to discern, if present; several secondary folds present on membrane based on rows of setae and relief of membrane. Hind wings not visible, although possibly present, maybe covered by forewings. Legs partly visible in ventral view, but encompassed by a complete coat of air (Fig. S1). Metasoma and genitalia not visible.

Discussion. The specimen CPT-4095 fits in the family Spathiopterygidae based on its general habitus, which is very similar to those of the other genera in this family. Many of the diagnostic characters for the family listed by Engel et al. (2013) are visible in the specimen, viz., head slightly wider than long, circular compound eyes with coarse ommatidia, thin antennae longer than the body length, scape longer than the remaining antennomeres, flagellomeres not expanded nor flattened and longer than wide, forewings with fringe setae not greatly elongated, membrane with scattered short setae, reduced venation represented by nebulous or spectral lines on the membrane, pterostigma absent, Rs+M bifurcating before the middle part of the wing, Rs parallel to R and the anterior wing margin, M directed towards the apico-posterior part of the wing, and Cu parallel to M. Other key characteristics of the spathiopterygid venation would be M+Cu fork (junction of B and Cu) shifted far basal, all veins distal of that fork lost as tubular, and presence of diverging folds often nested and partially of secondary nature (Alexandr P. Rasnitsyn pers. comm.). Several diagnostic characters of the family are poorly visible in the studied specimen due to its preservation, as it can be only seen from the dorsal view. We assign the specimen to a new genus and species within the family based on the diagnostic characteristics that differentiate it from the other genera. *Diameneura* gen. nov. has more than 40 ommatidia per eye, like *Mymaropsis* and *Spathopria*, and unlike *Spathiopteryx* and *Diaspathion*. Forewings with a marginal fringe of short setae are also present in *Spathiopteryx* and *Mymaropsis*, but not in *Spathopria*. *Diameneura* gen. nov. shares with *Mymaropsis* the sclerotised mid-basal section of the forewing margin (thick parastigma), unlike in *Spathiopteryx*, *Spathopria*, and *Diaspathion*. The wrinkled membrane of *Diameneura* gen. nov. is also present in *Spathopria* and *Diaspathion*, but not in *Spathiopteryx* and *Mymaropsis*. The forewing membrane of *Diameneura* gen. nov. is less setose than that of *Mymaropsis*. The specimen CPT-4095 shows unique characters in

Fig. 2. *Diameneura marveni* gen. et sp. nov. (Hymenoptera: Spathiopterygidae), sex unknown, late Albian, San Just (Teruel Province, Spain), holotype CPT-4095 (SJ-07-41): A, B) photograph and drawing from dorsal view, both at the same scale; C, D) venation and covering of setae in the right forewing; E) polygonal microsculpture on the back of the head and mesoscutum, with the ocelli indicated by the arrowheads; F) arrowheads indicate the sclerotisation of the mid-basal section of the costal margins of forewings (parastigma); arrows: indicate the veins Sc+R, B, M+Cu, Rs+M, and Cu. Scale bars = 0.5 mm (A, B), 0.2 mm (C, D), 0.1 mm (E, F).

the family, such as the gradient of setae on the forewing membrane and the polygonal rugulose microsculpture present on back of head and mesoscutum. An interpretation of the forewing venation of *Diameneura marveni* gen. et sp. nov. is proposed (Fig. 2D). Forewing venation is similar to that of *Mymaropsis*, although somewhat more sclerotised, with Rs+M not contacting M+Cu, Rs well defined and well distant from R, and Rs not contacting Rs+M (these venation characteristics are absent or dubious in *Mymaropsis*). Vein Rs is either absent or appressed to R in *Mymaropsis* (Engel et al., 2013). The new genus *Diameneura* might be closely related to *Mymaropsis*. We consider that CPT-4095 merits its determination as a new genus based on key differences with *Mymaropsis*: polygonal rugulose microsculpture on back of head and mesoscutum (vs. head and mesoscutum punctured in *Mymaropsis*), forewing membrane wrinkled (vs. smooth in *Mymaropsis*), and forewings moderately covered by setae with positive gradient from base to apex (vs. densely and homogeneously setose in *Mymaropsis*). Hind wings are not visible, but they cannot be considered absent, as they might be covered by the forewings. The presence vs. absence of hind wings is an unstable character in the family, as they are present in *Spathiopteryx* and *Mymaropsis*, but absent in *Spathopria* and *Diaspathion*.

Genus *Mymaropsis* Engel and Ortega-Blanco, 2013 (in Engel et al., 2013)
Type species: *Mymaropsis turolensis* Engel and Ortega-Blanco, 2013 (in Engel et al., 2013).
Other species: *Mymaropsis baabdaensis* Krogmann, Azar, Rajaei and Nel, 2016.

Original diagnosis (from Engel et al., 2013: 6–7). 'Head closely punctured, punctures not particularly coarse. Frontal shelf reduced but still present; toruli facing upward. Compound eyes not bulging (not as in *S. alavarommopsis*), with an apparent normal proportion of ommatidia. Pedicel with apicalmost margin rimmed; flagellomeres subequal in length and shape although II–IV slightly longer than remainder. Pronotum with fine vertical striate microsculpture. Propleuron laterally concave. Mesoscutum punctured; notauli faintly impressed, converging but not meeting posteriorly. Forewing membrane smooth, densely covered by short setae, with reduced venation distinct as weakly sclerotized lines, and with same veins present as in *Spathiopteryx*. Hind wing retaining a small portion of membrane with three distal marginal hamuli and a longer seta on apicalmost margin of membrane. Metasoma extremely short, shorter than mesosoma; second metasomal tergum largest, dorsally covering portions of subsequent terga.'
Remarks. Females of *Mymaropsis* are larger in size than males. The character 'flagellomeres subequal in length and shape although II–IV slightly longer than remainder' proposed in the original diagnosis should be modified to 'flagellomeres F1–F4 longer than the remainder except for F12', based on the observations of the new specimens. Females of *Mymaropsis turolensis* do not show forewings densely covered with setae, a character plausible due to the sexual dimorphism of the species, while females of *Mymaropsis baabdaensis* show forewings densely covered with setae. Females show a basitarsus longer than the remaining tarsomeres. The character 'metasoma extremely short, shorter than mesosoma' should be removed from the diagnosis, based on the observations of the new specimens, as the metasoma of the previously described specimen of *M. turolensis* seems to be incomplete (Engel et al., 2013: fig. 2).

Mymaropsis turolensis Engel and Ortega-Blanco, 2013 (in Engel et al., 2013)
Fig. 4

Material. CPT-4097 (SJ-07-43), female, from San Just amber. Housed at Museo Aragonés de Paleontología (Fundación Conjunto Paleontológico de Teruel-Dinópolis) in Teruel, Spain. Complete specimen preserved in an amber piece prepared in an epoxy prism of 24 × 14 mm.
Original diagnosis (from Engel et al., 2013). Same as that of the original diagnosis of the genus *Mymaropsis* (see above).
Emended diagnosis. Scape not ventrally expanded; pedicel almost globular (thinner than in *Mymaropsis baabdaensis*); flagellomeres with a similar width; forewing densely covered with setae in males and moderately covered with setae in females.
Description of new female specimen. Body 1.40 mm long (until the ovipositor tip) and completely preserved in transparent amber (Fig. 4A, B); integument black to dark brown without fine hairs. Head globular-ovoid, 0.19 mm long and 0.32 mm wide; head plus mesosoma 0.60 mm long; compound eyes not bulging and occupying large portion of head lateral surface, with number of ommatidia over 40; ocelli not visible; scape about twice as long as pedicel and slightly curved; pedicel elongated, with a rimmed distal margin; 12 flagellomeres covered with setae; last eight flagellomeres with more straight, distinct setae almost perpendicular to flagellomeres; distal flagellomere elongated and tapering toward apex; length:width of each antennomere, considering the mean of both antennae, from proximal to distal (in mm): scape 0.11:0.32, pedicel 0.69:0.26, F1 0.10:0.16, F2 0.81:0.18, F3 0.86:0.16, F4 0.81:0.18, F5 0.59:0.18, F6 0.61:0.22, F7 0.75:0.24, F8 0.76:0.21, F9 0.75:0.27, F10 0.70:0.22, F11 0.71:0.22, and F12 0.10:0.26; mouthparts not clearly discernible, hindered by small bubbles. Mesosoma 0.33 mm long and 0.21 mm wide, poorly visible from dorsal view; undetermined structure present left to mesosoma, possibly corresponding to a broken part of mesoscutum. Forewings smooth, 1.21 mm long and 0.52 mm wide; margin covered with rough, stiff setae; highly sclerotised mid-basal section of costal margin; membrane moderately covered with setae (not as dense as in the holotype of *Mymaropsis turolensis* described by Engel et al., 2013); pattern of venation unclear. Possible left hind wing visible (Fig. 4C), very reduced, hamuli not visible. Legs well-preserved; trochanters almost 2/3 length of femora; small rounded trochantellus present; femora and tibiae of fore- and mid-legs covered with a few small setae; femur and tibia of hind-leg densely covered with long, stiff setae; one distal spur on inner side of tibiae, with that of the protibia being curved and 0.05 mm long and those of the meso- and metatibiae being nearly straight and 0.03 mm long; five tarsomeres; basitarsus longer than remaining tarsomeres; lengths of tarsomeres from proximal to distal, forelegs: I 0.12 mm, II 0.05 mm, III 0.04 mm, IV 0.03 mm, and V 0.06 mm; midlegs: I 0.13 mm, II 0.05 mm, III 0.04 mm, IV 0.03 mm, and V 0.05 mm; and hindlegs: I 0.19 mm, II 0.07 mm, III 0.06 mm, IV 0.04 mm, and V 0.06 mm; distal tarsomeres with simple pretarsal claws; arolium large. Metasoma 0.77 mm long, 0.30 mm wide; nine visible sclerites; length of exposed part of ovipositor 0.063 mm (Fig. 4D).
Remarks. The specimen CPT-4097 shows most of the diagnostic characters for the genus *Mymaropsis*, such as the compound eyes not bulging with around 40 ommatidia, the pedicel presenting a rimmed distal margin, the forewing membrane being smooth with a marginal fringe of setae, and the venation reduced with weakly sclerotised parts of the forewings (Engel et al., 2013). Other diagnostic characters are not clearly visible in the specimen due to its preservation. The specimen is assigned to *Mymaropsis turolensis* based on the similarity of its habitus with that of the holotype. The adscription to *Mymaropsis baabdaensis* is discarded based on differences in the general dimensions (e.g., body and forewing lengths), the shape of the pedicel (globular and wider in *M.*

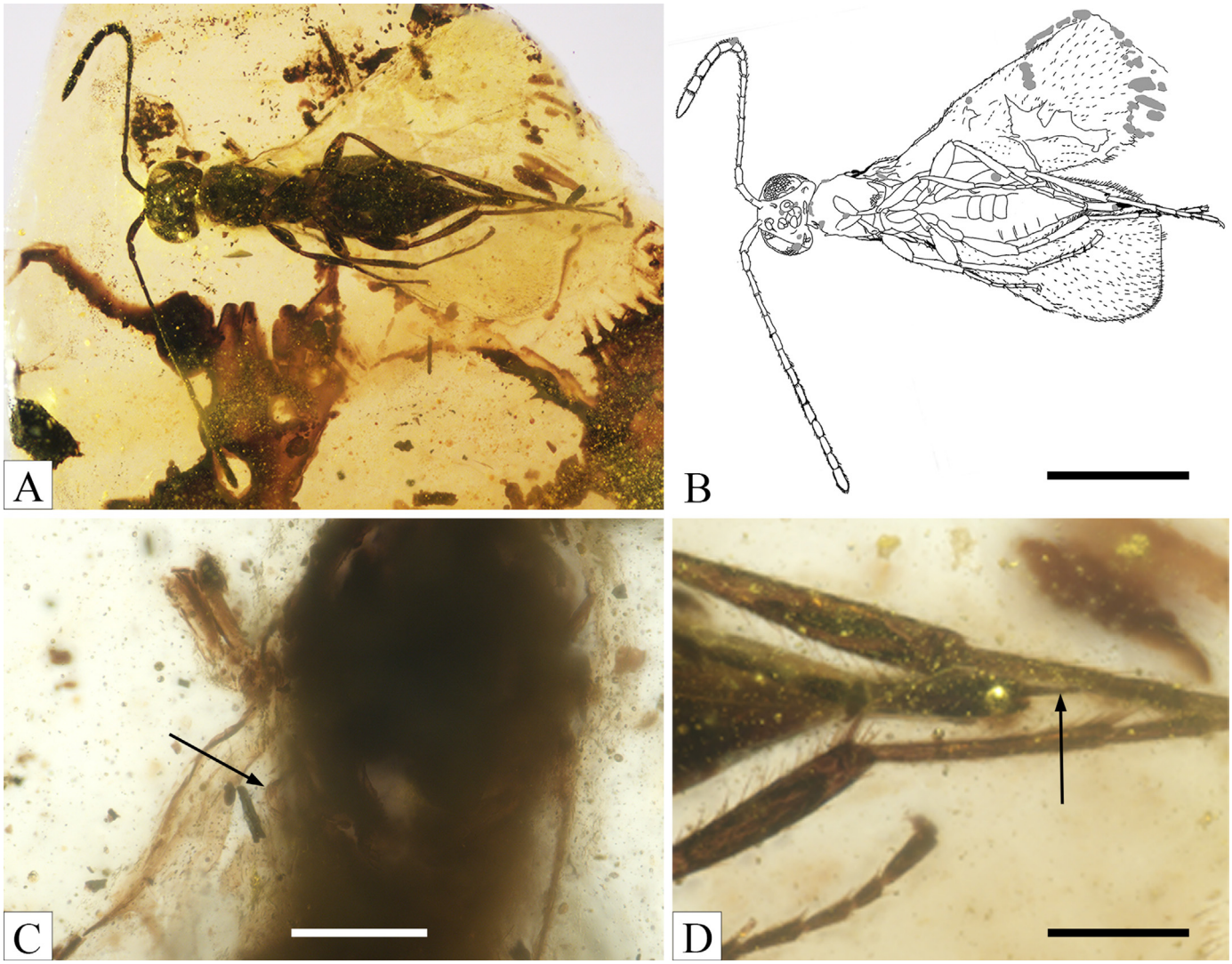

Fig. 4. *Mymaropsis turolensis* Engel and Ortega-Blanco, 2013 (Hymenoptera: Spathiopterygidae), female, late Albian, San Just (Teruel Province, Spain), specimen CPT-4097 (SJ-07-43): A, B) photograph and drawing in ventral view, both at the same scale; C) mesosoma from dorsal view; with the arrow indicating the possible left hind wing; D) ovipositor in ventral view; with the arrow indicating the tip of the ovipositor. Scale bars = 0.5 mm (A, B), 0.1 mm (C, D).

baabdaensis) and flagellomeres (wider in *M. baabdaensis*), and the dense covering of setae on the forewing in the female of *M. baabdaensis*. The differences between the studied specimen and the holotype of *M. turolensis* are as follows: general size (approximately 1.5 times larger than the holotype); flagellomeres F1–F4 longer than the remainder, except for F12, vs. flagellomeres F2–F4; thin flagellomeres vs. slightly wider flagellomeres; last eight flagellomeres bearing more setae than the remainder vs. more setae in the last five flagellomeres; and forewings moderately covered with setae vs. densely covered forewings. Although the genitalia are not visible in the holotype of *M. turolensis*, Engel et al. (2013) supposed that it is a male. Therefore, these minor differences could be explained by sexual dimorphism and intraspecific variability within *M. turolensis* instead of attributing the specimen to a new species. The basitarsi are longer than the remaining tarsomeres in the female of *M. turolensis* and *M. baabdaensis*, but not in the holotype of *M. turolensis*. Thus, this character can also be attributed to sexual dimorphism. The metasoma of the new specimen is similar in shape to that of *M. baabdaensis*, both females. Therefore, it could be a female character of the genus.

Mymaropsis baabdaensis Krogmann, Azar, Rajaei and Nel, 2016

Material. Holotype specimen 855, female, from the upper Barremian Hammana-Mdeyrij amber. Housed at the Natural History Museum of the Lebanese University (Faculty of Science II) in Fanar, Lebanon.

Diagnosis. Scape slightly expanded ventrally; pedicel globular (wider than in *Mymaropsis turolensis*); flagellomeres F5–F12 about twice as wide as remaining ones; forewing densely covered with setae in females.

Remarks. Based on the lack of an original diagnosis for *Mymaropsis baabdaensis* in Krogmann et al. (2016) and according to the requirements of article 13.1.1 of the International Code of Zoological Nomenclature (ICZN, 1999), we propose here a diagnosis to allow the name to be valid for the described species. The general size of the holotype specimen of *M. baabdaensis* is larger than that of the male of *Mymaropsis turolensis*, but smaller than that of the female of the latter. These differences are also present in forewing length (wing length generally suffer less from improper preservation than body length): 0.85 mm (*M. turolensis* male), 1.21 mm (*M. turolensis* female), 1.05 mm (*M. baabdaensis* female) (Engel et al., 2013;

Krogmann et al., 2016). The discovery and description of male specimens of *M. baabdaensis* would be quite useful to better understand the characters attributable to sexual dimorphism. Interestingly, the habitus of *M. baabdaensis* and *M. turolensis* is similar despite the time (more than 20 Ma; late Barremian to late Albian) and geographical distance between them.

4.2. Key to the genera and species of Spathiopterygidae

Characters between [ ] can be difficult to observe. Thus, they are considered to be of less importance than the others.

1. Forewing with a well-defined marginal fringe of setae..... 2
—. Forewing without a marginal fringe of setae..... 5
2. Compound eye bulging with few ommatidia; forewing slightly sclerotised on basal veins; thin parastigma [hind wing present as a veinal stub, without any remnants of a membrane; notauli meeting posteriorly]..... *Spathiopteryx alavarommopsis*
—. Compound eye with numerous ommatidia; forewing sclerotised on basal veins; thick parastigma..... 3
3. Forewing wrinkled, with visible venation and a positive gradient of setae towards the apex; less sclerotised M+Cu, highly sclerotised parastigma..... *Diameneura marveni* gen. et sp. nov.
—. Forewing smooth, with unclear venation, M vein not clearly defined and setae distribution on the membrane homogeneous; highly sclerotised M+Cu, less sclerotised parastigma; [hind wing present with a small membranous portion; notauli not meeting posteriorly]..... 4
4. Scape slightly expanded ventrally; pedicel globular; flagellomeres F5–F12 around twice as wide as the remainder..... *Mymaropsis baabdaensis*
—. Scape not ventrally expanded; pedicel almost globular; flagellomeres with similar widths..... *Mymaropsis turolensis*
5. Head coarsely punctured; antennae short, not longer than the total body length; metasoma globose, about as long as the mesosoma; [hind wing absent] ..... *Spathopria sayrevillensis*
—. Head imbricate; antennae elongated, longer than the total body length; metasoma ovoid, longer than the mesosoma; [hind wing absent]..... *Diaspathion ortegai*

5. Discussion

5.1. Taphonomy

The specimens from San Just amber studied here show different preservation. The holotype of *Diameneura marveni* gen. et sp. nov. (CPT-4095) is preserved in a milky amber piece, allowing good visualisation only from the dorsal view (Fig. 2A), while the *Mymaropsis turolensis* female (CPT-4097) is preserved in a transparent amber piece (Fig. 4A). Interestingly, some parts of the holotype of *Diameneura marveni* gen. et sp. nov. (e.g., the antennae) are covered by small bubbles, probably phloem sap drops (Lozano et al., 2020). These small bubbles could be due to wasp movement in the fluid resin before its death. Its legs are encompassed by a coat of air (Fig. S1). Usually, the bubbles around fossil insects preserved in amber have been linked to the escape of decay gases during necrolysis in resins or to bacterial activity (Martínez-Delclòs et al., 2004). Amber pieces with bioinclusions are related to aerial resin produced by the branches or trunks of resiniferous trees, and the different internal aspect might depend on the conditions of resin production such as stressful situations caused by palaeofires (Martínez-Delclòs et al., 2004). Internal dark marks in the amber piece including on the *M. turolensis* female (Fig. 4A) correspond to surfaces of desiccation in aerial conditions between different flows of the original resin.

5.2. Interrelationships in Spathiopterygidae

The six Spathiopterygidae species had a wide distribution from the upper Barremian to the Turonian (Table 1). Several character states of *Mymaropsis* seem to be plesiomorphic, such as the more developed forewing venation and the presence of hind wings with a membrane, as noted by Engel et al. (2015) and Krogmann et al. (2016). Therefore, *Mymaropsis* would be the most 'basal' member of the family. The other representatives show reductions in several structures related to putative apomorphic character states. However, the hind wings, which are extremely reduced in this family, could be challenging to observe in fossil specimens. Therefore, the character of the presence/absence of hind wings in each spathiopterygid species should be treated carefully in phylogenetic analyses. A general trend of reduction and simplification in morphology (e.g., miniaturisation and reduction of wing venation) among several hymenopteran lineages was proposed by Rasnitsyn (1969, 1980). This trend has been recently supported in some families by description of new taxa from Burmese amber (Li et al., 2015; Jouault et al., 2021a, b), and the spathiopterygids could be another example of this kind of evolutionary trend.

Engel et al. (2015) summarised the interrelationships of the family as [*Mymaropsis* (*Spathiopteryx* [*Diaspathion* + *Spathopria*])]. Based on current knowledge, this seems to be correct. Nonetheless, the description of new specimens of spathiopterygids is necessary (even corresponding to the known species) to better understand the plesiomorphic and apomorphic conditions of each character. *Diameneura* gen. nov. shows morphological similarities with the basal *Mymaropsis* (such as the forewings with a marginal fringe of short setae and sclerotised mid-basal section of the costal margin) and the derived representatives *Spathopria* and *Diaspathion* (such as the wrinkled forewing membrane). Furthermore, it has unique characters within the family, such as the gradient of setae on the forewing membrane and the polygonal rugulose microsculpture present on back of head and mesoscutum. Therefore, its phylogenetic position and relationships with the other genera are obscure, although it might be closely related to *Mymaropsis* based on the similar anatomic characteristics. A detailed phylogenetic analysis is required to resolve the interrelationships within Spathiopterygidae, as well as the relationships with the other families within Diaprioidea.

5.3. Sexual dimorphism and palaeobiology of Spathiopterygidae

Spathiopterygidae is currently represented by seven specimens from six species obtained from Cretaceous ambers, although only two of them are female (Table 1). Therefore, there is little information on sexual dimorphism and intraspecific variability within the family. Female hymenopterans are usually larger than males (Stubblefield and Seger, 1994). This sexual size dimorphism is also present in spathiopterygids based on the comparisons between the male and female specimens of *Mymaropsis turolensis* (Fig. S2). Furthermore, there are other characters that could be related to sexual dimorphism in *M. turolensis*, such as the width of the flagellomeres (thinner in females), the setae on the flagellomeres (F5–F12 with more setae in females vs. F8–F12 in males), and the setae covering the forewings (moderately in females vs. densely in males). The presence of abundant setae (acting as sensillae) on flagellomeres is possibly an adaptation to sense and identify prey for the gravid female searching a host. Interestingly, the diapriid *Trichopria drosophilae* Perkins, 1910 has the most developed

sensillae for host selection situated on the apical flagellomeres of the females (Romani et al., 2002), which maybe suggests a similar use of the sensillae in Spathiopterygidae. Females of both *M. turolensis* and *M. baabdaensis* show a similar morphology of the metasoma, probably related to the life habit of female parasitoid wasps that need a host to lay eggs. Basitarsi longer than the remaining tarsomeres in females of both species maybe facilitated the attaching to the host previously to the egg laying.

The putative extant sister group of Spathiopterygidae is Maamingidae (Engel et al., 2013), which is found today only in New Zealand (Early et al., 2001a), contrast with the wide distribution of spathiopterygids during the Cretaceous. *Maaminga rangi* Early, Masner, Naumann and Austin, 2001 inhabits *Agathis australis* (Araucariaceae) forests. *Maaminga marrisi* Early, Masner, Naumann and Austin, 2001 'is a leaf litter inhabitant of bushy scrub in exposed sites, from near the shoreline to montane shrubs and snow tussock' (Early et al., 2001a: 348–349). Even if the resin-producing trees of Spanish amber were araucarians related to *Agathis*, the diversity of the habitats of the extant Maamingidae and the putative sister grouping would stop us from making inferences from the biological data of these extant wasps for the Spathiopterygidae. An alternative sister group of Spathiopterygidae would be Diapriidae (Rasnitsyn and Öhm-Kühnle, 2020), with a worldwide distribution today (Masner, 1993).

The extant Diapriidae, Monomachidae, and Ismaridae are known to be parasitoid wasps (Masner, 1993; Perioto et al., 2016), and the Maamingidae are likely to have a similar life habits based on their morphology (Early et al., 2001a, b). More generally, this is also the case for the whole group Microprocta. Therefore, it is highly probable that spathiopterygids were also parasitoids, based on a simple phylogenetic inference (Nel, 1997). The Diapriidae are parasitoids of several insect groups (Masner, 1993), such as diverse families of dipterans (e.g., Mycetophilidae, Sciaridae, Syrphidae, and Calliphoridae), or secondarily change their hosts to beetles (Staphylinidae and Psephenidae) or ants (Formicidae). The biology of Monomachidae is poorly known, although some species are parasitoids of Stratiomyidae (Diptera) (Masner, 1993; Johnson and Musetti, 2012). The Ismaridae are known to be hyperparasitoids of planthoppers (Hemiptera: Cicadellidae) via the larvae of Dryinidae (Hymenoptera) (Masner, 1976, 1993). The hosts of the Maamingidae remain unknown (Early et al., 2001a, b), although the species *Maaminga marrisi* could be a parasitoid of Phoridae (Diptera) based on their abundance in the same habitat (Early et al., 2001a). The hosts of spathiopterygids could also have been some dipteran families, such as other families within Diaprioidea. However, this is not yet known as the morphological characters of the specimens have not shed light on this topic. Furthermore, all the specimens of the family have been found in amber pieces without the syninclusions that could indicate the putative host taxa. New descriptions of spathiopterygids and a detailed study and comparison of the female genitalia with that of other hymenopteran families might help to resolve this question. It is important to note that hymenopterans were the main driver of the Mid-Mesozoic Parasitoid Revolution (MMPR) described by Labandeira and Li (2021). Spanish amber, based on its chronological age, would be included in the final extension of Phase 2 of the MMPR after the diversification events that established six of the seven major parasitoid groups (Labandeira and Li, 2021). In Phase 3 after the MMPR, starting during the Cenomanian, the number of hymenopteran families within Proctotupomorpha and Aculeata greatly increased in diversity, and the insect parasitoid fauna was finally consolidated into food webs (Labandeira and Li, 2021). Interestingly, the latter authors suggested that spathiopterygids could have been endoparasitoids attacking the host at its egg stage.

An interesting characteristic of Spathiopterygidae is the bizarre reduction of the hind wings. In the case of *Mymaropsis*, the hind wings retain a small portion of the membrane and hamuli. In *Spathiopteryx*, they are reduced to a stalk without a membrane, while in *Spathopria* and *Diaspathion*, they are completely absent. Furthermore, as Engel et al. (2015) noted, they seem to represent a transitional series that correlate with age, with the absence of hind wings being a derived character of the younger representatives of the family. Nonetheless, as we indicate above, the hind wings could be difficult to observe due to preservation artefacts or other body parts covering them. Hind wings might have been present in *Diameneura marveni* gen. et sp. nov. considering its geological provenance (upper Albian). Hind wing reduction is also present in some other hymenopteran groups (e.g., Ortega-Blanco et al., 2011b), although a complete loss of hind wings is extremely unusual. Interestingly, the bizarre ceraphronoid family Aptenoperissidae known from Burmese amber is wingless (Rasnitsyn et al., 2017). Recently, a new Cretaceous monospecific family within Hymenoptera was described as showing morphological diptery (Rasnitsyn et al., 2019). The case of the spathiopterygids is even more exceptional, as diptery is only shared by two of the species, but not by all the members of the family. Morphological diptery is uncommon in active flying insects (Rasnitsyn et al., 2019), which clearly affected the flight mode of these bizarre insects.

6. Conclusions

The family Spathiopterygidae now contains six species in five genera thank to the description of *Diameneura marveni* gen. et sp. nov. that increases the known palaeodiversity of the family. The forewing venation of *Diameneura marveni* gen. et sp. nov. has been interpreted based on sclerotisation, nebulous veins, rows of setae, and reliefs of the membrane, providing a new framework for comparison with new undescribed specimens. The study of the sexual dimorphism of the family has been addressed from the description of the first known female of *Mymaropsis turolensis*, revealing characters that can be interpreted as differences between the sexes of the same species. The genus *Mymaropsis* would be the most basal member of the family as it retains plesiomorphic state characters, although a phylogenetic analysis is necessary to resolve the interrelationships of the family. As previously proposed, it is plausible that Spathiopterygidae belongs to Diaprioidea since it shares morphological similarities with Mymarommatoidea, Myanmarinidae, and Mymaridae, such as the peduncular forewing with nebulous venation and the reduced hind wings, could be explained as convergent evolution, as these families probably shared similar parasitoid biology. Despite the new information provided here, there are anatomical (presence vs. absence of hind wings) and phylogenetical (interrelationships of the family and with other families) uncertainties. The putative sister group, Maamingidae, is also not very well known. Key questions might be resolved after the monographic study of the new specimens from Burmese amber.

Acknowledgements

We are grateful to the Museo Aragonés de Paleontología and the staff of the Fundación Conjunto Paleontológico de Teruel-Dinópolis for providing the specimens, as well as to the Dirección General de Patrimonio Cultural of the Aragón Government (Spain) for the permission to excavate in San Just (exp. 171/2007). We are indebted to Rafael López del Valle for the preparation of the amber pieces. We thank Juli Pujade-Villar for their advice and discussion. We want to acknowledge the editor Eduardo Koutsoukos and the

reviewers Alexandr P. Rasnitsyn and Corentin Jouault for their comments and suggestions that have improved the manuscript text, and for their corrections on wing venation nomenclature and taxonomic issues. This study is a contribution to the project CRE CGL2017-84419 funded by the Spanish AEI/FEDER and the EU. The co-author S.Á.-P. acknowledges support from the Secretaria d'Universitats i Recerca de la Generalitat de Catalunya (Spain) and the European Social Fund (2020FI_B1 00002).

References

Álvarez-Parra, S., Pérez-de la Fuente, R., Peñalver, E., Barrón, E., Alcalá, L., Pérez-Cano, J., Martín-Closas, C., Trabelsi, K., Meléndez, N., López Del Valle, R., Lozano, R.P., Peris, D., Rodrigo, A., Sarto i Monteys, V., Bueno-Cebollada, C.A., Menor-Salván, C., Philippe, M., Sánchez-García, A., Peña-Kairath, C., Arillo, A., Espílez, E., Mampel, L., Delclòs, X., 2021. Dinosaur bonebed amber from an original swamp forest soil. Elife 10, e72477. https://doi.org/10.7554/eLife.72477.

Bover-Arnal, T., Moreno-Bedmar, J.A., Frijia, G., Pascual-Cebrian, E., Salas, R., 2016. Chronostratigraphy of the Barremian–Early Albian of the Maestrat Basin (E Iberian Peninsula): integrating strontium-isotope stratigraphy and ammonoid biostratigraphy. Newsletters on Stratigraphy 49, 41–68. https://doi.org/10.1127/nos/2016/0072.

Canerot, J., Crespo Zamorano, A., Navarro Vázquez, D., 1977. Cartografía geológica y memoria explicativa. In: Barnolas, A. (Ed.), Mapa geológico de España 1:50.000, Hoja 518 (28-20) Montalbán. Instituto Geológico y Minero de España, Madrid, p. 31.

Corral, J.C., López Del Valle, R., Alonso, J., 1999. El ámbar cretácico de Álava (Cuenca Vasco-Cantábrica, norte de España). Su colecta y preparación. Estudios del Museo de Ciencias Naturales de Álava 14, 7–21.

Dowton, M., Austin, A.D., 2001. Simultaneous analysis of 16S, 28S, COI and morphology in the Hymenoptera: Apocrita - evolutionary transitions among parasitic wasps. Biological Journal of the Linnean Society 74, 87–111. https://doi.org/10.1111/j.1095-8312.2001.tb01379.x.

Early, J.W., Masner, L., Naumann, I.D., Austin, A.D., 2001a. Maamingidae, a new family of proctotrupoid wasp (Insecta: Hymenoptera) from New Zealand. Invertebrate Taxonomy 15, 341–352. https://doi.org/10.1071/IT00053.

Early, J.W., Masner, L., Naumann, I.D., Austin, A.D., 2001b. Maamingidae, a new family of Proctotrupoidea unique to New Zealand. In: Melika, G., Thuroczy, C. (Eds.), Parasitic wasps: evolution, systematics, biodiversity and biological control. International symposium: "Parasitic Hymenoptera: Taxonomy and Biological Control". Agroinform Kiado & Nyomda KFT, Budapest, Hungary, Köszeg, Hungary, pp. 13–18.

Engel, M.S., Ortega-Blanco, J., Soriano, C., Grimaldi, D.A., Delclòs, X., 2013. A new lineage of enigmatic diaprioid wasps in Cretaceous amber (Hymenoptera: Diaprioidea). American Museum Novitates 3771, 1–23. https://doi.org/10.1206/3771.2.

Engel, M.S., Huang, D., Azar, D., Nel, A., Davis, S.R., Alvarado, M., Breitkreuz, L.C., 2015. The wasp family Spathiopterygidae in mid-Cretaceous amber from Myanmar (Hymenoptera: Diaprioidea). Comptes Rendus Palevol 14, 95–100. https://doi.org/10.1016/j.crpv.2014.11.002.

Fujiyama, I., 1994. Two parasitic wasps from Aptian (Lower Cretaceous) Choshi amber, Chiba, Japan. Natural History Research 3 (1), 1–5.

Haliday, A.H., 1833. An essay on the classification of the parasitic Hymenoptera of Britain, which correspond with the *Ichneumones minuti* of Linnaeus. Entomological Magazine 1, 259–276.

ICZN, 1999. International Code of Zoological Nomenclature, fourth ed. The International Trust for Zoological Nomenclature, London, UK, p. 306.

Johnson, N.F., Musetti, L., 2012. Genera of the parasitoid wasp family Monomachidae (Hymenoptera: Diaprioidea). Zootaxa 3188 (1), 31–41. https://doi.org/10.11646/zootaxa.3188.1.2.

Jouault, C., Ngô-Muller, V., Pouillon, J.M., Nel, A., 2021a. New Burmese amber fossils clarify the evolution of bethylid wasps (Hymenoptera: Chrysidoidea). Zoological Journal of the Linnean Society 191 (4), 1044–1058. https://doi.org/10.1093/zoolinnean/zlaa078.

Jouault, C., Perrichot, V., Nel, A., 2021b. New flat wasps from mid-Cretaceous Burmese amber deposits highlight the bethylid antiquity and paleobiogeography (Hymenoptera: Chrysidoidea). Cretaceous Research 123, 104772. https://doi.org/10.1016/j.cretres.2021.104772.

Jouault, C., Rasnitsyn, A.P., Perrichot, V., 2021c. Ohlhoffiidae, a new Cretaceous family of basal parasitic wasps (Hymenoptera: Stephanoidea). Cretaceous Research 117, 104635. https://doi.org/10.1016/j.cretres.2020.104635.

Krogmann, L., Azar, D., Rajaei, H., Nel, A., 2016. *Mymaropsis baabdaensis* sp. n. from Lower Cretaceous Lebanese amber—the earliest spathiopterygid wasp and the first female known for the family. Comptes Rendus Palevol 15, 483–487. https://doi.org/10.1016/j.crpv.2015.11.002.

Labandeira, C.C., Li, L., 2021. The history of insect parasitism and the Mid-Mesozoic Parasitoid Revolution. In: De Baeths, K., Huntley, J.W. (Eds.), The evolution and fossil record of parasitism: Identification and macroevolution of parasites, Topics in Geobiology, vol. 49(11). Springer, pp. 377–533. https://doi.org/10.1007/978-3-030-42484-8_11.

Li, L., Rasnitsyn, A.P., Shih, C., Ren, D., 2015. A new genus and species of Praeaulacidae (Hymenoptera: Evanioidea) from Upper Cretaceous Myanmar amber. Cretaceous Research 55, 19–24. https://doi.org/10.1016/j.cretres.2015.01.007.

Linnaeus, C., 1758. Systema naturae per regna tria Naturae, secundum classes, ordines, genera, species, cum characteribus, differentiis, synonymis, locis. Holmiae, Laur. Salvii, Editio Decima 1, 824. https://doi.org/10.5962/bhl.title.542.

Lozano, R.P., Pérez-de la Fuente, R., Barrón, E., Rodrigo, A., Viejo, J.L., Peñalver, E., 2020. Phloem sap in Cretaceous ambers as abundant double emulsions preserving organic and inorganic residues. Scientific Reports 10, 9751. https://doi.org/10.1038/s41598-020-66631-4.

Martín Fernández, M., Canerot, J., 1977. Cartografía geológica y memoria explicativa. In: Barnolas, A. (Ed.), Mapa geológico de España 1:50.000, Hoja 517 (27-20) Argente. Instituto Geológico y Minero de España, Madrid, p. 23.

Martínez-Delclòs, X., Briggs, D.E., Peñalver, E., 2004. Taphonomy of insects in carbonates and amber. Palaeogeography, Palaeoclimatology, Palaeoecology 203 (1–2), 19–64. https://doi.org/10.1016/S0031-0182(03)00643-6.

Masner, L., 1976. A revision of the Ismarinae of the New World (Hymenoptera, Proctotrupoidea, Diapriidae). The Canadian Entomologist 108, 1243–1266. https://doi.org/10.4039/Ent1081243-11.

Masner, L., 1993. Superfamily Proctotrupoidea. In: Goulet, H., Hubert, J.T. (Eds.), Hymenoptera of the world: an identification guide to families. Research Branch Agriculture Canada Publication, Ottawa, pp. 537–557.

McCoy, V.E., Barthel, H.J., Boom, A., Peñalver, E., Delclòs, X., Solórzano-Kraemer, M.M., 2021. Volatile and semi-volatile composition of Cretaceous amber. Cretaceous Research 127, 104958. https://doi.org/10.1016/j.cretres.2021.104958.

Nel, A., 1997. The probabilistic inference of unknown data in phylogenetic analysis. In: Grandcolas, P. (Ed.), The origin of biodiversity in insects: phylogenetic tests of evolutionary scenarios, vol. 173. Mémoires du Muséum National d'Histoire Naturelle de Paris, pp. 305–327.

Ortega-Blanco, J., Delclòs, X., Peñalver, E., Engel, M.S., 2011a. Serphitid wasps in Early Cretaceous amber from Spain (Hymenoptera: Serphitidae). Cretaceous Research 32 (2), 143–154. https://doi.org/10.1016/j.cretres.2010.11.004.

Ortega-Blanco, J., Peñalver, E., Delclòs, X., Engel, M.S., 2011b. False fairy wasps in early Cretaceous amber from Spain (Hymenoptera: Mymarommatoidea). Palaeontology 54 (3), 511–523. https://doi.org/10.1016/j.cretres.2010.11.004.

Peñalver, E., Delclòs, X., 2010. Spanish amber. In: Penney, D. (Ed.), Biodiversity of fossils in amber from the major world deposits, vol. 13. Siri Scientific Press, Manchester, pp. 236–270.

Peñalver, E., Grimaldi, D.A., Delclòs, X., 2006. Early Cretaceous spider web with its prey. Science 312 (5781), 1761–1761. https://doi.org/10.1126/science.1126628.

Peñalver, E., Delclòs, X., Soriano, C., 2007. A new rich amber outcrop with palaeobiological inclusions in the Lower Cretaceous of Spain. Cretaceous Research 28, 791–802. https://doi.org/10.1016/j.cretres.2006.12.004.

Perioto, N.W., Lara, R.I.R., Fernandes, D.P.R., De Bortoli, C.P., Salas, C., Netto, J.C., Perez, L.A., Trevisan, M., Kubota, M.M., Pereira, N.A., Gil, O.J.A., Dos Santos, R.F., Jorge, S.J., Laurentis, V.L., 2016. *Monomachus* (Hymenoptera, Monomachidae) from Atlantic rainforests in São Paulo State, Brazil. Revista Colombiana de Entomología 42, 171–175. https://doi.org/10.25100/socolen.v42i2.6688.

Perkins, R.C.L., 1910. Supplement to Hymenoptera. Fauna Hawaiiensis 6 (2), 600–686.

Peters, R.S., Krogmann, L., Mayer, C., Donath, A., Gunkel, S., Meusemann, K., Kozlov, A., Podsiadlowski, L., Petersen, M., Lanfear, R., Diez, P.A., Heraty, J., Kjer, K.M., Klopfstein, S., Meier, R., Polidori, C., Schmitt, T., Liu, S., Zhou, X., Wappler, T., Rust, J., Misof, B., Niehuis, O., 2017. Evolutionary history of the Hymenoptera. Current Biology 27, 1013–1018. https://doi.org/10.1016/j.cub.2017.01.027.

Peyrot, D., Rodríguez-López, J.P., Barrón, E., Meléndez, N., 2007. Palynology and biostratigraphy of the Escucha Formation in the Early Cretaceous Oliete Subbasin, Teruel, Spain. Revista Española de Micropaleontología 39, 135–154.

Rasnitsyn, A.P., 1969. The origin and evolution of Lower Hymenoptera, vol. 123. Trudy Paleontologicheskogo Instituta, pp. 1–196 [in Russian].

Rasnitsyn, A.P., 1980. Origin and evolution of Hymenoptera, vol. 174. Trudy Paleontologicheskogo Instituta, pp. 1–192 [in Russian].

Rasnitsyn, A.P., Öhm-Kühnle, C., 2020. Taxonomic revision of the infraorder Proctotrupomorpha (Hymenoptera). Palaeoentomology 3, 223–234. https://doi.org/10.11646/palaeoentomology.3.3.2.

Rasnitsyn, A.P., Poinar Jr., G., Brown, A.E., 2017. Bizzare wingless parasitic wasp from mid-Cretaceous Burmese amber (Hymenoptera, Ceraphronoidea, Aptenoperissidae fam. nov.). Cretaceous Research 69, 113–118. https://doi.org/10.1016/j.cretres.2016.09.003.

Rasnitsyn, A.P., Sidorchuk, E.A., Zhang, H., Zhang, Q., 2019. Dipterommatidae, a new family of parasitic wasps (Hymenoptera: Mymarommatoidea) in mid-Cretaceous Burmese amber: The first case of morphological diptery in flying Hymenoptera. Cretaceous Research 104, 104193. https://doi.org/10.1016/j.cretres.2019.104193.

Romani, R., Isidoro, N., Bin, F., Vinson, S.B., 2002. Host recognition in the pupal parasitoid *Trichopria drosophilae*: a morpho-functional approach. Entomologia Experimentalis et Applicata 105, 119–128. https://doi.org/10.1046/j.1570-7458.2002.01040.x.

Ross, A., Mellish, C., York, P., Crighton, B., 2010. Burmese amber. In: Penney, D. (Ed.), Biodiversity of fossils in amber from the major world deposits, vol. 12. Siri Scientific Press, Manchester, pp. 208–235.

Salas, R., Guimerà, J., 1996. Rasgos estructurales principales de la cuenca cretácica inferior del Maestrazgo (Cordillera Ibérica oriental). Geogaceta 20, 1704–1706.

Sharkey, M.J., 2007. Phylogeny and classification of Hymenoptera. In: Zhang, Z.-Q., Shear, W.A. (Eds.), Linnaeus tercentenary: Progress in invertebrate taxonomy, vol. 1668. Zootaxa, pp. 521–548. https://doi.org/10.11646/zootaxa.1668.1.25.

Sharkey, M.J., Carpenter, J.M., Vilhelmsen, L., Heraty, J., Liljeblad, J., Dowling, A.P., Schulmeister, S., Murray, D., Deans, A.R., Ronquist, F., Krogmann, L., Wheeler, W.C., 2012. Phylogenetic relationships among superfamilies of Hymenoptera. Cladistics 28, 80–112. https://doi.org/10.1111/j.1096-0031.2011.00366.x.

Stubblefield, J.W., Seger, J., 1994. Sexual dimorphism in the Hymenoptera. In: Short, R.V., Balaban, E. (Eds.), The differences between the sexes. Cambridge University Press, Cambridge, UK, pp. 77–103.

Villanueva-Amadoz, U., Pons, D., Diez, J.B., Ferrer, J., Sender, L.M., 2010. Angiosperm pollen grains of San Just site (Escucha Formation) from the Albian of the Iberian Range (north-eastern Spain). Review of Palaeobotany and Palynology 162, 362–381. https://doi.org/10.1016/j.revpalbo.2010.02.014.

Zhang, Q., Rasnitsyn, A.P., Wang, B., Zhang, H., 2018. Hymenoptera (wasps, bees and ants) in mid-Cretaceous Burmese amber: A review of the fauna. Proceedings of the Geologists' Association 129, 736–747. https://doi.org/10.1016/j.pgeola.2018.06.004.

Appendix A. Supplementary data

Supplementary data to this article can be found online at https://doi.org/10.1016/j.cretres.2021.105128.

Supplementary material

New insights into the enigmatic Cretaceous family Spathiopterygidae (Hymenoptera: Diaprioidea)

Maxime Santer, Sergio Álvarez-Parra *, André Nel, Enrique Peñalver, Xavier Delclòs

* Corresponding author email: sergio.alvarez-parra@ub.edu

Video 1. Animation showing a reconstructed living behaviour of *Diameneura marveni* gen. et sp. nov. (Hymenoptera: Spathiopterygidae), based on those of several living parasitoid wasps. The larva is a placeholder, as we do not know the host of the spathiopterygids. It is a mix of different insect larvae, viz. head taken from a xylophagous beetle larva, legless body taken from a maggot, and colours similar to caterpillar of *Papilio machaon*. The stinging movement is speculative. The real wasp could have stung without climbing on the larva. Note that the spathiopterygids could be parasitoids of egg stage, therefore the larva has been included for artistic purpose. Wasp forewing 1.05 mm long. Author of the animation: Maxime Santer.

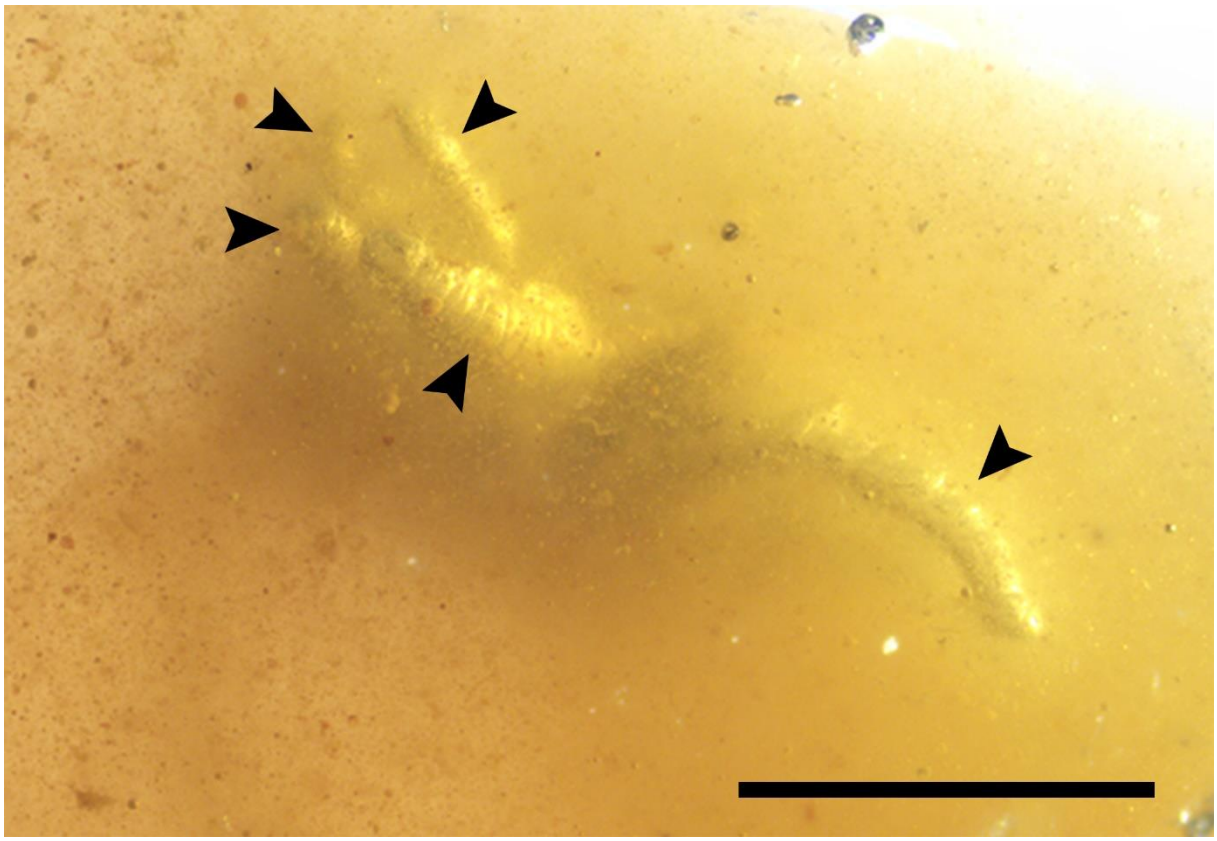

Supplementary Figure S1. Photograph from ventral view of *Diameneura marveni* gen. et sp. nov. (Hymenoptera: Spathiopterygidae), sex unknown, from the upper Albian amber-bearing outcrop of San Just (Teruel Province, Spain), holotype specimen CPT-4095 (SJ-07-41). The legs, indicated by arrowheads, are encompassed by bubbles. Scale bar = 0.5 mm.

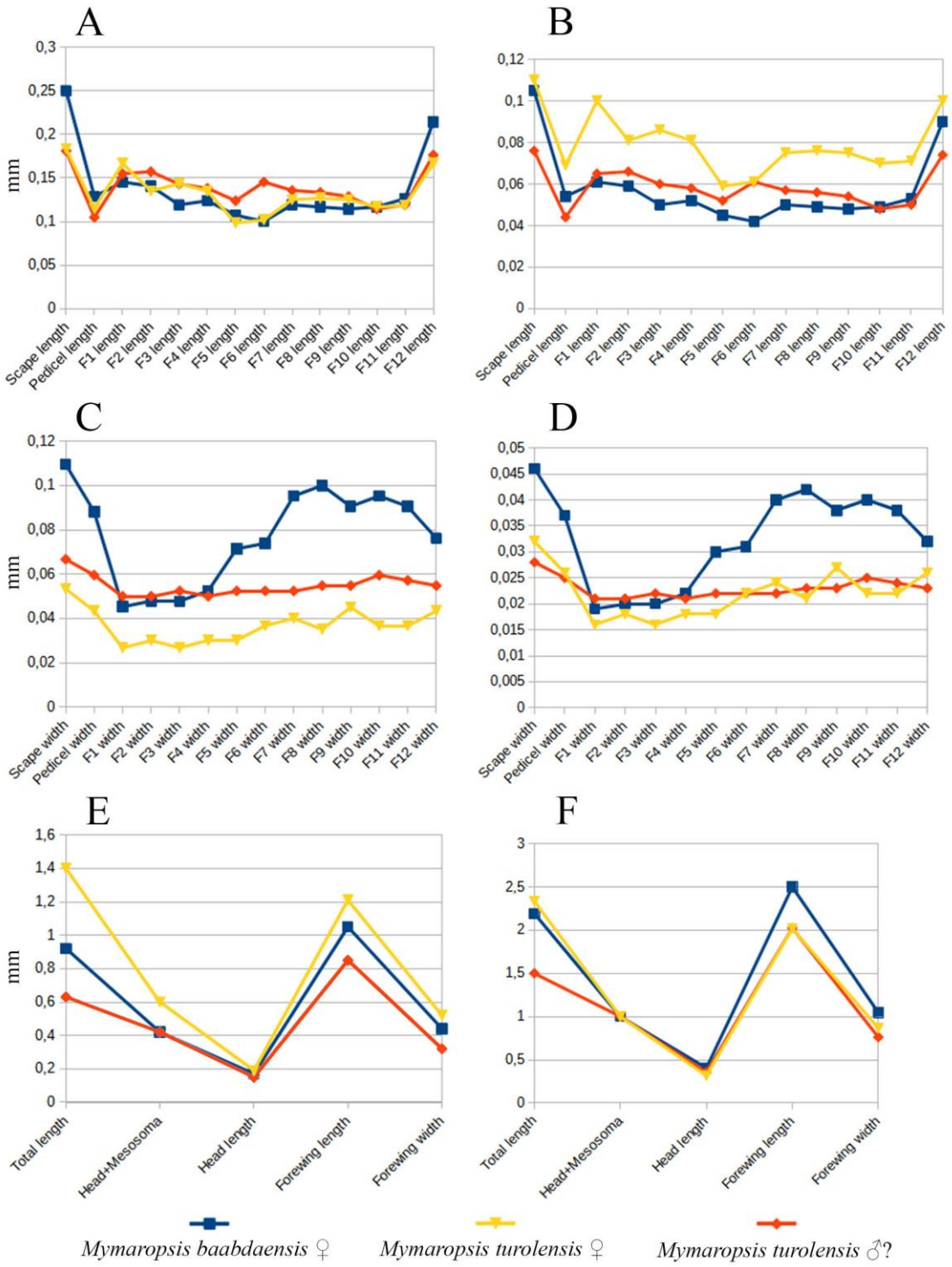

Supplementary Figure S2. Comparative graphics of measurements and ratios regarding the known Spathiopterygidae (Hymenoptera) specimens of *Mymaropsis baabdaensis* female (blue), *Mymaropsis turolensis* female (yellow) and *M. turolensis* probably male (red): A, B) Antenomeres length measurement and ratio antennomere length/head+mesosoma length, respectively. C, D) Antennomeres width measurement and ratio antennomere width/head+mesosoma length, respectively. E, F) Diverse measurements and ratio measurement/head+mesosoma length, respectively. F1–12 in A–D correspond to flagellomeres. The measurements have been obtained from Engel et al. (2013), Krogmann et al. (2016), and this paper.

Anexo 8.1.6

New barklice (Psocodea, Trogiomorpha) from Lower Cretaceous Spanish amber

Álvarez-Parra, S., Peñalver, E., Nel, A., Delclòs, X. 2022. New barklice (Psocodea, Trogiomorpha) from Lower Cretaceous Spanish amber. *Papers in Palaeontology*, **8**(3), e1436.

DOI: https://doi.org/10.1002/spp2.1436

Revista científica: *Papers in Palaeontology*
Factor de impacto: 3,349 (2021)
Categoría: *Paleontology*, Q1 (2021)

[Papers in Palaeontology, 2022, e1436]

New barklice (Psocodea, Trogiomorpha) from Lower Cretaceous Spanish amber

by SERGIO ÁLVAREZ-PARRA[1,*], ENRIQUE PEÑALVER[2], ANDRÉ NEL[3] *and* XAVIER DELCLÒS[1]

[1]Departament de Dinàmica de la Terra i de l'Oceà & Institut de Recerca de la Biodiversitat (IRBio), Facultat de Ciències de la Terra, Universitat de Barcelona, c/Martí i Franquès s/n, 08028 Barcelona, Spain; sergio.alvarez-parra@ub.edu
[2]Instituto Geológico y Minero de España-CSIC (Museo Geominero), c/Cirilo Amorós 42, 46004, Valencia, Spain
[3]Institut de Systématique, Évolution, Biodiversité (ISYEB), Muséum national d'Histoire naturelle, CNRS, Sorbonne Université, EPHE, Université des Antilles, CP50, 57 rue Cuvier, 75005 Paris, France
*Corresponding author

Typescript received 10 November 2021; accepted in revised form 2 February 2022

Abstract: Barklice are insects belonging to the order Psocodea. They are herbivorous or detritivorous, and inhabit a wide range of environments. Their oldest fossil record dates back to the late Carboniferous, but it was not until the Cretaceous that they became much more diverse. However, their fossil record could be affected by taphonomic processes due to their tiny size and soft bodies. Here, we present new psocid specimens from five amber-bearing outcrops in Spain that are Albian in age. One of the specimens, a well-preserved psocid nymph assigned to †Archaeatropidae, lacks evidence of debris-carrying behaviour. Some of the specimens belong to the previously known species *Archaeatropos alavensis* Baz & Ortuño and *Preempheria antiqua* Baz & Ortuño (Trogiomorpha: Atropetae), providing new anatomical and biogeographical information. Furthermore, we describe a new species, *Libanoglaris hespericus* sp. nov. (†Archaeatropidae). The diagnosis for the family †Archaeatropidae is emended. The abundance of psocids in Cretaceous amber and their virtual absence in compression outcrops could be due to taphonomic bias. Considerations on the phylogenetic placement of trogiomorphan families and the relationships between †Archaeatropidae and †Empheriidae are included. Today, the least diverse psocid suborder is Trogiomorpha, but this suborder comprises the majority of the Cretaceous psocodean species described to date, possibly due to palaeobiological or evolutionary constraints. Trogiomorphans could have been relegated to marginal habitats by niche competition with psocomorphans. Debris-carrying behaviour in response to predatory pressure might not have been widely distributed, geographically or phylogenetically, in the Cretaceous psocid nymphs.

Key words: Psocodea, Trogiomorpha, barklice, amber, Cretaceous.

PSOCIDS, commonly known as barklice and booklice, are hemimetabolous insects that are a few millimetres in length and are characterized by well-developed chewing mouthparts (Mockford 1993). They are considered cosmopolitan, inhabiting a wide range of habitats such as trees, rocks, caves, bird and mammal nests, ground litter, and domestic environments (New 1987). Psocids, accounting for more than 5000 living species, are herbivorous or detritivorous and feed on microorganisms and the remains of dead arthropods, thereby playing a key role as nutrient recyclers of organic matter (New 1987). Psocids are included in the order Psocodea alongside parasitic lice (Phthiraptera), with the previously known 'Psocoptera' forming a paraphyletic group (Johnson *et al.* 2018). Psocodea contains three suborders (Smithers 1972; De Moya *et al.* 2021): Trogiomorpha, Troctomorpha and Psocomorpha.

The oldest known psocodean record dates back to the late Carboniferous (Nel *et al.* 2013). A major diversification of the group took place during the Cretaceous, with 70 species described from amber dating to this period (Álvarez-Parra *et al.* 2020*a*, table 1; plus material subsequently described, including the new species described here). However, the lack of a pre-Cretaceous record could be due to taphonomic bias. The Cretaceous fossil record of psocids has expanded significantly in recent years with the description of the basal family †Cormopsocidae (Yoshizawa & Lienhard 2020), which has been found to be very diverse (Wang *et al.* 2021). The three psocodean suborders already existed during the Cretaceous (Álvarez-Parra *et al.* 2020*a*). Trogiomorpha includes the families †Cormopsocidae (not assigned to an infraorder, although its placement in a more basal clade outside Trogiomorpha cannot be excluded, *sensu* Yoshizawa & Lienhard 2020),

doi: 10.1002/spp2.1436

Prionoglarididae (within Prionoglaridetae), Psyllipsocidae (within Psyllipsocetae), †Archaeatropidae, †Empheriidae, Psoquillidae, Trogiidae and Lepidopsocidae (all five within Atropetae) (Yoshizawa *et al.* 2006). The fossil record of Trogiomorpha includes 57 species dating from the Barremian to the Quaternary (Table 1), most of which were found in amber and only four in copal. Trogiomorphan species from compression fossil sites are unknown to date. The families with the highest number of fossil species are the extinct families †Archaeatropidae and †Empheriidae. The former is a psocid family that has been identified only from Cretaceous ambers (Lebanon, Spain, France and Myanmar) and which includes 11 species in seven genera dating from the Barremian to the Cenomanian (Álvarez-Parra *et al.* 2020*a*; Cumming & Le Tirant 2021) (Table 1). †Empheriidae specimens are known from Cretaceous (Spain, Myanmar and Russia) and Eocene (France and Baltic) ambers, and comprise 11 species in eight genera dating from the Albian to the Priabonian (Hakim *et al.* 2021*a*) (Table 1). The phylogenetic position of both families might be more basal to the rest of the families belonging to the infraorder Atropetae (Yoshizawa & Lienhard 2020). The taxonomical relationships of †Archaeatropidae and †Empheriidae have been questioned, given that Li *et al.* (2020) described a new genus (assigned to †Empheriidae) with diagnostic characters of both families. The palaeobiology of archaeatropids and empheriids remains unknown.

The study of psocids from Spanish amber was initiated by Baz & Ortuño (2000), who erected the family †Archaeatropidae and later studied †Empheriidae and Manicapsocidae (Troctomorpha). Five psocid species from Spanish amber have been identified to date (all of them from Álava amber) (Baz & Ortuño 2000, 2001*a*, *b*): *Archaeatropos alavensis* Baz & Ortuño, 2000, *Empheropsocus arilloi* Baz & Ortuño, 2001*b*, *Empheropsocus margineglabrus* Baz & Ortuño, 2001*b*, *Manicapsocidus enigmaticus* Baz & Ortuño, 2001*a* and *Preempheria antiqua* Baz & Ortuño, 2001*b*. More than 100 psocids from Spanish amber are pending investigation, most of them from Álava amber.

Here, we describe new psocid specimens belonging to Trogiomorpha from five amber-bearing outcrops of the Iberian Peninsula. The first psocid nymph known from Spanish amber and a new species are described. Furthermore, the finding of new specimens belonging to known species adds further detail to previous anatomical information. We also address phylogenetic and palaeobiological topics regarding the Cretaceous Trogiomorpha.

GEOLOGICAL SETTING

The specimens studied here correspond to bioinclusions in amber pieces obtained from the El Soplao (Cantabria Autonomous Community) and Peñacerrada I (Burgos Province) fossil sites, and the Ariño, the Arroyo de la Pascueta and San Just fossil sites in Teruel Province. These amber-bearing outcrops are distributed along the north and east of the Iberian Peninsula, corresponding to the coastal areas of the Iberia Island during the Albian (Fig. 1).

El Soplao and Peñacerrada I are located in the Basque–Cantabrian Basin, which is related to the opening of the North Atlantic Ocean during the Oxfordian–Aptian rifting period (Martín-Chivelet *et al.* 2002). The El Soplao outcrop is in the western margin of the Basque–Cantabrian Basin and belongs to the Las Peñosas Formation, with the amber deposited in a deltaic–estuarine environment under a marine influence (Najarro *et al.* 2009). This outcrop is considered Albian in age (Najarro *et al.* 2009). Peñacerrada I (which, together with the Peñacerrada II outcrop was known as Álava amber) is located in the eastern margin of the Basque–Cantabrian Basin, belonging to the Utrillas Group (Barrón *et al.* 2015). The depositional environment corresponds to the top of the filling sequences of abandoned fluvial channels in interdistributary deltaic bays (Martínez-Torres *et al.* 2003). Peñacerrada I dates back to the late Albian based on its palynological content (Barrón *et al.* 2015).

The amber-bearing outcrops of Ariño, San Just and Arroyo de la Pascueta are in eastern Spain, located in the Maestrazgo Basin. Ariño amber is interesting because it appears to be associated with dinosaur bones in the bonebed level AR-1 (Alcalá *et al.* 2012; Álvarez-Parra *et al.* 2020*b*, 2021). This level belongs to the Escucha Formation and is early Albian in age based on the charophyte, ostracod and palynological assemblages it contains (Tibert *et al.* 2013; Villanueva-Amadoz *et al.* 2015). The palaeoenvironment corresponded to a freshwater swamp plain, including alkaline shallow lakes, with a marine influence in a subtropical or tropical climate (Tibert *et al.* 2013; Villanueva-Amadoz *et al.* 2015; Álvarez-Parra *et al.* 2021). The San Just outcrop is also attributed to the Escucha Formation and has been dated to the middle to lowermost upper Albian based on the palynological assemblage it contains (Peñalver *et al.* 2007; Villanueva-Amadoz *et al.* 2010). A recent palynological study constrained the dating to the upper Albian. The amber is found in a level that is rich in organic matter and fusinite, which is associated with a freshwater swamp plain (Peñalver *et al.* 2007; Villanueva-Amadoz *et al.* 2010). The little-studied Arroyo de la Pascueta amber outcrop is also assigned to the Escucha Formation and was initially dated to the lower–middle Albian (Gomez *et al.* 2000; Peñalver & Martínez-Delclòs 2002). However, as in the case of the San Just outcrop, a recent palynological study indicated the age to be late Albian. The sedimentology of the outcrop has been interpreted as a swamp in a lower

TABLE 1. Checklist of fossil species belonging to Trogiomorpha (Psocodea).

Infraorder	Family	Genus and species	Type locality	Age	Notes
Indet.	Indet.	*Empheriopsis vulnerata* Vishniakova, 1975	Yantardakh (Russia)	Santonian	Transferred to Trogiomorpha by Mockford *et al.* (2013)
	Indet.	*Parapsyllipsocus vergereaui* Perrichot *et al.*, 2003	Archingeay-Les Nouillers (France)	Albian–Cenomanian	–
	†Cormopsocidae	*Cormopsocus baleoi* Hakim *et al.*, 2021	Hukawng Valley (Myanmar)	Early Cenomanian	–
		Cormopsocus groehni Yoshizawa & Lienhard, 2020	Hukawng Valley	Early Cenomanian	–
		Cormopsocus neli Hakim, Azar & Huang *in* Hakim *et al.*, 2021*b*	Hukawng Valley	Early Cenomanian	–
		Cormopsocus perantiqua (Cockerell, 1919)	Hukawng Valley	Early Cenomanian	Transferred to *Cormopsocus* by Cumming & Le Tirant (2021)
		Longiglabellus edentatus Wang, Li & Yao *in* Wang *et al.*, 2021	Hukawng Valley	Early Cenomanian	–
		Longiglabellus pedhyalinus Wang, Li & Yao *in* Wang *et al.*, 2021	Hukawng Valley	Early Cenomanian	–
		Stimulopsocus jiewenae Liang & Liu, 2022	Hukawng Valley	Early Cenomanian	–
PRIONOGLARIDETAE	Prionoglarididae	*Palaeosiamoglaris burmica* Azar, Huang & Nel *in* Azar *et al.*, 2017	Hukawng Valley	Early Cenomanian	–
		Palaeosiamoglaris inexpectata Azar, Huang & Nel *in* Azar *et al.*, 2017	Hukawng Valley	Early Cenomanian	–
		Palaeosiamoglaris lienhardi Azar, Huang & Nel *in* Azar *et al.*, 2017	Hukawng Valley	Early Cenomanian	–
		Palaeosiamoglaris hkamtiensis Jouault *et al.*, 2021	Hkamti (Myanmar)	Early Albian	–
		Palaeosiamoglaris hammanaensis Hakim *et al.*, 2022	Hammana-Mdeyrij (Lebanon)	Barremian	–
PSYLLIPSOCETAE	Psyllipsocidae	*Psyllipsocus* sp.	Simojovel de Allende (Mexico)	Early–Middle Miocene	Nymph of *Psyllipsocus sensu* Mockford (1969)
		Psyllipsocus eocenicus Nel *et al.*, 2005	Le Quesnoy, Oise (France)	Ypresian	–
		Sinopsyllipsocus fushunensis Zhang *et al.*, 2016	Fushun (China)	Ypresian	–
		Khatangia inclusa Vishniakova, 1975	Yantardakh	Santonian	–
		Annulipsyllipsocus andreneli Hakim *et al.*, 2018*a*	Hukawng Valley	Early Cenomanian	–

(continued)

TABLE 1. (Continued)

Infraorder	Family	Genus and species	Type locality	Age	Notes
		Annulipsyllipsocus inexspectatus Hakim *et al.*, 2018*a*	Hukawng Valley	Early Cenomanian	–
		Concavapsocus parallelus Wang *et al.*, 2019	Hukawng Valley	Early Cenomanian	Probably does not belong to Psyllipsocidae *sensu* Jouault *et al.* (2021)
		Psyllipsocus myanmarensis Jouault *et al.*, 2021	Hukawng Valley	Early Cenomanian	–
		Psyllipsocus yangi Liang & Liu, 2021	Hukawng Valley	Early Cenomanian	–
		Psyllipsocus yoshizawai Álvarez-Parra *et al.*, 2020*a*	Hukawng Valley	Early Cenomanian	–
		Libanopsyllipsocus alexanderasnitsyni Azar & Nel, 2011	Hammana-Mdeyrij	Barremian	Belongs to Pachytroctidae (Troctomorpha) *sensu* Mockford *et al.* (2013)
ATROPETAE	†Archaeatropidae	*Proprionoglaris axioperierga* Azar *et al.*, 2015	La Garnache (France)	Cenomanian–Turonian	–
		Heliadesdakruon morganae Cumming & Le Tirant, 2021	Hukawng Valley	Early Cenomanian	–
		Proprionoglaris guyoti Perrichot *et al.*, 2003	Archingeay-Les Nouillers	Albian–Cenomanian	Transferred to †Archaeatropidae by Mockford *et al.* (2013)
		Prospeleketor albianensis Perrichot *et al.*, 2003	Archingeay-Les Nouillers	Albian–Cenomanian	Transferred to †Archaeatropidae by Mockford *et al.* (2013)
		Archaeatropos alavensis Baz & Ortuño, 2000	Peñacerrada I (Spain)	Late Albian	–
		Libanoglaris hespericus sp. nov.	Ariño (Spain)	Early Albian	–
		Archaeatropos randatae (Azar & Nel, 2004)	Jezzine (Lebanon)	Barremian	Transferred to *Archaeatropos* by Mockford *et al.* (2013)
		Bcharreglaris amunobi Azar & Nel, 2004	Bcharreh (Lebanon)	Barremian	Transferred to †Archaeatropidae by Mockford *et al.* (2013)
		Libanoglaris chehabi Azar & Nel, 2004	Hammana-Mdeyrij	Barremian	Transferred to †Archaeatropidae by Mockford *et al.* (2013)
		Libanoglaris mouawadi Azar, Perrichot, Néraudeau & Nel *in* Perrichot *et al.*, 2003	Hammana-Mdeyrij	Barremian	Transferred to †Archaeatropidae by Mockford *et al.* (2013)
		Setoglaris reemae Azar & Nel, 2004	Hammana-Mdeyrij	Barremian	Transferred to †Archaeatropidae by Mockford *et al.* (2013)
	†Empheriidae	*Empheria pertinens* (Enderlein, 1911)	Baltic amber	Lutetian	Transferred to *Empheria* by Roesler (1940)
		Empheria reticulata Hagen *in* Pictet-Baraban & Hagen, 1856	Baltic amber	Lutetian	–

(continued)

TABLE 1. (Continued)

Infraorder	Family	Genus and species	Type locality	Age	Notes
		Trichempheria villosa (Hagen, 1882)	Baltic amber	Lutetian	Transferred to *Trichempheria* by Enderlein (1911)
		Eoempheria intermedia Nel *et al.*, 2005	Le Quesnoy, Oise	Ypresian	–
		Jerseyempheria grimaldii Azar *et al.*, 2010	Sayreville (USA)	Turonian	–
		Empherium rasnitsyni Hakim *et al.* 2021*a*	Nizhnyaya Agapa (Russia)	Late Cenomanian	–
		Burmempheria densuschaetae Li, Wang & Yao *in* Li *et al.*, 2020	Hukawng Valley	Early Cenomanian	–
		Burmempheria raruschaetae Li, Wang & Yao *in* Li *et al.*, 2020	Hukawng Valley	Early Cenomanian	–
		Empheropsocus arilloi Baz & Ortuño, 2001*b*	Peñacerrada I (Spain)	Late Albian	–
		Empheropsocus margineglabrus Baz & Ortuño, 2001*b*	Peñacerrada I	Late Albian	–
		Preempheria antiqua Baz & Ortuño, 2001*b*	Peñacerrada I	Late Albian	–
	Psoquillidae	*Eorhyopsocus magnificus* Nel *et al.*, 2005	Le Quesnoy, Oise	Ypresian	–
	Trogiidae	*Paralepinotus fushunensis* Azar *et al.*, 2018	Fushun	Ypresian	–
		Cretolepinotus tankei Cockx *et al.*, 2020	Pipestone Creek (Canada)	Late Campanian	–
		Eolepinotus pilosus Vishniakova, 1975	Yantardakh	Santonian	–
		Eolepinotus zherikhini Hakim *et al.*, 2021*a*	Timmerdyakh-Khaya (Russia)	Late Cenomanian – Turonian	–
	Lepidopsocidae	*Nepticulomima mortua* (Hagen, 1865)	Zanzibar? copal	Quaternary	Transferred to *Nepticulomima* by Enderlein (1911)
		Perientomum incultum (Hagen, 1865)	Zanzibar? copal	Quaternary	Transferred to *Perientomum* by Enderlein (1911)
		Thylacella eversiana Enderlein, 1911	Zanzibar? copal	Quaternary	–
		Thylax fimbriatum Hagen, 1866	Zanzibar? copal	Quaternary	–
		Echmepteryx (*Loxopholia*) *dominicanus* Hakim *et al.*, 2018*b*	Dominican amber	Early–Middle Miocene	–
		Thylacella eocenica Nel *et al.*, 2005	Le Quesnoy, Oise	Ypresian	–

All fossil records correspond to amber or copal (for the limits of the term copal, see Solórzano-Kraemer *et al.* 2020). Undescribed trogiomorphans have been reported from Aptian Congolese amber (Bouju & Perrichot 2020) and Campanian Tilin (Myanmar) amber (Zheng *et al.* 2018). Note that there is controversy about the origin of the Zanzibar copal, which probably corresponds to copal obtained from different areas of East Africa (Delclòs *et al.* 2020). The new species described in this paper is shown in bold.

delta plain with freshwater and marine inputs (Gomez *et al.* 2000).

MATERIAL AND METHOD

Amber pieces were prepared following the methodology of Corral *et al.* (1999). They were cut, polished and embedded in prisms of epoxy resin, which facilitates the preservation and protection of amber pieces. Observations with reflected and transmitted light, photography and drawing of the specimens were acquired using an Olympus CX41 compound microscope with an attached sCMEX-20 digital camera and a camera lucida tube. ImageFocusAlpha version 1.3.7.12967.20180920 was used to take the photographs. Figures were prepared using Photoshop CS6. The anatomical nomenclature and systematic classification follow the works of Smithers (1972, 1990), Mockford (1993), Lienhard (1998) and Baz & Ortuño (2000).

This study includes 18 fossil psocid specimens. Their prefixes and provenances as well as the public Spanish institutions in which they are housed are given here.

Institutional abbreviations. AP, Arroyo de la Pascueta amber, housed in the Museo Aragonés de Paleontología, Teruel, Spain; AR-1-A, Ariño amber, housed in the Museo Aragonés de Paleontología (Fundación Conjunto Paleontológico de Teruel-Dinópolis), Teruel, Spain; CES, El Soplao amber, housed in the Colección Institucional del Laboratorio de la Cueva El Soplao in Celis, Cantabria, Spain; CPT, MAP, San Just amber, housed in the Museo Aragonés de Paleontología, Teruel, Spain; MCNA, Peñacerrada I amber, housed in the Museo de Ciencias Naturales de Álava in Vitoria-Gasteiz, Álava, Spain; SJ-10, SJNB2012, San Just amber, housed in the Museo Aragonés de Paleontología, Teruel, Spain.

SYSTEMATIC PALAEONTOLOGY

Order PSOCODEA Hennig, 1966
Suborder TROGIOMORPHA Roesler, 1940
Infraorder ATROPETAE Pearman, 1936
Family †ARCHAEATROPIDAE Baz & Ortuño, 2000

Type genus. *Archaeatropos* Baz & Ortuño, 2000.

Included genera and species. *Archaeatropos alavensis* Baz & Ortuño, 2000 (Albian, Spain); *Archaeatropos randatae* (Azar & Nel, 2004) (Barremian, Lebanon); *Bcharreglaris amunobi* Azar & Nel, 2004 (Barremian, Lebanon); *Heliadesdakruon morganae* Cumming & Le Tirant, 2021 (Cenomanian, Myanmar); *Libanoglaris chehabi* Azar & Nel, 2004 (Barremian, Lebanon); *Libanoglaris mouawadi* Azar, Perrichot, Néraudeau & Nel *in* Perrichot *et al.*, 2003 (Barremian, Lebanon); *Proprionoglaris axioperierga* Azar *et al.*, 2015 (Cenomanian–Turonian, France); *Proprionoglaris guyoti* Perrichot *et al.*, 2003 (Albian–Cenomanian, France); *Prospeleketor albianensis* Perrichot *et al.*, 2003 (Albian–Cenomanian, France); and *Setoglaris reemae* Azar & Nel, 2004 (Barremian, Lebanon).

Original diagnosis. Belonging to the suborder Trogiomorpha. Inner side of 2nd maxillary palpal segment with sensillum. Antennae with segments secondarily annulated. Forewing: veins (except Cu2) and margin with long setae. Basal sector of Sc well developed curving to meet R. Distal section of Sc directed backward. Pterostigma not thickened. M + Cu strongly curved. Crossvein from R1 to Rs. Areola postica long and slender, Cu1b shorter than Cu1a. Veins Cu2 and IA ending together on wing margin (nodulus). Hind wing: M 2-branched. Cu2 only slightly sinuous. Sc short, not passing into R. IA and 2A fused basally, dividing near margin, with IA strongly curved. Tarsi 3-segmented. Coxal organ present on hind legs. Hind tibia and tarsus together longer than abdomen. Claws without preapical tooth or, if present, very small. Ovipositor valvulae as follows: external valve (v3) as an elongate and setose lobe; dorsal valve (v2) small, rudimentary; ventral valve (v3) absent. Paraprocts with a strong posterior spine. Subgenital plate apparently membranous without sclerifications (Baz & Ortuño 2000).

Emended diagnosis. Antennae with 18 or more flagellomeres; inner side of the second maxillary palpomere possessing a sensillum; forewings: row of setae along the veins except Cu_2, basal sector of Sc well developed and curving to meet R_1, pterostigma not thickened, M + Cu strongly curved, crossvein from R_1 to Rs, areola postica long and slender, Cu_{1b} shorter than Cu_{1a}, veins Cu_2 and A ending together in a nodulus; hind wings: Sc short not passing into R, with Rs and M two-branched, basi-radial cell four-angled, 1A and 2A fused basally and dividing near the margin with 1A strongly curved; coxal organ present on hind legs; hind tibia and tarsus together longer than abdomen; tarsi three-segmented; ovipositor valvulae: external valve as an elongate and setose lobe, dorsal valve small and rudimentary, ventral valve absent; paraprocts with a strong posterior spine; subgenital plate apparently membranous without sclerifications.

Remarks. The original diagnosis of †Archaeatropidae proposed by Baz & Ortuño (2000) was based only on the species *Archaeatropos alavensis* due to monotypy. The diagnoses of the genus and the species were the same as the original diagnosis of the family. After the description of the family †Archaeatropidae, several genera and species have been identified that belong to this family. Therefore, an emended diagnosis was necessary to better accommodate the new taxa and to differentiate them from *A. alavensis*.

The character 'antennae with 18 or more flagellomeres' has been included in the emended diagnosis because this is typical in the species of the group (*Archaeatropos alavensis*, 20/21; *Archaeatropos randatae*, 22; *Bcharreglaris amunobi*, 25; *Heliadesdakruon morganae*, 25; *Libanoglaris chehabi*, 21; *Libanoglaris mouawadi*, 20; and *Proprionoglaris guyoti*, 18). *Setoglaris reemae* (with at least 10 flagellomeres) is an exception, but the antennae seem to be incomplete (Azar & Nel 2004). The number of

FIG. 1. Palaeogeographical reconstruction of western Europe from 100 Ma showing the location of the amber-bearing outcrops that yielded the studied specimens (psocid silhouettes). Map modified from Scotese (2001). Psocid silhouette redrawn from Lienhard *et al.* (2012, fig. 1).

flagellomeres in *Proprionoglaris axioperierga* and *Prospeleketor albianensis* is unknown. The characters 'secondary annulations on flagellomeres' and 'preapical tooth on pretarsal claws' are unstable in the family. All of the members of the family show a sensillum on the second maxillary palpomere, except for the genus *Proprionoglaris* (Perrichot *et al.* 2003). Fourth maxillary palpomere with hatchet-shaped apex is typical of both †Archaeatropidae and †Empheriidae. Regarding the forewing venation, the character 'distal section of Sc directed backward' is a putative autapomorphy of the genus *Archaeatropos*, as Mockford *et al.* (2013) indicated. Therefore, it has been removed from the emended diagnosis. The hind wings of archaeatropids show two-branched Rs and a four-angled basi-radial cell, with these two characters included in the emended diagnosis. The mention of the vein Cu_2 with a slightly sinuous path in the hind wings has been removed from the emended diagnosis because it is nearly straight or slightly curved in some specimens. In the original diagnosis the ventral valve of the ovipositor was incorrectly called 'v3' instead of 'v1'.

†ARCHAEATROPIDAE indet.

Figure 2

Material. SJNB2012-12-02: a complete nymph, sex unknown. The amber piece contains a total of 36 syninclusions: three psocids, one thrips, two hemipterans, nine hymenopterans, 15 dipterans, two undetermined insects, three spiders, and probable spiderweb threads.

Description. Complete immature specimen, sex unknown. Brown body 1.26 mm long, covered by fine hairs (Fig. 2A–D). Head 0.48 mm wide, with a broad vertex and two prominent compound eyes separated by 0.30 mm, lacking ocelli; left antenna incomplete with scape, pedicel and nine flagellomeres, with secondary annulations; right antenna completely preserved with scape, pedicel and 25 flagellomeres of similar lengths (*c.* 0.05 mm), with secondary annulations (Fig. 2E) and with a pair of distal, fine hairs; marked labrum and clypeus, with differentiable anteclypeus and postclypeus; maxillary palps four-segmented, covered by fine hairs, a sensillum visible on the left second maxillary palpomere, length of maxillary palpomeres: I 0.04 mm, II 0.08 mm, III 0.03 mm, IV 0.13 mm, fourth maxillary palpomere with hatchet-shaped apex; visible mentum, paraglosses and labial palps two-segmented with a round apex and covered by fine hairs, length of labial palpomeres: I 0.02 mmm, II 0.04 mm; lacinia not visible. Wing buds placed over the body; forewing buds 0.55 mm long, up to half the length of the abdomen, elongate and slender with a sharp apex, no visible venation, few fine hairs on costal and radial margins; hind wing buds 0.4 mm long, present under forewings, no visible venation

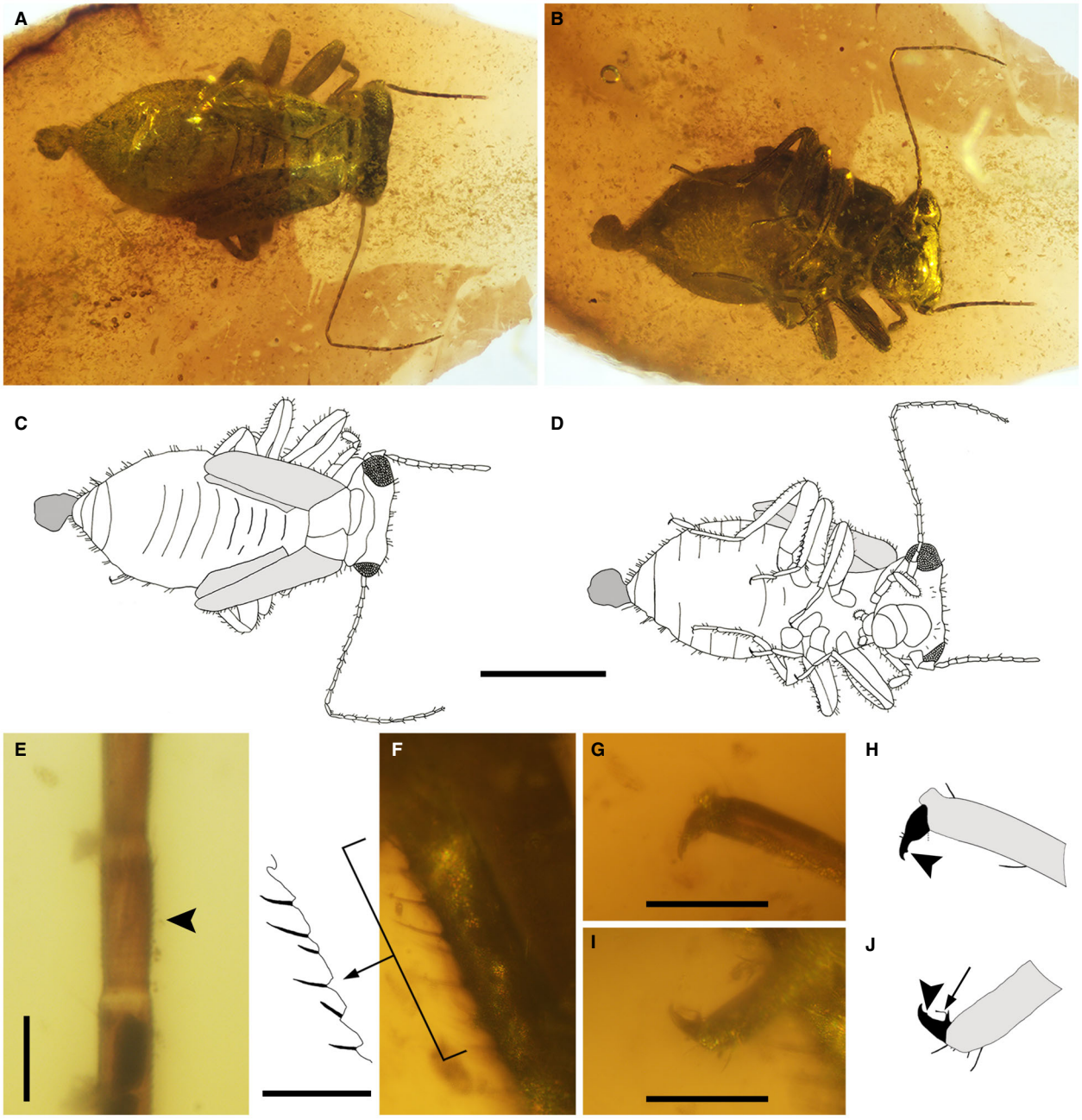

FIG. 2. Psocid nymph (Psocodea, Trogiomorpha, †Archaeatropidae) from the upper Albian amber of San Just (Teruel Province, Spain), SJNB2012-12-02, sex unknown. A–B, habitus in the dorsal and ventral view, respectively. C–D, camera lucida drawings of the habitus in dorsal and ventral view, respectively. E, detail of the left antenna in ventral view, with the secondary annulations indicated by an arrowhead. F, detail of the left midtibia and interpretation of the ctenidiobothria. G–H, detail of the pretarsal claw in the right hind leg, with the preapical tooth indicated by an arrowhead, both images are at the same scale. I–J, detail of the pretarsal claw in the left foreleg, with the preapical tooth indicated by an arrowhead and the pulvillus by an arrow, both images are at the same scale. A–D at the same scale. Scale bars represent: 0.5 mm (A–D); 0.05 mm (E–J).

or tracheation nor fine hairs. Legs completely preserved and covered by fine hairs, with thick femora, thin tibiae and two-segmented tarsi (typical for nymphs); a rounded mark on coxa of right hind leg (possibly coxal organ); two distal spurs on tibiae, and ctenidiobothria visible on midtibiae (Fig. 2F); length of tarsomeres of forelegs and midlegs: proximal 0.11 mm, distal

0.08 mm; tarsomeres of hind legs longer: proximal 0.20 mm, distal 0.09 mm; distal tarsomere with a pretarsal claw bearing one small preapical tooth, pulvillus present (Fig. 2G–J). Abdomen 0.84 mm long. Genitalia not visible. A structure at apex of abdomen could correspond to a coprolite.

Remarks. Nymphal stages of psocids resemble the adult body form and markings. They are characterized by a lack of ocelli, the presence of shorter antennae with fewer flagellomeres than in adults, and the presence of wing buds and two-segmented tarsi (Smithers 1972; Mockford 1993). The number of nymphal instars of psocids is usually six, but it is reduced in some species (New 1987). Wing buds emerge during the second instar (Smithers 1972). There are few reports of nymphal fossil psocids (e.g. Mockford 1969; Vishniakova 1975; Azar *et al.* 2015), and they are usually poorly preserved, hindering their study. Mockford (1969) described a psocid nymph from Miocene Mexican amber from Chiapas that had enough characters to assign it to the living genus *Psyllipsocus* (Trogiomorpha: Psyllipsocidae). Interestingly, Poinar & Vega (2020) identified a parasitic fungus adhering to a female psocid nymph (Troctomorpha: Troctopsocidae) that acted as the host. Recently, new psocid immatures have been described from Burmese amber (Kiesmüller *et al.* 2021; Xu *et al.* 2022).

The high number of flagellomeres (25) in SJNB2012-12-02 and the presence of a labial palpus with a minute proximal segment and a rounded distal segment led to its inclusion in Trogiomorpha (Smithers 1972; Mockford 1993). Considering that nymphs have fewer flagellomeres than adults, the imago of the corresponding species could show an extraordinarily high number of flagellomeres. The presence of a sensillum on the second maxillary palpomere links the specimen to the infraorder Atropetae or to the subfamily Speleketorinae (Prionoglaridetae: Prionoglarididae). Some species of the genera *Psyllipsocus* (Psyllipsocidae) and *Palaeosiamoglaris* (Prionoglarididae) also have a sensillum on the second maxillary palpomere (Lienhard & Ferreira 2015; Liang & Liu 2021; Hakim *et al.* 2022). Unfortunately, Atropetae and Prionoglaridetae are supported by the character states of the adults only (Yoshizawa *et al.* 2006). Speleketorinae is an interesting group in that some members show sex-reversed genital organs (female penis). The representatives of this subfamily are thought to have a Gondwanan origin (Yoshizawa *et al.* 2019). Specimens of this subfamily have secondarily annulated flagellomeres, trichobothria on the legs (absent in Prionoglaridinae) and a preapical tooth on the pretarsal claws, as observed in SJNB2012-12-02. Known Prionoglarididae specimens have half the number of flagellomeres or even fewer than the studied specimen, which would exclude it from this family (Lienhard 2000, 2004; Lienhard & Ferreira 2013). Speleketorinae lacks a fossil record to date, in contrast to the abundance of Atropetae specimens in Cretaceous amber. The assigning of SJNB2012-12-02 to Atropetae is reinforced by its somewhat triangular head, typical for this group. Furthermore, the extant nymphs of Speleketorinae are almost completely related to cave environments.

When comparing SJNB2012-12-02 to Atropetae specimens, the combination of 'flagellomeres with secondary annulations', 'sensillum on the second maxillary palpomere' and 'pretarsal claws bearing a preapical tooth and pulvillus' excludes it from the families Lepidopsocidae, Trogiidae, Psoquillidae and †Empheriidae (Smithers 1972; Mockford 1993; Baz & Ortuño 2001*b*). The SJNB2012-12-02 nymph meets the diagnostic characters of †Archaeatropidae (Baz & Ortuño 2000). The feature 'hatchet-shaped apex of fourth maxillary palpomere' is typical of archaeatropids and empheriids. Regarding the archaeatropid genera, the specimen resembles *Bcharreglaris* (which includes only the species *B. amunobi* from Barremian Lebanese amber), based on the characters that they share, including the same number of flagellomeres (Azar & Nel 2004). *Heliadesdakruon morganae* also shows 25 flagellomeres (Cumming & Le Tirant 2021). The species *Archaeatropos alavensis* is present in San Just, as discussed below. SJNB2012-12-02 differs from *A. alavensis* only by the number of flagellomeres, which could be variable (Baz & Ortuño 2000). Therefore, it is plausible that the nymph belongs to this species. Nonetheless, we prefer not to assign the specimen to a specific group given the lack of data on nymphal fossil psocids. Furthermore, the description of a new species based on a nymph would be problematic. This finding is interesting because the exceptionally well-preserved nymph is tentatively assigned to †Archaeatropidae, a psocid family restricted to the Cretaceous.

Genus ARCHAEATROPOS Baz & Ortuño, 2000

Type species. *Archaeatropos alavensis* Baz & Ortuño, 2000.

Other species. *Archaeatropos randatae* (Azar & Nel, 2004).

Emended diagnosis. Antennae with 20–22 flagellomeres; maxillary palps with the fourth palpomere longer than the second palpomere; forewings: distal sector of Sc straight or curved, directed towards the wing base; claws without a preapical tooth or, if present, a very small preapical tooth.

Archaeatropos alavensis Baz & Ortuño, 2000

Figures 3–5

Material. CES.445: an almost complete specimen, sex unknown. CES.465: a complete specimen, female. CES.495.4: wing remains, with three hymenopterans as syninclusions. CES.526.5: a partial specimen, sex unknown, with a cockroach, a mite, a hymenopteran, a dipteran, a psocid and a thrips as syninclusions. CES.586.2: forewings and partial body remains, with a psocid of the genus *Libanoglaris* as a syninclusion. MCNA-14912.1: an almost complete specimen, sex unknown, with an undetermined wing as a syninclusion. MAP-7812: a complete specimen, female, with two hymenopterans, a bethylid and a platygastrid as syninclusions. (SJ-10-50) SJ2: an almost complete specimen, sex unknown. AP-11.1: an almost complete specimen, sex unknown, with an undetermined larva, a cockroach and a dipteran as syninclusions.

Other material examined. MCNA-8834, holotype, female. MCNA-8646, allotype, male.

Emended diagnosis. Flagellomeres secondarily annulated; forewings: margin setose, distal sector of Sc curved and directed towards the wing base; hind wings: margin setose.

Description. Body length of the two completely preserved specimens is 1.35 mm (MAP-7812) and 1.62 mm (CES.465). Body covered by fine hairs. Head as long as wide and measuring *c.* 0.38 mm, with a broad vertex and two prominent compound eyes, ocelli not visible probably due to poor preservation of the vertex of the specimens; antennae incomplete with narrow and slightly elongate flagellomeres similar in shape, *c.* 0.05 mm long, secondarily annulated and with distal fine hairs (MAP-7812 has 20 flagellomeres); clypeus with a narrow anteclypeus and a bulging postclypeus; maxillary palp four-segmented, covered by fine hairs, with a sensillum on the second palpomere, fourth palpomere broadened preapically (hatchet-shaped apex) and longer than second palpomere, length of maxillary palpomeres in CES.465: I 0.03 mm, II 0.06 mm, III 0.04 mm, IV 0.10 mm; other mouthparts not visible. Thorax with slightly bulging pronotum; wings with complete venation; measurements and description of the wings mainly follow those of specimen MAP-7812. Forewing (Figs 3C, 4D) hyaline, 1.60–1.95 mm long and 0.60–0.70 mm wide, wing margin setose with closely packed linear spicules parallel to margin, one row of setae along veins; basal sector of Sc long, distally curved and directed towards R_1; distal sector of Sc curved and directed towards the wing base,

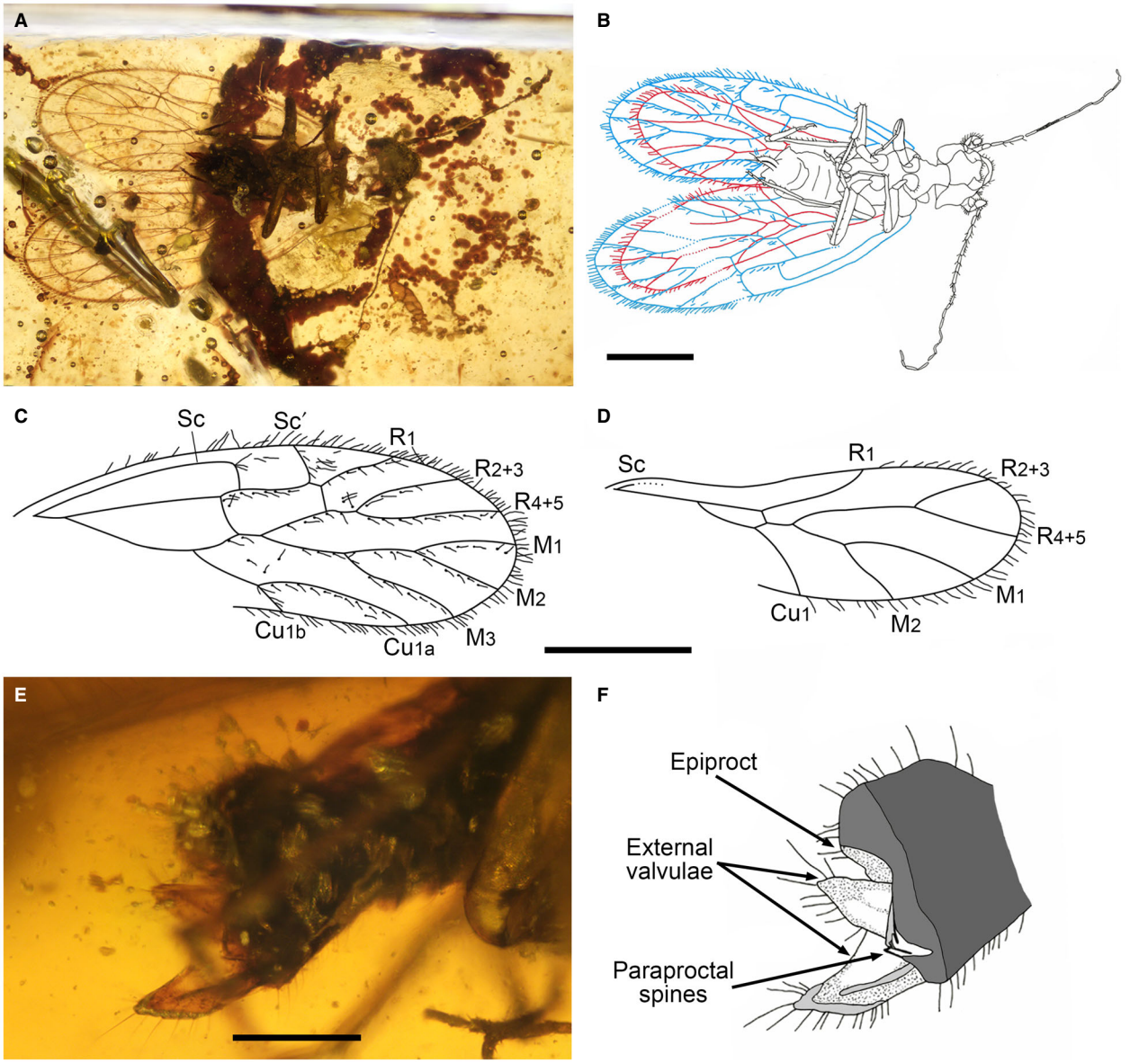

FIG. 3. New specimen of *Archaeatropos alavensis* Baz & Ortuño, 2000 (Psocodea, Trogiomorpha, †Archaeatropidae) from the upper Albian amber of San Just (Teruel Province, Spain), MAP-7812, female. A–B, photograph and drawing of the habitus in ventral view, with the forewings shown in blue and the hind wings in red. C–D, forewing and hind wing, respectively, both images are at the same scale. E–F, photograph and drawing of the female genitalia, respectively. Scale bars represent: 0.5 mm (A–D); 0.2 mm (E, F).

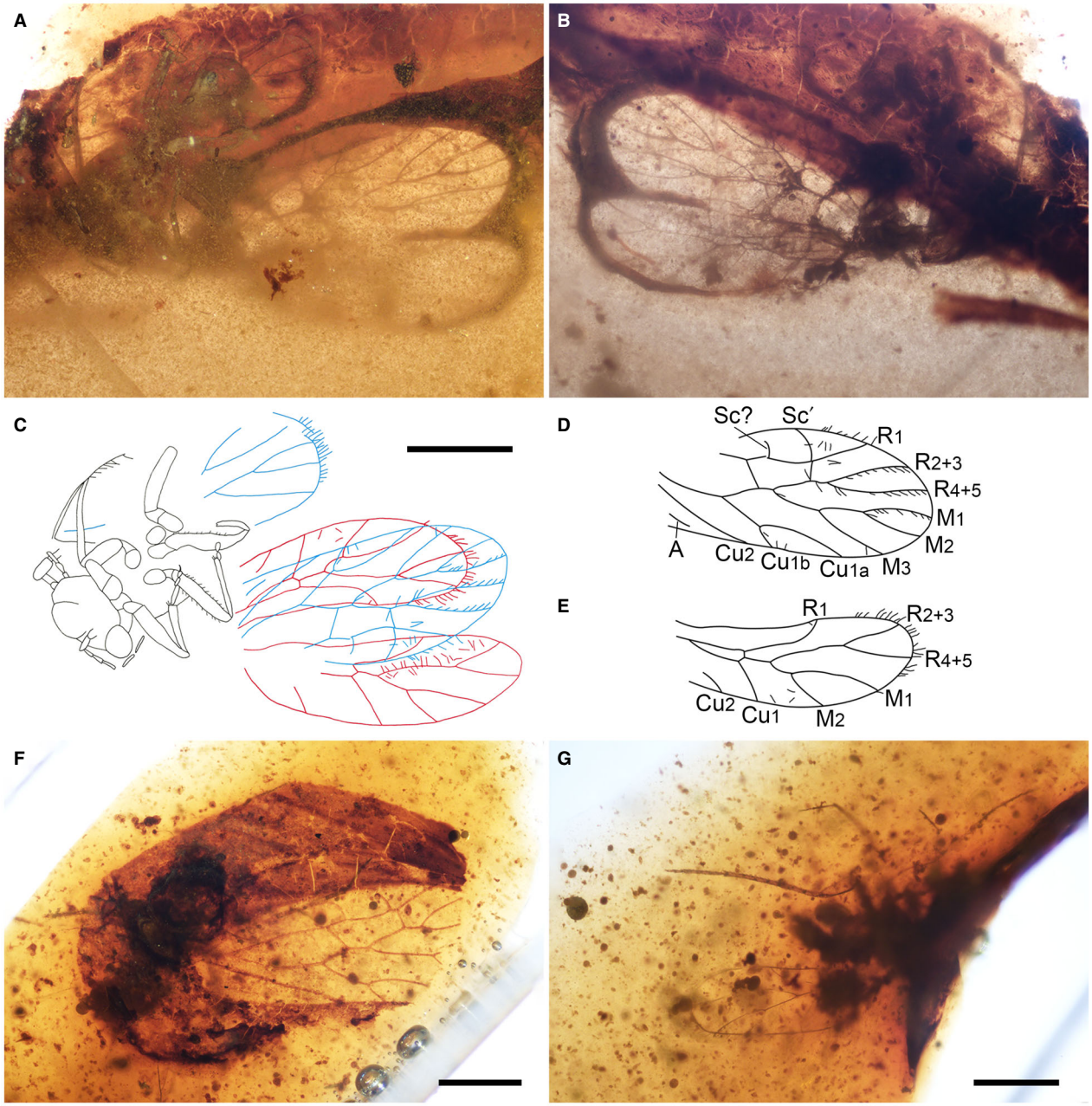

FIG. 4. New specimens of *Archaeatropos alavensis* Baz & Ortuño, 2000 (Psocodea, Trogiomorpha, †Archaeatropidae) from the upper Albian amber of San Just and Arroyo de la Pascueta (both in Teruel Province, Spain). A–E, specimen (SJ.10-50) SJ2, sex unknown: A–B, habitus in ventral and dorsal view, respectively; C, drawing of the habitus in ventral view, with the forewings shown in blue and the hind wings in red; D–E, left forewing and hind wing, respectively. F–G, habitus of the specimen AP-11.1 as preserved, sex unknown. A–E are at the same scale. Scale bars represent 0.5 mm.

joining margin at 1.00 mm from base; R_1 slightly sigmoidal, reaching margin at 1.33 mm from wing base; Rs perpendicular to M or slightly oblique at its base, joining M at 0.78 mm from wing base; straight crossvein between R_1 and Rs, forming a six-angled radial cell; Rs bifurcated into R_{2+3} and R_{4+5} at 1.18 mm from wing base, with both reaching the margin at 1.54 mm and 1.69 mm from wing base, respectively, R_{4+5} slightly sigmoidal; M_3 emerging from M at 1.16 mm from wing base, showing a sigmoidal path and reaching the margin at 1.56 mm from wing base; separation of M_1 and M_2 at 1.39 mm from wing base, both are nearly straight, reaching the margin at 1.74 mm and 1.69 mm from wing base, respectively; Cu_1 bifurcating into Cu_{1a} and Cu_{1b} at 0.89 mm from wing base, approximately at the same level as that of the bifurcation of Rs and M, areola postica

long and with a curved Cu_{1a} reaching the margin at 1.41 mm from wing base, while straight and short Cu_{1b} reaches the margin at 0.98 mm from wing base; nodulus between Cu_2 and A visible in CES.526.5 specimen at 0.67 mm from wing base, nodulus is also tentatively visible in CES.495.4 and MCNA-14912.1 specimens, while the paths of Cu_2 and A are compatible with the presence of a nodulus in the other specimens, although it is not visible in them. Hind wing (Figs 3D, 4E) hyaline, 1.12–1.45 mm long and 0.44–0.55 mm wide, with margin setose, membrane and veins without setae; Sc short and emerging near wing base, not reaching the wing margin or the other veins; elongate basi-radial cell four-angled; R_1 distally curved, reaching the margin at 0.90 mm from wing base; Rs fused to M only for 0.10 mm, bifurcating at 0.68 mm from wing base; Rs dividing into R_{2+3} and R_{4+5} at 1.09 mm from wing base, both veins slightly curved and reaching the margin at 1.33 mm and 1.43 mm from wing base, respectively; M dividing into M_1 and M_2 at 0.86 mm from wing base, M_1 is curved and reaches the margin at 1.31 mm from wing base, while M_2 is sigmoidal and reaches the margin at 1.07 mm from wing base; Cu_1 curved and reaching the margin at 0.78 mm from wing base; Cu_2 and A are not visible or only partly visible in the studied specimens due to the poor preservation of the cubito-anal region of the hind wings. Legs covered by fine hairs; tarsi three-segmented; one distal spur visible in tibiae; interestingly, the tibiae and first tarsomeres of the hind legs of CES.465 seem to be longer than in the other specimens; length of tarsomeres of right midleg of MAP-7812: proximal 0.16 mm, middle 0.04 mm, distal 0.04 mm; pretarsal claws of distal tarsomeres without a preapical tooth or pulvillus, although a very small preapical tooth can be seen in some specimens. Abdomen *c.* 0.83 mm long in CES.465. Female genitalia (Fig. 3E, F) visible in the MAP-7812 and CES.465 specimens; external valvulae are two elongate lobes covered by long setae at apex and sides, and seem to have a membrane along the midline; dorsal and ventral valves not visible; two marked paraproctal spines; membranous epiproct. Genitalia of the other studied specimens are obscure.

Remarks. The number of flagellomeres, the presence of a sensillum in the second maxillary palpomere and the arrangement of the ovipositor valvulae (with external valves as elongate lobes bearing long setae) confirm the assignment of *Archaeatropos alavensis* to Atropetae in Trogiomorpha (Smithers 1972; Mockford 1993). The secondarily annulated flagellomeres, the forewings with a row of setae along the veins, the basal sector of Sc curving to meet R_1 and the presence of a nodulus are characteristics of the family †Archaeatropidae, and differentiate it from the other families of Atropetae (Baz & Ortuño 2000). However, the recently described genus *Burmempheria*, belonging to †Empheriidae, shows some characters of †Archaeatropidae, such as the presence of a nodulus. Thus, the differences and putative relationships between these two families are discussed below. The diagnoses of the genus *Archaeatropos* and the species *A. alavensis* were the same as the original diagnosis of the family †Archaeatropidae (Baz & Ortuño 2000). Therefore, both have been emended to differentiate them from the other genera and species of the family.

As Mockford *et al.* (2013) indicated, the genus *Archaeatropos* is characterized by the distal sector of Sc being directed towards the wing base, a putative autapomorphy of the genus. This character is present in the two species of the genus. *Archaeatropos randatae*, from Barremian Lebanese amber, was first assigned to the genus *Libanoglaris* (Azar & Nel 2004), although its place in *Archaeatropos* (*sensu* Mockford *et al.* 2013) is suitable. *Archaeatropos randatae* differs from *A. alavensis* by having flagellomeres without secondary annulations (*A. alavensis* has secondary annulations), having a glabrous margin of the fore- and hind wing (setose in *A. alavensis*), and presenting a different shape of the areola postica (*A. alavensis* has a shorter Cu_{1b}). *Archaeatropos randatae* has one preapical tooth on the pretarsal claws but this character in *A. alavensis* shows intraspecies variability, given that it is present in some specimens and absent in others. The specimens assigned to *A. alavensis* in this study share the same habitus and autapomorphies of the species, despite some minor differences that can be explained by intraspecies variability. *Psylloneura perantiqua* Cockerell, 1919 was transferred to the genus *Archaeatropos* by Mockford *et al.* (2013) based on the distal sector of Sc being directed towards the wing base, which is straight and, therefore, different from that of the other species of the genus. This species was described by Cockerell (1919) based only on the characters of the poorly preserved forewings and a partial antenna. Moreover, there were many important characters that could not be visualized, such as the basal sector of Sc joining R_1, the areola postica, the nodulus and most of the body characters. Recently, this species was again transferred to the genus *Cormopsocus* (†Cormopsocidae) based on the finding of a new complete specimen from Burmese amber (Cumming & Le Tirant 2021).

Notably, *A. alavensis* is the most abundant psocid species found in Albian Spanish amber. It is present in the amber outcrops of El Soplao, Peñacerrada I, San Just and Arroyo de la Pascueta. Therefore, it was distributed at least along the northern Iberia Island during this period. Many of the undescribed psocids from Peñacerrada I have a morphotype similar to that of *A. alavensis*, although a detailed study is required for confirmation.

Genus LIBANOGLARIS Azar, Perrichot, Néraudeau & Nel *in* Perrichot *et al.*, 2003

Type species. Libanoglaris mouawadi Azar, Perrichot, Néraudeau & Nel *in* Perrichot *et al.*, 2003.

Other species. Libanoglaris chehabi Azar & Nel, 2004.

Libanoglaris hespericus sp. nov.

Figures 6–8

LSID. urn:lsid:zoobank.org:act:F9402FBD-5C80-419C-90AB-4254D82F8A3E

Derivation of name. After Hesperia, from the Greek *Εσπερία*, the ancient name for the western lands of the Mediterranean Sea, based on the location of the type locality of the new species

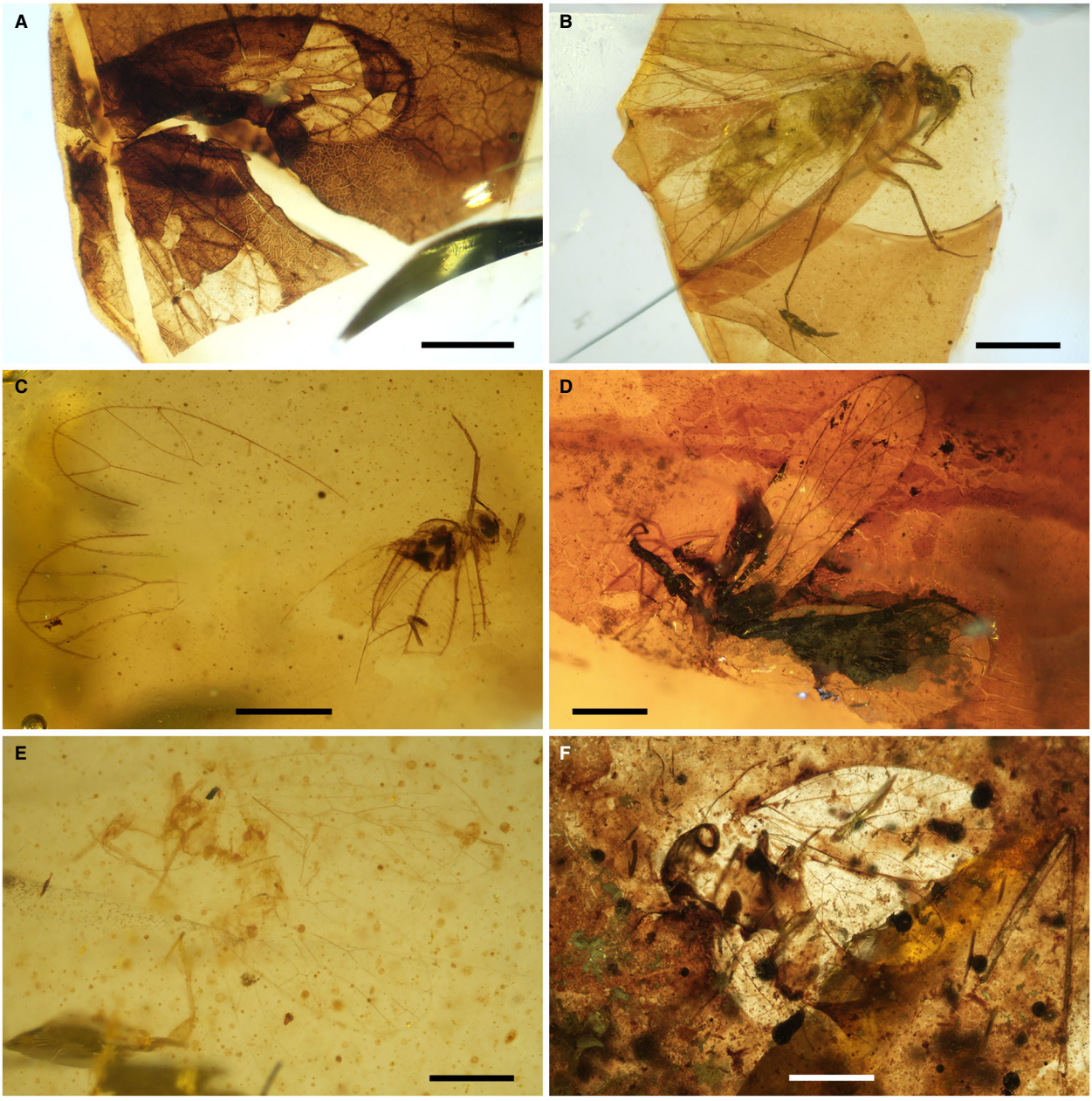

FIG. 5. New studied specimens of *Archaeatropos alavensis* Baz & Ortuño, 2000 (Psocodea, Trogiomorpha, †Archaeatropidae) from the Albian amber of El Soplao (Cantabria Autonomous Community, Spain) and the upper Albian amber of Peñacerrada I (Burgos Province, Spain). A, specimen CES.445, sex unknown. B, specimen CES.465, female. C, specimen CES.495.4, sex unknown. D, specimen CES.526.5, sex unknown. E, specimen CES.586.2, sex unknown. F, specimen MCNA-14912.1, sex unknown. Scale bars represent 0.5 mm.

in relation to that of the other species of the genus (from Lebanon).

Type specimens. Holotype AR-1-A-2019.35: an incomplete macropterous specimen with clearly visible venation (Fig. 6A, B), sex unknown. Paratype AR-1-A-2019.69.1: an almost complete specimen, the right forewing and some body characters are visible (Fig. 6C, D), sex unknown, with a specimen that could be a dipteran as a syninclusion. Both are housed at the Museo Aragonés de Paleontología (Fundación Conjunto Paleontológico de Teruel-Dinópolis).

Other material. CES.586.1: a complete specimen, the body is anterodorsally compressed (Fig. 7), the wings are folded roof-like so that the venation is unclear, sex unknown, with a psocid (*Archaeatropos alavensis*) as a syninclusion.

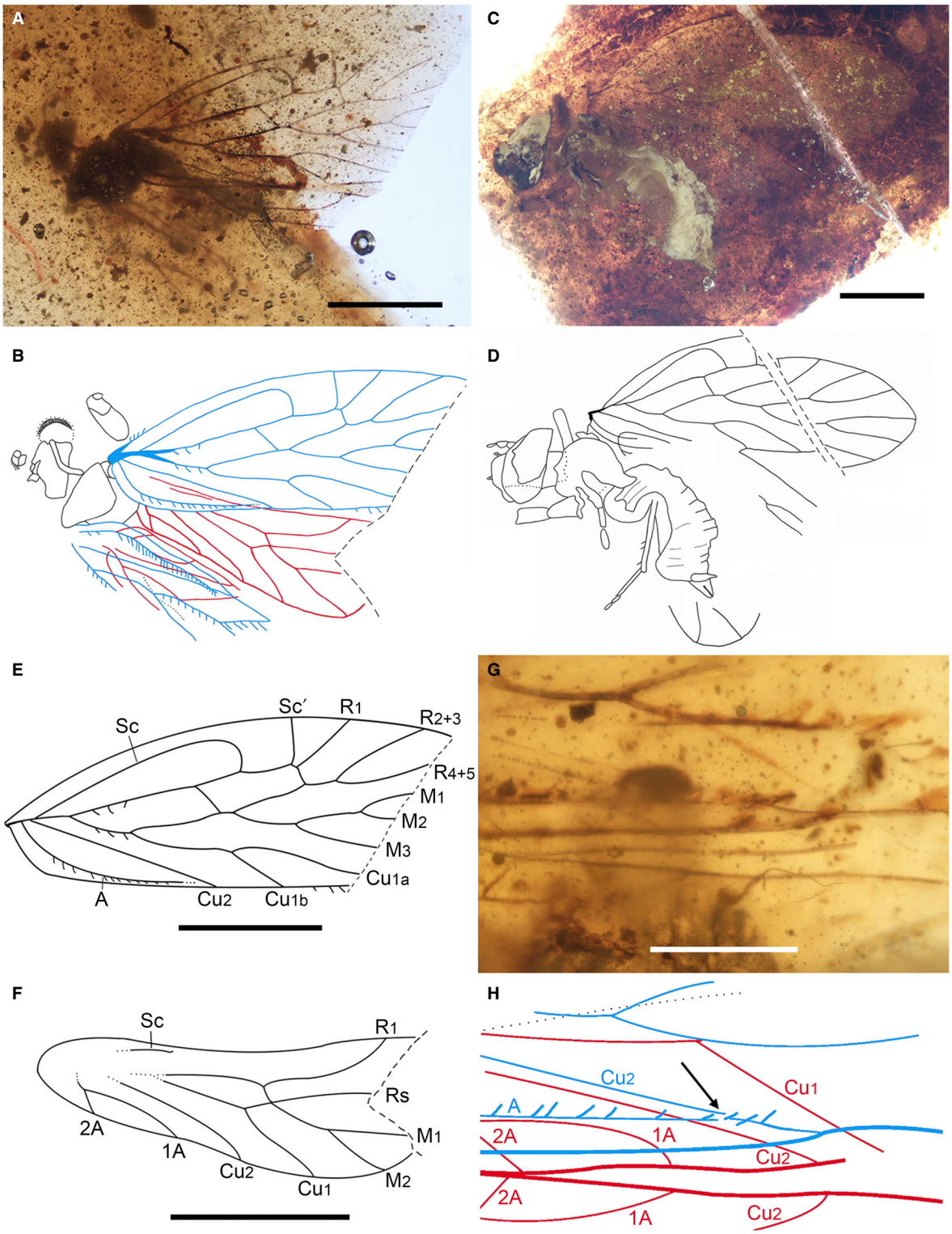

FIG. 6. Type specimens of *Libanoglaris hespericus* sp. nov. (Psocodea, Trogiomorpha, †Archaeatropidae) from the lower Albian amber of Ariño (Teruel Province, Spain). A–B, habitus of the holotype specimen AR-1-A-2019.35 in ventral view, sex unknown, with the forewings shown in blue and the hind wings in red in B. C–D, habitus of the paratype specimen AR-1-A-2019.69.1 in dorsal view, sex unknown. E–F, forewing and hind wing, respectively, of holotype AR-1-A-2019.35. G–H, detail and interpretive drawing of the nodulus of the right forewing of holotype AR-1-A-2019.35, respectively, with the nodulus indicated by an arrow in H, forewing is shown in blue and the hind wings in red. Scale bars represent: 0.5 mm (A–F); 0.2 mm (G, H).

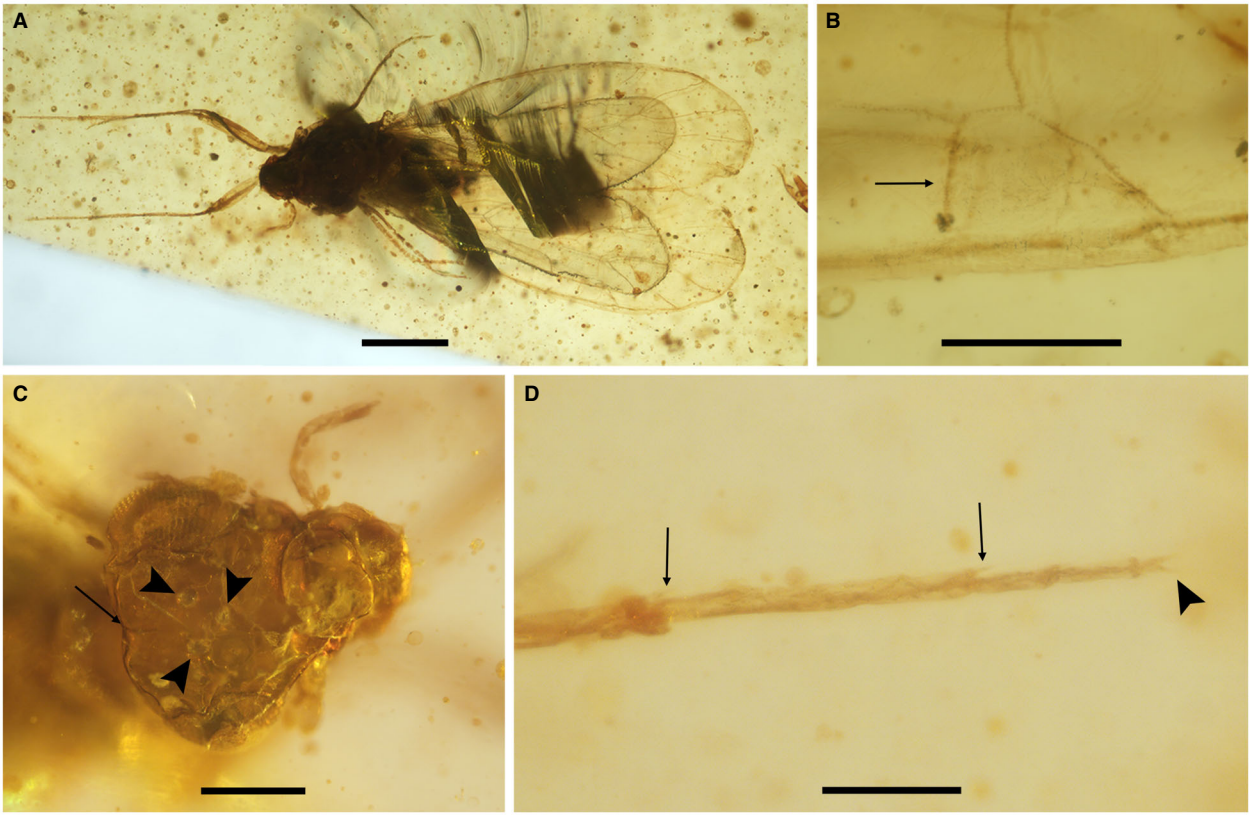

FIG. 7. *Libanoglaris hespericus* sp. nov. (Psocodea, Trogiomorpha, †Archaeatropidae) from the Albian amber of El Soplao (Cantabria Autonomous Community, Spain), CES.586.1, sex unknown. A, habitus in the dorsal view. B, pterostigma area of the left forewing, showing the straight distal sector of Sc (arrow) joining the wing margin at a right angle. C, head in the dorsal view (epicranial suture indicated by an arrow, ocelli indicated by arrowheads). D, right foreleg, distal spurs of the tibia and the proximal tarsomere are indicated by arrows, while the pretarsal claws lacking a preapical tooth are indicated by an arrowhead. Scale bars represent: 0.5 mm (A); 0.2 mm (B, C); 0.1 mm (D).

Diagnosis. Wings glabrous except for the forewings with fine hairs in the basal parts of R and M + Cu, and a row of setae along A; forewings: crossvein from R_1 to Rs straight, Rs oblique basally, bifurcation of Cu_{1a} and Cu_{1b} at the same level as that of the joining of Rs with M.

Description. Body almost glabrous or covered by a few fine hairs. Head 0.52 mm wide, with broad vertex showing three ocelli (Fig. 7C); prominent compound eyes separated by 0.32 mm; antennae preserved in AR-1-A-2019.69.1, showing scape, pedicel and first flagellomere of the right antenna without secondary annulations; bulging postclypeus; mouthparts obscure. Description of venation is based on the holotype AR-1-A-2019.35, which presents visible veins although it is lacking a wing apex (Fig. 6E–H); forewing 1.88–2.16 mm long and 0.60–0.71 mm wide (Fig. 6E), hyaline, with a glabrous margin except for a few fine hairs in the basal part of the costal margin of AR-1-A-2019.35; basal parts of R and M + Cu covered by fine hairs; basal sector of Sc long, showing a strong curve before fusion with R_1, to which it is fused for 0.18 mm, basal sector of Sc is not visible in CES.586.1; distal part of Sc straight and reaching the costal margin at 1.07 mm from the wing base to form almost a right angle; pterostigma area not thickened and without setae; straight crossvein from R_1 to Rs; length of R_1 from where the distal part of Sc emerges to the crossvein from R_1 to Rs is variable (Fig. 7B), longer in CES.586.1 than in the holotype AR-1-A-2019.35; Rs oblique basally and fused to M for 0.05 mm, emerging from M at 0.80 mm from wing base, and distally branching into R_{2+3} and R_{3+4} at 1.17 mm from the wing base, both veins slightly curved; radial cell closed, six-angled and elongate, more than threefold longer than wide; curved M + Cu_1, 0.22 mm long, bifurcating at 0.44 mm from wing base; M_3 emerging from M at 1.01 mm from wing base and continuing mostly straight, M branching into M_1 and M_2 at 1.24 mm from wing base; Cu_1 0.37 mm long, bifurcation of Cu_{1a} and Cu_{1b} at the same level as that of the joining of Rs with M, at 0.79 mm from wing base, Cu_{1a} showing a slight curve and extending towards the wing apex, Cu_{1b} straight, shorter than Cu_{1a} and reaching the margin at 0.99 mm from the wing base, both forming an elongate areola postica; straight Cu_2 extending towards the wing margin, which it reaches at 0.77 mm from the wing base; A covered by a row of setae, showing a strong curve and extending towards Cu_2, joining in a nodulus (Fig. 6G, H). Hind wing hyaline (Fig. 6F), without setae or fine hairs in the margin

or in the veins, 1.65 mm long in CES.586.1 (only specimen showing hind wings that are complete in length) and 0.34–0.45 mm wide; Sc does not reach the wing margin, ending free in wing membrane; R_1 reaching the margin at 0.98 mm from the wing base; Rs makes contact with M at a point, but they do not fuse, although Rs and M are fused for 0.23 mm in CES.586.1; Rs two-branched; basi-radial cell four-angled; M basally fused with Cu_1, length of M from its separation from Cu_1 to its joining with Rs is 0.08 mm, distal free part of M is 0.18 mm long, bifurcation of M_1 and M_2 is at 0.83 mm from wing base; Cu_1 separating from M and reaching the margin at 0.83 mm from wing base; slightly curved Cu_2 reaching the margin at 0.62 mm from wing base; A separating into 1A and 2A at 0.14 mm from wing base, 1A is curved and 2A is straight, both reaching the margin at 0.43 mm and 0.20 mm from the wing base, respectively. Forelegs of CES.586.1 are completely preserved; thick femora 0.43 mm long; thin tibiae 0.70 mm long; tarsi three-segmented (Fig. 7D); one distal spur in the tibiae and proximal tarsomere (Fig. 7D); length of tarsomeres: proximal 0.21 mm, middle 0.06 mm, distal 0.05 mm; two pretarsal claws in distal tarsomeres that lack a preapical tooth (Fig. 7D). Abdomen of AR-1-A-2019.69.1 and CES.586.1 poorly preserved; the former could be a female based on the morphology of the genitalia.

Remarks. *Libanoglaris hespericus* sp. nov. belongs to †Archaeatropidae (Trogiomorpha: Atropetae) based on the following characters: forewing with a well-developed basal sector of Sc that is curved and reaches R, a pterostigma area that is not thickened, a curved M + Cu, a crossvein from R_1 to Rs, a long and slender areola postica, a shorter Cu_{1b} compared with Cu_{1a}, the joining of Cu_2 and A in a nodulus, a short hind wing with Sc that does not reach R, a two-branched M, a four-angled basi-radial cell, basally fused 1A and 2A that branches near the wing margin, a curved 1A, and three-segmented tarsi. Within †Archaeatropidae, the three specimens are assigned to the genus *Libanoglaris* based on the lack of secondary annulations in the flagellomeres and the venation of the wings (Perrichot *et al.* 2003). Other archaeatropid genera without secondary annulations are *Prospeleketor* and *Proprionoglaris*, but the wing venations are clearly different (Perrichot *et al.* 2003). Both genera present forewings in which the distal sector of Sc is directed towards the wing apex (Perrichot *et al.* 2003), in contrast to the genus *Libanoglaris*, which presents a straight distal sector of Sc that joins nearly perpendicular to the anterior wing margin (Perrichot *et al.* 2003; Azar & Nel 2004). Furthermore, the three specimens fit within the genus *Libanoglaris* based on their wings without scales and without a sclerotized pterostigma, a forewing with the basal sector of Sc reaching R and fusing with it over a long stretch (basal sector of Sc not preserved in CES.586.1), an absence of a crossvein between the proximal sector of Sc and the wing margin, an elongate radial cell and an Rs that is oblique at its base, and a hind wing with a four-angled basi-radial cell (Perrichot *et al.* 2003). The number of flagellomeres, the characteristics of the mouthparts, and the absence of long sensillae in the median and posterior femora and tibiae, which are indicated in the diagnosis of *Libanoglaris* (Perrichot *et al.* 2003), cannot be observed in the specimens. The genus *Bcharreglaris* has forewings in which the distal sector of Sc is perpendicular to the wing margin (Azar & Nel 2004), but it has secondary annulations in the flagellomeres and a triangular pterostigma (vs a trapezoidal pterostigma in *Libanoglaris*). *Libanoglaris* includes two species from the Barremian Hammana-Mdeyrij locality (Lebanon), which are *Libanoglaris mouawadi* and *Libanoglaris chehabi*. Mockford *et al.* (2013) transferred *Libanoglaris randatae* Azar & Nel, 2004 (from the Jezzine locality in Lebanon) to the genus *Archaeatropos* based on the Sc′ being curved and directed towards the wing base, as commented above. The vein Sc′ is straight and reaches the costal margin, forming almost a right angle in *L. mouawadi*, which is different to the straight Sc′ in *L. chehabi* that is slightly directed towards the wing base, forming an obtuse angle with the costal margin (Fig. 8). The three

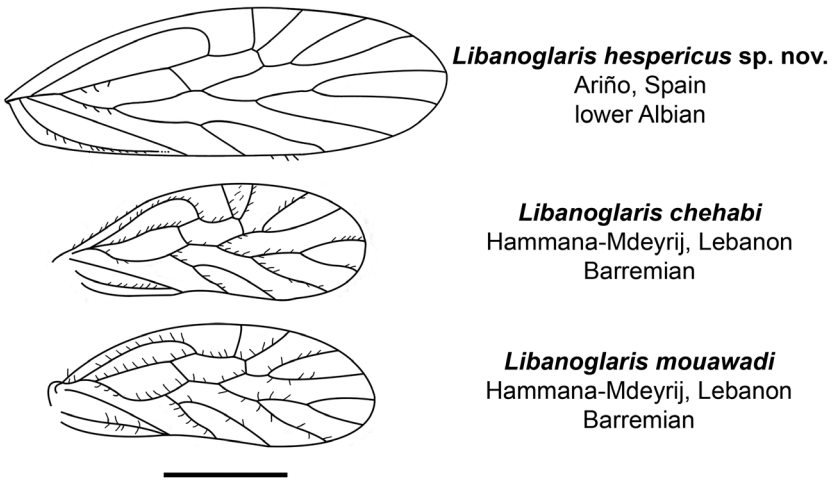

FIG. 8. Schematic drawings of the forewings of *Libanoglaris* spp. (Psocodea, Trogiomorpha, †Archaeatropidae). The forewing of *Libanoglaris hespericus* sp. nov. has been reconstructed from the specimens AR-1-A-2019.35 (holotype) and AR-1-A-2019.69.1 (paratype). The forewings of *Libanoglaris chehabi* and *Libanoglaris mouawadi* have been redrawn from Azar & Nel (2004) and Perrichot *et al.* (2003), respectively. All images are at the same scale. Scale bar represents 0.5 mm.

specimens are assigned to a new species, *L. hespericus*, based on the diagnostic characters that differentiate them from the other two species of the genus. They are conspecific based on the venation, mainly because they share the straight distal sector of Sc that joins the wing margin at almost a right angle. Furthermore, their wings are almost glabrous, both the margin and the membrane. *Libanoglaris hespericus* is separated from the other species of the genus by a time span of *c.* 20 myr (Perrichot *et al.* 2003; Azar & Nel 2004). Interestingly, the older Lebanese species would have been distributed throughout the south-eastern margin of the Tethys Sea, while the younger *L. hespericus* would have been present in the western margin (Iberia Island). Intraspecies variability of the wing venation has been noted when comparing the holotype AR-1-A-2019.35 from Ariño with the CES.586.1 specimen from El Soplao. The length of R_1 (in the forewings) from the emerging of the distal part of Sc to the crossvein from R_1 to Rs is longer in CES.586.1 than in AR-1-A-2019.35. Furthermore, in the hind wing of AR-1-A-2019.35, Rs makes slight contact with M at a point, but they do not fuse, whereas both veins are fused for 0.23 mm in CES.586.1. Despite these differences, we prefer to putatively assign CES.586.1 to *L. hespericus* rather than to establish a new species, based on the matching characters when compared with the Ariño specimens. The morphological differences can be explained by the spatial and temporal distance between the amber localities.

Type locality and horizon. Level AR-1 of the Ariño amber-bearing outcrop, Teruel Province, Spain; Escucha Formation, lower Albian (Álvarez-Parra *et al.* 2021).

Other localities. El Soplao amber-bearing outcrop, Cantabria Autonomous Community, Spain; Las Peñosas Formation, Albian.

Family †EMPHERIIDAE Kolbe, 1884

Type genus. *Empheria* Hagen *in* Pictet-Baraban & Hagen, 1856.

Included genera and species. *Burmempheria densuschaeate* Li, Wang & Yao *in* Li *et al.*, 2020 (Cenomanian, Myanmar); *Burmempheria raruschaetae* Li, Wang & Yao *in* Li *et al.*, 2020 (Cenomanian, Myanmar); *Empheria pertinens* (Enderlein, 1911) (Eocene, Baltic amber); *Empheria reticulata* Hagen *in* Pictet-Baraban & Hagen, 1856 (Eocene, Baltic amber); *Empherium rasnitsyni* Hakim *et al.*, 2021*a* (Cenomanian, Russia); *Empheropsocus arilloi* Baz & Ortuño, 2001*b* (Albian, Spain); *Empheropsocus margineglabrus* Baz & Ortuño, 2001*b* (Albian, Spain); *Eoempheria intermedia* Nel *et al.*, 2005 (Eocene, France); *Jerseyempheria grimaldii* Azar *et al.*, 2010 (Turonian, USA); *Preempheria antiqua* Baz & Ortuño, 2001*b* (Albian, Spain); and *Trichempheria villosa* (Hagen, 1882) (Eocene, Baltic amber).

Genus PREEMPHERIA Baz & Ortuño, 2001*b*

Type species. *Preempheria antiqua*; by monotypy.

Original diagnosis. Forewings oval. Forewing margin glabrous. Basal sector of Sc well developed, curving to meet R. Basal sector of Sc setose with the setae arranged as is typical for the family. Vein R1 reunites with Rs distally with a crossvein. Origin of the first branch of M distally to the crossvein R1–Rs. A transverse vein between R and Rs + M common trunk, forming a six-angled radial cell. (Baz & Ortuño 2001*b*)

Remarks. Based on the description of the new specimen from San Just assigned to *Preempheria antiqua*, several comments can be added to the original diagnosis of the genus. Besides the characters of the forewings indicated in the original diagnosis, the forewings show closely packed linear spicules that are parallel to the wing margin, rows of setae along both sides of the veins (typical in †Empheriidae), a short Cu_1 that divides into Cu_{1a} and Cu_{1b} at the same level as that of the joining of Rs and M, a long areola postica, a setose anal region, and an absent anal vein. The hind wings are completely glabrous, with a two-branched Rs and M. Given that the original diagnosis lacks body characters, we wanted to highlight the following: the presence of three ocelli that are close together and arranged into an inverted triangle, flagellomeres that are not secondarily annulated and of a similar length, four-segmented maxillary palps with the fourth palpomere elongate and showing a round and slightly widened apex, tibiae with three distal spurs, and distal tarsomeres with two pretarsal claws without a preapical tooth and bearing one pulvillus each that is widened at the tip.

Preempheria antiqua Baz & Ortuño, 2001*b*

Figure 9

Material. CPT-4117; a partial specimen, sex unknown.

Other material examined. MCNA-8888, holotype, female. MCNA-8872, paratype, female.

Description. Specimen covered by fine hairs and with head, thorax, proximal parts of wings and half of abdomen preserved (Fig. 9A, B). Macropterous with visible venation (Fig. 9C, D). Head 0.53 mm wide with two prominent compound eyes that are globular in shape, 0.17 mm in diameter and separated by 0.22 mm; vertex broad and covered by fine hairs, showing epicranial suture, with three ocelli close together and arranged into an inverted triangle (Fig. 9E); left antenna partially preserved with scape, pedicel and 16 flagellomeres preserved, lacking the distal ones, each *c.* 0.07 mm long and with a pair of distal fine hairs, without secondary annulations; right antenna with only scape, pedicel and five flagellomeres preserved; gibbous clypeus; maxillary palps four-segmented and covered by fine hairs, fourth palpomere with round and slightly widened apex, length of maxillary palpomeres: I 0.06 mm, II 0.04 mm, III 0.05 mm, IV 0.13 mm, a short conical sensillum is not visible on second palpomere; a thick elongate structure possibly corresponding to lacinia and galea can also be observed; labial palps two-segmented with a wide and round apex and covered by fine hairs, length of labial palpomeres: I 0.03 mm, II 0.04 mm. The

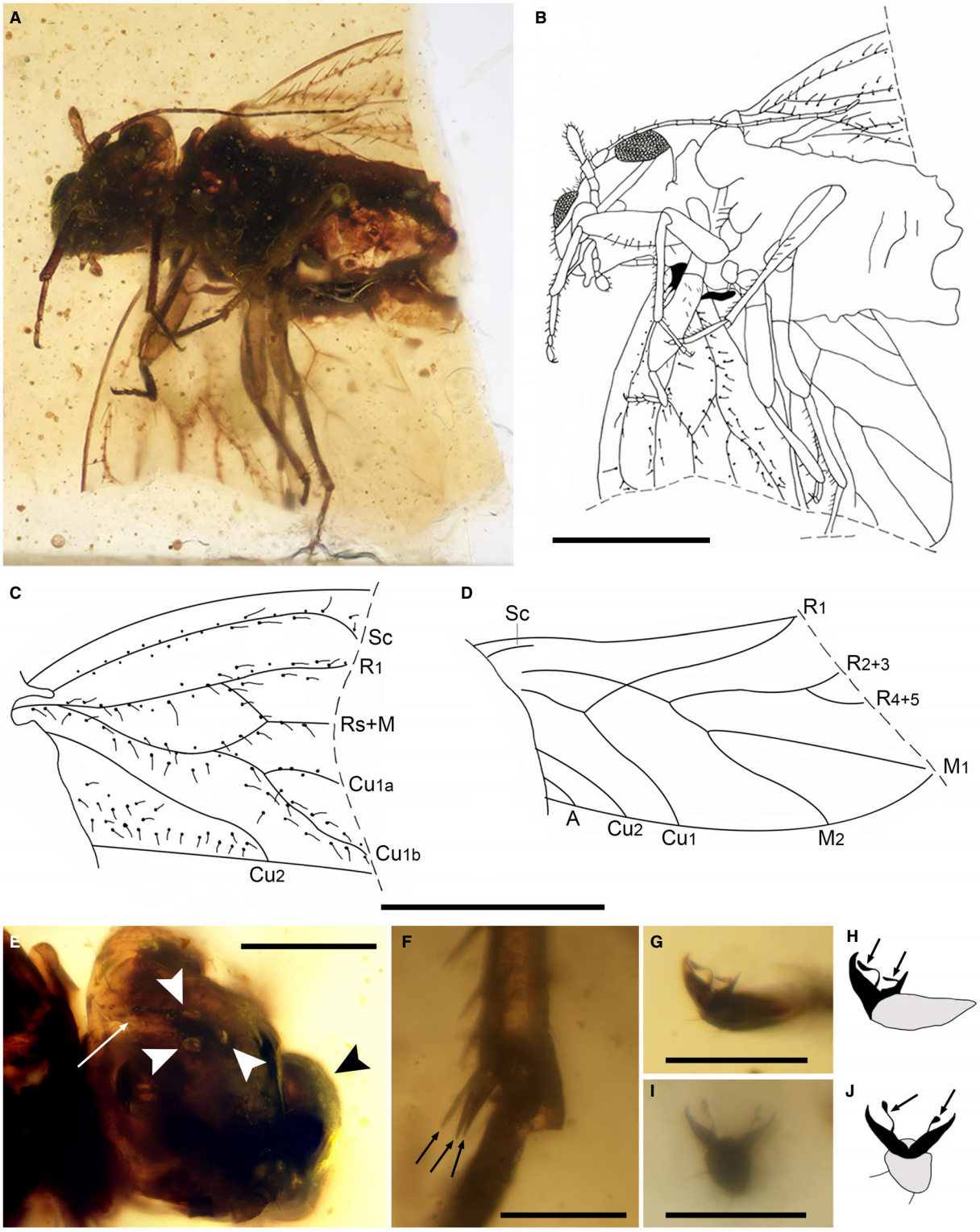

FIG. 9. New studied specimen of *Preempheria antiqua* Baz & Ortuño, 2001*b* (Psocodea, Trogiomorpha, †Empheriidae) from the upper Albian amber of San Just (Teruel Province, Spain), CPT-4117, sex unknown. A–B, photograph and drawing of the habitus. C–D, forewing and hind wing, respectively, both images are at the same scale. E, dorsal view of the head, with the epicranial suture indicated by an arrow, the ocelli indicated by white arrowheads, and the clypeus indicated by a black arrowhead. F, distal part of the tibia of the left hind leg, with the spurs indicated by arrows. G–J, details of the pretarsal claws bearing one pulvillus each, with the pulvilli indicated by arrows, G and H are from the right foreleg, while I and J are from the right midleg. Scale bars represent: 0.5 mm (A–D); 0.2 mm (E); 0.05 mm (F–J).

thorax is obscure and the wings are incomplete, but the legs are completely preserved, except for the distal part of the right hind leg. Forewings hyaline, 0.63 mm wide and with a glabrous margin (Fig. 9C); closely packed linear spicules parallel to the wing margin described by Baz & Ortuño (2001*b*) are clearly visible; setae are visible as rows along both sides of the veins; the basal sector of Sc is long and distally curved and directed towards R_1, although the joining is not preserved; Rs oblique, joining M at 0.58 mm from the wing base; Cu_1 short and dividing into Cu_{1a} and Cu_{1b} at the same level as that of the joining of Rs and M, Cu_{1b} shows a slightly sigmoidal path, areola postica is long; Cu_2 reaches the margin at 0.66 mm from the wing base; anal vein is not present, although the anal region is setose, a row of setae is directed towards Cu_2. Hind wings hyaline, 0.46 mm wide and completely glabrous, without setae (Fig. 9D); Sc short; R_1 showing a slightly sigmoidal path; basi-radial cell three-angled, triangular in shape; Rs and M two-branched; Cu_1, Cu_2 and A all present. Legs covered by fine hairs, thick femora, thin tibiae, and three-segmented tarsi; tibiae with two distal spurs, although three distal spurs can be seen in the tibia of the left hind leg (Fig. 9F); length of tarsomeres from proximal to distal: 0.13 mm, 0.04 mm, 0.05 mm; distal tarsomeres with two pretarsal claws, without a preapical tooth and bearing one pulvillus each that is widened at the tip (Fig. 9G–J). Abdomen is incomplete and genitalia are not preserved.

Remarks. Despite being incomplete the CPT-4117 specimen is assigned to a species. The short and broad head, flagellomeres that are not secondarily annulated, the two-segmented labial palps (with a minute basal segment and a rounded distal segment) and the three-segmented tarsi were used to assign the specimen to Atropetae belonging to Trogiomorpha (Smithers 1972; Mockford 1993). The presence of more than 18 flagellomeres and a sensillum on the second palpomere could not be determined due to preservation. Baz & Ortuño (2001*b*) stated that the following characters defined the †Empheriidae family: wings rounded at the apex, a forewing with a well-developed Sc whose basal sector joins with R, crossvein R_1–Rs, the forking of Cu close to the wing base, a long areola postica, setae arranged along both sides of the veins and a glabrous hind wing. The observable characters in CPT-4117 corresponded to those of †Empheriidae. Furthermore, an important character that differentiates †Empheriidae from †Archaeatropidae is the nodulus corresponding to the joint between Cu_2 and A (Baz & Ortuño 2000), which is absent in †Empheriidae and in CPT-4117. Considering the empheriid species, CPT-4117 belongs to *Preempheria antiqua* based on the preserved characters. The previously described *P. antiqua* specimen from the upper Albian Peñacerrada I amber-bearing outcrop has three distal spurs on the tibiae (Baz & Ortuño 2001*b*), but CPT-4117 has two distal spurs on the tibiae, except for one leg that has three, possibly due to a preservation artefact. Furthermore, the proximal tarsomere of CPT-4117 measures *c.* 0.13 mm, which is different to the length of 0.28 mm observed in the specimens from Peñacerrada I (Baz & Ortuño 2001*b*). These two characters constitute minor differences that would not justify the description of a new species. Although Baz & Ortuño (2001*b*) did not indicate it, the diagnosis of *P. antiqua* is the same as that of the genus *Preempheria*. The genus *Empheropsocus* could be related to *Preempheria* based on the absence of the A vein, which is an apomorphic character for both according to Mockford *et al.* (2013). The presence of a short vein from the basal sector of Sc directed towards the wing margin or to the distal sector of Sc in *Empheropsocus* and its absence in *Preempheria* is a key character for the differentiation of the two genera (Baz & Ortuño 2001*b*). The genus *Burmempheria* resembles *Empheropsocus* in that both show a short vein emerging from the basal sector of Sc. However, Li *et al.* (2020) indicated several additional characters that differentiate them. Therefore, *Empheropsocus* and *Preempheria* may form a subgroup in †Empheriidae that is characterized by the absence of the A vein as a putative synapomorphy (Mockford *et al.* 2013), which would be related to *Burmempheria*. The genus *Jerseyempheria* has a setose forewing margin, the presence of the A vein in the forewing, and a hind wing in which the M_1 and M_2 emerge from different branches of Rs + M, not forking from an M common trunk (Azar *et al.* 2010). Cretaceous empheriids have a forewing with a basal Rs–M vein and a hind wing with a closed cell, differing from Cenozoic empheriids (Mockford *et al.* 2013).

Indeterminate material

Four additional psocodean specimens were studied (Fig. 10), although they lack diagnostic characters to assign them to a group.

AR-1-A-2018.3.2. Wing remains of a psocid specimen (Fig. 10A, B). Antenna and abdomen poorly preserved. Genitalia can be seen in the distal part of the abdomen but they are obscure. Forewings and hind wings overlap, therefore their respective veins cannot be clearly resolved. A long pterostigma bounded by an oblique distal sector of Sc and an R_1 with a curved path seems to be similar to that of some Manicapsocidae (Troctomorpha) specimens.

AR-1-A-2019.42. This specimen is poorly preserved because it has only partial body remains and some blurred veins in wings with poorly defined margins (Fig. 10C, D). It could belong to †Archaeatropidae based on the basal sector of Sc being tentatively directed to R_1, but the latter is not preserved. The assignment to †Archaeatropidae is uncertain.

SJNB2012-12-06. Body 1.38 mm long, poorly preserved (Fig. 10E, F). Left prominent compound eye is visible; the postclypeus is bulging; antennae with at least 11 flagellomeres, hardly differentiable, lacking secondary annulations and covered by long, fine hairs; four-segmented maxillary palpus covered by fine hairs, a sensillum in the second maxillary palpomere seems to be absent. Forewings hyaline, 1.35 mm long and 0.45 mm wide; wing margin and membrane glabrous; a long basal section of Sc is tentatively visible in the left forewing; distal section of Sc might be present in both forewings, emerging from R_1 near the wing margin and forming a triangular pterostigma, although it is unclear whether it is a preservation artefact; the most distal parts of R_1, R_{2+3}, R_{4+5}, M_1, M_2, M_3 and Cu_{1a} are preserved. Hind wings hyaline and glabrous, 1.18 mm long and 0.35 mm wide; basi-radial

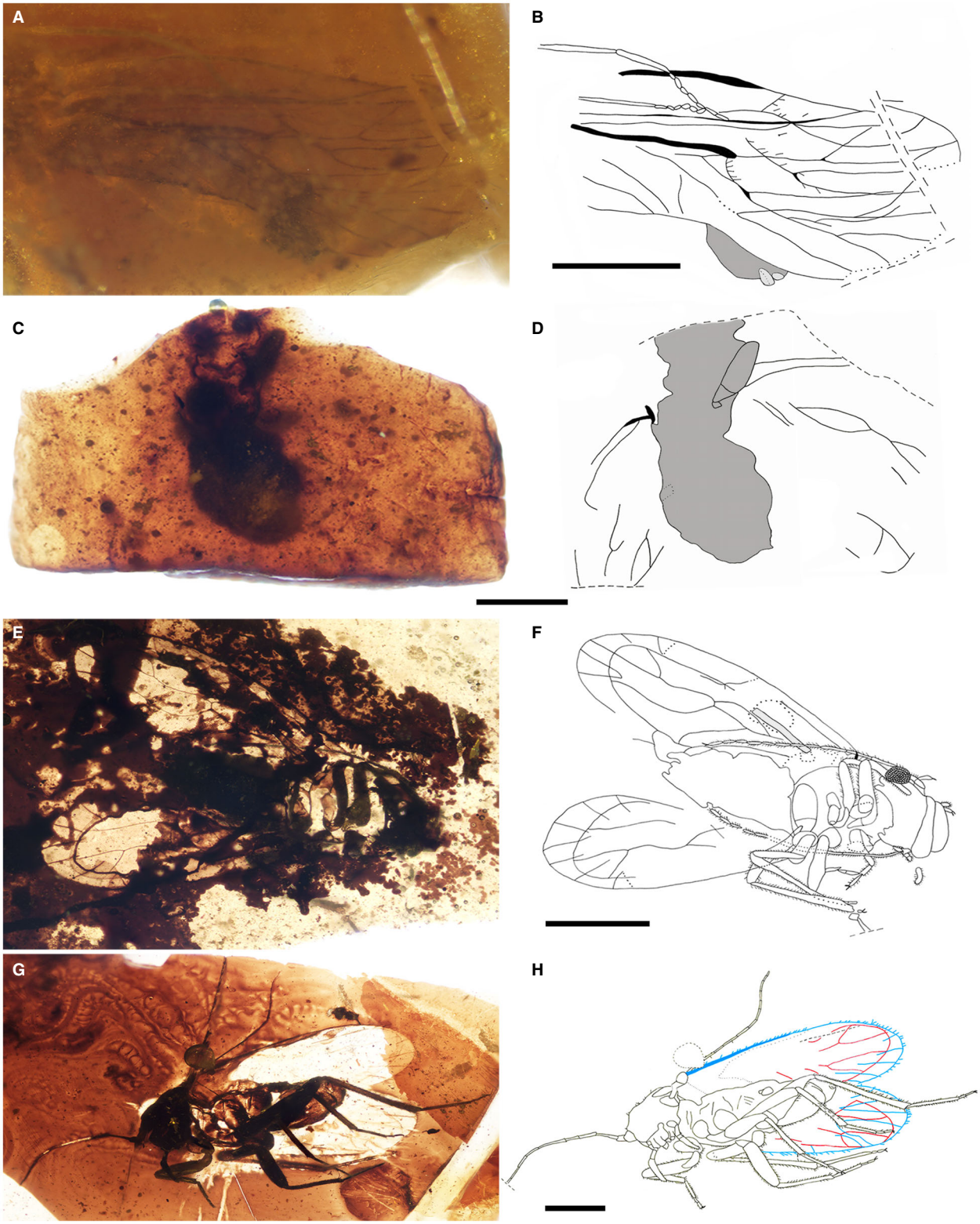

FIG. 10. Habitus of undetermined psocid (Psocodea) specimens from the lower Albian amber of Ariño and the upper Albian amber of San Just (both in Teruel Province, Spain). A–B, specimen AR-1-A-2018.3.2, similar to some Manicapsocidae (Troctomorpha) specimens. C–D, specimen AR-1-A-2019.42 putatively belonging to †Archaeatropidae. E–F, specimen SJNB2012-12-06 in dorsal view. G–H, specimen MAP-7822 in ventral view, with the forewings shown in blue and the hind wings in red. Scale bars represent: 0.5 mm.

cell four-angled; R_1 not visible; Rs two-branched; M not branched, showing a sigmoidal path; Cu_1 curved. Legs with preserved coxae, trochanters, femora, tibiae and tarsi and covered by fine hairs; tibiae with ctenidiobothria and two distal spurs; tarsi three-segmented; distal tarsomere with two pretarsal claws bearing one preapical tooth each. Abdomen obscure, the two external valvulae covered by setae of the female genitalia are visible.

MAP-7822. Body 1.75 mm long (Fig. 10G, H). Head covered by fine hairs; two prominent compound eyes; ocelli not visible; antennae with at least 12 flagellomeres lacking secondary annulations and fine hairs; mouthparts partly visible; maxillary palps four-segmented and covered by fine hairs, length of maxillary palpomeres: I 0.06 mm, II 0.09 mm, III 0.02 mm, IV 0.19 mm, distal maxillary palpomere thick and long and with a pointed apex, a sensillum in second maxillary palpomere seems to be absent. Forewing 1.81 mm long and 0.52 mm wide; forewing margin setose; right forewing might be presenting the distal sections of Sc and R_1; distal sections of R_{2+3}, R_{4+5}, M_1, M_2 and M_3 visible in both forewings. Hind wings hyaline and glabrous, 0.42 mm wide; Rs and M two-branched. Five legs completely preserved, covered by fine hairs; three distal spurs in tibiae (only two visible in some tibiae) and two distal spurs in proximal tarsomeres; tarsi three-segmented; proximal tarsomere with ctenidiobothria; two pretarsal claws with one preapical tooth each. Genitalia poorly preserved.

DISCUSSION

The fossil record of Psocodea from the Iberian Peninsula has been little studied and is represented only in Cretaceous amber and Miocene compression rock to date. Including the new addition described in this paper, the psocid record of Spanish amber consists of six species in five genera from five amber-bearing outcrops along the Basque–Cantabrian Basin and the Maestrazgo Basin. In addition to the new †Archaeatropidae and †Empheriidae specimens, there are several specimens of Trogiomorpha and Troctomorpha in Spanish amber that are currently under investigation (SÁ-P, pers. obs.) The only known compression fossil of a psocid from the Iberian Peninsula corresponds to an isolated forewing assigned to cf. *Mesopsocus* sp. (Psocomorpha: Mesopsocidae) that was found in the Lower Miocene laminated dolostones of the Ribesalbes–Alcora Basin from the La Rinconada outcrop (Peñalver *et al.* 1996). Cretaceous psocids from compression sites are virtually unknown and only a few finds have been reported, for example, two undetermined barklice from the Turonian Orapa site in Botswana (Brothers & Rasnitsyn 2003). Furthermore, some putative psocids from compression sites have been found to belong to closely related groups such as †Permopsocida and †Lophioneurida, as in the case of *Undacypha una* (Jell & Duncan 1986) from the Lower Cretaceous Koonwarra site in Australia that was most recently assigned to Lophioneurida (Ansorge 1996). Interestingly, the different preservation of psocids in amber and compression sites could be influenced by taphonomic bias (Martínez-Delclòs *et al.* 2004). Compression outcrops usually preserve large insect fossils, while amber preserves insects that were a few millimetres in size (Martínez-Delclòs *et al.* 2004). Additionally, the record of insects in compression sites depends on their buoyancy and the presence of predators and scavengers (Martínez-Delclòs *et al.* 2004). A detailed examination of the slabs could eventually increase the known fossil record of psocids, if there were not palaeoenvironmental constraints. Nevertheless, the three-dimensional preservation of insects in amber highlights the possibility of gaining further knowledge on Cretaceous and Cenozoic psocids.

The monophyly of Trogiomorpha is well supported by molecular data and anatomical autapomorphies (Yoshizawa *et al.* 2006; Johnson *et al.* 2018; Yoshizawa & Lienhard 2020). It is considered to be the most basal group within Psocodea because it retains plesiomorphic characters (Smithers 1972; Mockford 1993; Lienhard 1998; De Moya *et al.* 2021). The family †Cormopsocidae has been tentatively included in the suborder Trogiomorpha, although it may be phylogenetically located outside this group, basally to Psocodea, given that the female characters have not been described (Yoshizawa & Lienhard 2020). Despite this, the description of additional cormopsocid specimens supports its inclusion in Trogiomorpha (Hakim *et al.* 2021*b*; Wang *et al.* 2021). The families †Archaeatropidae and †Empheriidae have been placed basally to Atropetae (Yoshizawa & Lienhard 2020), retaining plesiomorphic characters that are also present in †Cormopsocidae and Prionoglarididae, such as the presence of a strongly curved Sc vein that makes contact with R_1 and the crossvein from R_1 to Rs in the forewings. To date, the relationships of Trogiomorpha indicated by Yoshizawa & Lienhard (2020) within Trogiomorpha seem to be plausible and can be summarized as follows: [Cormopsocidae (Prionoglaridetae [Psyllipsocetae (Atropetae)])].

Hagen (*in* Pictet-Baraban & Hagen 1856) described the genus *Empheria* as clearly lacking a nodulus. Kolbe (1883, p. 190) proposed the group 'Empheriini' without a diagnosis, while Kolbe (1884, p. 37) proposed the first diagnosis for the family. Enderlein (1911, p. 285) proposed the diagnosis for †Empheriidae as follows (translation from German), with these two characters possibly crucial in distinguishing between †Empheriidae and †Archaeatropidae: 'no nodulus and an absent maxillary palpus sensillum'. †Archaeatropidae specimens have a sensillum on the second maxillary palpomere, except for the genus *Proprionoglaris* (Perrichot *et al.* 2003). Unfortunately Li *et al.* (2020) indicated nothing about the presence versus absence of this structure in *Burmempheria*. Li *et al.* (2020,

p. 6) minimized the importance of the nodulus for family diagnoses: 'among the recent research, nodulus in forewing is an unstable character (Wang *et al.* 2019)'. However, Wang *et al.* (2019, p. 4) noticed this intrafamilial diversity in the two trogiomorphan families Lepidopsocidae and Psyllipsocidae only. We can add that the most basal trogiomorphan family †Cormopsocidae has no nodulus (Yoshizawa & Lienhard 2020; Hakim *et al.* 2021*b*), while the prionoglaridid genus *Siamoglaris* has one and *Sensitibilla* has none. Thus, the nodulus seems to be an unstable structure among trogiomorphans. Interestingly, despite the absent of the nodulus, an in-flight wing-coupling structure is present in *Cormopsocus groehni*, *Cormopsocus neli* and *Stimulopsocus* in the form of 12–14 separate and almost straight spines (Yoshizawa & Lienhard 2020; Hakim *et al.* 2021*b*; Liang & Liu 2022). The presence or absence of a sensillum on the second maxillary palpomere is more difficult to demonstrate for fossil taxa. For instance, Yoshizawa & Lienhard (2020) and Hakim *et al.* (2021*b*) said nothing about this structure for †Cormopsocidae, although it is clearly absent in *Cormopsocus baleoi* and *Stimulopsocus* (Hakim *et al.* 2021*c*; Liang & Liu 2022), while a sensillum on the fourth maxillary palpomere is present in *Longiglabellus* (Wang *et al.* 2021). As a result, the boundaries between †Archaeatropidae and †Empheriidae remain vague. †Archaeatropidae may be a junior synonym of †Empheriidae (Li *et al.* 2020). However, only a phylogenetic analysis including both extant and fossil taxa as well as morphological and molecular characters will help to solve this problem.

Today, the most diverse psocid suborder (excluding parasitic lice) is Psocomorpha, comprising 63% of psocid species, while Troctomorpha and Trogiomorpha contain 31% and 6% of psocid species, respectively (Yoshizawa *et al.* 2006; Zhang 2011; Yoshizawa & Johnson 2014) (Fig. 11A). Interestingly, current information about Cretaceous psocids shows the following relative diversity of the species for each suborder: 6%, Psocomorpha; 33%, Troctomorpha; and 61%, Trogiomorpha (Álvarez-Parra *et al.* 2020*a*, table 1; plus the new additions) (Fig. 11B). This different diversity might be explained by palaeobiological or evolutionary constraints. Furthermore, Trogiomorpha had a global distribution during the Cretaceous, while Psocomorpha has been found only in Eurasia (Fig. 11C) from French, Burmese and Taimyr ambers (Vishniakova 1975; Azar *et al.* 2015; Yoshizawa & Yamamoto 2021). Given that Trogiomorpha is the most basal suborder in Psocodea (De Moya *et al.* 2021), a preliminary diversification of this group during the Cretaceous could have occurred, which is supported by the fossil record (Fig. 11B). Later, the diversification of Psocomorpha probably occurred during the Cenozoic. Although some trogiomorphan species are cosmopolitan, most usually live in marginal habitats, such as ground litter in forests, caves and domestic environments (New 1987; Baz & Ortuño 2000). Therefore, the extant representatives may represent a relict group that evolved from generalist taxa into dwellers of marginal habitats to avoid competing with the more modern psocomorphans. This hypothesis was also stated by Thornton (1962) for cave barklice (Psyllipsocidae). Psyllipsocids are interesting because they include the only known extant psocid genus dating back to the Cretaceous (Álvarez-Parra *et al.* 2020*a*; Jouault *et al.* 2021; Liang & Liu 2021), showing a high grade of evolutionary stasis or bradytely that is typical of inhabitants of marginal environments (Peris & Háva 2016; Sánchez-García & Engel 2017; Arillo *et al.* 2022). †Cormopsocidae, †Archaeatropidae and †Empheriidae could have been generalists given their high diversity during the Cretaceous, but they probably began to decrease in abundance or became extinct when psocomorphans thrived due to niche competition. Troctomorphans have a similar relative diversity today as they did during the Cretaceous (Fig. 11A, B).

Taxonomic determination of fossil psocid immatures is challenging because the diagnostic characters are based on winged adult specimens (Kiesmüller *et al.* 2021). Furthermore, psocid nymphs are poorly known in the fossil record to date. However, the outstanding preservation of SJNB2012-12-02 enabled us to assign the specimen to †Archaeatropidae. It provides insights into the growth of psocid nymphs and the development of the wings, which are visible in the specimen. Kiesmüller *et al.* (2021) and Xu *et al.* (2022) described a debris-carrying behaviour in psocid nymphs from Burmese amber. This type of behaviour is also observed in extant immatures from diverse psocid families and has been linked to camouflage (Kiesmüller *et al.* 2021). The debris-carrying larval habit has also been reported in Cretaceous specimens of other insect groups (Pérez-de la Fuente *et al.* 2012, 2018). Therefore, it is assumed that psocid nymphs, inhabiting the ground litter or tree bark, developed this defensive strategy in response to predatory pressure (Kiesmüller *et al.* 2021). There is no evidence of debris-carrying behaviour in SJNB2012-12-02, suggesting three hypotheses: (1) debris-carrying behaviour and the related camouflage in psocids were restricted to the Burmese amber palaeoenvironment or were not globally distributed; (2) debris-carrying behaviour was not widely distributed phylogenetically in psocids; or (3) the lack of debris-carrying behaviour in SJNB2012-12-02 can be explained by a finding bias and it is also probable that it was present worldwide during the Cretaceous. Hypothesis 1 is plausible because psocid nymphs from French and Taimyr ambers do not show debris-carrying behaviour (Vishniakova 1975; Azar *et al.* 2015). Hypothesis 2 is also plausible. The diverse morphologies of psocid nymphs showing debris-carrying behaviour suggest that this could have

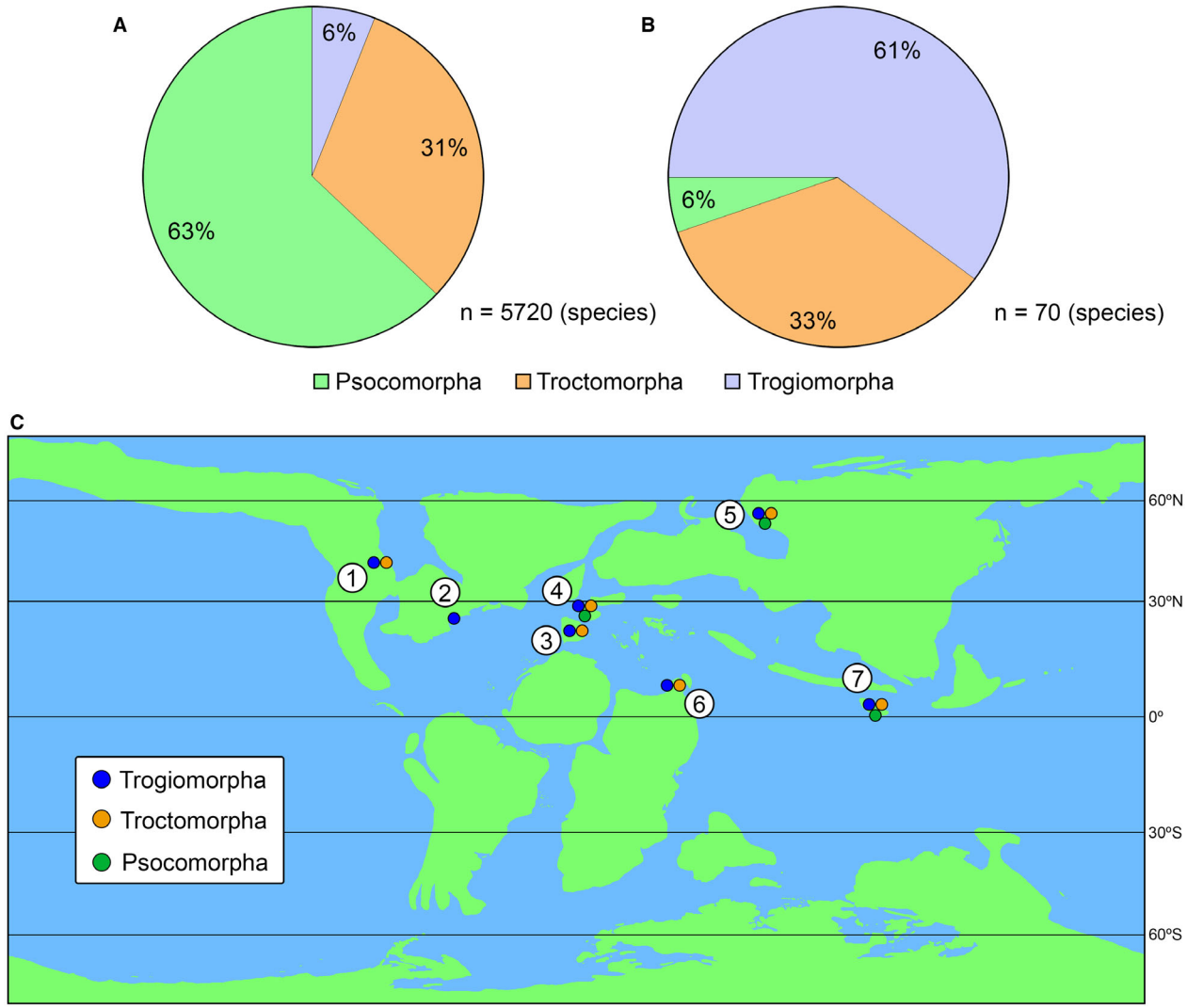

FIG. 11. Past and recent diversity and global palaeodistribution of the psocid (Psocodea) suborders. A–B, relative diversity of each of the psocid suborders today (A) and during the Cretaceous (B). C, Late Cretaceous global palaeogeographical reconstruction showing the presence of the described species of each psocid suborder in the amber sites: 1, Canadian amber (Cedar Lake and Pipestone Creek; Campanian); 2, Raritan amber (Sayreville; Turonian); 3, Spanish amber (Ariño, Arroyo de la Pascueta, El Soplao, Peñacerrada I and San Just; Albian); 4, French amber (Archingeay-Les Nouillers and La Garnache; Albian–Santonian); 5, Taimyr amber (Nizhnyaya Agapa, Timmerdyakh-Khaya and Yantardakh; Cenomanian–Santonian); 6, Lebanese amber (Bcharreh, Falougha, Hammana-Mdeyrij and Jezzine; Barremian); 7, Burmese amber (Hkamti and Tanai; Albian–Cenomanian). Undescribed psocids have been identified in Aptian Congolese amber (Bouju & Perrichot 2020) and Campanian Tilin (Myanmar) amber (Zheng *et al.* 2018). Parasitic lice (Phthiraptera) are excluded in A. Data for A and B were obtained from Yoshizawa *et al.* (2006), Zhang (2011), Yoshizawa & Johnson (2014) and Álvarez-Parra *et al.* (2020*a*), with the addition of the new species. Map modified from Scotese (2001).

been present in several families (Kiesmüller *et al.* 2021), but the family of the studied nymph (†Archaeatropidae) might not have shown this type of behaviour. Hypothesis 3, involving a finding bias, cannot be discarded either. It is possible that this behaviour was determined by both phylogenetical restrictions and environmental conditions.

CONCLUSION

Psocids were a widely distributed and diverse group of insects during the Cretaceous. The suborder Trogiomorpha comprises most of the described species from this period to date. The new specimens studied in this paper provide interesting data about the distribution

of the previously known species on the Iberia Island, as well as additional anatomical information and details about the development and growth of immature psocids based on the discovery of a well-preserved psocid nymph. A new species belonging to †Archaeatropidae is described and assigned to a genus previously known to occur only in northern Gondwana. Trogiomorpha is the most basal suborder within Psocodea. The phylogenetic placement of the extinct families †Archaeatropidae and †Empheriidae seems to be basal to the rest of the families within the infraorder Atropetae, although a phylogenetic analysis is needed to better understand their relationships with the other families. Furthermore, †Archaeatropidae could be a junior synonym of †Empheriidae based on recent findings. Trogiomorpha was the most diverse psocid suborder during the Cretaceous, unlike today when it is less diverse. Therefore, it is possible that the diversification of this basal group occurred during the Cretaceous, before the diversification of psocomorphans. Psocomorphans could have ecologically competed with trogiomorphans, relegating the latter to marginal habitats. It is also possible that palaeoenvironmental conditions could explain the different diversities of these groups. The study of Cenozoic psocids would provide interesting information about the evolutionary trends and niche competition in the history of Psocodea. Psocid nymphs showed debris-carrying behaviour, at least in the Burmese amber palaeoenvironment, although it is possible that this type of behaviour was not widely distributed, geographically or phylogenetically, among psocid immatures. This topic might be traced only in the amber record with further investigations.

Acknowledgements. We thank the participants in the palaeontological excavations in Peñacerrada I, Arroyo de la Pascueta, San Just, El Soplao and Ariño. We are grateful for the collaboration with the SAMCA Group and the Fundación Conjunto Paleontológico de Teruel-Dinópolis during our work in the Ariño outcrop. We thank the Consejería de Cultura, Turismo y Deporte del Gobierno de Cantabria (Spain) and the Dirección General de Patrimonio Cultural del Gobierno de Aragón (Spain) for giving us permission to excavate in the amber-bearing outcrops. We also thank the Museo de Ciencias Naturales de Álava, the Colección Institucional del Laboratorio de la Cueva El Soplao, and the Museo Aragonés de Paleontología for loaning their specimens. This work is part of the collaboration agreement between the Universitat de Barcelona and the public company El Soplao S.L. We are indebted to Rafael López del Valle, who prepared the amber pieces with the bioinclusions. We are very grateful for the useful and valuable comments of three anonymous reviewers and the editors Conrad C. Labandeira and Sally Thomas. This study is a contribution to the project CRE CGL2017-84419 funded by the Spanish AEI/FEDER and the EU. SÁ-P is a beneficiary of a grant from the Secretaria d'Universitats i Recerca de la Generalitat de Catalunya (Spain) and the European Social Fund (2020FI_B1 00002).

Author contributions. **Conceptualization** Sergio Álvarez-Parra; **Funding acquisition** Xavier Delclòs; **Investigation** Sergio Álvarez-Parra, Enrique Peñalver, André Nel, Xavier Delclòs; **Methodology** Sergio Álvarez-Parra; **Project administration** Xavier Delclòs; **Supervision** Enrique Peñalver, Xavier Delclòs; **Writing – original draft preparation** Sergio Álvarez-Parra; **Writing – review & editing** Sergio Álvarez-Parra, Enrique Peñalver, André Nel, Xavier Delclòs.

DATA ARCHIVING STATEMENT

This published work and the nomenclatural act it contains, have been registered in ZooBank: http://zoobank.org/References/0ABCDC39-0D0F-4268-A53E-1D97D328DE89

Editor. Conrad Labandeira

REFERENCES

ALCALÁ, L., ESPÍLEZ, E., MAMPEL, L., KIRKLAND, J. I., ORTIGA, M., RUBIO, D., GONZÁLEZ, A., AYALA, D., COBOS, A., ROYO-TORRES, R., GASCÓ, F. and PESQUERO, M. D. 2012. A new Lower Cretaceous vertebrate bonebed near Ariño (Teruel, Aragón, Spain); found and managed in a joint collaboration between a mining company and a palaeontological park. *Geoheritage*, **4**, 275–286.

ÁLVAREZ-PARRA, S., PEÑALVER, E., NEL, A. and DELCLÒS, X. 2020*a*. The oldest representative of the extant barklice genus *Psyllipsocus* (Psocodea: Trogiomorpha: Psyllipsocidae) from the Cenomanian amber of Myanmar. *Cretaceous Research*, **113**, 104480.

ÁLVAREZ-PARRA, S., DELCLÒS, X., SOLÓRZANO-KRAEMER, M. M., ALCALÁ, L. and PEÑALVER, E. 2020*b*. Cretaceous amniote integuments recorded through a taphonomic process unique to resins. *Scientific Reports*, **10**, 19840.

ÁLVAREZ-PARRA, S., PÉREZ-DE LA FUENTE, R., PEÑALVER, E., BARRÓN, E., ALCALÁ, L., PÉREZ-CANO, J., MARTÍN-CLOSAS, C., TRABELSI, K., MELÉNDEZ, N., LÓPEZ DEL VALLE, R., LOZANO, R. P., PERIS, D., RODRIGO, A., SARTO I MONTEYS, V., BUENO-CEBOLLADA, C. A., MENOR-SALVÁN, C., PHILIPPE, M., SÁNCHEZ-GARCÍA, A., PEÑA-KAIRATH, C., ARILLO, A., ESPÍLEZ, E., MAMPEL, L. and DELCLÒS, X. 2021. Dinosaur bonebed amber from an original swamp forest soil. *eLife*, **10**, e72477.

ANSORGE, J. 1996. Insekten aus dem oberen Lias von Grimmen (Vorpommern, Norddeutschland). *Neue Paläontologische Abhandlungen*, **2**, 1–132.

ARILLO, A., SUBÍAS, L. S. and ÁLVAREZ-PARRA, S. 2022. First fossil record of the oribatid family Liacaridae (Acariformes: Gustavioidea) from the lower Albian amber-

bearing site of Ariño (eastern Spain). *Cretaceous Research*, **131**, 105087.

AZAR, D. and NEL, A. 2004. Four new Psocoptera from Lebanese amber (Insecta: Psocomorpha: Trogiomorpha). *Annales de la Société Entomologique de France*, **40**, 185–192.

AZAR, D. and NEL, A. 2011. The oldest psyllipsocid booklice, in Lower Cretaceous amber from Lebanon (Psocodea, Trogiomorpha, Psocathropetae, Psyllipsocidae). *ZooKeys*, **130**, 153–165.

AZAR, D., NEL, A. and PETRULEVIČIUS, J. F. 2010. First psocodean (Psocodea, Empheriidae) from the Cretaceous amber of New Jersey. *Acta Geologica Sinica-English Edition*, **84**, 762–767.

AZAR, D., NEL, A. and PERRICHOT, V. 2015. Diverse barklice (Psocodea) from Late Cretaceous Vendean amber. *Paleontological Contributions*, **2014** (10C), 9–16.

AZAR, D., HUANG, D., EL-HAJJ, L., CAI, C., NEL, A. and MAKSOUD, S. 2017. New Prionoglarididae from Burmese amber (Psocodea: Trogiomorpha: Prionoglaridetae). *Cretaceous Research*, **75**, 146–156.

AZAR, D., MAKSOUD, S., NAMMOUR, C., NEL, A. and WANG, B. 2018. A new trogiid genus from lower Eocene Fushun amber (Insecta: Psocodea: Trogiomorpha). *Geobios*, **51**, 101–106.

BARRÓN, E., PEYROT, D., RODRÍGUEZ-LÓPEZ, J. P., MELÉNDEZ, N., LÓPEZ DEL VALLE, R., NAJARRO, M., ROSALES, I. and COMAS-RENGIFO, M. J. 2015. Palynology of Aptian and upper Albian (Lower Cretaceous) amber-bearing outcrops of the southern margin of the Basque-Cantabrian basin (northern Spain). *Cretaceous Research*, **52**, 292–312.

BAZ, A. and ORTUÑO, V. M. 2000. Archaeatropidae, a new family of Psocoptera from the Cretaceous amber of Alava, Northern Spain. *Annals of the Entomological Society of America*, **93**, 367–373.

BAZ, A. and ORTUÑO, V. M. 2001*a*. A new electrentomoid psocid (Psocoptera) from the Cretaceous amber of Alava (Northern Spain). *Deutsche Entomologische Zeitschrift*, **48**, 27–32.

BAZ, A. and ORTUÑO, V. M. 2001*b*. New genera and species of empheriids (Psocoptera: Empheriidae) from the Cretaceous amber of Alava, northern Spain. *Cretaceous Research*, **22**, 575–584.

BROTHERS, D. J. and RASNITSYN, A. P. 2003. Diversity of Hymenoptera and other insects in the Late Cretaceous (Turonian) deposits at Orapa, Botswana: a preliminary review. *African Entomology*, **11**, 221–226.

BOUJU, V. and PERRICHOT, V. 2020. A review of amber and copal occurrences in Africa and their paleontological significance. *BSGF – Earth Sciences Bulletin*, **191**, 17.

COCKERELL, T. D. A. 1919. Insects in Burmese amber. *The Entomologist*, **52**, 241–243.

COCKX, P., McKELLAR, R., TAPPERT, R., VAVREK, M. and MUEHLENBACHS, K. 2020. Bonebed amber as a new source of paleontological data: the case of the Pipestone Creek deposit (Upper cretaceous), Alberta, Canada. *Gondwana Research*, **81**, 378–389.

CORRAL, J. C., LÓPEZ DEL VALLE, R. and ALONSO, J. 1999. El ámbar cretácico de Álava (Cuenca Vasco-Cantábrica, norte de España). Su colecta y preparación. *Estudios del Museo de Ciencias Naturales de Álava*, **14** (2), 7–21.

CUMMING, R. T. and LE TIRANT, S. 2021. Review of the Cretaceous †Archaeatropidae and †Empheriidae and description of a new genus and species from Burmese amber (Psocoptera). *Faunitaxys*, **9** (16), 1–11.

DE MOYA, R. S., YOSHIZAWA, K., WALDEN, K. K., SWEET, A. D., DIETRICH, C. H. and KEVIN, P. J. 2021. Phylogenomics of parasitic and nonparasitic lice (Insecta: Psocodea): combining sequence data and exploring compositional bias solutions in next generation data sets. *Systematic Biology*, **70**, 719–738.

DELCLÒS, X., PEÑALVER, E., RANAIVOSOA, V. and SOLÓRZANO-KRAEMER, M. M. 2020. Unravelling the mystery of "Madagascar copal": age, origin and preservation of a Recent resin. *PLoS One*, **15** (5), e0232623.

ENDERLEIN, G. 1911. Die Fossilen Copeognathen und ihre Phylogenie. *Palaeontographica*, **58**, 279–360.

GOMEZ, B., MARTÍN-CLOSAS, C., BARALE, G. and THÉVENARD, F. 2000. A new species of *Nehvizdya* (Ginkgoales) from the Lower Cretaceous of the Iberian Ranges (Spain). *Review of Palaeobotany & Palynology*, **111**, 49–70.

HAGEN, H. 1865. On some aberrant genera of Psocina. *The Entomologist's Monthly Magazine*, **2**, 148–152.

HAGEN, H. 1866. Psocinorum et Embidonorum synopsis synonymica. *Verhandlungen Zoologische-Botanische Gesellschaft Wien*, **16**, 1–22.

HAGEN, H. 1882. Beitrage zur Monographie der Psociden. Über Psociden in Berstein. *Stettiner Entomologische Zeitung*, **43**, 217–237.

HAKIM, M., AZAR, S., MAKSOUD, S., HUANG, D.-Y. and AZAR, D. 2018*a*. New polymorphic psyllipsocids from Burmese amber (Psocodea: Psyllipsocidae). *Cretaceous Research*, **84**, 389–400.

HAKIM, M., HUANG, D.-Y. and AZAR, D. 2018*b*. First lepidopsocid from the mid Miocene Dominican amber (Psocodea: Trogiomorpha: Lepidopsocidae). *Palaeoentomology*, **1**, 58–64.

HAKIM, M., HUANG, D.-Y. and AZAR, D. 2021*a*. New fossil psocids from Cretaceous Siberian ambers (Psocodea: Trogiomorpha: Atropetae). *Palaeoentomology*, **4**, 186–198.

HAKIM, M., AZAR, D., FU, Y.-Z., CAI, C.-Y. and HUANG, D.-Y. 2021*b*. A new cormopsocid from mid-Cretaceous Burmese amber (Psocodea: Trogiomorpha: Cormopsocidae). *Palaeoentomology*, **4**, 178–185.

HAKIM, M., AZAR, D. and HUANG, D.-Y. 2021*c*. A new species of Cormopsocidae from Burmese amber (Psocodea; Trogiomorpha). *Palaeoentomology*, **4**, 213–217.

HAKIM, M., HUANG, D.-Y. and AZAR, D. 2022. Earliest record of Prionoglarididae from the Lower Cretaceous Lebanese amber (Psocodea; Trogiomorpha). *Cretaceous Research*, **132**, 105121.

HENNIG, W. 1966. *Phylogenetic systematics*. University of Illinois Press, 263 pp.

JELL, P. A. and DUNCAN, P. M. 1986. Invertebrates, mainly insects, from the freshwater, lower Cretaceous, Koonwarra fossil bed (Korumburra Group), south Gippsland, Victoria. *Memoirs of the Association of Australasian Palaeontologists*, **3**, 111–205.

JOHNSON, K. P., DIETRICH, C. H., FRIEDRICH, F., BEUTEL, R. G., WIPFLER, B., PETERS, R. S., ALLEN, J. M., PETERSEN, M., DONATH, A., WALDEN, K. K. O., KOZLOV, A. M., PODSIADLOWSKI, L., MAYER, C., MEUSEMANN, K., VASILIKOPOULOS, A., WATERHOUSE, R. M., CAMERON, S. L., WEIRAUCH, C., SWANSON, D. R., PERCY, D. M., HARDY, N. B., TERRY, I., LIU, S., ZHOU, X., MISOF, B., ROBERTSON, H. M. and YOSHIZAWA, K. 2018. Phylogenomics and the evolution of hemipteroid insects. *Proceedings of the National Academy of Sciences of the United States of America*, **115**, 12775–12780.

JOUAULT, C., YOSHIZAWA, K., HAKIM, M., HUANG, D. and NEL, A. 2021. New psocids (Psocodea: Prionoglaridídae, Psyllipsocidae) from Cretaceous Burmese amber deposits. *Cretaceous Research*, **126**, 104890.

KIESMÜLLER, C., HAUG, J. T., MÜLLER, P. and HÖRNIG, M. K. 2021. Debris-carrying behaviour of bark lice immatures preserved in 100 million years old amber. *PalZ*, 1–28. https://doi.org/https://doi.org/10.1007/s12542-021-00567-6

KOLBE, H. J. 1883. Neue Beiträge zur Kenntnis der Psociden der Bernstein-Fauna. *Stettiner Entomologische Zeitung*, **44**, 186–191.

KOLBE, H. J. 1884. Der Entwickelungsgang der Psociden im Individuum und in der Zeit. *Berliner Entomologische Zeitschrift*, **28**, 35–38.

LI, S., WANG, Q., REN, D. and YAO, Y. 2020. New genus and species of Empheriidae (Psocodea: Trogiomorpha) from mid-Cretaceous amber of northern Myanmar. *Cretaceous Research*, **110**, 104421.

LIANG, F. and LIU, X. 2021. A new species of *Psyllipsocus* (Psocodea: Trogiomorpha: Psyllipsocidae) from the mid-Cretaceous amber of Myanmar. *Zootaxa*, **5072**, 81–87.

LIANG, F. and LIU, X. 2022. A new genus and species of the family Cormopsocidae (Psocodea: Trogiomorpha) from mid-Cretaceous amber of Myanmar. *Cretaceous Research*, **130**, 105049.

LIENHARD, C. 1998. *Psocoptères Euro-Méditerranéens*. Fédération Française des Sociétés de Sciences Naturelles, Faune de France 83, 533 pp.

LIENHARD, C. 2000. A new genus of Prionoglaridídae from a Namibian cave (Insecta: Psocoptera). *Revue Suisse de Zoologie*, **107**, 871–882.

LIENHARD, C. 2004. *Siamoglaris zebrina* gen. n., sp. n., the first representative of Prionoglaridídae from the Oriental region (Insecta: Psocoptera). *Revue Suisse de Zoologie*, **111**, 865–875.

LIENHARD, C. and FERREIRA, R. L. 2013. A new species of *Neotrogla* from Brazilian caves (Psocodea: 'Psocoptera': Prionoglaridídae). *Revue Suisse de Zoologie*, **120**, 3–12.

LIENHARD, C. and FERREIRA, R. L. 2015. Review of Brazilian cave psocids of the families Psyllipsocidae and Prionoglaridídae (Psocodea: 'Psocoptera': Trogiomorpha) with a key to the South American species of these families. *Revue Suisse de Zoologie*, **122**, 121–142.

LIENHARD, C., FERREIRA, R. L., GNOS, E., HOLLIER, J., EGGENBERGER, U. and PIUZ, A. 2012. Microcrystals coating the wing membranes of a living insect (Psocoptera: Psyllipsocidae) from a Brazilian cave. *Scientific Reports*, **2**, 408.

MARTÍN-CHIVELET, J., BERASTEGUI, X., ROSALES, I., VILAS, L., VERA, T. A., CAUS, E., GRAFE, K.-U., MAS, R., PUIG, C., SEGURA, M., ROBLES, S., FLOQUET, M., QUESADA, S., RUIZ-ORTÍZ, P. A., FREGENAL-MARTÍNEZ, M. A., SALAS, R., ARIAS, C., GARCÍA, A., MARTÍN-ALGARRA, A., MELÉNDEZ, M. N., CHACÓN, B., MOLINA, J. M., SANZ, J. L., CASTRO, J. M., GARCÍA-HERNÁNDEZ, M., CARENAS, B., GARCÍA-HIDALGO, J. F., GIL, J. and ORTEGA, F. 2002. Chapter 12. Cretaceous. 255–292. *In* GIBBONS, W. and MORENO, M. T. (eds) *The geology of Spain*. Geological Society, London, 649 pp.

MARTÍNEZ-DELCLÒS, X., BRIGGS, D. E. and PEÑALVER, E. 2004. Taphonomy of insects in carbonates and amber. *Palaeogeography, Palaeoclimatology, Palaeoecology*, **203**, 19–64.

MARTÍNEZ-TORRES, L. M., PUJALTE, V. and ROBLES, S. 2003. Los yacimientos de ámbar del Cretácico inferior de Montoria-Peñacerrada (Álava, Cuenca Vasco-Cantábrica): estratigrafía, reconstrucción paleogeográfica y estructura tectónica. *Estudios del Museo de Ciencias Naturales de Alava*, **18** (sp. vol. 2), 9–32.

MOCKFORD, E. L. 1969. Fossil insects of the order Psocoptera from Tertiary amber of Chiapas, Mexico. *Journal of Paleontology*, **43**, 1267–1273.

MOCKFORD, E. L. 1993. *North American Psocoptera (Insecta)*. Sandhill Crane Press, Flora & Fauna Handbook, **10**, 455 pp.

MOCKFORD, E. L., LIENHARD, C. and YOSHIZAWA, K. 2013. Revised classification of 'Psocoptera' from Cretaceous amber, a reassessment of published information. *Insecta Matsumurana New series*, **69**, 1–26.

NAJARRO, M., PEÑALVER, E., ROSALES, I., PÉREZ-DE LA FUENTE, R., DAVIERO-GÓMEZ, V., GÓMEZ, B. and DECLÓS, X. 2009. Unusual concentration of Early Albian arthropod-bearing amber in the Basque-Cantabrian Basin (El Soplao, Cantabria, Northern Spain): palaeoenvironmental and palaeobiological implications. *Geologica Acta*, **7**, 363–388.

NEL, A., PROKOP, J., DE PLOËG, G. and MILLET, J. 2005. New Psocoptera (Insecta) from the lowermost Eocene amber of Oise, France. *Journal of Systematic Palaeontology*, **3**, 371–391.

NEL, A., ROQUES, P., NEL, P., PROKIN, A. A., BOURGOIN, T., PROKOP, J., SZWEDO, J., AZAR, D., DESUTTER-GRANDCOLAS, L., WAPPLER, T., GARROUSTE, R., COTY, D., HUANG, D., ENGEL, M. S. and KIREJTSHUK, A. G. 2013. The earliest known holometabolous insects. *Nature*, **503** (7475), 257–261.

NEW, T. R. 1987. Biology of the Psocoptera. *Oriental Insects*, **21**, 1–109.

PEARMAN, J. V. 1936. The taxonomy of the Psocoptera: preliminary sketch. *Proceedings of the Royal Entomological Society of London B*, **5**, 58–62.

PEÑALVER, E. and MARTÍNEZ-DELCLÒS, X. 2002. Importancia patrimonial de Arroyo de la Pascueta, un yacimiento de ámbar cretácico con insectos fósiles en Rubielos de Mora. 201–208. *In* MELÉNDEZ, G. and PEÑALVER, E. (eds) *El patrimonio paleontológico de Teruel*. Instituto de Estudios Turolenses, 447 pp.

PEÑALVER, E., NEL, A. and MARTÍNEZ-DELCLÒS, X. 1996. Insectos del Mioceno inferior de Ribesalbes (Castellón, España). Paleoptera y Neoptera poli- y paraneoptera. *Treballs del Museu de Geologia de Barcelona*, **5**, 15–95.

PEÑALVER, E., DELCLÒS, X. and SORIANO, C. 2007. A new rich amber outcrop with palaeobiological inclusions in the Lower Cretaceous of Spain. *Cretaceous Research*, **28**, 791–802.

PÉREZ-DE LA FUENTE, R., DELCLÒS, X., PEÑALVER, E., SPERANZA, M., WIERZCHOS, J., ASCASO, C. and ENGEL, M. S. 2012. Early evolution and ecology of camouflage in insects. *Proceedings of the National Academy of Sciences of the United States of America*, **109**, 21414–21419.

PÉREZ-DE LA FUENTE, R., PEÑALVER, E., AZAR, D. and ENGEL, M. S. 2018. A soil-carrying lacewing larva in Early Cretaceous Lebanese amber. *Scientific Reports*, **8**, 16663.

PERIS, D. and HÁVA, J. 2016. New species from Late Cretaceous New Jersey amber and stasis in subfamily Attageninae (Insecta: Coleoptera: Dermestidae). *Journal of Paleontology*, **90**, 491–498.

PERRICHOT, V., AZAR, D., NÉRAUDEAU, D. and NEL, A. 2003. New Psocoptera in the Early Cretaceous amber of SW France and Lebanon (Insecta: Psocoptera: Trogiomorpha). *Geological Magazine*, **140**, 669–683.

PICTET-BARABAN, F. and HAGEN, H. 1856. Die im Berstein befindlichen Neuropteren der Vorwelt. 57–64. *In* BERENDT, G. C. (ed.) *Die in Bernstein Befindlichen Organischen Reste der Vorwelt Gesammelt in Verbindung mit Mehreren Bearbeitetet und Herausgegeben*. Commission der Nicolaischen Buchhandlung, 434 pp.

POINAR, G. and VEGA, F. E. 2020. Entomopathogenic fungi (Hypocreales: Ophiocordycipitaceae) infecting bark lice (Psocoptera) in Dominican and Baltic amber. *Mycology*, **11**, 71–77.

ROESLER, R. 1940. Neue und wenig bekannte Copeognathengattungen. I. *Zoologischer Anzeiger*, **129**, 225–243.

SÁNCHEZ-GARCÍA, A. and ENGEL, M. S. 2017. Long-term stasis in a diverse fauna of Early Cretaceous springtails (Collembola: Symphypleona). *Journal of Systematic Palaeontology*, **15**, 513–537.

SCOTESE, C. R. 2001. *Atlas of Earth history, volume 1, paleogeography*. PALEOMAP Project, Arlington, Texas, 52 pp.

SMITHERS, C. N. 1972. The classification and phylogeny of the Psocoptera. *Australian Museum Memoir*, **14**, 1–349.

SMITHERS, C. N. 1990. Keys to the family and genera of Psocoptera (Arthropoda: Insecta). *Technical Reports of the Australian Museum*, **2**, 1–82.

SOLÓRZANO-KRAEMER, M. M., DELCLÒS, X., ENGEL, M. S. and PEÑALVER, E. 2020. A revised definition for copal and its significance for palaeontological and Anthropocene biodiversity-loss studies. *Scientific Reports*, **10**, 19904.

THORNTON, I. W. 1962. Psocids (Psocoptera) from the Batu Caves, Malaya. *Pacific Insects*, **4**, 441–455.

TIBERT, N. E., COLIN, J. P., KIRKLAND, J. I., ALCALÁ, L. and MARTÍN-CLOSAS, C. 2013. Lower Cretaceous nonmarine ostracodes from an Escucha Formation dinosaur bonebed in eastern Spain. *Micropaleontology*, **59**, 83–91.

VILLANUEVA-AMADOZ, U., PONS, D., DIEZ, J. B., FERRER, J. and SENDER, L. M. 2010. Angiosperm pollen grains of San Just site (Escucha Formation) from the Albian of the Iberian Range (north-eastern Spain). *Review of Palaeobotany & Palynology*, **162**, 362–381.

VILLANUEVA-AMADOZ, U., SENDER, L. M., ALCALÁ, L., PONS, D., ROYO-TORRES, R. and DIEZ, J. B. 2015. Paleoenvironmental reconstruction of an Albian plant community from the Ariño bonebed layer (Iberian Chain, NE Spain). *Historical Biology*, **27**, 430–441.

VISHNIAKOVA, V. N. 1975. Psocoptera in Late-Cretaceous insect-bearing resins from the Taimyr. *Entomological Review*, **54**, 63–75.

WANG, R., LI, S., REN, D. and YAO, Y. 2019. New genus and species of the Psyllipsocidae (Psocodea: Trogiomorpha) from mid-Cretaceous Burmese amber. *Cretaceous Research*, **104**, 104178.

WANG, Q., LI, S., REN, D. and YAO, Y. 2021. New genus and species of †Cormopsocidae (Psocodae: Trogiomorpha) from mid-Cretaceous amber of northern Myanmar. *Cretaceous Research*, **128**, 104992.

XU, C., WANG, B., FAN, L., JARZEMBOWSKI, E. A., FANG, Y., WANG, H., LI, W., ZHUO, D., DING, M. and ENGEL, M. S. 2022. Widespread mimicry and camouflage among mid-Cretaceous insects. *Gondwana Research*, **101**, 94–102.

YOSHIZAWA, K. and JOHNSON, K. P. 2014. Phylogeny of the suborder Psocomorpha: congruence and incongruence between morphology and molecular data (Insecta: Psocodea: 'Psocoptera'). *Zoological Journal of the Linnean Society*, **171**, 716–731.

YOSHIZAWA, K. and LIENHARD, C. 2020. †Cormopsocidae: a new family of the suborder Trogiomorpha (Insecta: Psocodea) from Burmese amber. *Entomological Science*, **23**, 208–215.

YOSHIZAWA, K. and YAMAMOTO, S. 2021. The earliest fossil record of the suborder Psocomorpha (Insecta: Psocodea) from mid-Cretaceous Burmese amber, with description of a new genus and species. *Insecta Matsumurana New series*, **77**, 1–15.

YOSHIZAWA, K., LIENHARD, C. and JOHNSON, K. P. 2006. Molecular systematics of the suborder Trogiomorpha (Insecta: Psocodea: 'Psocoptera'). *Zoological Journal of the Linnean Society*, **146**, 287–299.

YOSHIZAWA, K., LIENHARD, C., YAO, I. and FERREIRA, R. L. 2019. Cave insects with sex-reversed genitalia had their most recent common ancestor in West Gondwana (Psocodea: Prionoglarididae: Speleketorinae). *Entomological Science*, **22**, 334–338.

ZHANG, Z. Q. 2011. Animal biodiversity: an outline of higher-level classification and survey of taxonomic richness. *Zootaxa*, **3148**, 1–237.

ZHANG, Q., NEL, A., AZAR, D. and WANG, B. 2016. New Chinese psocids from Eocene Fushun amber (Insecta: Psocodea). *Alcheringa*, **40**, 366–372.

ZHENG, D., CHANG, S.-C., PERRICHOT, V., DUTTA, S., RUDRA, A., MU, L., KELLY, R. S., ZHANG, Q., ZHANG, Q. Q., WONG, J., WANG, J., WANG, H., FANG, Y., ZHANG, H. and WANG, B. 2018. A Late Cretaceous amber biota from central Myanmar. *Nature Communications*, **9**, 3170.

Anexo 8.1.7

A braconid wasp (Hymenoptera: Ichneumonoidea: Braconidae) from the Lower Cretaceous amber of San Just (E Iberian Peninsula)

Álvarez-Parra, S., Peñalver, E., Delclòs, X., Engel, M.S. 2022. A braconid wasp (Hymenoptera: Ichneumonoidea: Braconidae) from the Lower Cretaceous amber of San Just (E Iberian Peninsula). *ZooKeys*, **1103**, 65-78.

DOI: https://doi.org/10.3897/zookeys.1103.83650

Revista científica: *ZooKeys*
Factor de impacto: 1,492 (2021)
Categoría: *Zoology*, Q3 (2021)

ZooKeys 1103: 65–78 (2022)
doi: 10.3897/zookeys.1103.83650
https://zookeys.pensoft.net

RESEARCH ARTICLE

A peer-reviewed open-access journal
ZooKeys
Launched to accelerate biodiversity research

A braconid wasp (Hymenoptera, Braconidae) from the Lower Cretaceous amber of San Just, eastern Iberian Peninsula

Sergio Álvarez-Parra[1], Enrique Peñalver[2], Xavier Delclòs[1], Michael S. Engel[3,4,5]

1 *Departament de Dinàmica de la Terra i de l'Oceà and Institut de Recerca de la Biodiversitat (IRBio), Facultat de Ciències de la Terra, Universitat de Barcelona, c/ Martí i Franquès s/n, 08028, Barcelona, Spain* **2** *Instituto Geológico y Minero de España-CSIC, c/ Cirilo Amorós 42, 46004, Valencia, Spain* **3** *Division of Entomology, Natural History Museum, University of Kansas, 1501 Crestline Drive – Suite 140, Lawrence, Kansas 66045-4415, USA* **4** *Department of Ecology and Evolutionary Biology, University of Kansas, Lawrence, Kansas 66045, USA* **5** *Division of Invertebrate Zoology, American Museum of Natural History, Central Park West at 79th Street, New York, New York 10024-5192, USA*

Corresponding author: Sergio Álvarez-Parra (sergio.alvarez-parra@ub.edu)

Academic editor: Kees van Achterberg | Received 11 March 2022 | Accepted 22 April 2022 | Published 30 May 2022

http://zoobank.org/079C1F77-A3AA-4158-AE53-5F510C8FA0BE

Citation: Álvarez-Parra S, Peñalver E, Delclòs X, Engel MS (2022) A braconid wasp (Hymenoptera, Braconidae) from the Lower Cretaceous amber of San Just, eastern Iberian Peninsula. ZooKeys 1103: 65–78. https://doi.org/10.3897/zookeys.1103.83650

Abstract

Braconid parasitoid wasps are a widely diversified group today, while their fossil record from the Mesozoic is currently poorly known. Here, we describe *Utrillabracon electropteron* Álvarez-Parra & Engel, **gen. et sp. nov.**, from the upper Albian (Lower Cretaceous) amber of San Just in the eastern Iberian Peninsula. The holotype specimen is incomplete, although the forewing and hind wing venation are well preserved. The new taxon is assigned to the subfamily †Protorhyssalinae (Braconidae) and, based on characteristics of the wing venation, seems to be closely related to *Protorhyssalus goldmani* Basibuyuk & Quicke, 1999 and *Diorhyssalus allani* (Brues, 1937), both from Upper Cretaceous ambers of North America. We discuss the taxonomy of the Cretaceous braconids, considering †Seneciobraconinae as a valid subfamily. We also comment on possible relationships within †Protorhyssalinae, although a phylogenetic analysis is necessary. Additionally, a checklist is included of braconids known from Cretaceous ambers.

Keywords
Albian, fossil, Ichneumonoidea, Protorhyssalinae, Spanish amber, taxonomy, wasp diversity, wing venation

Introduction

Braconidae are the second largest family of Hymenoptera in terms of species numbers (Chen and van Achterberg 2019), trailing just behind the closely related family, Ichneumonidae. Like ichneumonids, braconids are parasitoid wasps, with their larvae developing within or externally on other insects, typically Coleoptera, Diptera, and Lepidoptera, but actually encompassing a considerable breadth of hosts from aphids to other wasps, and even adult stages (e.g., Euphorinae) (Wharton 1993). Given that braconids attack the immatures of many agriculturally important pest species, they have been heavily employed in sustainable pest management programs throughout the world (e.g., Nomano et al. 2015).

Braconids belong to the superfamily Ichneumonoidea, which comprises the extant families Ichneumonidae, Braconidae, and Trachypetidae (Quicke et al. 2020), along with the extinct †Praeichneumonidae, a monogeneric family including five species known from Early Cretaceous compression fossils (Rasnitsyn 1983, 1990; Kopylov 2012). A putative fifth group, †Ichneumonomimidae (Rasnitsyn 1975), has subsequently been considered to belong to Trigonalyidae (Rasnitsyn 1988), while the Trachypetidae has been recently restored as a non-cyclostome braconid subfamily (Jasso-Martínez et al. 2022a, 2022b). The fossil record of Ichneumonoidea is most diverse in Cenozoic deposits but extends well into the Early Cretaceous, with Mesozoic fossils representing early diverging lineages of both Ichneumonidae and Braconidae, several of which have been difficult to place phylogenetically or to even confirm as monophyletic (Kopylov et al. 2021; Spasojevic et al. 2021; Viertler et al. 2022).

One notable example of these early lineages is the braconid subfamily †Protorhyssalinae, a group of parasitoid wasps almost exclusively known by amber inclusions from the Albian to the Campanian (Li et al. 2021). Braconidae are currently represented by 21 genera and 22 species in Cretaceous ambers (Table 1), besides other specimens preserved as compressions in Cretaceous rocks (Belokobylskij 2012). Only two braconid species have been previously reported from Cretaceous Spanish amber (Ortega-Blanco et al. 2009, 2011) (Fig. 1). Furthermore, other specimens of the family were found in lower Miocene compression outcrops from the eastern Iberian Peninsula (Peñalver and Martínez-Delclòs 2000; Álvarez-Parra and Peñalver 2019). Here, we describe a new genus and species of fossil wasp belonging to the subfamily †Protorhyssalinae included in amber from the upper Albian San Just in the eastern Iberian Peninsula. Although the specimen is incomplete, the wings are extraordinarily well preserved and allow for its proper placement and characterization relative to other protorhyssalines. We provide a description of the new species and compare it with the previously known genera of †Protorhyssalinae. In addition, we append comments on the diversity of the subfamily and putative phylogenetic groups among this assemblage of wasps.

Table 1. Checklist of species of Braconidae (Hymenoptera, Ichneumonoidea) from Cretaceous ambers. The two species marked with an asterisk need taxonomic revision. For Cretaceous compression fossils see Belokobylskij (2012).

Subfamily	Genus and species	Locality	Age	Reference
Aphidiinae	*Archephedrus stolamissus* Ortega-Blanco, Bennett, Delclòs, & Engel, 2009	Peñacerrada I, Spain	late Albian	Ortega-Blanco et al. (2009)
Brachistinae	"*Neoblacus*" (=*Blacus*) *facialis* Brues, 1937 *	Cedar Lake, Canada	Campanian	Brues (1937)
Euphorinae	"*Pygostolus*" *patriarchicus* Brues, 1937 *	Cedar Lake, Canada	Campanian	Brues (1937)
†Megalyrhyssalinae	*Megalyrhyssalus clavicornis* Belokobylskij & Jouault, 2021	Hukawng Valley, Myanmar	early Cenomanian	Belokobylskij and Jouault (2021)
†Protobraconinae	*Rhetinorhyssalites emersoni* Engel, Thomas, & Alqarni, 2017	Sayreville, USA	Turonian	Engel et al. (2017); Chen et al. (2021b)
	Chainochora syntoma Chen & van Achterberg, 2021	Hukawng Valley, Myanmar	early Cenomanian	Chen et al. (2021a)
	Kleistochora dolichura Chen & van Achterberg, 2021	Hukawng Valley, Myanmar	early Cenomanian	Chen et al. (2021a)
	Protobracon robusticauda Chen & van Achterberg, 2021	Hukawng Valley, Myanmar	early Cenomanian	Chen et al. (2021b)
	Tibialobracon compressicornis Chen & van Achterberg, 2021	Hukawng Valley, Myanmar	early Cenomanian	Chen et al. (2021b)
†Protorhyssalinae	*Diorhyssalus allani* (Brues, 1937)	Cedar Lake, Canada	Campanian	Brues, (1937); Engel (2016); Chen et al. (2021b)
	Protorhyssalus goldmani Basibuyuk & Quicke, 1999	Sayreville, USA	Turonian	Basibuyuk et al. (1999)
	Protorhyssalodes arnaudi Perrichot, Nel, & Quicke, 2009	Cadeuil, France	early Cenomanian	Perrichot et al. (2009); Chen et al. (2021b)
	Archaeorhyssalus subsolanus Engel, 2016	Hukawng Valley, Myanmar	early Cenomanian	Engel and Wang (2016)
	Burmabracon gracilens Li, Shih, & Ren, 2021	Hukawng Valley, Myanmar	early Cenomanian	Li et al. (2021)
	Burmabracon grossus Li, Shih, & Ren, 2021	Hukawng Valley, Myanmar	early Cenomanian	Li et al. (2021)
	Protorhyssalopsis perrichoti Ortega-Blanco, Delclòs, & Engel, 2011	Peñacerrada I, Spain	late Albian	Ortega-Blanco et al. (2011)
	***Utrillabracon electropteron* Álvarez-Parra & Engel, gen. et sp. n.**	San Just, Spain	late Albian	This paper
†Seneciobraconinae	*Seneciobracon novalatus* Engel & Huang, 2018	Hukawng Valley, Myanmar	early Cenomanian	Engel et al. (2018)
Incertae sedis	*Aenigmabracon capdoliensis* Perrichot, Nel, & Quicke, 2009	Cadeuil, France	early Cenomanian	Perrichot et al. (2009)
	Pyramidibracon clypeatus Chen & van Achterberg, 2021	Hukawng Valley, Myanmar	early Cenomanian	Chen et al. (2021b)
	Rhetinorhyssalus morticinus Engel, 2016	Hukawng Valley, Myanmar	early Cenomanian	Engel (2016)
	Stephanorhyssalus longiscapus Belokobylskij & Jouault, 2021	Hukawng Valley, Myanmar	early Cenomanian	Belokobylskij and Jouault (2021)

Materials and methods

The amber material reported here comes from the San Just amber-bearing outcrop (Teruel Province, Aragón, Spain). The site is located near the Utrillas Municipality, in the Aliaga Sub-basin within the Maestrazgo Basin (Fig. 1). More than 30 amber-

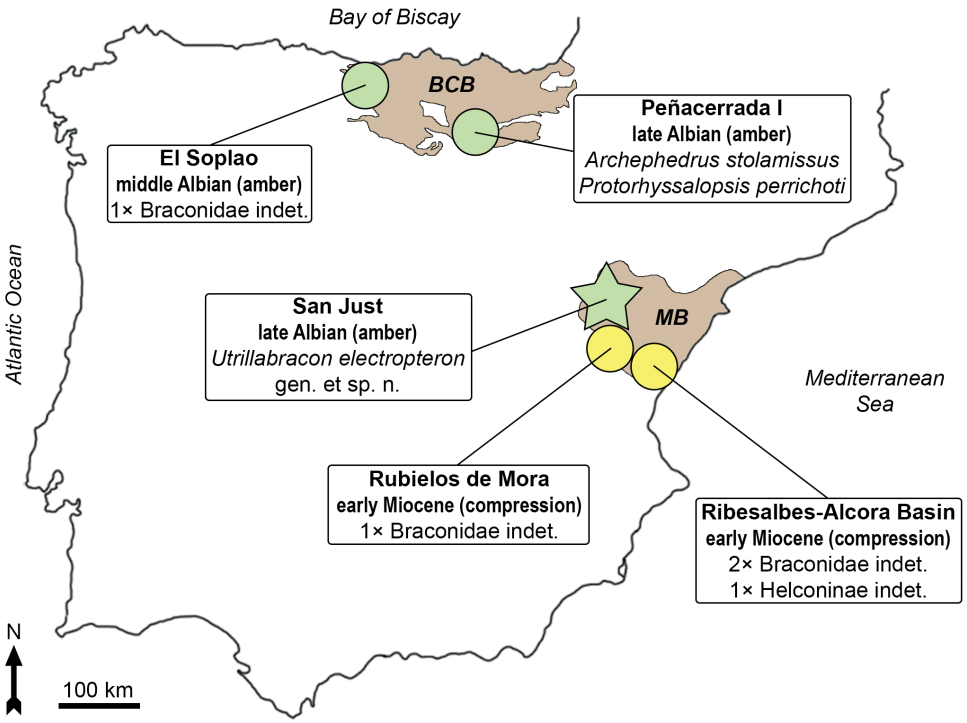

Figure 1. Map of the Iberian Peninsula showing the location of the amber and compression outcrops that have yielded braconid wasps. Basque-Cantabrian (BCB) and Maestrazgo (MB) basins are represented. The type locality the studied specimen is indicated with a star. The specimens from El Soplao and Rubielos de Mora are undescribed to date.

bearing outcrops have been reported in this basin, although only four of them have yielded bioinclusions (Álvarez-Parra et al. 2021). Stratigraphically, the San Just section has been assigned to the Escucha Formation (Peñalver et al. 2007). The amber-rich level is composed of grey-black marls with a high content of organic matter, charcoal, and fusinite and has been interpreted as a freshwater swamp plain (Peñalver et al. 2007; Villanueva-Amadoz et al. 2010). The site was dated as middle–earliest upper Albian based on palynological evidence (Villanueva-Amadoz et al. 2010). A new palynological study constrains the dating to the upper Albian (Eduardo Barrón pers. comm.). San Just is the type locality of 26 arthropod species (including the new species here described) and the Hymenoptera are represented by nine species in eight families (Santer et al. 2022). The amber piece was recovered during an excavation in 2012 (Government of Aragón permit 119/10-11-2012). The original amber piece was divided in four epoxy preparations to better examine the syninclusions. This process followed the methodology of Corral et al. (1999). The specimen was photographed and drawn using an Olympus CX41 compound microscope, with an attached digital camera sCMEX-20 and a camera lucida. Photographs were made using the software

ImageFocusAlpha v. 1.3.7.12967.20180920 and the figures were prepared using Photoshop CS6. Venational nomenclature is based on Huber and Sharkey (1993) and Ortega-Blanco et al. (2009). The specimen is deposited in the Museo Aragonés de Paleontología (Fundación Conjunto Paleontológico de Teruel-Dinópolis), Teruel, Spain. The fossil notation "MAP" corresponds to the number at the Museo Aragonés de Paleontología, while "SJE2012" is the field number.

Systematic paleontology

Family Braconidae Nees von Esenbeck, 1811

Subfamily †Protorhyssalinae Basibuyuk, Quicke, & van Achterberg, 1999

Protorhyssalinae Basibuyuk, Quicke, & van Achterberg, 1999: 211. Type genus: *Protorhyssalus* Basibuyuk & Quicke in Basibuyuk et al. (1999), by original designation.

Comments. Herein we restore the traditional concept of †Protorhyssalinae as recognized by Basibuyuk et al. (1999) and Chen and van Achterberg (2019). Belokobylskij and Jouault (2021) proposed a classification in which virtually all Cretaceous braconids are thrown into a paraphyletic group, rendering †Protorhyssalinae a meaningless grade. Admittedly, restoring †Protorhyssalinae still leaves the group paraphyletic but at least removes the more obviously derived groups and thereby narrows the challenge as to the affinities of the remaining genera. Nonetheless, while Belokobylskij and Jouault (2021) advocated for such a paraphyletic assemblage, they used plesiomorphic features along with autapomorphies to establish the subfamily †Megalyrhyssalinae. Unfortunately, †Megalyrhyssalinae is poorly justified and could be merely an autapomorphic form of the same protorhyssaline grade. By their own reasoning, they should have either not established such a subfamily or further divided †Protorhyssalinae to resolve the paraphyly. Under their conception of †Protorhyssalinae, †Megalyrhyssalinae would be a junior synonym. For now, we recognize the following subfamilies: †Protorhyssalinae, †Seneciobraconinae (*Seneciobracon*), and †Megalyrhyssalinae (*Megalyrhyssalus*), noting that the last may not be sufficiently justified but may well be worth considering once the full phylogeny of the genera comprising these groups is elucidated. Until such time it seems that further alterations of the subfamilial system in the absence of a cladistic framework would be unwarranted.

Included genera and species. *Archaeorhyssalus subsolanus* Engel, 2016; *Burmabracon gracilens* Li, Shih, & Ren, 2021; *B. grossus* Li, Shih, & Ren, 2021; *Diorhyssalus allani* (Brues, 1937); *Protorhyssalodes arnaudi* Perrichot, Nel, & Quicke, 2009; *Protorhyssalopsis perrichoti* Ortega-Blanco, Delclòs, & Engel, 2011; *Protorhyssalus goldmani* Basibuyuk & Quicke, 1999; and *Utrillabracon electropteron* Álvarez-Parra & Engel, gen. et sp. nov. *Cretorhyssalus brevis* Belokobylskij, 2012, *Magadanobracon rasnitsyni* Belokobylskij, 2012, and *M. zherikhini* Belokobylskij, 2012, known from compression fossils, were putatively assigned to †Protorhyssalinae *sensu* Belokobylskij (2012).

***Utrillabracon* Álvarez-Parra & Engel, gen. nov.**
http://zoobank.org/C6FE19C1-A5D0-4780-9860-F611198EF09C

Type species. *Utrillabracon electropteron* Álvarez-Parra & Engel, sp. nov.

Diagnosis. Forewing with margin bearing setae; pterostigma 4 × longer than wide; 1Rs relatively long and curved; r-rs oblique, arising medially from pterostigma; r-rs several times longer than abscissa of M between 2Rs and m-cu; marginal cell reaching wing apex; rs-m nebulous; elongate, five-sided second submarginal cell, 3 × longer than wide; 1M and m-cu of similar length; m-cu distinctly postfurcal; 2m-cu absent; cu-a slightly postfurcal and orthogonal. Hind wing with margin bearing setae; R1 distally widened with several hamuli beyond its apex; Sc + R not aligned with Rs; 2Cu present. Pretarsal claws present, without preapical tooth; arolium wide.

Etymology. The generic name is a combination of Utrillas, municipality where the San Just amber outcrop is located, and *Bracon* Fabricius, 1804, type genus of the family Braconidae. The gender of the name is masculine.

***Utrillabracon electropteron* Álvarez-Parra & Engel, sp. nov.**
http://zoobank.org/59B73E2C-0514-4DA4-8A87-ABF61D6EF2A8
Fig. 2

Material. ***Holotype***, MAP-7819 (SJE2012 49-04), sex unknown, from San Just amber. The holotype is largely preserved as the forewings and hind wings. Some parts of the head, an antenna, and a leg are next to the wings. Undetermined cuticular fragments are visible near the wings. Deposited in the Museo Aragonés de Paleontología (Fundación Conjunto Paleontológico de Teruel-Dinópolis) in Teruel, Spain. Syninclusions include three other hymenopterans (probable serphitid, platygastrid, and stigmaphronid wasps). The holotype is prepared isolated in an epoxy prism of 20 × 15 mm.

Locality and horizon. San Just amber-bearing outcrop, Utrillas, Teruel, Spain; Maestrazgo Basin, Escucha Formation, upper Albian (Peñalver et al. 2007).

Diagnosis. As for the genus (*vide supra*).

Description. Head deformed and incomplete as preserved (Fig. 2A, B); antenna partially preserved with 11 flagellomeres covered by setae, multiporous plate sensilla not visible; only distal two maxillary palpomeres preserved, covered by fine setae. Forewings and venation rather complete (Fig. 2C), forewing base not preserved, more than 1.31 mm long and 0.53 mm in its maximum width, margin bearing setae; C + Sc + R fused anterobasally, extending along wing margin to pterostigma; pterostigma 4 × longer than wide (0.33 mm vs 0.08 mm); elongate marginal cell, 3 × longer than wide (0.57 mm vs 0.19 mm), reaching wing apex; 1Rs relatively long and curved; Rs + M slightly sinuous; first submarginal cell 2 × longer than wide (0.31 mm vs 0.15 mm), pentagonal; 2Rs slightly sinuous; r-rs oblique, arising medially from pterostigma, 0.08 mm long; 3Rs extending nearly straight until wing margin, 0.55 mm long; r-rs several times longer than abscissa of M between 2Rs and m-cu; 1M curved, 2 × longer

than 1Rs (0.14 mm vs 0.07 mm); 2M straight, 0.38 mm long; almost straight 3M, disappearing before wing margin; rs-m nebulous, 0.13 mm long; elongate, pentagonal second submarginal cell, 3 × longer than wide (0.38 mm vs 0.13 mm); trapezoidal third submarginal cell, 0.31 mm long; first discal cell almost 2 × longer than wide (0.21 mm vs 0.12 mm); m-cu distinctly postfurcal (absence of a vein 2Rs + M), 0.12 mm long; lacking 2m-cu; elongate second discal cell, 0.63 mm long; cu-a (nervulus) slightly postfurcal (therefore presence of an exceptionally short $1Cu_a$), 0.06 mm long, perpendicular to 1Cu and A; 1Cu nearly straight, 0.14 mm long; 2Cu strongly curved basally separating $2Cu_a$ (0.05 mm long) and $2Cu_b$, latter curved and directed towards wing margin (but without meeting margin); first subdiscal cell 2 × longer than wide (0.13 mm vs 0.07 mm); elongate and narrow second subdiscal cell; A tubular and nearly straight; 1a and 2a not visible. Hind wings and venation rather complete

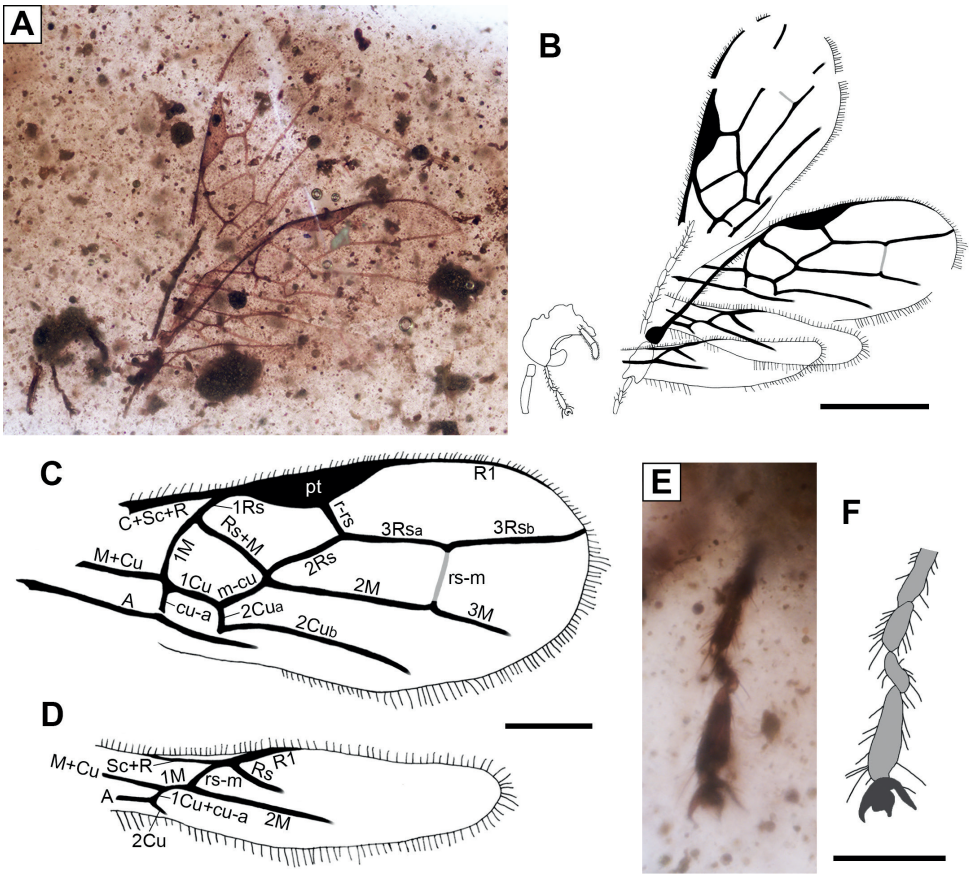

Figure 2. *Utrillabracon electropteron* Álvarez-Parra & Engel, gen. et sp. nov. (Braconidae, †Protorhyssalinae) from the upper Albian amber-bearing outcrop of San Just, specimen MAP-7819 (SJE2012 49-04). **A, B** photograph and drawing of preserved remains, both to the same scale **C** forewing venation **D** hind wing venation **E, F** photograph and drawing of tarsus and pretarsus, both to the same scale. Abbreviation: pt = pterostigma. Scale bars: 0.5 mm (**A, B**); 0.2 mm (**C, D**); 0.1 mm (**E, F**).

(Fig. 2D), hind wing base not preserved, more than 0.94 mm long and 0.23 mm at its maximum width, margin bearing setae; Sc + R fused anterobasally; R1 distally widened with several hamuli beyond its apex; Sc + R not aligned with Rs; 1M short, 0.05 long; rs-m oblique, 0.07 mm long; Rs and M ending as nebulous veins before margin; 1Cu + cu-a inclivitous, 0.03 mm long; short 2Cu, not contacting wing margin. Two fragments of legs visible: a partial femur and a tarsus; four distal tarsomeres preserved covered by fine setae (Fig. 2E, F), tarsomere III 0.06 mm long, tarsomere IV 0.04 mm long, tarsomere V 0.08 mm long; pretarsus with paired claws, preapical tooth absent, arolium wide.

Etymology. The specific epithet is a combination of the Greek *ἤλεκτρον* (élektron), meaning, "amber", and *πτηνόν* (ptéron), meaning, "winged creature", and referring to the fact that the holotype is mainly preserved by the wings in amber.

Discussion

The newly reported San Just amber wasp can be assigned to Braconidae quite easily owing to the characteristic wing venation: Rs + M present and 2m-cu absent in the forewing and rs-m proximal to bifurcation of R1 and Rs in the hind wing (Huber and Sharkey 1993; Belokobylskij and Jouault 2021). The absence of 2m-cu in the forewing also serves to exclude the fossil from the plesiomorphic †Praeichneumonidae. Additionally, the Trachypetinae (formerly as family Trachypetidae) have rs-m distal to the separation of R1 and Rs (Quicke et al. 2020), and therefore the current fossil also does not accord with the circumscription of this group. Although many have noted that braconid wing venation can be quite variable, the current fossil from San Just cannot be ascribed to any other clade and is quite readily attributable to Braconidae. In fact, several Cretaceous braconids possess 2m-cu in the forewing, such as *Aenigmabracon capdoliensis* Perrichot, Nel, & Quicke, 2009 (subfamily *incertae sedis*), *Stephanorhyssalus longiscapus* Belokobylskij & Jouault, 2021 (subfamily *incertae sedis*), and species of the subfamily †Eoichneumoninae, all of which likely retain this trait symplesiomorphically (Belokobylskij and Jouault 2021). Furthermore, some living species of the subfamilies Apozyginae, Doryctinae, and Rhyssalinae (all of crown-Braconidae) possess 2m-cu in the forewing (Tobias and Belokobylskij 1983), while some species of a few subfamilies of Ichneumonidae lack this vein (Tobias 1963). All of these cases are easily identified as secondary reappearances of the crossvein or "atavisms" based on the phylogenetic placement of the taxa in question (Belokobylskij and Jouault 2021).

The presence of a pentagonal (five-sided) second submarginal cell in the forewing and vein 2Cu in the hind wing indicates that *Utrillabracon electropteron* is currently best assigned to the subfamily †Protorhyssalinae (Basibuyuk et al. 1999; Chen et al. 2021b), despite the fact that this group, even in its restricted sense, may be paraphyletic. Indeed, the overall venation of *Utrillabracon* accords broadly with that of †Protorhyssalinae (Basibuyuk et al. 1999). The pentagonal second submarginal cell in the forewings is likely to be plesiomorphic in braconids. The other braconid subfamilies

with a Cretaceous record, such as Aphidiinae, †Seneciobraconinae, †Megalyrhyssalinae, and †Protobraconinae, lack 2Cu in the hind wing (Belokobylskij and Jouault 2021; Chen et al. 2021b). Several extant braconid subfamilies have 2Cu in the hind wing (Perrichot et al. 2009; Belokobylskij and Jouault 2021), and interestingly they are phylogenetically placed basal to all other crown-braconids (Apozyginae) or to the derived non-cyclostome lineage (Acampsohelconinae, Agathidinae, Meteorideinae, and Sigalphinae) (Chen and van Achterberg 2019). Furthermore, this character is also present in some †Eoichneumoninae (Braconidae), and in the ichneumonoid groups Trachypetinae (Braconidae), †Praeichneumonidae, and Ichneumonidae (Belokobylskij and Jouault 2021). Therefore, it is probable that the presence of 2Cu in the hind wing is symplesiomorphic across all of these lineages (Perrichot et al. 2009; Belokobylskij and Jouault 2021). The †Eoichneumoninae possess 2m-cu in the forewings (like the †Praeichneumonidae and the vast majority of Ichneumonidae) (Belokobylskij and Jouault 2021; Chen et al. 2021b), and quite unlike *U. electropteron*.

The San Just fossil may be easily distinguished from the two unplaced Canadian Late Cretaceous amber species "*Neoblacus*" (= *Blacus*) *facialis* Brues, 1937 and "*Pygostolus*" *patriarchicus* Brues, 1937. Both of these species need revision and likely do not belong to the genera to which Brues assigned them (Antropov et al. 2014; Chen et al. 2021b). Nonetheless, both are sufficiently known as to differentiate them from *U. electropteron*. The species *N.* (= *B.*) *facialis* lacks Rs + M and rs-m in the forewing (vs present), r-rs arises before the middle of the pterostigma and is perpendicular to the costal margin (vs inclivitous and arising pterostigmal midlength), and cu-a is distinctly postfurcal (vs slightly postfurcal) (Brues 1937). The pterostigma of *U. electropteron* seems to be similar to that of *N.* (= *B.*) *facialis*, as in both species it is 4 × longer than wide (Brues 1937). "*Pygostolus*" *patriarchicus* has a triangular pterostigma with basal and apical margins of equal length (vs pterostigma long and narrow), and cu-a postfurcal in the forewing (Brues 1937). The *incertae sedis* braconids *A. capdoliensis* and *S. longiscapus* differ from *U. electropteron* in the presence of 2m-cu and cu-a postfurcal in the forewing (Perrichot et al. 2009; Belokobylskij and Jouault 2021). *Pyramidibracon clypeatus* Chen & van Achterberg, 2021 and *Rhetinorhyssalus morticinus* Engel, 2016 are currently not assigned to a subfamily and differ from *U. electropteron* in several characters, such as cu-a strongly inclivitous in the forewing, Sc + R aligned with Rs, and both lack 2Cu in the hind wing (Engel 2016; Chen et al. 2021b).

Considering those genera currently assigned to †Protorhyssalinae, *U. electropteron* can be differentiated from them as summarized below. *Archaeorhyssalus subsolanus* lacks 1Rs (vs present), has a distinct 2Rs + M (vs absent), and m-cu antefurcal and contacting Rs + M (vs not contacting) in the forewing (Engel and Wang 2016). *Burmabracon gracilens*, *B. grossus*, and *Protorhyssalopsis perrichoti* have Sc + R aligned with Rs in the hind wing (vs not aligned), aside from a slew of further differences (Li et al. 2021; Ortega-Blanco et al. 2011). *Protorhyssalodes arnaudi* has cu-a distinctly postfurcal with $1Cu_a$ as long as cu-a (vs cu-a slightly postfurcal) in the forewing and also Sc + R aligned with Rs in the hind wing (Perrichot et al. 2009). The wing venation of *U. electropteron* is quite similar to that of *Protorhyssalus goldmani* and *Diorhyssalus allani* (Brues 1937; Basibuyuk et al. 1999; Engel 2016). *Utrillabracon electropteron*

shares with *P. goldmani* the marginal cell reaching the wing apex, vein m-cu postfurcal, and cu-a slightly postfurcal in the forewing, while differing in the length of the second submarginal cell (shorter in *P. goldmani*) and the length of r-rs in comparison to the abscissa of M between 2Rs and m-cu (similar length in *P. goldmani* and several times longer in *U.electropteron*) (Basibuyuk et al. 1999). Both species have Sc + R not aligned with Rs in the hind wing (Basibuyuk et al. 1999). In general, the venation of *U. electropteron* seems to be closest to that of *D. allani* (Brues 1937; Engel 2016). Particularly, the lengths of the second submarginal cell and r-rs (several times longer than the abscissa of M between 2Rs and m-cu) are similar in both, and they also have m-cu postfurcal (Brues 1937; Engel 2016). The characters present in *U. electropteron* that differ from *D. allani* are 1Rs curved (vs shorter and straight), rs-m nebulous (vs sclerotized), and cu-a orthogonal and slightly postfurcal (vs inclivitous and somewhat more postfurcal) (Brues 1937; Engel 2016). The hind wing of *D. allani* is poorly known (Engel 2016). Therefore, despite the similar venation of the San Just species with *D. allani*, we prefer to assign it to a new genus, as we think that the anatomical differences cannot be associated with variability between species. Furthermore, the San Just species and *D. allani* are separated by more than 20 Myr (Albian to Campanian), and a vast geographical distance (Iberian Peninsula vs western Canada).

Based on the similarities of the wing venations of *U. electropteron*, *P. goldmani*, and *D. allani*, it is possible that they were closely related. These three taxa may form a group within †Protorhyssalinae, supported by the following characters: 1Rs present, pterostigma long and narrow, r-rs arising medially from pterostigma, m-cu distinctly postfurcal, cu-a slightly postfurcal ($1Cu_a$ shorter than cu-a) in the forewing, and Sc + R not aligned with Rs in the hind wing. The latter character is tenuous for *D. allani*, as the hind wings are poorly documented (Brues 1937; Engel 2016). Nonetheless, it is probable that the hind wing of *D. allani* also had 2Cu, based on the other anatomical similarities with *P. goldmani* and *U. electropteron*. A revision of the holotype of *D. allani* or the discovery of new specimens of the same morphotype may demonstrate the presence of 2Cu (and Sc + R not aligned with Rs) for the hind wing, thus corroborating its placement to †Protorhyssalinae. *Archaeorhyssalus subsolanus* has m-cu antefurcal, a distinctive character among protorhyssalines, and it may be that this genus belongs to a more derived clade between the generally plesiomorphic †Protorhyssalinae and the more derived †Seneciobraconinae. We refrain, however, from establishing another monogeneric subfamily for this genus until such time as more critical cladistic work has been undertaken. *Burmabracon gracilens*, *B. grossus*, *P. arnaudi*, and *P. perrichoti* share Sc + R aligned with Rs in the hind wing, a character that could be a potential apomorphy of a group formed by these four species. In any case, these groupings are based solely on observations of wing venation and a phylogenetic analysis incorporating larger suites of data is necessary to resolve monophyly (or lack thereof) for †Protorhyssalinae, relationships among the constituent groups, as well as the placement of the various extinct subfamilies among early diverging Braconidae. Basibuyuk et al. (1999) noted that the subfamily †Protorhyssalinae lacks apomorphies, and it is likely that it will be discovered to be a grade (Engel 2016; Chen and van Achterberg 2019), necessitating the removal of some genera to other or even new subfamilies (e.g., *Archaeorhyssalus*).

An interesting breadth of early braconid diversity is documented from Cretaceous amber inclusions and compression fossils (Table 1). Nonetheless, this diversity is trivial by comparison to the overwhelming diversity of present-day Braconidae (Chen and van Achterberg 2019). This may be the result of a Late Cretaceous diversification of the family, with little diversity present prior to this time. This may be partly the case as an incredible diversity of new potential hosts for braconids were appearing during the Late Cretaceous and into the Paleogene owing to the rise of several flower-associated insects at the time (Labandeira and Li 2021). However, there is likely also a considerable taphonomic bias against the capture and preservation of early fossil Braconidae (Martínez-Delclòs et al. 2004). Their typically diminutive size means that preservation in sediments requires exceptionally fine grains in order to have sufficient fidelity for their proper identification as braconids and despite the rich number of wasps included in amber, Cretaceous braconids are rare. This could be owing to the fact that braconids have little reason to be near resin flows except in the case of seeking or emerging from a host that was somehow present on or in trees exuding resins. Certainly, the family was present and widespread during the Cretaceous owing to their occurrence in deposits spanning Canada to Myanmar, and so the combination of potentially low abundances, lower than present species diversity, typically small body size necessitating exceptional preservational conditions, and biases away from resin-producing sources may account for their rarity. If this is the case, then it would also render challenging any direct exploration of their earliest history as fossils would likely continue to be rare.

Acknowledgements

We thank the Museo Aragonés de Paleontología (Fundación Conjunto Paleontológico de Teruel-Dinópolis) for the loan of the material reported herein. We are grateful to the Dirección General de Patrimonio Cultural of the Government of Aragón (Spain) for the permission to excavate in the San Just outcrop, and to Rafael López del Valle for the preparation of the amber piece. We also thank Sergey Belokobylskij, two anonymous reviewers, and the subject editor Kees van Achterberg for their generous and helpful comments that improved the manuscript. This study is a contribution to the project CRE CGL2017-84419 funded by the Spanish AEI/FEDER and UE. S.Á.-P. is grateful for support from the Secretaria d'Universitats i Recerca de la Generalitat de Catalunya (Spain) and the European Social Fund (2021FI_B2 00003).

References

Álvarez-Parra S, Peñalver E (2019) Palaeoentomological study of the lacustrine oil-shales of the lower Miocene San Chils locality (Ribesalbes-Alcora Basin, Castellón province, Spain). Spanish Journal of Palaeontology 34(2): 187–203. https://doi.org/10.7203/sjp.34.2.16093

Álvarez-Parra S, Pérez-de la Fuente R, Peñalver E, Barrón E, Alcalá L, Pérez-Cano J, Martín-Closas C, Trabelsi K, Meléndez N, López Del Valle R, Lozano RP, Peris D, Rodrigo A,

Sarto i Monteys V, Bueno-Cebollada CA, Menor-Salván C, Philippe M, Sánchez-García A, Peña-Kairath C, Arillo A, Espílez E, Mampel L, Delclòs X (2021) Dinosaur bonebed amber from an original swamp forest soil. eLife 10: e72477. https://doi.org/10.7554/eLife.72477

Antropov AV, Belokobylskij SA, Compton SG, Dlussky GM, Khalaim AI, Kolyada VA, Kozlov MA, Perfilieva KS, Rasnitsyn AP (2014) The wasps, bees and ants (Insecta: Vespida = Hymenoptera) from the insect limestone (Late Eocene) of the Isle of Wight, UK. Earth and Environmental Science Transactions of the Royal Society of Edinburgh 104(3–4): 335–446. https://doi.org/10.1017/S1755691014000103

Basibuyuk HH, Rasnitsyn AP, van Achterberg K, Fitton MG, Quicke DLJ (1999) A new, putatively primitive Cretaceous fossil braconid subfamily from New Jersey amber (Hymenoptera, Braconidae). Zoologica Scripta 28(1–2): 211–214. https://doi.org/10.1046/j.1463-6409.1999.00006.x

Belokobylskij SA (2012) Cretaceous braconid wasps from the Magadan Province of Russia. Acta Palaeontologica Polonica 57(2): 351–361. https://doi.org/10.4202/app.2010.0120

Belokobylskij SA, Jouault C (2021) Two new striking braconid genera (Hymenoptera: Braconidae) from the mid-Cretaceous Burmese amber. Proceedings of the Geologists' Association 132(4): 426–437. https://doi.org/10.1016/j.pgeola.2021.04.003

Brues CT (1937) Superfamilies Ichneumonoidea, Serphoidea, and Chalcidoidea. In: Carpenter FM (Ed.) Fossil Insects in Canadian Amber. University of Toronto Studies, Geological Series 40: 27–44.

Chen XX, van Achterberg C (2019) Systematics, phylogeny, and evolution of braconid wasps: 30 years of progress. Annual Review of Entomology 64(1): 335–358. https://doi.org/10.1146/annurev-ento-011118-111856

Chen HY, van Achterberg C, Hong P (2021a) Two new genera of Protobraconinae (Hymenoptera, Braconidae) from mid-Cretaceous amber of northern Myanmar. Cretaceous Research 126: e104914. https://doi.org/10.1016/j.cretres.2021.104914

Chen HY, van Achterberg C, Pang H, Liu JX (2021b) Three new genera of Braconidae (Hymenoptera) from mid-Cretaceous amber of northern Myanmar. Cretaceous Research 118: e104669. https://doi.org/10.1016/j.cretres.2020.104669

Corral JC, López Del Valle R, Alonso J (1999) El ámbar cretácico de Álava (Cuenca Vasco-Cantábrica, norte de España). Su colecta y preparación. Estudios del Museo de Ciencias Naturales de Álava 14: 7–21.

Engel MS (2016) Notes on Cretaceous amber Braconidae (Hymenoptera), with descriptions of two new genera. Novitates Paleoentomologicae 15(15): 1–7. https://doi.org/10.17161/np.v0i15.5704

Engel MS, Wang B (2016) The first Oriental protorhyssaline wasp (Hymenoptera: Braconidae): A new genus and species in Upper Cretaceous amber from Myanmar. Cretaceous Research 63: 28–32. https://doi.org/10.1016/j.cretres.2016.02.012

Engel MS, Thomas JC, Alqarni AS (2017) A new genus of protorhyssaline wasps in Raritan amber (Hymenoptera, Braconidae). ZooKeys 711: 103–111. https://doi.org/10.3897/zookeys.711.20709

Engel MS, Huang D, Cai C, Alqarni AS (2018) A new lineage of braconid wasps in Burmese Cenomanian amber (Hymenoptera, Braconidae). ZooKeys 730: 75–86. https://doi.org/10.3897/zookeys.730.22585

Huber JT, Sharkey MJ (1993) Structure. In: Goulet H, Huber JT (Eds) Hymenoptera of the World: An Identification Guide to Families. Agriculture Canada, Ottawa, 13–59.

Jasso-Martínez JM, Quicke DLJ, Belokobylski SA, Santos BF, Fernández-Triana JL, Kula RR, Zaldívar-Riverón A (2022a) Mitochondrial phylogenomics and mitogenome organization in the parasitoid wasp family Braconidae (Hymenoptera: Ichneumonoidea). BMC Ecology and Evolution 22(1): e46. https://doi.org/10.1186/s12862-022-01983-1

Jasso-Martínez JM, Santos BF, Zaldívar-Riverón A, Fernandez-Triana J, Sharanowski BJ, Richter R, Dettman JR, Blaimer BB, Brady SG, Kula RR (2022b) Phylogenomics of braconid wasps (Hymenoptera, Braconidae) sheds light on classification and the evolution of parasitoid life history traits. Molecular Phylogenetics and Evolution 107452: e107452. https://doi.org/10.1016/j.ympev.2022.107452

Kopylov DS (2012) New species of Praeichneumonidae (Hymenoptera, Ichneumonoidea) from the lower Cretaceous of Transbaikalia. Paleontological Journal 46(1): 66–72. https://doi.org/10.1134/S0031030112010078

Kopylov DS, Zhang Q, Zhang HC (2021) The Darwin wasps (Hymenoptera: Ichneumonidae) of Burmese amber. Palaeoentomology 4(6): 592–603. https://doi.org/10.11646/palaeoentomology.4.6.8

Labandeira CC, Li L (2021) The history of insect parasitism and the Mid-Mesozoic Parasitoid Revolution. In: De Baets K, Huntley JW (Eds) The evolution and fossil record of parasitism: Identification and macroevolution of parasites. Springer, Topics in Geobiology 49(11): 377–533. https://doi.org/10.1007/978-3-030-42484-8_11

Li L, Shih C, Yang J, Wang L, Li D, Ren D (2021) New amber record of Braconidae (Insecta: Hymenoptera) from the mid-Cretaceous of Myanmar. Cretaceous Research 124: e104794. https://doi.org/10.1016/j.cretres.2021.104794

Martínez-Delclòs X, Briggs DE, Peñalver E (2004) Taphonomy of insects in carbonates and amber. Palaeogeography, Palaeoclimatology, Palaeoecology 203(1–2): 19–64. https://doi.org/10.1016/S0031-0182(03)00643-6

Nees von Esenbeck CG (1811) Ichneumonides Adsciti, in genera et familias divisi. Magazin Gesellschaft Naturforschender Freunde zu Berlin 5: 1–37.

Nomano FY, Mitsui H, Kimura MT (2015) Capacity of Japanese *Asobara* species (Hymenoptera; Braconidae) to parasitize a fruit pest *Drosophila suzukii* (Diptera; Drosophilidae). Journal of Applied Entomology 139(1–2): 105–113. https://doi.org/10.1111/jen.12141

Ortega-Blanco J, Bennett DJ, Delclòs X, Engel MS (2009) A primitive aphidiine wasp in Albian amber from Spain and a Northern Hemisphere origin for the subfamily (Hymenoptera: Braconidae: Aphidiinae). Journal of the Kansas Entomological Society 82(4): 273–282. https://doi.org/10.2317/JKES0812.08.1

Ortega-Blanco J, Delclòs X, Engel MS (2011) A protorhyssaline wasp in Early Cretaceous amber from Spain (Hymenoptera: Braconidae). Journal of the Kansas Entomological Society 84(1): 51–57. https://doi.org/10.2317/JKES100728.1

Peñalver E, Martínez-Delclòs X (2000) Insectos del Mioceno Inferior de Ribesalbes (Castellón, España). Hymenoptera. Treballs del Museu de Geologia de Barcelona 9: 97–153.

Peñalver E, Delclòs X, Soriano C (2007) A new rich amber outcrop with palaeobiological inclusions in the Lower Cretaceous of Spain. Cretaceous Research 28(5): 791–802. https://doi.org/10.1016/j.cretres.2006.12.004

Perrichot V, Nel A, Quicke DLJ (2009) New braconid wasps from French Cretaceous amber (Hymenoptera, Braconidae): Synonymization with Eoichneumonidae and implications for the phylogeny of Ichneumonoidea. Zoologica Scripta 38(1): 79–88. https://doi.org/10.1111/j.1463-6409.2008.00358.x

Quicke DLJ, Austin AD, Fagan-Jeffries EP, Hebert PD, Butcher BA (2020) Recognition of the Trachypetidae stat. n. as a new extant family of Ichneumonoidea (Hymenoptera), based on molecular and morphological evidence. Systematic Entomology 45(4): 771–782. https://doi.org/10.1111/syen.12426

Rasnitsyn AP (1975) Hymenoptera Apocrita of Mesozoic. Transactions of the Palaeontological Institute Academy of Sciences of the USSR 147: 1–134. [In Russian]

Rasnitsyn AP (1983) Ichneumonoidea (Hymenoptera) from the lower Cretaceous of Mongolia. Contributions of the American Entomological Institute 20: 259–265.

Rasnitsyn AP (1988) An outline of evolution of the hymenopterous insects (order Vespida). Oriental Insects 22(1): 115–145. https://doi.org/10.1080/00305316.1988.11835485

Rasnitsyn AP (1990) Hymenoptera. In: Ponomarenko AG (Ed.) Late Mesozoic insects of Eastern Transbaikalian. Transactions of the Palaeontological Institute Academy of Sciences of the USSR 239: 177–205. [In Russian]

Santer M, Álvarez-Parra S, Nel A, Peñalver E, Delclòs X (2022) New insights into the enigmatic Cretaceous family Spathiopterygidae (Hymenoptera: Diaprioidea). Cretaceous Research 133: e105128. https://doi.org/10.1016/j.cretres.2021.105128

Spasojevic T, Broad GR, Sääksjärvi IE, Schwarz M, Ito M, Korenko S, Klopfstein S (2021) Mind the outgroup and bare branches in total-evidence dating: A case study of pimpliform Darwin wasps (Hymenoptera, Ichneumonidae). Systematic Biology 70(2): 322–339. https://doi.org/10.1093/sysbio/syaa079

Tobias VI (1963) Ichneumonidae (Hymenoptera) with a venation type in the fore wings which resembles that in Braconidae. Zoologicheskij Zhurnal 42: 1513–1522. [In Russian with English summary]

Tobias VI, Belokobylskij SA (1983) Aberrant wing venation in Braconidae (Hymenoptera) and its significance in study of the phylogeny of the family. Entomologicheskoe Obozrenie 62: 341–347. [In Russian]

Viertler A, Klopfstein S, Jouault C, Spasojevic T (2022) Darwin wasps (Hymenoptera, Ichneumonidae) in Lower Eocene amber from the Paris basin. Journal of Hymenoptera Research 89: 19–45. https://doi.org/10.3897/jhr.89.80163

Villanueva-Amadoz U, Pons D, Diez JB, Ferrer J, Sender LM (2010) Angiosperm pollen grains of San Just site (Escucha Formation) from the Albian of the Iberian Range (northeastern Spain). Review of Palaeobotany and Palynology 162(3): 362–381. https://doi.org/10.1016/j.revpalbo.2010.02.014

Wharton RA (1993) Bionomics of the Braconidae. Annual Review of Entomology 38(1): 121–143. https://doi.org/10.1146/annurev.en.38.010193.001005

Anexo 8.1.8

A new genus of setose-winged barklice (Psocodea: Trogiomorpha: Lepidopsocidae) from the Eocene amber of Oise with notes on the biogeography of Thylacellinae

Álvarez-Parra, S., Nel, A. 2022. A new genus of setose-winged barklice (Psocodea: Trogiomorpha: Lepidopsocidae) from the Eocene amber of Oise with notes on the biogeography of Thylacellinae. *Historical Biology*, 1-10.

DOI: https://doi.org/10.1080/08912963.2022.2081566

Revista científica: *Historical Biology*
Factor de impacto: 1,942 (2021)
Categoría: *Paleontology*, Q2 (2021)

Historical Biology
An International Journal of Paleobiology

Taylor & Francis
Taylor & Francis Group

Historical Biology
An International Journal of Paleobiology

ISSN: (Print) (Online) Journal homepage: https://www.tandfonline.com/loi/ghbi20

A new genus of setose-winged barklice (Psocodea: Trogiomorpha: Lepidopsocidae) from the Eocene amber of Oise with notes on the biogeography of Thylacellinae

Sergio Álvarez-Parra & André Nel

To cite this article: Sergio Álvarez-Parra & André Nel (2022): A new genus of setose-winged barklice (Psocodea: Trogiomorpha: Lepidopsocidae) from the Eocene amber of Oise with notes on the biogeography of Thylacellinae, Historical Biology, DOI: 10.1080/08912963.2022.2081566

To link to this article: https://doi.org/10.1080/08912963.2022.2081566

HISTORICAL BIOLOGY
https://doi.org/10.1080/08912963.2022.2081566

Taylor & Francis
Taylor & Francis Group

A new genus of setose-winged barklice (Psocodea: Trogiomorpha: Lepidopsocidae) from the Eocene amber of Oise with notes on the biogeography of Thylacellinae

Sergio Álvarez-Parra[a] and André Nel[b]

[a]Departament de Dinàmica de la Terra i de l'Oceà and Institut de Recerca de la Biodiversitat (IRBio), Facultat de Ciències de la Terra, Universitat de Barcelona, Barcelona, Spain; [b]Institut de Systématique, Évolution, Biodiversité (ISYEB), Muséum national d'Histoire naturelle, CNRS, Sorbonne Université, EPHE, Université des Antilles, Paris, France

ABSTRACT

The members of the family Lepidopsocidae (Psocodea: Trogiomorpha) are commonly known as scaly-winged barklice based on the presence of scales on body and wings. Interestingly, the members of the subfamily Thylacellinae, which is the sister group to the remaining members of the family, lack scales and are characterised by densely setose body and wings. We describe the thylacelline *Parathylacella oisensis* gen. et sp. nov. from the Eocene amber of Oise (France), corresponding to the only known fossil genus of the family. We compare it with the other genera in the subfamily. It shows a similar habitus to the genus *Thylacella*, and both may be closely related. The description of the new taxon increases the poorly known palaeodiversity of the lepidopsocids. We comment on the putative palaeobiology of this group and discuss new insights into the palaeobiogeography and early diversification of the subfamily Thylacellinae. An association between the thylacelline barklice and Detarieae (Fabaceae: Caesalpinioideae) trees is plausible. The biogeographic distribution might be partially explained by this association, combined with oceanic currents. Studies on Cretaceous lepidopsocids, as well as other Cenozoic specimens, are crucial to understand the evolution of this group over time, and the possible vicariance process.

ARTICLE HISTORY
Received 21 April 2022
Accepted 19 May 2022

KEYWORDS
Lepidopsocidae; Thylacellinae; amber; Eocene; Detarieae; biogeography

Introduction

Barklice are hemimetabolous insects with herbivorous or detritivorous feeding habits and a wide, cosmopolitan distribution, occupying diverse habitats (Smithers 1972; Mockford 1993; New and Lienhard 2007). They are usually considered one of the most important nutrient recyclers of organic matter within the forest litter faunas (New 1987). They belong to the order Psocodea together with the booklice and parasitic lice (Johnson et al. 2018; Yoshizawa et al. 2018; de Moya et al. 2021). The oldest psocodean fossil record is from the Carboniferous (Nel et al. 2013); nonetheless, the major diversification is known from the Cretaceous (Mockford et al. 2013; Álvarez-Parra et al. 2020, 2022). Trogiomorpha is the sister group to the remaining members within Psocodea (Yoshizawa et al. 2006). The trogiomorphan families †Cormopsocidae, Prionoglarididae, Psyllipsocidae, †Archaeatropidae, †Empheriidae, and Trogiidae were present during the Cretaceous (Álvarez-Parra et al. 2022), whereas to date, the families Psoquillidae and Lepidopsocidae have only been studied from Cenozoic ambers (Nel et al. 2005; Hakim et al. 2018b; Álvarez-Parra et al. 2022). The Eocene Oise amber is one of the most significant sources of information on Cenozoic psocids, as it has yielded numerous specimens belonging to 11 species in 10 families within the three psocodean suborders (Nel et al. 2005; Brasero et al. 2009).

Lepidopsocidae are commonly known as scaly-winged barklice based on the presence of scales on body and wings (Smithers 1972; Mockford 1993), a character that is also present in the troctomorphan Amphientomidae (Smithers 1990; New and Lienhard 2007). The members of the subfamily Thylacellinae are peculiar within Lepidopsocidae, as they are characterised by densely setose body and wings, lacking scales (Smithers 1972; Mockford 1993), which is considered a plesiomorphic character (Yoshizawa et al. 2006). The family Lepidopsocidae includes about 200 extant species, but its fossil and subfossil record is barely known, being represented by only three species belonging to Thylacellinae, two species belonging to Perientominae, and one species belonging to Lepidopsocinae (Hakim et al. 2018b). At least one Cretaceous lepidopsocid has been reported from the Campanian Tilin amber (Myanmar), but to date, it remains unstudied (Zheng et al. 2018).

Currently, the subfamily Thylacellinae encompasses the extant genus *Thylacella* Enderlein, 1911 and the subfossil genus *Thylax* Hagen, 1866 (Smithers 1972). Seventeen extant species are included in the genus *Thylacella*, besides one fossil species (*Thylacella eocenica* Nel, Prokop, de Ploëg and Millet, 2005) from Eocene Oise amber and one subfossil species (*Thylacella eversiana* Enderlein, 1911) from Quaternary Zanzibar copal (Enderlein 1911; Broadhead and Richards 1982; García-Aldrete 2001; Nel et al. 2005). *Thylax fimbriatum* Hagen, 1866 was also described from Quaternary Zanzibar copal (Hagen 1866). There are issues regarding the origin of the Zanzibar copal, as its provenance might be several places from East Africa (Delclòs et al. 2020; Solórzano-Kraemer et al. 2020). The genus *Notolepium* Enderlein, 1910 is controversial. Initially placed within the subfamily Perientominae (Smithers 1972), it includes two extant species, *Notolepium paraguayense* Enderlein, 1910 and *Notolepium brasiliense* New, 1975. However, Mockford (2005) has suggested that the latter might be assigned to the genus *Thylacella*, and even that the genus *Notolepium*

CONTACT Sergio Álvarez-Parra sergio.alvarez-parra@ub.edu Departament de Dinàmica de la Terra i de l'Oceà and Institut de Recerca de la Biodiversitat (IRBio), Facultat de Ciències de la Terra, Universitat de Barcelona, c/ Martí i Franquès s/n, Barcelona 08028, Spain

Published online 01 Jun 2022

should be transferred to the subfamily Thylacellinae. Based on the lack of scales, the main characteristic of the Thylacellinae, we agree with Mockford (2005) on the transfer of *Notolepium* to this subfamily, although a detailed review of these species would be required.

Here, we describe a new genus and species of barklice from the Eocene amber of Oise. It is assigned to the subfamily Thylacellinae within the family Lepidopsocidae (Trogiomorpha). We discuss its taxonomic placement and compare its habitus with that of the other thylacelline genera. We also delve into the palaeobiology and biogeography of the subfamily.

Material and methods

The specimen studied here is included in an amber piece from Le Quesnoy outcrop, near Creil (Houdancourt village), in Oise Department (Hauts-de-France, France). Commonly known as Oise amber, the amber from this outcrop is found in a layer of thick brown sand (Nel and Brasero 2010). The palaeoenvironment has been inferred as a forest in a fluvio-lacustrine setting formed by a fluvial system with multiple channels and ponds, without apparent marine influence, and under a warm and wet seasonal climate (Nel et al. 2004). The diverse record of fossil vertebrates (including bones, teeth, and coprolites) recovered from the layer has enabled us to correlate it with the earliest Eocene reference locality (MP7) of Dormaal (Belgium) (Nel et al. 1999, 2004). The outcrop is dated as Sparnacian (Ypresian) in the earliest Eocene, c. 53 Ma (Nel et al. 1999, 2004; Nel and Brasero 2010). The Oise amber is usually yellowish and translucent, and it has yielded an enormous collection of more than 20,000 bioinclusions, including at least 17 insect orders, mites, spiders, pseudoscorpions, mammalian hairs and bird feathers (Nel et al. 2004; Brasero et al. 2009). The wood structure of the resin-producing tree is very similar to that of the extant genus *Daniellia* within the tribe Detarieae (Fabaceae: Caesalpinioideae), based on amber pieces associated with wood fragments (de Franceschi and de Ploëg 2003; Nel and Brasero 2010). This result is supported by geochemical analyses of the amber, which shows affinities with the subfamily Caesalpinioideae within the family Fabaceae (Nohra et al. 2015). The outcrop does not present the characteristics of an autochthonous amber site (Álvarez-Parra et al. 2021), as amber, plant, and vertebrate macro-remains show evidence of at least local transport, while carbonised wood could have undergone lengthy transport (Nel et al. 2004). Therefore, the Oise amber might be related to a combination of parautochthonous and allochthonous pieces.

After submersion in a dilution of sugar and water to improve visualisation, the studied specimen was photographed using a Nikon D800 digital camera attached to a Nikon SMZ25 stereomicroscope. The photographs were processed using Capture NX-D software, version 1.5.3. The software Helicon Focus 7.6.1 was used to stack and compile the photographs. The drawings were produced using a Leica M205 C stereomicroscope with a camera lucida. The figures were prepared using Adobe Photoshop CS6. The anatomical nomenclature follows the works of Smithers (1972) and Mockford (1993). The holotype specimen is housed at the Oise amber collection of the Muséum national d'Histoire naturelle (Paris, France) under the number MNHN-F.A71357.

Systematic palaeontology

Order **Psocodea** Hennig 1966

Suborder **Trogiomorpha** Roesler, 1940

Infraorder **Atropetae** Pearman 1936

Family **Lepidopsocidae** Enderlein 1903

Subfamily **Thylacellinae** Roesler 1944

Genus Parathylacella *Álvarez-Parra and Nel gen. nov.*

Type species: *Parathylacella oisensis* sp. nov., by present designation and monotypy, known exclusively from the Eocene amber of Oise (France).

LSID: urn:lsid:zoobank.org:act:6540C02C-6762-4D7C-BFBD-11A77BBB3B0D

Etymology

Name formed by 'para-', from the Greek παρά- (meaning 'beside', 'next to', or 'near'), and '*Thylacella*', type genus of the subfamily Thylacellinae. The name is feminine.

Diagnosis

Antennae with 21 flagellomeres; forewing: about 3.2× longer than wide, slightly pointed apex, costal and radial margin glabrous, rest of margin and membrane setose, basal section of Rs present, M_3 emerging far from bifurcation of Rs+M and nearly at the same level as crossvein r-rs; hind wing: margin setose, membrane mostly glabrous, closed basal cell, R_1 emerging slightly distal to the apex of basal cell, M_1 and M_2 arising together and bifurcating far from basal cell; two pretarsal claws lacking preapical teeth and pulvillus.

Parathylacella oisensis *Álvarez-Parra and Nel sp. nov.*

Figures 1–4

LSID: urn:lsid:zoobank.org:act:8D383BEE-9E55-4E41-BB80-13A47523A583

Type material

Holotype MNHN-F.A71357, adult specimen, sex unknown. A complete barklouse in a yellow, translucent amber piece measuring around 15 × 10 × 4 mm, with a partial *Thylacella eocenica* (Psocodea: Trogiomorpha: Lepidopsocidae) as syninclusion. Amber piece housed at the Oise amber collection of the Muséum national d'Histoire naturelle, Paris, France.

Locality and horizon

Le Quesnoy outcrop, near Creil, in Oise Department (Hauts-de-France, France), geologically corresponding to the Paris Basin (Nel et al. 1999, 2004; Nel and Brasero 2010). The amber-rich stratigraphic layer is thick brown sand from the lowermost Eocene, Sparnacian (Ypresian), c. 53 Ma, correlated with the MP7 mammal fauna of Dormaal (Belgium) (Nel et al. 1999, 2004; Nel and Brasero 2010).

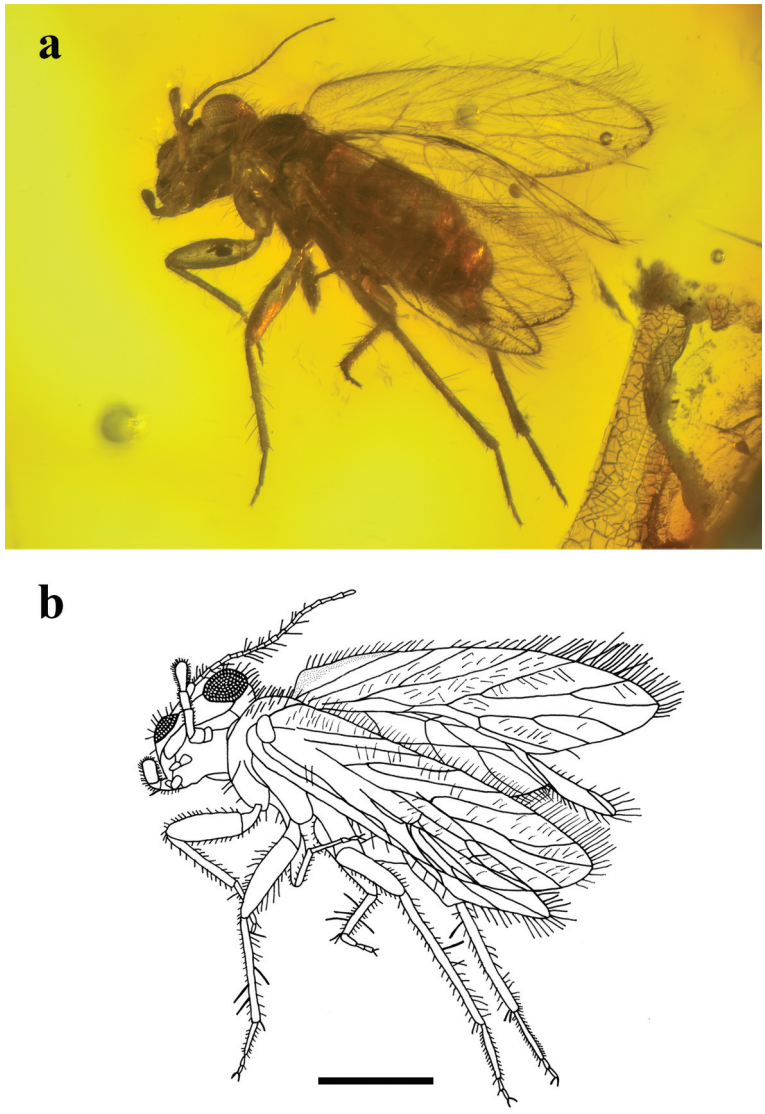

Figure 1. *Parathylacella oisensis* gen. et sp. nov. (Psocodea: Trogiomorpha: Lepidopsocidae), Eocene amber of Oise (France), holotype MNHN-F.A71357. (a) Photograph. (b) Drawing. Both in latero-dorsal view and at same scale. Scale bar: 0.5 mm.

Etymology

After Oise, the place that gives its name to the amber which yielded the type specimen.

Diagnosis

As for the genus.

Description

Body length 1.66 mm from clypeus to genitalia (Figure 1 and Figure 2). Body covered by fine hairs. Head nearly as long as wide (Figure 3 (a, b)), 0.43 mm and 0.40 mm, respectively, covered by setae; broad vertex 0.30 mm wide with punctured microsculpture; marked epicranial suture, indistinct anterior arms; three ocelli set close together, forming an inverted triangle (Figure 3(a)); anterior ocellus slightly smaller than the others; setose, prominent compound eyes 0.17 mm in diameter; left antenna with 19 flagellomeres (Figure 3(c)); right antenna with 21 flagellomeres; scape 0.07 mm long; pedicel 0.06 mm long; all flagellomeres of similar length, about 0.05 mm, distal ones narrower than proximal; proximal flagellomeres with long setae, whereas distal flagellomeres with a few fine hairs; flagellomeres not secondarily annulated; setose, bulging clypeus; maxillary palps four-segmented (Figure 3(b)), covered by fine hairs; length of maxillary palpomeres: I 0.06 mm, II 0.15 mm, III 0.08 mm, IV 0.13 mm; conical sensillum on second palpomere; distal palpomere with hatchet-shaped apex; labial palps two-segmented (Figure 3(b)), covered by fine hairs; length of labial palpomeres: I 0.05 mm, II 0.04 mm; lacinia not visible. Thorax 0.48 mm long; setose, bulging pronotum; macropterous, wings completely preserved. Forewing 1.47 mm long and 0.45 mm maximum wide (Figure 4(a, b)), about 3.2× longer than wide; slightly pointed apex; membrane hyaline and covered by numerous setae; punctured microsculpture in anal region; costal and radial margin glabrous, rest of margin setose; longest setae on medial margin; basal section of Sc evanescent, straight and long, curved distally, reaching margin at 0.72 mm from wing base; distal section of Sc sigmoidal, reaching margin at 0.89 mm from wing base; R_1 straight, reaching margin at 1.09 mm from wing base; basal section of Rs present; short crossvein r-rs 0.03 mm long; bifurcation of Rs into R_{2+3} and R_{4+5} at 0.98 mm from wing base; straight R_{2+3} reaching margin at 1.22 mm from wing base; curved R_{4+5} reaching margin at 1.35 mm from wing base; bifurcation of Rs and M at 0.66 mm from wing base; bifurcation of M into M_1 and M_2 at 1.13 mm from wing base, reaching margin at 1.45 mm and 1.34 mm from wing base,

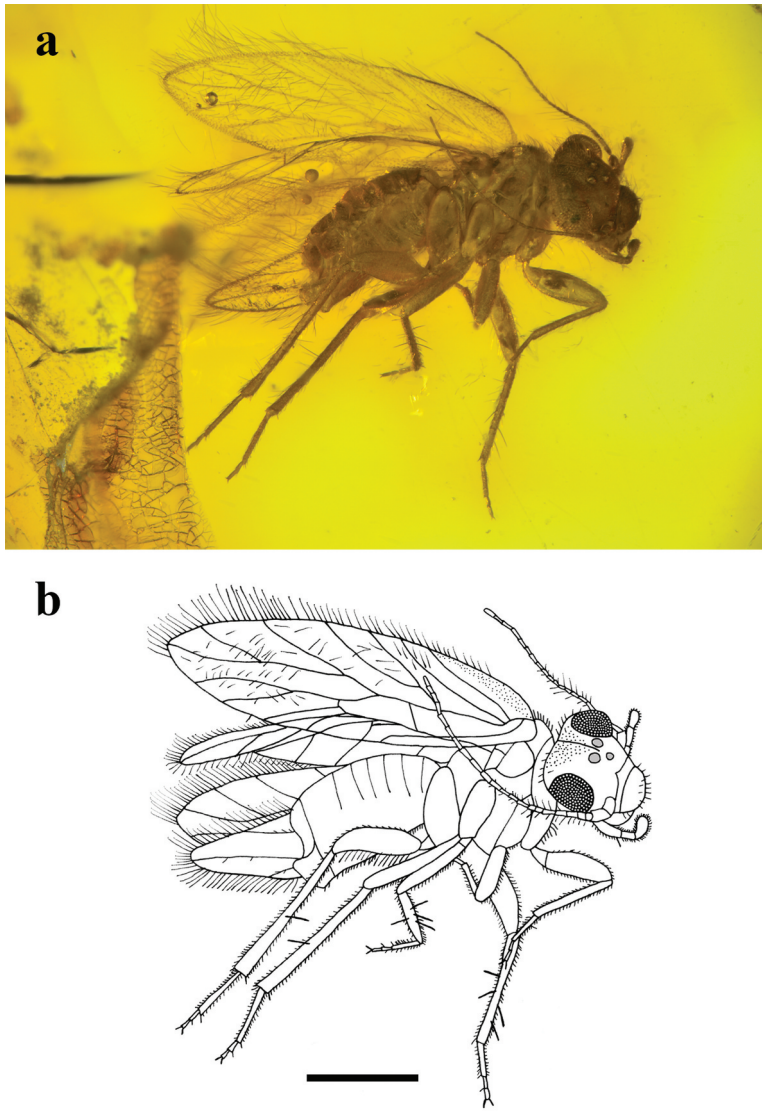

Figure 2. *Parathylacella oisensis* gen. et sp. nov. (Psocodea: Trogiomorpha: Lepidopsocidae), Eocene amber of Oise (France), holotype MNHN-F.A71357. (a) Photograph. (b) Drawing. Both in lateral view and at same scale. Scale bar: 0.5 mm.

respectively; M_1 reaching margin slightly below wing apex; M_3 emerging far from bifurcation of Rs+M and nearly at same level as crossvein r-rs; distance of 0.14 mm from bifurcation of Rs and M to emergence of M_3; M_3 reaching margin at 1.15 mm from wing base; bifurcation of Cu_1 into Cu_{1a} and Cu_{1b} at 0.49 mm from wing base; long and narrow areola postica; Cu_{1a} reaching margin at 0.98 mm from wing base; Cu_{1b} reaching margin at 0.76 mm from wing base; Cu_2 straight, reaching margin at 0.67 mm from wing base; anal vein evanescent and parallel to Cu_2, reaching margin at 0.48 mm from wing base. Hind wing 1.38 mm long and 0.31 mm maximum wide (Figure 4(a, c)); acute apex; membrane hyaline and mostly glabrous, only a few setae along some veins; margin setose; Sc not visible; basal cell closed, narrow and elongate, 0.20 mm long and 0.03 mm wide; R_1 emerging slightly distal to apex of basal cell; R_1 reaching margin at 0.88 mm from wing base; R_{2+3} reaching margin at 1.16 mm from wing base; R_{4+5} reaching margin at wing apex; short fusion of Rs+M 0.06 mm long; bifurcation of M into M_1 and M_2 far from basal cell, about 0.90 mm from wing base, arising together from Rs+M; M_1 reaching margin at 1.17 mm from wing base; M_2 reaching margin at 1.01 mm from wing base; curved Cu_1 and Cu_2; anal vein not visible. Legs covered by fine hairs, with thick femora and thin tibiae; four long, straight spurs nearly at the middle of mid tibia (Figure 3(d)); one long, straight spur nearly at the middle of hind tibia; two short spurs on apical mid and hind tibiae; three tarsomeres (Figure 3(d, e)); length of tarsomeres in foreleg: I 0.14 mm, II 0.05 mm, III 0.05 mm; length of tarsomeres in mid leg: I 0.15 mm, II 0.04 mm, III 0.05 mm; length of tarsomeres in hind leg: I 0.25 mm, II 0.06 mm, III 0.05 mm; distal tarsomeres bearing two pretarsal claws without preapical tooth or pulvillus (Figure 3(d, e)). Abdomen 0.82 mm long; several segments visible dorsally; genitalia not well visible hindered by hind wing and hind leg, sex unknown.

Discussion

Taxonomy

The studied specimen falls within the suborder Trogiomorpha based on the antennae with more than 20 flagellomeres (21 flagellomeres on right antenna), labial palps with minute proximal segment and rounded or somewhat elongate distal segment, macropterous, pterostigmal area not coloured (coloured only in †Cormopsocidae and in the psyllipsocid *Annulipsyllipsocus*

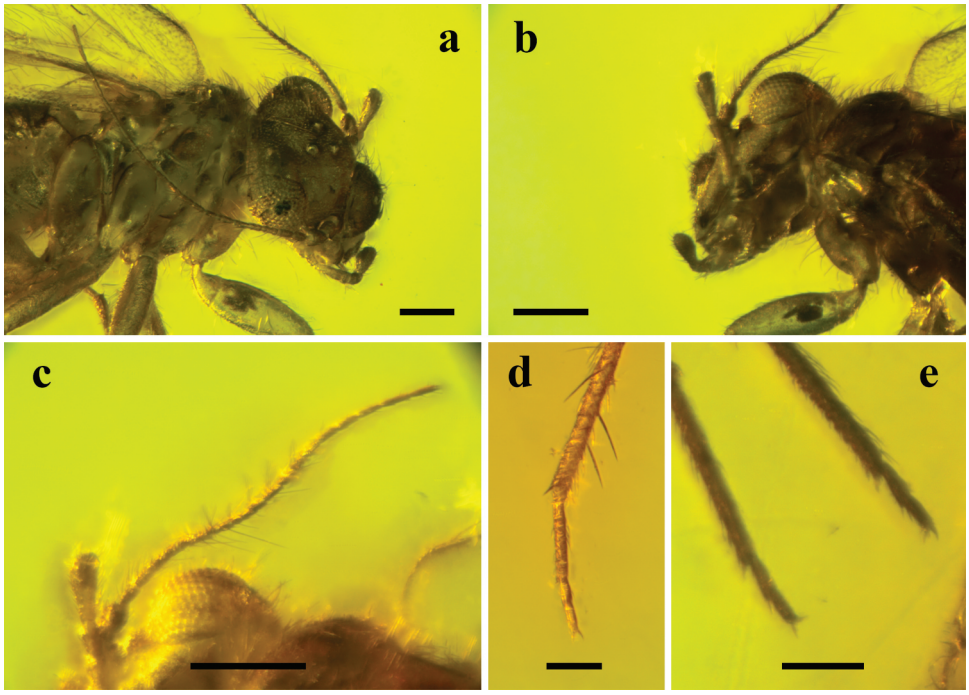

Figure 3. *Parathylacella oisensis* gen. et sp. nov. (Psocodea: Trogiomorpha: Lepidopsocidae), Eocene amber of Oise (France), holotype MNHN-F.A71357. (a) Head in latero-dorsal view. (b) Head in ventral view. (c) Left antenna. (d) Right mid leg. (e) Hind tarsi. Scale bars: 0.2 mm (a–c), and 0.1 mm (d, e).

inexspectatus Hakim et al. 2018a) and presence of three tarsomeres (Smithers 1972; Mockford 1993; Yoshizawa et al. 2006). It belongs to the infraorder Atropetae based on the presence of a conical sensillum on second maxillary palpomere and forewing without nodulus (only present in family †Archaeatropidae) (Smithers 1972; Mockford 1993; Yoshizawa et al. 2006). It is assigned to the family Lepidopsocidae based on densely setose body and wings, flagellomeres lacking secondary annulations, acuminate forewings, well-developed Sc, presence of r-rs cross-vein, Rs and M fused for a length, M branching near separation from Rs, and bifurcation of Cu_1 near to wing base, forming a long and narrow areola postica (Smithers 1972; Mockford 1993). The ocelli of lepidopsocids are usually widely separated (Smithers 1972), whereas they are close together in the studied specimen (Figure 3(a)). Interestingly, Smithers (1972) indicated for Lepidopsocidae that the hind wing has two M veins arising separately, while Mockford (1993) noted that they can also arise together. In the specimen MNHN-F.A71357, both M veins arise together from Rs+M (Figure 4(c)). Smithers (1972) pointed out the presence of claws with a strong apical curvature and at least one preapical tooth and pulvillus as characteristic for Lepidopsocidae. Nonetheless, the studied specimen lacks both preapical tooth and pulvillus (Figure 3(d,e)). Following the keys of Smithers (1990), the studied specimen would also be identified as a lepidopsocid based on the following characters: body and wings without flattened scales, distal flagellomeres without secondary annulations, second maxillary palpomere with a conical sensillum, macropterous, forewing apically pointed, forewing venation complex, pterostigmal area no more opaque than rest of membrane, no nodulus and three tarsomeres. The only character that indicates Lepidopsocidae but is absent in the studied specimen is the presence of a preapical tooth on pretarsal claws.

The presence of scales on the body surface and wings is distinctive of the Lepidopsocidae, except in the subfamily Thylacellinae, which is densely setose on the body surface and wings alike (Smithers 1972; Mockford 1993). Therefore, the studied specimen is identified as belonging to the Thylacellinae. The genus *Notolepium* has ocelli set relatively far apart (vs. close together), a slender forewing narrowing apically and ending in an acuminate point (vs. forewing not narrow apically), R_{4+5} that reaches the forewing margin at the apex (vs. R_{4+5} not reaching the apex), and pretarsal claws with one preapical tooth and three basal setae, but no pulvillus (vs. pretarsal claws without preapical tooth or pulvillus) (New 1975; Mockford 2005). *Thylax fimbriatum* was poorly described, and it seems to show a similar wing venation to *Thylacella*, although it has 40 antennomeres (Hagen 1866; Smithers 1972). It differs from the three genera in crucial characters; thus, we establish *Parathylacella oisensis* gen. et sp. nov. Peculiar characters such as 'proximal flagellomeres with long setae, while distal flagellomeres with few and short setae', 'three ocelli set close together, forming an inverted triangle and anterior ocellus slightly smaller than the others', 'four long, straight spurs nearly at the middle of mid tibiae', 'one long, straight spur nearly at the middle of hind tibiae', and 'two distal spurs on mid and hind tibiae' could be included in the diagnosis of the genus. Nonetheless, they might be related to inter- or intraspecific variability or even sexual dimorphism. Furthermore, they might not be observed in other specimens due to preservation. Therefore, we prefer to avoid their inclusion in the diagnosis until new specimens with a similar habitus are found.

Parathylacella oisensis resembles the *Thylacella* species, but several key differences support the description of a new genus. The characters of *Thylacella* species that differ from those of *Parathylacella oisensis* are (Enderlein 1911; Badonnel 1955, 1967; Smithers 1972; New 1975, 1976; Broadhead and Richards 1982; García-Aldrete 2001; Mockford 2005): ocelli widely spaced (vs. ocelli close together), forewing margin setose (vs. costal and radial margin glabrous), forewing M_3 emerging near bifurcation of Rs and M (vs. M_3 emerging far from bifurcation of Rs+M), hind wing membrane setose (vs. membrane mostly glabrous), hind wing M_1 and M_2 arising separately from Rs+M or together, but bifurcating close to basal cell (vs. M_1 and M_2 arising together and bifurcating

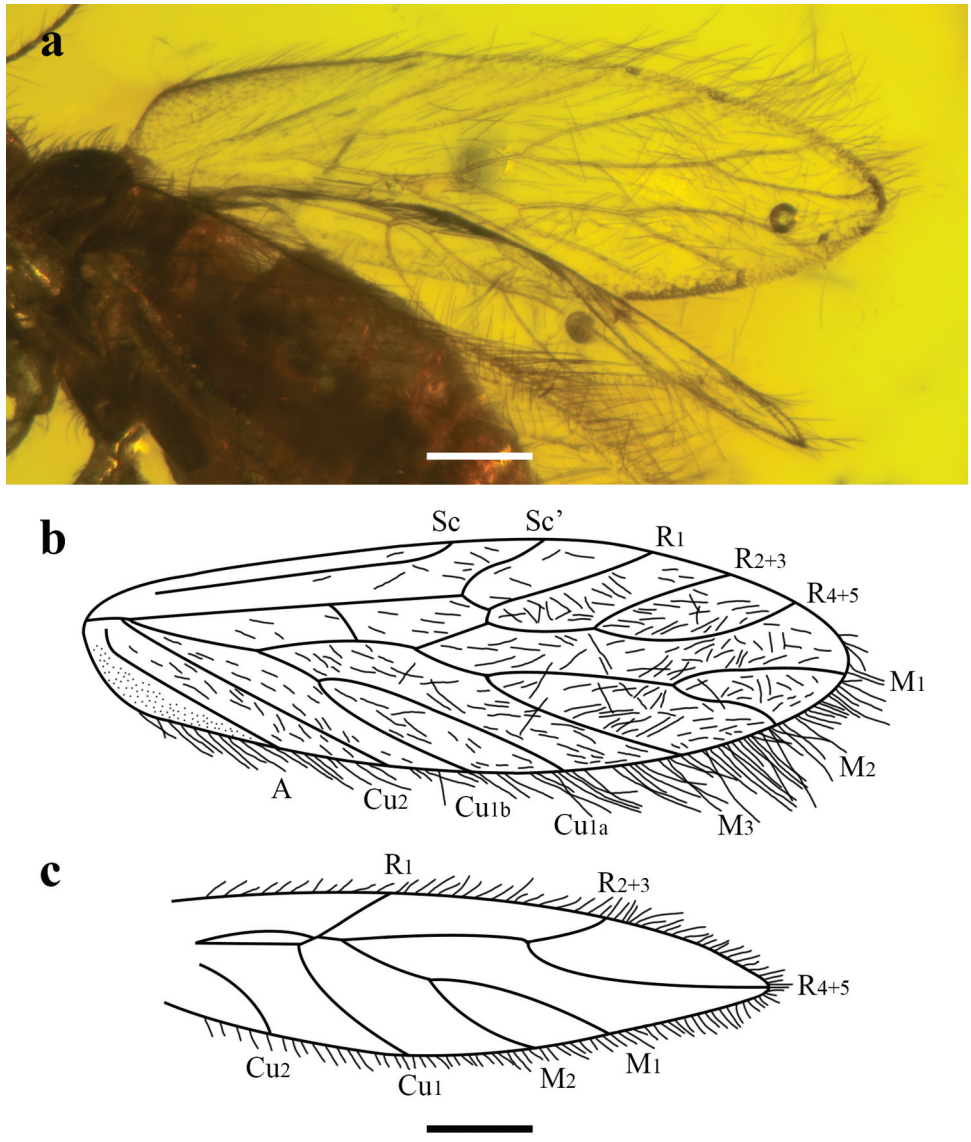

Figure 4. *Parathylacella oisensis* gen. et sp. nov. (Psocodea: Trogiomorpha: Lepidopsocidae) from the Eocene amber of Oise (France), holotype MNHN-F.A71357. (a) Photograph of right wings, the forewing is inverted. (b) Drawing of forewing. (c) Reconstructed drawing of hind wing. All at same scale. Scale bars: 0.2 mm.

far from basal cell), and pretarsal claws with two preapical teeth and pulvillus fairly broad (vs. pretarsal claws without preapical teeth or pulvillus, although *T. trifurcata* has a very small first preapical tooth and *T. huautlensis* García-Aldrete, 2001 has only one tooth). Forewings of *Thylacella* species are usually rather acuminate and distally narrow (Enderlein 1911; Badonnel 1955, 1967, 1976; García-Aldrete 2001), but *Parathylacella oisensis* has forewing apex only slightly pointed. Mockford (1993) noted that the *Thylacella* species have at least 26 flagellomeres, although there are some exceptions (e.g., Nel et al. 2005). We believe that these differences are sufficiently significant to support the description of a new genus within Thylacellinae, since the forewing margin not setose on costal and radial margin and only slightly pointed apex (not acuminate) are key characteristics of *Parathylacella* gen. nov. We do not think that the absence of setae on costal and radial margin is due to preservation artefact, as it would be a great coincidence the absence on the same margins of both forewings. In *Thylacella* species, marginal setae on costal and radial margins are nearly as long and numerous as those on medial and anal margins. Furthermore, a few isolated setae can be seen around the new specimen, but not the quantity that would be expected to find in case they would have fallen off at the time of resin inclusion. Mockford (1993) indicated 'forewing length about 4.1× forewing width' for Thylacellinae (considering *Thylacella* species), while forewings of *Parathylacella oisensis* are about 3.2× longer than wide. The character 'M_3 arising near separation of M from Rs and Cu_1' in forewing is crucial in the genus *Thylacella* (Smithers, 1972). In the new specimen, M_3 emerges far from the base of M. We note here how longer is the distance of M from the emerging of M_3 to bifurcation of M_1 and M_2 in relation to the distance from the base of M to the emerging of M_3 in some *Thylacella* species and the studied specimen (higher proportion indicates that the emerging of M_3 is closer to the base of M): 4.7× (*T. fasciifrons*♀), 3.6× (*T. fasciifrons*♂), 4.5× (*T. fasciata*♀), 7.2× (*T. huautlensis*♀), 3.8× (*T. angulifrons*♀), 7.2× (*T. similis*♀), 3.4× (*T. eversiana*♀), 12.7× (*T. eocenica*♀), 2.4× (*Parathylacella oisensis*). The proportion in *Parathylacella oisensis* is even less than 3×, and therefore M_3 emerges rather further from base of M than in the *Thylacella* species (Enderlein 1911; Badonnel 1955, 1967, 1976; García-Aldrete 2001; Nel et al. 2005). The arrangement of M in hind wing of

Parathylacella oisensis (M_1 and M_2 arising together and bifurcating far from basal cell) is clearly different to that of the *Thylacella* species. We consider that all of these differences are quite important, and they cannot be related to intraspecific or intrageneric variability.

Furthermore, the previously described lepidopsocid species from Eocene Oise amber (Nel et al. 2005), *Thylacella eocenica* shows different characters in comparison with *Parathylacella oisensis*, such as 22 flagellomeres (vs. 21 flagellomeres), forewing margin completely setose (vs. not setose on costal and radial margin), forewing M_3 arising just next to the emergence of M from Rs+M (vs. M_3 emerging far from bifurcation of Rs+M), hind wing membrane setose (vs. not setose), hind wing R_1 emerging from the apex of basal cell (vs. R_1 emerging slightly distal to basal cell), hind wing M_1 and M_2 arising separately (vs. M_1 and M_2 arising together) and pretarsal claws with a single small preapical tooth (vs. pretarsal claws without preapical tooth). The two diagnostic characters of *T. eocenica* (hind wing R_1 emerging at apex of basal cell and antennae with 24 segments) are not present in the studied specimen.

Palaeobiology and biogeography of Thylacellinae

The extant species within the family Lepidopsocidae are usually members of the forest litter fauna, associated with dead vegetation, rotten wood, or under stones, but also living under tree bark, on mosses and epiphytes, in bird nests, and in domestic habitats (Smithers 1972; New 1987; Mockford 1993; New and Lienhard 2007). A peculiar lepidopsocid species is the aberrant *Parasoa haploneura* Thornton, 1962, which inhabits the Malaysian Batu caves (Thornton 1962) and was transferred to its own subfamily (Mockford 2005). Regarding the setose-winged Thylacellinae, Smithers (1972) indicated that *Notolepium paraguayense* is found under bark, whereas *Thylacella* species are considered leaf litter dwellers, although they may also be present on tree trunks and branches, and some species even inhabit bird nests (Smithers 1972; Mockford 1993). The putative biology of the extinct *Thylax fimbriatum* and *Thylacella eversiana* from Zanzibar copal is unknown (Smithers 1972), although they may have occupied similar habitats to those of the other members of the family. The lepidopsocids from Oise amber may also have lived in the forest litter, together with psocids from other families, forming a diverse barklice litter fauna (Nel et al. 2005; Solórzano Kraemer et al. 2018). Interestingly, undescribed lepidopsocid specimens from Oise amber present characters similar to those typical of *Thylacella eocenica* (S.Á.-P. pers. obs.); thus, the habitus of the holotype of *Parathylacella oisensis* is unique in the Oise amber to date. Furthermore, the amber piece containing the studied specimen also has a partially preserved specimen of *T. eocenica*. Therefore, it is plausible that both lepidopsocid species shared the same habitat without niche competition.

Today, the representatives of the subfamily Thylacellinae show mainly Afrotropical and Neotropical distributions (Figure 5). Most of the known *Thylacella* species are present in Madagascar and continental eastern Africa (Kenya, Tanzania, Zimbabwe, and Mozambique), and a few species can also be found in western Africa (Togo, Nigeria, Congo, and Angola) (Smithers 1972). Interestingly, two *Thylacella* species have been described from America (Mockford 1993; García-Aldrete 2001). *Thylacella cubana* (Banks, 1941) is distributed throughout Mexico, southern Texas, Guatemala, Belize, Cuba, and the southern two-thirds of Florida (Mockford 1993). This species is even found on several islands off the Pacific coast of Mexico (García-Aldrete 1986; García-Aldrete et al. 1992). The controversial genus *Notolepium*, a putative member of Thylacellinae, has a peculiar distribution as it is present in the interior of South America, throughout Paraguay and in the Brazilian

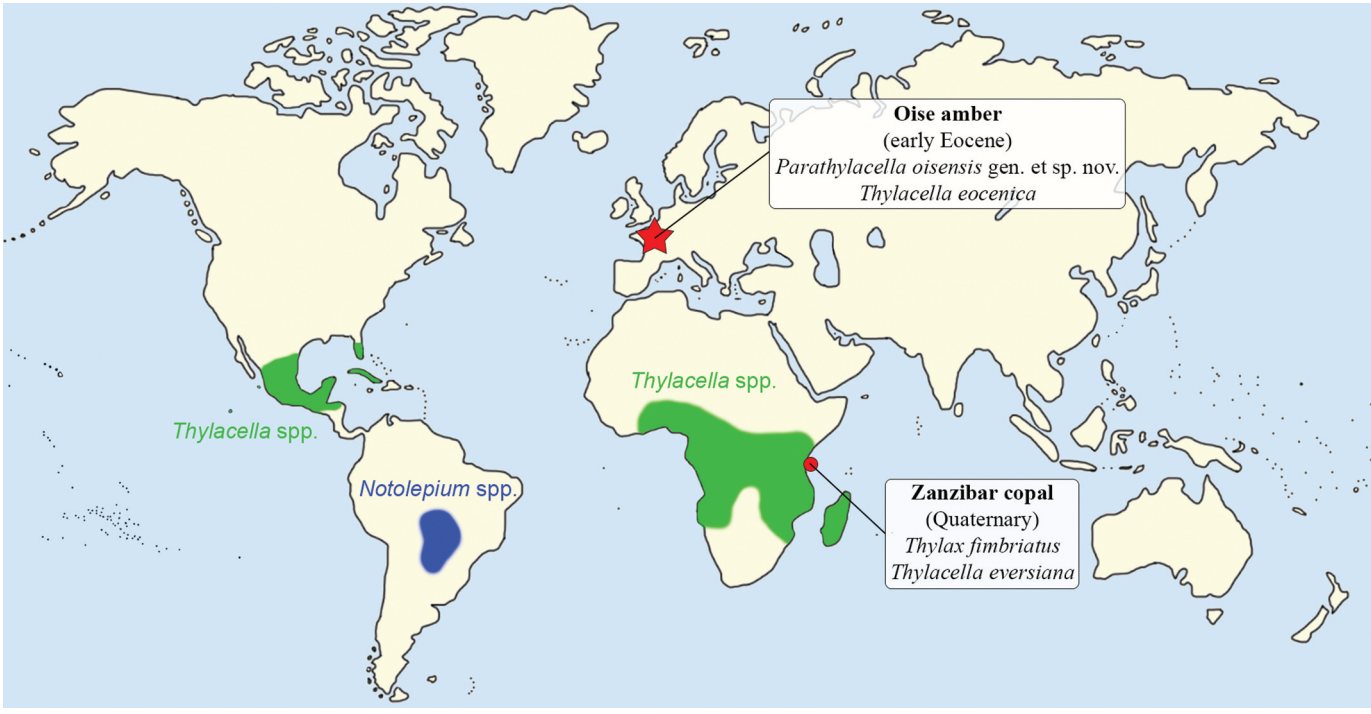

Figure 5. Approximate biogeographic distribution of representatives of Thylacellinae (Psocodea: Trogiomorpha: Lepidopsocidae) based on bibliographic information, and locations of known fossil and subfossil species of this subfamily. The two extant genera are *Thylacella* (green) and *Notolepium* (blue). The latter is putatively assigned to Thylacellinae.

region of Mato Grosso (Mockford 2005; García Aldrete and Mockford 2009). Broadhead and Richards (1982) suggested that *T. cubana* might have been introduced; however, the discovery of another *Thylacella* species in Mexico (García-Aldrete 2001) and the putative assignation of *Notolepium brasiliense* to the genus *Thylacella* (Mockford 2005) would indicate that this genus is also native of several regions in America.

One explanation for the biogeographic distribution of the subfamily might be vicariance (Wiley 1988). Thus, it is possible that the older members of Thylacellinae showed a wider distribution in the deep past, maybe even during the Cretaceous, at the time when America separated from Eurasia and Africa. The presence of *Thylacella eocenica* and *Parathylacella oisensis* in the Eocene Oise amber from Europe reinforces this hypothesis of an ancient wide distribution (Figure 5). Furthermore, it would also be supported by the divergence dates for the separation between Trogiidae and Lepidopsocidae, estimated in a range of 233.8–92.1 Ma (Yoshizawa et al. 2019). Nonetheless, a second hypothesis might arise to explain the biogeography of the extant Thylacellinae. The distribution of the resiniferous angiosperm *Hymenaea* (Fabaceae: Caesalpinioideae: Detarieae) trees is peculiar, as the species considered the most ancient in the genus is present in Madagascar and eastern Africa, whereas the other 13 species are Neotropical (Poinar and Brown 2002; Langenheim 2003). It is plausible that *Hymenaea* remains and *Hymenaea*-associated insects could have been transported from eastern Africa to South and Central America via oceanic currents (Peris et al. 2015). South Atlantic oceanic currents have changed little since the late Oligocene (Lawver and Gahagan 2003; Beal et al. 2011). Several previous studies have noted the similarities between Caribbean and African insect faunas (e.g., Bright 1972; Liebherr 1988; Cognato 2013; Peris et al. 2015). Therefore, if we assume a *Hymenaea* association for the Thylacellinae, the species belonging to this subfamily from South and Central America could have colonised these areas since late Oligocene after transport on *Hymenaea* or other wood remains from eastern Africa via oceanic currents along the coast of eastern and southern Africa and in the South Atlantic Ocean (Peris et al. 2015; van Sebille et al. 2020). The habitat of these barklice on tree trunks and branches or under bark would have facilitated their survival during a journey on buoyant wood remains. Thornton et al. (1988) indicated that the Lepidopsocidae are the most frequent barklice among the coastal trees 'facing directly on to a beach' in the Krakatau islands, strongly suggesting colonisation by sea.

Nevertheless, an association with *Hymenaea* cannot explain the entire extant distribution of Thylacellinae, as in the Afrotropical region, these trees only occupy areas of eastern Africa, but Thylacellinae species are present in both eastern and western Africa. The plant genus *Guibourtia*, closely related to *Hymenaea*, shows a distribution throughout regions of western Africa and America (Tosso et al. 2018). To date, no specimens belonging to Thylacellinae have been found in Miocene Mexican or Dominican ambers. The resin-producing tree of Oise amber has been related to the subfamily Caesalpinioideae (family Fabaceae) based on geochemical analyses (Nohra et al. 2015), and more specifically, on the wood structure very similar to that of the genus *Daniellia* (de Franceschi and de Ploëg 2003). Interestingly, *Daniellia, Guibourtia*, and *Hymenaea* belong to the tribe Detarieae (Fabaceae: Caesalpinioideae), which suggests an association between thylacelline barklice and Detarieae plants over the course of more than 50 million years. It is also important to mention the boreo-tropical corridor hypothesis to explain the possible dispersion of tropical groups from the Palaeotropical realm to the Neotropical realm via Eurasia during the Palaeocene–Eocene thermal maximum (PETM) (Wolfe 1985; Lavin and Luckow 1993). This was an episode of global warming when the rainforests expanded into high latitudes (Secord et al. 2010; Huurdeman et al. 2021). The presence of Thylacellinae species in Eocene Oise amber would be compatible with this hypothesis, indicating the expansion of these barklice to high latitudes. Later, a contraction in rainforest distribution due to cooling episode(s) would have caused a vicariance process, with the extinction of representatives of the subfamily in higher latitudes. Other two hypotheses that might explain peculiar distribution of barklice are transport on migrating birds (Mockford 1967) and transport by floating in wind currents (Glick 1957). Thylacellines are sometimes found in bird nests (Smithers 1972), so it would be plausible that they are also attached to feathers of living birds, explaining their presence in islands off the coast (García-Aldrete 1986; García-Aldrete et al. 1992). Nonetheless, thylacellines have not been reported from bird feathers or at high altitudes so far (Glick 1957; Mockford 1967, 2012). Here, we have made a first approximation for understanding of the biogeographic distribution of the members of Thylacellinae, but taxonomic and ecological studies together with phylogenetic analyses may provide more conclusive data on this matter.

The palaeoenvironmental conditions of the Oise amber, inferred as a warm and wet seasonal climate (Nel et al. 2004), are similar to those of the regions inhabited by extant Thylacellinae species (Peel et al. 2007). The discovery of *Thylax fimbriatum* and *Thylacella eversiana* in Zanzibar copal (Hagen 1866; Enderlein 1911) demonstrates that the East African Thylacellinae have inhabited the same area for at least a few thousand years.

Conclusions

The description of *Parathylacella oisensis* gen. et sp. nov. increases the scarcely known palaeodiversity of Thylacellinae and Lepidopsocidae. Furthermore, it is the only known fossil genus of the family, the holotype of *Thylax fimbriatum* being considered a subfossil as it is included in Quaternary Zanzibar copal. Despite the key differences between *Parathylacella* gen. nov. and *Thylacella*, both genera share a similar morphology; therefore, they may be closely related, and in a basal position, within Lepidopsocidae. A phylogenetic analysis of the Thylacellinae and a restudy of the holotypes of the *Notolepium* species and *Thylax fimbriatum* would help to resolve their relationships within the subfamily. Based on the known fossil record of lepidopsocids, it is possible that the members of Thylacellinae showed an early diversification during the Eocene, and maybe even during the Cretaceous, while the more derived scaly-winged barklice thrived later. A taxonomic study of Lepidopsocidae from Cretaceous and other Cenozoic ambers is required to advance further in our understanding of the evolution of this family. The biogeographic distribution of the Thylacellinae species might be the result of vicariance (during the Cretaceous or Palaeogene) or might partially be explained by an association with *Hymenaea* and related trees (within the tribe Detarieae) combined with oceanic circulation.

Acknowledgments

We thank Corentin Jouault for his technical help at the Muséum national d'Histoire naturelle (Paris, France) and Frédérick Legendre for access to the camera lucida. We are grateful to David Peris for discussion on insect biogeography. We also thank the comments of two anonymous reviewers, which have improved the manuscript. This study is a contribution to the project CRE CGL2017-84419 funded by the Spanish AEI/FEDER and the EU. It is part of the Ph.D. Thesis by S.Á.-P., who would also like to thank his supervisors Xavier Delclòs and Enrique Peñalver for their comments on the first draft of the manuscript.

Disclosure statement

No potential conflict of interest was reported by the author(s).

Funding

This study is the result of a research stay by S.Á.-P. at the Muséum national d'Histoire naturelle, funded by the project CRE CGL2017-84419 (Spanish AEI/FEDER and the EU) and a grant from the Fundació Montcelimar (Universitat de Barcelona, Spain). The first author, S.Á.-P., is the beneficiary of a grant from the Secretaria d'Universitats i Recerca de la Generalitat de Catalunya (Spain) and the European Social Fund (2021FI_B2 00003).

ORCID

Sergio Álvarez-Parra http://orcid.org/0000-0002-0232-1647
André Nel http://orcid.org/0000-0002-4241-7651

Data availability statement

The amber piece containing the type specimen studied here is housed at the Oise amber collection of the Muséum national d'Histoire naturelle (Paris, France), under the number MNHN-F.A71357. This manuscript has been registered in ZooBank under the number urn:lsid:zoobank.org:pub:F4B0CCCC-8A2D-4D8B-A251-0010899B58ED.

References

Álvarez-Parra S, Peñalver E, Nel A, Delclòs X. 2020. The oldest representative of the extant barklice genus *Psyllipsocus* (Psocodea: Trogiomorpha: Psyllipsocidae) from the Cenomanian amber of Myanmar. Cretac Res. 113:104480. DOI:10.1016/j.cretres.2020.104480.

Álvarez-Parra S, Pérez-de la Fuente R, Peñalver E, Barrón E, Alcalá L, Pérez-Cano J, Martín-Closas C, Trabelsi K, Meléndez N, López Del Valle R, et al. 2021. Dinosaur bonebed amber from an original swamp forest soil. eLife. 10: e72477. DOI:10.7554/eLife.72477.

Álvarez-Parra S, Peñalver E, Nel A, Delclòs X. 2022. New barklice (Psocodea, Trogiomorpha) from Lower Cretaceous Spanish amber. Pap Palaeontol. DOI:10.1002/spp2.1436.

Badonnel A. 1955. Psocoptères de l'Angola. Lisboa (PT): subsidio para o Estudo da Biologia na Lunda, Publicaçoes Culturais, Companhia de Diamantes de Angola (Diamang). Lunda (Angola): Serviços Culturais, Museo do Dundo. Vol. 26 p.1–266.

Badonnel A. 1967. Insectes Psocoptères. Fau Madagasc. 23:1–235.

Badonnel A. 1976. Compléments à l'étude des Psocoptères de Madagascar. Bull Mus Natl Hist Nat. 3(410, Zoologie 287):1143–1197.

Banks N. 1941. New neuropteroid insects from the Antilles. Mem Soc Cub Hist Nat. 15(4):385–402.

Beal LM, de Ruijter WPM, Biastoch A, Zahn R, Cronin M, Hermes J, Lutjeharms J, Quartly G, Tozuka T, Baker-Yeboah S. 2011. On the role of the Agulhas system in ocean circulation and climate. Nature. 472 (7344):429–436. DOI:10.1038/nature09983.

Brasero N, Nel A, Michez D. 2009. Insects from the Early Eocene amber of Oise (France): diversity and palaeontological significance. Denisia. 26:41–52.

Bright DE. 1972. The Scolytidae and Platypodidae of Jamaica (Coleoptera). B I Jam Ss. 21:1–106.

Broadhead E, Richards AM. 1982. The Psocoptera of East Africa – a taxonomic and ecological survey. Biol J Linn Soc. 17(2):137–216. DOI:10.1111/j.1095-8312.1982.tb01545.x.

Cognato AI. 2013. *Electroborus brighti*: the first Hylesinini bark beetle described from Dominican amber (Coleoptera: Curculionidae: Scolytinae). Canad Entomol. 145(5):501–508. DOI:10.4039/tce.2013.31.

de Franceschi D, de Ploëg G. 2003. Origine de l'ambre des faciès sparnaciens (Éocène inférieur) du Bassin de Paris: le bois de l'arbre producteur. Geodiversitas. 25(4):633–647.

de Moya RS, Yoshizawa K, Walden K, Sweet AD, Dietrich CH, Johnson KP . 2021. Phylogenomics of parasitic and nonparasitic lice (Insecta: Psocodea): combining sequence data and exploring compositional bias solutions in next generation data sets. Systematic Biol. 70(4):719–738. DOI:10.1093/sysbio/syaa075.

Delclòs X, Peñalver E, Ranaivosoa V, Solórzano-Kraemer MM . 2020. Unravelling the mystery of "Madagascar copal": age, origin and preservation of a Recent resin. PLoS One. 15(5):e0232623. DOI:10.1371/journal.pone.0232623.

Enderlein G. 1903. Die Copeognathen des indo-australischen Faunengebietes. Ann Hist Nat Mus Nat Hung. 1:179–344.

Enderlein G. 1910. Eine Dekade neuer Copeognathengattungen. Sitzungsber Ges Nat Fr Berlin. 1910(2):63–77.

Enderlein G. 1911. Die Fossilen Copeognathen und ihre Phylogenie. Palaeontographica. 58:279–360.

García Aldrete AN, Mockford EL. 2009. Listado de Psocoptera (Insecta: Psocodea) de Brasil. Rev Mex Biodiv. 80(3):665–673. DOI:10.22201/ib.20078706e.2009.003.163.

García-Aldrete AN. 1986. Especies de Psocoptera (Insecta), de las islas María Madre y San Juanito, Nayarit. Acta Zool Mex (Ns). 13:1–29.

García-Aldrete AN, Carrión AC, Peredo LC. 1992. Psocoptera (Insecta) of Socorro and Clarion Islands, Revillagigedo Archipelago, Mexico, species and comparisons with the continental and the Tres Marias Archipelago psocid faunas. Acta Zool Mex (Ns). 50:1–20.

García-Aldrete AN. 2001. A second sexual, Western Hemisphere species of *Thylacella* Enderlein (Insecta: Psocoptera: Lepidopsocidae). Reichenbachia. 34:57–60.

Glick PA. 1957. Collecting insects by airplane in southern Texas. US Dept Agric Tech Bull. 1158:1–28.

Hagen HA. 1866. Psocinorum et Embidonorum synopsis synonymica. Ver Zool Bot Ges Wien. 16:1–22.

Hakim M, Azar S, Maksoud S, Huang D, Azar D. 2018a. New polymorphic psyllipsocids from Burmese amber (Psocodea: Psyllipsocidae). Cretac Res. 84:389–400. DOI:10.1016/j.cretres.2017.11.027.

Hakim M, Huang D, Azar D. 2018b. First lepidopsocid from the mid Miocene Dominican amber (Psocodea: Trogiomorpha: Lepidopsocidae). Palaeoentomology. 1(1):58–64. DOI:10.11646/PALAEOENTOMOLOGY.1.1.8.

Hennig W. 1966. Phylogenetic systematics. Urbana (IL): University of Illinois Press.

Huurdeman EP, Frieling J, Reichgelt T, Bijl PK, Bohaty SM, Holdgate GR, Gallagher SJ, Peterse F, Greenwood DR, Pross J. 2021. Rapid expansion of meso-megathermal rain forests into the southern high latitudes at the onset of the Paleocene-Eocene Thermal Maximum. Geology. 49(1):40–44. DOI:10.1130/G47343.1.

Johnson KP, Dietrich CH, Friedrich F, Beutel RG, Wipfler B, Peters RS, Allen JM, Petersen M, Donath A, Walden KKO, et al. 2018. Phylogenomics and the evolution of hemipteroid insects. P Natl Acad Sci USA. 115 (50):12775–12780. DOI:10.1073/pnas.1815820115.

Langenheim JH. 2003. Plant resins, chemistry, evolution, ecology, ethnobotany. Portland (OR): Timber Press.

Lavin M, Luckow M. 1993. Origins and relationships of tropical North America in the context of the boreotropics hypothesis. Am J Bot. 80(1):1–14. DOI:10.1002/j.1537-2197.1993.tb13761.x.

Lawver LA, Gahagan LM. 2003. Evolution of Cenozoic seaways in the circum-Antarctic region. Palaeogeogr Palaeoclimatol Palaeoecol. 198(1–2):11–37. DOI:10.1016/S0031-0182(03)00392-4.

Liebherr JK. 1988. Zoogeography of Caribbean insects. Ithaca (NY): Cornell University Press.

Mockford EL. 1967. Some Psocoptera from the plumage of birds. Proc Entomol Soc Washington. 69:307–309.

Mockford EL. 1993. North American Psocoptera (Insecta). Gainesville (FL): Sandhill Crane Press, Flora & Fauna Handbook 10.

Mockford EL. 2005. A new genus of perientomine psocids (Psocoptera: Lepidopsocidae) with a review of the perientomine genera. T Am Entomol Soc. 31(1/2):201–215.

Mockford EL. 2012. Aspects of the biogeography of North American Psocoptera (Insecta). In: Stevens L, editor. Global advances in biogeography. Rijeka: IntechOpen; p. 307–328.

Mockford EL, Lienhard C, Yoshizawa K. 2013. Revised classification of 'Psocoptera' from Cretaceous amber, a reassessment of published information. Insect Matsum Ns. 69:1–26.

Nel A, de Ploëg G, Dejax J, Dutheil D, de Franceschi D, Gheerbrant E, Godinot M, Hervet S, Menier -J-J, Augé M, et al. 1999. Un gisement sparnacien exceptionnel à plantes, arthropodes et vertébrés (Éocène basal, MP7): le Quesnoy (Oise, France). C R Acad Sci II A. 329(1):65–72. DOI:10.1016/S1251-8050(99)80229-8.

Nel A, de Ploëg G, Milliet J, Menier JJ, Waller A. 2004. The French ambers: a general conspectus and the Lowermost Eocene amber deposit of Le Quesnoy in the Paris Basin. Geol Acta. 2(1):3–8. DOI:10.1344/105.000001628.

Nel A, Prokop J, de Ploëg G, Millet J. 2005. New Psocoptera (Insecta) from the lowermost Eocene amber of Oise, France. J Sys Palaeontol. 3(4):371–391. DOI:10.1017/S1477201905001598.

Nel A, Brasero N. 2010. Oise Amber. In: Penney D, editor. Biodiversity of fossils in amber from the major world deposits. Manchester: Siri Scientific Press; p. 137–148.

Nel A, Roques P, Nel P, Prokin AA, Bourgoin T, Prokop J, Szwedo J, Azar D, Desutter-Grandcolas L, Wappler T. 2013. The earliest known holometabolous insects. Nature. 503(7475):257–261. DOI:10.1038/nature12629.

New TR. 1975. Some Lepidopsocidae (Psocoptera) from Central Brazil. Rev Bras Entomol. 19:85–95.

New TR. 1987. Biology of the Psocoptera. Orient Insects. 21(1):1–109. DOI:10.1080/00305316.1987.11835472.

New TR, Lienhard C. 2007. The Psocoptera of tropical South-East Asia. Leiden: Brill.

Nohra YA, Perrichot V, Jeanneau L, Le Polles L, Azar D. 2015. Chemical characterization and botanical origin of French ambers. J Nat Prod. 78(6):1284–1293. DOI:10.1021/acs.jnatprod.5b00093.

Pearman JV. 1936. The taxonomy of the Psocoptera: preliminary sketch. Proc R Entomol Soc B. 5:58–62. DOI:10.1111/j.1365-3113.1936.tb00596.x.

Peel MC, Finlayson BL, McMahon TA. 2007. Updated world map of the Köppen-Geiger climate classification. Hydrol E Sys Sc. 11(5):1633–1644. DOI:10.5194/hess-11-1633-2007.

Peris D, Solórzano Kraemer MM, Peñalver E, Delclòs X. 2015. New ambrosia beetles (Coleoptera: Curculionidae: Platypodinae) from Miocene Mexican and Dominican ambers and their paleobiogeographical implications. Org Divers Evol. 15(3):527–542. DOI:10.1007/s13127-015-0213-y.

Poinar GO Jr, Brown AE. 2002. *Hymenaea mexicana* sp. nov. (Leguminosae: Caesalpinioideae) from Mexican amber indicates Old World connections. Bot J Linn Soc. 139(2):125–132. DOI:10.1046/j.1095-8339.2002.00053.x.

Roesler R. 1940. Neue und wenig bekannte Copeognathengattungen I. Zool Anz. 129(9/10):225–243.

Roesler R. 1944. Die Gattungen der Copeognathen. Stett. Entomol. Zeit. 105:117–166.

Secord R, Gingerich PD, Lohmann KC, MacLeod KG. 2010. Continental warming preceding the Paleocene-Eocene thermal maximum. Nature. 467(7318):955–958. DOI:10.1038/nature09441.

Smithers CN. 1972. The classification and phylogeny of the Psocoptera. Aust Mus Mem. 14:1–349. doi:10.3853/j.0067-1967.14.1972.424.

Smithers CN. 1990. Keys to the family and genera of Psocoptera (Arthropoda: Insecta). Tech Rep Aust Mus. 2:1–82. doi:10.3853/j.1031-8062.2.1990.77.

Solórzano Kraemer MM, Delclòs X, Clapham ME, Arillo A, Peris D, Jäger P, Stebner F, Peñalver E. 2018. Arthropods in modern resins reveal if amber accurately recorded forest arthropod communities. Proc Natl Acad Sci USA. 115(26):6739–6744. DOI:10.1073/pnas.1802138115.

Solórzano-Kraemer MM, Delclòs X, Engel MS, Peñalver E. 2020. A revised definition for copal and its significance for palaeontological and Anthropocene biodiversity-loss studies. Sci Rep. 10(1):19904. DOI:10.1038/s41598-020-76808-6.

Thornton IWB. 1962. Psocids (Psocoptera) from the Batu Caves, Malaya. Pacif. Insects. 4(2):441–455.

Thornton IWB, New TR, Vaughan PJ. 1988. Colonization of the Krakatau Islands by Psocoptera (Insecta). Philos Trans R Soc Lond B Biol. Sci. 322(1211):427–443. DOI:10.1098/rstb.1988.0136.

Tosso F, Hardy OJ, Doucet JL, Daïnou K, Kaymak E, Migliore J. 2018. Evolution in the Amphi-Atlantic tropical genus *Guibourtia* (Fabaceae, Detarioideae), combining NGS phylogeny and morphology. Mol Phyl Evol. 120:83–93. DOI:10.1016/j.ympev.2017.11.026.

van Sebille E, Aliani S, Law KL, Maximenko N, Alsina JM, Bagaev A, Bergmann M, Chapron B, Chubarenko I, Cózar A, et al. 2020. The physical oceanography of the transport of floating marine debris. Environ Res Lett. 15:023003. DOI:10.1088/1748-9326/ab6d7d.

Wiley EO. 1988. Vicariance biogeography. Ann Rev Ecol Syst. 19(1):513–542. DOI:10.1146/annurev.es.19.110188.002501.

Wolfe JA. 1985. Distribution of major vegetation types during the Tertiary. Geophys Monogr Ser. 32:357–375. DOI:10.1029/GM032p0357.

Yoshizawa K, Lienhard C, Johnson KP. 2006. Molecular systematics of the suborder Trogiomorpha (Insecta: Psocodea: 'Psocoptera'). Zool J Linn Soc. 146(2):287–299. DOI:10.1111/j.1096-3642.2006.00207.x.

Yoshizawa K, Johnson KP, Sweet AD, Yao I, Ferreira RL, Cameron SL. 2018. Mitochondrial phylogenomics and genome rearrangements in the barklice (Insecta: Psocodea). Mol Phylogenet Evol. 119:118–127. DOI:10.1016/j.ympev.2017.10.014.

Yoshizawa K, Lienhard C, Yao I, Ferreira RL. 2019. Cave insects with sex-reversed genitalia had their most recent common ancestor in West Gondwana (Psocodea: Prionoglarididae: Speleketorinae). Entomol Sci. 22(3):334–338. DOI:10.1111/ens.12374.

Zheng D, Chang S-C, Perrichot V, Dutta S, Rudra A, Mu L, Kelly RS, Zhang Q, Qin Z, Wong J. 2018. A Late Cretaceous amber biota from central Myanmar. Nat Comms. 9(1):3170. DOI:10.1038/s41467-018-05650-2.

Anexo 8.1.9

Biodiversity of ecosystems in an arid setting: the late Albian plant communities and associated biota from eastern Iberia

Barrón, E., Peyrot, D., Bueno-Cebollada, C.A., Kvaček, J., **Álvarez-Parra, S.**, Altolaguirre, Y., Meléndez, N. enviado tras revisión*. Biodiversity of ecosystems in an arid setting: the late Albian plant communities and associated biota from eastern Iberia. *PLOS One*.

Revista científica: *PLOS One*
Factor de impacto: 3,752 (2021)
Categoría: *Multidisciplinary Sciences*, Q2 (2021)

* El manuscrito se ha reenviado a la revista tras revisiones menores. Debido a la extensión en el número de páginas, no se ha incluido ni las tablas ni el material suplementario.

Biodiversity of ecosystems in an arid setting: the late Albian plant communities and associated biota from eastern Iberia

Eduardo Barrón[1]*, Daniel Peyrot[2], Carlos A. Bueno-Cebollada[1¶], Jiří Kvaček[3], Sergio Álvarez-Parra[4, 5], Yul Altolaguirre[6], Nieves Meléndez[7¶]

[1] Museo Geominero, Centro Nacional Instituto Geológico y Minero de España CN IGME-CSIC, Madrid, Spain
[2] School of Earth and Environment, Centre for Energy Geoscience, University of Western Australia, Crawley, Western Australia, Australia
[3] National Museum Prague, Praha, Czechia
[4] Departament de Dinàmica de la Terra i de l'Oceà, Facultat de Ciències de la Terra, Universitat de Barcelona, Barcelona, Spain
[5] Institut de Recerca de la Biodiversitat (IRBio), Universitat de Barcelona, Barcelona, Spain
[6] OCEEH Research Center 'The role of cultura in early expansions of humans', Heidelberg Academy of Sciences, Senckenberg Research Institute, Frankfurt am Main, Germany
[7] Deparment of Geodinámica, Estratigrafía y Paleontología, Facultad de Ciencias Geológicas, Universidad Complutense de Madrid, Spain

* Corresponding autor
E-mail: e.barron@igme.es (EB)

¶ These authors contributed equally to this work.

Data Availability: All relevant data are within the paper and its Supporting Information files.

Funding: This study is a contribution to the project CRE CGL2017-84419 AEI/FEDER, UE from the Ministerio de Ciencia, Innovación y Universidades (Spain) and the "Severo Ochoa" extraordinary grants for excellence IGME-CSIC (AECEX2021). The coauthor S.Á.-P. thanks the support from the Secretaria d'Universitats i Recerca de la Generalitat de Catalonia (Spain) and the European Social Fund (2021FI_B2 00003). The funders had no role in study design, data collection and analysis, decision to publish, or preparation of the manuscript.

Competing interests: The authors have declared that no competing interests exist.

Abstract

Deserts are stressful environments where the living beings must acquire different strategies to survive due to the water stress conditions. From the late Albian to the early Cenomanian, the northern and eastern parts of Iberia were the location of desert system represented by deposits assigned to the Utrillas Group, which bear abundant amber with numerous

bioinclusions, including diverse arthropods and vertebrate remains. In the Maestrazgo Basin (E Spain), the late Albian to early Cenomanian sedimentary succession represents the most distal part of the desert system (fore-erg) that was characterised by an alternation of aeolian and shallow marine sedimentary environments in the proximity of the Western Tethys palaeo-coast, with rare to frequent dinoflagellate cysts. The terrestrial ecosystems from this area were biodiverse, and comprised plant communities whose fossils are associated with sedimentological indicators of aridity. The palynoflora dominated by wind-transported conifer pollen are interpreted to reflect various types of xerophytic woodlands from the hinterlands and the coastal settings. Therefore, fern and angiosperm communities abundantly grew in wet interdunes and coastal wetlands (temporary to semi-permanent freshwater/salt marshes and water bodies). In addition, the occurrence of low diversity megafloral assemblages reflect the existence of coastal salt-influenced settings. The palaeobotanical study carried out in this paper which is an integrative work on palynology and palaeobotany, does not only allow the reconstruction of the vegetation that developed in the mid-Cretaceous fore-erg from the eastern Iberia, in addition, provides new biostratigraphic and palaeogeographic data considering the context of angiosperm radiation as well as the biota inferred in the amber-bearing outcrops of San Just, Arroyo de la Pascueta and La Hoya (within Cortes de Arenoso succesion). Importantly, the studied assemblages include *Afropollis*, *Dichastopollenites*, *Cretacaeiporites* together with pollen produced by Ephedraceae (known for its tolerance to arid conditions). The presence of these pollen grains, typical for northern Gondwana, associates the Iberian ecosystems with those characterizing the mentioned region.

Introduction

The Albian vegetation of western Europe has been studied in several works which described micro-, meso- and macroremains [1–7], and highlighting the prevalence of ferns and gymnosperms –mainly conifers (Araucariaceae-Podocarpaceae-Pinaceae-Cupressaceae-Cheirolepidiaceae)–, and the increasing representation of angiosperms. The distinctiveness of the western European flora has been recognised for a long time and several biogeographic provinces have been named on the basis of the nature of the fossil assemblages (i.e., palynological and megaremains [8–9]). The increased attention to the time-interval is justified by the rising of the dominance of the flowering plants in many ecosystems [10–13] including arid environments [14]. During the later part of the Early Cretaceous, SW Europe has been described as one of the probable migratory routes of angiosperms originating from a northern Gondwanan centre of radiation [15]. The successive northward migrations of angiosperms, well-characterised by both pollen and megaremain records, suggest broadly similar climate conditions in low to mid-latitude settings (i.e., low latitudinal climatic gradient) or selective migration of taxa able to tolerate a wide range of climatic conditions [16]. During most of the Albian, Iberia was part of a climatic zone referred to as the Northern Hot Arid (NHA) belt [17], where a desert system (erg) developed over an extensive area [18].

Arid environments, although less represented in fossil record have its examples over all Mesozoic. Semi-arid environments are, e.g., reconstructed for the Early Triassic of northeastern Spain and the Upper Jurassic Morison Formation based on presence of aeolian sandstones [19–20]. Arid environments were reconstructed for Early Cretaceous floras of Quedlinburg (Germany) and Las Hoyas (Central Spain) based on occurrence of dwarf lycopod *Nathorstiana* and fern *Weichselia* [21–22]. Reconstructions of Cretaceous continental ecosystems of Japan based on stable oxygen and carbon isotopes also suggest semi-arid conditions [23]. In addition, aeolian sandtones provide direct evidence of a desert environment during the mid-Cretaceous in mid- to low latitude Asia [24].

In Iberia, the eastern coastal margin consisted of a complex set of depositional environments comprising multifaceted vegetation types including conifer forests [14, 25]. Palaeobotanical studies of ancient desert successions (see i.e. [26–27]) report plant remains usually not preserved in sand-sized lithologies, which in turn constitute the bulk of their deposits. Assemblages belonging to this type of setting usually include remains that have experienced transport over varying, and sometimes considerable, distances to the site of burial. Considering this limitation and exploiting the characteristics of sets of fossils with distinct taphonomic histories (i.e., megaremains with limited transport vs. miospores disseminated over wider distances), the present work focuses on the reconstruction of the mid-Cretaceous plant communities that developed in the distal part of the desert system (or fore-erg) in the Maestrazgo Basin (Eastern Iberian Ranges, E Spain), considering specially the conifer-dominated ones. While the previous studies carried out in Albian deposits from the Maestrazgo Basin considered palaeobotanical and palynological data separately [28–37], this study represents the first attempt to integrate both data sets into a unified framework, aiming at the characterisation of the arid palaeoenvironmental and their link with the occurrence of amber.

The Cretaceous amber-bearing outcrops from the Maestrazgo Basin have been known for a long time [38] and were traditionally associated with the Escucha Formation [39], an Aptian–early Albian unit consisting of coal-bearing deposits [40] which sometimes also present amber [41]. Although more than 30 amber outcrops have been reported in the basin, the sites related to the desert system revealing the most diverse sets of bioinclusions and plant remains [29, 37, 42–44] are the successions of Arroyo de la Pascueta, San Just (both located in Teruel Province) and Cortes de Arenoso (Castellón Province) (Fig 1). The present study is the first to provide a comprehensive treatment of the palaeobotanical and palynological content of the three aforementioned mid-Cretaceous sites. This paper aims to: (i) document the micro- and macrofloral assemblages together with the entomological content recovered from highly significant amber-bearing outcrops; (ii) reassess the age of the successions on the basis of the presence of key biostratigraphic markers; (iii) reconstruct the corresponding ecosystems with a special focus on the plant communities and insects which thrived on them; and (iv) compare the vegetation with coeval floras from presumably wetter settings.

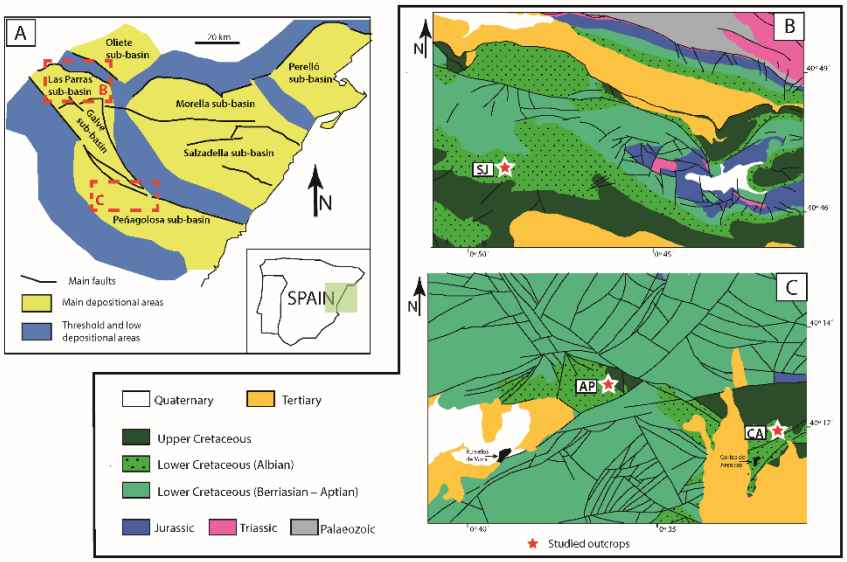

Fig 1. Location of the Maestrazgo Basin and its seven sub-basins (A) based on Aurell et al. [45]. The studied locations are indicated by coloured stars (San Just, SJ; Arroyo de la Pascueta, AP; Cortes de Arenoso, CA). (B) Detail of the geological map with the location of San Just (SJ) section in the Las Parras Sub-basin. Based on data from the geological map of Spain Magna 1:50000 [46]. (C) Detail of the geological map showing the location of Arroyo de la Pascueta (AP) and Cortes de Arenoso (CA) sections. Based on data from the geological map of Spain Magna 1:50000 [47].

Material and methods

Geological setting

The study area is located in the Maestrazgo Basin, on the eastern part of a palaeogeographic domain referred to as the Iberian Basin Rift System (IBRS), Spain (Fig 1A). The sedimentary succession was deposited during the transition from the Late Jurassic–Early Cretaceous syn-rift stage to the Late Cretaceous post rift stage, associated with the gradual opening of the Western Tethys and the North Atlantic Ocean [45, 48–49]. The Maestrazgo Basin forms a NW-SE-oriented depositional trough (Fig 1A), where the sedimentary succession generally becomes thicker towards the SE (Tethyan margin). During the Early Cretaceous the syn-rift sedimentary succession was dominated by thick, continental to coastal siliciclastic-dominated deposits (previously referred to as 'Weald facies') and marine carbonates ('Urgonian facies') [50–55] (Fig 2). Towards the end of the syn-rift stage (uppermost Aptian to early Albian), the sedimentary succession became more homogeneous across the basin, and coal-bearing strata attributed to the Escucha Formation were deposited [56–59]. The Escucha Formation has been interpreted as lagoons and marshes [59–60].

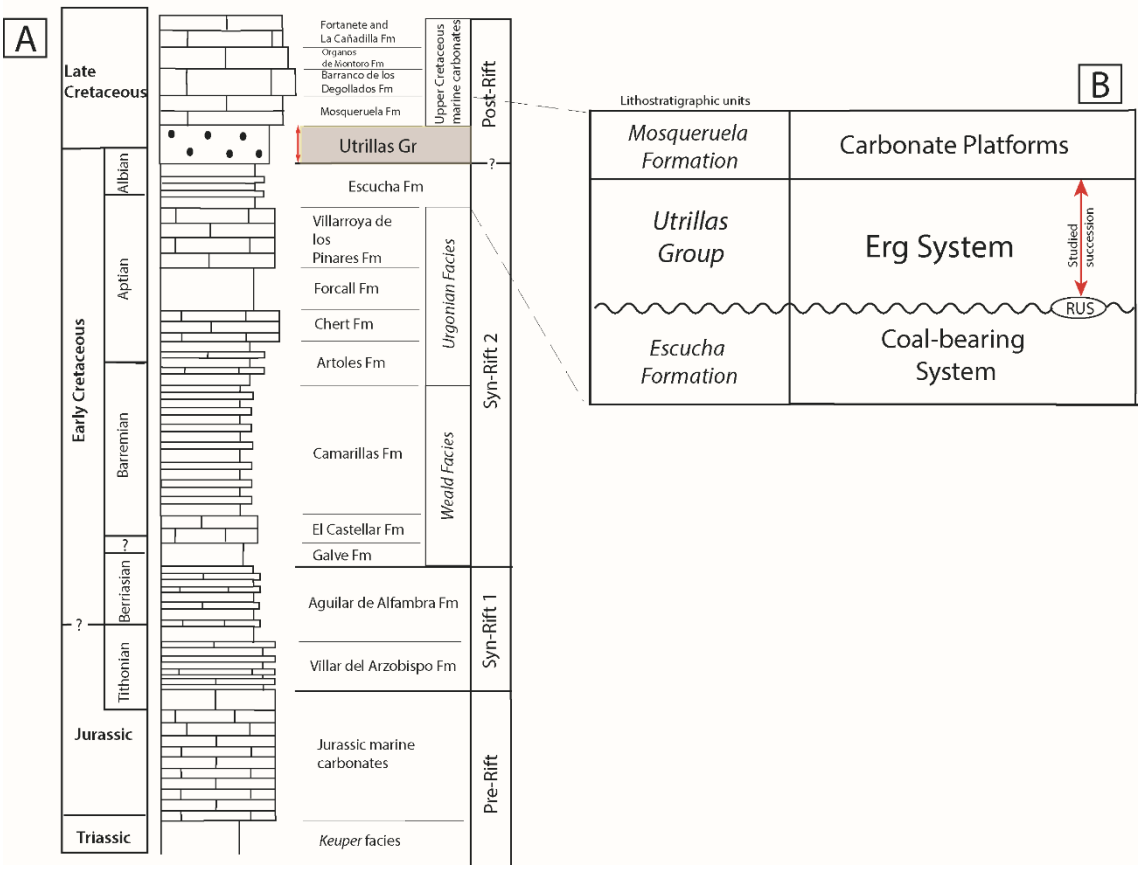

Fig 2. Synthetic stratigraphic log of the Maestrazgo Basin from the Triassic to the Upper Cretaceous. (A) The red arrow shows the location of the Utrillas Group in grey colour. Based on data from [52, 55]. (B) Detail of the lithostratigraphy of the studied succession, where the Utrillas Group Erg System overlies the coal-bearing deposits of the Escucha Formation by means of regional unconformity surface (RUS), which marks the onset of the Erg System. The Utrillas Group succession is, in turn, overlain by marine carbonate deposits of Mosqueruela Formation. Based on data from [59].

The Escucha Formation is overlain by strata forming the Utrillas Group, a highly diachronous unit widespread along the IBRS, which has been traditionally interpreted as the transition into the post-rift stage [57, 59, 61]. In the Maestrazgo Basin, the Utrillas Group spanned the middle Albian–earliest Cenomanian [59]. In the Maestrazgo Basin, this Group includes facies originally interpreted as tidally-influenced fluvial deposits [57, 62] and later reinterpreted as part of an erg system (aeolian dune desert), covering more than 16,000 km^2 on the eastern side of the Iberian Peninsula [18, 59].

According to [18, 59], this erg system (Fig 2B) displayed a threefold zonation developed along a NW–SE direction characterised by: (i) a back-erg area close to the main source area of siliciclastics (Iberian Massif), dominated by coarser-grained wadi sediments and minor aeolian accumulations; (ii) a central-erg area corresponding to the main locus of aeolian dune accumulation; and (iii) a fore-erg area characterised by the interplay between aeolian dunes and shallow marine deposits from the Western Tethys, giving rise to a complex interaction of tidally-reworked aeolian dune and subtidal facies associations.

In the Maestrazgo Basin, the Utrillas Group is overlain by the Mosqueruela Formation [50, 57, 59, 63] (Fig 2B), a marine carbonate unit, that represents the onset of carbonate sedimentation (Southern Iberian Ramp), which will prevail during most of the Late Cretaceous [48, 64]. The Maestrazgo Basin is divided into several sub-basins (Fig 1) that include: the Galve, Oliete, Las Parras, Morella, El Perelló, La Salzedella, and Peñagolosa sub-basins [49].

In this paper, three stratigraphic sections have been measured in three outcrops in the Maestrazgo Basin, namely: San Just (according to [31]: "left slope of San Just"), Arroyo de la Pascueta and Cortes de Arenoso (according to [40]: "La Hoya outcrop") sections. The San Just section is located in the Las Parras Sub-basin, about 70 km to the NNW from the other studied sections which crop out in the NNW sector of the Penyagolosa Sub-basin (Fig 1). The studied sedimentary succession is located in the distal part of the mid-Cretaceous desert system which is characterised by a fore-erg setting where aeolian strata interacted with shallow marine deposits in the coastal fringe of the Western Tethys.

San Just section (SJ). The 22 m-thick section is located in a roadside (N-420 road), approximately 3 km to the south of Utrillas village (Teruel Province) and overlain by the marine carbonates of the Mosqueruela Formation, dated as Cenomanian [46]. The succession can be divided into a lower part consisting mostly of dark siltstones and mudstones interspersed with cm- to dm-thick fine-grained sandstone layers with wavy to flaser heterolithic laminations (Fig 3), and an upper part dominated by fine-grained, cross-bedded, sandstones with thin (dm-thick) interbedded mudstones, which may include water deformation structures and slumps. The amber-bearing bed is located in the lower part of the section and is overlain by (large-scale) planar cross-bedded fine-grained sandstones exhibiting sharp basal contacts. Kindney-shaped amber pieces together with "stalactitic aerial" amber pieces, the latter with bioinclusions, are abundant in this bed [43] (Fig 4A–B).

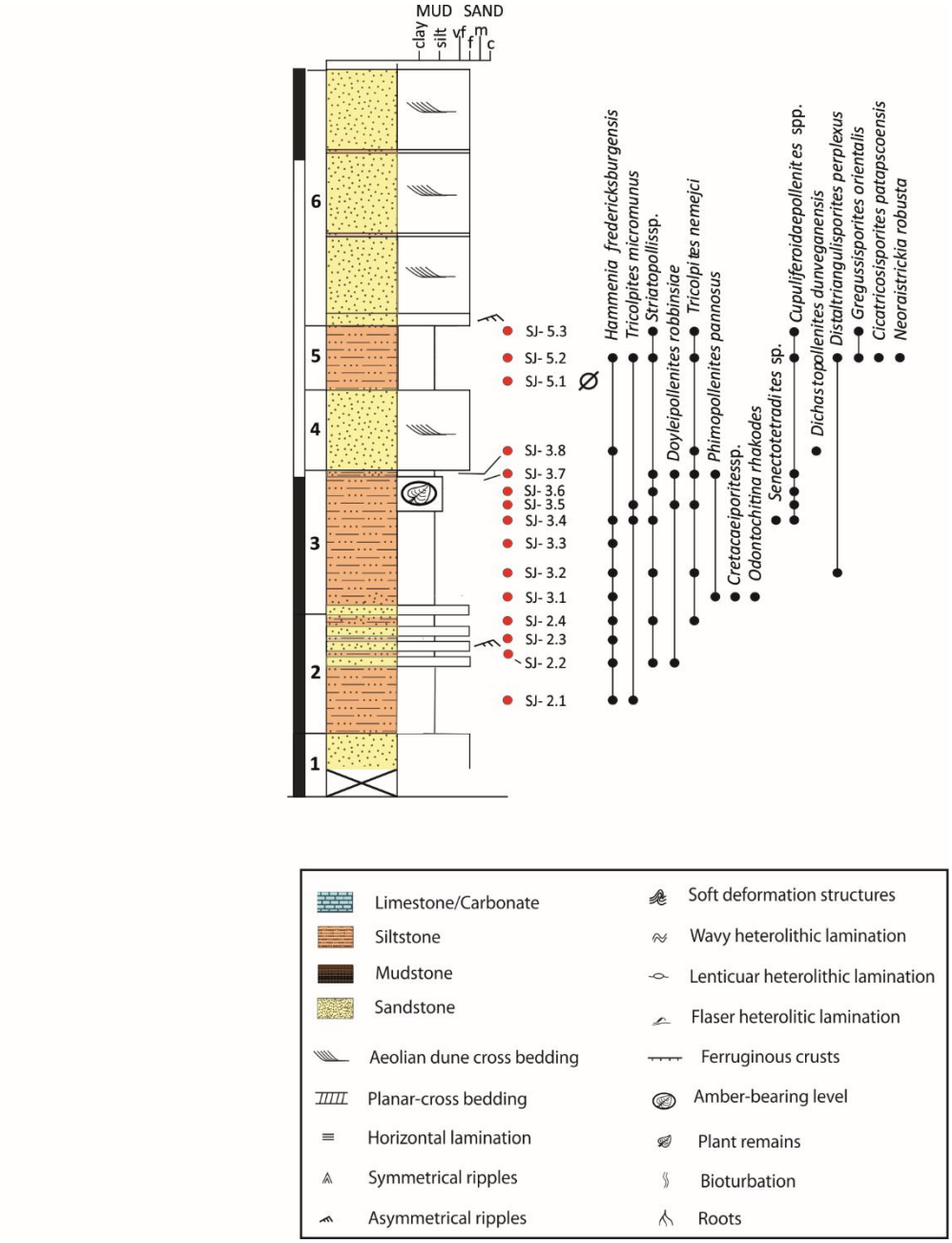

Fig 3. Stratigraphic log of the upper Albian San Just outcrop (SJ), showing the distribution of selected biostratigraphically relevant palynomorphs. San Just amber outcrop is at the top of the level 3. Red dots: location of the collected samples. Black dots: stratigraphic distribution of the selected taxa. Ø: barren sample.

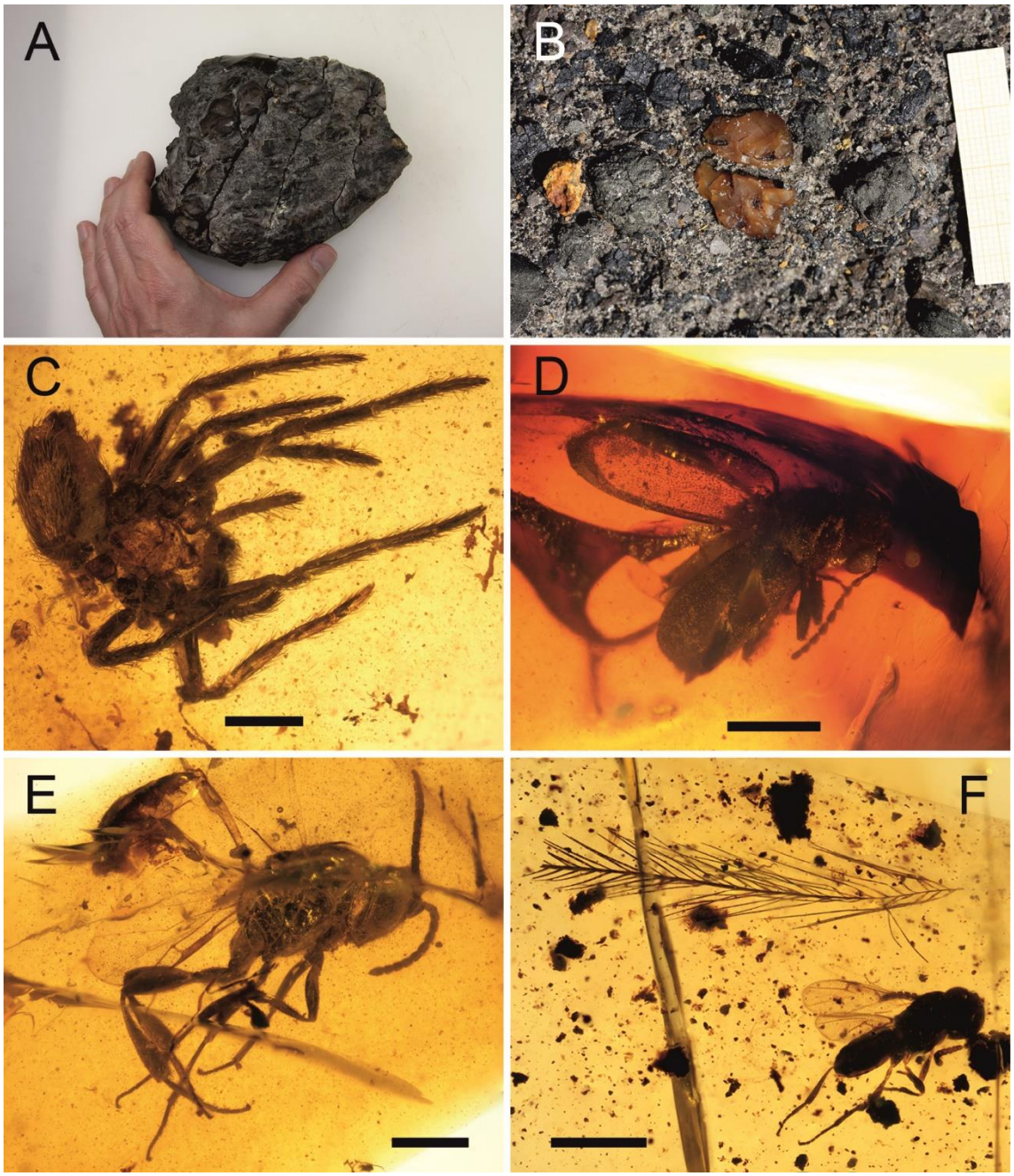

Fig 4. Amber from the late Albian San Just outcrop (Utrillas, Teruel) and its bioinclusions. (A) Big kidney-shaped amber mass of 640 g. (B) Unearthed amber pieces. (C) Undetermined Lagonomegopidae? spider (SJNB2012-12-07). (D) Holotype of *Actenobius magneoculus* (Coleoptera, Ptinidae) (MAP-7727). (E) Holotype of *Cretevania alcalai* (Hymenoptera, Evaniidae) (CPT-960). (F) Avian dinosaur feather barb close to an undetermined Platygastroidea wasp (CPT-4078 and CPT-4079, respectively). Scale bars C–F, 0.5 mm. Images A and B are provided by Enrique Peñalver. Acronyms SJNB, CPT and MAP correspond to amber pieces housed at the Museo Aragonés de Paleontología (Fundación Conjunto Paleontológico de Teruel-Dinópolis) in Teruel, Spain.

Cortes de Arenoso section (CA). This 172 m-thick section is cropping out in a ravine in the NNW of the Cortes de Arenoso locality (Castellón Province). The succession, sharply overlain

by marine carbonates attributed to the Mosqueruela Formation [47, 65], is dominated by fine-grained sandstones displaying large-scale planar cross-bedded sets, which laterally shift into dark mudstones and siltstones containing plant megaremains, especially abundant in the first 10–30 m of the logged section (Fig 4). The section includes heterolithic siltstone/mudstone and sansdtone deposits displaying subaqueous tidal sedimentary structures such as double mud drapes, lenticular, flaser and wavy laminations and cross-bedded sets depicting current bipolarity (herringbone-like cross-beddings). The amber-bearing level corresponds to the La Hoya amber outcrop (not to confuse it with the Barremian compression outcrop of Las Hoyas, also in Spain). Concretey, this level is located in the uppermost mudstone interval of the section and correlates with the amber-bearing stratum described in Arroyo de la Pascueta [40, 44].

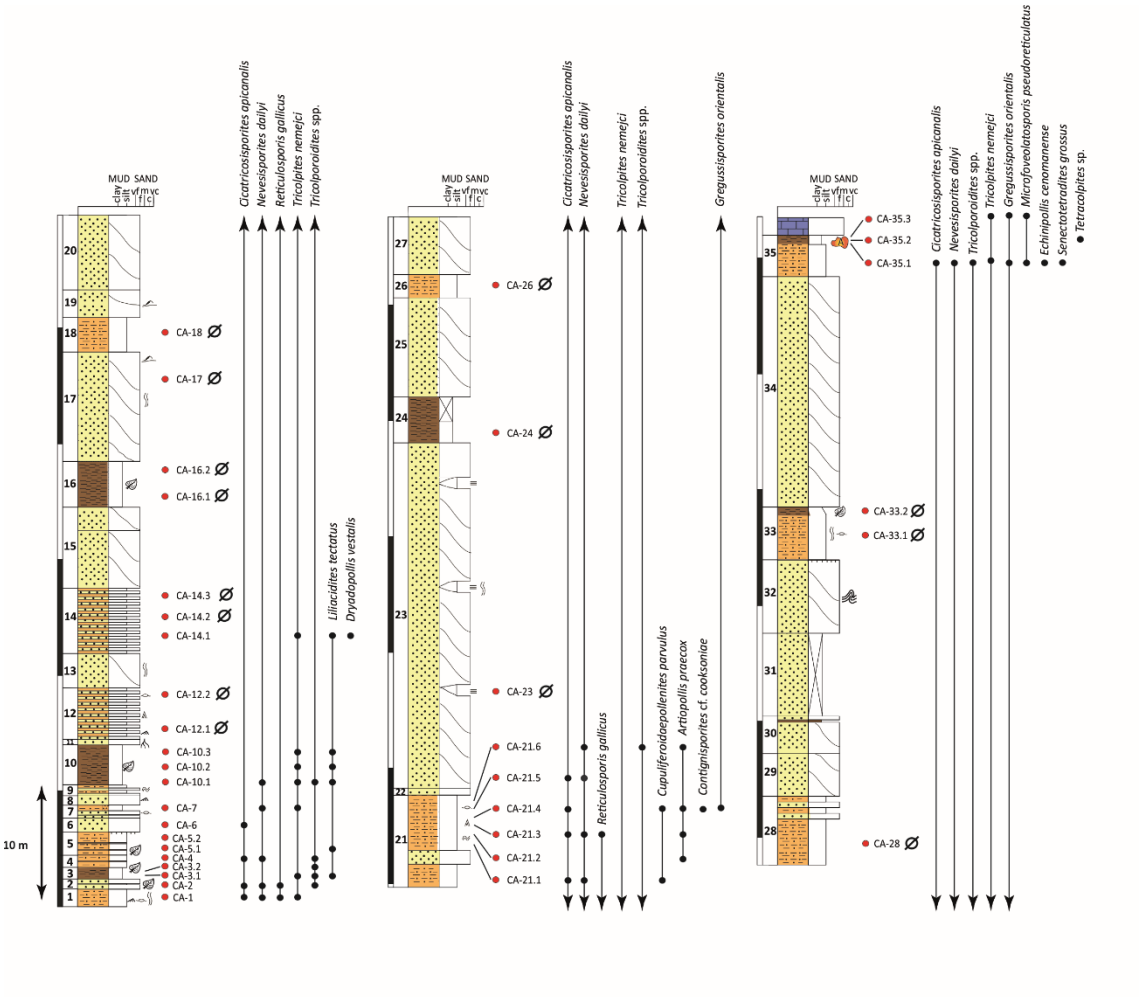

Fig 5. Stratigraphic log of the upper Albian/lower Cenomanian Cortes de Arenoso section (CA), showing the distribution of selected biostratigraphically relevant miospores (see the legend in Fig 3)**.** La Hoya amber outcrop is at the top of the section (level 35). Red dots: location of the collected samples. Black dots: stratigraphic distribution of the selected taxa. Ø: barren samples.

Arroyo de la Pascueta section (AP). The 182 m-thick section consists of an alternation of fine-grained homometric sandstone bodies with large-scale planar cross-bedding (Fig 6). The sandstone laterally shifts into dark siltstone to mudstone and heterolithic deposits with mud drapes and wavy to flaser laminations, showing similar characteristics to the heterolithic siltstone/mudstone described in the Cortes de Arenoso section (Fig 5). Despite plant remains being common and evenly distributed throughout the succession, only the lower part of the section (interval between 20 to 27 m in Fig 6) was sampled and analysed in previous palaeobotanical studies [29–30]. Amber fragments are abundant [40, 44] and recorded in a mudstone bed of the upper part of the succession, which is sharply overlain by the marine carbonates of the Mosqueruela Formation [47].

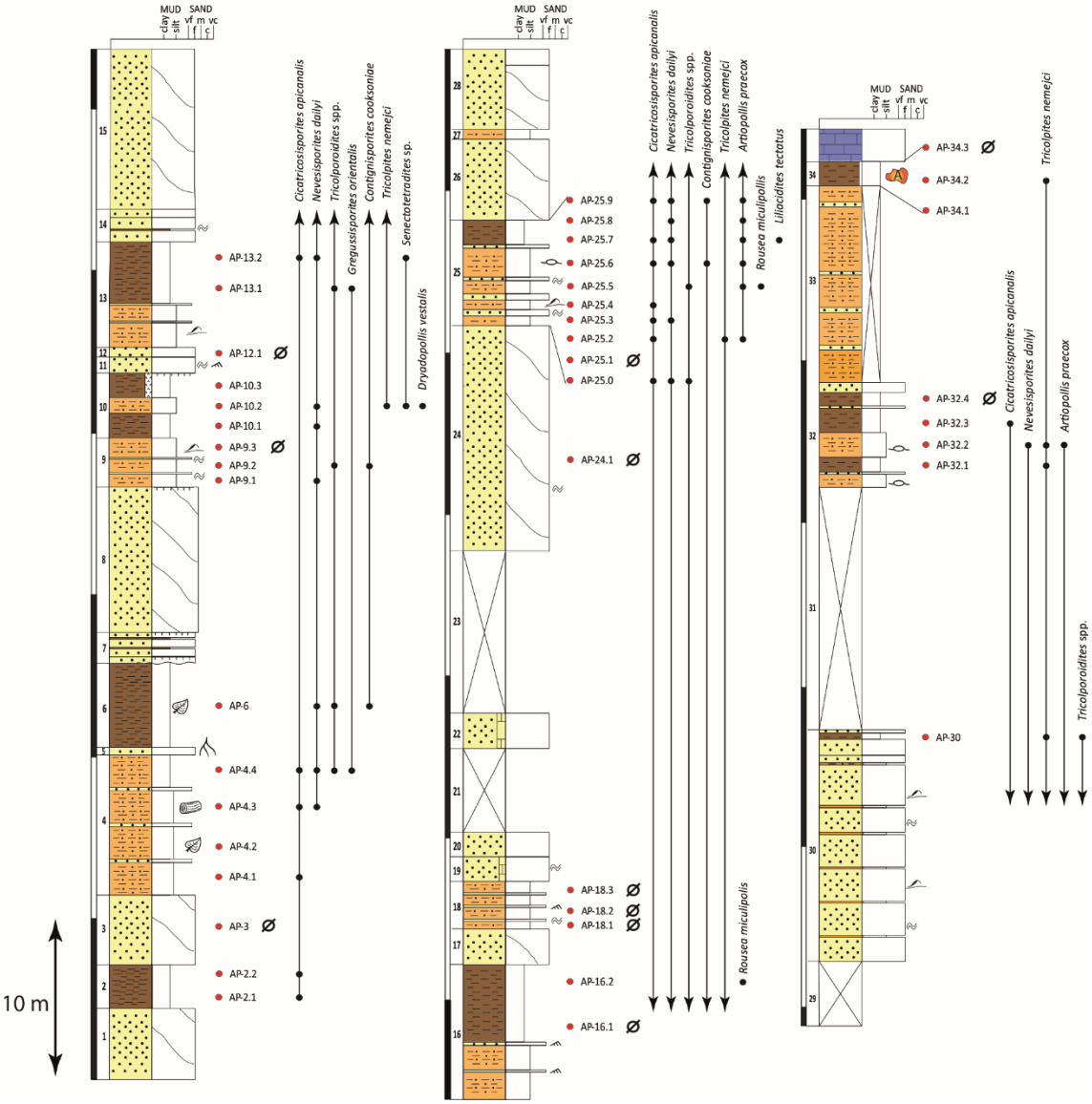

Fig 6. Stratigraphic log of the upper Albian Arroyo de la Pascueta section (AP), showing the distribution of selected biostratigraphically relevant miospores (see the legend in Fig 3). Arroyo de la Pascueta amber outcrop is at the top of the section (level 34). Red dots: location of the collected samples. Black dots: stratigraphic distribution of the selected taxa. Ø: barren samples.

Palynology

Ninety-two samples have been collected in the three cropping out successions described above (Fig 1). Although sampling primarily focused on amber-bearing strata, all suitable levels of the sections were carefully sampled (Figs 3–5) in order to obtain a more accurate and continuous biostratigraphic framework. The three logged sections were drawn using the software SedLog [66] in combination with Adobe Illustrator (www.adobe.com).

A total of 15 rock samples from the San Just, 36 from the Cortes de Arenoso and 41 from the Arroyo de la Pascueta sections were prepared for palynological analysis. Palynological residues were processed using acid digestion with HCl and HF at high temperatures [67–68]. When required, a short oxidation with HNO_3 ("nitric wash") was performed in some residues. The residues were then concentrated by sieving through 500, 250 and 10 μm sieves, mounted in glycerin jelly on strew slides. In order to include rare taxa with potential biostratigraphic value, between 500 and 1000 palynomorphs were identified per sample (S1 Appendix). Microscopic analysis of the palynological slides was performed with an Olympus BX51 microscope, incorporating a ColorView IIIu camera using a 100X oil immersion objective. Pollen diagrams were constructed by using Tilia/TGView 2.0.2 softwares [69–70]. All studied slides are provisionally stored in the museum of the Geological Survey of Spain (CN IGME-CSIC, Madrid). A list of the identified taxa along with their botanical affinity and occurrences in each section is given in Table 1 and S1 and S2 Appendices.

Mega and mesoflora

Megaflora was initially investigated and documented by using an Olympus SZX 12 stereomicroscope with DP 70 digital camera. Material with preserved morphological details was studied via Scanning Electron Microscopy (SEM). Specimens were mounted on cleaned aluminium stubs using nail polish, coated with gold and examined with a Hitachi S-3700N Environmental Scanning Electron Microscope at 2 kV, at the National Museum of Prague (Czechia), where the studied material is stored temporarily. Specimens from SJ and AP will be transferred in the future to the Museo Aragonés de Paleontología (Fundación Conjunto Paleontológico de Teruel-Dinópolis, Spain) as definitive repository.

Amber bioinclusions

In the Maestrazgo Basin, amber pieces with bioinclusions have been collected for research purposes since 1998. They have been prepared using epoxy resin [102], to improve the visualisation of the bioinclusions and their long-term preservation. The amber pieces from the San Just and Arroyo de la Pascueta outcrops are housed at the Museo Aragonés de Paleontología (Fundación Conjunto Paleontológico de Teruel-Dinópolis, Teruel), and the ones from La Hoya outcrop at the Museu de la Universitat de València d'Història Natural (Valencia). Bioinclusions have been photographed using a digital camera sCMEX-20 attached to a compound microscope Olympus CX41 with the software ImageFocusAlpha version

1.3.7.12967.20180920 (www.euromex.com) and processed with Photoshop CS6 version 13.0 (www.adobe.com). List of identified taxa is given in Table 2 and S2 Appendix.

Results

Palaeobotanical aspects

A total of 26 out of 92 samples processed for their palynological content were barren (1 in San Just section, 14 in Cortes de Arenoso section and 11 in the Arroyo de la Pascueta section). Productive samples showed an overall good recovery and well-preserved palynological content. Except on a few occasions, interpreted as reworking, miospores and dinocysts present a yellow to pale brown colour suggesting low thermal maturation [103]. A total of 367 palynomorph types (S2 Appendix) have been identified, mainly consisting of dinoflagellate cysts (dinocysts, 30 taxa; Fig 7C–H), bryophyte, lycophyte and pteridophyte spores (186 taxa; Fig 8), gymnosperms (53 taxa; Fig 7I–T) and angiosperms (88 taxa; Fig 9). A small number of acanthomorph acritarchs, phycomes of prasinophytes, freshwater algae (Fig 7A–B) and linings of foraminifers have also been recorded (S1 Appendix).

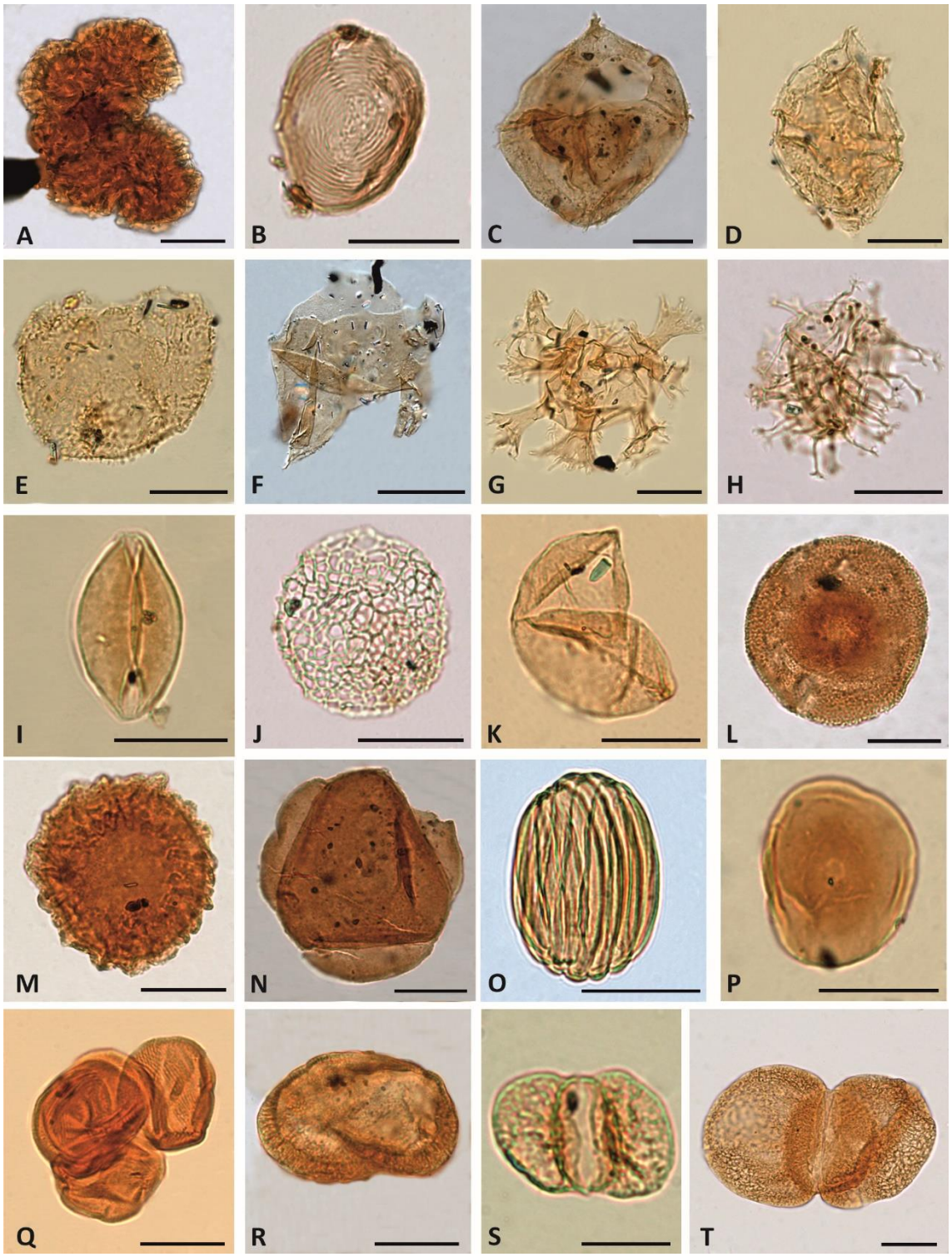

Fig 7. Light photomicrographs of selected aquatic palynomorphs and gymnosperm pollen grains. (A) *Botryococcus braunii*, level AP-34.1. (B) *Chomotriletes minor*, level AP-34.1. (C) *Cribroperidinium* sp., level AP-10.1. (D) *Ginginodinium* cf. *evittii*, level SJ-2.1. (E) *Tenua hystrix*, level SJ-2.1. (F) *Odontochitina rhakodes*, level SJ-3.1. (G) *Oligosphaeridium complex*, level SJ-2.1. (H) *Kiokansium unituberculatum*, level AP-13-1. (I) *Cycadopites* sp., level SJ-3.7. (J) *Afropollis jardinus*, level CA-5.2. (K) *Inaperturopollenites dubius*, level SJ-2.1. (L) *Uesuguipollenites callosus*, level AP-6. (M) *Callialasporites segmentatus*, level AP-6. (N) *Callialasporites trilobatus*, level AP-13.2. (O) *Gnetaceaepollenites oreadis*, level AP-16.2. (P)

Exesipollenites tumulus, level SJ-2.1. (Q) Tetrad of *Classopollis major*, level SJ-2.3. (R) *Parvisaccites radiatus*, level AP-4.3. (S) *Vitreisporites pallidus*, level SJ-2.2. (T) *Podocarpidites* sp., level AP-25.6. Specimens A–C, H, L–O, R, T are from the Arroyo de la Pascueta section; specimens D–G, I, K, P–Q, S are from the San Just section; the specimen J was found in a sample from the Cortes de Arenoso section. Scale bar equals 20 µm except in S when it equals 10 µm.

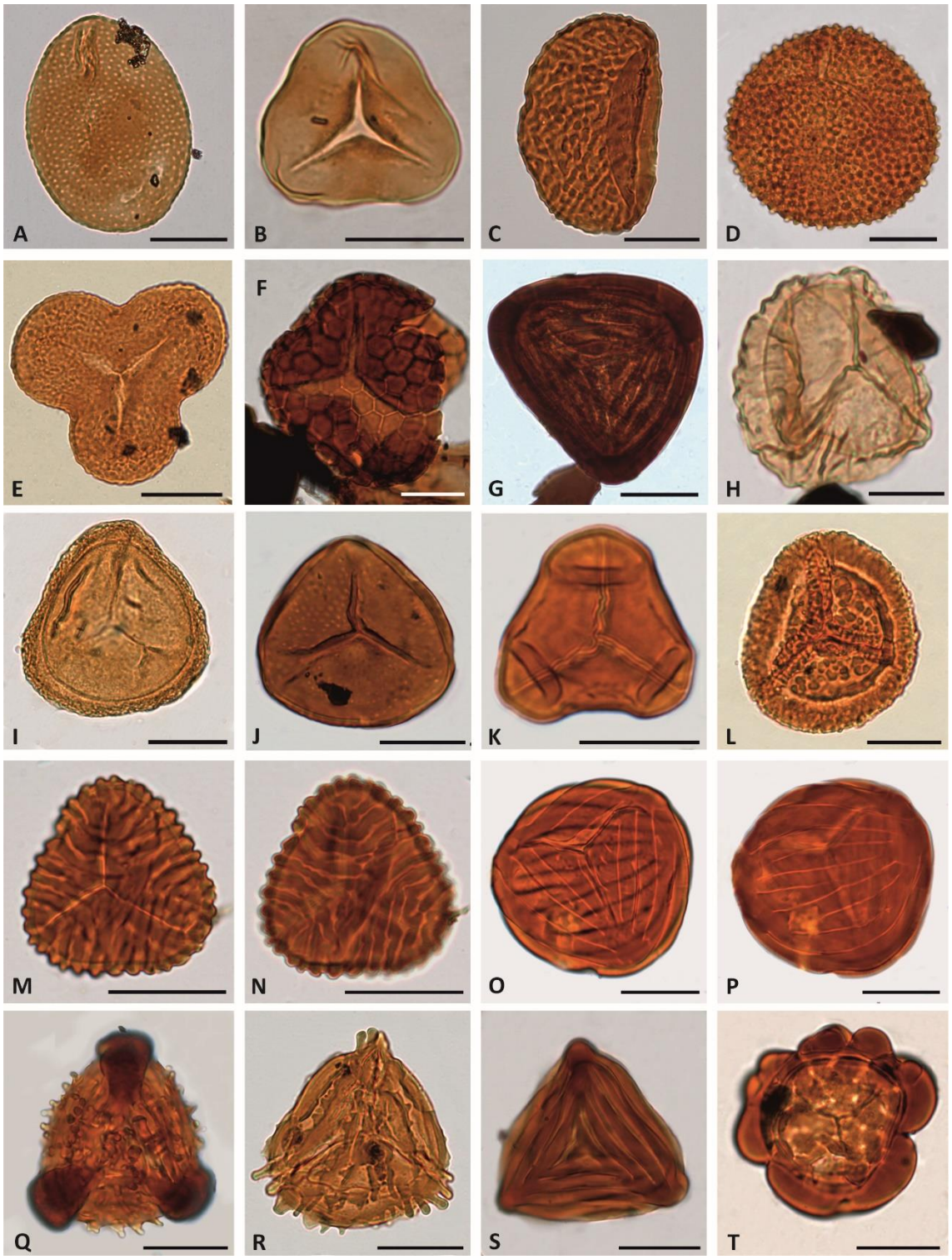

Fig 8. Light photomicrographs of selected spores of Bryophyta and Pteridophyta. (A) *Reticulosporis gallicus*, level CA-21.03. (B) *Cyathidites australis*, level SJ-2.1. (C) *Polypodiisporonites cenomanianus*, level CA-35.01. (D) *Verrucosisporites* sp., level AP-25.6. (E) *Concavissimisporites* cf. *crassatus*, level SJ-3.6. (F) *Gregussisporites orientalis*, level SJ-5.2. (G) *Contignisporites cooksoniae*, level AP-25.9. (H) *Staplinisporites caminus*, level AP-25.6. (I) *Densoisporites velatus*, level CA-2. (J) *Foveosporites* cf. *parviretus*, level AP-25.7. (K) *Cibotiumspora juriensis*, level CA-5.1. (L) *Taurocusporites segmentatus*, level SJ-3.1. (M–N) *Cicatricosisporites proxiradiatus*, level CA-21.04, (M) proximal side, (N) distal side. (O–P) *Cicatricosisporites potomacensis*, level AP-25.7, (O) proximal side, (P) distal side. (Q) *Nodosisporites segmentus*, sample AP-25.7. (R) *Appendicisporites* cf. *crenimurus*, level CA-10.01. (S) *Appendicisporites tricornitatus*, level AP-4.3. (T) *Patellasporites tavaredensis*, level SJ-5.2. Specimens A, C, I, K, M–N, R are from Cortes de Arenoso section; specimens B, E– F, L, T are from San Just section; specimens D, G, H, J, O–Q, S are from Arroyo de la Pascueta section. Scale bar equals 20 μm except in H when it equals 10 μm.

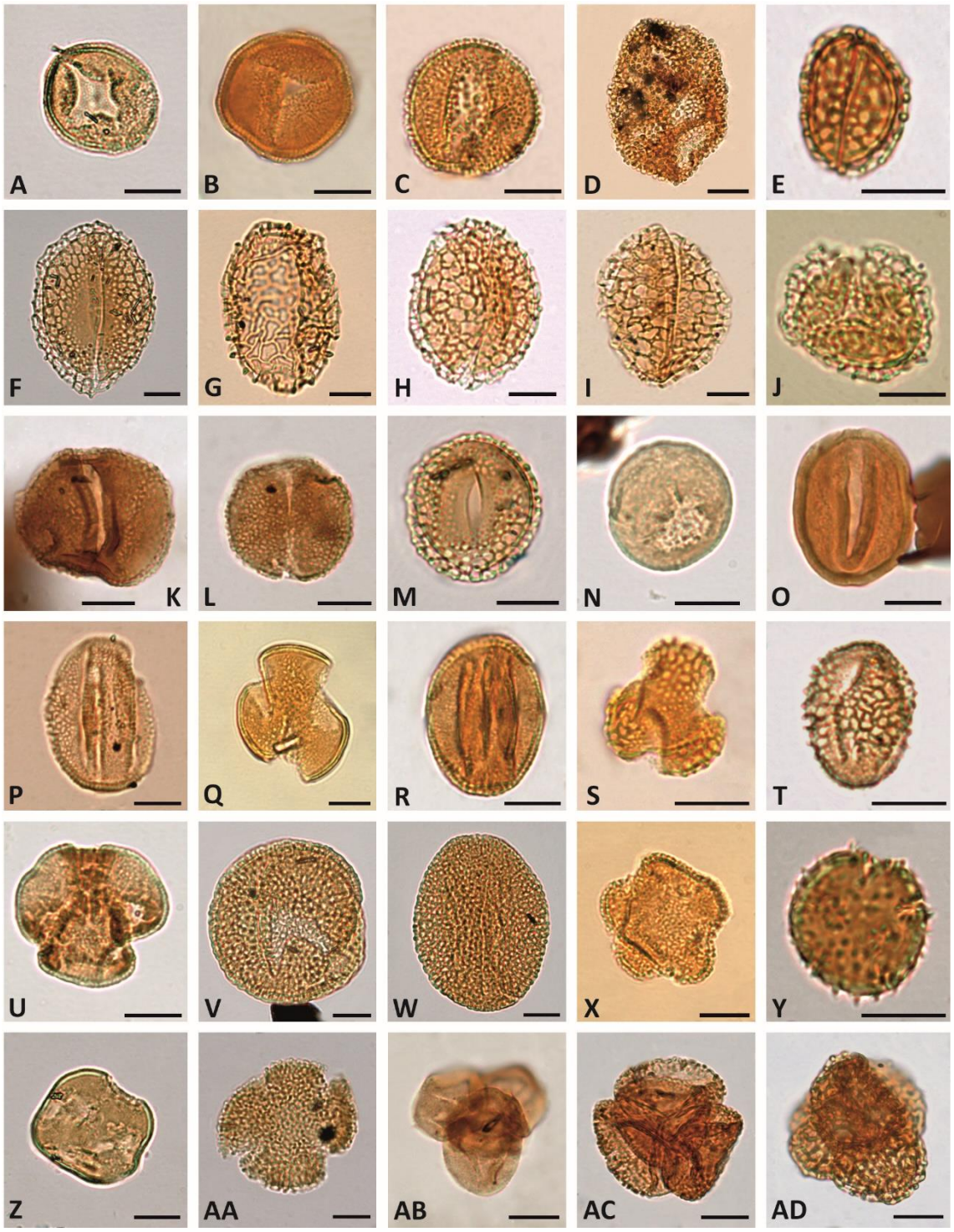

Fig 9. Light photomicrographs of selected pollen grains of angiosperms. (A) *Asteropollis asteroides*, level CA-2. (B) *Jusinghipollis* cf. *ticoensis*, level AP-10.2. (C) *Clavatipollenites tenellis*, level AP-32.3. (D) *Stellatopollis* cf. *barghoornii*, level SJ-5.2. (E) *Pennipollis reticulatus*, level CA-4. (F) *Liliacidites* cf. *clavatus*, level CA-14.01. (G) *Dichastopollenites* sp, level SJ-3.5. (H–I) *Dichastopollenites dunveganensis*, (H) level CA-7, (I) level SJ-3.8. (J) *Doyleipollenites robbinsiae*, level SJ-2.2. (K) *Retimonocolpites dividuus*, level AP-25.2. (L) *Dichastopollenites* cf. *reticulatus*, level AP-25.6. (M) *Liliacidites tectatus*, sample AP-25.7. (N) *Tucanopollis crisopolensis*, level CA-3.2. (O) *Transitoripollis* sp., level AP-25.6. (P) *Rousea*

georgensis, level SJ-3.8. (Q) *Phimopollenites pannosus*, level SJ-3.7. (R) *Tricolpites nemejci*, level AP-10.2. (S–T) *Dryadopollis vestalis*, (S) specimen in polar view, level AP-10.2, (T) specimen in equatorial view, level CA-14-01. (U) *Tricolpites*? *interangulus*, level AP-34.2. (V–W) *Tricolpites* cf. *maximus*, (V) specimen in polar view, level CA-3.1, (W) specimen in equatorial view, level CA-3.1. (X) *Hammenia fredericksburgensis*, level SJ-3.4. (Y) *Echinipollis cenomanensis*, level CA-35.01. (Z) *Penetetrapites mollis*, level CA-1. (AA) *Hammenia fredericksburgensis*, level CA-35.01. (AB) *Artiopollis praecox*, level AP-25.2. (AC) *Senectotetradites* sp., level AP-10.2. (AD) *Senectotetradites grossus*, level CA-35.01. Specimens A, E–F, H, N, V–W, Y–AA, AD are from Cortes de Arenoso section; specimens B–C, K–M, O, R–S, U, AB–AC are from Arroyo de la Pascueta section; specimens D, G, I–J, P–Q, T, X are from San Just section. Scale bar equals 10 μm.

Unlike the upper Albian–lower Cenomanian successions of the Basque-Cantabrian and Lusitanian basins [104–105], dinocysts were only scarcely recorded in the studied assemblages. The most frequently occurring taxa are *Cyclonephelium* spp., *Criboperidinium* spp. (Fig 7C), *Implestosphaeridium* spp., *Kiokansium unituberculatum* (Fig 7H) and *Oligosphaeridium complex* (Fig 7G). The remaining of the identified marine and freshwater palynomorphs are not numerically significant (S1 Appendix). Terrestrial assemblages are characterised by abundant conifers with *Classopollis* (mainly *Classopollis major*) and *Inaperturopollenites dubius* (Fig 7K, Q), constituting 80% of the total palynomorph sum at some levels. Other frequent gymnosperms include *Araucariacites australis*, *Exesipollenites tumulus* (Fig 7P) and *Monosulcites* spp. Bisaccate grains (Fig 7R–T) usually represent a minor component of the assemblages. Fern spores represented the most diversified group of miospores in all the studied sections and occasionally reached dominance, being *Cyathidites australis* and *C. minor* (Fig 8B) the most frequently occurring species. Angiosperms, mainly represented by the genera *Clavatipollenites* (Fig 9C) and *Retimonocolpites* (Fig 9K), were recorded in significant numbers at specific levels from the CA and AP sections. A low number of tricolpate grains were identified in the three successions (Fig 9P–W).

The PCA presents a variance of 33.8% in the first two dimensions (Fig 10). On the first axis (19.5% of variance), the taxa with negative coordinates were *Classopollis* spp., *Exesipollenites tumulus*, Araucariaceae, *Patellasporites tavaredensis*, *Cicatricosisporites* spp. and *Crassipollis chaloneri*. In contrast, *Inaperturopollenites dubius*, *Eucommiidites troedsonii*, *Peromonolites allenensis*, *Monosulcites* spp., *Cyathidites*/*Deltoidospora*, Gleicheniaceae, *Clavatipollenites* spp., *Pennipollis* spp., *Tucanopollis* spp. and the dinocysts presented positive coordinates in the PCA plot. The scattering of samples from AP and SJ along the first axis of the plot suggests the existence of an ecological gradient defining two vegetation types at the extremes. The second axis (14.3% of variance) discriminate spores in the negative extreme, from wind-transported gymnosperm pollen grains plus marine protists, in the positive one. While samples from AP and CA are majoritarily plotted against the negative side of the axis, levels from SJ are mainly restricted to the positive quadrant.

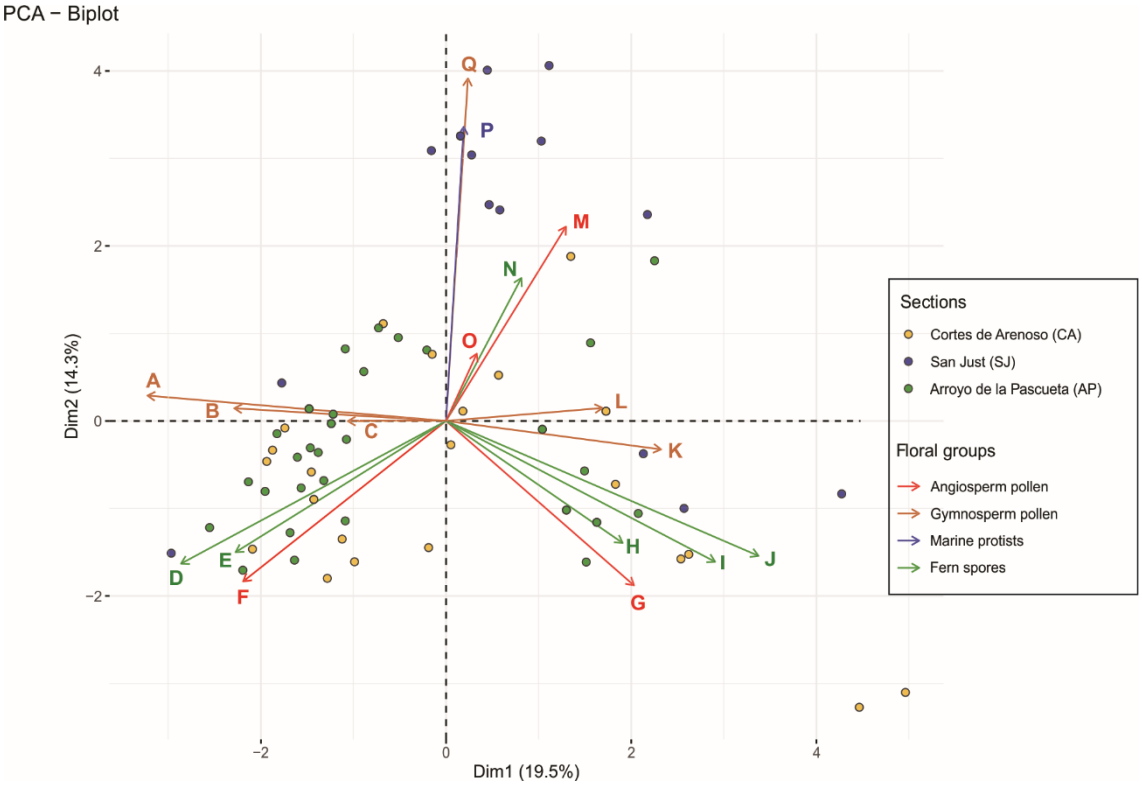

Fig 10. Principal Component Analysis (PCA) performed with the most relevant identified taxa and levels. (A) *Classopollis* spp. (B) *Exesipollenites tumulus*. (C) Araucariaceae. (D) *Patellasporites tavaredensis*. (E) *Cicatricosisporites* spp. (F) *Crassipollis chaloneri*. (G) *Clavatipollenites* spp. (H) *Plicifera* spp. (I) *Cyathidites*/*Deltoidospora*. (J) *Gleicheniidites senonicus*. (K) *Monosulcites* spp. (L) *Eucommiidites* sp. (M) *Pennipollis* spp. (N) *Peromonolites allenensis*. (O) *Tucanopollis* spp. (P) Marine protists. (Q) *Inaperturopollenites dubius*.

Mega- and mesoremains were collected in the three studied sections. Generally, they exhibit good preservation and occur more abundantly in levels with marine influence (i.e., associated with palynological samples containing dinocysts) and without amber (e.g., SJ-2.1, CA-2, AP-4.2; Figs 3–5). In sharp contrast with the palynofloras, the megafloral assemblages are poorly diverse and dominated by conifers, being *Frenelopsis* particularly abundant. Angiosperms represent only a minor part of the mesofossil assemblages. The megaremain assemblage of AP has been interpreted as mostly allochthonous due to the range of disarticulation and fragmentation of specimens of *Frenelopsis turolensis* [106]. The preservation of most of the fossil plants as compressions including well-preserved cuticle and the occurrence of ramified and articulated branches of *Frenelopsis* (Fig 11D), some of them presenting cones attached to their axes, would indicate, however, a parautochthonous production *sensu* [107].

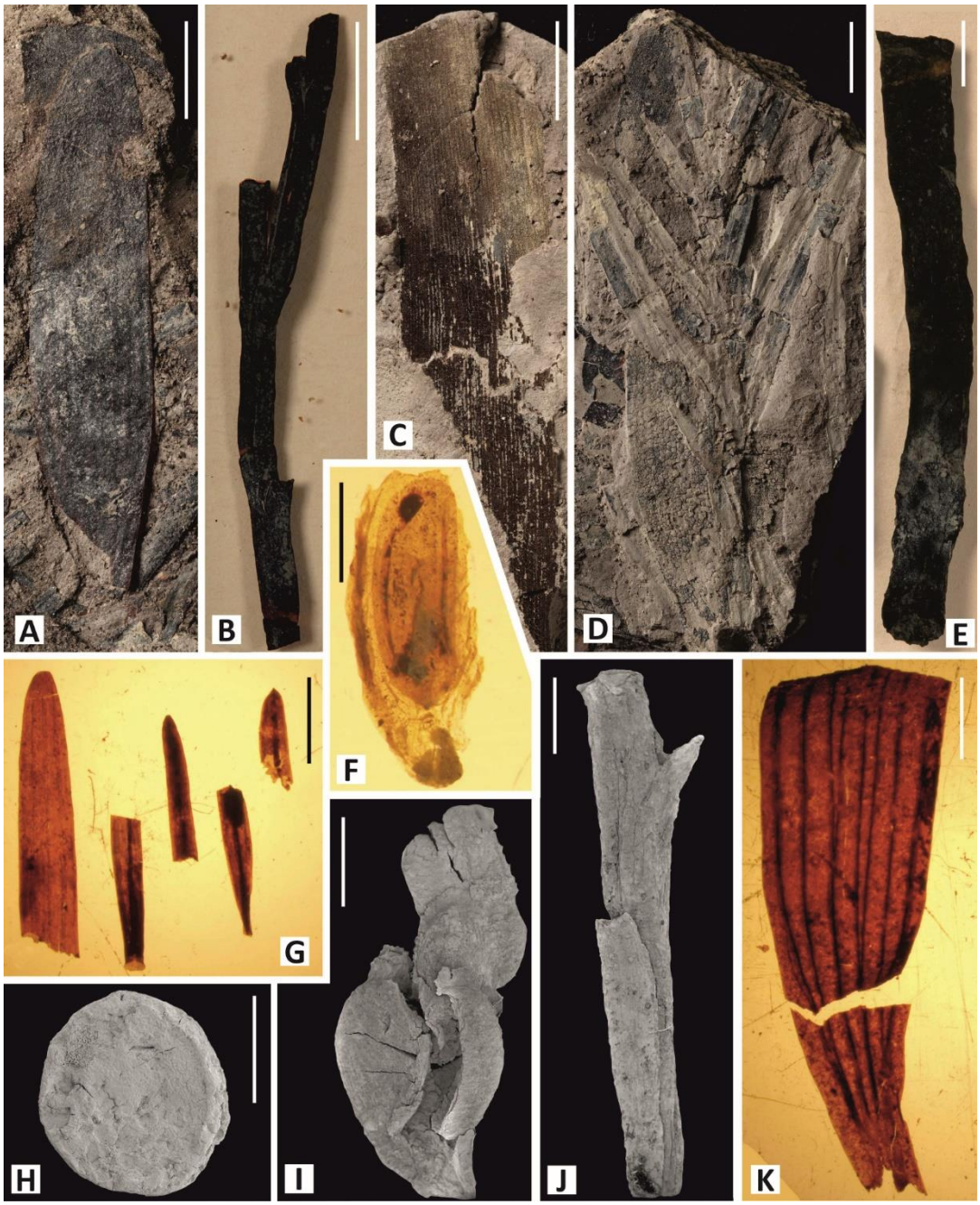

Fig 11. Selected plant macro and mesofossils from the El Maestrazgo Basin. (A) Leaf of *Nehvizdya* (=*Eretmophyllum*) *penalveri*, No. K 2788. (B) Shoot of *Frenelopsis turolensis*, No. K 2786. (C) Fragment of leaf of *Dammarites* cf. *albens*, No. K 2789. (D) Ramified shoot of *Frenelopsis* cf. *turolensis*, No. K 2797. (E) Shoot of *Frenelopsis justae*, No. K 2806. (F) Fruit fragment of *Montsechia*-type with orthotropous seed (*Spermatites*), No. K 2795. (G) Fragments of leaves of *Mirovia gothanii*, Nos. K 2807–2811. (H) Angiosperm fruit of cf. *Serialis* sp., SEM image, No. K 2803. (I) Shoot fragment of *Brachyphyllum* cf. *obesum*, SEM image, No. K 2804. (J) Shoot fragment of *Widdringtonites* sp., SEM image, No. K 2805. (K) Basal part of a leaf of *Nehvizdya* (=*Eretmophyllum*) *penalveri*, No. K 2794. Specimens A–C, G are from Arroyo de la Pascueta section; specimens D, F, K are from Cortes de Arenoso section; specimens E, H–J are from San Just section. Scale bars: A–D = 10 mm; E, G, K = 5 mm; F, H–J = 1 mm.

One of the most abundant taxon is *Frenelopsis*, which presents in the Maestrazgo Basin a vegetative morphology markedly xeromorphic with highly reduced leaves, thick cuticles and deeply sunken stomatas [37, 106]. Leaves of *Eretmophyllum*, *Mirovia* and *Dammarites*, as well as twigs of *Brachyphyllum* and *Widdringtonites*, have been commonly found.

San Just section (SJ). The lower palynological interval of this section (SJ-2.1–SJ-3.4; Fig 12 clusters I–II) is characterised by marine palynomorphs and high percentages of *Inaperturopollenites dubius* (Fig 7K) and *Classopollis* spp. (Fig 7Q). Its upper part (SJ-3.5–SJ-5.3; Fig 12 clusters III–V), corresponding with the amber outcrop, is devoid of dinocysts and reveals increasing abundances of fern spores (*Cyathidites/Deltoidospora* and Gleicheniaceae) and angiosperms (mainly *Pennipollis*). A renewed increase of *I. dubius* and *Classopollis*, this time accompanied by numerous Anemiaceae and spores of uncertain botanical affinities (*Patellasporites tavaredensis*, Fig 8T), is characterising the uppermost interval of the succession (Fig 12, cluster V).

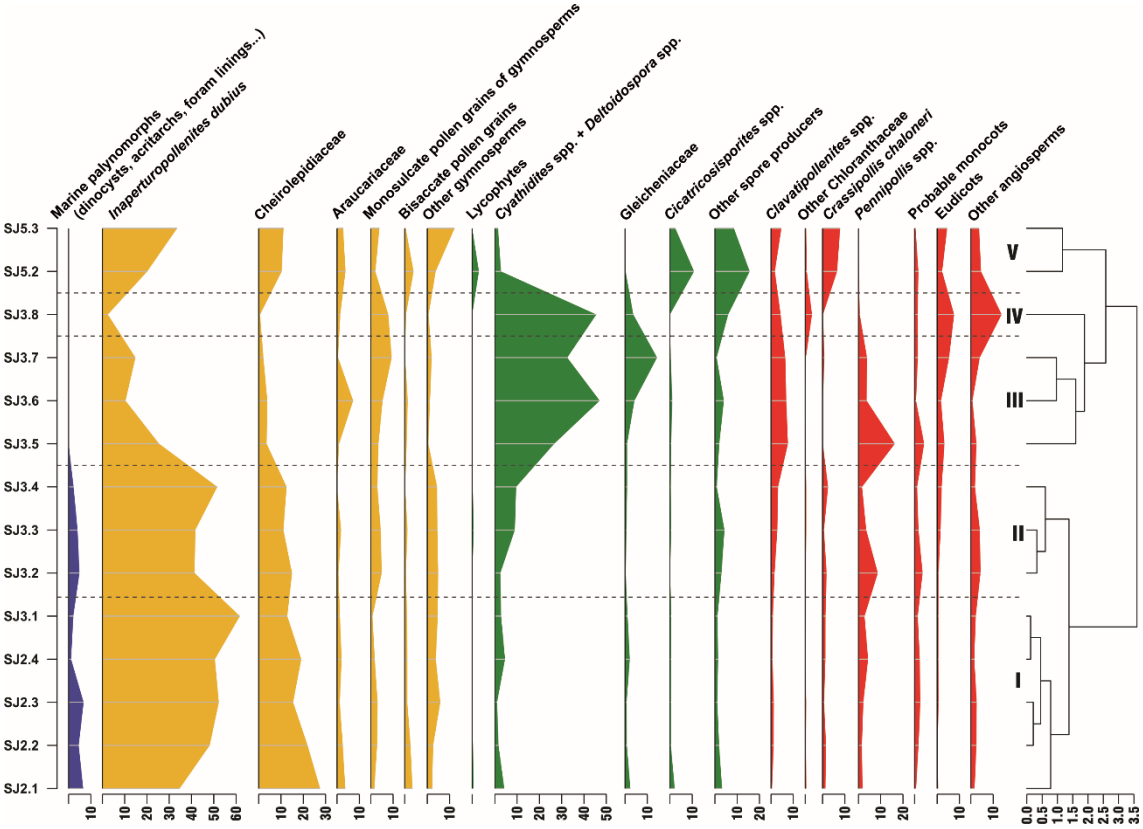

Fig 12. Detailed palynological chart for San Just section (SJ). Blue colour: marine palynomorphs; yellow colour: spores of ferns and allied; green colour: Gymnosperm pollen; red colour: Angiosperm pollen.

The megaflora collected in SJ (Fig 3) is the most diversified among the studied outcrops from the Maestrazgo Basin. *Frenelopsis justae* is numerically prevailing (Fig 11E).

This species shows robust axes consisting of nodes and internodes formed by three unified leaves [37]. In addition, scarce remains of *Brachyphyllum* cf. *obesum* (Fig 11I), *Eretmophyllum* sp., *Dammarites* sp. and *Widdringtonites* sp. (Fig 11J) have been found. Several small fruits of angiosperms were found as mesofossils. They mainly include fruits of *Montsechia*-type (Fig 11F) and segmented fruitlets of cf. *Serialis* sp. (Fig 11H).

Cortes de Arenoso section (CA). The lower palynological interval of CA (CA-1–CA-14.01; Fig 13, clusters I–IV) is characterised by fluctuating abundances of *Classopollis* and *Inaperturopollenites dubius.* The levels with the highest numbers of *Classopollis* usually include more dinocysts (*Cyclonephelium vannophorum* and *Kiokansium unituberculatum*) and other marine palynomorphs. In this interval, two levels with significantly high percentages of angiosperms (>40% of the total miospores) are noteworthy. The lower (CA-3.2) is characterised by the dominance of *Tucanopollis* spp. (Fig 9N), while the upper (CA-14.01; Fig 13, cluster IV) is characterised by a spike of "*Liliacidites*" *minutus,* and the near-complete absence of conifers. The overlying interval (CA-21.01–CA-35.03; Fig 13) includes high percentages of *Classopollis* (cluster V) and *Inaperturopollenites* (cluster VI), accompanied by moderate amounts of bisaccate grains and lower proportions of spores. The amber-bearing stratum (La Hoya amber outcrop) is restricted to the uppermost part of the succession (cluster VI).

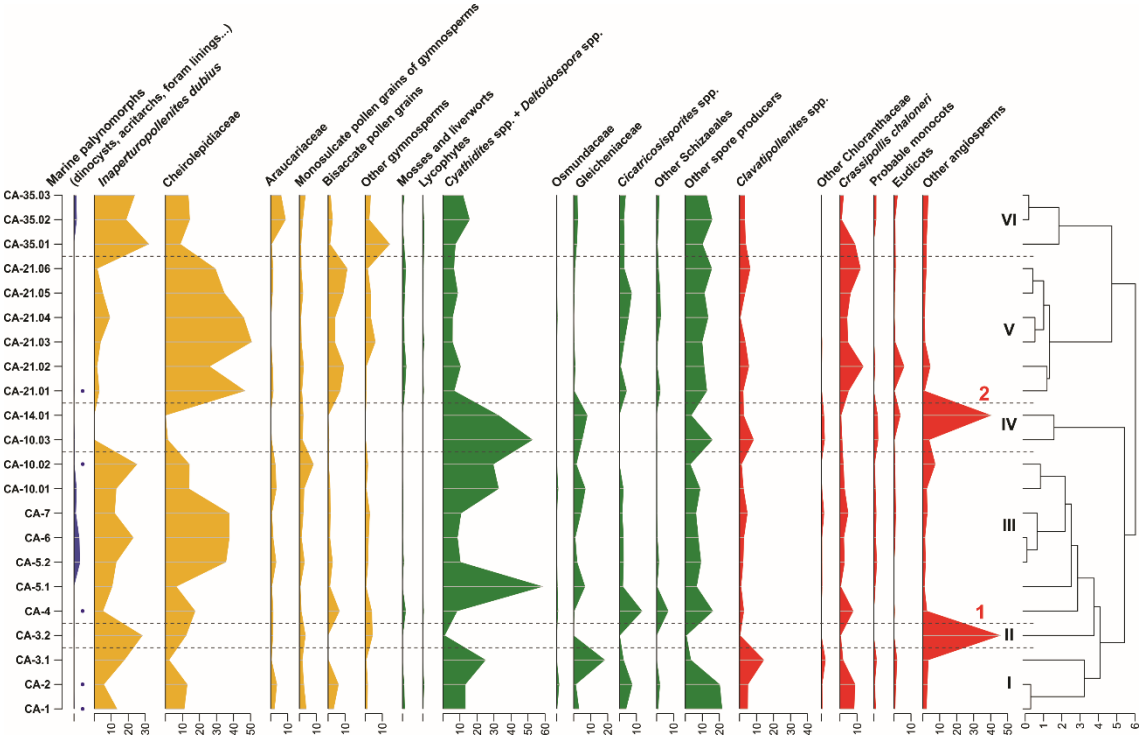

Fig 13. Detailed palynological chart for Cortes de Arenoso section (CA). Blue colour: marine palynomorphs; yellow colour: spores of ferns and allied; green colour: Gymnosperm pollen; red colour: Angiosperm pollen. 1. Pick due to the abundance of *Tucanopollis* spp. 2. Pick due to the abundance of "*Liliacidites*" *minutus*.

Over 90% of the plant megaremains of this section are attributed to *Frenelopsis* cf. *turolensis* (Fig. 11D). Particularly, this assemblage occurs in its lower part (levels CA-2, CA-3, CA-4, CA-10; Fig 5). Leaves of *Mirovia gothanii* and *Nehvizdya* (=*Eretmophyllum*) *penalveri* and elongated seeds of the *Spermatites*-type constitute the remaing of the assemblage.

Arroyo de la Pascueta outcrop (AP). In the palynological succession, *Cyathidites*/*Deltoidospora* and *Classopollis* exhibit antagonistic percentage fluctuations. Cheirolepidiaceae characterised the lower part of the succession (Fig 14, clusters I and III). Conversely, although defining a pattern slightly less pronounced, *Cyathidites*/*Deltoidospora* are more abundant in the upper part of the section (Fig 14, cluster V and cluster VI), and occur in assemblage devoid of marine palynomorphs. The two mentioned intervals are separated by a level with abundant angiosperms and common Anemiaceae (cluster IV). The amber-bearing stratum, typified by *Cyathidites/Deltoidospora*, is restricted to the uppermost part of the succession (cluster VI). Although not found in abundance, angiosperms are diverse in the amber-bearing bed and include various species associated with Chloranthaceae/Ceratophyllaceae, Laurales and eudicots (i.e., Fig 9U).

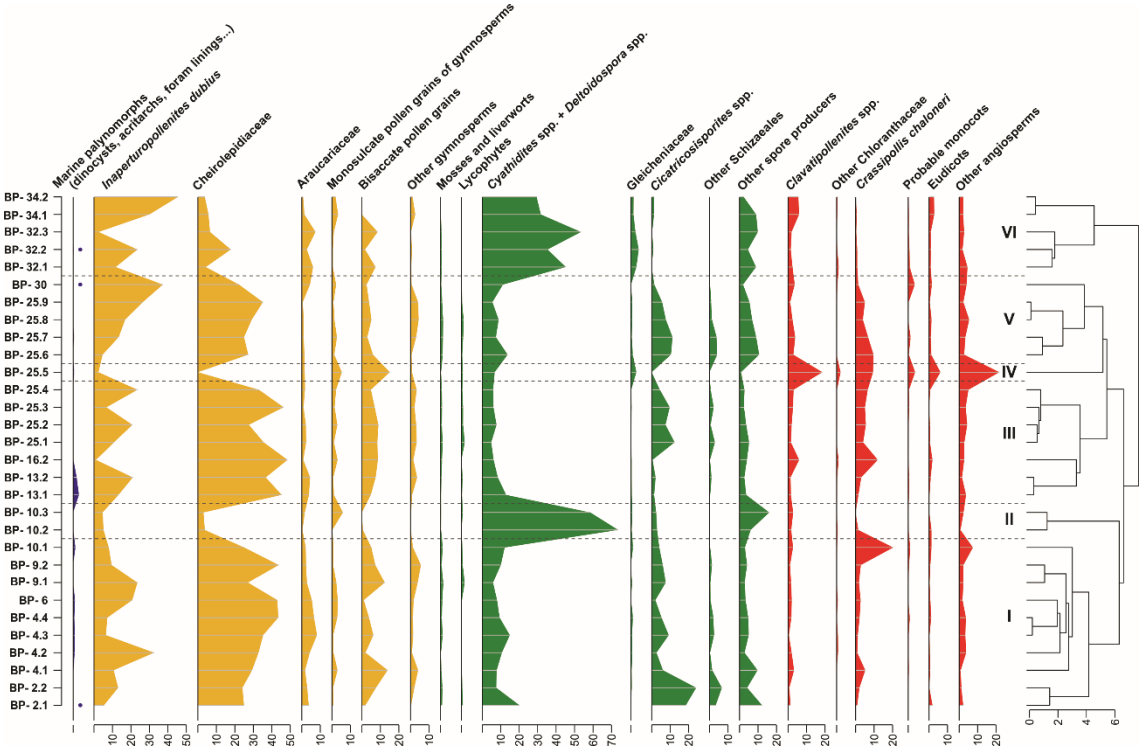

Fig 14. Detailed palynological chart for Arroyo de la Pascueta section (AP). Blue colour: marine palynomorphs; yellow colour: spores of ferns and allied; green colour: Gymnosperm pollen; red colour: Angiosperm pollen.

Mega and mesofossil plants from AP show a balanced representation of remains with thick cuticles. The megaflora includes narrowly elongated leaves of *Mirovia gothanii* (Fig 11C), broadly obtuse entire-margined leaves of the ginkgophyte *Nehvizdya* (=*Eretmophyllum*) *penalveri* (Fig 11A), shoots of the Cheirolepidiaceae *Frenelopsis turolensis*

(Fig 11B) and elongated leaves of *Dammarites* cf. *albens* (Fig 11C). While elongate seeds of the *Spermatites* type are common, the anecdotic presence of megaspores (two specimens) is noteworthy as it may reflect occasional floodings or high water table allowing the development of wetlands.

Insects and amber

The Cretaceous amber from the Maestrazgo Basin has provided an extensive arthropod record as bioinclusions from the San Just, Arroyo de la Pascueta and La Hoya outcrops (Table 2). San Just represents one of the most outstanding Cretaceous amber-bearing outcrops worldwide with diverse and abundant bioinclusions. Its entomological content has been the subject of extensive research over the last decades (i.e. [108–109] and references therein).

The arthropod assemblages from San Just include arachnids (Pseudoscorpions, Acari and Araneae; Fig 4C), non-insect hexapods (Collembola) and up to eleven orders of insects (Archaeognatha, Orthoptera, Blattodea, Mantodea, Psocodea, Thysanoptera, Hemiptera, Neuroptera, Coleoptera [Fig 4D], Hymenoptera [Fig 4E–F] and Diptera), together with a high number of arthropod ichnofossils such as spiderwebs and coprolites. The site is also the type locality of 22 arthropod taxa to date, most of them insects (Table 2). Hymenoptera (mainly platygastroids [Fig 4E]) and Diptera are the most abundant insects. Apart from arthropods, the amber from SJ also includes dinosaur feathers (Fig 4F), although the outcrop is devoid of faunal megaremains. Conversely, the bioinclusions from the Arroyo de la Pascueta and La Hoya outcrops are poorly known and only few amber pieces have been described so far. Additionally, new material collected from these two outcrops is currently being prepared and new findings are expected. Hymenoptera, including one new species [110], Hemiptera and Diptera have been reported from Arroyo de la Pascueta while Diptera and Blattodea have been recorded in La Hoya. Collectivelly, the amber from the three outcrops has delivered 40 arthropod taxa, presenting higher or similar level of diversity than other mid-Cretaceous amber-bearing sites of Iberia such as Peñacerrada and El Soplao (northern Spain).

Discussion

Palynomorph-based biostratigraphy

In the AP section, the presence of *Tricolporoidites* (Fig 6), *Artiopollis praecox* (Fig 9AB), *Dryadopollis vestalis* (Fig 9S), *Gnetaceaepollenites oreadis* (Fig 7O), *Liliacidites tectatus* (Fig 9M), *Rousea miculipollis*, *Senectotetradites* spp. (Fig 9AC) and *Tricolpites nemejci* (Fig. 9R) indicates a late Albian age (Fig 15) since none of these taxa have been identified in older strata [78, 93, 104, 111–113]. This age is significantly younger than the one inferred by [29] based on a long-distance correlation with palaeontological data from the neighbouring Morella Sub-basin.

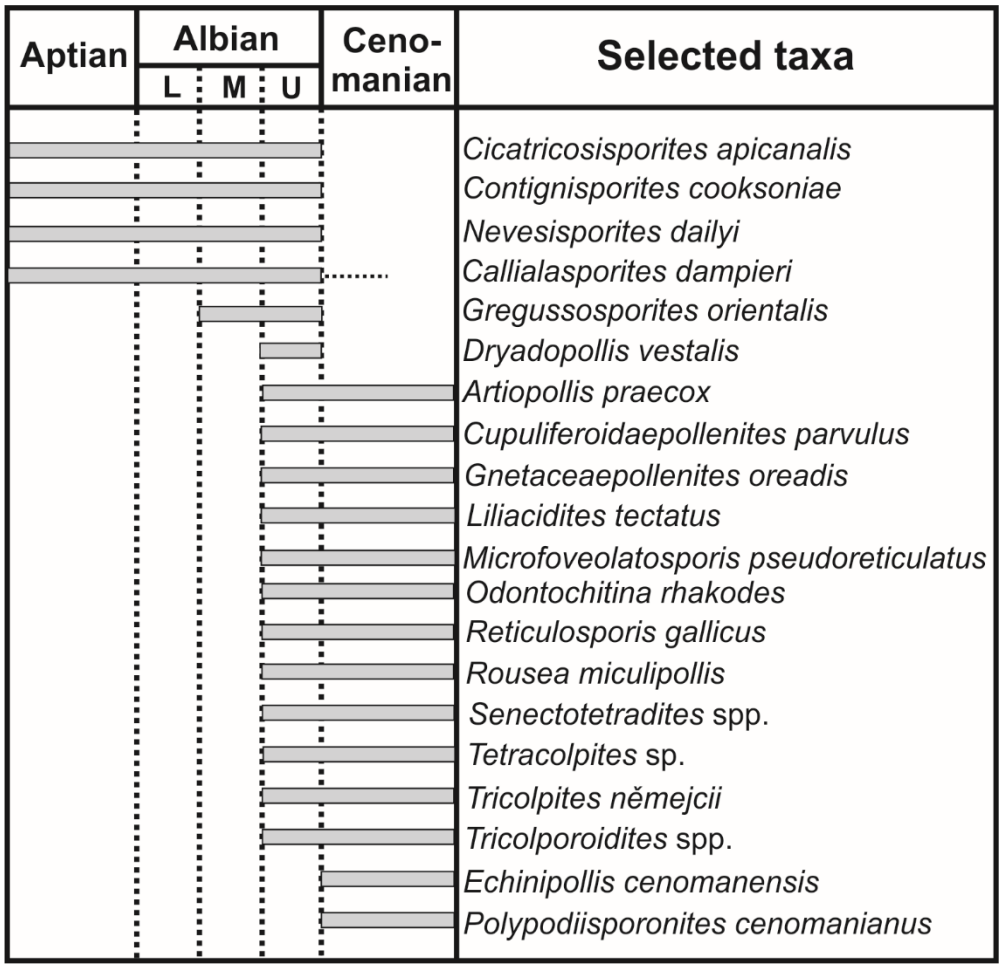

Fig 15. Composite range chart showing selected species of biostratigraphic interest identified in the Lower Cretaceous sections from the Maestrazgo Basin. L = lower; M = middle; U = upper.

The age of the SJ section can be independently dated as late Albian or younger based on the record of *Odontochitina rhakodes* (Fig 7F). This age is further supported by the presence of *Tricolpites nemejci* and *Senectotetradites* sp. [93, 104, 111, 114–116]. This age inference updates and refines the previously proposed middle to early late Albian age, which was based on a more limited palynological data set [32]. The presence of *Cicatricosisporites apicanalis*, *Contignisporites cooksoniae* (Fig 8G), *Gregussisporites orientalis* (Fig 8F) and *Nevesisporites dailyi* (Fig 15) in both SJ and AP, also allows defining an intra late Albian upper limit for the age interval as none of the taxa have been recorded in strata of different age in Europe [31, 113, 117].

In addition to the biostratigraphic markers already present in SJ and AP, the lower part of the CA section also includes *Reticulosporis gallicus* (Fig 8A), a taxon only recorded in France in strata independently dated as late Albian [90, 118], and *Microfoveolatosporis pseudoreticulatus* and *Cupuliferoidaepollenites parvulus* (Fig 15), both taxa presenting an oldest occurrence in strata of that age in North America and Western Europe [105, 112, 119]. A slightly younger early Cenomanian could be considered for the uppermost part of the CA section that corresponds to the La Hoya amber outcrop (CA-35.1–CA-35.3; Fig 5) as

Echinipollis cenomanensis (Fig 9Y)*, Polypodiisporonites cenomanianus* (Fig 8C) and *Senectotetradites grossus* (Fig 9AB) recorded therein have not been reported from older strata [111, 120–122]. The CA record could equally represent a range extension down into the late Albian for these taxa, which remain not widely distributed (i.e., rare species).

The updated new age for the sections has important implications for the local stratigraphy as it allows to confidently attribute them to the Utrillas Group [61], while previous studies considered them as part of the Escucha Formation [28–29, 31–32, 43]. The new biostratigraphic inferences are also supported by previous results obtained for the Utrillas Group in the Maestrazgo Basin based on indirect correlations [47, 50], palynological [123–124] and faunal data (ostracods) [61].

From a palaeoenvironmental perspective, the biostratigraphic markers recorded in the three studied sections suggest that resin production/deposition in the Maestrazgo Basin was either coeval or close in time. In that regard, the amber levels might represent a biostratigraphic event of regional significance. The marine carbonates of the Mosqueruela Formation [50], immediately overlying the amber-bearing strata at CA and AP, represent the regional expression of the flooding event described elsewhere in uppermost Albian strata (Mortoniceras rostratum/M. perinflatum ammonite zones) [125]. In eastern Iberia, this transgressive pulse led to the development of widespread marine platforms correlated across the Mesozoic basins of Iberia [48–49].

Environments and vegetation

The record of highly variable fossil remains, as well as amber with biological inclusions, suggests the presence of an ecosystem structurally framed by a multi-tiered vegetation [14, 28, 34–36] sustaining complex arthropod communities (Table 2). Terrestrial ecosystems of such complexity might seem surprising for deposits associated with a desert system. However, there are no reasons to believe that arid and semi-arid ecosystems from the Cretaceous were less complex than their modern counterparts, such as the Namib and Kalahari deserts [126–127]. The presence of palynological assemblages of varying composition in marine-influenced intervals is otherwise expected, given the taphonomic, palynological and palaeobotanical constraints [14, 128–131], and indicates the existence of mosaic vegetation types in the area with conifer-forests along the Tethyan coasts (Fig 16). The vegetation of this region was strongly conditioned by both the influence of the sea and the desert as well as other factors such as the palaeowildfires as the abundant charcoal found in the Spanish Cretaceous amber-bearing deposits indicates [40, 132].

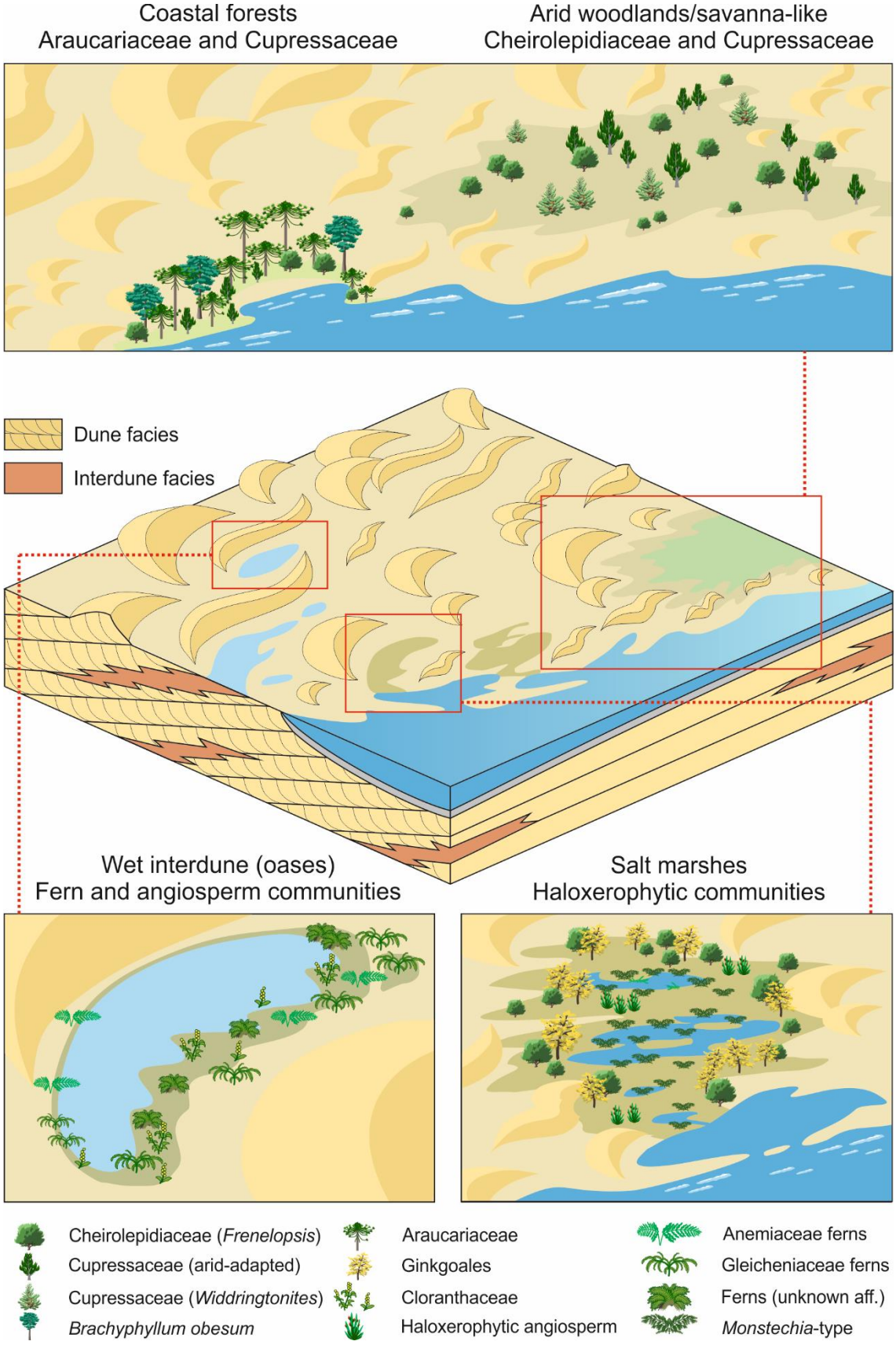

Fig 16. Schematic model of the late Albian fore-erg setting including the types of vegetation and their distribution in the different sub-environments.

A picture of the regional vegetation: Cheirolepidiaceae-Cupressaceae communities. The significant representation of *Classopollis* and *Inaperturopollenites dubius* in the studied assemblages reflects the importance of the families Cheirolepidiaceae and Cupressaceae in the vegetation. The increased numbers of these two taxa observed in assemblages with marine palynomorphs (Figs 12–14) and the correlation between *I. dubius* and dinocysts in the PCA (Fig 10), representing the most distal settings, indicate that their pollen-producers were widespread regionally, probably forming a significant part of the hinterland vegetation.

Cheirolepidiaceae was one of the most widespread conifer families among the Mesozoic vegetation. They colonised a wide range of environments ranging from low to high latitudes in both hemispheres [8, 133–135] and commonly assumed a dominant position in the vegetation from the Early Jurassic to the mid-Cretaceous [134, 136], especially in some low latitude settings associated with evaporites [8, 137]. While historically linked to arid environments and/or salty ones [79, 138–140], recent studies suggest broader ecological preferences for, at least, some representatives of the family [134, 141–142].

Inaperturopollenites dubius-producers are thought to belong to Cupressaceae, a conifer family with species widely distributed in present-day ecosystems of the Northern Hemisphere [143]. While some modern forms such as the bald cypress and the Chinese swamp cypress, mostly belonging to the *Glyptostrobus–Taxodium–Cryptomeria* clade (Taxodioideae), exhibit a marked ecological affinity toward wet environments [144], a significant number of Cupressaceae species prefer well-drained habitats [143]. Distinguishing moisture-loving forms from plants preferring well-drained substrates based solely on palynological evidence is complex due to the similarity of the pollen produced by both groups of plants. By analogy with modern pollen of *Taxodium*, fossil grains presenting a papilla such as *Taxodiaceaepollenites* are assumed to have been produced by trees preferring saturated soils and wetlands subjected to periodic floodings. Taxodioideae pollen is frequent in Cenozoic deposits and has also been found in high numbers in Cretaceous deposits from high latitude locations [135, 145]. These pollen grains have also been recorded in mid-latitude assemblages associated with spores produced by water ferns [90]. However, they are scarcely represented in the successions from the Maestrazgo Basin (Appendix 1). *Perinopollenites halonatus*, pollen with two distinct exine layers related to Taxodioideae [77], neither reaches a significant representation in the studied sections (S1 Appendix). Therefore, most Cupressaceae pollen recovered is assumed to have been produced by trees or shrubs that preferred well-drained substrates.

The presence of *Widdringtonites* sp. in SJ (Fig 11J) would support the presence of Cupressaceae linked to well-drained substrates as the specimens assigned to this taxon present well-developed Florin rings in their stomata, reflecting xerophytic conditions. Interestingly, the genus *Widdringtonites* has been related to the extant *Widdringtonia*, which presents species adapted to very hot, dry summers and recurring wildfires in South Africa [146].

If an arid/semi-arid environment can be inferred on the abundant number of Cupressaceae pollen and *Classopollis* as well as regional sedimentology, the presence of

localised thickets of Taxodioideae colonising the wettest parts of the landscape (i.e., wet interdunes, see below), while unlikely, cannot be discarded. The palynofloral data presented here and indicating the prevalence of Cupressaceae in local vegetation confirm the results obtained from fossil wood dataset for the Albian (T2 time bin in [5]).

Cheirolepidiaceae and Cupressaceae are often the co-dominant families in the studied palynofloras. Fluctuating frequencies of these taxa could, however, reflect drastic changes in vegetation which are difficult to ascertain. While, Cheirolepidiaceae are usually dominating in AP and CA (Figs 13–14), Cupressaceae remains are more abundant in SJ palynofloras and in the amber-bearing levels of AP and CA (Figs 12–14). Similar dominance of the palynofloras by these two taxa has been previously recorded in numerous mid-latitude Jurassic and Cretaceous deposits [25, 90, 104, 136, 142]. Present-day growth habits of Cupressaceae, as well as whole plant reconstructions of fossil representatives of Cheirolepidiaceae, suggest that these plants were dominantly, if not exclusively, arborescent during the Cretaceous. The corresponding shrubs and trees might have represented the sub-dominant and dominant components of open vegetation (savanna–woodlands; Fig 16) similar to those observed in modern arid to semi-arid climates [143]. This conifer-dominated plant community was very different of the Jurassic and Cretaceous fern savanna biome characterized by Escriba aquí la ecuación.the families Anemiaceae and Matoniaceae (Mohr et al., 2015; Hamad et al., 2016a y 2016b; Dettmann 2017; Blanco-Moreno et al., 2018; Halamski et al., 2020) which might have also grown on dunes.

The diversity of angiosperm pollen types and their varying abundance pattern (S2 Appendix), suggest that producers had distinct ecophysiologies allowing them to colonise not only moister habitats and, probably, water-logged, if not aquatic, environments [12, 35, 152–154] but also well-drained and/or dry edaphic settings. Originally associated to moist environments [155], angiosperms may have already radiated into more arid settings by the late Albian as their presence in deposits associated to desert system could suggest [14]. It is likely that the representation of flowering plants in pre-Cenomanian ecosystems is underestimated owing to morpho-functional and taphonomic biases (i.e., low production and dispersal of entomophilous pollen [156]). While the exact phenology of early angiosperms is poorly understood, the existence of short life cycles allowing flash flowering [152, 157] could explain the localised high abundance of this pollen.

Diversified local vegetation

- Coastal settings with Araucariaceae

Pollen of Araucariaceae is consistently recorded in the palynofloras of the three studied outcrops (S1 Appendix), albeit in low abundance (<5% of the total miospores). However, the presence and relative abundance of these conifers in the local vegetation may be underestimated since both modern [158–159] and fossil Araucariaceae pollen [136] are believed to present low dispersal capabilities. Several researchers [158] noted that modern palynological assemblages collected from Kauri (*Agathis australis*) forests only include relatively low percentages (<5–10%) of Araucariaceae pollen.

683 Palaeobotanical and geochemical evidence suggests a clear Araucariacean affinity for
684 the late Albian amber recovered in the Basque-Cantabrian Basin [90, 160]. However, a
685 geochemical analysis of the amber from San Just outcrop seems to support an
686 araucariacean-cheirolepidiacean affinity [161]. The ubiquity of Araucariaceae in
687 palynological assemblages and the record of presumed specialised insect pollen feeders
688 (nemonychid beetles) in amber inclusions from San Just outcrop [162] would represent
689 additional circumstantial evidence linking Araucariaceae to the resin production.
690 The precise role of Araucariaceae in Cretaceous vegetation and the structure of the
691 forest types they formed remain difficult to be ascertained given the characteristics of the
692 habitats colonised by modern forms. Apart from isolated occurrences in savanna-like
693 vegetation growing on mafic-ultramafic soils of New Caledonia (i.e., *Agathis ovata*; [163]),
694 modern araucarians are often part of evergreen rainforests where they act as emergents
695 (*Agathis microstachya* in Australia, *A. ovata* and *Araucaria schmidii* in New Caledonia,
696 *Agathis australis* in New Zealand), or constitute small thickets and discrete stands in low
697 altitude forests of New Zealand (*A. australis*) and Australia (*Araucaria heterophylla*) [164–
698 165]. Species distributed in low-fertility soils, ridgetops, and steep slopes reflect also
699 probably competitive exclusion by angiosperms, i.e., a derived, relictual, distribution (a
700 realised niche much more restricted than a potential niche sensu [166]). Some Recent
701 Araucariaceae such as *Araucaria columnaris*, *A. luxurians* and *A. nemorosa* are coastal trees
702 able to withstand the influence of salt wind [74, 167] and this ecological habit was probably
703 already exhibited by representatives of the family during the Mesozoic. The presence of
704 *Microphorites utrillensis* (Dolichopodidae: Microphorinae) in amber from the SJ outcrop
705 [168] would support a sandy coastal habitat for *Araucariacites*-producers, as living
706 microphorines are known to inhabit this type of habitats [169] (Figs 16–17).
707

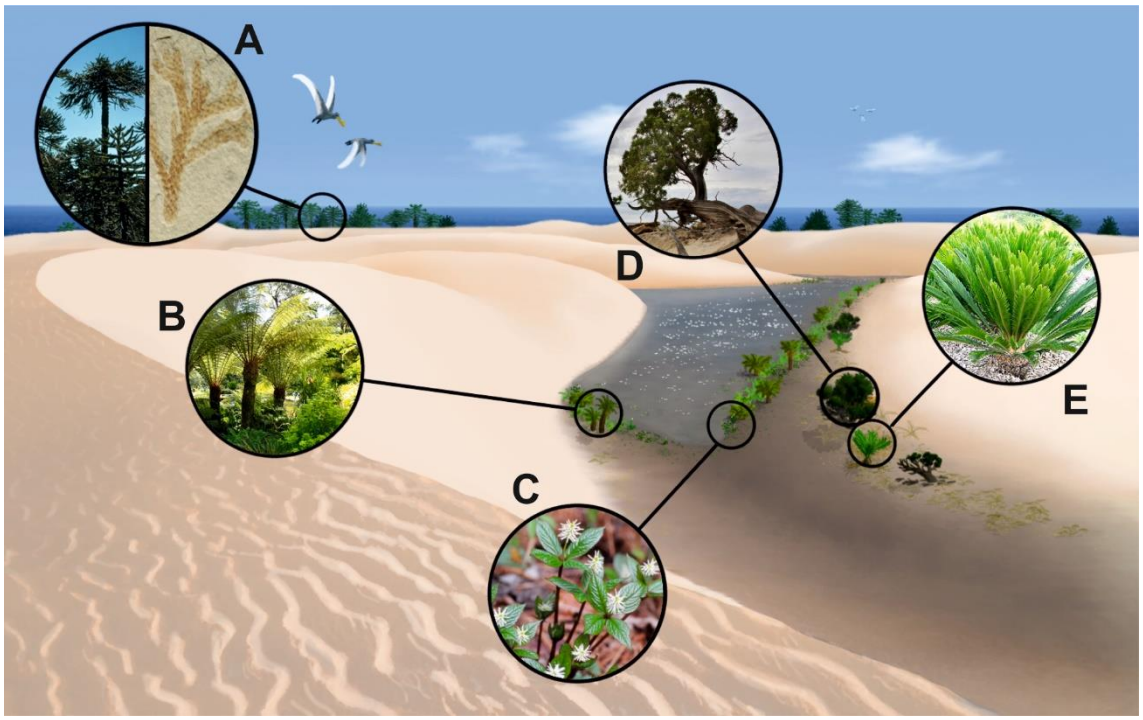

708

Fig 17. Conceptual palaeoartistic reconstruction of the late Albian wet interdunes in the fore-erg from the Maestrazgo Basin (eastern Spain). This environment developed near the Tethys where (A) coastal forests with Araucariaceae grew. The riparian places of the wet interdunes (oasis) (B) were covered by fern and angiosperm vegetation. (C) Fresh water/brackish aquatic angiosperms inhabited wet interdunes. (D–E) Xerophytic plant community involving Cheirolepidiaceae, Cupressaceae (D) and other gymnosperms groups as Bennettitales, Cycadales (*Monosulcites*/*Cycadopites*-producers) and Gnetales (*Equisetosporites*-producers) (E) that integrated arid woodlands.

It is interesting to mention the association of modern Araucariaceae with other conifers, mainly Podocarpaceae, but also Cupressaceae in the evergreen forests of New Zealand [165]. Associations among conifers, probably fortuitous within the context of modern vegetation dominated by angiosperms, should have been more frequent during most of the Mesozoic. The association of Araucariaceae with Cheirolepidiaceae and *Exesipollenites tumulus* in PCA (Fig 10) would support the existence of mixed-gymnosperm communities in the area. The spatial proximity of conifers from distinct families is also suggested by the megaremain assemblages where *Brachyphyllum* cf. *obesum* (Fig 11I), a species that indicates mesophytic to xerophytic conditions attributed to Araucariaceae, has been found together with the Cheirolepidiaceae *Frenelopsis justae* (Fig 11E).

Two types of plant formations involving Araucariaceae can be hypothesised: (i) thickets of limited lateral extent involving one or a few species of Araucariaceae as the dominant elements. This hypothesis, still not supported by *in situ* palaeobotanical evidence, could explain the low dispersion of pollen (i.e., underrepresentation in palynological assemblages), the resulting canopy acting as barrier to pollen transport in a fashion analogous to modern stands of *Araucaria columnaris* in New caledonia and *A. angustifolia* in Brazil [159] and a predicted poor species richness for the stand [170]); (ii) mixed conifer communities with Cupressaceae, Podocarpaceae or/and Cheirolepidiaceae conifers constituting single-tiered or two-tiered woodlands, the latter with emergent araucarians. It would be reasonable to assume the existence of a transition from woodlands to more open, savanna-like, vegetation structures constrained by local edaphic conditions and the presumed arid to semi-arid conditions at a regional scale.

The presence of Araucariaceae in hinterland vegetation could also be regarded as plausible but it is likely not to have produced the recovered palynological signal given the low transport capacity of the araucarian pollen. Conversely, the ubiquity of Cheirolepidiaceae in pollen assemblages suggests a more efficient dispersal and that their contribution to the mixed conifer association described above might not have been that significant.

- Salt marshes and swamps

Mega and mesofloral assemblages from the Maestrazgo Basin are characterised by abundant *Frenelopsis*. While the genus has been associated to brackish coastal marshes when found in mid-Cretaceous of Europe [106, 171–172], it seems likely that the

constituying species exhibited more diverse palaeoenvironmental affinities. In the three outcrops, the genus is represented by *F. turolensis* (Fig 11B), and/or *F. justae* (Fig 11E). While *F. turolensis* has been reconstructed as small ligneous plant or shrub growing in coastal salt-influenced environments [106, 173], *F. justae* [37] suggests more mesic settings [174–175].

The association of *F. turolensis* with *Nehvizdya* (=*Eretmophyllum*) *penalveri* [29] (Fig 11A, K), a ginkgoalean previously interpreted as halophytic [83, 176], supports colonisation of salt-influenced settings (Fig 16). This type of ginkgoalean constituted coastal vegetation associated with Cheirolepidiaceae [177]. These communities could thrive in supratidal coastal areas [174, 178]. A similar inference has also been proposed by [28–29] based on specimens collected in the AP succession. If not taphonomically-induced, the low diversity of *Frenelopsis-Eretmophyllum* could be interpreted as supporting evidence of ecological stressful conditions [179].

Similarly, the complex nature of the fruit of *Montsechia*-type with *Spermatites* seeds inside recorded in SJ and CA (Fig 11F), could reflect near-shore deposits as these seeds (*Spermatites*) have been recorded in physical association with *Pseudoasterophyllites cretaceous*, a Cenomanian angiosperm described in tidally-influenced deposits from Bohemia [180–182]. While still debated, *Montsechia* has been considered by some authors as a halophytic plant growing in periodically dessicated coastal marshes [183]. Irrespective of the specific ecological requirements of *Montsechia*, the existence of halophytic/xerophytic vegetation formation including angiosperms is supported by the presence of *Tucanopollis*. While this pollen has been recorded in European mid-Cretaceous deposits [184–186], it constitutes a key element of assemblages characterising arid settings of central [187–188] and NE Gondwana [16] and has been observed in stamens of *P. cretaceous* [181]. The high proportion of *Tucanopollis* in the lower part of the CA succession (representing the bulk of the 'other angiosperms' in level CA-3.2; Fig 13, cluster II; S1 Appendix) is assumed to reflect the proximity of a halophytic/xerophytic plant community also involving Cupressaceae (*Inaperturopollenites dubius*-producers), Ertmanithecales and Cheirolepidiaceae (*F. turolensis*) and probably *Monosulcites*-producers of uncertain botanical affinities (Fig. 17; S1 Appendix). This plant association would characterise coastal, salt-influenced, episodically (but not periodically) flooded, areas. The existence of mangroves (i.e., vegetation colonising habitats under *periodic* marine water influence) is possible, although currently not supported by anatomical evidence.

- Wet interdunes and wetlands

The presence of freshwater bodies in the study area during the late Albian to early Cenomanian has been inferred from both sedimentological and palaeobotanical evidence [189–190]. The existence of habitats with fluctuating humidity or with high moisture is also indicated in San Just by amber inclusions including the hemipteran *Iberofoveopsis miguelesi* [44], as well as the presence of edaphic fauna linked to the litter degradation and soils [191–193] (Table 2)

The high proportions of fern spores, in palynological assemblages devoid of marine palynomorphs and characterised by low numbers of gymnosperms (see Fig 12 clusters III and

IV; Fig 13 cluster IV; Fig 14 clusters II and VI), also indicate that freshwater was available, at least during part of the year, as spore producers need free water to complete their biological cycle. A series of fern-spikes, mainly consisting of abundant spores with smooth exine attributed to *Cyathidites* and *Deltoidospora*, are observed in the three sections.

The palynological signal corresponding to these spikes is difficult to interpret. Similar spikes have been recorded after the end-Permian, Triassic and Cretaceous events [194–196] and interpreted as fern-dominated pioneer vegetation characterising the early stage of recovery after the disruption of some terrestrial ecosystems. If the existence of a global adverse palaeoenvironmental event during the late Albian can be discarded on available evidence, the fern-spikes observed in the three sections could still be interpreted as riparian early successional developments [197] in the present context. Modern arid ecosystems are fragile and prone to significant vegetation shifts when disturbances such as draughts are occurring [198–199], and similar disruptions of vegetation could well have happened in similar past environments. A recovery vegetation reduced to pioneer ferns, and conifers and other resilient floral elements remains a plausible ecological scenario. It is interesting to highlight that palynofloras characterised by high proportion of *Cyathidites* and *Deltoidospora* (94% of the total miospore content) have already been recorded in other deposits associated to the Iberian Aptian–Albian desert system in SW Spain (Oliete Sub-basin) [2, 200]. If the palaeoenvironmental interpretation presented here is valid, the recurring fern-spikes suggest that episodes of accentuated draught were a common feature during the mid-Cretaceous at mid latitude locations and that the vegetation responded to palaeoenvironmental disturbance in a similar way. The high content in spores of palynofloras reflecting arid and disturbed vegetation may appear counter-intuitive but a significant number of modern spore-producers are able to withstand extended periods of drought, present a high tolerance to environmental stress or simply thrive in edaphically low-nutrient habitats [201–203]. This adaptability has also been inferred for several Palaeozoic and Mesozoic spore-producers (e.g. Pennsylvanian sphenophytes, Jurassic Gleicheniaceae, Late Cretaceous Matoniaceae [73, 151]) which are often presented as stress-tolerators. Periodic ecological disturbances are also thought to have been favoured by early angiosperms [155]. Besides *Tucanopollis*-producers, angiosperms colonising the Iberian Desert System included representative of the ANITA grade, Chloranthales of diverse affinities (*Clavatipollenites*, *Transitoripollis*, etc.), probable monocots (*Monocolpopollenites*, *Retimonocolpites*) and eudicots (Table 1). These angiosperms were probably well integrated in the landscape forming part of multiple vegetation types including terrestrial wetlands (wet interdunes, oases *sensu* [190]) and fresh-water aquatic ecosystems as helophytes and/or floating elements [4, 34, 36] (Fig 17).

The occurrence of high abundance of "*Liliacidites*" *minutus* in CA (Fig 13 clusters IV) could also reflect advanced stages of ecological succession, involving colonisation of settings dominated by ferns. This pollen type, currently related to Laurales [204], could have been produced by angiosperms of broad ecological tolerances similar to the one exhibited by

Eucalyptolaurus deprei, a representative of the family described from the Cenomanian of France [176, 205].

The high number of spores attributed to Anemiaceae (i.e., *Cicatricosisporites*) in the studied assemblages, indicates that ferns were probably still the dominant floral elements in wetlands and maybe in some arid places. Early Cretaceous representatives of the family have been previously associated to swamps and lacustrine and savanna environments [75, 150, 206] and a similar environment can be assumed for the Iberian Anemiaceae, along with other spore (*Patellasporites tavaredensis*) and pollen (*Crassipollis chaloneri*) producers (Fig 10). The inferred vegetation should have been of low-stature and have surrounded ephemerous or semi-permanent water bodies developed in interdunes, maybe as part of the understory of open woodlands [75, 189, 207].

- Hinterland vegetation

The presence of bisaccate grains in assemblages otherwise characterised by marine palynomorphs suggests that a fourth type of vegetation involving conifers could have constituted a more distant vegetation type. Bisaccate pollen grains present a high dispersal capability and their higher representation in distal, marine, settings is often interpreted to reflect a taphonomic (i.e., biostratinomic) bias [208–209], known as Neves effect in Palaeozoic floras [210]. In the present context, the higher abundance of bisaccate grains in marine assemblages could represent hinterland vegetation involving Pinaceae and/or Podocarpaceae that would have colonised topographically higher settings of the Iberian Massif [14].

Comparison with other localities

The palynological assemblages from the Maestrazgo Basin documented here are similar to coeval successions from the Las Parras and Oliete sub-basins [31, 33–35]. *Afropollis* (Fig 7J), ephedroid polyplicate pollen (Fig 7O) and several angiosperm taxa such as *Dichastopollenites* (Fig 9G–I, L) and *Cretacaeiporites* relate the Spanish successions to the palynofloras from North Gondwana (see i.e. [211–215]) and support Iberia as transitional zone between the floral provinces of NE Gondwana and Laurasia [104]. The Maestrazgo palynological assemblages can also be related to the ones described from the Basque-Cantabrian Basin [31, 87, 104, 132] as both basins share more than 90% of the identified miospore families and a great number of their respective species. The faunal record, particularly the arthropod assemblages characterising the two Iberian areas, reveals a series of common species [162]. Arthropods recorded in the Maestrazgo with a more widespread distribution include *Cretevania* (Hymenoptera: Evaniidae) documented in various outcrops across Europe and Asia [216], *Serphites* (Hymenoptera: Serphitidae) recorded in Europe, Asia, and North America [217] and *Microphorites* (Diptera: Dolichopodidae) found in ambers from France, Lebanon and Myanmar [168].

The coeval miospore assemblages from the Lusitanian Basin exhibit higher angiosperm abundance than the ones described herein [6, 105, 113, 218]. While this difference could likely reflect a vegetation with more angiosperms, the higher

representation of dinocysts of the Portuguese successions suggests the influence of facies as sedimentary successions on a passive margin can collect miospores from larger catchment area.

By contrasts, the megafloral record relates the flora from the Maestrazgo to Laurasian assemblages. Taxonomically similar, low-diversity, plant assemblages have been documented from mid-Cretaceous strata of southwestern and northern France [219–221] and the Czech Republic [83, 172]. These shared characteristics are interesting as they suggest that a low number of species of angiosperms were thriving on salt-influenced environments and that geographic and climatic barriers did not prevent a widespread distribution across Laurasia. Pathways allowing dispersal of taxa with such specialised ecological requirements could include coastal fringes surrounding the Tethys. The good representation of *Tucanopollis* in both NE Gondwana and southern Laurasia suggests that a significant number of halophytic angiosperms used this 'coastal pathway' to colonise new environments. However, a more direct, NS trending, migration routes following northern and southern Atlantic rift valleys, could also be considered to link central Gondwana floras of Gabon and Brazil to Laurasian floras.

In spite of the numerous similarities existing between floras from Gondwana, mid and northern Laurasia, it is probable that latitudinal migration of flora remained hindered by differences in climate. Floras from locations at equivalent palaeolatitudes, should always present more compositional and structural similarities than floras from distinct climatic belts. Late Albian–early Cenomanian floras from NW Europe and N America present higher percentages in Gleicheniaceae and *Cyathidites* but lower diversity in angiosperms than coetaneous floras from southern Europe.

Latitudinal effects influenced the composition of the mid-Cretaceous palynological assemblages from Western Europe and the Atlantic Coastal Plain of USA, since they belonged to the Northern Mid-latitude Warm humid belt (NMW belt) [17, 222]. Although the diversity of taxa was high in the palynological assemblages attributed to the NMW belt, the abundance of miospores is different from that of the Maestrazgo Basin (i.e., [90, 112, 223–227]), which was under the influence of the Northern Hot Arid (NHA) belt [17, 189] during the late Albian. More concretely, under the influence of the NMW belt, fern spores were generally abundant, showing conspicuous amounts of Gleicheniaceae and *Cyathidites*, the amounts of *Classopollis* indicate that it was a sub-dominant pollen type, bisaccate and inaperturate conifer pollen reaches conspicuous values, and angiosperm pollen exhibits high diversity and significant abundances (i.e., abundances of more than 30% of angiosperm pollen, and a diversity of around 47 taxa in Zone II of the Potomac Group [112]).

Additionally, the late Albian–early Cenomanian palynofloras from the Northern High-latitude Temperate Humid (NHT) belt are characterised by a high diversity of dinocysts, trilete spores and angiosperms (see i.e., [111, 228–230]). For example, the coeval existence of quite different plant communities from those described in eastern Iberia can be regarded if comparing the late Albian floras from Peace River Area (Alberta, Canada) [230]. These floras are characterised by scarce *Classopollis*, high amounts of bisaccate pollen grains of the

genera *Alisporites* and *Vitreisporites*, trilete spores such as *Cingutriletes*, *Gleicheniidites*, and *Stereisporites*, as well as conspicuous values of tricolpate angiosperm species (*Cupuliferoidaepollenites parvulus*, *Tricolpites sagax*, *T. vulgaris*).

Conclusions

The palaeobotanical study of three sections from the Utrillas Group in the Maestrazgo Basin (Iberian Ranges, eastern Spain) reveals the existence of ancient conifer woodlands and fern/angiosperm communities that thrived in the mid-Cretaceous Iberian Desert System. Four vegetation types have been inferred: the first one characterised by arid woodlands of Cheirolepidiaceae-Cupressaceae, the second was related to coastal settings with Araucariaceae, the third is related to salt marshes, and the fourth represents local fern and angiosperm communities linked to wet interdunes (oases) and wetlands. The existence of ponded areas linked to wet interdunes is interpreted based on the high percentages of fern spores, common occurrence of angiosperm pollen and lack of marine palynomorphs. The presence of spikes of *Tucanopollis* spp. and "*Liliacidites*" *minutus* in the CA section might be related to the relevant role of the angiosperms in the colonisation of xeric and disturbed habitats, and the ecological successions in arid settings.

The biostratigraphic markers recorded in the studied sections confirm a late Albian age, except for the uppermost levels of the Cortes de Arenoso section (La Hoya amber outcrop) in which an early Cenomanian age might be inferred based on the occurrence of *Echinipollis cenomanensis, Polypodiisporonites cenomanianus* and *Senectotetradites grossus*. Although the late Albian palynoflora from the Maestrazgo Basin was influenced by the palaeoclimatic conditions that prevailed in the Northern Hot Arid belt, the studied assemblages can generally be related to others from Europe and North America. However, the presence of pollen grains of the genera *Afropollis*, *Equisetosporites*, *Gnetaceapollenites*, *Steevesipollenites, Dichastopollenites* and *Cretacaeiporites* indicates that Iberia was a transitional area between the Northern Gondwanan and the Southern Laurasian provinces. In this sense, the studied macrofloristic assemblages from the Maestrazgo Basin show similatities to others from the European Laurasia.

Acknowlegements

The authors would like to thank to Rafael López del Valle for the preparation of the amber pieces with arthropod specimens, Juan Pedro Rodríguez López for his assistence in the fieldworks, Pepa Torres Matilla for her aid with the design of the figures, Xavier Delclòs as supervisor of the PhD Thesis of SÁP, Luis Somoza for the economical aid and the Dirección General de Patrimonio Cultural del Gobierno de Aragón (Spain) for permissions of excavation. We also thank the editor (Enrique Peñalver) and the two anonymous referees who provided valuable suggestions and discussion for the improvement of the manuscript.

Author Contributions

Conceptualization: Eduardo Barrón, Daniel Peyrot.

Data curation: Eduardo Barrón.

Formal analysis: Eduardo Barrón, Daniel Peyrot.

Funding acquisition: Eduardo Barrón.

Investigation: Eduardo Barrón, Daniel Peyrot, Carlos A. Bueno-Cebollada, Jiří Kvaček, Sergio Álvarez-Parra, Yul Altolaguirre, Nieves Meléndez.

Methodology: Eduardo Barrón, Daniel Peyrot, Jiří Kvaček, Sergio Álvarez-Parra, Nieves Meléndez.

Resources: Eduardo Barrón.

Supervision: Eduardo Barrón.

Visualization: Daniel Peyrot, Carlos A. Bueno-Cebollada, Jiří Kvaček, Sergio Álvarez-Parra, Yul Altolaguirre.

Writing – original draft: Eduardo Barrón, Daniel Peyrot, Carlos A. Bueno-Cebollada.

Writing – review & editing: Eduardo Barrón with inputs of the other authors.

References

1. Perrichot V. Environnements paraliques à ambre et à végétaux du Crétacé Nord-Aquitain (Charentes, Sud-Ouest de la France). PhD Thesis. Univ Rennes. 2003.
2. Peyrot D, Rodríguez-López JP, Barrón E, Meléndez N. Palynology and biostratigraphy of the Escucha Formation in the Early Cretaceous Oliete Sub-basin, Teruel, Spain. Rev Esp Micropaleontol. 2007; 39(1–2): 135–154.
3. Diéguez C, Peyrot D, Barrón E. Floristic and vegetational changes in the Iberian Peninsula during Jurassic and Cretaceous. Rev Palaeobot Palynol. 2010; 162: 325–340.
4. Coiffard C, Gomez B, Daviero-Gomez V, Dilcher D. Rise to dominance of angiosperm pioneers in European Cretaceous environments. PNAS. 2012; 109(51): 20955–20959.
5. Peralta-Medina E, Falcon-Lang HJ. Cretaceous forest composition and productivity inferred from a global fossil wood database. Geology. 2012; 40 (3): 219–222.
6. Heimhofer U, Hochuli PA, Burlas S, Oberli F, Adatte T, Dinis JL, Weissert H. Climate and vegetation history of western Portugal inferred from Albian near-shore deposits (Galé Formation, Lusitanian Basin). Geol Mag. 2012; 149: 1046–1064.
7. Heimhofer U, Wucherpfenning N, Adatte T, Schouten S, Schneebeli-Hermann E, Gardin S, Keller G, Kentsch S, Kujau A. Vegetation response to exceptional global warmth during Oceanic Anoxic Event 2. Nat Commun. 2018; 9: 3832.
8. Vakhrameev VA. Jurassic and Cretaceous floras and climates of the Earth. Cambridge: Cambridge Univ Press; 1991.
9. Herngreen GFW, Kedves M, Rovnina LV, Smirnova SB. Chapter 29C. Cretaceous palynofloral provinces: a review. In: Jansonius J, McGregor DC, editors. Palynology: Principles and Applications, vol. 3. Salt Lake City: Am Assoc Stratigr Palynol Found; 1996. pp. 1157–1188.
10. Lidgard S, Crane PR. Angiosperm diversification and Cretaceous floristic trends: a comparison of palynofloras and leaf macrofloras. Paleobiology. 1990; 16: 77–93.
11. Boyce CK, Brodribb TJ, Field TS, Zwieniecki MA. Angiosperm leaf vein evolution was physiologically and environmentally transformative. Proc R Soc Lond B. 2009; 276: 1771–1776.
12. Friis EM, Crane PR, Pedersen KR. Early flowers and angiosperm evolution. Cambridge: Cambridge Univ Press; 2011.
13. Herendeen PS, Friis EM, Perdersen KR, Crane PR. Palaeobotanical redux: revisiting the age of the angiosperms. Nat Plants. 2017; 17015.

14. Rodríguez-López JP, Peyrot D, Barrón E. Complex sedimentology and palaeohabitats of Holocene coastal deserts, their topographic controls, and analogues for the mid-Cretaceous of northern Iberia. Earth Sci Rev. 2020; 201: 103075.

15. Coiro M, Doyle JA, Hilton J. How deep is the conflict between molecular and fossil evidence on age of angiosperms? New Phytol. 2019; 223(1): 83–99.

16. Boukhamsin H, Peyrot D, Vecoli M. Angiosperm pollen assemblages from the Lower Cretaceous (Barremian–lower Aptian) of offshore Saudi Arabia and their implications for early patterns of angiosperm radiation. Palaeogeogr Palaeoeclimat Palaeoecol. 2022; 599: 111052.

17. Chumakov NM, Zharkov MA, Herman AB, Doludenko MP, Kalandadze NN, Lebedev EL, Ponomarenko AG, Rautian AS. Climatic belts of the mid-Cretaceous time. Stratigr Geol Correl. 1995; 3: 241–260.

18. Rodríguez-López JP, Meléndez N, de Boer PL, Soria AR, Liesa CL. Spatial variability of multi-controlled aeolian supersurfaces in central-erg and marine erg-margin systems. Aeolian Res. 2013; 11: 141–154.

19. Demko TM, Parrish JT. Paleoclimatic setting of the Upper Jurassic Morrison Formation. Mod Geol. 1998; 22: 283–296.

20. Galán-Abellán A-B, López-Gómez J, Barrenechea JF, Marzo M, De la Horra R, Arche A. 2013. The beginning of the Buntsandstein cycle (Early–Middle Triassic) in the Catalan Ranges, NE Spain: Sedimentary and palaeogeographic implications. Sediment Geol. 2013; 296:86–102.

21. Magdefrau K. Paläobiologie der Pflanzen (vierte Auflage). Jena: Gustav Fischer; 1968.

22. Blanco-Moreno C. Integrative approach to the Early Cretaceous ferns of Las Hoyas (upper Barremian, Cuenca, Spain) in the light of other European localities. PhD Thesis. Univ Autónoma Madrid. 2019.

23. Amiot R, Kusuhashi N, Saegusa H, Shibata M, Ikegami N. Paleoclimate and ecology of Cretaceous continental ecosystems of Japan inferred from the stable oxygen and carbon isotope compositions of vertebrate bioapatite. J Asian Earth Sci. 2021; 205: 104602.

24. Wu Ch, Kiu Ch, yi H, Xia G, Zhang H, Wang L, Li G, Wagreich M. Mid-Cretaceous desert system in the Simao Basin, southwestern China, and its implications for sea-level change during a greenhouse climate. Palaeogeogr Palaeoclimatol Palaeoecol. 2017; 468: 529–544.

25. Bueno-Cebollada CA, Barrón E, Peyrot D, Meléndez N. Palynostratigraphy and palaeoenvironmental evolution of the Aptian to lower Cenomanian succession in the Serranía de Cuenca (Eastern Spain). Cretaceous Res. 2021; 128: 104956.

26. Smith RMH, Mason TR. Sedimentary environments and trace fossils of Tertiary oasis deposits in the Central Namib Desert, Namibia. Palaios. 1998; 13: 547–559.

27. Parris JT, Falcon-Lang HJ. Coniferous trees associated with interdune deposits in the Jurassic Navajo Sandstone Formation, Utah, USA. Palaeontology. 2007; 50: 829–843.

28. Gomez B, Barale G, Martín-Closas C, Thévenard F, Philippe M. Découverte d'une flore à Ginkgoales, Bennettitales et Coniférales dans le Crétacé inférieur de la Formation Escucha (Chaîne Ibérique Orientale, Teruel, Espagne). Neues Jahr Geol Paläontol Monatsh. 1999; 1999(11): 661–675.

29. Gomez B, Martín-Closas C, Barale G, Thévenard F. A new species of *Nehvizdya* (Ginkgoales) from the Lower Cretaceous of the Iberian Ranges (Spain). Rev Palaeobot Palynol. 2000; 111: 49–70.

30. Gomez B. A new species of *Mirovia* (Coniferales, Miroviaceae) from the Lower Cretaceous of the Iberian Ranges (Spain). Cretaceous Res. 2002; 23: 761–773.

31. Villanueva-Amadoz U. Nuevas aportaciones palinostratigráficas para el intervalo Albiense-Cenomaniense en el Sector NE de la península Ibérica. Implicaciones paleogeográficas y paleoclimáticas. PhD Thesis. Univ Zaragoza. 2009.

32. Villanueva-Amadoz U, Pons D, Díez JB, Ferrer J, Sender LM. Angiosperm pollen grains of Sant Just site (Escucha Formation) from the Albian of the Iberian Range (north-eastern Spain). Rev Palaeobot Palynol. 2010; 162(3): 362–381.

33. Villanueva-Amadoz U, Sender LM, Díez JB, Ferrer J, Pons D. Palynological studies of the boundary marls unit (Albian–Cenomanian) from northeastern Spain. Paleophytogeographical implications. Geodiversitas. 2011; 33(1): 137–176.

34. Sender LM, Gomez B, Díez JB, Coiffard C, Martín-Closas C, Villanueva-Amadoz U, Ferrer J. *Ploufolia cerciforme* gen. et comb. nov.: Aquatic angiosperm leaves from the Upper Albian of north-eastern Spain. Rev Palaeobot Palynol. 2010; 161: 77–86.
35. Sender LM, Villanueva-Amadoz U, Díez JB, Sánchez-Pellicer R, Bercovici A, Pons D, Ferrer J. A new uppermost Albian flora from Teruel province, northeastern Spain. Geodiversitas. 2012; 34(2): 373–397.
36. Sender LM, Doyle JA, Upchurch GR, Villanueva-Amadoz U, Díez JB. Leaf and inflorescence evidence for near-basal Araceae and an unexpected diversity of other monocots from the late Early Cretaceous of Spain. J Syst Palaeontol. 2019; 17(15): 1093–1126.
37. Barral A, Gomez G, Daviero-Gomez V, Lécuyer C, Mendes MM, Ewin TAM. New insights into the morphology and taxonomy of the Cretaceous conifer *Frenelopsis* based on a new species from the Albian of San Just, Teruel, Spain. Cretaceous Res. 2019; 96: 21–36.
38. Vilanova y Piera J. Manual de Geología aplicada a la Agricultura y a las Artes Industriales, vol. 1. Madrid: Imprenta Nacional; 1860.
39. Delclòs X, Arillo A, Peñalver E, Barrón E, Soriano C, López del Valle R, Bernárdez E, Corral C, Ortuño VM. Fossiliferous amber deposits from the Cretaceous (Albian) of Spain. CR Palevol. 2007; 6: 135–149.
40. Peñalver E, Delclòs X. Spanish amber. In: Penney D., editor. Biodiversity of fossils in amber from the major world deposits. Manchester: Siri Scientific Press; 2010. pp. 236–270.
41. Álvarez-Parra S, Pérez-de la Fuente R, Peñalver E, Barrón E, Alcalá L, Pérez-Cano J, Martín-Closas C, Trabelsi K, Meléndez N, López del Valle R, Lozano RP, Peris D, Rodrigo A, Sarto i Monteys V, Bueno-Cebollada CA, Menor-Salván C, Philippe M, Sánchez-García A, Peña-Kairath C, Arillo A, Espílez E, Mampel L, Delclòs X. Dinosaur bonebed amber from an original swamp forest soil. eLife. 2021; 10:e72477.
42. Peñalver E, Martínez-Delclòs X. Importancia patrimonial de Arroyo de la Pascueta, un yacimiento de ámbar cretácico con insectos fósiles en Rubielos de Mora. In: Meléndez Hevia G, Peñalver Mollá E, editors. El patrimonio paleontológico de Teruel. Teruel: Instituto de Estudios Turolenses; 2002. pp. 201–208.
43. Peñalver E, Delclòs X, Soriano C. A new rich outcrop with palaeobiological inclusions in the Lower Cretaceous of Spain. Cretaceous Res. 2007; 28: 791–802.
44. Peñalver E, Ortega-Blanco J, Nel A, Delclòs X. Mesozoic Evaniidae (Insecta: Hymenoptera) in Spanish amber: reanalysis of the phylogeny of the Evanioidea. Acta Geol Sin 2010; 84 (4): 809–827.
45. Aurell M, Bádenas B, Gasca JM, Canudo JI, Liesa CL, Soria AR, Moreno-Azanza M, Najes L. Stratigraphy and evolution of the Galve sub-basin (Spain) in the middle Tithonian–early Barremian: implications for the setting and age of some dinosaur fossil sites. Cretaceous Res. 2016; 65: 138-162.
46. Canérot J, Crespo Zamorano A, Navarro Vázquez D. Hoja geológica nº 518 (Montalbán). Mapa Geológico de España 1:50.000. 2ª serie. Madrid: IGME; 1977.
47. Almera J, Anadón P, Godoy A. Mapa Geológico de España 1:50.000, hoja nº 591 (Mora de Rubielos). Madrid: IGME; 1972.
48. Sopeña A, Gutiérrez-Marco JC, Sánchez-Moya Y, Gómez JJ, Mas R, García A, Lago M. Cordillera Ibérica y Costero Catalana. In: Vera JA, editor. Geología de España. Madrid: SGE-IGME; 2004. pp. 465–527.
49. Martín-Chivelet J, López-Gómez J, Aguado R, Arias C, Arribas J, Arribas ME, Aurell M, Bádemas B, Benito MI, Bover-Arnal T, Casas-Sainz A, Castro JM, Coruña F, de Gea GA, Fornós JJ, Fregenal-Martínez M, García-Senz J, Garófano D, Gelabert B, Giménez J, González-Acebrón L, Guimerà J, Liesa CL, Mas R, Meléndez N, Molina JM, Muñoz JA, Navarrete R, Nebot M, Nieto LM, Omodeo-Salé S, Pedrera A, Peropadre C, Quijada IE, Quijano ML, Reolid M, Robador A, Rodríguez-López JM, Rodríguez-Perea A, Rosales I, Ruiz-Ortiz PA, Sàbat F, Salas R, Soria AR, Suárez-González P, Vilas L. The Late Jurassic–Early Cretaceous rifting. In: Quesada C, Oliveira JT, editors. The Geology of Iberia: A Geodynamic Approach. Volume 3: The Alpine cycle. Cham: Springer; 2019. pp. 169–249.
50. Canérot J, Cugny P, Pardo G, Salas R, Villena J. Ibérica central-maestrazgo. In: García A, editor. El Cretácico de España. Madrid: Univ Complutense; 1982. pp. 273–344.
51. Soria AR. La sedimentación en las cuencas marginales del Surco Ibérico durante el Cretácico Inferior y su control estructural. PhD Thesis. Univ Zaragoza. 1997.

52. Salas R, Guimerà J, Mas R, Martín-Closas C, Meléndez A, Alonso A. Evolution of the Mesozoic Central Iberian Rift System and its Cainozoic inversion (Iberian chain). Peri-Tethys Mem. 2001; 6: 145–185.

53. Peropadre C. El Aptiense del margen occidental de la Cuenca del Maestrazgo: controles tectónico, eustático y climático en la sedimentación. PhD Thesis. Madrid: Univ Complutense. 2011.

54. Peropadre C, Liesa CL, Meléndez N. High-frequency, moderate to high-amplitude sea-level oscillations during the late early Aptian: Insights into the mid-Aptian event (Galve Sub-basin, Spain). Sediment Geol. 2013; 294: 233–250.

55. Aurell M, Fregenal-Martínez M, Bádenas B, Muñoz-García MB, Élez J, Meléndez N, De Santisteban C. Middle Jurassic–Early Cretaceous tectono-sedimentary evolution of the southwestern Iberian Basin (central Spain): Major palaeogeographical changes in the geotectonic framework of the Western Tethys. Earth Sci Rev. 2019; 199: 1–33.

56. Cervera A, Pardo G, Villena J. Algunas precisiones litoestratigráficas sobre la formación «Lignitos de Escucha». Tecniterrae. 1976; 14: 25–33.

57. Pardo G. Estratigrafía y sedimentología de las formaciones detríticas del Cretácico Inferior terminal del Bajo Aragón Turolense. PhD Thesis. Univ Zaragoza. 1979.

58. Querol X, Salas R, Pardo G, Ardevol L. Albian coal-bearing deposits of the Iberian Range in northeastern Spain. . In: Mc. Cabe JP, Panish JT, editors. Coals. Geol Soc Am Spec Pap. 1992; 267: 193–208.

59. Rodríguez-López JP, Meléndez N, Soria AR, De Boer P. Reinterpretación estratigráfica y sedimentológica de las Formaciones Escucha y Utrillas de la Cordillera Ibérica. Rev Soc Geol Esp. 2009; 22(3–4): 163–219.

60. Rodríguez-López JP. Sedimentología y evolución del sistema desértico arenoso (erg) desarrollado en el margen occidental del Tethys durante el Cretácico Medio, Cordillera Ibérica. Provincias de Teruel y Zaragoza. PhD Thesis. Madrid: Univ Complutense. 2008.

61. Aguilar MJ, Ramírez del Pozo J, Riba O. Algunas precisiones sobre la sedimentación y paleocecología del Cretácico Inferior en la zona de Utrillas-Villarroya de los Pinares (Teruel). Estud Geol. 1971; 27(6): 497–512.

62. Pardo G, Ardevol L, Villena J. Mapa Geológico de España. 1:200.000, hoja nº40 (Daroca). Madrid: ITGE; 1991.

63. Liesa CL, Casas AM, Soria AR, Simón JL, Meléndez A. Estructura extensional cretácica e inversión terciaria en la región de Aliaga-Montalbán. Geo-Guías. 2004; 1: 151–180.

64. Martín-Chivelet J, Floquet M, García-Senz J, Callapez PM, López-Mir B, Muñoz JA, Barroso-Barcenilla F, Segura M, Soares AF, Dinis PM, Marques JF, Arbués P. Late Cretaceous Post-Rift to Convergence in Iberia. In: Quesada C, Oliveira JT, editors. The Geology of Iberia: A Geodynamic Approach. Volume 3: The Alpine cycle. Cham: Springer; 2019. pp. 285–376.

65. Altolaguirre Y. Estudio palinológico preliminar del Cretácico de Cortes de Arenoso, Castellón. MSc Thesis. Madrid: Univ Complutense; 2015.

66. Zervas D, Nichols GJ, Hall R, Smyth HR, Lüthje C, Murtagh F. SedLog: A shareware program for drawing graphic logs and log data manipulation. Comput Geosci. 2009; 35 (10): 2151–2159.

67. Batten DJ. Small palynomorphs. In: Jones TP, Rowe NP, editors. Fossil plant and spores modern techniques. London: Geol Soc; 1999. pp. 15–19.

68. Traverse A. Paleopalynology, Second ed. Dordrecht: Springer; 2007.

69. Grimm EC. Tilia, Version 2. Springfield: Illinois Stat Mus; 1992.

70. Grimm EC. TGView, Version 2.0.2. Springfield: Illinois Stat Mus; 2004.

71. Jansonius J. McGregor DC. Palynology: principles and applications. Volume 1. Principles. Salt Lake City: Am Assoc Stratigr Paynol Found; 1996.

72. Peyrot D. Late Cretaceous (late Cenomanian-early Turonian) dinoflagellate cysts from the Castilian Platform, northern Spain. Palynology. 2011; 35(2): 267–300.

73. Van Konijnenburg-Van Cittert JHA. Ecology of some Late Triassic to Early Cretaceous ferns in Eurasia. Rev Palaeobot Palynol. 2002; 119: 113–124.

74. Abbink OA, Van Konijnenburg-Van Cittert JHA, Visscher H. A sporomorph ecogroup model for the Northwest European Jurassic–Lower Cretaceous: concepts and framework. Geol Mijnbouw. 2004; 83: 17–31.

75. Mohr BAR, Bernardes-de-Oliveira MEC, Loveridge R, Pons D, Sucerquia PA, Castro-Fernandes MC. Ruffordia goeppertii (Schizaeales, Anemiaceae) – A common fern from the Lower Cretaceous Crato Formation of northeast Brazil. Cretaceous Res. 2015; 54: 17–26.

76. Lindström S, Irmis RB, Whiteside JH, Smith ND, Nesbitt SJ, Turner AH. Palynology of the upper Chinle Formation in northern New Mexico, U.S.A.: Implications for biostratigraphy and terrestrial ecosystem change during the Late Triassic (Norian–Rhaetian). Rev Palaeobot Palynol. 2016; 225: 106–131.

77. Thompson PW, Pflug H. Pollen und Sporen des Mitteleuropaïschen Tertiärs. Palaeontographica Abt B. 1953; 94 (1–4): 1–138.

78. Van Konijnenburg-Van Cittert JHA. In situ gymnosperm pollen from the Middle Jurassic of Yorkshire. Acta Bot Neerl. 1971; 20(1): 1–97.

79. Azéma C, Boltenhagen E. Pollen du Crétacé Moyen du Gabon attribué aux Ephedrales. Paléobiol Cont. 1974; 5(1): 1–37.

80. Alvin KL. Cheirolepidiaceae: Biology, structure and paleoecology. Rev Palaeobot Palynol. 1982; 37: 71–98.

81. Pedersen KR, Crane PR, Friis EM. Morphology and phylogenetic significance of Vardekloeftia Harris (Bennettitales). Rev Palaeobot Palynol. 1989; 60: 7–24.

82. Balme BE. Fossil in situ spores and pollen grains: an annotated catalogue. Rev Palaeobot Palynol. 1995; 87: 81–323.

83. Uličný D, Kvaček J, Svobodová M, Špičáková L. High-frequency sea-level fluctuations and plant habitats in Cenomanian fluvial to estuarine succession: Pecínov quarry, Bohemia. Palaeogeogr Palaeoclimatol Palaeoecol. 1997; 136: 165–197.

84. Stuchlik L, Ziembińska-Tworzydło M, Kohlman-Adamska A, Grabowska I, Ważyńska H, Sadowska A. Atlas of pollen and spores of the Polish Neogene. Volume 2 – Gymnosperms. Kraków: Polish Acad Sci; 2002.

85. Dejax J, Pons D, Yans J. Palynology of the dinosaur-bearing Wealden facies in the natural pit of Bernissart (Belgium). Rev Palaeobot Palynol. 2007; 144: 25–38.

86. Peyrot D, Barrón E, Comas-Rengifo MJ, Thouand E, Tafforeau P. A confocal laser scanning and conventional wide field light microscopy study of Circumpolles from the Toarcian-Aalenian of the Fuentelsaz section (Spain). Grana. 2007; 46: 217–226.

87. Peñalver E, Arillo A, Pérez de la Fuente R, Riccio M, Delclòs X, Barrón E, Grimaldi DA. Long-proboscid flies as pollinators of Cretaceous gymnosperms. Curr Biol. 2015; 25 (14): 1917–1923.

88. Pattemore GA, Rigby JF, Playford G. Triassic-Jurassic pteridosperms of Australasia: speciation, diversity and decline. Bol Geol Min. 2015; 126 (4): 689–722.

89. Peris D, Pérez de la Fuente R, Peñalver E, Delclòs X, Barrón E, Labandeira CC. False blister beetles and the expansion of gymnosperm-insect pollination modes before angiosperm dominance. Curr Biol. 2017; 27 (6): 897–904.

90. Kvaček J, Barrón E, Heřmanová Z, Mendes MM, Karch J, Žemlička J, Dudák J. Araucarian conifer from the late Albian amber of northern Spain. Pap Palaeont. 2018; 4(4): 643–656.

91. Peyrot D, Barrón E, Polette F, Batten DJ, Néraudeau D. Early Cenomanian palynofloras and inferred resiniferous forests and vegetation types in Charentes (southwestern France). Cretaceous Res. 2019; 94: 168–189.

92. Pacltová B. Some new pollen grains from the Bohemian Cenomanian. Rev Palaeobot Palynol. 1968; 7: 99–106.

93. Ward JV. Early Cretaceous angiosperm pollen from the Cheyenne and Kiowa Formations (Albian) of Kansas, U.S.A. Palaeontographica Abt B. 1986; 202 (1–6): 1–81.

94. Doyle JA, Endress PK, Upchurch GR. Early Cretaceous monocots: a phylogenetic evaluation. Acta Mus Natl Pragae B – Hist Nat. 2008; 64 (2–4): 59–87.

95. Raine JI, Mildenhall DC, Kennedy EM. New Zealand fossil spores and pollen: an illustrated catalogue. 4th edition. GNS Sci Misc Ser. 2011; 4. http://data.gns.cri.nz/sporepollen/index.htm

96. Stuchlik L, Ziembińska-Tworzydło M, Kohlman-Adamska A, Grabowska I, Słodkowska B, Worobiec E, Durska E. Atlas of pollen and spores of the Polish Neogene.

97. Doyle JA, Endress PK. Integrating Early Cretaceous fossils into the phylogeny of living angiosperms: ANITA lines and relatives of Chloranthaceae. Int J Plant Sci. 2014; 175: 555–600.
98. Kvaček J, Doyle JA, Endress PK, Daviero-Gomez V, Gomez B, Tekleva M. Pseudoasterophyllites cretaceous from the Cenomanian (Cretaceous) of the Czech Republic: A possible link between Chloranthaceae and Ceratophyllum. Taxon. 2016; 65(6): 1345–1373.
99. Llorens M, Pérez Loinaze VS. Late Aptian angiosperm pollen grains from Patagonia: Earliest steps in flowering plant evolution at middle latitudes in southern South America. Cretaceous Res. 2016; 57: 66–78.
100. Lê S, Josse J, Husson F. (2008). FactoMineR: An R Package for Multivariate Analysis. J Stat Soft. 2008; 25 (1): 1–18.
101. Juggins S. Rioja: Analysis of Quaternary Science Data. R package version 0.9-26, Newcastle: Newcastle Univ; 2020.
102. Corral JC, López Del Valle R, Alonso J. El ámbar cretácico de Álava (Cuenca Vasco-Cantábrica, norte de España). Su colecta y preparación. Estud Mus Cien Nat Álava. 1999; 14: 7–21.
103. Batten DJ. Chapter 26A. Palynofacies and Palaeoenvironmental interpretation. In: Jansonius J, McGregor DC, editors. Palynology: Principles and Applications, vol. 3. Salt Lake City: Am Assoc Stratigr Palynol Found; 1996. pp. 1011–1064.
104. Barrón E, Peyrot D, Rodríguez-López JP, Meléndez N, López del Valle R, Najarro M, Rosales I, Comas-Rengifo MJ. Palynology of Aptian and upper Albian (Lower Cretaceous) amber-bearing outcrops of the southern margin of the Basque-Cantabrian basin (northern Spain). Cretaceous Res. 2015; 52: 292–312.
105. Horikx M, Hochuli PA, Feist-Burkhardt S, Heimhofer U. Albian angiosperm pollen from shallow marine strata in the Lusitanian Basin, Portugal. Rev Palaeobot Palynol. 2016; 228: 67–92.
106. Gomez B, Martín-Closas C, Barale G, Solé de Porta N, Thévenard F, Guignard G. *Frenelopsis* (Coniferales: Cheirolepidiaceae) and related male organ genera from the Lower Cretaceous of Spain. Palaeontology. 2002; 45(5): 997–1036.
107. Behrensmeyer AK, Hook RW. Paleoenvironmental contexts and taphonomic modes in the terrestrial fossil record, in: Behrensmeyer AK, Damuth JD, DiMichele WA, Potts R, Sues H-D, Wing SL, editors. Terrestrial Ecosystems through Time. Evolutionary paleoecology of terrestrial plants and animals. Chicago: Univ Chicago Press; 1992. pp. 15–38.
108. Peñalver E, Grimaldi DA, Delclòs X. Early Cretaceous spider web with its prey. Science. 2006; 312: 1761–1761.
109. Delclòs X, Peñalver E, Arillo A, Engel MS, Nel A, Azar D, Ross A. 2016. New mantises (Insecta: Mantodea) in Cretaceous ambers from Lebanon, Spain, and Myanmar. Cretaceous Res. 2016; 60: 91–108.
110. Peñalver E, Ortega-Blanco J, Nel A, Delclòs X. Mesozoic Evaniidae (Insecta: Hymenoptera) in Spanish amber: reanalysis of the phylogeny of the Evanioidea. Acta Geol Sin 2010; 84 (4): 809–827.
111. Singh C. Cenomanian microfloras of the Peace River area, northwestern Alberta. Res Counc Alberta Bull. 1983; 44: 1–239.
112. Hochuli PA, Heimhofer U, Weissert H. Timing of early angiosperm radiation: recalibrating the classical succession. J Geol Soc Lond. 2006; 163: 587–594.
113. Hasenboehler B. Étude paléobotanique et palynologique de l'Albien et du Cenomanien du "Bassin Occidental Portugais" au Sud de l'Accident de Nazare (Province d'Estremadure, Portugal). PhD Thesis. Université Pierre et Marie Curie. 1981.
114. Bint AN. Fossil Ceratiaceae: A restudy and new taxa from the mid-Cretaceous of the Western Interior, U.S.A. Palynology. 1986; 10: 135–180.
115. Berthou PY, Leereveld H. Stratigraphic implications of palynological studies on Berriasian to Albian deposits from western and southern Portugal. Rev Palaeobot Palynol. 1990; 66: 313–344.
116. Schrank E, Ibrahim MIA. Cretaceous (Aptian–Maastrichtian) palynology of Foraminifera-dated wells (KRM-1, AG-18) in northwestern Egypt. Berl Geowiss Abh, Reihe A. 1995; 177: 1–44.
117. Leereveld H, de Haan PJ, Juhász M. Stratigraphic evaluation of spore/pollen assemblages from the Lower Cretaceous of the Alpine-Mediterranean Realm. Lab Palaeobot Palynol Contrib Ser. 1989; 89/07: 1–253+1–98.

118. Deák MH, Combaz A. “Microfossiles organiques" du Wealdien et du Cénomanien dans un sondage de Charente-Maritime. Rev Micropaléontol. 1967; 10(2): 69–96.
119. Ravn RL. Miospores from the Muddy Sandstone (upper Albian), Wind River Basin, Wyoming, U.S.A. Palaeontographica Abt B. 1995; 234: 41–91.
120. Pacltová B. Palynological study of Angiospermae from the Peruc Formation (?Albian-Lower Cenomanian) of Bohemia. Sb Geol Paleontol, řada P. 1971; 13: 105–139.
121. May FE. A survey of palynomorphs from several coal-bearing horizons of Utah. In: Doelling, H.H., editor. Utah Geol Min Surv Monogr Ser. 1972; 3: 497–542.
122. Ravn, RL, Witzke BJ. The palynostratigraphy of the Dakota Formation (?late Albian – Cenomanian) in its type area, northwestern Iowa and northeastern Nebraska, USA. Palaeontographica Abt B. 1995; 234(3–6): 93–171.
123. Boulouard C, Canérot J. Données nouvelles sur l’Aptien supérieur et l’Albien dans le Bas-Aragón et le Maestrazgo (Espagne). Bull Cent Rech Pau-SNPA. 1970; 4(2): 453–463.
124. Solé de Porta N, Salas R. Conjuntos microflorísticos del Cretácico Inferior de la Cuenca del Maestrazgo. Cordillera Ibérica Oriental (NE de España). Cuad Geol Ibér. 1994; 18: 355–368.
125. Haq B. Cretaceous eustasy revisited. Global Planet Change. 2014; 113: 44–58.
126. Jürgens N. Floristic biodiversity and history of African arid regions. Biodiversity Conserv. 1997; 6 (3): 495–514.
127. Cowling RM, Rundel PW, Desmet PG, Esler KJ. Extraordinary high regional-scale plant diversity in southern Africa arid lands: subcontinental and global comparisons. Divers Distrib. 1998; 4: 27–36.
128. Muller J. Palynology of recent Orinoco delta and shelf sediments: reports of the Orinoco Shelf Expedition; Volume 5. Micropaleontology. 1959; 5(1): 1–32.
129. Krasilov VA. Paleoecology of terrestrial plants. Basic principles and techniques. New York: John Wiley & sons, INC; 1975.
130. Spicer RA. Plant taphonomic processes. In: Allison PA, Briggs DE, editors. Taphonomy releasing: the data locked in the fossil record. New York: Plenum Press; 1991. pp. 71–113.
131. Davis MB. Palynology after Y2K - Understanding the source area of pollen in sediments. Annu Rev Earth Planet Sci. 2000; 28: 1–18.
132. Najarro M, Peñalver E, Pérez-de la Fuente R, Ortega-Blanco J, Menor-Salván C, Barrón E, Soriano C, Rosales I, López del Valle R, Velasco R, Tornos F, Daviero-Gomez V, Gomez B, Delclòs X. Review of the El Solplao amber outcrop, Early Cretaceous of Cantabria, Spain. Acta Geol Sin. 2010; 84 (4): 959–976.
133. Kimyai A. Palynology and biostratigraphy of the Lower Cretaceous sediments in the south barrow test well no. 1, point barrow, Alaska. Palynology. 2000; 24 (1): 201–215.
134. Tosolini A, McLoughlin S, Wagstaff B, Cantrill D, Gallagher S. Cheirolepidiacean foliage and pollen from Cretaceous high-latitudes of southeastern Australia. Gondwana Res. 2015; 27: 960–977.
135. Boukhamsin H, Peyrot D, Lang S, Vecoli M. Low-latitude ?upper Barremian-lower Aptian palynoflora and paleovegetation of the Biyadh Formation (Arabian Plate, eastern margin of northern Gondwana): evidence for a possible cold nap. Cretaceous Res. 2022a; 129: 104995.
136. Peyrot, D, Playford G, Mantle DJ, Backhouse J, Milne LA, Carpenter RJ, Foster C, Mory AJ, McLoughlin S, Vitacca J, Scibiorski J, Mack CL, Bevan J. The greening of Western Australian landscapes: the Phanerozoic plant record. J R Soc West Aust. 2019; 102: 52–82.
137. Boltenhagen, E., Salard-Cheboldaeff, M., 1987. Étude palynologique du sel aptien du Congo. Mém Trav Inst Montpellier Ecole Pratique Hautes Etud. 1987; 17: 273–293.
138. Watson J. Some Lower Cretaceous conifers of the Cheirolepidiaceae from the U.S.A. and England. Palaeontology. 1977; 20: 715–749.
139. Watson J. The Cheirolepidiaceae. In: Beck CB, editor. Origin and evolution of gymnosperms. New York: Columbia Univ Press; 1988. pp. 382–447.
140. Hotton CL, Baghai-Riding NL. Palynological evidence for conifer dominance within a heterogeneous landscape in the Late Jurassic Morrison Formation, U.S.A. In: Gee CT, editor. Plants in Mesozoic time: Morphological innovations, phylogeny, ecosystems. Bloomington: Indiana Univ Press; 2010. pp. 295–328.

141. Francis, JE. The dominant conifer of the Jurassic Purbeck Formation, England. Palaeontology. 1983; 26: 277–294.
142. McLoughlin S, Tosolini A-MP, Nagalingum NS, Drinnan AN. Early Cretaceous (Neocomian) flora and fauna of the lower Strzelecki Group, Gippsland Basin, Victoria. Mem Assoc Australasian Palaeontol. 2002; 26: 1–144.
143. Farjon A. A monograph of Cupressaceae and *Sciadopitys*. Kew: Royal Botanic Gardens; 2005.
144. Pelzer G, Riegel W, Wilde V. Depositional controls on the Lower Cretaceous Wealden coals of northwest Germany. In: McCabe PJ, Parrish JT, editors. Controls on the Distribution and Quality of Cretaceous Coals. Geol Soc Am Spec Pap. 1992; 267: 227–243.
145. Mays C. A Late Cretaceous (Cenomanian–Turonian) south polar palynoflora from the Chatham Islands, New Zealand. Mem Assoc Australas Palaeontol. 2015; 47: 1–92.
146. McIver EE. Cretaceous *Widdringtonia* Endl. (Cupressaceae) from North America. Int J Plant Sci. 2001; 162 (4): 937–961.
147. Hamad A, Abu M, Amireh B, Jasper A, Uhl D. New palaeobotanical data from the Jarash Formation (Aptian–Albian, Kurnub Group) of NW Jordan. The Palaeobotanist. 2016; 65: 19–29.
148. Hamad AMA, Amireh B, El Atfy H, Jasper A, Uhl D. Fire in a *Weichselia*-dominated coastal ecosystem from the Lower Cretaceous (Barremian) of the Kurnub Group in NW Jordan. Cretaceous Res. 2016; 66: 82–93.
149. Dettmann ME. Cretaceous vegetation: the microfossil record. In: Hill RS, editor. History of the Australian vegetation: Cretaceous to recent. Adelaide: Univ Adelaide Press; 2017. pp. 143–170.
150. Blanco-Moreno C, Gomez B, Buscalioni Á. Palaeobiogeographic and metric analysis of the Mesozoic fern *Weichselia*. Geobios. 2018; 51: 571– 578.
151. Halamski AT, Kvaček J, Svobodová M, Durska E, Heřmanová Z. Late Cretaceous mega-, meso-, and microfloras from Lower Silesia. Acta Palaeontol Pol. 2020; 65(4): 811–878.
152. Feild TS, Arens NC, Doyle JA, Dawson TE, Donoghue MJ. Dark and disturbed: a new image of early angiosperm ecology. Paleobiology. 2004; 30: 82–107.
153. Gomez B, Coiffard C, Sender LM, Martín-Closas C, Villanueva-Amadoz U, Ferrer J. *Klitzschophyllites*, aquatic basal eudicots (Ranunculales?) from the upper Albian (Lower Cretaceous) of northeastern Spain. Int J Plant Sci. 2009; 170 (8): 1075–1085.
154. Doyle JA, Endress PK. Integrating Early Cretaceous fossils into the phylogeny of living angiosperms: Magnoliidae and eudicots. J Syst Evol. 2010; 48(1): 1–35.
155. Feild T, Chatelet D, Brodribb T. Ancestral xerophobia: a hypothesis on the whole plant ecophysiology of early angiosperms. Geobiology. 2009; 7: 237–264.
156. Taylor DW, Hu S. Coevolution of early angiosperms and their pollinators: Evidence for pollen. Palaeontographica Abt B. 2010; 283: 103–135.
157. Vidiella PE, Armesto JJ, Gutiérrez JR. Vegetation changes and sequential flowering after rain in the southern Atacama Desert. J Arid Environ. 1999; 43: 449–458.
158. Elliot MB. Modern pollen–vegetation relationships in Northland, New Zealand. N Z J Bot. 1999; 37: 131–148.
159. Sousa VA, Hattemer HH. Pollen dispersal and gene flow by pollen in Araucaria angustifolia. Aust J Bot. 2003; 51: 309–317.
160. Chaler R, Grimalt JO. Fingerprint of Cretaceous higher plant resins by inferred spectroscopy and gas chromatography coupled to mass spectrometry. Phytochem Anal. 2005; 16(6): 446–450.
161. Dal Corso J, Roghi G, Ragazzi E, Angelini I, Giaretta A, Soriano C, Delclòs X, Jenkyns HC. Physico-chemical analysis of Albian (Lower Cretaceous) amber from San Just (Spain): implications for palaeoenvironmental and palaeoecological studies. Geol Acta. 2013; 11(3): 359–370.
162. Peris D, Davis SR, Engel MS, Delclòs X. An evolutionary history embedded in amber: reflection of the Mesozoic shift in weevil-dominated (Coleoptera: Curculionoidea) faunas. Zool J Linn Soc. 2014; 171: 534–553.
163. Jaffré T. Distribution and ecology of conifers in New Caledonia. In: Enright NJ, Hill RS, editors. Distribution and ecology of southern conifers. Carlton: Melbourne Univ Press; 1995. pp. 171–196.

164. Ogden J, Stewart GH. Community dynamics of the New Zealand conifers. In: Enright NJ, Hill RS, editors. Distribution and ecology of southern conifers. Carlton: Melbourne Univ Press; 1995. pp. 81–119.
165. Farjon A. A natural history of conifers. London: Timber Press; 2008.
166. Jackson ST, Overpeck JT. Responses of plant population and communities to environmental changes of the late Quaternary. Paleobiology. 2000; 26 (4): 194–220.
167. Pillon Y. Time and tempo of diversification in the flora of New Caledonia. Bot J Linn Soc. 2012; 170: 288–298.
168. Arillo A, Peñalver E, Delclòs X. *Microphorites* (Diptera: Dolichopodidae) from the Lower Cretaceous amber of San Just (Spain), and the co-occurrence of two ceratopogonid species in Spanish amber deposits. Zootaxa. 2008; 1920: 29–40.
169. Nel, A., Perrichot, V., Daugeron, C., Néraudeau, D. 2004. A new *Microphorites* in the Lower Cretaceous amber of the southwest of France (Diptera: Dolichopodidae, "Microphorinae"). Ann Soc Entomol Fr. 2004; 40 (1): 23–29.
170. Regal P. Ecology and the evolution of flowering plant dominance. Science. 1977; 1996: 622–629.
171. Upchurch Jr GR, Doyle JA. Paleoecology of the conifers *Frenelopsis* and *Pseudofrenelopsis* (Cheirolepidiaceae) from the Cretaceous Potomac Group of Maryland and Virginia. In: Romans RC, editor. Geobotany II. New York: Plenum Press; 1981. pp. 167–202.
172. Kvaček J. *Frenelopsis alata* and its microsporangiate and ovuliferous reproductive structures from the Cenomanian of bohemia (Czech Republic, Central Europe). Rev Palaeobot Palynol. 2000; 112: 51–78.
173. Daviero V, Gomez B, Philippe M. Uncommon branching pattern within conifers: *Frenelopsis turolensis*, a Spanish Early Cretaceous Cheirolepidiaceae. Can J Bot. 2001; 79: 1400–1408.
174. McElwain JC, Chaloner WG. The Fossil Cuticle as a Skeletal Record of Environmental Change. Palaios. 1996; 11(4): 376–388.
175. Haworth M, McElwain J. Hot, dry, wet, cold or toxic? Revisiting the ecological significance of leaf and cuticular micromorphology. Palaeogeogr Palaeoclimatol Palaeoecol. 2008; 262(1): 79–90.
176. Gomez B, Coiffard C, Dépré É, Daviero-Gomez V, Néraudeau D. Diversity and histology of a plant litter bed from the Cenomanian of Archingeay-Les Nouillers (southwestern France). CR Palevol. 2008; 7: 135–144.
177. Hluštík A. Eretmophyllous Ginkgoales from the Cenomanian. Acta Mus Natl Pragae, ser B Hist Nat. 1986; 42(1–2): 99–115.
178. Kvaček J, Falcon-Lang HJ, Dašková J. A new Late Cretaceous ginkgoalean reproductive structure *Nehvizdyella* gen. nov. from the Czech Republic and its whole-plant reconstruction. Am J Bot. 2005; 92(12): 1958–1969.
179. Hughes RG. Theories and models of species abundance. Am Nat. 1986; 128: 879–899.
180. Kvaček J, Gomez B, Zetter R. The early angiosperm *Pseudoasterophyllites cretaceus* from Albian-Cenomanian of the Czech Republic and France revisited. Acta Palaeontol Pol. 2012; 57(2): 437–443.
181. Kvaček J, Doyle JA, Endress PK, Daviero-Gomez V, Gomez B, Tekleva M. *Pseudoasterophyllites cretaceous* from the Cenomanian (Cretaceous) of the Czech Republic: A possible link between Chloranthaceae and *Ceratophyllum*. Taxon. 2016; 65(6): 1345–1373.
182. Kvaček J. Late Cretaceous floras in Central Europe and their palaeoenvironment. Praha: Univ Karlovy v Praze; 2017.
183. Krassilov VA. On *Montsechia*, an angiospermoid plant from Lower Cretaceous of Las Hoyas, Spain: new data and interpretations. Acta Palaeobot. 2011; 51(2): 181–205.
184. Friis EM, Pedersen K, Crane P. Cretaceous diversification of angiosperms in the western part of the Iberian Peninsula. Rev Palaeobot Palynol. 2010; 162: 341–361.
185. Heimhofer U, Hochuli PA, Burla S, Weissert H. New records of Early Cretaceous angiosperm pollen from Portuguese coastal deposits: Implications for the timing of the early angiosperm radiation. Rev Palaeobot Palynol. 2007; 144: 39–76.
186. Hughes N. The Enigma of Angiosperms origins. Cambridge: Cambridge Univ Press; 1994.
187. Regali M. *Tucanopollis*, a new genus of early angiosperms. Bol Geoci Petrobrás. 1989; 3: 395–402.

188. Doyle J. Revised palynological correlations of the lower Potomac Group (USA) and the Cocobeach sequence of Gabon (Barremian–Aptian). Cretaceous Res. 1992; 13: 337–349.
189. Rodríguez-López JP, Meléndez N, De Boer PL, Soria AR. Controls on marine–erg margin cycle variability: aeolian–marine interaction in the mid-Cretaceous Iberian Desert System, Spain. Sedimentology. 2012; 59(2): 466–501.
190. Rodríguez-López JP, Barrón E, Peyrot D, Hughes GB. Deadly oasis: Recurrent annihilation of Cretaceous desert bryophyte colonies; the role of solar, climate and lithospheric forcing. Geosci Front. 2021; 12: 1–12.
191. Engel MS, Delclòs X. Primitive termites in Cretaceous amber from Spain and Canada (Isoptera). J Kansas Entomol Soc. 2010; 83 (2): 111–128.
192. Peris D, Philips TK, Delclòs X. Ptinid beetles from the Cretaceous gymnosperm-dominated forests. Cretaceous Res. 2015; 52(Part B): 440–452.
193. Arillo A, Subías LS, Sánchez-García A. New species of fossil oribatid mites (Acariformes, Oribatida), from the Lower Cretaceous amber of Spain. Cretaceous Res. 2016; 63: 68–76.
194. Retallack G J. Permian–Triassic life crisis on land. Science. 1995; 267 (5194): 77–80.
195. Vajda V, Raine JI, Hollis CJ. Indication of global deforestation at the Cretaceous–Tertiary boundary by New Zealand fern spike. Science. 2001; 294 (5547): 1700–1702.
196. Van de Schootbrugge B, Quan TM, Lindstrom SL, Püttmann W, Heunisch C, Pross J, Fiebig J, Petschick R, Rohling HG. Floral changes across the Triassic/Jurassic boundary linked to flood basalt volcanism. Nat Geosci. 2009; 2 (8): 589–594.
197. Spicer RA. Changing climate and biota. In: Skelton PW, editor. The Cretaceous World. Cambridge: Cambridge Univ Press; 2003. pp. 85–162.
198. Brown JH, Valone TJ, Curtin CG 1997. Reorganization of an arid ecosystem in response to recent climate change. PNAS. 1997; 94 (18): 9729–9733.
199. Van de Koppel J, Rietkerk M. Spatial Interactions and Resilience in Arid Ecosystems. Am Nat. 2004; 163(1): 113–121.
200. Peyrot D, Rodríguez-López JP, Lassaletta L, Meléndez N, Barrón E. Contributions to the palaeoenvironmental knowledge of the Escucha Formation in the Lower Cretaceous Oliete Sub-basin, Teruel, Spain. CR Palevol. 2007; 6: 469–481.
201. Page CN. Ecological strategies in fern evolution: a neopteridological overview. Rev Palaeobot Palynol. 2002; 119: 1–33.
202. Hietz P. Fern adaptations to xeric environments. In: Mehltreter K, Walker L, Sharpe J, editors. Fern Ecology. Cambridge: Cambridge Univ Press; 2012. pp. 140–176.
203. Vitt DH, Crandall-Stotler B, Wood AJ. Bryophytes, survival in a dry world through tolerance and avoidance. In: Rajakaruna N, Boyd RS, Harris TB, editors. Plant Ecology and Evolution in Harsh Environments. New York: Nova Science; 2014. pp. 267–295.
204. Doyle J, Endress PK. Phylogenetic analyses of Cretaceous fossils related to Chloranthaceae and their evolutionary implications. Bot Rev. 2018; 84: 156–202.
205. Coiffard C, Gomez B, Thiébaut M, Kvaček J, Thévenard F, Néraudeau D. Inframarginal veined Lauraceae leaves from the Albian–Cenomanian of Charente-Maritime (western France). Palaeontology. 2009; 52(2): 323–336.
206. Crabtree DR. Mid-Cretaceous ferns in situ from the Albino member of the Mowry Shale, southwestern Montana. Palaeontographica Abt. B 1988; 209: 1–27.
207. Ahlbrandt TS, Fryberger SG. Sedimentary features and significance of interdune deposits. Soc Econ Paleontol Min Spec Publ. 1981; 31: 293–314.
208. Mudie PJ, McCarthy FMG. Late Quaternary pollen transport processes, western North Atlantic: Data from box models, cross-margin and N-S transects. Mar Geol. 1994; 118: 79–105.
209. Mudie PJ, McCarthy FMG. Marine palynology: potentials for onshore-offshore correlation of Pleistocene–Holocene records. Trans R Soc South Afr. 2006; 61: 139–157.
210. Chaloner WG, Muir M. Spores and Floras. In: Marendson L, Westord J, editors. Coal and coal-bearing strata. Edinburgh: Oliver and Boyd; 1968. pp. 127–146.

211. Ibrahim MIA. Aptian–Turonian palynology of the Ghazalat-1 Well (GTX-1) Qattara Depression, Egypt. Rev Palaeobot Palynol. 1996; 94: 137–168.
212. Ibrahim MIA. Late Albian–middle Cenomanian palynofacies and palynostratigraphy, Abu Gharadig-5 well, Western Desert, Egypt. Cretaceous Res. 2002; 2: 775–788.
213. El-Beialy S, El-Soughier M, Mohsen SA, El Atfy H. Palynostratigraphy and paleoenvironmental significance of the Cretaceous succession in the Gebel Rissu-1 well, north Western Desert, Egypt. J Afr Earth Sci. 2011; 59: 215–226.
214. Schrank E. Palaeoecological aspects of *Afropollis*/elaterates peaks (Albian–Cenomanian pollen) in the Cretaceous of northern Sudan and Egypt. In: Goodman DK, Clarke RT, editors. Proc IX Int Palynol Congress, Houston, Texas, USA, 1996. Am Assoc Stratigr Palynol Found; 2001. pp. 201–210.
215. Schrank E. Palynology of the Albian Makhtesh Qatan site, northern Negev (Israel), with descriptions of two new pollen species. Rev Palaeobot Palynol. 2017; 246: 185–215.
216. Shih PJ, Li L, Li D, Ren D. Application of geometric morphometric analyses to confirm three new wasps of Evaniidae (Hymenoptera: Evanioidea) from mid-Cretaceous Myanmar amber. Cretaceous Res. 2020; 109: 104249.
217. Engel MS, Perrichot V. The extinct wasp family Serphitidae in late Cretaceous Vendean amber (Hymenoptera). Paleontol Contrib. 2014; 10J: 46–51.
218. Médus J, Berthou PY. Palynoflores dans la coupe de l'Albien de Foz do Folcão (Portugal). Geobios. 1980; 13: 263–269.
219. Pons D, Vozenin-Serra C. Wood of Ginkgoales in the Cenomanian of Anjou, France. Cour Forchinst Senckenb. 1992; 147: 199–213.
220. Gomez B, Daviero-Gomez V, Perrichot V, Thévenard F, Coiffard C, Philippe M, Néraudeau D. Assemblages floristiques de l'Albien-Cénomanien de Charente-Maritime (SO France). Ann Paleontol. 2004; 90: 147–159.
221. Néraudeau D, Vullo R, Gomez B, Perrichot V, Videt B. Stratigraphie et paléontologie (plantes, vertébrés) de la série paralique Albien terminal-Cénomanian basal de Tonnay-Charente (Charente-Maritime, France). CR Palevol. 2005; 4: 79–93.
222. Spicer B, Skelton PW. The operation of the major geological carbon sinks. In: Skelton PW, editor. The Cretaceous World. Cambridge: Univ Press; 2003. pp. 249–271.
223. Brenner GJ. The spores and pollen of the Potomac Group of Maryland. Maryland Dep Geol Mines Water Res Bull. 1963; 27: 1–215.
224. Kemp EM. Aptian and Albian miospores from southern England. Palaeontographica Abt. B 1970; 131 (1–4): 73–143.
225. Svobodová M. Mid-Cretaceous palynomorphs from the Blansko Graben (Czech Republic): affinities to both Tethyan and Boreal bioprovinces. NR 58 Proc 4th EPPC: Mid-Cretaceous palynomorphs from the Blansko Graben; 1997. pp. 149–155.
226. Svobodová M, Hradecká L, Skupien P, Švábenická L. Microfossils of theAlbian and Cenomanian shales from the Stramberk area (Silesia unit, Outer Western Carpathians, Czech Republic). Geol Carpath. 2004; 55 (5): 371–388.
227. Polette F, Licht A, Cincotta A, Batten DJ, Depuydt P, Néraudeau D, Garcia G, Valentin X. Palynological assemblage from the lower Cenomanian plant-bearing Lagerstätte of Jaunay-Clan-Ormeau-Saint-Denis (Vienne, western France): Stratigraphic and paleoenvironmental implications. Rev Palaeobot Palynol. 2019; 271: 104102.
228. Norris G. Spores and pollen from the Lower Colorado Group (?Albian–Cenomanian) of central Alberta. Palaeontographica Abt B. 1967; 120 (1–4): 72–115.
229. Playford G. Palynology of Lower Cretaceous (Swan River) strata of Saskatchewan and Manitova. Palaeontology. 1971; 14 (4): 533–565.
230. Singh C. Lower Cretaceous microfloras of the Peace River Area, northwestern Alberta. Res Counc Alberta Bull. 1971; 28 (1): 1–299.

Anexo 8.1.10

A new genus of dance flies (Diptera: Empidoidea: Hybotidae) from Cretaceous Spanish ambers and introduction to the fossiliferous amber outcrop of La Hoya (Castellón Province, Spain)

Solórzano-Kraemer, M.M., Sinclair, B.J., Arillo, A., **Álvarez-Parra, S.** enviado tras revisión*. A new genus of dance flies (Diptera: Empidoidea: Hybotidae) from Cretaceous Spanish ambers and introduction to the fossiliferous amber outcrop of La Hoya (Castellón Province, Spain). *PeerJ*.

Revista científica: *PeerJ*
Factor de impacto: 3,061 (2021)
Categoría: *Multidisciplinary Sciences*, Q2 (2021)

* El manuscrito se ha reenviado a la revista tras revisiones menores. Dado que es un trabajo aún no publicado, se han retirado los nombres de los nuevos taxones descritos. Debido a la extensión en el número de páginas, no se ha incluido la Tabla 1.

A new genus of dance fly (Diptera: Empidoidea: Hybotidae) from Cretaceous Spanish ambers and introduction to the fossiliferous amber outcrop of La Hoya (Castellón Province, Spain)

Short Title: Hybotidae in Spanish ambers

Mónica M. Solórzano-Kraemer[1*], Bradley J. Sinclair[2], Antonio Arillo[3], Sergio Álvarez-Parra[4,5]

[1]Paläontologie und Historische Geologie, Senckenberg Forschungsinstitut und Naturmuseum, Frankfurt am Main, Germany.
[2]Canadian National Collection of Insects & Canadian Food Inspection Agency, OPL-Entomology, Ottawa, ON, Canada.
[3]Departamento de Biodiversidad, Ecología y Evolución, Facultad de Biología, Universidad Complutense, Madrid, Spain.
[4]Departament de Dinàmica de la Terra i de l'Oceà, Facultat de Ciències de la Terra, Universitat de Barcelona, Barcelona, Spain.
[5]Institut de Recerca de la Biodiversitat (IRBio), Universitat de Barcelona, Barcelona, Spain.

Corresponding Author:
Mónica M. Solórzano Kraemer[1]
Senckenberganlage 25, 60325 Frankfurt am Main, Germany
Email address: monica.solorzano-kraemer@senckenberg.de

Abstract

Hybotidae fly species, also known as dance flies, in Cretaceous ambers have been described from Lebanon, France, Myanmar, Russia, and Canada. Here we describe *AAA BBB* **gen. et sp. n.**, and recognize another two un-named species, in Spanish amber from the middle Albian El Soplao and lower Cenomanian La Hoya outcrops. The fore tibial gland is present in the new genus, which is characteristic of the family Hybotidae. We compare *AAA BBB* **gen. et sp. n.** with the holotypes of *Trichinites cretaceus* Hennig, 1970 and *Ecommocydromia difficilis* Schlüter, 1978, and clarify some morphological details present in the latter two species. Further taxonomic placement beyond family of the here described new genus was not possible and remains *incertae sedis* within Hybotidae until extant subfamilies are better defined. We provide new paleoecological data of the hybotids, together with paleogeographical and life paleoenvironmental notes. A table with the known Cretaceous Hybotidae is provided. Furthermore, the La Hoya amber-bearing outcrop is described in detail, filling the information gap for this deposit.

Keywords

Amber, new species, new genus, amber-bearing outcrop, *Trichinites*, *Ecommocydromia*

Introduction

The Empidoidea Latreille, 1809 (Insecta: Diptera) contain more than 10,000 described species (Pape et al., 2011), representing a diverse lineage within the 166,859 described species in the order Diptera (Evenhuis and Pape, 2022). The Empidoidea (dance flies and long-legged flies) consist of five families: Empididae Latreille, 1809; Hybotidae Fallén, 1816; Atelestidae Henning, 1970; Dolichopodidae Latreille, 1809; and Brachystomatidae *sensu* Sinclair and Cumming, 2006 (Sinclair and Cumming, 2006). However, Wahlberg and Johanson (2018) returned the latter family to a lineage of the Empididae and elevated Ragadinae Sinclair, 2016 to family rank. A couple of additional families are sometimes also recognized in the Empidoidea (Pape et al., 2011). The fossils studied here belong to the Hybotidae, a well-defined monophyletic group (Sinclair and Cumming, 2006; Wahlberg and Johanson, 2018) within the Empidoidea.

Most dance flies today are generalist predators, feeding on insects, but some also feed on dead insects (necrophagous). In addition, many species visit flowers and are known to feed on pollen and nectar (Downes and Smith, 1969). This behavior is also observable through the fossil record (Grimaldi and Engel, 2005). Predatory insects can be abundant in Defaunation resin, copal and amber because they are attracted by arthropods or vertebrates trapped by the resin (Solórzano Kraemer et al., 2015, 2018).

The Hybotidae currently include seven subfamilies: Trichininae Chvála, 1983; Ocydromiinae Schiner, 1862; Oedaleinae Chvála, 1983; Tachydromiinae Meigen, 1822; Hybotinae Meigen, 1820; Stuckenbergomyiinae Sinclair, 2019; and Bicellariinae Sinclair and Cumming, 2006 (Sinclair and Cumming, 2006; Wahlberg and Johanson, 2018; Sinclair, 2019). The subfamily Trichininae remains poorly defined and its relationships with the Oedaleinae, Ocydromiinae or Bicellariinae, or even its position within the Hybotidae, need to be further evaluated (Sinclair and Cumming, 2006; Wahlberg and Johanson, 2018).

The fossil record of the Cretaceous Hybotidae or unplaced hybotid-like species described in previous publications as *incertae sedis* is not extensive but diverse. Conversely, the Cenozoic fossils are abundant in Baltic, Dominican and Mexican ambers as well as compression fossils from the Oligocene of Brazil (EDNA Database, accessed November 2022). Cretaceous fossil hybotid species as bioinclusions have been described in amber from France, Lebanon, Myanmar, Russia, and Canada. Conversely, only one species based on a compression fossil is known from Orapa, Botswana (see Table 1). The species here described share characters with the genera *Trichinites* Hennig, 1970 and *Ecommocydromia* Schlüter, 1978.

Trichinites cretaceus Hennig, 1970 was described from Lebanese amber, which is Lower Cretaceous (Barremian, ~128 Ma) in age (Maksoud and Azar, 2020). It was described by Hennig (1970) based on a single female and placed as a stem-group to the subfamily group Ocydromioinea [Ocydromiinae+Hybotinae+Tachydromiinae], mainly based on wing characters. The position of the genus is currently assigned as the stem-group to the Hybotidae (Chvála, 1983; Grimaldi and Cumming, 1999). *Ecommocydromia difficilis* Schlüter, 1978 was described in amber from Bezonnais, France, which is Cenomanian (~100 Ma) in age (Schlüter, 1978; Perrichot et al., 2007). The most important characters of this genus are the costa not circumambient, cell dm emitting three veins, and legs with pronounced setation. The fossil was placed within the Ocydromiinae, which at the time included all Hybotidae genera exclusive of Hybotinae and Tachydromiinae (Schlüter, 1978). Both Lebanese and French ambers were characterized within the group of *Agathis*-like (Araucariaceae) resins (Perrichot et al., 2007; Azar et al., 2010)

The specimens studied in this work come from the El Soplao and La Hoya amber-bearing outcrops (Fig. 1A), in Spain. The El Soplao outcrop is located in the western margin of the Basque-Cantabrian Basin (northern Iberian Peninsula). It belongs to the Las Peñosas Formation, dated as lower–middle Albian based on foraminifera (García-Mondéjar, 1982), and the amber is most probably middle Albian in age. The sedimentary environment is related to a delta-estuary under marine influence (Najarro et al., 2009). El Soplao amber has been extensively studied and is one of the richest in bioinclusions in the Iberian Peninsula, yielding a diverse arthropod fauna (Najarro et al., 2010). The La Hoya locality (not to be mistaken with the Barremian compression outcrop of Las Hoyas, also in Spain) has been mentioned in several congress communications and scientific publications (Delclòs et al., 2007; Peñalver et al., 2007, 2010; Peñalver and Delclòs, 2010; Menor-Salván et al., 2016; Murillo-Barroso et al., 2018; Rodrigo et al., 2018; McCoy et al., 2021; Santer et al., 2022), but no detailed introduction about the general aspects of the outcrop has been published so far.

Here we describe more accurately the generalities of La Hoya outcrop. Furthermore, a new genus and species within Hybotidae are described and two additional, unnamed species are recognized. We compare our specimens with the holotypes of *Trichinites cretaceus* and *Ecommocydromia difficilis*, and clarify and add some anatomical details of these latter species. Finally, we discuss the classification of these three genera within the Empidoidea.

Materials & Methods

Six specimens of dance flies included in amber have been examined for this work. From the El Soplao amber-bearing outcrop (Cantabria Autonomous Community, Spain): CES.404.1 ♂, CES.404.2 ♂, CES.439 ♂, CES.372 ♀; housed at the Colección Institucional del Laboratorio de la Cueva El Soplao in Celis, Cantabria (acronym for the collections is **CES**); permissions of excavations PFC 83/08 and PFC 33/09 (Consejería de Cultura, Turismo y Deporte del Gobierno

de Cantabria). From the La Hoya amber-bearing outcrop (Castellón Province, Spain): MGUV-16348 (sex unknown) and MGUV-16349 ♀; housed at the Museu de la Universitat de València d'Història Natural (Burjassot, Valencia Province, Spain) (acronym for the collections is **MGUV**); permission of excavation 2003/0593-V (Conselleria d'Educació, Cultura i Esport de la Generalitat Valenciana). Amber pieces were cut and embedded in synthetic epoxy resin (EPO-TEK 301) and then polished (Corral et al., 1999; Nascimbene and Silverstein, 2000; Sadowski et al., 2021). Color photographs and Z-stack images were performed under a Nikon SMZ25 microscope, using Nikon SHR Plan Apo 0.5x and SHR Plan Apo 2x objectives with a Nikon DS-Ri2 camera and NIS-Element software (version 4.51.00 www.microscope.healthcare.nikon.com) and a digital camera attached to an Olympus BX51 compound microscope. Black White (Infrared reflected photomicrographs) were taken with a Nikon Eclipse ME600D (see Brocke and Wilde, 2001 for precise technical information). Photographs were Z-stacked using the NIS-Element software. Drawings were made with the aid of an Olympus U-DA drawing tube attached to an Olympus BX50 compound microscope and digitized using a Wacom drawing tablet. Figures were assembled using Adobe Photoshop software (CS6 version 13.0 www.adobe.com).

The electronic version of this article in Portable Document Format (PDF) will represent a published work according to the International Commission on Zoological Nomenclature (ICZN), and hence the new names contained in the electronic version are effectively published under that Code from the electronic edition alone. This published work and the nomenclatural acts it contains have been registered in ZooBank, the online registration system for the ICZN. The ZooBank LSIDs (Life Science Identifiers) can be resolved and the associated information viewed through any standard web browser by appending the LSID to the prefix http://zoobank.org/. The LSID for this publication is: [LSID urn:lsid:zoobank.org:pub:D36ECF93-C05E-4A9C-8AA2-C799ED04346D]. The online version of this work is archived and available from the following digital repositories: PeerJ, PubMed Central SCIE and CLOCKSS.

Synchrotron Radiation micro-Computed Tomography (SRμ-CT) scans were carried out; however, the samples did not produce enough contrast, and segmentation of the reconstructed scans was not successful.

The Fourier Transform Infrared Spectroscopy (FTIR) analysis of La Hoya amber was obtained using an IR PerkinElmer Frontier spectrometer that utilizes a diamond ATR system with a temperature stabilized DTGS detector and a CsI beam splitter at the Molecular Spectrometry Unit of the CCiTUB (University of Barcelona, Spain).

The anatomical terminology of the specimens follows Cumming and Wood (2017).

Results

Systematic paleontology

The specimens of the species described here are placed in the family Hybotidae, based on the following apomorphic ground plan characters: l) Costa runs to just below the apex of the wing, ending near or beyond distal end of M_1 or M_{1+2}; 2) Sc incomplete, not reaching the wing margin, ending freely in wing membrane; 3) R_{4+5} unbranched; 4) fore tibial gland present; 5) stylus with bare, terminal sensillum.

Order DIPTERA Linnaeus, 1758
Superfamily Empidoidea (*sensu* Chvála, 1983)
Family HYBOTIDAE Meigen, 1820

***AAA* n. gen.** (Figs. 2–5, 7, and 8)
LSID urn:lsid:zoobank.org:act:23818B66-56D4-4D7B-BFA5-1EB7D6995462

Type species. *A BBB* **n. sp.**

Etymology.

Diagnosis. Eyes meeting above antennae (holoptic) in males and dichoptic in females. Antenna with long, arista-like stylus, longer than postpedicel. R_{2+3} straight to costa. Cell dm slightly larger than cell cua, apices in same plane or linear. Cell dm with M_1, M_2 and M_4 extending to wing margin. Thoracic setae long and strong. Fore and hind tibiae more or less of the same thickness. Longitudinal furrow on mid and hind femora and tibiae. Fore tibial gland present. Symmetrical male hypopygium, slightly rotated. Hypandrium apically narrowly bilobed, with posterior apices pointed.

***AAA BBB* n. sp.** (Figs. 2–4, and 5A–C)
LSID urn:lsid:zoobank.org:act:9028DF70-F0B3-4A2C-B677-64F51C8CEC33

Etymology.

Diagnosis. As for the genus.

HOLOTYPE: **CES.404.1** ♂. Housed at the Colección Institucional del Laboratorio de la Cueva El Soplao in Celis (Cantabria, SPAIN).
PARATYPES: **CES.404.2** ♂**, CES.439** ♂

Description

Body. Holotype male CES.404.1 (Fig. 2A and B) body length about 1.79 mm, wing length 1.57 mm. Paratype male CES.404.2 (Fig. 2A right) body length 1.74 mm, wing length 1.53 mm. Paratype male CES.439 (Fig. 4A–E) body length 1.78 mm, wing length 1.42 mm.

Head. Eyes meeting above antennae (holoptic) (Fig. 3B); eyes do not meet below antenna (Fig. 3A); ommatrichia absent. Face flat level with eyes. Gena not extended below eye; ventral surface of head, posterior to mouth opening clothed in long, pale setulae. Two pairs of fine ocellar setulae, directed more upward than forward. One pair of outer vertical setae and one pair of inner vertical setae. Antenna inserted above middle of head; scape small, devoid of setulae; pedicel globose bearing long setulae; scape and pedicel similar in length; postpedicel pointed ovate to conical, apically tapered gradually to point, with two-articled apical arista-like stylus (Fig. 3A–C), longer than postpedicel; stylus 0.22 mm, pubescent with bare, terminal sensillum. Labrum large, almost as long as proboscis, apex of labrum rounded. Proboscis half as long as head. Palpus round, bearing 3–4 long setae; palpifer not visible or not present. Labellum covered with short setae on base and 4 strong, short setae visible in specimen CES.439 (Fig. 4B and C).

Thorax. Notum humpbacked (Fig. 2B), notum with 4 irregular rows of acrostichal and dorsocentral setulae; 2 pairs of larger dorsocentral setae posteriorly. One long, strong supra-alar seta, 2 long, strong notopleural setae, and 1 postalar seta on each side (Fig. 3F). Scutellum with 2 pairs of long setae. Legs long and unmodified, hindlegs longest; none of legs raptorial. Fore and hind femora slightly thicker than mid femur. Mid and hind femora and tibiae with longitudinal furrow (Fig. 4F). All femora and tibiae armed with rows of long, strong setae (Figs. 2A and 3G). Tarsus of all legs bearing short, strong setae. Fore tibia with posteroventral gland (Fig. 5).

Wing. Hyaline; with fine microtrichia over entire membrane. Pterostigma absent. Costa terminates between R_{4+5} and M_1 (Fig. 3H); Sc apically evanescent, ending slightly before costal margin; Rs arising distant from level of humeral crossvein; R_1 ending at or slightly beyond mid-length of wing; R_{2+3} straight to C, ending closer to apex of R_1 than R_{4+5}; R_{4+5} unbranched, parallel to M_1; cell dm slightly larger than cell cua, emitting three veins: M_1, M_2, and M_4; M_1 and M_4 only moderately divergent; CuA straight, aligned with apex of cell bm; apex of cell cua slightly truncate or acute. Anal lobe broad, well developed.

Abdomen. Abdomen scarcely broader near base, laterally compressed. Tergites and sternites bearing long, strong setae. Hypopygium symmetrical, slightly rotated (Figs. 3I–J, 4D and E). Hypandrium apically narrowly bilobed, with posterior apices pointed (Fig. 3I–J). Epandrium with pair of articulated surstyli; left surstylus slightly elongate, with inner long, strong setae. Cercus short, unmodified with pubescence.

Remarks. *AAA* n. gen. can be distinguished from *Trichinites* by the following combination of characters: position of vein r-m close to base of cell dm, R_{2+3} longer than in *Trichinites* and extending straight to wing margin (*T. cretaceus* is sharply curved prior to joining costa, Fig. 6A). Apices of cell bm and cua are aligned in *AAA* n. gen. In contrast, the apex of cell cua is obliquely projecting in *Trichinites*. *Trichinites* has an extra cell at the bifurcation of M_1 and M_2, but this is most probably an aberrant feature, thus it is not a diagnostic feature of the species, and is absent in all other specimens studied here. In the new genus, the fore tibia is slightly broader than the mid and hind tibiae and the fore tibial gland is present, distinguishable in three of the four specimens (Fig. 5). Furthermore, *Trichinites* lacks the fore tibial gland and is larger than the new species here described (body length 2.99 mm), including the telescopic abdomen, whereas the maximum length of *AAA BBB* gen. et sp. n. is 1.79 mm. The thorax of the paratype CES.439 appears somewhat flat, however, this is not considered here a differential character and could be due to the fossilization process.

***AAA* species 1**

(Fig. 7)

Female. CES.372 ♀. Body length 1.68 mm. Wing 1.22 mm. Stylus 0.22 mm. Postpedicel 0.16 mm. Similar to *AAA BBB* gen. et sp. n. male holotype, except for the following characters: eyes dichoptic (Fig. 7A and B); setae shorter and finer on thorax, abdomen and legs; labrum curved bearing pseudotracheae (Fig. 7C); proboscis 1/3 longer than head; thorax setae appears with seriated rings (Fig. 7B), possibly artifact of preservation; tergites bearing several shorter setae in comparison with males, first tergite with cluster of about 5 long setae on each side; apical abdominal segments exposed, gradually telescopic; cercus cylindrical, bearing 3 long setulae (Fig. 7F).

Remarks. *AAA* sp. 1 can be distinguished from *AAA* sp. 2 by the tergites bearing several shorter setae and the proboscis 1/3 longer than head.

***AAA* species 2**

(Fig. 8)

Female. MGUV-16348 (sex unknown), **MGUV-16349** ♀. Part of the abdomen of MGUV-16348 is not preserved; however, all other characters, such as the length of the proboscis, which is as long as the head, and dichoptic eyes indicate that it could be a female. Specimen MGUV-16349 only shows the end of the abdomen, which is telescopic, and one wing partially and badly preserved. MGUV-16348 and MGUV-16349 are included in the same amber piece as syninclusions. Similar to the male holotype of *AAA BBB* gen. et sp. n. except for the following characters: stylus 0.19 mm; postpedicel 0.10 mm; eyes dichoptic (Fig. 8D); setae long, strong on thorax, abdomen and legs, somewhat longer than in *AAA* sp. 1; labrum curved; proboscis 1/4 longer than head (Fig. 8D);

tergites and sternites bearing several long setae; setae on anal lobe of wing longer than in *AAA* sp. 1; apical abdominal segments exposed, gradually telescopic; cercus short, cylindrical.

Remarks. *AAA* sp. 2 can be distinguished from *AAA* sp. 1 by the long and strong setae on the thorax, abdomen and legs, somewhat longer than in species 1 and the proboscis is as long as the head.

As the females do not appear in any of the pieces containing males we cannot describe these as new species and they will remain unnamed until more specimens are found, that can be associated to the species with confidence.

Ecommocydromia difficilis Schlüter, 1978
(Fig. 9)

Complementary description

Head. Antenna inserted above middle of head. Right antenna broken, only scape, pedicel and part of postpedicel preserved. Left antenna preserved but base not visible. Scape longer than pedicel; pedicel short, slightly broader than scape with one long seta visible; postpedicel on one side appears pointed ovate to conical, however (as described by Schlüter, 1978) left postpedicel conical, with two-articled apical arista-like stylus (Fig. 9E and F).

Thorax. Laterotergite bare. Presence of tibial gland on foreleg not possible to ascertain. On right fore tibia, gland appears present, in abnormal position (Fig. 9H), but could be artifact due to preservation. On left foreleg, gland not visible, or absent. Fore tibia with anterodorsal row of strong setae, length nearly as long as width of tibia (Fig. 9G).

Abdomen. Shorter than thorax. Tergites and sternites bearing long, strong setae. Hypopygium nearly symmetrical, not rotated (Fig. 9C and D). Hypandrium apically narrowly bilobed, with posterior apices pointed (Fig. 9D). Epandrium with left surstylus broader, not articulated; long postgonites or phallic process (Fig. 9D). Cercus short, unmodified.

Remarks. In the original publication, the holotype of *E. difficilis* has the collection number Emp Ce Bez 1 (Paläontologisches Institut, FU-Berlin) (Fig. 9I). However, the holotype has been transferred to the Natur Museum für Naturkunde in Berlin, Germany under the Number MB.I.7927.

La Hoya amber-bearing outcrop

The La Hoya amber-bearing outcrop is located in the Penyagolosa Sub-basin within the Maestrazgo Basin in the eastern Iberian Peninsula (Salas and Guimerà, 1996). More than 30 amber

outcrops have been reported in this basin, although only four of them are fossiliferous (Peñalver and Delclòs, 2010; Álvarez-Parra et al., 2021): Ariño, San Just, Arroyo de la Pascueta and La Hoya. The amber outcrop of La Hoya is close to the Cortes de Arenoso town (Castellón Province, Valencian Community) and was named after the Font de l'Hoya ravine, where it is located. The Arroyo de la Pascueta amber outcrop is only a few kilometers from La Hoya (Fig. 1A). The oldest mention of amber in the Valencian Community corresponds to Cavanilles (1797), who indicated the presence of "succino" near the Quesa town (Valencia Province); since then, the number of amber outcrops detected in the region has increased. The amber of this area was traditionally used as incense by shepherds, but the livestock grazing has declined in the last decades, furthermore the access to the outcrop is difficult, so this locality could be currently free of anthropic alteration (Rodrigo et al., 2018). The La Hoya amber outcrop was discovered in 1998 and the first paleontological excavation took place in October 2003. La Hoya amber corresponds to the only known fossiliferous amber from the Valencian Community, including: two cockroaches (Blattodea), one platygastrid (Hymenoptera), one chironomid (Diptera), two hybotids (Diptera) here studied, and a few undetermined insect remains.

Geologically, the La Hoya amber outcrop is located at the top of the Cortes de Arenoso section (E. Barrón pers. comm.). This section has been dated as upper Albian–lower Cenomanian based on stratigraphic and palynological data, while the amber-bearing level is most probably lower Cenomanian (Upper Cretaceous) (E. Barrón pers. comm.). Therefore, La Hoya corresponds to the only known fossiliferous Cenomanian amber outcrop from the Iberian Peninsula, providing an interesting comparison framework with the Albian fossiliferous ambers from Iberia and with other Cenomanian ambers, such as those from the Hukawng Valley (Myanmar) and Charente-Maritime (France) (Grimaldi et al., 2002; Perrichot et al., 2007). The amber outcrops of San Just, Arroyo de la Pascueta, and La Hoya were initially assigned to the Escucha Formation (Delclòs et al., 2007), but they actually correspond to the Utrillas Group (E. Barrón pers. comm.). The amber-bearing level of La Hoya is a grey-black mudstone rich in organic matter about 50 cm thick at the top of grey mudstone about three meters thick (Fig. 1B). Below the grey mudstone there is a sandstone level, while above the amber-bearing level there is a limestone level (Fig. 1B). The amber-bearing rock is tough, and the amber pieces are usually broken and crumbled, so amber extraction is challenging (Fig. 1C). The aerial amber pieces (related to resin produced in branches or trunks) are scarcer than the nearly rounded kidney-shaped pieces (related to resin produced in roots). The aerial amber mainly corresponds to flow-shaped pieces, instead of droplet- or stalactitic-shaped morphologies. The color of the amber pieces is reddish-yellow.

The FTIR spectrum of the aerial amber from the La Hoya outcrop (Fig. 10) shows the typical characteristics of the amber (Grimalt et al., 1988): carbon-hydrogen stretching band about 2950 cm^{-1}, a prominent carbonyl band about 1700 cm^{-1}, and bending motions carbon-hydrogen bands about 1470 cm^{-1} and 1380 cm^{-1}. There are also hydroxyl bands about 3500 cm^{-1}. The absence of exocyclic methylenic bands at 1640 cm^{-1} and 880 cm^{-1} indicates a high degree of maturation,

related to the Cretaceous age of the amber (Alonso et al., 2000). The molecular composition of the La Hoya amber (through gas chromatography-mass spectrometry) was classified as Type 3, based on an absence of abietane type diterpenoids and higher proportion of amberene with relatively lower homoamberene (**III**) and trimethyltetralin (**II**) than the Type 1 amber (Menor-Salván et al., 2016). The amber Type 3 is compatible with an Araucariaceae origin (Menor-Salván et al., 2016; McCoy et al., 2021).

Finally, it is important to note that the La Hoya amber-bearing outcrop is designated as a LIG (*Lugar de Interés Geológico*, Site of Geological Interest), and it is protected under legislation for paleontological heritage, which means that the excavation requires previous permission from the regional government and that the extracted samples should be deposited in a public institution within the region (Rodrigo et al., 2018).

Discussion

Systematic position

The description of *Trichinites cretaceus* was based on a single female in Barremian amber from Jezzine (Lebanon) and is housed at the Staatliches Museum für Naturkunde (Stuttgart, Germany) (Holotype Nummer LB-617) (Fig. 6D). This holotype specimen was re-examined. *Trichinites* has been proposed as the sister group of the hybotids in which the fore tibial gland was not developed (Chvála, 1983) and was described with the following characters: arista-like stylus longer than postpedicel, with two, possibly three articles [Hennig (1970) suspected the distal basal article was an artifact and we can here confirm that the arista-like stylus of *Trichinites* consists of one basal article]. Fore tibial gland absent or not visible; notum with four irregular rows of acrostichal and dorsocentral setulae; two pairs of larger dorsocentral setae; wing with costal vein ending beyond apex of M_1; Sc incomplete; R_{4+5} not forked; cell dm with veins M_1, M_2 and M_4 branching separately off apex of cell, reaching wing margin; cell cua moderately long, subequal to length of cell bm, truncate apically; CuA projecting slightly obliquely; CuA+CuP reaching wing margin but becoming evanescent; anal lobe large. Terminal segments of female telescoping, without acanthophorite spines; cerci long.

We compared the female of *T. cretaceus* with our specimens of *AAA* n. gen. and noticed several differences: fore tibial gland present (absent or not visible in *Trichinites*), terminal abdominal segments telescoping but compact in comparison with *Trichinites*, tergite 8, syntergite 9+10 and cerci are half as long as in *Trichinites* (Fig. 6A). The wings also present some differences, including the length and apex of cell cua and the setae in the anal area are much larger in *AAA* n. gen. than in *Trichinites*, principally in *AAA* sp. 2. Accordingly, the specimens described herein could not be classified within *Trichinites*.

The most distinctive features of this new fossil genus are: three veins emitted from cell dm; unbranched R_{4+5}; truncate cell cua which is subequal in length with cell bm, both cells being apically aligned; and presence of the fore tibial gland. Furthermore, male specimens have symmetrical terminalia, which appears to be at most only slightly rotated. The presence of the fore tibial gland immediately assigns the genus to the Hybotidae, along with the slender apical sensillum on the stylus. The genus is excluded from the subfamilies Hybotinae and Tachydromiinae by the presence of cell dm emitting three veins. The long cell cua and the linear alignment with cell bm, excludes it from the Ocydromiinae, but it is most similar to the genera *Bicellaria* Macquart, 1823 (Bicellariinae) and *Trichinomyia* Tuomikoski, 1959 (Trichininae) (Chvála, 1983; figs 204, 206). These two genera also have similar nearly symmetrical male terminalia. The Bicellariinae is a distinct monophyletic lineage, defined on the basis of the loss of cell dm and the branches of M evanescent near mid wing, whereas the Trichininae is defined on the basis of symplesiomorphies (Sinclair and Cumming, 2006): dichoptic females, antennal stylus about half as long or shorter than the postpedicel, cell dm emitting three veins, proboscis short and directed downwards, ventral apodeme and postgonites absent. The subfamily contains only two genera, *Trichina* Meigen, 1830 and *Trichinomyia*. However, the position of Trichininae within Hybotidae remains unresolved. *AAA* spp. remain apart from this lineage on the basis of the elongate mouthparts and antennal stylus longer than the postpedicel. Furthermore, *AAA* n. gen. can be separated from *Trichinomyia* by the thoracic hairs and slender bristles, and wings without pterostigma. The male terminalia of *Trichina* is somewhat similar to *AAA BBB* gen. et sp. n., however the hypandrium in the latter seems to be symmetrically bilobed. Wing venation and mouthparts are similar to Oedaleinae; however, our genus can be excluded from the subfamily because of the long, apical antennal stylus, which is usually greatly shortened (shorter than postpedicel) in Oedaleinae.

The genus *Apterodromia* Oldroyd, 1949 was transferred from the Tachydromiinae to the tribe Ocydromiini (now subfamily Ocydromiinae) (Sinclair and Cumming, 2000) and excluded from Trichininae with the argument that an elongated cell cua represents the ground plan condition of the hybotid lineage and the male terminalia characters should be used. The male hypopygium of *AAA BBB* gen. et sp. n., as mentioned above, is symmetrical, not rotated, yet the genus *Trichinomyia*, classified in Trichininae by Sinclair and Cumming (2006) is hypothesized to be the sister group to the remaining Hybotidae on the basis of its symmetrical male hypopygium. Thus, we can assume that symmetrical male hypopygium and the absence of genital rotation in *Ecommocydromia difficilis* and *AAA BBB* gen. et sp. n. are primitive conditions. A similar condition has recently been described in the Ocydromiinae genus *Pseudoscelolabes* Collin, 1933 (Barros et al., 2022).

The phylogenetic position of *Ecommocydromia difficilis* remains uncertain in part mostly because several important characters are not visible, e.g., apex of the arista-like stylus, basal portion of the

wings, and mouthparts. However, the wing venation possibly indicates a close relationship with *AAA* n. gen. and *Trichinites*.

Ecology

The eyes of *AAA* n. gen. are holoptic in males, and dichoptic in females; this condition indicates that males probably formed aerial mating swarms (Chvála, 1976). The form of the females' mouthparts differs from that of males. This could be because of a natural dimorphism, common in Empidoidea, where the females have more prominent mouthparts than the males (Bletchly, 1954). We cannot exclude that the females belong to different species because they are found in separate amber pieces. Consequently, they are not described here as new species. However, the morphology of the mouthparts indicates the well-known predatory feeding habits of the empidoids. Diptera are very abundant in Defaunation resin, copal, and amber, and Empidoidea are among the most abundant Diptera within Cretaceous ambers (*e.g.*, Grimaldi and Cumming, 1999; Sinclair and Grimaldi, 2020; Ngô-Muller et al., 2021). We know that selected taxa trapped in resins represent the fauna living in and around the resin-producing tree and appear in resins because of their ecology and behavior (Solórzano Kraemer et al., 2018). In the case of the herein described specimens, their capture in resin is most probably due to swarming and predatory behaviors (Chvála, 1976; Daugeron, 1997).

The presence of *AAA* n. gen. in the amber-bearing outcrops of El Soplao and La Hoya points out to a wide distribution of the genus in the Cretaceous Iberia Island, along the northern and eastern coasts. This kind of distribution is compatible with that of other taxa found in amber from the Maestrazgo Basin (such as San Just) and in amber from the Basque-Cantabrian Basin (such as El Soplao and Peñacerrada I). Species of Psocodea, Coleoptera, Hymenoptera, and Diptera have been found in San Just and amber-bearing outcrops of northern Iberia (Arillo et al., 2008; Ortega-Blanco et al., 2011a, b; Peris et al., 2014; Álvarez-Parra et al., 2022). Thus, these paleogeographical distributions may indicate that the resiniferous forests in the Iberia Island were at least partly connected, not independently isolated, allowing the movement of entomofauna along the coastal forest environments. Furthermore, the finding of *AAA* n. gen. in the El Soplao amber middle Albian in age, and La Hoya amber most probably lower Cenomanian in age, shows that this genus inhabited the Iberia Island for an interval of about seven million years (~107–100 Ma). The finding of nearly rounded kidney-shaped amber pieces in the same level together with aerial amber pieces in La Hoya amber-bearing outcrop implies a parautochthonous accumulation in a transitional environment (Álvarez-Parra et al., 2021), similarly to El Soplao (Najarro et al., 2010). The La Hoya FTIR spectrum (Fig. 10) does not show significant differences with the spectra of other ambers from the Maestrazgo Basin, such as San Just and Ariño (Álvarez-Parra et al., 2021). The molecular composition of the amber from La Hoya, San Just, and Ariño relates the resin-producing tree to the Araucariaceae (Menor-Salván et al., 2016; Álvarez-Parra et al., 2021). Thus, the paleoenvironment could be similar in the three areas (E. Barrón pers. comm.). Interestingly, the geochemical analysis of the El Soplao

amber linked it to a resin-producing tree related to Cupressaceae or the extinct Cheirolepidiaceae, maybe the genus *Frenelopsis* (Menor-Salván et al., 2010). Therefore, the genus *AAA* n. gen. could inhabit in forests with different plant compositions.

Conclusions

The relevance of the new findings consists in providing new characters to the fossil character-pool of Hybotidae. Furthermore, a new genus and species are described, adding to the diversity of the family during the Cretaceous. This is critical in understanding the evolution of the family. The positions of *AAA* n. gen., *Trichinites*, and *Ecommocydromia* remain unresolved until the extant subfamilies are better defined, principally the Trichininae, and more specimens in Cretaceous amber are discovered that could provide more key information. It is not possible to infer subfamily assignment with the information here recovered. Because Empidoidea, especially Hybotidae are frequent in amber, it is probably only a matter of time before new findings are discovered. Furthermore, delving into taphonomical, geochemical, and paleobotanical data of the amber-bearing outcrops in which these insects are found provide key information about their paleoenvironment and paleoecology.

The search for new characters in the fauna included in amber is supported by technologies such as µ-CT or SRµ-CT. However, not all the inclusions in the different ambers offer good results. The different contrasts of amber specimens are probably a matter of preservation, not only of the diagenesis of the amber itself but also of the diagenesis of the organism. In the case of the amber studied here, SRµ-CT, which normally offers a better contrast than µ-CT, did not provide any signal. This made the segmentation and therefore the visualization of the specimens impossible, thus the character search was limited to light microscopy.

Acknowledgements

We would like to thank the colleagues who participated in fieldwork at the El Soplao and La Hoya amber outcrops. We thank the permissions of excavation and support from Consejería de Cultura, Turismo y Deporte del Gobierno de Cantabria (Spain) (permissions PFC 83/08 and PFC 33/09, research agreement #20963 with University of Barcelona) and Conselleria d'Educació, Cultura i Esport de la Generalitat Valenciana (Spain) (permission 2003/0593-V). We also thank Ascensión Jarque, owner of the land in which La Hoya outcrop is located, and Federico Alegre and Vicente Arnau, discoverers of this amber outcrop. We are indebted to Rafael López del Valle for preparation of the amber pieces. We are grateful to Robin Kunz (Senckenberg Research Institute) for helping with the digitalization of the drawings, and to Eduardo Barrón (Instituto Geológico y Minero de España, CSIC) for providing stratigraphic and dating information of the amber outcrops. Thanks also to Thomas Schlüter (University of Swaziland) for providing valuable information about *Ecommocydromia difficilis*, to Andreas Abele-Rassuly and Christian

Neumann (Museum für Naturkunde Berlin) for providing the holotype of *Ecommocydromia difficilis*, and Michael W. Rasser (Staatliches Museum für Naturkunde Stuttgart) for providing the holotype of *Trichinites cretaceus*. The coauthor S.Á-P. thanks the support of his supervisors Xavier Delclòs (Universitat de Barcelona) and Enrique Peñalver (Instituto Geológico y Minero de España, CSIC). Agnieszka Soszyńska-Maj (University of Lodz), an anonymous reviewer, and the editor Kennet de Baets (University of Warsaw) kindly commented on an earlier draft.

Additional Information and Declarations

Author Contributions

Mónica M. Solórzano-Kraemer, wrote the paper, performed the experiments, analyzed the data, prepared figures and/or tables, authored and reviewed drafts of the paper, and approved the final draft.

Bradley J. Sinclair, wrote the paper, analyzed the data, authored and reviewed drafts of the paper, and approved the final draft.

Antonio Arillo, analyzed the data, performed the experiments, prepared figures and/or tables, authored and reviewed drafts of the paper, and approved the final draft.

Sergio Álvarez-Parra, wrote the paper, analyzed the data, prepared figures and/or tables, authored and reviewed drafts of the paper, and approved the final draft.

References

Almera J, Anadón P, Godoy A. 1977. Cartografía geológica y memoria explicativa. In: Barnolas A, ed. *Mapa geológico de España 1:50.000, Hoja 591* Mora de Rubielos. Madrid: Instituto Geológico y Minero de España, 28–23.

Alonso J, Arillo A, Barrón E, Corral JC, Grimalt J, López JF, López R, Martínez-Delclòs X, Ortuño VM, Peñalver E, Trincão PR. 2000. A new fossil resin with biological inclusions in Lower Cretaceous deposits from Alava (northern Spain, Basque-Cantabrian Basin). *Journal of Paleontology* **74**:158–178. https://doi.org/10.1666/0022-3360(2000)074<0158:ANFRWB>2.0.CO;2

Álvarez-Parra S, Pérez-de la Fuente R, Peñalver E, Barrón E, Alcalá L, Pérez-Cano J, Martín-Closas C, Trabelsi K, Meléndez N, López Del Valle R, Lozano RP, Peris D, Rodrigo A, Sarto i Monteys V, Bueno-Cebollada CA, Menor-Salván C, Philippe M, Sánchez-García A, Peña-Kairath C, Arillo A, Espílez E, Mampel L, Delclòs X. 2021. Dinosaur bonebed amber from an original swamp forest soil. *eLife* **10**:e72477. https://doi.org/10.7554/eLife.72477

Álvarez-Parra S, Peñalver E, Nel A, Delclòs X. 2022. New barklice (Psocodea, Trogiomorpha) from Lower Cretaceous Spanish amber. *Papers in Palaeontology* **8**(**3**):e1436. https://doi.org/10.1002/spp2.1436

Arillo A, Peñalver E, Delclòs X. 2008. *Microphorites* (Diptera: Dolichopodidae) from the Lower Cretaceous amber of San Just (Spain), and the co-occurrence of two ceratopogonid species in Spanish amber deposits. *Zootaxa* **1920**(**1**):29–40. https://doi.org/10.11646/ZOOTAXA.1920.1.2

Azar D, Gèze R, Acra F. 2010. Lebanese amber. In: Penney D, ed. *Biodiversity of fossils in amber from the major world deposits*. Manchester: Siri Scientific Press, 271–298.

Barros LM, Soares MMM, Freitas-Silva RAP, Sinclair BJ, Ale-Rocha R. 2022. Revision of the New Zealand endemic genus *Pseudoscelolabes* Collin (Diptera: Hybotidae: Ocydromiinae). *Zootaxa* **5150**(**4**):516–528. https://doi.org/10.11646/zootaxa.5150.4.3

Bletchly JD. 1954. The mouth-parts of the dance fly, *Empis livida* L. (Diptera, Empididae). *Proceedings of the Zoological Society of London* **124**(**2**):317–334. https://doi.org/10.1111/j.1469-7998.1954.tb07785.x

Brocke R, Wilde V. 2001. Infrared video microscopy–an efficient-method for the routine investigation of opaque organic-walled microfossils. *Facies* **45**:157–164. https://doi.org/10.1007/BF02668109

Cavanilles AJ. 1797. *Observaciones sobre la historia natural, geografía, agricultura, población y frutos del Reyno de Valenci*a. Madrid: Imprenta Real.

Chvála M. 1976. Swarming, mating and feeding habits in Empididae (Diptera), and their significance in evolution of the family. *Acta Entomologica Bohemoslovaca* **73**:353–366.

Chvála M. 1983. The Empidoidea (Diptera) of Fennoscandia and Denmark. II. General Part. The families Hybotidae, Atelestidae and Microphoridae. *Fauna Entomologica Scandinavica* **12**:1–279.

Cockerell TDA. 1917. Insects in Burmese amber. *Annals of the Entomological Society of America* **10**(**4**):323–329. https://doi.org/10.1093/aesa/10.4.323

Corral JC, López Del Valle R, Alonso J. 1999. El ámbar cretácico de Álava (Cuenca Vasco-Cantábrica, norte de España). Su colecta y preparación. *Estudios del Museo de Ciencias Naturales de Álava* **14**(**2**):7–21.

Cumming JM, Wood DM. 2017. Adult morphology and terminology. In: Kirk-Spriggs AH, Sinclair BJ, eds. *Manual of Afrotropical Diptera. Volume 1. Introductory chapters and keys to Diptera families.* Pretoria: SANBI Graphics & Editing, 89–133.

Daugeron C. 1997. Evolution of feeding and mating behaviors in the Empidoidea (Diptera: Eremoneura). In: Grandcolas P, ed. *The origin of biodiversity in insects: tests of evolutionary scenarios*. Paris: Mémoires du Muséum National d'Histoire Naturelle, Zoologie, 163–182.

Delclòs X, Arillo A, Peñalver E, Barrón E, Soriano C, López del Valle R, Bernárdez E, Corral C, Ortuño VM. 2007. Fossiliferous amber deposits from the Cretaceous (Albian) of Spain. *Comptes Rendus Palevol* **6**(**1–2**):135–149. https://doi.org/10.1016/j.crpv.2006.09.003

Downes JA, Smith SM. 1969. New or little known feeding habits in Empididae (Diptera). *The Canadian Entomologist* **101**(**4**):404–408. https://doi.org/10.4039/Ent101404-4

Evenhuis NL, Pape T. 2022. *Systema Dipterum* Update. *Fly Times* **68**:34.

García-Mondéjar J. 1982. Aptiense y Albiense. In: Alonso A, Arias C, García A, Mas R, Rincón R, Vilas L, eds. *El Cretácico de España.* Madrid: Editorial Universidad Complutense de Madrid, 63–84.

Grimaldi DA, Cumming JM. 1999. Brachyceran Diptera in Cretaceous ambers and Mesozoic diversification of the Eremoneura. *Bulletin of the American Museum of Natural History* **239**:1–124.

Grimaldi D, Engel MS. 2005. *Evolution of the Insects*. England: Cambridge University Press.

Grimaldi DA, Engel MS, Nascimbene PC. 2002. Fossiliferous Cretaceous amber from Myanmar (Burma): its rediscovery, biotic diversity, and paleontological significance. *American Museum Novitates* **3361**:1–71. https://doi.org/10.1206/0003-0082(2002)361<0001:FCAFMB>2.0.CO;2

Grimalt JO, Simoneit BRT, Hatcher PG, Nissenbaum A. 1988. The molecular composition of ambers. *Organic Geochemistry* **13**(**4–6**):677–690. https://doi.org/10.1016/0146-6380(88)90089-7

Haggerty SE, Raber E, Naeser CW. 1983. Fission track dating of kimberlitic zircons. *Earth and Planetary Science Letters* **63(1)**:41–50.

Hennig W. 1970. Insektfossilien aus der unteren Kreide. II. Empididae (Diptera, Brachycera). *Stuttgarter Beiträge zur Naturkunde* **214**:1–12.

Jouault C, Ngô-Muller V, Zhang Q, Nel A. 2020. New empidoid flies (Diptera: Atelestidae; Dolichopodidae) from mid-Cretaceous Burmese amber. *Palaeoentomology* **3**(**2**):204–211. https://doi.org/10.11646/palaeoentomology.3.2.10

Kovalev VG. 1974. A new genus of the family Empididae (Diptera) and its phylogenetic relationships. *Paleontological Journal* **8**:196–220.

Kovalev VG. 1978. A new fly genus (Empididae) from the Cretaceous resinites of Taimyr. *Paleontological Journal* **12**:351–356.

Maksoud S, Azar D. 2020. Lebanese amber: latest updates. *Palaeoentomology* **3**(**2**):125–155. https://doi.org/10.11646/PALAEOENTOMOLOGY.3.2.2

McCoy VE, Barthel HJ, Boom A, Peñalver E, Delclòs X, Solórzano-Kraemer MM. 2021. Volatile and semi-volatile composition of Cretaceous amber. *Cretaceous Research* **127**:104958. https://doi.org/10.1016/j.cretres.2021.104958

McKellar RC, Wolfe AP. 2010. Canadian amber. In: Penney D ed. *Biodiversity of fossils in amber from the major world deposits*. Manchester: Siri Scientific Press, 149–166.

Menor-Salván C, Najarro M, Velasco F, Rosales I, Tornos F, Simoneit BR. 2010. Terpenoids in extracts of lower cretaceous ambers from the Basque-Cantabrian Basin (El Soplao, Cantabria, Spain): paleochemotaxonomic aspects. *Organic Geochemistry* **41**(**10**):1089–1103. https://doi.org/10.1016/j.orggeochem.2010.06.013

Menor-Salván C, Simoneit BR, Ruiz-Bermejo M, Alonso J. 2016. The molecular composition of Cretaceous ambers: Identification and chemosystematic relevance of 1, 6-dimethyl-5-alkyltetralins and related bisnorlabdane biomarkers. *Organic Geochemistry* **93**:7–21. https://doi.org/10.1016/j.orggeochem.2015.12.010

Murillo-Barroso M, Peñalver E, Bueno P, Barroso R, de Balbín R, Martiñón-Torres M. 2018. Amber in prehistoric Iberia: New data and a review. *PLOS ONE* **13**(**8**):e0202235. https://doi.org/10.1371/journal.pone.0202235

Najarro M, Peñalver E, Rosales I, Pérez-de la Fuente R, Daviero-Gómez V, Gómez B, Delclós X. 2009. Unusual concentration of Early Albian arthropod-bearing amber in the Basque-Cantabrian Basin (El Soplao, Cantabria, Northern Spain): Palaeoenvironmental and palaeobiological implications. *Geologica Acta* **7**(**3**):363–388. https://doi.org/10.1344/105.000001443

Najarro M, Peñalver E, Pérez-de la Fuente R, Ortega-Blanco J, Menor-Salván C, Barron E, Soriano C, Rosales I, López Del Valle R, Velasco F, Tornos F, Daviero-Gomez V, Gomez B, Delclos X. 2010. Review of the El Soplao amber outcrop, Early Cretaceous of Cantabria, Spain. *Acta Geologica Sinica* **84**(**4**):959–976. https://doi.org/10.1111/j.1755-6724.2010.00258.x

Nascimbene P, Silverstein H. 2000. The preparation of fragile Cretaceous ambers for conservation and study of organismal inclusions. In: Grimaldi D, ed. *Studies on Fossils in Amber, with particular reference to the Cretaceous of New Jersey*. Leiden: Backhuys Publishers, 93–102.

Ngô-Muller V, Engel MS, Garrouste R, Pouillon JM, Nel A. 2021. The first predatory dance fly of the subfamily Ocydromiinae with specialized, raptorial legs in mid–Cretaceous amber from Myanmar (Diptera: Hybotidae). *Cretaceous Research* **119**:104697. https://doi.org/10.1016/j.cretres.2020.104697

Ortega-Blanco J, Delclòs X, Engel MS. 2011a. Diverse stigmaphronid wasps in Early Cretaceous amber from Spain (Hymenoptera: Ceraphronoidea: Stigmaphronidae). *Cretaceous Research* **32**(**6**):762–773. https://doi.org/10.1016/j.cretres.2011.05.004

Ortega-Blanco J, Peñalver E, Delclós X, Engel MS. 2011b. False fairy wasps in early Cretaceous amber from Spain (Hymenoptera: Mymarommatoidea). *Palaeontology* **54**(**3**):511–523. https://doi.org/10.1111/j.1475-4983.2011.01049.x

Pape T, Blagoderov V, Mostovski MB. 2011. Order Diptera Linnaeus, 1758. In: Zhang, Z.-Q. (Ed.), *Animal biodiversity: An outline of higher-level classification and survey of taxonomic richness*. *Zootaxa* **3148**:222–229. https://doi.org/10.11646/zootaxa.3703.1.3

Peñalver E, Delclòs X. 2010. Spanish amber. In: Penney D, ed. *Biodiversity of fossils in amber from the major world deposits*. Manchester: Siri Scientific Press, 236–270.

Peñalver E, Delclòs X, Soriano C. 2007. A new rich amber outcrop with palaeobiological inclusions in the Lower Cretaceous of Spain. *Cretaceous Research* **28**(**5**):791–802. https://doi.org/10.1016/j.cretres.2006.12.004

Peñalver E, Ortega-Blanco J, Nel A, Delclòs X. 2010. Mesozoic Evaniidae (Insecta: Hymenoptera) in Spanish amber: reanalysis of the phylogeny of the Evanioidea. *Acta Geologica Sinica-English Edition* **84**(**4**):809–827. https://doi.org/10.1111/j.1755-6724.2010.00257.x

Peris D, Davis SR, Engel MS, Delclòs X. 2014. An evolutionary history embedded in amber: reflection of the Mesozoic shift in weevil-dominated (Coleoptera: Curculionoidea) faunas. *Zoological Journal of the Linnean Society* **171**(**3**):534–553. https://doi.org/10.1111/zoj12149

Perkovsky EE, Vasilenko DV. 2019. A summary of recent results in the study of Taimyr amber. *Paleontological Journal* **53(10):**984–993.

Perrichot V, Néraudeau D, Nel A, De Ploëg G. 2007. A reassessment of the Cretaceous amber deposits from France and their palaeontological significance. *African Invertebrates* **48**(**1**):213–227.

Rodrigo A, Peñalver E, López del Valle R, Barrón E, Delclòs X. 2018. The heritage interest of the Cretaceous amber outcrops in the Iberian Peninsula, and their management and protection. *Geoheritage* **10**(**3**):511–523. https://doi.org/10.1007/s12371-018-0292-1

Sadowski EM, Schmidt AR, Seyfullah LJ, Solórzano-Kraemer MM, Neumann C, Perrichot V, Hamann C, Milke R, Nascimbene PC. 2021. Conservation, preparation and imaging of diverse ambers and their inclusions. *Earth-Science Reviews* **220**:103653. https://doi.org/10.1016/j.earscirev.2021.103653

Salas R, Guimerà J. 1996. Rasgos estructurales principales de la cuenca cretácica inferior del Maestrazgo (Cordillera Ibérica oriental). *Geogaceta* **20**:1704–1706.

Santer M, Álvarez-Parra S, Nel A, Peñalver E, Delclòs X. 2022. New insights into the enigmatic Cretaceous family Spathiopterygidae (Hymenoptera: Diaprioidea). *Cretaceous Research* **133**:105128. https://doi.org/10.1016/j.cretres.2021.105128

Schlüter T. 1978. Zur Systematik und Palokologie harzkonservieter Arthropoda einer Taphozonose aus dem Cenomanium von NW-Frankreich. *Berliner Geo-wissenschaftliche Abhandlungen - Reihe A: Geologie und Palaontologie* **9**:1–150.

Shi G, Grimaldi DA, Harlow GE, Wang J, Wang J, Yang M, Lei W, Li Q, Li X. 2012. Age constraint on Burmese amber based on U–Pb dating of zircons. *Cretaceous research* **37**:155–163.

Sinclair BJ. 2019. Revision of the southern African genus *Stuckenbergomyia* Smith, 1971 (Diptera, Empidoidea) and proposal of a new subfamily. *African Invertebrates* **60**:133–145.

Sinclair BJ, Cumming JM. 2000. Revision of the genus *Apterodromia* (Diptera: Empidoidea), with a redefinition of the tribe Ocydromiini. *Records-Australian Museum* **52**(**2**):161–186. https://doi.org/10.3853/j.0067-1975.52.2000.1313

Sinclair BJ, Cumming JM. 2006. The morphology, higher-level phylogeny and classification of the Empidoidea (Diptera). *Zootaxa* **1180**(**1**):1–172. https://doi.org/10.11646/zootaxa.1180.1.1

Sinclair BJ, Grimaldi DA. 2020. Cretaceous diversity of the relict genus *Alavesia* Waters and Arillo (Diptera: Empidoidea: Atelestidae). *American Museum Novitates* **3961**:1–40. https://doi.org/10.1206/3961.1

Solórzano Kraemer MM, Delclòs X, Clapham M, Arillo A, Peris D, Jäger P, Stebner F, Peñalver E. 2018. Arthropods in modern resins reveal if amber accurately recorded forest arthropod communities. *Proceedings of the National Academy of Sciences* **115**(**26**):6739–6744. https://doi.org/10.1073/pnas.1802138115

Solórzano Kraemer MM, Solórzano KA, Stebner F, Bickel D, Rust J. 2015. Entrapment bias of insects in Miocene amber revealed by trapping experiments in a tropical forest in Chiapas, Mexico. *PLOS ONE* **10**(**3**):e.0118820. https://doi.org/10.1371/journal.pone.0118820

Wahlberg E, Johanson KA. 2018. Molecular phylogenetics reveals novel relationships within Empidoidea (Diptera). *Systematic Entomology* **43**(**4**):619–636. https://doi.org/10.1111/syen.12297

Waters SB. 1989. A new Hybotine dipteran from the Cretaceous of Botswana. *Palaeontology* **32**(**3**):657–667.

TABLE AND FIGURES

TABLE

Table 1. Checklist of the known Cretaceous Hybotidae and related genera (Diptera: Empidoidea), with indication of the provenance and age. The new taxa here described are in bold. The genus *Cretoplatypalpus* is doubtfully assigned to Empidoidea sensu Jouault et al. (2020). The genus *Ecommocydromia difficilis* was originally assigned to Ocydromiinae but later to the Empididae s.s. by Grimaldi and Engel (2005) and as *incertae sedis* within Empidoidea *sensu* Ngô-Muller et al. (2021) and in the present work. **Trichinites* has been proposed as the sister group of the hybotids, it is here included for practical reasons.

FIGURES

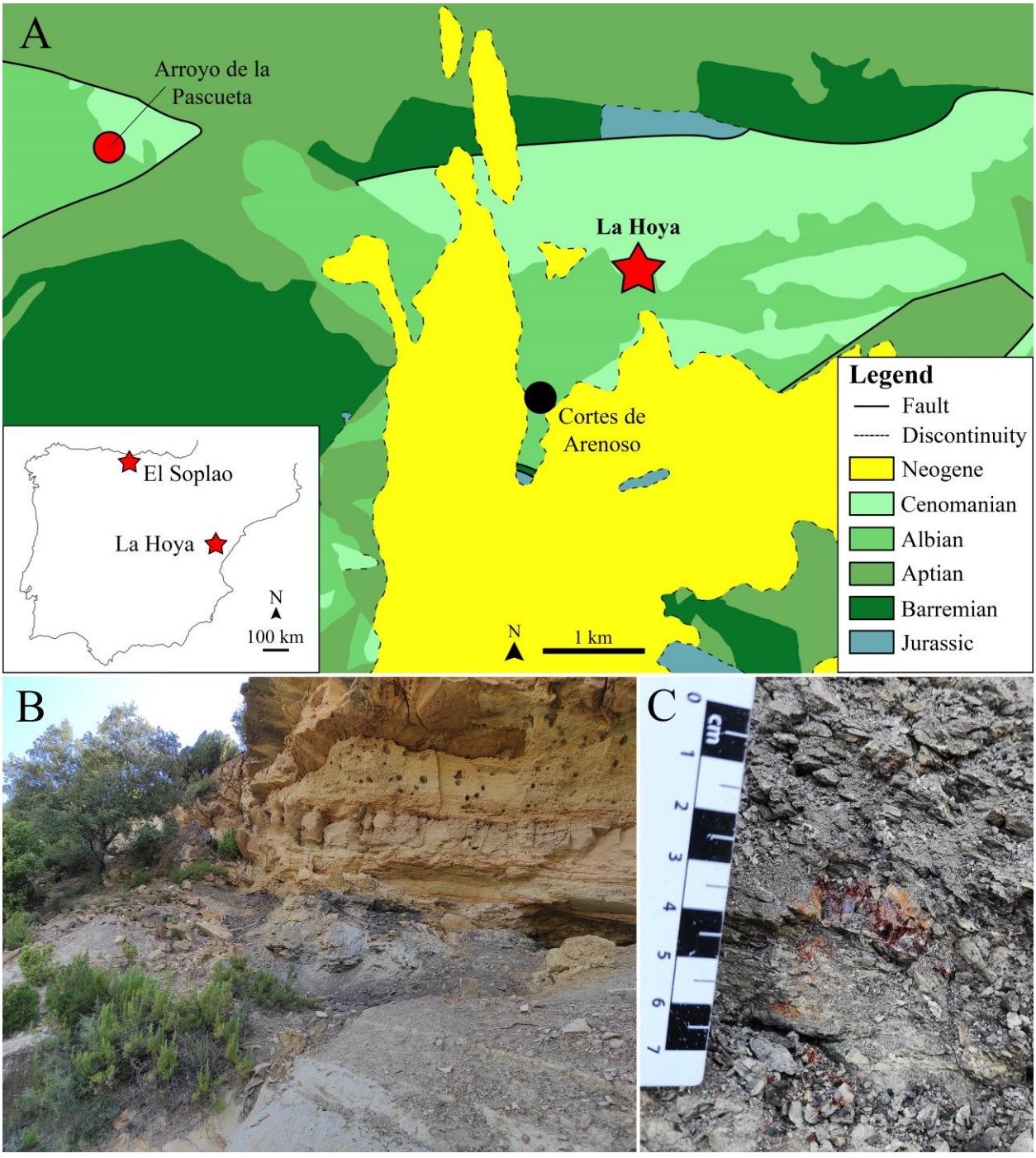

Figure 1. The lower Cenomanian (Upper Cretaceous) amber-bearing outcrop of La Hoya (Maestrazgo Basin, Castellón Province, Spain). (A) Geographical location within the Iberian Peninsula of the El Soplao (middle Albian) and La Hoya amber outcrops, and geological location of the La Hoya outcrop; Cortes de Arenoso village and the fossiliferous Arroyo de la Pascueta amber outcrop (late Albian) are also indicated in the geological map. (B) Amber-bearing level of the La Hoya outcrop, constituted by grey-black mudstone rich in organic matter, at the top of the

Cortes de Arenoso section. (C) An amber piece in the rock of the La Hoya outcrop. Geological map in A modified and simplified from Almera et al. (1977).

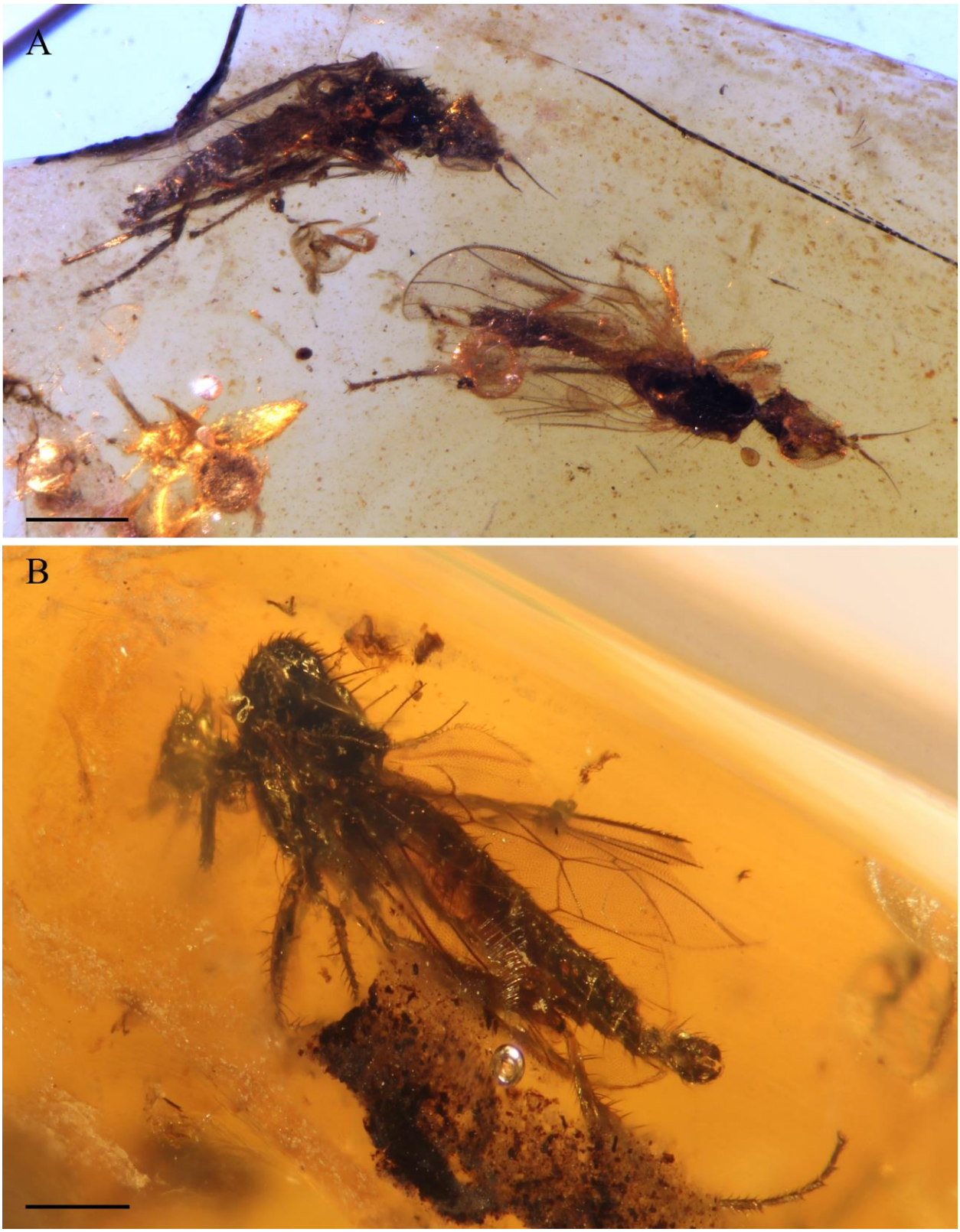

Figure 2. *AAA BBB* gen. et sp. n. (Diptera: Hybotidae), holotype male CES.404.1 and paratype male CES.404.2, from El Soplao outcrop, Cantabria, Spain (middle Albian in age). (A) Piece showing two specimens (holotype, left; paratype, right). (B) Habitus of holotype CES.404.1, lateral view. Scale bars 0.5 mm.

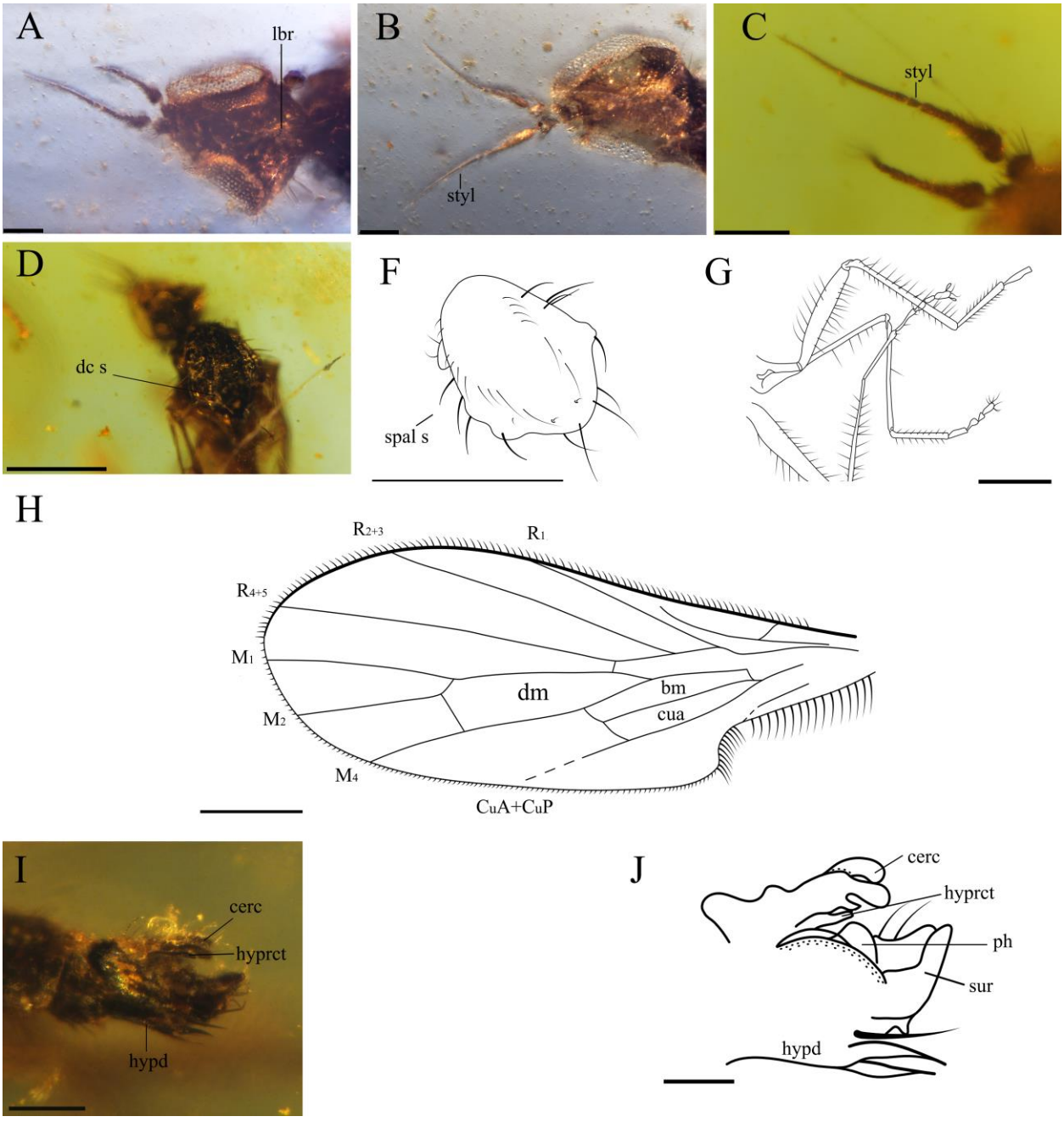

Figure 3. Important characters of *AAA BBB* gen. et sp. n. (Diptera: Hybotidae), holotype male CES.404.1 and paratype male CES.404.2, from El Soplao outcrop, Cantabria, Spain (middle Albian in age). (A) Head of holotype CES.404.1, ventral view. (B) Head of paratype male, dorsal view. (C) Antennae of holotype. (D) Thorax of holotype, dorsal view. (F) Drawing

of thorax of holotype, dorsal view. (G) Hindlegs of holotype. (H) Reconstruction of wing (I) Male terminalia of holotype, lateral view. (J) Male terminalia of holotype, lateroventral left. Scale bars A–C and H–J 0.1 mm, D–G 0.5 mm. Abbreviations: bm= basal medial cell, cerc= cercus, cua= anterior cubital cell, CuA+CuP= anterior branch of cubital vein + posterior branch of cubital vein, dc s= dorsocentral setae, dm= discal medial cell, hypd= hypandrium, hyprct= hypoproct, M= medial vein, lbr= labrum, ph= phallus, R= radial vein, Sc= subcostal, spal s= supra-alar seta, styl= stylus, sur= surstylus.

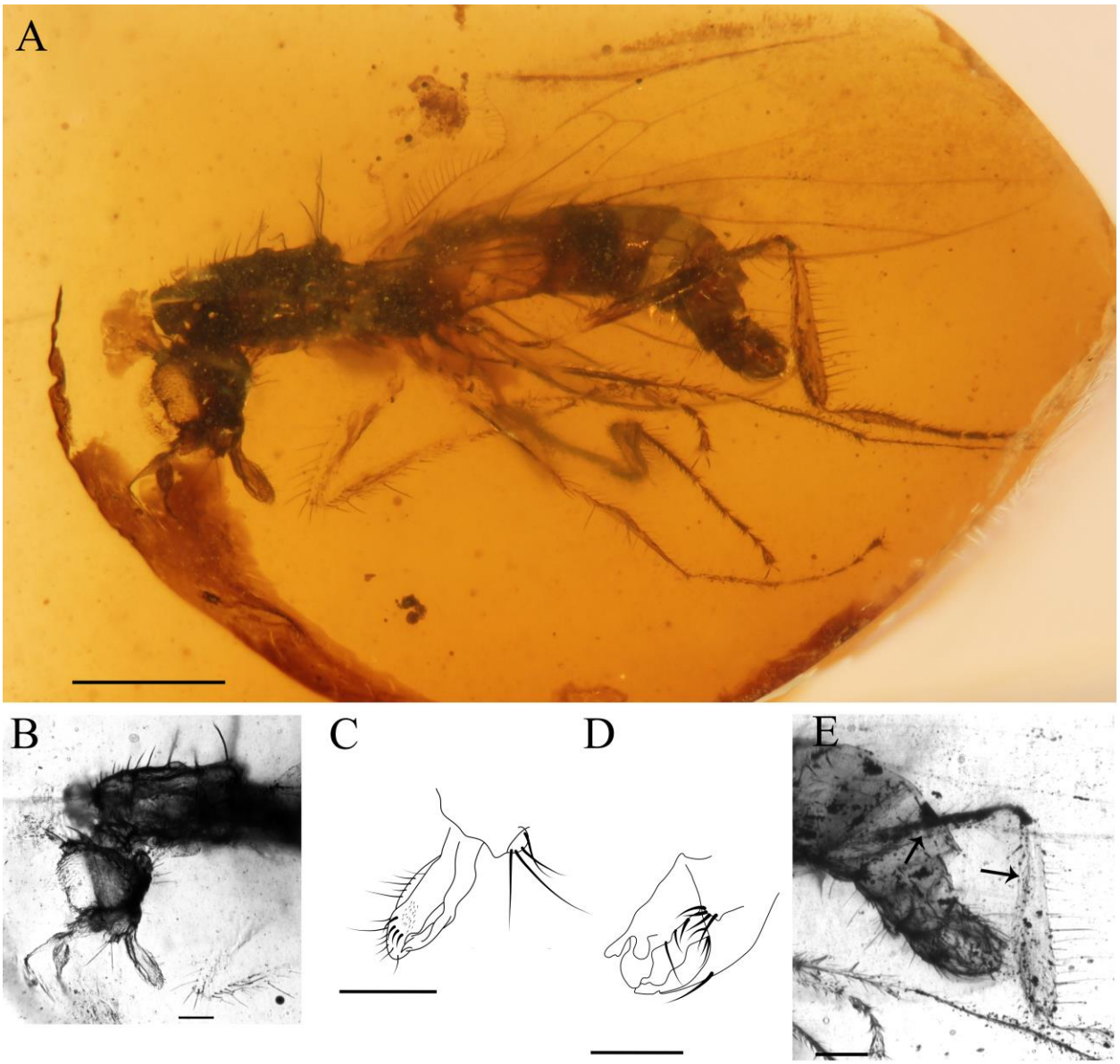

Figure 4. *AAA BBB* gen. et sp. n. (Diptera: Hybotidae), paratype male CES.439, from El Soplao outcrop, Cantabria, Spain (middle Albian in age). (A) Habitus, lateral view. (B) Head, ventrolateral view. (C) Mouthparts. (D) Male terminalia, laterodorsal view. (E) Photo of male

terminalia, laterodorsal view and hindleg. Black arrows show the longitudinal furrow on hind femur and tibia. Scale bars A 0.5 mm, B–E 0.1 mm.

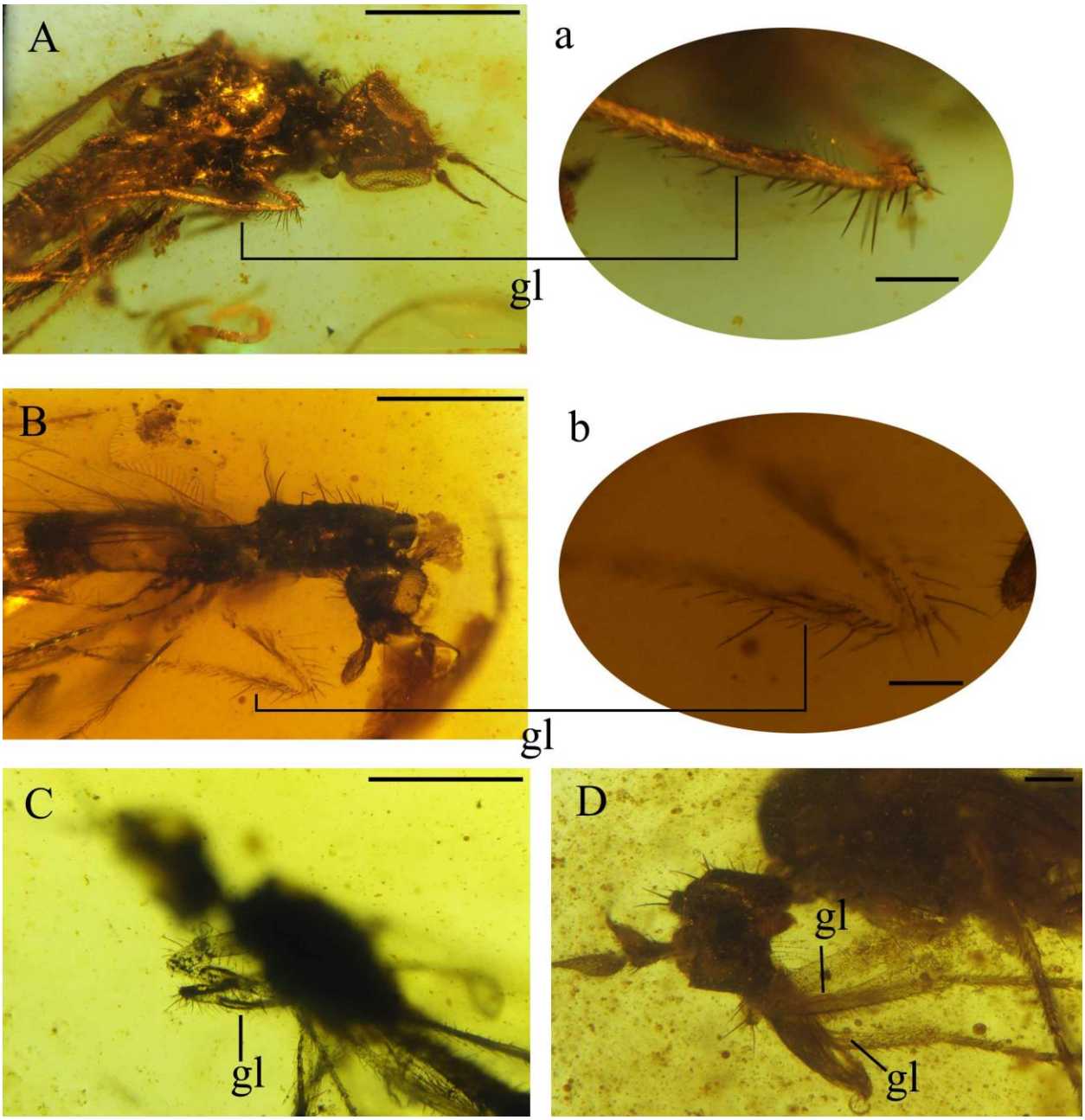

Figure 5. Fore tibial gland in *AAA BBB* gen. et sp. n. (Diptera: Hybotidae), from El Soplao outcrop, Cantabria, Spain (middle Albian in age). (A) Holotype CES.404.1, with close-up of gland. (B) Paratype CES.439, with close-up of gland. (C) Paratype CES.404.1. (D) Female, CES.372. Scale bars A–C 0.5 mm, a, b and D 0.1 mm. Abbreviation: gl= gland.

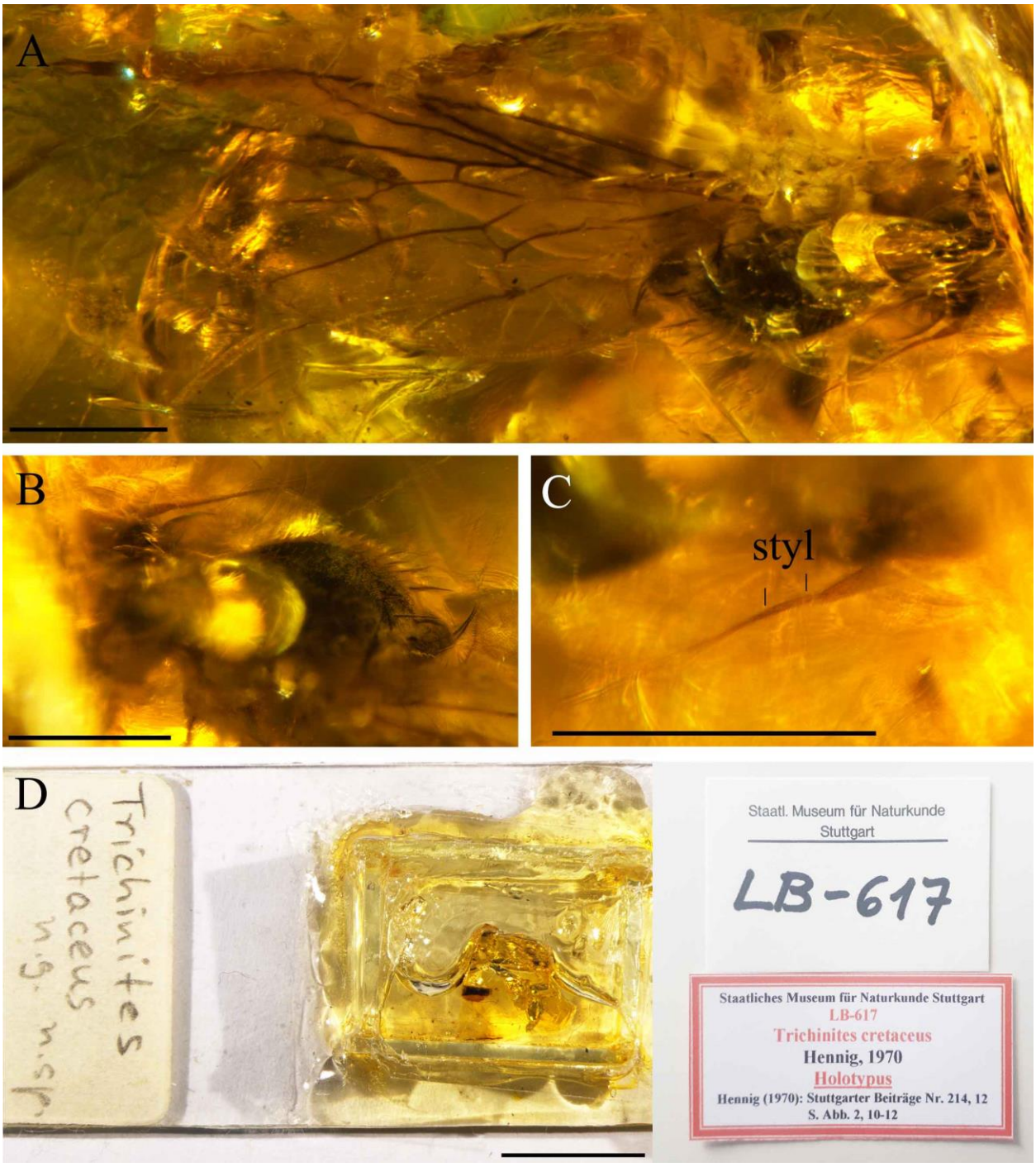

Figure 6. *Trichinites cretaceus* Hennig, 1970, holotype Number LB-617, from Jezzine outcrop, Lebanon (Barremian in age). (A) Scutum and wing, dorsal view. (B) Thorax, oblique lateral view. (C) Antenna with one basal article. (D) Holotype with labels. Scale bars A, B, C 0.5 mm, D 10 mm. Abbreviation: styl= stylus.

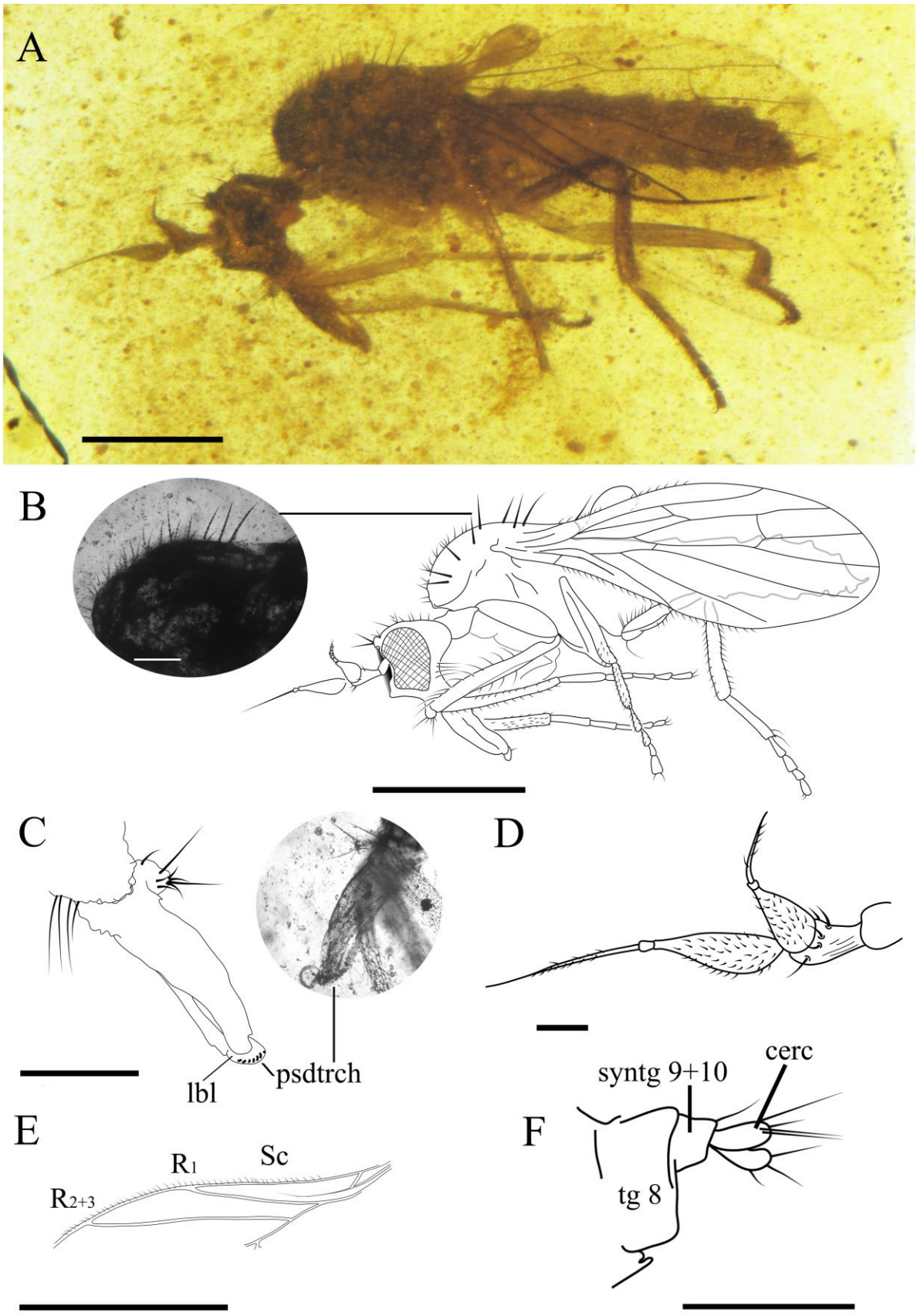

820

Figure 7. Female *AAA* sp. 1. (Diptera: Hybotidae), female CES.372, from El Soplao outcrop, Cantabria, Spain (middle Albian in age). (A) Habitus. (B) drawing of habitus with photo showing thoracic setae with apparent seriated rings (scale bar 0.1 mm). (C) Mouthparts. (D) Antennae. (E) Anterior part of wing. (F) Terminalia. Scale bars A, B, and E 0.5 mm; C, D and F 0.1 mm. Abbreviations: cerc= cercus, lbl= labrum psdtrch= pseudotrachea, R= radial vein, Sc= subcostal, syntg= tergite.

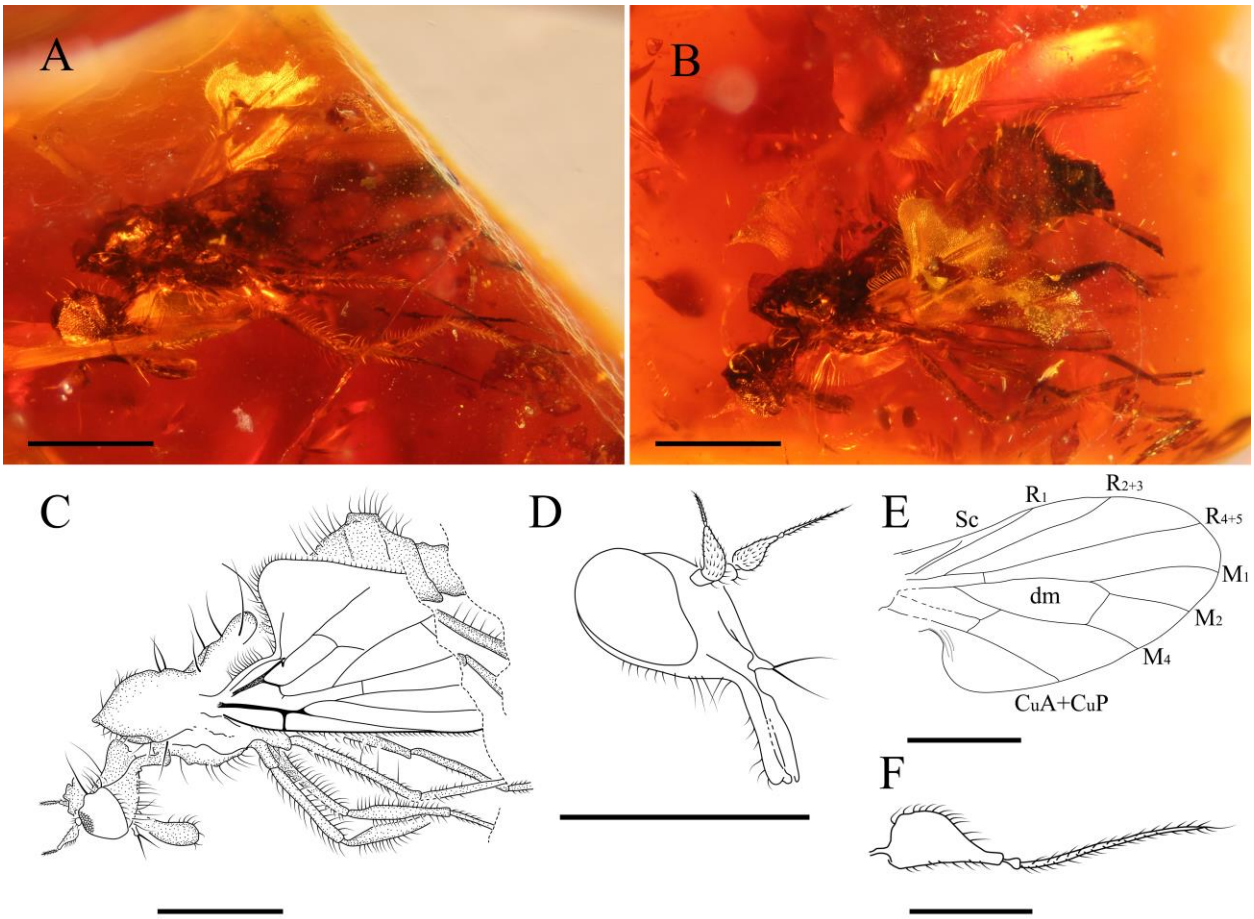

Figure 8. *AAA* sp. 2. (Diptera: Hybotidae), MGUV-16348 (sex unknown), from La Hoya outcrop, Castellón, Spain (early Cenomanian in age). (A) Habitus, lateral view right. (B) Habitus, lateral view left. (C) Drawing of habitus, lateral view. (D) Head, laterofrontal view. (E) Wing reconstruction. (F) Antenna. Scale bars A–E 0.5 mm; F 0.1 mm. Abbreviations: CuA+CuP= anterior branch of cubital vein + posterior branch of cubital vein, dm= discal medial cell, M= medial vein, R= radial vein, Sc= subcostal.

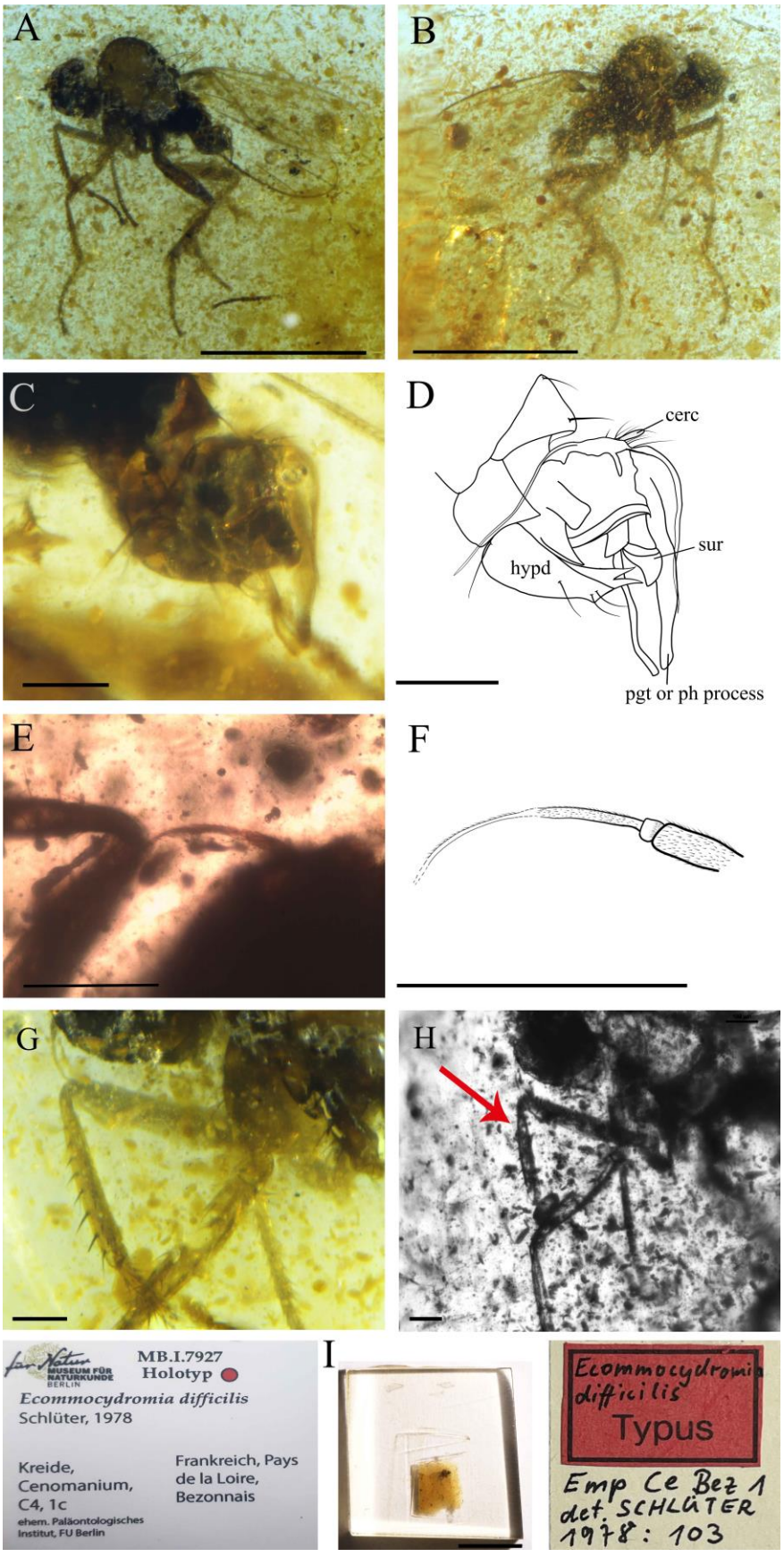
A
B
C
D
cerc
sur
hypd
pgt or ph process
E
F
G
H
MB.I.7927
Holotyp
Ecommocydromia difficilis
Schlüter, 1978
Kreide,
Cenomanium,
C4, 1c
Frankreich, Pays
de la Loire,
Bezonnais
ehem. Paläontologisches
Institut, FU Berlin
I
Ecommocydromia
difficilis
Typus
Emp Ce Bez 1
det. SCHLÜTER
1978: 103

836

Figure 9. *Ecommocydromia difficilis* Schlüter, 1978, from Écommoy, France (Cenomanian in age). (A) Habitus in left lateral view. (B) Habitus in right lateral view. (C) Terminalia in left lateral view. (D) Drawing of terminalia in left lateral view. (E) Antenna. (F) Drawing of antenna. (G) Foreleg. (H) Forelegs photographed with infrared camera, red arrow indicates possible posteroventral gland, however it could also be an artifact. (I) Holotype with labels. Scale bars A–B 0.5 mm, C–H 0.1 mm, I 5 mm. Abbreviations: cerc= cercus, hypd= hypandrium, pgt= postgonite, ph process = phallic process, sur= surstylus.

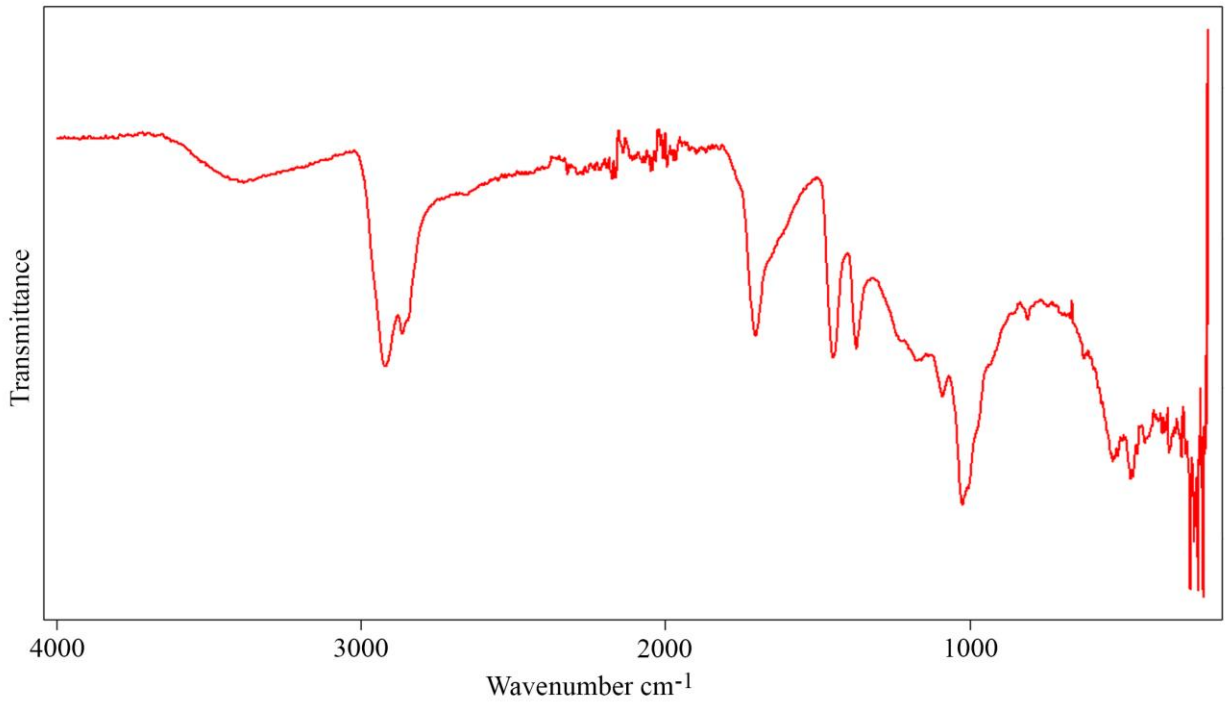

Figure 10. Infrared spectroscopy spectrum (FTIR) from an aerial amber piece of La Hoya outcrop (Castellón Province, Spain). Resolution = 4 cm^{-1}.

Anexo 8.1.11

Symbiosis between Cretaceous dinosaurs and feather-feeding beetles

Peñalver, E., Peris, D., **Álvarez-Parra, S.**, Grimaldi, D.A., Arillo, A., Chiappe, L., Delclòs, X., Alcalá, L., Sanz, J.L., Solórzano-Kraemer, M.M., Pérez-de la Fuente, R. en revisión*. Symbiosis between Cretaceous dinosaurs and feather-feeding beetles. *Proceedings of the National Academy of Sciences*.

Revista científica: *Proceedings of the National Academy of Sciences*
Factor de impacto: 12,779 (2021)
Categoría: *Multidisciplinary Sciences*, Q1 (2021)

* Se ha realizado el envío inicial a la revista y se encuentra en revisión. Debido a la extensión en el número de páginas, no se ha incluido el material suplementario.

PNAS
Manuscript for

Symbiosis between Cretaceous dinosaurs and feather-feeding beetles

Enrique Peñalver[a], David Peris[b,c], Sergio Álvarez-Parra[b,c], David A. Grimaldi[d], Antonio Arillo[e], Luis Chiappe[f], Xavier Delclòs[b,c], Luis Alcalá[g], José Luis Sanz[h,i], Mónica M. Solórzano-Kraemer[j] and Ricardo Pérez-de la Fuente[k]

[a]Instituto Geológico y Minero de España (IGME), CSIC; C/ Cirilo Amorós 42, 46004 Valencia, Spain.
[b]Departament de Dinàmica de la Terra i de l'Oceà, Facultat de Ciències de la Terra, Universitat de Barcelona, 08028 Barcelona, Spain.
[c]Institut de Recerca de la Biodiversitat (IRBio), Universitat de Barcelona, 08028 Barcelona, Spain.
[d]Division of Invertebrate Zoology, American Museum of Natural History; Central Park West at 79th St., New York, NY 10024-5192, USA.
[e]Departamento de Biodiversidad, Ecología y Evolución, Facultad de Biología, Universidad Complutense; Madrid, Spain.
[f]Dinosaur Institute, Natural History Museum of Los Angeles County; Los Angeles 90007, USA.
[g]Parque de las Ciencias de Andalucía, Av. de la Ciencia s/n, 18006 Granada, Spain.
[h]Unidad de Paleontología, Facultad de Ciencias, Universidad Autónoma de Madrid, Madrid, Spain.
[i]Real Academia Española de Ciencias Exactas, Físicas y Naturales; C/ Valverde 24, 28004, Madrid, Spain.
[j]Department of Palaeontology and Historical Geology, Senckenberg Research Institute; 60325 Frankfurt am Main, Germany.
[k]Oxford University Museum of Natural History; Parks Road, Oxford, OX1 3PW, UK.

Corresponding authors: Enrique Peñalver and Ricardo Pérez-de la Fuente

Emails: e.penalver@igme.es, ricardo.perez-de-lafuente@oum.ox.ac.uk
Author Contributions: E.P., and R.P.-d.l.F. designed research; E.P., D.P., S.Á.-P., A.A., D.A.G., L.Ch., X.D., L.A., J.L.S., M.M.S.-K. and R.P.-d.l.F. performed research and analyzed data; and E.P., D.P., A.A., D.A.G., L.Ch., and R.P.-d.l.F. wrote the paper.

Competing Interest Statement: Authors declare that they have no competing interests.

Classification: Biological Sciences/Evolution

Keywords: arthropod-dinosaur interaction / symbiosis / amber / Cretaceous / paleoecology

This PDF file includes:

Main Text
Figures 1 to 4

Abstract

Extant terrestrial vertebrates, including birds, show a panoply of symbiotic relationships −such as predatory or parasitic− with arthropods, namely insects and arachnids. Yet, identifying arthropod-vertebrate symbiotic relationships in the fossil record remains elusive, since such relationships are largely based on indirect evidence, and findings of direct association between arthropod (guest) and dinosaur (host) remains are exceedingly scarce. Here we present direct and indirect evidence demonstrating that beetle larvae fed on feathers from an undetermined theropod host 105 million years ago. The discovery involves an exceptional amber assemblage of larval molts (exuviae) intimately associated with plumulaceous feather portions and other remains, as well as three additional amber pieces preserving isolated conspecific exuviae. Samples were found in the roughly coeval Spanish amber deposits of El Soplao, San Just and Peñacerrada I. Integration of the morphological, systematic and taphonomic data shows that the beetle larval exuviae, belonging to three different developmental stages, can be most parsimoniously attributed to skin beetles (Dermestidae), a group with ecologically important extant keratophagous representatives and which commonly inhabit bird nests. Our findings shed light into early arthropod-dinosaur interactions, and show that a symbiotic relationship associated with keratophagy between beetles and birds, pervasive in modern ecosystems, was already present between their Early Cretaceous relatives.

Significance Statement

Vertebrates and arthropods are two of the most successful and frequently fossilized animal groups, but direct evidence of their interaction in deep time – entailing the joint, intimate fossilization of remains from both groups− is extremely rare. Our discoveries in fossilized plant resin (Cretaceous amber) from Spain

show that a symbiotic relationship, likely commensalistic/mutualistic, was established between beetle larvae feeding on detached feathers and feathered dinosaurs (theropods) more than a hundred million years ago. Only two previous records of arthropod-theropod symbiosis involving direct fossil evidence were known, both of the parasitic type. Our findings demonstrate that beetles and feathered theropods have interacted since the Mesozoic, and shed light on the evolutionary importance of early symbiotic relationships between arthropods and vertebrates.

Main Text

Introduction

Feathers, just like hair, are keratin-rich integumentary structures that today constitute a food source for highly-specialized arthropods able to digest tissues unavailable to most other animals due to their poor nutrient and/or water content, as well as complex metabolization (1, 2). Aside from its ecological importance, feeding on keratin-rich materials (keratophagy) has been significant from an evolutionary standpoint as well since in some instances has represented a transitional stage between free-living and parasitic forms, such as in the lice lineage (1). Keratophagy as a trophic specialization entails a parasitic symbiosis if the feeding arthropod guest causes damage in the plumage of the vertebrate host (3). On the other hand, keratophagy can also involve a commensalistic-mutualistic symbiosis between the host and the arthropod consuming the host's detached and/or accumulated integumentary structures, typically in a nest and at times possibly resulting advantageous to the host by cleaning its nest (4). In any case, symbiotic interactions are highly plastic, often not fitting into one of the traditional categories (3). Behaviors involving keratophagy do not necessarily represent trophic specializations, such as reptiles eating own shed skins or from conspecifics (5).

The plumage of diverse theropods has been well characterized in finely preserved Mesozoic compression fossils (6, 7). In Cretaceous amber, theropods are much less diverse but the feathers are preserved in unmatched detail (8−13). On the contrary, the only definitive keratophagous arthropod hitherto identified in the fossil record is a chewing louse (Amblycera) of the family Menoponidae, preserved as a compression fossil from the Eocene of the German outcrop of Messel; the remains of feather barbules preserved in its gut are direct evidence of keratophagy (14). Moreover, only a few Mesozoic (15, 16) and Cenozoic (17–20) amber records are known to contain arthropods associated with remains of the vertebrate host (feathers and hair) indicating symbiotic relationships. These

Mesozoic amber records represent direct evidence of an arthropod-dinosaur symbiotic relationship, all entailing instances of ectoparasitism (15, 16). A few Mesozoic records of arthropods associated with remains of the vertebrate host also exist in compression strata (21, 22), yet due to preservational and taphonomic limitations in that lithology the interpretation of these assemblages is ambiguous.

A recent, controversial report involves minute, wingless insects preserved adjacent to feathers in Burmese amber, reported as keratophagous ectoparasites, and placed in a new family, Mesophthiridae (23). Reassessment of the morphology, however, indicated that these are actually early instars (crawlers) of scale insects (Coccoidea), a group that today is wholly phytophagous, siphoning plant vascular fluids using long, very fine stylets (24). These stylets are coiled internally when at rest, forming a very distinctive structure called the crumena, which is apparent in the images from the original report along with other features diagnostic of coccoids. It was proposed that these insects may have been merely phoretic, but they definitely were not feeding on the feathers (24, 25), despite some portions presenting feeding damage (produced by other arthropods). In a rebuttal by the original authors, new images still did not resolve the putative chewing mandibles (26). The morphological evidence is unequivocal that "Mesophthiridae" are coccoids and thus could not have been keratophagous.

Here we present assorted evidence of keratophagy involving beetle and feather remains preserved in Cretaceous amber from Spain, representing a rare instance of arthropod-dinosaur symbiotic relationship in deep time.

Results

Amber samples studied. The amber piece SJNB2012-31 (Figs. 1 and 2; *SI Appendix*, Figs. S1–S3), from the San Just outcrop (upper Albian, NE Spain), was separated into two preparations, the principal one (SJNB2012-31-01) containing five amber fragments (largest about 8×6 mm). Altogether, the amber fragments contain abundant feather remains, exuvial (molt) remains of beetle larvae, fecal material and debris. Some amber fragments show desiccation surfaces typical of above-ground (aerial) resin (Fig. 1; *SI Appendix*, Figs. S1 and S3). The feather remains include abundant barbs of plumulaceous feather portions, an incomplete calamus (1.15 mm long as preserved, 0.40 mm greatest width), and two segments of rachises (0.4 mm wide) showing a rachidial ridge (Fig. 2). Plumulaceous barbs (up to 5.6 mm long as preserved) show brown pigmentation in barbule nodes. Exuvial remains in preparation SJNB2012-31-01 include a rather complete exuvium (Fig. 1 *B*–*E*) and other more fragmentary

remains; all of these are associated with a cloud of barbules (*SI Appendix*, Figs. S1 and S3; Movie S1) and were shed by at least two conspecific larval individuals of minute size (0.61 mm long as preserved, larvae ~1.5 mm as estimated) and early developmental stage. The six distinct exuvial remains preserved in different amber fragments (F#) of the preparation containing the feather-beetle assemblage (SJNB2012-31-01; *SI Appendix*, Fig. S1) are: [1] a rather intact exuvium lacking urogomphi due to disarticulation, in F2 (Fig. 1 *B* and *C*; *SI Appendix*, Fig. S2); [2] a fragment of a degraded abdominal projection, in F2; [3] a prementum portion, in F3 (*SI Appendix*, Fig. S2*D*); [4] a highly decayed fragment of an abdominal projection, in F3 (*SI Appendix*, Fig. S3*B*); [5] a thoracic leg fragment with tarsungulus, in F4 (*SI Appendix*, Fig. S3*A*); and [6] paired urogomphi, in F3 (Fig. 1*A*; *SI Appendix*, Fig. S3*C*). In addition, minute cuticle remains that may belong to degraded exuviae of this type are also present. The fecal material corresponds to several barrel-shaped structures (ca. 0.36×0.14 mm), most of them with fungal mycelia (~1 µm thick) growing on them.

Three isolated, two of them virtually complete, conspecific exuviae preserved in different amber pieces allow a more complete description of the beetle larval morphotype. The first isolated exuvium (SJNB2012-11: 0.83 mm body length) is an early developmental stage as the exuviae in SJNB2012-31, and belongs to the same amber-bearing stratum in San Just (Fig. 3 *A*–*D*; *SI Appendix*, Movie S1). The amber piece with the inclusion is a clear amber fragment lacking any other biological inclusions or desiccation surfaces. The second isolated larval exuvium, in piece ES-07-39, was found in the slightly older El Soplao outcrop (middle Albian, N Spain) (Fig. 3 *E* and *F*; *SI Appendix*, Figs. S4 and S5). The exuvium is very intact (only one antenna is lost, clypeus and labrum are largely undetected) and well preserved, and shows the three pairs of thoracic legs and the complete posterior body portion in excellent detail and in anatomic position. Although about two times larger and with a mandibular prostheca apparently double rather than simple (Fig. S4), this exuvium shows virtually the same morphological characters than those from the exuvial remains from San Just, and so it most likely represents a conspecific, later instar. The amber piece lacks any other biological inclusions or desiccation surfaces. The third exuvial specimen, in piece MCNA 12063, is partial and consists of a posterior body portion exceptionally preserved, and was found in the Peñacerrada I outcrop (upper Albian, N. Spain) (*SI Appendix*, Fig. S6). As the preserved body portion is significantly larger than the corresponding part from the El Soplao specimen and the visible features are consistent with those shown by the other exuviae, it could represent an even later instar of the same larval morphotype.

Although the exuviae from San Just represent the earliest developmental stage of the larval morphotype described herein, they are the most palaeoecologically significant remains due to their association with feather portions. For that reason, the descriptive account provided below focusses on these exuviae, with comparative notes on the increasingly more advanced larval instars found in El Soplao and Peñacerrada I localities, respectively.

***Description of the larval exuviae*.** Exuviae produced by early instar larvae (SJNB2012-11; SJNB2012-31). Setation abundant, dense (particularly on the thorax and abdomen), relatively long (ca. 10–20 µm); simple, without fine feathering, scales or plumosity. Cephalic capsule hypognathous, without visible stemmata, with setation distinctly shorter. Cephalic setational arrangement not discernible due to cuticular crumpling. Frontal arms of epicranial suture lyriform, likely contiguous at base (Fig. 3 *A* and C; *SI Appendix*, Fig. S2*A*). Antenna (*SI Appendix*, Fig. S2 *E* and *F*) relatively short, laterally arranged (this feature likely impacted by preservation), ~10 µm length, well sclerotized, three-segmented. Scape (first antennal segment) ring-like, diameter ca. 1.5 times that of pedicel, length half that of pedicel. Pedicel (second antennal segment) subcylindrical, slightly tapering distad, about 1.7 times longer than wide at base, bearing abundant fine setae and two thicker setae emerging from the subapical margin of the pedicel, about as long as half the length of the pedicel; sensorium emerging apically from pedicel, small, conical, almost or quite as long as flagellum; one strong seta also emerging from the apex of the pedicel. Flagellum (third antennal segment) spine-like, lacking a terminal seta. Clypeus with fine setae, slightly broader but shorter than labrum; frontoclypeal suture evident. Labrum free, approximately trapezoidal in shape, without subdivisions, wider than long, with short setae; setae on margin near mouth thicker. Mandibles (Figs. 1*E* and 3; *SI Appendix*, Fig. S2*C*) bidentate (a minute protrusion present at the external margin cannot be considered a third mandibular tooth seen smaller due to perspective), symmetrical; teeth subequal (inner tooth in left mandible slightly larger in appearance probably due to perspective), innermost tooth basally expanded at incisor edge; prostheca present, as a single unsclerotized process, lacking visible setae; molar area present, visible surface crenulated, oblique (at least distally), vertical portion (if present) not visible (in left mandible); base of mandibles with some fine, short setae. Maxilla (*SI Appendix*, Fig. S2*B*) with stipes well developed, longer than wide, slightly sclerotized, separation with cardo unapparent; maxillary palp three-segmented, with distinct palpifer, segment lengths 3>2>1; diameter of basal palpomere about twice that of apical one; apical palpomere with minute, clavate setula laterally; galea and lacinia separated; inner margin of lacinia spinose. Galea spiculate. Labium with

prementum (*SI Appendix*, Fig. S2 *A* and *D*) well developed, roughly quadrate, ligula absent; labial palp two-segmented, well separated from each other. Presence/absence of gula not visible. Tarsunguli well developed and sclerotized, simple, claw-like, with distal half tapering, setae absent (*SI Appendix*, Fig. S3*A*). Other thoracic leg parts present, disarticulated proximally and/or distally (truncated in shape). One pair of urogomphi evident, simple, unsegmented, relatively short, triangular, laterally flattened; slightly tapering distally, with minute spine at apex (Fig. 1*E*; *SI Appendix*, Fig. S2*H*); urogomphi in dorsal position and posteroventrally curved (Fig. 3*D*), slightly inclined towards each other (not upturned), covered with dense, fine setae. Additional abdominal structures (herein referred as 'abdominal projections') preserved as remains of their apices, but their exact configuration unclear.

The exuvium from El Soplao (ES-07-39), produced by a more advanced instar larva, has a configuration of the distal portion of the abdomen more completely preserved than in the earlier instar exuviae from San Just. The specimen presents three visible paired abdominal structures, the distalmost interpreted as a pair of urogomphi, medially placed on a plate in segment IX, and two pairs of projections in more lateral position, on segments VII and VIII. Although the urogomphi are in an apparent ventral position, they were likely displaced during molting, sharing the features of the above described urogomphi from the San Just exuviae. The distalmost pair of lateral abdominal projections are longer and conical in shape, bearing a few fine setae and with a rounded apex; the more proximal pair of projections are shorter and apparently more flattened in shape, bearing a few thick setae and having a notched apex. The abdominal projections preserved in a fragmentary way from the San Just specimens are compatible with the abdominal configuration of ES-07-39, although it is unknown if they matched. Yet, it is probable that the abdominal projections were less developed in earlier developmental stages.

Lastly, the partial exuvial specimen from Peñacerrada I (MCNA 12063), produced by a late instar, shows in the distalmost pair of lateral abdominal projections an inner, central tube with the surface finely striated (*SI Appendix*, Fig. S6). This structure is deemed as part of the tracheal system ending in a (putatively spiracular) opening at the apex of the projection. Moreover, the specimen shows additional lateral projections on more proximal abdominal segments.

Discussion

Affinities of the larvae. The morphology of the described larval exuviae, including those associated with feather remains, firmly place them as beetle

(Coleoptera) larvae. The more intact exuviae show powerful chewing mandibles with highly sclerotized teeth, and with a pair of dorsal abdominal processes identified as urogomphi that are slightly-recurved, cone-shaped. This type of urogomphus is typical of active, campodeiform beetle larvae inhabiting narrow spaces as it assists in locomotion (27). The character combination of the fossils is most consistent with that in extant representatives of the families Dermestidae and Derodontidae, namely in characters of the head, such as the orientation of the cephalic capsule, and the morphology of structures such as antennae, mouthparts and epicranial suture (*SI Appendix*, Table S1). The hypognathous head in the three more intact exuviae (both early and more advanced instars) is present in dermestid larvae and distinguishes them from other potential beetle groups to which they could be related based on morphology. Some mandibular characters present in the new fossils occur in larvae of scattered extant genera and other groupings of Dermestidae: the mandible is apically bidentate in *Orphilus*, Thorictinae, and most Trinodinae; the prostheca is diverse, sometimes a blunt process, but not sclerotized; and although a mola is usually absent, it is present in *Orphilus* (28). In contrast, although the frontal arms of the epicranial suture in extant dermestid larvae are V- or U-shaped (29), they are lyriform in the new fossils. The abdominal projections from the fossil exuviae, lateral in position as shown by the more advanced instar larvae, are absent from the known extant diversity of Dermestidae (28−31). Note that, although specialized setae such as spicisetae or hastisetae are absent in *Orphilus*, some dermestid species possess short, undulating (‘bent’) setae (30, 31); the absence of these can be confirmed in the fossils.

Derodontids have been considered either sister to dermestids (28) or relatively close phylogenetically yet classified in a different infraorder (27). However, recent phylogenomic studies consistently recover Derodontidae as phylogenetically distant from Dermestidae, sister to Clambidae and Eucinetidae (32–34). Although the frontal arms of the epicranial suture are lyriform in extant derodontid larvae, as in the fossil exuviae, their head is prognathous and their mandibles possess a falciform prostheca, both characters absent in the fossils.

The affiliation of these fossilized larval remains based on their morphology to yet other coleopteran lineages, such as Jacobsoniidae –currently classified in Staphyliniformia sensu Cai *et al*. (34)– or several cucujiformian families remains a possibility, although a less likely one based on the number of shared characters (*SI Appendix*, Table S1).

Taphonomy. Within the amber assemblage preserved in preparation SJNB2012-31-01, the exuvial remains are fully enveloped by the plumulaceous feather portions (Fig. 1; *SI Appendix*, Fig. S3). Based on such an intimate association, as

well as the rarity of feathers and these exuviae in amber, it is highly improbable that both remain types became independently trapped in resin and, thus, accidentally associated. Moreover, several elements in the amber fragments of the preparation show substantial degradation. The two more intact exuviae lack some body parts, and several fragmentary exuvial portions are present. Some fungal hyphae are present in feather barbules, the latter also showing degradation in some areas (Fig. 2; *SI Appendix*, Fig. S3). Lastly, the four coprolites were probably produced by the beetle larvae prior to molting and fungal hyphae subsequently grew on them (*SI Appendix*, Fig. S3). Therefore, the exuvial and feather remains were most likely associated for a period of time prior to becoming jointly immersed in resin.

Evidence of pervasive feeding damage (chewing) is absent in the feather portions surrounding the exuvial remains, but localized barbule damage is present in a few areas (*SI Appendix*, Fig. 2 *G* and *H*), although this degradation might be at least partly preservational. The tridimensional structure of the plumulaceous feather portions (not bidimensional as pennaceous feathers) and their twisted configuration might also prevent the identification of more evident feeding damage, as for instance present in the feather figured by Gao *et al*. (23) in their fig. 1a,k.

Keratophagy. The most compelling interpretation of the fossil exuviae, based on the preserved morphological, systematic and taphonomic data, is that they are remains of keratinophagous, dermestid (in the wide sense) beetle larvae that retained a few plesiomorphic characters, such as lyriform frontal arms of the epicranial suture, while also possessing apparently derived lateral abdominal processes. The minute to small size of the fossil exuviae is in line with keratin feeding, as this protein has a poor nutritional value.

Dermestid beetles are not particularly diverse at present, with only about 600 species (35), although they are nearly ubiquitous. The Mesozoic amber record of both adults and larvae is well represented in deposits worldwide. This includes some adults from Cretaceous ambers, both described (36) and undescribed (37, 38), as well as larvae, the latter as body records (1, 39) (Fig. 4*E*–*G*) or hastisetae (15, 40, 41). Extant dermestids, especially larvae, are xerophilic scavengers of animal materials, particularly dried matter including keratin-based tissues (29). These beetles are one of the most important pests of stored products and dried museum collections, and are also commonly found in extant vertebrate nests, the latter representing the ancestral habitats of many keratophagous insects (29, 42–44). Since extant dermestid beetles are typical inhabitants of bird nests (42, 43), and the assemblage reported herein implied a location close to a resin source, the most plausible microenvironment where

these remains were embedded together in resin is a nest. Extant bird and mammal nests are specialized microenvironments and rich sources of organic material inhabited by a diverse community of insects and arachnids (42, 43, 45). Many of these nest-inhabiting arthropods are generalist or specialist feeders on the organic remains, including shed keratin in the form of feathers, hair and skin, as well as feces. Extinct deinocrotonid ticks preserved in Burmese amber were considered nidicolous −living in their host's nest or in their own nest close to that of the host− after the presence of dermestid hastisetae attached to their bodies and other taphonomic features, which linked these hematophagous ectoparasites to a nest microenvironment (15).

Keratophagous arthropods are obligate symbionts that depend on their hosts for provisioning a reliable food source and shelter. Due to generalized morphology of the reported Early Cretaceous plumulaceous feather remains, it is not possible to determine the group of Cretaceous feathered theropod to which they belonged. However, modern birds (Neornithes) can be ruled out since they appeared much later in the fossil record (6). Also, the exact type of symbiotic relationship between the keratophagous beetle larvae and its feathered theropod host is challenging to address, even for extant fauna, given the mutualism-commensalism-parasitism spectrum (3, 46). A harmful impact (i.e., skewing towards parasitism) of the fossil dermestids to the feathered host was unlikely due to their lack of hastisetae or spicisetae. These specialized setae, present in some dermestid taxa, easily detach and can accumulate in great density in nests forming mats that entangle ants and other predators (47), but which can also irritate the nest hosts, in severe cases leading to death (48).

In sum, the most conservative stance is to consider this early arthropod-dinosaur interaction as commensalistic or mutualistic. Both the Eocene chewing louse from Messel preserved with feather fragments in its gut (14) and the assemblage described herein represent insect-theropod interactions but have significant differences (Fig. 4). The most remarkable of them is that the Eocene record involved modern birds and entailed a parasitic symbiotic relationship provided that chewing lice cause damage to the feathers while these are attached to the host, not as scavengers, thus impacting on the bird's fitness. On the contrary, our record involved detached feathers from a Cretaceous feathered theropod, thus most likely representing a commensalistic or mutualistic symbiotic relationship (Fig. 4).

Concluding remarks

The present research provides both direct and indirect evidence of early insect keratophagy and an arthropod-dinosaur symbiotic relationship of the commensalistic or mutualistic type during the late Mesozoic. The most plausible

scenario based on our taphonomic data is that the beetle larvae that produced the exuviae herein described fed on accumulated feathers in close proximity to a resiniferous tree, probably in a nest setting. Previous records of arthropod-theropod relationships based on direct evidence have been of the parasitic type, either of chewing lice (keratophagy) during the Eocene or of ixodid and deinocrotonid ticks (hematophagy) during the Cretaceous. The characteristics of amber fossilization, both its exceptional preservation of morphological structures and the ability that the resin had to capture remains almost instantly, enable detailed taphonomic and systematic studies aimed at reliably establishing symbiotic interactions in deep time.

Materials and Methods

Amber pieces. The four amber pieces come from three Spanish outcrops. Two of them were excavated from a level rich in amber and charcoal within the San Just outcrop (49, 50), upper Albian in age, during a paleontological excavation carried out in 2012 (Gobierno de Aragón permit: 119/10-11-2012). This outcrop is close to the village of Utrillas, Teruel Province (Autonomous Community of Aragón). Preparation SJNB2012-31-01 (Figs. 1 and 2; *SI Appendix*, Figs. S1, S2 in part, and S3) contains five small amber fragments (F1–F5, ranging from 2 to 7 mm in length) originally belonging to the same amber piece which fragmented during preparation, and which were embedded and polished in the same prism of synthetic resin (EPO-TEK 301; 24×16×4 mm in size) (51). An additional isolated fragment belonging to the same amber piece (F6; accession number SJNB2012-31-02) was prepared apart and only contains a wasp. Exuvial remains have a slightly fragmented and shriveled appearance. In total, this piece contains an incomplete beetle larva exuvium and four isolated, conspecific exuvial small portions at least one of them belonging to a different individual. Piece SJNB2012-11 (Fig. 2*A*–*D*; *SI Appendix*, Fig. S2 in part) contains an isolated, conspecific, almost complete beetle exuvium consisting of an amber portion (8×6×1 mm) embedded and polished in the same type of synthetic resin prism (20×14×1 mm in size). Both pieces are housed in the collection of the Museo Aragonés de Paleontología (Fundación Conjunto Paleontológico de Teruel-Dinópolis, Teruel city). The third amber piece, ES-07-39 (Fig. 3 *E* and *F*; *SI Appendix*, Figs. S4 and S5), was excavated from a rich level within El Soplao outcrop (Rábago village, Santander, Cantabria) (52, 53), middle Albian in age, during a paleontological prospection carried out in 2007 with a permit of the Gobierno de Cantabria. It contains a virtually complete beetle exuvium consisting of an amber portion (5×3×1 mm) embedded and polished in the same type of synthetic resin prism (23×10×2 mm in size). The piece is housed at the Institutional Collection from the

El Soplao Cave, Cantabria, Spain. The fourth amber piece, MCNA 12063 (*SI Appendix*, Fig. S6), was excavated by researchers of the Museo de Ciencias Naturales de Álava, in Peñacerrada I outcrop (Álava, Basque Country) (54), upper Albian in age (55). It contains a beetle exuvial portion, a rhagionid fly, a tipuloid fly, an indeterminate wasp, a fragment of wing of termite, arthropod coprolites and diverse minute debris, present in an amber portion (15×10×3 mm) embedded and polished in the same type of synthetic resin prism (20×15×4 mm in size). The piece is housed at the Museo de Ciencias Naturales de Álava, a Spanish public scientific institution.

Imaging. The specimens were examined with both Olympus BX51 and BX53 compound microscopes and the drawings were made using an Olympus U-DA drawing tube (camera lucida) attached to both compound microscopes at the Instituto Geológico y Minero de España (IGME, CSIC, Madrid and Valencia). Larval exuviae from San Just amber were described based on observation at 400X using a Nikon Eclipse compound scope with Plan Apo Extended Depth Working Distance lens at the AMNH (New York). Photomicrographs were made using a digital camera attached to both Olympus compound microscopes at the IGME; a movie sequence using selected images is included in Movie S1.

Confocal microscopy was used to image the exuvium in contact with feathers using a Leica TCS SPE-DM 5500 CSQ V-Vis (Manheim, D-68165, Germany) at the Museo Nacional de Ciencias Naturales (CSIC, Madrid). Images were acquired with a solid-state laser operating at 488 nm, a 10× eyepiece, an ACS APO 10×/0.3 objective, and the Leica Application Suite Advanced Fluorescence software (Leica MM AF 1.4). Fluorescence emission was collected from approximately 10 nm above the excitation wavelength up to 800 nm. Laser power for acquisition was set by viewing the fluorescence emission and increasing the power until the rate of increase in fluorescence slowed down. The photomultiplier gain for acquisition was then set by viewing the image and increasing the gain until signal overload was detected, at which point the gain was reduced slightly. Pixel matrices of 2048 × 2048, speed 400 Hz, and frame average of 4 were acquired for each Z-step at a zoom setting of 1.5–2×. An Airy unit setting of 1 was routinely used for the observation pinhole. No attempts were made to optimize image quality by minimization of the confocal pinhole diameter; however, high levels of signal averaging, high pixel resolution, and very small Z axis steps were used. A movie sequence using selected confocal microscopy images is included in Movie S1.

Acknowledgments. We are grateful to R. López del Valle for preparing the specimens and the 2012 San Just amber outcrop excavation team. The *Gobierno de Aragón* and *Unidad de Carreteras del Estado* in Teruel, and the *Gobierno de Cantabria* granted excavation permits. This work was supported by the project CRE, funded by the Spanish AEI/FEDER, UE Grant CGL2017-84419, the project PGC2018-094034-B-C22 (MCIU/AEI/FEDER, UE), the project CGL2014-52163, funded by the Spanish Ministry of Economy, Industry, and Competitiveness, and by the *Consejería de Industria, Turismo, Innovación, Transporte y Comercio* of the *Gobierno de Cantabria* through the public enterprise EL SOPLAO S.L. (research contract REF 030611220077 to IGME-CSIC and research agreement #20963 with University of Barcelona, both for the period 2022–2025). S.Á.-P. is funded by a grant from the Secretary of Universities and Research of the Government of Catalonia and European Social Fund (2021FI_B2 00003).

References

1. D. A. Grimaldi, M. S. Engel, *Evolution of the Insects* (Cambridge University Press, Cambridge, 2005).
2. R. Gupta, P. Ramnani, Microbial keratinases and their prospective applications: An overview. *Appl. Microbiol. Biotechnol.* **70**, 21–33 (2006).
3. S. J. N. Cooney, “Ecological Associations of the Hooded Parrot *(Psephotus dissimilis)*”, thesis, The Australian National University (2009).
4. D. F. Thomson, Some adaptations for the disposal of faeces. The hygiene of Australian birds. *Proc. Zool. Soc. Lond.* **1934**, 701–707 (1934).
5. J. C. Mitchell, J. D. Groves, S. C. Walls, Keratophagy in reptiles: Review, hypotheses, and recommendations. *South Am. J. Herpetol.* **1**, 42–53 (2006).
6. L. M. Chiappe, M. Qingjin, *Birds of Stone: Chinese Avian Fossils from the Age of Dinosaurs* (Johns Hopkins University Press, Baltimore, 2016).
7. N. R. Longrich, H. Tischlinger, Ch. Foth, “The feathers of the Jurassic Urvogel Archaeopteryx” in *The Evolution of Feathers*, Ch. Foth, O. W. M. Rauhut, Eds. (Springer, 2020), pp. 119–146.
8. R. C. McKellar, B. D. E. Chatterton, A. P. Wolfe, P. J. Currie, A diverse assemblage of Late Cretaceous dinosaur and bird feathers from Canadian amber. *Science* **333**, 1619–1622 (2011).
9. L. Xing *et al*., Mummified precocial bird wings in mid-Cretaceous Burmese amber. *Nat. Commun.* **7**, 12089 (2016). doi.org/10.1038/ncomms12089
10. L. Xing *et al*., A new enantiornithine bird with unusual pedal proportions found in amber. *Curr. Biol.* **29**, 2396–2401 (2019).

11. L. Xing *et al*., A fully feathered enantiornithine foot and wing fragment preserved in mid-Cretaceous Burmese amber. *Sci. Rep.* **9**, 927 (2019). doi.org/10.1038/s41598-018-37427-4
12. L. Xing, P. Cockx, R. C. McKellar, Disassociated feathers in Burmese amber shed new light on mid-Cretaceous dinosaurs and avifauna. *Gondwana Res.* **82**, 241–253 (2020).
13. N. R. Carroll, L. M. Chiappe, D. J. Bottjer, Mid-Cretaceous amber inclusions reveal morphogenesis of extinct rachis-dominated feathers. *Sci. Rep.* **9**, 18108 (2019). doi.org/10.1038/s41598-019-54429-y
14. T. Wappler, V. S. Smith, R. C. Dalgleish, Scratching an ancient itch: An Eocene bird louse fossil. *Proc. R. Soc. Lond*. B **271**, S255–S258 (2004). doi.org/10.1098/rsbl.2003.0158
15. E. Peñalver *et al*., Ticks parasitised feathered dinosaurs as revealed by Cretaceous amber assemblages. *Nat. Commun.* **8**, 1924 (2017). doi.org/10.1038/s41467-017-01550-z
16. L. Chitimia-Dobler, B. J. Mans, S. Handschuh, J. A. Dunlop, A remarkable assemblage of ticks from mid-Cretaceous Burmese amber. *Parasitology* **149**, 820–830 (2022). doi.org/10.1017/S0031182022000269
17. E. Peñalver, D. Grimaldi, Assemblages of mammalian hair and blood-feeding midges (Insecta: Diptera: Psychodidae: Phlebotominae) in Miocene amber. *Trans. R. Soc. Edinburgh, Earth Sciences* **96**, 177–195 (2006).
18. B. Kosmowska-Ceranowicz *et al*., Bird traces in Dominican amber. *International Amber Researcher Symposium, Amberif*, 62–66 (2013).
19. T. C. Fischer, Caterpillars and cases of Tineidae (Clothes Moths, Lepidoptera) from Baltic amber (Eocene). *Zitteliana* A **54**, 75–81 (2014).
20. E. A. Sidorchuk, A. V. Bochkov, T. Weiterschan, O. F. Chernova, A case of mite-on-mammal ectoparasitism from Eocene Baltic amber (Acari: Prostigmata: Myobiidae and Mammalia: Erinaceomorpha). *J. Syst. Palaeontol.* **17**, 331–347 (2019).
21. D. M. Martill, P. G. Davis, Did dinosaurs come up to scratch? *Nature* **396**, 528–529 (1998).
22. M. Qvarnström *et al*., Exceptionally preserved beetles in a Triassic coprolite of putative dinosauriform origin. *Curr. Biol.* **31**, 3374-3381 (2021). doi.org/10.1016/j.cub.2021.05.015
23. T. Gao *et al*., New insects feeding on dinosaur feathers in mid-Cretaceous amber. *Nat. Commun.* **10**, 5424 (2019). doi.org/10.1038/s41467-019-13516-4
24. D. A. Grimaldi, I. M. Vea, Insects with 100 million-year-old dinosaur feathers are not ectoparasites. *Nat. Commun.* **12**, 1469 (2021). doi.org/10.1038/s41467-021-21751-x
25. D. E. Shcherbakov, Crawlers of the Scale Insect *Mesophthirus* (Homoptera:

Xylococcidae) on Feathers in Burmese Amber – Wind Transport or Phoresy on Dinosaurs? *Paleontol. J.* **56**, 338–348 (2022).
26. T. P. Gao *et al*., Reply to: “Insects with 100 Million-Year-Old Dinosaur Feathers are not Ectoparasites” and “Crawlers of the Scale Insect *Mesophthirus* (Homoptera Xylococcidae) on Feathers in Burmese Amber—Wind Transport or Phoresy on Dinosaurs?”. *Paleontol. J.* **56**, 333–337 (2022).
27. J. F. Lawrence *et al*., Phylogeny of the Coleoptera based on morphological characters of adults and larvae. *Ann. Zool*. **61**, 1–217 (2011).
28. T. Kiselyova, J. V. McHugh, A phylogenetic study of Dermestidae (Coleoptera) based on larval morphology. *Syst. Entomol.* **31**, 469–507 (2006).
29. R. A. B. Leschen, B. G. Beutel, J. F. Lawrence, *Handbook of Zoology. Arthropoda: Insecta. Coleoptera, beetles. Volume 2: Morphology and Systematics (Elateroidea, Bostrichiformia, Cucujiformia partim* (Walter de Gruyter, Berlin, 2010).
30. R. S. Jr. Beal, Review of Nearctic species of *Orphilus* (Coleoptera: Dermestidae) with description of the larva of *O. subnitidus* LeConte. *Coleopt. Bull*. **39**, 265–271 (1985).
31. R. D. Zhantiev, Palaearctic dermestid beetles of the genus *Orphilus* Er. (Coleoptera, Dermestidae). *Entomol. Rev.* **81**, 200–210 (2001).
32. S. Zhang *et al*., Evolutionary history of Coleoptera revealed by extensive sampling of genes and species. *Nat. Commun*. **9**, 205 (2018). doi.org/10.1038/s41467-017-02644-4
33. D. D. McKenna *et al*., The evolution and genomic basis of beetle diversity. *Proc. Natl. Acad. Sci. U.S.A.* **116**, 24729–24737 (2019). doi.org/10.1073/pnas.190965511
34. C. Cai *et al*., Integrated phylogenomics and fossil data illuminate the evolution of beetles. *R. Soc. Open Sci.* **9**, 211771 (2022). doi.org/10.1098/rsos.211771
35. J. Háva, *Dermestidae world (Coleoptera)*. http://www.dermestidae.wz.cz (Accessed 09/04/2020) (2018).
36. D. Peris, Coleoptera in amber from Cretaceous resiniferous forests. *Cretac. Res.* **113**, 104484 (2020). doi.org/10.1016/j.cretres.2020.104484
37. A. G. Kirejtshuk, D. Azar, P. Tafforeau, R. Boistel, V. Fernandez, New beetles of Polyphaga (Coleoptera, Polyphaga) from Lower Cretaceous Lebanese amber. *Denisia* **26**, 119–130 (2009).
38. D. Peris, E. Ruzzier, V. Perrichot, X. Delclòs, Evolutionary and paleobiological implications of Coleoptera (Insecta) from Tethyan-influenced Cretaceous ambers. *Geosci. Front.* **7**, 695–706 (2016).

39. D. Peris, J. Rust, Cretaceous beetles (Insecta: Coleoptera) in amber: the palaeoecology of this most diverse group of insects. *Zool. J. Linn. Soc.* zlz118 (2019). doi.org/10.1093/zoolinnean/zlz118
40. G. O. Jr. Poinar, R. Poinar, Ancient hastisetae of Cretaceous carrion beetles (Coleoptera: Dermestidae) in Myanmar amber. *Arthropod Struct. Dev.* 45, 642–645 (2016).
41. A. P. Rasnitsyn, G. Jr. Poinar, A. E. Brown, Bizzare wingless parasitic wasp from mid-Cretaceous Burmese amber (Hymenoptera, Ceraphronoidea, Aptenoperissidae fam. nov.). *Cretac. Res.* **69**, 113–118 (2017).
42. E. A. Hicks, *Check-list and Bibliography on the Occurrence of Insects in Bird Nests* (Iowa State College Press, Iowa, 1959).
43. J. R. Philips, D. L. Dindal, Invertebrate populations in the nests of a screech owl (*Otus asio*) and an American kestrel (*Falco sparverius*) in central New York. *Entomol. News* **101**, 170–192 (1990).
44. J. F. Lawrence, A. Ślipiński, “6.1. Dermestidae Latreille, 1804” in *Morphology and systematics (Elateroidea, Bostrichiformia, Cucujiformia partim)*, R. Leschen, B. G. Beutel, J. F. Lawrence, Eds. (Walter de Gruyter, Berlin, 2010), vol. 2.
45. J. K. Waage, The evolution of insect/vertebrate associations. *Biol. J. Linn. Soc.* **12**, 187–224 (1979).
46. T. L. F. Leung, R. Poulin, Parasitism, commensalism, and mutualism: exploring the many shades of symbioses. *Vie Milieu* **58**, 107–115 (2008).
47. W. L. Nutting, H. G. Spangler, The hastate setae of certain dermestid larvae: an entangling defense mechanism. *Ann. Entomol. Soc. Am*. **62**, 763–769 (1969).
48. N. F. R. Snyder, J. C. Ogden, J. David Bittner, G. Grau, A. Larval dermestid beetles feeding on nestling snail kites, wood storks, and great blue herons. *Condor* **86**, 170–l74 (1984).
49. E. Peñalver, X. Delclòs, C. Soriano, A new rich amber outcrop with palaeobiological inclusions in the Lower Cretaceous of Spain. *Cretac. Res.* **28**, 791–802 (2007).
50. D. Penney, *Biodiversity of Fossils in Amber from the Major World Deposits* (Siri Scientific Press, Manchester, 2010).
51. D. Grimaldi, *Studies on Fossils in Amber, with Particular Reference to the Cretaceous of New Jersey* (Backhuys Publishers Leiden, Leiden, 2000).
52. M. Najarro *et al*., Unusual concentration of Early Albian arthropod-bearing amber in the Basque-Cantabrian Basin (El Soplao, Cantabria, Northern Spain): Palaeoenvironmental and palaeobiological implications. *Geol. Acta* **7**, 363–387 (2009).
53. M. Najarro *et al*., Review of the El Soplao amber outcrop, Early Cretaceous of Cantabria, Spain. *Acta Geol. Sin.* (English Edition) **84**, 959–976 (2010).

54. J. Alonso *et al*., A new fossil resin with biological inclusions in Lower Cretaceous deposits from Álava (Northern Spain, Basque-Cantabrian Basin). *J. Paleontol.* **74**, 158–178 (2000).
55. E. Barrón *et al*., Palynology of Aptian and upper Albian (Lower Cretaceous) amber-bearing outcrops of the southern margin of the Basque-Cantabrian basin (northern Spain). *Cretac. Res.* **52**, 292–312 (2015).

Figures

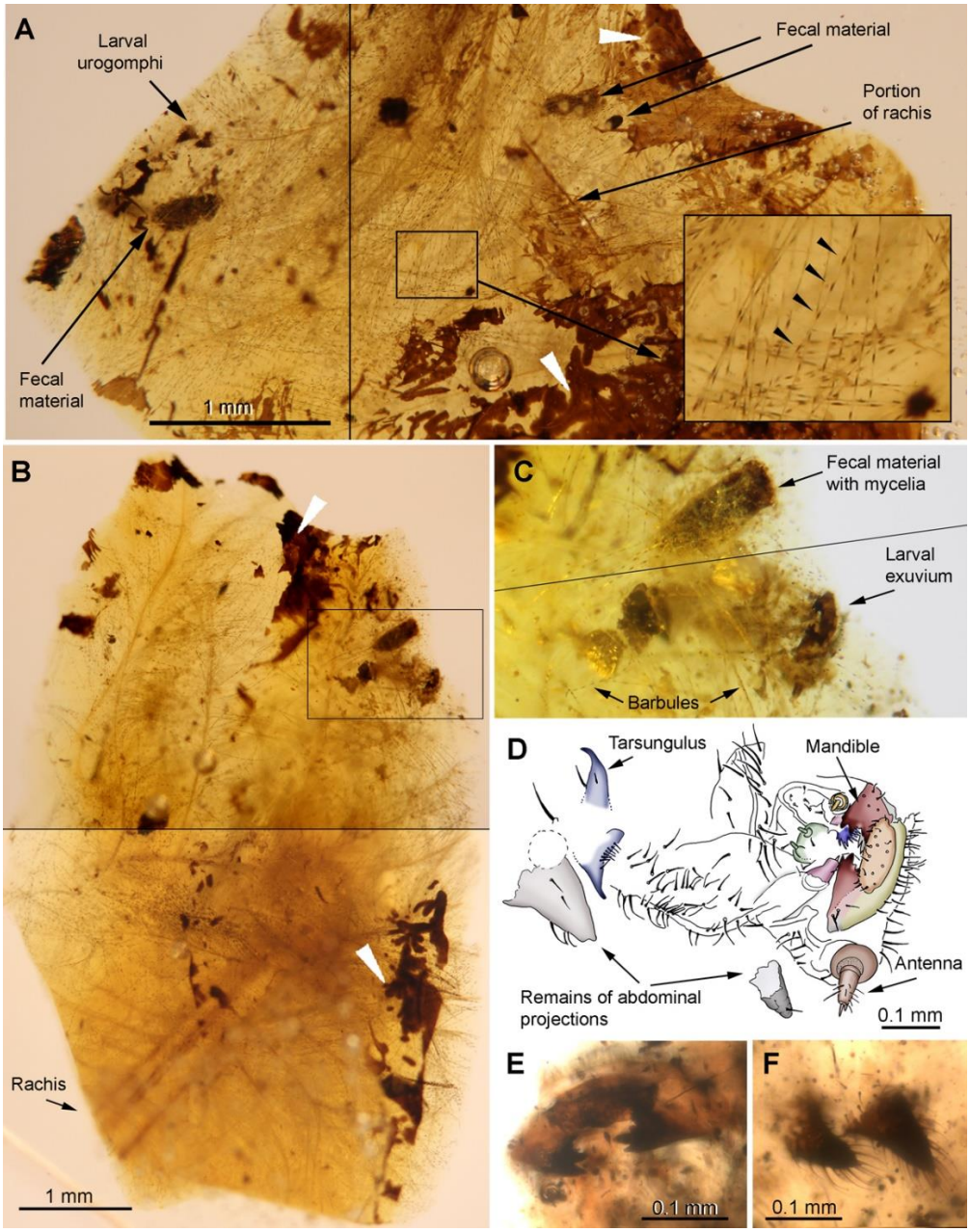

Figure 1. Exuvial remains from keratophagous beetle larvae intimately associated with plumulaceous feather remains in amber preparation SJNB2012-31-01 from the San Just outcrop

(NE Spain), upper Albian (Early Cretaceous) in age. (*A*) Amber fragment (F3, see *SI Appendix*, Fig. S1) with feather and exuvial remains, showing detail of the barbule node pigmentation (inset arrowheads). (*B*) Amber fragment (F2, see *SI Appendix*, Fig. S1) with partial plumulaceous feather and exuvial remains. (*C*) Detail of the almost intact larval exuvium in ventral view, and fecal material with fungal growth (mycelia; inset in (*B*)), both surrounded by barbules. (*D*) Larval exuvium in ventral view. (*E*) Larval head in frontal view showing mandibles. (*F*) Isolated pair of urogomphi (see (*A*) for location). Note the dark desiccation surfaces typical of aerial amber in (*A* and *B*) (white arrowheads). Images (*A*–*C*) composed of photographs taken at different focal planes.

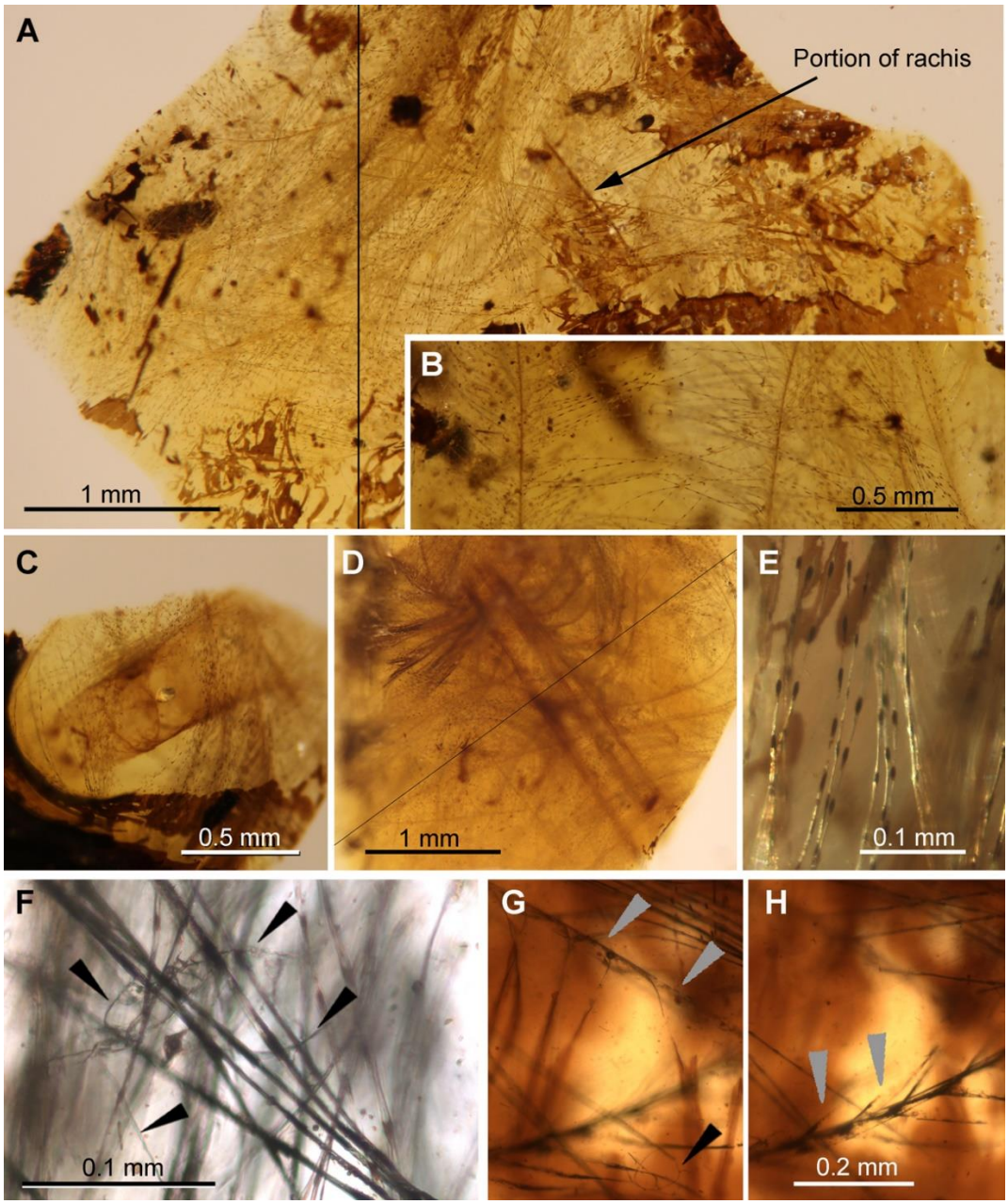

Figure 2. Morphological features and barb degradation of the feather portions associated with exuvial remains of beetle larvae in amber preparation SJNB2012-31-01 from the San Just outcrop (NE Spain), upper Albian (Early Cretaceous) in age. (*A*) Feather remains showing a

fragment of rachis and abundant barbs. (*B*) Two conspicuous barbs with abundant barbules. (*C*) Calamus and abundant surrounding barbs. (*D*) Portion of rachis showing abundant barbs arising from it. (*E*) Detail of the brown pigmentation concentrated in nodes of barbules. (*F*) Hyphae (black arrowheads) entangled or growing on the barbules. (*G*) and (*H*) Barb degradation showing hyphae on the barbules (black arrowhead) and barbule incompleteness (grey arrowheads) (both images of the same area at different focal planes and at the same scale). (*A* and *E*) from amber fragment F3; (*B* and *D*) from F2; (*C)* from F4. Note the dark desiccation surfaces typical of aerial amber in (*A*, *C* and *E*). Images (*A* and *D*) composed of photographs taken at different focal planes.

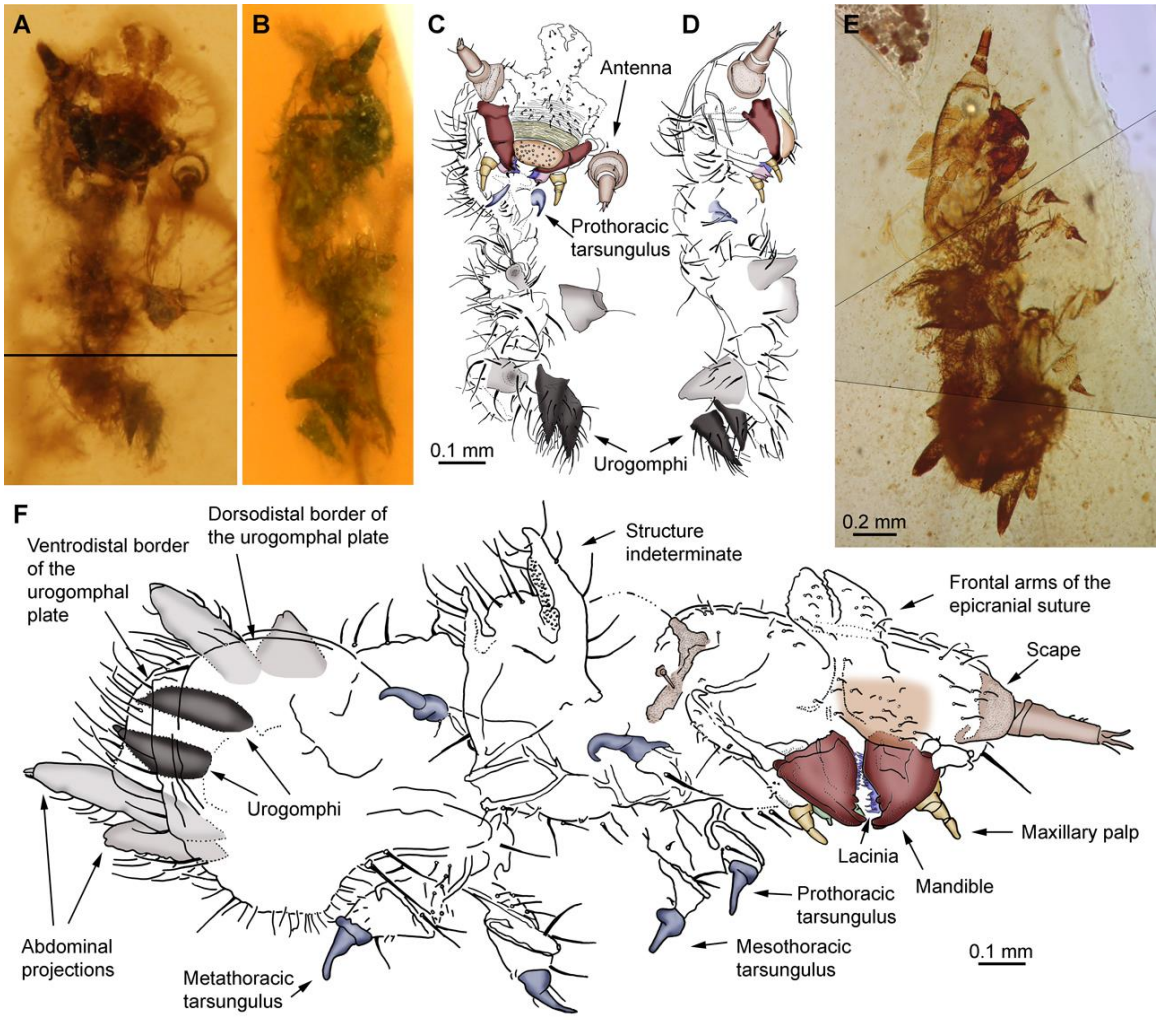

Figure 3. Isolated exuvium in amber piece SJNB2012-11 from the San Just outcrop (NE Spain), upper Albian (Early Cretaceous) in age (*A*–*D*), and isolated exuvium belonging to a putatively conspecific, more advanced instar from El Soplao amber (N Spain), middle Albian in age, piece ES-07-39 (*E* and *F*). (*A* and *B*) Ventral and lateral views, respectively. (*C* and *D*) Drawings of the former views. (*E*) Ventral oblique view. (*F*) Drawing of the same exuvium. (*A*–*D* and *F*) at the same scale for comparison. Images (*A* and *E*) composed of photographs taken at different focal planes.

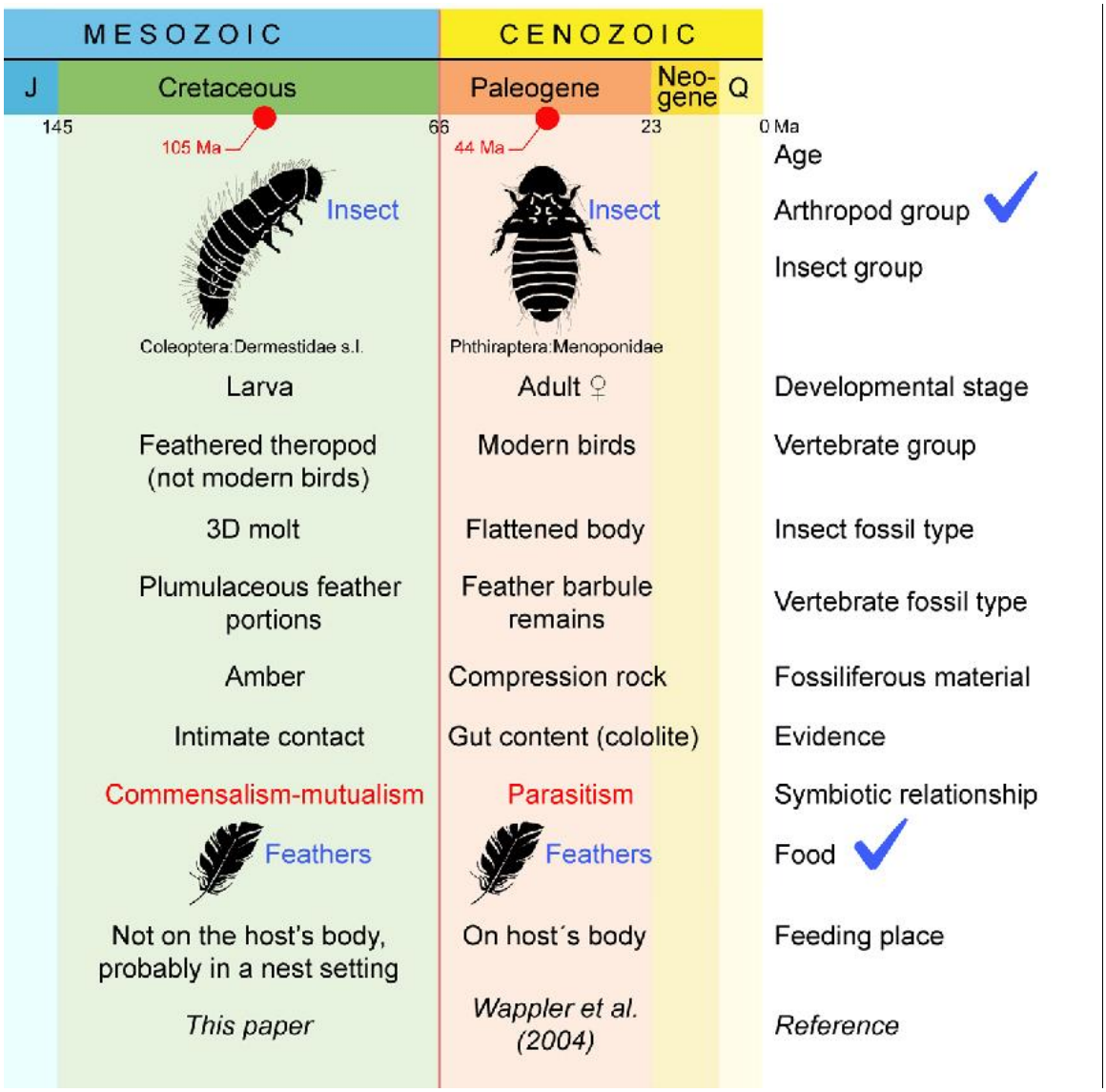

Fig. 4. Comparison of the two only records providing direct evidence of keratophagy in the current fossil record. The most relevant difference between the two records from the evolutionary standpoint is the type of symbiotic relationship recorded (in red). Only two important features are shared between the records, which are the arthropod group involved and integumentary food consumed (in blue). Abbreviations: J = Jurassic, Q = Quaternary.

Anexo 8.1.12

Barklice (Insecta: Psocodea) from Early Cretaceous resiniferous forests of Iberia (Spanish amber): new Troctomorpha and the oldest Psocomorpha

Álvarez-Parra, S., Peñalver, E., Nel, A., Delclòs, X. en preparación*. Barklice (Insecta: Psocodea) from Early Cretaceous resiniferous forests of Iberia (Spanish amber): new Troctomorpha and the oldest Psocomorpha.

* El manuscrito se encuentra en la fase final de su preparación. Dado que es un trabajo aún no publicado, se han retirado los nombres de los nuevos taxones descritos. No se han incluido las figuras ni los pies de figura.

Barklice (Insecta: Psocodea) from Early Cretaceous resiniferous forests of Iberia (Spanish amber): new Troctomorpha and the oldest Psocomorpha

Sergio Álvarez-Parra [1, 2 *], Enrique Peñalver [3], André Nel [4], Xavier Delclòs [1, 2]

[1] Departament de Dinàmica de la Terra i de l'Oceà and Institut de Recerca de la Biodiversitat (IRBio), Facultat de Ciències de la Terra, Universitat de Barcelona, c/ Martí i Franquès s/n, 08028, Barcelona, Spain

[2] Institut de Recerca de la Biodiversitat (IRBio), Universitat de Barcelona, Barcelona, Spain.

[3] Instituto Geológico y Minero de España-CSIC, c/ Cirilo Amorós 42, 46004, Valencia, Spain

[4] Institut de Systématique, Évolution, Biodiversité (ISYEB), Muséum national d'Histoire naturelle, CNRS, Sorbonne Université, EPHE, Université des Antilles, CP50, 57 rue Cuvier 75005 Paris, France

* Corresponding author: sergio.alvarez-parra@ub.edu (Sergio Álvarez-Parra)

Sergio Álvarez-Parra: https://orcid.org/0000-0002-0232-1647
Enrique Peñalver: https://orcid.org/0000-0001-8312-6087
André Nel: https://orcid.org/0000-0002-4241-7651
Xavier Delclòs: https://orcid.org/0000-0002-2233-5480

Abstract

Psocids, commonly known as barklice, are insects belonging to the order Psocodea, together with the parasitic lice. They usually inhabit forest litter or the bark of tree trunks and branches, showing herbivorous or detritivorous feeding habits. The Cretaceous psocid record is diverse, containing more than 70 described species. Here, we present new psocids (Troctomorpha and Psocomorpha) from two Spanish amber outcrops, both Albian in age (Early Cretaceous): El Soplao and Ariño. We describe the two new species *Azarpsocus AAA* Álvarez-Parra & Nel sp. nov. (Manicapsocidae) and *Burmacompsocus BBB* Álvarez-Parra & Nel sp. nov. (Compsocidae), and the new genus and species *CCC DDD* Álvarez-Parra & Nel gen. et sp. nov. (family *incertae sedis* within Psocomorpha). We discuss the taxonomic placement of the studied specimens and comment new data on the paleobiogeography of the Cretaceous psocids. The Cretaceous barklice fauna from Iberia shows more similarities with that from Lebanese (Barremian) and Burmese (Cenomanian) ambers than with that from the paleogeographically closer French amber (Cenomanian). This finding has been also reported in other insect groups from Spanish amber, and might be the consequence of several factors, such as the paleoenvironmental conditions of the ecosystems, the paleogeographical position of the Iberia Island during the latest Jurassic, closer to Gondwana than to Laurasia, and oceanic currents that facilitated or hindered the displacement of insect fauna between continental masses.

Keywords. Psocodea, barklice, Troctomorpha, Psocomorpha, paleobiogeography, Albian

Introduction

The order Psocodea encompasses barklice, booklice, and parasitic lice, forming part of the acercarian insects (Johnson et al., 2018). The first two are usually known as psocids, which correspond to a paraphyletic group previously known as 'Psocoptera' (Smithers, 1972; de Moya et al., 2021). There are more than 5,000 extant species of psocids, and they are present in a wide range of environments, including leaf litter, rotten wood, tree trunks and branches, bark, bird and mammal nests, rocks, caves, and domestic habitats. They are herbivorous and detritivorous, acting as nutrient recyclers of organic matter (New, 1987). Psocodea is divided into the suborders Trogiomorpha, Troctomorpha, and Psocomorpha (Smithers, 1972). The group Phthiraptera, which includes the parasitic lice, is considered an infraorder within Troctomorpha (de Moya et al., 2021). The Psocodea first appeared an estimated 375.7–292.4 Ma (Yoshizawa et al., 2019), supported by the oldest known fossil barklouse from the Late Carboniferous (Nel et al., 2013). The psocids underwent diversification during the Cretaceous, with more than 70 described species belonging to the three suborders (Álvarez-Parra et al., 2022). Furthermore, the extant genus *Psyllipsocus* is recorded from Cretaceous amber, showing the extraordinary evolutionary stasis or bradytely of this group of insects (Álvarez-Parra et al., 2020b; Jouault et al., 2021; Liang & Liu, 2021). Interestingly, the relative diversity of species in psocid suborders from the Cretaceous, albeit inferred from a fossil record biased toward resiniferous forests, is no longer reflected in present-day species (Álvarez-Parra et al., 2022). Nowadays, Psocomorpha is the most diverse suborder, but is only represented in the Cretaceous by four species described to date (Vishniakova, 1975; Azar et al., 2015; Yoshizawa & Yamamoto, 2021).

The suborder Troctomorpha was divided into the infraorders Amphientometae and Nanopsocetae (Smithers, 1972). Nonetheless, de Moya et al. (2021) proposed a rearrangement of this suborder, increasing the number of infraorders to five: Amphientometae, Sphaeropsocetae, Pachytroctetae, Liposcelidetae, and Phthiraptera. Thus, the parasitic lice are better accommodated as an infraorder, and the former suborders of Phthiraptera are now considered parvorders (de Moya et al., 2021). Therefore, Amphientometae includes the families Amphientomidae, Compsocidae, †Electrentomidae, Manicapsocidae, Musapsocidae, Troctopsocidae, and Protroctopsocidae; while Sphaeropsocetae, Pachytroctetae, and Liposcelidetae are monofamilial, including Sphaeropsocidae, Pachytroctidae, and Liposcelididae, respectively. The suborder Psocomorpha contains 27 families within six infraorders (Yoshizawa & Johnson, 2014; Yoshizawa & Yamamoto, 2021): Archipsocetae, Caeciliusetae, Homilopsocidea, Philotarsetae, Epipsocetae, and Psocetae.

The fossil record of Psocodea in the Iberian Peninsula is poorly known and mainly represented by specimens in Spanish Cretaceous amber. To date, only six species within five genera have been described (Baz & Ortuño, 2000, 2001a, b; Álvarez-Parra et al., 2022). Furthermore, an only partial record assigned to cf. *Mesopsocus* sp. (Psocomorpha: Mesopsocidae) has been described from Spanish Miocene laminated mudstones (Peñalver et al., 1996). The study of the psocids in Spanish amber was revived by Álvarez-Parra et al. (2022), providing the descriptions of new Trogiomorpha specimens from five amber-bearing outcrops. Here, we present new troctomorphan specimens and the oldest known Psocomorpha

from two amber-bearing outcrops of the Iberian Peninsula, and discuss their taxonomic placements and their paleobiological implications.

Material and methods

The specimens studied in this work are included in amber pieces from two Cretaceous (Albian) amber-bearing outcrops in Spain: El Soplao (Cantabria Autonomous Community), also known as Rábago-El Soplao, and Ariño (Teruel Province). El Soplao is located in the north of the Iberian Peninsula, while Ariño is in the east (Fig. 1).

El Soplao outcrop is geologically located on the western margin of the Basque-Cantabrian Basin belonging to the Las Peñosas Formation (Najarro et al., 2009), which is dated as middle Albian based on foraminifera (García-Mondéjar, 1982). The amber-bearing level is related to a deltaic-estuarine paleoenvironment (Najarro et al., 2009). Ariño amber is found in the bonebed level AR-1 within the Santa María open-pit coal mine located in the Maestrazgo Basin (Alcalá et al., 2012; Álvarez-Parra et al., 2021). The level AR-1 belongs to the Escucha Formation, and is dated as lower Albian based on the charophyte, ostracod, and palynological content (Tibert et al., 2013; Villanueva-Amadoz et al., 2015 Vajda et al., 2016; Álvarez-Parra et al., 2021). The Ariño amber paleoenvironment is related to a freshwater swamp plain with shallow alkaline lakes and marine influence under a subtropical or tropical climate, inhabited by a highly diverse range of organisms (Alcalá et al., 2012; Álvarez-Parra et al., 2020a, 2021; Arillo et al., 2022).

Amber pieces were cut, polished, and embedded in epoxy resin prisms following the methodology of Corral et al. (1999), ensuring their preservation and protection. The specimens were examined using an Olympus CX41 compound microscope with reflected and transmitted light. Photographs and drawings of the specimens were acquired using the same compound microscope with an attached sCMEX-20 digital camera and a camera lucida. The softwares ImageFocusAlpha version 1.3.7.12967.20180920 and Photoshop CS6 were used to take the photographs and prepare the figures, respectively. The anatomical nomenclature and systematics follow the works of Smithers (1972, 1990), Mockford (1993), and New & Lienhard (2007). Vein notation is as follows: Sc, Sc', subcostal veins; Rs, R_1, R_{2+3}, R_{4+5}, radial veins; M, M_1, M_2, M_3, medial veins; Cu_1, Cu_2, cubital veins; A, 1A, 2A, anal veins.

This study includes five fossil psocid specimens. Their acronyms and provenances as well as the Spanish public institutions where they are housed are indicated below. The type locality of the new taxa is also indicated in the corresponding section of the systematic paleontology.

Acronym CES: El Soplao amber. Housed in the Colección Institucional del Laboratorio de la Cueva El Soplao in Celis, Cantabria.

Acronym AR-1-A: Ariño amber. Housed in the Museo Aragonés de Paleontología (Fundación Conjunto Paleontológico de Teruel-Dinópolis) in Teruel.

Systematic paleontology

Order **Psocodea** Hennig, 1966

Suborder **Troctomorpha** Roesler, 1940

Infraorder **Amphientometae** Pearman, 1936

Family **Manicapsocidae** Mockford, 1967

Genus ***Azarpsocus*** Maheu & Nel, 2020

Type species: *Azarpsocus perreaui* Maheu & Nel, 2020.

Original diagnosis (from Maheu & Nel, 2020): "Forewing: three-branched vein M, areola postica as long as high; vein A1 closely parallel to posterior wing margin; no crossvein between M and areola postica; A2 not fused with A1; pterostigma very long; hind wing: basal segment of Rs present; median vein simple."

Remarks: Based on the new specimens here assigned to the genus *Azarpsocus*, the diagnosis is maintained as in the original except for one character that would be related to specific variability. Maheu & Nel (2020) indicated the same characters as being diagnostic for *Azarpsocus perreaui*, adding 'maxillary palp 2 (mx2) as long as maxillary palp 4 (mx4)'. We consider that 'areola postica as long as high' should be included in the diagnosis of *A. perreaui* and excluded from that of the genus *Azarpsocus*.

Azarpsocus AAA Álvarez-Parra & Nel **sp. nov.**

Figs. 2–4

LSID:

Type material: Holotype CES.057.3; a complete specimen (Fig. 2), sex unknown; syninclusion with one arachnid, two beetles, and three hymenopterans. Housed in the Colección Institucional del Laboratorio de la Cueva El Soplao in Celis, Rábago, Cantabria.

Other material: AR-1-A-2019.58.1; a partial specimen (Fig. 3c, d), sex unknown; syninclusion with a hymenopteran. AR-1-A-2019.60.1, a partial specimen (Fig. 3a, b), sex unknown; syninclusion with a beetle and a dipteran.

Locality and horizon: El Soplao amber-bearing outcrop, Cantabria Autonomous Community, Spain; Las Peñosas Formation, Albian, Early Cretaceous (Najarro et al., 2009).

Other localities: Ariño amber-bearing outcrop, Teruel Province, Spain; Escucha Formation, early Albian (Álvarez-Parra et al., 2021).

Etymology:

Diagnosis: Forewing with R_1 strongly curved at its distal part forming a long and bulging pterostigma, areola postica 2× longer than wide, Cu_{1a} strongly curved, forming a bulging areola postica.

Description: Body length of the holotype CES.057.3 from clypeus to distal part of abdomen is 0.97 mm (Fig. 2a, b). No setae or fine hairs on body surface. Head 0.34 mm wide; epicranial suture or ocelli not visible; small and bulging compound eyes 0.06 mm in diameter; number of ommatidia indiscernible; antenna with 13 flagellomeres covered by fine hairs; first flagellomere long and slightly curved; length of flagellomeres: I 0.18 mm, II 0.15 mm, III 0.14 mm, IV 0.10 mm, V 0.10 mm, VI 0.08 mm, VII 0.08 mm, VIII 0.08 mm, IX 0.06 mm, X 0.04 mm, XI 0.04 mm, XII 0.04 mm, XIII 0.4 mm; secondary annulations uncertain; bulging clypeus; mouthparts obscure, only left distal maxillary palpomere and probably lacinia visible. Thorax 0.35 mm long. Forewing completely preserved in the holotype CES.057.3 (Fig. 2c) and in AR-1-A-2019.60.1 (Fig. 3a, b), partially preserved in AR-1-A-2019.58.1 (Fig. 3c, d); length

and maximum width (in mm) of forewing 1.92:0.73 (holotype CES.057.3), 2.84:1.06 (AR-1-A-2019.60.1); membrane hyaline; margin and membrane glabrous; microsculpture of small points; basal section of Sc short and curved, joining R; distal section of Sc short and slightly curved; R_1 strongly curved at its distal part, forming a long and bulging pterostigma; pterostigma not colored; pterostigma of AR-1-A-2019.60.1 apparently with an area close to costal margin more marked than rest of the membrane; highly sclerotized point emerging of distal of Sc in AR-1-A-2019.58.1; basal section of Rs straight in the holotype CES.057.3, while curved in the other specimens; Rs and M fused for a short distance; Rs bifurcating into R_{2+3} and R_{4+5} nearly at level of R_1, reaching margin; M three-branched; bifurcation of M_1 and M_2 slightly distal to bifurcation of Rs; emerging of M_3 slightly basal to bifurcation of Rs; areola postica free, 2× longer than wide; Cu_{1a} strongly curved, forming a bulging areola postica; Cu_{1b} short; Cu_2 and A joining in a nodulus close to margin; A parallel to posterior margin; second anal vein not visible in any specimen. Hind wing completely preserved in the holotype CES.057.3 (Fig. 3d), partly preserved in AR-1-A-2019.58.1 (Fig. 3c, d) and AR-1-A-2019.60.1 (Fig. 3a, b); length and maximum width (in mm) of hind wing 1.46:0.49 (holotype CES.057.3), 2.45:0.74 (AR-1-A-2019.60.1); membrane hyaline; margin and membrane glabrous; microsculpture of small points; Sc not visible; R_1 reaching margin closer to base of Rs in the holotype CES.057.3 and AR-1-A-2019.58.1 than in AR-1-A-2019.60.1; Rs and M fused for a short distance; Rs two-branched; M unbranched; Cu_1 and Cu_2 present; bifurcation of anal vein near margin visible in AR-1-A-2019.60.1. Legs covered by fine hairs; one distal spur on tibiae visible in the holotype CES.057.3 and in AR-1-A-2019.58.1; three tarsomeres; proximal tarsomere the longest; pulvillus and one preapical tooth unclear in the specimens. Abdomen obscure; five segments can be observed in the holotype CES.057.3; genitalia not visible in any specimen.

Discussion: The holotype specimen CES.057.3 fits within the family Manicapsocidae based on the characters: body and wings without scales, 15 antennomeres (13 flagellomeres), macropterous, forewing venation not reduced, pterostigma not colored and closed basally (distal section of Sc present), nodulus present, hind wing with M unbranched, and tarsi three-segmented (Mockford, 1967; Smithers, 1972, 1990). Key characters, such as presence of second anal vein in forewings and one preapical tooth on pretarsal claws, as well as characters of the genitalia, are challenging to observe in fossil specimens that are not exceptionally well-preserved. Considering the genera within Manicapsocidae, the holotype CES.057.3 shows a similar venation to *Azarpsocus perreaui* from Burmese amber (Fig. 4). Furthermore, most of the diagnostic characters of the genus (Maheu & Nel, 2020) are present in CES.057.3, such as forewing with very long pterostigma, M three-branched, vein 1A closely parallel to posterior wing margin, no crossvein between M and areola postica, and hind wing with basal segment of Rs present and M simple. The only diagnostic characters of the genus absent in CES.057.3 are 'second anal not fused with first anal vein' (second anal vein not visible) and 'areola postica as long as high'. We propose to move the latter to the diagnostic characters of the species *A. perreaui* (see above). The main differences between CES.057.3 and *A. perreaui* concern the shape of the pterostigma and the areola postica. Therefore, we consider that these data support the description of a new species, *Azarpsocus AAA* sp. nov., closely related to *A. perreaui*. Unfortunately, the secondary annulations described in *A. perreaui* cannot be observed in the holotype of the new species. The other two studied specimens, not in the type series, show the same wing venation as the holotype, thus they are considered conspecific. Nonetheless, these

specimens are poorly preserved and few body characters are visible; furthermore, some parts of the wings cannot be observed either. It is interesting to note the difference in size of all these specimens, the holotype being the smallest, similar in size to the holotype of *A. perreaui* (Maheu & Nel, 2020). Furthermore, in the holotype and AR-1-A-2019.58.1, R_1 in hind wing reaches the wing margin closer to base of Rs than in AR-1-A-2019.60.1. These differences might be explained by intraspecific variability.

The genus *Azarpsocus* shows a venation similar to the *Caecilius*-type present in several groups within Psocomorpha (Smithers, 1972); most notably, it is strikingly similar to that of the family Lachesillidae (infraorder Homilopsocidea). Furthermore, they share glabrous wings and the presence of a preapical tooth on pretarsal claws (Smithers, 1972). The placement of the genus *Azarpsocus* within Lachesillidae is ruled out based on several characters (Smithers, 1972, 1990; Mockford, 1993; New & Lienhard, 2007): 15 antennomeres (psocomorphans have 13 or fewer), flagellomeres secondarily annulated at least in the species *Azarpsocus perreaui* (not secondarily annulated in psocomorphans), ocelli not grouped in a tubercle (ocelli in a tubercle is typical of homilopsocideans), pterostigma not colored (usually colored in psocomorphans), short basal section of Sc joining R in forewing (character typical of manicapsocids), hind wing with Rs fused with M for a short distance (fused for a relatively long distance in lachesillids), and three-segmented tarsi (two-segmented in lachesillids). Nonetheless, the colored pterostigma might be a character depending on intraspecific variability; in addition, the lachesillid *Eolachesilla chilensis* Badonnel, 1967 shows three-segmented tarsi (New & Lienhard, 2007). Therefore, we prefer to maintain the bispecific genus *Azarpsocus* as belonging to Manicapsocidae. It is possible that new psocid specimens with *Caecilius*-type venation will be described from Cretaceous amber, thus helping to discern the anatomical differences between manicapsocids and psocomorphans.

Azarpsocus AAA sp. nov. is present in El Soplao (probably middle Albian) and Ariño (early Albian) ambers. These findings thus suggest morphological stasis for this species in Iberia throughout the Albian, despite minor differences in some characters and size.

Superfamily Electrentomoidea Enderlein, 1911
Family **Compsocidae** Mockford, 1967
Genus ***Burmacompsocus*** Nel & Waller, 2007

Type species: *Burmacompsocus perreaui* Nel & Waller, 2007.
Other species: *Burmacompsocus banksi* (Cockerell, 1916), *B. coniugans* Sroka & Nel, 2017, and *B. pouilloni* Ngô-Muller, Garrouste & Nel, 2020.

Burmacompsocus BBB Álvarez-Parra & Nel **sp. nov.**
Fig. 5

LSID:

Type material: Holotype CES.315.8; incomplete macropterous specimen with poorly preserved body but nearly complete venation preserved (Fig. 5a, b), sex unknown; syninclusion with one beetle, two hymenopterans, and four dipterans. Housed in the Colección Institucional del Laboratorio de la Cueva El Soplao in Celis, Rábago, Cantabria.

Locality and horizon: El Soplao amber-bearing outcrop, Cantabria Autonomous Community, Spain; Las Peñosas Formation, Albian, Early Cretaceous (Najarro et al., 2009).

Etymology:

Diagnosis: Forewing with short basal section of Sc, Rs contacting M in a point, bulging areola postica with Cu_{1a} strongly curved, areola postica 1.5× longer than pterostigma; hind wing with Sc long fused to R_1, Cu_1 strongly curved before reaching margin.

Description: No flattened scales on body or wings. One antenna partly preserved, with at least nine visible flagellomeres; length of the basal flagellomeres around 0.08 mm; length of the distal flagellomeres around 0.04 mm; secondary annulations not visible on flagellomeres. Forewing 1.90 mm long and 0.80 mm maximum wide (Fig. 5c); membrane hyaline; margin and membrane glabrous; microvestiture on forewing membrane in form of small points; basal section of Sc short and strongly curved, joining R at 0.44 mm from wing base; closed pterostigma 0.26 mm long and 0.08 mm wide, not colored, formed by a short distal section of Sc reaching margin at 1.21 mm from wing base, and slightly curved R_1 reaching margin at 1.40 mm from wing base; Rs showing a single point of contact with M, neither fused; no crossvein between R_1 and Rs; bifurcation of Rs into R_{2+3} and R_{4+5} at 1.20 mm from wing base; both veins long, slightly curved and reaching margin at 1.70 mm and 1.81 mm from wing base, respectively; M three-branched; M_3 emerging at 1.36 mm from wing base, running almost straight to margin, joining at 1.64 mm from wing base; bifurcation of M_1 and M_2 not visible; both veins nearly straight; M_1 reaching wing apex; M_2 reaching wing margin at 1.80 mm from wing base; areola postica 0.39 mm long and 0.17 mm wide; crossvein between M and areola postica not present; Cu_{1a} bulging and strongly curved, reaching wing margin at 1.43 mm from wing base; Cu_{1b} short and reaching wing margin at 1.04 mm from wing base; Cu_2 and A veins present, apparently joining in a nodulus, but not clearly visible. Hind wing 1.56 mm long and 0.55 mm wide (Fig. 5d); membrane hyaline; margin and membrane glabrous; Sc long fused to R_1, emerging at 0.59 mm from wing base; R_1 slightly curved; basal section of Rs not present; Rs two-branched and bifurcating into R_{2+3} and R_{4+5} at 1.11 mm from wing base; M two-branched and bifurcating into M_1 and M_2 at 0.98 mm from wing base; Cu_1 and Cu_2 present; Cu_1 with a strong curve before reaching margin. Legs partly preserved; two distal spurs on hind tibia; right hind tibia 0.74 mm long; right hind tarsus 0.43 mm long; three-segmented tarsi; length of tarsomeres of right hind leg: proximal 0.29 mm, middle 0.07 mm, distal 0.07 mm; pretarsal claws not visible. Abdomen partly preserved; characters of genitalia cannot be described.

Discussion: The holotype specimen CES.315.8 belongs to the family Compsocidae, within Amphientometae (Troctomorpha), based on body and wings without flattened scales, macropterous wings, complex forewing venation, pterostigma that is closed basally and not colored, hind wing with M two-branched, and three-segmented tarsi (Smithers, 1972; Nel & Waller, 2007). Interestingly, Mockford (1967) and Smithers (1972) indicated hind wing with unbranched M, even though the drawings in Banks (1930, plate 9: figure 4) and Mockford (1967) clearly show M two-branched in the type genus *Compsocus* and in *Electrentomopsis*. Some diagnostic body characters (Mockford, 1967) are not visible in the studied specimen. The presence of a nodulus is a key character of the family (Nel & Waller, 2007), but unfortunately, although it might be present, it is not clearly visible. Members of Compsocidae show forewings with two anal veins, 2A joining 1A, and two preapical teeth on pretarsal claws (Mockford,

1967). CES.315.8 only shows one anal vein and pretarsal claws are not visible, both probably due to preservation. Within Compsocidae, CES.315.8 falls in the genus *Burmacompsocus* based on venation similar to the previously described species (Nel & Waller, 2007; Sroka & Nel, 2017; Ngô-Muller et al., 2020). The diagnosis of *Burmacompsocus* includes forewing with microvestiture in the form of small points and hind wing without basal section of Rs (Nel & Waller, 2007), as in CES.315.8. The shape of the areola postica, its proportional length in relation to the pterostigma, and hind wing with Sc long fused to R_1, and strongly curved Cu_1, as observed in CES.315.8, are unique characters within the genus, supporting the description of *Burmacompsocus BBB* sp. nov. The basal section of Sc in forewings is longer in *B. perreaui* and *B. pouilloni* than in the new species; furthermore, Sc is briefly fused to R_1 in hind wings of *B. perreaui* and *B. pouilloni* (Nel & Waller, 2007; Ngô-Muller et al., 2020). *Burmacompsocus BBB* sp. nov. differs from *B. coniugans* in the Rs showing a single point of contact with M in forewings (vs. briefly fused) (Sroka & Nel, 2017). *Burmacompsocus banksi* was included in the genus *Psyllipsocus* by Cockerell (1916), but later transferred to the genus *Burmacompsocus* by Mockford et al. (2013), who noted the similarity with *B. perreaui*. The Cretaceous species *Paraelectrentomopsis chenyangcaii* has a crossvein between Rs and M, and M bifurcates into M_1 and M_2+M_3 (Azar et al., 2016); these two characters differ from *B. BBB* sp. nov. The family Compsocidae comprises only two extant species (Mockford, 1967): *Compsocus elegans* Mockford, 1967 and *Electrentomopsis variegatus* Mockford, 1967. The character 'basal section of Rs in hind wing' is present in *C. elegans*, but not in *E. variegatus* (Mockford, 1967). Anal veins 1A and 2A join in *E. variegatus*, differing from *Burmacompsocus* (Nel & Waller, 2007). The total number of antennomeres, secondary annulations on flagellomeres, and preapical teeth on preapical claws are not visible in the holotype of *B. BBB* sp. nov. due to preservation, therefore the description of new complete specimens with the same venation morphotype may support the erection of a new genus within Compsocidae. Notably, the extant species of the family are only found in Central America, whereas the fossil representatives come from Cretaceous deposits in Spain and Myanmar, indicating an ancient wide distribution of the group. The living species would correspond to a relict fauna.

The members of Manicapsocidae and Compsocidae show similarities and are probably phylogenetically closely related (Mockford, 1967), diverging during the Early Cretaceous (Baz & Ortuño, 2001a). Interestingly, the wing venation of *Manicapsocidus enigmaticus* is strikingly similar to that of *Burmacompsocus BBB* sp. nov., sharing the shape of the pterostigma and the areola postica, but differing in the presence of vein rs-m and the arrangement of M branches in *M. enigmaticus* forewing. Furthermore, the hind wing of the new species shows Sc emerging from R_1 and M is two-branched (vs. Sc not present and M unbranched).

Suborder **Psocomorpha** Badonnel, 1951

Family ***incertae sedis***

CCC Álvarez-Parra & Nel **gen. nov.**

Figs. 6, 7

LSID:

Type species: *CCC DDD* sp. nov., by present designation and monotypy.

Etymology:

Diagnosis: Wing margin and membrane glabrous; wing membrane with microsculpture of small points; forewings with long and flat pterostigma somewhat bulging at its distal part, 1.8× longer than areola postica, Rs showing a single point of contact with M, Rs and M two-branched, bifurcation of M slightly distal to that of Rs, short and bulging areola postica, nodulus present; hind wings with R_1 short, crossvein rs-m present, five-angled basi-radial cell, Rs two-branched, M unbranched; tarsi two-segmented; pretarsal claws without preapical tooth.

CCC DDD Álvarez-Parra & Nel **sp. nov.**

Figs. 6, 7

LSID:

Type material: Holotype AR-1-A-2019.50.3; partial macropterous specimen, sex unknown; syninclusion with two dipterans. Housed in the Museo Aragonés de Paleontología (Fundación Conjunto Paleontológico de Teruel-Dinópolis).

Locality and horizon: Ariño amber-bearing outcrop, Teruel Province, Spain; Escucha Formation, early Albian, Early Cretaceous (Álvarez-Parra et al., 2021).

Etymology:

Diagnosis: Same as for the genus.

Description: Body length from frontal part of clypeus to distal part of abdomen, 1.44 mm (Fig. 6a, b). Setae or fine hairs not visible on body surface. Head 0.39 mm wide; no ocelli visible; bulging compound eyes, some ommatidia visible in right eye; bulging clypeus; antennae spectrally preserved with the total number of flagellomeres difficult to discern; scape, pedicel, and some flagellomeres visible, apparently covered by a few fine hairs; first and second flagellomeres apparently longer than rest; secondary annulations cannot be observed; mouthparts not visible. Thorax preserved as a hollow structure. Right wings preserved. Forewing 1.67 mm long and 0.62 maximum wide (Fig. 7a, c); membrane hyaline; margin and membrane glabrous; microsculpture on membrane in form of small points; costal margin partly thickened; basal section of Sc poorly visible, but it seems to end in the membrane, not joining R or margin; pterostigma long and flat, with distal part somewhat bulging, 0.45 mm long and 0.08 mm maximum wide; short distal section of Sc arising from a highly sclerotized point of R, reaching margin at 0.91 mm from wing base; R_1 reaching margin at 1.34 mm from wing base; Rs only showing a single point of contact with M, these are not fused and there is no crossvein between the two veins; Rs bifurcating into R_{2+3} and R_{4+5} at 1.23 mm from wing base; R_{2+3} and R_{4+5} slightly curved, reaching margin at 1.56 mm and 1.63 mm from wing base, respectively; M two-branched, bifurcating into M_1 and M_2 at 1.29 mm from wing base, slightly distal to bifurcation of Rs; M_1 reaching margin at 1.63 mm from wing base; M_2 reaching margin at 1.46 mm from wing base; area between branches of M 1.5× wider than that between branches of Rs (at maximum width of both areas); Cu emerging from M+Cu at nearly the same level as Rs emerges from R; areola postica short and bulging, 0.25 mm long and 0.15 mm wide; strongly curved Cu_{1a} reaching margin at 1.23 mm from wing base; straight Cu_{1b} reaching margin at 0.96 mm from wing base; Cu_{1b} 2.5× longer than shortest distance between M and Cu_{1a}; Cu2 and 1A joining in a nodulus at 0.59 mm from wing base (Fig. 6c, d); 2A partly visible, joining margin near wing base. Hind wing 1.27 mm long and 0.43 mm maximum wide (Fig. 7b, d); membrane

hyaline; margin and membrane glabrous; microsculpture on membrane in form of small points; Sc not visible; curved R; short and straight R_1 reaching margin at 0.64 mm from wing base; crossvein rs-m 0.03 mm long; Rs two-branched, bifurcating at 0.97 mm from wing base; R_{4+5} reaching margin at wing apex; M unbranched; five-angled basi-radial cell; Cu_1 and Cu_2 present; anal veins not visible. Legs partly visible; thin femorae and tibiae; tarsi seem to be two-segmented (Fig. 6e), covered by fine hairs; proximal tarsomere of hind leg 0.18 mm long; distal tarsomere of mid-leg 0.10 mm long; one distal spur on proximal tarsomere; pretarsal claws without preapical tooth or pulvillus (Fig. 6e). Abdomen incomplete and observation hindered by left wings; genitalia cannot be described.

Discussion: The holotype specimen AR-1-A-2019.50.3 shows a peculiar venation in forewing and hind wing that is not known from other Cretaceous psocids. Nonetheless, due to poor preservation, it lacks key characters required to obtain an accurate identification, such as the number of flagellomeres (and the presence or absence of secondary annulations on them). Regarding the families within Trogiomorpha and Troctomorpha, the holotype is only similar to the Pachytroctidae, based on forewing with M two-branched and hind wing with unbranched M (Smithers, 1972). It also shares these characters with *Libanopsyllipsocus alexanderasnitsyni* Azar & Nel, 2011 from Barremian Lebanese amber, assigned to the family Psyllipsocidae by Azar & Nel (2011), but belonging to Pachytroctidae *sensu* Mockford et al. (2013). The holotype differs with both in the shape of the pterostigma and the areola postica. Furthermore, the family Pachytroctidae lacks a nodulus (Smithers, 1972; Mockford, 1993). The presence of a nodulus in forewing and the two-segmented tarsi links the studied specimen to the suborder Psocomorpha (Smithers, 1972; Mockford, 1993). Within Psocomorpha, the wing venation of *CCC* gen. nov. is strikingly similar to that of the genera *Mepleres* Enderlein, 1926 and *Scottiella* Enderlein, 1931 (Fig. 7e, f) (Enderlein, 1926, 1931; Smithers, 1972; New & Lienhard, 2007), which both belong to the family Pseudocaeciliidae (infraorder Philotarsetae).

The genus *Mepleres* comprises more than 60 species distributed in Jamaica, Africa, South-East Asia, and Oceania (New & Lienhard, 2007). The genus *Scottiella* includes three species from Seychelles (Enderlein, 1931). Currently, they are the only two genera of pseudocaeciliids showing a M two-branched on the forewing, following the synonymy of *Pseudoscottiella* and *Meniscopsocus* under *Mepleres* (Yoshizawa, 2000). The most important difference between these two genera and *CCC* gen. nov. is the presence of setae on the forewing margin and veins and on the margin of the hind wing (Enderlein, 1931; New & Lienhard, 2007), while the wings of the new genus are completely glabrous. Other minor forewing differences are the Rs and M fused for a length (vs. showing a single point of contact in the new genus) and the absence of a second anal vein (vs. partly visible). The hind wings of *Mepleres* and *Scottiella* show a long R_1 until reaching the margin (vs. short in the new genus), Rs and M fused for a length (vs. not fused and presence of a crossvein rs-m); the presence of Sc and an anal vein in these wings is a character that is not visible in the holotype, the only known specimen of the new genus. The main differences between *Mepleres* and *Scottiella* are the forewing costa (thickened in *Mepleres* vs. not thickened in *Scottiella*) and areola postica (somewhat flat and long vs. semicircular). Considering these characters, *CCC* gen. nov. would be 'intermediate' as it has partly thickened forewing costa (as in *Mepleres*) and a nearly semicircular areola postica (as in *Scottiella*). The three genera share the absence of a preapical tooth in pretarsal claws. The differences between the studied specimen and these genera prevent its inclusion within any of

them, while the lack of setae on wings and Rs and M not fused in forewing or hind wing rule out its membership of the Pseudocaeciliidae (Smithers, 1972). Considering this information, and the substantial difference from the other Cretaceous psocid genera, we describe a new genus and species within Psocomorpha based on the specimen AR-1-A-2019.50.3. Nonetheless, we prefer to maintain this new taxon as family *incertae sedis* because several key characters are not visible in the holotype and no clear affinities can be discerned with the currently established psocomorphan families. New discoveries of specimens with similar venation may help to determine the phylogenetic placement of *CCC DDD* gen. et sp. nov.

To date, only four Cretaceous psocomorphan species have been described (Vishniakova, 1975; Azar et al., 2015; Yoshizawa & Yamamoto, 2021): *Cretapsocus capillatus* Vishniakova, 1975 (*incertae sedis*) and *Archaelachesis granulosa* Vishniakova, 1975 (Lachesillidae), both from Santonian Yantardakh amber, *Burmesopsocus lienhardi* Yoshizawa, 2021 (Homilopsocidea *incertae sedis*) from Cenomanian Burmese amber, and *Mesopsocoides dupei* Azar, Nel & Perrichot, 2015 (Mesopsocidae) from Cenomanian–Turonian Vendean amber. Considering these species, *CCC DDD* gen. et sp. nov. shares some characters with *C. capillatus*, such as the forewing with M two-branched, hind wing with crossvein rs-m and unbranched M, two-segmented tarsi, and preapical tooth not present (Vishniakova, 1975). Nevertheless, *C. capillatus* has a densely hairy margin and membrane on both wings, Sc is absent on the forewing, Rs and M are fused for a length, the areola postica is elongate, and there is no nodulus (Vishniakova, 1975). Therefore, *CCC DDD* gen. et sp. nov. is clearly different to all the previously described Cretaceous psocomorphans, supporting the description of a new genus and species.

Discussion

The known diversity of the Cretaceous psocids has rapidly increased in recent years following the description of new taxa mainly from Burmese amber (Myanmar), but also from other ambers around the world, such as Canadian, Spanish, French, Lebanese, and Taimyr (Russia) ambers (Azar et al., 2015; Álvarez-Parra et al., 2020b, 2022; Cockx et al., 2020; Hakim et al., 2021, 2022). Interestingly, the suborder Trogiomorpha accounts for most of the Cretaceous psocid species, whereas today it is the least diverse (Álvarez-Parra et al., 2022). To date, Troctomorpha encompasses 25 Cretaceous species. The study of Cretaceous troctomorphans sheds light on the origin of the parasitic lice, which may have occurred around 115 Ma, during the Early Cretaceous (de Moya et al., 2021). Until now, only one fossil louse species has been identified, *Megamenopon rasnitsyni* Wappler, Smith & Dalgleish, 2004 (Menoponidae), from the Eocene Eckfeld Maar in Germany (Wappler et al., 2004; Dalgleish et al., 2006). Another undescribed fossil louse has been reported from the Pleistocene Locality 49 of the Ziegler Reservoir fossil site in the USA (Elias, 2014). Lice-like insects, supposedly ectoparasitic, have turned out to be hemipterans unrelated to Phthiraptera (Grimaldi & Vea, 2021). The psocid family most closely related to the parasitic lice is Liposcelididae (de Moya et al., 2021), which has a fossil record with representatives from the Cretaceous, Eocene, and Miocene (Nel et al., 2004; Grimaldi & Engel, 2006). The origin of parasitism in Psocodea remains obscure, based on differences between the anatomic morphology of parasitic and non-parasitic members of the order (de Moya et al., 2021). Nonetheless, the study of dinosaur feathers and associated

entomofauna from Cretaceous ambers may yield key information about the general morphotype of the ancient lice, similarly to other groups of parasitic arthropods (e.g., Peñalver et al., 2017). Furthermore, it is expected that new 'transitional' specimens will be described from Cretaceous ambers, showing a combination of characters typical of different families, such as the recently described genus *Burmempheria* (Trogiomorpha: †Empheriidae) shows characters typical of †Archaeatropidae and †Empheriidae (Li et al., 2020), and has led to synonymize the first family under the second one (Li et al., 2022). These taxa, although challenging to place systematically, help to understand the relationships between the psocid families and the evolution of the group during the Cretaceous.

The description of *Azarpsocus AAA* sp. nov. in Manicapsocidae and *Burmacompsocus BBB* sp. nov. in Compsocidae expands our knowledge of the early diversification and paleogeographical distribution of these families. They are the first Cretaceous representatives of their corresponding families to be found in an amber other than the rich in bioinclusions Cenomanian Burmese amber. Furthermore, they are also the oldest records of both Manicapsocidae and Compsocidae, providing new calibration points for phylogenetic analyses. The Manicapsocidae correspond to eight extant species mainly found in South and Central America and an additional species from south-eastern inland Africa (Mockford, 1996; Hakim et al., 2020). The fossil record of the family includes six Cretaceous species in four genera (adding *A. AAA* sp. nov.) and two Eocene species in two genera (Nel et al., 2005; Hakim et al., 2020). The genus *Burmacompsocus* was highly diverse during the Cretaceous, containing five species (including *B. BBB* sp. nov.). Interestingly, the family Compsocidae includes six Cretaceous species, but only two extant species, which inhabit Central America (Mockford, 1967; Azar et al., 2016). Thus, it is plausible that these families showed a high diversity and wide distribution during the Cretaceous and then underwent vicariance and extinction processes, probably due to niche competition with the more derived psocomorphans, relegating them to the current restricted distribution, similarly to other Cretaceous trogiomorphan families (Álvarez-Parra et al., 2022).

The Burmese amber, containing specimens belonging to Manicapsocidae and Compsocidae, is related to resiniferous trees from the Burma Terrane, which was a near-equatorial Tethyan island during the mid-Cretaceous, explaining the high degree of endemism (Westerweel et al., 2019). It is thought to have been located between the Indian and Australian blocks in East Gondwana during the Early Jurassic and then displaced northward during the Late Jurassic–Early Cretaceous (Heine et al., 2004; Westerweel et al., 2019). Nonetheless, the proposed hypothesis on the Gondwanan origin of part of the Burmese amber biota is controversial (Clarke et al., 2019; Peris & Jelínek, 2020; Morley et al., 2021). The lack of fossil manicapsocids and compsocids in other Gondwanan ambers would discard their Gondwanan origin. Consequently, the migration of these psocid families from south-eastern Asia to the Burma Terrane cannot be ruled out. Therefore, the discovery of new troctomorphans in African (Bouju & Perrichot, 2020) or Australian (Stilwell et al., 2020) Cretaceous ambers would help to determine the evolutionary origin of these groups. Interestingly, although the Iberia Island was geographically close to Laurasia, the psocid fauna from Spanish amber seems to be more similar to that from Lebanese and Burmese ambers. The genera *Archaeatropos* and *Libanoglaris* (both within †Archaeatropidae in Trogiomorpha) are also present in Barremian Lebanese amber (Álvarez-Parra et al., 2022), while the genera studied here, *Azarpsocus* and

Burmacompsocus, are found in Cenomanian Burmese amber. Thus, the psocid fauna of Iberia (Albian in age) shares more similarities with the fauna from these distant amber deposits than with that from the geographically closer French amber (Cenomanian). In the Albian, resiniferous forests were distributed throughout north and eastern Iberia, whereas during the Cenomanian, the resiniferous forests were present in the southern and western Armorica-French Central Massif, both regions separated by an oceanic strait of around a few hundred kilometers (Álvarez-Parra et al., 2022, figure 1). Thus, a certain similarity between psocid faunas would be expected. The differences might be explained by the paleobarrier that this strait represented, maybe reinforced by the oceanic currents connecting the Tethys Sea and the North Atlantic Ocean, as occurred from the Miocene in the Channel of Mozambique, between Africa and Madagascar (Delclòs et al., 2020). Nevertheless, further study is required of the reasons for these anomalous relations among psocid faunas, following the description of new specimens from these provenances. The co-occurrence of insect genera from Lebanese or Burmese ambers with Spanish amber has been noted previously for groups such as springtails, beetles, wasps, and dipterans (e.g., Ortega-Blanco et al., 2011; Pérez-de la Fuente et al., 2011; Peris et al., 2014, 2016; Sánchez-García & Engel, 2016; Arillo et al., 2018; Santer et al., 2022), whereas there are few similarities between the Cretaceous insect faunas from Spanish amber and French amber (Peris et al., 2016). A study of the Spanish Cretaceous palynoflora has also revealed differences with that from the upper Albian–middle Cenomanian of western France (Barrón et al., 2015). The paleoenvironmental and paleoclimatic conditions and the botanical assemblages of the amber deposits together with the Cretaceous paleogeography might help to explain the differences and similarities between the arthropod faunas inhabiting resiniferous forests (Peris et al., 2016). As mentioned above, the flow of oceanic currents around Iberia during the mid-Cretaceous might have facilitated or hindered arthropodo-faunal displacements through some areas.

Psocomorpha is the most diverse psocid suborder today, although its representatives are almost unknown from the Cretaceous (Yoshizawa & Yamamoto, 2021; Álvarez-Parra et al., 2022). The species described here, *CCC DDD* gen. et sp. nov., corresponds to the oldest known Psocomorpha to date, providing a new calibration point for phylogenetic analyses at 110 Ma (early Albian). The relatively poor preservation of the holotype prevents its assignation to a known family, although it seems to share similarities regarding wing venation, with the pseudocaeciliid genus *Scotiella*. Therefore, the wing venation of *CCC DDD* gen. et sp. nov. seems to be somewhat derived, despite its antiquity. The only known psocomorphan from Burmese amber, *Burmesopsocus lienhardi*, also shows derived characters for Psocomorpha (Yoshizawa & Yamamoto, 2021). This information is interesting, as one would expect to find 'basal' psocomorphans, such as Archipsocidae (de Moya et al., 2021), in Cretaceous ambers, whereas the oldest known records of this family are from the Eocene (Nel et al., 2005). As Yoshizawa & Yamamoto (2021) have noted, it is likely that new psocomorphan specimens will be described from Cretaceous ambers, revealing the early evolution of the group and providing insights into its origin.

Conclusions

The description of one new genus and three new species in Albian Spanish amber strongly supports the idea that the psocids showed relatively high diversity during the Cretaceous. The barklice fauna of resiniferous forests in Iberia was diverse, with the three psocodean suborders present, and accounting for nine species within eight genera. Information about their paleobiology remains poor, but they probably had a similar lifestyle to the extant representatives of the group, inhabiting forest litter and the bark of the trunk and branches of resiniferous trees. More globally, barklice fauna was diverse during the Early Cretaceous, with the oldest representatives of several extant families (such as Prionoglarididae, Manicapsocidae, Compsocidae, Pachytroctidae, and Sphaeropsocidae), but also some extinct families (such as †Archaeatropidae and †Empheriidae). Unfortunately, while the Eocene psocid fauna is relatively well known thanks to the Oise, Baltic, and Rovno ambers, our knowledge of the latest Cretaceous and Paleocene psocids is very poor. Bridging this crucial gap will require considerable research effort in the coming years and investigation into new amber outcrops and Konservat-Lagerstätten of continental compression rocks covering this interval, which comprises the Cretaceous–Cenozoic crisis. The exact impact of this crisis on the Psocodea remains totally unknown.

Acknowledgments. We would like to thank the colleagues who participated in paleontological excavations at El Soplao and Ariño. We are grateful for the collaboration of the SAMCA Group and Fundación Conjunto Paleontológico de Teruel-Dinópolis during fieldwork at Ariño, and for the support of the Consejería de Cultura, Turismo y Deporte del Gobierno de Cantabria (Spain) and the Dirección General de Patrimonio Cultural del Gobierno de Aragón (Spain). We also thank the Museo de Ciencias Naturales de Álava and Colección Institucional del Laboratorio de la Cueva El Soplao for access to fossil specimens. This work was supported by the Consejería de Industria, Turismo, Innovación, Transporte y Comercio of the Gobierno de Cantabria through the public enterprise EL SOPLAO S.L. (research agreement #20963 with University of Barcelona and research contract REF 030611220077 to IGME-CSIC, both for the period 2022–2025). We are also grateful to Rafael López del Valle for preparing the amber pieces. This study is a contribution to the project CRE CGL2017-84419 funded by the Spanish AEI/FEDER and the EU. The first author, S.Á.-P., acknowledges the support of the Secretaria d'Universitats i Recerca de la Generalitat de Catalunya (Spain) and the European Social Fund (2021FI_B2 00003).

Author contributions. Conceptualisation: Sergio Álvarez-Parra; Funding acquisition: Xavier Delclòs; Investigation: Sergio Álvarez-Parra, Enrique Peñalver, André Nel, Xavier Delclòs; Methodology: Sergio Álvarez-Parra; Project administration: Xavier Delclòs; Writing – original draft: Sergio Álvarez-Parra; Writing – review and editing: Sergio Álvarez-Parra, Enrique Peñalver, André Nel, Xavier Delclòs.

Data and material availability. The institutions that housed the studied specimens are indicated in the Material and methods section.

Conflict of interest. The authors declare no competing interests.

References

Alcalá, L., Espílez, E., Mampel, L., Kirkland, J. I., Ortiga, M., Rubio, D., González, A., Ayala, D., Cobos, A., Royo-Torres, R., Gascó, F., & Pesquero, M.D. (2012). A new Lower Cretaceous vertebrate bonebed near Ariño (Teruel, Aragón, Spain); found and managed in a joint collaboration between a mining company and a palaeontological park. *Geoheritage*, *4*(4), 275–286. https://doi.org/10.1007/s12371-012-0068-y

Álvarez-Parra, S., Delclòs, X., Solórzano-Kraemer, M. M., Alcalá, L., & Peñalver, E. (2020a). Cretaceous amniote integuments recorded through a taphonomic process unique to resins. *Scientific Reports*, *10*, 19840. https://doi.org/10.1038/s41598-020-76830-8

Álvarez-Parra, S., Peñalver, E., Nel, A., & Delclòs, X. (2020b). The oldest representative of the extant barklice genus *Psyllipsocus* (Psocodea: Trogiomorpha: Psyllipsocidae) from the Cenomanian amber of Myanmar. *Cretaceous Research*, *113*, 104480. https://doi.org/10.1016/j.cretres.2020.104480

Álvarez-Parra, S., Pérez-de la Fuente, R., Peñalver, E., Barrón, E., Alcalá, L., Pérez-Cano, J., Martín-Closas, C., Trabelsi, K., Meléndez, N., López Del Valle, R., Lozano, R. P., Peris, D., Rodrigo, A., Sarto i Monteys, V., Bueno-Cebollada, C. A., Menor-Salván, C., Philippe, M., Sánchez-García, A., Peña-Kairath, C., Arillo, A., Espílez, E., Mampel, L., & Delclòs, X. (2021). Dinosaur bonebed amber from an original swamp forest soil. *eLife*, *10*, e72477. https://doi.org/10.7554/eLife.72477

Álvarez-Parra, S., Peñalver, E., Nel, A., & Delclòs, X. (2022). New barklice (Psocodea: Trogiomorpha) from Lower Cretaceous Spanish amber. *Papers in Palaeontology*, *8*(3), e1436. https://doi.org/10.1002/spp2.1436

Arillo, A., Blagoderov, V., & Peñalver, E. (2018). Early Cretaceous parasitism in amber: A new species of *Burmazelmira* fly (Diptera: Archizelmiridae) parasitized by a *Leptus* sp. mite (Acari, Erythraeidae). *Cretaceous Research*, *86*, 24–32. https://doi.org/10.1016/j.cretres.2018.02.006

Arillo, A., Subías, L. S., & Álvarez-Parra, S. (2022). First fossil record of the oribatid family Liacaridae (Acariformes: Gustavioidea) from the lower Albian amber-bearing site of Ariño (eastern Spain). *Cretaceous Research*, *131*, 105087. https://doi.org/10.1016/j.cretres.2021.105087

Azar, D., & Nel, A. (2011). The oldest psyllipsocid booklice, in Lower Cretaceous amber from Lebanon (Psocodea, Trogiomorpha, Psocathropetae, Psyllipsocidae). *ZooKeys*, *130*, 153–165. https://doi.org/10.3897/zookeys.130.1430

Azar, D., Nel, A., & Perrichot, V. (2015). Diverse barklice (Psocodea) from Late Cretaceous Vendean amber. *Paleontological Contributions*, *2014*(10C), 9–15. https://doi.org/10.17161/PC.1808.15983

Azar, D., Hakim, M., & Huang, D. (2016). A new compsocid booklouse from the Cretaceous amber of Myanmar (Psocodea: Troctomorpha: Amphientometae: Compsocidae). *Cretaceous Research*, *68*, 28–33. https://doi.org/10.1016/j.cretres.2016.08.003

Badonnel, A. (1951). Psocoptères. In P. -P. Grassé (Ed.), *Traité de Zoologie* (pp. 1301–1340). Masson & Cie, vol. 10, fasc. 2.

Badonnel, A. (1967). Psocoptères édaphiques du Chili (2e note). *Biologie de l'Amérique australe*, *3*, 541–585.

Banks, N. (1930). Some new Neotropical neuropteroid insects. *Psyche*, *37*, 183–191. https://doi.org/10.1155/1930/89823

Barrón, E., Peyrot, D., Rodríguez-López, J. P., Meléndez, N., López Del Valle, R., Najarro, M., Rosales, I., & Comas-Rengifo, M. J. (2015). Palynology of Aptian and upper Albian (Lower Cretaceous) amber-bearing outcrops of the southern margin of the Basque-Cantabrian basin (northern Spain). *Cretaceous Research*, *52*, 292–312. https://doi.org/10.1016/j.cretres.2014.10.003

Baz, A., & Ortuño, V. M. (2000). Archaeatropidae, a new family of Psocoptera from the Cretaceous amber of Alava, Northern Spain. *Annals of the Entomological Society of America*, *93*(3), 367–373. https://doi.org/10.1603/0013-8746(2000)093[0367:AANFOP]2.0.CO;2

Baz, A., & Ortuño, V. M. (2001a). A new electrentomoid psocid (Psocoptera) from the Cretaceous amber of Alava (Northern Spain). *Deutsche Entomologische Zeitschrift*, *48*, 27–32. https://doi.org/10.1002/dez.200100004

Baz, A., & Ortuño, V. M. (2001b). New genera and species of empheriids (Psocoptera: Empheriidae) from the Cretaceous amber of Alava, northern Spain. *Cretaceous Research*, *22*(5), 575–584. https://doi.org/10.1006/cres.2001.0275

Bouju, V., & Perrichot, V. (2020). A review of amber and copal occurrences in Africa and their paleontological significance. *BSGF-Earth Sciences Bulletin, 191*(1), 17. https://doi.org/10.1051/bsgf/2020018

Clarke, D. J., Limaye, A., McKenna, D. D., & Oberprieler, R. G. (2019). The weevil fauna preserved in Burmese amber—snapshot of a unique, extinct lineage (Coleoptera: Curculionoidea). *Diversity, 11*(1), 1. https://doi.org/10.3390/d11010001

Cockerell, T. D. A., (1916). Insects in Burmese amber. *American Journal of Science, 42*, 135–138. https://doi.org/10.2475/ajs.s4-42.248.135

Cockx, P., McKellar, R., Tappert, R., Vavrek, M., & Muehlenbachs, K. (2020). Bonebed amber as a new source of paleontological data: The case of the Pipestone Creek deposit (Upper Cretaceous), Alberta, Canada. *Gondwana Research, 81*, 378–389. https://doi.org/10.1016/j.gr.2019.12.005

Corral, J. C., López Del Valle, R., & Alonso, J. (1999). El ámbar cretácico de Álava (Cuenca Vasco-Cantábrica, norte de España). Su colecta y preparación. *Estudios del Museo de Ciencias Naturales de Álava, 14*, 7–21.

Dalgleish, R. C., Palma, R. L., Price, R. D., & Smith, V. S. (2006). Fossil lice (Insecta: Phthiraptera) reconsidered. *Systematic Entomology, 31*(4), 648–651. https://doi.org/10.1111/j.1365-3113.2006.00342.x

Delclòs, X., Peñalver, E., Ranaivosoa, V., & Solórzano-Kraemer, M. M. (2020). Unravelling the mystery of "Madagascar copal": Age, origin and preservation of a Recent resin. *PLOS ONE, 15*(5), e0232623. https://doi.org/10.1371/journal.pone.0232623

de Moya, R. S., Yoshizawa, K., Walden, K. K., Sweet, A. D., Dietrich, C. H., & Kevin P. J. (2021). Phylogenomics of parasitic and nonparasitic lice (Insecta: Psocodea): Combining sequence data and exploring compositional bias solutions in next generation data sets. *Systematic Biology, 70*, 719–738. https://doi.org/10.1093/sysbio/syaa075

Elias, S. A. (2014). Environmental interpretation of fossil insect assemblages from MIS 5 at Ziegler Reservoir, Snowmass Village, Colorado. *Quaternary Research, 82*(3), 592–603. https://doi.org/10.1016/j.yqres.2014.01.005

Enderlein, G. (1905). Morphologie, Systematik und Biologie der Atropiden und Troctiden, sowie Zusammenstellung aller bisher bekannten recenten und fossilen Formen. In L. A. Jägerskiöld (Ed.), *Results of the Swedish Zoological Expedition to Egypt and the White Nile, 1901* (pp. 1–58). The Library of the Royal University of Uppsala, vol. 2, n. 18.

Enderlein, G. (1911). Die Fossilen Copeognathen und ihre Phylogenie. *Palaeontographica, 58*, 279–360.

Enderlein, G. (1926). Die Copeognathen-Fauna Javas. *Zoologische Mededeelingen, 9*, 50–70.

Enderlein, G. (1931). Die Copeognathen Fauna der Seychellen. *Transactions of the Linnean Society of London 2nd Series Zoology, 19*(2), 207–240. https://doi.org/10.1111/j.1096-3642.1931.tb00127.x

García-Mondéjar, J. (1982). Aptiense y Albiense. In A. Alonso, C. Arias, A. García, R. Mas, R. Rincón, & L. Vilas (Eds.), *El Cretácico de España (pp. 63–84)*. Editorial Universidad Complutense de Madrid.

Grimaldi, D., & Engel, M. S. (2006). Fossil Liposcelididae and the lice ages (Insecta: Psocodea). *Proceedings of the Royal Society B: Biological Sciences, 273*(1586), 625–633. https://doi.org/10.1098/rspb.2005.3337

Grimaldi, D. A., & Vea, I. M. (2021). Insects with 100 million-year-old dinosaur feathers are not ectoparasites. *Nature Communications, 12*, 1469. https://doi.org/10.1038/s41467-021-21751-x

Hakim, M., Azar, D., & Huang, D. (2020). A unique manicapsocid (Psocodea: Amphientometae) from the mid-Cretaceous Burmese amber. *Cretaceous Research, 107*, 104278. https://doi.org/10.1016/j.cretres.2019.104278

Hakim, M., Huang, D. -Y., & Azar, D. (2021). New fossil psocids from Cretaceous Siberian ambers (Psocodea: Trogiomorpha: Atropetae). *Palaeoentomology, 4*(2), 186–198. https://doi.org/10.11646/PALAEOENTOMOLOGY.4.2.8

Hakim, M., Huang, D. -Y., & Azar, D. (2022). Earliest record of Prionoglarididae from the Lower Cretaceous Lebanese amber (Psocodea; Trogiomorpha). *Cretaceous Research, 132*, 105121. https://doi.org/10.1016/j.cretres.2021.105121

Heine, C., Müller, R. D., Gaina, C., Clift, P., Kuhnt, W., Wang, P., & Hayes, D. (2004). Reconstructing the lost eastern Tethys ocean basin: Convergence history of the SE Asian margin and marine gateways. *Continent-Ocean Interactions Within East Asian Marginal Seas*. *Geophysical Monograph Series, 149*, 37–54. https://doi.org/10.1029/149GM03

Hennig, W. (1966). *Phylogenetic systematics*. University of Illinois Press.

Johnson, K. P., Dietrich, C. H., Friedrich, F., Beutel, R. G., Wipfler, B., Peters, R. S., Allen, J. M., Petersen, M., Donath, A., Walden, K. K. O., Kozlov, A. M., Podsiadlowski, L., Mayer, C., Meusemann, K., Vasilikopoulos,

A., Waterhouse, R. M., Cameron, S. L., Weirauch, C., Swanson, D. R., Percy, D. M., Hardy, N. B., Terry, I., Liu, S., Zhou, X., Misof, B., Robertson, H. M., & Yoshizawa, K. (2018). Phylogenomics and the evolution of hemipteroid insects. *Proceedings of the National Academy of Sciences*, *115*(50), 12775–12780. https://doi.org/10.1073/pnas.1815820115

Jouault, C., Yoshizawa, K., Hakim, M., Huang, D., & Nel, A. (2021). New psocids (Psocodea: Prionoglarididae, Psyllipsocidae) from Cretaceous Burmese amber deposits. *Cretaceous Research*, *126*, 104890. https://doi.org/10.1016/j.cretres.2021.104890

Li, S., Wang, Q., Ren, D., & Yao, Y. (2020). New genus and species of Empheriidae (Psocodea: Trogiomorpha) from mid-Cretaceous amber of northern Myanmar. *Cretaceous Research*, *110*, 104421. https://doi.org/10.1016/j.cretres.2020.104421

Li, S., Yoshizawa, K., Wang, Q., Ren, D., Bai, M., & Yao, Y. (2022). New genus and species of† Empheriidae (Insecta: Psocodea: Trogiomorpha) and their implication for the phylogeny of infraorder Atropetae. *Frontiers in Ecology and Evolution*, *10*, 907903. https://doi.org/10.3389/fevo.2022.907903

Liang, F., & Liu, X. (2021). A new species of *Psyllipsocus* (Psocodea: Trogiomorpha: Psyllipsocidae) from the mid-Cretaceous amber of Myanmar. *Zootaxa*, *5072*(1), 81–87. https://doi.org/10.11646/zootaxa.5072.1.9

Maheu, A., & Nel, A. (2020). A new fossil booklouse (psocodea: Troctomorpha: Amphientometae: Manicapsocidae) from the mid-Cretaceous amber of northern Myanmar. *Cretaceous Research*, *106*, 104222. https://doi.org/10.1016/j.cretres.2019.104222

Mas, R., García, A., Salas, R., Meléndez, A., Alonso, A., Aurell, M., Bádenas, B., Benito, M. I., Carenas, B., García-Hidalgo, J. F., Gil, J., & Segura, M. (2004). Segunda fase de rifting: Jurásico Superior-Cretácico Inferior. In J. A. Vera (Ed.), Geología de España (pp. 503–551). Sociedad Geológica de España and Instituto Geológico y Minero de España.

Mockford, E. L. (1967). The electrentomoid Psocids (Psocoptera). *Psyche*, *74*, 118–163. https://doi.org/10.1155/1967/862560

Mockford, E. L. (1993). *North American Psocoptera (Insecta)*. Sandhill Crane Press.

Mockford, E. L. (1996). Character analysis of the Western Hemisphere genera of family Manicapsocidae (Psocoptera): Genus *Epitroctes* reinstated with descriptions of four new species. *Insecta Mundi*, *10*, 169–180.

Mockford, E. L., Lienhard, C., & Yoshizawa, K. (2013). Revised classification of 'Psocoptera' from Cretaceous amber, a reassessment of published information. *Insecta Matsumurana New series*, *69*, 1–26.

Morley, C. K., Chantraprasert, S., Kongchum, J., & Chenoll, K. (2021). The West Burma Terrane, a review of recent paleo-latitude data, its geological implications and constraints. *Earth-Science Reviews*, *220*, 103722. https://doi.org/10.1016/j.earscirev.2021.103722

Najarro, M., Peñalver, E., Rosales, I., Pérez-de la Fuente, R., Daviero-Gómez, V., Gómez, B., & Delclós, X. (2009). Unusual concentration of Early Albian arthropod-bearing amber in the Basque-Cantabrian Basin (El Soplao, Cantabria, Northern Spain): Palaeoenvironmental and palaeobiological implications. *Geologica Acta*, *7*(3), 363–388. https://doi.org/10.1344/105.000001443

Nel, A., & Waller, A. (2007). The first fossil Compsocidae from Cretaceous Burmese amber (Insecta, Psocoptera, Troctomorpha). *Cretaceous Research*, *28*, 1039–1041. https://doi.org/10.1016/j.cretres.2007.02.002

Nel, A., De Ploëg, G., & Azar, D. (2004). The oldest Liposcelididae in the lowermost Eocene amber of the Paris Basin (Insecta: Psocoptera). *Geologica Acta*, *2*(1), 31–36.

Nel, A., Prokop, J., De Ploëg, G., & Millet, J. (2005). New Psocoptera (Insecta) from the lowermost Eocene amber of Oise, France. *Journal of Systematic Palaeontology*, *3*(4), 371–391. https://doi.org/10.1017/S1477201905001598

Nel, A., Roques, P., Nel, P., Prokin, A. A., Bourgoin, T., Prokop, J., Szwedo, J., Azar, D., Desutter-Grandcolas, L., Wappler, T., Garrouste, R., Coty, D., Huang, D., Engel, M. S., & Kirejtshuk, A. G. (2013). The earliest known holometabolous insects. *Nature*, *503*(7475), 257–261. https://doi.org/10.1038/nature12629

New, T. R. (1987). Biology of the Psocoptera. *Oriental Insects*, *21*(1), 1–109. https://doi.org/10.1080/00305316.1987.11835472

New, T. R., & Lienhard, C. (2007). *The Psocoptera of tropical South-east Asia*. National Museum of Natural History Naturalis, Brill.

Ngô-Muller, V., Garrouste, R., & Nel, A. (2020). Small but important: A piece of mid-Cretaceous Burmese amber with a new genus and two new insect species (Odonata: Burmaphlebiidae & 'Psocoptera': Compsocidae). *Cretaceous Research*, *110*, 104405. https://doi.org/10.1016/j.cretres.2020.104405

Ortega-Blanco, J., Delclòs, X., & Engel, M. S. (2011). Diverse stigmaphronid wasps in Early Cretaceous amber from Spain (Hymenoptera: Ceraphronoidea: Stigmaphronidae). *Cretaceous Research, 32*(6), 762–773. https://doi.org/10.1016/j.cretres.2011.05.004

Pearman, J. V. (1936). The taxonomy of the Psocoptera: Preliminary sketch. *Proceedings of the Royal Entomological Society of London (B), 5*, 58–62. http://doi.org/10.1111/j.1365-3113.1936.tb00596.x

Peñalver, E., Nel, A., & Martínez-Delclòs, X. (1996). Insectos del Mioceno inferior de Ribesalbes (Castellón, España). Paleoptera y Neoptera poli- y paraneoptera. *Treballs del Museu de Geologia de Barcelona, 5*, 15–95.

Peñalver, E., Arillo, A., Delclòs, X., Peris, D., Grimaldi, D. A., Anderson, S. R., Nascimbene, P. C., & Pérez-de la Fuente, R. (2017). Ticks parasitised feathered dinosaurs as revealed by Cretaceous amber assemblages. *Nature Communications, 8*, 1924. https://doi.org/10.1038/s41467-017-01550-z

Pérez-de la Fuente, R., Delclòs, X., Peñalver, E., & Arillo, A. (2011). Biting midges (Diptera: Ceratopogonidae) from the Early Cretaceous El Soplao amber (N Spain). *Cretaceous Research, 32*(6), 750–761. https://doi.org/10.1016/j.cretres.2011.05.003

Peris, D., & Jelínek, J. (2020). Syninclusions of two new species of short-winged flower beetle (Coleoptera: Kateretidae) in mid-Cretaceous Kachin amber (Myanmar). *Cretaceous Research, 106*, 104264. https://doi.org/10.1016/j.cretres.2019.104264

Peris, D., Chatzimanolis, S., & Delclòs, X. (2014). Diversity of rove beetles (Coleoptera: Staphylinidae) in Early Cretaceous Spanish amber. *Cretaceous Research, 48*, 85–95. https://doi.org/10.1016/j.cretres.2013.11.008

Peris, D., Ruzzier, E., Perrichot, V., & Delclòs, X. (2016). Evolutionary and paleobiological implications of Coleoptera (Insecta) from Tethyan-influenced *Cretaceous ambers. Geoscience Frontiers*, *7*(4), 695–706. https://doi.org/10.1016/j.gsf.2015.12.007

Roesler, R. (1940). Neue und wenig bekannte Copeognathengattungen. I. *Zoologischer Anzeiger, 129*, 225–243.

Sánchez-García, A., & Engel, M. S. (2016). Springtails from the Early Cretaceous amber of Spain (Collembola: Entomobryomorpha), with an annotated checklist of fossil Collembola. *American Museum Novitates, 2016*(3862), 1–47. https://doi.org/10.1206/3862.1

Santer, M., Álvarez-Parra, S., Nel, A., Peñalver, E., & Delclòs, X. (2022). New insights into the enigmatic Cretaceous family Spathiopterygidae (Hymenoptera: Diaprioidea). *Cretaceous Research, 133*, 105128. https://doi.org/10.1016/j.cretres.2021.105128

Smithers, C. N. (1972). The classification and phylogeny of the Psocoptera. *Australian Museum Memoir, 14*, 1–349.

Smithers, C. N. (1990). Keys to the families and genera of Psocoptera (Arthropoda, Insecta). *Technical Reports of the Australian Museum, 2*, 1–82.

Sroka, P., & Nel, A. (2017). New species of Compsocidae (Insecta, Psocodea) from Cretaceous Burmese amber. *Zootaxa, 4320*, 597–600. https://doi.org/10.11646/zootaxa.4320.3.12

Stilwell, J. D., Langendam, A., Mays, C., Sutherland, L. J., Arillo, A., Bickel, D. J., De Silva, W. T., Pentland, A. H., Roghi, G., Price, G. D., Cantrill, D. J., Quinney, A., & Peñalver, E. (2020). Amber from the Triassic to Paleogene of Australia and New Zealand as exceptional preservation of poorly known terrestrial ecosystems. *Scientific Reports, 10*, 5703. https://doi.org/10.1038/s41598-020-62252-z

Tibert, N. E., Colin, J. P., Kirkland, J. I., Alcalá, L., & Martín-Closas, C. (2013). Lower Cretaceous nonmarine ostracodes from an Escucha Formation dinosaur bonebed in eastern Spain. *Micropaleontology, 59*(1), 83–91.

Vajda, V., Pesquero Fernández, M. D., Villanueva-Amadoz, U., Lehsten, V., & Alcalá, L. (2016). Dietary and environmental implications of Early Cretaceous predatory dinosaur coprolites from Teruel, Spain. *Palaeogeography, Palaeoclimatology, Palaeoecology, 464*, 134–142. https://doi.org/10.1016/j.palaeo.2016.02.036

Villanueva-Amadoz, U., Sender, L. M., Alcalá, L., Pons, D., Royo-Torres, R., & Diez, J. B. (2015). Paleoenvironmental reconstruction of an Albian plant community from the Ariño bonebed layer (Iberian Chain, NE Spain). *Historical Biology, 27*(3–4), 430–441. https://doi.org/10.1080/08912963.2014.895826

Vishniakova, V. N. (1975). Psocoptera in Late-Cretaceous insect-bearing resins from the Taimyr. *Entomological Review, 54*, 63–75.

Wappler, T., Smith, V. S., & Dalgleish, R. C. (2004). Scratching an ancient itch: an Eocene bird louse fossil. *Proceedings of the Royal Society of London. Series B: Biological Sciences 271*(Suppl. 5), S255–S258. https://doi.org/10.1098/rsbl.2003.0158

Westerweel, J., Roperch, P., Licht, A., Dupont-Nivet, G., Win, Z., Poblete, F., Ruffet, G., Swe, H. H., Thi, M. K., & Aung, D. W. (2019). Burma Terrane part of the Trans-Tethyan arc during collision with India according to palaeomagnetic data. *Nature Geoscience, 12*, 863–868. https://doi.org/10.1038/s41561-019-0443-2

Yoshizawa, K. (2000). Redescription of *Mepleres suzukii* (Okamoto), with comments on synonymy among *Mepleres*, *Pseudoscottiella* and *Meniscopsocus* (Psocodea: 'Psocoptera': Pseudocaeciliidae). *Entomological Science, 3*, 669–674.

Yoshizawa, K., & Yamamoto, S. (2021). The earliest fossil record of the suborder Psocomorpha (Insecta: Psocodea) from mid-Cretaceous Burmese amber, with description of a new genus and species. *Insecta Matsumurana New series, 77*, 1–15.

Yoshizawa, K., Lienhard, C., Yao, I., & Ferreira, R. L. (2019). Cave insects with sex-reversed genitalia had their most recent common ancestor in West Gondwana (Psocodea: Prionoglarididae: Speleketorinae). *Entomological Science, 22*(3), 334–338. https://doi.org/10.1111/ens.12374

Anexo 8.1.13

Serphitid wasps (Hymenoptera: Serphitidae) from Early Cretaceous amber of eastern Spain with comments on the evolution and palaeobiology of Serphitoidea

Álvarez-Parra, S., Santer, M., *et al.* en preparación*. Serphitid wasps (Hymenoptera: Serphitidae) from Early Cretaceous amber of eastern Spain with comments on the evolution and palaeobiology of Serphitoidea.

* El manuscrito se encuentra en la fase intermedia de su preparación. Dado que es un trabajo aún no publicado, se han retirado los nombres de los nuevos taxones descritos. No se han incluido las figuras ni los pies de figura. Se ha preferido no indicar los nombres ni el orden de todos los autores.

Serphitid wasps (Hymenoptera: Serphitidae) from Early Cretaceous amber of eastern Spain with comments on the evolution and palaeobiology of Serphitoidea

Sergio Álvarez-Parra [a, b *], Maxime Santer [a, b], et al.

[a] Departament de Dinàmica de la Terra i de l'Oceà, Facultat de Ciències de la Terra, Universitat de Barcelona, c/ Martí i Franquès s/n, 08028, Barcelona, Spain
[b] Institut de Recerca de la Biodiversitat (IRBio), Universitat de Barcelona, Barcelona, Spain

[*] Corresponding author email: sergio.alvarez-parra@ub.edu

Abstract

Keywords:

1. Introduction

[Section not finished]

The Serphitidae Brues, 1937 are a small family of extinct wasps, including 23 species in 8 genera (Table 1). This family contains three subfamilies, Microserphitinae Engel, 2015, Supraserphitinae Rasnitsyn and Öhm-Kühnle, 2018 and Serphitinae Brues, 1937, the Serphitidae lived in the Cretaceous period and were present in all the northern hemisphere, having been found in ambers from Lebanon, Myanmar, Russia, Spain, France, Canada, and the USA. The oldest known representatives are known from the Barremian (Rasnitsyn et al., 2022), and they are found up to the Campanian (Brues, 1937, McKellar and Engel, 2011).

Serphitids are described as parasitoids by phylogenic inferences. Even though relatively few specimens are currently described, Serphitidae were common, and a lot of specimens are undescribed. The family was poorly known until 2011, when several papers started to be published, with an acceleration in the release of studies since 2018, with 6 papers released in 4 years. Serphitidae are within the superfamily Serphitoidea (Brues, 1935), alongside Archaeoserphitidae (Engel, 2015). They are included in Bipetiolarida (Engel, 2015), alongside Mymarommatoidea according to Engel (2015).

The behaviour of many fossil families is assumed based solely on phylogenetic inferences, without further investigation of whether these assumptions are consistent with the morphology of these animals.

Here we describe a new genus and species of Serphitidae, and two new species of *Serphites*. These specimens come from the upper Albian San Just amber-bearing outcrop (eastern Iberian Peninsula). The new genus represents the ninth genus described from this family, and the two new species of *Serphites* are the thirteenth and fourteenth species of this genus, respectively. Four *Serphites* species are now known from the Albian of Spain, for a total of seven species within Serphitoidea, and it shows the diversity of this family in deep times. We discuss the phylogeny and the supposed paleoethology of the family, providing new comments on the paleobiology. We also add new insights on the general evolution of the family.

2. Material and methods

The specimens studied here are included in amber from the outcrops of Ariño and San Just, both in Teruel Province (Aragón, Spain). These amber-bearing outcrops are located in the Maestrazgo Basin in eastern Spain (Fig. 1), corresponding to the Aragonese Branch of the Iberian Chain (Salas and Guimerà, 1996). Although more than 30 amber-bearing outcrops have been reported in the basin, only the ambers from Ariño, San Just, Arroyo de la Pascueta and La Hoya have yielded bioinclusions (Peñalver and Delclòs, 2010; Álvarez-Parra et al., 2021). The Ariño outcrop is within the Santa María open-pit coal mine in the Oliete Sub-basin and has provided a rich and diverse fossil record from the level AR-1 (Alcalá et al., 2012). This level belongs to the Escucha Formation and has been dated as lower Albian (Alcalá et al., 2012; Villanueva-Amadoz et al., 2015; Álvarez-Parra et al., 2021). Interestingly, aerial amber rich in bioinclusions and dinosaur bones have been found together in this level, moreover the root amber pieces show characteristics indicating that they are in situ (Álvarez-Parra et al., 2021). The palaeoenvironment was inferred as a resiniferous forest in a freshwater swamp plain with marine influence under subtropical or tropical climate (Tibert et al., 2013; Villanueva-Amadoz et al., 2015; Álvarez-Parra et al., 2021). The record of bioinclusions from Ariño amber includes plant remains, arachnids, 11 insect orders, a fragment of dinosaur feather, and mammalian hair (Álvarez-Parra et al., 2020, 2021, 2022b; Arillo et al., 2022). The San Just amber-bearing outcrop is in the Las Parras (or Aliaga) Sub-basin (Peñalver et al., 2007). Firstly, it was assigned to the Escucha Formation, dated as was dated as middle–earliest upper Albian, and the palaeoenvironment was interpreted as a freshwater swamp plain (Peñalver et al., 2007; Villanueva-Amadoz et al., 2010). Nonetheless, a new biostratigraphic and palynological study would point out to an upper Albian age, an assignment to the Utrillas Group, and a different environmental interpretation. San Just amber has provided a record of fungal and plant remains, arachnids, 11 insect orders, and dinosaur feathers (Peñalver et al., 2007). Several hymenopteran species have been described from San Just amber (Álvarez-Parra et al., 2022a; Santer et al., 2022). Both Ariño and San Just ambers have been related to an Araucariaceae origin (Menor-Salván et al., 2016; Álvarez-Parra et al., 2021).

The amber pieces were cut, polished, and embedded in epoxy resin for allowing the visualisation and protection of the pieces (Corral et al., 1999). The specimens were examined using an Olympus CX41 compound microscope with camera lucida tube and sCMEX-20 digital camera attached. Photographs were processed with ImageFocusAlpha version 1.3.7.12967.20180920. The figures were prepared with Photoshop CS6. The descriptions follow the nomenclature from Goulet and Huber (1993) and Herbert and McKellar (2022). Here we consider that the pterostigma is delimited by Sc in its proximal edge and R in its hypostigmal edge, thus fuscous area extends from pterostigma midlength over crossvein r-rs to its joining with Rs. The studied material is deposited in the Museo Aragonés de Paleontología (Fundación Conjunto Paleontológico de Teruel-Dinópolis), Teruel, Spain.

3. Systematic palaeontology

Order Hymenoptera Linnaeus, 1758

Clade Bipetiolarida Engel, 2005

Superfamily Serphitoidea Brues, 1937
Family **Serphitidae** Brues, 1937
Subfamily Serphitinae Brues, 1937

Type genus: *Serphites* Brues, 1937.

Other genera: *Aposerphites* Kozlov and Rasnitsyn, 1979, *Buserphites* Herbert and McKellar, 2022, *Jubaserphites* McKellar and Engel, 2011, and *Mesoserphites* Herbert and McKellar, 2022.

Genus ***AAA*** gen. nov.

Type species: *AAA BBB* sp. nov., by present designation and monotypy.

Etymology.

Diagnosis. Body length of 1.40 mm; head nearly spherical; compound eyes small, occupying only nearly a third part of the head lateral length, dorsoventrally elongate; lateral ocellus rounded, broad and separated from eye margin by more than two times the ocellar diameter; antennae 9-segmented, filiform, emerging ventrally to the compound eyes; flagellomeres globular; pedicel curved; mesosoma slightly longer than gaster; metanotum with surface dorsally convex; forewing with narrow costal cell and highly pigmented pterostigma, triangular equilateral in shape; Rs reaching wing margin one pterostigmal width from apical margin of pterostigma in forewing; metacoxae globous about 1.5× longer than wide; trochantelli rectangular and elongate; metatarsus nearly as longer as metafemur; combined longitudes of second to fifth tarsomeres about 1.3× longer than basitarsus; first petiolar segment 1.5× longer than second petiolar segment; first petiolar segment rimmed posteriorly; first petiolar segment cylindrical, second petiolar segment globular; gaster dorsoventrally flattened.

AAA BBB sp. nov.
Figures 2 and 3

Type material. Holotype: SJ-10-12, sex unknown, syninclusion with a Diptera and a fragment of dinosaur feather. Housed at Museo Aragonés de Paleontología (Fundación Conjunto Paleontológico de Teruel Dinópolis) in Teruel, Spain.

Locality and horizon. San Just amber-bearing outcrop, Utrillas, Teruel Province, Spain; Escucha Formation or Utrillas Group, upper Albian (Peñalver et al., 2007).

Etymology.

Diagnosis. As for the genus.

Description. Body 1.40 mm long. Integument black, setae are not visible. Head globous, nearly spherical, 0.28 mm long; compound eyes small, occupying only nearly a third part of the head lateral length, dorsoventrally elongate, 0.08 mm long and 0.11 mm wide, numerous minute ommatidia are visible; right lateral ocellus rounded, broad, and separated from eye margin by more than two times the ocellar diameter: ocellar diameter of 0.02 mm, distance to compound eye of 0.05 mm; antennae 9-segmented, filiform (not clubbed), and emerging ventrally to the compound eyes; elongate scape, rectangular in shape, 0.09 mm long, 3× longer than wide; pedicel chalice-like in shape, curved, 0.06 mm long and 0.03 mm maximum wide; flagellum complete, but cut by a microfracture in the amber; first flagellomere chalice-like in shape; second to sixth flagellomeres globular; terminal flagellomere elongate and with a rounded apex; length-maximum width in mm of flagellomeres: 1f: 0.04-0.03, 2f: 0.05-0.04, 3f: 0.04-0.05, 4f: 0.03-0.04, 5f: 0.04-0.05, 6f: 0.05-0.05, 7f: 0.07-0.05; genae inflated; mouthpart not visible. Mesosoma 0.51 mm long, difficult to observed as it is covered by particles; mesoscutum prominent showing a humped aspect; metanotum with surface dorsally convex. Forewings with a marginal fringe of short setae and membrane covered by numerous microtrichia; thick and pigmented C and Sc+R, delimiting a narrow costal cell about 0.02 mm maximum wide; pterostigma triangular (equilateral) in shape and highly pigmented, about 0.15 mm wide; broad fuscous are extending form pterostigma midlength over r-rs to its join with Rs; vein Rs tubular and as pigmented as pterostigma, extending curved to wing margin, reaching obliquely; distance from apical part of pterostigma to Rs joining margin equal as pterostigma width; triangular radial cell delimited by Sc+R, M+Cu, and 1M, the latter reaching an expansion adjacent to the pterostigma together with Sc+R; vein Rs+M absent; vein M showing a slightly sinuous path; crossvein m-cu not visible; CuA curved, nebulous distal section close to wing margin; a thick sclerotisation along anal margin might correspond to A. Hind wings not preserved or obscure. Right midleg and left hind leg mostly complete, the other legs are partially preserved; legs thin and relatively long; mesocoxae rectangular, metacoxae globous about 1.5× longer than wide; trochantelli rectangular and elongate; femorae slightly swollen; tibiae thin and widened apically, apical spurs are not visible; tarsi pentamerous, poorly visible due to turbid amber; metatarsus nearly as longer as metafemur; combined longitudes of second to fifth tarsomeres about 1.3× longer than basitarsus; pretarsal claws and arolium not visible. Metasoma bipetiolate; first petiolar segment cylindrical and rimmed posteriorly, longitudinal striation not visible, maybe hindered by preservation darkening; first petiolar segment 1.5× longer than second petiolar segment, 0.12 mm and 0.08 mm long respectively; second petiolar segment globular; gaster dorsoventrally flattened, 0.41 mm long, segmentation undiscernible; genitalia obscure.

Discussion. [Section not finished]. The specimen bears resemblances with the genus *Aposerphites*, as the presence of a distinct pterostigma coupled with the first petiolar segment being less than twice the size that of the second petiolar segment, and having the lateral ocellus separated from eye margin more than one-half diameter or more. However, some characteristics are different enough to justify a new genus, as the head shape, the highly reduced diameter of the eyes, and the distance between the eye and the lateral ocellus, being separated from eye margin more than 2 ocellus diameters.

Genus ***Serphites*** Brues, 1937

Type species: *Serphites paradoxus* Brues, 1937.

Other species: *Serphites bruesi* McKellar and Engel, 2011, *Serphites dux* Kozlov and Rasnitsyn, 1979, *Serphites fannyae* Engel and Perrichot, 2014, *Serphites gigas* Kozlov and Rasnitsyn, 1979, *Serphites hynemani* McKellar and Engel, 2011, *Serphites kuzminae* McKellar and Engel, 2011, *Serphites lamiak* Ortega-Blanco, Delclòs, Peñalver and Engel, 2011, *Serphites navesinkae* Engel and Grimaldi, 2011 (in Engel et al., 2011), *Serphites pygmaeus* McKellar and Engel, 2011, *Serphites raritanensis* Engel and Grimaldi, 2011 (in Engel et al., 2011), *Serphites silban* Ortega-Blanco, Delclòs, Peñalver and Engel, 2011.

Serphites CCC sp. nov.
Figures 4 and 5

Type material. Holotype: SJNB2012-17, complete specimen, male, syninclusion with spiderweb strands (at least one in contact with the wasp). From San Just amber. Housed at Museo Aragonés de Paleontología (Fundación Conjunto Paleontológico de Teruel Dinópolis) in Teruel, Spain.

Locality and horizon. San Just amber-bearing outcrop, Utrillas, Teruel Province, Spain; Escucha Formation or Utrillas Group, upper Albian (Peñalver et al., 2007).

Etymology.

Diagnosis. Body length of 2.45 mm; antennae 12-segmented, clubbed from flagellomeres fifth to terminal; mesosoma and gaster nearly the same longitude; forewings with highly pigmented pterostigma, triangular equilateral in shape; straight distal sections of Rs and M in forewings; metacoxae 2× longer than wide; metatrochantelli globous; tibiae with one sharp, apical spur; metatarsus about 1.3× longer than metafemur; combined longitudes of second to fifth tarsomeres about 1.4× longer than basitarsus; first segment of petiole rimmed and longitudinally striated, about 2.2× longer than second segment; gaster nearly as long as mesosoma, 2× longer than wide.

Description. Male. Body 2.45 mm long. Integument dark brown or black, covered by fine setae. Head globous 0.41 mm long and 0.57 mm wide; large compound eyes covering most of the sides of the head about 0.27 mm in diameter, formed by numerous minute ommatidia; central ocellus prominent and larger than lateral ocelli, the latter separated about 0.05 mm from compound eyes; antennae 12-segmented; elongate scape, rectangular in shape, 0.17 mm long, 3× longer than wide; pedicel slightly narrowed at the base, 0.07 mm long and 0.04 mm maximum wide; first flagellomere chalice-like in shape; second to ninth flagellomeres nearly square in shape, slightly wider than long; terminal flagellomere elongate and with a rounded and acute apex; fifth to terminal flagellomeres forming a club; length-maximum width in mm of flagellomeres: 1f: 0.05-0.04, 2f: 0.03-0.04, 3f: 0.03-0.04, 4f: 0.04-0.05, 5f: 0.04-0.06, 6f:

0.05-0.07, 7f: 0.05-0.08, 8f: 0.07-0.07, 9f: 0.05-0.07, 10f: 0.08-0.05; genae inflated; black, prominent mandibles, with a metallic sheen; right mandible with three long, sharp, and curved teeth, central one slightly shorter and broader; left mandible bidentate, covered by thin setae or spines, two teeth shorter and broader in base that those from right mandible, both curved and with the same longitude; other mouthparts obscure, although labial palps might be discerned. Mesosoma 0.86 mm long, dorsal and ventral surfaces difficult to observe due to preservation darkening. Forewings with a marginal fringe of short setae and membrane covered by numerous microtrichia; thick, slightly pigmented C along margin reaching a highly pigmented, black pterostigma triangular (equilateral) in shape, 0.21 mm wide; Sc+R slightly curved and extending to the pterostigma forming a closed costal cell about 0.04 mm maximum wide; tubular fuscous area extending from pterostigmal midlength and adjacent to the joining of crossvein r-rs and Rs; triangular radial cell delimited by highly pigmented Sc+R, M+Cu, and 1M, the latter reaching an expansion adjacent to the pterostigma together with Sc+R; vein Rs+M absent; straight distal section of Rs, reaching margin; distance from apical part of pterostigma to the joining of Rs with margin about the same length of pterostigma; straight distal section of M, reaching margin; anterior section of Cu highly pigmented; crossvein m-cu nebulous; straight CuA reaching margin; veins CuP and A indiscernible. Hind wings with marginal fringe of short setae and membrane covered by numerous microtrichia; vein C+Sc+R highly pigmented along costal margin, with three apical hamuli. Legs thin and covered by fine setae, right anterior leg is missing; metacoxae 2× longer than wide; metatrochantelli globous, pro- and mesotrochantelli thinner and longer; femorae swollen; tibiae thin although widened towards apical part, with one sharp apical spur; tarsi pentamerous; metatarsus about 1.3× longer than metafemur; all tarsomeres with two apical, short spurs; combined longitudes of second to fifth tarsomeres about 1.4× longer than basitarsus; two pretarsal claws simple with wide arolium. Metasoma bipetiolate; first petiolar segment striate (visible under high incident light) and rimmed anteriorly; first petiolar segment about 2.2× longer than second segment, 0.24 mm and 0.11 mm long respectively; first petiolar segment rectangular in shape, second segment nearly square; elongate gaster 0.83 mm long, nearly as long as mesosoma, 2× longer than maximum wide; terga and sterna smooth, although several punctures at midlength of gaster in terga; gaster apparently 5-segmented in dorsal view, with first two segments longer than the rest; genitalia covered by setae longer than the rest of the gaster, with an acute protuberance in the right side and an structure than might correspond to the aedeagus.

Discussion. [Section not finished]. Clubbed antenna would indicate that it is a male. The habitus of the holotype allows to assign it to the genus *Serphites*, within Serphitidae. The holotype shows key differences with the other *Serphites* species from Spanish amber.

***Serphites DDD* sp. nov.**

Figures 6–8

Type material. Holotype: AR-1-A-2019.94.8, sex unknown, syninclusion with five Hymenoptera, two Diptera, one Thysanoptera, one Coleoptera, and other specimen of the new species.

Additional material. AR-1-A-2019.43.2, sex unknown, syninclusion with a Diptera and a Hymenoptera; AR-1-A-2019.94.5, sex unknown. Both amber pieces are milky and highly turbid, so many anatomic characters are obscure. Housed at Museo Aragonés de Paleontología (Fundación Conjunto Paleontológico de Teruel Dinópolis) in Teruel, Spain.

Locality and horizon. Level AR-1 of the Ariño amber-bearing outcrop, in mina Santa María, Ariño, Teruel Province, Spain; Escucha Formation, lower Albian (Álvarez-Parra et al. 2021).

Etymology.

Diagnosis. Body length 1.98mm; head antero-posteriorly flattened; gaster approximately equals to mesosoma; forewings with highly pigmented pterostigma, triangular equilateral in shape; Rs slightly curved at the wing margin, Rs before pterostigma basally truncated without contact with M, forewing length/forewing width ratio equals or greater than 2 (1.64 in *S. bruesi*), hindwing length/hindwing width ratio approximately 3.5 (6 in *S. bruesi*); metacoxae 1.5× longer than wide metatrochantelli slightly elongated; mesotibiae with one sharp apical spur; metatarsus longer than metafemur; first petiolar segment rectangular in shape, rimmed anteriorly, and longitudinally striated, about 2.8× longer than second segment; gaster nearly as long as mesosoma, nearly rounded in dorsal view and dorsoventrally flattened in lateral view.

Description. Holotype AR-1-A-2019.94.8 body length of 1.98 mm, specimen AR-1-A-2019.43.2 body length of 2.10 mm, and specimen AR-1-A-2019.94.5 body length of 2.39 mm. Integument dark brown, covered by fine setae. Head of holotype AR-1-A-2019.94.8 and specimen AR-1-A-2019.94.5 difficult to see due to turbid amber; head of specimen AR-1-A-2019.43.2 antero-posteriorly flattened, vertex seemingly with minute polygonal microsculpture, lateral ocelli oval 0.05×0.03 mm, separated for 0.04 mm from large compound eyes 0.23 mm in diameter; antennae of specimen AR-1-A-2019.43.2 composed by 12 antennomeres somewhat clubbed, antennae of holotype AR-1-A-2019.94.8 and specimen AR-1-A-2019.94.5 with at least 8 flagellomeres, although difficult to discern at base, not clubbed in the two latter; in specimen AR-1-A-2019.43.2 basal flagellomeres seem to be longer than apical ones, scape and pedicel difficult to see, forth to ninth flagellomeres are nearly square in shape, terminal flagellomere elongate and with a rounded and acute apex, length-width in mm of clearly visible flagellomeres: 4f: 0.05-0.05, 5f: 0.06-0.06, 6f: 0.05-0.07, 7f: 0.05-0.07, 8f: 0.05-0.07, 9f: 0.06-0.06, 10f: 0.09-0.05; genae inflated; mandibles visible in specimen AR-1-A-2019.43.2, right mandible tridentate, although one lateral tooth is broken, central tooth shorter than lateral, left mandible bidentate, one tooth seems to be shorter than the other, interestingly right mandible is black, while left mandible is white, probably due to preservation; other mouthpart obscure on the three specimens. Mesosoma 0.63 mm long in holotype AR-1-A-2019.94.8 and 0.79 mm long in specimen AR-1-A-2019.43.2, both with mesoscutum prominent, a polygonal microsculpture can be seen in propodeum of holotype AR-1-A-2019.94.8. Description of wings is based on holotype AR-1-A-2019.94.8. Forewings approximately 1.20 mm long and 0.54 mm wide, with a marginal fringe of short setae and membrane covered by numerous microtrichia; vein C pigmented and extending along margin

to pterostigma, delimiting with a highly pigmented Sc+Rs narrow costal cell 0.02 mm maximum wide; pterostigma triangular (equilateral) in shape, 0.23 mm wide; tubular fuscous area covering crossvein r-rs and extending to its joining with Rs; triangular and relatively narrow radial cell; veins M+Cu and 1M highly pigmented; vein Rs+M absent; Rs extending curved and reaching wing margin obliquely; distance from apical part of pterostigma to joing of Rs with margin longer than pterostigma width; vein M extending straight and curved distally towards anterior margin, reaching margin; crossvein m-cu present; vein CuA extending straight and distally curved towards posterior margin; veins CuP and A not visible; interestingly the forewing venation of specimen AR-1-A-2019.43.2 seems to be somewhat different probably due to preservation artefact, lacking radial cell; forewing venation of AR-1-A-2019.94.5 is very similar to that of the holotype. Hind wings 0.7 mm long and 0.20 mm wide, with marginal fringe of short setae and membrane covered by numerous microtrichia; vein C+Sc+R highly pigmented along costal margin; hamuli cannot be discerned. Legs poorly visible and partially preserved in the three specimens; metacoxae 1.5× wider than long; mesotrochatelli seem to be somewhat elongate, while metatrochantelli are nearly globular in shape; tibiae as wide as femora; one apical tibial spur can be seen in left mesotibia of holotype AR-1-A-2019.94.8; tarsi pentamerous; hind leg of AR-1-A-2019.94.5 with combined longitudes of second to fifth tarsomeres about 1.2× longer than basitarsus; two pretarsal claws and wide arolium present. Petiole well visible in holotype AR-1-A-2019.94.8; first petiolar segment rectangular in shape, rimmed anteriorly, and longitudinally striated; second petiolar segment globular; first petiolar segment about 2.8× longer than second petiolar segment; gaster 0.65 mm long in holotype AR-1-A-2019.94.8 and 0.73 mm long in specimen AR-1-A-2019.43.2, nearly as long as mesosoma in both specimens; gaster nearly rounded in dorsal view and dorsoventrally flattened in lateral view; gaster covered by fine setae and apparently 5-segmented in dorsal view, with first segment longer than the rest; genitalia obscure, although there is an acute protuberance at the distal part of gaster in holotype AR-1-A-2019.94.8 and specimen AR-1-A-2019.43.2.

Discussion. [Section not finished]. The slightly clubbed antennae on specimen AR-1-A-2019.43.2 might indicate that this specimen is a male. However, the shape of the gaster is like that of holotype AR-1-A-2019.94.8. The holotype is the smallest one, typical of males, but it does not bear clubbed antennae. The poor preservation of the other two specimens makes their identification difficult, so they were not used as paratypes. The specimen AR-1-A-2019.94.5 is present in the same amber piece as the holotype specimen, and the preserved characteristics are compatible with the description of *Serphites DDD* sp. nov., so the specimen is considered conspecific. The specimen AR-1-A-2019.43.2 have a combination of characteristics compatible with *S. DDD* sp. nov. Nonetheless, due to the poor preservation of the specimen and the impossibility of checking key characters, we prefer to determine it as *S. DDD*? sp. nov. We reach to this conclusion by maximum parsimony, instead of describing another *Serphites* species, until further specimens showing the habitus of *S. DDD* sp. nov. are found. The three specimens share the same ratio between forewing length and forewing width, and hindwing length and hindwing width (except for AR-1-A-2019.43.2 in which the hindwings are absent). The characteristics mentioned above are close to the characteristics found in *Serphites kuzminae*, from the Campanian Canadian amber, except for the metatarsus is longer than the metafemur. This difference, together with the geographical and temporal distance between *S.*

kuzminae and the new species described here are sufficient to justify the belonging to a different species.

***Serphites* sp.**

Figure 9

Material. SJ-10-03, incomplete specimen with head and anterior part of the forewings only preserved, sex unknown, syninclusion with a fragment of dinosaur feather. From San Just amber. Housed at Museo Aragonés de Paleontología (Fundación Conjunto Paleontológico de Teruel Dinópolis) in Teruel, Spain.

Description. Dark brown integument of the head. Head about 0.21 mm long and 0.31 mm wide; right compound eye about 0.11 mm in diameter; antennae 9-segmented; scape slightly curved, rectangular in shape, 0.09 mm long, 3× longer than wide; pedicel globous, 0.05 mm long and 0.04 mm wide; first flagellomere chalice-like in shape; second to sixth flagellomeres almost square in shape, broader than longer; terminal flagellomere elongate and with a rounded and acute apex; length-maximum width in mm of flagellomeres: 1f: 0.04-0.03, 2f: 0.03-0.04, 3f: 0.03-0.04, 4f: 0.04-0.04, 5f: 0.04-0.05, 6f: 0.04-0.05, 7f: 0.07-0.04; mouthparts obscure, a 3-segmented labial palpus is visible. Forewings with marginal fringe of setae and membrane covered by microtrichia; triangular (equilateral) pterostigma highly pigmented and sclerotised; rectangular fuscous area extending from pterostigmal midlength and adjacent to the joining of crossvein r-rs and Rs; costal cell delimited by C along anterior margin and tubular Sc+R; C slightly pigmented and thicker than Sc+R; radial cell triangular in shape, delimited by Sc+R, M+Cu, and 1M, the latter reaching an expansion adjacent to the pterostigma together with Sc+R; vein Rs+M absent; distal sections of Rs and M not tubular, reaching wing margin; the anterior section of Cu is visible.

Remarks. The specimen shows the typical serphitid-type forewing venation, including a triangular dark pterostigma, allowing its assignment to Serphitidae. Within this family, the subfamily Supraserphitinae presents antennae 11 or 12-segmented (Rasnitsyn et al., 2022), while the studied specimen has antennae 9-segmented. The subfamily Microserphitinae is characterised by an indistinct pterostigma (Kozlov and Rasnitsyn, 1979), represented by a fuscous area, while the pterostigma of the studied specimen is clearly distinct from the forewing membrane. Considering the subfamily Serphitinae, although partial, it shows typical characters of the genus *Serphites*, such as head wider than long, large triangular pterostigma, fuscous area extending from pterostigmal midlength and adjacent to the joining of crossvein r-rs and Rs, C thicker and less sclerotised than Sc+R, vein M curved apically and reaching an expansion adjacent to the pterostigma, and Rs reaches margin about one pterostigmal width from apical margin of pterostigma (McKellar and Engel, 2011). Thus, we putatively consider the specimen SJ-10-03 as belonging to the genus *Serphites*, based also on the similar pterostigma shape to other *Serphites* species. Within Serphitinae, *Jubaserphites* is unique possessing antennae 8-segmented (McKellar and Engel, 2011). The other serphitine genera *Aposerphites*, *Buserphites*, and *Mesoserphites* are characterised by structures not visible in the studied specimen, such as the arrangement of the ocelli and lengths of the petiolar segments (Herbert and McKellar, 2022).

Serphites silban from San Just has antennae apparently 12-segmented, while the number of antennomeres of *Serphites lamiak* from El Soplao is unknown, but the shape its pterostigma is different to that of SJ-10-03 (Ortega-Blanco et al., 2011). A new *Serphites* species described in this paper show antennae 12-segmented, while that of the other new species is difficult to discern. The description of a new species based on SJ-10-03 is discouraged due to the lack diagnostic characters. Antennae 9-segmented, as in the studied specimen, are also present in *Serphites fannyae* (male) from French amber, *Serphites navesinkae* (female), and *Serphites raritanensis* (female), both from New Jersey amber (Engel et al., 2011; Engel and Perrichot, 2014).

4. Discussion

4.1. Taphonomy and life palaeoenvironment of the studied specimens

[Section not finished]

The amber pieces from Ariño are usually very turbid and makes the description of the specimens difficult, as some parts are missing or hidden by debris. This turbidity might be related to stressful conditions underwent by the resiniferous trees. Two serphitids from San Just are found in syninclusion with dinosaur feather fragments, and the other one is attached to a spiderweb strand. This can provide a context for these insects in their environment and the relationships they have with other organisms in the same environment.

4.2. Phylogenetic relationships and evolution of Serphitoidea

[Section not finished]

Engel (2015) considers that the wing venation of Serphitinae is a secondary reversion, and so Serphitoidea and Mymarommatoidea are sister groups. While Rasnitsyn et al. (2019) considers that Mymarommatoidea evolved from Microserphitinae, thus Serphitoidea and Serphitidae would be paraphyletic. Following Engel's proposal, Microserphitinae and Mymarommatoids might show convergent evolution in size, body shape, and wing venation.

The Serphitidae was an extremely diverse group, placed as the second most diverse non-aculeate Cretaceous Hymenoptera group after the Evaniidae (Rasnitsyn and Öhm-Kühnle, 2021), but the description of 12 new species (including in this paper) places it in first place, with the Braconidae gaining only 8 species (Belokobylskij et Jouault, 2021, Chen et al. 2021a, Chen et al. 2021b, Álvarez-Parra et al., 2022a) and the Evaniidae, Scelionidae, and Stigmaphronidae gaining no new species. However, the diversity collapsed at the end of the Cretaceous, maybe related to the extinction of the host species.

4.3. Sexual dimorphism and palaeobiology of Serphitoidea

[Section not finished]

Sexual dimorphism in Serphitoidea is not very marked, being mainly the length of the antennae, as well as the shape of the abdomen, which would be more elongated in females. However, the holotype of *S. pygmaeus* is a male, and has an elongated abdomen, contradicting

this. To date, nine species of the family are known by representatives of both sexes (Table 1), allowing the comparison to confirm their sexual determination.

Based on phylogenetical inference, Serphitidae are supposed to be parasitoids. However, the previous articles do not explore the characteristics of this lifestyle in more detail.

The wings of Serphitoidea have undergone many changes over time, varying by genus. There is a tendence to reduce the length of the forewing in relation to the length of the body. At the same time, the width of the forewing remains relatively constant, resulting in a slight change in forewing shape from a long, thin wing to a shorter, wider wing. We also observe a complexification of the forewing veins, with notably the increase in size of the pterostigma in Serphitinae, as well as a reduction of the pre-pterostigmal angle observed in Archaeoserphitidae and Microserphitinae (Fig 12). This reduction, allowing straightening of the C and Sc veins, is accompanied by a more important sclerification in *Serphites*, *Mesoserphites*, *Buserphites* as well as in a convergent way in Supraserphites, not being found in *Leptoserphites* nor *Microserphites*. In these specimens, we observe a curvature at the level of the vein A, which allows to follow the shape of the thorax when the wings are placed at rest horizontally above the abdomen, while keeping a high wing surface.

The pterostigma is known in many insects to work as a wing stabilizer, reducing the vibrations (Norberg, 1972). This increases the flapping speed of the wing, allowing for increase flight speed and maneuverability, and is found in species requiring more precise flight. Its development in Serphitoidea seems to be different from Mymarommatoidea whose wings are provided with bristles used to take advantage of the viscosity of the wind at small scale (Shen et al., 2022). The round wing shape is also associated with a higher flight speed (Perrard, 2019).

Serphitoidea are also characterized by the presence of a two-segmented petiole, characteristics they share with their sister group Mymarommatoidea, some groups of Formicidae, Nevaniinae as well as to some extent Chalcididae, the latter having a second petiolar segment very reduced compared to the first. This second petiolar segment increases the flexibility of the abdomen and can also be compared to the constrictions found on the abdomen of certain hymenopterans such as Scoliidae, Tiphiidae and Mutillidae, for which no petiole differentiation is observed (Hashimoto, 1996). By moving the mass of the abdomen away from the center of the insect, it increases the moment of inertia of abdominal movements, which increases the maneuverability of flight (Perrard, 2019).

We also noted similarities between the rim in the first petiolar segment present in some species of Serphitidae, and the petiolar bumps of Formicidae, used as muscle attachments (Perrard, 2019). It is possible that they are used in a similar manner in Serphitidae, implying increased muscle mass at these parts, anterior in some species and posterior in others.

Complex parasitoid behaviours, as known from living wasps, would be difficult to determine from the fossil record and should therefore be kept in mind when theorizing about the behaviour of extinct wasps.

5. Conclusions

Acknowledgements

We thank Museo Aragonés de Paleontología (Fundación Conjunto Paleontológico de Teruel-Dinópolis) for providing the specimens, and the support from the Dirección General de Patrimonio Cultural of the Aragón Government (Spain). We are indebted to Rafael López del Valle for preparation of the amber pieces. This work is a contribution to the project CRE CGL2017-84419 funded by the Spanish AEI/FEDER and the EU. The first author S.Á.-P. acknowledges the support from the Secretaria d'Universitats i Recerca de la Generalitat de Catalunya (Spain) and the European Social Fund (2021FI_B2 00003). The second author M.S. acknowledges the support of the Erasmus+ programme of the European Union.

References

[Not all references are included in the list]

Alcalá, L., Espílez, E., Mampel, L., Kirkland, J.I., Ortiga, M., Rubio, D., González, A., Ayala, D., Cobos, A., Royo-Torres, R., Gascó, F., Pesquero, M.D., 2012. A new Lower Cretaceous vertebrate bonebed near Ariño (Teruel, Aragón, Spain); found and managed in a joint collaboration between a mining company and a palaeontological park. Geoheritage 4, 275–286. https://doi.org/10.1007/s12371-012-0068-y

Álvarez-Parra, S., Delclòs, X., Solórzano-Kraemer, M.M., Alcalá, L., Peñalver, E., 2020. Cretaceous amniote integuments recorded through a taphonomic process unique to resins. Scientific Reports 10, 19840. https://doi.org/10.1038/s41598-020-76830-8

Álvarez-Parra, S., Pérez-de la Fuente, R., Peñalver, E., Barrón, E., Alcalá, L., Pérez-Cano, J., Martín-Closas, C., Trabelsi, K., Meléndez, N., López Del Valle, R., Lozano, R.P., Peris, D., Rodrigo, A., Sarto i Monteys, V., Bueno-Cebollada, C.A., Menor-Salván, C., Philippe, M., Sánchez-García, A., Peña-Kairath, C., Arillo, A., Espílez, E., Mampel, L., Delclòs, X., 2021. Dinosaur bonebed amber from an original swamp forest soil. eLife 10, e72477. https://doi.org/10.7554/eLife.72477

Álvarez-Parra, S., Peñalver, E., Delclòs, X., Engel, M.S., 2022a. A braconid wasp (Hymenoptera, Braconidae) from the Lower Cretaceous amber of San Just, eastern Iberian Peninsula. ZooKeys 1103, 65–78. https://doi.org/10.3897/zookeys.1103.83650

Álvarez-Parra, S., Peñalver, E., Nel, A., Delclòs, X., 2022b. New barklice (Psocodea, Trogiomorpha) from Lower Cretaceous Spanish amber. Papers in Palaeontology 8 (3), e1436. https://doi.org/10.1002/spp2.1436

Arillo, A., Subías, L.S., Álvarez-Parra, S., 2022. First fossil record of the oribatid family Liacaridae (Acariformes: Gustavioidea) from the lower Albian amber-bearing site of Ariño (eastern Spain). Cretaceous Research 131, 105087. https://doi.org/10.1016/j.cretres.2021.105087

Brues, C., 1937. Superfamilies Ichneumonoidea, Serphoidea, and Chalcidoidea. University of Toronto Studies, Geological Series 40, 27–44.

Corral, J.C., López Del Valle, R., Alonso, J., 1999. El ámbar cretácico de Álava (Cuenca Vasco-Cantábrica, norte de España). Su colecta y preparación. Estudios del Museo de Ciencias Naturales de Álava 14, 7–21.

Engel, M.S., 2005. The crown wasp genus *Electrostephanus* (Hymenoptera: Stephanidae): discovery of the female and a new species. Polskie Pismo Entomologiczne 74 (3), 317–332.

Engel, M.S., Perrichot, V., 2014. The extinct wasp family Serphitidae in late Cretaceous Vendean amber (Hymenoptera). Paleontological Contributions 2014 (10J), 46–51. https://doi.org/10.17161/PC.1808.15990

Engel, M.S., Grimaldi, D.A., Ortega-Blanco, J., 2011. Serphitid wasps in Cretaceous amber from New Jersey (Hymenoptera: Serphitidae). Insect Systematics & Evolution 42 (2), 197–204. https://doi.org/10.1163/187631211X560892

García-Penas, A., Aurell, M., Zamora, S., 2022. Progressive opening of a shallow-marine bay (Oliete Subbasin, Spain) and the record of possible eustatic fall events near the Barremian-Aptian boundary. Palaeogeography, Palaeoclimatology, Palaeoecology 594, 110938. https://doi.org/10.1016/j.palaeo.2022.110938

Goulet, H., Huber, J.T., 1993. Hymenoptera of the world: an identification guide to families. Research Branch Agriculture Canada, Ottawa, 668 pp.

Herbert, M.C.M., McKellar, R.C., 2022. New genera *Buserphites* and *Mesoserphites* (Hymenoptera: Serphitidae) from mid-Cretaceous amber of Myanmar. Cretaceous Research 130, 105025. https://doi.org/10.1016/j.cretres.2021.105025

Kozlov, M., Rasnitsyn, A., 1979. On the limits of the family Serphitidae (Hymenoptera, Proctotrupoidea). Entomologicheskoe Obozrenie 58 (2), 402–416. [In Russian with English summary]. https://doi.org/10.5281/zenodo.26382

Linnaeus, C., 1758. Systema naturae per regna tria Naturae, secundum classes, ordines, genera, species, cum characteribus, differentiis, synonymis, locis. Holmiae, Laur. Salvii, Editio Decima, 1, 824 pp. https://doi.org/10.5962/bhl.title.542

McKellar, R.C., Engel, M.S., 2011. The serphitid wasps (Hymenoptera: Proctotrupomorpha: Serphitoidea) of Canadian Cretaceous amber. Systematic Entomology 36 (1), 192–208. https://doi.org/10.1111/j.1365-3113.2010.00559.x

Menor-Salván, C., Simoneit, B.R.T., Ruiz-Bermejo, M., Alonso, J., 2016. The molecular composition of Cretaceous ambers: identification and chemosystematic relevance of 1, 6-dimethyl-5-alkyltetralins and related bisnorlabdane biomarkers. Organic Geochemistry 93, 7–21. https://doi.org/10.1016/j.orggeochem.2009.05.002

Ortega-Blanco, J., Delclòs, X., Peñalver, E., Engel, M.S., 2011. Serphitid wasps in early Cretaceous amber from Spain (Hymenoptera: Serphitidae). Cretaceous Research 32 (2), 143–154. https://doi.org/10.1016/j.cretres.2010.11.004

Peñalver, E., Delclòs, X., 2010. Spanish amber. In: Penney, D. (Ed.), Biodiversity of fossils in amber from the major world deposits, vol. 13. Siri Scientific Press, Manchester, pp. 236–270.

Peñalver, E., Delclòs, X., Soriano, C., 2007. A new rich amber outcrop with palaeobiological inclusions in the Lower Cretaceous of Spain. Cretaceous Research 28 (5), 791–802. https://doi.org/10.1016/j.cretres.2006.12.004

Rasnitsyn, A.P., Maalouf, M., Maalouf, R., Azar, D., 2022. New Serphitidae and Gallorommatidae (Insecta: Hymenoptera: Microprocta) in the Early Cretaceous Lebanese amber. Palaeoentomology 5 (2), 120–136.

Salas, R., Guimerà, J., 1996. Rasgos estructurales principales de la cuenca cretácica inferior del Maestrazgo (Cordillera Ibérica oriental). Geogaceta 20 (7), 1704–1706.

Santer, M., Álvarez-Parra, S., Nel, A., Peñalver, E., Delclòs, X., 2022. New insights into the enigmatic Cretaceous family Spathiopterygidae (Hymenoptera: Diaprioidea). Cretaceous Research 133, 105128. https://doi.org/10.1016/j.cretres.2021.105128

Tibert, N.E., Colin, J.P., Kirkland, J.I., Alcalá, L., Martín- Closas, C., 2013. Lower Cretaceous nonmarine ostracodes from an Escucha Formation dinosaur bonebed in eastern Spain. Micropaleontology 59, 83–91.

Villanueva-Amadoz, U., Pons, D., Diez, J.B., Ferrer, J., Sender, L.M., 2010. Angiosperm pollen grains of San Just site (Escucha Formation) from the Albian of the Iberian Range (north-eastern Spain). Review of Palaeobotany and Palynology 162 (3), 362–381. https://doi.org/10.1016/j.revpalbo.2010.02.014

Villanueva-Amadoz, U., Sender, L.M., Alcalá, L., Pons, D., Royo-Torres, R., Diez, J.B., 2015. Paleoenvironmental reconstruction of an Albian plant community from the Ariño bonebed layer (Iberian Chain, NE Spain). Historical Biology 27 (3–4), 430–441. https://doi.org/10.1080/08912963.2014.895826

Anexo 8.1.14

Amber and the Cretaceous Resinous Interval: hypotheses on causes

Delclòs, X., Peñalver, E., Barrón, E., Pérez-de la Fuente, R., Grimaldi, D.A., Holz, M., Labandeira, C., Scotese, C.R., Solórzano-Kraemer, M.M., **Álvarez-Parra, S.**, *et al.*, Peris, D. Amber and the Cretaceous Resinous Interval: hypotheses on causes.

* El manuscrito se encuentra en la fase final de su preparación. No se han incluido las figuras, los pies de figura ni el material suplementario. Se ha preferido no indicar los nombres ni el orden de todos los autores.

Amber and the Cretaceous Resinous Interval: hypotheses on causes

Delclòs, X.[a,b*], Peñalver, E.[c*], Barrón, E.[c], Pérez-de la Fuente, R.[d], Grimaldi, D.A.[e], Holz, M.[f], Labandeira, C.[g–i], Scotese, C.R.[j], Solórzano-Kraemer, M.M.[k], Álvarez-Parra, S.[a,b], et al., Peris, D.[a,b]

[a]Departament de Dinàmica de la Terra i de l'Oceà, Facultat de Ciències de la Terra, Universitat de Barcelona, Spain
[b]Institut de Recerca de la Biodiversitat (IRBio), Universitat de Barcelona, Spain
[c]Instituto Geológico y Minero de España (IGME), CSIC, Madrid, Spain
[d]Oxford University Museum of Natural History, Oxford, UK
[e]Division of Invertebrate Zoology, American Museum of Natural History, New York, USA
[f]Instituto de Geociências, Universidade Federal da Bahia, Salvador da Bahia, Brazil
[g]National Museum of Natural History, Smithsonian Institution, Washington, D.C, USA
[h]Department of Entomology, University of Maryland, Maryland, USA
[i]College of Life Sciences & Academy for Multidisciplinary Studies, Capital Normal University, Beijing, China
[j]Department of Earth & Planetary Sciences, Northwestern University, Evanston, IL, USA
[k]Senckenberg Forschungsinstitut und Naturmuseum, Frankfurt, Frankfurt am Main, Germany

(*) Corresponding authors. These contributed equally to this work.
E-mail address: xdelclos@ub.edu (X. Delclòs) and e.penalver@igme.es (E. Peñalver).

Abstract. Amber is fossilized resin well known for containing biological remains in exceptional preservation. The study of amber has revolutionized knowledge on past terrestrial organisms and habitats since the Early Cretaceous. Prolific amber-bearing outcrops are more pervasive in the Northern Hemisphere and are richly represented in time during an interval of about 60 million years, from the Barremian to the Maastrichtian stages of the Cretaceous period. The extensive resin production that must have taken place to account for this remarkable amber record is related to conifer groups that produced copious resin and to the growth of resiniferous forests in proximity to transitional sedimentary environments that accumulated and preserved the resin, among other variables such as the nature and dynamics of the atmosphere during the Cretaceous. Here we discuss the potential set of interrelated abiotic and biotic factors involved in these processes and explore their possible global nature. We name this period of mass resin production by conifers during the late Mesozoic, paramount for documenting the evolution of life since then, the Cretaceous Resinous Interval (CREI).
Keywords. Cretaceous; Amber; Copal; Resin; Mass resin production, Conifers.

1. Introduction

Resins are secondary metabolites synthesized by specialized cells of gymnosperm and angiosperm plants, whose composition consist of amorphous mixtures of carboxylic acids, essential oils and isoprene-based hydrocarbons (Langenheim, 2003). Resin production is highly conditioned by the amount of water in the environment inhabited by the resiniferous plants (Allen et al., 2010). The main functions of resins relate to defense against herbivores and pathogens as well as acting as a healing mechanism, sealing wounds and vulnerable parts after herbivore attack or physical damage (Langenheim, 2003; Seyfullah et al., 2018). Resins remain sticky from just hours to several months after being secreted, allowing the ability to entrap

organisms or parts of them —known as bioinclusions— found in the same ecosystem of the resin-producing plant (Solórzano Kraemer et al., 2018). The crosslinking of resin takes place over millions of years, resulting in gradual hardening, decrease in thermal denaturation and loss of free methyl groups, all of which leading to a relatively inert, hardened form called amber (Langenheim, 1990; Anderson et al., 1992; McCoy et al., 2015; Solórzano-Kraemer et al., 2020). Only a few types of resins can fossilize based on their chemical composition (Anderson and Crelling, 1995; Langenheim, 2003).

Most amber deposits have yielded a few or no bioinclusions. The reasons for that are variable, yet usually relate to where the resin was produced and/or how long retained its stickiness (Solórzano Kraemer et al., 2018). Amber-bearing outcrops that preserve bioinclusions are a type of Konservat-Lagerstätte; indeed, the preservation of organisms in amber is exceptional, different from any other organic or inorganic mechanism retaining organismic detail for millions of years (Martínez-Delclòs et al., 2004; Grimaldi and Ross, 2017). Despite the biases that resin entrapment entails (Solórzano Kraemer et al., 2018), amber provides high anatomical detail —both external and internal— of the bioinclusions and even evidence of past animal behaviors (Labandeira, 2014a; Grimaldi, 2019), providing extraordinary data on diverse terrestrial organisms and ecosystems in deep time. Amber deposits are typically parautochthonous-allochthonous, where resin was dislodged by gravity, and transported and concentrated by water, being accumulated in a primary or secondary location (Martínez-Delclòs et al., 2004). However, a few autochthonous-parautochthonous deposits are known where resin suffered minimal or virtually no transport (Schmidt et al., 2012; Seyfullah et al., 2018; Álvarez-Parra et al., 2021). Resin crosslinking, which begins once the resin is exuded by the plant, continues after becoming buried in sealed, anoxic sediments (e.g., within or under layers of clay) and little interaction with meteoric water (Martínez-Delclòs et al., 2004). Moreover, resin has almost the same density as freshwater but is buoyant in sea water and/or that with sediments in suspension, being easily transported by flotation. For these reasons, transitional settings with large accumulations of continental organic matter such as deltas, oxbow lakes, estuaries or swamps, are the most favorable sedimentary environments for resin fossilization (Grimaldi et al., 2000b; Martínez-Delclòs et al., 2004; Iturralde-Vinent and McPhee, 2019). Resiniferous trees are often located on emergent topography within these transitional environments (Álvarez-Parra et al., 2021) or close to areas where resin primarily accumulated by low-energy transport, indicated by the preservation of fragile resin structures (Grimaldi et al., 2000b; Perrichot, 2005; Rust et al. 2010; Veltz et al., 2013). The formation of many of the amber-bearing deposits associated with coal or other rocks rich in organic matter coincides with episodes of marine transgression that flooded inland environments (Najarro et al., 2009; Rodríguez-López et al., 2020).

Although resin is exuded by different tissues and organs of plants, amber deposits —at least those from the Cretaceous— were formed by resin produced by root tissues and generally lacking bioinclusions (root resin) and, usually in a minor amount, by that produced by the trunk, branches or and other exposed parts (aerial resin) (Langenheim, 1995; Álvarez-Parra et al., 2021); the latter type has the potential to contain abundant bioinclusions. Although the oldest fossil resin dates from the Carboniferous (Bray and Anderson, 2008), amber with the oldest bioinclusions dates from the Late Triassic, which preserves a few minute arthropods (Schmidt et al., 2012; Sidorchuk et al., 2015). Jurassic amber is highly scarce and apparently associated with low latitudes within the tropical-equatorial zone from the Northern

Hemisphere, as it has namely been found in Thailand, Italy and Lebanon; no macroscopic bioinclusions have hitherto been reported from it (Nohra et al., 2013; Neri et al., 2016). The oldest deposits rich in highly fossiliferous amber are Barremian (Early Cretaceous) (Maksoud et al., 2017).

The Cretaceous (~145.5–66.0 Ma) represents a time of rapid evolutionary turnover and radiation of organisms. From a macroecological perspective, the Cretaceous was a key period in the Earth history in which the Angiosperm Terrestrial Revolution (*ca.* 100 to 50 Ma), inclusive of the formerly defined Cretaceous Terrestrial Revolution (Lloyd et al., 2008; Benton et al., 2022), took place. This time interval represented a replacement of a Mesophytic paleobiome dominated by gymnosperms by a Cenophytic paleobiome dominated by angiosperms (Labandeira, 2014b; McElwain, 2018; Birks, 2020; Condamine et al., 2020). This turnover altered the bases of the trophic networks of continental ecosystems (Labandeira, 2014b), substantially modifying the communities of herbivores (Labandeira, 2007; Kergoat et al., 2014) and, therefore, affecting the composition and evolutionary patterns of continental biotas (Meredith et al., 2011; McKenna et al., 2015; Peris et al., 2017; Benson et al., 2021). Cretaceous climate was warmer and more humid than that of today, probably due to very active, sustained volcanism associated with unusually extensive seafloor spreading that promoted higher atmospheric CO_2 and O_2 values than at present (Poulsen and Zhou, 2013; Royer et al., 2014). During most of the Cretaceous period, polar regions were virtually devoid of ice (Scotese, 2021) and continental masses were largely occupied by forests dominated by conifers (Hay and Floegel, 2012; Peralta-Medina and Falcon-Lang, 2012), thereby entailing a significant reduction in albedo. The decrease of latitudinal desert belts during the Early Cretaceous and long-lasting humid conditions during the Late Cretaceous were driven by the breakup of Pangea (Chaboureau et al., 2014; Landwehrs et al., 2021).

Cretaceous amber-bearing deposits, at least those currently documented, have a limited temporal and geographical distribution (Martínez-Delclòs et al., 2004; Labandeira, 2014a; Solórzano-Kraemer et al., 2020). They date from the Barremian to the Maastrichtian stages (dated from ~129 to 66 Ma at present), and although numerous and widely distributed, they are clearly biased towards the Northern Hemisphere (Fig. 1A). Several Cretaceous amber-bearing deposits yield abundant amber and bioinclusions (Martínez-Delclòs et al., 2004; Penney, 2010; Seyfullah et al., 2018). The most studied fossiliferous amber-bearing outcrops from the Cretaceous are found in Lebanon (Barremian), Congo (Aptian), Spain (Albian), France (Cenomanian), Myanmar (Cenomanian), New Jersey in the USA (Turonian), Taimyr in Russia (Santonian) and Canada (Campanian). In addition to these outcrops, amber (with or without bioinclusions) has been reported from Cretaceous deposits in many other regions worldwide (Fig. 2; Supplementary material Y). These amber-bearing deposits display similar taphonomic and depositional characteristics along a relatively continuous time interval.

Molecular analysis of amber, Pleistocene and Holocene copals and Defaunation resin (produced after the beginning of the Industrial Revolution, see Solórzano-Kraemer et al., 2020) is a valuable tool for interpreting the botanical origin of amber (McCoy et al., 2017; 2021). However, the identity of Cretaceous resin-producing plants is unknown in most cases. The taxonomic affinities of the Cretaceous trees that produced abundant resin remain elusive due to a variety of factors. These include the extensive chemical variation observed in the composition of the Cretaceous amber samples (Menor-Salván et al., 2016; McCoy et al., 2021), cases of molecular convergence (Bray and Anderson, 2009) and the usually scarce record of

plant remains in amber as bioinclusions (Kvaček et al., 2018; Moreau et al., 2020). Nevertheless, geochemical studies have ruled out angiosperms as resin-producing plants during the Cretaceous (Anderson et al., 1992; Lambert et al., 1996; Menor-Salván et al., 2016), with a few minor exceptions (Grimaldi et al., 2000a). Most likely, angiosperms did not acquire the ability to produce resin in sufficient quantity to form amber-bearing deposits until the Eocene (Jossang et al., 2008). As for gymnosperms, the coniferous tree families of Araucariaceae, Cheirolepidiaceae†, Cupressaceae s.l., Podocarpaceae and Pinaceae were widely distributed during the Cretaceous (Peralta-Medina and Falcon-Lang, 2012) (Fig. 2) and they have been identified as the likely resin sources of the Cretaceous amber deposits (Azar et al., 2010; Peñalver and Delclòs, 2010; Perrichot et al., 2010; Nohra et al., 2014; Menor-Salván et al., 2016; McCoy et al., 2021) (Supplementary Material X). Although modern Pinaceae resin poorly crosslinks due to its molecular composition, a few moderate-size amber deposits resulting from this resin have been found (Bray and Anderson, 2008; Menor-Salván et al., 2016). Cretaceous Cupressaceae produced resin but generally in small amounts (e.g. Otto et al., 2000). Cheirolepidiaceae conifers lack resiniferous structures except some forms presenting traumatic resin canals (Bodnar et al., 2013; Rombola et al., 2022). Actuo-taphonomic studies (Peñalver et al., 2018), plant amber fossils (Kvaček et al., 2018; Moreau et al., 2020) (Fig. 3A−B) and examination of wood logs and cone scales with embedded amber found in amber-rich levels (Perrichot, 2005; Mays et al., 2019) provide important evidence for determining the conifer taxa involved in resin mass production during the Cretaceous.

In this contribution we define and outline the Cretaceous Resinous Interval (CREI) by integrating diverse lines of evidence and analyzing the potential set of interrelated abiotic and biotic factors that characterize this interval. Current knowledge limitations and future directions are also discussed. The data presented herein was gathered and integrated both from the literature and our own data based on fieldwork in Cretaceous amber localities from Lebanon, Jordan, Congo, Ecuador, Spain, France, Myanmar, USA and New Zealand; in Cenozoic amber localities from France, Mexico, Dominican Republic, New Zealand, India, China and Ethiopia; and in copal and Defaunation resin deposits from Colombia, Dominican Republic, New Caledonia, New Zealand and Madagascar. In the three latter areas, fieldwork focused on actuotaphonomic processes aimed at understanding the conditions of production and conservation of Defaunation resins, as well as the formation of copal deposits. All the material obtained during fieldwork (amber prospections and excavations) is housed at free-access, public institutions and comply with the authorization of the corresponding national and local administrations. The material used and figured in this work is housed at … Data used in the figures is our own when not specified in the captions. For Figure 2, present-day spatial coordinates and age from a total of 239 Cretaceous amber outcrops and XXX paleobotanical records worldwide were obtained from a bibliographic survey (Supplementary Material Y). Present coordinates of amber outcrops and paleobotanic occurrences were rotated to paleocoordinates using R 4.0.4 and GPlates 2.2.0. Paleogeographic maps were sourced from Scotese (2001). Map visualization and imaging was made using the QGIS 3.22.3 software.

2. Definition of the Cretaceous Resinous Interval

We define the Cretaceous Resinous Interval (CREI) as *a global continental mass resin production and burial which occurred from the Barremian to the Maastrichtian stages of the Cretaceous period*. We posit that, during a relatively continuous time interval of about 60

million years, a series of factors led to the formation of rich amber deposits of similar characteristics and wide geographic distribution (Figs 1, 2). This time-delimited interval is based on the known geological record providing evidence of numerous amber-bearing deposits from the Barremian (Early Cretaceous) to the Maastrichtian (latest Cretaceous) (DePalma et al., 2010; Penney, 2010; Maksoud and Azar, 2020). Most of these amber deposits occur in the Northern Hemisphere, between 5° and 75° N latitude, and are especially important in low to mid latitudes between the Barremian and Coniacian and in mid to high latitudes between the Santonian and the Maastrichtian (Fig. 1A). Some Cretaceous amber-bearing deposits are found in the Southern Hemisphere between the Aptian–Turonian and in the Maastrichtian, but they are scarce (Fig. 1A). Significant Cenozoic amber deposits are essentially absent until the Paleocene of Wyoming, USA (~61 Ma) and Alaska, USA (~57 Ma) (Grimaldi et al., 2000a; 2018), and the Eocene of Oise, France (~53 Ma), Fushun, China (53–50 Ma) and Cambay, India (~52–50 Ma) (Jossang et al., 2008; Rust et al., 2010; Wang et al., 2014a).

The major shared characteristics among amber deposits generated during the CREI are: (a) the plants potentially involved in the production of resin are restricted to conifers (Araucariaceae, Cheirolepidiaceae†, Cupressaceae s.l., Podocarpaceae and Pinaceae) (Lagenheim, 2003; Menor-Salván et al., 2010; Seyfullah et al., 2018); (b) the occurrence of charcoal resulting from plant material charred by wildfires at the same levels that contain amber, particularly in the Northern Hemisphere (Brown et al., 2012; Tappert et al., 2013), is common (Fig. 3C); (c) when bioinclusions are preserved, they correspond to similar fauna and flora under comparable biases (Penney, 2010; Solórzano Kraemer et al., 2018), although in some instances bioinclusions are absent likely due to taphonomic reasons; (d) all amber deposits are originated in transitional sedimentary environments under subtropical and temperate paleoclimates; and (e) amber-bearing deposits coincide with periods of demonstrable marine transgression (Bowen and Jux, 1987; Villagómez et al., 1996; Najarro et al., 2009) (Fig. 1B). Spatially, we regard the CREI global in nature since amber-bearing outcrops are distributed worldwide throughout the Cretaceous, although they are particularly concentrated in Laurasia and the northern margin of Gondwana (Figs 1,2).

3. Conditional factors on resin production and preservation

Two basic conditions need to co-occur in time and space in order to generate an accumulation of resin with the potential to become an amber-bearing deposit. First, the existence of resin-producing plants with the capacity to secrete a large amount of resin. And second, the occurrence of a suitable sedimentary setting –namely a transitional environment– that buries resin under anoxic conditions. Known Cretaceous amber-bearing deposits are restricted geographically despite that resin-producing conifers were distributed worldwide during various Cretaceous stages (Fig. 2). Consequently, one would assume that the lack of suitable depositional environments leading to the accumulation and preservation of the resin must have been involved in such discrepancy. Yet, transitional sedimentary environments during major marine transgressions were equally probable anywhere on Earth's surface, and have occurred cyclically throughout time (Haq, 2014). Thus, the two basic conditions noted above alone would not fully explain the observed distribution of the Cretaceous amber-bearing deposits. It seems reasonable to assume that a third condition for mass resin production and accumulation must have been at play – the existence of, at least, one abiotic or biotic factor,

likely the confluence of several factors, that promoted the production of resin by trees and/or its subsequent accumulation and preservation. These factors could be global or more localized in spatial scale, and are not necessarily mutually exclusive, thus may have acted simultaneously.

3.1. Abiotic factors

Multiple abiotic factors were potentially related to mass production and/or accumulation of resin during the CREI. Although these factors are interrelated, affecting other factors directly or indirectly, they are grouped in the following points below to facilitate discussion. These are: (1) atmospheric gas composition, temperature and wildfires; (2) volcanism and changes in sea level; and (3) oceanic physicochemical properties and hurricanes. An overview on the global climatic circumstances throughout the CREI is given at the end of this subsection.

3.1.1. Atmospheric gas composition, temperature and wildfires

Atmospheric gas composition (Fig. 4A–B) has had a major impact on climatic variables. Atmospheric greenhouse gases such as carbon dioxide (CO_2), methane (CH_4) and atmospheric oxygen (O_2), must have had direct or indirect impact on the global resin production. Although atmospheric CO_2 concentration during the Cretaceous varied according to the authors and proxies used (Tappert et al., 2013; Landwehrs et al., 2021), it is considered to have remained greater than twice that of preindustrial values, between 560 and 1680 ppm (Barral et al., 2017). Such high levels are due to extensive volcanic emissions during the Cretaceous from Large Igneous Provinces (LIPs, Fig. 4C) and seafloor formation (Condie et al., 2021). Wildfires, changes in ocean chemistry, biotic respiration and organic matter decomposition also released significant amounts of CO_2 to the atmosphere during the Cretaceous (Hu et al., 2012; Wang et al., 2014b; Scott, 2018). Methane has a greater greenhouse potential than CO_2, and it is likely to have notably increased the greenhouse effect during the Cretaceous (Jahren et al., 2001; Chang et al., 2022). Higher CH_4 levels were related to the liberation of methane hydrate from the seafloor by rising water temperatures (Wagner et al., 2007) and from seafloor spreading. The global temperature fluctuated (Holz, 2015; Landwehrs et al., 2021) during the here defined CREI (Fig. 4C), with generally elevated temperatures and reduced latitudinal temperature gradients between the equator and the poles, of about ≤35°C mean annual temperature (MAT) in both hemispheres (O'Brien et al., 2017; Huber et al., 2018). The Northern Hemisphere thermal gradient showed a ca. 5°C decrease from the Late Jurassic into the Late Cretaceous due to an increase of CO_2 and associated warming, while the Southern Hemisphere temperature gradient increased during this time due to the migration of Antarctica towards the South Pole (Landwehrs et al., 2021). Higher temperatures also brought more extreme atmospheric precipitation regimes and the establishment of more extensive regions under arid or monsoonic climates (Hasegawa et al., 2012), although the latter would have been more influenced by paleogeography than by atmospheric gas concentrations (Farnsworth et al., 2019). Zhou et al. (2012) showed using coupled ocean-atmosphere general circulation simulations that during the mid-Cretaceous continental precipitation had a roughly mirrored distribution between Northern and Southern Hemispheres, with the maximum continental precipitation taking place around the equator, then steeply decreasing and reaching a relatively minimum surrounding the 30° latitude N/S and then reaching high continental precipitation peaks at around 50° latitude N/S. This pattern situates the main bulk

of amber deposits bearing bioinclusions known from the Cretaceous (particularly the mid-Cretaceous) (Fig. 1A) in areas of moderate or relatively low average rainfall. The occurrence of the first significant Triassic amber deposits with inclusions in northern Italy coincides with the Carnian Pluvial Episode, associated with an important gymnosperm evolutionary event and radiation (Roghi et al., 2022).

The increase in atmospheric CO_2 below the RuBisCo (the enzyme ribulose-1,5-bisphosphate carboxylase/oxygenase, involved in the first major step of carbon fixation) saturation limit accelerates plant photosynthesis and growth under present conditions (Dalling et al., 2016; Olivoto et al., 2017). In principle, such acceleration would also indicate that an increase in atmospheric CO_2 levels could result in higher metabolic rates and so increased production of secondary metabolites such as resin (Trapp and Croteau, 2001; Novick et al., 2012). However, even related plant species may show opposite responses to CO_2 changes due to differences in physiological plasticity (Berini et al., 2018; Kurepin et al., 2018), thereby limiting the ability to infer resin production of fossil plant species based on CO_2 concentration. Even so, CO_2 and O_2 values might be indirectly linked with resin production because elevated levels would be expected to impact plant physiologic features that, in turn, could increase the herbivorous, wood-boring or pathogenic activity of other organisms such as arthropods or fungi (Lake and Wade, 2009; Labandeira, 2013; Couture et al., 2015; see section 3.2 below).

Numerous proxies suggest that atmospheric O_2 increased continuously from the Barremian to the Cenomanian (Fig. 4A), reaching a level of 29% (Berner, 2006; Glasspool and Scott, 2010; Brown et al., 2012), which decreased during the Eocene until reaching the current value of 21% (Wade et al., 2019). The high O_2 content in the atmosphere during the Cretaceous favored recurrent wildfires in coniferous forests (Belcher and McElwain, 2008), which were also promoted by increased electrical storms and intensive volcanism (Scott, 2018). Charcoal is indicative of wildfires (Brown et al., 2012; Scott, 2018) and it is abundant in most Cretaceous amber-bearing deposits (Peñalver and Delclòs, 2010; Shi et al., 2012; De Lima et al., 2019) (Fig. 3C), including the presence of charcoalified remains within amber (Grimaldi et al., 2000b; Najarro et al., 2010). Partially burned amber pieces have also been occasionally found together with charcoalified plant material (Grimaldi et al., 2000b). Extant trees increase resin exudation if injured by fire (Fig. 3D) as a physiological response that prevents pathogenic activity or arthropod invasion (Langenheim, 2003; Della Prasetya et al., 2017). Fire has had a key role in reshaping ecosystems, particularly after the accumulation of flammable biomass arising from increased productivity of terrestrial ecosystems linked to the predominance of angiosperms (Bond and Scott, 2010) as well as an altered ignitability and flammability of potential angiospermous fuels (Belcher and Hudspith, 2017). Different groups of Cretaceous conifers exhibit pyrophilous modifications linked to recurrent wildfires (He et al., 2016), a lifestyle (e.g., serotiny) that has endured into the present (Pausas, 2018). Moreover, there are diverse instances of organisms intimately associated with fire preserved in Cretaceous ambers (Ortega-Blanco et al., 2008; Pérez-de la Fuente et al., 2012; Shi et al., 2022) (Fig. 3E–G). All the above indicates that during the CREI wildfires played a role in the genesis of resins, at least of some deposits, by favoring their exudation but also in their subsequent accumulation, as deforested soils experience increased erosion. In any case, based on the global occurrence of paleowildfires (Brown et al., 2012; Scott, 2018) and the widespread distribution of potential resiniferous plants during the CREI, a uniform distribution of Cretaceous amber deposits on Earth would be expected. However, that is not the case (Fig. 2). Wildfires were involved in local

and regional resin production and accumulation during the CREI (e.g., the Raritan Fm. amber in New Jersey, USA), but appear to not be a definitive cause of resin production on a global scale. The abundant record of volcanic rocks associated directly or laterally with Cretaceous amber-bearing deposits such as those in Lebanon (Velz et al., 2013), Myanmar (Shi et al., 2012), Ecuador (Balseca et al., 1993) and Canada (Eberth, 2005) is evidence that resin mass production took place in environments with local volcanic influence, this factor being intimately related with wildfires (see above).

3.1.2. Volcanism and changes in sea level

Aside from increasing the levels of atmospheric gases such as CO_2 and promoting wildfires, large amounts of volcanic emissions over a long period of time could have also affected the global climate in multiple other ways (Macdonald et al., 2018; Johansson et al., 2018). The maximum development of LIPs during the last 2,500 million years occurred during the Cretaceous (Eldholm and Coffin, 2000; Condie et al., 2021). This peak of LIP development (Fig. 4C) altered the composition and circulation patterns of both the atmosphere and the hydrosphere and changed the geometry of sedimentary basins and sea level.

LIP formation and seafloor spreading, when considered jointly with increased global MATs during the Cretaceous due to the higher greenhouse gas levels of CO_2 and CH_4, led to the melting of polar ice caps (Zhou et al., 2008; Hay, 2017) and to significant reduction of the Earth's albedo (Kent and Muttoni, 2022). These effects produced a global marine transgression (Fig. 1C) from the Valanginian to the Turonian stages (Wagreich et al., 2020). This global transgression was only interrupted by a regression during the Aptian−Albian boundary after a decrease in global temperature (Haq, 2014), with global MATs of 12^{o}C (Hay, 2017). Maximum transgression was reached in the Turonian and regained high levels in the Campanian (Olde et al., 2015). All amber-bearing deposits coincide with second-order transgressive periods of the long-term curve (Grimaldi et al., 2000b; Perrichot, 2005; Najarro et al., 2009) (Fig. 1C); the resin-bearing strata developed during maximum regressive episodes which punctuated the overall transgressive trend. The global high sea level present during the CREI increased the insularization, changing the extent and distribution of land masses and epicontinental seas (e.g., the Late Cretaceous European archipelago or the Midcontinental Seaway of North America). Extensive areas were flooded, establishing new areas of deposition and even flooding coastal forests, reducing terrestrial biotopes and increasing flooding stress (Erwin, 2009). The general marine transgression trend during the Cretaceous and the paleogeographic changes that brought a greater proportion of emerged land mass at mid-high latitudes of the Northern Hemisphere (Landwehrs et al., 2021) entailed a greater availability of land that was colonized by plants (Klages et al., 2020). In the Southern Hemisphere, the proportion of emerged land masses at mid-high latitudes was similarly lower during the Cretaceous as it is at present (Figs 1, 2).

3.1.3. Oceanic physicochemical properties and hurricanes

As amber-bearing deposits are frequently associated with transitional sea to land environments, the physicochemical properties of the oceanic waters (salinity, temperature) and their paleocirculation patterns affected their formation. Water salinity probably controlled the formation of amber deposits because resin has a lower density than seawater, rendering it buoyant and making its burial and preservation in environments with high salinity difficult. Hyper-saline conditions did occur in regions where currently amber-bearing deposits are found

in the Northern Hemisphere, such as in Myanmar and New Jersey of the USA (Poulsen et al., 1998; Topper et al., 2011), as well as in the Southern Hemisphere such as in Brazil and Congo (Pérez-Díaz and Eagles, 2017). The formation of resin deposits in hyper-salinity zones suggests only temporary marine influence. The record of frequent, yet rarely diverse, marine protists and plant megaremains in amber deposits (Néraudeau et al., 2008; Barrón et al., 2015; Peyrot et al., 2019) would support this type of depositional setting. Alternatively, disparate data exist regarding the surface sea temperature (SST) during the CREI (Hay and Floegel, 2012) (Fig. 4D), so no definitive conclusions can be drawn beyond that the global average SST during the mid-Cretaceous was >6^{o}C higher than that of today (Hay, 2009; Torsvik and Cocks, 2016). Global ocean circulation changed significantly during the Cretaceous due to progressive opening of the South Atlantic Ocean and the Tethyan Circumglobal Current providing E to W flow around the globe at low latitudes of the Northern Hemisphere; both factors conditioned global temperature and climate during the CREI (Hay, 2009; Wohlwend et al., 2015). In addition, the transfer of heat from the hydrosphere to the atmosphere from water vapor played an important role in cooling the tropics and in warming at high latitudes, establishing the smooth latitudinal gradient of temperature noted earlier.

Linked to the high average SST during the Cretaceous, heavy rainfall and winds such as those occurring in hurricanes have been also proposed as an abiotic cause of resin production to seal damage and minimize opportunistic insect attacks or pathogenic infections (Lanhengeim, 1993; Seyfullah et al., 2018). Climate models based on marine and continental distribution and topography suggest that winds were generally weaker during the Cretaceous than at present (Cousin-Rittemard et al., 2002; Hay, 2009), but the high SST throughout annual seasons could have promoted the development of hurricanes in low to medium latitudes. The absence of high topographic relief (Hay et al., 2019) would have allowed the wind to circulate without diverting its zonal flow (Scotese et al., 2021).

3.1.4. Climatic overview throughout the CREI

Based on paleoclimate data (Chumakov et al., 1995), most Cretaceous amber-bearing deposits originated in the Northern Mid-latitude Warm Humid Belt. Nevertheless, during the Albian, Santonian and Maastrichtian, some resin deposits developed within the Northern High-latitude Temperate Humid Belt, and during the Albian and Cenomanian other resin deposits originated within the Equatorial Humid Belt and the Northern Hot Arid Belt, respectively. Based on global circulation models, the depositional environments that gave rise to amber-bearing deposits in Lebanon (Barremian) were located in the tropical climate belt (Sewall et al., 2007; Ohba and Ueda, 2010). During the lower to middle Aptian, a cold stage developed globally (Mutterlose et al., 2010), which coincides with an important reduction in the record of amber deposits, although this cold interval has recently been questioned (Huber and O'Brien, 2020). At the Aptian–Albian boundary, the conditions of the warm greenhouse were re-established due to intense volcanism returning significant amounts of CO_2 to the atmosphere, coinciding with amber deposits in Brazil, Ecuador and Congo at low latitudes of the Southern Hemisphere (Pereira et al., 2009; Cadena et al., 2018; Bouju and Perrichot, 2020). During the Albian, an extensive subtropical arid belt developed in the equatorial zone, which subsequently migrated poleward (Scotese, 2021). Abundant resin accumulations were common in tropical mid latitudes in areas such as the Iberian Peninsula, leading to the present Spanish amber deposits (Peñalver and Delclòs, 2010). During the Cenomanian–Turonian,

climate zones began to structure latitudinally (Sewall et al., 2007), although under hothouse conditions and the influence of intense volcanism (Kidder and Worsley, 2010; Mills et al., 2017), enabling tropical biota to migrate poleward of 40°N latitude. Forests of resiniferous trees from this period grew in tropical regions, with a MAT of around 30°C (Hay and Floegel, 2012); these originated the resin corresponding to the amber-bearing deposits from the lower Cenomanian of France (Perrichot et al., 2010) and Myanmar (Ross et al., 2010), and from the Turonian of New Jersey in the USA (Grimaldi and Nascimbene, 2010). During the upper Turonian–Maastrichtian, climate changed considerably (Tabor et al., 2016). The simulated global mean surface air temperatures (GMST) show decreased values of 21.2°C–19.5°C during the Campanian. These trends are associated with changes in the fraction of Earth's surface occupied by land (Fig. 1B), which has a higher average albedo than the ocean, affected by the general lowered sea levels that resulted in greater exposure of continental areas (Landwehrs et al., 2021). The Maastrichtian temperature trends are controversial. Some data suggest global cooling (Linert et al., 2014), while others indicate cooling in the South Atlantic and contemporary warming of the North Atlantic, with an average of 25.9°C ± 2°C (Tagliavento et al., 2019).

3.2. Biotic factors

The mass production of resin during the CREI was probably also promoted by potential biotic factors acting at a regional scale (Martínez-Delclòs et al., 2004; Seyfullah et al., 2018). These include arthropod damage, pathogenic activity and the emission of volatile compounds by the resins which attract insects.

Terrestrial arthropods (insects, mites) can cause severe damage to plants through feeding- or development-related activity. Different wood-boring insects, namely beetles (Coleoptera) but also some wasps (Hymenoptera) such as wood wasps (Siricidae) and moths (Lepidoptera) such as cossid millers (Cossidae) or clearwing moths (Sesiidae) bore into wood for nest building and offspring development, at times cultivating fungi as a food source in galleries within woody tissues (Hulcr and Stelinski, 2017; Peris et al., 2021). The diseased tree reacts against invasive agents by developing secondary defensive compounds such as terpene-rich oleoresins in conifers, which flood the area to physically repel the invasion, while different toxins and volatiles act as a chemical defense (Raffa, 2014; Krokene, 2015). The influence of massive attacks of wood-boring beetles on resiniferous ancient forests has been widely cited in the literature based on their abundance in Cenozoic ambers, Pleistocene and Holocene copals, and Defaunation resins (Martínez-Delclòs et al., 2004; Labandeira, 2014a; Seyfullah et al., 2018; Peris, 2020). However, there is no significant direct evidence of beetle infestations in Cretaceous ambers yet found, despite the scarce occurrence of the families of auger beetles (Bostrichidae), spider beetles (Ptinidae), ship timber beetles (Lymexylidae) and weevils (Curculionidae) (Peris and Rust, 2020; Peris, 2020) (Fig. 5A−B). On the contrary, herbivorous insect groups such as true bugs (Hemiptera), thrips (Thysanoptera) (Fig. 5D), grasshoppers and crickets (Orthoptera), and termites (Isoptera) have been found in the major Cretaceous amber deposits and include taxa that currently cause significant damage to plants. In any case, little evidence exists of intense arthropod herbivory during the CREI (Labandeira, 1998, 2014b; Xiao et al., 2022a, b), and the approach has not been used in amber studies due to the scarcity of damaged leaves and other photosynthetic structures (such as cheirolepidiacean axes) as

bioinclusions and the relative temporal and spatial limitation of amber-bearing deposits when compared to rock deposits preserving plant material.

Pathogenic organisms can invade plant tissues directly or through a vector. Aside from their ability to cause direct harm, some extant species from the insect groups noted above and others transmit pathogens to their plant hosts, including viruses, bacteria, fungi, oomycetes and nematodes (Labandeira and Prevec, 2014). The development of insect-borne pathogens depends on population dynamics, dispersal ability, host selection behavior and the feeding behavior of the insect vectors (Labandeira and Prevec, 2014; Eigenbrode et al., 2018). Bacteria and fungi are chiefly spread by adhering to the insect's body, so their vector relationship is not specific, but the transmission of viral diseases entails a higher specificity (Jones, 2005). Oomycetes are remarkable plant pathogens because infection by these fungus-like microorganisms can induce copious resin exudation, as observed in the genus *Agathis* in New Zealand (Fig. 5E−G), which produces a particular variation in the coloration of large resin exudates (Weir et al., 2015). Unfortunately, this type of resin would be difficult to recognize once transformed into amber; future studies may be able to distinguish this resin isotopically or by the presence of oomycete spores as bioinclusions.

Plants are known to emit volatile compounds to attract or repel insects (Raffa, 2014; Cantúa Ayala et al., 2019). On the other hand, many insect species are attracted to volatile plant mixtures which indicate tree stress, as these signaling allows entering tissues free of defense and, potentially, competition (Hulcr and Dunn, 2011). Resin terpenoids may be able to attract pollinators (Pichersky and Gershenzon, 2020; Zhou and Pichersky, 2020). Highly specialized pollination relationships between some groups of insects and gymnosperms have been discovered in amber since the Albian (Fig. 5C), in some instances lacking extant representatives of such pollination interactions (Peñalver et al., 2012, 2015; Peris et al., 2017, 2020; Peña-Kairath et al., in press). Resin exudation by conifers during the CREI could be related to the attraction of certain groups of insects to assist in the pollination. This idea was proposed for Cenozoic ambers produced by angiosperms (Armbruster, 1993). Nevertheless, this hypothesis is challenging to test at present, and the absence of Cretaceous insects with attached conifer pollen (Peris et al., 2020) renders it unlikely. Nevertheless, cheirolepidiaceous pollen has been found on the mouthparts of insects in compression–impression deposits from non-amber producing environments of the Middle Jurassic to the Early Cretaceous (Labandeira et al., 2016), indicating that insect pollination of at least one reproductively specialized cheirolepidiaceous conifer was an exception (Labandeira et al., 2007).

4. Present limitations

We propose that the CREI represented a distinct mass resin production that took place over a continuous time interval from the Barremian to the Maastrichtian despite differences in the known record of amber-bearing deposits between different Cretaceous stages (Fig. 1A). If these records reflect a variable degree of resin production and/or accumulation throughout time, the causes underlying these fluctuations are not well understood at present, although they may relate to specific circumstances that must be addressed on a case by case basis by integrating multiple approaches. We hypothesize that the same set of general processes that promoted resin mass production (and accumulation) acted for the entirety of the CREI, but under possible local or regional circumstances that determined the intensity of the effect. Note that the CREI is established using the stage level as the temporal framework. A higher

temporal resolution would add considerable noise to the analyses at present, as many amber deposits and conventional paleobotanical deposits are far from accurately dated. Thus, this circumstance remains a fundamental constraint when addressing the CREI.

The amber deposits during the CREI are numerous and widely distributed, although skewed towards the Northern Hemisphere according to their current occurrences, especially those from the Albian and Cenomanian (Figs 1, 2). Such a distribution may reflect sampling (or study) biases, for instance due to the impossibility to access sedimentary outcrops in extensive areas covered by vegetation or deserts in the Southern Hemisphere. However, the unequal amber deposit distribution between hemispheres might also be explained by the greater proportion of emerged land mass in the Northern Hemisphere when compared to the Southern Hemisphere (Landwehrs et al., 2021) (Fig. 1). Moreover, the distribution of charcoal during the Cretaceous was scarcer in the Southern Hemisphere (Brown et al., 2012; appendix 2), suggesting a much lower prevalence of forest fires than in the Northern Hemisphere during that time. Therefore, it is also possible that resin-producing forests were more widespread in the Northern Hemisphere during the Cretaceous, leading to the formation of a greater number of amber deposits.

5. Conclusions

The Cretaceous distribution of amber-bearing deposits is clustered around an interval of roughly 60 Ma, from the Barremian to the Maastrichtian, and reflects global, massive resin production during the late Mesozoic. Prior to that, since the Carboniferous and during the Triassic, Jurassic and the earliest Cretaceous (the ca. 15 Ma from the Berriasian to Hauterivian), amber is remarkably scarce, appears in small pieces and, save from some Triassic amber, it has not hitherto yielded macroscopic bioinclusions. Shared characteristics of Cretaceous amber deposits are herein used to formally establish the Cretaceous Resinous Interval, or CREI, and are distinct from the Cenozoic amber deposits. The resin that originated the amber deposits during the CREI was produced by conifers and was accumulated in transitional sedimentary environments from subtropical and temperate regions, commonly associated with charcoal and coinciding with periods of marine transgression. Moreover, the fauna and flora preserved within the CREI amber share similar characteristics and suffered comparable taphonomic biases. The set of factors potentially involved in the CREI are complex and often interrelated. Abiotic conditions that we relate to massive resin production and accumulation that took place during the CREI include: (1) the increase of global average temperatures, (2) a reduced latitudinal temperature gradient, (3) higher values of greenhouse atmospheric gases (carbon dioxide, methane) and oxygen, (5) greater wildfire activity, (6) moderate or relatively low average rainfall, (7) increased volcanic activity, (8) transgressive changes in the sea level, (9) changes in the ocean physicochemical properties (high sea surface temperatures, hyper-salinity), (10) a more globalized ocean circulation pattern due to seafloor spreading and (11) increased storm and hurricane activity. Biotic factors partially explaining the CREI at a more localized scale could have included arthropod damage, pathogenic activity and the emission of insect-attracting compounds by the resins.

Despite establishing a single interval at present for the mass production and accumulation of resin during the Cretaceous, distinct subintervals or even events might be distinguished within the CREI in the future if a greater temporal resolution was gained when more locality and dating data is available. It will be necessary to substantially increase

reconnaissance efforts in areas of the Southern Hemisphere to determine whether the scarcity of amber deposits there is just apparent or rather obeys to reasons linked with a comparatively lower proportion of emerged land area during the Cretaceous and consequent lesser extension of resiniferous forests.

We hope that our multidisciplinary approach to define a time interval of mass production and burial of resin will stimulate future research efforts aimed at shedding light on the past dynamics between the geosphere and the biosphere. Although several abiotic and biotic factors influencing resin production and accumulation during the Cretaceous have been proposed herein, the relative importance of each factor as well as their geographical scale, among other variables, will need to be determined in future studies. Equally paramount will be expanding the taphonomic work focused on ascertaining the formation processes of amber deposits, and those features related to resin-producing plants based on geochemical and plant meso-/macroremains, including wood studies. Increased knowledge of when, how and why the CREI took place will shed light on its global impact for the Cretaceous terrestrial ecology and the establishment of modern ecosystems. The exceptionally preserved record that was trapped in resin during the Cretaceous Resinous Interval is crucial to unravel the evolutionary history of many key lineages, including plants, terrestrial arthropods and vertebrates, and for the understanding of life, as we know it, in a moment of critical change for terrestrial ecosystems at the transition from the Mesozoic to the Cenozoic.

Declaration of Competing Interest

The authors declare that they have no known competing financial interests or personal relationships that could have appeared to influence the work reported in this paper.

Acknowledgements

This study is a contribution to the projects CRE CGL2017-84419 AEI/FEDER, UE from the Ministerio de Ciencia, Innovación y Universidades (Spain), and has been partially supported by the *Consejería de Industria, Turismo, Innovación, Transporte y Comercio* of the *Gobierno de Cantabria* through the public enterprise EL SOPLAO S.L. (research agreement #20963 with University of Barcelona and research contract REF 030611220077 to IGME-CSIC, both 2022–2025). This is contribution no. 6 of the postdoctoral fellowships program Beatriu de Pinós project 2020 BP 00015, *The flowering plant success – Influence of beetles*, funded to DP by the Secretary of Universities and Research (Government of Catalonia) and by the Horizon 2020 program of research and innovation of the European Union under the Marie-Curie grant agreement no. 801370. This is also a contribution to the project GEFNE 127-14 by the National Geographic Global Exploration Fund Northern Europa, to the project SO 894/6-1 by the Deutsche Forschungsgemeinschaft (DFG), to the project 90946 by the VolkswagenStiftung and a contribution of the activity of the laboratory “Advanced Micropalaeontology, Biodiversity and Evolution Researches” (AMBER) led by DA at the Lebanese University. The coauthor SÁ-P thanks the support from the Secretaria d’Universitats i Recerca de la Generalitat de Catalunya (Spain) and the European Social Fund (2021FI_B2 00003).

Data availability: All data generated or analyzed during this study are included in the manuscript and supporting files.

References

Allen, C.D., Macalady, A.K., Chenchouni, H., Bachelet, D., McDowell, N. et al., 2010. A global overview of drought and heat-induced tree mortality reveals emerging climate change risks for forests. Forest Ecology and Management 259, 660–684. DOI: https://doi.org/10.1016/j.foreco.2009.09.001

Álvarez-Parra, S., Pérez-de la Fuente, R., Peñalver, E., Barrón, E., Alcalá, L. et al., 2021. Dinosaur bonebed amber from an original swamp forest soil. eLife 10, e72477. DOI: https://doi.org/10.7554/eLife.72477

Anderson, K.B., Crelling, J.C. (Eds.) 1995. Amber, Resinite, and Fossil Resins. ACS Symposium Series No. 617, Washington, p. 297.

Anderson, K.B., Winans, R.E., Botto, R.E., 1992. The nature and fate of natural resins in the geosphere–II. Identification, classification and nomenclature of resinites. Organic Geochemistry 18, 829–841. DOI: https://doi.org/10.1016/0146-6380(92)90051-X

Armbruster, W.S., 1993. Evolution of Plant Pollination Systems: Hypotheses and Tests with the Neotropical Vine *Dalechampia*. Evolution 47, 1480–1505.DOI: https://doi.org/10.1111/j.1558-5646.1993.tb02170.x

Azar, D., Gèze, R., Acra, F., 2010. Lebanese amber. In: Penney, D. (Ed.), Biodiversity of Fossils in Amber from the Major World Deposits. Siri Scientific Press, pp. 271–298.

Balseca, W., Ferrari, L., Pasquare, G., Tibaldi, A., 1993. Structural evolution of the Northern sub-Andes of Ecuador: the Napo uplift. Second ISAG, Oxford (UK) 9, 163–166.

Barral, A., Gomez, B., Fourel, F., Daviero-Gomez, V., Lécuyer, Ch., 2017. CO_2 and temperature decoupling at the million-year scale during the Cretaceous Greenhouse. Scientific Reports 7, 8310. DOI: https://doi.org/10.1038/s41598-017-08234-0

Barrón, E., Peyrot, D., Rodríguez-López, J.P., Meléndez, N., López Del Valle, R. et al., 2015. Palynology of Aptian and upper Albian (Lower Cretaceous) amber-bearing outcrops of the southern margin of the Basque-Cantabrian basin (northern Spain) Cretaceous Research 52, 292–312. DOI: https://doi.org/10.1016/j.cretres.2014.10.003

Belcher, C.A., Hudspith, V.A., 2017. Changes to Cretaceous surface fire behaviour influenced the spread of the early angiosperms. New Phytologist 213, 1521–1532. DOI: https://doi.org/10.1111/nph.14264

Belcher, C.M., McElwain, J.C., 2008. Limits for combustion in low O_2 redefine paleoatmospheric predictions for the Mesozoic. Science 321, 1197–1200. DOI: http://doi.org/10.1126/science.1160978

Benson, R.B.J., Butler, R., Close, R.A., Saupe, E., Rabosky, D.L., 2021. Biodiversity across space and time in the fossil record. Current Biology 31, R1225–R1236. DOI: https://doi.org/10.1016/j.cub.2021.07.071

Benton, M.J., Wilf, P., Sauquet, H., 2022. The Angiosperm Terrestrial Revolution and the origins of modern biodiversity. New Phytologist 233, 2017–2035. DOI: https://doi.org/10.1111/nph.17822

Berini, J.L. Brockman, S.A., Hegeman, A.D., Reich, P.B., Muthukrishnan, R. et al., 2018. Combinations of Abiotic Factors Differentially Alter Production of Plant Secondary Metabolites in Five Woody Plant Species in the Boreal-Temperate Transition Zone. Frontiers in Plant Science 9, 1257. DOI: https://doi.org/10.3389/fpls.2018.01257

Berner, R.A., 2006. GEOCARBSULF: A combined model for Phanerozoic atmospheric O_2 and CO_2. Geochimica et Cosmochimica Acta 70, 5653–5664. DOI: https://doi.org/10.1016/j.gca.2005.11.032

Birks, H.J.B., 2020. Angiosperms versus gymnosperms in the Cretaceous. Proceedings of the National Academy of Sciences 117, 30879–30881. DOI: https://doi.org/10.1073/pnas.2021186117

Bodnar, J., Escapa, I, Cúneo, N.R., Gnaedinger, S., 2013. First Record of Conifer Wood from the Cañadón Asfalto Formation (Early-Middle Jurassic), Chubut Province, Argentina. Ameghiniana 50, 227–239. DOI: https://doi.org/10.5710/AMGH.26.04.2013.620

Bouju, V., Perrichot, V., 2020. A review of amber and copal occurrences in Africa and their paleontological significance. BSGF - Earth Sciences Bulletin 191, 1–11. DOI: https://doi.org/10.1051/bsgf/2020018

Bowen, R., Jux, U., 1987. Afro-Arabian Geology. A kinematic view. Chapman & Hall, London, New York, p. 296.

Bray, P.S., Anderson, K.B., 2008. The nature and fate of natural resins in the geosphere XIII: a probable pinaceous resin from the early Cretaceous (Barremian), Isle of Wight. Geochemical Transactions 9, 1–5. DOI: https://doi.org/10.1186/1467-4866-9-3

Bray, P.S., Anderson, K.B. 2009. Identification of Carboniferous (320 million years old) class Ic amber. Science, 326(5949), 132−134. https://doi.org/10.1126/science.1177539

Brown, S.A.E., Scott, A.C., Glasspool, I.J., Collinson, M.E., 2012. Cretaceous wildfires and their impact on the Earth system. Cretaceous Research 36, 162–190. DOI: https://doi.org/10.1016/j.cretres.2012.02.008

Cadena, E.A., Mejia-Molina, A., Brito, C.M., Peñafiel, S., Sanmartin, K.J. et al., 2018. New Mesozoic and Cenozoic fossils from Ecuador: Invertebrates, vertebrates, plants, and microfossils. Journal of South American Earth Sciences 83, 27–36. DOI: https://doi.org/10.1016/j.jsames.2018.02.004

Cantúa Ayala, J.A., Flores Olivas, A., Valenzuela Solo, J.H., 2019. Volatile organic compounds of plants induced by insects: current situation in Mexico. Revista Mexicana de Ciencias Agrícolas 10, 729–742. DOI: https://doi.org/10.29312/remexca.v10i3.678

Chang, B., Huang, J., Algeo, Th., J., Pancost, R.D., Wan, X. et al., 2022. Episodic massive release of methane during the mid-Cretaceous greenhouse. The Geological Society American Bulletin. DOI: https://doi.org/10.1130/B36169.1

Chumakov, N.M., Zharkov, M.A., Herman, A.B., Doludenko, M.P., Kalandadze, N.N. et al., 1995. Climatic Belts of the Mid-Cretaceous Time. Stratigraphy and Geological Correlation 3, 241–260.

Condamine, F.L., Silvestro, D., Koppelhus, E.B., Antonelli, A., 2020. The rise of angiosperms pushed conifers to decline during global cooling. Proceedings of the National Academy of Sciences 117, 28867–28875. DOI: https://doi.org/10.1073/pnas.2005571117

Condie, K.C., Pisarevsky, S.A., Puetz, S.J., 2021. LIPs, orogens and supercontinents: The ongoing saga. Gondwana Research 96, 105–121. DOI: https://doi.org/10.1016/j.gr.2021.05.002

Cousin-Rittemard, N.M.M., Dijkstra, H.A., Zwagers, T., 2002. Was there a wind-driven Tethys Circum-global Current in the Late Cretaceous? Earth and Planetary Science Letters 203, 741–753. DOI: https://doi.org/10.1016/S0012-821X(02)00899-3

Couture, J., Meehan, T., Kruger, E., Lindroth R.L., 2015. Insect herbivory alters impact of atmospheric change on northern temperate forests. Nature Plants 1, 15016. DOI: https://doi.org/10.1038/nplants.2015.16

Chaboureau, A.C., Sepulchre, P., Donnadieu, Y., Franc, A., 2014. Tectonic-driven climate change and the diversification of angiosperms. Proceedings of the National Academy of Sciences 111, 14066–14070. DOI: https://doi.org/10.1073/pnas.1324002111

Dalling, J.W., Cernusak, L.A., Winter, K., Aranda, J., Garcia, M. et al., 2016. Two tropical conifers show strong growth and water-use efficiency responses to altered CO_2 concentration. Annals of Botany 118, 1113–1125. DOI: https://doi.org/10.1093/aob/mcw162

De Lima, F.J., Pires, E.F., Jasper, A., Uhl, D., Feitosa Saraiva, A.A. et al., 2019. Fire in the paradise: evidence of repeated palaeo-wildfires from the Araripe Fossil Lagerstätte (Araripe Basin, Aptian-Albian), Northeast Brazil. Palaeobiodiversity and Palaeoenvironments 99, 367–378. DOI: https://doi.org/10.1007/s12549-018-0359-7

Della Prasetya, Ch., Syaufina, L., Santosa, G., 2017. The effect of various types of forest fires on pine resin productivity in Gunung Walat University Forest, Sukabumi, Indonesia. Biodiversitas 18, 476–482. DOI: https://doi.org/10.13057/biodiv/d180105

DePalma, R., Cichocki, F., Dierick, M., Feeney, R., 2010. Preliminary Notes on the First Recorded Amber Insects from the Hell Creek Formation. The Journal of Paleontological Sciences JPS. C.10.0001, 1–7.

Eberth, D.A., 2005. The Geology. In: Currie, P.J. and Koppelhus, E.B. (Eds.), Dinosaur Provincial Park: A Spectacular Ancient Ecosystem Revealed. Indiana University Press, pp. 54–82.

Eigenbrode, S.D., Bosque-Pérez, N.A., Davis, Th.S., 2018. Insect-Borne Plant Pathogens and Their Vectors: Ecology, Evolution, and Complex Interactions. Annual Review of Entomology 63, 169–191. DOI: https://doi.org/10.1146/annurev-ento-020117-043119

Eldholm, O., Coffin, L.F., 2000. Large Igneous Provinces and Plate Tectonics. In: Richards, M.A., Gordon, R.G., and Van Der Hilst, R.D. (Eds.), The History and Dynamics of Global Plate Motions. American Geophysical Union, Geophysical Monograph Series 121, 309–326. DOI: https://doi.org/10.1029/GM121p0309

Erwin, D.H., 2009. Climate as a Driver of Evolutionary Change. Current Biology 19, 575–583. DOI: https://doi.org/10.1016/j.cub.2009.05.047

Farnsworth, A., Lunt, D.J., Robinson, S.A., Valdes, P.J., Roberts, W.H.G. et al., 2019. Past East Asian monsoon evolution controlled by paleogeography, not CO_2. Science Advances 5, eaax169. DOI: https://doi.org/10.1126/sciadv.aax1697

Glasspool, I.J., Scott, A.C., 2010. Phanerozoic concentrations of atmospheric oxygen reconstructed from sedimentary charcoal. Nature Geoscience 3, 627–630. DOI: https://doi.org/10.1038/ngeo923

Grimaldi, D.A., 2019. Amber. Current Biology 29, 861–862. DOI: https://doi.org/10.1016/j.cub.2019.08.047

Grimaldi, D.A., Nascimbene, P., 2010. Raritan (New Jersey) amber. In: Penney, D. (Ed.), Biodiversity of Fossils in Amber from the Major World Deposits. Siri Scientific Press, pp. 167–191.

Grimaldi, D.A., Ross, A.J., 2017. Extraordinary Lagerstätten in Amber, with particular reference to the Cretaceous of Burma. In: Fraser, N.C. and Sues, H.-D. (Eds.), Terrestrial Conservation Lagerstätten: Windows into the Evolution of Life on Land. Dunedin Academic Press Ltd, pp. 287–342.

Grimaldi, D.A., Lillegraven, J.A., Wampler, T., Bookwalter, D., Shedrinsky, A.M., 2000a. Amber from Upper Cretaceous through Paleocene strata of the Hanna Basin, Wyoming, with evidence for source and taphonomy of fossil resins. Rocky Mountain Geology 35, 163–204.

Grimaldi, D.A., Shedrinsky, A., Wampler, Th.P., 2000b. A remarkable deposit of fossiliferous amber from the Upper Cretaceous (Turonian) of New Jersey. In: Grimaldi, D. (Ed.), Studies on fossils in amber, with particular reference to the Cretaceous of New Jersey. Backhuys Publishers, pp. 1–76.

Grimaldi, D.A., Sunderlin, D., Aaroe, G.A., Dempsky, M.R., Parker, N.E. et al., 2018. Biological Inclusions in Amber from the Paleogene Chickaloon Formation of Alaska. American Museum Novitates 3908, 1–37. DOI: https://doi.org/10.1206/3908.1

Haq, B.U., 2014. Cretaceous eustasy revisited. Global and Planetary Change 113, 44–58. DOI: https://doi.org/10.1016/j.gloplacha.2013.12.007

Hasegawa, H., Tada, R., Jiang, X., Suganuma, Y., Imsamut, S. et al., 2012. Drastic shrinking of the Hadley circulation during the mid-Cretaceous Supergreenhouse. Climate of the Past 8, 1323–1337. DOI: https://doi.org/10.5194/cp-8-1323-2012

Hay, W.W., 2009. Cretaceous Oceans and Ocean Modelling. In: Hu., X., Wang, Ch., Scott, R.W., Wagreich, M., nd Jansa, L. (Eds.), Cretaceous Oceanic Red Beds: Stratigraphy, Composition, Origins, and Paleoceanographic and Paleoclimatic Significance. SEPM Special Publication 91, 243–271. DOI: https://doi.org/10.2110/sepmsp.091.233

Hay, W.W., 2017. Toward understanding Cretaceous climate—An updated review. Science China Earth Sciences 60, 5–19. DOI: https://doi.org/10.1007/s11430-016-0095-9

Hay, W.W., Floegel, S., 2012. New thoughts about the Cretaceous climate and oceans. Earth-Science Reviews 115, 262–272. DOI: https://doi.org/10.1016/j.earscirev.2012.09.008

Hay, W.W., DeConto, R.M., de Boer, P. Flögel, S., Song, Y. et al., 2019. Possible solutions to several enigmas of Cretaceous climate. International Journal Earth Sciences 108, 587–620. DOI: https://doi.org/10.1007/s00531-018-1670-2

He, T., Lamont, B., Manning, J.A., 2016. Cretaceous origin for fire adaptations in the Cape flora. Scientific Reports 6, 34880. DOI: https://doi.org/10.1038/srep34880

Holz, M., 2015. Mesozoic paleogeography and paleoclimates – A discussion of the diverse greenhouse and hothouse conditions of an alien world. Journal of South American Earth Sciences 61, 91–107. DOI: https://doi.org/10.1016/j.jsames.2015.01.001

Hu, X., Scott, R.W., Cai, Y., Wang, Ch., Melinte-Dobrinescu, M.C., 2012. Cretaceous oceanic red beds (CORBs): Different time scales and models of origin. Earth-Science Reviews 115, 217–248. DOI: https://doi.org/10.1016/j.earscirev.2012.09.007

Huber, B.T., O'Brien, Ch.L., 2020. Cretaceous Climate. In: Scott, E., and Alderton, D. (Eds.), Encyclopedia of Geology, 2nd edition, Elsevier, pp. 497–503.

Huber, B.T., MacLeod, K.G., Watkins, D.K., Coffin, M.F., 2018. The rise and fall of the Cretaceous Hot Greenhouse climate. Global and Planetary Change 167, 1–23. DOI: https://doi.org/10.1016/j.gloplacha.2018.04.004

Hulcr, J., Dunn, R.R., 2011. The sudden emergence of pathogenicity in insect–fungus symbioses threatens naive forest ecosystems. Proceedings of the Royal Society B: Biological Sciences, 278(1720), 2866–2873. DOI: https://doi.org/10.1098/rspb.2011.1130

Hulcr, J., Stelinski, L.L., 2017. The Ambrosia Symbiosis: From Evolutionary Ecology to Practical Management. Annual Review of Entomology 62, 285–303. DOI: https://doi.org/10.1146/annurev-ento-031616-035105

Iturralde-Vinent, M.A., MacPhee, R.D.E., 2019. Remarks on the age of Dominican amber. Palaeoentomology 2, 236–240. DOI: https://doi.org/10.11646/PALAEOENTOMOLOGY.2.3.7

Jahren, H., Arens, N.C., Sarmiento-Pérez, G.A., Guerrero, J., Amundson, R., 2001. Terrestrial record of methane hydrate dissociation in the Early Cretaceous. Geology 29, 159–162. DOI: https://doi.org/10.1130/0091-7613(2001)029<0159:TROMHD>2.0.CO;2

Johansson, L., Zahirovic, S., Dietmar Müller, R., 2018. The Interplay Between the Eruption and Weathering of Large Igneous Provinces and the Deep-Time Carbon Cycle. Geophysical Research Letters 45, 5380–5389. DOI: https://doi.org/10.1029/2017GL076691

Jones, D.R., 2005. Plant Viruses Transmitted by Thrips. European Journal Plant Pathology 113, 119–157. DOI: https://doi.org/10.1007/s10658-005-2334-1

Jossang, J., Bel-Kassaoui, H., Jossang, A., Seuleiman, M., Nel, A., 2008. Quesnoin, a Novel Pentacyclic ent-Diterpene from 55 Million Years Old Oise Amber. The Journal of Organic Chemistry 73, 412–417. DOI: https://doi.org/10.1021/jo701544k

Kent, D.V., Muttoni, G., 2022. Latitudinal land–sea distributions and global surface albedo since the Cretaceous. Palaeogeography, Palaeoclimatology, Palaeoecology 585, 110718. DOI: https://doi.org/10.1016/j.palaeo.2021.110718

Kergoat, G.J., Bouchard, P., Clamens, A.-L., Abbate, J.L., Jourdan, H. et al., 2014. Cretaceous environmental changes led to high extinction rates in a hyperdiverse beetle family. BMC Evolutionary Biology 14, 1–13. DOI: https://doi.org/10.1186/s12862-014-0220-1

Kidder, D.L., Worsley, T.R., 2010. Phanerozoic Large Igneous Provinces (LIPs), HEATT (Haline Euxinic Acidic Thermal Transgression) episodes, and mass extinctions. Palaeogeography, Palaeoclimatology, Palaeoecology 295, 162–191. DOI: https://doi.org/10.1016/j.palaeo.2010.05.036

Klages, J.P., Salzmann, U., Bickert, T., Hillenbrand, C.-D., Gohl, K. et al., 2020. Temperate rainforests near the South Pole during peak Cretaceous warmth. Nature 580, 81–86. DOI: https://doi.org/10.1038/s41586-020-2148-5

Krokene, P., 2015. Conifer Defence and Resistance to Bark Beetles. In: Vega, F.E., and Hofstetter, R.W. (Eds.), Bark Beetles: Biology and Ecology of Native and Invasive Species. Academic Press, Elsevier, London, pp. 177–207.

Kurepin, L.V., 2018. Contrasting acclimation abilities of two dominant boreal conifers to elevated CO_2 and temperature. Plant, Cell & Environment 41, 1331–1345. DOI: https://doi.org/10.1111/pce.13158

Kvaček, J., Barrón, E., Hermanová, Z., Mendes, M.M., Karch, J. et al., 2018. Araucarian conifer from late Albian amber of northern Spain. Papers in Palaeontology 4, 643–656. DOI: https://doi.org/10.1002/spp2.1223

Labandeira, C.C., 1998. The role of insects in late Jurassic to Middle Cretaceous ecosystems. In: Lucas, S.G., Kirkland, J.I., and Estep, J.W. (Eds.), Lower and Middle Cretaceous Terrestrial Ecosystems. New Mexico Museum of Natural History and Science Bulletin 14, 105–124. DOI: http://hdl.handle.net/10088/5968

Labandeira, C.C., 2007. The origin of herbivory on land: Initial patterns of plant tissue consumption by arthropods. Insect Science 14, 259–275. DOI: https://doi.org/10.1111/j.1744-7917.2007.00141.x-i1

Labandeira, C.C., 2013. A paleobiologic perspective on plant–insect interactions. Current Opinion in Plant Biology 16, 414–421. DOI: https://doi.org/10.1016/j.pbi.2013.06.003

Labandeira, C.C., 2014a. Amber. In: LaFlamme, M., Schiffbauer, J.D., and Darroch, S.A.F. (Eds.), Reading and Writing of the Fossil Record: Preservational Pathways to Exceptional Fossilization. Paleontological Society Papers 20, pp. 163–215. DOI: https://repository.si.edu/handle/10088/24696

Labandeira, C.C., 2014b. Why Did Terrestrial Insect Diversity Not Increase During the Angiosperm Radiation? Mid-Mesozoic, Plant-Associated Insect Lineages Harbor Clues. In: Pontarotti, P. (Ed.), Evolutionary Biology: Genome Evolution, Speciation, Coevolution and Origin of Life. Springer International Publishing, pp. 261–299. DOI: https://doi.org/10.1007/978-3-319-07623-2_13

Labandeira, C.C., Kvaček, J., Mostovski, M.B., 2007. Pollination drops, pollen, and insect pollination of Mesozoic gymnosperms. Taxon 56, 663–695. DOI: https://doi.org/10.2307/25065852

Labandeira, C.C., Prevec, R., 2014. Plant paleopathology and the roles of pathogens and insects. International Journal of Paleopathology 4, 1–16. DOI: https://doi.org/10.1016/j.ijpp.2013.10.002

Labandeira, C.C., Yang, Q., Santiago-Blay, J.A., Hotton, C.L., Monteiro, A. et al., 2016. The evolutionary convergence of mid-Mesozoic lacewings and Cenozoic butterflies. Proceedings of the Royal Society B 283, 20152893. DOI: http://dx.doi.org/10.1098/rspb.2015.2893

Lake, J.A., Wade, R.N., 2009. Plant–pathogen interactions and elevated CO_2: morphological changes in favour of pathogens. Journal of Experimental Botany 60, 3123–3131. DOI: https://doi.org/10.1093/jxb/erp147

Lambert, J.B., Johnson, S.C., Poinar, G.O. Jr., 1996. Nuclear magnetic resonance characterization of Cretaceous amber. Archaeometry 38, 325–335. DOI: https://doi.org/10.1111/j.1475-4754.1996.tb00780.x

Landwehrs, J., Feulner, G., Petri, S., Sames, B., Wagreich, M., 2021. Investigating Mesozoic Climate Trends and Sensitivities With a Large Ensemble of Climate Model Simulations. Paleoceanography and Paleoclimatology 36, e2020PA004134. DOI: https://doi.org/10.1029/2020PA004134

Langenheim, J.H., 1990. Plant resins. American Scientist 78, 16–24.

Langenheim, J.H., 1995. Biology of Amber-Producing Trees: Focus on Case Studies of *Hymenaea* and *Agathis*. In: Anderson, K.B, and Crelling, J.C. (Eds.), Amber, Resinite, and Fossil Resins. ACS Symposium Series 617, pp. 1–31.

Langenheim, J.H., 2003. Plant Resins: Chemistry, Evolution, Ecology, Ethnobotany. Timber Press, Portland, Cambridge, p. 586.

Linnert, C., Robinson, S., Lees, J., Brown, P.R., Pérez-Rodríguez, I., et al., 2014. Evidence for global cooling in the Late Cretaceous. Nature Communications 5, 4194. DOI: https://doi.org/10.1038/ncomms5194

Lloyd, G.T., Davis, K.E., Pisani, D., Tarver, J.E., Ruta, M. et al., 2008. Dinosaurs and the Cretaceous Terrestrial Revolution. Proceedings of the Royal Society B 275, 2483–2490. DOI: https://doi.org/10.1098/rspb.2008.0715

Macdonald, F., Wordsworth, R., Swanson-Hysell, N., 2018. LIPs and climate change. Goldschmidt2018 Abstract. DOI: https://goldschmidt.info/2018/abstracts/abstractView?id=2018003432

Maksoud, S., Azar, D., 2020. Lebanese amber: latest updates. Palaeoentomology 3, 125–155. DOI: 10.11646/palaeoentomology.3.2.2

Maksoud, S., Azar, D., Granier, B., Gèze, R., 2017. New data on the age of the Lower Cretaceous amber outcrops of Lebanon. Palaeoworld 26, 331–338. DOI: https://doi.org/10.1016/j.palwor.2016.03.003

Marcilly, Ch.M., Torsvika, T.H., Conrad, P., 2022. Global Phanerozoic sea levels from paleogeographic flooding maps. Gondwana Research 110, 128–142. DOI: https://doi.org/10.1016/j.gr.2022.05.011

Martínez-Delclòs, X., Briggs, D.E.G., Peñalver, E., 2004. Taphonomy of insects in carbonates and amber. Palaeogeography, Palaeoclimatology, Palaeoecology 203, 19–64. DOI: https://doi.org/10.1016/S0031-0182(03)00643-6

Mays, Ch., Coward, A.J., O'Dell, L.A., Tappert, R., 2019. The botanical provenance and taphonomy of Late Cretaceous Chatham amber, Chatham Islands, New Zealand. Review of Palaeobotany and Palynology 260, 16–26. DOI : https://doi.org/10.1016/j.revpalbo.2018.08.004

McCoy, V.E, Barthel, J.H., Boom, A., Peñalver, E., Delclòs, X. et al., 2021. Volatile and semi-volatile composition of Cretaceous amber. Cretaceous Research 127, 104958. DOI: https://doi.org/10.1016/j.cretres.2021.104958

McCoy, V.E., Boom, A., Kraemer, M.M.S., Gabbott, S.E., 2017. The chemistry of American and African amber, copal, and resin from the genus *Hymenaea*. Organic Geochemistry 113, 43–54. DOI: https://doi.org/10.1016/j.orggeochem.2017.08.005

McElwain, J.C., 2018. Paleobotany and Global Change: Important Lessons for Species to Biomes from Vegetation Responses to Past Global Change. Annual Review of Plant Biology 69, 761–787. DOI: https://doi.org/10.1146/annurev-arplant-042817-040405

McKenna, D.D., Wild, A., Kanda, K., Bellamy, C., Beutel, R.G. et al., 2015. The beetle tree of life reveals that Coleoptera survived end-Permian mass extinction to diversify during the Cretaceous terrestrial revolution. Systematic Entomology 40, 835–880. DOI: https://doi.org/10.1111/syen.12132

Menor-Salván, C., Najarro, M., Velasco, F., Rosales, I., Tornos, F. et al., 2010. Terpenoids in extracts of Lower Cretaceous ambers from the Basque-Cantabrian Basin (El Soplao, Cantabria, Spain): Paleochemotaxonomic aspects. Organic Geochemistry 41, 1089–1103. DOI: https://doi.org/10.1016/j.orggeochem.2010.06.013

Menor-Salván, C., Simoneit, B.R.T., Ruíz-Bermejo, M., Alonso, J., 2016. The molecular composition of Cretaceous ambers: Identification and chemosystematic relevance of 1,6-dimethyl-5-alkyltetralins and related bisnorlabdane biomarkers. Organic Geochemistry 93, 7–21. DOI: https://doi.org/10.1016/j.orggeochem.2015.12.010

Meredith, R.W., Janečka, J.E., Gatesy, J., Ryder, O.A., Fisher, C.A. et al., 2011. Impacts of the Cretaceous Terrestrial Revolution and KPg Extinction on Mammal Diversification. Science 334, 521–524. DOI: https://doi.org/10.1126/science.1211028

Mills, J.V., Gomes, M.L., Kristall, B., Sageman, B.B., Jacobson, A.D. et al., 2017. Massive volcanism, evaporite deposition, and the chemical evolution of the Early Cretaceous ocean. Geology 45, 475–478. DOI: https://doi.org/10.1130/G38667.1

Moreau, J.-D., Néraudeau, D., Perrichot, V., 2020. Conifers from the Cenomanian amber of Fouras (Charente-Maritime, western France). BSGF – Earth Sciences Bulletin 191, 1–5. DOI: https://doi.org/10.1051/bsgf/2020017

Najarro, M., Peñalver, E., Rosales, I., Pérez-de-la-Fuente, R., Daviero-Gomez, V. et al., 2009. Unusual concentration of Early Albian arthropod-bearing amber in the Basque-Cantabrian Basin (El Soplao, Cantabria, Northern Spain): Palaeoenvironmental and palaeobiological implications. Geologica Acta 7, 363–387. DOI: https://doi.org/10.1344/105.000001443

Néraudeau, D., Perrichot, V., Colin, J.-P., Girard, V., Gomez, B. et al., 2008. A new amber deposit from the Cretaceous (uppermost Albian-lowermost Cenomanian) of southwestern France. Cretaceous Research 29, 925–929. DOI: https://doi.org/10.1016/j.cretres.2008.05.009

Neri, M., Roghi, G., Ragazzi, E., Papazzonia, C.A., 2016. First record of Pliensbachian (Lower Jurassic) amber and associated palynoflora from the Monti Lessini (northern Italy). Geobios 50, 49–63. DOI: https://doi.org/10.1016/j.geobios.2016.10.001

Nohra, Y.A., Azar, D., Gèze, R., Maksoud, S., El-Samrani, A. et al., 2013. New Jurassic amber outcrops from Lebanon. Terrestrial Arthropod Reviews 6, 27–51. DOI: https://doi.org/10.1163/18749836-06021056

Nohra, Y.A., Perrichot, V., Boura, A., Jeanneau, L., Néraudeau, D. et al., 2014. Cupressacean origin of the Cretaceous Vendean amber (northwester France): evidence from fossil wood and chemical signatures. 9th European Palaeobotany-Palynology Conference, 189, Padova. https://archivesic.ccsd.cnrs.fr/GR1/insu-01068204v1

Novick, K., Katul, G.G., McCarthy, H.R., Oren, R., 2012. Increased resin flow in mature pine trees growing under elevated CO_2 and moderate soil fertility. Tree Physiology 32, 752–763. DOI: https://doi.org/10.1093/treephys/tpr133

O'Brien, C.L., Robinson, S.A., Pancost, R.D., Sinninghe Damsté, J.S., Schouten, S. et al., 2017. Cretaceous sea-surface temperature evolution: Constraints from TEX_{86} and planktonic foraminiferal oxygen isotopes. Earth-Science Reviews 172, 224–247. DOI: https://doi.org/10.1016/j.earscirev.2017.07.01

Ohba, M., Ueda, H., 2010. A GCM Study on Effects of Continental Drift on Tropical Climate at the Early and Late Cretaceous. Journal of the Meteorological Society of Japan 88, 869–881. DOI: https://doi.org/10.2151/jmsj.2010-601

Olde, K., Jarvis, I., Uličný, D., Pearce, M.A., Trabucho-Alexandre, J. et al., 2015. Geochemical and palynological sea-level proxies in hemipelagic sediments: A critical assessment from the Upper Cretaceous of the Czech Republic. Palaeogeography, Palaeoclimatology, Palaeoecology 435, 222–243. DOI: https://doi.org/10.1016/j.palaeo.2015.06.018

Olivoto, T., Nardino, M., Carvalho, I.R., Follmann, D.N., Szareski, V.J. et al., 2017. Plant secondary metabolites and its dynamical systems of induction in response to environmental factors: A review. African Journal of Agricultural Research 12, 71–84. DOI: https://doi.org/10.5897/AJAR2016.11677

Ortega-Blanco, J., Rasnitsyn, A., Delclòs, X., 2008. First record of anaxyelid woodwasps (Hymenoptera: Anaxyelidae) in Lower Cretaceous Spanish amber. Zootaxa 1937, 39–50. DOI: http://doi.org/10.11646/zootaxa.1937.1.3

Otto, A., Kvaček, J., Goth, K. 2000. Biomarkers from the taxodiaceous conifer *Sphenolepis pecinovensis* Kvaček and resin from Bohemian Cenomanian. Acta Palaeobotanica Suppl. 2, 153–157.

Pausas, J.G., 2018. Generalized fire response strategies in plants and animals. Oikos 128, 147–153. DOI: https://doi.org/10.1111/oik.05907

Penney, D. (Ed.) 2010. Biodiversity of Fossils in Amber from the Major World Deposits. Siri Scientific Press, Manchester, p. 304.

Peñalver, E., Delclòs, X., 2010. Spanish Amber. In: Penney, D. (Ed.), Biodiversity of Fossils in Amber from the Major World Deposits. Siri Scientific Press, pp. 236–270.

Peñalver, E., Arillo, A., Pérez-de la Fuente, R., Riccio, M.L., Delclòs, X. et al., 2015. Long-Proboscid Flies as Pollinators of Cretaceous Gymnosperms. Current Biology 14, 1917–1923. DOI: https://doi.org/10.1016/j.cub.2015.05.062

Peñalver, E., Delclòs, X., Solórzano Kraemer, M.M., 2018. A new approach to determine the resiniferous trees involved in the origin of the Cretaceous amber deposits. 1st Paleontological Virtual Congress, 140, Valencia. https://www.uv.es/everlab/PUBLICACIONES/1stSVP%20BOOK%20OF%20ABTRACTS.pdf

Peñalver, E., Labandeira, C.C., Barrón, E., Delclòs, X., Nel, P. et al., 2012. Thrips pollination of Mesozoic gymnosperms. Proceedings of the National Academy of Sciences 109, 8623–8628. DOI: https://doi.org/10.1073/pnas.1120499109

Peralta-Medina, E., Falcon-Lang, H.J., 2012. Cretaceous forest composition and productivity inferred from a global fossil wood database. Geology 40, 219–222. DOI: https://doi.org/10.1130/G32733.1

Pereira, R., de Souza Carvalho, I., Simoneit, B.R.T., de Almeida Azevedo, D., 2009. Molecular composition and chemosystematic aspects of Cretaceous amber from the Amazonas, Araripe and Recôncavo basins, Brazil. Organic Geochemistry 40, 863–875. DOI: https://doi.org/10.1016/j.orggeochem.2009.05.002

Pérez-de la Fuente, R., Delclòs, X., Peñalver, E., Speranza, M., Wierzos, J. et al., 2012. Early evolution and ecology of camouflage in insects. Proceedings of the National Academy of Sciences 109, 21414–21419. DOI: https://doi.org/10.1073/pnas.121377511

Pérez-Diaz, L., Eagles, G., 2017. South Atlantic paleobathymetry since early Cretaceous. Scientific Reports 7, 11819. DOI: https://doi.org/10.1038/s41598-017-11959-7

Peris, D., 2020. Coleoptera in amber from Cretaceous resiniferous forests. Cretaceous Research 113, 104484. DOI: https://doi.org/10.1016/j.cretres.2020.104484

Peris, D., Rust, J., 2020. Cretaceous beetles (Insecta: Coleoptera) in amber: the palaeoecology of this most diverse group of insects. Zoological Journal of the Linnean Society 189, 1085–1104. DOI: https://doi.org/10.1093/zoolinnean/zlz118

Peris, D., Delclòs, X., Jordal, B.H., 2021. Origin and evolution of fungus farming in wood-boring Coleoptera – a palaeontological perspective. Biological Reviews 96, 2476–2488. DOI: https://doi.org/10.1111/brv.12763

Peris, D., Labandeira, C.C., Barrón, E., Delclòs, X., Rust, J. et al., 2020. Generalist Pollen-Feeding Beetles during the Mid-Cretaceous. iScience 23, 100913. DOI: https://doi.org/10.1016/j.isci.2020.100913

Peris, D., Pérez-de la Fuente, Peñalver, E., Delclòs, X., Barrón, E. et al., 2017. False Blister Beetles and the Expansion of Gymnosperm-Insect Pollination Modes before Angiosperm Dominance. Current Biology 27, 897–904. DOI: https://doi.org/10.1016/j.cub.2017.02.009

Perrichot, V., 2005. Environnements paraliques à ambre et à végétaux du Crétacé Nord-Aquitain (Charentes, Sud-Ouest de la France). Mémoires Géosciences Rennes, Thèse de l'Université de Rennes 2003, 118, 213 pp. + annexes. https://tel.archives-ouvertes.fr/tel-00011639

Perrichot, V., Néraudeau, D., Tafforeau, P., 2010. Charentese Amber. In: Penney, D. (Ed.), Biodiversity of Fossils in Amber from the Major World Deposits. Siri Scientific Press, pp. 193–208.

Peyrot, D., Barrón, E., Polette, F., Batten, D.J., Néraudeau, D., 2019. Early Cenomanian palynofloras and inferred resiniferous forests and vegetation types in Charentes (southwestern France). Cretaceous Research 94, 168–189. DOI: https://doi.org/10.1016/j.cretres.2018.10.011

Pichersky, E., Gershenzon, J., 2020. The formation and function of plant volatiles: Perfumes for pollinator attraction and defense. Current Opinion in Plant Biology 5, 237–243. DOI: https://doi.org/10.1016/S1369-5266(02)00251-0

Poinar, G., Jr., Lambert, J.B, Wu, Y., 2007. Araucarian source of fossiliferous Burmese amber: Spectroscopic and anatomical evidence. Journal of The Botanical Research Institute of Texas 1, 449–455.

Poulsen, C.J., Zhou, J., 2013. Sensitivity of Arctic Climate Variability to Mean State: Insights from the Cretaceous. Journal of Climate 26, 7003–7022. DOI: https://doi.org/10.1175/JCLI-D-12-00825.1

Poulsen, C.J., Seidov, D., Barron, E.J., Peterson, W.H., 1998. The impact of paleogeographic evolution on the surface oceanic circulation and the marine environment within the mid-Cretaceous Tethys. Paleoceanography and Paleoclimatology 13, 546–559. DOI: https://doi.org/10.1029/98PA01789

Raffa K.F., 2014. Terpenes tell different tales at different scales: glimpses into the Chemical Ecology of conifer – bark beetle – microbial interactions. Journal of Chemical Ecology 40, 1–20. DOI: https://doi.org/10.1007/s10886-013-0368-y

Ray, D.C., van Buchem, F.S.P., Baines, G., Davies, A., Gréselle, B. et al., 2019. The magnitude and cause of short-term eustatic Cretaceous sea-level change: A synthesis. Earth-Science Reviews 197, 102901. DOI: https://doi.org/10.1016/j.earscirev.2019.102901

Rodríguez-López, J.P., Peyrot, D., Barrón, E., 2020. Complex sedimentology and palaeohabitats of Holocene coastal deserts, their topographic controls, and analogues for the mid-Cretaceous of northern Iberia. Earth-Science Reviews 201, 103075. DOI: https://doi.org/10.1016/j.earscirev.2019.103075

Roghi, G., Gianolla, P., Kustatscher, E., Schmidt, A.R., Seyfullah, L.J. 2022. An Exceptionally Preserved Terrestrial Record of LIP Effects on Plants in the Carnian (Upper Triassic) Amber-Bearing Section of

the Dolomites, Italy. Frontiers in Earth Science 10, 900586, 1–18. DOI: https://doi.org/10.3389/feart.2022.900586

Rombola, C.F., Greppi, C.D., Pujana, R.R., García Massini, J.L, Bellosi, E.S., Marenssi, S.A., 2022. Brachyoxylon fossil woods with traumatic resin canals from the Upper CretaceousCerro Fortaleza Formation, southern Patagonia (Santa Cruz Province, Argentina). Cretaceous Research 130, 105065. DOI: https://doi.org/10.1016/j.cretres.2021.105065

Ross, A., Mellish, C., York, P., Crighton, B., 2010. Burmese Amber. In: Penney, D. (Ed.), Biodiversity of Fossils in Amber from the Major World Deposits. Siri Scientific Press, pp. 208–225.

Royer, D.L., Berner, A., Montañez, I.P., Tabor, N.J., Beerling, D.J., 2015. CO_2 as a primary driver of Phanerozoic climate. GSA Today 14, 4–10. DOI: htpps://doi.org/10.1130/1052-5173(2004)014<4:CAAPDO>2.0.CO;2

Rust, J., Singh, H., Rana, R.S., McCann, T., Singh, L. et al., 2010. Biogeographic and evolutionary implications of a diverse paleobiota in amber from the Early Eocene of India. Proceedings of the National Academy of Sciences 107, 18360–18365. DOI: http://dx.doi.org/10.1073/pnas.1007407107

Scotese, C.R., Song, H., Mills, B.J.W., van der Meer, D., 2021. Phanerozoic paleotemperatures: The earth's changing climate during the last 540 million years. Earth-Science Reviews 215, 103503. DOI: https://doi.org/10.1016/j.earscirev.2021.103503

Scotese, C.R., 2021. An Atlas of Phanerozoic Paleogeographic Maps: The Seas Come In and the Seas Go Out. Annual Reviews of Earth and Planetary Sciences 49, 669–718. DOI: https://doi.org/10.1146/annurev-earth-081320-064052

Scott, A.C., 2018. Burning Planet: The Story of Fire Through Time. Oxford University Press, Oxford, p. 256.

Schmidt, A.R., Jancke, S., Lindquist, E.E., Ragazzi, E., Roghi, G. et al., 2012. Arthropods in amber from the Triassic Period. Proceedings of the National Academy of Sciences 109, 14796–14801. DOI: https://doi.org/10.1073/pnas.1208464109

Sewall, J.O., van de Wal, R.S.W., van der Zwan, K., van Oosterhout, C., Dijkstra, H.A. et al., 2007. Climate model boundary conditions for four Cretaceous time slices. Climate of the Past, European Geosciences Union (EGU) 3, 647–657. DOI: https://doi.org/10.5194/cp-3-647-2007

Seyfullah, L.J., Beimforde, Ch., Dal Corso, J., Perrichot, V., Rikkinen, J. et al., 2018. Production and preservation of resins – past and present. Biological Reviews 93, 1684–1714. DOI: https://doi.org/10.1111/brv.12414

Shi, C., Wang, S., Cai, H., Zhang, H, Long, X. et al., 2022. Fire-prone Rhamnaceae with South African affinities in Cretaceous Myanmar amber. Nature Plants 8, 125–135. DOI: https://doi.org/10.1038/s41477-021-01091-w

Shi, G., Grimaldi, D.A., Harlow, G.E., Wang, J., Wang, M. et al., 2012. Age constraint on Burmese amber based on U–Pb dating of zircons. Cretaceous Research 37, 155–163. DOI: https://doi.org/10.1016/j.cretres.2012.03.014

Snedden, J.W., Liu, Ch., 2010. A Compilation of Phanerozoic Sea-Level Change, Coastal Onlaps and Recommended Sequence Designations. On internet: ExxonMobil Production Deutschland GmbH.

Solórzano Kraemer, M.M., Delclòs, X., Clapham, M.E., Arillo, A., Peris, D. et al., 2018. Arthropods in modern resins reveal if amber accurately recorded forest arthropod communities. Proceedings of the National Academy of Sciences 115, 6739–6744. DOI: https://doi.org/10.1073/pnas.1802138115

Solórzano-Kraemer, M.M., Delclòs, X., Engel, M., Peñalver, E., 2020. A revised definition for copal and its significance for palaeontological and Anthropocene biodiversity-loss studies. Scientific Reports 10, 19904. DOI: https://doi.org/10.1038/s41598-020-76808-6

Tabor, C.R., Poulsen, C.J., Lunt, D.J., Rosenbloom, N.A., Otto-Bliesner, B.L. et al., 2016. The cause of Late Cretaceous cooling: A multimodel-proxy comparison. Geology 44, 963–966. DOI: https://doi.org/10.1130/G38363.1

Tagliavento, M., John, C.M., Stemmerik, L., 2019. Tropical temperature in the Maastrichtian Danish Basin: Data from coccolith Δ_{47} and $\delta^{18}O$. Geology 47, 1074–1078. DOI: https://doi.org/10.1130/G46671.1

Tappert, R., McKellar, R.C., Wolfe, A.P., Tappert, M.C., Ortega-Blanco, J. et al., 2013. Stable carbon isotopes of C3 plant resins and ambers record changes in atmospheric oxygen since the Triassic. Geochimica et Cosmochimica Acta 121, 240–262. DOI: https://doi.org/10.1016/j.gca.2013.07.011

Topper, M., Trabucho Alexandre, J., Tuenter, E., Meijer, P.Th., 2011. A regional ocean circulation model for the mid-Cretaceous North Atlantic Basin: implications for black shale formation. Climate of the Past 7, 277–297. DOI: https://doi.org/10.5194/cp-7-277-2011

Torsvik, T., Cocks, L., 2016. Cretaceous. In: Torsvik, T.H., and Cocks, L.R.M. (Eds.), Earth History and Palaeogeography. Cambridge University Press, pp. 219–239. DOI: https://doi.org/10.1017/9781316225523.014

Trapp, S., Croteau, R., 2001. Defensive Resin Biosynthesis in Conifers. Annual Review of Plant Physiology and Plant Molecular Biology 52, 689–724. DOI: https://doi.org/10.1146/annurev.arplant.52.1.689

Veltz, I., Paicheler, J.-C., Maksoud, S., Gèze, R., Azar, D., 2013. Context and genesis of the Lebanese amberiferous palaeoenvironments at the Jurassic-Cretaceous transition. Terrestrial Arthropod Reviews 6, 11–26. DOI: https://doi.org/10.1163/18749836-06021055

Villagómez, R., Jaillard, E., Bulot, L., Rivadeneira, M., Vera, R., 1996. The Aptian–Late Albian marine transgression in the Oriente Basin of Ecuador. Third ISAG. St Malo (France), 521–524.

Wade, D.C., Abraham, N.L., Farnsworth, A., Valdes, P.J., Bragg, F. et al., 2019. Simulating the climate response to atmospheric oxygen variability in the Phanerozoic: a focus on the Holocene, Cretaceous and Permian. Climate of the Past 15, 1463–1483. DOI: https://doi.org/10.5194/cp-15-1463-2019

Wagner, Th., Wallmann, K., Herrle, J.O., Hofmann, P., Stuesser, I., 2007. Consequences of moderate ~25,000 yr lasting emission of light CO_2 into the mid-Cretaceous ocean. Earth and Planetary Science Letters 259, 200–211. DOI: https://doi.org/10.1016/j.epsl.2007.04.045

Wagreich, M., Hart, M.B., Sames, B., Yilmaz, I.O. (Eds.) 2020. Cretaceous Climate Events and Short-Term Sea-Level Changes. Geological Society, London, Special Publications 498, 1–8. DOI: https://doi.org/10.1144/SP498-2019-156

Wang, B., Rust, J., Engel, M.S., Szwedo, J., Dutta, S. et al. 2014a. A Diverse Paleobiota in Early Eocene Fushun Amber from China. Current Biology 24, 1606–1610. DOI: http://dx.doi.org/10.1016/j.cub.2014.05.048

Wang, Y., Huang, Ch., Sun, B., Quan, Ch., Wu, J., Lin, Z., 2014b. Paleo-CO_2 variation trends and the Cretaceous greenhouse climate. Earth-Science Reviews 129, 136–147. DOI: https://doi.org/10.1016/j.earscirev.2013.11.001

Weir, B.S., Paderes, E.P., Anand, N., Uchida, J.Y., Pennycook, S.R. et al., 2015. A taxonomic revision of *Phytophthora* Clade 5 including two new species, *Phytophthora agathidicida* and *P. cocois*. Phytotaxa 205, 21–38. DOI: http://dx.doi.org/10.11646/phytotaxa.205.1.2

Wilkinson, D.M., Nisbet, E.G., Ruxton, G.D., 2012. Could methane produced by sauropod dinosaurs have helped drive Mesozoic climate warmth? Current Biology 22, 292–293. DOI: https://doi.org/10.1016/j.cub.2012.03.042

Wohlwend, S., Hart, M., Weissert, H., 2015. Ocean current intensification during the Cretaceous oceanic anoxic event 2 – evidence from the northern Tethys. Terra Nova 27, 147–155. DOI: https://doi.org/10.1111/ter.12142

Xiao, L.F., Labandeira, C.C., Dilcher, D.L., Ren, D. 2022a. Arthropod and fungal herbivory at the dawn of angiosperm diversification: The Rose Creek plant assemblage of Nebraska, U.S.A. Cretaceous Research 131, 105088. DOI: https://doi.org/10.1016/j.cretres.2021.105088

Xiao, L.F., Labandeira, C.C., Dilcher, D.L., Ren, D. 2022b. Data, metrics, and methods for arthropod and fungal herbivory at the dawn of angiosperm diversification: The Rose Creek plant assemblage of Nebraska, U.S.A. Data in Brief 42, 108170. DOI: https://doi.org/10.1016/j.dib.2022.108170

Zhou, F., Pichersky, E., 2020. More is better: the diversity of terpene metabolism in plants. Current Opinion in Plant Biology 55, 1–10. DOI: https://doi.org/10.1016/j.pbi.2020.01.005

Zhou, J., Poulsen, C.J., Pollard, D., White, T.S., 2008. Simulation of modern and middle Cretaceous marine $\delta^{18}O$ with an ocean-atmosphere general circulation model. Paleoceanography and Paleoclimatology 23, PA3223. DOI: https://doi.org/10.1029/2008PA001596

Zhou, J., Poulsen, C.J., Rosenbloom, N., Shields, C., Briegleb, B., 2012. Vegetation-climate interactions in the warm mid-Cretaceous. Climate of the Past 8, 565–576. DOI: https://doi.org/10.5194/cp-8-565-2012

8.2. Listado de bioinclusiones de los ámbares de la Cuenca del Maestrazgo

A continuación, se indican los géneros y especies presentes en los ámbares de la Cuenca del Maestrazgo por orden alfabético. Todos los taxones indicados se corresponden con artrópodos (arácnidos e insectos). Se han incluido únicamente los géneros y especies que hayan resultado de un estudio detallado y publicado, no se han considerado determinaciones preliminares. En la columna "Localidad tipo" se indica en verde si el yacimiento es localidad tipo de cada especie.

Género y especie	Familia	Orden	Localidad tipo
Ariño (Albiense inferior)			
Liacarus (*Procorynetes*) *shtanchaevae*	Liacaridae	Acari: Oribatida	
Libanoglaris hespericus	†Empheriidae	Psocodea	
San Just (Albiense superior)			
Actenobius magneoculus	Ptinidae	Coleoptera	
Alavaromma orchamum	†Alavarommatidae	Hymenoptera	
Ametroproctus valeriae	Ametroproctidae	Acari: Oribatida	
Aragomantispa lacerata	Mantispidae	Neuroptera	
Aragonimantis aenigma	*Incertae sedis*	Mantodea	
Aragonitermes teruelensis	*Incertae sedis*	Blattodea: Isoptera	
Archaeatropos alavensis	†Empheriidae	Psocodea	
Archiculicoides skalskii	Ceratopogonidae	Diptera	
Arra legalovi	Nemonychidae	Coleoptera	
Burmaphron jentilak	†Stigmaphronidae	Hymenoptera	
Burmazelmira grimaldii	†Archizelmiridae	Diptera	
Cretaceobodes martinezae	Otocepheidae	Acari: Oribatida	
Cretaceomma turolensis	†Gallorommatidae	Hymenoptera	
Cretevania alcalai	Evaniidae	Hymenoptera	
Cretevania montoyai	Evaniidae	Hymenoptera	
Diameneura marveni	†Spathiopterygidae	Hymenoptera	
Hispanothrips utrillensis	Stenurothripidae	Thysanoptera	
Helius turolensis	Limoniidae	Diptera	
Hypovertex hispanicus	Scutoverticidae	Acari: Oribatida	
Iberofoveopsis miguelesi	†Perforissidae	Hemiptera	
Leptoconops zherikhini	Ceratopogonidae	Diptera	
Leptus sp.	Erythraeidae	Acari: Trombidiformes	
Litoleptis fossilis	Rhagionidae	Diptera	
Microphorites utrillensis	Dolichopodidae	Diptera	
Mymaropsis turolensis	†Spathiopterygidae	Hymenoptera	
Orchestina sp.	Oonopidae	Araneae	
Preempheria antiqua	†Empheriidae	Psocodea	
Protoculicoides hispanicus	Ceratopogonidae	Diptera	
Protoculicoides sanjusti	Ceratopogonidae	Diptera	
Serphites silban	†Serphitidae	Hymenoptera	
Spinomegops aragonensis	†Lagonomegopidae	Araneae	
Tenuelamellarea estefaniae	Lamellareidae	Acari: Oribatida	
Trhypochthonius lopezvallei	Trhypochthoniidae	Acari: Oribatida	
Utrillabracon electropteron	Braconidae	Hymenoptera	
Arroyo de la Pascueta (Albiense superior)			
Archaeatropos alavensis	†Empheriidae	Psocodea	
Cretevania rubusensis	Evaniidae	Hymenoptera	

A continuación, se indica el total de bioinclusiones identificadas en los ámbares de Ariño, San Just, Arroyo de la Pascueta y La Hoya. En estos listados se incluyen únicamente las bioinclusiones en el ámbar, no otras muestras obtenidas a partir de los trabajos en los yacimientos. Por ello, las siglas pueden no ser consecutivas. Las bioinclusiones que se corresponden con sininclusiones en la misma pieza de ámbar (separada o no en diferentes preparaciones de epoxi) se indican en amarillo en la columna denominada "Sin". Cuando ha sido posible, se ha añadido la sigla institucional de la colección donde se encuentran depositadas las piezas: CPT y MAP (Museo Aragonés de Paleontología), y MGUV (Museu de la Universitat de València d'Història Natural). Se indican las siglas de trabajo de campo con las que se denominaron inicialmente las bioinclusiones: AR-1-A (ámbar de Ariño), SJ-07, SJ-10, SJNB2012, SJE2012, SJY22012, SJNB2021 (las seis para ámbar de San Just), AP (ámbar de Arroyo de la Pascueta) y LH (ámbar de La Hoya).

Ámbar de Ariño:

Sigla	Identificación/ clase	Orden	Familia	Género y especie	Sin
AR-1-A-2018.2.1	Insecta	Diptera?			
AR-1-A-2018.2.2	Insecta	Neuroptera	Berothidae?		
AR-1-A-2018.3.1	Planta?				
AR-1-A-2018.3.2	Insecta	Psocodea			
AR-1-A-2019.32.1	Insecta	Diptera			
AR-1-A-2019.32.2	Planta?				
AR-1-A-2019.33	Arachnida	Araneae?			
AR-1-A-2019.34	Insecta	Hymenoptera			
AR-1-A-2019.35	Insecta	Psocodea	†Empheriidae	*Libanoglaris hespericus*	
AR-1-A-2019.36	Insecta	Orthoptera	†Elcanidae?		
AR-1-A-2019.37.1	Insecta	Diptera?			
AR-1-A-2019.37.2	Insecta	Diptera	Cecidomyiidae		
AR-1-A-2019.38.1	Insecta	Blattodea	†Blattulidae		
AR-1-A-2019.38.2	Telaraña				
AR-1-A-2019.39	Insecta	Hymenoptera			
AR-1-A-2019.40	Insecta	Thysanoptera			

AR-1-A-2019.41	Arachnida				
AR-1-A-2019.42	Insecta	Psocodea			
AR-1-A-2019.43.1	Insecta	Diptera	Scatopsidae		
AR-1-A-2019.43.2	Insecta	Hymenoptera	†Serphitidae		
AR-1-A-2019.43.3	Insecta	Hymenoptera			
AR-1-A-2019.44	Insecta	Coleoptera	Ptinidae?		
AR-1-A-2019.45	Arachnida: Acari	Oribatida	Liacaridae	*Liacarus* (*Procorynetes*) *shtanchaevae*	
AR-1-A-2019.46	Insecta	Archaeognatha			
AR-1-A-2019.47.1	Insecta	Diptera	Chironomidae		
AR-1-A-2019.47.2	Arachnida				
AR-1-A-2019.48	Insecta	Diptera	Ceratopogonidae		
AR-1-A-2019.49	Insecta	Diptera			
AR-1-A-2019.50.1	Insecta	Diptera	Rhagionidae?		
AR-1-A-2019.50.2	Insecta	Diptera	Psychodidae?		
AR-1-A-2019.50.3	Insecta	Psocodea			
AR-1-A-2019.51	Insecta	Hymenoptera?			
AR-1-A-2019.52	Insecta	Hymenoptera	Scelionidae?		
AR-1-A-2019.53	Fragmento de pluma				
AR-1-A-2019.54	Insecta	Diptera			
AR-1-A-2019.55	Insecta	Hemiptera?			
AR-1-A-2019.56	Planta o coprolito				
AR-1-A-2019.57.1	Insecta	Coleoptera			
AR-1-A-2019.57.2	Insecta				
AR-1-A-2019.58.1	Insecta	Psocodea	Manicapsocidae	*Azarpsocus* sp. nov.	
AR-1-A-2019.58.2	Insecta	Hymenoptera	Scelionidae?		
AR-1-A-2019.59	Insecta	Hymenoptera	†Stigmaphronidae?		
AR-1-A-2019.60.1	Insecta	Psocodea	Manicapsocidae	*Azarpsocus* sp. nov.	
AR-1-A-2019.60.2	Insecta	Diptera			

AR-1-A-2019.60.3	Insecta	Coleoptera			
AR-1-A-2019.61	Insecta	Hymenoptera	†Gallorommatidae	*Cretaceomma turolensis*?	
AR-1-A-2019.62	Arachnida: Acari				
AR-1-A-2019.63	Insecta	Diptera			
AR-1-A-2019.64	Insecta	Hemiptera			
AR-1-A-2019.65.1	Insecta	Hymenoptera			
AR-1-A-2019.65.2	Insecta	Thysanoptera			
AR-1-A-2019.65.3	Insecta	Thysanoptera			
AR-1-A-2019.65.4	Insecta	Thysanoptera			
AR-1-A-2019.66	Insecta	Diptera			
AR-1-A-2019.67.1	Insecta				
AR-1-A-2019.67.2	Insecta				
AR-1-A-2019.67.3	Insecta				
AR-1-A-2019.68	Insecta	Diptera	Mycetophilidae		
AR-1-A-2019.69.1	Insecta	Psocodea	†Empheriidae	*Libanoglaris hespericus*	
AR-1-A-2019.69.2	Insecta	Diptera?			
AR-1-A-2019.70.1	Insecta				
AR-1-A-2019.70.2	Insecta	Hymenoptera	Scelionidae?		
AR-1-A-2019.71	Arachnida: Acari	Trombidiformes	Rhagidiidae		
AR-1-A-2019.72	Insecta	Hymenoptera?			
AR-1-A-2019.73	Coprolito				
AR-1-A-2019.74	Insecta	Diptera?			
AR-1-A-2019.75	Arachnida	Araneae?			
AR-1-A-2019.76	Arachnida	Araneae			
AR-1-A-2019.77	Coprolitos				
AR-1-A-2019.80	Insecta?				
AR-1-A-2019.81	Insecta	Diptera?			
AR-1-A-2019.82	Planta				
AR-1-A-2019.83	Insecta	Neuroptera			

AR-1-A-2019.88.1	Pelos de mamífero				
AR-1-A-2019.88.2	Insecta				
AR-1-A-2019.88.3	Insecta?				
AR-1-A-2019.89	Insecta?				
AR-1-A-2019.90	Planta				
AR-1-A-2019.91	Insecta				
AR-1-A-2019.94.1	Insecta	Hymenoptera	Scelionidae?		
AR-1-A-2019.94.2	Insecta	Hymenoptera	Scelionidae?		
AR-1-A-2019.94.3	Insecta	Thysanoptera			
AR-1-A-2019.94.4	Insecta	Coleoptera			
AR-1-A-2019.94.5	Insecta	Hymenoptera	†Serphitidae		
AR-1-A-2019.94.6	Insecta	Hymenoptera	Scelionidae?		
AR-1-A-2019.94.7	Insecta	Hymenoptera	Cecidomyiidae?		
AR-1-A-2019.94.8	Insecta	Hymenoptera	†Serphitidae		
AR-1-A-2019.94.9	Insecta	Diptera	Rhagionidae		
AR-1-A-2019.94.10	Insecta	Hymenoptera	Scelionidae?		
AR-1-A-2019.94.11	Insecta	Hymenoptera			
AR-1-A-2019.95.1	Insecta	Lepidoptera			
AR-1-A-2019.95.2	Insecta	Diptera	†Archizelmiridae: †Burmazelmirinae	*Burmazelmira* sp.	
AR-1-A-2019.95.3	Insecta	Hymenoptera	Scelionidae		
AR-1-A-2019.95.4	Arachnida: Acari	Trombidiformes	Pyemotidae?		
AR-1-A-2019.95.5	Telaraña				
AR-1-A-2019.95.6	Telaraña				
AR-1-A-2019.95.7	Planta				
AR-1-A-2019.95.8	Planta				
AR-1-A-2019.96	Insecta?				
AR-1-A-2019.97.1	Insecta	Hymenoptera	Scelionidae?		
AR-1-A-2019.97.2	Insecta	Hymenoptera			

AR-1-A-2019.98.1	Insecta	Hymenoptera			
AR-1-A-2019.98.2	Insecta				
AR-1-A-2019.99	Insecta				
AR-1-A-2019.100.1	Insecta	Hemiptera	Aleyrodidae: Aleurodicinae		
AR-1-A-2019.100.2	Insecta	Hemiptera	Aleyrodidae: Aleurodicinae		
AR-1-A-2019.100.3	Insecta	Hemiptera	Aleyrodidae: Aleurodicinae		
AR-1-A-2019.100.4	Insecta				
AR-1-A-2019.101	Insecta	Hymenoptera: Mymarommatoidea			
AR-1-A-2019.102	Insecta	Hemiptera			
AR-1-A-2019.103	Insecta	Hemiptera: Aphidoidea			
AR-1-A-2019.104	Insecta	Diptera			
AR-1-A-2019.105	Insecta	Diptera	Ceratopogonidae?		
AR-1-A-2019.106	Insecta	Diptera			
AR-1-A-2019.107.1	Insecta	Thysanoptera			
AR-1-A-2019.107.2	Insecta	Thysanoptera			
AR-1-A-2019.108	Insecta	Orthoptera	†Elcanidae?		
AR-1-A-2019.109	Arachnida				
AR-1-A-2019.110.1	Insecta	Hymenoptera			
AR-1-A-2019.110.2	Planta				
AR-1-A-2019.111	Insecta	Hymenoptera	Scelionidae?		
AR-1-A-2019.112	Insecta	Hymenoptera	†Stigmaphronidae?		
AR-1-A-2019.113.1	Insecta	Hymenoptera	Scelionidae?		
AR-1-A-2019.113.2	Insecta	Hymenoptera	Scelionidae?		

AR-1-A-2019.114.1	Insecta	Thysanoptera			
AR-1-A-2019.114.2	Insecta	Thysanoptera			
AR-1-A-2019.114.3	Planta				
AR-1-A-2019.115	Insecta	Thysanoptera			
AR-1-A-2019.116	Insecta	Hymenoptera	Scelionidae?		
AR-1-A-2019.117	Insecta	Hymenoptera?			
AR-1-A-2019.118.1	Insecta	Coleoptera	Cantharidae?		
AR-1-A-2019.118.2	Insecta	Hymenoptera	†Stigmaphronidae?		
AR-1-A-2019.119	Arachnida: Acari				
AR-1-A-2019.120	Insecta	Diptera	Rhagionidae?		
AR-1-A-2019.121	Insecta	Hymenoptera			
AR-1-A-2019.122	Insecta	Hymenoptera			
AR-1-A-2019.123	Insecta	Hymenoptera	Scelionidae?		
AR-1-A-2019.124	Insecta	Hymenoptera			
AR-1-A-2019.125	Insecta?				
AR-1-A-2019.126	Insecta	Hymenoptera?			
AR-1-A-2019.127	Insecta?				
AR-1-A-2019.128.1	Insecta	Neuroptera	Sisyridae: †Paradoxosisyrinae		
AR-1-A-2019.128.2	Insecta	Thysanoptera			
AR-1-A-2019.128.3	Insecta		†Umenocoleidae		
AR-1-A-2019.128.4	Telaraña				

Ámbar de San Just:

Sigla	Identificación /clase	Orden	Familia	Género y especie	Sin
CPT-955	Arachnida	Araneae			
CPT-956	Arachnida	Araneae			
CPT-957	Insecta	Hymenoptera	Evaniidae	*Cretevania montoyai*	
CPT-960	Insecta	Hymenoptera	Evaniidae	*Cretevania alcalai*	
CPT-961	Insecta	Hymenoptera	†Stigmaphronidae		
CPT-963	Insecta	Diptera	Dolichopodidae	*Microphorites utrillensis*	
CPT-964	Arachnida: Acari	Oribatida?			
CPT-965	Insecta	Coleoptera	Cryptophagidae		
CPT-966	Insecta	Hymenoptera	Scelionidae		
CPT-967	Insecta	Hymenoptera	Scelionidae		
CPT-968	Insecta	Hymenoptera	Scelionidae		
CPT-969	Insecta	Hymenoptera	Scelionidae		
CPT-970	Insecta	Diptera	Ceratopogonidae	*Archiculicoides skalskii*	
CPT-971	Insecta	Thysnaoptera	Stenurothripidae		
CPT-3341 (SJ-07-4)	Arachnida: Acari	Oribatida	Ametroproctidae	*Ametroproctus valeriae*	
CPT-3342 (SJ-07-9)	Insecta	Diptera	†Archizelmiridae: †Burmazelmirinae	*Burmazelmira grimaldii*	
CPT-3343 (SJ-07-15)	Insecta	Diptera	Ceratopogonidae	*Archiculicoides skalskii*	
CPT-3344 (SJ-07-26)	Insecta	Diptera	Rhagionidae	*Litoleptis fossilis*	
CPT-3345 (SJ-07-71)	Insecta	Diptera	Ceratopogonidae	*Leptoconops zherikhini*	
CPT-4059 (SJ-07-1)	Insecta	Hymenoptera	†Serphitidae	*Serphites silban*	
CPT-4060 (SJ-07-2)	Insecta	Coleoptera			
CPT-4061 (SJ-07-3)	Insecta	Diptera	Dolichopodidae	*Microphorites* sp.	
CPT-4062 (SJ-07-5)	Arachnida: Acari	Oribatida	Otocepheidae	*Cretaceobodes martinezae*	
CPT-4066 (SJ-07-10)	Insecta	Diptera	Ceratopogonidae	*Protoculicoides* sp.	
CPT-4067 (SJ-07-11)	Insecta	Diptera	Phoridae		
CPT-4068 (SJ-07-12)	Arachnida: Acari	Oribatida	Scutoverticidae	*Hypovertex hispanicus*	
CPT-4069 (SJ-07-13)	Coprolito				
CPT-4070 (SJ-07-14)	Coprolito				
CPT-4071 (SJ-07-16)	Insecta	Diptera	Mycetophilidae		
CPT-4072 (SJ-07-17)	Insecta	Diptera	Scatopsidae		

CPT-4073 (SJ-07-18)	Insecta	Hymenoptera			
CPT-4074 (SJ-07-19)	Insecta	Diptera	Ceratopogonidae	*Lectonops* cf. *zherikhini*	
CPT-4075 (SJ-07-20) (30-SJ)	Insecta	Hymenoptera	†Stigmaphronidae	*Burmaphron jentilak*	
CPT-4078 (SJ-07-23)	Fragmento de pluma				
CPT-4079 (SJ-07-24)	Insecta	Hymenoptera	Scelionidae		
CPT-4080 (SJ-07-25)	Telaraña				
CPT-4063 (SJ-07-6)	Insecta	Diptera	Rhagionidae		
CPT-4064 (SJ-07-7)	Collembola?				
CPT-4065 (SJ-07-8)	Insecta	Blattodea: Isoptera	*Incertae sedis*	*Aragonitermes teruelensis*	
CPT-4081 (SJ-07-27)	Insecta	Diptera	Chironomidae		
CPT-4082 (SJ-07-28)	Insecta				
CPT-4083 (SJ-07-28)	Insecta	Orthoptera	†Elcanidae?		
CPT-4084 (SJ-07-30)	Insecta	Hymenoptera	Scelionidae		
CPT-4085 (SJ-07-31)	Coprolitos				
CPT-4086 (SJ-07-32)	Arachnida: Acari				
CPT-4087 (SJ-07-33)	Insecta	Hymenoptera	Scelionidae		
CPT-4090 (SJ-07-36)	Insecta	Hymenoptera	Scelionidae		
CPT-4091 (SJ-07-37)	Insecta	Hymenoptera	Scelionidae		
CPT-4092 (SJ-07-38)	Insecta	Hymenoptera	Scelionidae		
CPT-4093 (SJ-07-39)	Insecta	Hymenoptera	Scelionidae		
CPT-4094 (SJ-07-40)	Insecta	Hymenoptera	Scelionidae		
CPT-4095 (SJ-07-41)	Insecta	Hymenoptera	†Spathiopterygidae	*Diameneura marveni*	
CPT-4096 (SJ-07-42)	Insecta	Hymenoptera	Scelionidae		
CPT-4097 (SJ-07-43)	Insecta	Hymenoptera	†Spathiopterygidae	*Mymaropsis turolensis*	
CPT-4098 (SJ-07-44)	Insecta	Hymenoptera	Scelionidae		
CPT-4099 (SJ-07-45)	Insecta	Thysanoptera	Stenurothripidae	*Hispanothrips utrillensis*	
CPT-4100 (SJ-07-46)	Arachnida	Araneae	Oonopidae	*Orchestina* sp.	
CPT-4101 (SJ-07-47	Insecta	Hymenoptera			

CPT-4102 (SJ-07-48)	Insecta	Thysanoptera	Stenurothripidae	*Hispanothrips utrillensis*	
CPT-4103 (SJ-07-49)	Insecta	Thysanoptera	Stenurothripidae	*Hispanothrips utrillensis*	
CPT-4104 (SJ-07-50)	Arachnida	Araneae			
CPT-4105 (SJ-07-51)	Insecta	Coleoptera	Silvanidae		
CPT-4106 (SJ-07-52)	Insecta	Coleoptera	Nemonychidae	*Arra legalovi*	
CPT-4107 (SJ-07-53)	Insecta	Diptera	Chironomidae		
CPT-4108 (SJ-07-54)	Insecta	Blattodea	†Mesoblattinidae		
CPT-4109 (SJ-07-55)	Insecta	Blattodea	†Blattulidae		
CPT-4110 (SJ-07-56)	Coprolito				
CPT-4111 (SJ-07-57)	Insecta	Thysanoptera			
CPT-4112 (SJ-07-58)	Insecta	Thysanoptera			
CPT-4113 (SJ-07-59)	Insecta	Thysanoptera			
CPT-4114 (SJ-07-60)	Insecta	Diptera	Chironomidae		
CPT-4115 (SJ-07-61)	Collembola?				
CPT-4116 (SJ-07-62)	Arachnida	Araneae			
CPT-4117 (SJ-07-63)	Insecta	Psocodea	†Empheriidae	*Preempheria antiqua*	
CPT-4118 (SJ-07-64)	Insecta	Hemiptera			
CPT-4119 (SJ-07-65)	Insecta	Hemiptera			
CPT-4120 (SJ-07-66)	Insecta	Diptera	Chironomidae		
CPT-4121 (SJ-07-67)	Insecta	Diptera			
CPT-4122 (SJ-07-68)	Insecta	Blattodea	Corydiidae?		
CPT-4123 (SJ-07-69)	Coprolito				
CPT-4124 (SJ-07-70)	Coprolito				
CPT-4125 (SJ-07-72)	Insecta	Hymenoptera	Scelionidae		
CPT-4127 (SJ-07-74)	Insecta	Hymenoptera	Scelionidae		
CPT-4128 (SJ-07-75)	Insecta	Diptera			
CPT-4129 (SJ-07-76)	Insecta	Coleoptera	Eucinetidae		
CPT-4130 (SJ-07-77)	Insecta	Hemiptera			
CPT-4131 (SJ-07-78)	Insecta				

CPT-4133 (SJ-07-80)	Insecta	Neuroptera			
CPT-4135 (SJ-07-82)	Insecta	Diptera			
CPT-4139 (SJ-07-86)	Insecta	Hymenoptera	†Gallorommatidae	*Cretaceomma turolensis*	
CPT-4140 (SJ-07-87)	Insecta	Hymenoptera	†Alavarommatidae	*Alavaromma orchamum*	
CPT-4141 (SJ-07-88)	Insecta	Hemiptera			
CPT-4142 (SJ-07-89)	Insecta	Hymenoptera	Scelionidae		
CPT-4143 (SJ-07-90)	Insecta	Hymenoptera	Bethylidae		
CPT-4144 (SJ-07-91)	Insecta	Neuroptera	Berothidae		
CPT-4145 (SJ-07-92)	Insecta	Diptera	Phoridae		
CPT-4146 (SJ-07-93)	Insecta	Diptera	Chironomidae		
CPT-4147 (SJ-07-94)	Insecta	Diptera	Chironomidae		
CPT-4148 (SJ-07-95)	Insecta	Hymenoptera			
CPT-4149 (SJ-07-96)	Planta				
CPT-4150 (SJ-07-97)	Insecta	Diptera	Chironomidae		
CPT-4076 (SJ-07-21) (28-SJ)	Insecta	Hymenoptera	Sierolomorphidae?		
CPT-4077 (SJ-07-22 (21-SJ)	Insecta	Hymenoptera	†Spathiopterygidae	*Mymaropsis turolensis*	
CPT-4088 (SJ-07-34) (23-SJ)	Insecta	Hymenoptera	Scelionidae		
CPT-4089 (SJ-07-35) (24-SJ)	Insecta	Hymenoptera	Scelionidae		
CPT-4126 (SJ-07-73) (20-SJ)	Insecta	Hymenoptera	Scelionidae		
CPT-4132 (SJ-07-79)	Insecta	Hemiptera	†Perforissidae	*Iberofoveopsis miguelesi*	
CPT-4151 (SJ-07-98)	Insecta	Diptera	Keroplatidae		
CPT-4152 (SJ-07-99)	Insecta	Diptera	Keroplatidae		
CPT-4153 (SJ-07-100)	Insecta	Diptera	Keroplatidae		
CPT-4154 (SJ-07-101)	Insecta	Diptera	Ceratopogonidae	*Archiculicoides skalskii*	
CPT-4155 (SJ-07-102)	Arachnida	Araneae	†Lagonomegopidae	*Spinomegops aragonensis*	
CPT-4156 (SJ-07-103)	Insecta	Diptera			

CPT-4157 (SJ-07-104)	Insecta	Hymenoptera	†Stigmaphronidae		
CPT-4158 (SJ-07-105)	Insecta	Blattodea: Isoptera			
CPT-4159 (SJ-07-106)	Insecta	Diptera	Psychodidae		
CPT-4160 (SJ-07-107)	Insecta	Diptera	Psychodidae		
CPT-4161 (SJ-07-108)	Arachnida: Acari	Oribatida	Trhypochthoniidae	*Trhypochthonius lopezvallei*	
CPT-4162 (SJ-07-109)	Arachnida: Acari				
CPT-4163 (SJ-07-110)	Insecta	Hymenoptera			
CPT-4164 (SJ-07-111)	Indet.				
CPT-4165 (SJ-07-112)	Arachnida: Acari	Oribatida	Lamellareidae	*Tenuelamellarea estefaniae*	
CPT-4166 (SJ-07-113)	Insecta	Diptera	†Archizelmiridae: †Burmazelmirinae	*Burmazelmira grimaldii*	
CPT-4167 (SJ-07-114)	Arachnida: Acari	Trombidiformes	Erythraeidae	*Leptus* sp.	
CPT-4168 (SJ-07-115)	Insecta	Hymenoptera	Scelionidae		
CPT-4169 (SJ-07-116)	Planta				
CPT-4170 (SJ-07-117)	Planta				
CPT-4171 (SJ-07-118)	Planta				
CPT-4172 (SJ-07-119)	Planta				
CPT-4173 (SJ-07-120)	Micelio fúngico				
CPT-4174 (SJ-07-121)	Arachnida	Araneae			
CPT-4175 (SJ-07-122)	Insecta	Hymenoptera	Scelionidae		
CPT-4176 (SJ-07-123)	Insecta	Hymenoptera	Scelionidae		
CPT-4177 (SJ-07-124)	Insecta	Hymenoptera			
CPT-4178 (SJ-07-125)	Insecta	Diptera	Chironomidae		
CPT-4179 (SJ-07-126)	Insecta	Hymenoptera: †Serphitoidea/ Mymarommatoidea			
CPT-4180 (SJ-07-127)	Planta				
CPT-4181 (SJ-07-128)	Insecta	Hymenoptera	Scelionidae		
CPT-4182 (SJ-07-129)	Insecta				
CPT.4183 (SJ-07-130)	Insecta				
CPT-4184 - (SJ-07-131)	Insecta	Hymenoptera	Scelionidae		

CPT-4185 (SJ-07-132)	Insecta	Diptera			
CPT-4186 (SJ-07-133)	Coprolito				
CPT-4187 (SJ-07-134)	Insecta	Hymenoptera	Scelionidae		
CPT-4188 (SJ-07-135)	Insecta	Blattodea			
CPT-4189 (SJ-07-136)	Insecta	Hymenoptera			
CPT-4190 (SJ-07-137)	Insecta	Diptera			
CPT-4191 (SJ-07-138)	Insecta	Hymenoptera	Scelionidae		
CPT-4192 (SJ-07-139)	Indet.				
CPT-4193 (SJ-07-140)	Insecta	Blattodea	†Liberiblattinidae?		
CPT-4194 (SJ-07-141)	Insecta	Hemiptera			
CPT-4195 (SJ-07-142)	Telaraña				
CPT-4196 (SJ-07-143)	Telaraña				
CPT-4197 (SJ-07-144)	Telaraña				
CPT-4198 (SJ-07-145)	Insecta	Diptera			
CPT-4199 (SJ-07-146)	Insecta	Hymenoptera			
CPT-4200 (SJ-07-147)	Fragmentos de plumas				
CPT-4201 (SJ-07-148)	Insecta	Hymenoptera	Scelionidae		
CPT-4202 (SJ-07-149)	Planta				
SJ-10-01	Insecta	Diptera	†Chimeromyiidae		
MAP-7843 (SJ-10-02)	Insecta	Blattodea	†Skokidae?		
SJ-10-03	Insecta	Hymenoptera	†Serphitidae	*Serphites* sp.	
SJ-10-04	Fragmento de pluma				
SJ-10-05	Insecta	Diptera	Ceratopogonidae	*Leptoconops* sp.	
SJ-10-06	Insecta	Hymenoptera	Scelionidae		
SJ-10-07	Insecta	Diptera	Ceratopogonidae		
SJ-10-08	Insecta	Diptera: Empidoidea			
SJ-10-09	Insecta	Hymenoptera	Sapygidae?		
SJ-10-10	Arachnida	Araneae			
SJ-10-11	Insecta	Diptera	Chironomidae		
SJ-10-12	Insecta	Hymenoptera	†Serphitidae		
SJ-10-13	Fragmento de pluma				
SJ-10-14	Insecta	Thysanoptera	Stenurothripidae		
SJ-10-15	Telaraña				
SJ-10-16	Arachnida: Acari	Trombidiformes	Erythraeidae	*Leptus* sp.	

SJ-10-17	Insecta	Mantodea	*Incertae sedis*	*Aragonimantis aenigma*	
MAP-7727 (SJ-10-18)	Insecta	Coleoptera	Ptinidae	*Actenobius magneoculus*	
MAP-7728 (SJ-10-19)	Insecta	Hymenoptera			
MAP-7729 (SJ-10-20)	Arachnida	Araneae			
SJ-10-21	Insecta	Diptera	Ceratopogonidae		
SJ-10-22	Insecta	Neuroptera	Mantispidae	*Aragomantispa lacerata*	
SJ-10-23	Telaraña				
SJ-10-24	Indet.				
SJ-10-25	Insecta	Neuroptera	Berothidae?		
SJ-10-26	Insecta	Diptera	Dolichopodidae	*Microphorites* sp.	
SJ-10-27	Insecta	Diptera	Rhagionidae		
SJ-10-29	Insecta	Hemiptera	†Perforissidae		
SJ-10-30	Insecta	Diptera			
SJ-10-31	Insecta	Diptera	Ceratopogonidae		
SJ-10-32	Insecta	Hymenoptera?			
SJ-10-33	Insecta	Hymenoptera	Scelionidae		
SJ-10-34	Insecta	Hymenoptera	Scelionidae		
SJ-10-35	Insecta	Hymenoptera	Scelionidae		
SJ-10-36	Insecta	Diptera	Anisopodidae		
SJ-10-37	Insecta	Diptera			
SJ-10-38	Arachnida: Acari	Trombidiformes	Erythraeidae	*Leptus* sp.	
SJ-10-39	Telaraña				
SJ-10-40	Insecta	Hymenoptera			
SJ-10-41	Insecta	Hymenoptera			
SJ-10-42	Insecta	Blattodea	†Mesoblattinidae		
SJ-10-43	Micelio fúngico				
SJ-10-44	Diplura?				
SJ-10-45	Insecta	Hymenoptera			
SJ-10-46	Insecta	Thysanoptera			
SJ-10-47	Insecta	Hymenoptera	Scelionidae		
SJ-10-48	Insecta	Coleoptera			
SJ-10-49	Insecta	Diptera	Ceratopogonidae	*Archiaustroconops* sp.	
SJ-10-50	Insecta	Psocodea	†Empheriidae	*Archaeatropos alavensis*	
SJ-10-51	Insecta	Coleoptera	Silvanidae		
SJ-10-52	Insecta	Diptera	Chironomidae		
SJ-10-53	Fragmento de pluma				
SJ-10-54	Insecta	Diptera	Limoniidae	*Helius turolensis*	
SJ-10-55	Insecta	Hemiptera			
SJ-10-56	Insecta	Hemiptera?			
SJ-10-57	Insecta	Hymenoptera	Sapygidae?		
SJ-10-58	Insecta	Diptera	Lonchopteridae		
SJ-10-59	Insecta	Diptera	Chironomidae		
SJ-10-60	Insecta	Diptera			
SJ-10-61	Insecta	Neuroptera			
SJ-10-62	Indet.				
SJ-10-63	Insecta	Neuroptera	Berothidae?		
SJ-10-64	Planta				

MAP-7866 (SJ-10-65)	Insecta	Blattodea			
SJ-10-66	Insecta	Coleoptera			
SJ-10-67	Insecta	Coleoptera			
SJ-10-68	Insecta	Hymenoptera	Scelionidae		
SJ-10-69	Micelio fúngico				
SJ-10-70	Planta				
SJ-10-71	Insecta				
SJ-10-72	Planta				
MAP-7873 (SJ-10-73)	Insecta	Blattodea	Corydiidae		
SJ-10-74	Insecta	Blattodea: Isoptera			
SJNB2012-01-01	Arachnida: Acari				
SJNB2012-01-02	Insecta	Coleoptera			
SJNB2012-01-03	Insecta	Diptera			
MAP-7743 (SJNB2012-01-04)	Insecta	Hymenoptera	Scelionidae		
MAP-7744 (SJNB2012-02)	Insecta	Hymenoptera	Scelionidae		
MAP-7745 (SJNB2012-03)	Insecta	Hymenoptera	Scelionidae		
SJNB2012-04	Insecta	Neuroptera: Mantispoidea/ Dilaroidea			
MAP-7746 (SJNB2012-05)	Insecta	Hymenoptera	Sapygidae?		
SJNB2012-06	Insecta	Hemiptera			
SJNB2012-07	Insecta	Thysanoptera			
SJNB2012-08	Insecta	Diptera	Keroplatidae		
MAP-7750 (SJNB2012-09)	Insecta	Hymenoptera	Scelionidae		
MAP-7751 (SJNB2012-10)	Insecta	†Lophioneurida	†Lophioneuridae	*Jantardachus* cf. *reductus*	
SJNB2012-11	Insecta	Coleoptera	Dermestidae		
SJNB2012-12-01	Insecta	Hemiptera			
SJNB2012-12-02	Insecta	Psocodea	†Empheriidae		
SJNB2012-12-03	Insecta	Psocodea			
SJNB2012-12-04	Insecta	Hymenoptera	Scelionidae		
SJNB2012-12-05	Insecta	Hymenoptera	Scelionidae		

SJNB2012-12-06	Insecta	Psocodea			
SJNB2012-12-07	Arachnida	Araneae	†Lagonomegopidae		
SJNB2012-12-08	Insecta				
SJNB2012-12-09	Insecta	Diptera	Chironomidae		
SJNB2012-12-10	Insecta	Diptera	Ironomyiidae		
SJNB2012-12-11	Insecta	Diptera	Ceratopogonidae		
SJNB2012-12-12	Arachnida	Araneae			
SJNB2012-12-13	Insecta	Hymenoptera	Scelionidae		
SJNB2012-12-14	Insecta	Hemiptera			
SJNB2012-12-15	Insecta	Hymenoptera	Scelionidae		
SJNB2012-12-16	Insecta				
SJNB2012-12-17	Insecta	Thysanoptera			
SJNB2012-12-18	Insecta	Hemiptera			
SJNB2012-12-19	Arachnida	Araneae			
SJNB2012-12-20	Insecta	Hymenoptera	Scelionidae		
SJNB2012-12-21	Insecta	Hymenoptera	Scelionidae		
SJNB2012-12-22	Insecta	Hymenoptera	Scelionidae		
SJNB2012-12-23	Insecta	Hymenoptera	Scelionidae		
SJNB2012-12-24	Insecta	Diptera	Rhagionidae	*Litoleptis fossilis*	
SJNB2012-12-25	Insecta	Diptera	Ceratopogonidae	*Protoculicoides hispanicus*	
SJNB2012-12-26	Insecta	Diptera	Ceratopogonidae	*Protoculicoides hispanicus*	
SJNB2012-12-27	Insecta	Diptera	Ceratopogonidae	*Protoculicoides hispanicus*	
SJNB2012-12-28	Insecta	Diptera	Ceratopogonidae	*Protoculicoides hispanicus*	
SJNB2012-12-29	Telaraña				
SJNB2012-12-30	Insecta	Diptera	Ceratopogonidae	*Protoculicoides hispanicus*	
SJNB2012-12-31	Insecta	Diptera	Ceratopogonidae	*Protoculicoides sanjusti*	
SJNB2012-12-32	Insecta	Diptera	Ceratopogonidae	*Protoculicoides hispanicus*	
SJNB2012-12-33	Insecta	Diptera			
SJNB2012-12-34	Insecta	Diptera	Ceratopogonidae	*Protoculicoides hispanicus*	

SJNB2012-12-35	Insecta	Diptera	Ceratopogonidae	*Protoculicoides hispanicus*	
SJNB2012-12-36	Insecta	Diptera	Ceratopogonidae	*Protoculicoides sanjusti*	
MAP-7752 (SJNB2012-13)	Insecta	Hymenoptera	Scelionidae		
MAP-7753 (SJNB2012-14-01)	Insecta	Blattodea			
MAP-7754 (SJNB2012-14-02)	Collembola?				
SJNB2012-15	Insecta	Blattodea	†Mesoblattinidae?		
SJNB2012-16	Insecta	Diptera	Chironomidae		
SJNB2012-17	Insecta	Hymenoptera	†Serphitidae	*Serphites* sp.	
SJNB2012-18	Insecta	Diptera	Rhagionidae		
SJNB2012-19	Insecta	Diptera	Psychodidae		
SJNB2012-20	Insecta	Diptera			
MAP-7759 (SJNB2012-21)	Insecta	Hymenoptera	Scelionidae		
MAP-7760 (SJNB2012-22)	Insecta	Hymenoptera	Scelionidae		
SJNB2012-23-01	Insecta	Hemiptera			
SJNB2012-23-02	Insecta	Hemiptera			
SJNB2012-23-03	Insecta	Hemiptera			
SJNB2012-23-04	Insecta	Hemiptera			
SJNB2012-24	Insecta	Thysanoptera			
SJNB2012-25	Micelio fúngico				
SJNB2012-26	Arachnida	Araneae			
MAP-7768 (SJNB2012-27)	Insecta	Hymenoptera			
SJNB2012-28	Arachnida	Araneae			
SJNB2012-29	Insecta	Hemiptera			
SJNB2012-30	Telaraña				
SJNB2012-31-01	Fragmentos de pluma				

MAP-7772 (SJNB2012-31-02)	Insecta	Hymenoptera			
SJNB2012-32-01	Insecta	Diptera?			
SJNB2012-32-02	Insecta	Diptera	Ceratopogonidae		
SJNB2012-33-01	Arachnida: Acari	Trombidiformes	Bdellidae		
SJNB2012-33-02	Arachnida: Acari	Trombidiformes	Erythraeidae	*Leptus* sp.	
MAP-7776 (SJNB2012-34-01)	Insecta	Blattodea	†Mesoblattinidae		
MAP-7777 (SJNB2012-34-02)	Insecta	Hymenoptera			
MAP-7778 (SJNB2012-35-01)	Insecta	Hymenoptera	Scelionidae		
MAP-7779 (SJNB2012-35-02)	Insecta	Hymenoptera	Scelionidae		
MAP-7780 (SJNB2012-35-03)	Insecta	Hymenoptera			
MAP-7781 (SJNB2012-35-04)	Insecta	Hymenoptera	Scelionidae		
SJNB2012-36-01	Insecta	Thysanoptera			
SJNB2012-36-02	Insecta	Hemiptera			
SJNB2012-37-01	Insecta	Diptera			
MAP-7785 (SJNB2012-37-02)	Insecta	Hymenoptera	Scelionidae		
SJNB2012-38-01	Insecta	Hemiptera			
SJNB2012-38-02	Insecta	Hemiptera?			
SJNB2012-39-01	Insecta	Coleoptera			
SJNB2012-39-02	Insecta	Diptera			
SJNB2012-39-03	Insecta	Thysanoptera			
SJNB2012-39-04	Insecta	Diptera	Phoridae		
SJNB2012-40	Insecta	Coleoptera	Staphylinidae		
SJNB2012-41	Insecta	Coleoptera	Dermestidae?		
SJNB2012-42	Insecta	Cryptophagidae			
SJNB2012-43	Insecta	Coleoptera	Staphylinidae		

SJNB2012-44	Arachnida	Pseudoscorpiones			
MAP-7791 (SJE2012-45-01)	Insecta	Diptera	Dolichopodidae	*Microphorites* sp.	
MAP-7792 (SJE2012-45-02)	Insecta	Diptera	Dolichopodidae	*Microphorites* sp.	
MAP-7793 (SJE2012-45-03)	Insecta	Diptera	Dolichopodidae	*Microphorites* sp.	
MAP-7794 (SJE2012-45-04)	Insecta	Diptera	Dolichopodidae	*Microphorites* sp.	
MAP-7795 (SJE2012-45-05)	Insecta	Diptera	Dolichopodidae	*Microphorites* sp.	
MAP-7796 (SJE2012-45-06)	Insecta	Diptera	Dolichopodidae	*Microphorites* sp.	
MAP-7797 (SJE2012-45-07)	Arachnida: Acari				
MAP-7798 (SJE2012-45-08)	Insecta	Blattodea			
MAP-7799 (SJE2012-45-09)	Insecta	Archaeognatha			
SJE2012-46-01	Collembola?				
SJE2012-46-02	Insecta	Hemiptera			
SJE2012-46-03	Insecta	Hemiptera			
SJE2012-46-04	Insecta	Hemiptera			
SJE2012-46-05	Insecta	Hemiptera			
SJE2012-46-06	Insecta	Hemiptera			
SJE2012-46-07	Insecta	Hemiptera			
SJE2012-46-08	Insecta	Hemiptera			
SJE2012-46-09	Insecta	Hemiptera			
SJE2012-47-01	Insecta	Coleoptera			
MAP-7810 (SJE2012-47-02)	Insecta	Hymenoptera	Bethylidae		
MAP-7811 (SJE2012-47-03)	Insecta	Hymenoptera	Scelionidae		
MAP-7812 (SJE2012-47-04)	Insecta	Psocodea	†Empheriidae	*Archaeatropos alavensis*	

MAP-7813 (SJE2012-48-01)	Insecta	Hymenoptera	Scelionidae		
MAP-7814 (SJE2012-48-02)	Insecta	Hymenoptera	Scelionidae		
MAP-7815 (SJE2012-48-03)	Insecta	Hymenoptera	Scelionidae		
SJE2012-49-01	Arachnida	Araneae			
MAP-7817 (SJE2012-49-02)	Insecta	Hymenoptera			
MAP-7818 (SJE2012-49-03)	Insecta	Hymenoptera	Scelionidae		
MAP-7819 (SJE2012-49-04)	Insecta	Hymenoptera	Braconidae	*Utrillabracon electropteron*	
MAP-7820 (SJE2012-49-05)	Insecta	Hymenoptera	†Stigmaphronidae		
SJY22012-01	Indet.				
MAP-7822 (SJY22012-02)	Insecta	Psocodea			
SJY22012-03	Insecta	Diptera	Ceratopogonidae		
SJY22012-04-01	Insecta	Diptera	Ceratopogonidae	*Archiaustroconops*? sp.	
SJY22012-04-02	Insecta	Diptera	Ceratopogonidae	*Archiaustroconops*? sp.	
SJNB2021-1	Insecta	Diptera			
SJNB2021-2.1	Fragmento de pluma				
SJNB2021-2.2	Insecta	Hymenoptera	Scelionidae?		
SJNB2021-2.3	Insecta	Diptera			
SJNB2021-3	Fragmentos de plumas				
SJNB2021-4	Insecta	Diptera	Ceratopogonidae?		
SJNB2021-5	Insecta	Diptera	Ceratopogonidae?		
SJNB2021-6.1	Insecta	Hymenoptera			
SJNB2021-6.2	Insecta	Diptera	Ceratopogonidae?		
SJNB2021-7	Insecta	Hymenoptera	Sceliondae?		
SJNB2021-8	Insecta	Diptera	Ceratopogonidae?		
SJNB2021-9	Insecta	Hymenoptera	Scelionidae?		
SJNB2021-10	Insecta	Hymenoptera			
SJNB2021-11	Insecta	Hymenoptera			
SJNB2021-12	Insecta	Blattodea: Isoptera			

SJNB2021-13	Arachnida: Acari	Oribatida?			
SJNB2021-14	Arachnida: Acari				
SJNB2021-15	Insecta	Coleoptera			
SJNB2021-16	Insecta	Diptera	Ceratopogonidae?		
SJNB2021-17	Insecta	Thysanoptera?			
SJNB2021-18	Insecta	Coleoptera?			
SJNB2021-19	Insecta	Coleoptera	Staphylinidae?		
SJNB2021-20	Insecta	Coleoptera			
SJNB2021-21.1	Fragmentos de plumas				
SJNB2021-21.2	Insecta	Blattodea			
SJNB2021-21.3	Arachnida: Acari	Oribatida?			
SJNB2021-22	Arachnida	Araneae			
SJNB2021-23	Indet.				
SJNB2021-24	Insecta	Coleoptera			
SJNB2021-25	Insecta	Hymenoptera	Scelionidae?		
SJNB2021-26	Insecta	Psocodea			
SJNB2021-27	Insecta	Hymenoptera	Scelionidae?		
SJNB2021-28	Insecta	Diptera			
SJNB2021-29	Insecta	Blattodea			
SJNB2021-30	Insecta	Hymenoptera	†Stigmaphronidae?		
SJNB2021-31	Insecta	Diptera	Chironomidae?		
SJNB2021-32.1	Insecta	Neuroptera	Sisyridae: †Paradoxosisyrinae?		
SJNB2021-32.2	Insecta	Coleoptera			
SJNB2021-33	Insecta	Hymenoptera?			
SJNB2021-34	Insecta	Psocodea	†Empheriidae		
SJNB2021-35	Insecta	Coleoptera			
SJNB2021-36	Insecta	Diptera	Ceratopogonidae?		
SJNB2021-37	Insecta	Diptera	†Chimeromyiidae	*Chimeromyia alava*	
SJNB2021-38.1	Insecta	Diptera	Ceratopogonidae?		

SJNB2021-38.2	Insecta	Diptera	Ceratopogonidae?		
SJNB2021-39	Insecta	Hymenoptera	Scelionidae		
SJNB2021-40	Insecta	Hymenoptera:			
SJNB2021-41	Insecta				
SJNB2021-42	Insecta	Hymenoptera			
SJNB2021-43	Insecta	Hymenoptera	Scelionidae		
SJNB2021-44.1	Insecta	Diptera	Ceratopogonidae?		
SJNB2021-44.2	Insecta	Diptera	Ceratopogonidae?		
SJNB2021-45.1	Insecta	Diptera	Dolichopodidae?		
SJNB2021-45.2	Insecta	Hemiptera			
SJNB2021-45.3	Arachnida	Araneae			
SJNB2021-46	Insecta	Hemiptera			
SJNB2021-47	Insecta	Hemiptera			
SJNB2021-48	Insecta	Hymenoptera	Scelionidae		
SJNB2021-49	Arachnida: Acari				
SJNB2021-50	Insecta	Diptera	Ceratopogonidae?		
SJNB2021-51	Insecta	Blattodea: Isoptera			
SJNB2021-52	Insecta	Blattodea: Isoptera			

Ámbar de Arroyo de la Pascueta:

Sigla	Identificación/clase	Orden	Familia	Género y especie	Sin
CPT-2260	Insecta	Hymenoptera	Evaniidae	*Cretevania rubusensis*	
CPT-3334 (AP-1)	Insecta	Hemiptera	Cixiidae?		
CPT-3336 (AP-3)	Insecta	Hymenoptera	Scelionidae		
CPT-3337 (AP-4)	Insecta	Hymenoptera	Scelionidae		
CPT-3338 (AP-5)	Insecta	Hymenoptera	Scelionidae		
CPT-3339 (AP-6)	Insecta	Hymenoptera	Scelionidae		
CPT-3340 (AP-7)	Insecta	Diptera			
AP-8	Insecta	Diptera	Ceratopogonidae?		
AP-9	Insecta	Diptera	Chironomidae		
AP-10	Insecta	Psocodea	†Empheriidae		
AP-11.1	Insecta	Psocodea	†Empheriidae	*Archaeatropos alavensis*	
AP-11.2	Insecta	Raphidioptera			
AP-11.3	Insecta	Blattodea	Corydiidae		
AP-11.4	Insecta	Diptera			

Ámbar de La Hoya:

Sigla	Identificación/clase	Orden	Familia	Género y especie	Sin
MGUV-16234	Insecta	Blattodea			
MGUV-16240	Insecta				
MGUV-16345	Insecta				
MGUV-16346	Insecta				
MGUV-16347	Insecta				
MGUV-16348	Insecta	Diptera	Hybotidae	Gen. nov. sp. 2	
MGUV-16349	Insecta	Diptera	Hybotidae	Gen. nov. sp. 2	
LH-1	Insecta	Blattodea	†Mesoblattinidae?		
LH-2	Insecta	Hymenoptera	Scelionidae		
LH-3	Insecta	Diptera	Chironomidae		

8.3. Divulgación y difusión social

Durante la Tesis Doctoral se ha prestado especial atención a las actividades de divulgación y difusión social de las campañas de excavación y de los resultados de las investigaciones. Es muy importante que la información resultante de los estudios científicos llegue al público general y no quede limitada al ámbito científico. Se han realizado diferentes actividades por medio de diversas vías, como redacción de notas de prensa, entrevistas, colaboración con periodistas y preparación de contenido divulgativo. A continuación, se indican las principales actividades que se han llevado a cabo:

Actividad	Medio de difusión	Link / Nombre del evento
Nota de prensa	Universitat de Barcelona	https://www.ub.edu/web/ub/es/menu_eines/noticies/2020/11/026.html
Nota de prensa	Universitat de Barcelona	https://www.ub.edu/web/ub/es/menu_eines/noticies/2021/11/031.html
Nota de prensa	Institut de Recerca de la Biodiversitat	http://www.ub.edu/irbio/descubiertos-nuevos-insectos-emparentados-con-los-piojos-en-el-ambar-cretaceo-de-la-peninsula-iberica-n-967-es
Entrevista	Diario de Teruel	https://www.diariodeteruel.es/entrevistas/sergio-alvarez-parra-investigador-en-formacion-en-la-universitat-de-barcelona-el-yacimiento-de-ambar-de-arino-dara-mas-cosas-pero-los-pelos-han-sido-la-bomba
Entrevista	Aragón TV	https://www.youtube.com/watch?v=cLDOh4NZ6lA
Entrevista	Podcast Nomen Dubium	https://www.ivoox.com/23-paleoentrevista-a-sergio-alvarez-el-ambar-como-audios-mp3_rf_66030272_1.html
Colaboración con periodistas	New Scientist	https://www.newscientist.com/article/2300530-dinosaur-era-swamp-ecosystem-preserved-in-amber/
Divulgación	Sociedad Española de Paleontología	https://sepaleontologia.es/una-depilacion-cretacica-plumas-de-dinosaurio-y-pelos-de-mamifero-en-ambar-de-teruel/
Divulgación	Sociedad Española de Paleontología	https://sepaleontologia.es/una-nueva-especie-de-peculiares-avispas-cretacicas-nombrada-en-honor-al-divulgador-cientifico-nigel-marven/
Divulgación	Twitter	https://mobile.twitter.com/SrAmbarez/status/1384855415519842305
Divulgación	I Congreso Online Pangea. Youtube: El Pakozoico	https://www.youtube.com/watch?v=8dFCqJFElQo&t=5782s (min 40:10)
Divulgación	Universitat de Barcelona	"Els fòssils una finestra al passat" en la VIII Festa de la Ciència de la Universitat de Barcelona. 27/05/22-28/05/22
Divulgación	Oxford University Museum of Natural History	"Fossil Minibeast!" en el Super Science Saturday del Oxford University Museum of Natural History. 12/03/2022

UNIVERSITAT DE BARCELONA

Instituto Geológico y Minero de España

IRBio

Institut de Recerca de la Biodiversitat
UNIVERSITAT DE BARCELONA